MEDICINAL PLANTS FOR CARDIOVASCULAR AND NEURODEGENERATIVE AGING-RELATED DISEASES: FROM BENCH TO BEDSIDE

EDITED BY: Yue Liu, Valentina Echeverria Moran and Youhua Xu
PUBLISHED IN: Frontiers in Pharmacology

frontiers Research Topics

frontiers

ISSN 1664-8714
ISBN 978-2-88966-160-2
DOI 10.3389/978-2-88966-160-2

About Frontiers

Frontiers is more than just an open-access publisher of scholarly articles: it is a pioneering approach to the world of academia, radically improving the way scholarly research is managed. The grand vision of Frontiers is a world where all people have an equal opportunity to seek, share and generate knowledge. Frontiers provides immediate and permanent online open access to all its publications, but this alone is not enough to realize our grand goals.

Frontiers Journal Series

The Frontiers Journal Series is a multi-tier and interdisciplinary set of open-access, online journals, promising a paradigm shift from the current review, selection and dissemination processes in academic publishing. All Frontiers journals are driven by researchers for researchers; therefore, they constitute a service to the scholarly community. At the same time, the Frontiers Journal Series operates on a revolutionary invention, the tiered publishing system, initially addressing specific communities of scholars, and gradually climbing up to broader public understanding, thus serving the interests of the lay society, too.

Dedication to Quality

Each Frontiers article is a landmark of the highest quality, thanks to genuinely collaborative interactions between authors and review editors, who include some of the world's best academicians. Research must be certified by peers before entering a stream of knowledge that may eventually reach the public - and shape society; therefore, Frontiers only applies the most rigorous and unbiased reviews.
Frontiers revolutionizes research publishing by freely delivering the most outstanding research, evaluated with no bias from both the academic and social point of view. By applying the most advanced information technologies, Frontiers is catapulting scholarly publishing into a new generation.

What are Frontiers Research Topics?

Frontiers Research Topics are very popular trademarks of the Frontiers Journals Series: they are collections of at least ten articles, all centered on a particular subject. With their unique mix of varied contributions from Original Research to Review Articles, Frontiers Research Topics unify the most influential researchers, the latest key findings and historical advances in a hot research area! Find out more on how to host your own Frontiers Research Topic or contribute to one as an author by contacting the Frontiers Editorial Office: researchtopics@frontiersin.org

MEDICINAL PLANTS FOR CARDIOVASCULAR AND NEURODEGENERATIVE AGING-RELATED DISEASES: FROM BENCH TO BEDSIDE

Topic Editors:
Yue Liu, Xiyuan Hospital, China
Valentina Echeverria Moran, Bay Pines VA Healthcare System, United States
Youhua Xu, Macau University of Science and Technology, Macau

Citation: Liu, Y., Moran, V. E., Xu, Y., eds. (2020). Medicinal Plants for Cardiovascular and Neurodegenerative Aging-related Diseases: From Bench to Bedside. Lausanne: Frontiers Media SA. doi: 10.3389/978-2-88966-160-2

Table of Contents

frontiers in Pharmacology

EDITORIAL
published: 23 September 2020
doi: 10.3389/fphar.2020.585155

Editorial: Medicinal Plants for Cardiovascular and Neurodegenerative Aging-Related Diseases: From Bench to Bedside

Yue Liu[1,2]*, *Valentina Echeverria*[3,4] *and Youhua Xu*[5]

[1] Cardiovascular Disease Centre, Xiyuan Hospital of China Academy of Chinese Medical Sciences, Beijing, China, [2] Cardiovascular Disease Centre, National Clinical Research Center for Chinese Medicine Cardiology, Beijing, China, [3] Laboratorio de Neurobiología, Facultad de Ciencias de la Salud, Universidad San Sebastián, Concepción, Chile, [4] Research and Development Department, Bay Pines VA Healthcare System, Bay Pines, FL, United States, [5] State Key Laboratory of Quality Research in Chinese Medicines, Macau University of Science and Technology, Macau, Macau

Keywords: medicinal plants, aging, age-related diseases, cardiovascular disease, neurodegenerative diseases

Editorial on the Research Topic Medicinal

Medicinal Plants for Cardiovascular and Neurodegenerative Aging-Related Diseases: From Bench to Bedside

OPEN ACCESS

Edited and reviewed by:
Javier Echeverria,
University of Santiago, Chile

***Correspondence:**
Yue Liu
liuyueheart@hotmail.com

Specialty section:
This article was submitted to Ethnopharmacology, a section of the journal Frontiers in Pharmacology

Received: *19 July 2020*
Accepted: *11 September 2020*
Published: *23 September 2020*

Citation:
Liu Y, Echeverria V and Xu Y (2020) Editorial: Medicinal Plants for Cardiovascular and Neurodegenerative Aging-Related Diseases: From Bench to Bedside. Front. Pharmacol. 11:585155. doi: 10.3389/fphar.2020.585155

Aging is a progressive and multi-step degeneration in the physiological functions and metabolic processes of living organisms until death. It represents the main risk factors for a number of debilitating diseases and contributes to increase in mortality (Ahadi et al., 2020). With increasing life expectancy, the number of patients with aging related diseases will continue to rise, leading to an increased healthcare burden. There is a need for new therapies to treat this growing number of patients in a manner that is effective and sustainable (Liu and Chen, 2012). Aging presents profound physiological changes in the cardiovascular system and the relationship between cardiovascular pathology and neurodegenerative diseases is well known (Luo et al., 2020). Ischemic events due to cardiac pathology or stroke can lead to cardiovascular dementia and the development of Alzheimer's disease (Daniele et al., 2020). Cardiac pathology has also been found to be associated with other neurodegenerative conditions such as Huntington's disease (Critchley et al., 2018). Interestingly, it is hypothesized that factors systemically linking these pathologies are associated with neuroinflammation and oxidative stress pathways (Liu et al., 2019; Tian et al., 2019). While the underlying mechanisms in the aging heart or brain are still unclear, greater research is needed to test the potential for pharmacological interventions in these pathways.

Natural plants have been associated with traditional medical approaches for thousands of years all over the world. Great varieties of plants have persisted in such usage for medicinal treatments in various cultures and many new drugs have been discovered from herbal sources (Liu et al., 2013; Liu and Liu, 2020). The 2015 Nobel Prize awarded to Professor Tu, a Chinese pharmaceutical scientist, for the discovery of artemisinin renewed global interest in herbal medicine, and potential integration of such approaches into evidence-based medical systems (Tu, 2011). Medicinal plants have shown to be beneficial in decreasing the occurrence or delay of the neurodegenerative process induced by cardiovascular and mixed pathological events. It is believed that many of the medicinal herbs have anti-aging properties (Zhao et al., 2020), but the mechanisms and safety remain unclear.

This Research Topic is a collection of nineteen articles adapting a critical approach designed to robustly test the clinical effects, mechanisms and safety of adequately-characterized herbal medicine and their active components for aging-related diseases, in particular, cardiovascular and neurodegenerative diseases.

Alzheimer's disease (AD) is the most common neurodegenerative disorder associated with aging that causes memory, thinking and behavior disorders. Currently, FDA-approved anti-AD drugs (rivastigmine, galantamine, donepezil, memantine) are potential effective in the short term but are unable to halt or reverse disease progression (Dong et al., 2019). In November 2019, Sodium oligomannate received its first approval in China for the treatment of mild to moderate AD to improve cognitive function (Syed Yahiya, 2020), therapeutically remodels gut microbiota and suppresses gut bacterial amino acids-shaped neuroinflammation to inhibit AD progression (Wang et al., 2019), but there is some controversy in China (Rao, 2020; Wang et al., 2020). In this Research Topic, there are three research articles and two review articles describing the potential efficacy and related mechanisms of medicinal plants for AD or brain aging. An research article by Yang et al. evaluated the *in vitro* and *in vivo* effects of a traditional Chinese medicinal formula named *Yizhiqingxin formula* (YQF) on autophagy, the authors found that YQF could improve spatial learning in APP/PS1 mice and ameliorate the accumulation of Aβ while promoting autophagy *via* mTOR pathway modulation. Peng et al.'s article studied the molecular mechanisms of another traditional Chinese medicinal formula, *Baizhu decoction* (BZD) for AD, they found that middle- and high-doses of BZD ameliorated the behavioral aspects of 5xFAD transgenic mice in elevated plus maze, Y maze and Morris water maze tests with reduced BACE1 and PS1, resulting in a reduction of Aβ plaques and oxidative damage. Study by Wang et al. showed that β-Asarone, the main constituent of *Acorus tatarinowii Schott*, significantly dose-dependently increased cell proliferation and decreased cytotoxicity, inhibited SA-bGal and improved cell senescence in PC12 cell AD model. In a literature review, Balkrishna et al. reviewed the phytochemical profile, pharmacological attributes and medicinal information of *Convolvulus prostratus* (a nootropic herb used in traditional medicinal systems) with comprehensive research gap analysis, *Convolvulus prostratus* is mainly endowed with neuroprotective, nootropic and neuro-modulatory activities without any signs of toxicity and neurodegeneration up to a dose of 2000 mg/kg in mice. Another review article by Martínez-Coria et al. analyzed the most important pharmacological actions of *dihydromyricetin* (one of the main flavonoids of some Asian medicinal plants), including its antioxidant, anti-inflammatory and neuroprotective actions, as well as its ability to restore GABA neurotransmission, improve motor and cognitive behavior.

One research article by Fu et al. studied neuroprotective effects of *Qingnao dripping pills*(QNDP), a traditional Chinese prescription, for Ischemic stroke. The authors found that QNDP had neuroprotective effects against cerebral ischemia *via* inhibiting NLRP3 inflammasome signaling pathway, and was a potential candidate for the future treatment of ischemic stroke.

Heart failure (HF) is the terminal state of all cardiovascular diseases, and there is limited effective drug up to now (McMurray et al., 2019; Triposkiadis et al., 2019). The discovery of potential drugs for the treatment of heart failure from medicinal plants is of great clinical value. Lu et al. explore the effect of *Qishen Granule* (an effective Chinese medicine for treating heart failure) on the release of splenic monocytes, the recruitment of monocytes into heart tissues and the differentiation of macrophages under ischemic conditions. The authors reported that compounds of Chinese medicine have synergistic effects on cardiac and splenic organs through regulating differentiation of monocytes/macrophages in inhibiting myocardial remodeling. Li et al. reported that administration of Shengmai (used to treat acute and chronic heart failure in China), a traditional Chinese medicine extracted from *Panax ginseng C.A. Mey., Ophiopogon japonicus (Thunb.) Ker Gawl., and Schisandra chinensis (Turcz.) Baill.*, suppressed ang II–induced cardiomyocyte hypertrophy and apoptosis *via* activation of the AMPK signaling pathway through an energy dependent mechanisms. Another TCM, *Shenfu injection* (SFI) has been widely used for the treatment of shock and HF in China. The study by Zhu et al. showed that the vasodilation effect of SFI in thoracic aorta is mediated entirely by enhancing eNOS, activity through the PI3K/Akt signaling pathway, providing novel knowledge on the effect of SFI on shock and HF for future clinical applications. *Yixinshu Capsules* (YXSC) are widely used in China for the treatment of heart failure (HF) with better clinical efficacy, but the therapeutic mechanisms are not well understood. In the study by Xu et al., a metabonomic approach based on integrated UPLC-Q/TOF-MS technique and MALDI-MS was utilized to explore potential metabolic biomarkers increasing the understanding of HF and assessing the potential mechanisms of YXSC against HF, they proposed strategy may contribute to the understanding of the complex pathogenesis of ischemia-induced HF and the potential mechanism of YXSC.

Many medicinal plants do not enter the blood after they are taken orally, growing evidence suggest the role of the gut microbiota as targets for the multifunctional role of medicinal plants for cardiovascular diseases (CVD) (Gong et al., 2020). There are three research articles focused on the changing characteristics of gut microbiota to elucidate the mechanisms of medicinal plants in the treatment of cardiovascular disease. Zhang et al. reported that long-term administration of *Naoxintong* capsule, a Chinese medicine, increased the diversity of gut microbiota, influenced the microbiome structure and composition stably, and revered the increase of the ratio of the Firmicutes to Bacteroidetes in relative abundance, inhibited the development of cardiovascular diseases by ameliorating high-fat diet-induced metabolic disorders and partly through improving gut microbiota. Wu M. et al. observe the effects of high or low doses of *berberine* on atherosclerosis and gut microbiota modulation, their study found that anti-atherosclerotic action of berberine may be partly attributed to changes in composition and functions of gut microbiota which

may be associated with anti-inflammatory and metabolism of glucose and lipid. The study by Wu D. et al. provides for the first time the morphological, biochemical, and molecular evidence supporting the protective effects of *baicalin* (the major flavonoid component of *S. baicalensis Georgi*) on the intestinal integrity in the spontaneously hypertensive rats, which may help better understand the therapeutic actions of *S. baicalensis Georgi* in the treatment of hypertension.

An important feature of this Research Topic collection, many well-known scholars have contributed a lot of wonderful literature reviews about medicinal plants for aging-related cardiovascular and neurodegenerative diseases. Souza-Junior et al. discuss the ethnobotanical characteristics, phytochemical constitution, and cardiovascular and neurological properties of *A. canelilla*, systematizing the knowledge about the species and proposing new perspectives for research and development. Shaito et al. overview the data on the ethnopharmacological therapeutic potentials and medicinal properties against CVDs (myocardial infarction, hypertension, peripheral vascular diseases, coronary heart disease, cardiomyopathies, and dyslipidemias) of *Ginseng, Ginkgo biloba, Ganoderma lucidum, and Gynostemma pentaphyllum*. Michel et al. reviewed the potential use of medicinal plants from Asteraceae and Lamiaceae Plant Family in CVDs. Atherosclerosis is the main pathological mechanism of aging-related cardiovascular and neurodegenerative diseases, characterized by changes of blood lipids profile and inflammation in vessel wall. Kirichenko et al. reviewed the databases PubMed and Scopus (until November, 2019) to investigate the medicinal plants possessing anti-atherosclerotic activity in experimental and clinical studies. Wu M. et al. summarize the blood lipid lowering, anti-oxidative, anti-inflammatory, and vascular endothelial protection by hawthorn and its extracts, providing a potential use for atherosclerosis. This Research Topic also includes a systematic preclinical review of the effect of Notoginsenoside R1 (NGR1) for ischemia/reperfusion injury. The study by Tong et al. showed the organ protection effect of NGR1 after I/R injury, suggesting that NGR1 can potentially become a novel drug candidate for ischemic diseases.

From the above-mentioned 19 articles, this Research Topic provides recent evidence about efficacy, mechanisms, and safety of medicinal plants for cardiovascular and neurodegenerative aging-related diseases. We hope this topic will help to achieve a deeper understanding of the effect of medicinal plants for aging-related diseases.

AUTHOR CONTRIBUTIONS

All authors listed have made a substantial, direct, and intellectual contribution to the work, and approved it for publication.

FUNDING

VE was supported by a Grant Fondecyt 1190264 from ANID, Chile.

ACKNOWLEDGMENTS

The guest editors of this Research Topic acknowledges the efforts and contribution of authors, reviewers, and journal senior editors for their sincere efforts.

REFERENCES

Ahadi, S., Zhou, W., Schüssler-Fiorenza Rose, S. M., Sailani, M. R., Contrepois, K., Avina, M., et al. (2020). Personal aging markers and ageotypes revealed by deep longitudinal profiling. *Nat. Med.* 26 (1), 83–90. doi: 10.1038/s41591-019-0719-5

Critchley, B. J., Isalan, M., and Mielcarek, M. (2018). Neuro-Cardio Mechanisms in Huntington's Disease and Other Neurodegenerative Disorders. *Front. Physiol.* 9, 559. doi: 10.3389/fphys.2018.00559

Daniele, G., DiLucia, S., Masci, P. G., and Del Monte, F. (2020). Heart and Brain: Complex Relationships for Left Ventricular Dysfunction. *Curr. Cardiol. Rep.* 22 (8), 72. doi: 10.1007/s11886-020-01318-w

Dong, Y., Li, X., Cheng, J., and Hou, L. (2019). Drug development for Alzheimer's disease: microglia induced neuroinfammation as a target? *Int. J. Mol. Sci.* 20 (3), 558. doi: 10.3390/ijms20030558

Gong, X., Li, X., Bo, A., Shi, R.-Y., Li, Q.-Y., Lei, L.-J., et al. (2020). The interactions between gut microbiota and bioactive ingredients of traditional Chinese medicines: A review. *Pharmacol. Res.* 157, 104824. doi: 10.1016/j.phrs.2020.104824

Liu, Y., and Chen, K. J. (2012). Atherosclerosis, vascular aging and therapeutic strategies. *Chin. J. Integr. Med.* 18 (2), 83–87. doi: 10.1007/s11655-012-0996-z

Liu, Y., and Liu, Y. (2020). Herbal Medicine for Slowing Aging and Cardiovascular Risk: Mechanisms and Safety. *Curr. Vasc. Pharmacol.* 18 (4), 305–306. doi: 10.2174/1570161118042005070756O6

Liu, Y., Yin, H., and Chen, K. (2013). Platelet proteomics and its advanced application for research of blood stasis syndrome and activated blood circulation herbs of Chinese medicine. *Sci. China Life Sci.* 56 (11), 1000–1006. doi: 10.1007/s11427-013-4551-8

Liu, Y., Weng, W., Gao, R., and Liu, Y. (2019). New Insights for Cellular and Molecular Mechanisms of Aging and Aging-Related Diseases: Herbal Medicine as Potential Therapeutic Approach. *Oxid. Med. Cell Longev.* 2019, 4598167. doi: 10.1155/2019/4598167

Luo, H., Zhang, R., Krigman, J., McAdams, A., Ozgen, S., and Sun, N. (2020). A Healthy Heart and a Healthy Brain: Looking at Mitophagy. *Front. Cell Dev. Biol.* 8, 294. doi: 10.3389/fcell.2020.00294

McMurray, J. J. V., Solomon, S. D., Inzucchi, S. E., Køber, L., Kosiborod, M. N., Martinez, F. A., et al. (2019). Dapagliflozin in Patients with Heart Failure and Reduced Ejection Fraction. *N. Engl. J. Med.* 381 (21), 1995–2008. doi: 10.1056/NEJMoa1911303

Rao, Y. (2020). Omission of previous publications by an author should be corrected. *Cell Res.* 30 (9), 819. doi: 10.1038/s41422-020-0344-3

Syed Yahiya, Y. (2020). Sodium Oligomannate: First Approval. *J. Drugs* 80 (4), 441–444. doi: 10.1007/s40265-020-01268-1

Tian, J., Popal, M. S., Zhao, Y., Liu, Y., Chen, K., and Liu, Y. (2019). Interplay between Exosomes and Autophagy in Cardiovascular Diseases: Novel Promising Target for Diagnostic and Therapeutic Application. *Aging Dis.* 10 (6), 1302–1310. doi: 10.14336/AD.2018.1020

Triposkiadis, F., Xanthopoulos, A., and Butler, J. (2019). Cardiovascular Aging and Heart Failure: JACC Review Topic of the Week. *J. Am. Coll. Cardiol.* 74 (6), 804–813. doi: 10.1016/j.jacc.2019.06.053

Tu, Y. (2011). The discovery of artemisinin (qinghaosu) and gifts from Chinese medicine. *Nat. Med.* 17 (10), 1217–1220. doi: 10.1038/nm.2471

Wang, X., Sun, G., Feng, T., Zhang, J., Huang, X., Wang, T., et al. (2019). Sodium oligomannate therapeutically remodels gut microbiota and suppresses gut bacterial amino acids-shaped neuroinflammation to inhibit Alzheimer's disease progression. *Cell Res.* 29 (10), 787–803. doi: 10.1038/s41422-019-0216-x

Wang, X., Sun, G., Feng, T., Zhang, J., Huang, X., Wang, T., et al. (2020). Geng et al. reply. *Cell Res.* 30 (9), 820. doi: 10.1038/s41422-020-0377-7

Zhao, J., Lan, X., Liu, Y., Liu, Y., Xian, Y., Lin, Z., et al. (2020). Anti-aging role of Chinese herbel medicine: an overview of scientific evidence from 2008 to 2018. *Ann. Palliat. Med.* 9 (3), 1230–1248. doi: 10.21037/apm.2020.04.09

Conflict of Interest: The authors declare that the research was conducted in the absence of any commercial or financial relationships that could be construed as a potential conflict of interest.

frontiers in Pharmacology

ORIGINAL RESEARCH
published: 17 September 2019
doi: 10.3389/fphar.2019.01041

Yizhiqingxin Formula Alleviates Cognitive Deficits and Enhances Autophagy *via* mTOR Signaling Pathway Modulation in Early Onset Alzheimer's Disease Mice

Yang Yang[1†], Zhiyong Wang[1†], Yu Cao[1], Jiangang Liu[1], Peng Li[2], Hao Li[1] and Meixia Liu[1*]*

[1] Institute of Geriatrics, Xiyuan Hospital, China Academy of Chinese Medical Sciences, Beijing, China, [2] Beijing Key Laboratory of Pharmacology of Chinese Materia Region, Institute of Basic Medical Sciences of Xiyuan Hospital, China Academy of Chinese Medical Sciences, Beijing, China

OPEN ACCESS

Edited by:
Yue Liu,
Xiyuan Hospital,
China

Reviewed by:
Jun Xu,
Capital Medical University,
China
Yan-Fang Xian,
The Chinese University of
Hong Kong, Hong Kong

***Correspondence:**
Hao Li
xyhplihao1965@126.com
Meixia Liu
18701522362@126.com

†These authors have contributed equally to this work

Specialty section:
This article was submitted to Ethnopharmacology, a section of the journal Frontiers in Pharmacology

Received: 07 June 2019
Accepted: 16 August 2019
Published: 17 September 2019

Citation:
Yang Y, Wang Z, Cao Y, Liu J, Li P, Li H and Liu M (2019) Yizhiqingxin Formula Alleviates Cognitive Deficits and Enhances Autophagy via mTOR Signaling Pathway Modulation in Early Onset Alzheimer's Disease Mice. Front. Pharmacol. 10:1041. doi: 10.3389/fphar.2019.01041

Alzheimer's disease (AD) is the most common type of dementia worldwide. The deposition of amyloid β (Aβ) is one of the most important pathological changes in AD. Autophagy, which mediates degradation of toxic proteins and maintains normal neuronal function, is dysfunctional in AD; dysfunctional autophagy is believed to be a critical pathological feature of AD. Here, we evaluated the *in vitro* and *in vivo* effects of a traditional Chinese medicinal formula called Yizhiqingxin formula (YQF) on autophagy. We determined that treatment with a high dose of YQF improved spatial memory and decreased the hippocampal Aβ burden in *APP/PS1* mice, an early onset AD model. Transmission electron microscopy and immunohistochemical data revealed that YQF enhanced autophagosome formation and also increased the levels of LC3II/LC3I and Beclin1. Further, we found that YQF treatment promoted autophagic activity by inhibiting the phosphorylation of the Mammalian target of rapamycin (mTOR) at the Ser2448 site. Moreover, the level of 4EBP1 increased after YQF intervention, indicating a suppression of mTOR signaling. YQF was also found to promote autophagosome degradation, as indicated by the decreased p62 levels and increased cathepsin D and V-ATPase levels. Taken together, YQF could improve spatial learning in *APP/PS1* mice and ameliorate the accumulation of Aβ while promoting autophagy *via* mTOR pathway modulation.

Keywords: Alzheimer's disease, Yizhiqingxin formula, autophagy, mTOR, APP/PS1 mice

INTRODUCTION

Alzheimer's disease (AD), manifested by core clinical features of progressive memory loss and executive dysfunction, is the most common type of dementia worldwide. In China, the current prevalence of AD in people over 65 is 3.21% (Jia et al., 2014). The aggravating trend of aging population also drives the increasing number of AD patients. According to the World Alzheimer Report 2018, it is estimated that there are about 47 million Alzheimer's patients worldwide, with 10 million new cases each year (Alzheimer's Association, 2018). As the disease progresses, most patients eventually need constant care and help with most basic daily activities, exacting a heavy

burden on families and society (Jia et al., 2018). AD therapy is reported to be the most expensive treatment in the U.S. (Souchet et al., 2018).

Autophagy is an evolutionarily conserved intracellular process responsible for the lysosomal degradation and removal of degraded and aggregated proteins, and damaged intracellular organelles to maintain cellular homeostasis (Ryter et al., 2013). This robust quality control mechanism is critical in neurons to support their long-term viability and functionality. Multiple studies have identified defective autophagic activity in several neurodegenerative diseases, especially in AD, which is characterized by amyloid β (Aβ) peptide aggregation. Moreover, both *in vitro* and *in vivo* studies have shown that autophagy retards neuronal degeneration and age-associated cognitive disorders by the clearance of accumulated toxic proteins. An abnormal alteration of autophagy and Aβ deposition has been observed in AD patients, along with a hyperactivation of the mammalian target of rapamycin (mTOR) pathway (Sun et al., 2014; Tramutola et al., 2017). Consistent with these clinical findings, overwhelming data suggest a vicious cycle between Aβ deposition and mTOR hyperactivity (Oddo, 2012; Talboom et al., 2015).

Yizhiqingxin formula (YQF; previously called Fuzheng Quxie Decoction **Supplementary Data Sheet 1**) is a traditional Chinese formula composed of *Panax ginseng* (radix), *Coptis chinensis* (rhizome), and *Conioselinum anthriscoides 'Chuanxiong'* (rhizome). Our previous work found that YQF could alleviate cognitive deficits and tau hyperphosphorylation in SAMP8 mice (Yang et al., 2017); vascular endothelial growth factor (VEGF) and VEGF receptor were the other molecular targets of YQF (Wang et al., 2018). However, the effects of YQF on autophagy and the underlying mechanisms are not clear. In the present study, we investigate the potential roles of YQF on autophagy and mTOR signaling in *APP/PS1* mice and *APP/PS1* double transgenic HEK293 cells. Data revealed that YQF could ameliorate cognitive deficits and decrease Aβ deposition, suggesting that YQF is a potential candidate for the treatment of AD.

MATERIALS AND METHODS

Animals

Sixty 3-month-old male *APP/PS1* transgenic mice were randomly divided into five groups: Model group, Rapa group (2.24 mg·kg^{-1}·d^{-1}), YQF high dose group (YQF-H, 10.4 g·kg^{-1}·d^{-1} raw drugs), YQF medium dose group (YQF-M, 5.2 g·kg^{-1}·d^{-1} raw drugs), and YQF low dose group (YQF-L, 2.6 g·kg^{-1}·d^{-1} raw drugs). Twelve male C57BL/6 mice with the same genetic background at 3 months of age were used as control. Each group was given 24 weeks of gavage intervention. Drugs used in Rapa and YQF-L groups were equivalent doses suggested in the clinic. The Control and Model groups were given equal volumes of distilled water. The other groups were given corresponding drugs. Mice were all housed in groups of three to four per cage and maintained in a specific pathogen-free conditions at 22 ± 2°C with automatic light cycles (12 h light/dark) and relative humidity of 50–70%. Animals received food and water *ad libitum* and were allowed to adapt to the environment for 1 week before experiment. All experiments were carried out in accordance with the guidelines for animal care and were approved by the animal ethics committee of the Ethics Committee of Xiyuan Hospital, China Academy of Chinese Medical Sciences (NO. 2018XLC004-1).

Reagents

Rabbit monoclonal anti-beta amyloid 1–42 (ab201060) antibody and rabbit polyclonal anti-LC3 II (ab48394), anti-p62 (ab91526), anti-mTOR (ab2732), and anti-cathepsin D (ab75852) antibodies were procured from Abcam (UK). Rabbit polyclonal anti-ATPase (sc-28801) antibody was procured from Santa Cruz (USA). Rabbit polyclonal anti-p-mTOR (5536S), anti-4EBP1 (9644S), anti-P70S6K (2708S), anti-Beclin 1 (3738S), and anti-LAMP1 (3243S) antibodies were procured from Cell Signaling Technology (USA). Mouse monoclonal anti-GAPDH (YM3029) antibody was purchased from Immunoway (USA). Mouse monoclonal anti-*β-actin* (sc-69879) antibody was purchased from Santa Cruz (USA). Aβ ELISA kit (DAB142) was purchased from RD (USA).

Drug Preparation

YQF is composed of *Panax ginseng* (radix), *Coptis chinensis* (rhizome), and *Conioselinum anthriscoides 'Chuanxiong'* (rhizome), with a weight ratio of 9:5:6. Raw drugs were purchased from Beijing Kangrentang Pharmaceutical Co. Ltd. They were deposited at the Herbarium of National Resource Center for Chinese Materia Medica (CMMI), China Academy of Chinese Medical Sciences. The codes for *Panax ginseng* (radix), *Coptis chinensis* (rhizome), and *Conioselinum anthriscoides 'Chuanxiong'* (rhizome) specimens were 0220582LY0015, 420528LY0075, and 331127LY0805, respectively. The extraction was done by the Department of Pharmaceutics of Xiyuan Hospital, China Academy of Chinese Medical Sciences. Per gram extraction was obtained from 3.71 grams raw drug mixture. Seven major bioactive compounds (gginsenoside Rg1, ginsenoside Re, ginsenoside Rb1, coptisine, berberine, ligustilide, and ferulic acid) were identified using HPLC (high performance liquid chromatography) (Yang et al., 2017).

Cell Culture, Gene Transfection, and Drug Intervention Protocols

The human embryonic kidney cell line (HEK293 cells) was purchased from National Infrastructure of Cell Line Resource (NO: 3111C0001CCC000128). Cells were cultured in Dulbecco's modified Eagle medium (DMEM; Hyclone, USA) supplemented with penicillin–streptomycin (100 IU/ml and 100 μg/ml, Gibco, USA) and 10% fetal bovine serum (Gibco, USA) in a humidified atmosphere of 5% CO_2 at 37°C. Cells were passaged using 0.25% trypsin with 0.02% EDTA every 3–4 days. During transfection, HEK293 cells were cultured in Opti-MEM I Serum Medium (Gibco, USA) and transfected with APP695 plasmid (Addgene, USA) with Lipofectamine 2000 (Invitrogen, USA) following manufacturers' instructions. The *APP695* gene HEK293 (APP-HEK293) cell clones were selected using puromycin (4 μg/ml, Amresco, USA). PSEN1dE9 plasmids (Beijing Borui Technology Co., Ltd., China) were transfected into the APP-HEK293 cells [clones were selected using G418 (1 mg/ml, Amresco, USA)],

and then the *APP/PS1* double gene transfected HEK293 cells stably expressing *APP695* and *PSEN1dE9* genes (*APP*/*PS1* double transgenic HEK293 cells) were obtained.

After gene transfection, HEK293 cells were divided into the Control group (treated with Control group serum), and *APP*/*PS1* double transgenic HEK293 cells were divided into the Model group, YQF-H group, YQF-M group, and YQF-L group and were treated with serum containing YQF.

Cell Viability Assay

Cell viabilities were measured by the Cell Counting Kit-8/WST-8 kit (CCK8, Dojindo, Japan) following the manufacturer's instruction. Briefly, cells were plated in a 96-well plate at a density of 1×10^5/ml. CCK8 mixed with DMEM without phenol red at a ratio of 1:9 was added to the 96-well plate, and then the plate was incubated in an incubator for 1–2 h. Optical density readings were measured with a Microplate Reader (Bio Tek, USA) at 450 nm wavelength.

Preparation of Serum Containing YQF (YQF-Serum)

Forty 3-month-old male Sprague Dawley rats purchased from Huafukang Biological Technologies [Beijing, China, NO: SCXK (Beijing) 2014-0004] were divided into four groups: YQF high dose group (YQF-H, 18 $g \cdot kg^{-1} \cdot d^{-1}$, herbal medicine), YQF medium dose group (YQF-M, 9 $g \cdot kg^{-1} \cdot d^{-1}$, herbal medicine), YQF low dose group (YQF-L, 1.8 $g \cdot kg^{-1} \cdot d^{-1}$, herbal medicine), and Control group (control, equal volume of distilled water) with 10 rats in each group. Rats in the four groups received a daily gavage with the respective treatment for 1 week. Subsequently, the rats were anaesthetized by intraperitoneal injection with pentobarbital sodium. Blood was drawn from the abdominal aorta and centrifuged at 3000 rpm for 10 min. The YQF-Serum so obtained was used for further experiments.

Morris Water Maze Tests

Spatial memory was assessed using the Morris water maze (MWM) test, as described previously (Yang et al., 2017). Briefly, a tank (diameter 120 cm, height 50 cm, painted white) filled with water (22°C) to the depth of 40 cm was used. The water was stained with nontoxic white dye. A white platform (diameter, 10 cm; height, 15 cm) was placed in the center of the target quadrant 1 cm beneath the water. The place navigation trial consisted of five training days and four trials per day with a 20-min inter-trial interval. Mice were placed into the water from four different starting positions facing the wall, and each trial lasted for 60 s. If a mouse did not reach the platform within 60 s, it was guided to the platform where it had to remain for 10 s. The swimming distance and escape latencies were recorded. One day after the task acquisition (day 5), a probe trial was performed in order to assess the spatial memory. The platform was removed. Animals were put into the tank from the position opposite to the platform and allowed to swim freely for 60 s. The percentage of total time spent in each quadrant and the number of crossings where the platform had been previously located were recorded.

Analysis of Blood and Brain Tissue for Active Components of YQF

After the MWM experiments, blood samples were collected from rats being transcardially perfused with ice-cold physiological saline for brain tissue isolation. Brains were quickly removed on ice; cerebral cortices were then separated and homogenized in ice-cold physiological saline (2 ml saline per 1 g cortex). Plasma was isolated from the blood samples of each group. Subsequently, liquid chromatography tandem mass spectrometry (LC-MS/MS) was used to detect the active components of YQF present in the blood plasma and brain tissue homogenate.

Transmission Electron Microscopy Analysis

Cells from *in vitro* experiments and hippocampal tissues obtained from the sacrificed mice, post MWM tests, were fixed with 2.5% glutaraldehyde and washed three times in phosphate-buffered saline (PBS) (pH 7.2), following which they were post fixed in 1% osmium tetroxide, dehydrated in graded ethanol and acetone solution, and embedded in epoxy resin. Sectioning and staining were subsequently performed under general electron microscopy supervision. Autophagosomes in cells of different samples were observed and imaged under a transmission electron microscope at 4000× magnification.

Immunohistochemistry Assays

After the behavior test, five mice from each group were anesthetized with pentobarbital sodium (30 mg/kg) and were perfused by intracardiac puncture with PBS (4°C) and 4% paraformaldehyde. Immunohistochemistry staining was conducted on 20 mm thick coronal sections as previously reported (Wang et al., 2010). Briefly, the sections were dewaxed, rehydrated, and incubated in PBS containing 3% H_2O_2 for 10 min. After washing with tris-buffered saline (TBS), sections were boiled in citric acid buffer for 5 min in a microwave oven and then incubated overnight at 4°C with rabbit antibody against $A\beta_{1\text{-}42}$ antibody (1:1000 dilutions). After rinsing, sections were incubated with biotinylated secondary antibody for 1 h, followed by streptavidin peroxidase for 1 h at room temperature. Subsequently, the sections were visualized with 3, 3-diaminobenzidine and analyzed using an inverted microscope (OLYMPUS CKX41, Tokyo, Japan).

To assess the Aβ burden in the cortex and hippocampus, five sections with the same reference position were selected from each mouse (n = 5). The percentage of the total area of Aβ-positive areas compared with the total area of the hippocampus was quantified (in square micrometers). The data were analyzed with the image analysis system (Image-Pro Plus 6.0).

ELISA

Cell cultures were treated with YQF-serum at the indicated concentrations for the specified durations. The conditioned medium was then collected and subjected to a sandwich ELISA for the $A\beta_{42}$ levels according to the manufacturer's guidelines.

Western Blot Analysis

The hippocampus was lysed on ice in lysis buffer and then centrifuged at 12,000g for 10 min at 4°C. The protein content was determined using a BCA protein assay kit (Pierce, Rockford, IL). Proteins (40 mg) were separated by SDS-PAGE electrophoresis and then transferred to 0.45 μm polyvinylidene difluoride membranes (Millipore, Bedford, MA). The membranes were blocked for 2 h in 5% BCA and were then incubated overnight at 4°C with the primary antibody (1:1000 dilutions) followed by a horseradish peroxidase-conjugated secondary antibody (1:2000 dilutions). The blots of proteins of interest were visualized using an ECL advanced Western blotting detection kit (Thermo Fisher Scientific, MA, USA). Quantitative analyses of the protein bands were performed with a Molecular Imager Carestream MI SE system (Rochester, NY, USA).

Statistical Analysis

Data are expressed as mean ± SEM and were analyzed by GraphPad Prism 7.0 (GraphPad Software, San Diego, CA). MWM latencies were analyzed using two-way analysis of variance (ANOVA) with repeated measures. All the other data were analyzed using one-way ANOVA. Fisher's least significant difference *post hoc* test was used to test the differences between two groups. Significance level was set at $p < 0.05$.

RESULTS

Analysis of Blood and Brain Tissue for Active Components of YQF

Our previous HPLC study revealed that the important active components of YQF are ginsenoside Rg1, ginsenoside Re, ginsenoside Rb1, coptisine, berberine, ligustilide, and ferulic acid (Yang et al., 2017). Here, the LC-MS/MS analyses of active components of YQF in the plasma and brain tissue (**Table 1** and **Supplementary DataTable 1**) showed that many alkaloids like berberine, palmatine, worenine, and protopine, and ginsenosides like Rg1, Re, Rb1, Rd, and Rc were found in plasma, while berberine, palmatine, epiberberine, coptisine, and ginsenoside Rb1 were found in brain tissue and ferulic acid of *Conioselinum anthriscoides 'Chuanxiong'* (rhizome) was found in the plasma but not brain tissue. Since many of the active components of *Conioselinum anthriscoides 'Chuanxiong'* (rhizome) are volatile, we believe that not all of its components were detected by this method.

YQF Treatment Alleviates Spatial Memory Deficits in *APP/PS1* Mice

APP/PS1 mice cognitive–behavioral changes occur at 3 months of age (Garcia-Alloza et al., 2006), APP/PS1 mice have a substantial number of amyloid deposits by 6 months of age. The plaque burden increases progressively with time (Jankowsky et al., 2004). Therefore, APP/PS1 mice have well simulated the main pathological changes of AD and are currently recognized as the international animal model of AD. To investigate whether a long-term YQF treatment could ameliorate spatial learning deficits in transgenic *APP/PS1* mice, MWM tests were performed. As shown in **Figure 1A**, all mice exhibited a significant decrease in escape latency over time. Two-way ANOVA reported a significant treatment effect on the escape latency [$F(5, 53) = 3.237$, $p = 0.013$]. However, *APP/PS1* mice spent more time searching for the hidden platform than controls ($p < 0.01$ model group vs. control group), indicating a significant cognitive decline. After high dose YQF treatment, the escape latency was shortened remarkably ($p < 0.01$ YQF-H group vs. model group). Rapamycin also reduced the mean latency significantly ($p < 0.05$ Rapa group vs. model group) (**Figure 1A**).

Moreover, in the probe trial, *APP/PS1* mice failed to remember the accurate location of the platform, and the crossover times were remarkably less than the Control group [$F(5, 54) = 3.615$ $p = 0.007$, $p < 0.01$ model group vs. control group]. Administration of rapamycin or high dose YQF significantly mitigated the deficits ($p < 0.05$ Rapa group vs. model group and $p < 0.05$ YQF-H group vs. model group). Besides, the mice treated with medium dose of YQF spent significantly more time in the target quadrant [$F(5, 52) = 3.359$ $p = 0.011$, $p < 0.05$ YQF-M group vs. model group]. The low

TABLE 1 | Active components of YQF in the serum and brain tissue of SD rats.

Sample name	Content (ng/mL)				
	Serum-L	Serum-M	Serum-H	Brain-H	Brain-M
Berberine	5.79	6.79	19.3	14.2	6.62
Palmatine	1.37	2.28	1.77	7.07	1.55
Worenine	0.818	0.923	2.18	1.91	ND
Protopine	ND	0.947	1.2	3.69	ND
Epiberberine	1.79	2.42	35.2	8.12	1.99
Coptisine	6.13	8.56	29.6	16.7	4.33
Jatrorrhizine	10.9	ND	19.6	13.4	3.85
Dehydrocorydaline	ND	ND	ND	9.73	ND
Tetrahydrojatrorrhizine	ND	ND	ND	9.12	1.12
Ginsenoside Rg1	ND	ND	22.7	ND	ND
Ginsenoside Re	ND	ND	18.8	ND	ND
Ginsenoside Rb1	87.9	232	514	5.89	ND
Ginsenoside Rd	ND	21.1	48.9	ND	ND
Ginsenoside Rc	31.7	78.9	147	ND	ND
Ferulic acid	1.71	3.96	113	ND	ND

ND, no detected. n = 3. Serum and brains were obtained from SD rats treated with low, medium, or high dose of YQF, and named as Serum-L, Serum-M, Serum-H, Brain-M, and Brain-H, respectively.

dose-treated group also showed a higher percentage of the swimming distance and time in the target quadrant than the Model group [$F(5, 52) = 3.712$ p = 0.006, $p < 0.01$ YQF-L group vs. model group and $F(5, 52) = 3.359$ $p = 0.011$, $p < 0.05$ YQF-L group vs. model group]. These results indicate that YQF treatment improves the spatial learning and memory function in *APP/PS1* mice (**Figures 1B–D**).

YQF Reduces Aβ Levels in the Hippocampus of *APP/PS1* Mice and *APP/PS1* Double Transgenic HEK293 Cells

To investigate the effect of YQF treatment on Aβ deposition and senile plaque formation, brain slices were stained with a monoclonal antibody against $A\beta_{1\text{-}42}$ and quantitative image analysis was performed (**Figures 2A**, **B**). Results show that in 9-month-old *APP/PS1* mice, immuno-positive diffuse plaques occupied a great deal of the hippocampal areas compared to non-transgenic mice [$F(5, 24) = 11.618$ $p = 0.000$, $p < 0.01$ model group vs. control group]. After YQF treatment, all YQF groups had significantly reduced Aβ burden ($p < 0.05$ YQF-L group vs. model group and $p < 0.01$ YQF-M/H group vs. model group). Rapamycin group also showed a remarkable reduction in Aβ burden ($p < 0.01$ Rapa group vs. model group).

In vitro (**Figure 2C**), we also found that *APP/PS1* double transgenic HEK293 cells expressed the highest level of $A\beta_{1\text{-}42}$ compared with the other groups [$F(5,18) = 130.531$ p = 0.000, $p < 0.01$ model group vs. control group]; YQF could reduce the expression of $A\beta_{1\text{-}42}$, especially in the YQF-M and YQF-H groups ($p < 0.01$ YQF-M/H group vs. model group).

YQF Promotes the Formation and Degradation of Autophagosome *In Vivo* and *In Vitro*

By transmission electron microscopy (**Figure 3**), we found using *in vivo* and vitro experiments that many large autophagosomes are assembled in *APP/PS1* mice and cells compared with non-transgenic animals and cells. Mitochondria and other cytoplasmic components could be found in the autophagosomes. Furthermore, rapamycin could assemble large number of autophagosomes in neuronal cells and transgenic HEK293 cells as compared to the Model group. Every cell in the YQF groups exhibited autophagosomes more than that in Model groups but less than in Rapamycin groups. Moreover, we could also find that contents in the autophagic vacuoles of YQF groups were partly degraded, especially in the YQF-H group; apparently, a portion of the autophagic vacuoles were autophagolysosomes.

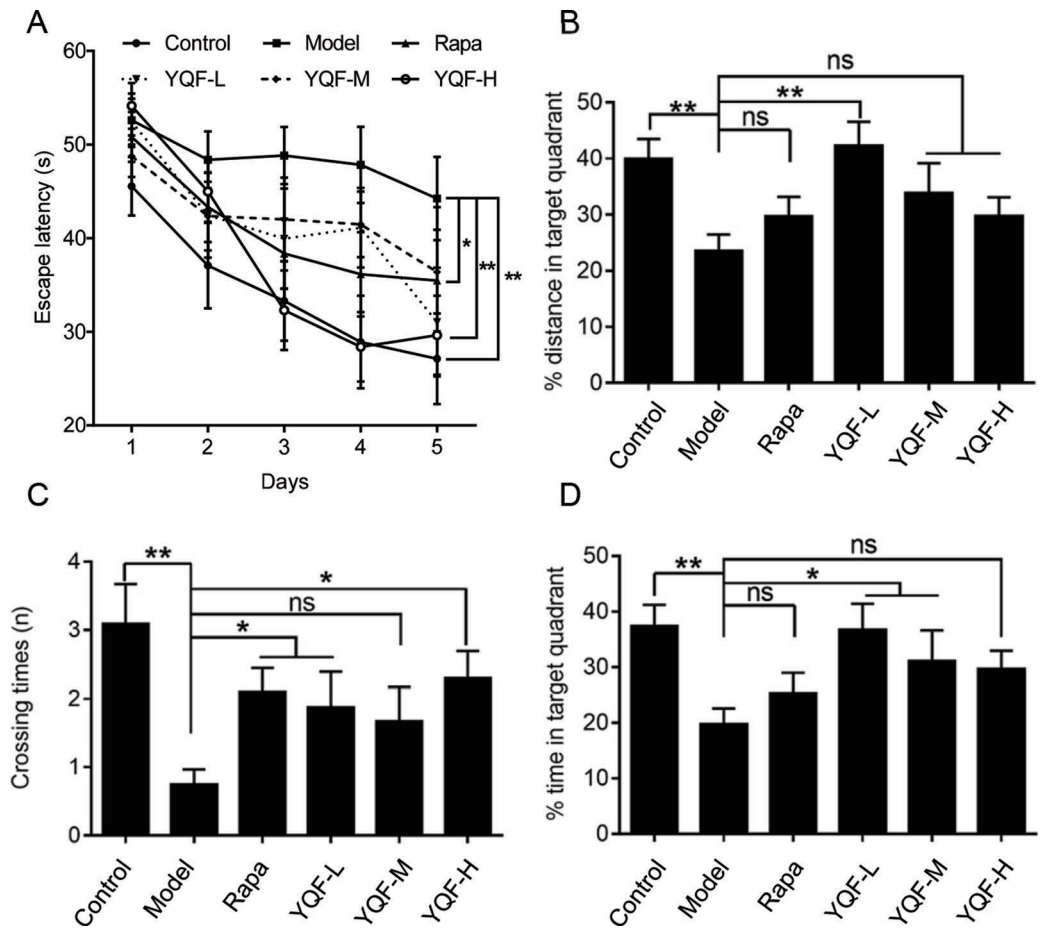

FIGURE 1 | YQF alleviates spatial memory deficits of APP/PS1 mice **(A)** Escape latency, **(B)** Distance in the target quadrant, **(C)** Crossing times, **(D)** Time spent in the target quadrant, n = 8–12; *$p < 0.05$; **$p < 0.01$; ns, no significant difference.

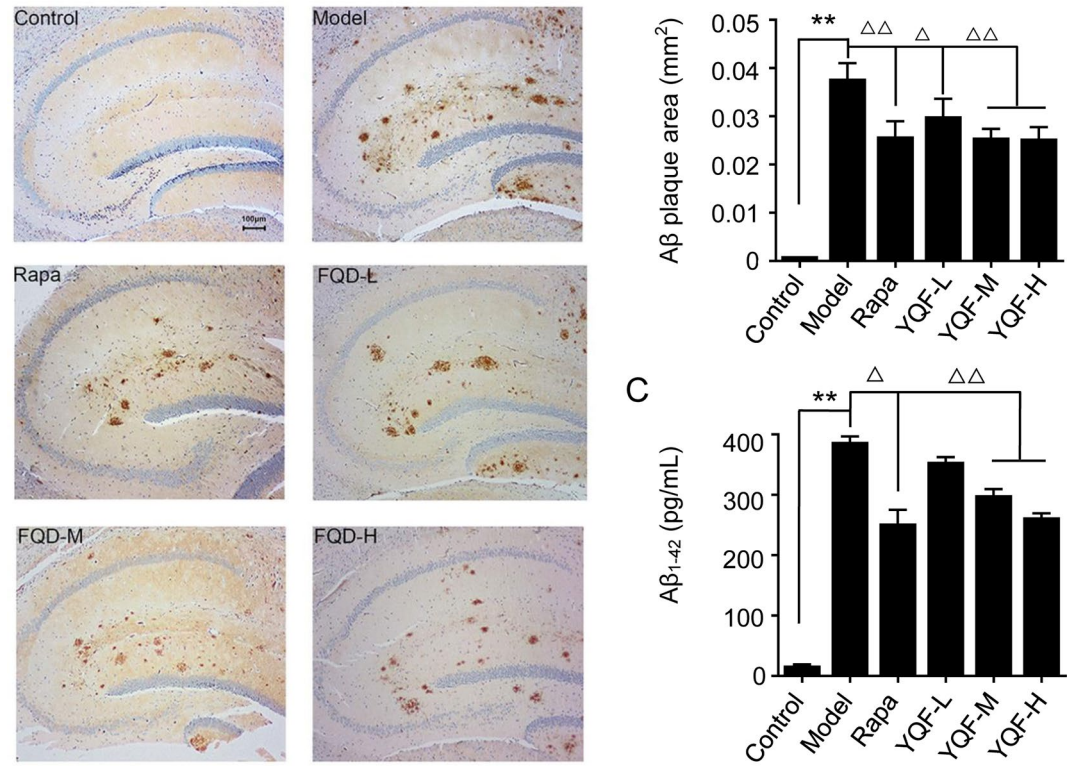

FIGURE 2 | Expression of $A\beta_{1\text{-}42}$ in hippocampus of mice **(A** and **B)** and HEK293 cells **(C)**. Data are expressed as mean ± SEM, n = 5, $^{**}p < 0.01$ compared with the control group, $^{\triangle}p < 0.05$ and $^{\triangle\triangle}p < 0.01$ compared with the model group.

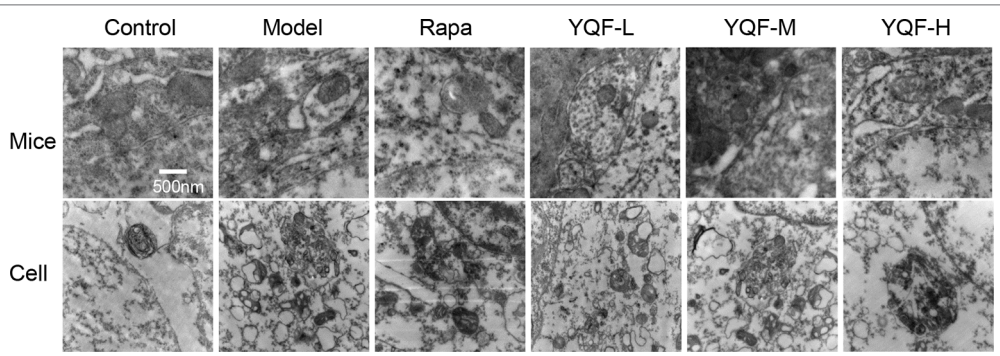

FIGURE 3 | Ultrastructure of hippocampus of 9-month-old APP/PS1 transgenic mice, C57BL/6J mice, HEK293 cells, and APP/PS1 HEK293 cells. Autophagy vesicles were detected by transmission electron microscope after the treatment of rapamycin and YQF (500nm).

YQF Treatment Promotes Autophagy Activity *In Vivo* and *In Vitro*

Beclin 1, LC3, and P62 are protein markers of autophagy activity. *In vitro* and *in vivo* experiments revealed that Beclin 1 levels decreased significantly in Model group mice and cell lines [$\chi^2 = 15.565$ $p = 0.008$, $p < 0.05$ model group vs. control group *in vivo* and $F(5,12) = 5.142$, $p = 0.009$, $p < 0.01$ model group vs. control group *in vitro*]. With the formation and maturation of the autophagosome, LC3I converts to LC3II, and here, we take the LC3II/LC3I ratio as the sign of the formation of autophagosome. Although we did not find any differences *in vivo* between Model group mice and Control group mice, the LC3II/LC3I ratio of *in vitro* model cell lines decreased significantly [$F(5,12) = 10.263$, $p = 0.001$, $p < 0.01$ model group vs. control group]. Rapamycin could promote the expression of Beclin 1 ($\chi^2 = 15.565$ $p = 0.008$, $p < 0.05$ Rapa group vs. model group *in vivo*) and LC3II [$F(5,12) = 10.263$, $p = 0.001$, $p < 0.05$ Rapa group vs. model group *in vitro*], similar to the *in vivo* and *in vitro* effects of YQF (Beclin 1 $p < 0.05$ YQF-H group vs. model

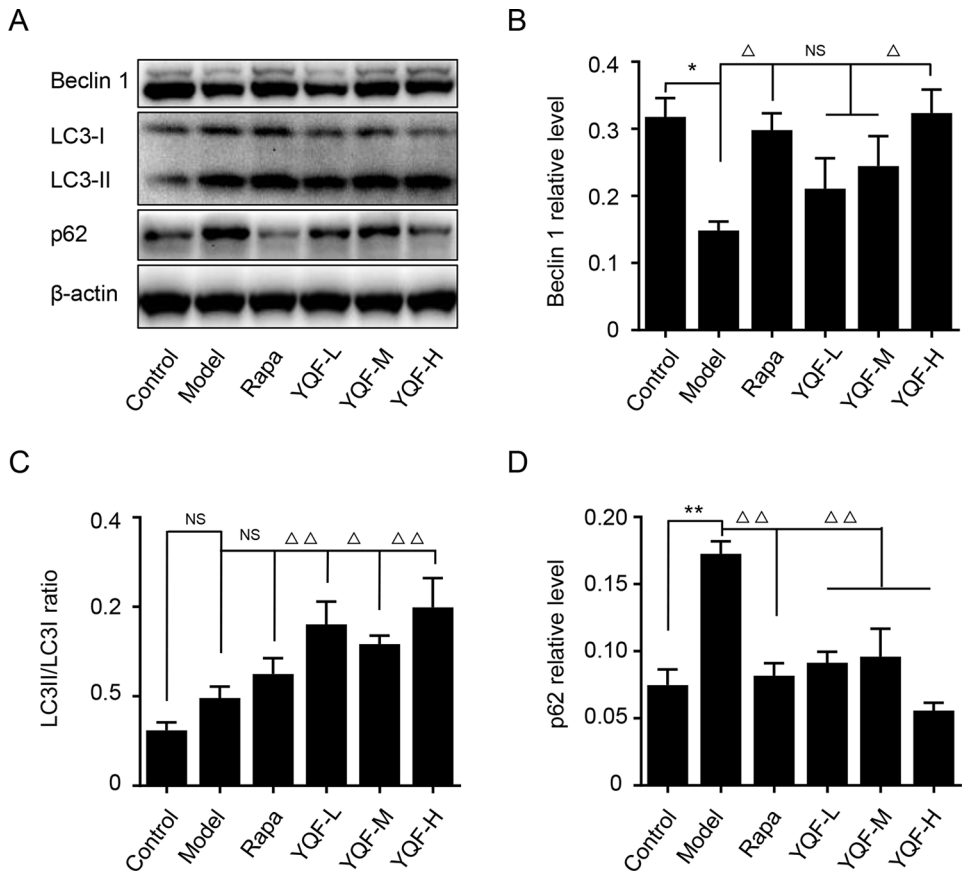

FIGURE 4 | The expression of autophagy related proteins in APP/PS1 and C57BL/6J mice hippocampus intervened with YQF. **(A)** Western blot bands, **(B)** Beclin 1, **(C)** LC3/LC3, **(D)** P62. Data are expressed as mean ± SEM, n = 5, $^{*}p < 0.05$ and $^{**}p < 0.01$ compared with the control group, $^{\triangle}p < 0.05$ and $^{\triangle\triangle}p < 0.01$ compared with the model group, NS, no significant difference.

group *in vivo*, $p < 0.01$ YQF-L/H group vs. model group *in vitro* and LC3II, $p < 0.01$ YQF-L/H group vs. model group *in vivo*, $p < 0.05$ YQF-M/H group vs. model group *in vitro*) (**Figure 4** and **Figures 5A–C**). P62 expresses rapidly with the formation and maturation of the autophagosome but decreases with the formation and degradation of autolysosomes. In this study, we found that P62 levels increased in Model groups [$\chi^2 = 16.298$ $p = 0.006$, $p < 0.01$ Rapa group vs. model group *in vivo* and $F(5, 12) = 11.783$ p = 0.000, $p < 0.05$ Rapa group vs. model group *in vitro*] but decreased in Rapamycin ($p < 0.01$ *in vivo*, $p < 0.05$ *in vitro*) and YQF groups ($p < 0.01$ YQF-L/M/H group vs. model group *in vivo*, $p < 0.01$ YQF-M/H group vs. model group *in vitro*) (**Figure 4** and **Figures 5A**, **D**).

YQF Treatment Suppresses the Activity of mTOR Signaling Pathway

Autophagy is regulated by the mTOR signaling pathway, so we studied how it is affected by YQF. Our results showed that YQF could significantly suppress the activity of this pathway (**Figure 6** and **Figure 7**). We considered p-mTOR/mTOR ratio as the indicator of mTOR activity, and we found significantly elevated mTOR activity in model mice and cells [$F(5,24) = 7.950$ $p = 0.000$, $p < 0.05$ model group vs. control group *in vivo* and $F(5,12) = 1.990$ $p = 0.153$, $p < 0.05$ model group vs. control group *in vitro*]. Rapamycin and YQF could reverse this condition ($p < 0.05$ Rapa group vs. model group *in vivo* and *in vitro*, $p < 0.05$ YQF-H group vs. model group *in vivo* and *in vitro*), in effect suppressing the activity of mTOR. P70S6K and 4EBP1 are two major downstream signaling molecules of mTOR; with the activation of mTOR, P70S6K is activated and 4EBP1 is suppressed. Here, we found that in each group, P70S6K varied directly with pmTOR/mTOR ratio and had an indirect relationship with 4EBP1 levels. However, we did not find significant differences in P70S6K levels between the different study groups. Although rapamycin could significantly promote the expression of 4EBP1, we did not find any difference between YQF groups and the Model group.

YQF Treatment Promotes the Degradation of Autolysosome *In Vitro*

To further explore the effect of YQF on the whole process of autophagy, we analyzed the levels of autolysosome related proteins like lysosomal-associated membrane protein 1 (LAMP-1), cathepsin D, and vacuolar-type H^+-ATPase (V-ATPase) (**Figure 8**). We found that the levels of LAMP-1 in the Model group and the Control group were not significantly different [$F(5,12) = 4.257$ $p = 0.019$, $p > 0.05$ model group vs. control group]. Rapamycin could promote LAMP-1 expression ($p < 0.05$ Rapa group vs. model group). Although YQF could promote LAMP-1 expression, non-significant differences were

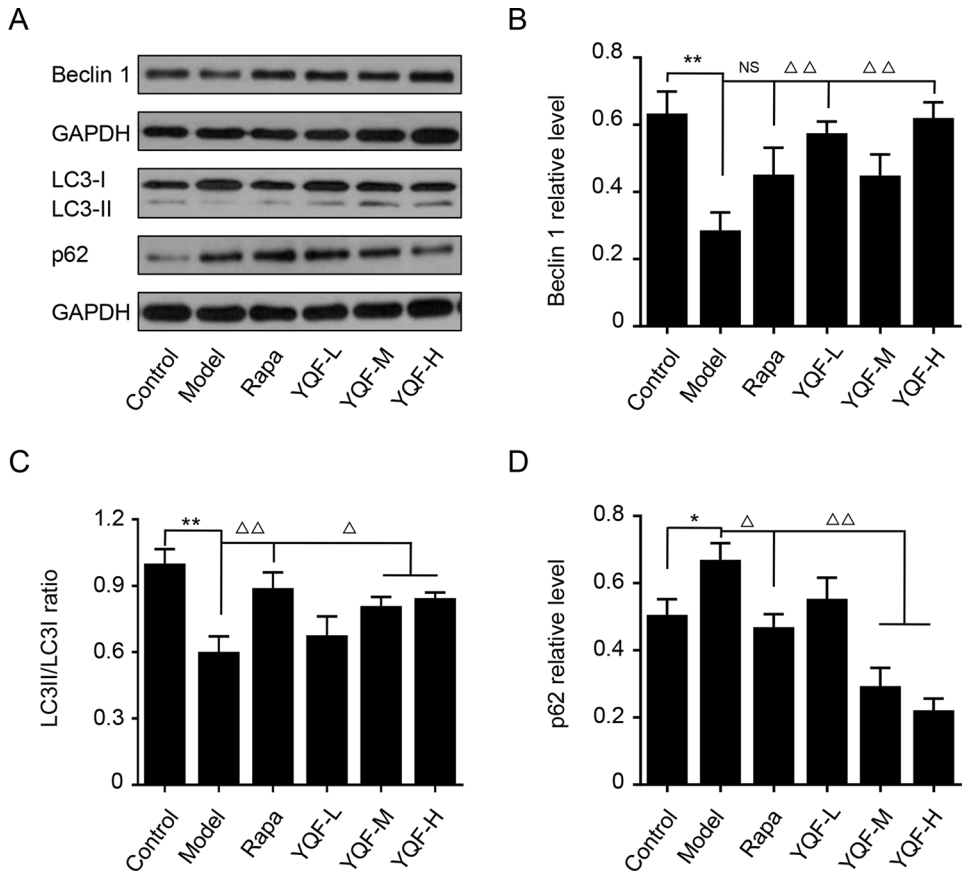

FIGURE 5 | The expression of autophagy related proteins in APP/PS1 and HEk293 cells intervened with YQF. **(A)** Western blot bands, **(B)** Beclin 1, **(C)** LC3II/LC3I, **(D)** P62. Data are expressed as mean ± SEM, n = 3, $^{*}p < 0.05$ and $^{**}p < 0.01$ compared with the control group, $^{\triangle}p < 0.05$ and $^{\triangle\triangle}p < 0.01$ compared with the model group, NS, no significant difference.

found. Cathepsin D and V-ATPase were found to be significantly decreased in the Model group compared with the Control group [$F(5,12) = 4.322$ $p = 0.018$, $p < 0.05$ model group vs. control group and $F(5,12) = 2.237$ $p = 0.113$, $p < 0.05$ model group vs. control group]. Rapamycin could increase the cathepsin D and V-ATPase levels; however, the differences were non-significant. YQF could significantly enhance the expression of cathepsin D ($p < 0.05$ YQF-H group vs. model group) and V-ATPase ($p < 0.05$ YQF-L group vs. model group and $p < 0.01$ YQF-M/H group vs. model group).

DISCUSSION

Under physiological conditions, autophagy, by recycling damaged organelle and defective proteins, is crucial for the homeostasis of energy metabolism in neural cells. During normal aging or the progression of AD, autophagy activity gradually declines, attributing to the aggregation of Aβ (Pickford et al., 2008; Uchiyama et al., 2008), which is now widely considered as a prominent feature found in AD brain. The impairment of autophagy in AD has been substantiated by the accumulation of autophagosomes in dystrophic neurites (Tanida et al., 2005). Consistent with these results, activation of the autophagy pathway by rapamycin retards Aβ and Tau pathology and enhances cognitive functions (Caccamo et al., 2010; Majumder et al., 2011). Apart from these data, previous study also reported that autophagy participates in the extracellular Aβ secretion, thereby directly affecting Aβ plaque formation (Nilsson et al., 2013). Therefore, considerable efforts have been focusing on autophagy to discover potential targets for AD therapeutic interventions (Zhu et al., 2013; Jiang et al., 2014). Beclin 1, the mammalian orthologue of the yeast Vps30/Apg6 gene, functioning as a scaffold, is necessary for the formation of autophagosome. Previous study showed a reduction of Beclin 1 level in the entorhinal cortex of AD patients (Pickford et al., 2008). In APP transgenic mice, Beclin 1 deficiency exacerbates Aβ deposition and promotes synaptodendritic degeneration. On the contrary, Beclin 1 overexpression reduces amyloid pathology (Pickford et al., 2008). Our results suggest a significant reduction of Beclin 1, accompanied with an increased Aβ accumulation in the brain of *APP/PS1* mice and *APP/PS1* HEK293 cells. Furthermore, results demonstrate that YQF or rapamycin treatment elevates the level of Beclin 1 and reduces the formation of Aβ and amyloid plaques.

Microtubule-associated protein 1 light chain 3 (LC3 I) plays a key role in autophagosome biogenesis/maturation. During autophagy, a cytosolic form of LC3 (LC3 I) is converted from a nonlipidated

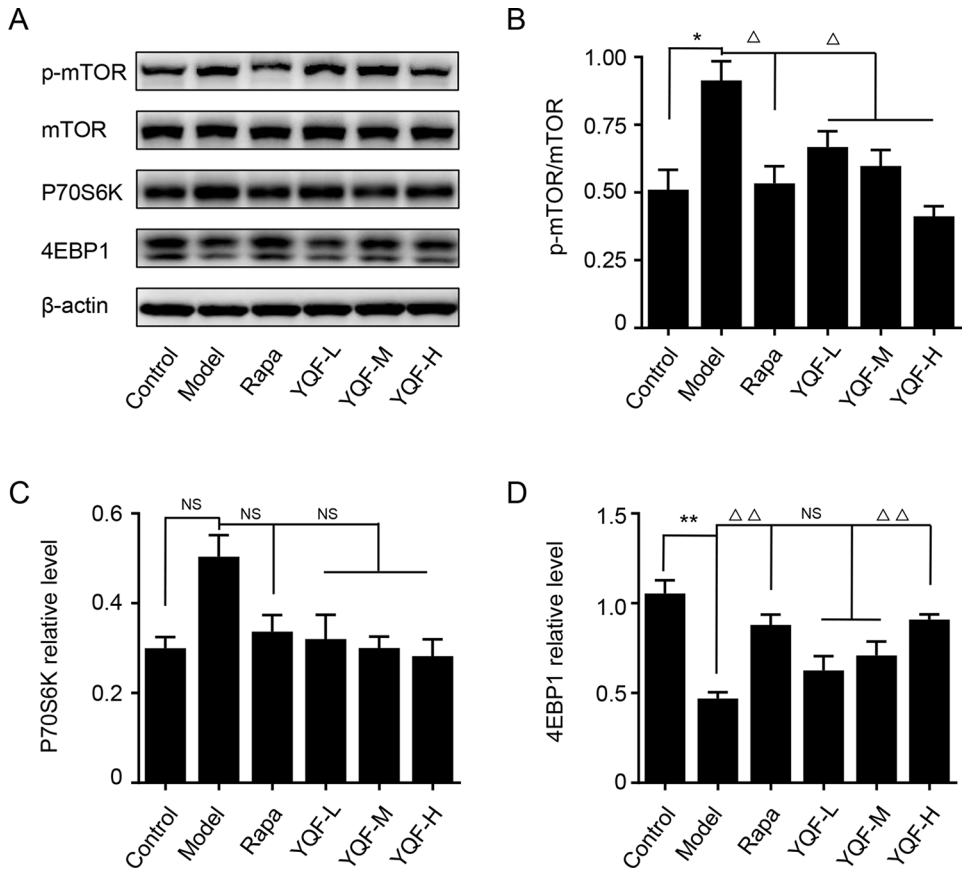

FIGURE 6 | The expression of mTOR, 4EBP1, and P70S6K in APP/PS1 mice intervened with YQF. **(A)** Western blot bands, **(B)** p-mTOR/mTOR, **(C)** P70S6K, **(D)** 4EBP1. Data are expressed as mean ± SEM, n = 3, $^{*}p < 0.05$ and $^{**}p < 0.01$ compared with the control group, $^{\triangle}p < 0.05$ and $^{\triangle\triangle}p < 0.01$ compared with the model group, NS, no significant difference.

form (LC3 I) to a phosphatidylethanolamine (PE)-conjugated form (LC3 II), which is recruited to autophagosomal membranes. LC3 II specifically localizes in autophagosome membranes, and it is therefore considered a specific autophagy marker (Lai and Devenish, 2012). Sequestosome-1 (SQSTM1)/p62 is a ubiquitin-LC3-binding protein and also an adaptor protein for the autophagic degradation of misfolded proteins or organelles. p62 itself is a selective autophagy substrate targeted by the autophagy–lysosome degradation system. Hence, the level of p62 inversely correlates with autophagy activity and is considered as an important biomarker for autophagy degradation (Tanida et al., 2005). In accordance with previous data (Lee et al., 2014; Guo et al., 2015), here we show that an impaired autophagic flux is present, as indicated by an increase of LC3 II/LC3 I and p62 level *in vivo* in model mice, whereas with the *in vitro* study, LC3 II/LC3 I decreased but the level of p62 increased in *APP/PS1* double transgenic HEK293 cells, indicating that both the formation and degradation of autophagosome are obstructed in AD. Importantly, in this study, treatment with different doses of YQF rectified the aberrant autophagy activity. Our results show that YQF treatment increases the LC3 II/LC3 I ratio and reduces p62 levels.

In order to explore the underlying mechanism, we evaluated the phosphorylation of mTOR and the lysosomal function. mTOR is a critical negative regulator of autophagy, which senses and integrates signals under various conditions including growth factors, amino acids, hypoxia, and energy levels (Liang, 2010; Kim and Guan, 2015). In the brain, it is primarily expressed in neurons and is involved in synaptic plasticity and cognition (Talboom et al., 2015). In AD, there is ample evidence suggesting that hyperactive mTOR contributes to the accumulation of Aβ and cognitive impairment. mTOR inhibitors reduce AD hallmarks and protect cognitive function (Godoy et al., 2014; Tramutola et al., 2017). In this study, we found that 9-month-old *APP/PS1* mice and *APP/PS1* double transgenic HEK293 cells exhibit hyperphosphorylated mTOR compared with age-matched wild-type control C57BL/6J mice and non-transfected HEK293 cells, which is in accordance with previous study (Zhou et al., 2008). Our study found that YQF and rapamycin treatments retard the abnormal phosphorylation, and thus inhibit the activity of mTOR and promoted autophagy. By phosphorylating the downstream signaling molecules, mTOR activates P70S6K and inactivates 4EBP1, thereby exerting intracellular signal transduction (Perluigi et al., 2015). Although we did not find significant changes in P70S6K activity in each group, we found that the levels of 4EBP1 decreased significantly in Model groups and increased after the *in vivo* YQF treatment, further proof that YQF inhibits the activity of mTOR.

Formation of autolysosomes by the fusion of autophagosome and lysosome is needed for the subsequent completion of substrate

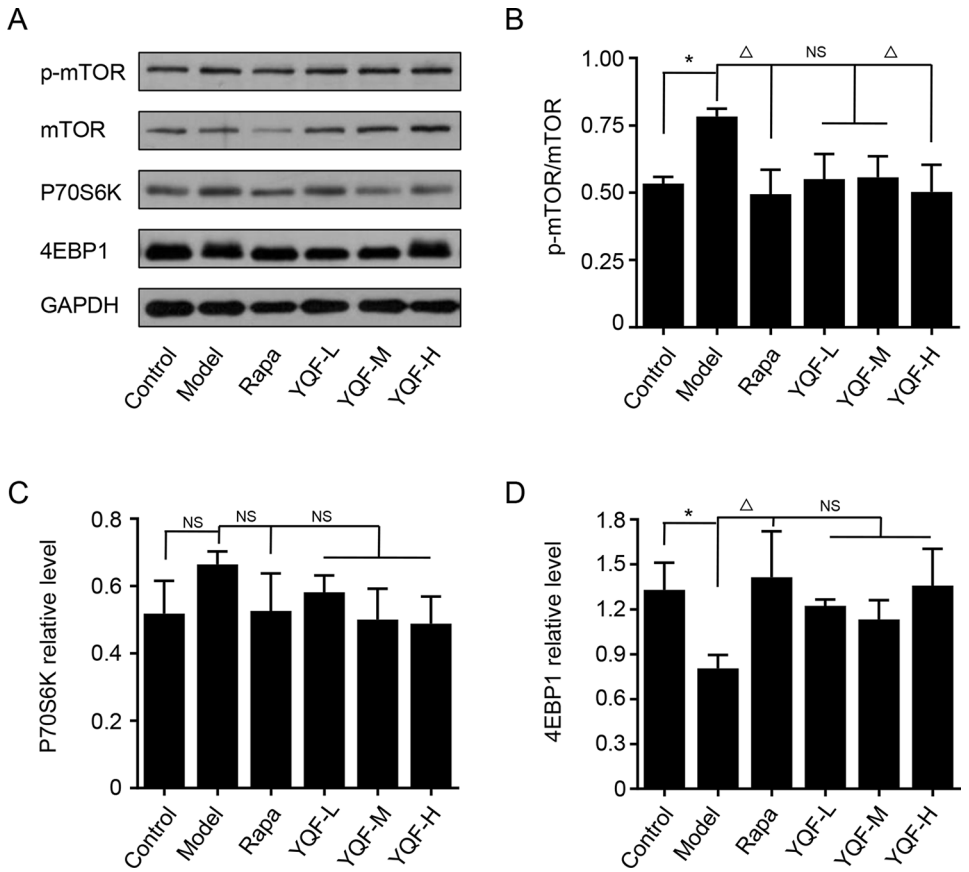

FIGURE 7 | The expression of mTOR, 4EBP1, and P70S6K in HEk293 cells intervened with YQF. **(A)** Western blot bands, **(B)** p-mTOR/mTOR, **(C)** P70S6K, **(D)** 4EBP1. Data are expressed as mean ± SEM, n = 3, $^{*}p < 0.05$ compared with the control group, $^{\triangle}p < 0.05$ compared with the model group, NS, no significant difference.

clearance. Lysosome function is crucial in this step. Studies found that lysosome dysfunction may be the most important point in the autophagy disorder in AD (Bordi et al., 2016; Ma et al., 2017). LAMP-1 is a lysosome-associated membrane glycoprotein, cathepsin D is an aspartic endo-protease that is ubiquitously distributed in lysosomes, and V-ATPase is an ATP-dependent proton pump (transporting H^+ ions into the lysosome) that maintains the acidity of lysosomes. Our *in vitro* studies revealed that LAMP-1 levels were largely the same between different groups, but the levels of cathepsin D and V-ATPase decreased significantly in the Model groups, while YQF could increase their levels. This phenomenon indicates that while the levels of lysosomes are not significantly changed in different groups, their functions changed; lysosome function was impaired in Model groups, and YQF could alleviate this defect.

In conclusion, in the present study, we show that long-term administration of YQF ameliorates learning and memory deficits in the *APP/PS1* mice. The presence of Aβ plaques is a key pathological feature of AD. Here, immunohistochemistry results demonstrate that YQF treatment mitigates the formation of amyloid plaques and decreases the levels of Aβ. The results from ELISA assays show that YQF could up-regulate Beclin-1 and LC3 II, down-regulate p62, and inhibit the activity of the mTOR signaling pathway, *in vivo* and *in vitro*. Thus, we conclude that YQF can improve cognitive function and promote Aβ clearance by activating autophagy function *via* suppressing the mTOR pathway, which may provide new insight in the treatment of AD. We have detected several active components of YQF, but we cannot sure which one play the critical role. We will do some more work to research which active components play the key role in YQF.

DATA AVAILABILITY

The datasets generated for this study are available on request to the corresponding author.

ETHICS STATEMENT

The animal study was reviewed and approved by the animal ethics committee of the Ethics Committee of Xiyuan Hospital, China Academy of Chinese Medical Sciences.

AUTHOR CONTRIBUTIONS

YY and ZW contributed equally to this work. YY and ZW performed experiments and data analysis and wrote the

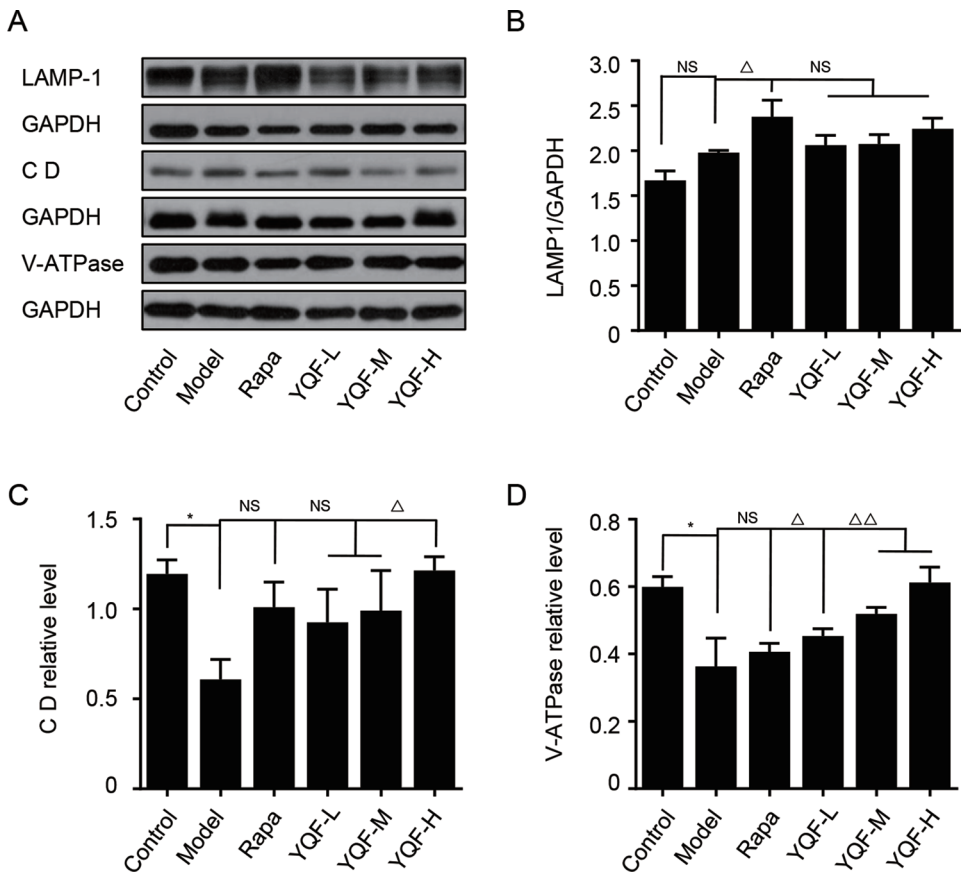

FIGURE 8 | The expression of LAMP-1, Cathepsin D CD and V-ATPase in HEK293 cells intervened with YQF. **(A)** Western blot bands, **(B)** LAMP-1, **(C)** Cathepsin D, **(D)** V-ATPase. Data are expressed as mean ± SEM, n = 3, *p < 0.05 compared with the control group, △p < 0.05 and △△p < 0.01 compared with the model group, NS, no significant difference.

manuscript. YC assisted in the *in vivo* experiments and manuscript writing. PL assisted in the *in vitro* experiments. HL and JL supervised the experiments. HL and ML conceived the study and designed the experiments. All the authors reviewed and approved the manuscript.

FUNDING

The study was funded by the National Natural Science Foundation of China (No. 81503628, 81573819, and 81873350).

ACKNOWLEDGMENTS

The authors thank the National Natural Science Foundation of China for the financial support.

SUPPLEMENTARY MATERIAL

The Supplementary Material for this article can be found online at: https://www.frontiersin.org/articles/10.3389/fphar.2019.01041/full#supplementary-material

REFERENCES

Alzheimer's Association (2018). Alzheimer's Association Report 2018 Alzheimer's disease facts and figures. *Alzheimers Dement.* 14, 367–429. doi: 10.1016/j.jalz.2018.02.001

Bordi, M., Berg, M. J., Mohan, P. S., Peterhoff, C. M., Alldred, M. J., Che, S., et al. (2016). Autophagy flux in CA1 neurons of Alzheimer hippocampus: increased induction overburdens failing lysosomes to propel neuritic dystrophy. *Autophagy* 12, 2467–2483. doi: 10.1080/15548627.2016.1239003

Caccamo, A., Majumder, S., Richardson, A., Strong, R., and Oddo, S. (2010). Molecular interplay between mammalian target of rapamycin (mTOR), amyloid-β, and tau effects on cognitive impairments. *J. Biol. Chem.* 285, 13107–13120. doi: 10.1074/jbc.M110.100420

Garcia-Alloza, M., Robbins, E. M., Zhang-Nunes, S. X., Purcell, S. M., Betensky, R. A., Raju, S., et al. (2006). Characterization of amyloid deposition in the APPswe/PS1dE9 mouse model of Alzheimer disease. *Neurobiol Dis.* 24 (3), 516–524. doi: 10.1016/j.nbd.2006.08.017

Godoy, J. A., Rios, J. A., Zolezzi, J. M., Braidy, N., and Inestrosa, N. C. (2014). Signaling pathway cross talk in Alzheimer's disease. *Cell Commun. Signal.* 12, 23. doi: 10.1186/1478-811X-12-23

Guo, Z., Sun, H., Zhang, H., and Zhang, Y. (2015). Anti-hypertensive and renoprotective effects of berberine in spontaneously hypertensive rats. *Clin. Exp. Hypertens.* 37, 332–339. doi: 10.3109/10641963.2014.972560

Jankowsky, J. L., Fadale, D. J., Anderson, J., Xu, G. M., Gonzales, V., Jenkins, N. A., et al. (2004). Mutant presenilins specifically elevate the levels of the 42 residue beta-amyloid peptide *in vivo*: evidence for augmentation of

a 42-specific gamma secretase. *Hum. Mol. Genet.* 13, 159–170. doi: 10.1093/hmg/ddh019

Jia, J., Wang, F., Wei, C., Zhou, A., Jia., X., Li, F., et al. (2014). The prevalence of dementia in urban and rural areas of China. *Alzheimers Dement.* 10, 1–9. doi: 10.1016/j.jalz.2013.01.012

Jia, J., Wei, C., Chen, S., Li, F., Tang, Y., Qin, W., et al. (2018). The cost of Alzheimer's disease in China and re-estimation of costs worldwide. *Alzheimers Dement.* 14, 483–491. doi: 10.1016/j.jalz.2017.12.006

Jiang, T., Yu, J. T., Zhu, X. C., Tans, M. S., Wang, H. F., Cao, L., et al. (2014). Temsirolimus promotes autophagic clearance of amyloid-β and provides protective effects in cellular and animal models of Alzheimer's disease. *Pharmacol. Res.* 81, 54–63. doi: 10.1016/j.phrs.2014.02.008

Kim, Y. C., and Guan, K. L. (2015). MTOR: a pharmacologic target for autophagy regulation. *J. Clin. Invest.* 125, 25–32. doi: 10.1172/JCI73939

Lai, S. C., and Devenish, R. J. (2012). LC3-associated phagocytosis (LAP): connections with host autophagy. *Cells* 1, 396–408. doi: 10.3390/cells1030396

Lee, J. K., Jin, H. K., Park, M. H., Kim, B. R., Lee, P. H., Nakauchi, H., et al. (2014). Acid sphingomyelinase modulates the autophagic process by controlling lysosomal biogenesis in Alzheimer's disease. *J. Exp. Med.* 211, 1551–1570. doi: 10.1084/jem.20132451

Liang, C. (2010). Negative regulation of autophagy. *Cell Death Differ.* 17, 1807–1815. doi: 10.1038/cdd.2010.115

Ma, L. Y., Lv, Y. L., Huo, K., Liu, J., Shang, S. H., Fei, Y. L., et al. (2017). Autophagy-lysosome dysfunction is involved in Abeta deposition in STZ-induced diabetic rats. *Behav. Brain Res.* 320, 484–493. doi: 10.1016/j.bbr.2016.10.031

Majumder, S., Richardson, A., Strong, R., and Oddo, S. (2011). Inducing autophagy by rapamycin before, but not after, the formation of plaques and tangles ameliorates cognitive deficits. *PLoS One* 6, e25416. doi: 10.1371/journal.pone.0025416

Nilsson, P., Loganathan, K., Sekiguchi, M., Matsuba, Y., Hui., K., Tsubuki, S., et al. (2013). Aβ secretion and plaque formation depend on autophagy. *Cell Rep.* 5, 61–69. doi: 10.1016/j.celrep.2013.08.042

Oddo, S. (2012). The role of mTOR signaling in Alzheimer disease. *Front. Biosci. (Schol Ed)* 4, 941–952. doi: 10.2741/s310

Perluigi, M., Di Domenico, F., and Butterfield, D. A. (2015). mTOR signaling in aging and neurodegeneration: at the crossroad between metabolism dysfunction and impairment of autophagy. *Neurobiol. Dis.* 84, 39–49. doi: 10.1016/j.nbd.2015.03.014

Pickford, F., Masliah, E., Britschqi, M., Lucin, K., Narsimhan, R., Jaegar, P. A., et al. (2008). The autophagy-related protein beclin 1 shows reduced expression in early Alzheimer disease and regulates amyloid β accumulation in mice. *J. Clin. Invest.* 118, 2190–2199. doi: 10.1172/JCI33585

Ryter, S. W., Cloonan, S. M., and Choi, A. M. (2013). Autophagy: a critical regulator of cellular metabolism and homeostasis. *Mol. Cells* 36, 7–16. doi: 10.1007/s10059-013-0140-8

Souchet, B., Audrain, M., Billoir, B., Lecanu, L., Tada, S., Braudeau, J., et al. (2018). Is it time to rethink the Alzheimer's disease drug development strategy by targeting its silent phase? *Neural Regen Res.* 13, 224–225. doi: 10.4103/1673-5374.226389

Sun, Y. X., Ji, X., Mao, X., Xie, L., Jia, J., Galvan, V., et al. (2014). Differential activation of mTOR complex 1 signaling in human brain with mild to severe Alzheimer's disease. *J. Alzheimers Dis.* 38, 437–444. doi: 10.3233/JAD-131124

Talboom, J. S., Velazquez, R., and Oddo, S. (2015). The mammalian target of rapamycin at the crossroad between cognitive aging and Alzheimer's disease. *NPJ Aging Mech. Dis.* 1, 15008. doi: 10.1038/npjamd.2015.8

Tanida, I., Minematsu-Ikeguchi, N., Ueno, T., and Kominami, E. (2005). Lysosomal turnover, but not a cellular level, of endogenous LC3 is a marker for autophagy. *Autophagy* 1, 84–91. doi: 10.4161/auto.1.2.1697

Tramutola, A., Lanzillotta, C., and Di Domenico, F. (2017). Targeting mTOR to reduce Alzheimer-related cognitive decline: from current hits to future therapies. *Expert Rev. Neurother.* 17, 33–45. doi: 10.1111/jnc.13037

Uchiyama, Y., Shibata, M., Koike, M., Yoshimura, K., and Sasaki, M. (2008). Autophagy–physiology and pathophysiology. *Histochem. Cell Biol.* 129, 407–420. doi: 10.1007/s00418-008-0406-y

Wang, F., Feng, J., Yang, Y., Liu, J., Liu, M., Wang, Z., et al. (2018). The Chinese herbal formula Fuzheng Quxie decoction attenuates cognitive impairment and protects cerebrovascular function in SAMP8 mice. *Neuropsychiatr Dis. Treat.* 14, 3037–3051. doi: 10.2147/NDT

Wang, X., Zheng, W., Xie, J. W., Wang, T., Wang, S. L., Teng, W. P., et al. (2010). Insulin deficiency exacerbates cerebral amyloidosis and behavioral deficits in an Alzheimer transgenic mouse model. *Mol. Neurodegener.* 5, 46. doi: 10.1186/1750-1326-5-46

Yang, Y., Jia, X., Feng, J., Wang, Z., Cao, Y., Liu, J., et al. (2017). Fuzheng Quxie decoction ameliorates learning and memory impairment in SAMP8 mice by decreasing tau hyperphosphorylation. *Evid. Based Complement. Alternat. Med.* 2017, 5934254. doi: 10.1155/2017/5934254

Zhou, X. W., Tanila, H., and Pei, J. J. (2008). Parallel increase in p70 kinase activation and tau phosphorylation (S262) with Aβ overproduction. *FEBS Lett.* 582, 159–164. doi: 10.1016/j.febslet.2007.11.078

Zhu, X. C., Yu, J. T., Jiang, T., and Tan, L. (2013). Autophagy modulation for Alzheimer's disease therapy. *Mol. Neurobiol.* 48, 702–714. doi: 10.1007/s12035-013-8457-z

Conflict of Interest Statement: The authors declare that the research was conducted in the absence of any commercial or financial relationships that could be construed as a potential conflict of interest.

The handling editor declared a shared affiliation, though no other collaboration, with the authors HL, YY, ZW, YC, JL, PL, ML at the time of the review.

frontiers in Pharmacology

ORIGINAL RESEARCH
published: 20 September 2019
doi: 10.3389/fphar.2019.01095

Shengmai Injection Suppresses Angiotensin II-Induced Cardiomyocyte Hypertrophy and Apoptosis *via* Activation of the AMPK Signaling Pathway Through Energy-Dependent Mechanisms

*Yiping Li[1,2], Xiaofen Ruan[1,2], Xiaowen Xu[2], Cha Li[2], Tingting Qiang[2], Hua Zhou[1,2], Junjie Gao[1] and Xiaolong Wang[1,2]**

[1] Cardiovascular Department of Traditional Chinese Medicine, Shuguang Hospital Affiliated to Shanghai University of Traditional Chinese Medicine, Shanghai, China, [2] Cardiovascular Research Institute of Traditional Chinese Medicine, Shuguang Hospital Affiliated to Shanghai University of Traditional Chinese Medicine, Shanghai, China

OPEN ACCESS

Edited by:
Yue Liu,
Xiyuan Hospital, China

Reviewed by:
Hongyi Qi,
Southwest University, China
Jun Ren,
University of Wyoming, United States

***Correspondence:**
Xiaolong Wang
wxlqy0214@163.com

Specialty section:
This article was submitted to Ethnopharmacology, a section of the journal Frontiers in Pharmacology

Received: *22 May 2019*
Accepted: *26 August 2019*
Published: *20 September 2019*

Citation:
Li Y, Ruan X, Xu X, Li C, Qiang T, Zhou H, Gao J and Wang X (2019) Shengmai Injection Suppresses Angiotensin II-Induced Cardiomyocyte Hypertrophy and Apoptosis via Activation of the AMPK Signaling Pathway Through Energy-Dependent Mechanisms. Front. Pharmacol. 10:1095. doi: 10.3389/fphar.2019.01095

Shengmai injection (SMI), a traditional Chinese herbal medicine extracted from *Panax ginseng* C.A. Mey., *Ophiopogon japonicus* (Thunb.) Ker Gawl., and *Schisandra chinensis* (Turcz.) Baill., has been used to treat acute and chronic heart failure. This study aimed to further clarify the effects of SMI on energy metabolism. SMI could improve cell-survival rate and also reduce myocardial cell hypertrophy and apoptosis. Mitochondria are important sites of cellular energy metabolism, and SMI protects mitochondrial function which was evaluated by mitochondrial ultrastructure, mitochondrial respiratory control ratio (RCR), and mitochondrial membrane potential ($\Delta\Psi m$) in this study. The expression levels of adenosine triphosphate (ATP), adenosine diphosphate (ADP), and phosphocreatine (PCr) increased. The expression levels of free fatty acid oxidation [carnitine palmitoyltransferase-1 (CPT-1)], glucose oxidation [glucose transporter-4 (GLUT-4)], and mitochondrial biogenesis-related genes (peroxisome proliferator-activated receptor-γ coactivator-1α [PGC-1α]) were upregulated after SMI treatment. AMP-activated protein kinase (AMPK) is an important signaling pathway regulating energy metabolism and also can regulate the above-mentioned indicators. In the present study, SMI was found to promote phosphorylation of AMPK. However, the effects of SMI on fatty acid, glucose oxidation, mitochondrial biogenesis, as well as inhibiting apoptosis of hypertrophic cardiomyocytes were partly blocked by AMPK inhibitor–compound C. Moreover, decreased myocardial hypertrophy and apoptosis treated by SMI were inhibited by AMPK knockdown with shAMPK to a certain degree and AMPK knockdown almost abolished the SMI-induced increase in the expression of GLUT-4, CPT-1, and PGC-1α. These data suggest that SMI suppressed Ang II–induced cardiomyocyte hypertrophy and apoptosis *via* activation of the AMPK signaling pathway through energy-dependent mechanisms.

Keywords: Shengmai injection, cardiomyocyte hypertrophy, apoptosis, energy metabolism, AMPK signaling pathway

INTRODUCTION

Heart failure (HF) is a major public health concern, affecting more than 6.2 million people in the USA (Benjamin et al., 2019) and more than 23 million people worldwide (Go et al., 2013). The pathogenesis of HF is pathological cardiac remodeling, manifested as left ventricular dilatation, myocardial cell hypertrophy, and interstitial fibrosis (Opie et al., 2006; Shah et al., 2012). Among them, cardiomyocyte hypertrophy is the main cause of decreased myocardial cell contractility and decreased blood supply capacity (Roman et al., 1997). A previous study confirmed the activation of the neuroendocrine system, especially the renin–angiotensin–aldosterone system (RAAS), which is a key mechanism leading to cardiomyocyte hypertrophy. Cutting off RAAS to reduce cardiomyocyte hypertrophy has become the basis for preventing and treating of HF (Tamura et al., 2000). Classical HF treatments, in particular angiotensin-converting enzyme indicators/angiotensin receptor blockers and beta-blockers, have been successfully conducted. However, the 1-year mortality rate of HF has only slightly declined, and its 5-year mortality rate has not declined during the last 10 years (Benjamin et al., 2019).

Alterations in cardiac energy metabolism contribute to the severity of HF and cardiac hypertrophy. Myocardial oxygen consumption is very high in HF and cardiac hypertrophy, exhibiting an energy deficit (containing 30–40% less ATP compared with a healthy heart) due to altered energy substrate availability and impaired mitochondrial oxidative metabolism (De Jong and Lopaschuk, 2017). At the same time, important factors are involved in fatty acid metabolism and ATP synthesis, such as carnitine palmitoyl transferase 1 (CPT-1), peroxisome proliferator–activated receptorγ coactivator1α (PGC-1α), and malonyl-CoA decarboxylase, which were abnormally expressed during cardiac hypertrophy (Haynes and Campbell, 2014; Torrens et al., 2017). Among them, CPT-1 controls the rate-limiting step of mitochondrial fatty acid oxidation, and PGC-1α controls mitochondrial biosynthesis and the entire pathway of ATP synthesis (Hoppel et al., 2009). In addition to fatty acid oxidation, glycolysis is an alternate source of ATP production. Glucose is taken up by cardiomyocytes *via* glucose transporter1 (GLUT-1) and glucose transporter4 (GLUT-4); GLUT-4 is primarily responsible for the insulin-dependent uptake of glucose (Fan et al., 2011; Dolinsky et al., 2016; De Jong and Lopaschuk, 2017). After knocking out the glucose carrier GLUT-4 in mice, the heart gradually develops into a hypertrophic phenotype (Luo et al., 2018). Consequently, metabolic agents may be a complementary effective strategy for treating HF (Rosano and Vitale, 2018).

Shengmai is a traditional Chinese herbal medicine. It is a mixture extracted from three herbs: *Panax ginseng* C.A. Mey., *Ophiopogon japonicus* (Thunb.) Ker Gawl., and *Schisandra chinensis* (Turcz.) Baill. It is the most important rescue agent for patients before wide prescription of Western medicine in China. Nowadays, Shengmai is typically produced as a patented drug on the basis of a standardized formula in different forms, including capsule, powder, oral liquid, and injection. It is also typically prescribed in China as a complementary treatment compared with Western medicine recommended for acute HF and chronic HF. Although the poor quality of trials compromised the reliability of the evidence, the efficacy of Shengmai against HF has been demonstrated in several studies (Zhou et al., 2014). A recent clinical trial further confirmed the efficacy that the patients with CHF and coronary artery disease (CAD) could benefit from the integrative treatments with standard medicines plus Shengmai injection (SMI) with respect to the New York Heart Association (NYHA) functional classification, 6-min walking distance (6MWD), 36-item short-form health survey (SF-36) (SF-36) score, and traditional Chinese medicine (TCM) syndrome score (Xian et al., 2016). Previous basic studies have proved that SMI protected myocardial ischemia-reperfusion injury and doxorubicin-induced cardiomyopathy related to improving myocardial energy metabolism (Quaini et al., 2015; Zhan et al., 2015). However, whether it can improve the cardiac function *via* improving the mitochondrial energy metabolism of cardiac hypertrophy remains elusive.

Cardiac hypertrophy is characterized by increased cardiomyocyte size, a higher degree of sarcomere organization, and enhanced gene transcription and translation levels, all of which are closely associated with energy metabolism (Tham et al., 2015). This study established the model of cardiomyocyte hypertrophy induced by Angiotensin (Ang) II to investigate the protective effects of SMI on myocardial energy metabolism and the underlying mechanism, so as to provide a new complementary target for the energy metabolism of HF.

MATERIALS AND METHODS

Chemicals and Treatments

SMI (10 ml/tablet, H17050402; Shanghai Hutchison Pharmaceuticals, Shanghai, China), Ang II (Sigma–Aldrich, St. Louis, MO, USA), and the AMP-activated protein kinase (AMPK) inhibitor compound C (S7306, Selleck Chemicals, Houston, TX, USA) were purchased. All animals used in this study were 1- to 4-day old Sprague–Dawley (SD) rats (Experimental Animal Center, Shanghai University of Traditional Chinese Medicine, Shanghai, China).

Cardiomyocytes were randomly assigned into three groups: blank, Ang II (0.8 μM), and SMI groups (Ang II 0.8 μM + SMI 1/4,000). The cardiomyocytes were pretreated with phosphate-buffered saline (PBS) or SMI for 1 h and then stimulated with 0.8 μM Ang II for 48 h.

To prove that SMI regulates glycolipid metabolism and mitochondrial synthesis through the AMPK pathway, we later divided the cardiomyocytes into five groups: blank, Ang II (0.8 μM), compound C (Ang II 0.8 μM + compound C 0.1uM), SMI (Ang II 0.8 μM + SMI 1/4,000), and SMI + compound C (Ang II 0.8 μM + SMI 1/4,000 + compound C 0.1 μM). Also, the levels of proteins related to energy metabolism were examined, besides flow cytometry analysis of cell apoptosis and apoptosis-related proteins.

Preparation and Quality Control Standard of SMI

The quality control standard of SMI conformed to the National Drug Standard of the Ministry of Health of China, which specifies

that the total amount of ginsenoside Rg1 and ginsenoside Re should not be lower than 0.08 and 0.04mg in a 1 ml injection respectively, as analyzed by high-performance liquid chromatography (HPLC).

To guide the rational use of SMI in clinic, an increasing number of studies focused on the fingerprint analysis of SMI and showed that more than 10 components were determined, including ginsenoside Rg1, ginsenoside Re, ginsenoside Rf, ginsenoside Rb1, ginsenoside Rc, ginsenoside Rh1, ginsenoside Rd, schisandrin, ginsenoside Rg5 (Rk1), and ginsenoside Rh3 (**Supplementary Figures 2–3** and **Supplementary Tables 1–2**).

Isolation of Neonatal Cardiomyocyte and Cell Models for Hypertrophy

Neonatal rat ventricular myocytes were isolated and cultured from the ventricles of postnatal days 1–3 SD rats. The hearts were removed from mice aseptically, and large vessels and atria were discarded. The ventricles were washed, cut into small pieces in Dulbecco's modified Eagle's medium (DMEM), and then digested in 0.25% trypsin in a CO_2 incubator at 37°C for 15 min. To enrich cardiomyocytes and deplete nonmyocytes, the cells were centrifuged and cultured in DMEM for 2 h, allowing the attachment of nonmyocytes. After the purification process, the cardiomyocytes were resuspended and cultured in DMEM supplemented with 15% fetal bovine serum. The culture medium was renewed after 48 h, and the cardiomyocytes were further cultured for 24 h. Next, the culture medium was changed with serum-free DMEM, and the cardiomyocytes were pretreated with PBS, SMI, or compound C (both diluted with PBS) for 1 h and then stimulated with Ang II (0.8 μM) for 48 h.

Quantitative Reverse Transcription Polymerase Chain Reaction (RT-qPCR)

Quantitative analysis of mRNA expression of atrial natriuretic peptide (ANP), brain natriuretic peptide (BNP), and β-myosin heavy chain (β-MHC) in cardiomyocytes and cardiac tissues was conducted using RT-qPCR. Total RNA was extracted from cardiomyocytes by using TRIzol reagent (15596-026; Invitrogen, Carlsbad, CA, USA) according to the manufacturer's protocols. Next, 0.5 μg of total RNA was reversely transcribed using the SuperScript III Reverse Transcriptase (R250-01; Invitrogen, Carlsbad, CA, USA) to obtain cDNA. The SYBR Green PCR Master Mix Kit (CS7561; Invitrogen, Carlsbad, CA, USA) was used to quantify the RNA levels of the hypertrophic markers, such as ANP, BNP, and β-MHC in cardiomyocytes, with glyceraldehyde-3-phosphate dehydrogenase (GAPDH) as an internal control. The RT-qPCR was performed by CFX96TM Real-Time System (Bio-Rad Laboratories, CA, USA) for 40 cycles. The sequences of primers used for amplification were as follows: ANP, 5'-CTC CGATAGATCTGCCCTCTTGAA-3' and 5'-GGTACCGGAA GCTGTTGCAGCCTA-3'; BNP, 5'-TGATTCTGCTCCTGCT TTTC-3' and 5'-GTGGATTGTTCTGGAGACTG-3'; β-MHC, 5'-CAGCAGCCCAGTACCTCCGA-3' and 5'-TGTCATCAGG CACGAAGCAC-3'; GLUT-4, 5'-GCCGGGACACTATACCC TATTC-3' and 5'-AAGGACCAGTGTCCCAGTCA-3'; CPT-1, 5'-GCAGCTCGCACATTACAAGG-3' and 5'-CGTTGACTT GGGGTCCATCA-3'; PGC-1α, 5'-CATTCAGGAGCTGGATG GCT-3' and 5'-TATGTTCGCGGGCTCATTGT-3'; and GAP DH,5'-AAGAATGGTGAAGCAGGC-3' and 5'-TCCACCAC CAGTTGCTGTA-3.' Data were analyzed using 2ΔΔCt method for relative quantification. In this study, ΔCt was calculated as Ct (detected mRNA) − Ct (GAPDH), and ΔΔCt was calculated as ΔCt (drug treated) − ΔCt (control), where the control is the group treated with non-drugs. The relative value was obtained by 2-ΔΔCt.

Cell Viability Assay

The CellTiter-Glo Luminescent Cell Viability Assay Kit (C0068M; Beyotime Institute of Biotechnology, Shanghai, China) was used to test the cell viability according to manufacturer's protocol. Briefly, the cells were seeded on 96-well plates at 1×10^5 cells/well overnight. The reagent was reconstituted and added to the cells. After mixing on an orbital shaker for 2 min to lyse the cells, the plate was incubated at room temperature for 10 min, and then the luminescent signals were recorded.

Determination of Cardiomyocyte Area

The cells with a satisfactory growth rate were digested and re-suspended the previous day. They were inoculated in a six-well plate and treated in different groups for 48 h after the liquid exchange. Then, 1 ml of carboxyfluorescein diacetate succinimidyl ester (CFDA-SE) (C0051, Beyotime Institute of Biotechnology, Shanghai, China) was added; stock solution (2×) was added for 10 min at 37°C. The cells were washed one to two times with 1× PBS. After adding 1–2 ml of complete cell culture medium and incubating for 5 min at 37°C, the cells washed one to two times again with 1× PBS. Further 4% paraformaldehyde (1 ml) was added to fix for 30 min, and the cells were washed with 2× PBS two to three times. The cell nuclei were stained with Hoechst 33342 (C1022; Beyotime Institute of Biotechnology, Shanghai, China) solution (final concentration of 1 μg/ml) at room temperature for 5–10 min and washed two to three times with 1× PBS. Next, 1 ml of 1× PBS was added to each well, and the cells were observed and photographed under a fluorescence microscope; Image-Pro Plus software was used to calculate the total area and number of cardiomyocytes in the same field of view and the number of cardiomyocytes in the same field of view.

Average cell area in the same field of view = (total area of the same field of view)/(the number of core cells in the same field of view).

Detecting Protein Content of Cardiomyocytes by Bicinchoninic Acid Assay

Depending on the number of samples, 50 parts of bicinchoninic acid (BCA) reagent A plus 1 volume of BCA reagent (50:1, P0012, Beyotime Institute of Biotechnology) were mixed to configure the appropriate amount of BCA working solution. Then, 10 μl of protein standard diluted with 100 μl of PBS to a final concentration of 0.5 mg/ml. The standard was added to a 96-well plate and diluted to 20 μl. The sample to be tested was

added to the 96-well plate, and the standard was diluted to 20 µl. Further, 200 µl of BCA working solution was added to each well and placed at 37°C for 30 min. The optical density (OD) value at 562 nm. The protein concentration was calculated from the standard curve.

Bromodeoxyuridine (BrdU) Incorporation

The cells were incubated with culture media containing 10µM 5-bromo-20-deoxybromouridine (BrdU) (Cat. No. B23151, Invitrogen, USA), for 6 h at 37°C; fixed with 3.7% formaldehyde for 15 min; and treated according to the BrdU experimental protocol. Briefly, the medium was removed, and the cells were washed with PBS. The PBS was replaced with 1 ml of Triton X-100 permeabilization buffer for 20 min at room temperature. The permeabilization buffer was removed, and 1 ml of 1N HCl was added, which was incubated for 10 min on ice. The cells were then incubated with 2N HCl for 10 min at room temperature. The acid solution was removed, and the cells were washed three times with Triton X-100 permeabilization buffer. The buffer was then removed and replaced with the staining solution. After an incubation period of 24 h, the anti-BrdU primary antibody (Cat. No. B35130, Invitrogen, USA) was removed, and the cells were washed three times with Triton X-100 permeabilization buffer. Each well was incubated with fluorescently labeled secondary antibody (Cat. No. A-11001, Invitrogen, USA) for 1 h at room temperature. Finally, the cells were imaged with appropriate filters.

Mitochondria Extraction and Determination of Oxidative Respiratory Function

Genmed medium (2.5 ml) was added into the reaction glass tank, mixed, and sealed. Further, mitochondria, state IV substrate solution, and state III substrate solution were added in a proper sequence following the manufacturer's protocol. Mitochondrial state III and state IV respiration rates in the closed reaction system were determined using dissolved oxygen electrolytic solution (Orion 4-tar; Thermo Fisher Scientific, MA, USA). The mitochondrial respiratory control ratio (RCR) was calculated according to the following formula: RCR, state III respiration rate/state IV respiration rate.

Transmission Electron Microscopy

The adherent cells were directly scraped off, and the cell suspension was centrifuged (1,000 rpm, 5 min). The supernatant was discarded, washed twice with PBS, and pelleted by centrifugation. Further, 2.5% glutaraldehyde was added for fixation at 4°C overnight. After washing with 0.1M PBS three times, the supernatant was incubated with 1% citric acid (Pelco, CA, USA) at 4°C for 3 h, washed with buffer three times, and dehydrated with ethanol step by step, followed by the replacement of propylene oxide. The Spurr resin (SPI-Chem, Structure Probe, Inc., PA, USA) was impregnated and embedded. Finally, it was polymerized in an oven at 70°C. The embedded blocks of different materials were placed on an ultrathin slicer (EM UC6; Leica, Wetzlar, Germany) for sectioning. The ultrathin section was 70 nm thick; it was stained with uranyl acetate (SPI-Chem, Structure Probe, Inc. A) and lead citrate (SPI-Chem, Structure Probe, Inc.) and then observed under a transmission electron microscope (JEM1230; JEOL Ltd., Tokyo, Japan).

JC-1 Stain for Mitochondrial Membrane Potential ($\Delta\psi m$)

Neonatal mouse ventricular myocytes in three groups were cultured in 24-well plates and treated as mentioned earlier. The cells were washed with PBS once, and 0.25 ml of fresh medium was added into each well. JC-1 dye (0.25 ml, C2006; Beyotime Institute of Biotechnology) was added to each well and mixed well. The cells were then incubated in an incubator at 37°C for 20 min. At the end of incubation, the supernatant was discarded, and the cells were washed. The cell culture medium (0.5 ml) was added, and the cells were observed under a fluorescence microscope. Integrated OD (IOD), as calculated by multiplying the area and average density of the fluorescence, was evaluated using Image-Pro Plus 7 software (Media Cybernetics Inc., MD, USA).

Detection of ATP, ADP, AMP, and PCr Levels in Cardiomyocytes by HPLC Assay

The supernatant (400 µl) was collected from different groups and centrifuged again at 4,000 rpm for 10 min at 4°C; the supernatant was filtered with a 0.45-µm membrane. The prepared supernatant was loaded onto a 10-A HPLC detector (Monolithic RP-C18, 2.0 × 50 mm^2; Merck, Darmstadt, Germany with Waters UPLC Q-trap5500 [1024985-AX; AB SCIEX, MA, USA]), followed by separation and detection at a wavelength of 254 nm. The levels of adenosine triphosphate (ATP) (99%, Sigma–Aldrich, MO, USA), adenosine diphosphate (ADP) (99%, Sigma), adenosine monophosphate (AMP) (99%, Sigma), and phosphocreatine (PCr) (99%, Merck) were calculated according to the elution peak area and standard concentrations.

Sample ATP/ADP/AMP/PCr concentration (µg/L) = [sample peak area × standard ATP/ADP/AMP/PCr concentration]/peak area of the standard ATP/ADP/AMP/PCr concentration.

Flow Cytometry Analysis of Cell Apoptosis

Five groups as mentioned earlier (see "Chemicals and Treatments" section) were investigated. Apoptotic rates were examined 48 h after the treatment. In accordance with the Annexin V/Propidium Iodide (PI) Apoptosis Kit (BioVision, CA, USA), 5 × 10^5 cells were collected in each tube and 1 ml of annexin V binding buffer was added, followed by thorough mixing. Subsequently, 5 ml of annexin V–fluorescein isothiocyanate and 10 ml of PI were added. After mixing, the tube was incubated in the dark at 37°C for 15 min. For the early apoptotic cells, the membrane phosphatidylserine was exposed and combined with annexin V, without PI. For the late apoptotic cells, the membranes were permeable to PI and the cells were stained with annexin V and PI. The dead cells were stained only with PI. The samples were analyzed using a FACScan flow cytometer (BD Biosciences, NJ, USA) within 1 h. Flow

cytometry (BD FACSAria; BD Biosciences) was performed to detect cell apoptosis.

Western Blot Analysis

The primary antibodies to AMPK (1:1,000 dilution, sc-25792; Santa Cruz Biotechnology, Inc., TX, USA), p-AMPKα1/2 (Thr183/172) (1:1,000 dilution, sc-101630; Santa Cruz Biotechnology, Inc.), peroxisome proliferator-activated receptor-γ (PPAR-γ, 1:1,000 dilution, ab209350; Abcam, Cambridge, UK), CPT-1 (H40) (1:1,000 dilution, sc-98834; Santa Cruz Biotechnology, Inc.), GLUT-4 (1:500 dilution, bs-0384R; Bioss Antibodies, MA, USA), PGC-1α (1:500 dilution, bs-1832R; Bioss Antibodies), Bax (1:1,000 dilution, ab32503; Abcam), Bcl-2 (1:500 dilution, bs-0032R; Bioss Antibodies), caspase-3 (1:500 dilution, bs-2593R; Bioss Antibodies), and horseradish peroxidase (HRP) goat anti-rabbit (IgG) secondary antibody (1:5,000 dilution, BV-S8008; BIOVAL, CA, USA) were used. To document the loading controls, the membrane was reported with a primary antibody against anti-rabbit HRP secondary antibody. The signals were quantified by scanning densitometry and computer-assisted image analysis.

Recombinant Lentivirus

The recombinant lentivirus plasmid expressing short hairpin (sh) RNA targeting both AMPKα1 and AMPKα2 (TGAATTAAATCCACAGAAA) and the control shRNA (ACGACGTCAGCTGGTGCATGT) were created as described earlier (Tangeman et al., 2012). Lentiviruses were packaged in rat neonatal cardiomyocytes.

Statistical Analysis

The experimental results were presented as mean ± standard error. One-way analysis of variance was used to compare differences among the three groups, followed by the Bonferroni *post hoc* test for multiple comparisons. P values <0.05 were considered statistically significant. Statistical analyses were performed using GraphPad Prism 7.0 software (GraphPad Software Inc., CA, USA).

RESULTS

Selection of SMI Concentration and Its Effects on Cell Viability

Consistent with the findings of previous studies, cardiac hypertrophy could be induced by Ang II (Patrucco et al., 2014; Liu et al., 2015; Dong et al., 2017). RT-qPCR was used to quantify the RNA levels of the hypertrophic markers, such as ANP, BNP, and β-MHC, in cardiomyocytes to determine the concentrations of Ang II and SMI. For this purpose, the effects of Ang II (0.4, 0.8, and 1.2 μM) on the expression levels of these proteins in cardiomyocytes were first investigated. In addition, Ang II (0.8 μM) caused the maximum increase in the mRNA expression of ANP, BNP, and β-MHC compared with the blank group (**Figure 1A-a**). In contrast, 1/4,000 SMI significantly attenuated Ang II–induced expression levels of ANP, BNP, and β-MHC (**Figure 1A-b**). A sharp drop in NPPA after treatment with Ang II (1,200 nM) might be related to the cytotoxicity of high-dose Ang II, and NPPA was more sensitive.

To assess the effects of SMI on the viability of cardiomyocytes at different time points and concentrations, a CellTiter-Glo Luminescent Cell Viability Assay Kit (Promega, WI, USA) was used. The results showed that 1/4,000 SMI had the best cardiomyocyte viability after incubating with Ang II for 48 h (**Figure 1B**).

SMI Attenuated Ang II–Induced Cardiac Hypertrophy in Rat Neonatal Cardiomyocytes

To investigate whether SMI could attenuate Ang II–induced cardiac hypertrophy, neonatal mouse cardiomyocytes were treated with SMI (1/4,000) and/or Ang II (0.8 μM) as described in the Materials and Methods section. Ang II markedly increased the area of cardiomyocytes ($P < 0.05$), and SMI could reverse the effects of Ang II ($P < 0.05$) (**Figure 2A**).

To further investigate the effects of SMI on cardiac hypertrophy, the effects of SMI on the average protein content of cardiac hypertrophy were examined with BCA. Ang II significantly increased the average protein content of cardiomyocytes ($P < 0.05$), and SMI could reverse the effects of Ang II ($P < 0.05$) (**Figure 2B**).

Nascent DNA synthesis in replicating cells is traditionally measured with synthetic thymidine analogs such as BrdU. BrdU antibody staining showed a significant difference between BrdU nonproliferating cells and BrdU proliferating cells. Compared with the blank group, the proportion of $BrdU^+$ in the Ang II group decreased significantly ($P < 0.05$). However, the SMI treatment group showed an improved increase ($P < 0.05$) (**Figure 2C**). Collectively, these observations indicated that the decreased average protein content of cardiomyocytes in the SMI group was not related to the inhibition of cardiomyocyte proliferation. Thus, SMI attenuated the hypertrophy of cardiomyocytes induced by Ang II.

SMI Attenuated Mitochondria Dysfunction

Next, the effects of SMI on the mitochondrial structure and function of myocardial cells were assessed. Ultrastructural changes were induced in cardiomyocytes and mitochondria in hypertrophic cardiomyocytes by Ang II treatment for 48 h, as detected by transmission electron microscopy. Compared with the blank group, the myocardial cell structure of the Ang II group was severely damaged, with several vacuole-like structures. The mitochondria became rounded and swollen, the sputum ruptured or even disappeared, the matrix became deep, some mitochondria dissolved and ruptured, and the membrane disappeared. The SMI group might improve the damage in mitochondrial structure to a certain degree (**Figure 3A**).

The mitochondrial membrane potential acts as an electrochemical gradient necessary to maintain mitochondrial structure and function and is capable of reflecting the mitochondrial functional status, which is also an indication of early apoptosis in cardiomyocytes. Thus, fluorescence was used to observe the effects of SMI on mitochondrial membrane potential.

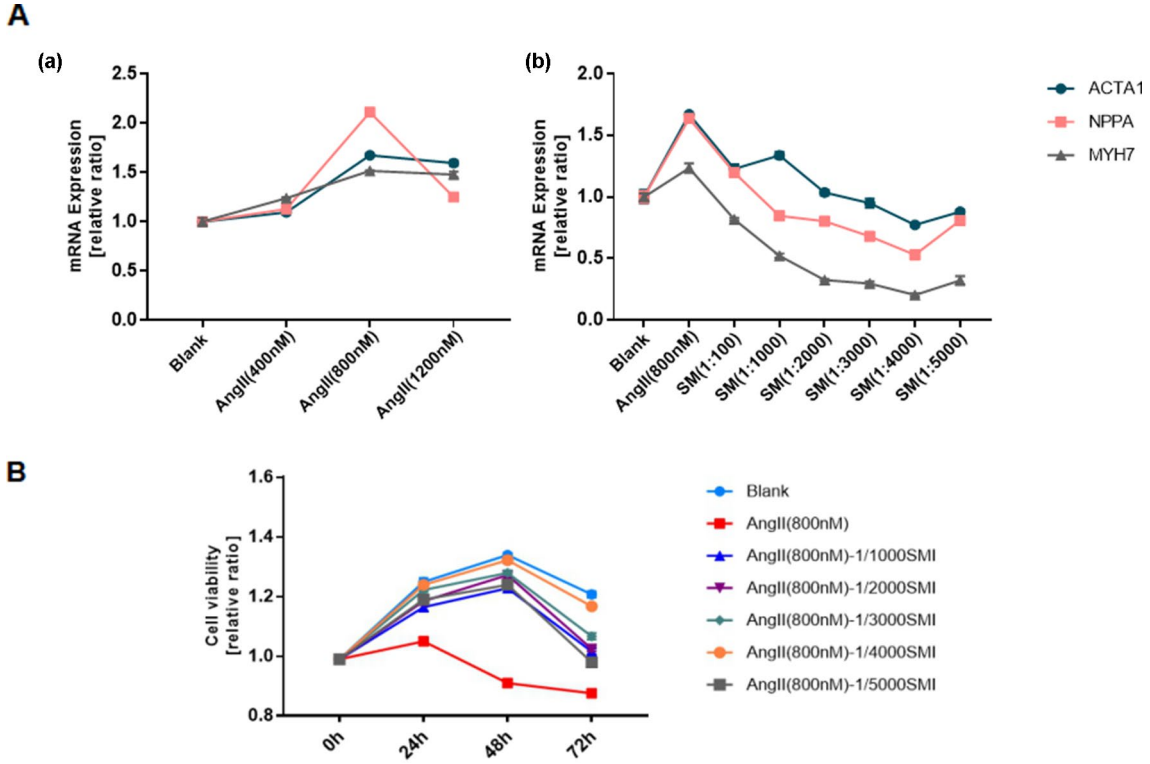

FIGURE 1 | Selection of SMI concentration and its effects on cell viability. **(A)** (a) Selection of Ang II concentration (n = 3); (b) Selection of SMI concentration (n = 3). **(B)** Effects of SMI on cell viability at different time points and concentrations (n = 3).

As shown in **Figure 3B**, when the heart function was normal, the mitochondrial membrane potential was relatively stable, with mostly red fluorescence. The myocardial cell mitochondria were damaged in the Ang II group, and the mitochondrial membrane potential notably decreased ($P < 0.05$). SMI played a significant role in stabilizing mitochondrial membrane potential ($P < 0.05$) (**Figure 3B**).

The RCR is one of the parameters reflecting mitochondrial function that can be used to measure mitochondria (Fatini et al., 2010). The myocardial mitochondrial RCR values were found to be significantly lower than those after HF, suggesting that the mitochondria's ability to make use of oxygen was reduced. Compared with the blank group, the myocardial mitochondrial membrane potential declined in the Ang II group ($P < 0.05$). The SMI treatment group showed an improved mitochondrial respiratory function and increased RCR ($P < 0.05$) (**Figure 3C**).

Changes in Expression Levels of ADP, ATP AMP, and PCr in Hypertrophic Cardiomyocytes

The continuous production of ATP by heart is a prerequisite for maintaining its own pump function, and ATP production is achieved mainly by oxidative phosphorylation in the mitochondrial electron transport chain. The energy in the cells is stored mainly in the form of PCr (Chen et al., 2012). Therefore, the energy level of cardiomyocytes and the function of mitochondria were measured by detecting the expression levels of ADP, ATP, AMP, and PCr *via* HPLC. Compared with the blank group, the expression levels of ATP, ADP, and PCr in the Ang II group were significantly lower ($P < 0.05$), revealing a disturbance in the supply of energy for cardiomyocytes in the Ang II group. Compared with the model group, the levels of ATP, ADP, and PCr remarkably increased in the SMI intervention group ($P < 0.05$). No significant difference was found in the expression level between the three groups ($P > 0.05$) (**Figures 4A–D**).

SMI Regulates the Levels of Fatty Acid Metabolism, Glucose Oxidation, and Mitochondrial Biogenesis With CPT-1, GLUT-4, and PPARγ/PGC-1α Through the AMPK Signaling Pathway

SMI was found to regulate the expression level of p-AMPK consistent with the expression trends of CPT-1, GLUT4, and PGC-1α (**Supplementary Figure 1**). Previous studies showed that AMPK could regulate the expression level of CPT-1 (Kim et al., 2017), GLUT-4 (Manna et al., 2017; Niu et al., 2017), and PGC-1α (Guo et al., 2018). Therefore, it was speculated that SMI regulated the levels of fatty acid metabolism, glucose oxidation, and mitochondrial synthesis probably by activating the AMPK signaling pathway. The effects of AMPK inhibitor compound C on cardiomyocyte viability

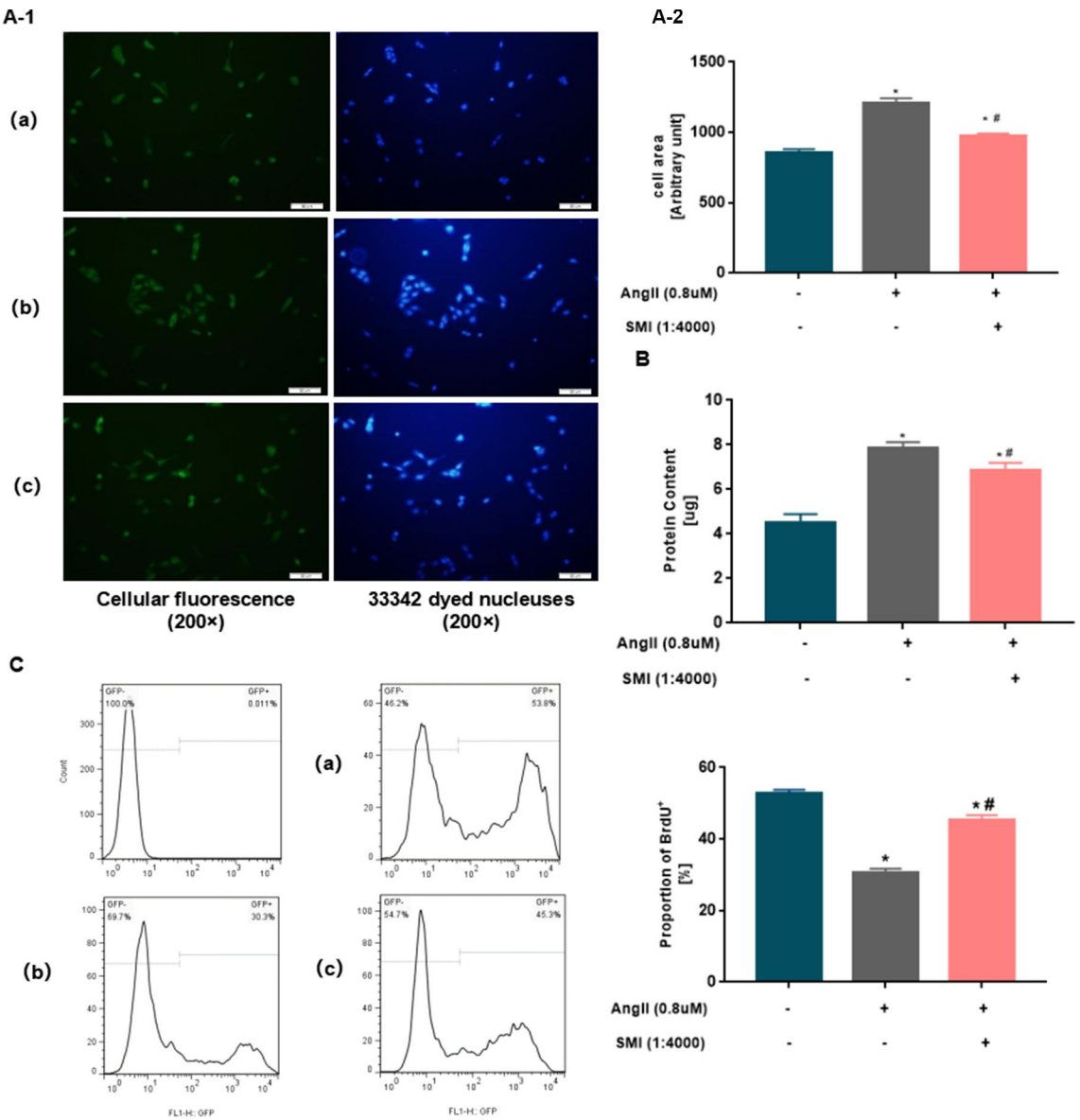

FIGURE 2 | SMI attenuated Ang II–induced cardiac hypertrophy in rat neonatal cardiomyocytes. **(A)** Cell surface in three groups was assessed using an inverted microscope (200×). **(B)** Average protein content of cardiomyocytes in three groups was assessed using BCA. $^{*}P < 0.05$, compared with the blank group; $^{\#}P < 0.05$, compared with the Ang II group. **(C)** Percentages of BrdU^{+} cells assayed by BrdU incorporation. Numbers represent the percentage of BrdU^{+} cells in rat neonatal cardiomyocytes. $^{*}P < 0.05$, compared with the blank group; $^{\#}P < 0.05$, compared with the Ang II group. (a) Blank group, (b) Ang II group (Ang II 0.8μM), and (c) SMI group (Ang II 0.8μM + SMI 1/4,000).

were evaluated at different concentrations. When the concentration of compound C was 0.1μM, the cell viability was the worst after incubation with Ang II for 48 h (**Figure 5A**).

As illustrated in **Figure 5B**, after adding Ang II into cardiomyocytes, the expression level of CPT-1 protein significantly decreased compared with the control group ($P < 0.05$). During the process of Ang II–induced cardiac hypertrophy, the expression level of CPT-1 protein increased in the SMI group compared with the Ang II group. Compound C could reverse the effects of SMI ($P < 0.05$), indicating that SMI regulated CPT-1 *via* activating the AMPK signaling pathway. Consistent with fatty acid metabolism, the expression levels of GLUT-4 and PPARγ/PGC-1α proteins significantly decreased ($P < 0.05$) during Ang II–induced cardiomyocyte hypertrophy, but when SMI was added, these expression levels increased ($P < 0.05$). However, treating cells with AMPK inhibitor compound C notably decreased the expression levels of GLUT-4 and PPARγ/PGC-1α proteins ($P < 0.05$). These data indicated that SMI regulated the expression levels of CPT-1, GLUT-4, and PPARγ/PGC-1α *via* activating the AMPK signaling pathway.

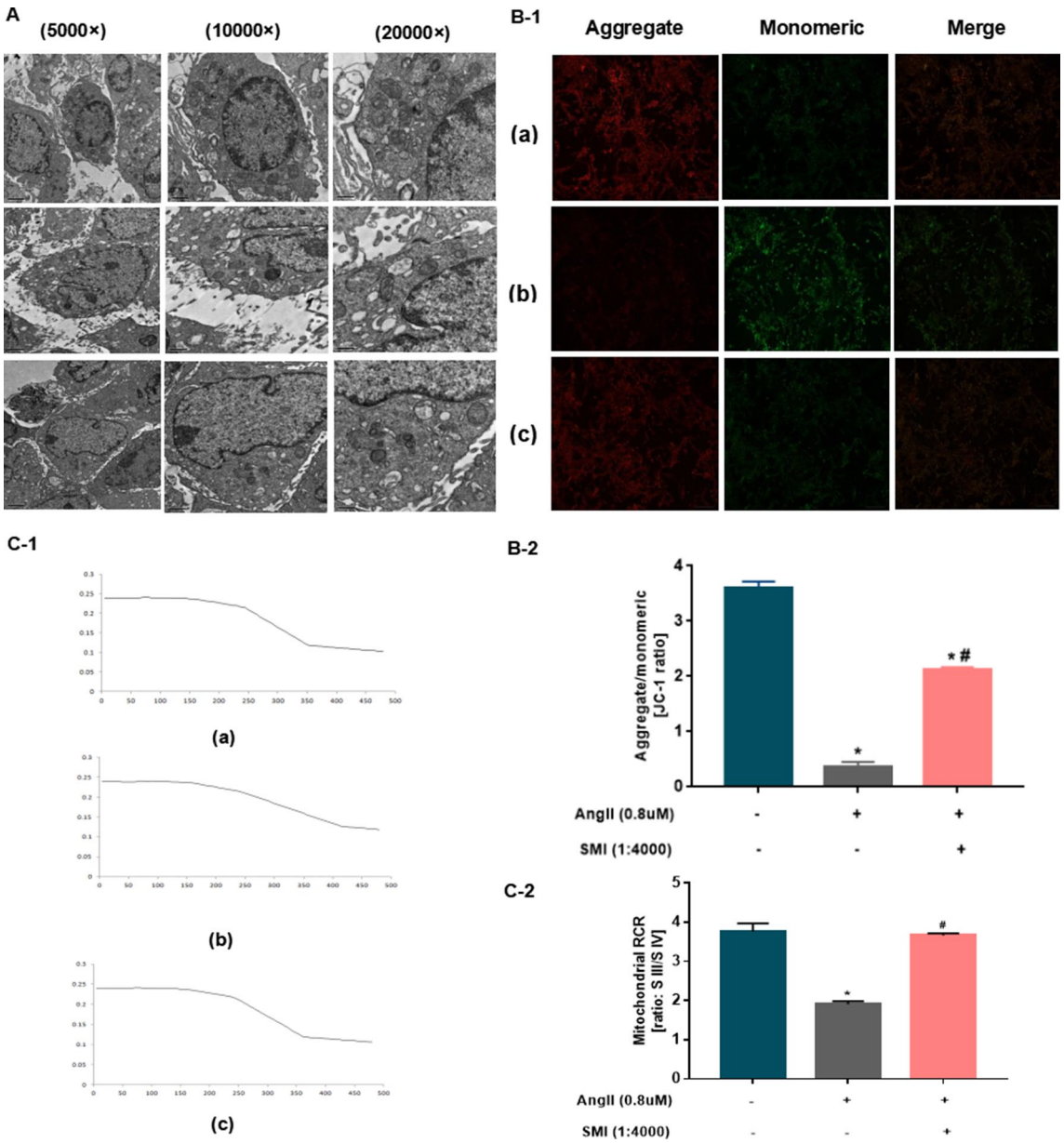

FIGURE 3 | SMI had protective effects on mitochondria (n = 3). **(A)** Effects of SMI on the ultrastructural changes in cardiomyocytes and mitochondria assessed by TEM. **(B)** Effects of SMI on mitochondrial membrane potential assessed by JC-1 staining. **(C)** Effects of SMI on RCR assessed by dissolved oxygen electrolytic analyzer. *P < 0.05, compared with the blank group; #P < 0.05, compared with the Ang II group. (a) Blank group, (b) Ang II group (Ang II 0.8 uM), (c) SMI group (Ang II 0.8uM + SMI 1/4,000).

SMI Inhibited Apoptosis of Hypertrophic Cardiomyocytes *via* the AMPK Signaling Pathway

Apoptosis is a key feature of the progression of heart diseases, and the elimination of pro-apoptotic stimulation or inhibition of the apoptotic cascade can rescue damaged myocardium and prevent the progression of adverse remodeling and HF (Abbate and Narula, 2012). Cardiomyocyte apoptosis may be the cause of cardiac hypertrophy to HF (Abbate et al., 2003). SMI could increase mitochondrial membrane potential (ΔΨm). However, the decline or disappearance of ΔΨm is an early event of myocardial cell apoptosis (Wlodkowic et al., 2012). Therefore, the effects of SMI on cardiomyocyte apoptosis were evaluated. Ang II markedly decreased the rate of apoptosis (P < 0.05), and compound C could reverse the protective effects of SMI on cardiomyocyte apoptosis partly (P < 0.05) (**Figure 6A**).

To further reveal the role of SMI in inhibiting cardiomyocyte apoptosis, the levels of apoptosis-related proteins were examined

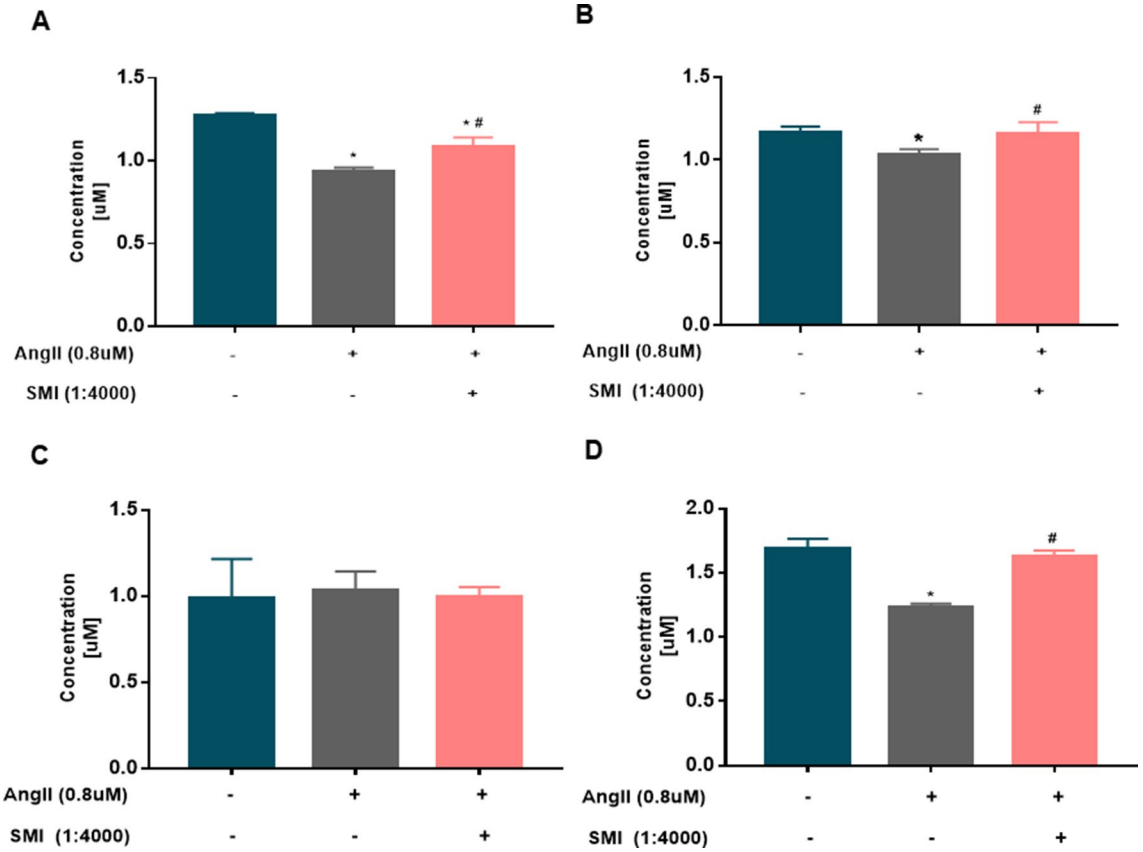

FIGURE 4 | Changes in the levels of ADP, ATP, AMP, and PCr in hypertrophic cardiomyocytes ($n = 6$). **(A)** Changes in the ADP level in the three groups were assessed by HPLC. **(B)** Changes in the ATP level in the three groups were assessed by HPLC. **(C)** Changes in the AMP level in the three groups were assessed by HPLC. **(D)** Changes in the PCr level in the three groups were assessed by HPLC. $^{*}P < 0.05$, compared with the blank group; $^{\#}P < 0.05$, compared with the Ang II group.

by Western blot analysis. As displayed in **Figure 6B**, compared with the blank group, the expression levels of Bax and caspase-3 proteins in the Ang II group were significantly higher, while the expression level of Bcl-2 was lower ($P < 0.05$), demonstrating that cardiomyocyte apoptosis occurred in the Ang II–induced cardiomyocyte hypertrophy group. Compared with the model group, the expression levels of Bax and caspase-3 increased and the expression level of Bcl-2 decreased in the SMI intervention group ($P < 0.05$). Compound C could reverse the effects of SMI on the expression levels of Bax and Bcl-2 ($P < 0.05$) (**Figure 6B**).

Effect of AMPK on SMI-Mediated Cardiomyocyte Hypertrophy and Apoptosis

To further validate the effects of AMPK in inhibiting cardiomyocyte hypertrophy and apoptosis treated with SMI, AMPK knockdown experiments were performed using shRNA. Thus, lentivirus vectors expressing shRNA to both AMPK alpha1 and alpha2 were constructed (Tangeman et al., 2012) (**Supplementary Figure 4**). Decreased myocardial hypertrophy and apoptosis treated with SMI were partly inhibited by AMPK knockdown (**Figures 7A**, **B**). AMPK knockdown almost abolished the SMI-induced increase in the expression of GLUT-4, CPT-1, and PGC-1α (**Figure 7C**). The mechanism underlying increased levels of fatty acid metabolism, glucose oxidation, and mitochondrial biogenesis with CPT-1, GLUT-4, and PGC-1α was dependent on an SMI-mediated increase in AMPK expression. These observations corresponded with the experiments on AMPK inhibitor compound C.

DISCUSSION

The present study demonstrated that SMI not only reduced the cardiomyocyte hypertrophy and cell apoptosis induced by Ang II but also protected the mitochondrial function in hypertrophic cardiomyocytes. In addition, SMI improved energy metabolism by activating the expression levels of related factors in Ang II–induced cardiomyocyte hypertrophy, such as energy metabolism (AMPK), fatty acid metabolism (CPT-1), mitochondrial biogenesis factor (PGC-1α), and glucose oxidation (GLUT-4). These data suggested the phosphorylation of AMPK as a metabolic switch reconstituting fatty acid metabolism, glucose metabolism, and mitochondrial biogenesis to prevent cardiomyocyte hypertrophy and cell apoptosis. A previous study

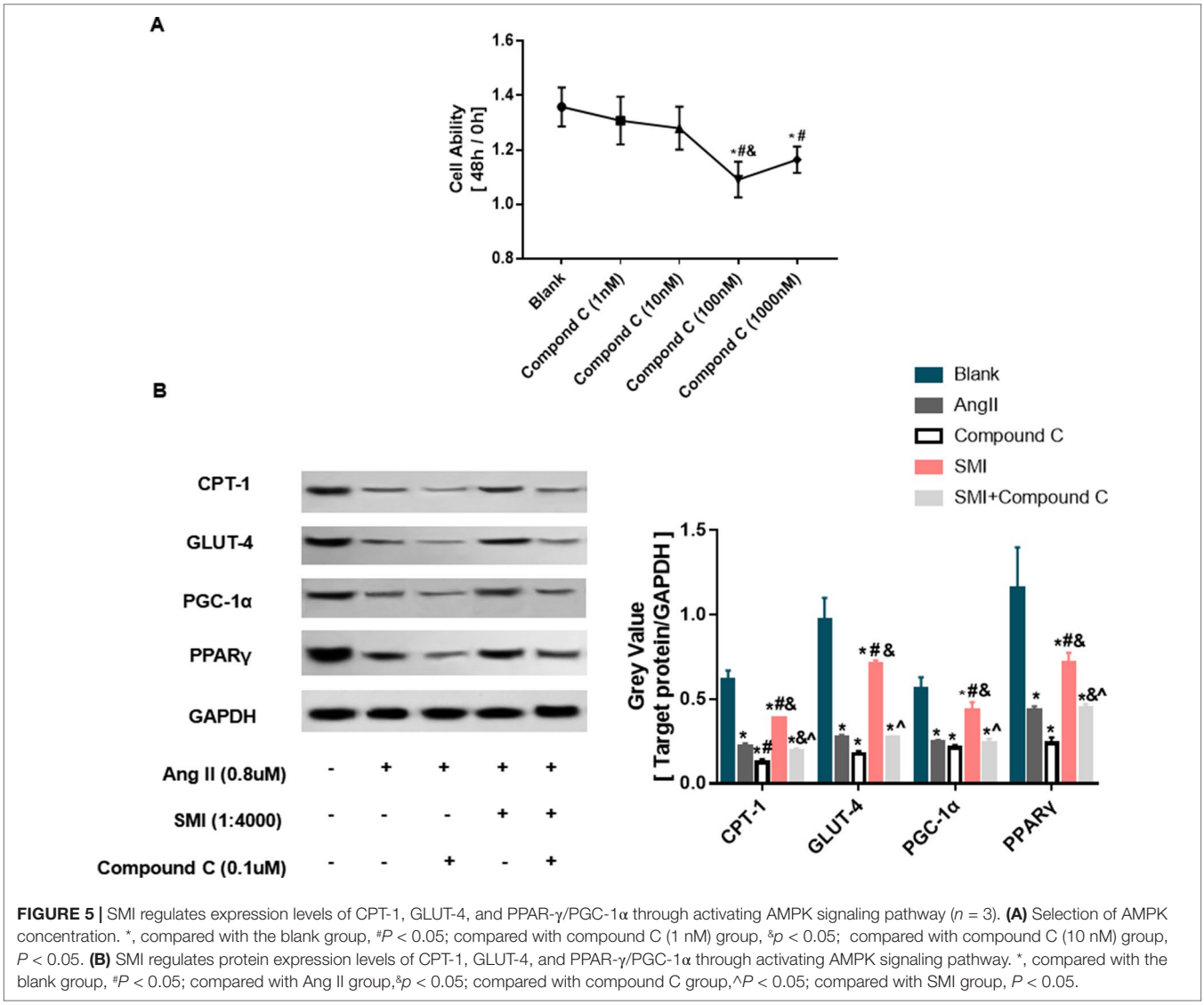

FIGURE 5 | SMI regulates expression levels of CPT-1, GLUT-4, and PPAR-γ/PGC-1α through activating AMPK signaling pathway ($n = 3$). **(A)** Selection of AMPK concentration. *, compared with the blank group, $^{\#}P < 0.05$; compared with compound C (1 nM) group, $^{\&}p < 0.05$; compared with compound C (10 nM) group, $P < 0.05$. **(B)** SMI regulates protein expression levels of CPT-1, GLUT-4, and PPAR-γ/PGC-1α through activating AMPK signaling pathway. *, compared with the blank group, $^{\#}P < 0.05$; compared with Ang II group,$^{\&}p < 0.05$; compared with compound C group,^$P < 0.05$; compared with SMI group, $P < 0.05$.

found that cardiac hypertrophy was both an intermediate step and a determinant of HF (Meijs et al., 2007). This was of great significance to identify alternative therapeutic approaches for HF.

The main source of normal adult myocardial energy is FFA oxidation. FFA oxidation disorder and increased glucose utilization occur in hypertrophic and failing myocardium, in which the direct consequence of this transformation is the reduction of fatty acid utilization. Although the oxidation of glucose needs less oxygen, it produces much less energy compared with FFA oxidation, causing the heart to remain in an energy-starved state, ultimately leading to a lack of myocardial energy. Due to the high energy demand of the heart, a fine balance in energy substrate (glucose and fatty acid) use is crucial in maintaining metabolic flexibility (Karwi et al., 2018). A key metabolic regulator is AMPK; a heterotrimeric protein is centrally involved in controlling cellular energy homeostasis. Its activation through metabolic stress stimulates energy-generating processes and has been shown to regulate hypertrophy-regulating genes in several models. The activation of the AMPK signaling pathway increases FFA oxidation by phosphorylating ACC, in turn decreasing the malonyl-CoA content and activating CPT-1. AMPK stimulates GLUT-4 translocation and increases the whole-body use of glucose (Yamaguchi et al., 2005). However, knowledge about the influence of Ang II on cardiac energy metabolism is limited. In the present study, when the action time reached 48 h, the expression levels of p-AMPK, CPT-1, and GLUT-4 decreased, suggesting that glucose metabolism and fatty acid metabolism were weakened. To validate further the effects of AMPK in SMI-mediated energy metabolism, AMPK knockdown experiments were performed using shRNA. The findings were consistent with the results of previous studies (Liu et al., 2018). Mitochondrial biogenesis is regulated by a complex regulatory system. PGC-1α, a transcription coactivator of nuclear receptors and master regulator of metabolism, plays a pivotal role in mediating metabolic alterations in both physiological and pathological hypertrophies. PGC-1α is also involved in mitochondrial

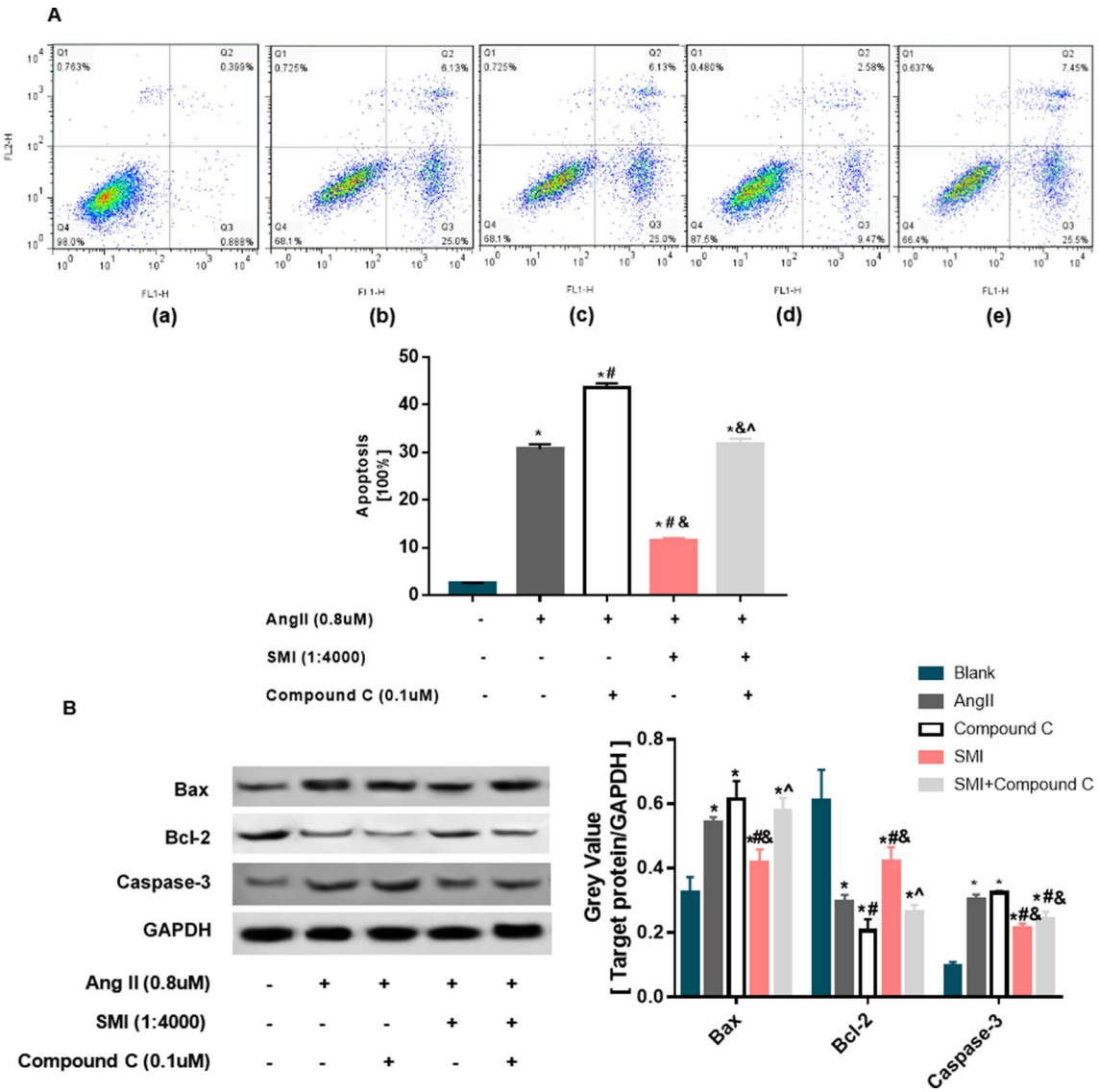

FIGURE 6 | SMI inhibited the apoptosis of hypertrophic cardiomyocytes (n = 3). **(A)** Effects of SMI on cardiomyocyte apoptosis in hypertrophic cardiomyocytes. 3 Control group; (b) Ang II group; (c) compound C group; (d) SMI group; and (e) SMI + compound C group. Dead cells were labeled with annexin V (–) propidium iodide (PI) (+) and are shown in the Q1 area; late apoptotic cells were labeled with annexin V (+) PI (+) and are shown in the Q2 area; early apoptotic cells were labeled with annexin V (+) PI (–) and are shown in the Q3 area; live cells were labeled with annexin V (–) PI (–) and are shown in the Q4 area. Summarized data for TMRE fluorescence intensity measured with confocal microscopy. **(B)** Effects of SMI on apoptosis-related proteins in hypertrophic cardiomyocytes. $^{*}P < 0.05$, compared with the blank group; $^{\#}P < 0.05$, compared with the Ang II group; $^{\&}P < 0.05$, compared with the compound C group; $^{\wedge}P < 0.05$, compared with the SMI group.

biogenesis, which is vital for cell survival (Kulikova et al., 2018). The present study confirmed that SMI activated the AMPK signaling pathway and upregulated the expression levels of PGC-1α, CPT-1, and GLUT-4 compared with the model group. Thus, SMI regulated energy metabolism by activating the AMPK/PPARγ/PGC-1α signaling pathway. Specifically, SMI regulated fatty acid and glucose metabolism *via* activating the AMPK signaling pathway.

The energy metabolism in cardiomyocytes is closely associated with the status of mitochondrial function. Mitochondrial dysfunction can be caused by the intermediate metabolite accumulation in HF. In the present study, SMI was found to reduce mitochondrial structural damage, decrease respiratory function, and reduce membrane potential, which were induced by Ang II induction. The cardiac hypertrophic program was accompanied by progressive mitochondrial remodeling, and particularly by mitochondrial permeability transition pore opening (Javadov and Karmazyn, 2007; Javadov et al., 2009). When the membrane potential decreased the uncoupling of oxidative phosphorylation, ATP was depleted, and the number of oxygen radicals increased,

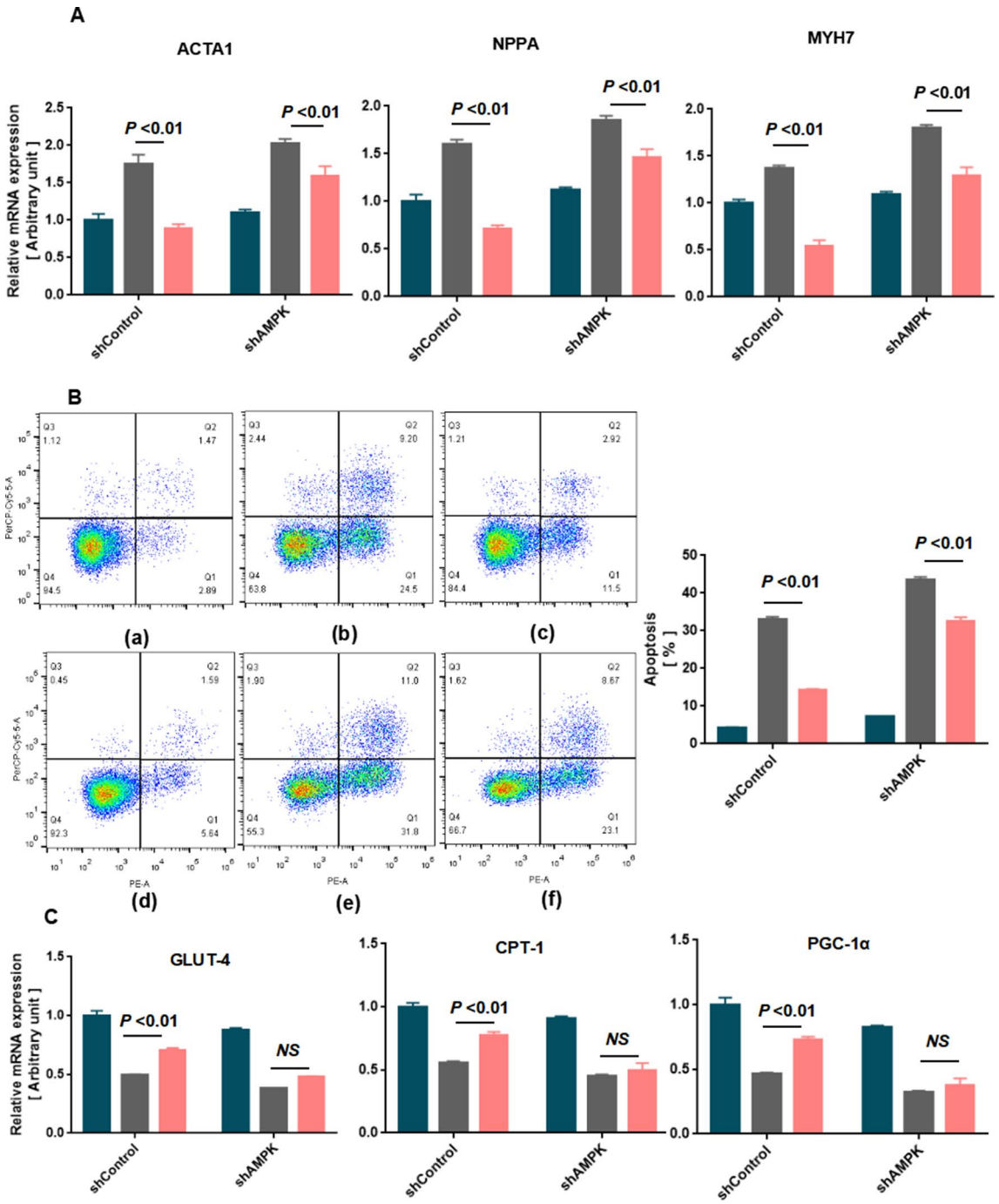

FIGURE 7 | Knockdown of AMPK aggravated SMI-mediated cardiomyocyte hypertrophy and apoptosis in rat neonatal cardiomyocytes (n = 3). **(A)** Quantification of RT-qPCR was used to quantify the RNA levels of the hypertrophic markers in blank, Ang II-treated, or SMI-treated rat neonatal cardiomyocytes with shCtrol or shAMPK. **(B)** Annexin V/PI apoptosis kit was used to quantify cardiomyocyte apoptosis in blank, Ang II-treated, or SMI-treated rat neonatal cardiomyocytes with shCtrol or shAMPK. (a) Blank + shCtrol; (b) Ang II (0.8 μM) + shCtrol; (c) SMI (1/4,000) + Ang II (0.8 μM) + shCtrol; (d) Blank + shAMPK; (e) Ang II (0.8 μM) + shAMPK; (f) SMI (1/4,000) + Ang II (0.8 μM) + shCtrol. **(C)** Quantification of RT-qPCR was used to quantify the RNA levels of GLUT-4, CPT-1, and PGC-1α.

leading to the irreversible apoptosis of cardiac myocytes. Cell proliferation, apoptosis, and cell hypertrophy are interrelated and interacted with each other during ventricular remodeling (Sun et al., 2013). Cardiomyocyte hypertrophy assembly leads to apoptosis, resulting in myocardial failure–induced cardiovascular disease. Thus, cardiac hypertrophy and apoptosis are closely related to cardiovascular diseases, such as HF (Freundlich et al., 2013). The expression levels of Bax and caspase-3 increased while

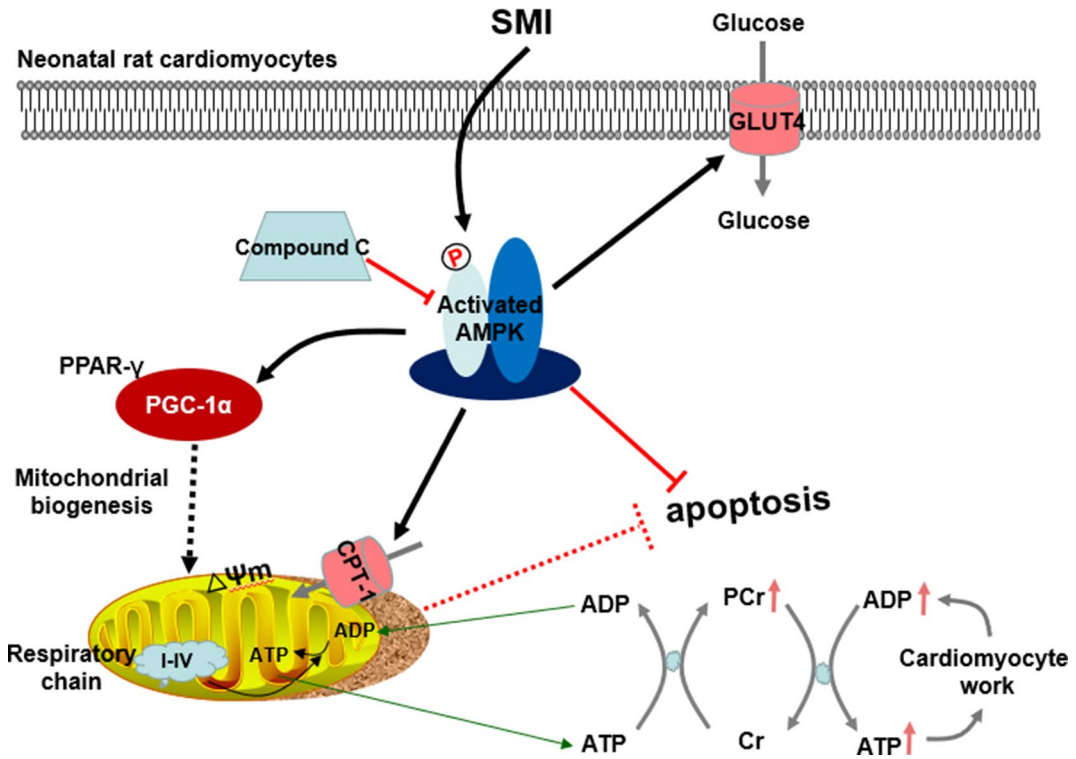

FIGURE 8 | SMI suppressed Ang II–induced cardiomyocyte hypertrophy and apoptosis through the activation of the AMPK signaling pathway *via* energy-dependent mechanisms.

the expression level of Bcl-2 decreased in the Ang II group, thus justifying the increase in the rate of apoptosis; this result was consistent with the finding of a previous study (Hutchinson et al., 2008; Day et al., 2011).

ATP is produced in mitochondria, and it needs to be continuously produced to maintain their function. Studies have shown that mitochondria in cardiomyocytes account for about one third of the total cardiomyocytes (Ventura-Clapier et al., 2011), indirectly indicating that the supply of myocardial energy is inseparable from mitochondria with normal function and structure. Mitochondrial dysfunction may affect the function of myocardium (Guzun et al., 2011). When cardiomyocytes were induced by Ang II, the mitochondrial structure, respiratory function, and membrane potential were notably damaged. Therefore, a decline in the ATP level was noted in the Ang II group. A study suggested that an increased intracellular AMP/ATP ratio was the primary mechanism for the activation of AMPK (Oakhill et al., 2011). Recent studies have shown other sensitive AMPK activators besides the activation of AMPK signaling pathway. Also, the deletion and decline in FDP can directly activate AMPK rather than being dependent on AMP (Kemp and Oakhill, 2017). The present study revealed for the first time that FBP was associated with the activation mechanism of AMPK, with no dependence on AMP and ADP. The AMP content did not change in Ang II–induced hypertrophic cardiomyocytes compared with the blank group, and SMI did not increase the expression level of AMP. Thus, it was suggested that SMI might directly activate the AMPK signaling pathway to increase the expression levels of ATP, ADP, and PCr in hypertrophic cardiomyocytes.

However, this study had many limitations. It did not deeply investigate the specific mechanism by which SMI regulated the mitochondrial function, glucose metabolism, and fatty acid metabolism. No animal experiments were conducted to verify the results. SMI itself is a compound preparation of TCM, which is extracted from three herbs: *Panax ginseng* C.A. Mey, *Ophiopogon japonicus* (Thunb.) Ker Gawl., and *Schisandra chinensis* (Turcz.) Baill. More than 28 ginsenosides have been extracted from ginseng, which could delay cardiac mitochondrial impairment (Scott et al., 2001; Wang and Ren, 2002). SMI was found to have more than 10 components using HPLC in the present study, including ginsenoside Rg1, ginsenoside Re, ginsenoside Rf, ginsenoside Rb1, ginsenoside Rc, ginsenoside Rh1, ginsenoside Rd, schisandrin, ginsenoside Rg5 (Rk1), and ginsenoside Rh3. Which specific component of SMI regulated energy metabolism was not studied. These issues will be addressed in future studies.

CONCLUSIONS

This study showed that SMI suppressed Ang II–induced cardiomyocyte hypertrophy and apoptosis through activating the AMPK signaling pathway *via* energy-dependent mechanisms (**Figure 8**). SMI can be considered to be an alternative therapeutic approach for HF.

DATA AVAILABILITY

The datasets generated for this study can be found in the ANP: GenBank, NC_005104; BNP: GenBank, NC_005104;β-MHC: GenBank, NC_005114.

ETHICS STATEMENT

This study was carried out in accordance with the principles of the Basel Declaration and recommendations of the Care and Use of Laboratory Animals Center of Shanghai University of Traditional Chinese Medicine. The protocol was approved by the 'Experimental Animal Welfare and Ethics Committee of Shanghai University of Traditional Chinese Medicine' (Permit No. PZSHUTCM190329013).

AUTHOR CONTRIBUTIONS

YL and XW designed the experiment, analyzed the data, and wrote the paper. YL, XR, XX, TQ and CL performed the experiments. HZ, XR and JG commented the manuscript. All authors have read and approved the manuscript.

FUNDING

This study was supported by a grant from the National Natural Science Foundation of China (Grant No. 81803887, 81573647 and 81703743).

SUPPLEMENTARY MATERIAL

The Supplementary Material for this article can be found online at: https://www.frontiersin.org/articles/10.3389/fphar.2019.01095/full#supplementary-material

REFERENCES

Abbate, A., Biondi-Zoccai, G. G. L., Bussani, R., Dobrina, A., Camilot, D., Feroce, F., et al. (2003). Increased myocardial apoptosis in patients with unfavorable left ventricular remodeling and early symptomatic post-infarction heart failure. *J. Am. Coll. Cardiol.* 41 (5), 753–760. doi: 10.1016/S0735-1097(02)02959-5

Abbate, A., and Narula, J. (2012). Role of apoptosis in adverse ventricular remodeling. *Heart Fail. Clin.* 8 (1), 79–86. doi: 10.1016/j.hfc.2011.08.010

Benjamin, E. J., Muntner, P., Alonso, A., Bittencourt, M. S., Callaway, C. W., Carson, A. P., et al. (2019). Heart disease and stroke statistics—2019 update: a report from the american heart association. *Circulation* 139 (10), e56-e528. doi: 10.1161/CIR.0000000000000659

Chen, Y., Wang, Y., Chen, J., Chen, X., Cao, W., Chen, S., et al. (2012). Roles of transcriptional corepressor RIP140 and coactivator PGC-1α in energy state of chronically infarcted rat hearts and mitochondrial function of cardiomyocytes. *Mol. Cell. Endocrinol.* 362 (1-2), 11–18. doi: 10.1016/j.mce.2012.03.023

Day, R. M., Lee, Y. H., Han, L., Kim, Y. C., and Feng, Y. H. (2011). Angiotensin II activates AMPK for execution of apoptosis through energy-dependent and -independent mechanisms. *Am. J. Physiol. Lung Cell Mol. Physiol.* 301 (5), L772–L781. doi: 10.1152/ajplung.00072.2011

De Jong, K. A., and Lopaschuk, G. D. (2017). Complex energy metabolic changes in heart failure with preserved ejection fraction and heart failure with reduced ejection fraction. *Can. J. Cardiol.* 33 (7), 860–871. doi: 10.1016/j.cjca.2017.03.009

Dolinsky, V. W., Cole, L. K., Sparagna, G. C., and Hatch, G. M. (2016). Cardiac mitochondrial energy metabolism in heart failure: role of cardiolipin and sirtuins. *Biochim. Biophys. Acta Mol. Cell Biol. Lipds.* 1861 (10), 1544–1554. doi: 10.1016/j.bbalip.2016.03.008

Dong, Z. X., Wan, L., Wang, R. J., Shi, Y. Q., Liu, G. Z., Zheng, S. J., et al. (2017). (−)-Epicatechin suppresses angiotensin II-induced cardiac hypertrophy via the activation of the SP1/SIRT1 signaling pathway. *Cell Physiol. Biochem.* 41 (5), 2004–2015. doi: 10.1159/000475396

Fan, X. J., Yu, H., and Ren, J. (2011). Homeostasis and compensatory homeostasis: bridging Western medicine and traditional Chinese medicine. *Curr. Cardiol. Rev.* 7 (1), 43–46. doi: 10.2174/157340311795677671

Fatini, C., Sticchi, E., Marcucci, R., Verdiani, V., Nozzoli, C., Vassallo, C., et al. (2010). S38G single-nucleotide polymorphism at the KCNE1 locus is associated with heart failure. *Heart Rhythm* 7 (3), 363–367. doi: 10.1016/j.hrthm.2009.11.032

Freundlich, M., Li, Y. C., Quiroz, Y., Bravo, Y., Seeherunvong, W., Faul, C., et al. (2013). Paricalcitol downregulates myocardial renin-angiotensin and fibroblast growth factor expression and attenuates cardiac hypertrophy in uremic rats. *Am. J. Hypertens.* 27 (5), 720–726. doi: 10.1093/ajh/hpt177

Go, A. S., Mozaffarian, D., Roger, V. L., Benjamin, E. J., Berry, J. D., Borden, W. B., et al. (2013). Executive summary: heart disease and stroke statistics—2013 update: a report from the American Heart Association. *Circulation* 127 (1), 143–152. doi: 10.1161/CIR.0b013e318282ab8f

Guo, X., Jiang, Q., Tuccitto, A., Chan, D., Alqawlaq, S., Won, G.-J., et al. (2018). The AMPK-PGC-1α signaling axis regulates the astrocyte glutathione system to protect against oxidative and metabolic injury. *Neurobiol. Dis.* 113, 59–69. doi: 10.1016/j.nbd.2018.02.004

Guzun, R., Timohhina, N., Tepp, K., Gonzalez-Granillo, M., Shevchuk, I., Chekulayev, V., et al. (2011). Systems bioenergetics of creatine kinase networks: physiological roles of creatine and phosphocreatine in regulation of cardiac cell function. *Amino Acids* 40 (5), 1333–1348. doi: 10.1007/s00726-011-0854-x

Haynes, P., and Campbell, K. S. (2014). Myocardial hypertrophy reduces transmural variation in mitochondrial function. *Front. Physiol.* 5, 178. doi: 10.3389/fphys.2014.00178

Hoppel, C. L., Tandler, B., Fujioka, H., and Riva, A. (2009). Dynamic organization of mitochondria in human heart and in myocardial disease. *Int. J. Biochem. Cell Biol.* 41 (10), 1949–1956. doi: 10.1016/j.biocel.2009.05.004

Hutchinson, D. S., Summers, R. J., and Bengtsson, T. (2008). Regulation of AMP-activated protein kinase activity by G-protein coupled receptors: potential utility in treatment of diabetes and heart disease. *Pharmacol. Ther.* 119 (3), 291–310. doi: 10.1016/j.pharmthera.2008.05.008

Javadov, S., and Karmazyn, M. (2007). Mitochondrial Permeability transition pore opening as an endpoint to initiate cell death and as a putative target for cardioprotection. *Cell Physiol. Biochem.* 20, 01–22. doi: 10.1159/000103747

Javadov, S., Rajapurohitam, V., Kilić, A., Zeidan, A., Choi, A., and Karmazyn, M. (2009). Anti-hypertrophic effect of NHE-1 inhibition involves GSK-3β-dependent attenuation of mitochondrial dysfunction. *J. Mol. Cell Cardiol.* 46 (6), 998–1007. doi: 10.1016/j.yjmcc.2008.12.023

Karwi, Q. G., Uddin, G. M., Ho, K. L., and Lopaschuk, G. D. (2018). Loss of metabolic flexibility in the failing heart. *Front. Cardiovasc. Med.* 5, 68. doi: 10.3389/fcvm.2018.00068

Kemp, B. E., and Oakhill, J. S. (2017). Energy sensing through a sugar diphosphate. *Nature* 548 (7665), 36–37. doi: 10.1038/nature23099

Kim, B., Woo, M.-J., Park, C.-S., Lee, S.-H., Kim, J.-S., Kim, B., et al. (2017). Hovenia Dulcis extract reduces lipid accumulation in oleic acid-induced steatosis of Hep G2 cells *via* activation of AMPK and PPARα/CPT-1 pathway

and in acute hyperlipidemia mouse model. *Phytother. Res.* 31 (1), 132–139. doi: 10.1002/ptr.5741

Kulikova, T. G., Stepanova, O. V., Voronova, A. D., Valikhov, M. P., Sirotkin, V. N., Zhirov, I. V., et al. (2018). Pathological remodeling of the myocardium in chronic heart failure: role of PGC-1α. *Bull. Exp. Biol. Med.* 164 (6), 794–797. doi: 10.1007/s10517-018-4082-1

Liu, B. L., Cheng, M., Hu, S., Wang, S., Wang, L., Hu, Z. Q., et al. (2018). Effect of the Shensong Yangxin Capsule on energy metabolism in angiotensin ii-induced cardiac hypertrophy. *Chin. Med. J. (Engl.)* 131 (19), 2287–2296. doi: 10.4103/0366-6999.241819

Liu, L., Wang, C., Sun, D., Jiang, S., Li, H., Zhang, W., et al. (2015). Calhex 231 Ameliorates cardiac hypertrophy by inhibiting cellular autophagy in Vivo and in Vitro. *Cell Physiol. Biochem.* 36 (4), 1597–1612. doi: 10.1159/000430322

Luo, Y., Xu, Y., Liang, C., Xing, W., and Zhang, T. (2018). The mechanism of myocardial hypertrophy regulated by the interaction between mhrt and myocardin. *Cell Signalling* 43, 11–20. doi: 10.1016/j.cellsig.2017.11.007

Manna, P., Achari, A. E., and Jain, S. K. (2017). Vitamin D supplementation inhibits oxidative stress and upregulate SIRT1/AMPK/GLUT4 cascade in high glucose-treated 3T3L1 adipocytes and in adipose tissue of high fat diet-fed diabetic mice. *Arch. Biochem. Biophys.* 615, 22–34. doi: 10.1016/j.abb.2017.01.002

Meijs, M. F., de Windt, L. J., de Jonge, N., Cramer, M. J., Bots, M. L., Mali, W. P., et al. (2007). Left ventricular hypertrophy: a shift in paradigm. *Curr. Med. Chem.* 14, 157–171. doi: 10.2174/092986707779313354

Niu, Y., Wang, T., Liu, S., Yuan, H., Li, H., and Fu, L. (2017). Exercise-induced GLUT4 transcription *via* inactivation of HDAC4/5 in mouse skeletal muscle in an AMPKα2-dependent manner. *Biochim. Biophys. Acta Mol. Basis Dis.* 1863 (9), 2372–2381. doi: 10.1016/j.bbadis.2017.07.001

Oakhill, J.S., Steel, R., Chen, Z. P., Scott, J. W., Ling, N., Tam, S. et al. (2011). AMPK is a direct adenylate charge-regulated protein kinase. *Science* 322 (6036), 1433–1435. doi: 10.1126/science.1200094

Opie, L. H., Commerford, P. J., Gersh, B. J., and Pfeffer, M. A. (2006). Controversies in ventricular remodelling. *Lancet* 367 (9507), 356–367. doi: 10.1016/S0140-6736(06)68074-4

Patrucco, E., Domes, K., Sbroggio, M., Blaich, A., Schlossmann, J., Desch, M., et al. (2014). Roles of cGMP-dependent protein kinase I (cGKI) and PDE5 in the regulation of Ang II-induced cardiac hypertrophy and fibrosis. *Proc. Natl. Acad. Sci.* 111 (35), 12925–12929. doi: 10.1073/pnas.1414364111

Quaini, F., Chen, Y., Tang, Y., Zhang, Y.-C., Huang, X.-H., Xie, Y.-Q., et al. (2015). A Metabolomic study of rats with doxorubicin-induced cardiomyopathy and Shengmai injection treatment. *PloS One* 10 (5), e0125209. doi: 10.1371/journal.pone.0125209

Roman, M. J., Ganau, A., Saba, P. S., and Devereux, R. B. (1997). Left ventricular hypertrophy, arterial compliance, and aging. *Adv. Exp. Med. Biol.* 432, 13–22. doi: 10.1007/978-1-4615-5385-4_2

Rosano, G. M., and Vitale, C. (2018). Metabolic modulation of cardiac metabolism in heart failure. *Cardiac Fail. Rev.* 4 (2), 99–103. doi: 10.15420/cfr.2018.18.2

Scott, G. I., Colligan, P. B., Ren, B. H., and Ren, J. (2001). Ginsenosides Rb1 and Re decrease cardiac contraction in adult rat ventricular myocytes: role of nitric oxide. *Br. J. Pharmacol.* 134 (6), 1159–1165. doi: 10.1038/sj.bjp.0704377

Shah, A. M., Shin, S. H., Takeuchi, M., Skali, H., Desai, A. S., Kober, L., et al. (2012). Left ventricular systolic and diastolic function, remodelling, and clinical outcomes among patients with diabetes following myocardial infarction and the influence of direct renin inhibition with aliskiren. *Eur. J. Heart Fail.* 14 (2), 185–192. doi: 10.1093/eurjhf/hfr125

Sun, B., Huo, R., Sheng, Y., Li, Y., Xie, X., Chen, C., et al. (2013). Bone morphogenetic protein-4 mediates cardiac hypertrophy, apoptosis, and fibrosis in experimentally pathological cardiac hypertrophy. *Hypertension* 61 (2), 352–360. doi: 10.1161/HYPERTENSIONAHA.111.00562

Tamura, T., Said, S., Harris, J., Lu, W., and Gerdes, A. M. (2000). Reverse remodeling of cardiac myocyte hypertrophy in hypertension and failure by targeting of the renin-angiotensin system. *Circulation* 102 (2), 253–259. doi: 10.1161/01.CIR.102.2.253

Tham, Y. K., Bernardo, B. C., Ooi, J. Y. Y., Weeks, K. L., and McMullen, J. R. (2015). Pathophysiology of cardiac hypertrophy and heart failure: signaling pathways and novel therapeutic targets. *Arch. Toxicol.* 89 (9), 1401–1438. doi: 10.1007/s00204-015-1477-x

Tangeman, L., Wyatt, C. N., and Brown, T. L. (2012). Knockdown of AMP-activated protein kinase alpha 1 and alpha 2 catalytic subunits. *J. RNAi Gene Silencing* 8 (1), 470–478.

Torrens, C., Ghnenis, A. B., Odhiambo, J. F., McCormick, R. J., Nathanielsz, P. W., and Ford, S. P. (2017). Maternal obesity in the ewe increases cardiac ventricular expression of glucocorticoid receptors, proinflammatory cytokines and fibrosis in adult male offspring. *PloS One* 12 (12), e0189977. doi: 10.1371/journal.pone.0189977

Ventura-Clapier, R., Garnier, A., Veksler, V., and Joubert, F. (2011). Bioenergetics of the failing heart. *Biochim. Biophys. Acta Mol. Cell Res.* 1813 (7), 1360–1372. doi: 10.1016/j.bbamcr.2010.09.006

Wang, Z. G., and Ren, J. (2002). Current status and future direction of Chinese herbal medicine. *Trends Pharmacol. Sci.* 23 (8), 347–348. doi: 10.1016/S0165-6147(02)02051-5

Wlodkowic, D.I., Skommer, J., and Darzynkiewicz, Z. (2012). Cytometry of apoptosis. Historical perspective and new advances. *Exp. Oncol.* 34 (3), 255–262.

Xian, S., Yang, Z., Lee, J., Jiang, Z., Ye, X., Luo, L., et al. (2016). A randomized, double-blind, multicenter, placebo-controlled clinical study on the efficacy and safety of Shengmai injection in patients with chronic heart failure. *J. Ethnopharmacol.* 186, 136–142. doi: 10.1016/j.jep.2016.03.066

Yamaguchi, S., Katahira, H., Ozawa, S., Nakamichi, Y., Tanaka, T., Shimoyama, T., et al. (2005). Activators of AMP-activated protein kinase enhance GLUT4 translocation and its glucose transport activity in 3T3-L1 adipocytes. *Am. J. Physiol.-Endocrinol. Metab.* 289 (4), E643–E649. doi: 10.1152/ajpendo.00456.2004

Zhan, S., Fan, X., Zhang, F., Wang, Y., Kang, L., and Li, Z. (2015). A proteomic study of Shengmai injection's mechanism on preventing cardiac ischemia-reperfusion injury *via* energy metabolism modulation. *Mol. BioSyst.* 11 (2), 540–548. doi: 10.1039/C4MB00161C

Zhou, Q., Qin, W.-Z., Liu, S.-B., Kwong, J. S. W., Zhou, J., Chen, J. et al. (2014). Shengmai (a traditional Chinese herbal medicine) for heart failure. *Cochrane Database Syst. Rev.* (4), CD005052. doi: 10.1002/14651858.CD005052.pub5

Conflict of Interest Statement: The authors declare that the research was conducted in the absence of any commercial or financial relationships that could be construed as a potential conflict of interest.

frontiers in Pharmacology

ORIGINAL RESEARCH
published: 03 October 2019
doi: 10.3389/fphar.2019.01128

Naoxintong Capsule Inhibits the Development of Cardiovascular Pathological Changes in Bama Minipig Through Improving Gut Microbiota

Wei-jian Zhang[1], Wei-wei Su[1,2], Pei-bo Li[1], Hong-yu Rao[1], Qing-wei Lin[1], Xuan Zeng[1], Tao-bin Chen[1], Zeng-hao Yan[1], Hong Liu[1] and Hong-liang Yao[1,3]**

[1] Guangdong Engineering & Technology Research Center for Quality and Efficacy Reevaluation of Post-market Traditional Chinese Medicine, Guangdong Key Laboratory of Plant Resources, State Key Laboratory of Biocontrol, School of Life Sciences, Sun Yat-sen University, Guangzhou, China, [2] Key Laboratory of Traditional Chinese Medicine Quality Standards, Guangxi Institute of Traditional Medical and Pharmaceutical Sciences, Nanning, China, [3] Guangdong Key Laboratory of Animal Conservation and Resource Utilization, Guangdong Public Laboratory of Wild Animal Conservation and Utilization, Drug Synthesis and Evaluation Center, Guangdong Institute of Applied Biological Resources, Guangzhou, China

OPEN ACCESS

Edited by:
Yue Liu,
Xiyuan Hospital, China

Reviewed by:
Yaozu Xiang,
Tongji University, China
Hein Min Tun,
The University of Hong Kong, Hong Kong
Jihong Han,
Nankai University, China

***Correspondence:**
Hong Liu
liuhong29@mail.sysu.edu.cn
Hong-liang Yao
yhlsysu@126.com

Specialty section:
This article was submitted to Ethnopharmacology, a section of the journal Frontiers in Pharmacology

Received: *16 May 2019*
Accepted: *30 August 2019*
Published: *03 October 2019*

Citation:
Zhang W-j, Su W-w, Li P-b, Rao H-y, Lin Q-w, Zeng X, Chen T-b, Yan Z-h, Liu H and Yao H-l (2019) Naoxintong Capsule Inhibits the Development of Cardiovascular Pathological Changes in Bama Minipig Through Improving Gut Microbiota. Front. Pharmacol. 10:1128. doi: 10.3389/fphar.2019.01128

Naoxintong capsule (NXT), a Chinese medicine, has performed excellent effects on the prevention and treatment against cardiovascular diseases. NXT is a fine powder mixture without any herb extraction, and there must be lots of ingredients hard to be absorbed. However, little is known about the correlation between the NXT's cardioprotective effects and gut microbiota. Herein, we report the effect of NXT on the development of cardiovascular diseases and clarify the correlation between NXT's cardioprotective effects and gut microbiota. In the current study, minipigs were selected and fed with high-fat diet and NXT daily for successive 8 months. During the process, up to 18 biomedical parameters were monthly determined to observe the dynamic changes after NXT treatment. At the end of experimental process, pathological examinations of heart, coronary artery, carotid artery, thoracic aorta, and abdominal aorta were conducted by HE staining and 16SrDNA sequencing, and analyzing of gut microbiota were conducted. Our results showed that NXT's effects against cardiovascular diseases were through regulating blood lipid profiles, inhibiting vascular inflammation, enhancing antioxidant capacity, and alleviating myocardial injury, without damages on liver and kidney particularly. Concurrently, we also found that long-term administration of NXT increased the diversity of gut microbiota, influenced the microbiome structure and composition stably, and revered the increase of the ratio of the *Firmicutes* to *Bacteroidetes* (F/B ratio) in relative abundance. Specifically, our results revealed some key bacterium of *Caproiciproducens (enhanced)*, *Sutterella (enhanced)*, *Erysipelotrichaceae (enhanced)*, and *Romboutsia (decreased)* that were closely involved in NXT's effects. Taken together, our study demonstrates that NXT can inhibit the development of cardiovascular diseases by ameliorating high-fat diet–induced metabolic disorders and partly through improving gut microbiota.

Keywords: Naoxintong capsule (NXT), Bama minipig, cardiovascular diseases, blood lipid metabolism, gut microbiota

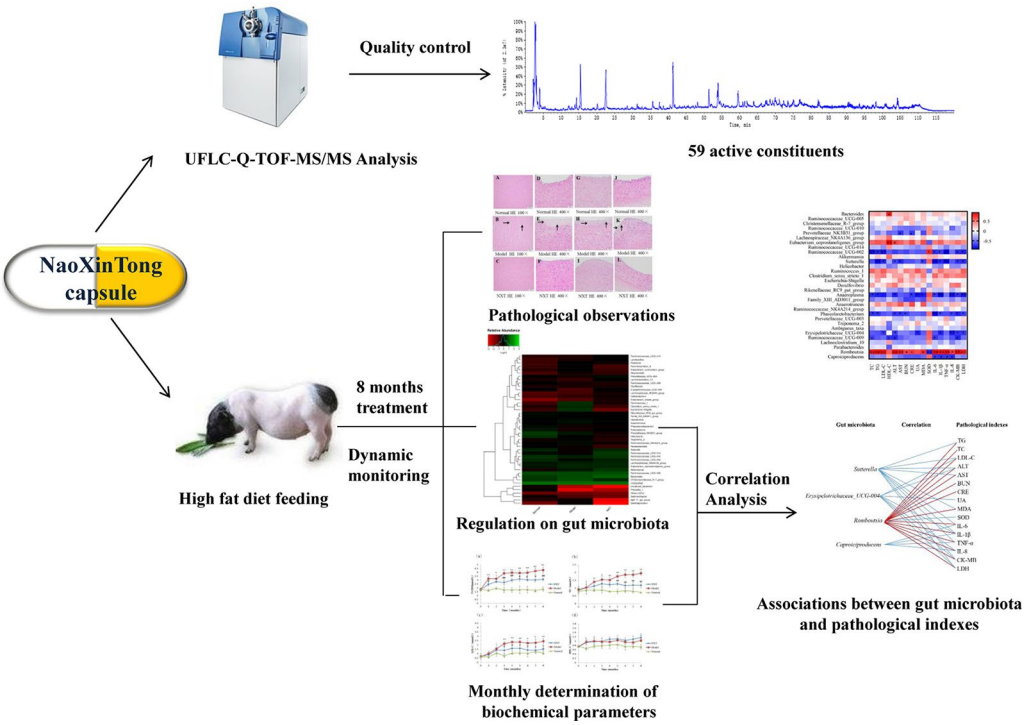

GRAPHICAL ABSTRACT | The graphic abstract of the study.

INTRODUCTION

Atherosclerotic cardiovascular diseases are the leading cause of morbidity and mortality worldwide. Dyslipidemia is one of the most common risk factors leading to cardiovascular diseases (Besli et al., 2017). High-fat diet is considered to be the indispensable factor to induce lipid metabolism disorder and result in atherosclerotic cardiovascular disease. Studies *in vivo* and *in vitro* have demonstrated that high-fat feeding could cause inflammation (Jakobsdottir et al., 2013), induce oxidative stress (Paula et al., 2016), generate endothelial dysfunctions (Knight et al., 2008), as well as exacerbate hepatic and renal injuries (Michal et al., 2004; Pinhal et al., 2013). Such high-fat diet–induced metabolic disorders are closely associated with the generation and development of atherosclerotic cardiovascular disease.

Minipigs, smaller than domestic swine, are becoming increasingly attractive experimental animal for research. Minipigs have been proven to be recommended model for hyperlipidemia, atherosclerosis, and cardiovascular studies because the morphology and function of their cardiovascular system closely resemble that of humans. More importantly, minipigs have lipoprotein profiles and metabolism similar to humans, and they develop atherosclerosis with increased age spontaneously (Smith et al., 1990; Bergen and Mersmann, 2005; Casellas et al., 2013). And giving minipigs high-fat diet feeding can induce hyperlipidemia and atherosclerosis similar to that of humans (Shoumin et al., 2004; Miyoshi et al., 2010).

In recent years, numerous studies have demonstrated that gut microbiota played a key role in the maintenance of human health, and many inflammatory and metabolic diseases are related to the imbalance of intestinal microecology (Nadja et al., 2010; Vrieze et al., 2010). Long-term high-fat diet intervention can change the intestinal microecology, and the imbalance of gut microbiota could cause the disorder of lipid metabolism, thus leading to cardiovascular disease (Zhang et al., 2010; Murphy et al., 2015).

NXT has been widely used in the prevention and treatment of coronary heart disease, stroke, and other vascular diseases since it was listed in 1993. It is composed of 16 kinds of traditional Chinese medicines, including *Astragalus membranaceus*, *Salvia miltiorrhiza*, *Ligusticum*, *Radix paeoniae rubra*, *Szechwan lovage Rhizome*, *Semen persicae*, *Carthamus tinctorius* L., *Frankincense*, *myrrh*, *Spatholobus suberectus*, *Achyranthes root*, *Cassia Twig*, *Mulberry Twig*, *Buthus martensii*, *Hirudo nipponica*, and *Pheretima aspergillum*. Numerous studies *in vivo* have demonstrated that NXT had protective effects in vascular diseases through different actions such as lowering glucose and lipid, improving ischemia reperfusion injury, stabilizing vulnerable plaques, etc. (Wang et al., 2017; Yang et al., 2017; Yang et al., 2018). Ma X H et al. analyzed the absorbable components of NXT and used the network pharmacology method to discuss the mechanism of NXT in the treatment of heart diseases, and their result showed that NXT significant regulated 123 targets and related pathways (Ma et al., 2016). Recently, Yang X X et al. summarized the cardioprotective properties and the involved mechanisms of NXT, and the review shows that multiple protective effects of NXT on cardiovascular diseases can be correlated to the actions of NXT on inflammation, oxidative stress, and lipid/glucose metabolism (Han et al., 2019).

Different from general Chinese traditional medicine, NXT is a fine powder mixture containing herbs without any extraction. Therefore, there are some components hard to be absorbed, such as a large number of dietary fibers. Accordingly, this study was designed on the hypothesis that NXT's effects against the cardiovascular diseases are partly through ameliorating high-fat diet–induced metabolic disorders and partly through improving gut microbiota. Consequently, we attempted to perform long-term dynamic observation of NXT against the development of cardiovascular pathological changes, including the effects of NXT on blood lipid profiles, inflammation, oxidative stress, liver and kidney functions, myocardial enzyme, as well as the change of gut microbiota in Bama minipigs, along with long-term high-fat diet feeding and medication treatment.

MATERIALS AND METHODS

Drugs and Reagents

NXT (Med-drug permit no. Z20025001) was kindly provided by Buchang Pharmaceutical Co., Ltd. NXT is composed of 16 herbs including *A. membranaceus* (165 g/kg, g weight of herb/kg weight of NXT powder), *Radix paeoniae rubra* (67.5 g/kg), *Salvia miltiorrhiza* (67.5 g/kg), *Ligusticum* (67.5 g/kg), *Szechwan lovage Rhizome* (67.5 g/kg), *Semen persicae* (67.5 g/kg), *Achyranthes root* (67.5 g/kg), *Mulberry twig* (67.5 g/kg), *P. aspergillum* (67.5 g/kg), *Hirudo nipponica* (67.5 g/kg), *Spatholobus suberectus* (50 g/kg), *Cassia Twig* (50 g/kg), *Carthamus tinctorius* L. (32.5 g/kg), *Frankincense* (32.5 g/kg), *myrrh* (32.5 g/kg), and *Buthus martensii* (32.5 g/kg). All the above herbs, in the radios of 66: 27:27:27:27:27:27:27:27:27:20:20:13:13:13:13 (dry weight), are crushed into fine powder, screened through mesh size of 80, and mixed homogeneously, without any extraction (Chinese Pharmacopoeia Commission, 2015). Assay kits for total cholesterol (TC), triglyceride (TG), high-density lipoprotein cholesterol (HDL-C), low-density lipoprotein (LDL-C), alanine transaminase (ALT), aspartate transaminase (AST), blood urea nitrogen (BUN), creatinine (CRE), uric acid (UA), methane dicarboxylic aldehyde (MDA), superoxide dismutase (SOD), lactic dehydrogenase (LDH), and creatine kinase-MB (CK-MB) were purchased from Nanjing Jiancheng Bioengineering Institute Co., Ltd, China. ELISA kits for interleukin-1β (IL-1β), interleukin-8 (IL-8), interleukin-6 (IL-6), and tumor necrosis factor-α (TNF-α) were purchased from cloud-clone Corp., USA. Eosin, hematoxylin, and oil red O were purchased from Shanghai Aladdin Bio-Chem Technology Co., Ltd.; cholesterol was purchased from Guangzhou NOCIKAR Biotechnology Co., Ltd.; butter was purchased from Jieshou Yutu Edible Oil Co., Ltd.; peanut oil was purchased from Shandong Luhua Co., Ltd.; bile salt was purchased from China National Pharmaceutical Group Corporation Chemical Reagent Co., Ltd.; and basic feed were all provided by Dongguan Pearl Lab Animal Sci & Tech Co., Ltd.

Instruments

BS-3000A electronic analytical balance (Shanghai Yousheng Weighing Apparatus Co., Ltd.), DS-261 Automatic Biochemical Analyzer (Jiangsu SINNOWA Co., Ltd.), KDC-2046 low-speed refrigerated centrifuge (USTC Zonkia Scientific Instruments Co., Ltd.), Haier DW-86L628 Ultra-Low Temperature Refrigerator (Qingdao Haier), OLYMPUS® Biological Microscope (Beijing Cnrico Technology Co., Ltd.), hybrid triple quadrupole time-of-flight mass spectrometer (AB SCIEX Triple TOF™ 5600 plus).

UFLC-Q-TOF-MS/MS Analysis of NXT

The capsule of NXT was completely removed, and the powder was weighed 1g precisely. The powder was treated by ultrasonic wave in 50ml of 75% methanol for 30 min. The supernatant was filtrated and then injected into ultra-fast liquid chromatography/quadrupole-time-of-flight tandem mass spectrometry system for analysis (UFLC-Q-TOF-MS/MS). The column was a Ultimate XB-C18 (4.6×250mm, 5μm, Welch), which is maintained at 30°C. The mobile phases were composed of acetonitrile (A) and water with 0.1% formic acid (B) using a multi-step linear gradient elution of 10% A at 0–5min, 10–25% A at 5–35min, 25–60% A at 35–65min, 60–67% A at 65–70min, 67% A at 70–80min, 67–90% A at 80–95min, 90% A at 95–105min, 90–10% A at 105–110min, and 10% A at 110–120min with the flow rate kept at 1.0 ml/min. Other MS parameters were adopted same as published work (Zeng et al., 2018). The sample volume injected was set at 20μl. All the acquisition and analysis of data were controlled by the PeakView Software TM V. 1.1 (AB SCIEX, Foster City, CA).

Ethical Statement and Animals

Nine male Bama minipigs aged 6 months, weighing 13~18 kg, were provided by Dongguan Pearl Lab Animal Sci & Tech Co., Ltd. (Certification No. SYXK (Yue) 2017-0123). The animals were maintained at the Animal Center of Dongguan Pearl Lab Animal Sci & Tech Co., Ltd. Animals were individually housed in pens under controlled conditions (temperature was maintained at 18~26°C, and the relative humidity at 40~70%, with a 12-h light/dark cycle). All the experimental procedures were carried out in accordance with the National Institutes of Health guide for the care and use of laboratory animals and were approved by Animal Care and Use Committee of School of Life Sciences of Sun Yat-sen University. During the experiment, appropriate procedures were taken to minimize the harm to the animals.

Modeling and Grouping Administration

Bama minipigs were randomly divided into three groups (3/group) and received the following treatment for 8 months: normal group, normal diet; model group, high-fat diet; and NXT group, high-fat diet containing NXT powder (110 mg/kg/day). Food, 3% of body weight/day, was supplied twice a day, and body weights were measured once a month. Normal diet was composed of corn 48%, wheat bran 20%, soybean meal 15%, rice bran 12%, and fish powder 5%. High-fat diet was formed from a mixture of 3% cholesterol, 10% butter, 6% peanut oil, and 0.5% bile salt with normal diet. In order to avoid stress reaction in animals fed with high-fat diet, the proportion of fat was gradually increased in the first 10 days. After the animals get used to the high-fat diet, we started the experiment.

Determination of Biochemical Parameters

During the experiment, blood samples for measuring biochemical parameters of blood lipid metabolism, hepatic and renal functions, oxidative stress, inflammatory, and myocardial enzyme were collected every month. The animals were anesthetized by intramuscular injection of pentobarbital sodium (30 mg/kg) fasted overnight, and blood was drawn from precaval vein. Ten milliliters of non-anticoagulant blood was standing for 30min at room temperature, and serum was separated from blood by centrifugation for 15min at 3,000 rpm. Six hundred microliters of serum was put into DS-261 automatic biochemical analyzer to detect the TC, TG, HDL-C, LDL-C, ALT, AST, BUN, CRE, CK-MB, and LDH. Four hundred microliters of serum was used to detect the IL-6, IL-8, IL-1β, and TNF-α through the ELISA kits. Fifty microliters was used to detect the SOD and MDA through the colorimetric-assay kits. All the detection operations were conducted in strict according to the corresponding kit instructions.

Collection of Tissues and Pathological Observation

At the end of the experiment, animals were sacrificed by phlebotomy under anesthesia with intramuscular Injection of pentobarbital sodium (30 mg/kg). The tissues including fresh heart, coronary artery, carotid artery, and abdominal aorta were removed and fixed in 4% paraformaldehyde. And these tissues were made into routine paraffin sections and stained routinely with hematoxylin and eosin (HE) and then examined histopathologically.

Extraction and Detection of Fecal Genomic DNA and 16SrDNA Gene Sequencing

Fresh fecal samples were collected from each minipig at the end of the experiment, and the fecal DNA was extracted using PowerSoil DNA Extraction Kit (MO BIO Laboratories, Inc., Carlsbad, CA, USA). The quality and concentration of extracted DNA was detected using a Nanodrop ND-1000 Spectrophotometer (Thermo Electron Corporation, USA). PCR amplification of 16SrDNA sequences was performed using primer sets specific for v3–v4 variable regions. Final PCR products were purified from unincorporated nucleotides and primers using the QIAquick PCR Purification Kit (Qiagen, Valencia, USA). Purified samples were normalized to equal DNA concentration and sequenced using the Illumina MiSeq sequencer (Illumina, USA).

Statistical Analysis

16SrDNA gene sequence data were analyzed using the Quantitative Insights into Microbial Ecology (QIIME) 1.8.0 software (Caporaso et al., 2010). The operational taxonomic units (OTUs) were selected by clustering sequences with a similarity of >97% using USEARCH 7.0.1090 software (Edgar, 2013), and subsequently, chimera detection was performed using the UCHIME method (Edgar et al., 2011). OTUs were annotated with taxonomic information based on RDP classifier version 2.2 algorithm using the Greengenes database.

Alpha diversity indexes were calculated by Mothur v1.31.2 software, and the difference of alpha diversity was evaluated by Kruskal–Wallis test. Beta diversity was measured by calculating the Bray–Curtis. Nonmetric multidimensional scaling (NMDS) was applied on the distance metrics to generate two-dimensional plots in QIIME v1.80. The significant changed bacteria were tested by Metastats (http://metastats.cbcb.umd.edu/). P-value was corrected by p.adjust in the R (v3.0.3) with the method of Benjamini–Hochberg. Correlation between pharmacological indexes and 16SrDNA sequence data are presented in the form of a heatmap diagram based on Spearman's correlation coefficient. At the genus level, the correlation coefficient of R value was color-mapped onto the gut microbiota, showing how correlated each gut microbiota was with the pharmacological indexes. R values are presented in different colors, and the color card as the color partition of different r values ($p < 0.05^{*}$, $p < 0.01^{**}$).

Apart from the gut microbiota analysis, all the other data were statistically analyzed by Student's t-test using SPSS software (version: 21.0). The data were expressed as mean ± SD, and a P value less than 0.05 or 0.01 was considered to be statistically significant.

RESULTS

Identification of Major Components in NXT

This study employed UFLC-Q-TOF-MS/MS detection to investigate the ingredients of NXT for the quality control. As a result, a total of 59 compounds were identified in NXT based on high-accuracy protonated precursors and multi-stage mass spectrometry according to the reported literature (Wang et al., 2015; Ma et al., 2016) and online databases such as ChemSpider (www.chemspider.com) and the Mass Bank (www.massbank.jp) (details in **Table 1**). These compounds mainly included flavones, flavone glycosides, phenanthraquinones, and terpenoids. Most of these constituents have been reported to show potentially important therapeutic activities for CVDs (Ma et al., 2016). In addition, to ensure the identity of chemical constituents of NXT, the comparison of chemical constituents in three different batches of NXT was carried out, and the results showed the above ingredients of NXT could stably recur (details in **Figure S1**).

Monthly Determination of Biochemical Parameters

The dynamic graph of changes of biochemical parameters in this study can be found at **Supplementary Material** (dynamic changes bubble chart in parameters with time).

Body Weight

Body weights were measured at monthly intervals to compare weight gain in the different groups. As shown in **Table 2**, high-fat diet feeding resulted in a faster increase in body weight than that observed in the normal group. After 4 months of feeding, animals in NXT group showed significantly lower body weight compared with the model animals ($p<0.05$ or $p<0.01$).

TABLE 1 | Identification of the chemical constituents of NXT by UFLC-Q-TOF-MS/MS.

T_R(min)	Formula	$[M+H]^+$ (error, ppm)	$[M-H]^-$ (error, ppm)	Fragment ions in positive (+) ion mode	Fragment ions in negative (–) ion mode	Identification
4.02	$C_{10}H_{13}N_5O_4$	268.1043 (1)		136.0644$[M+H-C_5H_2N_5]^+$		Adenosine
5.03	$C_7H_6O_5$		169.0151 (5.2)		125.0243$[M-H-C_2H_4O]^-$	Gallic acid
12.21	$C_{19}H_{28}O_{11}$		431.1559 (0.1)		269.1029$[M-H-C_6H_{10}O_5]^-$	Benzyl-β-gentiobioside
12.22	$C_{26}H_{32}O_{14}$		567.1721 (0.2)		405.1124$[M-H-C_6H_{10}O_5]^-$, 243.0652$[M-H-2C_6H_{10}O_5]^-$	Mulberroside A
13.05	$C_{23}H_{28}O_{12}$		495.1511 (0.5)		333.1036$[M-H-C_6H_{10}O_5]^-$	Oxypaeoniflorin
13.39	$C_7H_6O_3$		137.0260 (10)		108.0206$[M-H-CHO]^-$	Protocatechuic aldehyde
13.91	$C_{16}H_{18}O_9$		353.0883 (1.1)		191.0573$[M-H-C_6H_{10}O_5]^-$	Chlorogenic acid
14.27	$C_{15}H_{14}O_6$	291.0866 (0.9)	289.0721 (1.3)	165.0565$[M+H-C_6H_6O_3]^+$, 139.0401$[M+H-C_8H_6O_3]^+$, 123.0477$[M+H-C_8H_7O_4]^+$	245.0859$[M-H-CO_2]^-$, 203.0734$[M-H-CO_2-C_2H_2O]^-$, 161.0602$[M-H-CO_2-2C_2H_2O]^-$, 151.0422$[M-H-C_6H_6O_2-CO]^-$	Catechin
14.34	$C_{27}H_{32}O_{16}$		611.1622 (0.8)		491.1219$[M-H-C_4H_8O_4]^-$, 473.0862$[M-H-C_4H_8O_4-H_2O]^-$, 403.1008$[M-H-C_7H_{10}O_6-H_2O]^-$, 325.0727$[M-H-C_5H_8O_5-H_2O]^-$, 283.0646$[M-H-C_4H_8O_4-C_7H_{10}O_6-H_2O]^-$	Hydroxysafflor yellow A
14.44	$C_8H_8O_5$		183.0308 (3.3)		124.0148$[M-H-C_2H_5O_2]^-$	Methyl gallate
15.43	$C_{20}H_{27}NO_{11}$		456.1512 (0.1)		323.0964$[M-H-C_8H_7NO]^-$	Amygdalin
19.34	$C_{15}H_{14}O_6$	291.0866 (0.8)	289.0723 (1.8)	165.0565$[M+H-C_6H_6O_3]^+$, 139.0401$[M+H-C_8H_6O_3]^+$, 123.0477$[M+H-C_8H_7O_4]^+$	245.0832$[M-H-CO_2]^-$, 205.0552$[M-H-2C_2H_2O]^-$, 203.0735$[M-H-CO_2-C_2H_2O]^-$, 151.0443$[M-H-C_6H_6O_2-CO]^-$, 125.0230$[M-H-C_9H_8O_3]^-$	Epicatechin
20.13	$C_{23}H_{28}O_{11}$	481.1704 (0)	479.1560 (0.3)	197.0807$[M+H-C_6H_{10}O_5-C_7H_5O_2]^+$, 179.0696$[M+H-C_6H_{10}O_5-C_7H_5O_2-H_2O]^+$	121.0311$[M-H-C_{15}H_{18}O_{10}]^-$	Albiflorin
22.04	$C_{27}H_{30}O_{17}$	627.1550 (–1)	625.1420 (1)	465.1050$[M+H-C_6H_{10}O_5]^+$, 303.0474$[M+H-2C_6H_{10}O_5]^+$	463.0879$[M-H-C_6H_{10}O_5]^-$, 301.0346$[M-H-2C_6H_{10}O_5]^-$	6-Hydroxy kaempferol-di-O-glucoside
22.54	$C_{23}H_{28}O_{11}$		479.1560 (0.3)		327.1174$[M-H-C_7H_6O_2-CH_2O]^-$, 165.0577$[M-H-C_{17}H_{14}O_6]^-$, 121.0298$[M-H-C_{16}H_{22}O_9]^-$	Paeoniflorin
25.12	$C_{27}H_{30}O_{16}$	611.1601 (–0.9)	609.1471 (0.8)	465.0915$[M+H-C_6H_{10}O_4]^+$, 303.0479$[M+H-C_{12}H_{20}O_9]^+$	301.0356$[M-H-C_{12}H_{20}O_9]^-$, 272.0279$[M-H-C_{13}H_{22}O_{10}]^-$	Rutin
26.18	$C_{21}H_{20}O_{12}$	465.1029 (0.2)	463.0887 (1)	303.0490$[M+H-C_6H_{10}O_5]^+$	301.0365$[M-H-C_6H_{10}O_5]^-$	Isoquercitrin
27.2	$C_{22}H_{22}O_{10}$	447.1285 (–0.3)		285.0746$[M+H-C_6H_{10}O_5]^+$, 270.0514$[M+H-C_6H_{10}O_5-CH_3]^+$, 253.0474$[M+H-C_6H_{10}O_5-CH_3OH]^+$, 225.0520$[M+H-C_6H_{10}O_5-CH_3OH-CO]^+$, 137.0250$[M+H-C_6H_{10}O_5-C_9H_8O_2]^+$		Calycosin-7-O-β-D-glycoside

(Continued)

TABLE 1 | Continued

T_R(min)	Formula	[M+H]$^+$ (error, ppm)	[M–H]$^-$ (error, ppm)	Fragment ions in positive (+) ion mode	Fragment ions in negative (–) ion mode	Identification
27.93	$C_{10}H_{10}O_4$	195.0650 (–0.9)	193.0512 (3)	177.0527[M+H–H_2O]$^+$, 149.0594[M+H–H_2O–CO]$^+$, 145.0283[M+H–H_2O–CH_3OH]$^+$, 134.0390[M+H–H_2O–CO–CH_3]$^+$, 117.0380[M+H–H_2O–CO–CH_3OH]$^+$, 89.0445[M+H–H_2O–CH_3OH–2CO]$^+$	178.0258[M–H–CH_3]$^-$, 134.0371[M–H–CO_2]$^-$, 89.0411[M–H–CH_3–CO_2]$^-$	Ferulic acid
28.45	$C_{27}H_{44}O_7$	481.3157 (–0.5)		445.2911[M+H–2H_2O]$^+$, 427.2891[M+H–3H_2O]$^+$, 371.2204[M+H–3H_2O–CO_2]$^+$		β-Ecdysterone
29.88	$C_{30}H_{32}O_{15}$		631.1679 (1.6)		613.1554[M–H–H_2O]$^-$, 491.0970[M–H–$C_7H_5O_2$–H_2O]$^-$, 313.0580[M–H–$C_{17}H_{16}O_5$–H_2O]$^-$	Galloylpaeoniflorin
31.01	$C_{15}H_{12}O_7$		303.0515 (1)		285.0535[M–H–H_2O]$^-$, 125.0231[M–H–$C_6H_4O_3$–3H_2O]$^-$	Taxifolin
31.46	$C_{41}H_{32}O_{26}$		939.1140 (2.2)		769.0530[M–H–$C_7H_6O_5$]$^-$	Pentagalloylglucose
32.19	$C_{15}H_{10}O_6$	287.0551 (0.4)		258.0529[M+H–CHO]$^+$, 213.0552[M+H–H_2O–2CO]$^+$, 165.0163[M+H–$C_7H_6O_2$]$^+$		Kaempferol
32.19	$C_{21}H_{20}O_{11}$	449.1074 (–0.9)		287.0532[M+H–$C_6H_{10}O_5$]$^+$		Kaempferol-3-O-glucoside
32.24	$C_{27}H_{30}O_{15}$	595.1653 (–0.8)	593.1521 (0.8)	287.0548[M+H–$C_{12}H_{20}O_9$]$^+$	285.0410[M–H–$C_{12}H_{20}O_9$]$^-$	Kaempferol-3-O-rutinoside
33.37	$C_{14}H_{12}O_4$	245.0810 (0.8)	243.0668 (2.3)	199.0777[M+H–C_2H_6O]$^+$, 181.0603[M+H–C_2H_6O–H_2O]$^+$, 161.0606[M+H–$C_4H_4O_2$]$^+$, 107.0544[M+H–$C_7H_4O_2$–H_2O]$^+$	225.0572[M–H–H_2O]$^-$, 199.0766[M–H–C_2H_4O]$^-$, 175.0763[M–H–C_4H_4O]$^-$, 159.0459[M–H–$C_4H_4O_2$]$^-$	Oxyresveratrol
35.71	$C_{25}H_{24}O_{13}$	533.1284 (–1)		285.0759[M+H–$C_6H_{10}O_5$–$C_3H_2O_3$]$^+$		Calycosin-7-O-β-D-glc-6"-O-malonate
36.01	$C_9H_{16}O_4$		187.0989 (4.5)		125.0970[M–H–CO_2–H_2O]$^-$	Skinorim
37.33	$C_9H_6O_2$	147.0442 (1)		103.0596[M+H–CO_2]$^+$, 91.0593[M+H–2CO]$^+$, 77.0471[M+H–$C_3H_2O_2$]$^+$, 65.0479[M+H–$C_4H_2O_2$]$^+$, 51.0300[M+H–$C_5H_4O_2$]$^+$		Coumarin
37.56	$C_{18}H_{16}O_8$		359.0778 (1.6)		197.0474[M–H–$C_9H_6O_3$]$^-$, 179.0358[M–H–$C_9H_6O_3$–H_2O]$^-$, 161.0247[M–H–$C_9H_6O_3$–2H_2O]$^-$, 123.0419[M–H–$C_{11}H_8O_6$]$^-$	Rosmarinic acid
38.19	$C_{12}H_{14}O_3$	207.1018 (0.9)		189.0890[M+H–H_2O]$^+$, 179.1067[M+H–CO]$^+$, 165.0873[M+H–C_2H_2O]$^+$, 161.0943[M+H–H_2O–CO]$^+$		Senkyunolide F
38.71	$C_{26}H_{22}O_{10}$		493.1151 (2.2)		295.0623123.0419[M–H–$C_9H_{10}O_5$]$^-$, 159.0453[M–H–$C_9H_{10}O_5$–$C_8H_8O_2$]$^-$, 109.0290[M–H–$C_9H_{10}O_5$–$C_{11}H_6O_3$]$^-$	Salvianolic acid A
40.71	$C_{22}H_{22}O_9$	431.1338 (0.2)		269.0813[M+H–$C_6H_{10}O_5$]$^+$, 254.0563[M+H–$C_6H_{10}O_5$–CH_3]$^+$, 237.0533[M+H–$C_6H_{10}O_5$–CH_3OH]$^+$, 213.0902[M+H–$C_6H_{10}O_5$–2CO]$^+$		Ononin

(Continued)

TABLE 1 | Continued

T_R(min)	Formula	[M+H]$^+$ (error, ppm)	[M–H]$^-$ (error, ppm)	Fragment ions in positive (+) ion mode	Fragment ions in negative (–) ion mode	Identification
41.36	$C_{36}H_{30}O_{16}$	719.1602 (–0.7)	717.1488 (3.2)	521.0991[M+H–$C_9H_{10}O_5$]$^+$, 341.0605[M+H–$C_9H_{10}O_5$–$C_9H_8O_4$]$^+$, 323.0536[M+H–2$C_9H_{10}O_5$]$^+$	519.0952[M–H–$C_9H_{10}O_5$]$^-$, 339.0531[M–H–$C_9H_{10}O_5$–$C_9H_8O_4$]$^-$, 321.0413[M–H–2$C_9H_{10}O_5$]$^-$, 295.0630[M–H–$C_9H_{10}O_5$–$C_9H_8O_4$–CO_2]$^-$, 279.0307[M–H–2$C_9H_{10}O_5$–C_2H_2O]$^-$	Salvianolic acid B
45.27	$C_{16}H_{12}O_5$	285.0760 (0.9)	283.0620 (3)	270.0516[M+H–CH_3]$^+$, 253.0470[M+H–CH_3OH]$^+$, 225.0540[M+H–CH_3OH–CO]$^+$, 197.0580[M+H–CH_3OH–2CO]$^+$, 137.0245[M+H–$C_9H_8O_5$]$^+$	268.0385[M–H–CH_3]$^-$, 195.0483[M–H–CH_3OH–2CO]$^-$, 135.0056[M–H–$C_9H_8O_5$]$^-$	Calycosin
46.93	$C_{17}H_{16}O_5$	301.1073 (0.9)	299.0933 (2.7)	167.0714[M+H–$C_8H_6O_2$]$^+$,		(6aR,11aR)-3-Hydroxy-9,10-dimethoxypterocarpan
48.25	$C_{30}H_{32}O_{12}$		583.1829 (1.4)		165.0501[M–H–$C_{24}H_{18}O_7$]$^-$, 121.0278[M–H–$C_{23}H_{26}O_{10}$]$^-$	Benzoylpaeoniflorin
49.21	C_9H_8O	133.0648 (0.4)		115.0581[M+H–H_2O]$^+$, 105.0755[M+H–CO]$^+$, 91.0609[M+H–C_2H_2O]$^+$, 77.0468[M+H–C_3H_4O]$^+$		Cinnamaldehyde
51.46	$C_{43}H_{42}O_{22}$		909.2125 (3.3)		501.1065[M–H–$C_{19}H_{20}O_{10}$]$^-$, 407.0936[M–H–$C_{24}H_{22}O_{12}$]$^-$	Carthamin
53.9	$C_{42}H_{66}O_{14}$		793.4401 (2.7)		631.3946[M–H–$C_6H_{10}O_5$]$^-$	Chikusetsusaponin IVa
54.24	$C_{47}H_{72}O_{20}$		955.4577 (3.4)		835.4515[M–H–$C_4H_8O_4$]$^-$, 793.4461[M–H–$C_6H_{10}O_5$]$^-$	Achyranthoside C
54.26	$C_{47}H_{70}O_{20}$		953.4443 (4.8)		909.4571[M–H–CO_2]$^-$, 851.4411[M–H–$C_4H_8O_4$]$^-$, 793.4462[M–H–$C_5H_4O_6$]$^-$	Achyranthoside A
54.46	$C_{12}H_{14}O_3$		205.0874 (2.1)		161.0962[M–H–CO_2]$^-$	3-Butyl-4-hydroxyphthalide
54.82	$C_{16}H_{12}O_4$	269.0810 (0.8)	267.0666 (1.3)	254.0567[M+H–CH_3]$^+$, 237.0527[M+H–CH_3OH]$^+$, 213.0892[M+H–2CO]$^+$	252.0428[M–H–CH_3]$^+$	Formononetin
60.83	$C_{19}H_{18}O_4$	311.1281 (1)		267.1380[M+H–CO_2]$^+$		Hydroxytanshinone IIA
62.89	$C_{12}H_{16}O_2$	193.1225 (0.9)		147.1187[M+H–H_2O–CO]$^+$, 137.0624[M+H–C_4H_8]$^+$, 105.0745[M+H–H_2O–CO–C_3H_6]$^+$, 91.0606[M+H–H_2O–CO–C_4H_8]$^+$		Senkyunolide A
67.87	$C_{12}H_{18}O_2$	195.1378 (–0.7)		177.1309[M+H–H_2O]$^+$, 149.1345[M+H–H_2O–CO]$^+$		Neocnidilide
68.04	$C_{18}H_{14}O_3$	279.1018 (0.8)		261.0910[M+H–H_2O]$^+$, 233.0959[M+H–H_2O–CO]$^+$, 205.1012[M+H–H_2O–2CO]$^+$, 190.0776[M+H–H_2O–2CO–CH_3]$^+$		Dihydrotanshinone I
68.42	$C_{12}H_{14}O_2$	191.1066 (–0.4)		173.0976[M+H–H_2O]$^+$, 163.1125[M+H–C_2H_4]$^+$, 155.0866[M+H–2H_2O]$^+$, 149.0612[M+H–C_3H_6]$^+$, 145.1029[M+H–H_2O–CO]$^+$, 135.0462[M+H–C_4H_8]$^+$		Ligustilide

(Continued)

TABLE 1 | Continued

T_R(min)	Formula	[M+H]$^+$ (error, ppm)	[M–H]$^-$ (error, ppm)	Fragment ions in positive (+) ion mode	Fragment ions in negative (–) ion mode	Identification
70.72	$C_{20}H_{18}O_5$	339.1230 (1)		279.1003[M+H–$C_2H_4O_2$]$^+$, 261.0908[M+H–$C_2H_4O_2$–H_2O]$^+$, 233.0956[M+H–$C_2H_4O_2$–H_2O–CO]$^+$, 205.0994[M+H–$C_2H_4O_2$–H_2O–2CO]$^+$, 190.0763[M+H–$C_2H_4O_2$–H_2O–2CO–CH_3]$^+$		Methyl tanshinonate
74.36	$C_{19}H_{20}O_3$	297.1492 (2.1)		279.1372[M+H–H_2O]$^+$, 268.1080[M+H–C_2H_4]$^+$, 251.1422[M+H–H_2O–CO]$^+$, 237.0896[M+H–H_2O–C_3H_6]$^+$, 209.0957[M+H–H_2O–C_5H_{10}]$^+$		Cryptotanshinone
74.79	$C_{18}H_{32}O_3$		295.2292 (3.9)		277.2176[M–H–H_2O]$^-$, 195.1400[M–H–$C_6H_{12}O$]$^-$	13-Hydroxy-9,11-hexadecadienoic acid
75.02	$C_{18}H_{12}O_3$	277.0862 (0.8)		249.0908[M+H–CO]$^+$, 231.0756[M+H–CO–H_2O]$^+$, 221.0990[M+H–C_3H_4O]$^+$, 193.1013[M+H–2CO]$^+$		Tanshinone I
83.42	$C_{24}H_{28}O_4$	381.2063 (0.2)		191.1069[M+H–$C_{12}H_{14}O_2$]$^+$, 173.0970[M+H–$C_{12}H_{14}O_2$–H_2O]$^+$, 149.0623[M+H–$C_{12}H_{14}O_2$–C_3H_6]$^+$, 135.0470[M+H–$C_{12}H_{14}O_2$–C_4H_8]$^+$		Levistilide A
84.62	$C_{19}H_{18}O_3$	295.1335 (0.9)		280.1076[M+H–CH_3]$^+$, 277.1222[M+H–H_2O]$^+$, 262.0984[M+H–CH_3–H_2O]$^+$, 249.1267[M+H–H_2O–CO]$^+$		Tanshinone IIA
87.2	$C_{19}H_{22}O_2$	283.1695 (0.9)		265.1598[M+H–H_2O]$^+$, 223.1107[M+H–H_2O–C_3H_6]$^+$, 207.1137[M+H–H_2O–C_3H_6–CH_3]$^+$		Miltirone
97.22	$C_{18}H_{35}NO$	282.2796 (1.5)		265.2540[M+H–NH_3]$^+$, 247.2422[M+H–H_2O–NH_3]$^+$		(Z)-9-Octadecenamide
100.6	$C_{32}H_{48}O_5$	513.3578 (0.7)		407.3295[M+H–CH_2O_2–$C_2H_4O_2$]$^+$, 173.1321[M+H–$C_{25}H_{24}O$]$^+$		Acetyl-11-keto-β-boswellic acid

TABLE 2 | Changes of body weight in different groups.

Time (months)	Normal group	Model group	NXT group
0	13.97 ± 0.80	15.83 ± 1.63	15.73 ± 0.93
1	17.43 ± 1.24	17.20 ± 0.72	15.43 ± 1.97
2	21.40 ± 1.25	25.03 ± 1.52	21.17 ± 2.47
3	26.10 ± 3.86	32.17 ± 1.53	25.73 ± 2.77
4	34.20 ± 1.73	44.87 ± 1.50**	33.73 ± 1.70#
5	40.63 ± 1.38	51.93 ± 1.76**	42.90 ± 2.10##
6	45.43 ± 2.10	57.13 ± 1.75**	51.67 ± 3.23##
7	50.83 ± 1.15	62.90 ± 1.57**	60.00 ± 2.76
8	54.53 ± 0.61	71.23 ± 1.99**	68.57 ± 0.80

*Data represent mean ± SD. **$P < 0.01$ vs. normal group. #$P < 0.05$ vs. model group. ##$P < 0.01$ vs. model group. $n = 3$.*

Effect of NXT on Lipid Metabolism

The parameters of lipid metabolism were determined every month during the study. As shown in **Figure 1**, TC, TG, and LDL-C levels in the model group were increased significantly with time and were also significantly higher compared with normal group ($p < 0.05$ or $p < 0.01$) suggesting that the high-fat diet had induced hyperlipemia in minipigs. After drug administration, NXT significantly decreased the TC, TG, and LDL-C levels from the third month ($p < 0.05$ or $p < 0.01$).

Effect of NXT on Liver and Kidney Function

The liver and kidney function indexes of each group were examined once a month. As shown in **Figure 2**. The levels of ALT, AST, BUN, CRE, and UA in the model group increased significantly with time, and the levels of these indexes were significantly higher than those in the normal group ($P < 0.05$ or $P < 0.01$), indicating that minipigs in the model group exhibited liver and kidney dysfunction. From the fourth month, ALT, AST, BUN, CRE, and UA levels in NXT group were significantly lower than those in the model group ($p < 0.05$ or $p < 0.01$), indicating that NXT could play a role in protecting liver and kidney.

Effect of NXT on Oxidative Stress

SOD and MDA levels of each group were determined once a month. As shown in **Figure 3**, MDA level in the model group increased significantly with time, while the activity of SOD decreased. After 4 months high-fat diet feeding, MDA level in the model group was significantly higher than that in normal group, while SOD activity was significantly lower ($P < 0.05$ or $P < 0.01$), indicating that

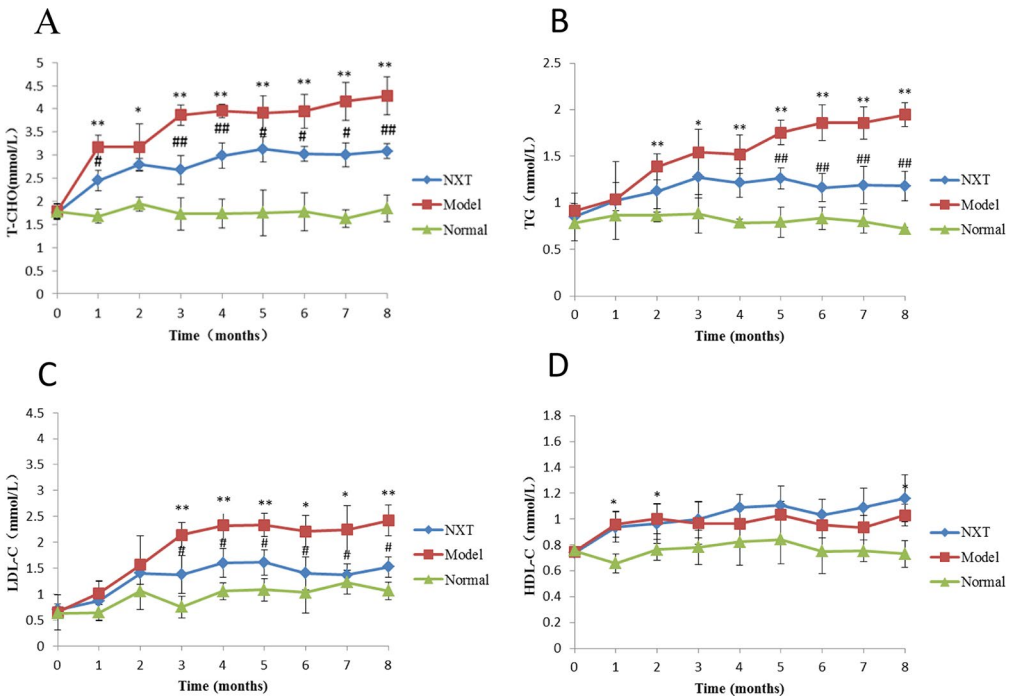

FIGURE 1 | Changes in serum cholesterol (T-CHO) **(A)**, triglyceride (TG) **(B)**, low density lipoprotein (LDL-C), **(C)** and high-density lipoprotein (HDL-C) **(D)**. Data represent mean ± SD. *P < 0.05 vs. normal group. **P < 0.01 vs. normal group. #P < 0.05 vs. model group. ##P < 0.01 vs. model group. n = 3.

high-fat diet could induced oxidative stress disorders in minipigs. From the fifth month, NXT significantly decreased the MDA level and increased SOD activity ($P < 0.05$ or $P < 0.01$).

Effect of NXT on Inflammatory Responses

Serum inflammatory cytokines were determined every month. As shown in **Figure 4**, IL-6, IL-1β, TNF-α, and IL-8 levels in model group were increased with time, and the levels of these inflammatory cytokines were significantly higher than those in the normal group ($P < 0.05$ or $P < 0.01$), suggesting that high-fat diet caused obvious inflammation reaction in minipigs. From the fourth month, NXT significantly decreased the IL-6, IL-1β, TNF-α, and IL-8 levels ($P < 0.05$ or $P < 0.01$), indicating that NXT had the remarkable anti-inflammatory effect.

Effect of NXT on Myocardial Enzymes

CK-MB and LDH levels of each group were determined once a month. As shown in **Figure 5**, the CK-MB and LDH levels in model group significantly increased over time, and were significantly higher than those in normal group ($P < 0.05$ or $P < 0.01$), suggesting the minipigs in model group exhibited myocardial injury. From the third month, CK-MB and LDH levels in NXT group were significantly lower than those in the model group ($P < 0.05$ or $P < 0.01$), indicating that the long-term administration of NXT could improve the myocardial injury.

Pathological Observations of Tissues

HE staining results of cardiac tissue sections showed that the myocardial fibers of model group were loose. And fibrous tissue hyperplasia in the interstitium, a small amount of local myocardial fiber necrosis and inflammatory cell infiltration appeared in cardiac tissue in the model group (**Figure 6B**).The results of HE staining of arteries showed that subintimal lipid necrotic material deposition and a small amount of macrophage infiltration appeared in the carotid artery (**Figure 6E**), abdominal aorta (**Figure 6H**), and coronary artery (**Figure 6K**) in the model group. No abnormalities were observed in the normal group (**Figure 6A**, **D**, **G**, **J**) and NXT group (**Figure 6C**, **F**, **I**, **L**). Such pathological observation results indicated that NXT could inhibit the above vascular lesions caused by the long-term high-fat feeding.

Effects of NXT on Intestinal Microecology

Diversity of Intestinal Microflora in the Minipigs After NXT Treatment

To investigate how NXT influenced the diversity of gut microbiota, the observed species index, Chao index, Ace index, Shannon index, and Simpson index were calculated to estimate the alpha diversity. The observed species index, Chao index, and Ace index are used to estimate the OUT number in microflora representing species richness. Shannon and Simpson indices are quantitative measures of bacterial diversity reflecting both species richness and evenness. The bigger the first four indexes are, as well as the smaller the Simpson index is, indicating that species in the sample is more abundant. As shown in **Figure 7**, the above indexes of each group suggested that the diversity of intestinal microbial of minipigs in the model group was significantly decreased. And the long-term

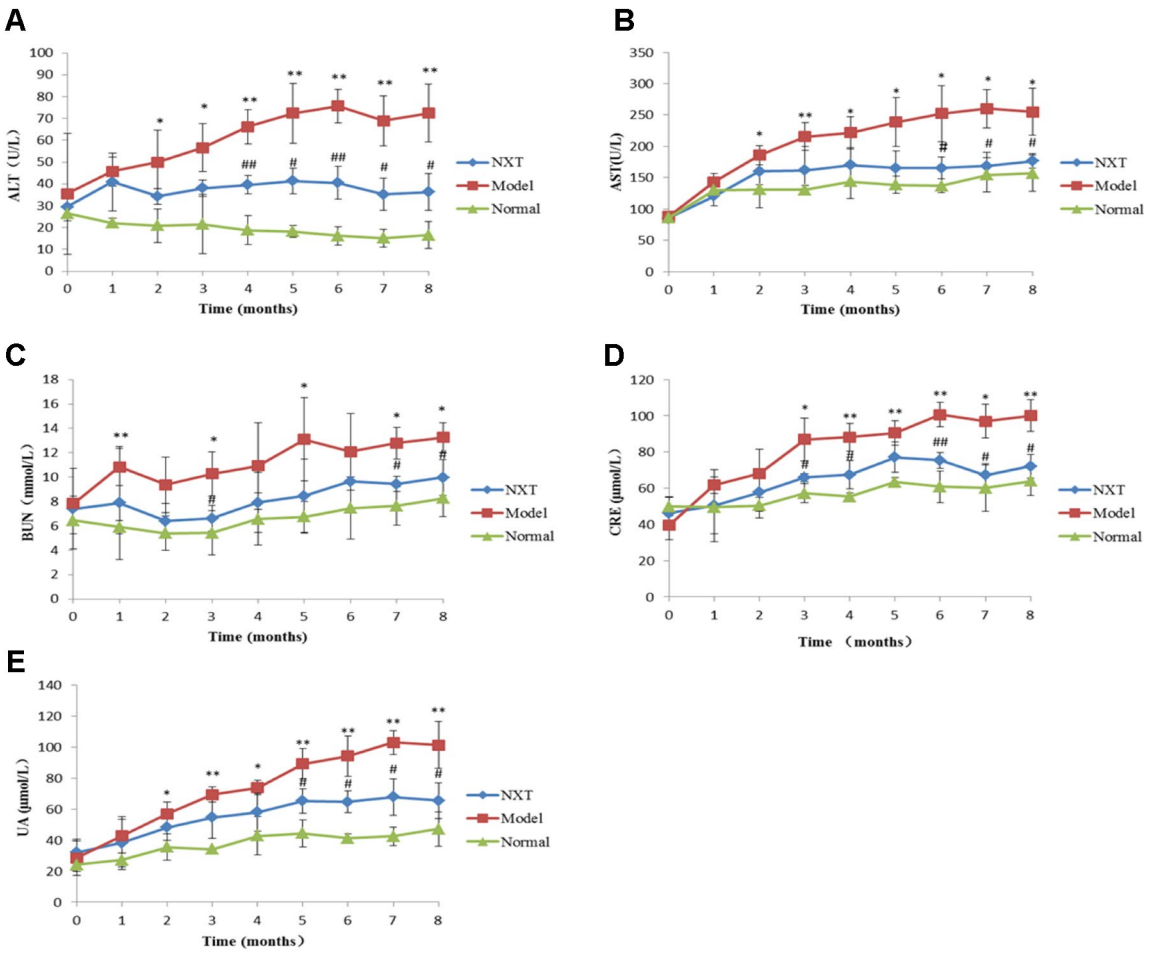

FIGURE 2 | Changes in glutamic–oxalacetic transaminase (AST) **(A)**, glutamic–pyruvic transaminase (ALT) **(B)**, creatinine (Cr) **(C)**, urea nitrogen (BUN) **(D)**, uric acid (UA) **(E)**. Data represent mean ± SD. *P < 0.05 vs. normal group. **P < 0.01 vs. normal group. #P < 0.05 vs. model group. ##P < 0.01 vs. model group. n = 3.

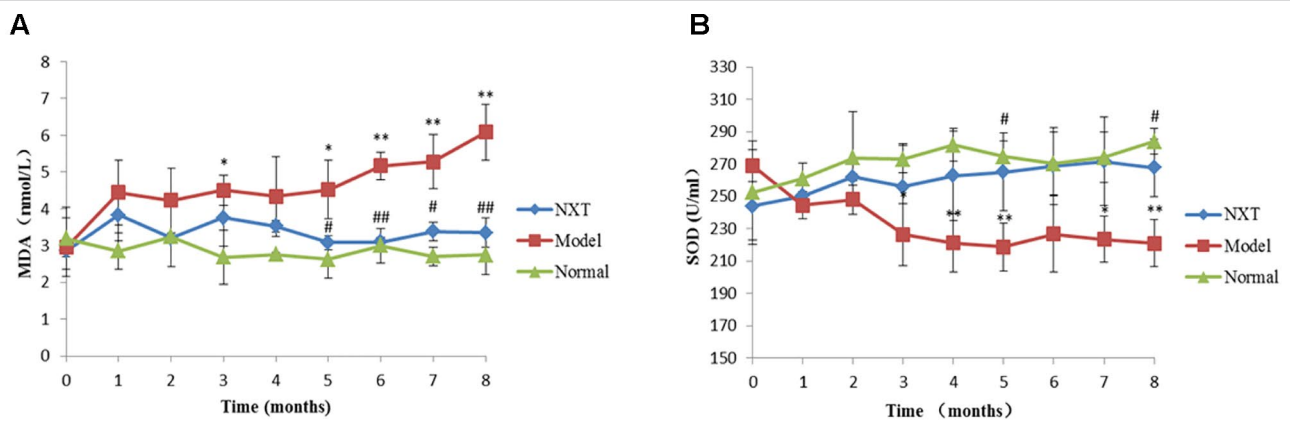

FIGURE 3 | Changes in methane dicarboxylic aldehyde (MDA) **(A)**, superoxide dismutase (SOD) **(B)**. Data represent mean ± SD. *P < 0.05 *vs*. normal group. **P < 0.01 *vs*. normal group. #P < 0.05 *vs*. model group. ##P < 0.01 *vs*. model group. n = 3.

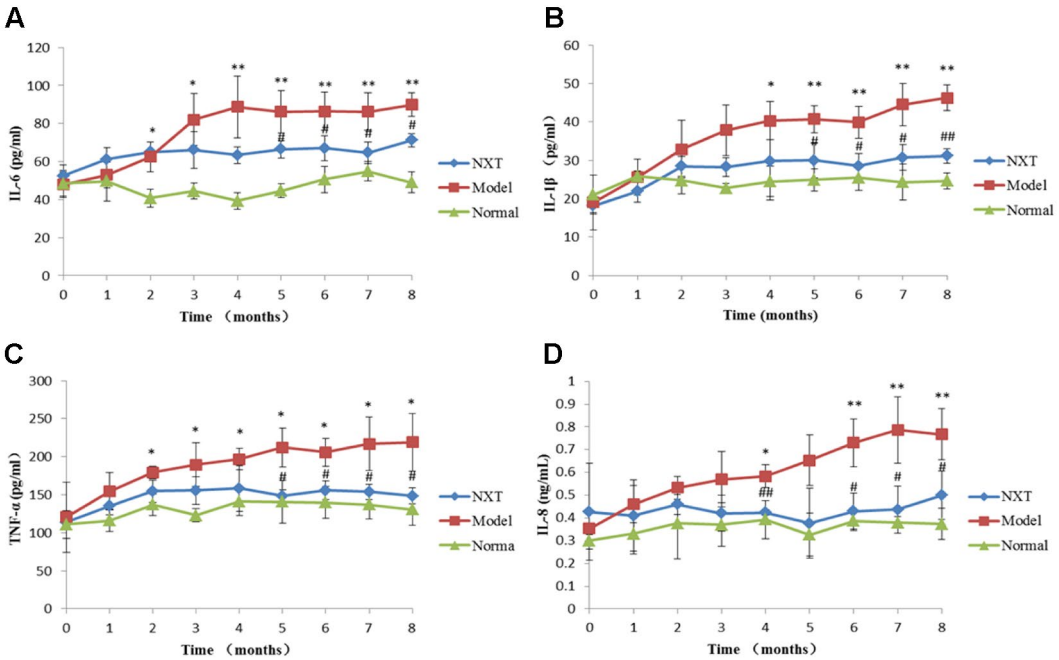

FIGURE 4 | Changes in interleukin-6 (IL-6) **(A)**, interleukin-1β (IL-1β) **(B)**, tumor necrosis factor-α (TNF-α) **(C)**, and interleukin-8 (IL-8) **(D)**. Data represent mean ± SD. *P < 0.05 vs. normal group. **P < 0.01 vs. normal group. #P < 0.05 vs. model group. ##P < 0.01 vs. model group. n = 3.

administration of NXT could play a role in restoring the gut microbiota species diversity.

Beta Diversity Changes Due to the NXT Treatment

The three groups were clearly distinguished in NMDS (**Figure 8**), indicating that the composition of the gut microbiota differed between them. More importantly, the result showed that the distance differences among minipigs in the NXT group were very small, indicating the composition of gut microbiota in each minipig in NXT group was very similar. This finding suggested that the long-term administration of NXT had significant effect on regulating the microflora structure and the microflora structure in NXT group tend to be stable in our study.

Relative Abundances of Different Bacteria After NXT Treatment

At the phylum level, the decreased abundance of *Bacteroidetes* and the increased abundance of *Firmicutes* were observed in the model group (**Figure 9A**), suggesting that the long-term high-fat diet feeding could cause the increase of the ratio of the *Firmicutes* to *Bacteroidetes* (F/B ratio) in relative abundance. The long-term administration of NXT increased the abundance of *Bacteroidetes* and decreased the abundance of *Firmicutes* in minipigs with high-fat diet feeding (**Figure 9A**). Our results showed that NXT treatment could revered the increase of the ratio of the *Firmicutes* to *Bacteroidetes*. Moreover, NXT treatment could reduce the relative abundance of *Proteobacteria* (**Figure 9A**). The result of relative abundances

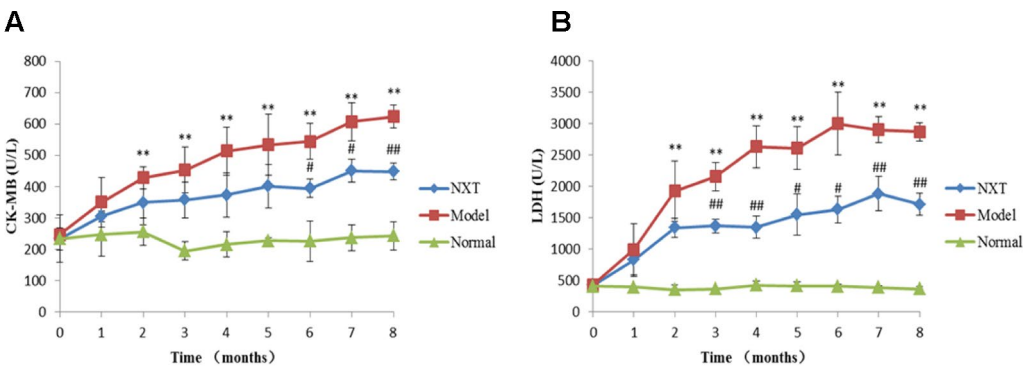

FIGURE 5 | Changes in creatine kinase-MB **(A)** and lactic dehydrogenase **(B)**. Data represent mean ± SD. *P < 0.05 vs. normal group. **P < 0.01 vs. normal group. #P < 0.05 vs. model group. ##P < 0.01 vs. model group. n = 3.

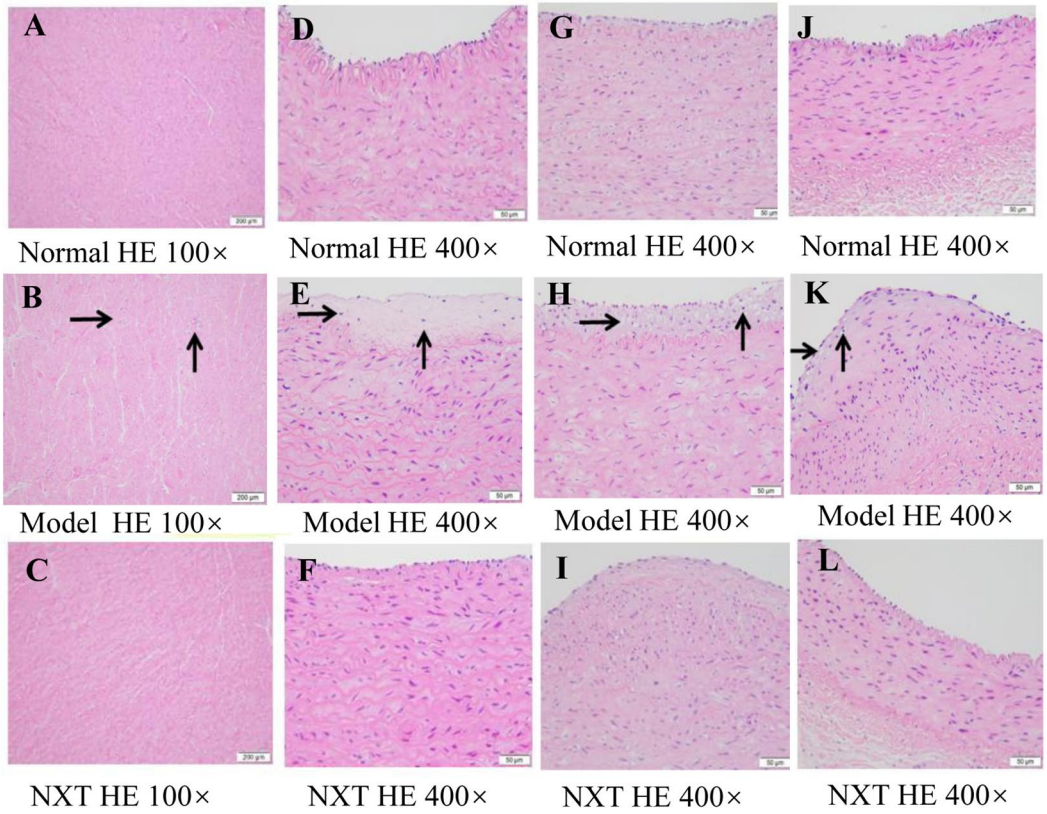

FIGURE 6 | Pathological observations with hematoxylin-eosin (HE) staining on heart **(A-C)**, carotid artery **(D-F)**, abdominal aorta **(G-I)**, and coronary artery **(J-L)** of minipigs in each group.

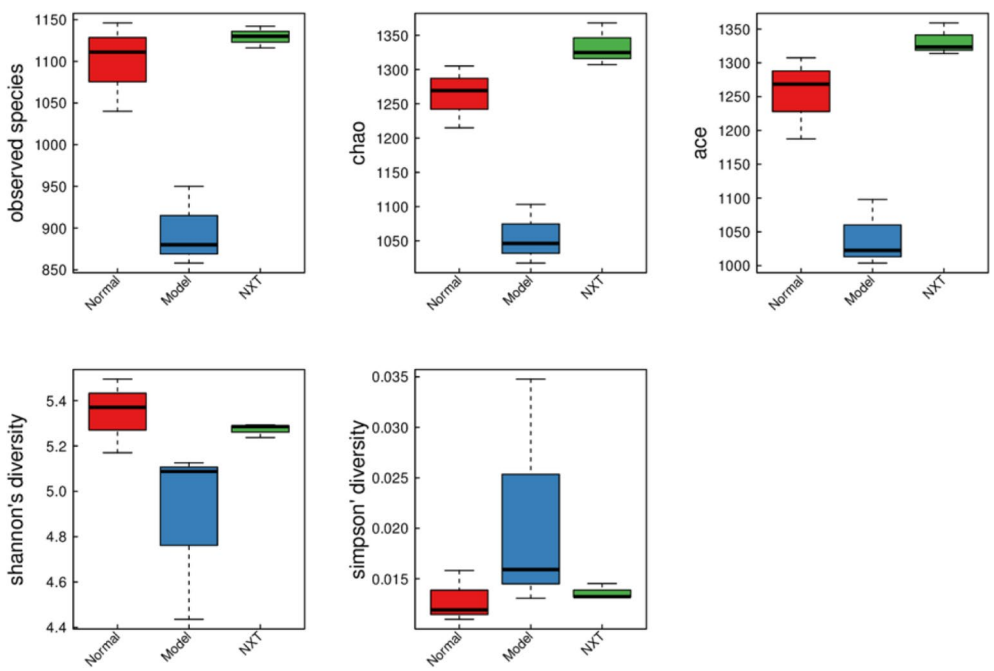

FIGURE 7 | Box chart of alpha diversity between groups.

of different bacteria in each minipig (**Figure 9B**) showed that the microflora structure tended to be stable in NXT group, indicating that the long-term administration of NXT could steadily regulates the gut microbiota.

Gut microbes species abundance distribution at the genus level were shown in **Figure 10A**. *Caproiciproducens*, *Sutterella*, and *erysipelotrichaceae_ucg-004* abundances were significantly reduced in model group compared to the normal group ($P < 0.05$, $P < 0.01$, $P < 0.05$), whereas the *Romboutsia* abundance was significantly elevated in the model group ($P < 0.05$). *Caproiciproducens*, *Sutterella,* and *erysipelotrichaceae_ucg-004* abundances were all significantly elevated by NXT treatment ($P < 0.05$, $P < 0.01$, $P < 0.01$), and *Romboutsia* abundance was significantly reduced by NXT treatment ($P < 0.01$, $P < 0.05$) (**Figure 10B**).

Correlation Between Bacterial Taxa and Pathological Measurements

As shown in **Figure 11**, the covariation between pathological indexes and 16SrDNA data are presented in the form of a heatmap diagram. Most of the gut microbiota had the correlation with multiple pathological indexes. For the gut microbiota, NXT significantly affect; *Sutterella* had a negative correlation with TG, LDL-C, ALT, AST, MDA, IL-6, IL-1β, TNF-α, CK-MB, and LDH. *Erysipelotrichaceae_UCG-004* had a negative correlation with LDL-C, ALT, UA, IL-1β, IL-8, CK-MB, and LDH. *Caproiciproducens* had a negative correlation with IL-6, IL-1β, TNF-α, and IL-8. While *Romboutsia* had a positive correlation with TC, TG, LDL-C, ALT, AST, BUN, CRE, MDA, IL-6, IL-1β, TNF-α, IL-8, CK-MB, and LDH (**Figure 12**).

DISCUSSION

In the present study, UFLC-Q-TOF-MS/MS was used to identify constituents in NXT. A total of 59 compounds were identified, and most of these active components were reported to have potential anti-CVD effects. In addition, we observed and evaluated the effect of long-term administration of NXT on minipigs with high-fat diet feeding. And we found that, in the course of time, NXT treatment effectively improved the blood lipid metabolism, inhibited vascular inflammation, enhanced antioxidant capacity, and alleviated myocardial injury. Moreover, NXT treatment could restore the imbalance of gut microbiota caused by the high-fat diet. And, we found some key bacterium of *Caproiciproducens* (enhanced), Sutterella (enhanced), *Erysipelotrichaceae* (enhanced), and *Romboutsia* (decreased) were closely involved in NXT's effects in our study.

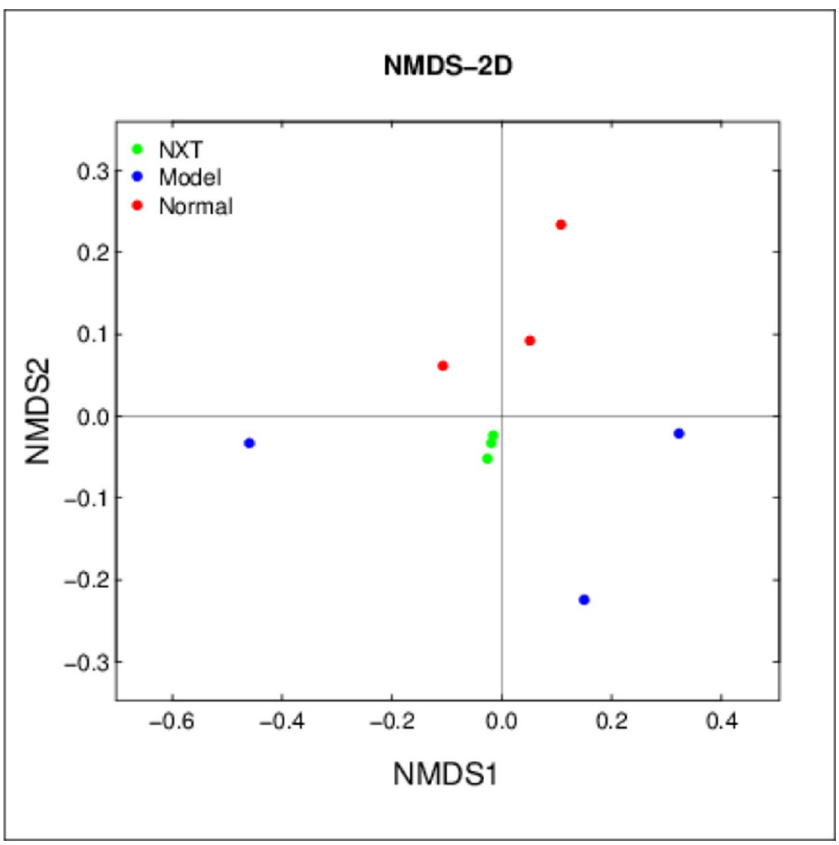

FIGURE 8 | Beta diversity changes due to the NXT treatment. Samples of the same color belong to the same group (green, NXT group; blue, model group; red, normal group). The closer the samples are, indicating that the more similar the composition of the samples.

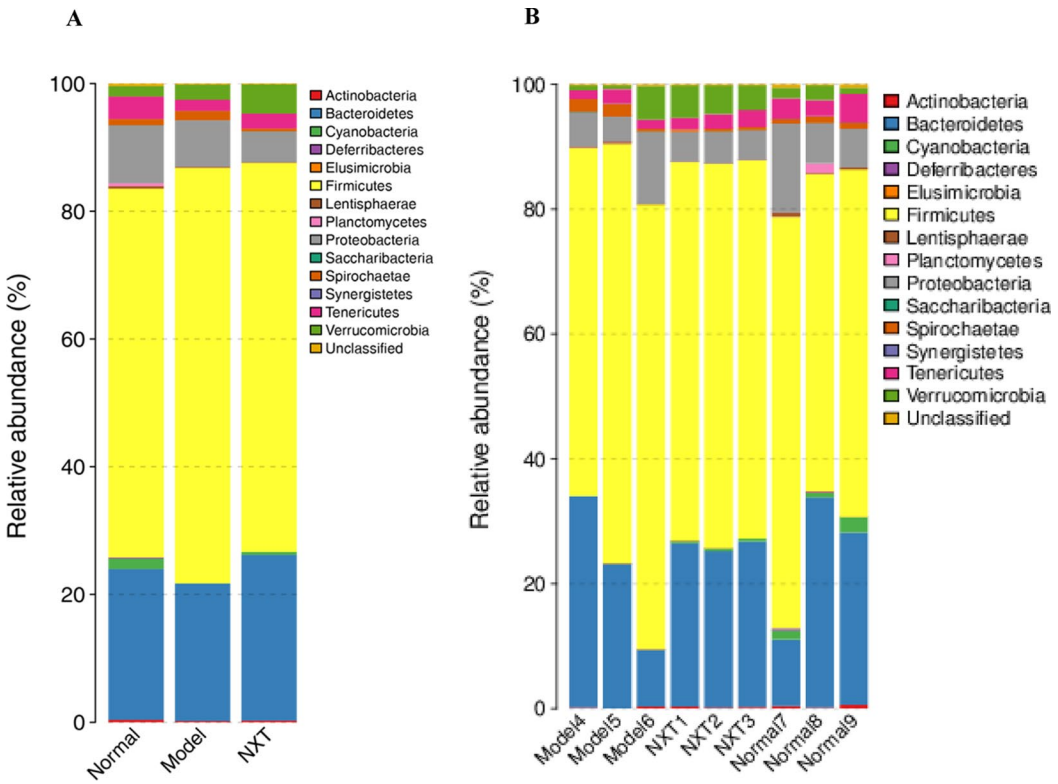

FIGURE 9 | Relative abundances of different bacteria at phylum level of each group **(A)** and each animal **(B)**.

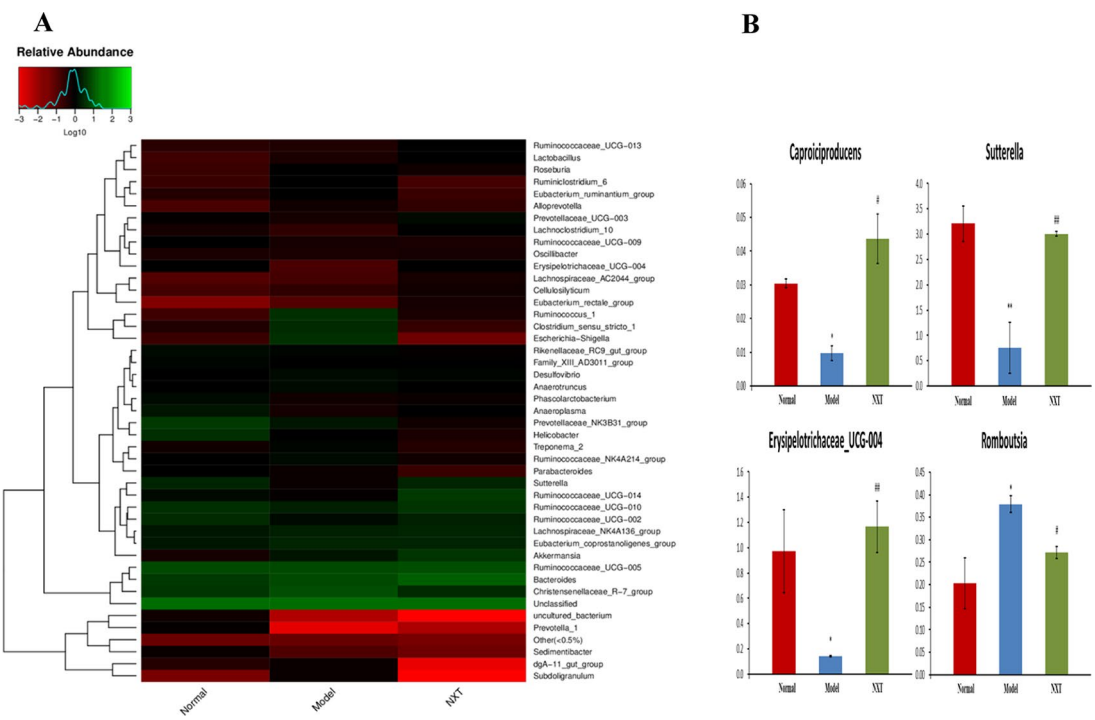

FIGURE 10 | Effect of NXT on the recovery of dysbiosis of gut microbiota **(A)** and key bacteria **(B)** at genus level. For **(A)**, the higher red degree means the less the relative abundance, while the higher green degree means the more the relative abundance. For **(B)**, data represent mean ± SD. *P < 0.05 vs. normal group. #P < 0.05 vs. model group.

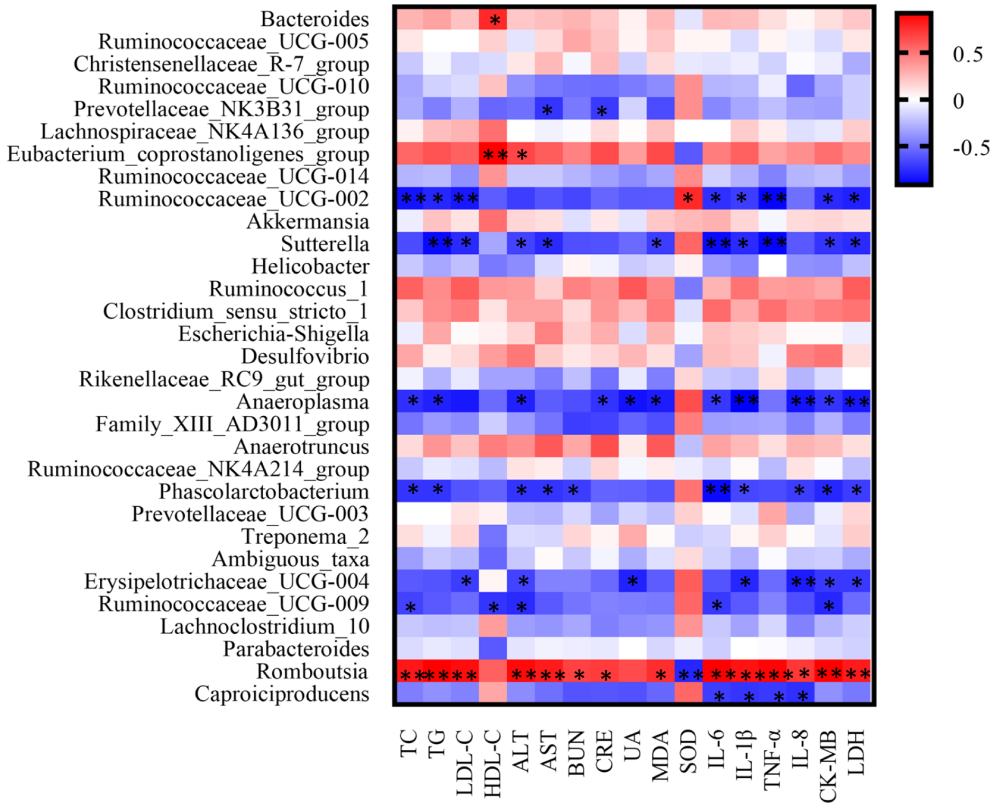

FIGURE 11 | The correlation heatmap of identifying associations between the gut microbiota structure (genus level) and the pathological indexes. The red color means positive correlation while the blue color shows a negative correlation. The deeper color means the greater correlation ($p < 0.05$*, $p < 0.01$**).

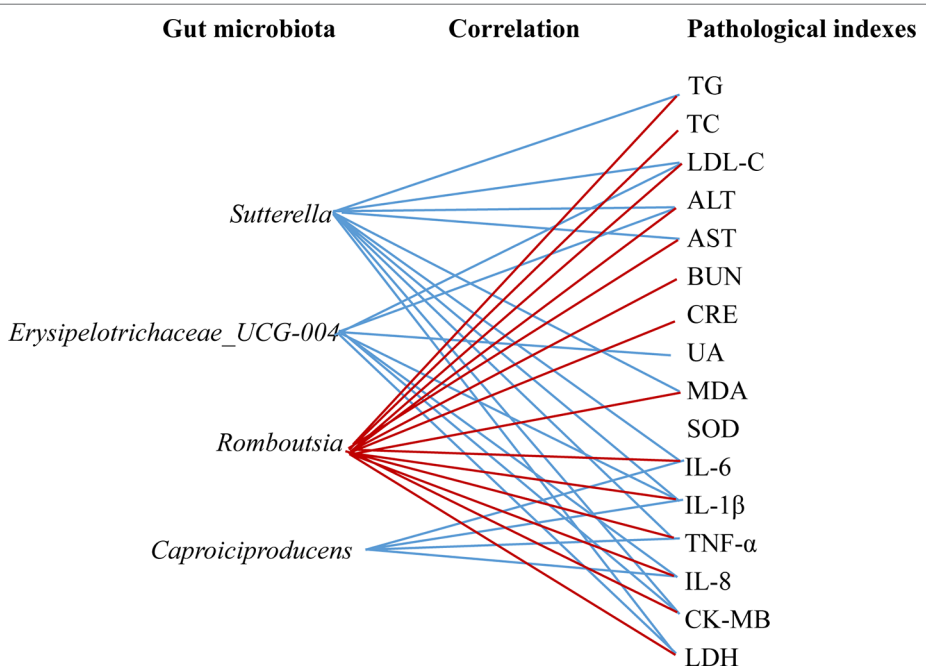

FIGURE 12 | Associations between the gut microbiota (NXT significantly affect) and the pathological indexes. Associations with the pathological indexes are shown for each genus microbiota with the direction of correlation indicated by red (positive) or blue (negative) lines.

Serum TC refers to the sum of all lipoprotein cholesterol in the blood; the increased content of TC has become the independent risk factor for coronary heart disease (Cui et al., 2007). Higher TG level is closely associated with the risk of atherosclerotic cardiovascular disease (Bittner, 2001). LDL contributes to the deposition of cholesterol in blood vessel wall, and the increased content of LDL could lead to cardiovascular disease (Jeppesen et al., 2006). In the present study, in model animals with high-fat diet feeding, the TC, TG, and LDL-C levels increased significantly with breeding time, and from 4th month, the contents were significantly higher than those of normal group. Our results showed that high-fat feeding for 4 months could cause the lipid metabolic abnormalities in minipigs. And, long-term administration of NXT significantly inhibited the increase of TC, TG, and LDL-C thus improved hyperlipemia effectively.

IL-1β is an important mediator in the inflammatory response, which can be secreted and synthesized by a variety of cells (Prantner et al., 2009). It can aggravate the tissue damage mediated by cellular immunity and humoral immunity, promote the expression of endothelial leukocyte adhesion molecule, and stimulate the migration of inflammatory cells into the lesion site. IL-6 is an inflammatory factor that plays an important role in vascular injury and acute myocardial ischemia (Ridker et al., 2000). The increase of IL-6 caused by the injury of vascular endothelium could induce a large number of corresponding antibodies to form immune complexes and result in thrombosis. IL-8 is a cytokine involved in immune regulation and inflammatory response, which plays an important role in the aggregation and activation of neutrophils in various inflammatory processes, and its level is associated with the stability of atherosclerotic plaques (Frostegård et al., 1999). TNF-α is a polypeptide produced by the activated monocytes and lymphocytes, which can promote blood coagulation and inhibit fibrinolysis, and it is closely related to the occurrence and development of atherosclerosis (Leboeuf and Schreyer, 1998). In our study, the serum IL-6, IL-8, IL-1, and TNF-α levels of minipigs in model group increased continuously with the passage of high-fat feeding time, suggesting that vascular endothelium of minipigs suffered from damage during high-fat diet feeding, thus leading to the up-regulation of inflammatory factors. Long-term administration of NXT inhibited the gradual increase of the above inflammatory factors, indicating that NXT could protect the vascular endothelium and had remarkable anti-inflammatory effect.

The activity of ALT and AST would sensitively increase when the liver cells are injured or necrotic. Serum ALT and AST levels were significantly increased in the model group, indicating that prolonged high-fat diet feeding caused the liver dysfunction in minipigs. The long-term administration of NXT could reduce the levels of ALT and AST in serum, indicating that NXT had a certain protective effect on liver. In addition, the significant increased levels of Cr, BUN, and UA in minipigs in the model group suggested the dysfunction of glomerular filtration and renal tubular secretion. NXT treatment inhibited the abnormal elevated levels of Cr, BUN, and UA, which indicated that NXT had the protective effect on the kidney. The increase of reactive oxygen species (ROS) and the damage of endogenous antioxidants would cause the imbalance of redox state and inflammation, which further aggravate the damage to tissues and organs. A significant reduction in the antioxidant capacity of the minipigs with long-term high-fat diet was determined as the increase of MDA content and the decrease of SOD activity. NXT inhibited both the rise of MDA content and the decrease of SOD activity, suggesting that NXT could inhibit the aggravation of oxidative stress disorder. CK-MB is released into the bloodstream when myocardial cells are injured, so its level can reflect the degree of injury to myocardial cells (Adams et al., 1994). LDH is commonly used to diagnose the occurrence of myocarditis in clinic (Snodgrass et al., 1959). In the model animals, the levels of CK-MB and LDH were significantly increased, and hyperplasia of cardiac fibrosis, myocardial fibrosis necrosis, and inflammatory cell infiltration were observed in the heart issue (**Figure 6B**). The NXT treatment could effectively decrease the level of CK-MB and LDH and thus prevent the relevant lesion in the myocardial issue (**Figure 6C**).

In recent years, the increasing number of studies have revealed a close relationship between gut microbiota and blood lipid metabolism (Fava et al., 2006; Velagapudi et al., 2010). Some studies found that *Bifidobacterium*, *Lactobacillus*, *Enterococcus*, and etc. could produce conjugated bile acid hydrolytic enzyme. Such enzyme can transform conjugated bile acid into free bile acid; thereby, the enterohepatic circulation of bile acid will be affected, and the synthesis of bile acid in the liver will be promoted, which makes the cholesterol level in the blood reduce (Hlivak et al., 2005; Mishra and Prasad, 2005; Wang et al., 2009). On the other hand, the intestinal microecology will be changed when hyperlipidemia developed. The changes in intestinal microecology will affect the metabolism and reproduction of some normal gut microbiota and thus make their quantity decreased significantly, such as *Bifidobacteria*, *Lactobacillus*, *Enterococcus*, and etc., whereas, the relative abundance of *Enterobacteriaceae* increases, thereby the dysbacteriosis developed. The long-term high-fat diet feeding can cause the prolong and continuous changes in intestinal microecology (Ley et al., 2006). In the present study, minipigs were fed with high-fat diet up to 8 months, and blood lipid metabolism disorder developed. Alpha diversity results showed that the diversity of gut microbiota of minipigs in the model group was significantly decreased (**Figure 7**). Our result was consistent with the finding of De WIT N et al., which demonstrated that high-fat diet could reduce the diversity of gut microbiota (De et al., 2012). And, the long-term administration of NXT could restore the diversity of gut microbiota in our study, suggesting that NXT might improve the blood lipid metabolism disorder by ameliorating the dysbacteriosis.

Various kinds of diseases have been shown to be associated with the gut microbiota recently. It has been reported that an elevated ratio of *Firmicutes* to *Bacteroidetes* was significantly associated with cardiovascular disease, obesity, and diabetes (Mariat et al., 2009; Everard and Cani, 2013; Chang et al., 2017). In this study, the high-fat diet for up to 8 months could decrease the abundance of *Bacteroidetes*, increase the abundance of *Firmicutes*, and elevate ratio of *Firmicutes* to *Bacteroidetes* in minipigs in

the model group (**Figure 10A**). Our results were in accordance with the previous studies. Ley R E *et al*. found that, compared with lean people, the abundance of *Bacteroidetes* in the obese people was lower, and the abundance of *Firmicutes* was higher, and the proportion of *Firmicutes*/*Bacteroidetes* was significantly increased (Ley et al., 2006). Guo et al. compared the abundance of *Bacteroidetes* and *Firmicutes* in obese and thin minipigs and found that the abundance of *Bacteroidetes* was significantly reduced in obese minipigs (Guo et al., 2010). And, in the present study, our results showed that the long-term administration of NXT could increase the abundance of *Bacteroidetes* and reduce the abundance of *Firmicutes* thus revered the increase of the ratio of the *Firmicutes* to *Bacteroidetes* in relative abundance caused by the high-fat diet.

More importantly, at the phylum level, the result of relative abundances of different bacteria in each minipig in NXT group (**Figure 10B**) showed that the microflora structure tended to be stable after 8 months of treatment. And the result of Beta diversity also showed that the composition of gut microbiota in each minipig in NXT group was very similar (**Figure 8**). In other words, the long-term NXT treatment could improve the composition of gut microbiota stably. This exciting finding suggested that the long-term administration of NXT was capable of reversing varied compositional abnormalities (dysbiosis) of gut microbiota associated with blood lipid metabolism disorders by steadily modulating the composition of gut microbiota instead of altering the composition of intestinal microbial community simply.

At the genus level, we found that NXT treatment significantly increased *Caproiciproducens*, *Sutterella*, and *Erysipelotrichaceae_UCG-004* abundance while reduced *Romboutsia* abundance (**Figure 10B**). *Caproiciproducens* is an acid-producing bacterium that can use galactose as the carbon source. The end products of its anaerobic fermentation are hydrogen, carbon dioxide, ethanol, acetic acid, butyric acid, and caproic acid (Liu et al., 2017). Caproic acid has many effects, such as inhibiting pathogenic bacteria, improving gut microbiota, promoting animal growth, and enhancing animal immunity (Van et al., 2004). This result indicated that NXT might improve the body's immune by increasing *Caproiciproducens* abundance to produce more caproic acid. And, by this way, NXT could inhibit pathogenic bacteria and improve the gut microbiota. Moreover, the long-term high-fat diet feeding could result in a significant higher abundance of *Romboutsia* in minipigs (**Figure 10B**). This result was consistent with the experimental results of Liu Han *et al*., which demonstrated that a high-sugar and high-fat diet could increase the relative abundance of *Romboutsia* (Han et al., 2018). And NXT treatment could reduce the relative abundance of *Romboutsia* in our study. The result of correlation analysis between gut microbiota and pathological indexes showed that *Romboutsia* had a positive correlation with blood lipid profiles, hepatic and renal functions, inflammation cytokine, and myocardial enzyme. While *Caproiciproducens*, *Sutterella*, and *Erysipelotrichaceae_UCG-004* had a negative correlation with blood lipid profiles, inflammation cytokine, and myocardial enzyme (**Figures 11**, **12**). These results suggested that the modulation of gut microbiota might be one mechanism by which NXT prevent and treat cardiovascular diseases, which warrants a further investigation on the specific involvement of gut microbiota in NXT's cardioprotective effects.

CONCLUSIONS

The present study demonstrated that NXT was effective in reducing blood lipids, inhibiting vascular inflammation, enhancing antioxidant capacity, and alleviating myocardial injury, without damages on liver and kidney particularly. On the other hand, NXT played an important role in recovering the imbalance of intestinal microecology. These results indicated that NXT had integrated regulating effect on the prevention and treatment in cardiovascular diseases partly through ameliorating high-fat diet–induced metabolic disorders and partly through stably improving gut microbiota. The findings of this study would provide a further reference for the clinical application of NXT.

DATA AVAILABILITY STATEMENT

The datasets generated for this study can be found in Genebank using the accession number KDAE00000000.

ETHICS STATEMENT

The animal study was reviewed and approved by Animal Ethics Committee of the School of Life Sciences in Sun Yat-sen University.

AUTHOR CONTRIBUTIONS

W-JZ, HL, H-LY and W-WS conceived and designed the experiments; Q-WL, H-YR, Z-HY and XZ conducted experiments; W-JZ, T-BC and HL analyzed the data; W-JZ, HL and P-BL wrote the manuscript.

FUNDING

This work was supported by the grants of Secondary Development Projects of Traditional Chinese Medicine (2017-No.19), Project funded by China Postdoctoral Science Foundation under grant number (2018T110857, 2018M643036) and Guangzhou Major Special Projects of People's Livelihood (201704020119, 201803010082). The funders had no role in the study design, data collection and analysis, decision to publish, or preparation of the manuscript.

SUPPLEMENTARY MATERIAL

The Supplementary Material for this article can be found online at: https://www.frontiersin.org/articles/10.3389/fphar.2019.01128/full#supplementary-material

FIGURE S1 | The identity of chemical constituents of NXT in different batches (A: positive ionization mode, B: negative ionization mode)

REFERENCES

Adams, J. E., Schechtman, K. B., Landt, Y., Ladenson, J. H., and Jaffe, A. S. (1994). Comparable detection of acute myocardial infarction by creatine kinase MB isoenzyme and cardiac troponin I. *Clin. Chem.* 40 (1), 1291–1295.

Bergen, W. G., and Mersmann, H. J. (2005). Comparative aspects of lipid metabolism: impact on contemporary research and use of animal models. *J. Nutr.* 135 (11), 2499–2502. doi: 10.1093/jn/135.11.2499

Besli, F., Ilter, A., and Gungoren, F. (2017). The link between mean platelet volume to lymphocyte ratio and complexity of coronary artery disease. *Angiology* 69 (4), 3319717743315. doi: 10.1177/0003319717743315

Bittner, V. (2001). Treatment of dyslipidemia in pre- and postmenopausal women with and without known atherosclerotic cardiovascular disease. *Curr. Cardiol. Rep.* 3 (5), 401–407. doi: 10.1007/s11886-001-0057-2

Caporaso, J., Kuczynski, J., Stombaugh, J., Bittinger, K., Bushman, F., Costello, E. et al. (2010). QIIME allows analysis of high-throughput community sequencing data. *Nat Methods.* 7 (5), 335–336. (1548-7105 (Electronic)). doi: 10.1038/nmeth.f.303

Casellas, J., Vidal, O., Pena, R. N., Gallardo, D., Manunza, A., Quintanilla, R., et al. (2013). Genetics of serum and muscle lipids in pigs. *Anim. Genet.* 44 (6), 609–619. doi: 10.1111/age.12049

Chang, C. J., Lin, C. S., Lu, C. C., Martel, J., Ko, Y. F., Ojcius, D. M., et al. (2017). Corrigendum: Ganoderma lucidum reduces obesity in mice by modulating the composition of the gut microbiota. *Nat. Commun.* 6, 7489. doi: 10.1038/ncomms8489

Chinese Pharmacopoeia Commission (2015). *Pharmacopoeia of the people's republic of China* Vol. I. China: China Medical Science Press.

Cui, R., Iso, H., Toyoshima, H., Date, C., Yamamoto, A., Kikuchi, S., et al. (2007). Serum total cholesterol levels and risk of mortality from stroke and coronary heart disease in Japanese: the JACC study. *Atherosclerosis* 194 (2), 415. doi: 10.1016/j.atherosclerosis.2006.08.022

De, W. N., Derrien, M., Bosch-Vermeulen, H., Oosterink, E., Keshtkar, S., Duval, C., et al. (2012). Saturated fat stimulates obesity and hepatic steatosis and affects gut microbiota composition by an enhanced overflow of dietary fat to the distal intestine. *AJP Gastrointest. Liver Physiol.* 303 (5), G589. doi: 10.1152/ajpgi.00488.2011

Edgar, R. C. (2013). UPARSE: highly accurate OTU sequences from microbial amplicon reads. *Nat. Methods* 10 (10), 996. doi: 10.1038/nmeth.2604

Edgar, R. C., Haas, B. J., Clemente, J. C., Christopher, Q., and Rob, K. (2011). UCHIME improves sensitivity and speed of chimera detection. *Bioinformatics* 27 (16), 2194. doi: 10.1093/bioinformatics/btr381

Everard, A., and Cani, P. D. (2013). Diabetes, obesity and gut microbiota. *Best Pract. Res. Clin. Gastroenterol.* 27 (1), 73–83. doi: 10.1016/j.bpg.2013.03.007

Fava, F., Lovegrove, J. R., Jackson, K. G., and Tuohy, K. M. (2006). The gut microbiota and lipid metabolism: implications for human health and coronary heart disease. *Curr. Med. Chem.* 13 (25), 3005–3021. doi: 10.2174/092986706778521814

Frostegård, J., Ulfgren, A. K., Nyberg, P., Hedin, U., Swedenborg, J., Andersson, U., et al. (1999). Cytokine expression in advanced human atherosclerotic plaques: dominance of pro-inflammatory (Th1) and macrophage-stimulating cytokines. *Atherosclerosis* 145 (1), 33–43. doi: 10.1016/S0021-9150(99)00011-8

Jakobsdottir, G., Xu, J., Molin, G., Ahrné, S., and Nyman, M. (2013). High-fat diet reduces the formation of butyrate, but increases succinate, inflammation, liver fat and cholesterol in rats, while dietary fibre counteracts these effects. *Plos One* 8 (11), e80476. doi: 10.1371/journal.pone.0080476

Guo, X., Xia, X., Tang, R., Zhou, J., Zhao, H., and Wang, K. (2010). Development of a real-time PCR method for Firmicutes and Bacteroidetes in faeces and its application to quantify intestinal population of obese and lean pigs. *Lett. Appl. Microbiol.* 47 (5), 367–373. doi: 10.1111/j.1472-765X.2008.02408.x

Han, J., Tan, H., Duan, Y., Chen, Y., Zhu, Y., Zhao, B., et al. (2019). The cardioprotective properties and the involved mechanisms of NaoXinTong capsule. *Pharmacol. Res.* 141, 409–417. doi: 10.1016/j.phrs.2019.01.024

Han, L., Yunqian, W. U., Huifeng, L. I., and Weimin, W. (2018). Effects of high-fat-high-carbohydrate diet on liver and composition of gut microbiota in blunt snout bream. *J. Huazhong Agric.Univ.* 37 (4), 85–92. doi: 10.13300/j.cnki.hnlkxb.2018.04.012

Hlivak, P., Odraska, J., Ferencik, M., Ebringer, L., Jahnova, E., and Mikes, Z. (2005). One-year application of probiotic strain Enterococcus faecium M-74 decreases serum cholesterol levels. *Bratisl. Lek. Listy* 106 (2), 67–72.

Jeppesen, J., Hansen, T. W., Rasmussen, S., Ibsen, H., and Torp-Pedersen, C. (2006). Metabolic syndrome, low-density lipoprotein cholesterol, and risk of cardiovascular disease: a population-based study. *Atherosclerosis* 189 (2), 369–374. doi: 10.1016/j.atherosclerosis.2005.12.010

Knight, S., Quigley, J., Roy, S., Elmarakby, A., and Imig, J. (2008). Endothelial dysfunction and the development of renal injury in spontaneously hypertensive rats fed a high-fat diet. *Hypertension* 51 (2), 352. doi: 10.1161/HYPERTENSIONAHA.107.099499

Leboeuf, R. C., and Schreyer, S. A. (1998). The role of tumor necrosis factor-α receptors in Atherosclerosis. *Trends Cardiovasc. Med.* 8 (3), 131–138. doi: 10.1016/S1050-1738(97)00142-4

Ley, R. E., Turnbaugh, P. J., Samuel, K., and Gordon, J. I. (2006). Microbial ecology: human gut microbes associated with obesity. *Nature* 444 (7122), 1022–1023. doi: 10.1038/4441022a

Liu, M. K., Tang, Y. M., Guo, X. J., Zhao, K., Tian, X. H., Liu, Y., et al. (2017). Deep sequencing reveals high bacterial diversity and phylogenetic novelty in pit mud from Luzhou Laojiao cellars for Chinese strong-flavor Baijiu. *Food Res. Int.* 102, 68–76. doi: 10.1016/j.foodres.2017.09.075

Ma, X., Lv, B., Li, P., Jiang, X., Zhou, Q., Wang, X., et al. (2016). Identification of "multiple components-multiple targets-multiple pathways" associated with Naoxintong Capsule in the treatment of heart diseases using UPLC/Q-TOF-MS and network pharmacology. *J. Evid. Based Complementary Altern. Med.* 2016 (12), 9468087. doi: 10.1155/2016/9468087

Mariat, D., Firmesse, O., Levenez, F., Guimarães, V. D., Sokol, H., Doré, J., et al. (2009). The Firmicutes/Bacteroidetes ratio of the human microbiota changes with age. *BMC Microbiol.* 9 (1), 123. doi: 10.1186/1471-2180-9-123

Michal, C. H., Cederbaum, A. I., and Natalia, N. (2004). A high-fat diet leads to the progression of non-alcoholic fatty liver disease in obese rats. *FASEB J.* 19 (1), 136–138. doi: 10.1096/fj.04-2291fje

Mishra, V., and Prasad, D. N. (2005). Application of *in vitro* methods for selection of Lactobacillus casei strains as potential probiotics. *Int. J. Food Microbiol.* 103 (1), 109–115. doi: 10.1016/j.ijfoodmicro.2004.10.047

Miyoshi, N., Horiuchi, M., Inokuchi, Y., Miyamoto, Y., Miura, N., Tokunaga, S., et al. (2010). Novel microminipig model of atherosclerosis by high fat and high cholesterol diet, established in Japan. *Vivo* 24 (24), 671–680.

Murphy, E. A., Velazquez, K. T., and Herbert, K. M. (2015). Influence of high-fat diet on gut microbiota: a driving force for chronic disease risk. *Curr. Opin. Clin. Nutr. Metab. Care* 18 (5), 515. doi: 10.1097/MCO.0000000000000209

Nadja, L., Vogensen, F. K., van den Berg, F. W. J., Nielsen, D. S., Andreasen, A. S., Pedersen, B. K., et al. (2010). Gut microbiota in human adults with type 2 diabetes differs from non-diabetic adults. *Plos One* 5 (2), e9085. doi: 10.1371/journal.pone.0009085

Paula, M. T. D., Silva, M. R. P., Araujo, S. M., Bortolotto, V. C., Meichtry, L. B., Zemolin, A. P. P., et al. (2016). High-fat diet induces oxidative stress and MPK2 and HSP83 gene expression in Drosophila melanogaster. *Oxid. Med. Cell. Longevity* 2016 (6), 1–12. doi: 10.1155/2016/4018157

Pinhal, C. S., Lopes, A., Torres, D. B., Felisbino, S. L., Rocha Gontijo, J. A., and Boer, P. A. (2013). Time-course morphological and functional disorders of the kidney induced by long-term high-fat diet intake in female rats. *Nephrol. Dial. Transplant.* 28 (10), 2464–2476. doi: 10.1093/ndt/gft304

Prantner, D., Darville, T., Sikes, J. D., Andrews, C. W., Jr., Brade, H., Rank, R. G., et al. (2009). Critical role for interleukin-1β (IL-1β) during Chlamydia muridarum genital infection and bacterial replication-independent secretion of IL-1β in mouse macrophages. *Infect. Immun.* 77 (12), 5334–5346. doi: 10.1128/IAI.00883-09

Ridker, P. M., Rifai, N., Stampfer, M. J., and Hennekens, C. H. (2000). Plasma concentration of interleukin-6 and the risk of future myocardial infarction among apparently healthy men. *Circulation* 101 (15), 1767. doi: 10.1161/01.CIR.101.15.1767

Shoumin, X., Weidong, Y., Zongbao, W., Masataka, K., Xin, L., Tomonari, K., et al. (2004). A minipig model of high-fat/high-sucrose diet-induced diabetes and atherosclerosis. *Int. J. Exp. Path.* 85 (4), 223–231. doi: 10.1111/j.0959-9673.2004.00394.x

Smith, A. C., Spinale, F. G., and Swindle, M. M. (1990). Cardiac function and morphology of Hanford miniature swine and Yucatan miniature and micro swine. *Lab. Anim. Sci.* 40 (1), 47–50.

Snodgrass, P. J., Wacker, W. E., Eppinger, E. C., and Vallee, B. L. (1959). Metalloenzymes and myocardial infarction. III. Lactic dehydrogenase activity

of serum-a determinate diagnostic measure. *New Engl. J. Med.* 261 (11), 1259. doi: 10.1056/NEJM195912172612502

Van, I. F., De, B. J., Boyen, F., Bohez, L., Pasmans, F., Volf, J., et al. (2004). Medium-chain fatty acids decrease colonization and invasion through hilA suppression shortly after infection of chickens with Salmonella enterica serovar Enteritidis. *Appl. Environ. Microbiol.* 70 (6), 3582. doi: 10.1128/AEM.70.6.3582-3587.2004

Velagapudi, V. R., Hezaveh, R., Reigstad, C. S., Gopalacharyulu, P., Yetukuri, L., Islam, S., et al. (2010). The gut microbiota modulates host energy and lipid metabolism in mice. *J. Lipid Res.* 51 (5), 1101–1112. doi: 10.1194/jlr.M002774

Vrieze, A., Holleman, F., Zoetendal, E. G., Vos, W. M. D., Hoekstra, J. B. L., and Nieuwdorp, M. (2010). The environment within: how gut microbiota may influence metabolism and body composition. *Diabetologia* 53 (4), 606–613. doi: 10.1007/s00125-010-1662-7

Wang, S., Xu, H., Yan, M., Wang, X., Yang, S., Huang, B., et al. (2015). Characterization and rapid identification of chemical constituents of NaoXinTong capsules by UHPLC-linear ion trap/Orbitrap mass spectrometry. *J. Pharm. Biomedic. Anal.* 111, 104–118. doi: 10.1016/j.jpba.2015.01.020

Wang, Y., Xu, N., Xi, A., Ahmed, Z., Zhang, B., and Bai, X. (2009). Effects of Lactobacillus plantarum MA2 isolated from Tibet kefir on lipid metabolism and intestinal microflora of rats fed on high-cholesterol diet. *Appl. Microbiol. Biotechnol.* 84 (2), 341–347. doi: 10.1007/s00253-009-2012-x

Wang, Y., Yan, X., Mi, S., Li, Z., Wang, Y., Zhu, H., et al. (2017). Naoxintong attenuates Ischaemia/reperfusion injury through inhibiting NLRP3 inflammasome activation. *J. Cell. Mol. Med.* 21 (1), 4–12. doi: 10.1111/jcmm.12915

Yang, S., Liu, M., Chen, Y., Ma, C., Liu, L., Zhao, B., et al. (2018). NaoXinTong capsules inhibit the development of diabetic nephropathy in db/db mice. *Sci. Rep.* 8 (1), 9158–. doi: 10.1038/s41598-018-26746-1

Yang, X., Li, Y., Sun, L., Liu, Y., Ma, C., Chen, Y., et al. (2017). NaoXinTong enhances atorvastatin-induced plaque stability while ameliorating atorvastatin-induced hepatic inflammation. *J. Cardiovasc. Pharmacol.* 69 (1), 55–64. doi: 10.1097/FJC.0000000000000441

Zeng, X., Su, W., Zheng, Y., Liu, H., Li, P., Zhang, W., et al. (2018). UFLC-Q-TOF-MS/MS-based screening and identification of flavonoids and derived metabolites in human urine after oral administration of Exocarpium Citri Grandis Extract. *Molecules* 23 (4), 895. doi: 10.3390/molecules23040895

Zhang, C., Zhang, M., Wang, S., Han, R., Cao, Y., Hua, W., et al. (2010). Interactions between gut microbiota, host genetics and diet relevant to development of metabolic syndromes in mice. *ISME J.* 4 (2), 232–241. doi: 10.1038/ismej.2009.112

Conflict of Interest: The authors declare that the research was conducted in the absence of any commercial or financial relationships that could be construed as a potential conflict of interest.

frontiers in Pharmacology

SYSTEMATIC REVIEW
published: 17 October 2019
doi: 10.3389/fphar.2019.01204

Notoginsenoside R1 for Organs Ischemia/Reperfusion Injury: A Preclinical Systematic Review

Qiang Tong[1†], Peng-chong Zhu[1†], Zhuang Zhuang[1], Li-hui Deng[1], Zi-hao Wang[1], Hua Zeng[2], Guo-qing Zheng[2] and Yan Wang[1*]*

[1] Department of Cardiology, The Second Affiliated Hospital and Yuying Children's Hospital of Wenzhou Medical University, Wenzhou, China, [2] Department of Neurology, The Second Affiliated Hospital and Yuying Children's Hospital of Wenzhou Medical University, Wenzhou, China

Notoginsenoside R1 (NGR1) exerts pharmacological actions for a variety of diseases such as myocardial infarction, ischemic stroke, acute renal injury, and intestinal injury. Here, we conducted a preclinical systematic review of NGR1 for ischemia reperfusion (I/R) injury. Eight databases were searched from their inception to February 23rd, 2019; Review Manager 5.3 was applied for data analysis. CAMARADES 10-item checklist and cell 10-item checklist were used to evaluate the methodological quality. Twenty-five studies with 304 animals and 124 cells were selected. Scores of the risk of bias in animal studies ranged from 3 to 8, and the cell studies ranged from 3 to 5. NGR1 had significant effects on decreasing myocardial infarct size in myocardial I/R injury, decreasing cerebral infarction volume and neurologic deficit score in cerebral I/R injury, decreasing serum creatinine in renal I/R injury, and decreasing Park/Chiu score in intestinal I/R injury compared with controls (all $P < 0.05$ or $P < 0.01$). The multiple organ protection of NGR1 after I/R injury is mainly through the mechanisms of antioxidant, anti-apoptosis, and anti-inflammatory, promoting angiogenesis and improving energy metabolism. The findings showed the organ protection effect of NGR1 after I/R injury, and NGR1 can potentially become a novel drug candidate for ischemic diseases. Further translation studies are needed.

Keywords: notoginsenoside R1, ischemia, reperfusion, organ, preclinical systematic review, meta-analysis

OPEN ACCESS

Edited by:
Yue Liu,
Xiyuan Hospital, China

Reviewed by:
Yun K. Tam,
Sinoveda Canada Inc., Canada
Sefirin Djiogue,
University of Yaounde I, Cameroon

***Correspondence:**
Guo-qing Zheng
gq_zheng@sohu.com
Yan Wang
wywzchina@sina.com

†These authors have contributed equally to this work

Specialty section:
This article was submitted to Ethnopharmacology, a section of the journal Frontiers in Pharmacology

Received: *13 June 2019*
Accepted: *17 September 2019*
Published: *17 October 2019*

Citation:
Tong Q, Zhu P-c, Zhuang Z, Deng L-h, Wang Z-h, Zeng H, Zheng G-q and Wang Y (2019) Notoginsenoside R1 for Organs Ischemia/Reperfusion Injury: A Preclinical Systematic Review. Front. Pharmacol. 10:1204. doi: 10.3389/fphar.2019.01204

INTRODUCTION

Ischemia and reperfusion (I/R) injury, featuring as an interruption of organ blood flow and the following re-oxygenation after reperfusion, is a common pathological phenomenon in ischemic diseases. These mainly include myocardial infarction (MI), ischemic stroke, acute renal injury, and intestinal injury (Eltzschig and Eckle 2011). Although these pathological processes are involved in a variety of diseases, these diseases share common molecular mechanisms. The main mechanisms of I/R injury include inflammation (Chen and Nuñez, 2010), oxidative stress (Ohsawa et al., 2007), apoptosis (Shiva et al., 2007), energy metabolism disorder (Wang and Ma, 2018), microvascular dysfunction (Eltzschig and Collard, 2004), and leucocyte-endothelial cell adhesion (Eltzschig and Eckle 2011). Owing to the chronic organ injury, the ischemia organ will ultimately develop into the pathological outcomes with tissue fibrosis and organ failure (Friedman et al., 2013). In 2016, the two main ischemic diseases, ischemic heart disease (IHD) and stroke, were the leading causes of human death globally, accounting for more than 85.1% of all cardiovascular and cerebrovascular

diseases and death (Murray Christopher 2017). Over the past three decades, great progress has been made in the therapy of ischemic diseases, especially in MI and ischemic stroke. Nevertheless, there exist disadvantages in safety and efficacy in main and promising therapy approaches. In acute management, the timely revascularization therapies such as percutaneous coronary intervention (PCI) and thrombolysis can recover the supply of oxygen and blood for ischemic organs or tissues. However, irreversible ischemia from delayed administration and reperfusion injury can result in chronic organ failure and a shortened lifespan (Alex et al., 2017). Currently antiplatelet drugs have good effects on anti-platelet adhesion and aggregation in clinic, but they have little efficacy in energy metabolism disorder and oxidative stress (Han et al., 2017). Studies have shown that ischemic preconditioning and ischemic postconditioning can reduce MI size caused by I/R injury, whereas the mechanism of the conditioning phenomenon with the most robust cardioprotective procedure through interventions reducing MI size is still largely unknown in the human heart (Heusch and Rassaf 2016; Heusch and Gersh, 2016; Heusch, 2017). Currently, recanalization therapy for acute ischemic stroke (AIS) is mainly through recombinant tissue plasminogen activator (rt-PA). However, rt-PA is accepted by a minority of patients due to narrow time window of thrombolysis and hemorrhage (Hacke et al., 2004; Khandelwal et al., 2016). Unfortunately, the reocclusion after thrombolysis led to neurological function impairment and higher in-hospital mortality (Lee et al., 2001). Considering the limitations of these therapies, we need to seek new therapy to improve organ damage induced by I/R injury.

Panax notoginseng (*P. notoginseng*), one of the most valuable traditional Chinese medicine (TCM), is derived from the roots and rhizomes of *P. notoginseng* (Burkill) F.H. Chen (Ng, 2006; Peng et al., 2018). Over the past several centuries, *P. notoginseng* showed good efficacy in controlling internal and external bleeding and improving blood stasis (Wang T. et al., 2016). With the advancing of pharmacology, the studies of *P. notoginseng* demonstrate that it is widely used in cardiovascular diseases (CVDs) mainly because of its vasodilatory and antihypertensive functions (Yang et al., 2014). Notoginsenoside R1 (NGR1) (the specific chemical structure of NGR1 is shown in **Figure 1**) is the main effective component isolated from *P. notoginseng*, and NGR1 belongs to protopanaxatriol (PPT) type of saponins (Leung et al., 2007). Previous studies indicated that NGR1 is easily dissolved in water, but shows low bio-availability and poor permeability in the gastrointestinal tract (Liang and Hua, 2005; Liu et al., 2009; Ruan et al., 2010). In absorption property, Liang et al. (2005) revealed that the optimal site for absorption of NGR1 is the upper extremity of the intestine. Guo et al. (2014) first described the detection of NGR1 in brain tissue by the way of nasally applying drugs. To improve the oral bioavailability of NGR1, sodium N-[8-(2-hydroxybenzoyl) amino] caprylate (SNAC, a novel absorption enhancer) was used (Li et al., 2018). It has been reported that NGR1 significantly improves prognosis of other disease models such as atherosclerosis, diabetic nephropathy, and diabetic cardiomyopathy (Su et al., 2015; Zhang et al., 2018; Zhang B. et al., 2019). NGR1 also plays a protective role in ischemic diseases (Liu et al., 2010; Li et al., 2014; Yu et al., 2016; Tu et al., 2018). Although NGR1 has been widely used for the treatment of ischemic diseases, the efficacy and mechanisms of NGR1 for ischemic organs such as heart, cerebral, kidney, intestinal, and liver have not been systematically analyzed. Animal experiment, the most important approach of basic research, is a bridge between the bench and bedside (Olesen et al., 2012). The conclusions derived from preclinical studies are of little evaluation, and using these conclusions as inadequate evidence for conducting clinical trials has resulted in a high cost in clinical research or withdrawal of the drug from the market later (Perel et al., 2006). Systematic reviews (SRs) are usually used in clinical study, which provided available resources for performing clinical practice guidelines and policies. SR of preclinical studies also plays a significant role in many aspects, including: 1) improving the methodological quality of studies, 2) choosing suitable animal models, 3) translating the experimental data from preclinical to clinical, and 4) implementing the 3Rs (reduction, replacement, and refinement) (De Vries et al., 2014). In addition, SR of preclinical experiments is of significance to elucidate the mechanism and treatment of human diseases (Sena et al., 2014). SR can further evaluate the preclinical evidence objectively and reduce the bias of experimental results (Roberts

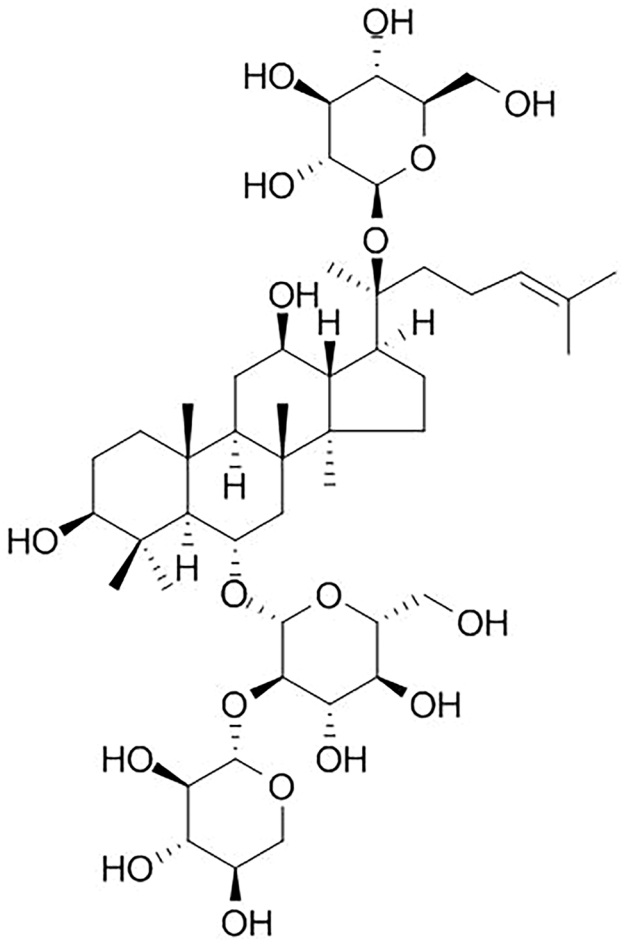

FIGURE 1 | Chemical structure of notoginsenoside R1.

et al., 2002; Perel et al., 2006). SRs for preclinical study that could offer crucial information for clinical research are quite scarce (Judith et al., 2014; Tsujimoto et al., 2017). Thus, we conducted an SR on preclinical studies of NGR1 for I/R injury.

METHODS

Search Strategy

We searched PubMed, Cochrane Library, EMBASE, Web of Science, Chinese National Knowledge Infrastructure (CNKI), Wanfang Data Information Site, VIP information database, and Chinese Biomedical Literature Database from their inception to February 23rd, 2019. The following terms were used: 1) "notoginsenoside" AND "infarction OR ischem* OR reperfusion" limited on animals; and 2) "notoginsenoside" AND "Oxygen–glucose deprivation OR hypoxia" limited on cells.

Inclusion Criteria/Exclusion Criteria

Inclusion criteria were prespecified as follows: 1) experimental animal models of I/R; 2) experimental cell models established by oxygen and glucose deprivation/reoxygenation (OGD/R); 3) treatment group received the NGR1 therapy merely; 4) control group received vehicle, non-functional liquid with equal volume, no treatment or positive control; 5) the primary outcome measures were MI size, creatine kinase (CK) or creatine kinase isoenzymes MB (CKMB), left ventricular ejection fraction (LVEF) and cardiac troponin I/T (cTnI/T) in myocardial I/R studies; cerebral infarct volume and neurologic deficit score in cerebral I/R studies; myeloperoxidase (MPO), glucose/water clearance and Park/Chiu score in intestinal I/R studies; MPO, serum creatinine (Scr), glomerular filtration rate (GFR), and blood urea nitrogen (BUN) in renal I/R studies, and alanine aminotransferase (ALT) and aspartate aminotransferase (AST) in liver I/R studies; cell viability, lactate dehydrogenase (LDH), superoxide dismutase (SOD), malondialdehyde (MDA), apoptosis rate and/or TUNEL positive rate in cell models; 6) the secondary outcome measures were mechanisms of NGR1 intervention in both animal and cell models. Exclusion criteria were prespecified as follows: 1) treatment group received non-NGR1; 2) comparing NGR1 with other herbal medicine or herbal active compounds; 3) no control group; 4) master dissertation or doctoral dissertation; 5) case report or review; 6) NGR1 for other disease models; 7) NGR1 in combination with other drugs; 8) duplicate publication.

Data Extraction

A data extraction form was used to collect the following items from each included study: 1) first author, year of publication; 2) detailed information about the experimental subjects such as animal species, number, sex and weight, and cell number, organism, age, tissue, and primary/subcultured; 3) administration method and duration of NGR1 treatment; 4) the types and administration methods of anesthetics; 5) the outcome measures including type, timing, and mean and standard deviations.

Only the last time point and the highest dose were recorded if there were many different time points of outcome measures or the experimental animals received different doses of the drug. The data were measured by the digital ruler software if the data were presented with graphs. Further information was retrieved by contacting with the authors when the primary data were incomplete.

Assessment of the Risk of Bias

Minor modified CAMARADES 10-item scale was used to assess the risk of bias in animal studies (Macleod et al., 2004). The modified item is the use of anesthetic with no intrinsic organ-protective activity. Our newly developed scale specially designed for cell studies was used for the assessment of risk of bias in cell experiments (Bao et al., 2018).

Statistical Analysis

All data analysis was implemented by RevMan 5.3 (https://community.cochrane.org). We calculated the standard mean difference (SMD) with 95% confidence intervals (CIs). Heterogeneity was assessed using the Cochrane Q-statistic test ($P < 0.05$ was considered statistically effective) and the I^2-statistic test. A random-effects model would be adopted if $I^2 > 50\%$, which indicates substantial heterogeneity. Conversely, a fixed-effects model would be used if $I^2 < 50\%$. Sources of heterogeneity were searched as far as possible, and subgroup analysis was carried out when necessary. The sensitivity analysis was performed in order to improve the robustness of the results.

RESULTS

Study Selection

For animal studies, a total of 473 potentially relevant hints were identified, of which 401 were duplicated. After screening of the titles and abstracts, seven studies were excluded because of the following reasons: 1) case report; 2) clinical trial; and 3) review article. Then secondary screening was conducted by reading the full text of the remaining 65 studies; 51 studies were excluded because of at least one of the following reasons: 1) failed to obtain full text; 2) non-NGR1 treatment; 3) inappropriate animal model; 4) compared with Chinese herbal medicine or herbal active compounds; 5) no control group; 6) master dissertation or doctoral dissertation; and 7) no available data. Finally, 14 papers (Liu et al., 2010; Deng and Lai, 2013; Han, 2014; He et al., 2014; Li et al., 2014; Meng et al., 2014; Yu et al., 2014; Dong et al., 2015; Xia et al., 2015; Wang et al., 2016; Yu et al., 2016; Zhao et al., 2017; Zou et al., 2017; Tu et al., 2018) were included (**Figure 2A**).

For cell studies, a total of 112 potentially relevant hints were identified, of which 47 were duplicated. After screening of the titles and abstracts, 13 studies were excluded because of the following reasons: 1) case report; 2) clinical trial; and 3) review article. Then secondary screening was conducted by reading the full text of the remaining 52 studies; 28 studies were excluded because of at least one of the following reasons: 1) failed to obtain full text; 2) non-NGR1 treatment; 3) inappropriate cell model; 4) compared with Chinese herbal medicine or herbal active compounds; 5) no control group; 6) master dissertation or doctoral dissertation; and 7) no

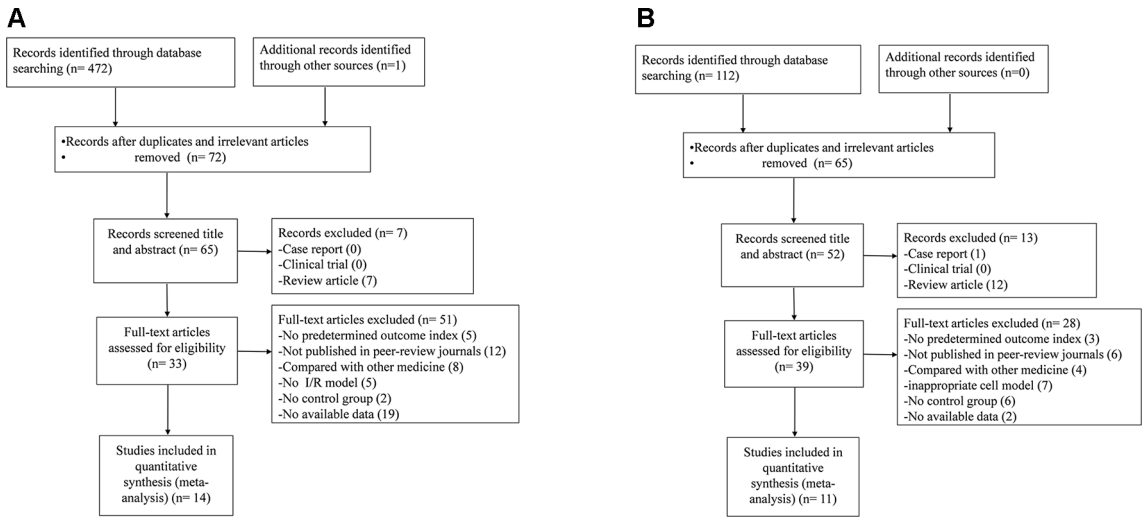

FIGURE 2 | Summary of the process for identifying candidate studies. **(A)** Search strategy for animal experiments: 473 potentially relevant studies were identified; after removal of duplicates and the application of inclusion and exclusion criteria, 14 studies were included in the meta-analysis. **(B)** Search strategy for cell experiments: 112 potentially relevant studies were identified; after removal of duplicates and the application of inclusion and exclusion criteria, 11 studies were included in the meta-analysis.

available data. Finally, 11 papers (He et al., 2014; Meng et al., 2014; Wan et al., 2015; Yu et al., 2016; Zhou et al., 2016; Wang et al., 2016; Hou et al., 2017; Wang et al., 2017; Zhou et al., 2017; Liu et al., 2019; Tu et al., 2018) were included (**Figure 2B**).

Characteristics of Included Studies

Animal Experiments

Fourteen animal experiments between 2010 and 2018 were included. Five studies (Deng and Lai, 2013; Han, 2014; Yu et al., 2014; Dong et al., 2015; Zhao et al., 2017) were published in Chinese, and nine studies (Liu et al., 2010; He et al., 2014; Li et al., 2014; Meng et al., 2014; Xia et al., 2015; Wang et al., 2016; Yu et al., 2016; Zou et al., 2017; Tu et al., 2018) were published in English. Eleven studies (Liu et al., 2010; Deng and Lai, 2013; Han, 2014; He et al., 2014; Li et al., 2014; Meng et al., 2014; Dong et al., 2015; Xia et al., 2015; Yu et al., 2016; Zhao et al., 2017; Zou et al., 2017) used healthy adult Sprague-Dawley (SD) male rats, while one study (Yu et al., 2014) used male Wistar rat and two studies (Wang et al., 2016; Tu et al., 2018) used 7-day-old SD rats. The body weight of adult SD rats ranged from 180 to 300 g. To induce anesthesia, pentobarbital were used in five studies (Liu et al., 2010; He et al., 2014; Yu et al., 2014; Xia et al., 2015; Zhao et al., 2017); chloral hydratein in two studies (Dong et al., 2015; Zhou et al., 2017); isofluranein in two studies (Wang et al., 2016; Tu et al., 2018); urethane in one study (Yu et al., 2016); ulatanin in one study (Han, 2014); ketaminein in one study (Meng et al., 2014); and noanesthetic in one study (Deng and Lai, 2013). To establish animal models of myocardial I/R injury, ligation of left anterior descending coronary artery (LAD) was used in four studies (Han, 2014; He et al., 2014; Yu et al., 2014; Xia et al., 2015); ligation of LAD for 40 min followed by 60 min of reperfusion in one study (Yu et al., 2016); ligation of LAD for 30 min followed by 30, 60, and 90 min of reperfusion in one study (Han, 2014). One study (Deng and Lai, 2013) reported that AMI model induced by injecting pituitrin (0.65 U/kg) into sublingual. To establish cerebral I/R injury models, occlusion of middle cerebral artery (MCA) was used in three studies (Meng et al., 2014; Dong et al., 2015; Zhao et al., 2017); ligation of common carotid artery (CCL) in two studies (Wang et al., 2016; Tu et al., 2018); and bilateral common carotid artery occlusion (BCCAO) in one study (Zou et al., 2017). One study (Liu et al., 2010) induced renal I/R animal models by clamping left renal artery and vein, and one study (Li et al., 2014) induced intestinal I/R animal models by clamping superior mesenteric artery. For outcome measures, the MI size was used in four studies (Deng and Lai, 2013; Han 2014; He et al., 2014; Xia et al., 2015), serum CK in three studies (Deng and Lai, 2013; Xia et al., 2015; Yu et al., 2016), serum MDA in two studies (Xia et al., 2015; Yu et al., 2016), cerebral infarction volume in five studies (Meng et al., 2014; Dong et al., 2015; Wang et al., 2016; Zou et al., 2017; Tu et al., 2018), neurologic deficit score in two studies (Meng et al., 2014; Dong et al., 2015), serum creatinine in one study (Liu et al., 2010), and Park/Chiu score in one study (Li et al., 2014). The detailed characteristics of the included studies were generalized in **Table 1**.

Cell Experiments

Eleven studies involved in cell experiments between 2014 and 2018 were included, of which four studies (Wan et al., 2015; Zhou et al., 2016; Hou et al., 2017; Zhou et al., 2017) were published in Chinese and seven studies (He et al., 2014; Meng et al., 2014; Wang et al., 2016; Yu et al., 2016; Wang et al., 2017; Liu et al., 2019; Tu et al., 2018) in English. Wistar Suckling mice cardiomyocytes were used in three studies (Wan et al., 2015; Zhou et al., 2016; Zhou et al., 2017), and embryonic cardiomyoblast-derived cardiomyocytes (H9C2) of rat were used in two studies (He et al., 2014; Yu et al., 2016). The methods of establishing I/R model in cardiomyocytes

TABLE 1 | Characteristics of the 14 included animal studies.

Study (years)	Species (sex; n = experimental/ control group)	Weight	Model(method)	Anesthetic	Treatment group(Method to astraddle sides)	Control group	Outcome index (time)	Intergroup differences
Deng and Lai 2013	SD rats (Half male and female; 10/10)	180–220 g	Sublingual vein injection of pituitrin	—	NGR1 (10 mg/kg/day; i.g.) for 4 days before ischemia and 7 days after ischemia	Negative control group, isometric normal saline (i.g.) for 4 days before ischemia and 7 days after ischemiaPositive control group, diltiazem (i.g.) for 4 days before ischemia and 7 days after ischemia	1. ST-segment and inversion rate of T-wave 2. AST 3. CK 4. CK-MB 5. LDH 6. LDH1 7. Myocardial infarct size 8. Bcl-2 9. Bax	1. $P < 0.01$ 2. $P < 0.05$ 3. $P < 0.05$ 4. $P < 0.05$ 5. $P < 0.05$ 6. $P < 0.05$ 7. $P < 0.05$ 8. $P < 0.01$ 9. $P < 0.01$
Han, 2014	SD rats (male; 6/6)	240–260 g	Block LAD 30 min after reperfusion	20%Ulatan (1.25 g/kg)	NGR1 (5 mg/kg/h; i.v.) 20 min before ischemia	Intravenous infusion of the equal volume of normal saline	1. Venular RBC velocity (%) 2. Albumin leakage (%) 3. Coronary blood flow (%) 4. Myocardial infarct size 5. Heart rat (bpm) 6. LVDP 7. LVSP 8. +dP/dtmax 9. – dP/dtmax 10. MPO 11. ICAM-1 12. CD18 13. Positive percent of TUNEL (%) 14. ATP 15. ADP 16. AMP 17. ADP/ATP 18. AMP/ATP 19. ATPα/GAPDH 20. ATP5D/GAPDH 21. ATPβ/GAPDH 22. ZO-1/GAPDH 23. VE/GAPDH 24. JAM-1/GAPDH 25. Claudin-5/GAPDH 26. Cav-1/GAPDH 27. Cav-3/GAPDH 28.p-Src/Src 29.Src/GAPDH	1. $P < 0.05$ 2. $P < 0.05$ 3. $P < 0.05$ 4. $P < 0.05$ 5. $P > 0.05$ 6. $P > 0.05$ 7. $P < 0.05$ 8. $P < 0.05$ 9. $P < 0.05$ 10. $P < 0.05$ 11. $P < 0.05$ 12. $P < 0.05$ 13. $P < 0.05$ 14. $P < 0.05$ 15. $P > 0.05$ 16. $P > 0.05$ 17. $P < 0.05$ 18. $P < 0.05$ 19. $P > 0.05$ 20. $P < 0.05$ 21. $P > 0.05$ 22. $P < 0.05$ 23. $P < 0.05$ 24. $P < 0.05$ 25. $P < 0.05$ 26. $P < 0.05$ 27. $P < 0.05$ 28. $P < 0.05$ 29. $P > 0.05$
Yu et al., 2014	Wistar rats (male; 13/13)	220–280 g	Block LAD	1% Pentobarbital sodium(40 mg/kg)	NGR1 (2.5 mg/kg/day; i.p.)for 4 weeks after ischemia	Intraperitoneal injection of equal volume of saline after ischemia	1. MVC 2. MVD 3. VEGF 4. bFGF	1. $P < 0.05$ 2. $P < 0.05$ 3. $P < 0.05$ 4. $P < 0.05$
He et al., 2014	SD rats (male; 8/8)	240–260 g	Block LAD 30 min after reperfusion	2% Pentobarbital sodium	NGR1 (5mg/kg/h; i.v.) for 30 min before ischemia; 30 min during ischemia; and 90 min after ischemia	Continuous injection of saline (1 ml/h)	1. AAR/LV 2. Myocardial infarct size/AAR 3.+dP/dtmax 4.– dP/dtmax 5. LVSP 6. LVDP 7. TUNEL-positive 8. Bcl-2/Bax 9. Cleaved caspase-3/procaspase-3 10. ATP 11. AMP 12. P-AMPK/β-actin 13. ATP synthase-α/β-actin 14. ATP synthase-β/β-actin 15. ATP 5D/β-actin 16. ROCK/β-actin 17. P-MYPT1/MYPT1	1. $P > 0.05$ 2. $P < 0.05$ 3. $P > 0.05$ 4. $P < 0.05$ 5. $P > 0.05$ 6. $P > 0.05$ 7. $P < 0.05$ 8. $P < 0.05$ 9. $P < 0.05$ 10. $P < 0.05$ 11. $P > 0.05$ 12. $P < 0.05$ 13. $P > 0.05$ 14. $P > 0.05$ 15. $P < 0.05$ 16. $P < 0.05$ 17. $P < 0.05$
Xia et al., 2015	SD rats (male; 6/6)	250–300 g	Block LAD 30 min after reperfusion	Pentobarbital sodium (30 mg/kg)	NGR1 (60 mg/kg; i.g.) for 5 days	No treatment	1. Myocardial infarct size 2. CK 3. LDH 4. T-SOD 5. MDA 6. IL-1β 7. IL-8 8. TNF-α 9. p-NF-κBP65/NF-κBP65 10. p-IκBα/IκBα 11. VDUP1/GAPDH	1. $P < 0.01$ 2. $P < 0.01$ 3. $P < 0.05$ 4. $P < 0.001$ 5. $P < 0.01$ 6. $P < 0.01$ 7. $P < 0.01$ 8. $P < 0.01$ 9. $P < 0.01$ 10. $P < 0.01$ 11. $P < 0.01$
Yu et al., 2016	SD rats (male; 10/10)	200–220 g	The isolated Langendorff-perfused rat hearts received ischemia/reperfusion(40 min/60 min)	Urethane	NGR1 (20 μM) for 15 min before the ischemia	No treatment	1. LVSP 2. Heart rate 3. +dp/dtmax 4. -dp/dt min 5. MDA 6. SOD 7. CAT 8. CK 9. GSH-Px activities 10. P-JNK/JNK 11. CHOP/β-actin 12. Bcl-2/BAX 13. GRP78/β-actin 14. P-PERK/PERK 15. P-elf2α/elf2α 16. IRE1/β-actin 17. ATF6/β-actin 18. Caspase-12/β-actin 19. BAX/β-actin	1. $P < 0.01$ 2. $P < 0.05$ 3. $P < 0.01$ 4. $P < 0.01$ 5. $P < 0.01$ 6. $P < 0.01$ 7. $P < 0.01$ 8. $P < 0.001$ 9. $P < 0.001$ 10. $P < 0.001$ 11. $P < 0.001$ 12. $P < 0.001$ 13. $P < 0.01$ 14. $P < 0.001$ 15. $P < 0.001$ 16. $P < 0.001$ 17. $P < 0.01$ 18. $P < 0.001$ 19. $P < 0.001$

(Continued)

TABLE 1 | Continued

Study (years)	Species (sex; n = experimental/ control group)	Weight	Model(method)	Anesthetic	Treatment group(Method to astraddle sides)	Control group	Outcome index (time)	Intergroup differences
Meng et al., 2014	SD rats (male; 40/40)	250–300 g	MCAO	Ketamine (80 mg/ kg; i.p.)	NGR1 (20 mg/kg; i.p) before ischemia	Given the same amount of saline	1. Infarction volumes 2. Neurologic deficit score 3. TUNEL-positive cells rate 4. Caspase-3 activity 5. NADPH oxidase activity 6. Superoxide levels 7. Mitochondrial superoxide levels 8. MDA 9. Protein carbonyl levels 10. 8-OHdG levels 11. HO-1 activity	1. $P < 0.01$ 2. $P < 0.01$ 3. $P < 0.01$ 4. $P < 0.01$ 5. $P < 0.01$ 6. $P < 0.01$ 7. $P < 0.01$ 8. $P < 0.01$ 9. $P < 0.01$ 10. $P < 0.01$ 11 . $P< 0.01$
Dong et al., 2015	SD rats (male; 8/8)	180–200 g	MCAO	10% Chloral hydrate (300 mg/ kg; i.p.)	NGR1 (7.0 mg/kg; i.p.) for 14 days after ischemia	Given the same amount of saline	1. Infarction volumes 2. Neurologic deficit score 3. Population spike 4. Escape latency 5. Target quadrant dwell time	1. $P < 0.01$ 2. $P < 0.01$ 3. $P < 0.01$ 4. $P < 0.01$ 5. $P < 0.01$
Wang et al., 2016	7-day-old SD rats (male; 5/5)	–	The common carotid artery (CCL)	Isoflurane (2.5%)	NGR1 (15 mg/kg· 12 h; i.p.) after CCL; before exposure to the hypoxic environment	No treatment	1. Infarction volumes 2. Ratio of GRP78/β-actin 3. Ratio of P-PERK/PERK 4. Ratio of P-IRE1α/IRE1α 5. Ratio of CHOP/β-actin	1. $P < 0.05$ 2. $P < 0.05$ 3. $P < 0.05$ 4. $P < 0.05$ 5. $P < 0.05$
Zhao et al., 2017	SD rats (male; 10/10)	–	MCAO	3% Pelltobarbitalum Natricum (0.2 ml/100 g)	NGR1 (5 mg/ml; i.v.) for 3 days	Given the same amount of saline	1. The number of TUNEL-positive cells 2. TNF-α mRNA	1. $P < 0.05$ 2. $P < 0.05$
Zou et al., 2017	SD rats(male; 15/15)	250–300 g	BCCAO (ischemia; 20 min; reperfusion; 3 h)	Chloral hydrate (350 mg/kg; i.p.)	NGR1 (100 mg/kg; i.g.) after ischemia	Intragastric administrationof 0.5 ml saline	1. Cerebral infarction size 2. Relative expression of BDNF mRNA 3. Relative expression of Bcl-2 to β-actin 4. Relative expression of Bax to β-actin	1. $P < 0.01$ 2. $P < 0.01$ 3. $P < 0.01$ 4. $P < 0.01$
Tu et al., 2018	7-day-old SD rats (male; 9/9)	–	CCL	Isoflurane (2.5%)	NGR1 (15 mg/kg; i.p.; q12 h) for 2 days after ischemia	Not mentioned	1. The water content of brain tissue 2. Volume of brain infarction 3. TUNEL positive nuclei 4. Brain weight ratio 5. The score of balance beam 6. Percent in the target quadrant 7. PI3K/β-actin 8. P-Akt/T-Akt 9. P-mTOR/T-mTOR 10. P-P70S6K/ P70S6K 11. P-4EBP-1/4EBP-1 12. P-JNK/T-JNK 13. P-c-JUN/c-JUN	1. $P < 0.05$ 2. $P < 0.01$ 3. $P < 0.01$ 4. $P < 0.01$ 5. $P < 0.05$ 6. $P < 0.01$ 7. $P < 0.01$ 8. $P < 0.05$ 9. $P < 0.05$ 10. $P < 0.05$ 11. $P < 0.05$ 12. $P < 0.01$ 13. $P < 0.05$
Liu et al., 2010	SD rats (male; 6/6)	230–250 g	Clamping left renal arteryand vein (ischemia; 45 min; reperfusion; 72 h)	Pentobarbital sodium (50 mg/ kg)	NGR1 (40 mg/kg; i.p.) before ischemia and for 3 days after reperfusion	Receiving the same amount of saline	1. Serum levels of creatinine 2. MPO 3. Relative TNF-α band intensity 4. TUNEL-positive cells 5. Relative p38MAPK band intensity 6. NF-κB band intensity	1. $P < 0.05$ 2. $P <0.05$ 3. $P < 0.05$ 4. $P < 0.05$ 5. $P < 0.05$ 6. $P < 0.05$
Li et al., 2014	SD rats (male; 6/6)	200–220 g	Clamping superior mesenteric artery (90 min/1 or 72 h)	Pentobarbital sodium (50 mg/ kg)	NGR1 (10 mg/kg/h; IVgtt) for 170 min after reperfusion	Receiving the same amount of saline	1. IκB-α change (%) 2. NF-κB change (%) 3. ATP5D change (%) 4. Zonulaoccludens -1 change (%) 5. Occludin change (%) 6. Claudin-5 change (%)	1. $P < 0.05$ 2. $P < 0.05$ 3. $P < 0.05$ 4. $P < 0.05$ 5. $P < 0.05$ 6. $P < 0.05$

SD rats, Sprague-Dawley rats; LAD, the left anterior descending coronary artery; SOD, superoxide dismutase; MDA, malondialdehyde; CK, creatine kinase; LDH, lactate dehydrogenase; CK-MB, creatine kinase-MB; TNF-α, tumor necrosis factor-α; GSH-Px, glutathione peroxidase; CAT, catalase; AST, aspartate aminotransferase; AAR/LV, area at risk/left ventricle;+dp/dtmax, maximum ascending rate of left ventricular pressure; –dP/dtmax, maximum descending rate of left ventricular pressure; LVSP, left ventricular systolic pressure; LVDP, left ventricular diastolic pressure; MVC, miniature blood vessel; MVD, microvascular density; VEGF, vascular endothelial growth factor; bFGF, basic fibroblast growth factor; ATP, adenosine triphosphate; AMP, adenosine monophosphate; IL-1, interleukin-1; IL-8, interleukin-8; NF-κBp65, nuclear factor-kappa Bp65; AMPK, AMP-activated protein kinase; ROCK, Rho-associated coil kinase; MYPT1, myosin phosphatase target subunit-1; NF-κBP65, nuclear factor-κBp65; IκBα, nuclear factor of kappa light polypeptide gene enhancer in B-cells inhibitor; alpha; VDUP1, vitamin D3 upregulated protein 1; GAPDH, glyceraldehyde-3-phosphate dehydrogenase; c-JNK, c-Jun N-terminal kinase; Bcl-2, B-cell lymphoma-2; MCAO; middle cerebral artery occlusion; BCCAO, bilateral common carotid artery occlusion; BDNF, brain-derived neurotrophic factor; NGR1, notoginsenoside R1; AMI, acute myocardial ischemia; bax, Bcl-2-associated X protein; RBC, red blood cell; MPO, myeloperoxidase; ICAM-1, intercellular cell adhesion molecule-1; TUNEL, TdT-mediated dUTP nick-end labeling; ADP, adenosine diphosphate; GAPDH, glyceraldehyde-3-phosphate dehydrogenase; ZO-1, Zonula occludens-1; JAM-1, recombinant junctional adhesion molecule 1; Cav-1, caveolin 1; Cav-3, caveolin 3; AAR, area at risk; T-SOD, total superoxide dismutase; IL-1β, interleukin 1 beta; CHOP, C/EBP homologous protein; GRP78, glucose regulated protein 78; PERK, protein kinase R-like ER kinase; p-PERK, phospho-protein kinase R-like ER kinase; elf2α, eukaryotic initiation factor 2α; IRE1, inositol-requiring enzyme-1α; ATF6, activating transcription factor 6; 8-OHdG, 8-hydroxydeoxyguanosine; HO-1, heme oxygenase-1; PI3K, p-mTOR, phospho-mammalian target of rapamycin; T-mTOR, P70S6K, protein S6 kinase; P-P70S6K, phospho-protein S6 kinase; P-4EBP-1, phospho-4EBP1.

include the application of hydrogen peroxide (H_2O_2) (Wan et al., 2015; Zhou et al., 2016; Zhou et al., 2017) and OGD/R (He et al., 2014; Yu et al., 2016). The dosages of NGR1 were 10 μmol/L in two studies (Zhou et al., 2016; Zhou et al., 2017), 20 μmol/L in one study (Yu et al., 2016), and 100 μmol/L in two studies (He et al., 2014; Wan et al., 2015). Cell viability and TUNEL-positive rate were used as outcome measures in six studies (He et al., 2014; Wan et al., 2015; Zhou et al., 2016; Yu et al., 2016; Zhou et al., 2017; Liu et al., 2019), LDH in seven studies (He et al., 2014; Meng et al., 2014; Wang et al., 2016; Zhou et al., 2016; Zhou et al., 2017; Hou et al., 2017; Tu et al., 2018), SOD in three studies (Wan et al., 2015; Zhou et al., 2016; Zhou et al., 2017), and MDA in four studies (Meng et al., 2014; Wan et al., 2015; Zhou et al., 2016; Zhou et al., 2017). The detailed characteristics of the included studies were generalized in **Table 2**.

In addition, seven studies (Liu et al., 2010; Meng et al., 2014; Yu et al., 2014; Xia et al., 2015; Yu et al., 2016; Zou et al., 2017; Tu et al., 2018) reported chemical analysis of NGR1 in animal studies. Seven studies (Meng et al., 2014; Wan et al., 2015; Wang et al., 2016; Wang et al., 2016; Liu et al., 2019; Tu et al., 2018) reported chemical analysis of NGR1 in cell studies. The characteristics of NGR1 were shown in **Table 3**.

Study Quality

Animal Studies

The scores of study quality ranged from 3 to 8 in a total of 10 points. All included studies were peer-reviewed publication. All the studies reported that the animals were allocated randomly to treatment or control group, and the anesthetics used in the experiments with no intrinsic organ-protective activity. However, sample size calculation, blinded induction of model, and blinded assessment of outcome were not reported in all included studies. Seven studies (He et al., 2014; Meng et al., 2014; Xia et al., 2015; Wang et al., 2016; Yu et al., 2016; Zou et al., 2017; Tu et al., 2018) stated compliance with animal welfare regulations and eight studies (He et al., 2014; Meng et al., 2014; Yu et al., 2014; Dong et al., 2015; Xia et al., 2015; Wang et al., 2016; Yu et al., 2016; Tu et al., 2018) declared no potential conflict of interests. The methodological quality of included studies was shown in **Table 4**.

Cell Studies

The scores of study quality ranged from 3 to 5 in a total of 10 points. All included studies were peer-reviewed publication. All the studies reported control of experimental conditions, the effect or safety of treatment, and statement of no potential conflict of interests. Nine studies (Meng et al., 2014; Wan et al., 2015; Wang et al., 2016; Zhou et al., 2016; Hou et al., 2017; Wang et al., 2017; Zhou et al., 2017; Liu et al., 2019; Tu et al., 2018) used primary cultured cells and two studies (He et al., 2014; Yu et al., 2016) used subcultured cells. However, sample size calculation and blinded assessment of outcome were not reported in all included studies. The methodological quality was shown in **Table 5**.

Effectiveness

Myocardial I/R Injury

MI Size

Meta-analysis of four studies (Deng and Lai, 2013; Han, 2014; He et al., 2014; Xia et al., 2015) showed NGR1 had significant effect on reducing MI size compared with control group [n = 60, SMD: -2.01, 95% CI: -2.67 to -1.35, P < 0.00001; heterogeneity $\chi^2 = 1.24$, df = 3 (P = 0.74), $I^2 = 0\%$] (**Figure 3A**).

Cardiac Enzyme

Meta-analysis of three studies (Deng and Lai, 2013; Xia et al., 2015; Yu et al., 2016) showed NGR1 had significant effect on decreasing CK compared with the control group [$n = 52$, SMD: -5.05, 95% CI: -8.83 to -1.28, $P = 0.009$; heterogeneity: $\chi^2 = 22.94$, df = 2 ($P < 0.0001$), $I^2 = 91\%$]. Owing to the obvious heterogeneity, we conducted a sensitivity analyses and removed one study (Yu et al., 2016) that utilized Langendroff-perfused rat hearts. Meta-analysis of the remaining two studies (Deng and Lai, 2013; Xia et al., 2015) showed NGR1 had significant effect on decreasing CK compared with the control group [$n = 32$, SMD: -2.06, 95% CI: -2.96 to -1.15, $P< 0.00001$; heterogeneity: $\chi^2 = 0.02$, df = 1 ($P = 0.89$), $I^2 = 0\%$] (**Figure 3B**). We failed to conduct meta-analysis of serum MDA in the two studies (Xia et al., 2015; Yu et al., 2016) because of high heterogeneity. However, both of them favored that NGR1 treatment could reduce the level of serum MDA compared with the control group ($P < 0.05$).

Cardiomyocyte Apoptosis Rate

Meta-analysis of six studies (He et al., 2014; Wan et al., 2015; Yu et al., 2016; Zhou et al., 2016; Zhou et al., 2017; Liu et al., 2019) showed NGR1 had significant effect on reducing TUNEL-positive cell rate compared with the control group [$n = 72$, SMD: -10.94, 95% CI: -14.77 to -7.11, $P < 0.00001$; heterogeneity: $\chi^2 = 13.83$, df = 5 ($P = 0.02$), $I^2 = 64\%$]. Owing to the obvious heterogeneity, we conducted a sensitivity analyses and removed two studies (He et al., 2014; Yu et al., 2016) that utilized subcultured cells. Meta-analysis of the remaining four studies (Wan et al., 2015; Zhou et al., 2016; Zhou et al., 2017; Liu et al., 2019) showed NGR1 had significant effect on decreasing TUNEL-positive cell rate compared with the control group [$n = 48$, SMD: -9.51,95% CI: -12.80 to -6.23, $P < 0.00001$; heterogeneity: $\chi^2 = 5.27$, df = 3 ($P = 0.15$), $I^2 = 43\%$] (**Figure 3C**).

Cardiomyocyte Viability

Meta-analysis of six studies (He et al., 2014; Wan et al., 2015; Yu et al., 2016; Zhou et al., 2016; Zhou et al., 2017; Liu et al., 2019) showed NGR1 had significant effect on increasing cell viability compared with the control group [$n = 36$, SMD: 9.31, 95% CI: 7.21 to 11.41, $P < 0.00001$; heterogeneity: $\chi^2 = 5.65$, df = 5 ($P = 0.34$), $I^2 = 12\%$] (**Figure 4**).

Cardiomyocytes LDH

Meta-analysis of four studies (He et al., 2014; Yu et al., 2016; Zhou et al., 2016; Zhou et al., 2017) showed NGR1 had significant effect on decreasing cell LDH compared with the control group [$n = 48$, SMD: -13.57, 95% CI: -21.27 to -5.88, $P = 0.0005$;

TABLE 2 | Characteristics of the 11 included cell studies.

Study (years)	Appellation (n = experimental/ control group)	Organism age tissue	Primary cells or subcultured cells	Model (method)	Treatment group (method to astragal sides)	Control group	Outcome index (time)	Intergroup differences
Zhou et al., 2016	RCM (6/6)	WistarSuckling miceMyocardium	Primary cells	Received H_2O_2 (50 μmol/L)	NGR1 (10 μmol/L; 24 h) before molding	No treatment	1. LDH 2. SOD 3. MDA 4. Cell viability 5. Apoptosis rate 6. p-ERK1/2 7. ERK1/2 8. p-p38 9. p38	1. $P < 0.01$ 2. $P < 0.01$ 3. $P < 0.01$ 4. $P < 0.01$ 5. $P < 0.01$ 6. $P < 0.01$ 7. $P < 0.01$ 8. $P < 0.01$ 9. $P < 0.01$
Zhou et al., 2017	RCM (6/6)	WistarSuckling miceMyocardium	Primary cells	Received H_2O_2 (50 μmol/L)	NGR1 (10 μmol/L; 24 h) before molding	No treatment	1. LDH 2. SOD 3. MDA 4. Cell viability 5. Apoptosis rate	1. $P < 0.01$ 2. $P < 0.01$ 3. $P < 0.01$ 4. $P < 0.01$ 5. $P < 0.01$
Wan et al., 2015	RCM (6/6)	WistarSuckling miceMyocardium	Primary cells	Received H_2O_2 (1 mmol/L)	Received NGR1 (100 μmol/L; 24 h) before molding	No treatment	1. Cell viability 2. Apoptosis rate 3. MDA 4. SOD5. p-JNK 6. Bax 7. Bcl -2	1. $P < 0.05$ 2. $P < 0.05$ 3. $P < 0.05$ 4. $P < 0.05$ 5. $P < 0.05$ 6. $P < 0.05$ 7. $P < 0.05$
Yu et al., 2016	H9C2 (6/6)	Rat embryonic cardiomyoblast-derived H9c2 cardiomyocytes	Subcultured cells	H/R (6 h/12 h)	NGR1 (20 μmol/L; 24 h) before molding	No treatment	1. Cell viability2. Extracellular LDH3. ROS4. Relative intensity of red/green fluorescence5. PIP positive cell rate6. TUNEL-positive7. GRP78/β-actin8. P-PERK/PERK9. P- elf2α/elf2α10. IRE1/β-actin11. ATF6/β-actin	1. $P < 0.001$ 2. $P < 0.001$ 3. $P < 0.01$ 4. $P < 0.001$ 5. $P < 0.01$ 6. $P < 0.001$ 7. $P < 0.01$ 8. $P < 0.001$ 9. $P < 0.001$ 10. $P < 0.01$ 11. $P < 0.001$
He et al., 2014	H9C2 (6/6)	A rat cardiac myoblast cell line	Subcultured cells	OGD/R(15 h)	NGR1 (100 μmol/L)	No treatment	1. TUNEL-positive2. Cell viability3. LDH4. Bcl-2/Bax5. Cleaved caspase-3/ procaspase-36. ATP7. AMP8. ATP synthase activity9. P-AMPK/β-actin10. ATPsynthase-α/β-actin11. ATP synthase-β/β-actin12. ATP 5D/β-actin13. ROCK/β-actin14. P-MYPT1/MYPT1	1. $P < 0.05$ 2. $P < 0.05$ 3. $P < 0.05$ 4. $P < 0.05$ 5. $P < 0.05$ 6. $P < 0.05$ 7. $P < 0.05$ 8. $P < 0.05$ 9. $P < 0.05$ 10. $P > 0.05$ 11. $P > 0.05$ 12. $P < 0.05$ 13. $P < 0.05$ 14. $P < 0.05$
Liu et al., 2019	RCM	NeonatalSD rats Myocardium	Primary cells	OGD (6 h)	NGR1 (20 μmol/L) for 24 h	No treatment	1. Cell viability2. Apoptotic cells3. RNA level expression of miR-214. mRNA and protein levels of PTEN	1. $P < 0.05$ 2. $P < 0.05$ 3. $P < 0.05$ $P < 0.05$
Meng et al., 2014	Primary cortical neurons (6/6)	SD rats embryo cerebral cortices	Primary cells	OGD/R (2 h/24 h)	NGR1 (25 μM) for 24 h before ischemia	Treated with DMSO (final concentration was 0.1%)	1. Intracellular ROS2. NADPH oxidase activity3. Superoxide levels4. Mitochondrial superoxide5. MDA6. Protein carbonyl7. 8-OHdG8. TUNEL-positive cells rate9. Apoptosis rate10. Ratio of red to green fluorescence intensity11.Cell viability12. LDH13. Caspase-3 activity	1. $P < 0.01$ 2. $P < 0.01$ 3. $P < 0.01$ 4. $P < 0.01$ 5. $P < 0.01$ 6. $P < 0.01$ 7. $P < 0.01$ 8. $P < 0.01$ 9. $P < 0.01$ 10. $P < 0.01$ 11. $P < 0.01$ 12. $P < 0.01$ 13. $P < 0.01$
Wang, 2016	Primary cortical neurons (5/5)	SD rats embryo cerebral cortices	Primary cells	OGD/R (1.5 h/24 h)	NGR1 (10 μmol/L)	DMSO (1%)	1. Cell viability2. LDH3. Ratio of GRP78/β-actin4. Ratio of P-PERK/PERK5. Cleaved-caspase-12/caspase-126. Ratio of P-IRE1α/IRE1α7. Ratio of BCL-2/β-actin	1. $P < 0.05$ 2. $P < 0.05$ 3. $P < 0.05$ 4. $P < 0.05$ 5. $P < 0.05$ 6. $P < 0.05$ 7. $P < 0.05$
Hou et al., 2017	Primary cortical neurons (5/5)	SD rats embryo cerebral cortices	Primary cells	OGD/R (1.5 h/24 h)	NGR1 (10 μmol/L)		1. Cell viability2. LDH3. ATF6/Akt4. P-Akt/Akt5. Cleaved Caspase-3/β-actin6. Bax/β-actin	1. $P < 0.05$ 2. $P < 0.05$ 3. $P < 0.05$ 4. $P < 0.05$ 5. $P < 0.05$ 6. $P < 0.05$

(Continued)

TABLE 2 | Continued

Study (years)	Appellation (n = experimental/ control group)	Organism age tissue	Primary cells or subcultured cells	Model (method)	Treatment group (method to astragal sides)	Control group	Outcome index (time)	Intergroup differences
Wang et al., 2017	Primary cortical neuron (5/5)	SD rats embryo cerebral cortices	Primary cells	OGD/R (1.5 h/24 h)	NGR1 (10 μmol/L)	DMSO (1%)	1. Cell viability2. Ratio of p-PLCβ/PLCβ3. Ratio of p-PLCγ/PLCγ4. Ratio of IP3R1/β-actin5. Ratio of p-PERK/β-actin6. Ratio of p-IRE1/β-actin7. Ratio of CHOP/β-actin8. Ratio of p-CaMKII/β-actin9. Ratio of p-P38/β-actin10. Ratio of p-JNK/β-actin11. Ratio of TUNEL-positive cells	1. P < 0.05 2. P < 0.05 3. P < 0.05 4. P < 0.05 5. P < 0.05 6. P < 0.05 7. P < 0.05 8. P < 0.05 9. P < 0.05 10. P < 0.05 11. P < 0.05
Tu et al., 2018	Primary cortical neuron (5/5)	Rats embryo cerebral cortices	Primary cells	OGD/R (1.5 h/24 h)	NGR1 (10 μmol/L)		1. Cell viability2. LDH3. Ratio of PI3K/β-actin4. P-Akt/T-Akt5. P-mTOR/T-mTOR6. P-P70S6K/P70S6K7. P-4EBP-1/4EBP-18. P-JNK/T-JNK9. P-c-JUN/c-JUN	1. P < 0.05 2. P < 0.05 3. P < 0.05 4. P < 0.05 5. P < 0.05 6. P < 0.05 7. P < 0.05 8. P < 0.05 9. P < 0.05

RCM, rat cardiac myocytes; OGD/R, oxygen glucose deprivation/reoxygenation; LDH, lactic dehydrogenase; SOD, superoxide dismutase; MDA, TUNEL, terminal deoxynucleotidyl transferase-mediated dUTP nick end labelling; p-ERK1/2, phospho extracellular regulated protein kinases; p-JNK, phospho c-Jun N-terminal kinase; ERK1/2, extracellular regulated protein kinase; Bax, Bcl-2 Associated X protein; Bcl-2, B-cell lymphoma-2; ROS, reactive oxygen species; GRP78, glucose-regulated protein 78; P-PERK, phospho protein kinase RNA-like endoplasmic reticulum kinase; PERK, PKR-like endoplasmic reticular kinase; P-eIf2α, phospho-eukaryotic initiation factor 2α; eIf2α, eukaryotic initiation factor 2; IRE1, inositol-requiring enzyme-1α; ATF6, activating transcription factor 6; P-AMPK, phosphorylation of AMP-activated protein kinase; ROCK, Rho-associated kinase protein; P-MYPT1, phosphorylating myosin light chain phosphatase; MYPT1, myosin light chain phosphatase; ATP, adenosine triphosphate; AMP, adenosine monophosphate; SD rats, Sprague-Dawley; DMSO, dimethyl sulfoxide; OGD, oxygen-glucose deprivation; NADPH, nicotinamide adenine dinucleotide phosphate; 8-OHdG, 8-hydroxy-2'-deoxyguanosine; P-IRE1α, phosphoinositol requiring enzyme 1α; Akt, protein kinase B; P-Akt, phosphorylated Akt; p-PLCβ, phospho phospholipase Cβ; PLCβ, phospholipase C β; p-PLCγ, phospho phospholipase Cγ; PLCγ, phospholipase Cγ; IP3R1, inositol 1;4;5-triphosphate receptor type 1; p-IRE1, inositol-requiring enzyme 1; CHOP, C/EBP homologous protein; p-CaMKII, phospho Ca2+/calmodulin-dependent protein kinase II; PI3K, phosphoinositide 3-kinase; P-mTOR, phosphorylated mammalian target of rapamycin; T-mTOR, mammalian target of rapamycin; P-P70S6K, P70S6K P-4EBP-1, phosphorylated 4E-binding protein 1; 4EBP-1, 4E-binding protein 1.

heterogeneity: χ^2 = 16.3, df = 3 (P = 0.001), I^2 = 82%].Owing to high heterogeneity, we conducted a sensitivity analyses and removed one study (He et al., 2014) for non-pretreatment with NGR1. Meta-analysis of the remaining three studies (Yu et al., 2016; Zhou et al., 2016; Zhou et al., 2017) showed that NGR1 had significant effect on reducing cell LDH compared with the control group [n = 36, SMD: -16.22, 95% CI: -20.93 to -11.51, P < 0.00001; heterogeneity: χ^2 = 1.92, df = 2 (P = 0.38), I^2 = 0%] (**Figure 5**).t

Cerebral Injury

Cerebral Infarction Volume

Meta-analysis of five studies (Meng et al., 2014; Dong et al., 2015; Wang et al., 2016; Zou et al., 2017; Tu et al., 2018) demonstrated NGR1 had significant effect on decreasing cerebral infarction volume compared with the control group [n = 94, SMD: -5.25, 95% CI: -6.24 to -4.27, P < 0.00001; heterogeneity: χ^2 = 13.65, df = 4 (P = 0.009), I^2 = 71%]. Owing to the obvious heterogeneity, we conducted a sensitivity analyses and removed two studies (Wang et al., 2016; Tu et al., 2018) that utilized 7-day-old SD rats. Meta-analysis of the remaining three studies (Meng et al., 2014; Dong et al., 2015; Zou et al., 2017) demonstrated NGR1 had significant effect on reducing cerebral infarction volume compared with the control group [n = 66, SMD: -6.43, 95% CI: -7.76 to -5.11, P < 0.00001; heterogeneity: χ^2 = 3.06, df = 2 (P = 0.22), I^2 = 35%] (**Figure 6**).

Neurologic Deficit Score

Meta-analysis of two studies (Meng et al., 2014; Dong et al., 2015) demonstrated NGR1 had significant effect on reducing neurologic deficit score compared with the control group [n = 26, SMD: -1.58, 95% CI: -1.87 to -1.28, P< 0.00001; heterogeneity: χ^2 = 0.35, df = 1 (P = 0.56), I^2 = 0%] (**Figure 7**).

Cerebral Cell Viability

Meta-analysis of five studies (Wang et al., 2016; Wang et al., 2017; Hou et al., 2017; Tu et al., 2018) demonstrated NGR1 had significant effect on increasing cell viability compared with the control group [n = 54, SMD: 4.34, 95% CI: 3.16 to 5.52, P < 0.00001; heterogeneity: χ^2 = 2.19, df = 4 (P = 0.70), I^2 = 0%] (**Figure 8**).

Renal Injury

One study (Liu et al., 2010) reported that NGR1 had significant effect on reducing MPO and serum creatinine compared with the control group (P < 0.05).

Intestinal Injury

One study (Li et al., 2014) reported that NGR1 had significant effect on reducing MPO and Park/Chiu score compared with the control group (P < 0.05).

Organ-Protection Mechanisms

For animal experiments, meta-analysis of two studies (Han, 2014; He et al., 2014) showed NGR1 had significant effect on increasing ATP compared with the control group [n = 28, SMD: 20.20, 95%

TABLE 3 | Statement of the characteristics of NGR1.

Study	Source	Species, concentration	Quality control reported? (Y/N)	Chemical analysis reported? (Y/N)
Liu et al., 2010	Chinese National Institute for the Control of Pharmaceutical and Biological Products	*Panax notoginseng*40 mg/kg	N	Y-HPLC
Deng and Lai 2013	Guangxi Wuzhou Pharmaceutical (Group) Co., Ltd	*P. notoginseng*, 10 mg/kg	Y(120502)	N
Han, 2014	Fengshanjian Medicine Research Co. Ltd. (Kunming, Yunnan, China)	*P. notoginseng*, 5 mg/kg	N	N
He et al., 2014	Feng-Shan-Jian Medical, Kunming, China	*P. notoginseng,* 20 mg/kg	N	N
He et al., 2014	Feng-Shan-Jian Medical, Kunming, China	*P. notoginseng*, 0.1 mM	N	N
Li et al., 2014	Feng-Shan-Jian Medical (Kunming, China)	*P. notoginseng*, 10 mg/kg	N	N
Meng et al., 2014	Shanghai Winherb Medical S & T Development (China)	*P. notoginseng*, 20 mg/kg	N	Y-HPLC
Meng et al., 2014	Shanghai Winherb Medical S & T Development (China)	*P. notoginseng*, 25 μM	N	Y-HPLC
Yu et al., 2014	Chengdu Must Bio-Technology Co., Ltd	*P. notoginseng*, 2.5 mg/kg/d	Y(MUST-23091001)	Y-HPLC
Dong et al., 2015	Nanjing ZeLang Medicine Photochemistry Technology Co., Ltd	*P. notoginseng*, 7 mg/kg	N	N
Xia et al., 2015	National Institutes for Food andDrug Control (Beijing, China)	*P. notoginseng*, 60 mg/kg	N	Y-HPLC
Wan et al., 2015	Chengdu Must Bio-Technology Co., Ltd	*P. notoginseng*, 100 μM	N	Y-HPLC
Wang et al., 2016	SigmaAldrich	*P. notoginseng*	N	N
Yu et al., 2016	Shanghai Winherb Medical S&T Development (Shanghai, China)	*P. notoginseng*, 15 mg/kg	N	Y-HPLC
Yu et al., 2016	Shanghai Winherb Medical S&T Development (Shanghai, China)	*P. notoginseng*, 20 μM	N	Y-HPLC
Zhou et al., 2016	Guangzhou Institute for drug control	*P. notoginseng*, 10 μmol/L	N	N
Wang et al., 2016	SigmaAldrich	*P. notoginseng*, 20 mmol/L	N	Y-HPLC
Hou et al., 2017	Nanjing Jiancheng Bioengineering Institute	*P. notoginseng*, 20 μmol/L	N	N
Wang et al., 2017	Sigma-Aldrich	*P. notoginseng*, 10 μmol/L	N	Y-HPLC
Zhao et al., 2017	Shanghai Yuanye Biological Technology Co. Ltd	*P. notoginseng*, 5mg/ml	N	N
Zhou et al., 2017	Guangzhou Institute for drug control	*P. notoginseng*, 10 μM	N	N
Zou et al., 2017	Shanghai Ronghe Pharmaceutical Technology Development Co., Ltd	*P. notoginseng*, 100 mg/kg	N	Y-HPLC
Liu et al., 2019	Sigma-Aldrich	*P. notoginseng*, 80μM	N	Y-HPLC
Tu et al., 2018	Sigma-Aldrich	*P. notoginseng*, 15 mg/kg	N	Y-HPLC
Tu et al., 2018	Sigma-Aldrich	*P. notoginseng*, 10 μmol/l	N	Y-HPLC

CI: 13.91 to 26.50, $P < 0.00001$; heterogeneity: $\chi^2 = 0.16$, df = 1 ($P = 0.69$), $I^2 = 0\%$] (**Figure 9**). One study (He et al., 2014) showed that NGR1 increased the proportion of anti-apoptosis proteins such as Bcl-2/Bax and cleaved caspase-3/procaspase-3 compared with the control group ($P < 0.05$); one study (Yu et al., 2014) showed that NGR1 increased the density of neovasculature and improved the expression of angiogenesis protein such as VEGF and bFGF compared with the control group ($P < 0.05$); one study (He et al., 2014) showed that NGR1 improved the production of ATP and ATP5D compared with the control group ($P < 0.05$); one study (He et al., 2014) demonstrated that NGR1 reduced the protein level of phosphorylation-AMP-activated protein kinase (P-AMPK), Rho-associated coil kinase (ROCK), and phosphorylation-myosin phosphatase target subunit-1 (P-MYPT1) compared with the control group ($P < 0.05$); one study (Xia et al., 2015) indicated that NGR1 decreased the inflammatory mediators such as IL-1β and IL-8 compared with the control group ($P < 0.05$); one study (Xia et al., 2015) indicated that NGR1 decreased the expression of phosphorylation-nuclear factor-κBp65 (p-NF-κBp65) and phosphorylation-nuclear factor of kappa light polypeptide gene enhancer in B-cells inhibitor alpha (p-IκBα) compared with the control group ($P < 0.05$); one study (Yu et al., 2016) indicated that NGR1 lowered the level of ERS-responsive proteins, such as glucose regulated protein 78 (GRP78), phospho-protein kinase R-like ER kinase (P-PERK), activating transcription factor 6 (ATF6), and inositol-requiring enzyme-1α (IRE1) compared with the control group ($P < 0.05$); one study (Meng et al., 2014) indicated that NGR1 decreased the expression of 8-hydroxy-2 deoxyguanosine (8-OHDG) compared with the control group ($P < 0.05$); one study (Tu et al., 2018) demonstrated that NGR1 increased the synthesis of ribosomal translation regulatory proteins such as phospho-mammalian target of rapamycin (P-mTOR), phospho-protein S6 kinase (P-P70S6K), and phospho-eukaryotic initiation factor 4E binding protein 1 (P-4EBP-1) compared with the control group ($P < 0.05$); one study (Tu et al., 2018) demonstrated that NGR1 reduced the expression of pro-apoptotic proteins, such as phospho-c-Jun N-terminal kinase (P-JNK) compared with the control group ($P < 0.05$); one study (Zhou et al., 2016) showed that NGR1 decreased the level of extracellular regulated protein kinases (ERK1/2) and p38-mitogen-activated protein kinase (p38MAPK) compared with the control group ($P < 0.01$).

TABLE 4 | Risk of bias of the included *in vivo* studies.

Study	A	B	C	D	E	F	G	H	I	J	Total
Deng and Lai 2013	√		√			√					3
Han, 2014	√	√	√			√					4
He et al., 2014	√	√	√	√		√			√	√	7
Yu et al., 2014	√		√	√		√				√	5
Xia et al., 2015	√	√	√	√		√			√	√	7
Yu et al., 2016	√	√	√	√	√	√			√	√	8
Tu et al., 2018	√	√				√			√	√	5
Meng et al., 2014	√	√	√		√	√			√	√	7
Zou et al., 2017	√	√	√			√			√		5
Wang et al., 2016	√	√				√			√	√	5
Zhao et al., 2017	√	√				√					3
Dong et al., 2015	√	√				√				√	4

Studies fulfilling the criteria of: A, peer reviewed publication; B, control of temperature; C, random allocation to treatment or control; D, blinded induction of model; E, blinded assessment of outcome; F, use of anesthetic without significant intrinsic vascular protection activity; G, appropriate animal model (aged, diabetic, or hypertensive); H, sample size calculation; I, compliance with animal welfare regulations; J, statement of potential conflict of interests.

TABLE 5 | Risk of bias of the included *in vitro* studies.

Study	A	B	C	D	E	F	G	H	I	J	Total
He et al., 2014	√			√	√					√	4
Wan et al., 2015	√				√					√	3
Zhou et al., 2016	√	√			√					√	4
Zhou et al., 2017	√	√			√					√	4
Liu, 2018	√	√		√	√					√	5
Meng et al., 2014	√	√		√	√					√	5
Wang, 2016	√	√		√	√					√	5
Wang et al., 2017	√	√		√	√					√	5
Hou et al., 2017	√	√		√	√					√	5
Tu et al., 2018	√	√		√	√					√	5

Studies fulfilling the criteria of: A, peer-reviewed publication; B, use of appropriate primary cells to study; C, cell lines with reliable source or validated by appropriate methods; ,D, assess toxicity of treatment on cells; E, culture environment (culture media/sera, pH/CO_2 and temperature); F, random allocation to treatment or control; G, blinded induction of model; H, blinded assessment of outcome; I, calculation of the sample size necessary to achieve sufficient power; and J, statement of potential conflict of interests. Each item was awarded one point.

We summarized a schematic representation for the possible intrinsic mechanisms of NGR1 protection for organ I/R injury (**Figure 10**).

DISCUSSION

Summary of Evidence

To our knowledge, this is a first SR to assess the preclinical evidences of NGR1 for I/R injury both *in vivo* and *in vitro*. Twenty-five studies with 304 animals and 124 cells were selected. The quality of the included studies was generally moderate. In the present study, NGR1 exerts multiple organ protection in I/R injury, mainly through antioxidant, anti-apoptosis, and anti-inflammatory, promoting angiogenesis and improving energy metabolism.

Limitations

None of these studies had used animals with comorbidities such as diabetes, hypertension, or hyperlipidemia. Primary cells were considered to be the suitable subjects to validate organ protective function *in vitro*, while only two studies (Xia et al., 2015; Yu et al., 2016) used subcultured cells (H9C2). None of these studies reported the blindness of ischemia induction, randomized allocation to treatment, or control group and sample size calculation. In most studies, the signal pathways investigated could not fully validate the therapeutic targets.

Implications

Our findings demonstrated that NGR1 could attenuate I/R-induced organ injuries by a variety of pathways. For myocardial I/R injury, NGR1 could reduce MI size, increase cardiomyocyte viability, and exert cardioprotective function by the following mechanisms: 1) anti-inflammatory effect by activating the VDUP1/NF-κB signaling pathway (Xia et al., 2015) and decreasing the expression of ICAM-1 and CD18 (Han, 2014); 2) improving energy metabolism *via* up-regulation of ROCK signaling pathway (He et al., 2014); 3) promoting angiogenesis by increasing the expression of VEGF and bFGF (Yu et al., 2014); 4) inhibiting apoptosis by decreasing the expression level of ERS-responsive proteins such as GRP78, P-PERK, ATF6,

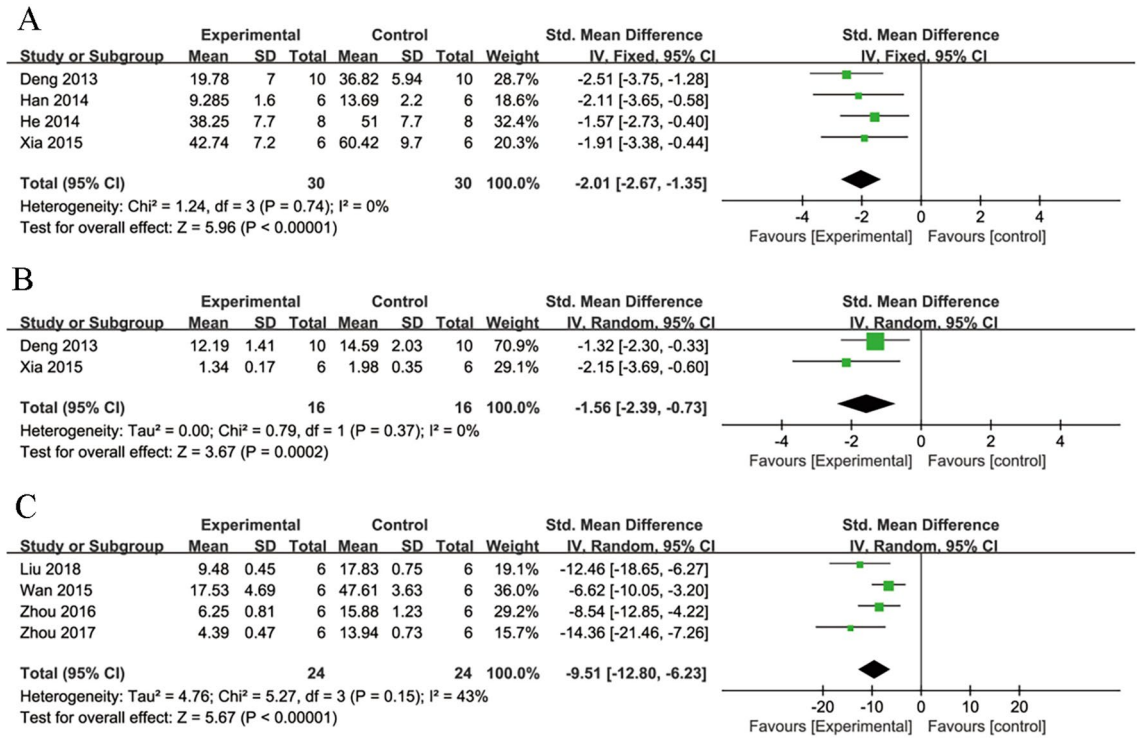

FIGURE 3 | The forest plot: **(A)** effects of notoginsenoside R1 for reducing the myocardial infarction size compared with the control group (n = 30 per group). **(B)** Effects of notoginsenoside R1 for reducing the creatine kinase compared with the control group (n = 16 per group). **(C)** The forest plot: effects of notoginsenoside R1 for reducing cardiomyocytes apoptosis rate compared with the control group (n = 24 per group).

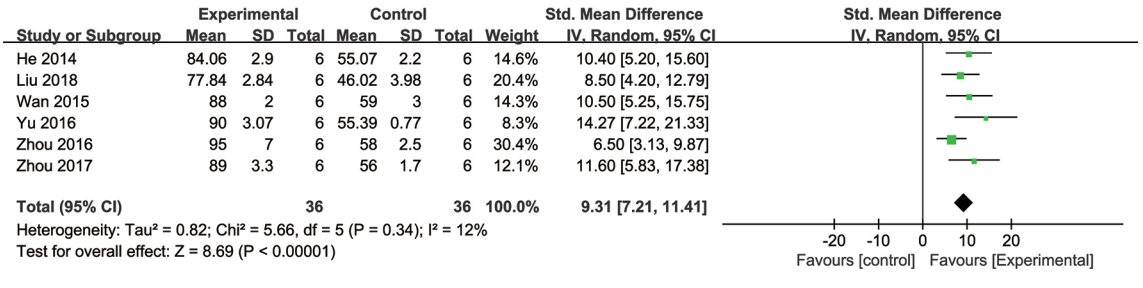

FIGURE 4 | The forest plot: effects of notoginsenoside R1 for increasing cardiomyocytes cell viability compared with the control group (n = 36 per group).

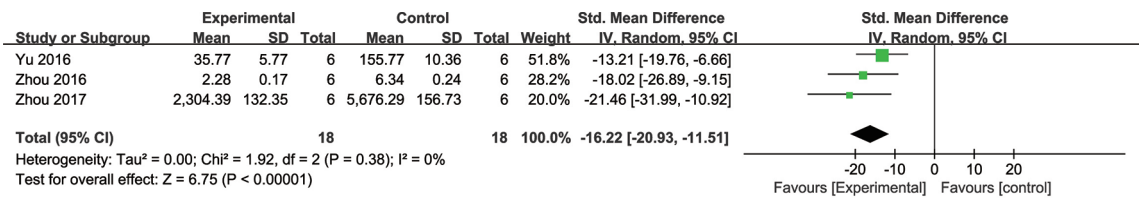

FIGURE 5 | The forest plot: effects of notoginsenoside R1 for reducing cardiomyocytes LDH release compared with the control group (n = 18 per group).

and IRE, and reducing the expression of pro-apoptosis proteins such as CHOP, Caspase-12, and P-JNK (Yu et al., 2016); and 5) improving microvascular dysfunction by increasing the expression of tight junction proteins such as ZO-1, VE, JAM-1, and Claudin-5 and reducing the level of embrane intrinsic protein of Cav-1 and Cav-3 (Han, 2014). For cerebral I/R injury, NGR1 could decrease cerebral infarction volume (Meng et al., 2014; Dong et al., 2015; Wang et al., 2016; Zou et al., 2017; Tu et al., 2018) and neurological deficit score (Meng et al., 2014; Dong et al., 2015) and increase cerebral cell viability

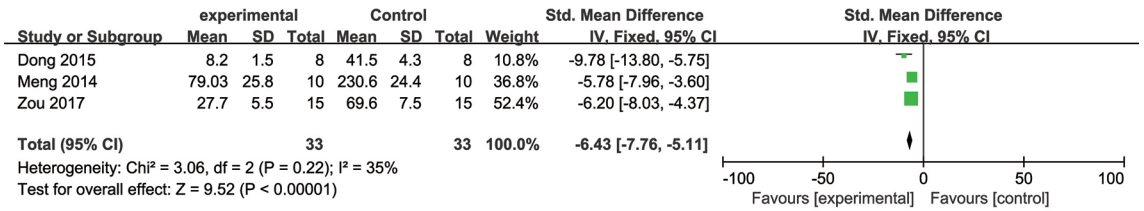

FIGURE 6 | The forest plot: effects of notoginsenoside R1 for reducing cerebral infarction volume compared with the control group (n = 33 per group).

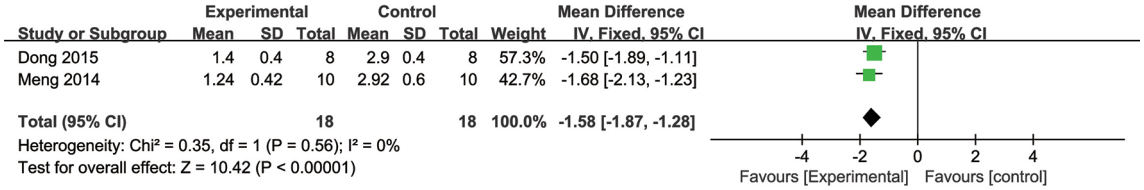

FIGURE 7 | The forest plot: effects of notoginsenoside R1 for reducing neurologic deficit score compared with the control group (n = 18 per group).

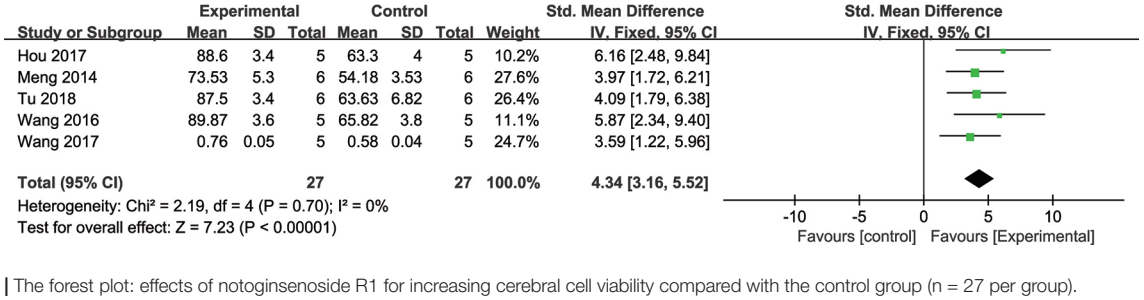

FIGURE 8 | The forest plot: effects of notoginsenoside R1 for increasing cerebral cell viability compared with the control group (n = 27 per group).

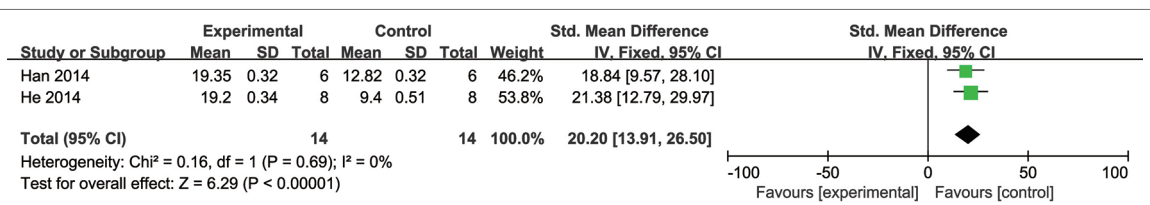

FIGURE 9 | The forest plot: effects of notoginsenoside R1 for increasing ATP compared with the control group (n = 14 per group).

(Wang et al., 2016; Hou et al., 2017; Wang et al., 2017; Tu et al., 2018). The neuroprotective effect of NGR1 was mainly due to anti-apoptosis effect by regulating the Akt/Nrf2 and Akt/mTOR/JNK pathways (Tu et al., 2018). For renal I/R injury, NGR1 had an anti-inflammatory effect through the p38MAPK/NFκB pathway and also increased the proportion of bcl-2/bax, which could produce anti-apoptosis effect (Liu et al., 2010). For intestinal I/R injury, NGR1 could attenuate the production of inflammatory cytokine by inhibiting the NF-κB pathway and reduce the expression of loss of tight junction proteins such as zonula occluden-1 (ZO-1), occludin, and claudin-5. It was also reported that NGR1 could improve the energy metabolism *via* depressing ATP5D expression during intestinal I/R injury (Li et al., 2014). Although NGR1 could exert organ-protective effect in I/R injury *via* multiple signal pathways, the validation of NGR1 therapeutic target is insufficient. In the process of drug discovery, it is common to perform target validation to illustrate 1) the function of the potential target in disease phenotype 2) and the therapeutic efficacy of drug-like molecules through modulating the activities of the potential target (Zhu et al., 2012; Gashaw et al., 2012). The approach of validation generally included gene knockout/knockdown *in vivo*, pharmacological inhibitors, and small interfering RNA (SiRNA) of cells *in vitro* (Overall and Kleifeld 2006). In the present study, four studies (He et al., 2014; Meng et al., 2014; Yu et al., 2016; Tu et al., 2018) used signal pathway inhibitors to validate the drug targets. However, the remaining studies were not verified. Although inhibitors enjoy strong suppression functions and high selectivity, the severe side effects in organisms mean that this is not the best way to study potential targets for drugs (May et al., 2011; Yan 2016).

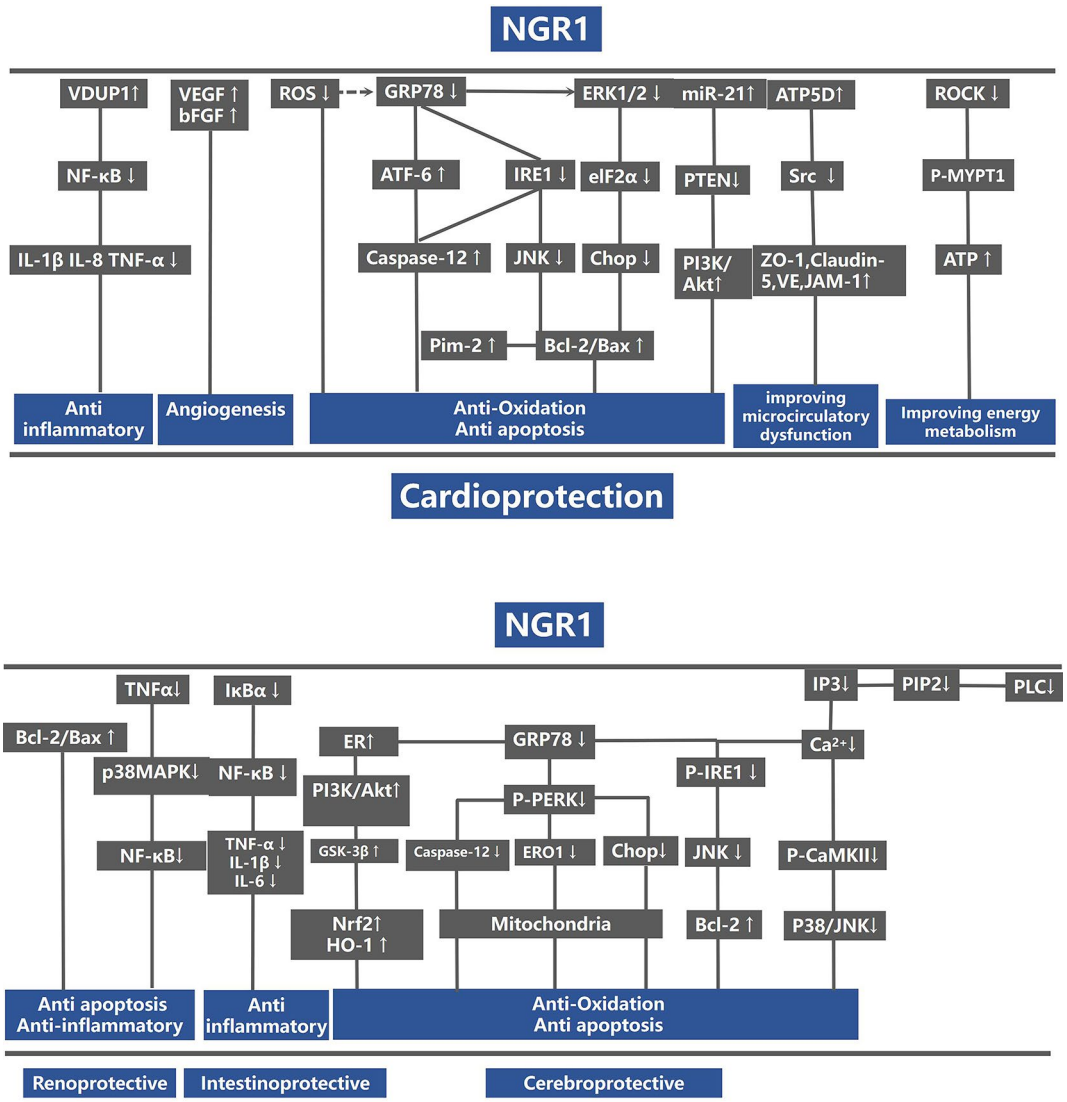

FIGURE 10 | A schematic representation of cardioprotective mechanisms of NGR1 for organs ischemia/reperfusion injury. VDUP1, vitamin D3 up-regulated protein 1; NF-κB, nuclear factor-kappa; IL-1, interleukin-1; IL-1β, interleukin 1 beta; IL-8, interleukin-8; TNF-α, tumor necrosis factor-α; VEGF, vascular endothelial growth factor; bFGF, basic fibroblast growth factor; GRP78, glucose regulated protein 78; PERK, protein kinase R-like ER kinase; ATF-6, activating transcription factor 6; IRE1, inositol-requiring enzyme-1α; JNK, Jun N-terminal kinase; CHOP, C/EBP homologous protein; B-cell lymphoma-2; Bax, BCL2-associated X protein; elf2α, eukaryotic initiation factor 2α; PTEN, phosphatase and tensin homolog deleted on chromosome ten; PI3K, p-mTOR, phospho-mammalian target of rapamycin; ZO-1, Zonula occludens-1; JAM-1, recombinant junctional adhesion molecule 1; Cav-1, caveolin 1; Cav-3, caveolin 3; MYPT1, myosin phosphatase target subunit-1; ATP, adenosine triphosphate; ROCK, Rho-associated kinase; GSK-3β, glycogen synthase kinase-3 beta; IκBα, nuclear factor of kappa light polypeptide gene enhancer in B-cells inhibitor; alpha; HO-1, heme oxygenase-1; Nrf2, nuclear factor erythroid 2-related factor 2; IP3, inositol 1, 4, 5-trisphosphate; PLC, phospholipase C.

Owing to different isoforms may hold different functions, gene knockout technique effectively eliminates all isoforms possessing alternative splicing of the precursor messenger RNAs (mRNAs) and post-translational modifications compared with RNA interference (Smith, 2003). Unfortunately, it is widespread that off-target effects highly occurred in gene knockdown (Kok et al., 2015). Thus, a call for researchers should utilize animal with gene knockout to validate the drug target.

A multitude of preclinical researches showed that many available medical treatment strategies share good efficacy on animal models, while they have poor efficacy in clinical practice (Worp and Sandercock, 2012). High-quality preclinical study can provide vital information for justifying clinical advancement (Henderson et al., 2013). An SR of preclinical research is a novel method that offers important information for future clinical trials. According to CAMARADES 10-item checklist, the score of the included studies was medium. They are similar to other animal studies, and the main limitations were that no study reported sample size calculation, allocation concealment, and blinding of outcome assessment (Bao et al., 2018). Inadequate

sample size could not reach the approximately threshold with sufficient power and efficacy (Bacchetti 2010). Blinding of the ischemia model refers to establishing ischemia models for experimental animals firstly and then assigning randomly. This method can avoid selection bias in allocating the animals to the treatment groups and makes it more likely that the intergroups are comparable (Festing and Altman, 2002). An overview study involving seven meta-analyses demonstrated that unblinded induction of ischemia had a greater effect size (about 13.1%) than studies that included blinding (Crossley et al., 2008). Thus, the poor blinding of the ischemia model induction and outcome evaluation may lead to overestimating efficacy in preclinical studies (Crossley et al., 2008). Those who were attacked with IHD tend to possess an advanced age and coexist with diabetes mellitus, hyperglycemia, and hypertension (Heusch 2017; Davidson et al., 2019). However, investigators prefer to utilize young healthy animals to conduct research. This may overestimate the efficacy of intervention compared with clinical administration (Sanne et al., 2014). Accordingly, researchers should take the following factors into account: 1) improving the quality of study design; 2) blinding for induction of ischemia models and evaluation of outcomes; 3) reporting completely experimental program (sample size calculation, allocation concealment) and result; and 4) utilizing animals with comorbidities that can maximally mimic the ischemia patients suffering from hypertension, hyperlipidemia, and diabetes.

The animal model that holds maximum replication of important functional, structural, and molecular pathological characteristics of human disease is crucial to clinical translation (Saulnier-Blache et al., 2018). LAD ligation in rats is the most common I/R injury model (Nishina et al., 2001; Macarthur et al., 2013). MCA occlusion is a widely accepted model to mimic human stroke and to explore the mechanism of stroke (Durukan and Tatlisumak 2007). In the present study, most of the included studies selected these two recognized models, except one study (Deng and Lai, 2013) by injecting pituitrin and three studies (Wang et al., 2016; Tu et al., 2018; Zou et al., 2017) *via* ligating one or bilateral common carotid artery. Small animals such as mice and rats are the most commonly used vertebrate species because of their small size, low cost, easy handling, and fast reproduction rate (Seabrook et al., 2017). However, compared with humans, small animals have some limitations with small body size, short lifetime, and fundamentally distinct physiology (Cibelli et al., 2013). Large animal models are highly similar with human anatomy and pharmacodynamics, which can provide a choice of appropriate animal models for particular human disease conditions and medical applications (Van Hout et al., 2015). However, it also has weaknesses such as more expensive, difficult to manipulate, and ethical issues. Thus, we should select an ideal model that usually is a biological representative of human disease, inexpensive, reproducible, easily manipulated, and ethically sound according to experimental purpose.

A powerful outcome measure is essential to certify the efficacy of new therapy (Hietamies et al., 2018). In MI research, LVEF is the strongest predictor factor for post-MI both clinically (Barthel et al., 2013) and preclinically (Kanelidis et al., 2017). Cardiac troponins, especially the cTnI and cTnT, are the preferred biomarkers for the diagnosis and prognosis of MI clinically (Thygesen et al., 2012; Hall et al., 2015). Plasma cTnI can also serve as a predictor for myocardial injury in small animal models (Frobert et al., 2015). In cerebral ischemia, perfusion-weighted magnetic resonance imaging is an identified predictor, which can evaluate the ischemic stroke patients with perfusion abnormalities (Sasaki et al., 2011; Powers et al., 2018). In renal ischemia, GFR is an essential indicator to predict prognosis for renal injury, which can reflect the efficacy of intervention through renal blood flow and regional perfusion in the clinical setting (Dagher et al., 2003). However, few present included studies selected these important outcomes. Thus, they should be selected in priority of further myocardial I/R injury studies.

Primary cell with wild-type and unadulterated nature more closely mimics the physiological state of cells *in vivo* and generates more relevant data representing living systems (Astashkina et al., 2012; Egger et al., 2013). In nerve cell I/R models, all cells were harvested from the cerebral cortices of rat fetuses. However, in cardiomyocytes I/R models, two studies (He et al., 2014; Wan et al., 2015) used cell lines (H9C2), which did not accurately simulate the physiological and pathological state of the cells *in vivo*. Cell viability examination is a routine assay that can quantitatively assess cell reaction to drug administration. Meanwhile, the optimal drug concentration is vital for pharmacological research in cellular models, which can achieve maximum efficacy while ensuring drug safety, providing a reference for further *in vivo* experiments (Astashkina et al., 2012; Bao et al., 2018). 3-(4,5-Dimethyl-2-thiazolyl)-2,5-diphenyl-2Htetrazolium bromide (MTT) and Cell Counting Kit-8 (CCK-8) are two classical assay methods used to detect cell viability and sift the optimal drug concentration. Eight studies (Zhou et al., 2016; Wan et al., 2015; Yu et al., 2016; Wang et al., 2016; Hou et al., 2017; Wang et al., 2017; Zhou et al., 2017; Tu et al., 2018) used MTT assay, and two studies (He et al., 2014; Meng et al., 2014; Liu et al., 2019) used the CCK-8 assay. However, one study (He et al., 2014) did not conduct the assay of screening the optimal drug concentration. OGD/R is a good method for mimicking the general pathophysiological process of I/R injury at the cellular level (Jones et al., 2004). However, there are various methods for constructing cell hypoxia. Many home-made devices or chemical agents are used to create hypoxia environment. The oxygen concentration is not uniform, and the time of hypoxia varies greatly, which makes the research results to lack comparability. In addition, all included studies did not report allocation concealment, blinding of model induction, and blinding of outcome assessment. Thus, we recommend that researchers should utilize primary cells and the appropriate methods of induction in study, select optimal drug concentration, and report experimental protocols with complete information. Standardized preclinical research reporting, suitable animal/cell models, and appropriate primary outcome measures are crucial to translation from bench to bed. In order to better explore the protective function of NGR1 in I/R injury of multiple organs, researchers should add more animal/cell experiments in other less studied organs such as the liver, lung, renal, and intestinal ischemia.

To date, there has been no available therapy clinically that can alleviate I/R injury (Cung et al., 2015). An enduring ischemia leads to irreversible damage for cardiomyocytes and neurons with the low ability to regenerate or renew (Galluzzi et al., 2009; Jennings 2013). And delayed reperfusion is associated with high mortality in patients after primary PCI (Terkelsen et al., 2010). In the present study, seven studies (Deng and Lai, 2013; Li et al., 2014; Li et al., 2014; Han, 2014; He et al., 2014; Meng et al., 2014; Dong et al., 2015; Xia et al., 2015) had reported that experimental subjects were pretreated with NGR1 before modeling, and the rest of the studies had not exploited pretreatment methods. Owing to the slow onset time of herbal efficacy, administration of herbs before the induction of models was often used for herbal pharmacological researches in order to reach the effective plasma concentration. Thus, pretreatment of NGR1 before molding establishment exerts a therapeutical role rather than an approach of preventive treatment. In addition, the treatment at post-model induction is more in line with clinical practice. Definitely, it is more appropriate to study herbal pharmacology in both two different administrations.

NGR1 belongs to 20(S)-protopanaxatriol type ginsenoside, which possesses glycosides moieties at C-6 and/or C-20. NGR1 has a poor bioavailability due to fast elimination from plasma and low permeability (Zhang et al., 2019). And the direct absorption of natural ginsenosides is quite not easy due to the fact that they need to be transformed into secondary saponins *via* the metabolism of gut, and then they can be easily absorbed and utilized in the blood (Liu et al., 2009). Previous study showed a low permeability of the main metabolites of NGR1 across the Caco-2 cell monolayer, which implies a poor absorption (<1%) in humans after being taken orally; however, the permeability of the metabolites of NGR1 in intestinal bacteria is higher than that in the Caco-2 cell monolayer (Ruan et al., 2010). These findings may suggest that metabolites of NGR1 forming by intestinal bacteria have a better effect than NGR1. They are eliminated from the gastrointestinal tract to produce a series of disaccharide glycosides, including ginsenoside Rg1, notoginseng saponins R2, ginseng saponins Rh1, ginsenosides F1, and glycoside ligand proglycerol (Liu et al., 2009). The four metabolites of NGR1, including ginsenoside Rg1, notoginsenoside R2, ginsenoside Rh1, ginsenoside F1, and the aglycone protopanaxatriol, have been identified and display relative high exploration in rat plasma (Zhang et al., 2019). *In vitro* experiments mainly include the following functions: 1) carrying on experiment in Caco-2 cell to evaluate the absorption of compounds through the inner layer of the gastrointestinal tract (Artursson et al., 2001); 2) identifying the disposition of compounds among organs to study the distribution mechanism; and 3) studying and quantitating the metabolism of chemicals (Pelkonen and Turpeinen 2007). The role of experimental studies *in vitro* of the review mainly sifts the optimum concentration and explores the signaling pathway, while experimental studies *in vivo* mainly focus on the change of infarct size and the indicator relating to clinical trials (such as creatine kinase, neurologic deficit score). Previous studies have shown that the results of intervention in vitro extrapolating to the observation in vivo remains very challenging. (Wienkers and Heath, 2005; Joris et al., 2013; Hadjidemetriou et al., 2015). In the present review, the included studies did not test the metabolites of NGR1 to explore the protection mechanism on ischemic diseases. Recent studies have shown that ginsenoside metabolites share better biological effects than those of ginsenosides (Feng et al., 2017). Studies have shown that the metabolites of ginsenosides Rb1 can form rare ginsenosides such as Rg3, Rd, F2, and compound K with high bioactive functions by physical and biological treatments (Oh and Kim 2016; Fu et al., 2017). Ginsenosides Rg3 has a strong protection on cerebral ischemia compared with other ginsenosides such as Rg1, Rh2, and Rg5 (Cheng et al., 2019). Compound K showed great protection on Alzheimer's disease and cerebral ischemia *via* enhancing cognition effects and decreasing inflammatory biomarkers (Oh and Kim 2016), and has protective effects on myocardial IR injury *via* reducing infarct size and activating the PI3K pathway (Tsutsumi et al., 2011). Similarly, ginsenoside and notoginsenoside belong to same group of triterpenoid saponins, and thus we extrapolated that NGR1 should own the same property: the metabolites of NGR1 have a greater efficacy than NGR1. Owing to the lack of direct evidence of the metabolites of NGR1, they should be further tested directly in order to extend the findings of animal models to the clinic. Currently, the application of metabolomics in herbal medicine is a research focus (Wang et al., 2017; Bi et al., 2017). So, further study should test the metabolites of NGR1 directly and one of the proper methods through using metabolomics.

CONCLUSION

The findings of the present study demonstrated that NGR1 exerts organ protective functions for I/R injury, mainly through antioxidant, anti-inflammatory, and anti-apoptosis, increasing energy metabolism and angiogenesis. Further translation studies are needed.

DATA AVAILABILITY STATEMENT

The datasets generated for this study are available on request to the corresponding author.

AUTHOR CONTRIBUTIONS

QT, P-CZ, ZZ, L-HD, Z-HW, HZ, G-QZ, and YW designed the study. ZZ, L-HD, and Z-HW collected the data. QT, P-CZ, HZ, and ZZ performed all analyses. QT and P-CZ wrote the manuscript.

FUNDING

This work was supported by the grant of the National Natural Science Foundation of China (81573750/81473491/81173395/H2902).

REFERENCES

Alex, D., Felipe, D. P., Giovanni, S., Lach, A. B., Galfo, F., Mendonca, B. P., et al. (2017). Ammonium tetrathiomolybdate following ischemia/reperfusion injury: Chemistry, pharmacology, and impact of a new class of sulfide donor in preclinical injury models. *PLOS Med.* 14 (7), e1002310–. doi: 10.1371/journal.pmed.1002310

Artursson, P., Palm, K., and Luthman, K. (2001). Caco-2 monolayers in experimental and theoretical predictions of drug transport. *Adv. Drug Deliv. Rev.* 46. doi: 10.1016/S0169-409X(00)00128-9

Astashkina, A., Mann, B., and Grainger, D. W. (2012). A critical evaluation of *in vitro* cell culture models for high-throughput drug screening and toxicity. *Pharmacol. Ther.* 134 (1), 82–106. doi: 10.1016/j.pharmthera.2012.01.001

Bacchetti, P. (2010). Current sample size conventions: flaws, harms, and alternatives. *BMC Med.* 8 (1), 17–10. doi: 10.1186/1741-7015-8-17 8,1(2010-03-22).

Bao, X. Y., Zheng, Q., Tong, Q., Zhu, P. C., Zhuang, Z., Zheng, G. Q., et al. (2018). Danshensu for Myocardial Ischemic Injury: Preclinical Evidence and Novel Methodology of Quality Assessment Tool. *Front. Pharmacol.* 9, 1445. doi: 10.3389/fphar.2018.01445

Barthel, P., Wensel, R., Bauer, A., Muller, A., Wolf, P., Ulm, K., et al.. (2013). Respiratory rate predicts outcome after acute myocardial infarction: a prospective cohort study. *Eur. Heart J.* 34 (22), 1644–1650. doi: 10.1093/eurheartj/ehs420

Bi, W., Liu, H., Shen, J., Zhang, L. H., Li, P., Peng, B., et al. (2017). Chemopreventive effects of ku-jin tea against aom-induced precancerous colorectal lesions in rats and metabolomic analysis. *Sci. Rep.* 7 (1), 15893. doi: 10.1038/s41598-017-16237-0

Chen, G. Y., and Nuñez, G. (2010). Sterile inflammation: sensing and reacting to damage. *Nat. Rev. Immunol.* 10 (12), 826–837. doi: 10.1038/nri2873

Cheng, Z. K., Zhang, M., Ling, C. L., Zhu, Y., Ren, H. W., Hong, C., et al. (2019). Neuroprotective Effects of Ginsenosides against Cerebral Ischemia. *Molecules* 2019, 24(6). doi: 10.3390/molecules24061102

Cibelli, J., Emborg, M. E., Prockop, D. J., Roberts, M., Schatten, G., Rao, M., et al. (2013). Strategies for improving animal models for regenerative medicine. *Cell Stem Cell* 12 (3), 271–274. doi: 10.1016/j.stem.2013.01.004

Crossley, N. A., Sena, E., Goehler, J., Horn, J., Bart, V. D. W., Bath, P. M. W., et al. (2008). Empirical evidence of bias in the design of experimental stroke studies: a metaepidemiologic approach. *Stroke* 39 (3), 929–934. doi: 10.1161/STROKEAHA.107.498725

Cung, T. T., Morel, O., Cayla, G., Rioufol, G., Garcia-Dorado, D., Angoulvant, D., et al. (2015). Cyclosporine before PCI in Patients with Acute Myocardial Infarction. *N. Engl. J. Med.* 373, 1021–1031. doi: 10.1056/NEJMoa1505489

Dagher, P. C., Herget-Rosenthal, S., Ruehm, S. G., Jo, S. K., Star, R. A., and Agarwal, R. (2003). Newly developed techniques to study and diagnose acute renal failure. *J. Am. Soc. Nephrol.* 14 (8), 2188–2198. doi: 10.1097/01.ASN.0000079790.91292.4A

Davidson, S. M., Ferdinandy, P., Andreadou, I., Bøtker, H. E., Heusch, G., Ibáñez, B., et al. (2019). Multitarget Strategies to Reduce Myocardial Ischemia/Reperfusion Injury: JACC Review Topic of the Week. *J. Am. Coll. Cardiol.* 73, 89–99. doi: 10.1016/j.jacc.2018.09.086

De Vries, R. B. M., Wever, K. E., Avey, M. T., Stephens, M. L., Sena, E. S., and Leenaars, M. (2014). The usefulness of systematic reviews of animal experiments for the design of preclinical and clinical studies. *ILAR J.* 55 (3), 427–437. doi: 10.1093/ilar/ilu043

Deng, H. Y., and Lai, W. G. (2013). Protective Effect of Notoginsenoside R1 on Acute Myocardial Ischemia in Rats Model. *Chin. J. Exp. Tradit. Med. Formulae* (10). doi: 10.11653/syfj2013100265

Dong, X. H., Zhang, C. L., Wu, Z. G., Shen, L. X., Zhang, D. S., and Meng, X. Y. (2015). Protective effect of notoginsenoside R1 on cerebral ischemia-reperfusion injury in rats. *Chin. J. Gerontol.* v.35 (07), 1940–1942. doi: 10.3969/j.issn.1005-9202.2015.07.093

Durukan, A., and Tatlisumak, T. (2007). Acute ischemic stroke: overview of major experimental rodent models, pathophysiology, and therapy of focal cerebral ischemia. *Pharmacol. Biochem. Behav.* 87 (1), 179–197. doi: 10.1016/j.pbb.2007.04.015

Egger, B., Van Giesen, L., Moraru, M., Sprecher, S. G. (2013). *In vitro* imaging of primary neural cell culture from drosophila. *Nat. Protoc.* 8 (5), 958–65 doi: 10.1038/nprot.2013.052

Eltzschig, H. K., and Eckle, T. (2011). Ischemia and reperfusion—from mechanism to translation. *Nat. Med.* 17.11, 1391–1401. doi: 10.1038/nm.2507

Eltzschig, H. K., and Collard, C. D. (2004). Vascular ischaemia and reperfusion injury. *Br. Med. Bull.* 70 (1), 71–86. doi: 10.1093/bmb/ldh025

Fan, Q., Zhang, Y., Hou, X., Li, Z., Zhang, K., Shao, Q., et al. (2018). Improved oral bioavailability of notoginsenoside r1 with sodium glycocholate-mediated liposomes: preparation by supercritical fluid technology and evaluation *in vitro* and *in vivo*. *Intl. J. Pharm.* doi: 10.1016/j.ijpharm.2018.10.005

Feng, R., Liu, J., Wang, Z., Zhang, J., Cates, C., Rousselle, T., et al. (2017). The structure-activity relationship of ginsenosides on hypoxia-reoxygenation induced apoptosis of cardiomyocytes. *Biochem. Biophys. Res. Commun.*, S0006291X1732034X. doi: 10.1016/j.bbrc.2017.10.056

Festing, M. F. W., and Altman, D. G. (2002). Guidelines for the design and statistical analysis of experiments using laboratory animals. *Ilar J.* 43 (4), 244. doi: 10.1093/ilar.43.4.244

Friedman, S. L., Sheppard, D., Duffield, J. S., and Violette, ,. S. (2013). Therapy for Fibrotic Diseases: Nearing the Starting Line. *Sci. Transl. Med.* 5 (167), 167sr1–167sr1. doi: 10.1126/scitranslmed.3004700

Frobert, A., Valentin, J., Jean-Luc, M., Erwin, R., Cook, S., and Marie-Noëlle, G. (2015). Prognostic value of troponin i for infarct size to improve preclinical myocardial infarction small animal models. *Front. Physiol.* 6. doi: 10.3389/fphys.2015.00353

Fu, Y., Yin, Z., and Yin, C. (2017). Biotransformation of ginsenoside Rb1 to ginsenoside Rg3 by endophytic bacterium *Burkholderia* sp. GE 17-7 isolated from Panax ginseng. *J. Appl. Microbiol.* doi: 10.1111/jam.13435

Furie, K. L., and Jayaraman, M. V. (2018). guidelines for the early management of patients with acute ischemic stroke. *Stroke*. doi: 10.1161/STROKEAHA.118.020176

Galluzzi, L., Blomgren, K., and Kroemer, G. (2009). Mitochondrial membrane permeabilization in neuronal injury. *Nat. Rev. Neurosci.* 10 (7), 481–494. doi: 10.1038/nrn2665

Gashaw, I., Ellinghaus, P., Sommer, A., and Asadullah, K. (2012). What makes a good drug target? *Drug Disc. Today* 17 (supp-S), 0–0. doi: 10.1016/j.drudis.2011.12.008

Guo, Q., Li, P., Wang, Z., Cheng, Y., Wu, H., Yang, B., et al. (2014). Brain distribution pharmacokinetics and integrated pharmacokinetics of *Panax* notoginsenoside r1, ginsenosides rg1, rb1, re and rd in rats after intranasal administration of *Panax notoginseng* saponins assessed by uplc/ms/ms. *J. Chromatogr. B.* 969, 264–271. doi: 10.1016/j.jchromb.2014.08.034

Hacke, W., Donnan, G., Fieschi, C., Kaste, M., von Kummer, R., Broderick, J. P., et al. (2004). Association of outcome with early stroke treatment: pooled analysis of ATLANTIS, ECASS, and NINDS rt-PA stroke trials. *Lancet* 363, (9411). doi: 10.1016/S0140-6736(04)15692-4

Hadjidemetriou, M., Al-Ahmadi, Z., Mazza, M., Collins, R. F., and Kostarelos, K. (2015). In vivo biomolecule corona around blood-circulating, clinically-used and antibody-targeted lipid bilayer nanoscale vesicles. *ACS Nano* 9 (8), 8142–8156. doi: 10.1021/acsnano.5b03300

Hall, T. S., Hallén, J., Krucoff, M. W., Roe, M. T., Brennan, D. M., Agewall, S., et al. (2015). Cardiac troponin i for prediction of clinical outcomes and cardiac function through 3-month follow-up after primary percutaneous coronary intervention for st-segment elevation myocardial infarction. *Am. Heart J.* 169 (2), 257–265.e1. doi: 10.1016/j.ahj.2014.10.015

Han, J. Y., Li, Q., Ma, Z. Z., and Fan, J. Y. (2017). Effects and mechanisms of compound Chinese medicine and major ingredients on microcirculatory dysfunction and organ injury induced by ischemia/reperfusion. *Pharmacol. Ther.* 2017, S0163725817300852. doi: 10.1016/j.pharmthera.2017.03.005

Han, J. Y. (2014). The protective effect of Notoginsenoside R1 on the heart. Application Number: CN201310175976.8.

He, K., Yan, L., Pan, C. S., Liu, Y. Y., Cui, Y. C., Hu, B. H., et al. (2014). ROCK-dependent ATP5D modulation contributes to the protection of notoginsenoside NR1 against ischemia-reperfusion-induced myocardial injury. *Am. J. Physiol. Heart Circ. Physiol.* 307, H1764–H1776. doi: 10.1152/ajpheart.00259.2014

Henderson, V. C., Kimmelman, J., Fergusson, D., Grimshaw, J. M., Hackam, D. G., and Ioannidis, J. P. (2013). Threats to validity in the design and conduct of preclinical efficacy studies: a systematic review of guidelines for *in vivo* animal experiments. *PLoS Med.* 10 (7), e1001489. doi: 10.1371/journal.pmed.1001489

Heusch, G., and Rassaf, T. (2016). Time to Give Up on Cardioprotection?: A Critical Appraisal of Clinical Studies on Ischemic Pre-, Post-, and Remote Conditioning. *Circ. Res.* 119 (5), 676–695. doi: 10.1161/CIRCRESAHA.116.308736

Heusch, G. (2017). Critical Issues for the Translation of Cardioprotection. *Circ. Res.* 120 (9), 1477–1486. doi: 10.1161/CIRCRESAHA.117.310820

Heusch, G., and Gersh, B. J. (2016). The pathophysiology of acute myocardial infarction and strategies of protection beyond reperfusion: a continual challenge. *Eur. Heart J.* 38 (11), ehw224. doi: 10.1093/eurheartj/ehw224

Hietamies, T. M., Caroline, O., Zhong, P., Luyang, F., Christopher, M. C., Work, L. M., et al. (2018). Variability of functional outcome measures used in animal models of stroke and vascular cognitive impairment – a review of contemporary studies. *J. Cereb. Blood Flow Metab.*, 0271678X1879985–. doi: 10.1177/0271678X18799858

Hou, Q. L., Wang, Y., Li, Y. B., Hu, X. L., and Wang, S. L. (2017). Protective effect of notoginsenoside R1 on neuron injury induced by OGD/R through ATF6/Akt signaling pathway. *Chin. J. Chin. Mater. Med.* (6). doi: 10.19540/j.cnki.cjcmm.20170121.014

Jennings, R. B. (2013). Historical perspective on the pathology of myocardial ischemia/reperfusion injury. *Circ. Res.* 113 (4), 428–438. doi: 10.1161/CIRCRESAHA.113.300987

Jones, P. A., May, G. R., Mcluckie, J. A., Iwashita, A., and Sharkey, J. (2004). Apoptosis is not an invariable component of *in vitro* models of cortical cerebral ischaemia. *Cell Res.* 14 (3), 241–250. doi: 10.1038/sj.cr.7290225

Joris, F., Manshian, B. B., Peynshaert, K., De Smedt, S. C., Braeckmans, K., and Soenen, S. J. (2013). Assessing nanoparticle toxicity in cell-based assays: influence of cell culture parameters and optimized models for bridging the *in vitro–in vivo* gap. *Chem. Soc. Rev.* 42 (21), 8339. doi: 10.1039/c3cs60145e

Judith, V. L., Brenda, B., Rovers, M. M., Merel, R. H., De, V. R. B. M., Marlies, L., et al. (2014). Systematic reviews of animal studies; missing link in translational research? *PLoS ONE* 9 (3), e89981–. doi: 10.1371/journal.pone.0089981

Kanelidis, A., Premer, C., Lopez, J. G., Balkan, W., and Hare, J. M. (2017). Route of delivery modulates the efficacy of mesenchymal stem cell therapy for myocardial infarction: a meta-analysis of preclinical studies and clinical trials. *Circ. Res.* 120 (7), 1139. doi: 10.1161/CIRCRESAHA.116.309819

Khandelwal, P., Yavagal, D. R., and Sacco, R. L. (2016). Acute ischemic stroke intervention. *J. Am. Coll. Cardiol.* 67 (22), 2631–2644. doi: 10.1016/j.jacc.2016.03.555

Kok, F., Shin, M., Ni, C. W., Gupta, A., Grosse, A., van Impel, A., et al. (2015). Reverse genetic screening reveals poor correlation between morpholino-induced and mutant phenotypes in zebrafish. *Dev. Cell* 32 (1), 97–108. doi: 10.1016/j.devcel.2014.11.018

Lee, K. Y., Heo, J. H., Lee, S. I., and Yoon, ,. P. H. (2001). Rescue treatment with abciximab in acute ischemic stroke. *Neurology* 56 (11), 1585–1587. doi: 10.1212/WNL.56.11.1585

Leung, S. Y., Chan, K., Bensoussan, A., and Munroe, M. J. (2007). Application of atmospheric pressure chemical ionisation mass spectrometry in the identification and differentiation of Panax Species. *Phytochem. Analysis* 18 (2), 146–150. doi: 10.1002/pca.962

Li, C., Li, Q., Liu, Y. Y., Wang, M. X., Pan, C. S., Yan, L., et al. (2014). Protective effects of notoginsenoside r1 on intestinal ischemia-reperfusion injury in rats. *Am. J. Physiol. Gastrointest. Liver Physiol.* 306 (2), G111. doi: 10.1152/ajpgi.00123.2013

Li, Y., Yang, D., and Zhu, C. (2018). Impact of sodium n-[8-(2-hydroxybenzoyl) amino]- caprylate on intestinal permeability for notoginsenoside r1 and salvianolic acids in caco-2 cells transport and rat pharmacokinetics. *Molecules* 23 (11), 2990. doi: 10.3390/molecules23112990

Liang, F. and Hua, J. X. (2005). Absorption profiles of sanchinoside R1 and ginsenoside Rg1 in the rat intestine. *Eur. J. Drug Metab. Pharmacokinet.* 30 (4), 261–268. doi: 10.1007/BF03190630

Liu, H., Yang, J., Du, F., Gao, X., Ma, X., Huang, Y., et al.. (2009). Absorption and disposition of ginsenosides after oral administration of *Panax notoginseng* extract to rats. *Drug Metab. Dispos.* 37 (12), 2290–2298. doi: 10.1124/dmd.109.029819

Liu, W. J., Tang, H. T., Jia, Y. T., Ma, B., Fu, J. F., Wang, Y., et al. (2010). Notoginsenoside r1 attenuates renal ischemia-reperfusion injury in rats. *Shock* 34 (3), 314–320. doi: 10.1097/SHK.0b013e3181ceede4

Liu, Z. j., Wang, H. Y., Hou, G. L., Cao, H. L., Zhao, Y., and Yang, B. F. (2019). Notoginsenoside R1 protects oxygen and glucose deprivation-induced injury by upregulation of miR-21 in cardiomyocytes. *J. Cell. Biochem.* 120, 9181–9192. doi: 10.1002/jcb.28194

Macarthur, J. W., Purcell, B. P., Shudo, Y., Cohen, J. E., Fairman, A., Trubelja, A., et al. (2013). Sustained release of engineered stromal cell-derived factor 1-α from injectable hydrogels effectively recruits endothelial progenitor cells and preserves ventricular function after myocardial infarction. *Circulation* 128 (11_suppl_1), S79–S86. doi: 10.1161/CIRCULATIONAHA.112.000343

Macleod, M. R., O'Collins, T., Howells, D. W., and Donnan, G. A. (2004). Pooling of animal experimental data reveals influence of study design and publication bias. *Stroke* 35 (5), 1203–1208. doi: 10.1161/01.STR.0000125719.25853.20

May, P. C., Dean, R. A., Lowe, S. L., Martenyi, F., Sheehan, S. M., Boggs, L. N., et al.. (2011). Robust central reduction of amyloid-β in humans with an orally available, non-peptidic β-secretase inhibitor. *J. Neurosci.* 31, 16507–16516. doi: 10.1523/JNEUROSCI.3647-11.2011

Meng, X., Wang, M., Wang, X., Sun, G., Ye, J., Xu, H., et al. (2014). Suppression of nadph oxidase-and mitochondrion-derived superoxide by notoginsenoside r1 protects against cerebral ischemia–reperfusion injury through estrogen receptor-dependent activation of akt/nrf2 pathways. *Free Radic. Res.* 48 (7), 823–838. doi: 10.3109/10715762.2014.911853

Peng, M., Yi, Y. X., Zhang, T., Ding, Y., Le. J. (2018). Stereoisomers of Saponins in *Panax notoginseng* (Sanqi): A Review. *Front. Pharmacol.* 9, 188–. doi: 10.3389/fphar.2018.00188

Murray Christopher, J. L. (2017). Global, regional, and national age-sex specific mortality for 264 causes of death, 1980-2016: a systematic analysis for the Global Burden of Disease Study 2016. *Lancet* 390, 1151–1210. doi: 10.1016/S0140-6736(17)32152-9

Ng, T. B. (2006). Pharmacological activity of sanchi ginseng (Panax notoginseng). *J. Pharm. Pharmacol.* 58 (8), 1007–1019. doi: 10.1211/jpp.58.8.0001

Nishina, T., Nishimura, K., Yuasa, S., Miwa, S., Nomoto, T., Sakakibara, Y., et al. (2001). Initial effects of the left ventricular repair by plication may not last long in a rat ischemic cardiomyopathy model. *Circulation* 104 (Supplement 1), I–241-I-245. doi: 10.1161/hc37t1.094522

Oh, J., and Kim, J. S. (2016). Compound k derived from ginseng: neuroprotection and cognitive improvement. *Food Funct.* 7 (11). doi: 10.1039/C6FO01077F

Ohsawa, I., Ishikawa, M., Takahashi, K., Watanabe, M., Nishimaki, K., Yamagata, K., et al.. (2007). Hydrogen acts as a therapeutic antioxidant by selectively reducing cytotoxic oxygen radicals. *Nat. Med.* 13 (6), 688–694. doi: 10.1038/nm1577

Olesen, A. E., Andresen, T., Staahl, C., Drewes, A. M., et al. (2012). Human Experimental Pain Models for Assessing the Therapeutic Efficacy of Analgesic Drugs. *Pharmacol. Rev.* 64 (3), 722–779. doi: 10.1124/pr.111.005447

Overall, C. M., and Kleifeld, O. (2006). Tumour microenvironment-Opinion: Validating matrix metalloproteinases as drug targets and anti-targets for cancer therapy. *Nat. Rev. Cancer* 6 (3), 227–239. doi: 10.1038/nrc1821

Pelkonen, O., and Turpeinen, M. (2007). In vitro-*in vivo* extrapolation of hepatic clearance: biological tools, scaling factors, model assumptions and correct concentrations. *Xenobiotica* 37, 1066–1089. doi: 10.1080/00498250701620726

Perel, P., Roberts, I., Sena, E., Wheble, P., Briscoe, C., Sandercock, P., et al. (2006). Comparison of treatment effects between animal experiments and clinical trials: systematic review. *BMJ* 334. doi: 10.1136/bmj.39048.407928.BE

Powers, W. J., Rabinstein, A. A., Ackerson, T., Adevoe, O. M., Bambakidis, N. C., Becker, K., et al. (2018). guidelines for the early management of patients with acute ischemic stroke: a guideline for healthcare professionals from the american heart association/american stroke association. Stroke. 49 (3), e46–e110. doi: 10.1161/STR.0000000000000158

Roberts, I., Kwan, I., Evans, P., and Haig, S. (2002). Does animal experimentation inform human healthcare? Observations from a systematic review of international animal experiments on fluid resuscitation. *BMJ* 324 (7335), 474–476. doi: 10.1136/bmj.324.7335.474

Ruan, J. Q., Leong, W. I., Yan, R., and Wang, Y. T. (2010). Characterization of metabolism and\r, *in vitro*\r, permeability study of notoginsenoside r1 from radix notoginseng. *J. Agric. Food Chem.* 58 (9), 5770–5776. doi: 10.1021/jf1005885

Sanne, J. O. L., Eding, J., Tycho, V. D. S., Vesterinen, H., Sena, E., Doevendans, P., et al. (2014). Similar effect of autologous and allogeneic cell therapy for ischemic heart disease: results from a meta-analysis of large animal studies. *J. Am. Coll. Cardiol.* 63 (12), A1762. doi: 10.1016/S0735-1097(14)61765-4

Sasaki, M., Kudo, K., Honjo, K., Hu, J. Q., Wang, H. B., and Shintaku, K. (2011). Prediction of infarct volume and neurologic outcome by using automated multiparametric perfusion-weighted magnetic resonance imaging in a primate model of permanent middle cerebral artery occlusion. *J. Cereb. Blood Flow Metab.* 31 (2), 448. doi: 10.1038/jcbfm.2010.106

Saulnier-Blache, J. S., Rory, ,. W., Kristaps, K., Delyth, G., Ioana, A., Kastenmüller, G., et al. (2018). Ldlr-/- and ApoE-/- mice better mimic the

human metabolite signature of increased carotid intima media thickness compared to other animal models of cardiovascular disease. *Atherosclerosis* 276, 140–147. doi: 10.1016/j.atherosclerosis.2018.07.024

Seabrook, T. A., Burbridge, T. J., Crair, M. C., and Huberman, A. D. (2017). Architecture, function, and assembly of the mouse visual system. *Annu. Rev. Neurosci.* 40 (1), 499–538. doi: 10.1146/annurev-neuro-071714-033842

Sena, E. S., Currie, G. L., Mccann, S. K., Macleod, M. R., and Howells, D. W. (2014). Systematic reviews and meta-analysis of preclinical studies: why perform them and how to appraise them critically. *J. Cereb. Blood Flow Metab.* 34 (5), 737–742. doi: 10.1038/jcbfm.2014.28

Shiva, S., Sack, M. N., Greer, J. J., Duranski, M., Ringwood, L. A., et al. (2007). Nitrite augments tolerance to ischemia/reperfusion injury *via the* modulation of mitochondrial electron transfer. *J. Exp. Med.* 204 (9), 2089–2102. doi: 10.1084/jem.20070198

Smith, C. (2003). Drug target validation: Hitting the target. *Nature* 422, 341, 343, 345 passim. doi: 10.1038/422341a

Su, P., Du, S., Li, H., Li, Z., Xin, W., Zhang, W., et al. (2015). Notoginsenoside R1 inhibits oxidized low-density lipoprotein induced inflammatory cytokines production in human endothelial EA.hy926 cells. *Eur. J. Pharmacol.* 770, 9–15. doi: 10.1016/j.ejphar.2015.11.040

Terkelsen, C. J., Sørensen, J.,. T., Maeng, M., Jensen, L. O., Tilsted, H. H., Trautner, S., et al. (2010). System delay and mortality among patients with stemi treated with primary percutaneous coronary intervention. *JAMA* 304 (7), 763. doi: 10.1001/jama.2010.1139

Thygesen, K., Alpert, J. S., Jaffe, A. S., Simoons, M. L., Chaitman, B. R., and White, H. D. (2012). Third universal definition of myocardial infarction. *Circulation* 126 (16), 2020–2035. doi: 10.1161/CIR.0b013e31826e1058

Tsujimoto, Y., Tsutsumi, Y., Kataoka, Y., Tsujimoto, H., Yamamoto, Y., Papola, D., et al. (2017). Association between statistical significance and time to publication among systematic reviews: a study protocol for a meta-epidemiological investigation. *BMJ Open* 7 (10), e018856. doi: 10.1136/bmjopen-2017-018856

Tsutsumi, Y. M., Tsutsumi, R., Mawatari, K., Nakaya, Y., Kinoshita, M., Tanaka, K., et al. (2011). Compound k, a metabolite of ginsenosides, induces cardiac protection mediated nitric oxide *via* akt/pi3k pathway. *Life Sci.* 88 (15-16), 0–729. doi: 10.1016/j.lfs.2011.02.011

Tu, L., Wang, Y., Chen, D., Xiang, P., and Wang, S. (2018). Protective effects of notoginsenoside r1 *via* regulation of the pi3k-akt-mtor/jnk pathway in neonatal cerebral hypoxic–ischemic brain injury. *Neurochem. Res.* 43 (9), 1210–1226. doi: 10.1007/s11064-018-2538-3

Van Hout, G. P. J., Jansen, O. L. S. J., Wever, K. E., Sena, E., Kouwenberg, L. H. J. A., Van Solinge, W. W., et al. (2015). Translational failure of anti-inflammatory compounds for myocardial infarction. *Cardiovasc. Res.* 109 (2), 240. doi: 10.1093/cvr/cvv239

Wan, Q., Pan, Y. Y., Jia, Y. H., and Liu, Z. Y. (2015). Notoginsenoside R1 Reduced Cardiomyocytes Injury Induced by Hydrogen Peroxide through JNK Signal Pathway. *Lishizhen Med. Materia Med. Res.* (9), 2061–2064. doi: 10.3969/j.issn.1008-2015.09.005

Wang, L., and Ma, Q. (2018). Clinical benefits and pharmacology of Scutellarin: A comprehensive review. *Pharmacol. Ther.*, S0163725818300809. doi: 10.1016/j.pharmthera.2018.05.006

Wang, Y., Tu, L., Li, Y., Chen, D., Liu, Z., Hu, X., et al. (2017). Notoginsenoside r1 alleviates oxygen–glucose deprivation/reoxygenation injury by suppressing endoplasmic reticulum calcium release *via* plc. *Sci. Rep.* 7 (1), 16226. doi: 10.1038/s41598-017-16373-7

Wang, Y., Tu, L., Li, Y., Di, C., and Wang, S. (2016). Notoginsenoside r1 protects against neonatal cerebral hypoxic-ischemic injury through estrogen receptor-dependent activation of endoplasmic reticulum stress pathways. *J. Pharmacol. Exp. Ther.* doi: 10.1124/jpet.115.230359

Wang, T., Guo, R., Zhou, G., Zhou, X., Kou, Z., Sui, F., et al. (2016). Traditional uses, botany, phytochemistry, pharmacology and toxicology of *Panax notoginseng* (Burk.) F. H. Chen: A review. *J. Ethnopharmacol.* 2016, S0378874116302665. doi: 10.1016/j.jep.2016.05.005

Wienkers, L. C., and Heath, T. G. (2005). Predicting *in vivo* drug interactions from *in vitro* drug discovery data. *Nat. Rev. Drug Disc.* 4 (10), 825–833. doi: 10.1038/nrd1851

Worp, H. B. V. D., and Sandercock, P. A. G. (2012). Improving the process of translational research. *BMJ* 345, e7837–e7837. doi: 10.1136/bmj.e7837

Wozniak, A. W. (2004). Association of outcome with early stroke treatment: Pooled analysis of ATLANTIS, ECASS, and NINDS rt-PA stroke trials. *Lancet* 13 (5), 19. doi: 10.1016/j.accreview.2004.04.032

Xia, K. P., Cao, H. M., and Shao, C. Z. (2015). Protective effect of Notoginsenoside r1 in a rat model of myocardial ischemia reperfusion injury by regulation of vitamin d3 upregulated protein 1/nf-κb pathway. *Die Pharm. Intl. J. Pharm. Sci.* doi: 10.1691/ph.2015.5694

Yan, R. Q. (2016). Stepping closer to treating Alzheimer's disease patients with BACE1 inhibitor drugs. *Transl. Neurodegener.* 5 (1), 13. doi: 10.1186/s40035-016-0061-5

Yang, X. C., Xiong, X.,. J., Wang, H.,. R., and Wang, J. (2014). Protective Effects of *Panax Notoginseng* Saponins on Cardiovascular Diseases: A Comprehensive Overview of Experimental Studies. *Evid. Based Complementary Altern. Med.* 2014, 1–13. doi: 10.1155/2014/204840

Yu, J. M., Ju, L., Wang, H. D., Wan, X. J., Yang, J. S., and Wang., Q. (2014). Effects of Notoginsenoside R1 on VEGF and bFGF Expression in Ischemic Myocardium of Rats. *Prog. Mod. Biomed.* 14 (30), 5845–5848. doi: 10.13241/j.cnki.pmb.2014.30.012

Yu, Y., Sun, G., Luo, Y., Wang, M., Chen, R., Zhang, J., et al.. (2016). Cardioprotective effects of notoginsenoside r1 against ischemia/reperfusion injuries by regulating oxidative stress-and endoplasmic reticulum stress-related signaling pathways. *Sci. Rep.* 6, 21730. doi: 10.1038/srep21730

Zhao, Z. X., Hu, X. M., Wang, J., Cai, H. F. (2017). The effects of Notoginsenoside R1 on TNF-α mRNA after cerebral ischemia and reperfusion in rats. *Zhejiang J. Trauma Surg.* 22 (1). doi: 10.3969/j.issn.1009-7147.2017.01.005

Zhang, B., Zhang, J., Zhang, C., Zhang, X., Ye, J. X., Kuang, S. H., et al.. (2018). Notoginsenoside R1 Protects Against Diabetic Cardiomyopathy Through Activating Estrogen Receptorα and Its Downstream Signaling. *Front. Pharmacol.* 9, 1227. doi: 10.3389/fphar.2018.01227

Zhang, B., Zhang, X. L., Zhang, C. Y., Shen, Q., Sun, G. B., and Sun, X. B. (2019). Notoginsenoside R1 Protects db/db Mice against Diabetic Nephropathy *via* Upregulation of Nrf2-Mediated HO-1 Expression. *Molecules* 24. doi: 10.3390/molecules24020247 undefined.

Zhang, S., Ju, Z., Guan, H., Yu, L., Wang, Z., and Zhao, Y. (2019). Dose-dependent exposure profile and metabolic characterization of notoginsenoside R in rat plasma by ultra-fast liquid chromatography-electrospray ionization-tandem mass spectrometry. *Biomed. Chromatogr.*, e4670. doi: 10.1002/bmc.4670 undefined.

Zhou, F. H., Pan, Y. Y., Cui, X. B., and Jia, ,. Y.,. H. (2016). Notoginsenoside R1 Alleviates Cardiomyocytes Injury Induced By H2O2 Through ERK1/2 And p38 Signal Pathway. *Chin. J. Herb. Pharmacology.* (2), 17–20. doi: 10.13412/j.cnki.zyyl.2016.02.006

Zhou, F. H., Pan, Y. Y., Jia, Y.,. H., and Sun., X. G. (2017). Effect of Pim-2 in Cardiomyocytes Injury Induced by H2O2 and Prevention of Notoginsenoside R1. *Liaoning J. Tradit. Chin. Med.* (03), 176–180. doi: 10.13192/j.issn.1000_1719.2017.03.056

Zhu, F., Shi, Z., Qin, C., Tao, L., Liu, X., Xu, F., et al.. (2012). Therapeutic target database update 2012: a resource for facilitating target-oriented drug discovery. *Nucleic Acids Res.* 40 (D1), D1128–D1136. doi: 10.1093/nar/gkr797

Zou, S., Zhang, M. X., Feng, L. M., Zhou, Y. F., Li, L., and Ban, L. L. (2017). Protective effects of notoginsenoside R1 on cerebral ischemia-reperfusion injury in rats. *Exp. Ther. Med.* 14, 6012–6016. doi: 10.3892/etm.2017.5268

Conflict of Interest: The authors declare that the research was conducted in the absence of any commercial or financial relationships that could be construed as a potential conflict of interest.

frontiers in Pharmacology

ORIGINAL RESEARCH
published: 28 October 2019
doi: 10.3389/fphar.2019.01271

Baicalin Protects Against Hypertension-Associated Intestinal Barrier Impairment in Part Through Enhanced Microbial Production of Short-Chain Fatty Acids

Dandan Wu[1], Liliqiang Ding[1], Xiaoting Tang[1], Wenjian Wang[2], Yu Chen[1,2] and Teng Zhang[1,2]**

[1] Clinical Research Institute of Integrative Medicine, Yueyang Hospital, Shanghai University of Traditional Chinese Medicine, Shanghai, China, [2] Clinical Research Institute of Integrative Medicine, Shanghai Academy of Traditional Chinese Medicine, Shanghai, China

OPEN ACCESS

Edited by:
Yue Liu,
Xiyuan Hospital, China

Reviewed by:
Xudong Liao,
Case Western Reserve University, United States
Cai-Guang Yang,
Shanghai Institute of Materia Medica (CAS), China

***Correspondence:**
Yu Chen
chenyu@shyueyanghospital.com
Teng Zhang
zhangteng@shyueyanghospital.com

Specialty section:
This article was submitted to Ethnopharmacology, a section of the journal Frontiers in Pharmacology

Received: *27 August 2019*
Accepted: *04 October 2019*
Published: *28 October 2019*

Citation:
Wu D, Ding L, Tang X, Wang W, Chen Y and Zhang T (2019) Baicalin Protects Against Hypertension-Associated Intestinal Barrier Impairment in Part Through Enhanced Microbial Production of Short-Chain Fatty Acids. Front. Pharmacol. 10:1271. doi: 10.3389/fphar.2019.01271

Impaired intestinal barrier plays an important role in the pathogenesis of hypertension primarily through promoting the development of chronic low-grade inflammation. Baicalin *is the major flavonoid component of Scutellaria baicalensis* Georgi, a medicinal plant commonly used for the treatment of inflammatory intestinal disorders and hypertension in traditional Chinese medicine. However, it remains to be elucidated whether baicalin alleviates hypertension-associated intestinal barrier impairment. The current study thus investigated the effects of baicalin on the intestinal barrier integrity, the intestinal expression of genes encoding proinflammatory factors and tight junction proteins, the serum levels of the inflammatory markers, the amount of fecal short-chain fatty acids (SCFAs) and the abundance of SCFAs-producing bacteria in the spontaneously hypertensive rats (SHRs). The results showed that baicalin alleviated the pathological lesions in the ilium and the proximal colon in the SHRs. Baicalin treatment resulted in decreased ileal and colonic expression of proinflammatory genes in the SHRs. In addition, baicalin treatment attenuated hypertension-associated intestinal hyperpermeability and decreased the serum levels of inflammatory indicators such as high-sensitivity C-reactive protein (hs-CRP), interleukin 1 beta, and IL-6 in the SHRs. The protective effect of baicalin on the intestinal integrity was also supported by well-preserved intestinal ultrastructure and increased intestinal expression of genes encoding tight junction proteins such as zonula occludens-1 (ZO-1), cingulin, and occludin in the SHRs. Lastly, baicalin treatment increased the amount of fecal SCFAs and the abundance of SCFAs-producing bacteria in the SHRs. In conclusion, the work here provides for the first time the morphological, biochemical, and molecular evidence supporting the protective effects of baicalin on the intestinal integrity in the SHRs, which may help better understand the therapeutic effects of *S. baicalensis* Georgi in the treatment of hypertension.

Keywords: baicalin, hypertension, intestinal barrier, short-chain fatty acids, gut microbiota

INTRODUCTION

Hypertension is the leading risk factor for the development of cardiovascular diseases (Ahluwalia and Bangalore, 2017). Intestinal barrier impairment has recently been noted as an important pathological element implicated in the progression of hypertension (Jaworska et al., 2017; Santisteban et al., 2017). Intestinal barrier serves as a critical internal defense to restrict the systemic entry of luminal contents. Intestinal barrier impairment therefore is implicated in the pathogenesis of chronic low-grade inflammation that perpetuates the hypertensive state, exacerbates hypertensive target organ damages, and promotes the development of resistant hypertension (Fukui, 2016; Solak et al., 2016). Therapeutic agents protecting the intestinal barrier integrity under hypertensive conditions may help better control the progression of hypertension.

Baicalin is a major flavone component found in *Scutellaria baicalensis* Georgi, a medicinal herb with a long history of clinical application in the treatment of a host of diseases primarily including intestinal disorders and hypertension (Zhao et al., 2016). Anti-inflammatory and anti-hypertensive activities of baicalin have been previously documented (Zhao et al., 2016; Ding et al., 2019). However, whether baicalin is pharmacologically active at preserving the intestinal barrier integrity under hypertensive conditions remains to be investigated.

The current study thus assessed the effects of baicalin on the intestinal lesions and the intestinal expression of proinflammatory factors in SHRs. In addition, the intestinal permeability, systemic levels of hs-CRP and proinflammatory factors, the ileal and colonic ultrastructure, and the expression of genes encoding tight junction proteins were examined. Furthermore, the amount of fecal SCFAs and the abundance of SCFAs-producing bacteria in the gut were analyzed to better understand the intestinal effects of baicalin under hypertensive conditions.

MATERIALS AND METHODS

Chemicals

Baicalin was purchased from Shanghai Yuanye Biotechnology Co., Ltd (Shanghai, China) and the purity was validated to be over 98% as previously described (Ding et al., 2019).

Animals and Treatments

Age-matched male SHRs and Wistar-Kyoto (WKY) rats were purchased from Beijing Vital River Laboratory Animal Technology Co., Ltd. (Beijing, China). SHRs and WKY rats were housed under a controlled condition of temperature, humidity, and light (12 h light/dark cycles) and free access to food and water was allowed. The study was carried out in accordance with the recommendations of the NIH Guide for the Care and Use of Laboratory Animals. The protocol was approved by the Institutional Animal Care and Use Committee at Yueyang Hospital, Shanghai University of Traditional Chinese Medicine. Baicalin was dissolved in sterile water with the assistance of Na_2CO_3. SHRs were either treated with baicalin solution through oral gavage at the dose of 100 mg/kg body weight (bw) per day or received vehicle treatment in the same manner. WKY controls were gavaged with the vehicle as well. The indicated treatments were applied to 6-week animals and delivered for 6 or 14 weeks as indicated.

Blood Pressure Measurement

The blood pressure was measured using a non-invasive tail-cuff method (Softron, Beijing, China) as previously described (Ding et al., 2019). Briefly, conscious rats were conditioned before systolic blood pressure (SBP) and diastolic blood pressure (DBP) were taken. For each measurement, at least five readings within 5–10 mm Hg range were recorded to acquire the mean of SBP and DBP.

Histological Examination

At the end of the indicated treatments, the ileum and proximal colon specimens in the length of 3 mm were procured from the euthanized animals and subject to 4% paraformaldehyde fixation, paraffin embedding and sectioning. Paraffin sections 4 μm thick were then stained with hematoxylin and eosin (H&E) or Masson's trichrome solution. Histopathology was recorded using a light microscope (DM2000, Leica, Germany). The number of goblet cells, the thickness of tunica muscularis, the length of the villi, and the mucosal thickness were measured after H&E staining. Masson's trichrome positivity was quantified using Image-Pro Plus 6.

Immunohistochemistry

At the end of the indicated treatments, the ilium and proximal colon specimens were fixed in 4% paraformaldehyde and processed for cryosectioning. Cryosections 8 μm thick were subject to immunohistochemical examination using rabbit polyclonal anti-ZO-1 (Novus Biologicals, USA) or anti-Cgn (Novus Biologicals, USA) primary antibody in conjunction with a cy3-conjugated goat-anti-rabbit secondary antibody (Sigma, USA). Counterstaining of 4-6-diamidino-2-phenylindole (DAPI) was performed to visualize the nucleus. The immunopositivity of the indicated antibody labeling was recorded by fluorescent microscopy (DM6000B, Leica, Germany).

Transmission Electron Microscopy

To assess the intestinal ultrastructure, the ileum and the proximal colon specimens were collected after 6 weeks of the indicated treatments, fixed in 2.5% glutaraldehyde solution, followed by gradient acetone dehydration and embedding in epoxy resin. Ultrathin sections 50 nm thick were then made and subject to transmission electron microscopy (TEM) observation (Tecnai G2 Spirit Bio TWIN, FEI company, USA).

Real-Time Reverse Transcriptase Polymerase Chain Reaction Analysis

Total RNA was isolated from the ileum and proximal colon using miRNeasy Mini Kit (Qiagen, USA), followed by reverse transcription using miScript Reverse Transcription Kit (Qiagen, USA). Real-time polymerase chain reaction (PCR) was subsequently performed to analyze the expression of genes

of interest using SYBR Green PCR Master Mix (ABI, USA) on LightCycler 480 System (Roche, USA). Primer sequences are indicated in **Table 1**. Glyceraldehyde 3-phosphate dehydrogenase was included as an internal control for normalization purposes. The fold change in the gene expression was calculated according to $2^{-[Ct\ (specific\ gene)-Ct\ (GAPDH)]}$.

Enzyme-Linked Immunosorbent Assay

At the end of the indicated experiments, serum samples were prepared from the blood samples by centrifugation at 3,000 rpm for 10 min. The level of LBP, hs-CRP, IL-1β, and IL-6 was measured using ELISA Kits (Shanghai Yuanye Biotechnology Co., Ltd, China) according to the manufacturer's instructions. The optical density value was measured at 450 nm using a microplate reader (BioTek, USA). For each assay, a standard cure was generated to calculate the concentration of LBP, hs-CRP, IL-1β, and IL-6 in the samples.

Gas Chromatography-Mass Spectrometry Analysis

Fecal samples were dissolved in distilled water, vortexed, and centrifuged at 10,000 rpm for 5 min. The supernatant was filtered through 0.45 μm syringe filter, followed by extraction using 50% sulfuric solution and ether. Supernatant was collected after centrifugation at 10,000 rpm for 5 min and subject to the quantification of SCFAs by GC-MS (Agilent 6890N, USA).

Fecal 16s Recombinant Deoxyribonucleic Acid Sequencing

Fecal samples were collected from 20-week old vehicle-treated WKY, vehicle-treated SHRs, and baicalin-treated SHRs, followed by deoxyribonucleic acid (DNA) isolation using QIAamp Fast DNA Stool Mini Kit. After PCR amplification, 16S recombinant deoxyribonucleic acid (rDNA) sequencing was performed using MiSeq System (Illumina, USA). Community and phylogenesis analysis and beta analysis were performed to assess the differences in the gut microbiota among the indicated experimental groups. The project was deposited at the European Molecular Biology Laboratory database with the accession number PRJEB34365.

TABLE 1 | Real-Time Reverse Transcriptase Polymerase Chain Reaction Analysis.

Gene name	Forward primer (3'-5')	Reverse primer (3'-5')
Cgn	ACTCCTGGCGAAAAGCTTCC	GTCTGCAGGTTGCTCTCAGT
GAPDH	ACAGCAACAGGGTGGTGGAC	TTTGAGGGTGCAGCGAACTT
HMGB1	TTTCCACACACCCTGCATA	GAGTCCTCAGGTAAGGAGCAG
IL-1β	GCTTCCTTGTGAAGTGTCT	TCTGGACAGCCCAAGTCAAG
IL-23	ATCTCTGCACACTAGCCTGG	ATCTTTGCAAACAGAACTGGC
Ocln	GATCTAGAGCCTGGAGCAACG	ATTGGGTTTGAATTCATCCGGC
RAGE	CTCCCTGAGGTAGGGCATGA	TCATCACCGGTTTCTGTGACC
TLR2	TGGAGGTCTCCAGGTCAAATCT	TTTTGCTGTGAGTCCCGAG
TLR4	CTCTGCCCTGCCACCATTTA	AGGAAGTACCTCTATGGGGAT
TNF-α	ATGGGCTCCCTCTCATCAGT	GCTTGGTGGTTTGCTACGAC
ZO-1	TCGAGGTCTTCGTAGCTCCA	GCAACATCAGCAATCGGTCC

Statistical Analysis

The experimental data were expressed as the mean ± S.E.M. The statistical analyses were performed using SPSS. 21.0. Data were analyzed by one-way ANOVA with Dunnett's post-test. Statistically significance was designated if $p < 0.05$.

RESULTS

Baicalin Treatment Attenuates the Necrotic and Ulcerative Intestinal Lesions and Impairment of the Mechanical Intestinal Barrier in the Spontaneously Hypertensive Rats

Anti-hypertensive effect of baicalin has been demonstrated in our previous study (Ding et al., 2019). To further investigate the impact of baicalin treatment on hypertension-associated impairment of the intestinal barrier, 6-week old SHRs were subject to a 6-week treatment regimen including either vehicle or baicalin administered at 100 mg/kg bw, a dose with a partial blood pressure-lowering effect (Ding et al., 2019), followed by histological examination of the ileal and colonic pathologies. As shown in **Supplemental Figure 1**, both SBP (**Supplemental Figure 1A**) and DBP (**Supplemental Figure 1B**) were progressively increased in the vehicle-treated SHRs compared to that from the vehicle-treated WKYs. Consistent with our previous findings (Ding et al., 2019), baicalin treatment resulted in a partial decrease in the SBP and DBP in the SHRs. In addition, as shown in **Figure 1A**, necrotic and ulcerative lesions were readily detected in the ilium in the 12-week old vehicle-treated SHRs compared to the intact ileal histology manifested by the vehicle-treated WKY controls. In contrast, baicalin treatment attenuated the ileal lesions in the SHRs (**Figure 1A**). Measurement of the number of goblet cells, villi length and the thickness of tunica muscularis further revealed that the vehicle-treated SHRs was characterized by decreased number of goblet cells, reduced villi length, and decreased thickness of tunica muscularis compared to the vehicle-treated WKY controls, whereas baicalin treatment increased the number of goblet cells, the length of the villi, and the thickness of tunica muscularis compared to that from the vehicle-treated SHRs (**Figures 1B–D**). The necrotic and ulcerative lesions were also observed in the proximal colon in the 12-week old vehicle-treated SHRs compared to that from the age-matched vehicle-treated WKY rats. Meanwhile, baicalin treatment attenuated the pathological alterations in the proximal colon in the 12-week old SHRs (**Figure 2A**). In addition, while no significant changes in the thickness of tunica muscularis were observed, the number of goblet cells and the mucosal thickness were significantly decreased in the proximal colon in the vehicle-treated SHRs compared to the vehicle-treated WKY controls. In contrast, the number of goblet cells and the mucosal thickness were significantly increased in the proximal colon in the baicalin-treated SHRs compared to their vehicle-treated SHR counterparts (**Figures 2B–D**). These results indicate that baicalin treatment ameliorates the necrotic and ulcerative intestinal lesions and impairment of the mechanical intestinal barrier in the SHRs.

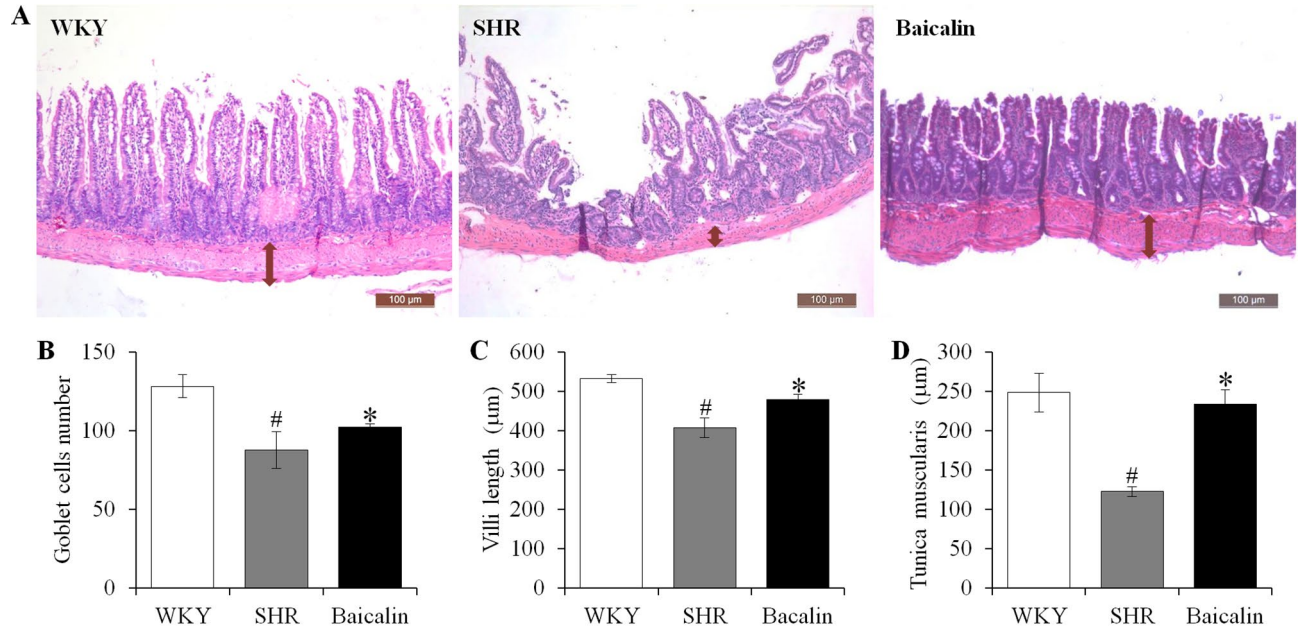

FIGURE 1 | Baicalin treatment alleviates the pathological lesions in the ileum in spontaneously hypertensive rats (SHRs). The ileum specimens were collected from 12-week old vehicle-treated Wistar-Kyoto controls (WKY), vehicle-treated SHRs (SHR), and baicalin-treated SHRs (baicalin) after 6-week of the indicated treatments. The paraffin sections made from the ilium specimens were then subject to hematoxylin and eosin (H&E) staining and the ileal histology were observed and documented using a light microscope **(A)**. The number of the goblet cells **(B)** was counted and the length of the villi **(C)** and the thickness of the tunica muscularis **(D)** were measured in H&E-stained sections. Scale bar: 100 μm. Data were expressed as mean ± S.E.M (n = 6 per group). # Compared to that from the vehicle-treated WKY rats, $p < 0.05$; * compared to that from the vehicle-treated SHRs, $p < 0.05$.

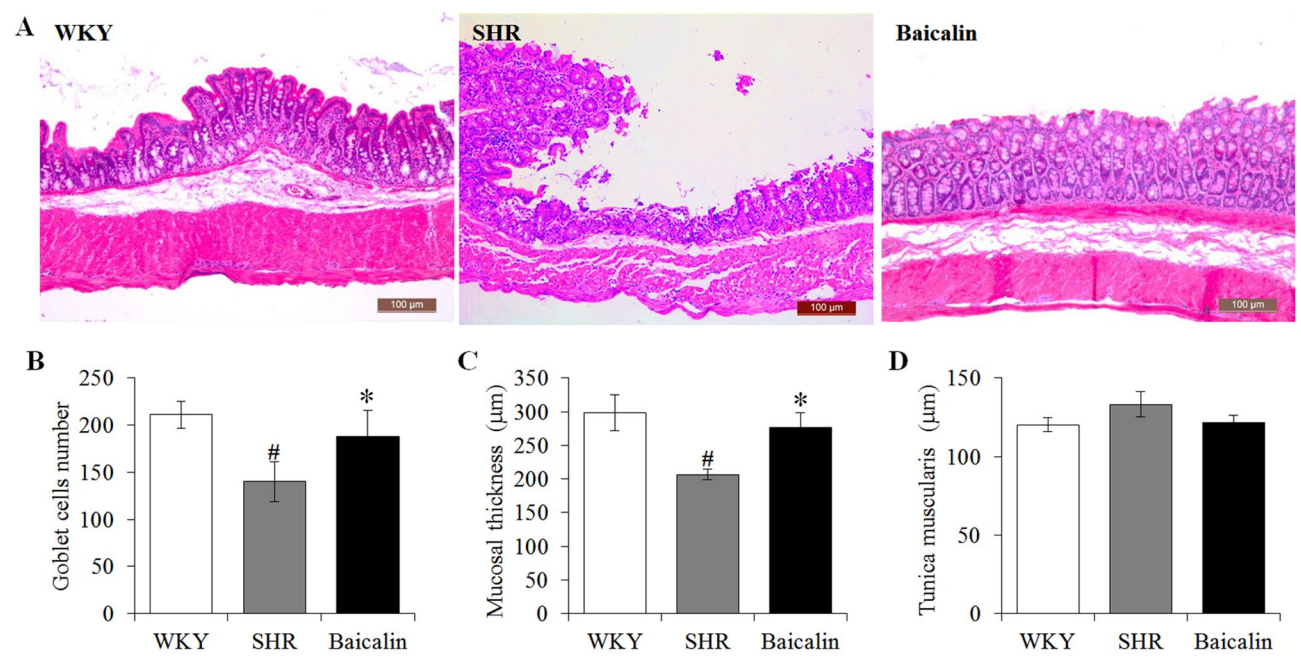

FIGURE 2 | Baicalin treatment alleviates the pathological lesions in the colon in spontaneously hypertensive rats (SHRs). At the end of 6-week treatment of baicalin or vehicle, the proximal colons were collected from 12-week old vehicle-treated Wistar-Kyoto controls (WKY), vehicle-treated SHRs (SHR), and baicalin-treated SHRs (baicalin) and were processed for paraffin embedding and sectioning. Hematoxylin and eosin (H&E) staining was then performed to assess the colonic histology **(A)**. The number of the goblet cells **(B)** was counted and the thickness of the mucosal **(C)** and the tunica muscularis **(D)** were measured in H&E-stained sections. Scale bar: 100 μm. Data were expressed as mean ± S.E.M (n = 6 per group). # Compared to that from the vehicle-treated WKY rats, $p < 0.05$; * compared to that from the vehicle-treated SHRs, $p < 0.05$.

Baicalin Treatment Decreases the Ileal and Colonic Expression of Pro-Inflammatory Genes in the Spontaneously Hypertensive Rats

Given that necrotic and ulcerative intestinal lesions were noted in the SHRs, the ileal and colonic expression of genes implicated in inflammatory responses were further analyzed, including *Tlr4, Tlr2, HMGB1, RAGE, IL-1β, TNF-α, and IL-23*. As shown in **Figure 3A**, although no significant changes in the ileal expression of *Tlr2, HMGB1, RAGE, IL-1β, and IL-23* were observed, significantly increased ileal expression of *Tlr4* and *TNF-α* was noted in the 12-week old vehicle-treated SHRs compared to that from the vehicle-treated WKY controls. In contrast, baicalin treatment resulted in significantly decreased ileal expression of not only *Tlr4* and *TNF-α*, but also *Tlr2, HMGB1, RAGE, IL-1β,* and *IL-23* in the SHRs compared to that from the vehicle-treated SHRs. Furthermore, the colonic expression of these proinflammatory genes was analyzed. As shown in **Figure 3B**, increased expression of *Tlr2, HMGB1, IL-1β, TNF-α,* and *IL-23* was observed in the 12-week old vehicle-treated SHRs compared to that from the vehicle-treated WKY controls. Baicalin treatment, however, led to significantly decreased colonic expression of *Tlr2, IL-1β, TNF-α, and IL-23* in the SHRs. These results indicate that baicalin treatment is effective at restricting the intestinal inflammatory response in the SHRs.

Baicalin Treatment Attenuates the Fibrotic Lesions in the Ilium and the Colon in the Spontaneously Hypertensive Rats

Next, given that intestinal fibrotic lesions have been noted as hypertension-associated pathological changes as well (Santisteban et al., 2017), Masson's trichrome staining, a method visualizing the collagen fibers in the tissue, was adopted to assess the effect of baicalin treatment on the fibrotic alterations in the ileum and the proximal colon in the SHRs. As shown in **Figures 4A**, **B**, increased Masson's trichrome positivity was observed in the ileum in the 12-week old vehicle-treated SHRs compared to that from the vehicle-treated WKY rats, whereas baicalin treatment decreased Masson's trichrome positivity in the ileum in the SHRs. Similar observations were made in the proximal colon. As shown in **Figures 4C**, **D**, increased Masson's trichrome positivity was detected in the proximal colon in the 12-week old vehicle-treated SHRs compared to that from the vehicle-treated WKY controls, which was significantly attenuated in the baicalin-treated SHRs. These results indicate that baicalin treatment attenuates the fibrotic lesions in the ileal and proximal colon in SHRs.

Baicalin Treatment Mitigates Intestinal Hyperpermeability and Systemic Inflammatory Response in the Spontaneously Hypertensive Rats

Hypertension is associated with increased intestinal permeability due to impaired intestinal barrier (Jaworska et al., 2017; Santisteban et al., 2017). As shown above, baicalin treatment alleviates the pathological lesions of the mechanical intestinal barrier in the SHRs, the impact of baicalin on the intestinal permeability was further assessed. Decreased serum level of LBP serves as an indirect index of increased intestinal permeability (Gutsmann et al., 2001; Forsyth et al., 2011; Wu et al., 2019). Therefore, the serum level of LBP was analyzed to assess the effect of baicalin treatment on hypertension-associated intestinal hyperpermeability. As shown in **Figure 5A**, the serum level of LBP was found to be decreased in the 12-week old vehicle-treated SHRs compared to that from the vehicle-treated WKY controls. In contrast, baicalin treatment resulted in elevated level of serum LBP in the SHRs. Given that increased intestinal permeability is causally associated with the development of low-grade chronic inflammation, the serum levels of hs-CRP, an indicator of systemic inflammation as well as proinflammatory cytokines IL-1β and

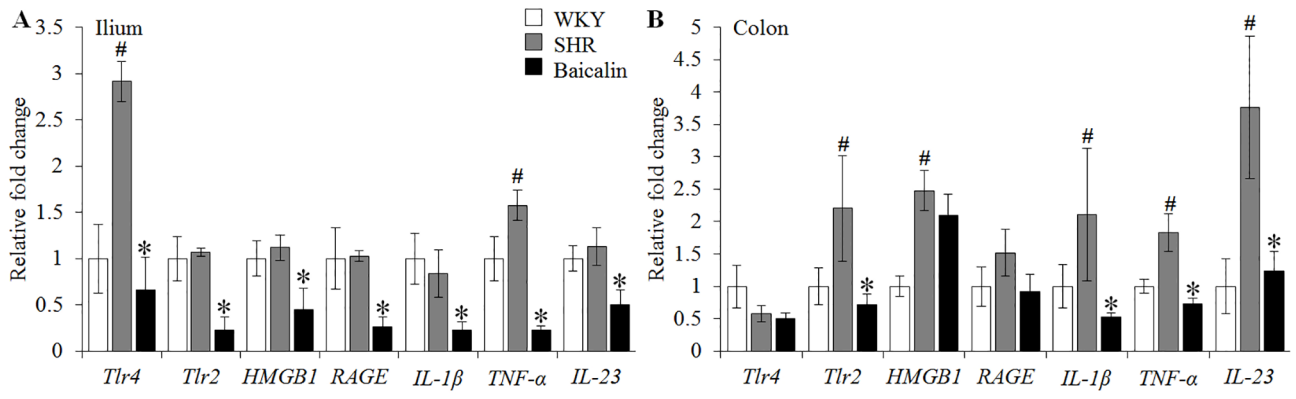

FIGURE 3 | Baicalin treatment decreases the ileal and colonic expression of proinflammatory genes in spontaneously hypertensive rats (SHRs). Six-week Wistar-Kyoto (WKY) controls or SHRs received the indicated treatment for 6 weeks, followed by real-time polymerase chain reaction to analyze the ileal **(A)** and colonic **(B)** expression of *Tlr4, Tlr2, HMGB1, RAGE, interleukin 1 beta, tumor necrosis factor alpha,* and *IL-23*. Relative fold change of these genes in the vehicle-treated SHRs and baicalin-treated SHRs against that from the vehicle-treated WKYs was presented. The expression of glyceraldehyde 3-phosphate dehydrogenase was included as the internal control. Data were expressed as mean ± S.E.M (n = 6 per group). # Compared to that from the vehicle-treated WKY rats, $p < 0.05$; * compared to that from the vehicle-treated SHRs, $p < 0.05$.

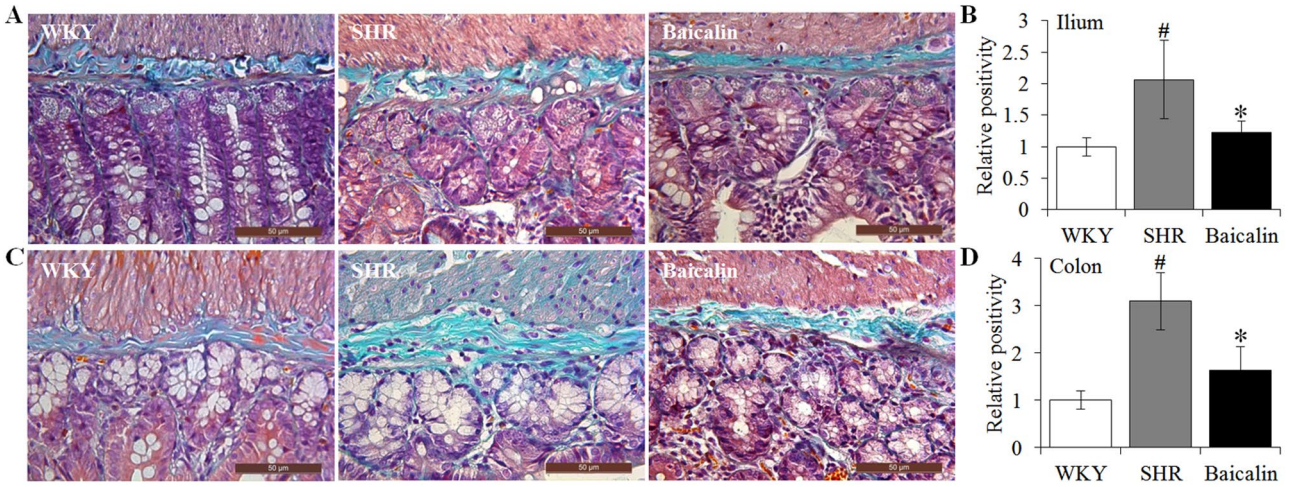

FIGURE 4 | Baicalin treatment alleviates the intestinal fibrotic lesions in spontaneously hypertensive rats (SHRs). The ilium and proximal colon specimens were collected from 12-week-old vehicle-treated Wistar-Kyoto rats (WKY), vehicle-treated SHRs (SHR), and baicalin-treated SHRs (baicalin) after 6 week of the indicated treatments. Paraffin sections were then made and subject to Masson's trichrome staining to assess the fibrotic changes in the ilium **(A)** and colon **(C)**. Masson's trichrome positivity in the ilium **(B)** and colon sections **(D)** was then measured and expressed as the relative positivity against that from the WKY controls. Scale bar: 50 μm. Data were expressed as mean ± S.E.M (n = 6 per group). # Compared to that from the vehicle-treated WKY rats, $p < 0.05$; * compared to that from the vehicle-treated SHRs, $p < 0.05$.

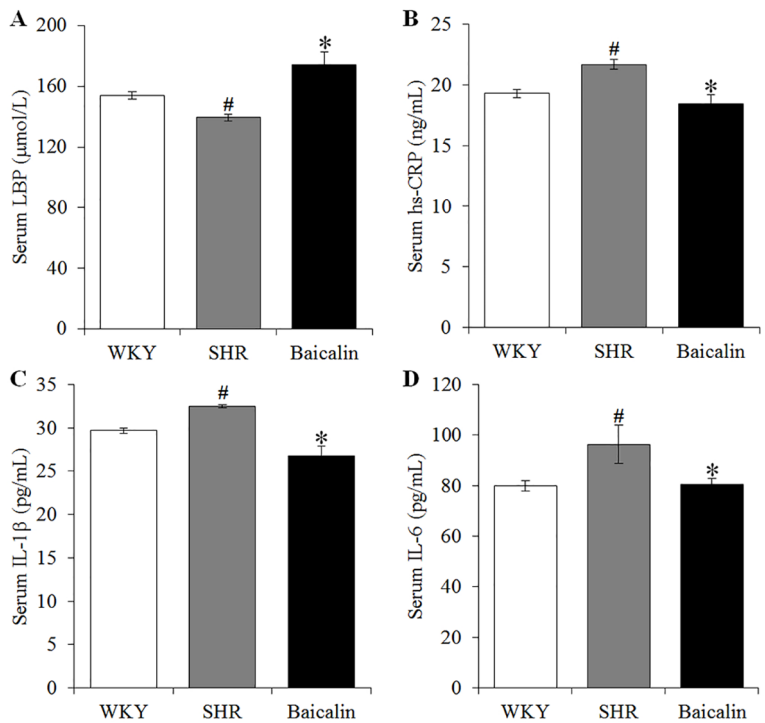

FIGURE 5 | Baicalin treatment attenuates the intestinal hyperpermeability and systemic inflammatory response in the spontaneously hypertensive rats (SHRs). After 6 weeks of the indicated treatments, enzyme-linked immunosorbent assay was performed to analyze the serum levels of LBP **(A)**, high-sensitivity C-reactive protein **(B)**, interleukin 1 beta **(C)**, and IL-6 **(D)** in the vehicle-treated WKY controls (WKY), vehicle-treated SHRs (SHR) and baicalin-treated SHRs (Baicalin). Data were expressed as mean ± S.E.M (n = 10 per group). # Compared to that from the vehicle-treated WKY rats, $p < 0.05$; * compared to that from the vehicle-treated SHRs, $p < 0.05$.

IL-6 were further analyzed. The results showed that compared to that from the vehicle-treated WKY controls, the serum levels of hs-CRP (**Figure 5B**), IL-1β (**Figure 5C**), and IL-6 (**Figure 5D**) were increased in the vehicle-treated SHRs, whereas significantly decreased serum levels of hs-CRP, IL-1β, and IL-6 were observed in the baicalin-treated SHRs. These results collectively indicate that baicalin treatment attenuates intestinal hyperpermeability and systemic inflammatory response in the SHRs.

Baicalin Treatment Preserves the Intestinal Tight Junction in the Spontaneously Hypertensive Rats

The intestinal permeability is regulated by tight junctions. Next, the ileal and colonic expression of genes encoding tight junction proteins including ZO-1, cingulin (Cgn), and occludin (Ocln) was analyzed to better understand the protective effect of baicalin against intestinal hyperpermeability in the SHRs. As shown in **Figure 6A**, compared to that from the vehicle-treated WKY rats, the ileal expression of *ZO-1*, *Cgn,* and *Ocln* was remarkably decreased in the 12-week old vehicle-treated SHRs. In distinct contrast, significantly increased ileal expression of *ZO-1*, *Cgn,* and *Ocln* was observed in the baicalin-treated SHRs compared to that from the vehicle-treated SHRs. Meanwhile, as shown in **Figure 6B**, significantly decreased colonic expression of *ZO-1*, *Cgn,* and *Ocln* was observed in the vehicle-treated SHRs compared to the vehicle-treated WKY controls. Baicalin treatment, however, resulted in increased expression of *ZO-1*, *Cgn,* and *Ocln* in the colon in the SHRs. Immunohistochemistry was also performed to visualize the changes in the intestinal tight junction proteins *in situ*. As shown in **Figures 7A, B**, decreased immunopositivity of ZO-1 was observed in the ilium in the vehicle-treated SHRs compared to that from the vehicle-treated WKY controls. On the contrary, compared to that from the vehicle-treated SHRs, increased ZO-1 immunopositivity was observed in the ilium in the baicalin-treated SHRs. In addition, baicalin treatment resulted in increased immunopositivity of Cgn in the ilium in SHRs compared to that from the vehicle-treated SHRs, in which the immunopositivity of Cgn was found to be decreased compared to the vehicle-treated WKY controls (**Figures 7C, D**). Similar observation was also made in the proximal colon (**Figure 8**). Furthermore, TEM was adopted to examine the ultrastructure of the ilium and the proximal colon. As shown in **Figure 9A**, compared to that from the vehicle-treated WKY controls, the ileal tight junction was disrupted in the vehicle-treated SHRs, which was found to be intact in the baicalin-treated SHRs. In the colonic tissue, in addition to loosened tight junction, shortened villi structure was observed in the vehicle-treated SHRs compared to that from the vehicle-treated WKYs. In contrast, baicalin treatment preserved the tight junction and the villi structure in the SHRs (**Figure 9B**). Taken together, these results indicate that baicalin treatment exerts protective effects on the intestinal integrity, in particular, intestinal tight junction under hypertensive conditions.

Baicalin Treatment Increases the Microbial Production of Short-Chain Fatty Acids in Spontaneously Hypertensive Rats

SCFAs are produced in the gut and are essential for the maintenance of the intestinal barrier integrity (Sakata, 1987; Peng et al., 2009). Therefore, the amount of the fecal SCFAs was further analyzed to better understand the mechanisms underlying the protective effect of baicalin on the intestinal barrier. As shown in **Figure 10A**, although no significant changes in the amount of fecal SCFAs were observed in the 12-week old vehicle-treated SHRs compared to that from the vehicle-treated WKY controls, significantly increased amount of acetic acid, propionic acid, butyric acid, isobutyric acid, valeric acid, and isovaleric acid was noted in the baicalin-treated SHRs compared to the vehicle-treated SHRs, suggesting a direct effect of baicalin on the microbial production of SCFAs in the SHRs. To validate the effect of baicalin on SCFAs production, the amount of fecal SCFAs was also analyzed in the 20-week old SHRs along with the vehicle-treated WKY controls. By 20 week of age, although without statistical significance, the amount of acetic acid and propionic acid was decreased by

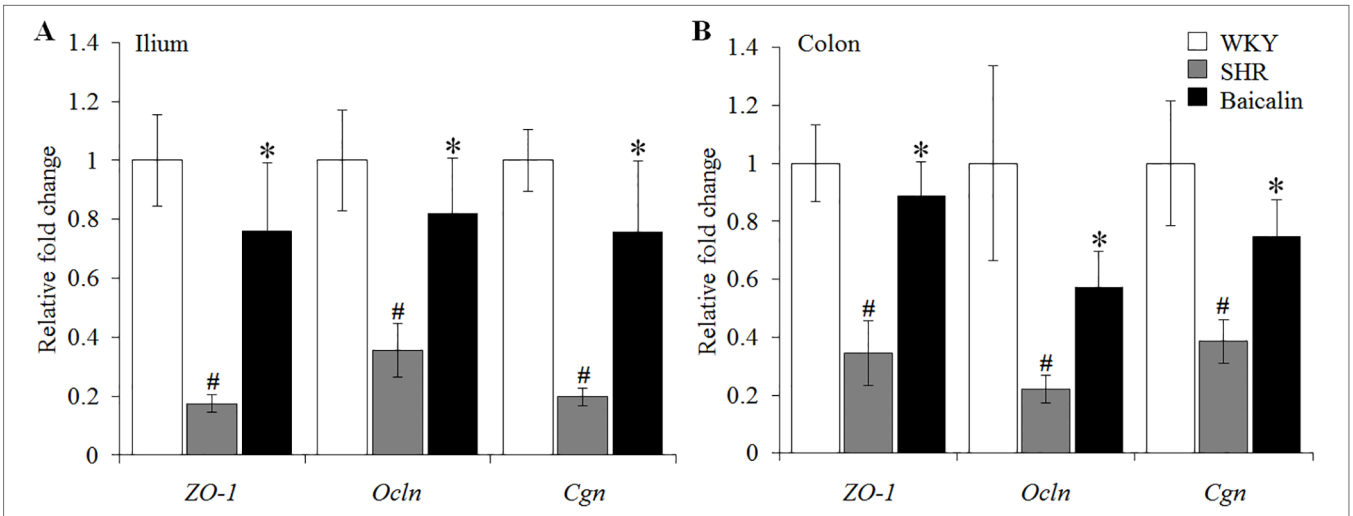

FIGURE 6 | Baicalin treatment increases the ileal and colonic expression of the genes encoding zonula occludens-1 (ZO-1), Ocln, and Cgn. Real-time polymerase chain reaction was performed after 6 weeks of the indicated treatment to analyze the ileal **(A)** and colonic **(B)** expression of ZO-1, Ocln, and Cgn. The expression of glyceraldehyde 3-phosphate dehydrogenase was included as the internal control. Relative fold change of ZO-1, cingulin, and occludin in the vehicle-treated spontaneously hypertensive rats (SHRs) and baicalin-treated SHRs against that from the vehicle-treated Wistar-Kyoto (WKYs) was presented. Data were expressed as mean ± S.E.M (n = 6 per group). # Compared to that from the vehicle-treated Wistar-Kyoto rats, $p < 0.05$; * compared to that from the vehicle-treated SHRs, $p < 0.05$.

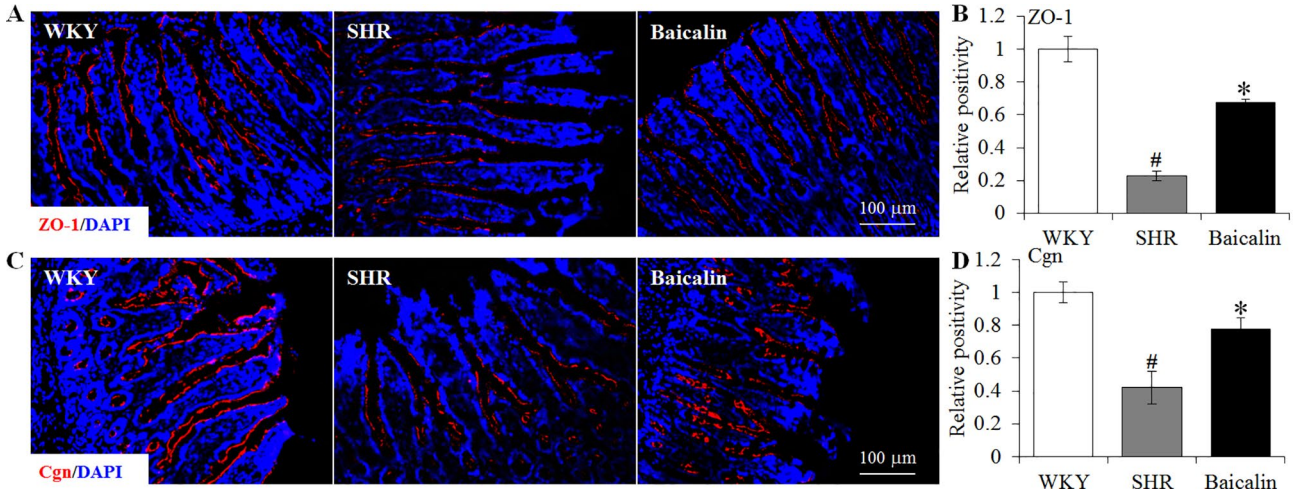

FIGURE 7 | Baicalin treatment increases immunopositivity of zonula occludens-1 (ZO-1) and Cgn in the ilium in the spontaneously hypertensive rats (SHRs). Immunohistochemistry was performed at the end of the 6 weeks of the indicated treatment to reveal the expression of ZO-1 **(A)** and cingulin (Cgn) **(C)** in the ilium *in situ*. Counterstaining of 4-6-diamidino-2-phenylindole was performed to visualize the nucleus. The immunopositivity was recorded using a fluorescent microscope and analyzed using ImageJ. Relative immunopositivity of ZO-1 **(B)** and Cgn **(D)** in the vehicle-treated SHRs and baicalin-treated SHRs against that from the vehicle-treated Wistar-Kyotos (WKYs) was presented. Scale bar: 100 μm. Data were expressed as mean ± S.E.M (n = 6 per group). # Compared to that from the vehicle-treated WKY rats, $p < 0.05$; * compared to that from the vehicle-treated SHRs, $p < 0.05$.

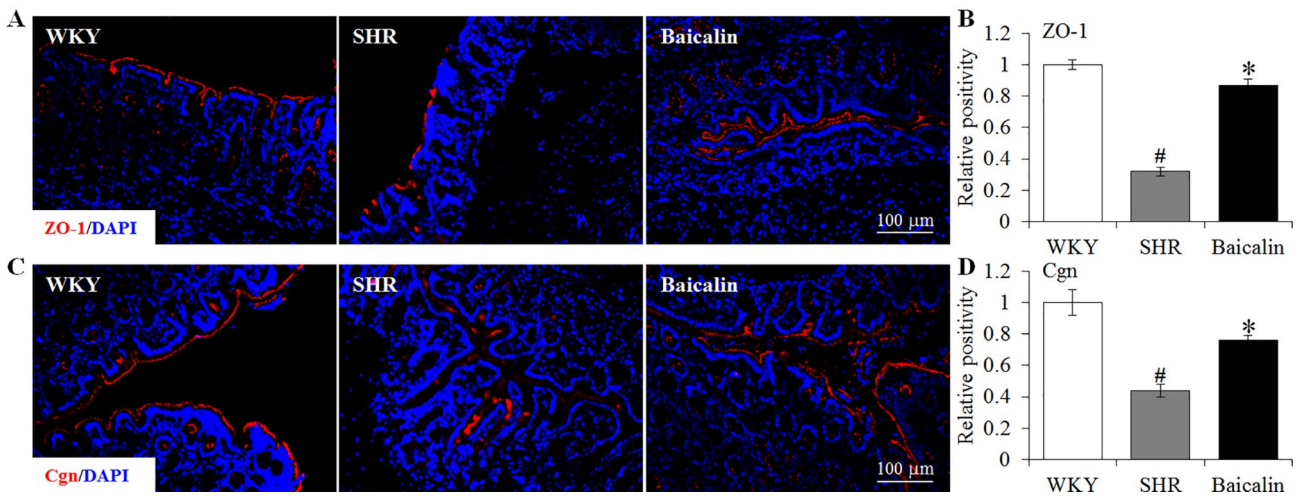

FIGURE 8 | Baicalin treatment increases immunopositivity of zonula occludens-1 (ZO-1) and cingulin (Cgn) in the proximal colon in the spontaneously hypertensive rats (SHRs). Immunohistochemistry was performed at the end of the 6 weeks of the indicated treatment to reveal the expression of ZO-1 **(A)** and cingulin (Cgn) **(C)** in the proximal colon *in situ*. Counterstaining of 4-6-diamidino-2-phenylindole was performed to visualize the nucleus. The immunopositivity was recorded using a fluorescent microscope and analyzed using ImageJ. Relative immunopositivity of ZO-1 **(B)** and Cgn **(D)** in the vehicle-treated SHRs and baicalin-treated SHRs against that from the vehicle-treated Wistar-Kyoto (WKYs) was presented. Scale bar: 100 μm. Data were expressed as mean ± S.E.M (n = 6 per group). # Compared to that from the vehicle-treated WKY rats, $p < 0.05$; * compared to that from the vehicle-treated SHRs, $p < 0.05$.

approximately 20 and 30%, respectively, in the vehicle-treated SHRs compared to that from the vehicle-treated WKY controls, whereas a remarkable increase in the amount of acetic acid, propionic acid, butyric acid, isobutyric acid, valeric acid, and isovaleric acid was observed in the baicalin-treated SHRs (**Figure 10B**). These results confirm that baicalin may have a direct impact on the microbial production of SCFAs in the SHRs. Thus, the abundance of SCFAs-producing bacteria was further analyzed by 16S rDNA sequencing of the fecal samples. As shown in **Table 2**, SCFAs-producing bacteria including the genus *Faecalitalea* and *Streptococcus* were not detected in the vehicle-treated SHRs compared to that from the vehicle-treated WKY controls. Baicalin treatment resulted in significantly increased abundance of *Streptococcus* in the SHRs. It is also noted that although not at a statistically significant level, the genus *Faecalitalea* was detected in the fecal samples from the

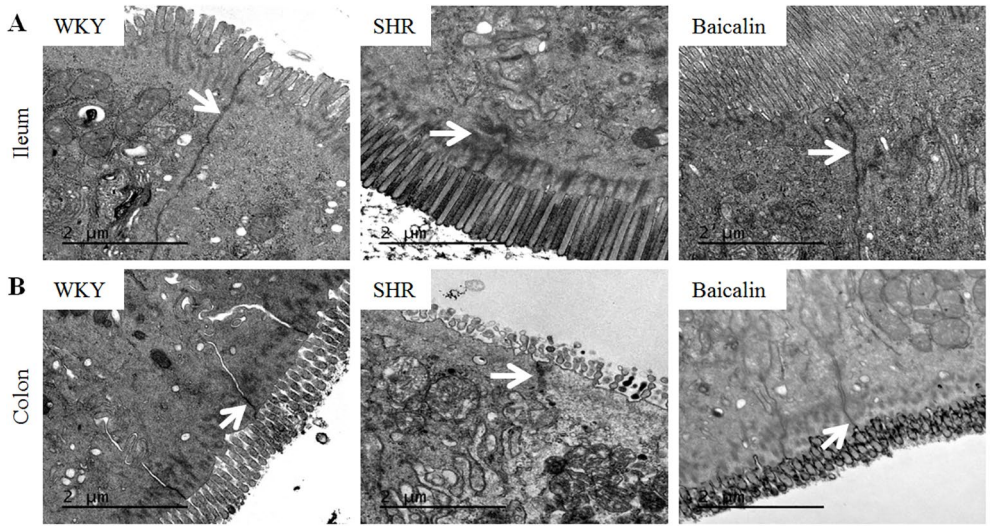

FIGURE 9 | Baicalin treatment alleviates the impairment of the intestinal ultrastructure in the spontaneously hypertensive rats (SHRs). At the end of the 6-week treatment, ilium and proximal colon specimens were collected, which was followed by transmission electron microscopy to assess the changes in the ileal **(A)** and colonic **(B)** ultrastructure in the vehicle-treated Wistar-Kyoto controls (WKY), vehicle-treated SHRs (SHR), and baicalin-treated SHRs (baicalin). Scale bar: 2 μm. White arrows indicate tight junctions.

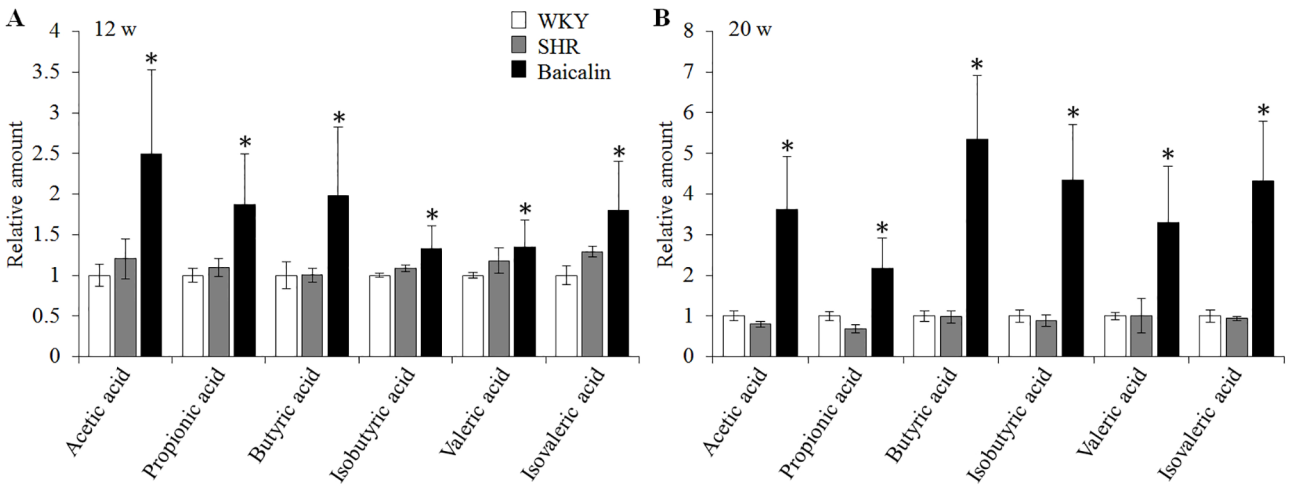

FIGURE 10 | Baicalin treatment increases the fecal level of SCFAs in the spontaneously hypertensive rats (SHRs). Six-week old SHRs were treated with or baicalin for 6 weeks or 14 weeks. At the end of the indicated treatments, fecal samples were collected from 12 or 20-week old vehicle-treated Wistar-Kyoto (WKY) controls, vehicle-treated SHRs and baicalin-treated SHRs. GC-MS analyses were performed to quantify the amount of fecal SCFAs. **(A)** The relative amount of the fecal short-chain fatty acids (SCFAs) from the rats that were treated for 6 weeks. **(B)**. The relative amount of the fecal SCFAs from the rats that received the indicated treatments for 14 weeks. Data were expressed as mean ± S.E.M (n = 5 per group). * compared to that from the vehicle-treated SHRs, $p < 0.05$.

baicalin-treated SHRs. In addition, the abundance of the genus *Akkermansia*, *Allobaculum*, *Bifidobacterium*, *Lachnospiraceae_NK4B4_group,* and *Roseburia* exhibited a tendency of reduction in the vehicle-treated SHRs compared to that from the vehicle-treated WKYs, in particular, the genera *Bifidobacterium* and *Lachnospiraceae_NK4B4_group* were undetectable in the vehicle-treated SHRs. However, significantly increased abundance of these genera was observed in the baicalin-treated SHRs. These results indicate baicalin treatment increases the abundance of SCFAs-producing bacteria in the SHRs.

DISCUSSION

The current study mainly demonstrates that baicalin protects against the impairment of the intestinal barrier and increases

TABLE 2 | Baicalin treatment increases the abundance of short-chain fatty acids-producing bacteria in the spontaneously hypertensive rats.

Genus	Mean ± SEM			p value	
	WKY (%)	SHR (%)	Baicalin (%)	SHR *vs*. WKY	Baicalin *vs*. SHR
Akkermansia	0.0008 ± 0.0008	0.0030 ± 0.0030	0.0189 ± 0.0061	0.37	0.03*
Allobaculum	0.0257 ± 0.0114	0.0083 ± 0.0057	0.0280 ± 0.0066	0.20	0.04*
Bifidobacterium	0.0408 ± 0.0215	0	0.0922 ± 0.0385	0.08	0.03*
Faecalitalea	0.0121 ± 0.0051	0	0.003 ± 0.0014	0.03#	0.13
Lachnospiraceae_NK4B4_group	0.0023 ± 0.0015	0	0.0113 ± 0.0048	0.25	0.03*
Roseburia	0.1391 ± 0.0363	0.0673 ± 0.0122	0.1739 ± 0.0441	0.08	0.03*
Ruminococcaceae_UCG-009	0.2805 ± 0.0537	0.2238 ± 0.0425	0.375 ± 0.0403	0.50	0.02*
Ruminococcaceae_UCG-010	0.224 ± 0.0295	0.2495 ± 0.0693	0.4468 ± 0.0612	0.77	0.05*
Ruminococcaceae_UCG-014	1.5747 ± 0.0431	2.2370 ± 0.3456	3.3461 ± 0.3607	0.08	0.04*
Ruminococcus_2	0.0181 ± 0.0172	0.0265 ± 0.0117	0.0900 ± 0.0270	0.73	0.04*
Streptococcus	0.0076 ± 0.0032	0	0.0083 ± 0.0028	0.03#	0.01*

#*Compared to that from the vehicle-treated WKY rats, $p < 0.05$; * compared to that from the vehicle-treated SHRs, $p < 0.05$.*

the microbial production of SCFAs under hypertensive conditions. Baicalin treatment provides partial protection against the development of hypertension-associated necrotic, ulcerative, and fibrotic changes in the intestine, suppresses the intestinal expression of proinflammatory genes, ameliorates intestinal hyperpermeability and systemic inflammation, attenuates tight junction disruption, and increases the abundance of SCFAs-producing bacteria as well as the fecal amount of SCFAs in the SHRs.

In addition to absorbing the nutrients and water, the intestine also serves as the internal barrier preventing the invasion of pathogens and limiting the systemic exposure to harmful luminal contents (Gutsmann et al., 2001; Konig et al., 2016). Disruption of the intestinal barrier increases the intestinal permeability and leads to systemic exposure of luminal endotoxins, pathogens, and antigens. This often results in altered innate immunity and triggers systemic inflammatory responses. Impaired intestinal barrier integrity is thus mechanistically implicated in the development of inflammatory state encountered in various intestinal and extra-intestinal diseases including hypertension (Cani et al., 2008; Cani et al., 2009; Fukui, 2016; Jaworska et al., 2017; Santisteban et al., 2017). Given that chronic low-grade inflammation not only is a risk factor for hypertension, but also perpetuates hypertension and promotes the development of hypertensive target organ damages and treatment resistance, maintaining the intestinal barrier integrity is important for the optimal control of hypertension. One of the major components of the intestinal barrier is the mechanical barrier primarily composed of the intestinal epithelium. The current study reveals that baicalin protects the ileal and colonic tissues from developing necrotic, ulcerative, and fibrotic lesions in the SHRs. The ileal and colonic expression of proinflammatory gene in the SHRs is decreased as a result of baicalin treatment. Meanwhile, the ultrastructure of the intestinal tight junction in the SHRs is preserved by baicalin treatment, which is paralleled by increased expression of genes encoding tight junction proteins in the intestine, decreased intestinal permeability and lower levels of inflammatory biomarkers in the serum. These results collectively support the notion that baicalin is pharmacologically active at maintaining the intestinal epithelial barrier integrity under hypertensive conditions.

The intestinal protective effects of baicalin in the SHRs may in part be attributed to its anti-inflammatory effect. Anti-inflammatory effects of baicalin have been experimentally established in different cell types. For instance, baicalin suppresses LPS-induced production of proinflammatory IL-6 and TNF-α in HBE16 airway epithelial cells (Dong et al., 2015). Baicalin inhibits TLR4 signaling in LPS-stimulated peripheral blood mononuclear cells (Ye et al., 2015). Baicalin suppresses TLR4-mediated neuroinflammation *in vivo* and in microglial cells *in vitro* (Guo et al., 2019). Baicalin also alleviates the colonic lesions in an experimental inflammatory bowel disease model *in vivo* (Zhu et al., 2016). Our current study further demonstrates that under hypertensive conditions, baicalin treatment alleviates the necrotic and ulcerative lesions and decreases the expression of proinflammatory genes in the ilium and colon. It is also noted that increased expression of proinflammatory genes in the ileum and colon appears to be affected by hypertension in a different manner. While significantly increased expression of *Tlr4* and *TNF-α* is observed in the ilium, increased expression of *Tlr2*, *HMGB1*, *TNF-α*, *IL-1β,* and *IL-23* is noted in the colon in the 12-week old SHRs. However, baicalin treatment not only counteracts hypertension-associated increase in the expression of *Tlr4* and *TNF-α* in the ilium, but also significantly decreases the ileal expression of *Tlr2*, *HMGB1*, *RAGE*, *IL-1β,* and *IL-23* in the SHRs although the expression of these genes is not altered in the vehicle-treated SHRs. In the colon, however, baicalin treatment counteracts hypertension-associated increases in the expression of *Tlr2*, *TNF-α*, *IL-1β,* and *IL-23* but not *HMGB1* in the SHRs. These results suggest that baicalin treatment may have differential impacts on the expression of proinflammatory genes in the ilium and colon. In particular, baicalin may directly decrease the basal expression of *Tlr2*, *HMGB1*, *RAGE*, *IL-1β,* and *IL-23* in the ilium, which remains to be elucidated in the future studies.

In addition, the intestines in the SHRs are characterized by disrupted intestinal tight junction structure and decreased expression of genes encoding tight junction proteins, which is attenuated as a result of baicalin treatment. These observations provide morphological and molecular evidence further supporting the protective effects of baicalin on the intestinal

epithelial integrity under hypertensive conditions, which may in part result from enhanced expression of tight junction proteins as a result of baicalin treatment. In agreement with the protective effect of baicalin on the intestinal tight junctions observed in the current study, similar effect of baicalin on tight junctions has been reported by other studies. It has been demonstrated that baicalin protects against TNF-α-induced downregulation of ZO-1 expression in rat small intestinal epithelial cells *in vitro* (Wang et al., 2017). Another study has shown that baicalin restores the blood-brain barrier function through promoting the expression of tight junction proteins in cultured brain microvascular cells (Zhu et al., 2012). Therefore, the findings from our current study provide additional *in vivo* evidence supporting the protective effect of baicalin on the tight junctions. Given that baicalin treatment results in decreased intestinal expression of *TNF-α* in the SHRs, it is likely that the observed effect of baicalin on the intestinal tight junctions is in part derived from its anti-inflammatory effect.

Meanwhile, it is worth noting that baicalin treatment increases the fecal level of SCFAs under hypertensive conditions. The results from the current study also imply a direct effect of baicalin on the microbial production of SCFAs given that baicalin treatment increases the fecal level of SCFAs in the SHRs even when no significant alterations of the fecal SCFAs are noted in the vehicle-treated SHRs compared to that from the vehicle-treated WKY controls. Gut microbiota-produced metabolites play important roles in regulating normal intestinal homeostasis and multiple extra-intestinal physiological processes in the host. SCFAs, generated in the colon through microbial fermentation of undigested dietary carbohydrates, have a diverse range of health-promoting properties (Bond and Levitt, 1976). SCFAs may reduce the intestinal hyperpermeability and preserve the intestinal integrity in part through increasing the expression of tight junction proteins, thereby alleviating systemic inflammation and endotoxemia caused by intestinal hyperpermeability. For instance, as the primary energy source of colonocytes, butyrate regulates tight junctions and preserves intestinal barrier integrity (Peng et al., 2009). Butyrate also coordinates intestinal barrier protection through stabilizing hypoxia-inducible factor (Kelly et al., 2015). Relevant to the findings from the current study, increased SCFAs may in part contribute to the effect of baicalin at protecting the intestinal tight junctions and alleviating the intestinal permeability and systemic inflammation in the SHRs.

It is worth noting that the results from the current study reveal that the abundance of SCFAs-producing bacteria is increased as a result of baicalin treatment, including the genus *Roseburia*, *Ruminococcaceae UCG-009*, *Ruminococcaceae UCG-010*, *Ruminococcaceae UCG-014*, *Bifidobacterium*, *Akkermansia*, *Allobaculum,* and *Ruminococcus 2* (Ohira et al., 2017). The family *Ruminococcaceae* constitutes a type of common commensal gut bacteria that digests complex carbohydrates, serving as one of the predominant bacteria for the production of SCFAs, in particularly butyrate (Koh et al., 2016). *Bifidobacterium* spp. produces acetate and butyrate (Riviere et al., 2016). *Akkermansia*, produces butyrate and propionate (Naito et al., 2018). *Ruminococcus* spp. or *Streptococcus* generates butyrate (Riviere et al., 2016). Most members in the genus *Allobaculum* are SCFAs-producing bacteria (Everard et al., 2014). *Roseburia* spp. is among a group of dominant butyrate-producing *Firmicutes* (Takahashi et al., 2016; La Rosa et al., 2019) and plays an important role in controlling the inflammatory response in the gut primarily through the production of butyrate (Tamanai-Shacoori et al., 2017). Increased abundance of the above-mentioned SCFAs-producing bacteria in part explains elevated fecal level of SCFAs in the baicalin-treated SHRs. In addition, the effect of baicalin on increasing the abundance of SCFAs-producing bacteria and the microbial production of SCFAs is also corroborated by a recent report showing that baicalin increases the microbial production of SCFAs in mice fed with long-term high fat diet (Ju et al., 2019). However, to what extent the enhanced microbial production of SCFAs contributes baicalin-mediated intestinal barrier protection in the SHRs remains to be investigated in the future studies.

Meanwhile, vasodilatory effects of SCFAs have been reported (Mortensen et al., 1990; Nutting et al., 1991). SCFAs are involved in the blood pressure regulation *in vivo* (Pluznick, 2017). Meta-analyses have also shown that probiotic treatment or increased dietary fiber intake lowers the blood pressure presumably due to increased microbial production of SCFAs (Whelton et al., 2005; Khalesi et al., 2014). Therefore, in addition to the possible implication in baicalin-conferred intestinal barrier protection, increased production of SCFAs might in part contribute to the blood pressure-lowering effect of baicalin in the SHRs, which remains to be clarified in the future studies.

As shown in the current work, baicalin protects against hypertension-associated intestinal impairment. However, it remains to be clarified whether baicalin exerts a primary impact on the hypertensive gut or the intestinal protection occurs in a secondary manner as baicalin treatment results in a partial decrease in the blood pressure. Our results show that baicalin treatment decreases the ileal expression of *Tlr2*, *HMGB1*, *RAGE*, *IL-1β,* and *IL-23* in the SHRs when no significant changes in the expression of these genes are noted in the vehicle-treated SHRs. In addition, baicalin treatment enhances the microbial production of SCFAs prior to any hypertension-associated changes in the SCFAs are observed in the vehicle-treated SHRs. Although these results suggest a direct impact of baicalin on the hypertensive gut, it is still likely that baicalin treatment exerts a beneficial effect on the gut in part through lowering the blood pressure. Future studies are worth pursuing to clarify the intestinal effect and the associated mechanisms of baicalin under hypertensive conditions.

CONCLUSION

In conclusion, the current study demonstrates for the first time that baicalin exerts protective effect on the intestinal integrity under hypertensive conditions. Most notably, baicalin treatment increases the abundance of SCFAs-producing bacteria in the gut, thereby promoting the production of SCFAs in the SHRs.

Thus, the current work provides novel experimental evidence enriching the pharmacological understanding of baicalin. In addition, given that baicalin is the signature chemical component of *S. baicalensis* Georgi, the findings here may help better understand the traditional application of *S. baicalensis* Georgi in the treatment of hypertension.

DATA AVAILABILITY STATEMENT

The project was deposited at EMBL database with the accession number PRJEB34365.

ETHICS STATEMENT

The animal study was reviewed and approved by Institutional Animal Care and Use Committee at Yueyang Hospital, Shanghai University of Traditional Chinese Medicine.

AUTHOR CONTRIBUTIONS

TZ and YC designed and supervised the study. DW, LD, and XT performed the experiments. DW, WW, TZ, and YC analyzed the data. TZ, DW, and YC wrote the manuscript.

FUNDING

This work was supported by the Program for Professor of Special Appointment (Eastern Scholar) at Shanghai Institutions of Higher Learning (GZ2015011 and GZ2017064, TZ and YC).

SUPPLEMENTARY MATERIAL

The Supplementary Material for this article can be found online at: https://www.frontiersin.org/articles/10.3389/fphar.2019.01271/full#supplementary-material

REFERENCES

Ahluwalia, M., and Bangalore, S. (2017). Management of hypertension in 2017: targets and therapies. *Curr. Opin. Cardiol.* 32, 413–421. doi: 10.1097/HCO.0000000000000408

Bond, J. H., and Levitt, M. D. (1976). Fate of soluble carbohydrate in the colon of rats and man. *J. Clin. Invest.* 57, 1158–1164. doi: 10.1172/JCI108383

Cani, P. D., Bibiloni, R., Knauf, C., Waget, A., Neyrinck, A. M., Delzenne, N. M., et al. (2008). Changes in gut microbiota control metabolic endotoxemia-induced inflammation in high-fat diet-induced obesity and diabetes in mice. *Diabetes.* 57, 1470–1481. doi: 10.2337/db07-1403

Cani, P. D., Possemiers, S., Van de Wiele, T., Guiot, Y., Everard, A., Rottier, O., et al. (2009). Changes in gut microbiota control inflammation in obese mice through a mechanism involving GLP-2-driven improvement of gut permeability. *Gut.* 58, 1091–1103. doi: 10.1136/gut.2008.165886

Ding, L., Jia, C., Zhang, Y., Wang, W., Zhu, W., Chen, Y., et al. (2019). Baicalin relaxes vascular smooth muscle and lowers blood pressure in spontaneously hypertensive rats. *Biomed. Pharmacother.* 111, 325–330. doi: 10.1016/j.biopha.2018.12.086

Dong, S. J., Zhong, Y. Q., Lu, W. T., Li, G. H., Jiang, H. L., and Mao, B. (2015). Baicalin inhibits lipopolysaccharide-induced inflammation through signaling NF-kappaB pathway in HBE16 Airway epithelial cells. *Inflammation* 38, 1493–1501. doi: 10.1007/s10753-015-0124-2

Everard, A., Lazarevic, V., Gaia, N., Johansson, M., Stahlman, M., Backhed, F., et al. (2014). Microbiome of prebiotic-treated mice reveals novel targets involved in host response during obesity. *ISME J.* 8, 2116–2130. doi: 10.1038/ismej.2014.45

Forsyth, C. B., Shannon, K. M., Kordower, J. H., Voigt, R. M., Shaikh, M., Jaglin, J. A., et al. (2011). Increased intestinal permeability correlates with sigmoid mucosa alpha-synuclein staining and endotoxin exposure markers in early Parkinson's disease. *PLoS One.* 6, e28032. doi: 10.1371/journal.pone.0028032

Fukui, H. (2016). Increased Intestinal Permeability and Decreased Barrier Function: Does It really influence the risk of inflammation? *Inflamm. Intest. Dis.* 1, 135–145. doi: 10.1159/000447252

Guo, L. T., Wang, S. Q., Su, J., Xu, L. X., Ji, Z. Y., Zhang, R. Y., et al. (2019). Baicalin ameliorates neuroinflammation-induced depressive-like behavior through inhibition of toll-like receptor 4 expression via the PI3K/AKT/FoxO1 pathway. *J. Neuroinflammation.* 16, 95. doi: 10.1186/s12974-019-1474-8

Gutsmann, T., Muller, M., Carroll, S. F., MacKenzie, R. C., Wiese, A., and Seydel, U. (2001). Dual role of lipopolysaccharide (LPS)-binding protein in neutralization of LPS and enhancement of LPS-induced activation of mononuclear cells. *Infect. Immun.* 69, 6942–6950. doi: 10.1128/IAI.69.11.6942-6950.2001

Jaworska, K., Huc, T., Samborowska, E., Dobrowolski, L., Bielinska, K., Gawlak, M., et al. (2017). Hypertension in rats is associated with an increased permeability of the colon to TMA, a gut bacteria metabolite. *PLoS One.* 12, e0189310. doi: 10.1371/journal.pone.0189310

Ju, M., Liu, Y., Li, M., Cheng, M., Zhang, Y., Deng, G., et al. (2019). Baicalin improves intestinal microecology and abnormal metabolism induced by high-fat diet. *Eur. J. Pharmacol.* 857, 172457. doi: 10.1016/j.ejphar.2019.172457

Kelly, C. J., Zheng, L., Campbell, E. L., Saeedi, B., Scholz, C. C., Bayless, A. J., et al. (2015). Crosstalk between microbiota-derived short-chain fatty acids and intestinal epithelial hif augments tissue barrier function. *Cell Host Microbe.* 17, 662–671. doi: 10.1016/j.chom.2015.03.005

Khalesi, S., Sun, J., Buys, N., and Jayasinghe, R. (2014). Effect of probiotics on blood pressure: a systematic review and meta-analysis of randomized, controlled trials. *Hypertension* 64, 897–903. doi: 10.1161/HYPERTENSIONAHA.114.03469

Koh, A., De Vadder, F., Kovatcheva-Datchary, P., and Backhed, F. (2016). From dietary fiber to host physiology: short-chain fatty acids as key bacterial Metabolites. *Cell.* 165, 1332–1345. doi: 10.1016/j.cell.2016.05.041

Konig, J., Wells, J., Cani, P. D., Garcia-Rodenas, C. L., MacDonald, T., Mercenier, A., et al. (2016). Human Intestinal Barrier Function in Health and Disease. *Clin. Transl. Gastroenterol.* 7, e196. doi: 10.1038/ctg.2016.54

La Rosa, S. L., Leth, M. L., Michalak, L., Hansen, M. E., Pudlo, N. A., Glowacki, R., et al. (2019). The human gut Firmicute Roseburia intestinalis is a primary degrader of dietary beta-mannans. *Nat. Commun.* 10, 905. doi: 10.1038/s41467-019-08812-y

Mortensen, F. V., Nielsen, H., Mulvany, M. J., and Hessov, I. (1990). Short chain fatty acids dilate isolated human colonic resistance arteries. *Gut.* 31, 1391–1394. doi: 10.1136/gut.31.12.1391

Naito, Y., Uchiyama, K., and Takagi, T. (2018). A next-generation beneficial microbe: Akkermansia muciniphila. *J. Clin. Biochem. Nutr.* 63, 33–35. doi: 10.3164/jcbn.18-57

Nutting, C. W., Islam, S., and Daugirdas, J. T. (1991). Vasorelaxant effects of short chain fatty acid salts in rat caudal artery. *Am. J. Physiol.* 261, H561–H567. doi: 10.1152/ajpheart.1991.261.2.H561

Ohira, H., Tsutsui, W., and Fujioka, Y. (2017). Are short chain fatty acids in gut microbiota defensive players for inflammation and atherosclerosis? *J. Atheroscler. Thromb.* 24, 660–672. doi: 10.5551/jat.RV17006

Peng, L., Li, Z. R., Green, R. S., Holzman, I. R., and Lin, J. (2009). Butyrate enhances the intestinal barrier by facilitating tight junction assembly via activation of AMP-activated protein kinase in Caco-2 cell monolayers. *J. Nutr.* 139, 1619–1625. doi: 10.3945/jn.109.104638

Pluznick, J. L. (2017). Microbial short-chain fatty acids and blood pressure regulation. *Curr. Hypertens. Rep.* 19, 25. doi: 10.1007/s11906-017-0722-5

Riviere, A., Selak, M., Lantin, D., Leroy, F., and De Vuyst, L. (2016). Bifidobacteria and Butyrate-producing colon bacteria: importance and strategies for their stimulation in the human gut. *Front. Microbiol.* 7, 979. doi: 10.3389/fmicb.2016.00979

Sakata, T. (1987). Stimulatory effect of short-chain fatty acids on epithelial cell proliferation in the rat intestine: a possible explanation for trophic effects of fermentable fibre, gut microbes and luminal trophic factors. *Br. J. Nutr.* 58, 95–103. doi: 10.1079/BJN19870073

Santisteban, M. M., Qi, Y., Zubcevic, J., Kim, S., Yang, T., Shenoy, V., et al. (2017). Hypertension-linked pathophysiological alterations in the gut. *Circ. Res.* 120, 312–323. doi: 10.1161/CIRCRESAHA.116.309006

Solak, Y., Afsar, B., Vaziri, N. D., Aslan, G., Yalcin, C. E., Covic, A., et al. (2016). Hypertension as an autoimmune and inflammatory disease. *Hypertens. Res.* 39, 567–573. doi: 10.1038/hr.2016.35

Takahashi, K., Nishida, A., Fujimoto, T., Fujii, M., Shioya, M., Imaeda, H., et al. (2016). Reduced abundance of butyrate-producing bacteria species in the fecal microbial community in crohn's disease. *Digestion.* 93, 59–65. doi: 10.1159/000441768

Tamanai-Shacoori, Z., Smida, I., Bousarghin, L., Loreal, O., Meuric, V., Fong, S. B., et al. (2017). Roseburia spp.: a marker of health? *Future Microbiol.* 12, 157–170. doi: 10.2217/fmb-2016-0130

Wang, L., Zhang, R., Chen, J., Wu, Q., and Kuang, Z. (2017). Baicalin protects against TNF-alpha-Induced injury by down-regulating mir-191a that targets the tight junction protein ZO-1 in IEC-6 Cells. *Biol. Pharm. Bull.* 40, 435–443. doi: 10.1248/bpb.b16-00789

Whelton, S. P., Hyre, A. D., Pedersen, B., Yi, Y., Whelton, P. K., and He, J. (2005). Effect of dietary fiber intake on blood pressure: a meta-analysis of randomized, controlled clinical trials. *J. Hypertens.* 23, 475–481. doi: 10.1097/01.hjh.0000160199.51158.cf

Wu, D., Tang, X., Ding, L., Cui, J., Wang, P., Du, X., et al. (2019). Candesartan attenuates hypertension-associated pathophysiological alterations in the gut. *Biomed. Pharmacother.* 116, 109040. doi: 10.1016/j.biopha.2019.109040

Ye, L., Tao, Y., Wang, Y., Feng, T., and Li, H. (2015). The effects of baicalin on the TLR2/4 signaling pathway in the peripheral blood mononuclear cells of a lipopolysaccharide-induced rat fever model. *Int. Immunopharmacol.* 25, 106–111. doi: 10.1016/j.intimp.2014.12.028

Zhao, Q., Chen, X. Y., and Martin, C. (2016). Scutellaria baicalensis, the golden herb from the garden of Chinese medicinal plants. *Sci. Bull. (Beijing).* 61, 1391–1398. doi: 10.1007/s11434-016-1136-5

Zhu, H., Wang, Z., Xing, Y., Gao, Y., Ma, T., Lou, L., et al. (2012). Baicalin reduces the permeability of the blood-brain barrier during hypoxia in vitro by increasing the expression of tight junction proteins in brain microvascular endothelial cells. *J. Ethnopharmacol.* 141, 714–720. doi: 10.1016/j.jep.2011.08.063

Zhu, W., Jin, Z., Yu, J., Liang, J., Yang, Q., Li, F., et al. (2016). Baicalin ameliorates experimental inflammatory bowel disease through polarization of macrophages to an M2 phenotype. *Int. Immunopharmacol.* 35, 119–126. doi: 10.1016/j.intimp.2016.03.030

Conflict of Interest: The authors declare that the research was conducted in the absence of any commercial or financial relationships that could be construed as a potential conflict of interest.

frontiers in Pharmacology

MINI REVIEW
published: 11 November 2019
doi: 10.3389/fphar.2019.01334

Preclinical Research of Dihydromyricetin for Brain Aging and Neurodegenerative Diseases

*Hilda Martínez-Coria[1,2], Martha X. Mendoza-Rojas[3], Isabel Arrieta-Cruz[4] and Héctor E. López-Valdés[1,3]**

[1] División de Investigación, Facultad de Medicina, Universidad Nacional Autónoma de México (UNAM), Ciudad de México, México, [2] Laboratorio Experimental de Enfermedades Neurodegenerativas, UNAM-INNyN, Instituto Nacional de Neurología y Neurocirugía "Manuel Velasco Suárez",Ciudad de México, Mexico, [3] Unidad Periférica de Neurociencias, UNAM-INNyN, Instituto Nacional de Neurología y Neurocirugía "Manuel Velasco Suárez",Ciudad de México, Mexico, [4] Departamento de Investigación Básica, Instituto Nacional de Geriatría,Ciudad de México, Mexico

Brain aging and neurodegenerative diseases share the hallmarks of slow and progressive loss of neuronal cells. Flavonoids, a subgroup of polyphenols, are broadly present in food and beverage and numerous studies have suggested that it could be useful for preventing or treating neurodegenerative diseases in humans. Dihydromyricetin (DHM) is one of the main flavonoids of some Asian medicinal plants that are used to treat diverse illness. The effects of DHM have been studied in different *in vitro* systems of oxidative damage and neuroinflammation, as well as in animal models of several neurodegenerative diseases, such as Alzheimer's disease, Parkinson's disease, and Huntington's disease. Here we analyzed the most important effects of DHM, including its antioxidant, anti-inflammatory, and neuroprotective effects, as well as its ability to restore GABA neurotransmission and improve motor and cognitive behavior. We propose new areas of research that might contribute to a better understanding of the mechanism of action of this flavonoid, which could help develop a new therapy for aging and age-related brain diseases.

Keywords: dihydromyricetin, ampelopsin, aging, neurodegenerative diseases, Alzheimer's disease, Parkinson's disease, Huntington's disease

OPEN ACCESS

Edited by:
Valentina Echeverria Moran, Bay Pines VA Healthcare System, United States

Reviewed by:
Marta Llansola, Centro de Investigación Príncipe Felipe, Spain
Subhalakshmi Ghosh, Independent Researcher, Kolkata, India

***Correspondence:**
Héctor E. López-Valdés
helopezv@gmail.com

Specialty section:
This article was submitted to Ethnopharmacology, a section of the journal Frontiers in Pharmacology

Received: *22 July 2019*
Accepted: *18 October 2019*
Published: *11 November 2019*

Citation:
Martínez-Coria H, Mendoza-Rojas MX, Arrieta-Cruz I and López-Valdés HE (2019) Preclinical Research of Dihydromyricetin for Brain Aging and Neurodegenerative Diseases. Front. Pharmacol. 10:1334. doi: 10.3389/fphar.2019.01334

INTRODUCTION

Aging is a major risk factor for developing brain illnesses such as Alzheimer's disease (AD) (Lindsay et al., 2002; Katz et al., 2012), Parkinson's disease (PD) (Collier et al., 2011), and other age-related dementias (López-Valdés and Martínez-Coria, 2016), as well as cerebrovascular disorders (Choi et al., 1998). These diseases share pathophysiological mechanisms with aging such as oxidative stress and chronic inflammation.

Dihydromyricetin (DHM), also known as ampeloptin, rac-ampelopsin, and ampelopsin, is a flavonoid isolated mainly from Japanese raisin trees (*Hovenia dulcis* Thum) and Chinese Rattan tea [*Ampelopsis grossedentata* (Hand.-Mazz.) W.T.Wang]. These plants have been used for a long time in Asian traditional medicine to treat different health problems (Hyun et al., 2010; Kou and Chen, 2012). DHM is one of the main flavonoids found in the Japanese raisin tree and Chinese Rattan tea, together with myricetin and quercetin (Zhang et al., 2007; Hyun et al., 2010).

In the few past decades, scientific knowledge about the effects of DHM has increased considerably. This molecule has a wide range of positive effects, including anti-oxidative, anti-inflammatory and neuroprotective properties, and has been shown to cause motor and memory improvements, all of which can help treat dysfunctions associated with brain aging and some neurodegenerative diseases such as AD and PD.

This work summarizes and analyzes the current scientific information on the pharmacology of DHM, with a particular focus on the pathological processes of age-related brain diseases and on animal models of these diseases. We suggest some areas of research in which this compound could be shown to beneficial effects on human aging and age-related diseases.

DHM Structure, Pharmacokinetics and Toxicity

Dihydromyricetin (2*R*,3*R*)-3,5,7-trihydroxy-2-(3,4,5- trihy droxyphenyl)-2,3-dihydrochromen-4-one is a flavanonol, a subgroup of flavonoids (PubChem CID: 161557 and ChEBI: 28429). This subgroup is a class of secondary plant metabolites that perform many physiological functions in plants as antioxidants, pigments, etc. (Tsao, 2010).

The pharmacokinetic parameters of DHM have so far been identified in rats after oral administration, the results indicating that DHM is poorly absorbed into the bloodstream, with a bioavailability of only 4.02%. Furthermore, the time required for it reaches peak plasma concentration is 2.67 h after oral administration at a dose of 20 mg/kg (Liu et al., 2017). A recent *in vitro* study using the human intestinal Caco-2 cell model, a common tool used to predict, *in vivo*, the absorption of drugs in humans, showed that the uptake and transport of DHM occurs mainly through a passive diffusion mechanism, which can partially explain the low bioavailability of DHM after oral administration (Xiang et al., 2018).

After ingestion by animals, some DHM is metabolized in the gastrointestinal tract and liver, and the rest is absorbed into the bloodstream and is widely distributed throughout the body, including the heart, lungs, kidney, etc., even crossing the blood–brain barrier and spreading through brain tissue (Fan et al., 2017). DHM is completely excreted in urine and feces after 12 h. Seven to eight DHM metabolites have been identified in urine, feces, and blood (Fan et al., 2017), all of them produced by common metabolic routes such as dihydroxylation, methylation, glucuronidation, reduction, and isomerization (Zhang et al., 2007; Fan et al., 2017). Whether these metabolites have any pharmacologic effect is still unknown.

Although there have been few DHM toxicity studies, some important information has already been obtained. For example, the lethal dose 50% for oral administration in mice is >5 g/kg (Zhou and Zhou, 1996). At concentrations ranging from 150 mg/kg (500 mmol/L) to 1.5 g/kg (5,000 mmol/L), DHM did not cause any acute toxicity or had significant side effects on mice (Zhang et al., 2014), which suggests that DHM has very low toxicity (OECD, 2001a; OECD, 2001b); however, more *in vitro* and *in vivo* tests are needed to establish reliable safety limits.

Since low bioavailability limits the pharmacologic value, several research groups have been made diverse preparations with better solubility or permeability, mainly tested on the *in vitro* studies. For example, microemulsion (Solanki et al., 2012), nanoparticles (Ameen et al., 2018), soluble cocrystals (Wang et al., 2016), nanoencapsulation (Dalcin et al., 2019), and solid dispersions and inclusion complex (Ruan et al., 2005). Additionally, Zhao et al. (2019) showed that a nanoscale DHM-phospholipid complex significantly increased oral bioavailability in rats. All these developments can improves the oral bioavailability and facilitate their possibly use against brain aging and neurodegenerative diseases.

Anti-Oxidative Effects of DHM (*In Vitro* Models)

Oxidative damage to cells is a common and important part of the pathology of many diseases such as AD, PD, Huntington's disease (HD), and aging (López-Otín et al., 2013; Singh et al., 2019). The molecules responsible for oxidative damage, known as reactive oxygen species (ROS) and reactive nitrogen species (RNS), are mainly produced by the mitochondrial respiratory chain. Several *in vitro* studies have shown that DHM inhibits lipid-peroxidation (He et al., 2003a; He et al., 2003b; Zhang et al., 2003; Yang et al., 2009), which suggest that DHM can protect cell membrane lipids against the damage induced by an excess of ROS and RNS. Moreover, DHM may reduce oxidative damage to cells through different mechanisms such as direct radical-scavenging and Fe^{2}-chelation (Li et al., 2016), as well as by increasing the enzymatic activity of superoxide dismutase (SOD), which mainly catalyzes the dismutation of superoxide anion (O2•–) to molecular oxygen (Mu et al., 2016; Song et al., 2017). Moreover, DHM also exerts antioxidant effects by activating phosphatidylinositol 3-kinase (PI3K/Akt) and modulating the nuclear transcription factor-erythroid 2-related factor 2 (Nrf2), which participates in the induction of genes encoding detoxifying and antioxidant enzymes (Luo et al., 2017; Hu et al., 2018). Another study suggests that DHM modulate AMP-activated protein kinase to cause inhibition of the oxidative stress response (Jiang et al., 2014). Taking all the above into account, DHM seems to reduce the oxidative stress by modulating several molecules of this signaling pathway.

Anti-Inflammatory Effects of DHM (*In Vitro* Models)

Although some aspects of the anti-inflammatory effect of DHM are still unknown, some *in vitro* studies have shown that it decreases the production of different molecules that are part of the pro-inflammatory cascade, such as interleukin IL-1β and IL-6, the tumor necrosis factor-alpha (TNF-α) and nitric oxide (Qi et al., 2012; Hou et al., 2015), while also increasing the production of anti-inflammatory IL-10. Moreover, DHM downregulates the expression of TNF-α by inhibiting nuclear factor-kappa B (NF-kB), a protein complex that controls cytokine production and is involved in many processes, including inflammation and apoptosis (Tang et al., 2016).

Moreover, another research found that DHM decrease dysfunction (tube formation and migration) of Human Umbilical Vein Endothelial Cells (HUVECs) Culture, induced by TNF- α through repressing miR-21 expression (Yang et al., 2018), a microRNA which increased expression was observed in human atherosclerosis (Raitoharju et al., 2011).

Effects of DHM in Animal Models of Aging

A common model for the study of aging is the D-galactose-induced aging rats, produced by the chronic administration of D-galactose (D-gal), which causes mitochondrial dysfunction and increases apoptosis, inflammation and oxidative stress in the brain. These animals show alterations such as poor immune response, a shortened lifespan, and learning and memory deficits (Shwe et al., 2018). In this animal model, DHM has been shown to cause a significant reduction astrogliosis, apoptosis and dysfunctional autophagy in neurons of the hippocampus through the up-regulation of sirtuin 1 (SIRT1) and p53/p21, and the down-regulation of the mammalian target of rapamycin (mTOR) in a miR-34a-dependent manner (Kou et al., 2016). These results suggest that DHM ameliorate cognitive impairments and aging by modulate excessive apoptosis and dysfunctional autophagy of hippocampal neurons, and astrogliosis.

Effects of DHM in Animal Models of AD

A few years ago we published a study (Liang et al., 2014) about the chronic effects of DHM in two different transgenic mouse models of AD (TG2576 and TG-SwDI). We used 20 months-old male animals divided into transgenic and control groups. The animals were treated with 2mg/Kg/day during 3 months and we analyzed the effects of DHM on their behavior and pathology. The results showed that chronic treatment with DHM improves memory, decreases the accumulation of Aβ1–40 and Aβ1–42 (markers for AD), and restores Gamma-Aminobutyric Acid (GABA) neurotransmission and the levels of gephyrin, an anchor protein for the postsynaptic GABAA receptor. These results suggest that chronic treatment with DHM improves cognitive deficits, reverses the progressive accumulation of Aβ peptides, and restores GABAergic transmission and functional synapses. Recently, Feng et al. (2018) used another Alzheimer's mouse model, termed APP/PS1 double-transgenic, in which the mouse/human amyloid precursor protein and the mutant human presenilin-1 are overexpressed. They showed that DHM treatment also improves memory and decreases the number of activated microglia and the NLRP3 inflammasome, the activation of which plays an important role in chronic brain neuroinflammation (Heneka et al., 2018). Another recent study (Sun et al., 2019) done in an AD rat model induced by intracerebroventricular injection of Aβ1–42, found that DHM (100 and 200 mg/kg for 21 days) improves learning and memory, decreased hippocampal neuronal apoptosis, IL-1β, IL-6, and TNF-α in serum and hippocampus and changes in different proteins such as decreased pro-apoptotic Bax and NF-κB and increased anti-apoptotic Bcl-2, pAMPK, AMPK, and SIRT1, suggesting that beneficial effects of DHM are mediated by up-regulation of AMPK/SIRT1 pathway.

Effects of DHM in Animal Models of PD

A common animal model of PD is based on the administration of the protoxicant MPTP (1-methyl-4-phenyl-1, 2, 3, 6-tetrahydropyridine) for several days. After MPTP crosses the blood-brain barrier, it is metabolized by glial cells, which produce and release the toxic metabolite MPP+(1-methyl-4-phenylpyridinium ion), which is selectively transported into dopaminergic neurons of the substantia nigra pars compacta, where it reduces ATP production and increases the production of ROS (Blandini and Armentero, 2012). Recently, Ren et al. (2017) used the MPTP animal model of PD to study the effects of DHM and found that the administration of DHM for thirteen days (tree days before the start of MPTP, seven days during MPTP administration and three days after the end of MTPT) significantly decreased dopaminergic neuronal loss and motor impairments (evaluated using the climbing pole and rotarod tests) by a mechanism that involves the inhibition of ROS production as well as a reduction in the production of the toxicant MPP+ through the inhibition of glycogen synthase kinase-3β (GSK-3β), the activity of which is associated with dopaminergic neuronal death caused by MPTP and by the neuroinflammation process associated with PD (Golpich et al., 2015).

Effects of DHM in Animal Models of HD

In a 3-NP rat model of HD, treatment with DHM (10mg/kg/day for five consecutive days) reduced significantly the initial and total time in the balance beam task, the hang time in the grip-strength test, and escape latency and time in the target quadrant in the Morris water-maze test, all together suggest that DHM reduced motor, learning, and memory impairments. Moreover, DHM increased the striatal metabolic rate, and reduced oxidative stress and apoptosis. The mechanisms behind these effects include the down-regulation of the pro-apoptotic Bax protein and the up-regulation of the anti-apoptotic Bcl-2 protein, increased SOD activity and decreased Malondialdehyde, a final product of polyunsaturated fatty acids peroxidation (Mu et al., 2016).

Last Considerations

It is worthwhile to note, that DHM it is not the only flavanonol that has been studied as a potential neuroprotective agent. Taxifolin, also known as Dihydroquercetin or Distylin (PubChem CID: 439533), shows neuroprotective effects such as reduction of Aβ1–40 and Aβ1–42 formation, improves cognition in a transgenic mouse model of cerebral amyloid angiopathy and in AD mouse model induced by injection of Aβ1–42 on the hippocampus (Davis et al., 2004; Sato et al., 2013; Saito et al., 2017; Wang et al., 2018). Although, DHM and Taxifolin have a similar molecular structure and they share some activation pathways (e.g. BDNF and SIRT1) more research is needed to establish a structure-activity relationship of flavanonols.

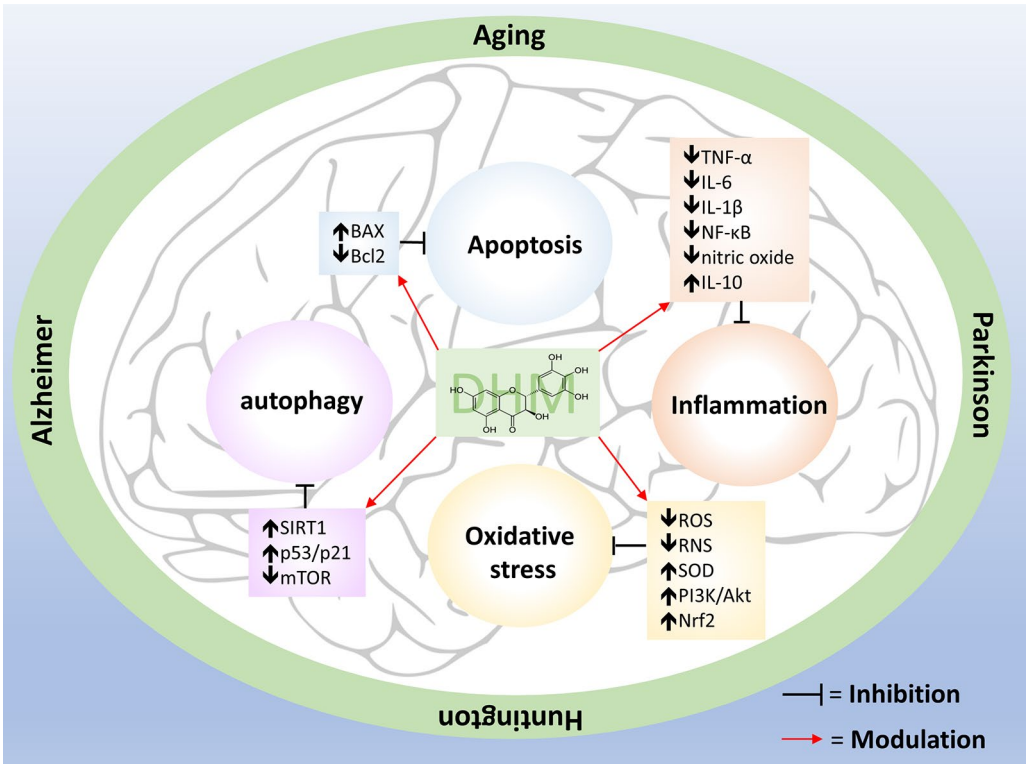

FIGURE 1 | Pleiotropic effects of DHM. Aging, AD, HD and PD have several dysfunctional responses such as oxidative stress, chronic inflammation, apoptosis, and autophagy impairment. DHM counteract these alterations by modulate specific molecules (showed inside the boxes) that are part of those pathways.

Conclusions and Future Prospects

In this review, we showed that DHM has a wide range of beneficial effects, both *in vitro* and *in vivo* models of human diseases, including anti-oxidative, anti-inflammatory and neuroprotective properties (**Figure 1**), restoration of GABA neurotransmission, and improvements in motor and cognitive behavior, which suggests that this compound may be useful for treating human aging and neurodegenerative diseases. However, further research is required to assess the clinical potential of DHM. For example: several studies have indicated that DHM is absorbed in the gastrointestinal tract, crosses the blood-brain barrier and does not have toxic effects, suggesting that it could exert positive effects on the brain without risk of toxicity; however, more pharmacokinetic studies are required to provide more robust evidence. Although we have a good understanding of some of the effects of DHM on cells found outside of the brain, we still do not understand completely the basic mechanisms of neuroprotection and neuroplasticity of DHM in neurons and glial cells, particularly in microglia and astrocytes, which play a very important role in the homeostatic maintenance of the brain. Besides this, senescent cells are also always present in aging and neurodegenerative diseases, and we need to know whether DHM can modulate cellular senescence and the inducers of this process. Anti-inflammatory effects of DHM have been broadly studied, mainly *in vitro* and *in vivo* models, and a clinical trial has shown some similar results. A randomized, double-blind, placebo-controlled trial in humans showed a significant decrease in seric TNF-α after 12 weeks of consuming 600 mg of DHM per day (Chen et al., 2015), supporting the idea that DHM has positive effects on human health.

AUTHOR CONTRIBUTIONS

Conceptualization, HM-C and HEL-V. Writing original draft preparation, HM-C, HEL-V, MM-R, and IA-C. Writing review and editing, HM-C, HEL-V, MM-R, and IA-C. Supervision, HEL-V and HM-C.

FUNDING

This project was supported by a grant from the Secretaria de Educación, Ciencia, Tecnología e Innovación de la Ciudad de México SECITI/042/2018 (INGER-DI-CRECITES-002-2018 to IA-C) "Red Colaborativa de Investigación Traslacional para el Envejecimiento Saludable de la Ciudad de México (RECITES)".

REFERENCES

Ameen, F., AlYahya, S. A., Bakhrebah, M. A., Nassar, M. S., and Aljuraifani, A. (2018). Flavonoid dihydromyricetin-mediated silver nanoparticles as potential nanomedicine for biomedical treatment of infections caused by opportunistic fungal pathogens. *Res. Chem. Intermed.* 44, 5063–5073. doi: 10.1007/s11164-018-3409-x

Blandini, F., and Armentero, M.-T. (2012). Animal models of Parkinson's disease. *FEBS J.* 279, 1156–1166. doi: 10.1111/j.1742-4658.2012.08491.x

Chen, S., Zhao, X., Wan, J., Ran, L., Qin, Y., Wang, X., et al. (2015). Dihydromyricetin improves glucose and lipid metabolism and exerts anti-inflammatory effects in nonalcoholic fatty liver disease: A randomized controlled trial. *Pharmacol. Res.* 99, 74–81. doi: 10.1016/j.phrs.2015.05.009

Choi, J. Y., Morris, J. C., and Hsu, C. Y. (1998). Aging and cerebrovascular disease. *Neurol. Clin.* 16, 687–711. doi: 10.1016/S0733-8619(05)70089-X

Collier, T. J., Kanaan, N. M., and Kordower, J. H. (2011). Ageing as a primary risk factor for Parkinson's disease: evidence from studies of non-human primates. *Nat. Rev. Neurosci.* 12, 359–366. doi: 10.1038/nrn3039

Dalcin, A. J. F., Vizzotto, B. S., Bochi, G. V., Guarda, N. S., Nascimento, K., Sagrillo, M. R., et al. (2019). Nanoencapsulation of the flavonoid dihydromyricetin protects against the genotoxicity and cytotoxicity induced by cationic nanocapsules. *Colloids Surf. B Biointerfaces* 173, 798–805. doi: 10.1016/j.colsurfb.2018.10.066

Davis, J., Xu, F., Deane, R., Romanov, G., Previti, M. L., Zeigler, K., et al. (2004). Early-onset and robust cerebral microvascular accumulation of amyloid beta-protein in transgenic mice expressing low levels of a vasculotropic Dutch/Iowa mutant form of amyloid beta-protein precursor. *J. Biol. Chem.* 279, 20296–20306. doi: 10.1074/jbc.M312946200

Fan, L., Tong, Q., Dong, W., Yang, G., Hou, X., Xiong, W., et al. (2017). Tissue Distribution, Excretion, and Metabolic Profile of Dihydromyricetin, a Flavonoid from Vine Tea (Ampelopsis grossedentata) after Oral Administration in Rats. *J. Agric. Food Chem.* 65, 4597–4604. doi: 10.1021/acs.jafc.7b01155

Feng, J., Wang, J., Du, Y., Liu, Y., Zhang, W., Chen, J., et al. (2018). Dihydromyricetin inhibits microglial activation and neuroinflammation by suppressing NLRP3 inflammasome activation in APP/PS1 transgenic mice. *CNS Neurosci. Ther.* 24, 1207–1218. doi: 10.1111/cns.12983

Golpich, M., Amini, E., Hemmati, F., Ibrahim, N. M., Rahmani, B., Mohamed, Z., et al. (2015). Glycogen synthase kinase-3 beta (GSK-3β) signaling: Implications for Parkinson's disease. *Pharmacol. Res.* 97, 16–26. doi: 10.1016/j.phrs.2015.03.010

He, G., Du, F., Yang, W., Pei, G., and Zhu, Y. (2003a). Effects of tengcha flavonoids on scavenging oxygen free radicals and inhibiting lipid-peroxidation. *Zhong Yao Cai Zhongyaocai J. Chin. Med. Mater.* 26, 338–340.

He, G., Yang, W., Pei, G., Zhu, Y., and Du, F. (2003b). Studies on the effect of dihydromyricetin on antilipid-peroxidation. *Zhongguo Zhong Yao Za Zhi Zhongguo Zhongyao Zazhi China J. Chin. Mater. Med.* 28, 1188–1190.

Heneka, M. T., McManus, R. M., and Latz, E. (2018). Inflammasome signalling in brain function and neurodegenerative disease. *Nat. Rev. Neurosci.* 19, 610–621. doi: 10.1038/s41583-018-0055-7

Hou, X. L., Tong, Q., Wang, W. Q., Shi, C. Y., Xiong, W., Chen, J., et al. (2015). Suppression of inflammatory responses by dihydromyricetin, a flavonoid from ampelopsis grossedentata, *via* inhibiting the activation of NF-κB and MAPK Signaling Pathways. *J. Nat. Prod.* 78, 1689–1696. doi: 10.1021/acs.jnatprod.5b00275

Hu, Q., Zhang, T., Yi, L., Zhou, X., and Mi, M. (2018). Dihydromyricetin inhibits NLRP3 inflammasome-dependent pyroptosis by activating the Nrf2 signaling pathway in vascular endothelial cells. *BioFactors Oxf. Engl.* 44, 123–136. doi: 10.1002/biof.1395

Hyun, T., Eom, S., Yu, C., and Roitsch, T. (2010). Hovenia dulcis – An Asian Traditional Herb. *Planta Med.* 76, 943–949. doi: 10.1055/s-0030-1249776

Jiang, B., Le, L., Pan, H., Hu, K., Xu, L., and Xiao, P. (2014). Dihydromyricetin ameliorates the oxidative stress response induced by methylglyoxal *via the* AMPK/GLUT4 signaling pathway in PC12 cells. *Brain Res. Bull.* 109, 117–126. doi: 10.1016/j.brainresbull.2014.10.010

Katz, M. J., Lipton, R. B., Hall, C. B., Zimmerman, M. E., Sanders, A. E., Verghese, J., et al. (2012). Age-specific and sex-specific prevalence and incidence of mild cognitive impairment, dementia, and Alzheimer dementia in blacks and whites: a report from the Einstein Aging Study. *Alzheimer Dis. Assoc. Disord.* 26, 335–343. doi: 10.1097/WAD.0b013e31823dbcfc

Kou, X., and Chen, N. (2012). Pharmacological potential of ampelopsin in Rattan tea. *Food Sci. Hum. Wellness* 1, 14–18. doi: 10.1016/j.fshw.2012.08.001

Kou, X., Liu, X., Chen, X., Li, J., Yang, X., Fan, J., et al. (2016). Ampelopsin attenuates brain aging of D-gal-induced rats through miR-34a-mediated SIRT1/mTOR signal pathway. *Oncotarget* 7, 74484–74495. doi: 10.18632/oncotarget.12811

Li, X., Liu, J., Lin, J., Wang, T., Huang, J., Lin, Y., et al. (2016). Protective Effects of Dihydromyricetin against •OH-Induced Mesenchymal Stem Cells Damage and Mechanistic Chemistry. *Mol. Basel Switz.* 21, 604. doi: 10.3390/molecules21050604

Liang, J., López-Valdés, H. E., Martínez-Coria, H., Lindemeyer, A. K., Shen, Y., Shao, X. M., et al. (2014). Dihydromyricetin ameliorates behavioral deficits and reverses neuropathology of transgenic mouse models of Alzheimer's disease. *Neurochem. Res.* 39, 1171–1181. doi: 10.1007/s11064-014-1304-4

Lindsay, J., Laurin, D., Verreault, R., Hébert, R., Helliwell, B., Hill, G. B., et al. (2002). Risk factors for Alzheimer's disease: a prospective analysis from the Canadian Study of Health and Aging. *Am. J. Epidemiol.* 156, 445–453. doi: 10.1093/aje/kwf074

Liu, L., Yin, X., Wang, X., and Li, X. (2017). Determination of dihydromyricetin in rat plasma by LC-MS/MS and its application to a pharmacokinetic study. *Pharm. Biol.* 55, 657–662. doi: 10.1080/13880209.2016.1266669

López-Otín, C., Blasco, M. A., Partridge, L., Serrano, M., and Kroemer, G. (2013). The hallmarks of aging. *Cell* 153, 1194–1217. doi: 10.1016/j.cell.2013.05.039

López-Valdés, H. E., and Martínez-Coria, H. (2016). The Role of Neuroinflammation in Age-Related Dementias. *Rev. Investig. Clin. Organo Hosp. Enfermedades Nutr.* 68, 40–48.

Luo, Y., Lu, S., Dong, X., Xu, L., Sun, G., and Sun, X. (2017). Dihydromyricetin protects human umbilical vein endothelial cells from injury through ERK and Akt mediated Nrf2/HO-1 signaling pathway. *Apoptosis Int. J. Program. Cell Death* 22, 1013–1024. doi: 10.1007/s10495-017-1381-3

Mu, S., Li, Y., Liu, B., Wang, W., Chen, S., Wu, J., et al. (2016). Dihydromyricetin Ameliorates 3NP-induced Behavioral Deficits and Striatal Injury in Rats. *J. Mol. Neurosci. MN* 60, 267–275. doi: 10.1007/s12031-016-0801-0

OECD. (2001a). Guidance Document on Acute oral Toxicity Testing: Organisation for Economic Co-operation and Development (OECD) Paris (FR); 2001; Report No.: ENV/JM/MONO(2001)4.

OECD. (2001b). Guideline for the Testing of Chemicals: Acute Oral Toxicity—Up-and Down Procedure (TG 425): Organisation for Economic Co-operation and Development (OECD) Paris (FR); 2001; adopted: 21st September 1998; revised method adopted: 17th December 2001.

Qi, S., Xin, Y., Guo, Y., Diao, Y., Kou, X., Luo, L., et al. (2012). Ampelopsin reduces endotoxic inflammation *via* repressing ROS-mediated activation of PI3K/Akt/NF-κB signaling pathways. *Int. Immunopharmacol.* 12, 278–287. doi: 10.1016/j.intimp.2011.12.001

Raitoharju, E., Lyytikäinen, L.-P., Levula, M., Oksala, N., Mennander, A., Tarkka, M., et al. (2011). miR-21, miR-210, miR-34a, and miR-146a/b are up-regulated in human atherosclerotic plaques in the Tampere Vascular Study. *Atherosclerosis* 219, 211–217. doi: 10.1016/j.atherosclerosis.2011.07.020

Ren, Z., Zhao, Y., Cao, T., and Zhen, X. (2017). Erratum: Dihydromyricetin protects neurons in an MPTP-induced model of Parkinson's disease by suppressing glycogen synthase kinase-3 beta activity. *Acta Pharmacol. Sin.* 38, 733. doi: 10.1038/aps.2017.40

Ruan, L.-P., Yu, B.-Y., Fu, G.-M., and Zhu, D. (2005). Improving the solubility of ampelopsin by solid dispersions and inclusion complexes. *J. Pharm. Biomed. Anal.* 38, 457–464. doi: 10.1016/j.jpba.2005.01.030

Saito, S., Yamamoto, Y., Maki, T., Hattori, Y., Ito, H., Mizuno, K., et al. (2017). Taxifolin inhibits amyloid-β oligomer formation and fully restores vascular integrity and memory in cerebral amyloid angiopathy. *Acta Neuropathol. Commun.* 5, 26. doi: 10.1186/s40478-017-0429-5

Sato, M., Murakami, K., Uno, M., Nakagawa, Y., Katayama, S., Akagi, K., et al. (2013). Site-specific inhibitory mechanism for amyloid β42 aggregation by catechol-type flavonoids targeting the Lys residues. *J. Biol. Chem.* 288, 23212–23224. doi: 10.1074/jbc.M113.464222

Shwe, T., Pratchayasakul, W., Chattipakorn, N., and Chattipakorn, S. C. (2018). Role of D-galactose-induced brain aging and its potential used for therapeutic interventions. *Exp. Gerontol.* 101, 13–36. doi: 10.1016/j.exger.2017.10.029

Singh, A., Kukreti, R., Saso, L., and Kukreti, S. (2019). Oxidative Stress: A Key Modulator in Neurodegenerative Diseases. *Mol. Basel Switz.* 24, 1583. doi: 10.3390/molecules24081583

Solanki, S. S., Sarkar, B., and Dhanwani, R. K. (2012). Microemulsion drug delivery system: for bioavailability enhancement of ampelopsin. *ISRN Pharm.* 2012, 108164. doi: 10.5402/2012/108164

Song, Q., Liu, L., Yu, J., Zhang, J., Xu, M., Sun, L., et al. (2017). Dihydromyricetin attenuated Ang II induced cardiac fibroblasts proliferation related to inhibitory of oxidative stress. *Eur. J. Pharmacol.* 807, 159–167. doi: 10.1016/j.ejphar.2017.04.014

Sun, P., Yin, J.-B., Liu, L.-H., Guo, J., Wang, S.-H., Qu, C.-H., et al. (2019). Protective role of Dihydromyricetin in Alzheimer's disease rat model associated with activating AMPK/SIRT1 signaling pathway. *Biosci. Rep.* 39. doi: 10.1042/BSR20180902

Tang, N., Ma, J., Wang, K. S., Mi, C., Lv, Y., Piao, L. X., et al. (2016). Dihydromyricetin suppresses TNF-α-induced NF-κB activation and target gene expression. *Mol. Cell. Biochem.* 422, 11–20. doi: 10.1007/s11010-016-2799-6

Tsao, R. (2010). Chemistry and Biochemistry of Dietary Polyphenols. *Nutrients* 2, 1231–1246. doi: 10.3390/nu2121231

Wang, C., Tong, Q., Hou, X., Hu, S., Fang, J., and Sun, C. C. (2016). Enhancing Bioavailability of Dihydromyricetin through Inhibiting Precipitation of Soluble Cocrystals by a Crystallization Inhibitor. *Cryst. Growth Des.* 16, 5030–5039. doi: 10.1021/acs.cgd.6b00591

Wang, Y., Wang, Q., Bao, X., Ding, Y., Shentu, J., Cui, W., et al. (2018). Taxifolin prevents β-amyloid-induced impairments of synaptic formation and deficits of memory *via the* inhibition of cytosolic phospholipase A2/prostaglandin E2 content. *Metab. Brain Dis.* 33, 1069–1079. doi: 10.1007/s11011-018-0207-5

Xiang, D., Fan, L., Hou, X.-L., Xiong, W., Shi, C.-Y., Wang, W.-Q., et al. (2018). Uptake and Transport Mechanism of Dihydromyricetin Across Human Intestinal Caco-2 Cells. *J. Food Sci.* 83, 1941–1947. doi: 10.1111/1750-3841.14112

Yang, D., Tan, S., Yang, Z., Jiang, P., Qin, C., Yuan, Q., et al. (2018). Dihydromyricetin attenuates TNF-α-induced endothelial dysfunction through miR-21-mediated DDAH1/ADMA/NO signal pathway. *BioMed. Res. Int.* 2018. doi: 10.1155/2018/1047810

Yang, J.-G., Liu, B.-G., Liang, G.-Z., and Ning, Z.-X. (2009). Structure-activity relationship of flavonoids active against lard oil oxidation based on quantum chemical analysis. *Mol. Basel Switz.* 14, 46–52. doi: 10.3390/molecules14010046

Zhang, Q., Liu, J., Liu, B., Xia, J., Chen, N., Chen, X., et al. (2014). Dihydromyricetin promotes hepatocellular carcinoma regression *via a* p53 activation-dependent mechanism. *Sci. Rep.* 4, 4628. doi: 10.1038/srep04628

Zhang, Y., Ning, Z., Yang, S., and Wu, H. (2003). Antioxidation properties and mechanism of action of dihydromyricetin from Ampelopsis grossedentata. *Yao Xue Xue Bao* 38, 241–244.

Zhang, Y., Que, S., Yang, X., Wang, B., Qiao, L., and Zhao, Y. (2007). Isolation and identification of metabolites from dihydromyricetin. *Magn. Reson. Chem. MRC* 45, 909–916. doi: 10.1002/mrc.2051

Zhao, X., Shi, C., Zhou, X., Lin, T., Gong, Y., Yin, M., et al. (2019). Preparation of a nanoscale dihydromyricetin-phospholipid complex to improve the bioavailability: *in vitro* and *in vivo* evaluations. *Eur. J. Pharm. Sci. Off. J. Eur. Fed. Pharm. Sci.* 138, 104994. doi: 10.1016/j.ejps.2019.104994

Zhou, T., and Zhou, X. (1996). Isolation, structure determination and pharmacological activity of flavanonol from ampelopsis grossedentata. *Chin. Pharm. J.* 458–461.

Conflict of Interest: The authors declare that the research was conducted in the absence of any commercial or financial relationships that could be construed as a potential conflict of interest.

frontiers in Pharmacology

ORIGINAL RESEARCH
published: 25 November 2019
doi: 10.3389/fphar.2019.01399

Qishen Granule Improved Cardiac Remodeling *via* Balancing M1 and M2 Macrophages

Wenji Lu[1†], Qiyan Wang[2†], Xiaoqian Sun[1], Hao He[2], Qixin Wang[3], Yan Wu[4], Yue Liu[5], Yong Wang[1]* and Chun Li[3]**

[1] College of Chinese Medicine, Beijing University of Chinese Medicine, Beijing, China, [2] School of Life Sciences, Beijing University of Chinese Medicine, Beijing, China, [3] Modern Research Center for Traditional Chinese Medicine, School of Chinese Materia Medica, Beijing University of Chinese Medicine, Beijing, China, [4] Center of Scientific Experiment, Beijing University of Chinese Medicine, Beijing, China, [5] Cardiovascular Disease Center, Xiyuan Hospital, China Academy of Chinese Medical Sciences, Beijing, China

OPEN ACCESS

Edited by:
George Qian Li,
Western Sydney University,
Australia

Reviewed by:
Geng Wenye,
Fudan University, China
Yi Ding,
Fourth Military Medical University,
China

***Correspondence:**
Yue Liu
liuyueheart@hotmail.com
Yong Wang
doctor_wangyong@163.com
Chun Li
lichun19850204@163.com

†These authors have contributed equally to this work

Specialty section:
This article was submitted to Ethnopharmacology, a section of the journal Frontiers in Pharmacology

Received: 03 July 2019
Accepted: 01 November 2019
Published: 25 November 2019

Citation:
Lu W, Wang Q, Sun X, He H, Wang Q, Wu Y, Liu Y, Wang Y and Li C (2019) Qishen Granule Improved Cardiac Remodeling via Balancing M1 and M2 Macrophages. Front. Pharmacol. 10:1399. doi: 10.3389/fphar.2019.01399

Macrophages play a pivotal role in myocardial remodeling (MR) process which could eventually lead to heart failure. Splenic monocytes could be mobilized and recruited under inflammatory conditions and differentiated into different types of macrophages in heart tissues. Inflammatory M1 macrophages could aggravate tissue damage whereas M2 macrophages could promote angiogenesis and tissue repair process. Unbalanced ratio of M1/M2 macrophages may eventually lead to adverse remodeling. Therefore, regulating differentiation and activities of macrophages are potential strategies for the management of myocardial remodeling. Qishen Granule (QSG) is an effective Chinese medicine for treating heart failure. Our previous studies demonstrated that QSG could inhibit myocardial fibrosis through regulating secretion of cytokines and activation of macrophages. However, the detailed effects of QSG on had not been elucidated yet. In this study, we aimed to explore the effect of QSG on the release of splenic monocytes, the recruitment of monocytes into heart tissues and the differentiation of macrophages under ischemic conditions. Our results showed that QSG could suppress the release of monocytes from the spleen and recruitment of monocytes to heart tissues *via* inhibiting splenic angiotensin (Ang) II/AT1-cardiac monocyte chemotactic protein (MCP)-1/CC chemokine receptor 2 (CCR2) pathway. The anti-fibrotic effect of QSG was exerted by inhibiting M1 macrophage-activated transforming growth factor (TGF)-β1/Smad3 pathway. Meanwhile, QSG could promote angiogenesis by promoting differentiation of M1 macrophages into M2 macrophages. Our results suggest that compounds of Chinese medicine have synergistic effects on cardiac and splenic organs through regulating differentiation of monocytes/macrophages in inhibiting myocardial remodeling.

Keywords: Qishen Granule, myocardial fibrosis, splenic monocytes, macrophages, angiogenesis

INTRODUCTION

Myocardial remodeling (MR) is an important pathophysiological change after myocardial infarction, and is a common pathological change during the development of heart failure (HF) (Pryds et al., 2019). Macrophage-mediated inflammation contributes greatly to fibrosis and prolonged inflammation will eventually lead to MR. Macrophages also participate in the healing process after myocardial infarction. Therefore, regulating differentiation and activities of macrophages are potential strategies for the management of MR to prevent HF (Honold and Nahrendorf, 2018).

The myocardium is mainly composed of cardiomyocytes, fibroblasts, endothelial cells and macrophages (Hu et al., 2017). Macrophages are involved in myocardial injury, repair and remodeling processes during the inflammatory response (Hulsmans et al., 2018). In steady state, most cardiac macrophages are derived from local progenitors and their functions remain largely unknown. It is speculated that these resident macrophages may play roles in guarding against infection, regulating angiogenesis and directing matrix turnover (Jablonski et al., 2015). Under inflammatory condition, such as myocardial infarction, circulating monocytes will be abundantly recruited to ischemic heart tissues through monocyte chemotactic protein-1 (MCP-1)/CC chemokine receptor 2 (CCR2) interactions. Once recruited, monocytes can differentiate into different types of macrophages which participate either in inflammatory or repairing process. According to surface markers and functions, macrophages can be roughly classified into inflammatory M1 and less inflammatory M2 types. M1 macrophages participate in inflammatory response by secreting pro-inflammatory cytokines interleukin (IL)-6 and chemokines, which aggravate tissue damage (Momtazi-Borojeni et al., 2019). M2 macrophages have only weak antigen-presenting ability, and they secrete vascular endothelial growth factor (VEGF) which promotes angiogenesis and tissue repair (Wu et al., 2010). The dynamic regulation and balance between M1 and M2 macrophages will determine the ventricular remodeling process.

The spleen is the largest organ in the immune system. Besides, it is a huge reservoir of more than half of the body's monocytes (Halade et al., 2018). About 40–70% of monocytes that are recruited to myocardial infarct site are derived from the spleen (Sager et al., 2017). The resting spleen contains a large reservoir of bona fide monocytes (Robbins and Swirski, 2010). Under inflammatory condition, angiotensin (Ang) II activates the Ang II type I receptor (AT1) in the spleen, allowing a large number of monocytes to be released into the blood. The role that spleen plays in myocardial infarction remains to be fully investigated. Inhibiting release of monocytes from spleen could reduce the number of macrophages in heart tissues and ameliorate inflammation (Partha D. Nahrendorf, 2015). Therefore, spleen is a potential target in the management of MR.

Qishen Granule (QSG) is prepared from the combination of the classic prescription Zhenwu Tang and Si Miao Yong An Tang in traditional Chinese medicine (Li et al., 2014). QSG mainly consists of six Chinese herbs including *A. membranaceus* (Fisch.) Bunge., *S. Miltiorrhiza* Bunge., *L. japonica* Thunb., *S. aestivalis* Griseb., *A. fischeri* Rchb. and *G. uralensis* Fisch (Li et al., 2016). The chemical component of QSG has been verified by liquid chromatography-mass spectrometry techniques (Guo et al., 2016). Preclinical studies have proven that QSG can effectively improve cardiac function and inhibit myocardial fibrosis (Wang et al., 2019). It has also been reported that QSG could protect against myocardial damage after macrophage activation (Liu et al., 2016). However, it hasn't been clarified if QSG could inhibit activation of macrophages through inhibiting release of monocytes from spleen. The regulative effect of QSG on differentiation of macrophages is also unclear. In this study, we aimed to explore if QSG could ameliorate myocardial remodeling through suppressing release of monocytes from spleen and inhibiting macrophage recruitment in a HF rat model. The roles of QSG on macrophage differentiation and splenic AngII/AT1-cardiac MCP-1/CCR2 pathway were investigated. This study will provide alternative targets in the management of macrophage-induced myocardial remodeling.

Abbreviations: Ang II, angiotensin II; CCR2, CC chemokine receptor 2; EF, ejection fraction; FS, fractional shortening; HF, heart failure; IL-6, Interleukin-6; LAD, left anterior descending; LVAW;s, left ventricular anterior wall; systole; LVAW;d, left ventricular anterior wall; diastole; LVID;d, left ventricular internal diameter; diastole; LVID;s, left ventricular internal diameter; systole; LVPW;s, left ventricular posterior wall; systole; LVPW;d, left ventricular posterior wall; diastole; MR, myocardial remodeling; MCP-1, monocyte chemotactic protein-1; MMP2, Matrix metallopeptidase 2; QSG, Qishen Granule; RAAS, renin angiotensin aldosterone system; TGF-β1, transforming growth factor-β1; VEGF, vascular endothelial growth factor.

MATERIALS AND METHODS

Animals

All animal experimental protocols were approved by the Ethics Committee of Beijing University of Chinese Medicine and conformed to the Guide for the Care and Use of Laboratory Animals published by the U.S. National Institute of Health (NIH Publication No. 85-23, revised 1996). 60 male Sprague–Dawley (SD) healthy rats (220 ± 20 g) in Specific Pathogen Free (SPF) grade used in this study were obtained from Beijing Vital River Laboratory Animal Technology Co. Ltd (China). The rats were housed in the cages under standard laboratory conditions (12 h light/dark cycle, controlled temperature of 25°C).

Drugs

Qishen Qranule is composed of *A. membranaceus* (Fisch.) Bunge., *S. Miltiorrhiza* Bunge., *L. japonica* Thunb., *S. aestivalis* Griseb., *A. fischeri* Rchb. and *G. uralensis* Fisch, purchased from Beijing Tongrentang (Group) Co., Ltd. and all the authentication of plant materials was identified by Dr. Jian Ni at Beijing University of Chinese Medicine. The voucher specimens (Voucher numbers: *A. membranaceus* (Fisch.) Bunge-2016-007; *S. Miltiorrhiza* Bunge-2016-008; *L. japonica* Thunb-2016-009; *S. aestivalis* Griseb-2016-010; *A. fischeri* Rchb-2016-011; *G. uralensis* Fisch-2016-012) were submitted to Department of Chinese medicine teaching and Research, School of Traditional Chinese Medicine, Beijing University of Chinese Medicine (Wang et al., 2017). The previous team tested the chemical composition of QSG by

Ultra-high performance liquid chromatography coupled with hybridion trap-time of flight mass spectrometry (UHPLC-IT-TOF-MS), and the results showed that Glycyrrhizic acid, Formononetin, Dihydrotanshinone I, Cryptotanshinone, Tanshinone I, Tanshinone I, Glycyrrhetic acid, and Tanshinone IIA were the main component (Guo et al., 2016). The fingerprint of QSG was analyzed by HPLC and the typical chromatograms were shown in **Supplementary Data 1**. Fosinopril was provided by Sino-US Shanghai Squibb Pharmaceutical Co. Ltd. Country Medicine Accurate Character Number: H19980197.

Animal Model of Heart Failure and Drug Administration

Left anterior descending (LAD) coronary artery of rats was ligated to induce the HF model as described in our previous studies (Wang et al., 2013). Briefly, 60 SD rats underwent left thoracotomy between the third and fourth intercostal space. After exposure of heart tissues, the LAD was ligated with a sterile suture 1 mm below the left atrium in 50 rats. Rats in sham group only underwent thoracotomy and threading in the same position of the heart. Ten rats that underwent LAD ligation were randomly chosen for splenectomy surgery using previously published method (Schwarz and Hiserodt. 1990). Approximately 1 cm incision was made by midline laparotomy, hepatic hilum was clamped, spleen was removed, and the muscles and skin were sutured with silk suture.

The main causes of mortality in myocardial infarction rats were anesthesia, laryngeal edema, excessive blood loss, arrhythmia, lung injury, pneumothorax, etc (Degabriele et al., 2004). Within 1 day after surgery, 8 rats died (1 rat in the splenectomy group) and 52 survived. The survival rate was 86.7%. 52 rats were randomly divided into five groups: 10 rats in the sham group, 11 rats in the model group, 9 rats in the splenectomy group, 11 rats in the QSG group, and 11 rats in the fosinopril group.

Rats in QSG group were treated with QSG at the dosage of 235.2 mg/kg per day and rats in fosinopril group were treated with fosinopril at the dosage of 4.67 mg/kg per day for 21 d. All the drugs were gavaged with the amount of l ml/100 g. Rats in the sham group, model group and splenectomy group were administrated with the same volume of water for 21 d.

Evaluation of Echocardiographic Parameters

21 d after treatment, rats inhaled anesthetic isoflurane and vevo 2100 was applied to observe the echocardiographic parameters of rats to assess the cardiac functions (Vevo TM 2100, Visual Sonics, Canada). Short axis was used to measure the length of left ventricular anterior wall; systole (LVAW;s), left ventricular anterior wall; diastole (LVAW;d), left ventricular internal diameter; diastole (LVID;d), left ventricular internal diameter; systole (LVID;s), left ventricular posterior wall; systole (LVPW;s), left ventricular posterior wall; diastole (LVPW;d). The values of ejection fraction (EF) and fractional shortening (FS) were calculated according to the following equation: FS% = [(LVID;d − LVID;s)/LVID;d] × 100%; EF% = [(LVEDV − LVESV)/LVEDV] × 100%.

Histological Examination

The heart and spleen tissues were fixed in 4% paraformaldehyde for 48 h, and then embedded in paraffin and cut into 5 μm sections. The spleen tissues were stained with hematoxylin–eosin (HE) staining to assess the basic structure. The heart tissues were stained with Masson staining and Sirius red staining to assess the extent of inflammatory infiltration and myocardial fibrosis.

Measurement of angiotensin II in the serum by radioimmunoassay

The level of angiotensin II was quantified directly from prepared plasma using radioimmunoassay (RIA) kits (Beijing Sino-UK institute of biological technology, Beijing, China) according to protocol of the manufacturer.

Measurement of Indicators by Immunohistochemistry

The heart sections were deparaffinized in xylene, rehydrated in alcohol gradient and then rinsed in PBS. The samples were incubated with primary antibody (Anti-CD31, GB12063, Servicebio, China) for 12 h at 4°C after being blocked with 0.3% hydrogen peroxide, avidin biotin blocking reagent, and biotin blocking reagent for 15 min. The slides were then incubated with the biotinylated secondary antibody for 2 h and the stained with hematoxylin for 30 s. The slides were then dehydrated by graded ethanol and xylene and fixed with resin glue. The positive area was specifically stained brown-yellow.

Measurement of Indicators by Immunofluorescence

The sections were sequentially dewaxed in xylene I and II, rehydrated in an alcohol gradient, and then placed in a citrate antigen retrieval buffer (pH 8.0) for antigen retrieval. Normal serum was added to the slides and blocked at room temperature for 30 min. After blocking, sections were incubated overnight with anti-CD68 (ab201340, Abcam, United States), anti-CD86 (ab53004, Abcam, United States), anti-CD163 (ab182422, Abcam, United States) primary antibody at 4°C and with fluorescent secondary antibody for 1 h at 37°C. The sections were further stained with DAPI staining for 5 min in the dark. Finally, the sections were sealed on cover slips and fluorescence images were captured using fluorescence microscope.

Measurement of Indicators by Western Blot

Tissue protein of heart and spleen was lysed by the RIPA lysate (50:1) and tissue disrupter and quantified by the BCA method. The quantified homogenate was added to loading buffer, and the mixture was boiled and denatured at 99°C. Each lane was loaded with 10 ul of proteins. After electrophoresis at 100 V for 1–1.5 h, proteins were transferred to PVDF membranes at 300 mA for 1–1.5 h. Afterwards, the membrane blocked with 5% skim milk for 1–1.5 h at room temperature, incubated on a shaker, and washed with TBS-T. Western blot analysis was conducted using anti-AT1 (ab18801; Abcam, United States),

anti-MCP-1 (ab25124, Abcam, United States), anti-CCR2 (PAI-27409), anti-TGF-β1 (3711s, Cell Signaling Technology, Germany), anti-Smad3 (ab28379, Abcam, United States), anti-MMP2 (ab86607, Abcam, United States), anti-Col III (ab7778, Abcam, United States), anti-VEGF (ab10972, Abcam, United States), anti-CD31 (ab24590, Abcam, United States) and anti-GAPDH (ab8245, Abcam, United States) at 4°C overnight. After incubation with the appropriate secondary antibodies at 37°C for 2 h at room temperature, the membrane treated with ECL for 1 min at room temperature. The final expression of each protein was normalized by GAPDH and grayscale analysis was performed using Image J software.

Statistical Analysis

All data were expressed as mean ± standard deviation (SD). One-way analysis of variance (ANOVA) and Dunnett's test were used to compare differences among multiple groups. The values of $P < 0.05$ were considered as statistically significant. All analyses were performed using SPSS 17.0 or GraphPad Prism 7.

RESULTS

QSG Inhibited the Release of Monocytes From the Spleen

Heart failure results in increased motility of monocytes in the spleen (Swirski FK et al., 2009). First, we assessed the number of monocyte in the spleen on 21 d after LAD ligation. The subcapsular region is the site where monocytes are stored in the spleen. HE staining showed that the number of monocytes in the marginal zone of the spleen was decreased after LAD ligation compared with the sham group, indicating that after LAD ligation, spleen released a large number of monocytes. Second, the effect of QSG on the release of monocytes from spleen was investigated. QSG could significantly increase the number of monocytes in red pulp under the capsule and marginal zone of the spleen as compared with those in the model group (**Figure 1A**). Fosinopril, an angiotensin-converting enzyme inhibitor (ACEI), was applied as the positive control drug. Circulatory level of angiotensin II in model group was increased compared with sham group. Consistently, levels of AT1 and MCP-1 in the spleen were also up-regulated in the model group. Treatment of QSG and fosinopril could significantly down-regulate the levels of AngII, AT1 and MCP-1, indicating that QSG could suppress the release of monocytes from the spleen *via* inhibiting Ang II/AT1 signaling pathway (**Figures 1B**, **C**).

QSG Inhibited Recruitment of Monocytes and M1 Macrophages-Induced Activation of Transforming Growth Factor (TGF)-B1/Smad3 in the Border Zone of Infarcted Heart

The effect of QSG on the recruitment of monocytes to infarcted heart tissues was further examined. Immunofluorescence results showed that the number of M1 macrophages (CD68 + CD86 positive cells) increased significantly in the model group relative to the sham group. QSG could reduce the number of M1 macrophages in the border zone of infarcted heart as compared with the model group. Splenectomy was applied to investigate whether the increased macrophages in heart were originated from the spleen. After splenectomy, the number of M1 macrophages

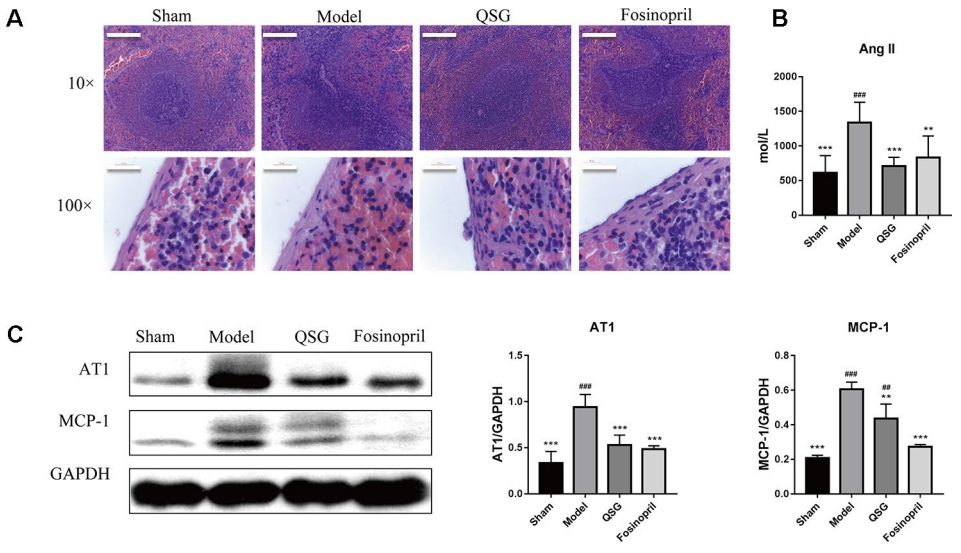

FIGURE 1 | QSG inhibited the release of monocytes from the spleen. **(A)** HE staining showed that monocytes in the marginal zone of the spleen were released in the model group, and QSG could exert the protective effect by increasing the number of monocytes in red pulp under the capsule and marginal zone of the spleen. **(B)**. QSG significantly decreased the circulatory level of angiotensin II. **(C)** Western blot showed that QSG reduced the expressions of AT1 and MCP-1 in splenic tissues. All data were presented as means ± SD from independent experiments performed in triplicate. $^{\#\#}P < 0.01$, $^{\#\#\#}P < 0.001$ vs the sham group; $^{**}P < 0.01$, $^{***}P < 0.001$ vs the model group. N = 3 per group.

was reduced significantly (**Figure 2A**). Splenectomy could also significantly alleviate inflammation and fibrosis in the heart tissues, demonstrating that splenic monocytes played important role in myocardial remodeling (**Figure 2B**). Since AT1 receptor-activated MCP-1/CCR2 interaction is critically involved in the recruitment of monocytes to heart tissues (França et al., 2017), the effects of QSG on the expressions of AT1, MCP-1 and CCR2 were then examined. Results showed that the levels of AT1, MCP-1 and CCR2 were significantly increased in the model group, as compared with the sham group. After treatment with QSG, expressions of AT1, MCP-1 and CCR2 were down-regulated, indicating that QSG could inhibit recruitment of monocytes through MCP-1/CCR2 interactions. Splenectomy and fosinopril had similar effects as QSG treatment (**Figure 2C**).

When monocytes are recruited to heart tissues, they could differentiate into M1 macrophages, which are able to stimulate production of TGF-β1 by fibroblasts, activate Smad3 and induce production of collagens and MMPs, thereby promoting fibrosis and myocardial remodeling (Shivshankar et al., 2014). Western blot showed that QSG could down-regulate expressions of TGF-β1 and Smad3 in the border zone of myocardial infarction. Levels of collagen III and matrix metallopeptidase 2 (MMP2) were

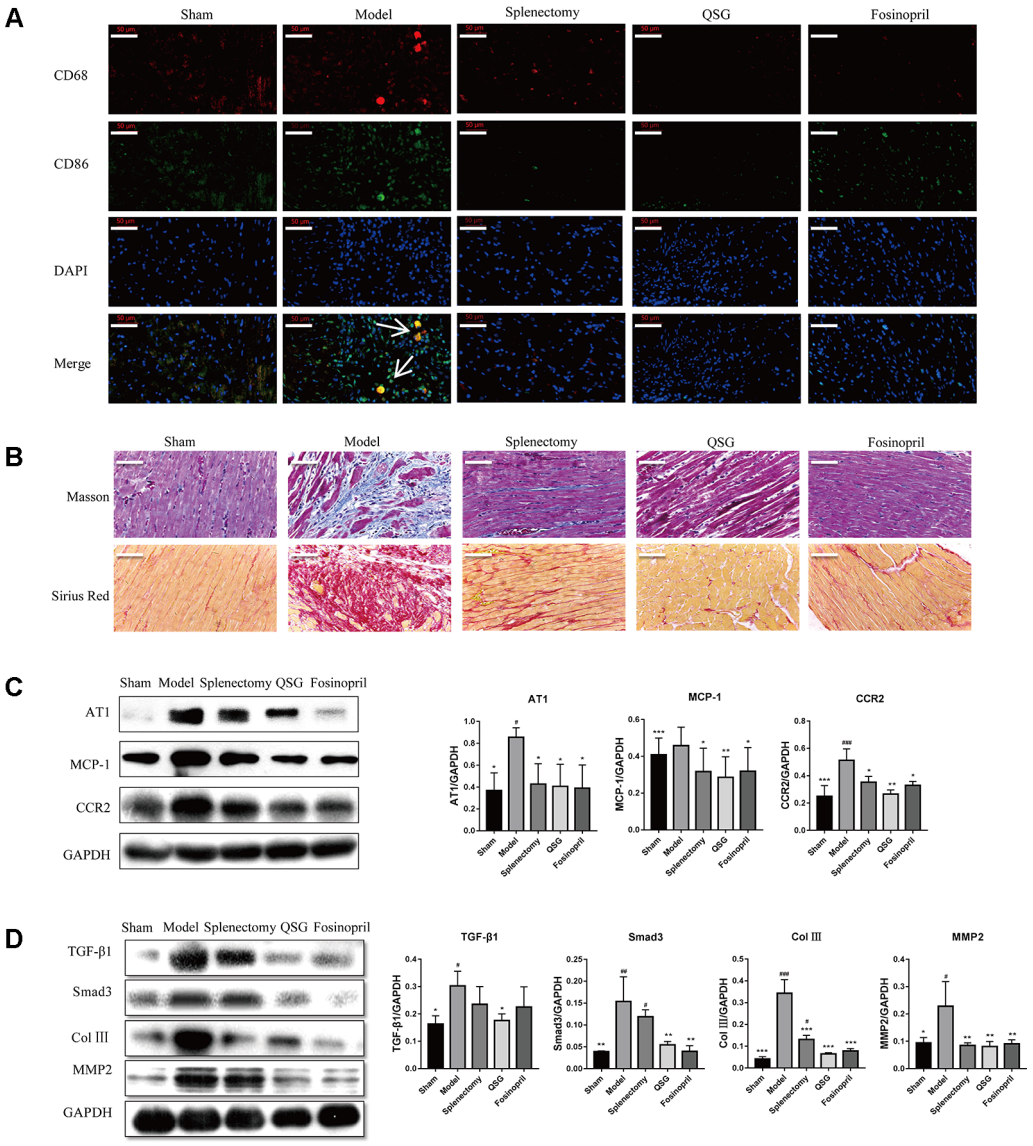

FIGURE 2 | QSG inhibited activation of TGF-β1/Smad3 through reducing the recruitment of M1 macrophages in myocardial tissue. **(A)** IF staining showed that splenectomy reduced the recruitment of M1 macrophages in myocardial tissue; QSG treatment decreased the recruitment of M1 macrophages. **(B)** Masson and Sirius Red staining showed that QSG inhibited cardiac fibrosis. **(C)** Western blot showed that QSG down-regulated the expressions of AT1, MCP-1 and CCR2 in myocardial tissue compared with that in the model group. **(D)** Western blot showed that QSG decreased the expressions of TGF-β1, Smad3, collagen III and MMP2 in cardiac tissue. All data were presented as means ± SD from independent experiments performed in triplicate. $^{\#}P < 0.05$, $^{\#\#}P < 0.01$, $^{\#\#\#}P < 0.001$ vs the sham group; $^{*}P < 0.05$, $^{**}P < 0.01$, $^{***}P < 0.001$ vs the model group. N = 3 per group.

also reduced by QSG treatment. Splenectomy and fosinopril had similar effects (**Figure 2D**). These results suggested that QSG could ameliorate myocardial remodeling by inhibiting macrophage-activated TGF-β1/Smad3 pathway.

QSG Induced Differentiation of M2 Macrophages and Promoted Angiogenesis in Myocardial Tissue

In contrast to M1 macrophages, M2 macrophages are involved in inflammation suppression, tissue repair and angiogenesis (Ribeiro et al., 2018). Therefore, the effect of QSG on differentiation of M2 macrophages was further investigated. Immunofluorescence staining (labeled by CD86 and CD163) showed that the number of M2 macrophages in QSG group was increased compared with model group. In splenectomy group, there were no detectable M2 macrophages (**Figure 3A**). Immunohistochemical staining of CD31 showed that the number of microvessels was significantly up-regulated after treatment with QSG. However, the effect of splenectomy group was less significant than of QSG group (**Figure 3B**). Western blot showed that compared with the sham group, the expression levels of VEGF and CD31 were significantly down-regulated in the model group. After treatments with QSG, the expression levels of VEGF and CD31 were increased (**Figure 3C**), demonstrating that QSG might promote angiogenesis through M2 macrophages. Fosinopril had similar effect with QSG. Echocardiography showed that compared with the sham group, left ventricular ejection fraction (EF) and fractional shortening (FS) of the model group were significantly decreased ($P < 0.001$). QSG increased EF by 56%, demonstrating that QSG could improve the left ventricular contractility. Splenectomy and fosinopril could also improve heart function (**Figure 4**).

DISCUSSION

Myocardial remodeling occurs in a variety of cardiovascular diseases and can be caused by inflammatory response, which

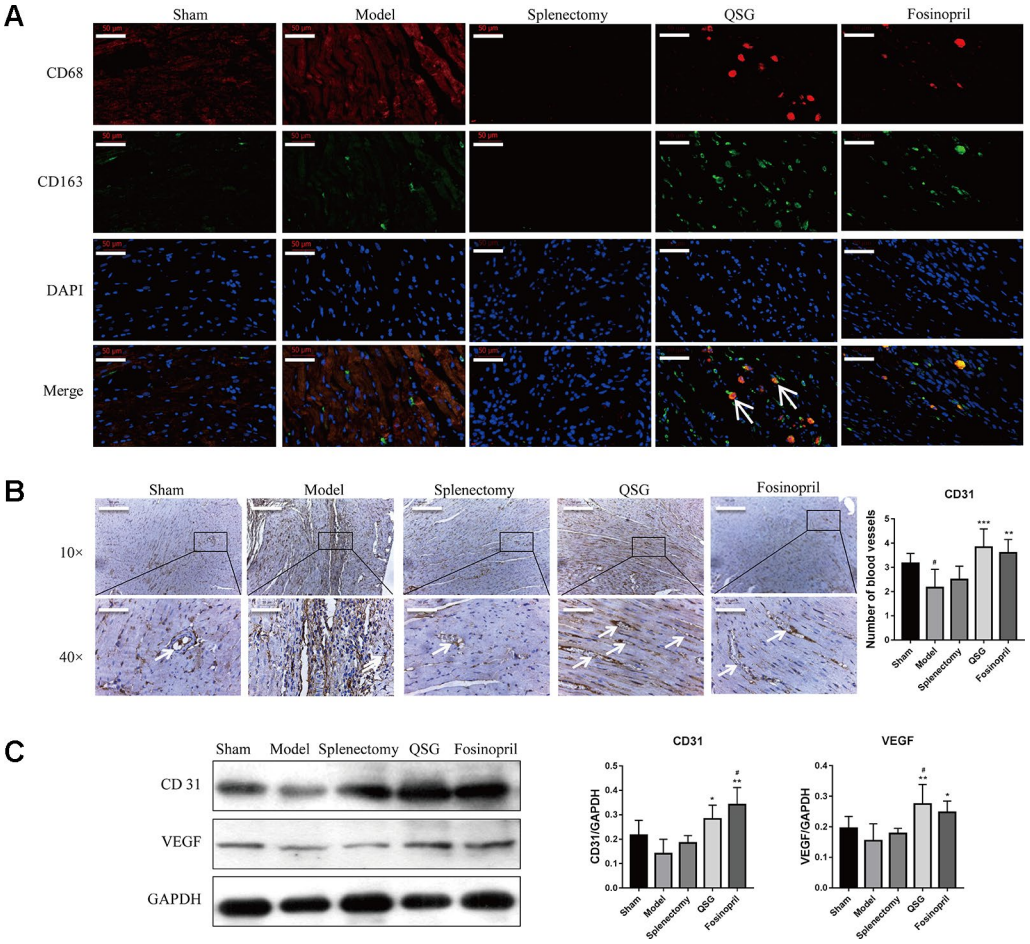

FIGURE 3 | QSG promoted angiogenesis through inducing the number of M2 macrophages in myocardial tissue. **(A)** IF staining showed that QSG treatment up-regulated the M2 macrophages. After splenectomy, the number of M2 macrophages remained unchanged relative to the model group. **(B)** CD31 staining showed that QSG could promote angiogenesis. **(C)** Western blot showed that QSG increased the expressions of CD31 and VEGF in myocardial tissue compared with model group. All data were presented as means ± SD from independent experiments performed in triplicate. $^{\#}P < 0.05$ vs the sham group; $^{*}P < 0.05$, $^{**}P < 0.01$, $^{***}P < 0.001$ vs the model group. N = 3 per group.

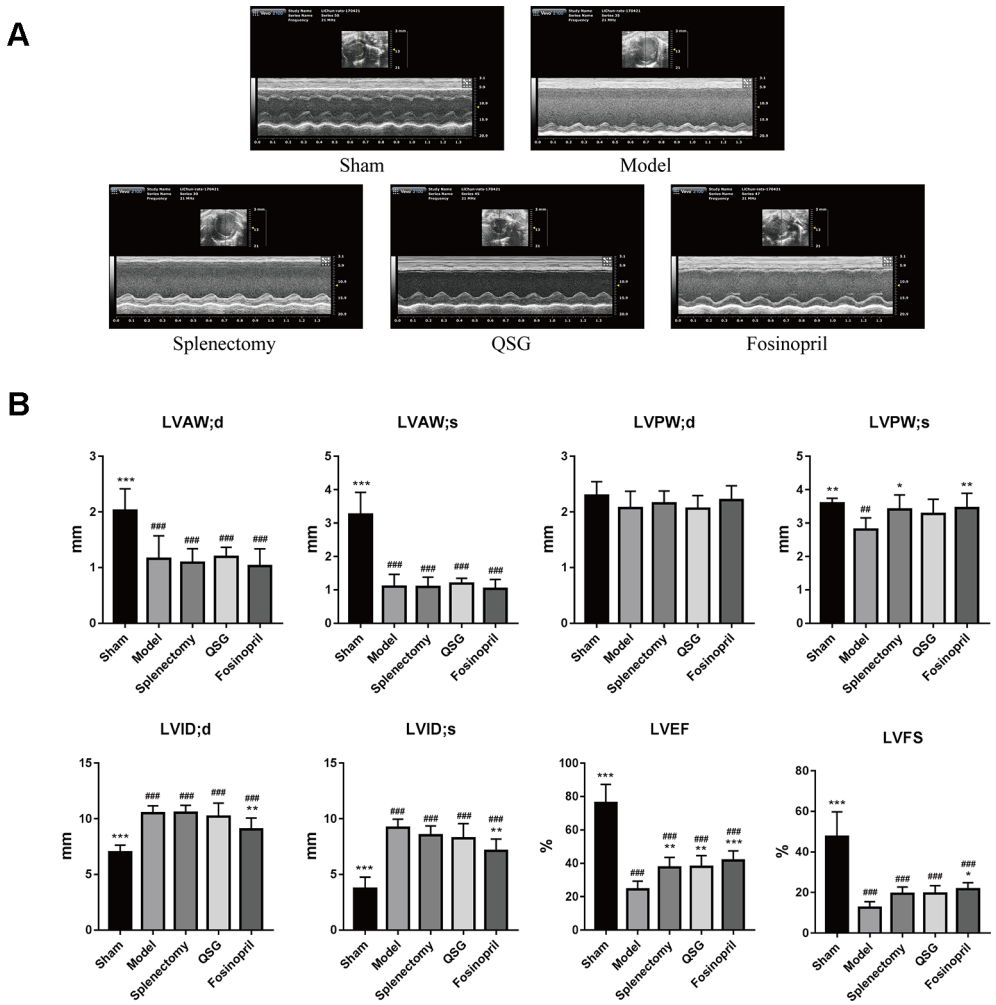

FIGURE 4 | QSG improves cardiac function by echocardiography. **(A)** Representative images of echocardiography exhibiting the changes in cardiac function in each group. **(B)** Echocardiography results showed that QSG and splenectomy improved left ventricular ejection fraction, and cardiac function of HF rats. $^{\#\#}P < 0.01$, $^{\#\#\#}P < 0.001$ vs the sham group; $^{*}P < 0.05$, $^{**}P < 0.01$, $^{***}P < 0.001$ vs the model group. N = 7 per group.

is closely related to infiltration of macrophages (Frantz and Nahrendorf, 2014). Macrophage is an important cell population in healthy heart tissues. Macrophages have multiple phenotypes and functions. It is speculated that macrophages guard against infection and regulate matrix turnover under steady state, although the source of macrophages in healthy heart remains unclear (Davies and Taylor. 2015). Under inflammatory conditions, such as acute infarction, circulatory monocytes will be recruited to heart tissues and differentiate into different types of macrophages. These macrophages play critical roles in inflammation, fibrosis, angiogenesis and myocardial remodeling. Therefore, regulating the recruitment of monocytes and differentiation of macrophages is considered to be promising target for managing myocardial remodeling. In this study, we explored the effect of traditional Chinese medicine QSG on monocytes/macrophages in infarct heart and spleen tissues and investigated the mechanism by which QSG inhibited fibrosis and myocardial remodeling.

A rat model of LAD ligation was induced in this study. LAD ligation led to myocardial infarction, remodeling and eventual heart failure. We firstly explored the source of macrophages in the border zone of infarction site. In addition to bone marrow, the spleen is a reservoir of monocytes and may supply large amount of monocytes that can be recruited to heart tissues under inflammatory conditions. Studies have shown that 40–70% of the macrophages in myocardial infarct site are recruited from spleen (Okizaki et al., 2015). Some experiments have demonstrated that removal of the spleen could inhibit the release of splenic monocytes and protect heart function (Pinto et al., 2012). Therefore, we performed splenectomy to explore the role of splenic monocytes under myocardial infarction conditions. It was shown that 21 d after LAD ligation, there were infiltrations of M1 macrophages (inflammatory type) in heart tissues. Myocardial fibrosis and compromised heart function were also observed. Furthermore, the number of monocytes in the spleen was significantly reduced in the model group. After removal of

spleen, the number of M1 macrophages in myocardial tissue was significantly reduced and fibrosis was attenuated. Heart function was also improved by splenectomy. These results demonstrate that spleen is an important source of M1 macrophages after occurrence of myocardial infarction. Inhibition of release of splenic monocytes could attenuate fibrosis and protect against heart failure.

Furthermore, release of splenic monocytes is dependent on activation of renin-angiotensin-aldosterone system (RAAS). Angiotensin II activates release of splenic monocytes through AT1 receptor, and ACE inhibitor can attenuate release of monocytes from spleen (Leuschner et al.2010). Our previous studies have indicated that QSG has anti-inflammatory effects (Wang et al, 2015). Therefore, the effect of QSG on release of splenic monocytes was investigated in current study. Impressively, we found that QSG treatment could inhibit release of monocytes from spleen in rats with LAD ligation, and circulatory level of angiotensin II was also reduced accompanied by the suppression of AT1 and MCP-1. These data suggest that QSG exerts anti-inflammatory effect by suppressing release of splenic monocytes through the AT1-MCP-1 pathway in spleen. Under myocardial infarction conditions, the monocytes released by spleen will be recruited to heart through MCP-1/CCR2 interaction. In heart tissues, monocytes will be differentiated into inflammatory M1 macrophages and alternative activated M2 macrophages (Moore and Tabas. 2011). M1 macrophages contribute to myocardial fibrosis by stimulating production of TGF-β1, which contributes to tissue fibrosis by stimulating Smads signaling and releasing extracellular matrix from myocardial myofibroblasts (Zhang et al., 2016). In our study, we found that QSG could reduce the number of M1 macrophages in the border zone of myocardial infarction and inhibit deposition of collagens. The expressions of AT1, MCP-1 and CCR2 in heart tissues were reduced accordingly. Furthermore, the levels of TGF-β1 and Smad3 were also suppressed. ACE inhibitor had similar effect as those of QSG. These data indicate that QSG may inhibit monocyte recruitment *via* MCP-1/CCR2 interaction and suppress M1 macrophage-induced fibrosis *via* TGF-β1/Smad3 pathway.

In addition, studies have shown that M1 macrophages are inflammatory whereas M2 macrophages participate in tissue repair, angiogenesis and resolution of inflammation (Liao et al., 2018). Promoting differentiation of monocytes into M2 macrophages might be beneficial for heart function (Singla et al, 2017). In this study, we observed that the number of M2 macrophages was up-regulated by QSG treatment. Intriguingly, there were no M2 macrophages observed in heart tissues in rats with splenectomy, as the reservoirs of monocytes, the spleen had been removed. Previous studies showed that M2 macrophages could promote angiogenesis by excreting VEGF (Oka et al., 2014). We found that the number of microvessels was significantly up-regulated after QSG treatment and the expressions of CD31 and VEGF were also increased by QSG. These results demonstrate that QSG could exert angiogenic effects through up-regulating differentiation of M2 macrophages.

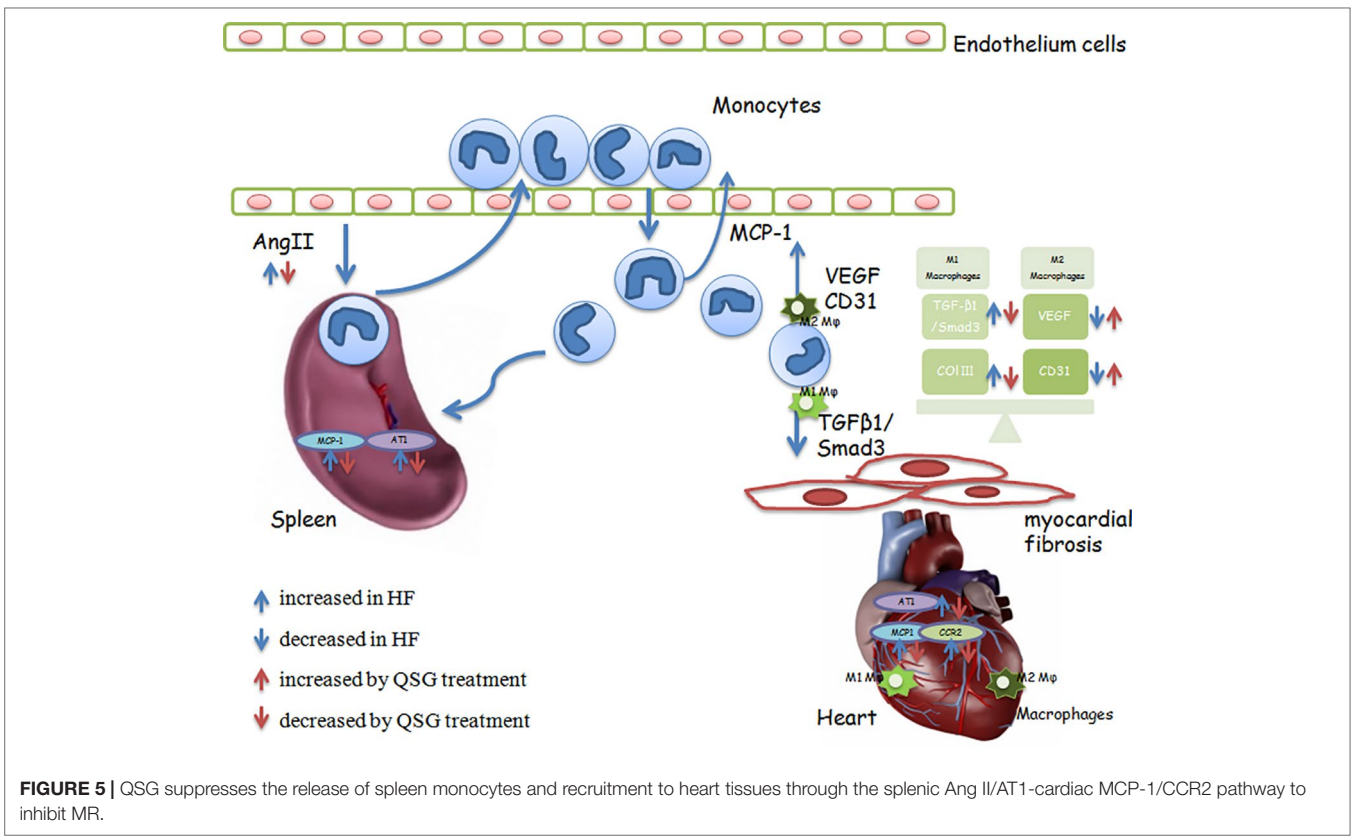

FIGURE 5 | QSG suppresses the release of spleen monocytes and recruitment to heart tissues through the splenic Ang II/AT1-cardiac MCP-1/CCR2 pathway to inhibit MR.

In conclusion, QSG attenuated myocardial fibrosis through restoring the unbalance of M1 and M2 macrophages in heart tissues. Monocytes released by spleen could be recruited to heart tissues while QSG could suppress splenic release of monocytes. QSG could inhibit M1 macrophages-activated TGF-β1/Smad3 pathway and promote M2 macrophage-dependent angiogenesis (**Figure 5**). This study provides evidence that compounds of Chinese medicine have synergistic effect on cardiac and splenic organs. Moreover, restoring the balance of M1 and M2 macrophages can be a promising strategy for the management of myocardial remodeling.

DATA AVAILABILITY STATEMENT

All datasets generated for this study are included in the article/ **Supplementary Material**.

ETHICS STATEMENT

All animal experimental protocols were approved by the Ethics Committee of Beijing University of Chinese Medicine and conformed to the Guide for the Care and Use of Laboratory Animals published by the U.S. National Institute of Health (NIH Publication No. 85-23, revised 1996).

AUTHOR CONTRIBUTIONS

CL, YWa and YL designed the study. WL and QiyW did majority of experimental work and interpretation throughout the experiments. XS, HH and QixW analyzed the data. YWu operated cardiac ultrasound. All authors read and approved the final manuscript.

FUNDING

This work was supported by the Grants from the National Natural Science Foundation of China (Nos. 81673802, 81530100, 81673712, and 81822049), Fok Ying Tung Education Foundation (No. 151044), Beijing Nova program (No. Z171100001117028), Talent Young Scientist of China Association for Science and Technology (No. CACM-2017-QNRC2-C13, No. CACM-2018-QNRC2-C07), the Fundamental Research Funds for the Central Universities (2017-JYB-JS-020).

SUPPLEMENTARY MATERIAL

The Supplementary Material for this article can be found online at: https://www.frontiersin.org/articles/10.3389/fphar.2019.01399/full#supplementary-material

REFERENCES

Davies, L. C., and Taylor, P. R. (2015). Tissue-resident macrophages: then and now. *Immunol.* 144 (4), 541–548. doi: 10.1111/imm.12451

Degabriele, N. M., Griesenbach, U., Sato, K., Post, M. J., Zhu, J., Williams, J., et al. (2004). Critical appraisal of the mouse model of myocardial infarction. *Exp. Physiol.* 89 (4), 497–505. doi: 10.1113/expphysiol.2004.027276

França, C. N., Izar, M. C. O., Hortêncio, M. N. S., Do Amaral, J. B., Ferreira, C. E. S., Tuleta, I. D., et al. (2017). Monocyte Subtypes and the CCR2 Chemokine Receptor in Cardiovascular Disease. *Clin. Sci. (Lond)* 131, 1215–1224. doi: 10.1042/CS20170009

Frantz, S., and Nahrendorf, M. (2014). Cardiac Macrophages and Their Role in Ischaemic Heart Disease. *Cardiovasc. Res.* 102 (2), 240–248. doi: 10.1093/Cvr/Cvu025

Guo, S., Li, P., Fu, B., Chuo, W., Gao, K., Zhang, W., et al. (2016). Systems-Biology Dissection of Mechanisms and Chemical Basis of Herbal Formula in Treating Chronic Myocardial Ischemia. *Pharmacol. Res.* 114, 196–208. doi: 10.1016/J.Phrs.2016.10.026

Halade, G. V., Norris, P. C., Kain, V., Serhan, C. N., and Ingle, K. A. (2018). Splenic Leukocytes Define the Resolution of Inflammation in Heart Failure. *Sci. Signaling* 11 (520), Eaao1818. doi: 10.1126/Scisignal.Aao1818

Honold, L., and Nahrendorf, M. (2018). Resident and Monocyte-Derived Macrophages in Cardiova-scular Disease. *Circ. Res.* 122 (1), 113–127. doi: 10.1161/CIRCRESAHA.117.311071

Hu, Y., Jiang, S., Lu, S., Xu, R., Huang, Y., Zhao, Z., et al. (2017). Echocardiography and Electrocardiography Variables Correlate With the New York Heart Association classification: An Observational Study of Ischemic Cardiomyopathy Patients. *Med* 96 (26), e7071. doi: 10.1097/MD.0000000000007071

Hulsmans, M., Sager, H. B., Roh, J. D., Valero-Muñoz, M., Houstis, N. E., Iwamoto, Y., et al. (2018). Cardiac macrophages promote diastolic dysfunction. *J. Exp. Med.* 215 (2), j423–j440. doi: 10.1084/jem.20171274

Jablonski, K. A., Amici, S. A., Webb, L. M., Ruiz-Rosado Jde, D., Popovich, P. G., Partida-Sanchez, S., et al. (2015). Novel Markers to Delineate Murine M1 and M2 Macrophages. *PloS One* 10 (12), E0145342. doi: 10.1371/Journal.Pone.0145342

Leuschner, F., Panizzi, P., Chico-Calero, L., Lee, W. W., Ueno, T., Cortez-Retamozo, V., et al. (2010). ACE Inhibition Prevents the Release of Monocytes From Their Splenic Reservoir in Mice With Myocardial Infarction. *Circ. Res.* 107 (11), 1364–1373. doi: 10.1161/CIRCRESAHA.110.227454

Li, C., Wang, Y., Qiu, Q., Shi, T., Wu, Y., Han, J., et al. (2014). Qishenyiqi Protects Ligation-Induced Left Ventricular Remodeling by Attenuating Inflammation and Fibrosis *via* STAT3 and NF-κB Signaling Pathway. *PloS One* 9 (8), e104255. doi: 10.1371/journal.pone.0104255

Li, C., Wang, J., Wang, Q., Zhang, Y., Zhang, N., Lu, L., et al. (2016). Qishen granules inhibit myocardial inflammation injury through regulating arachidonic acid metabolism. *Sci. Rep.* 6, 36949. doi: 10.1038/srep36949

Liao, X., Shen, Y., Zhang, R., Sugi, K., Vasudevan, N. T., Alaiti, M. A., et al. (2018). Distinct Roles of Resident and Nonresident Macrophages in Nonischemic Cardiomyopathy. *Proc. Natl. Acad. Sci.* 115 (20), E4661–E4669. doi: 10.1073/Pnas.1720065115

Liu, Z., Guo, F., Wang, Y., Li, C., Zhang, X., Li, H., et al. (2016). BATMAN-TCM: a Bioinformatics Analysis Tool for Molecular mechANism of Traditional Chinese Medicine. *Sci. Rep 2016* 6, 21146. doi: 10.1038/srep21146

Momtazi-Borojeni, A. A., Abdollahi, E., Nikfar, B., Chaichian, S., Ekhlasi-Hundrieser, M. et al. (2019). Curcumin as a potential modulator of M1 and M2 macrophages: new insights in atherosclerosis therapy. *Heart Failure Rev.* 24 (3), 399–409. doi: 10.1007/s10741-018-09764-z

Moore, K. J., and Tabas, I. (2011). Macrophages in the pathogenesis of atherosclerosis. *Cell.* 145 (3), 341–355. doi: 10.1016/j.cell.2011.04.005

Oka, T., Akazawa, H., and Naito, A. T. (2014). Angiogenesis and Cardiac Hypertrophy: Maintenance of Cardiac Function and Causative Roles in Heart Failure. *Circ. Res.* 114 (3), 565–571. doi: 10.1161/CIRCRESAHA.114.300507

Okizaki, S., Ito, Y., Hosono, K., Oba, K., Ohkubo, H., Amano, H., et al. (2015). Suppressed recruitment of alternatively activated macrophages reduces TGF-β1 and impairs wound healing in streptozotocin-induced diabetic mice. *Biomed Pharmacother* 70, 317–325. doi: 10.1016/j.biopha.2014.10.020

Partha D. Nahrendorf, M. (2015). Monocytes in Myocardial Infarction. *Arterioscler. Thromb. Vasc. Biol.* 35 (5), 1066–1070. doi: 10.1161/ATVBAHA.114.304652

Pinto, A. R., Paolicelli, R., Salimova, E., Gospocic, J., Slonimsky, E., Bilbao-Cortes, D. et al. (2012). An Abundant Tissue Macrophage Population in the Adult Murine Heart with a distinct alternatively-activated macrophage profile. *PloS One* 7 (5), e36814. doi: 10.1371/journal.pone.0036814

Pryds, K., Rahbek Schmidt, M., Bjerre, M., Thiel, S., Refsgaard, J., Bøtker, H. E., et al. (2019). Effect of long-term remote ischemic conditioning on inflammation and cardiac remodeling. *Scand Cardiovasc. J.* 5, 1–9. doi: 10.1080/14017431.2019.1622770

Ribeiro, K. C., Campelo, R. P., Rodrigues, D. D. R. F., Mattos, E. C., Brandão, I. T., da Silva, C. L., et al. (2018). Immunization with plasmids encoding M2 acetylcholine muscarinic receptor epitopes impairs cardiac function in mice and induces autophagy in the myocardium. *Autoimmunity* 51 (5), 245–257. doi: 10.1080/08916934.2018.1514389

Robbins, C. S., and Swirski, F. K. (2010). The multiple roles of monocyte subsets in steady state and inflammation. *Cell. Mol. Life Sci.* 67 (16), 2685–2693. doi: 10.1007/s00018-010-0375-x

Sager, H. B., Kessler, T., and Schunkert, H. (2017). Monocytes and macrophages in cardiac injury and repair. *J. Thoracic Dis.* 9 (Suppl 1), S30–S35. doi: 10.21037/jtd.2016.11.17

Schwarz, R. E., and Hiserodt, J. C. (1990). Effects of splenectomy on the development of tumor-specific immunity[J]. *J. Surg. Res.* 48 (5), 448–453. doi: 10.1016/0022-4804(90)90011-P

Shivshankar, P., Halade, G. V., Calhoun, C., Escobar, G. P., Mehr, A. J., Jimenez, F., et al. (2014). Caveolin-1 deletion exacerbates cardiac interstitial fibrosis by promoting M2 macrophage activation in mice after myocardial infarction. *J. Mol. Cell. Cardiol.* 76, 84–93. doi: 10.1016/j.yjmcc.2014.07.020

Singla, D. K., Wang., Jing, and Reetu, S. (2017). Primary human monocytes differentiate into M2 macrophages and involve Notch-1 pathway. *Can. J. Physiol. pharamacology* 95 (3), 288–294. doi: 10.1139/cjpp-2016-0319

Swirski, FK1, Nahrendorf, M., Etzrodt, M., Wildgruber, M., Cortez-Retamozo, V., Panizzi, P., et al. (2009). Identification of splenic reservoir monocytes and their deployment to inflammatory sites. *Sci* 325 (5940), 612–616. doi: 10.1126/science.1175202

Wang, J., Lu, L., Wang, Y., Wu, Y., Han, J., Wang, W., et al. (2015). Qishenyiqi Dropping Pill attenuates myocardial fibrosis in rats by inhibiting RAAS-mediated arachidonic acid inflammation. *J. ethnopharmacol* 176, 375–384. doi: 10.1016/j.jep.2015.11.023

Wang, Y., Lin, W., Li, C., Singhai, S., Jain, G., Zhu, R., et al. (2017). Multipronged Therapeutic Effects of Chinese Herbal Medicine Qishenyiqi in the Treatment of Acute Myocardial Infarction. *Front. In Pharmacol.* 2; 8, 98. doi: 10.3389/fphar.2017.00098

Wang, Y., Li, C., Ouyang, Y., Shi, T., Yang, X., Yu, J., et al. (2013). QSYQ attenuates oxidative stress and apoptosis induced heart remodeling rats through different subtypes of NADPH-oxidase. *Evid. Based Complement Alternat. Med.* 2013, 824960. doi: 10.1155/2013/824960

Wang, Y., Li, C., Ouyang, Y., Yu, J., Guo, S., Liu, Z., et al. (2019). Cardioprotective Effects of Qishenyiqi Mediated by Angiotensin II Type 1 Receptor Blockade and Enhancing Angiotensin-Converting Enzyme 2. *Evidence-Based Complement Altern Med.* 2019, 9791436. doi: 10.1155/2019/9791436

Wu, W. K., Llewellyn, O. P., Bates, D. O., Nicholson, L. B., and Dick, A. D. (2010). IL-10 regulation of macrophage VEGF production is dependent on macrophage polarisation and hypoxia. *Immunobiol* 215 (9-10), 796–803. doi: 10.1016/j.imbio.2010.05.025

Zhang, F., Dang, Y., Li, Y., Hao, Q., Li, R., Qi, X., et al. (2016). Cardiac Contractility Modulation Attenuate Myocardial Fibrosis by Inhibiting TGF-β1/Smad3 Signaling Pathway in a Rabbit Model of Chronic Heart Failure. *Cell. Physiol. Biochem.* 39 (1), 294–302. doi: 10.1159/000445624

Conflict of Interest: The authors declare that the research was conducted in the absence of any commercial or financial relationships that could be construed as a potential conflict of interest.

frontiers in Pharmacology

ORIGINAL RESEARCH
published: 27 November 2019
doi: 10.3389/fphar.2019.01391

Bazhu Decoction, a Traditional Chinese Medical Formula, Ameliorates Cognitive Deficits in the 5xFAD Mouse Model of Alzheimer's Disease

Axiang Peng[1†], Yuehong Gao[2†], Xiaomei Zhuang[1†], Yaoqi Lin[1], Wencan He[2], Yannan Wang[3], Wenfan Chen[1], Tingting Chen[1], Xiaoqing Huang[1], Renzhi Yang[1], Yuanpeng Huang[1], Shengyan Xi[3]* and Xian Zhang[2]**

[1] Department of Traditional Chinese Medicine, Zhongshan Hospital, Xiamen University, Xiamen, China, [2] Fujian Provincial Key Laboratory of Neurodegenerative Disease and Aging Research, Institute of Neuroscience, School of Medicine, Xiamen University, Xiamen, China, [3] Department of Traditional Chinese Medicine, School of Medicine, Xiamen University, Xiamen, China

Alzheimer's disease (AD) is the most common neurodegenerative disorder associated with aging. There are currently no effective treatments for AD. Bazhu decoction (BZD), a traditional Chinese medicine (TCM) formula, has been employed clinically to alleviate AD. However, the underlying molecular mechanisms are still unclear. Here we found that middle- and high-doses of BZD ameliorated the behavioral aspects of 5xFAD transgenic mice in elevated plus maze, Y maze and Morris water maze tests. Moreover, BZD reduced the protein levels of BACE1 and PS1, resulting in a reduction of Aβ plaques. We also identified a beneficial effect of BZD on oxidative stress by attenuating MDA levels and SOD activity in the brains of 5xFAD mice. Together, these results indicate that BZD produces a dose-dependent positive effect on 5xFAD transgenic mouse model by decreasing APP processing and Aβ plaques, and by ameliorating oxidative damage. BZD may play a protective role in the cognitive and anxiety impairments and may be a complementary therapeutic option for AD.

Keywords: Bazhu decoction, Alzheimer's disease (AD), 5xFAD mice, β-amyloid (Aβ), traditional Chinese medicine (TCM)

OPEN ACCESS

Edited by:
Valentina Echeverria Moran, Bay Pines VA Healthcare System, United States

Reviewed by:
Andrei Mocan, Iuliu Haţieganu University of Medicine and Pharmacy, Romania
Zhi-Yuan Zhang, Nanjing Medical University, China

***Correspondence:**
Yuanpeng Huang
huangyp998@xmu.edu.cn
Shengyan Xi
xishengyan@xmu.edu.cn
Xian Zhang
xianzhang@xmu.edu.cn

†These authors have contributed equally to this work

Specialty section:
This article was submitted to Ethnopharmacology, a section of the journal Frontiers in Pharmacology

Received: *15 May 2019*
Accepted: *31 October 2019*
Published: *27 November 2019*

Citation:
Peng A, Gao Y, Zhuang X, Lin Y, He W, Wang Y, Chen W, Chen T, Huang X, Yang R, Huang Y, Xi S and Zhang X (2019) Bazhu Decoction, a Traditional Chinese Medical Formula, Ameliorates Cognitive Deficits in the 5xFAD Mouse Model of Alzheimer's Disease. Front. Pharmacol. 10:1391. doi: 10.3389/fphar.2019.01391

INTRODUCTION

Alzheimer's disease (AD), the most common cause of dementia in the elderly, is an age-related neurodegenerative disease characterized by progressive loss of memory, cognitive dysfunction, and other executive deficits (Mattson, 2004; Stokin et al., 2005). According to the World Alzheimer Report 2018 (Patterson, 2018), 50 million people are currently affected by AD, and this number is expected to increase to more than 152 million by 2050. AD, therefore places a huge economic burden on society and on many families.

Pathologically, the classic hallmarks of AD include the accumulation of extracellular senile plaques constituted of aggregated β-amyloid (Aβ), intracellular neurofibrillary tangles (NFTs), and synapse loss (Alzheimer et al., 1995). Since Aβ is one of the primary components of amyloid plaques in the brains of patients with AD, hypotheses have been proposed regarding the key contribution of Aβ in the pathological alterations and cognitive impairment in AD (Hardy and Allsop, 1991;

Hardy and Higgins, 1992). Multiple lines of evidence show that Aβ accumulation leads to neurotoxicity and memory deterioration. Aβ is generated from the proteolytic processing of amyloid precursor protein (APP) by β-secretase (BACE1) and γ-secretase (Checler, 1995; Zhang et al., 2014). Presenilin-1 (PS1) functions as the catalytic subunit of γ-secretase (Zhang et al., 2014).

Previous studies have suggested that Aβ plaques can induce activation of glial cells including astrocytes and microglia, leading to inflammation and oxidative stress (Lu et al., 2009; Li et al., 2011; Zhou et al., 2014). This may hinder neurotransmitter release, induce neuronal apoptosis and/or neuronal degeneration, and eventually contribute to cognitive impairment in AD. Malondialdehyde (MDA), a metabolite of lipid peroxidation, reflects the levels of free radicals and cellular damage (higher lipid peroxidation correlates to higher levels of MDA) (Giera et al., 2012). Superoxide dismutase (SOD) is a critical antioxidant, which can effectively eliminate the superoxide anion, protecting against neuronal toxicity (Batinic-Haberle et al., 2014).

Despite its high impact, the drugs (including donepezil HCl, rivastigmine, galanthamine, and memantine) commonly prescribed to treat AD patients merely relieve symptoms temporarily instead of decelerating the progression of disease (Wang et al., 2014; Cao et al., 2018). Preliminary clinical and preclinical studies have suggested that some traditional Chinese medicines (TCM) are beneficial to the prevention and control of AD. For instance, Fumanjian, a classic Chinese herbal formula, could ameliorate the impairment of spatial learning and memory by modulating the apoptotic signaling pathway in the hippocampus of rats with $A\beta_{1-40}$-induced AD (Hu et al., 2014). TCM Shen-Zhi-Ling oral liquid not only improved behavioral and neuropsychological symptoms of dementia in AD patients, but also ameliorated memory impairment in AD mice by modulating the HO-1/BVR system (Xing et al., 2017). In addition, components of certain herbal formulations may constitute an alternative complementary approach to alleviate symptoms and delay the progression of AD (Jesky and Hailong, 2011; May et al., 2016). Oral administration of alpha-asarone, an active substance of Rhizoma Acori Tatarinowii (Shichangpu), improved working spatial memory in AD-like preclinical models (Limon et al., 2009). In the same study, the authors also suggested that this effect may be attributed to the protection of neuronal cells from oxidative stress, owing to decreases in NO production and Aβ-neurotoxicity. Therefore, TCM may represent an effective therapeutic option for AD, and warrants further investigation.

Bazhu decoction (BZD) is a formula of TCM that includes Radix Morindae Officinalis (Bajitian), Fructus Corni (Shanzhuyu), Pheretima (Dilong), Rhizoma Acori Tatarinowii (Shichangpu) and Arisaema cum Bile (Dannanxing). These compounds may enhance memory and ameliorate cognitive dysfunction in patients with AD (Li et al., 2016; Peng and Huang, 2017). Moreover, previous studies have suggested that water extracts from the respective herbs contained in BZD significantly improve learning and memory in AD-like animals *via* antioxidation, scavenging free radicals, neuroprotection, immunity enhancement, and by reducing the deposition of senile plaques (Jin et al., 2009; Wen and Chen, 2009; Li et al., 2013; Wang et al., 2013). Nevertheless, the mechanisms by which BZD may ameliorate AD remain elusive. In this study, we sought to explore the effect of BZD in 5xFAD mice (Oakley et al., 2006), a recognized transgenic mouse model of AD, by investigating the biological mechanisms underlying its potential therapeutic effect.

MATERIALS AND METHODS

Experimental Animals

5xFAD transgenic mice and wild-type littermates (50% females; weight: 25 ± 3 g; age: 3 months) were from the Jackson Laboratory. 5xFAD (APP and PS1 double-transgenic) mice co-express five familial AD mutations, namely, APP K670N/M671L (Swedish), I716V (Florida), V717I (London), PS1 M146L, and L286V, and have been shown to develop major pathological features of AD more rapidly than other transgenic AD-like animal models (Oakley et al., 2006). These animals present with increased amyloid plaque deposits and memory impairments in the Y and Morris water mazes at the ages of 2 and 4 months, respectively (Oakley et al., 2006; Wang et al., 2014). All animals were fed, cared for, and handled in accordance with the Guide for the Care and Use of Laboratory Animals of the Xiamen University, and the Animal Ethics Committee Guidelines of the Animal Facility of the Zhongshan Hospital Xiamen University. The animals were acclimatized to the facilities for one week before the beginning of the treatment.

Drug Preparation and Reagents

Chinese medicines used for the concoction of BZD were supplied by the Zhongshan Hospital Xiamen University (Xiamen, China). Each herb was identified by the experts in the School of Pharmaceutical Sciences of Xiamen University. All voucher specimens were deposited at the Xiamen Botanical Garden (http://sweetgum.nybg.org/science/ih/herbarium-details/?irn=249232) (Herbarium Code: XMBG) for future reference. BZD containing Radix Morindae Officinalis, Fructus Corni, Pheretima, Rhizoma Acori Tatarinowii, and Arisaema cum Bile (3:2:3:3:2) (see **Table 1**) was strictly decocted in accordance with the standards of Chinese medicine, and 3 concentrations (0.211 g/ml, 0.423 g/ml, and 0.845 g/ml) were prepared using a heat cycle oven. Additionally, donepezil HCl (Aricept) was purchased from Eisai pharmaceutical Co., Ltd. Donepezil HCl was dissolved in a 1% solution of sodium carboxymethyl cellulose to obtain a concentration of 0.0325 mg/ml.

Antibodies against APP (369) and PS1-NTF (Ab14) were generated in-house (Thinakaran et al., 1996; Xu et al., 1997). Anti-BACE1 (3D5) antibody was kindly provided by Professor Robert Vassar (Northwestern University). Anti-β-actin antibody was purchased from ZEN bioscience, and anti-β-amyloid antibody was obtained from Abcam. Horseradish peroxidase labeled secondary goat anti-rat IgG antibody and goat anti-rabbit

TABLE 1 | Information of components in BZD.

Chinese name	Botanical name	Common name	Weight (g)	Voucher numbers	Part used
Ba Ji Tian	*Morinda officinalis* How	Radix Morindae Officinalis	15	180901	Root
Shan Zhu Yu	*Cornus officinalis* Sieb. et Zucc.	Asiatic Cornelian Cherry Fruit	10	180221	Matured sarcocarp
Shi Chang Pu	*Acorus tatarinowii* Schott	Grassleaf Sweetflag Rhizome	15	180901	Rhizome
Di Long	*Pheretima aspergillum* (E. Perrier), *Pheretima vulgaris* Chen, *Pheretima guillelmi* (Michaelsen) or *Pheretima Pectinifera* Michaelsen	Earth Worm	15	181121	Dried body
Dan Nan Xing	*Arisaema erubescens* (Wall.) Schott, *Arisaema heterophyllum* B1. or *Arisaema amurense* Maxim	Arisaema Cum Bile	10	171203	Powder

IgG antibody were purchased from Pierce, and polyvinylidene difluoride (PVDF) membranes were purchased from Millipore. The protein loading marker was purchased from Fermentas, and the protease inhibitors were purchased from Roche. X-ray blue films were purchased from Kodak; BSA and TEMED were purchased from Sigma.

UHPLC-MS

The major chemical constituents of BZD were profiled by ultra-high performance liquid chromatography (UHPLC) coupled with a high resolution electrospray ionization mass (HR-ESI-MS) detector. 10 mg lyophilized powder was dissolved in 1 mL of ultrapure water through ultrasonic method. The solution was filtered with 0.22 μm nylon filter membrane before injection into the UHPLC. The UHPLC separation was performed over a C18Kinetex column (100 × 2.1 mm i.d., 2.6 μm, Phenomenex Inc., Torrance, USA) at 35 °C on the Thermo UltiMate 3000 LC system (Thermo Fisher Scientific, Bremen, Germany). The mobile phases were acetonitrile (A) and 0.1% formic acid with water (*v/v*) (B). Samples were eluted by gradients according to the elution program as follows: A from 5% to 35% and B from 95% to 65% during 0–30 min, A from 35 to 100% and B from 65 to 0% during 30–35 min, A and B were kept at 100 and 0% respectively during 35–45 min. The column was maintained at 35 °C and eluted at a flow rate of 0.3 mL/min. The injected volume was 5 μL. A diode array detector with detection wavelength of 254 nm, and a high resolution ESI-MS detector were used to record the HPLC chromatograms. After UHPLC, samples were analyzed by MS spectra on a Thermo Q-Exactive system. The mass spectrometer with positive and negative ionizations was calibrated across *m/z* 100–1,500 using the manufacturer's calibration standards mixture (caffeine, MRFA and Ultramark 1621 in anacetonitrile–methanol–water solution containing 1% acetic acid) allowing mass fluctuation of no more than 5 ppm in the external calibration mode. The ionization voltage was 3.5 kV, and the capillary temperature was set at 300 °C.

Grouping and Treatment

The 5xFAD mice were randomly allocated to 5 groups, namely, control (5xFAD-Control), low-dose BZD (5xFAD-BZD-L), medium-dose BZD (5xFAD-BZD-M), high-dose BZD (5xFAD-BZD-H), and donepezil HCl (5xFAD-Donep) (n = 8/group). Wild-type littermates, used as control mice, were randomly allocated to control (WT-Control), BZD (WT-BZD), and donepezil HCl (WT-Donep) groups (n = 8/group).

The clinical dosing of BZD and Donepezil HCl was determined in accordance with the Pharmacopoeia of the People's Republic of China (2015). Mice in the control groups were administered 20 mL/(kg·d) double distilled water by gavage. The 5xFAD-Donep and WT-Donep mice were administered 20 mL/(kg·d) donepezil HCl at a dose of 0.65 mg/(kg·d) and concentration of 0.0325 mg/mL. In addition, mice in the 5xFAD-BZD-L, 5xFAD-BZD-M, 5xFAD-BZD-M, and WT-BZD groups were orally administered 20 mL/(kg·d) BZD at doses of 4,225 g/(kg·d), 8,450 g/(kg·d), 16,900 g/(kg·d), and 16,900 g/(kg·d), respectively. All mice received treatment once daily by gavage for 12 weeks.

Behavioral Tests

The behavioral tests were initiated 10 days before the end of treatment (n = 8/group). On a normal test day, mice were allowed to adapt to the experimental environment for 30 min. Only one behavioral test was performed on each day. The order of the tests was organized so that easy to difficult tests could be performed in standard room-lighting conditions. Mazes were cleaned with 75% alcohol immediately after the end of the test to minimize scent trails. Smart 3.0 software, a data collection system, and an overhead camera were used to monitor the activity of the mice.

The methods for the open field test and elevated plus maze used in our study have been described in detail elsewhere (Liu et al., 2014). For the open field test, mice were placed in an arena measuring 40 cm × 40 cm × 40 cm divided into 16 squares, for 10 min. The total distance moved in the arena and the time spent in the central arena (central 4 squares) were analyzed for each mouse. For the elevated plus maze, the apparatus, which was elevated 40 cm above the ground, consisted of two opposing open arms (30 cm × 6 cm) and two opposing closed arms (30 cm 6 cm × 15 cm) with an open roof. Each mouse was placed at the center of the maze facing an open arm. Then the experimenter exited the room, allowing the mouse to freely explore for 5 min. The frequencies of entries to the open arms, and the time spent in the open arms were recorded as an index of anxiety (higher index, lower anxiety).

Study has shown that (Ohno et al., 2004), the procedure for the Y Maze did not involve any training, reward, or punishment and allowed researchers to evaluate the rodents' spontaneous spatial working memory. This test mostly assesses the function of the hippocampus. The Y maze comprised 3 symmetrical arms (30 cm × 6 cm × 15 cm) separated by 120 degrees. Every mouse was placed in the center of Y maze, with the head in the same direction, and was allowed to explore the arms freely for 5 min. The sequence and total number of arm entries were recorded. Data were analyzed using the percentage of alternation triplet, which was the number of triads containing entries into all 3 arms divided by the maximum possible number of alternations (the total number of arms entered - 2) × 100.

For the Morris water maze, the task was carried out in strict accordance with the protocol described by Geda (Vorhees and Williams, 2006). The maze consisted of a 1.2 m diameter, light blue, plastic, circular pool filled with water to a depth of 31 cm with a temperature of 22 ± 1°C. The maze was divided into four quadrants (SW, SE, NE, and WN). A transparent platform was placed at the SW quadrant and was submerged ~1 cm beneath the surface of the water. The test included two phases: spatial navigation training and probe experiments. During spatial navigation training, mice were first placed in one of the four starting locations facing the pool wall, and were allowed to swim until finding the platform in 60 s. The time that each mouse took to find the hidden platform was recorded. If the mice did not find the platform within 60 s, they were guided to the platform by the experimenter and were allowed to remain at the platform for 10 s. For the probe experiments, each trial was conducted when the animal's latency to reach the platform tended to stabilize. The hidden platform was removed, and mice were placed in the pool at the opposite quadrant of the platform, and were allowed to swim freely for 60 s. Time spent in each quadrant, frequencies of crossings to the previous location of the target platform, and motion tracings were obtained using an automated video tracking software from Smart 3.0.

Collection of Brain Tissues

Experimental mice were sacrificed after completing the Morris water maze test. Briefly, the animals were anesthetized with 1.5% pentobarbital sodium, perfused with phosphate buffered saline (PBS), and the brains were rapidly harvested on ice. Six mice were randomly selected from each group, and the left hemi-brains were fixed in fresh 4% paraformaldehyde and were used for immunohistochemistry analysis. The right hemi-brains were immediately frozen in liquid nitrogen for storage until homogenization for other biochemical assays.

Immunohistochemistry

Immunohistochemistry was performed as previously described (Hu et al., 2015) (n = 6/group). In summary, the brains were fixed for 48 h at 4°C in 4% paraformaldehyde and were then transferred to 30% sucrose for 2–3 days. O.C.T., a tissue freezing medium, was employed to freeze the brains and the tissue was then sectioned into 10-μm slices using a freezing microtome. Immunohistochemistry staining was used to determine Aβ plaques in the cortex and hippocampus. Anti-β-amyloid antibody (ab126649) was employed at a concentration of 1:500. The signal was revealed using the DAB chromogenic reagent kit. Light microscopy was used to capture the images. Densitometry analysis of the images was conducted using Image Pro Plus 6.0 software.

Oxidative Stress Assay

In summary, the hippocampal and cortical tissues were separated from the right hemi-brains (n = 6/group), homogenized in phosphate buffered saline (PBS) (mass ratio of 1:1) and were then divided into two parts, one for detecting SOD/MDA, and the other for detecting protein by western blot analysis. PBS (mass ratio of 1:10) was added to the homogenates and homogenization was repeated using a Polytron homogenizer. The homogenates were centrifuged at 3,000 r/min for 10 min at 4°C and the supernatants were collected. The SOD activity and MDA levels were determined according to the manufacturers' instructions for Total Superoxide Dismutase (T-SOD) assay kit (Hydroxylamine method) or Malondialdehyde (MDA) assay kit (TBA method) from Nanjing Jiancheng Bioengineering Institute.

Western Blot

The other part of homogenates from hippocampal and cortical tissues (n = 6/group) was homogenized again in a buffer solution containing a protease inhibitor mix (Roche). Samples were centrifuged at 12,000g for 20 min at 4°C. The supernatant was collected and the proteins in the final elute were quantified using a BCA protein assay kit according to the manufacturer's protocol. Equivalent amounts of protein were separated in 10% sodium dodecyl sulphate polyacrylamide gel (SDS-PAGE) and were then electrophoretically transferred to a PVDF membrane. The membranes were blocked with Tris-buffered saline containing 0.05% Tween-20 (TBST) and 5% skimmed milk for 2 h. The membranes were then probed with primary antibodies (anti-APP, anti-PS1-NTF and anti-BACE1) overnight at 4 °C, followed by incubation with horseradish peroxidase-linked secondary antibodies at room temperature (23 ± 2 °C) for 1 h. Signals were revealed using enhanced chemiluminescence western blotting detection reagents. Relative protein levels were normalized to β-actin. The intensity of the immunoreactive bands was quantified using Image J software.

Statistical Analysis

Data have been expressed as mean ± standard deviation (SD). Statistical analyses were performed using GraphPad Prism 7.0 (GraphPad Software Inc., La Jolla, United States). One-way analyses of variance (One-Way ANOVA) was used to compare the means of multiple groups. The least significant difference (LSD) method was selected for *post hoc* analysis. $P < 0.05$ was considered statistically significant.

RESULTS

Analysis of BZD

BZD was separated using the UHPLC-MS system and its chromatographic fingerprinting established. Comparing the retention time, UV and MS spectra with reference samples, the following twenty major components were identified: leucine (peak R1, Rt = 3.76 min), adenine (peak R2, Rt = 4.92 min), phenylalanine (peak R3, Rt = 5.27 min), 5-hydroxymethyl-2-furaldehyde (peak C1, Rt = 6.23 min), tryptophan (peak R4, Rt = 6.76 min), morroniside (peak C2, Rt = 7.96 min), asperuloside (peak M1, Rt = 8.82 min), loganin (peak C3, Rt = 9.41 min), sweroside (peak C4, Rt = 9.60 min), cornuside (peak C5, Rt = 12.81 min), taurochenodeoxycholic acid (peak A1, Rt = 14.43 min), glycohyodeoxycholic acid (peak A2, Rt = 14.85 min), 2,4,5-trimethoxybenzaldehyde (peak G1, Rt = 16.31 min), β-asarone (peak G2, Rt = 16.99 min), cholic acid (peak A3, Rt = 20.21 min), rubiadin (peak M2, Rt = 20.86 min), physcion (peak M3, Rt = 21.31 min), hyodeoxycholic acid (peak A4, Rt = 22.28 min), rubiadin-1-methyl ether (peak M4, Rt = 22.94 min), and 1,6-dihydroxy-2-methoxyanthraquinone (peak M5, Rt = 24.21 min) as shown in **Figures 1** and **2**. Detailed information of BZD's components identified by UHPLC is provided in the **Supplementary Table**.

BZD Improves Learning and Memory Abilities and Alleviated Anxiety-Related Behaviors in 5xFAD Mice

To evaluate the impact of BZD treatment on locomotor activity and anxiety-related behaviors, we performed open field and elevated plus maze tests. In the open field test, there was no significant difference in the percentage of time spent in the center of the arena, or in the total distance traveled among groups ($P > 0.05$) (**Figures 3A**, **B**), indicating that locomotor activity of 6-month-old 5xFAD mice is not altered. In the elevated plus maze, the 5xFAD-Control mice spent greater time in the open arms and had a larger number of entries in the open arms ($P < 0.01$) (**Figures 3C**, **D**) than the mice in the WT-Control group, suggesting that at 6-months, 5xFAD mice showed attenuated anxiety in dangerous environments, with enhanced behavioral disinhibition (Olausson et al., 1999). BZD or donepezil HCl had no effect on anxiety in wild-type mice. Interestingly, we observed that the 5xFAD-BZD-M, 5xFAD-BZD-H, and 5xFAD-Donep groups exhibited a marked decrease in the percentage of time spent in the open arms, and in the frequency of entries into the open arms when compared to the 5xFAD-control group ($P < 0.05$ or $P < 0.01$) (**Figures 3C**, **D**), confirming that medium and high doses of BZD attenuated the behavioral disinhibition of 5xFAD mice.

To investigate the effects of BZD on the pathological features related to learning and memory, we also tested the animals in the Y and Morris water mazes. In the Y maze, the 5xFAD-Control group showed a pronounced decrease in the percentage of triple alternations compared to the WT-Control group ($P < 0.01$) (**Figure 4A**), suggesting that spontaneous spatial working memory is impaired in 5xFAD mice. BZD and Donepezil increased the percentage of triple alternations in 5xFAD mice ($P < 0.05$) (**Figure 4A**), suggesting that medium and high doses of BZD improved spontaneous spatial working memory in 5xFAD mice. In the Morris water maze, as anticipated, we found that training shortened the escape latency time (ELT) of mice across groups (**Figure 4B**). On the sixth day of training, the mean ELT of the wild-type mice was under 20 s, while the 5xFAD mice presented with values of 20 s or higher. Nevertheless, both wild-type and 5xFAD mice presented with stable values of ELT in the last two training days, suggesting that the probe experiment could be conducted on the seventh day. During the probe trials, the 5xFAD-Control mice showed a dramatic decrease in spatial learning and memory compared to wild-type mice ($P < 0.01$ or $P < 0.001$) (**Figures 4C**, **D**). Medium- and high-dose BZD and donepezil reduced this deficit, as demonstrated by the increased number of target (platform) crossing events and the percentage of time spent in the target quadrant, compared to the 5xFAD-control group ($P < 0.05$ or $P < 0.01$) (**Figures 4C**, **D**). Thus, Medium and high doses of BZD improved spatial learning and memory in 5xFAD mice.

BZD Reduces Aβ Deposition

Cumulative evidence suggests that aggregation of Aβ in the brain is a causative factor for AD pathogenesis. Aβ plaques were determined in the cortex and hippocampus of 5xFAD Mice and wild type littermates by immunostaining. The results showed that no positive staining was observed in the cortex or hippocampus of wild-type mice, whereas the 5xFAD mice presented with a high number of Aβ plaques (**Figure 5A**). Low-dose BZD did not affect the quantity of Aβ plaques ($P > 0.05$) (**Figure 5B**). However, donepezil HCl and medium- and high-dose BZD significantly reduced the burden of Aβ plaques in 5xFAD mice ($P < 0.01$) (**Figure 5B**).

BZD Modulates APP Processing

β-secretase and γ-secretase are two key elements of the amyloidogenic pathway of APP processing associated with the production of Aβ. To investigate whether BZD could affect APP processing, we checked the protein levels of APP, BACE1 and PS1-NTF in the lysates from hippocampal and cortical tissues of the experimental mice (5xFAD-Control, 5xFAD-BZD-L, 5xFAD-BZD-M, 5xFAD-BZD-H, 5xFAD-Donep, WT-Control, WT-BZD and WT-Donep) (**Figure 6A**). As expected, 5xFAD mice presented with significantly higher proteins levels of APP, BACE1 and PS1-NTF compared to the wild-type mice (**Figures 6B**–**D**). BZD and donepezil had no effect on APP protein levels ($P > 0.05$) (**Figure 6B**). High-dose BZD and donepezil decreased BACE1 protein levels in 5xFAD mice ($P < 0.05$); and medium and low-dose BZD had no effect (**Figure 6C**). PS1-NTF is the catalytic subunit of γ-secretase, an enzyme that plays an important role during APP processing. We found that Donepezil HCl and high but not medium or low doses of BZD, reduced the levels of PS1-NTF ($P < 0.05$) (**Figure 6D**). These results indicate that BZD may reduce Aβ level by modulating APP processing.

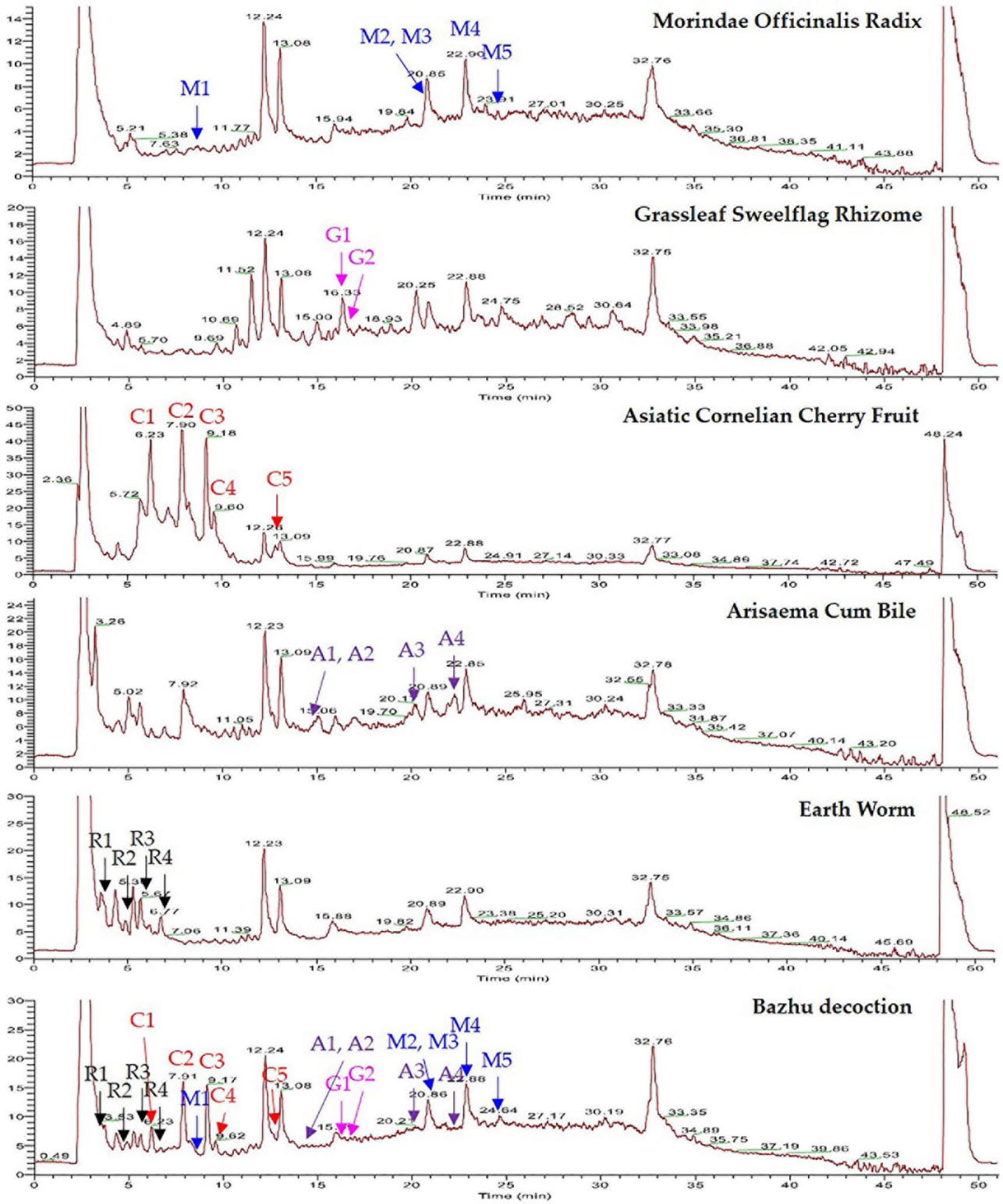

FIGURE 1 | UHPLC-MS chemical fingerprint of BZD. Asperuloside (M1), rubiadin (M2), physcion (M3), rubiadin-1-methyl ether (M4), 1,6-dihydroxy-2-methoxyanthraquinone (M5), 2,4,5-trimethoxybenzaldehyde (G1), β-asarone (G2), 5-hydroxymethyl-2-furaldehyde (C1), morroniside (C2), loganin (C3), sweroside (C4), cornuside (C5), taurochenodeoxycholic acid (A1), glycohyodeoxycholic acid (A2), cholic acid (A3), hyodeoxycholic acid (A4), leucine (R1), adenine (R2), phenylalanine (R3), and tryptophan (R4).

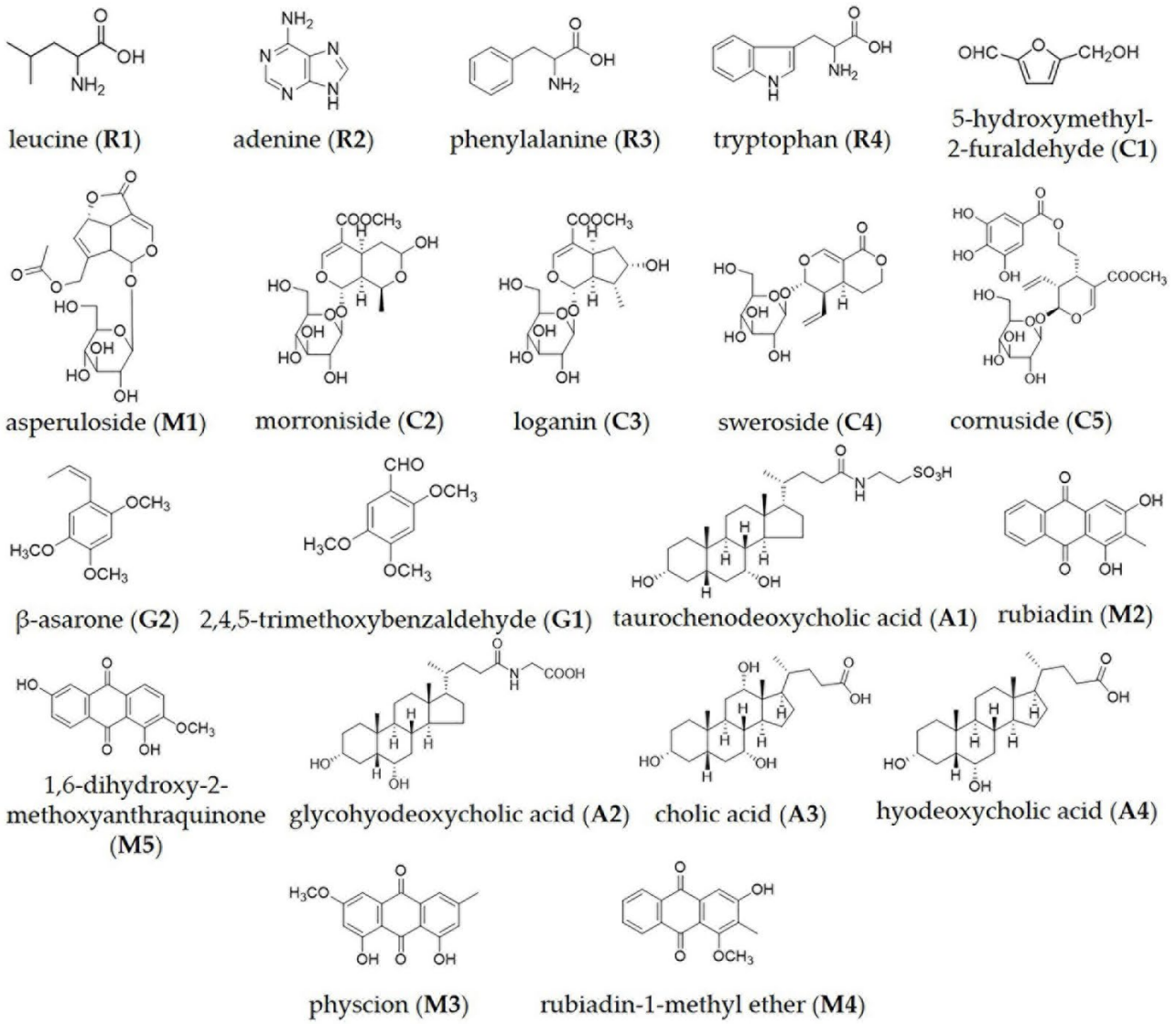

FIGURE 2 | Chemical structure of the major identified components in BZD by UHPLC-MS: leucine, adenine, phenylalanine, tryptophan, 5-hydroxymethyl-2-furaldehyde, asperuloside, morroniside, loganin, sweroside, cornuside, β-asarone, 2,4,5-trimethoxybenzaldehyde, taurochenodeoxycholic acid, rubiadin, 1,6-dihydroxy-2-methoxyanthraquinone, glycohyodeoxycholic acid, cholic acid, hyodeoxycholic acid, physcion and rubiadin-1-methyl ether.

BZD Decreases Oxidative Damage in the Cortex and Hippocampus of 5xFAD Mice

Oxidative stress is implicated in the pathogenesis of AD. Recent studies have shown that increases in MDA content and the fluctuant activity of SOD are associated with the aggregation of Aβ plaques and AD (Zhou et al., 2014). To explore whether BZD could have an impact on MDA/SOD, we quantified MDA levels and SOD activity in homogenates of the cortical and hippocampal tissue samples. 5xFAD mice presented with higher levels of MDA and greater SOD activity than those in the WT-Control group ($P < 0.01$) (**Figures 7A**, **B**), suggesting that 5xFAD mice present with higher levels of free radicals and cellular damage. Interestingly, high- and medium-dose BZD and donepezil HCl reduced both MDA levels and SOD activity ($P < 0.05$) (**Figures 7A**, **B**). These results indicate that BZD decreases oxidative damage in the cortex and hippocampus of 5xFAD Mice.

DISCUSSION

In this study, we evaluated the potential impact of BZD, an alternative Chinese medicine formulation, on behavioral alterations in a transgenic mouse model of AD, including its key molecular hallmarks. We found that BZD exerted a dose-dependent beneficial effect in 5xFAD mice. Medium and high doses of BZD not only ameliorated behaviors related to the disease, but also reduced the production and aggregation of Aβ plaques, probably by reducing the levels of BACE1 and PS1.

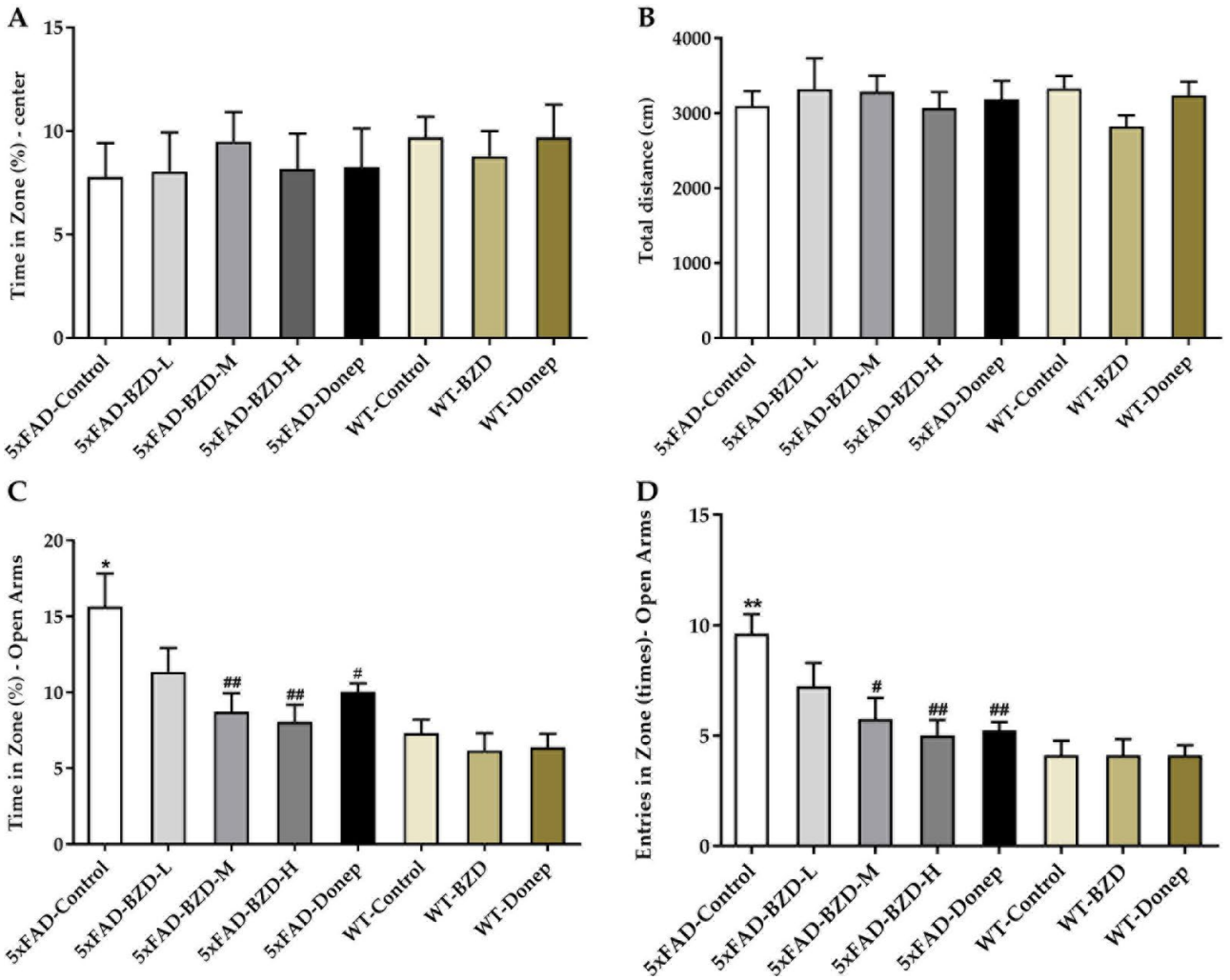

FIGURE 3 | BZD alleviates anxiety-related behaviors in 5xFAD mice. **(A**, **B)** Mice (5xFAD-Control, 5xFAD-BZD-L, 5xFAD-BZD-M, 5xFAD-BZD-H, 5xFAD-Donep, WT-Control, WT-BZD and WT-Donep) were analyzed for duration in the center **(A)** and total travel distance **(B)** in the open field test. Data are expressed as the mean ± SD from 8 mice per group, not significant, One-Way ANOVA. **(C**, **D)** Mice (5xFAD-Control, 5xFAD-BZD-L, 5xFAD-BZD-M, 5xFAD-BZD-H, 5xFAD-Donep, WT-Control, WT-BZD and WT-Donep) were analyzed for time in zone – open arms **(C)** and entries in zone – open arms **(D)** in elevated plus maze. Data are expressed as the mean ± SD from 8 mice per group. $^{*}P < 0.05$, $^{**}P < 0.01$ compared with WT-Control group; $^{\#}P < 0.05$, $^{\#\#}P < 0.01$ compared with 5xFAD-Control group, One-Way ANOVA.

We also identified a beneficial effect on oxidative stress (SOD/MDA) in the hippocampi of 5xFAD mice. We suggest that BZD represent a therapeutic option for AD patients that is worth to be explored in randomized clinical studies.

According to the theory of TCM, AD results from insufficiency of kidney essence, intermingling of phlegm and blood, and fluid stasis (Peng and Huang, 2017). AD may, therefore, benefit from treatments invigorating the qi of the kidney, stimulating elimination of phlegm and promoting blood circulation to remove obstruction and dredge collaterals (Zhu and Hu, 2007). Based on this assumption, Morinda officinalis How. (Bajitian), Cornus officinalis Sieb. et Zucc. (Shanzhuyu), Earthworm (Dilong), Acori Tatarinowii Rhizoma (Shichangpu), and Arisaema cum Bile (Dannanxing) were selected to compound the BZD formula. Bajitian is the sovereign drug that warms and recuperates the yang of the kidney, Shanzhuyu is the minister drug, nourishing and invigorating the yin and qi of the kidney, respectively, Shichangpu and Dannanxing are assistant drugs, that increase the elimination of phlegm, and Dilong is the envoy drug, which not only promotes blood circulation and removes obstruction in the collaterals, but also assists other drugs to penetrate into the diseased areas (Li et al., 2016; Peng and Huang, 2017). Therefore, BZD is consistent with the TCM prescription theory

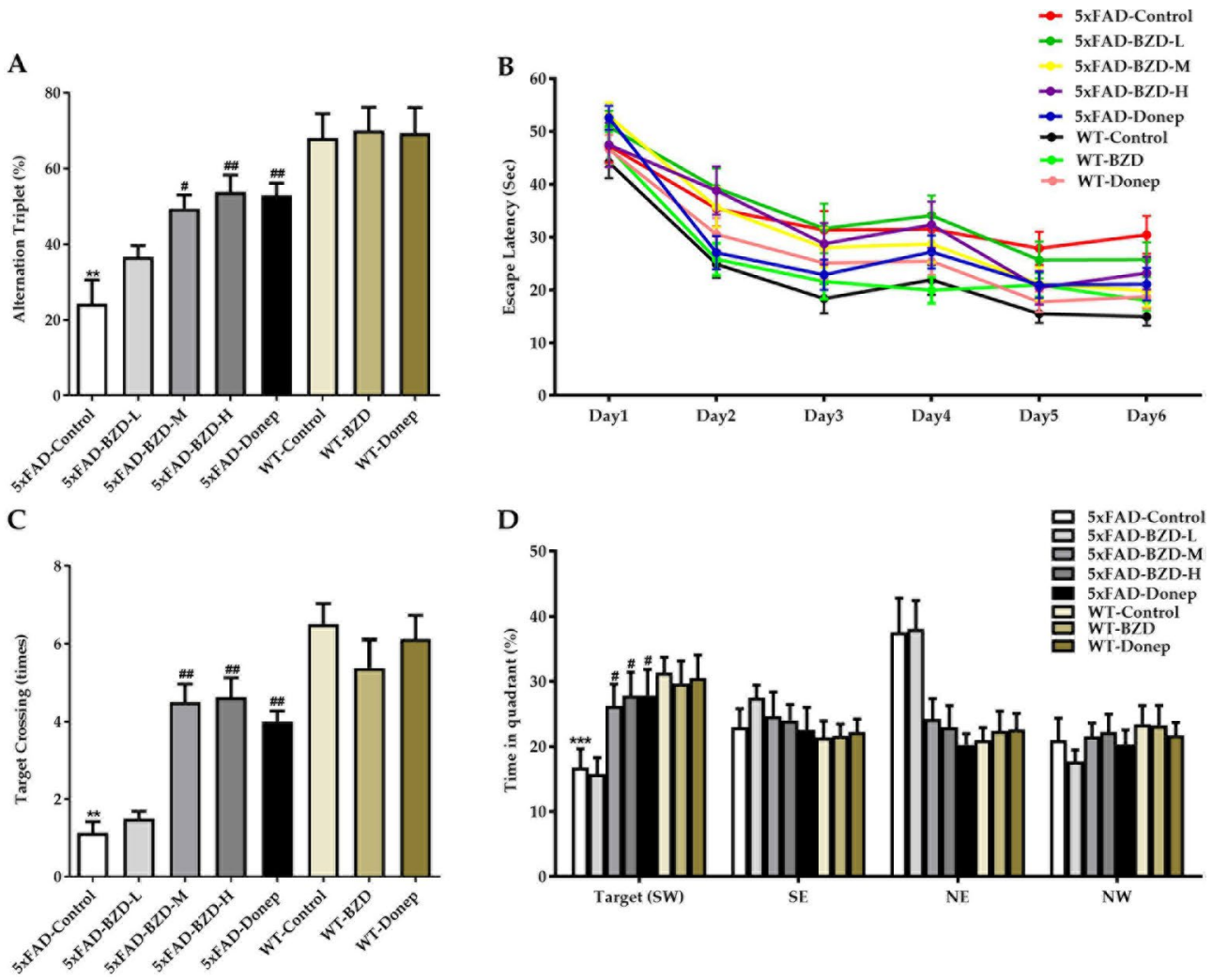

FIGURE 4 | BZD improves learning and memory abilities in 5xFAD mice. **(A)** Mice (5xFAD-Control, 5xFAD-BZD-L, 5xFAD-BZD-M, 5xFAD-BZD-H, 5xFAD-Donep, WT-Control, WT-BZD and WT-Donep) were analyzed for spontaneous alternation behavior by Y-maze tests. Data are expressed as the mean ± SD from 8 mice per group. $^{**}P < 0.01$ compared with WT-Control group; $^{\#}P < 0.05$, $^{\#\#}P < 0.01$ compared with 5xFAD-Control group, One-Way ANOVA. **(B–D)** Mice (5xFAD-Control, 5xFAD-BZD-L, 5xFAD-BZD-M, 5xFAD-BZD-H, 5xFAD-Donep, WT-Control, WT-BZD and WT-Donep) were analyzed for spatial learning and memory in Morris water maze tests. Mice were analyzed for escape latency within a 6-day training period **(B)**. On the 7th day, mice were assayed for the number of crossings over the target platform region **(C)** and time spent in target quadrant **(D)**. Data are expressed as the mean ± SD from 8 mice per group. $^{**}P < 0.01$, $^{***}P < 0.001$ compared with WT-Control group; $^{\#}P < 0.05$, $^{\#\#}P < 0.01$ compared with 5xFAD-Control group, One-Way ANOVA.

for AD, which aims to adjust the patients' habitus including the syndromes of intermingled deficiency and excess, heat and cold, or phlegm and blood stasis. BZD may optimize the rapid aging internal environment and mobilize immune function, thereby extending life and improving intelligence. An increasing number of studies have suggested that single components of BZD are beneficial for AD. Oligosaccharides from Radix Morindae Officinalis improve memory function of AD animal models (Yang et al., 2018). Isolated compounds from Radix Morindae Officinalis ameliorate AD (Lee et al., 2017). Other pharmacological studies have also demonstrated that extracts of Radix Morindae Officinalis have anti-Alzheimer's, anti-fatigue, anti-aging, cardiovascular protective, anti-oxidative, immune-regulatory, and anti-inflammatory activities (Zhang et al., 2018). Studies using Fructus Corni have suggested a wide range of therapeutic properties for this compound, including neuroprotection, anti-amnesia, anti-aging, anti-inflammation, analgesia, antioxidation, anti-osteoporosis, and immunoregulation (Huang et al., 2018a). Rhizoma Acori Tatarinowii reduces amyloid plaques and tau phosphorylation, and has anti-inflammatory effects (Deng et al., 2015; Song et al., 2018). Therefore, the anti-inflammatory and immunity-enhancing effects may contribute to its therapeutic effects in AD. Arisaema cum Bile is useful for treating diseases associated with oxidative imbalance, such as AD, Parkinson's disease, heart disease, rheumatoid arthritis and diabetes (Ahn et al., 2012).

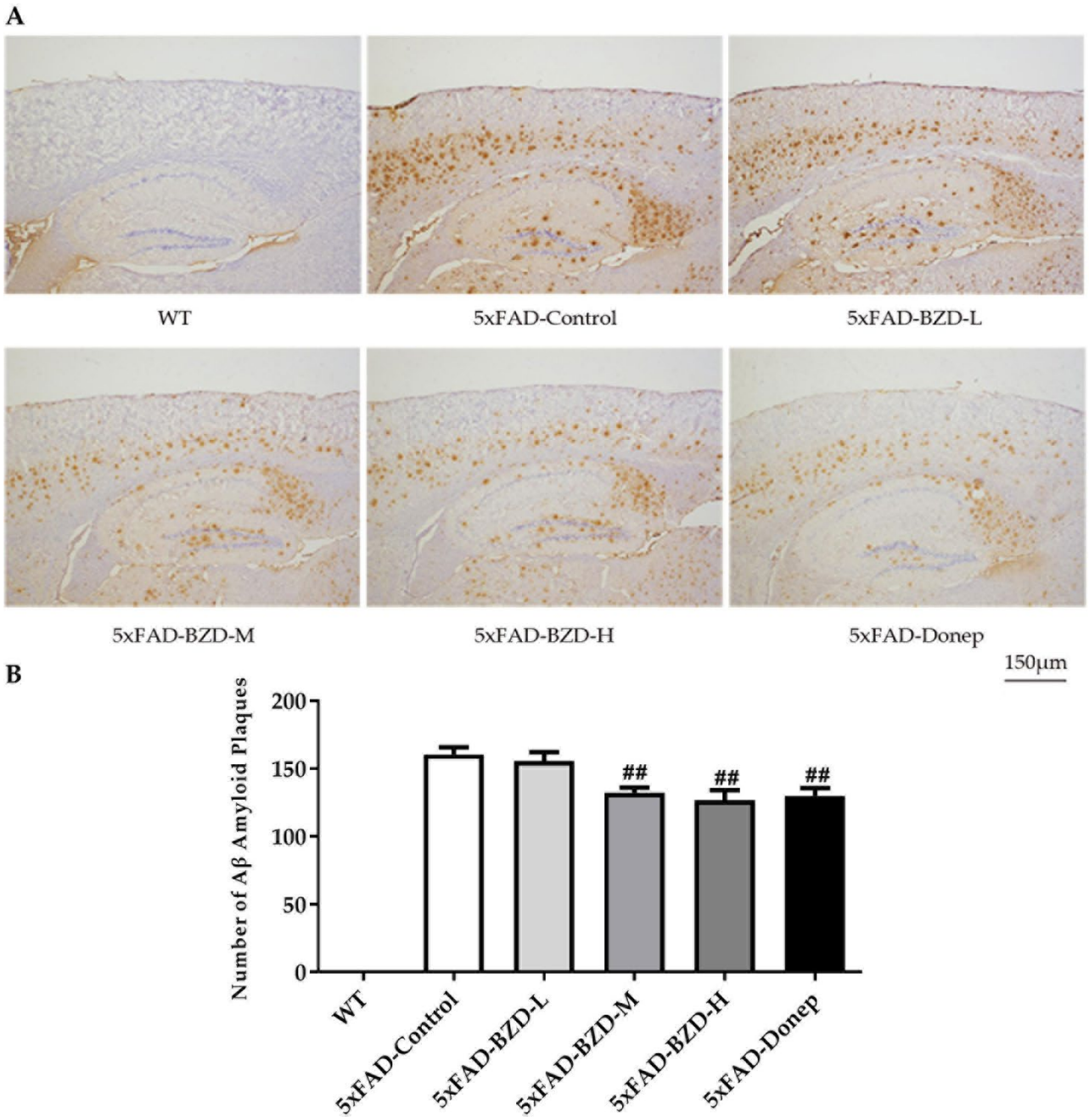

FIGURE 5 | BZD Reduces Aβ Deposition. **(A)** Immunohistochemistry analysis of Aβ plaques in the cortex and hippocampus of 5xFAD Mice (5xFAD-Control, 5xFAD-BZD-L, 5xFAD-BZD-M, 5xFAD-BZD-H and 5xFAD-Donep) and wild type (WT) littermates. Representative images of Aβ plaques; Scale bar, 150 μm. **(B)** Quantification of Aβ plaques in A. Data are expressed as the mean ± SD from 6 mice per group. $^{\#\#}P < 0.01$ compared with 5xFAD-Control group, One-Way ANOVA.

Earthworm may have immune regulatory, anti-inflammatory, anti-bacterial and anti-oxidative properties, which are closely related to AD (Huang et al., 2018b). BZD therapeutic effects are likely to benefit from the synergistic effects of these compounds when administered concomitantly. However, empirical evidence supporting this hypothesis is still scarce.

In this study, BZD was separated using the UHPLC-MS system and 20 major chemical components were identified. Taurochenodeoxycholic acid, as a signaling molecule, shows obvious anti-inflammatory and immune regulation properties. Taurochenodeoxycholic acid plays a role in the PKC/JNK signaling pathway, and may be a latent effective pharmaceutical product for

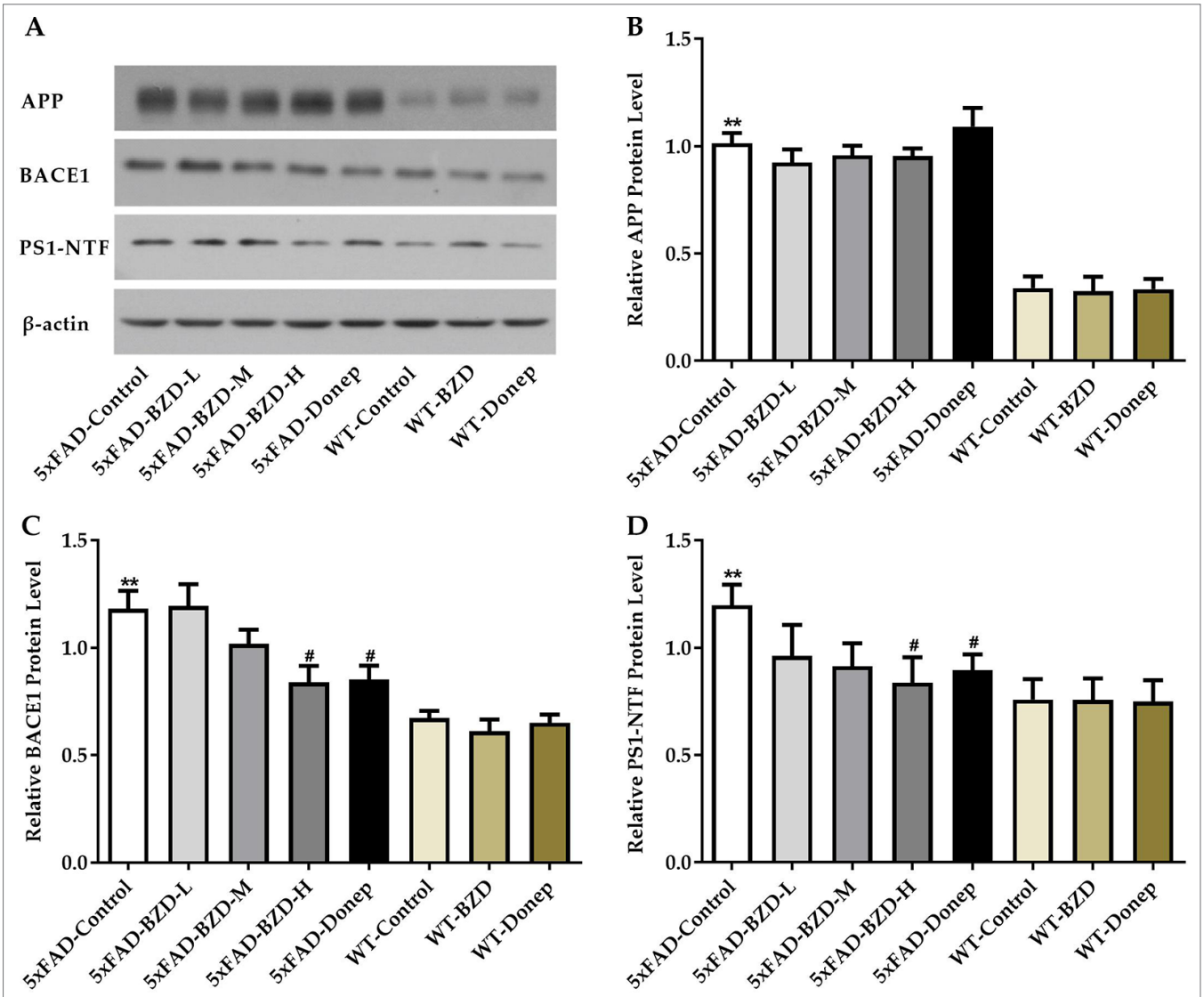

FIGURE 6 | BZD Modulates APP Processing. **(A)** Equal protein quantities of lysates from hippocampal and cortical tissues of mice (5xFAD-Control, 5xFAD-BZD-L, 5xFAD-BZD-M, 5xFAD-BZD-H, 5xFAD-Donep, WT-Control, WT-BZD and WT-Donep) were subjected to western blot with antibodies against APP, BACE1, PS1-NTF, and β-actin. APP **(B)**, BACE1 **(C)** and PS1-NTF **(D)** protein intensities were quantified by densitometry, and normalized to respective β-actin levels. Data are expressed as the mean ± SD from 6 mice per group. $^{**}P < 0.01$ compared with WT-Control group; $^{\#}P < 0.05$ compared with 5xFAD-Control group, One-Way ANOVA.

apoptosis- or age-related diseases (Wang et al., 2016). Tryptophan is converted *via* the 5-hydroxyindole pathway to serotonin, a neurotransmitter in the brain, paracrine and endocrine signal in the gut, and a paracrine signal and vasoconstrictor released by platelets. It is also converted by endocrine and other cells *via* serotonin to the hormone melatonin, which may improve mood and sleep (Fernstrom, 2016). Rubiadin-1-methyl ether may be a therapeutic candidate for bone diseases characterized by enhanced bone resorption (He et al., 2018a). Asperuloside and sweroside both can exert an anti-inflammatory effect *via* suppression of the NF-κB signaling pathways in LPS-induced RAW 264.7 cells (He et al., 2018b; Wang et al., 2019). Rubiadin, a dihydroxy anthraquinone, isolated from alcoholic extract of Rubia cordifolia, possesses potent antioxidant property (Tripathi et al., 1997). Hyodeoxycholic acid protects the neurovascular unit against oxygen-glucose deprivation and reoxygenation-induced injury *in vitro* (Li et al., 2019). 2,4,5-trimethoxybenzaldehyde, a bitter principle in plants, suppresses adipogenesis through the regulation of ERK1 (Wang and Kuo, 2014). Physcion blocks cell cycle and induces apoptosis in human B cell precursor acute lymphoblastic leukemia cells by downregulating HOXA5 (Gao et al., 2017). Morroniside protects against cerebral ischemia/reperfusion injury by inhibiting neuron apoptosis and MMP2/9 expression (Zeng et al., 2018). Loganin exerts sedative and hypnotic effects *via* modulation of the serotonergic system and GABAergic neurons (Shi et al., 2019). Cornuside attenuates apoptosis and ameliorates mitochondrial energy metabolism in rat cortical neurons (Jiang et al., 2009; Jiang et al., 2014).

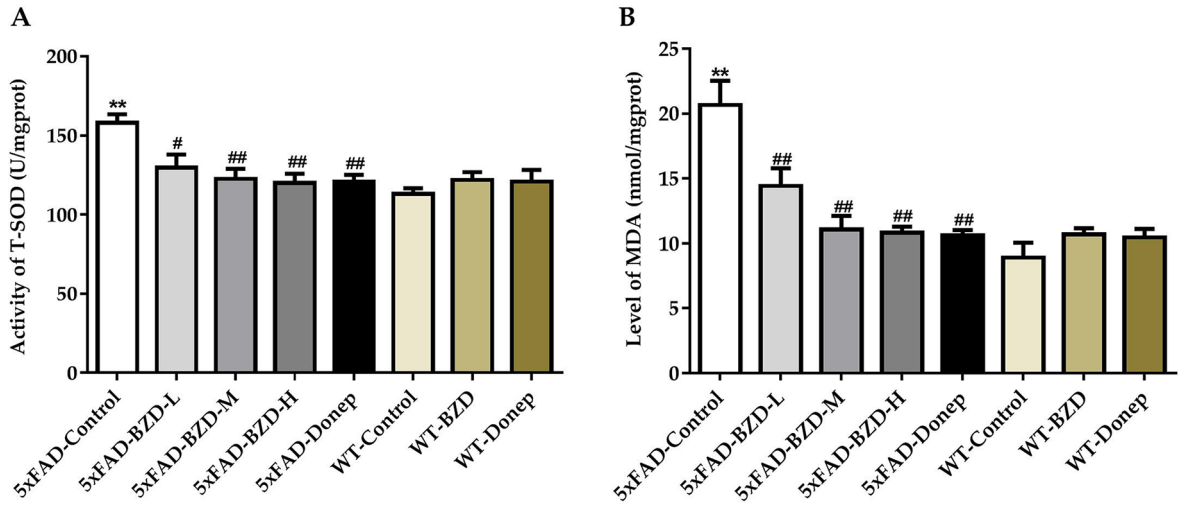

FIGURE 7 | BZD Decreases MDA Levels and SOD Activity in the Cortex and Hippocampus of 5xFAD Mice. **(A)** Activities of SOD were measured in the cortical and hippocampal tissue samples of mice (5xFAD-Control, 5xFAD-BZD-L, 5xFAD-BZD-M, 5xFAD-BZD-H, 5xFAD-Donep, WT-Control, WT-BZD and WT-Donep). Data are expressed as the mean ± SD from 6 mice per group. $^{**}P < 0.01$ compared with WT-Control group; $^{\#\#}P < 0.05$, $^{\#\#}P < 0.01$ compared with 5xFAD-Control group, One-Way ANOVA. **(B)** MDA levels were measured in the cortical and hippocampal tissue samples of mice (5xFAD-Control, 5xFAD-BZD-L, 5xFAD-BZD-M, 5xFAD-BZD-H, 5xFAD-Donep, WT-Control, WT-BZD and WT-Donep). Data are expressed as the mean ± SD from 6 mice per group. $^{**}P < 0.01$ compared with WT-Control group; $^{\#\#}P < 0.01$ compared with 5xFAD-Control group, One-Way ANOVA.

Cholic acid can be used as a treatment for cerebrotendinous xanthomatosis in adults (Mandia et al., 2019). 5-hydroxymethyl-2-furaldehyde (5-HMF) may block scopolamine-induced learning deficit and enhance cognitive function *via* the activation of NMDA receptor signaling, including CaMKII and ERK, and would be an effective candidate against cognitive disorders, such as Alzheimer's disease (Lee et al., 2015). Leucine-rich repeat kinase 2 is associated with activation of the paraventricular nucleus of the hypothalamus and stress-related gastrointestinal dysmotility (Maekawa et al., 2019). All of these chemical components have anti-aging, anti-inflammatory, anti-oxidative, immune-regulatory, anti-tumor, and neuroregulatory properties, among others.

AD is characterized by memory loss and cognitive impairment, and various neuropsychiatric symptoms including depression, anxiety, hallucination, irritability, indifference and disinhibition (Geda et al., 2013). Here the potential effects of BZD on locomotor activity and anxiety were assessed by the open field and elevated plus maze tests; while the effect of BZD on learning and memory was assessed using the Y and Morris water maze tests. The open field test reflects locomotor activity, spontaneous exploration, and anxiety levels of mice in a novel environment (typically, the greater is the time spent in the central arena, the less is the anxiety; greater distances traveled are associated with greater locomotor activity) (Heredia et al., 2014). In this cohort, 6-month-old 5xFAD mice and the wild-type littermates did not differ with respect to general locomotor activity. BZD had no effect on the locomotor activity of 5xFAD mice.

To further assess the effects o on anxiety levels, we used the elevated plus maze. Since mice have an innate fear of elevated open places, when allowed to freely explore the maze, they typically enter less and spend shorter time in the open arms as compared to the closed arms of the maze (Walf and Frye, 2007). Therefore, a greater number of entries and time spent in the open arms indicate low anxiety levels and behavioral disinhibition (Walf and Frye, 2007). Moreover, 6-month-old 5xFAD mice presented with lower anxiety in dangerous environments, indicating a tendency toward disinhibition. This result concurs with that of previous reports suggesting that approximately 35% of mild AD patient's exhibit disinhibition, which manifests as impulsive behavior, talking to strangers like acquaintances, ignoring dangers, and excessive euphoria (Olausson et al., 1999; Starkstein et al., 2004). Importantly, medium and high doses of BZD attenuated this behavioral alteration by increasing vigilance and attenuating behavioral disinhibition in the 5xFAD mice.

The Y maze is typically used to assess spontaneous spatial working memory in rodents (Ohno et al., 2004) by analyzing the percentage of alternation triplet (the higher the percentage of alternation triplets, the better the spontaneous spatial working memory). In our study, 5xFAD mice exhibited impaired spontaneous spatial working memory. We found that medium and high doses of BZD improved memory impairments in 5xFAD mice, as shown by an increase in the percentage of alternation triplets. The Morris water maze is one of the classic behavioral tests for spatial learning and memory capacity in rodents (Barnhart et al., 2015). The escape latency time acquired after spatial navigation training reflects the learning capacity. A short ELT indicates strong learning capacity; conversely, a long ELT indicates poor learning capacity. As anticipated, 5xFAD mice showed marked impairment in spatial learning and

memory. However, medium and high doses of BZD significantly ameliorated this deficit.

One of the most critical pathological features of AD is accumulation of Aβ, which is derived from APP through sequential cleavage by β-secretase and γ-secretase (Jiang et al., 2014). Here we showed that Aβ plaques were significantly reduced in the cortex and hippocampus of 5xFAD mice when treated with medium- and high-dose BZD, as well as donepezil HCl. Further, we showed that high-dose BZD decreased BACE1 and PS1 protein levels in 5xFAD mice, indicating that reduction of Aβ may be due to altered APP processing.

Increased activity of SOD typically indicates enhanced protection against oxidative stress and damage. However, at early stages of the inflammatory reaction (compensation stage), SOD activity is known to increase owing to the overproduction of free radicals. As anticipated, we found increased levels of MDA and higher SOD activity in the 5xFAD mice, suggesting that although these animals may suffer from damage caused by oxidative stress, they are likely to remain in the compensatory period. Interestingly, medium and high doses of BZD attenuated both MDA levels and SOD activity, suggesting beneficial effects on hippocampal oxidative stress.

Our results show the potential preventive effects of BZD during an early stage of AD (6-month-old 5xFAD mice), which may not be generalized to include later stages of the disease, where the pathology is already fully established and is more severe. Further studies evaluating the extent of benefits of BZD in more advanced stages of the disease are warranted, to fully unravel its therapeutic potential in AD. In addition, future studies are required to directly compare different therapeutic schemes that vary in the timing of administration, and to determine the best time-window for BZD administration. This knowledge may aid in designing future clinical studies to evaluate whether BZD is a viable treatment option in AD.

DATA AVAILABILITY STATEMENT

The data used to support the findings of this study are available from the corresponding authors upon request.

ETHICS STATEMENT

All animal procedures were approved by the Laboratory Animal Management and Ethics Committee of Xiamen University, and the Animal Ethics Committee Guidelines of the Animal Facility of the Zhongshan Hospital Xiamen University.

AUTHOR CONTRIBUTIONS

YH and XZha conceived and designed the experiments, AP, XZhu, YG, YL, WH, SX, YW, WC, XH, TC, and RY performed the experiments, AP and YG analyzed the data, AP and XZhu prepared the manuscript, and SX wrote the contents and constructed the figures involved UHPLC-MS, and critically revised this manuscript as well as XZha. All authors have read and approved the manuscript.

ACKNOWLEDGMENTS

The authors would like to thank Dr. Robert Vassar from Northwestern University for providing the BACE1 antibody for this study, thank Dr. Jie Zhang from Institute of Neuroscience of Xiamen University for providing expertise on the animal experiments, and thank Dr. Yingkun Qiu from School of Pharmaceutical Sciences of Xiamen University for his attentive guidance in the experiment of UHPLC-MS. The authors would also like to acknowledge the support from the National Natural Science Foundation of China (No. 81674041), the Foundation of Science and Technology Department of Xiamen (No.3502Z20164013), and the Natural Science Foundation of Fujian Province (No. 2018J01395) for this study.

SUPPLEMENTARY MATERIAL

The Supplementary Material for this article can be found online at: https://www.frontiersin.org/articles/10.3389/fphar.2019.01391/full#supplementary-material

REFERENCES

Ahn, C. B., Shin, T. S., Seo, H. K., and Je, J. Y. (2012). Phenolic composition and antioxidant effect of aqueous extract of arisaema cum bile, the oriental herb medicine, in human fibroblast cells. *Immunopharmacol. Immunotoxicol.* 34, 661–666. doi: 10.3109/08923973.2011.649289

Alzheimer, A., Stelzmann, R. A., Schnitzlein, H. N., and Murtagh, F. R. (1995). An English translation of Alzheimer's 1907 paper, uber eine eigenartige erkankung der hirnrinde. *Clin. Anat.* 8, 429–431. doi: 10.1002/ca.980080612

Barnhart, C. D., Yang, D., and Lein, P. J. (2015). Using the morris water maze to assess spatial learning and memory in weanling mice. *PloS One* 10, e0124521. doi: 10.1371/journal.pone.0124521

Batinic-Haberle, I., Tovmasyan, A., Roberts, E. R., Vujaskovic, Z., Leong, K. W., and Spasojevic, I. (2014). SOD therapeutics: latest insights into their structure-activity relationships and impact on the cellular redox-based signaling pathways. *Antioxid. Redox Sign.* 20, 2372–2415. doi: 10.1089/ars.2012.5147

Cao, J., Hou, J., Ping, J., and Cai, D. (2018). Advances in developing novel therapeutic strategies for Alzheimer's disease. *Mol. Neurodegener.* 13, 64. doi: 10.1186/s13024-018-0299-8

Checler., F. (1995). Processing of the β-amyloid precursor protein and its regulation in Alzheimer's disease. *J. Neurochem.* 65, 1431–1444. doi: 10.1046/j.1471-4159.1995.65041431.x

Deng, M. Z., Huang, L. P., and Fang, Y. Q. (2015). Effects of total Ginsenosides and Volatile oil of Acorus tatarinowii co-administration on ability of learning and memory and apoptosis in Alzheimer's disease mice model induced by d-galactose and aluminium chloride. *J. Chin. Med. Mater.* 8, 1018–1023.

Fernstrom, J. D. (2016). A Perspective on the safety of supplemental tryptophan based on its metabolic fates. *J. Nutr.* 146, 2601S–2608S. doi: 10.3945/jn.115.228643

Gao, F., Liu, W., Guo, Q., Bai, Y., Yang, H., and Chen, H. (2017). Physcion blocks cell cycle and induces apoptosis in human B cell precursor acute lymphoblastic leukemia cells by downregulating HOXA5. *Biomed. Pharmacother.* 94, 850–857. doi: 10.1016/j.biopha.2017.07.149

Geda, Y. E., Schneider, L. S., Gitlin, L. N., Miller, D. S., Smith, G. S., and Bell, J. (2013). Neuropsychiatric symptoms in Alzheimer's disease: past progress and anticipation of the future. *Alzheimers Dement.* 9, 602–608. doi: 10.1016/j.jalz.2012.12.001

Giera, M., Lingeman, H., and Niessen, W. M. (2012). Recent advancements in the LC- and GC-based analysis of malondialdehyde (MDA): a brief overview. *Chromatographia* 75, 433–440. doi: 10.1007/s10337-012-2237-1

Hardy, J., and Allsop, D. (1991). Amyloid deposition as the central event in the aetiology of Alzheimer's disease. *Trends Pharmacol. Sci.* 12, 383–388. doi: 10.1016/0165-6147(91)90609-V

Hardy, J. A., and Higgins, G. A. (1992). Alzheimer's disease: the amyloid cascade hypothesis. *Science* 256, 184–185. doi: 10.1126/science.1566067

He, Y. Q., Zhang, Q., Shen, Y., Han, T., Zhang, Q. L., and Zhang, J. H. (2018a). Rubiadin-1-methyl ether from Morinda officinalis How. inhibits osteoclastogenesis through blocking RANKL-induced NF-κB pathway. *Biochem. Biophys. Res. Commun.* 506, 927–931. doi: 10.1016/j.bbrc.2018.10.100

He, J., Lu, X., Wei, T., Dong, Y., Cai, Z., and Tang, L. (2018b). Asperuloside and asperulosidic acid exert an anti-inflammatory effect via suppression of the NF-κB and MAPK signaling pathways in LPS-induced RAW 264.7 macrophages. *Int. J. Mol. Sci.* 19 (7), E2027. doi: 10.3390/ijms19072027

Heredia, L., Torrente, M., Colomina, M. T., and Domingo, J. L. (2014). Assessing anxiety in C57BL/6J mice: a pharmacological characterization of the open-field and light/dark tests. *J. Pharmacol. Toxicol. Methods* 69, 108–114. doi: 10.1016/j.vascn.2013.12.005

Hu, H. Y., Cui, Z. H., Li, H. Q., Wang, Y. R., Chen, X., and Li, J. H. (2014). Fumanjian, a classic Chinese herbal formula, can ameliorate the impairment of spatial learning and memory through apoptotic signaling pathway in the hippocampus of rats with Aβ 1-40 -induced Alzheimer's disease. *Evid-Based Compl. Alt. Med.* 2014, 942917. doi: 10.1155/2014/942917

Hu, J., Liu, C. C., Chen, X. F., Zhang, Y. W., Xu, H., and Bu, G. (2015). Opposing effects of viral mediated brain expression of apolipoprotein E2 (apoE2) and apoE4 on apoE lipidation and Aβ metabolism in apoE4-targeted replacement mice. *Mol. Neurodegener.* 10, 1–11. doi: 10.1186/s13024-015-0001-3

Huang, J., Zhang, Y. W., Dong, L., Gao, Q. H., Yin, L., and Quan, H. F. (2018a). Ethnopharmacology, phytochemistry, and pharmacology of Cornus officinalis Sieb. et Zucc. *J. Ethnopharmacol.* 213, 280–301. doi: 10.1016/j.jep.2017.11.010

Huang, J. W., Gao, H. W., and Duan, J. F. (2018b). Research on chemical composition and pharmacological effects of geosaurus. *Guiding J. Tradit. Chin. Med. Pharm.* 24, 104–107. doi: 10.13862/j.cnki.cn43-1446/r.2018.12.034

Jesky, R., and Hailong., C. (2011). Are herbal compounds the next frontier for alleviating learning and memory impairments? An integrative look at memory, dementia and the promising therapeutics of traditional Chinese medicines. *Phytother. Res.* 25, 1105–1118. doi: 10.1002/ptr.3388

Jiang, W. L., Chen, X. G., Zhu, H. B., Hou, J., and Tian, J. W. (2009). Cornuside attenuates apoptosis and ameliorates mitochondrial energy metabolism in rat cortical neurons. *Pharmacology* 84 (3), 162–170. doi: 10.1159/000235621

Jiang, S., Li, Y., Zhang, X., Bu, G., Xu, H., and Zhang, Y. W. (2014). Trafficking regulation of proteins in Alzheimer's disease. *Mol. Neurodegener.* 9, 6. doi: 10.1186/1750-1326-9-6

Jin, H., Ou, Q., and Wang, D. D. (2009). Effects of dogwood polysaccharides on the learning and memory capabilities in aging model rats. *Chin. J. Gerontol.* 29, 1467–1469. doi: 10.3969/j.issn.1005-9202.2009.12.005

Lee, Y., Gao, Q., Kim, E., Lee, Y., Park, S. J., and Lee, H. E. (2015). Pretreatment with 5-hydroxymethyl-2-furaldehyde blocks scopolamine-induced learning deficit in contextual and spatial memory in male mice. *Pharmacol. Biochem. Behav.* 134, 57–64. doi: 10.1016/j.pbb.2015.04.007

Lee, Y. K., Bang, H. J., Oh, J. B., and Whang, W. K. (2017). Bioassay-Guided isolated compounds from Morinda officinalis inhibit Alzheimer's disease pathologies. *Molecules* 22, 1638. doi: 10.3390/molecules22101638

Li, C., Zhao, R., Gao, K., Wei, Z., Yin, M. Y., and Lau, L. T. (2011). Astrocytes: implications for neuroinflammatory pathogenesis of Alzheimer's disease. *Curr. Alzheimer Res.* 8, 67–80. doi: 10.2174/156720511794604543

Li, J., Nie, J., and Zhang, M. (2013). Intervention activity of curcuma against rats with Alzheimer disease and its mechanisms. *J. Med. Res.* 42, 173–176. doi: 10.3969/j.issn.1673-548X.2013.06.049

Li, L. Q., Peng, A. X., Zhang, X., Chen, T. T., and Huang, Y. P. (2016). The clinical therapy of Bazhu Decoction in 36 patients of AD with kidney deficient encephala reduce pattern. *China J. Fujian J. T.C.M.* 47,, 14– 16. doi: 10.13260/j.cnki.jfjtcm.011057

Li, C. X., Wang, X. Q., Cheng, F. F., Yan, X., Luo, J., and Wang, Q. G. (2019). Hyodeoxycholic acid protects the neurovascular unit against oxygen-glucose deprivation and reoxygenation-induced injury *in vitro*. *Neural. Regen. Res.* 14 (11), 1941–1949. doi: 10.4103/1673-5374.259617

Limon, I. D., Mendieta, L., Diaz, A., Chamorro, G., Espinosa, B., and Zenteno, E. (2009). Neuroprotective effect of alpha-asarone on spatial memory and nitric oxide levels in rats injected with amyloid-beta (25-35). *Neurosci. Lett.* 453, 98–103. doi: 10.1016/j.neulet.2009.02.011

Liu, C. C., Tsai, C. W., Deak, F., Rogers, J., Penuliar, M., and Sung, Y. M. (2014). Deficiency in LRP6-mediated Wnt signaling contributes to synaptic abnormalities and amyloid pathology in Alzheimer's disease. *Neuron* 84, 63–77. doi: 10.1016/j.neuron.2014.08.048

Lu, L., Mak, Y. T., Fang, M., and Yew, D. T. (2009). The difference in gliosis induced by β-amyloid and Tau treatments in astrocyte cultures derived from senescence accelerated and normal mouse strains. *Biogerontology* 10, 695–710. doi: 10.1007/s10522-009-9217-3

Maekawa, T., Tsushima, H., Kawakami, F., Kawashima, R., Kodo, M., and Imai, M. (2019). Leucine-rich repeat kinase 2 is associated with activation of the paraventricular nucleus of the hypothalamus and stress-related gastrointestinal dysmotility. *Front. Neurosci.* 13, 905. doi: 10.3389/fnins.2019.00905

Mandia, D., Chaussenot, A., Besson, G., Lamari, F., Castelnovo, G., and Curot, J. (2019). Cholic acid as a treatment for cerebrotendinous xanthomatosis in adults. *J. Neurol.* 266 (8), 2043–2050. doi: 10.1007/s00415-019-09377-y.

Mattson, M. P. (2004). Pathways towards and away from Alzheimer's disease. *Nature* 430, 631–639. doi: 10.1038/nature02621

May, B. H., Feng, M., Zhou, I. W., Chang, S. Y., Lu, S. C., and Zhang, A. L. (2016). Memory impairment, dementia, and Alzheimer's disease in classical and contemporary traditional Chinese medicine. *J. Alt. Compl. Med.* 22, 695–705. doi: 10.1089/acm.2016.0070

Oakley, H., Cole, S. L., Logan, S., Maus, E., Shao, P., and Craft, J. (2006). Intraneuronal beta-amyloid aggregates, neurodegeneration, and neuron loss in transgenic mice with five familial Alzheimer's disease mutations: potential factors in amyloid plaque formation. *J. Neurosci.* 26, 10129–10140. doi: 10.1523/JNEUROSCI.1202-06.2006

Ohno, M., Sametsky, E. A., Younkin, L. H., Oakley, H., Younkin, S. G., and Citron, M. (2004). BACE1 deficiency rescues memory deficits and cholinergic dysfunction in a mouse model of Alzheimer's disease. *Neuron* 41, 27–33. doi: 10.1016/S0896-6273(03)00810-9

Olausson, P., Engel, J. A., and Soderpalm, B. (1999). Behavioral sensitization to nicotine is associated with behavioral disinhibition; counteraction by citalopram. *Psychopharmacology* 142, 111–119. doi: 10.1007/s002130050869

Peng, A. X., and Huang, Y. P. (2017). Thought of Bazhu Mixture treating on Alzheimer's disease. *China J. Tradit. Chin. Med. Pharm.* 32, 5442–5445.

Patterson, C. (2018). World Alzheimer Report 2018—The State of the Art of Dementia Research: New Frontiers. London: Alzheimer's Disease International (ADI). Available online at: https://www.alz.co.uk/research/WorldAlzheimerReport2018.pdf

Shi, R., Han, Y., Yan, Y., Qiao, H. Y., He, J., and Lian, W. W. (2019). Loganin exerts sedative and hypnotic effects via modulation of the serotonergic system and GABAergic neurons. *Front. Pharmacol.* 10, 409. doi: 10.3389/fphar.2019.00409

Song, Z. Y., Yin, F., Xiang, B., Lan, B., and Cheng, S. W. (2018). Systems pharmacological approach to investigate the mechanism of Acori Tatarinowii Rhizoma for Alzheimer's disease. *Evid-Based Compl. Alt. Med.* 2018, 5194016. doi: 10.1155/2018/5194016

Starkstein, S. E., Garau, M. L., and Cao, A. (2004). Prevalence and clinical correlates of disinhibition in dementia. *Cogn. Behav. Neurol.* 17, 139–147. doi: 10.1097/01.wnn.0000119241.65522.90

Stokin, G. B., Lillo, C., Falzone, T. L., Brusch, R. G., Rockenstein, E., and Mount, S. L. (2005). Axonopathy and transport deficits early in the pathogenesis of Alzheimer's disease. *Science* 307, 1282–1288. doi: 10.1126/science.1105681

Thinakaran, G., Borchelt, D. R., Lee, M. K., Slunt, H. H., Spitzer, L., and Kim, G. (1996). Endoproteolysis of presenilin 1 and accumulation of processed derivatives *in vivo*. *Neuron* 17, 181–190. doi: 10.1016/s0896-6273(00)80291-3

Tripathi, Y. B., Sharma, M., and Manickam, M. (1997). Rubiadin, a new antioxidant from Rubia cordifolia. *Indian J. Biochem. Biophys.* 34 (3), 302–306. doi: 10.1016/S1367-5931(97)80119-6

Vorhees, C. V., and Williams, M. T. (2006). Morris water maze: procedures for assessing spatial and related forms of learning and memory. *Nat. Protoc.* 1, 848–858. doi: 10.1038/nprot.2006.116

Walf, A. A., and Frye, C. A. (2007). The use of the elevated plus maze as an assay of anxiety-related behavior in rodents. *Nat. Protoc.* 2, 322–328. doi: 10.1038/nprot.2007.44

Wang, Y. W., and Kuo, C. F. (2014). 2,4,5-trimethoxybenzaldehyde, a bitter principle in plants, suppresses adipogenesis through the regulation of ERK1. *J. Agric. Food Chem.* 62 (40), 9860–9867. doi: 10.1021/jf503344v

Wang, X., Li, J., Liao, Y. L., and Deng, C. L. (2013). Study on protective effect of water extract from Morindae officinalis on Alzheimer disease model rats. *China Pharm.* 24, 2908–2910.

Wang, Q., Xiao, B., Cui, S. Q., Song, H. L., Qian, Y. J., and Dong, L. (2014). Wang, Triptolide treatment reduces Alzheimer's disease (AD)-like pathology through inhibition of BACE1 in a transgenic mouse model of AD. *Dis. Model. Mech.* 7, 1385–1395. doi: 10.1242/dmm.018218

Wang, X., Zhang, Z. Y., He, X. L., Mao, W., Zhou, L., and Li, P. F. (2016). Taurochenodeoxycholic acid induces NR8383 cells apoptosis *via* PKC/JNK-dependent pathway. *Eur. J. Pharmacol.* 786, 109–115. doi: 10.1016/j.ejphar.2016.06.007

Wang, R., Dong, Z., Lan, X., Liao, Z., and Chen, M. (2019). Sweroside alleviated LPS-induced inflammation via SIRT1 mediating NF-κB and FOXO1 signaling pathways in RAW264.7 cells. *Molecules* 24 (5), 872. doi: 10.3390/molecules24050872

Wen, Z. J., and Chen, H. W. (2009). The election for the effective fractions extracted from Acorus Gramineus on restoring consciousness and inducing resuscitation of model mice. *Chin. Arch. Tradit. Chin. Med.* 27, 2203–2205. doi: 10.3969/j.issn.1008-0805.2002.05.002

Xing, S. L., Shen, D. Z., Chen, C., Wu, B. L., and Chi., H. Y. (2017). Effect of the herbal formulation Shen-Zhi-Ling on an APP/PS1 mouse model of Alzheimer's disease by modulating the biliverdin reductase/heme oxygenase 1 system. *Exp. Ther. Med.* 14, 1961–1966. doi: 10.3892/etm.2017.4732

Xu, H., Sweeney, D., Wang, R., Thinakaran, G., Lo, A. C., and Sisodia, S. S. (1997). Generation of Alzheimer beta-amyloid protein in the trans-Golgi network in the apparent absence of vesicle formation. *Proc. Natl. Acad. Sci. U. S. A.* 94, 3748–3752. doi: 10.1073/pnas.94.8.3748

Yang, X., Chen, D. L., Yang, J., Liu, T., Hu, G. Y., and Liang, H. L. (2018). Effects of oligosaccharides from Morinda officinalis on gut microbiota and metabolome of APP/PS1 transgenic mice. *Front. Neurol.* 15, 412. doi: 10.3389/fneur.2018.00412

Zeng, G., Ding, W., Li, Y., Sun, M., and Deng, L. (2018). Morroniside protects against cerebral ischemia/reperfusion injury by inhibiting neuron apoptosis and MMP2/9 expression. *Exp. Ther. Med.* 16 (3), 2229–2234. doi: 10.3892/etm.2018.6457

Zhang, X., Li, Y., Xu, H., and Zhang, Y. W. (2014). The γ-secretase complex: from structure to function. *Front. Cell. Neurosci.* 8, 427. doi: 10.3389/fncel.2014.00427

Zhang, J. H., Xin, H. L., Xu, Y. M., Shen, Y., He, Y. Q., and Hsien-Yeh (2018). Morinda officinalis How. -A comprehensive review of traditional uses, phytochemistry and pharmacology. *J. Ethnopharmacol.* 213, 230–255. doi: 10.1016/j.jep.2017.10.028

Zhou, W. W., Lu, S., Su, Y. J., Xue, D., Yu, X. L., and Wang, S. W. (2014). Decreasing oxidative stress and neuroinflammation with a multifunctional peptide rescues memory deficits in mice with Alzheimer disease. *Free Rad. Bio. Med.* 74, 67–80. doi: 10.1016/j.freeradbiomed.2014.06.013

Zhu, W.M. and Hu, H.Y. (2007). A survey of TCM treatment for Alzheimer's disease. *J. Tradit. Chin. Med.* 27, 226–232.

Conflict of Interest: The authors declare that the research was conducted in the absence of any commercial or financial relationships that could be construed as a potential conflict of interest.

frontiers in Pharmacology

ORIGINAL RESEARCH
published: 06 December 2019
doi: 10.3389/fphar.2019.01474

Integrated UPLC-Q/TOF-MS Technique and MALDI-MS to Study of the Efficacy of YiXinshu Capsules Against Heart Failure in a Rat Model

Jing Xu[1†], Xianyu Li[2†], Fangbo Zhang[1†], Liying Tang[1], Junying Wei[1], Xiaoqing Lei[3], Huanhuan Wang[1], Yi Zhang[1], Defeng Li[1], Xuan Tang[1], Geng Li[3], Shihuan Tang[1]*, Hongwei Wu[1]* and Hongjun Yang[1]*

[1] Institute of Chinese Materia Medica, China Academy of Chinese Medical Sciences, Beijing, China, [2] Experimental Research Centre, China Academy of Chinese Medical Sciences, Beijing, China, [3] Cardiovascular Center, China-Japan Friendship Hospital, Beijing, China

OPEN ACCESS

Edited by:
Yue Liu,
Xiyuan Hospital, China

Reviewed by:
Yong Wang,
Beijing University of Chinese Medicine, China
Victoria Samanidou,
Aristotle University of Thessaloniki, Greece

***Correspondence:**
Hongwei Wu
whw9905012@163.com
Geng Li
13810507641@163.com
Shihuan Tang
shtang@icmm.ac.cn

[†]These authors have contributed equally to this work

Specialty section:
This article was submitted to Ethnopharmacology, a section of the journal Frontiers in Pharmacology

Received: *12 August 2019*
Accepted: *13 November 2019*
Published: *06 December 2019*

Citation:
Xu J, Li X, Zhang F, Tang L, Wei J, Lei X, Wang H, Zhang Y, Li D, Tang X, Li G, Tang S, Wu H and Yang H (2019) Integrated UPLC-Q/TOF-MS Technique and MALDI-MS to Study of the Efficacy of YiXinshu Capsules Against Heart Failure in a Rat Model. Front. Pharmacol. 10:1474. doi: 10.3389/fphar.2019.01474

Background: Yixinshu Capsules (YXSC) are widely used in Chinese medicine for the treatment of cardiovascular diseases. However, the therapeutic mechanisms of action are not well understood.

Method: In this study, a metabonomic approach based on integrated UPLC-Q/TOF-MS technique and MALDI-MS was utilized to explore potential metabolic biomarkers that may help increase the understanding of heart failure (HF) and in order to assess the potential mechanisms of YXSC against HF. Plasma metabolic profiles were analyzed by UPLC-Q/TOF-MS with complementary hydrophilic interaction chromatography and reversed-phase liquid chromatography. Moreover, time-course analysis at the 2nd, 4th, and 10th week after permanent occlusion was conducted. In an effort to identify a more reliable potential metabolic marker, common metabolic markers of the 2nd, 4th, and 10th week were selected through multivariate data analysis. Furthermore, MALDI-MS was applied to identify metabolic biomarkers in the blood at apoptotic positions of heart tissues.

Results: The results showed that HF appeared at the fourth week after permanent occlusion based on echocardiographic assessment. Clear separations were observed between the sham and model group by loading plots of orthogonal projection to latent structure discrimination analysis (OPLS-DA) at different time points after permanent occlusion. Potential markers of interest were extracted from the combining S-plots, variable importance for the projections values (VIP > 1), and t-test ($p < 0.05$). Twenty-one common metabolic markers over the course of the development and progression of HF after permanent occlusion were identified. These were determined to be mainly related to disturbances in fatty acids, phosphatidylcholine, bile acids, amino acid metabolism, and pyruvate metabolism. Of the metabolic markers, 16 metabolites such as palmitoleic acid, arachidonic acid, and lactic acid showed obvious changes ($p < 0.05$) and a tendency for returning to baseline values in YXSC-treated HF rats at the 10th week. Moreover, four biomarkers, including palmitoleic acid, palmitic acid, arachidonic, acid and lactic acid, were further validated at the apoptotic position of heart tissue using MALDI-MS, consistent to the variation trends in the plasma.

Conclusions: Taken in concert, our proposed strategy may contribute to the understanding of the complex pathogenesis of ischemia-induced HF and the potential mechanism of YXSC.

Keywords: heart failure, YiXinShu capsules, UPLC-Q/TOF-MS, MALDI-MS, metabonomic studies

INTRODUCTION

Heart failure (HF), a common clinical syndrome, is commonly associated with high morbidity and, if survived, may result in lifelong and often devastating health conditions (Doenst et al., 2013; Jackson et al., 2015; Ponikowski et al., 2016). As the end stage of various heart diseases, HF manifestation is characterized with architectural changes or functional disorders, including changes in electrophysiology, inflammatory responses, oxidative stress, energy metabolism, etc. (Doenst et al., 2013; Tanai and Frantz, 2015). Even though modern state-of-the art treatment options may be used to improve clinical symptoms and slow the progression of contractile dysfunction (Ohn and Ognoni, 2001; Pfeffer, 2003; Savarese et al., 2013), no significant breakthroughs have been made to improve the overall outcome of HF patients, indicating that HF prognosis and treatment remain poorly controlled (Guo et al., 2014; Yang et al., 2015).

Traditional Chinese medicine (TCM) has long been practiced using multiple components to treat as well as prevent various complex and refractory disease states. Yixinshu Capsule (YXSC), recorded in the Chinese Pharmacopoeia (Chinese Pharmacopoeia Commission, 2015), has been used for the treatment of HF in order to improve clinical symptoms such as chest pain, palpitation, shortness of breath, and cyanosis (Carubelli et al., 2015; Sun et al., 2017). YXSC, derived from a classic TCM prescription named Sheng-Mai-San, contains seven Chinese herbal medicines including *Salvia miltiorrhiza* Bunge, radix and rhizome; *Panax ginseng* C.A.Mey., radix and rhizome; *Ophiopogon japonicus (*Thunb.) Ker Gawl, radix; *Crataegus pinnatifida* Bunge, fructus; *Astragalus membranaceus* (Fisch.) Bunge, radix.; *Ligusticum chuanxiong* S.H.Qiu, Y.Q.Zeng, K.Y.Pan, Y.C.Tang & J.M.Xu, rhizome; *Schisandra chinensis* (Turcz.) Baill., fructus. The ratios of the above botanical materials in the preparation were 2:1.5:1.5:1.5:1.5:1:1. In our previous studies, a total of 276 components in the YXSC were identified mainly including ginsenosides, astragalus saponins, lignans, phenolic acids, and tanshinones (Wang et al., 2015). The quality control and evaluation of YXSC in this study can be seen in the **Supplementary Materials**. Moreover, previously conducted studies have shown that YXSC, as a standardized product, has been able to reduce mitochondrial-mediated apoptosis (Zhao et al., 2016), oxidative stress injury (Zhang et al., 2017), and myocardial dysfunction (Zhang et al., 2017). Even though numerous clinical trials have shown that YXSC exhibits a protective function against HF, the mechanism of YXSC used as a treatment option for HF remains unclear.

HF as a metabolic syndrome has been shown to be accompanied by metabolic derangements such as systemic and myocardial insulin resistance, mitochondrial dysfunction, and myocardial energetic failure associated with biosynthesis and metabolism of ATP, glycolysis, TCA cycle, and related metabolic pathways (Stanley et al., 2005). There is growing evidence to support the concept that alterations in substrate metabolism of HF significantly contribute to contractile dysfunction and the progression of LV remodeling (Birkenfeld et al., 2018). Therefore, metabolomics offers a suitable way to understand disease pathogenesis and the mechanisms of YXSC from the standpoint of a metabolic evaluation. Furthermore, some specific molecular targets (e.g., fatty acid–binding protein 3 and cytoskeleton-associated protein 5), regulated by YXSC against HF, were identified by proteomic analysis in a study reported by us previously (Wei et al., 2019). However, the metabolic phenotype of HF as well as the metabolic regulation of YXSC against HF remains incomplete and therefore unclear.

In this study, an untargeted metabolic profile approach based on UPLC-Q/TOF-MS with complementary hydrophilic interaction chromatography (HILIC) as well as reversed-phase liquid chromatography was used to investigate the metabolic changes of plasma in rats subjected to ischemia-induced HF. In an effort to identify more reliable potential metabolic biomarkers, common metabolic markers of different time points after myocardial infarction (MI) were selected through multivariate data analysis. These potential metabolic markers related to the perturbed metabolic pathways in HF rats were identified in order to develop an improved understanding of HF pathogenesis as well as the underlying mechanisms of YXSC. Moreover, MALDI-MS was further applied to track the identified metabolic biomarkers in the blood at the apoptotic position of the heart tissue. Compared with conventional analytical techniques, MALDI-MSI has the ability of *in situ* localization of a wide range of biomolecules in a simultaneous fashion from a tissue specimen in one single run. As a consequence, MALDI-MSI has become one of the most powerful techniques in the field of biomedical research and exhibits further applicability in disease diagnosis and prognosis, biomarker discovery, and drug development (Wang et al., 2015). Hopefully, this study will provide a useful approach for exploring the mechanism of ischemia-induced HF and evaluating the efficacy of YXSC in regards to the study of metabolites associated with HF.

MATERIALS AND METHODS

Animals, Chemicals, and Reagents

A total of 28 adult male Sprague-Dawley rats (body weight: 260–270 g) were provided by the Animal Breeding Centre of Beijing Vital River Laboratories Company (Beijing, China). All

experimental animal procedures were approved by the Academy of Chinese Medical Science's Administrative Panel on Laboratory Animal Care and performed in accordance with institutional guidelines and ethics of the committee as part of the China Academy of Chinese Medical Sciences (February 1st, 2016).

YXSC was obtained from Guizhou Xinbang Pharmaceutical Co., Ltd (Guizhou, China); Valsartan was purchased from HaiNan Aumei Pharmaceutical Co., Ltd (Hainan, China). All organic solvents used throughout the studies were of HPLC-grade and were purchased from Fisher Scientific (Shanghai, China). All other chemicals used were of analytical grade and purchased from Sigma-Aldrich (Shanghai, China) unless stated otherwise.

Animal Models, Drugs Treatment, and Echocardiography

Male Sprague-Dawley rats were kept inside an animal room at a temperature of 22 ± 2°C and a relative humidity of 50 ± 10%, with a 12 h light/12 h dark cycle. All animals were acclimatized for 1 week prior to surgery. The animals had free access to water and fodder (Beijing Keaoxieli Co, Ltd.). A total of 28 rats were randomly divided into sham rats (n = 8) and rats with MI (n = 20). According to previously published methods, ischemia-induced HF was performed by ligation of the left anterior descending coronary artery near its origin from the left coronary artery (Huang et al., 2006; Turer, 2013). Rats in the sham group were subjected to a similar procedure except for the left coronary artery ligation. At the fourth week after permanent occlusion, HF appeared based on the value of ejection fraction (EF). Then, rats with MI were randomly divided into two groups of model group and YXSC group. Meanwhile, the YXSC group was orally administered YXSC (0.32 g· kg^{-1}· day^{-1}) equivalent to clinical doses for six consecutive weeks. Before occlusion and at the 4th and 10th week after occlusion, 2-D echocardiography (Visual Sonics, Canada) was employed to measure echocardiographic parameters; the left ventricular end-diastolic volume (LVEDV) and left ventricular end-systolic volume (LVESV) were calculated. Then, the values of EF of the LV were calculated from the LV dimensions as follows: EF (%) = (LVEDV - LVESV)/LVEDV × 100% (Zhang et al., 2014). Of the 20 rats with MI, 4 rats with MI died after surgery. Moreover, one rat in model group died at the 4th week and one rat died in sham group at the 10th week after occlusion.

Sample Collection and Preparation

Preparation of plasma samples. In order to investigate the metabolic changes during the period from occlusion to HF, blood plasma samples were collected from the ophthalmic vein at the 2nd, 4th, and 10th week after occlusion. After centrifugation at 3,500 rpm for 10 min at 4 °C, the plasma was collected and stored at – 80 °C prior to metabonomic profiling analysis. Before UPLC-Q/TOF–MS analysis, 100 µl plasma was mixed with 300 µl of cold acetonitrile and then vortexed vigorously for 30 s. The resulting mixture was then centrifuged at 4 °C at 12,000 rpm for 10 min and the supernatant was injected into the UPLC-Q/TOF–MS analytical system.

Tissue sectioning. At the 10th week after occlusion, Sprague–Dawley rats were euthanized with pentobarbital (0.55 mg/kg, i.p.) and the heart tissues were explanted. Left and right atria were resected respecting anatomic landmarks. Then heart tissue was divided into two parts along the long axis section of left ventricle and snap-frozen in liquid nitrogen for further study. The slices of all tissues samples were sectioned at 10 µm thickness using a Leica CM1950 cryostat (Leica Microsystems GmbH, Wetzlar, Germany) at −17 °C and thaw mounted onto indium tin oxide (ITO) coated glass slides. The glass slides were then placed into a vacuum desiccator for approximately 1 h before matrix application. For MALDI-MS, the matrix solution, i.e., 1,5-DAN hydrochloride in 50% ethanol/water prepared as reported in the literature (Liu et al., 2014), was sprayed onto the tissue sections mounted onto ITO coated glass slides using an automatic matrix sprayer (ImagePrep, Bruker Daltonics). During this procedure, homogeneous matrix coverage was ensured over the entire tissue surface. For locating the apoptosis site of the left ventricle of the heart section, a TUNEL assay (11684795910, Roche) was performed according to the manufacturer's specifications. Briefly, after dewaxing and hydrating, the parallel sections were treated with protease-K and freshly prepared TdT enzyme in a dark place, followed by sealing using the sealing fluid, color development with DAB. Images were obtained with a DP72 digital camera (Olympus, Tokyo, Japan).

Untargeted Metabolic Profiles Analysis by UPLC-Q/TOF-MS

An untargeted metabonomics approach based on complementary HILIC and reversed-phase liquid chromatography (RPLC) combined with Q-TOF mass spectrometry was implemented in order to select more potential biomarkers in the plasma of HF rats.

For HILIC-MS analysis, the separation was performed using a Waters UPLC BEH amide column (2.1 mm × 100 mm, 1.7 µm particle size). The mobile phase consisted of solvent A (0.1% formic acid–acetonitrile, containing 1 mM ammonium formate) and solvent B (0.1% formic acid–water, containing 2 mM ammonium formate). Gradient elution was employed (0–1 min, 95% A; 1–9 min, 95–50% A; 9.1–13 min, 50–95% A). The flow rate of the mobile phase was 0.3 ml min^{-1}, the column temperature was 40 °C, and the injection volume was 1 µl. For RPLC-MS analysis, the separation procedure was carried out using s Waters ACQUITY HSS T3 (2.1 mm × 100 mm, 1.8 µm) system. The mobile phase consisted of solvent A (0.1% formic acid–water) and solvent B (0.1% formic acid–methanol). Gradient elution was employed (0–1 min, 100% A; 1–4 min, 100–30% A; 4–12 min, 30–0% A; 12.1–14 min, 0–100% A). The flow rate of the mobile phase was 0.3 ml min^{-1} and the injection volume was 1 µl.

The conditions of MS analysis were as follows: RPLC-MS and HILIC-MS spectra were acquired on a hybrid quadrupole-time-of-flight (Q-TOF) mass spectrometer (Xevo G2 Q-TOF MS systems, Waters Corp., Milford, MA, USA), equipped with an electrospray ionization (ESI) source. The full-scan data were acquired from 50 to 1,200 Da, with a scan time of 0.2 s using a capillary voltage of 3.0 kV for positive mode and 2.2 kV for negative mode, a desolvation temperature of 350 °C, sample cone voltage of 40 V, extraction cone voltage of 4 V, source temperature of 100 °C, cone gas flow of 40 L/h, and desolvation gas flow of 800 L/h. The mass spectrometer was calibrated across a mass range of 50–1,200 Da using a solution

of sodium formate. The mass was corrected during acquisition using an external reference (Lock-Spray™) consisting of a 0.2 ng ml^{-1} solution of leucine enkephalin, infused at a flow rate of 5 µl min^{-1} *via* a lock spray interface and generating a reference ion at 556.2771 Da ($[M+H]^+$) or 554.2615 Da ($[M-H]^-$). The lock spray scan time was set to 0.5 s, with an interval of 15 s, and the acquired data were averaged over three scans. RPLC-MS spectra were obtained in positive and negative ion modes, respectively. For HILIC-MS analysis, only positive mode was employed. The system was controlled by the software package Masslynx V4.1.

Matrix Assisted Laser Desorption Ionization Mass Spectrometry

MALDI-MS experiments were performed on an Ultraflextreme MALDI-TOF/TOF MS (Bruker Daltonics, Billerica, MA) equipped with a smartbeam Nd: YAG 355 nm laser operating at 2,000 kHz. Medium focus was set for the laser spot size (laser spot diameter: ~50 µm); the laser power was optimized prior to each run and then fixed during the entire experiment. The mass spectra were acquired in negative reflectron mode, with a pulsed ion extraction time of 130 ns, an accelerating voltage of 20.00 kV, an extraction voltage of 17.95 kV, a lens voltage of 7.5 kV, and a reflector voltage of 21.10 kV. The mass spectra data were acquired at a mass range of m/z = 50–1,360 Da. The imaging data for each array position consisted of 200 laser shots, with spatial resolution of 200 µm for all heart tissue sections. External mass calibration was performed with standards before data acquisition. MALDI mass spectra were normalized with the total ion current (TIC). The signal intensity of each imaging data displayed was the normalized intensity. MS/MS fragmentations observed on the MALDI-TOF/TOF MS instrument in the LIFTTM mode were used for further detailed structural confirmation of the identified metabolites (Liu et al., 2014).

Data Processing and Statistical Analysis

UPLC-Q/TOF-MS data processing was performed using the Progenesis QI software, which was developed for processing metabolic profiling data. Raw data obtained from the Masslynx 4.1 workstation of UPLC-Q/TOF-MS were imported to Progenesis QI. The detailed workflow included retention time correction, experimental design setup, peak picking, normalization, deconvolution, and alignment. Retention time (t_R)-m/z datasets were used to characterize the detected ions. The rule of a coefficient of variation (CV) less than 30% was used to filter the consistent ions. The intensity of each t_R-m/z variable was normalized and further imported into the SIMCA-P 13.0 software package for orthogonal partial least squares discriminant analysis (OPLS-DA). The OPLS-DA data were then used to identify the different metabolites responsible for the separation between the groups.

For MALDI-MS, regions of interest (ROIs) were located at the apoptotic area according to TUNEL staining results and the corresponding average intensity of metabolites was acquired. A two-tailed Student's t-test was performed to compare the average intensity of metabolites between the different regions of the heart tissue. p-values ≤ 0.05 were considered statistically significant.

All other values measured *in vivo* were presented as means ± standard error. Statistical significance was determined *via* a one-way ANOVA test, followed by Tukey multiple comparison test or Student's *t*-tests. A value of $p \leq 0.05$ was considered statistically significant.

RESULTS AND DISCUSSION

Echocardiographic Assessment

HF generally describes a final syndrome before mortality, triggered by a variety of factors. Decreased EF has already been recognized as a prominent standard in the diagnosis of HF and guiding HF management (Fu et al., 2015; Bloom et al., 2017). In our previous study (Wei et al., 2019), the protective effect of varying doses of YXSC on cardiac performance was evaluated by dynamic changes of EF. Here the dose of 0.32 g· kg^{-1}· day^{-1} exhibited a beneficial effect and was therefore selected for further studies. As shown in **Figure 1** and **Table 1**, rats in model group significantly decreased in fractional shortening (FS) and EF at the 4th and 10th week after permanent occlusion compared to those of the sham group ($p < 0.01$). The results indicated heart dysfunction occurred. At the 10th week after myocardial ischemia, the YXSC group exhibited a reversed increase in FS and EF compared to the model group ($p < 0.05$), indicating that administration of YXSC had an effective cardio-protective effect against HF.

Plasma Untargeted Metabolic Profiles Analysis

HF is not an independent disease, but a progressive clinical syndrome and, unfortunately, represents the end stage of heart disease development. In this study reported herein, the obvious appearance of HF induced by ischemia occurred at the fourth week after permanent occlusion. In an effort to shed further light on metabolic profiling, various plasma metabolites were analyzed dynamically at the 2nd, 4th, and 10th week after permanent occlusion. The identification of common metabolic markers between sham and model groups at different time points may provide a dynamic view of the underlying pathological process of HF. Different types of mobile phases, including 0.05% and 0.1% formic and acetic acid in water, acetonitrile, and methanol were screened for plasma sample analysis. Optimized conditions of mobile phases for HILIC-MS and RPLC-MS were obtained as detailed in the section *Untargeted Metabolic Profiles Analysis by UPLC-Q/TOF-MS*. Typical total ion chromatograms (TICs) of plasma samples for HILIC-MS in the positive ionization mode as well as RPLC-MS chromatograms in the positive and negative ionization modes are shown in **Figure 2**.

QC samples were used to monitor the stability of the UPLC-Q/TOF-MS system. The QC samples were analyzed in the positive and negative ionization mode at regular intervals (every 10 samples) throughout the entire sequence. The RSDs of the peak areas and retention times of the detected ion signals were calculated. More than 80% of the RSDs were less than 30% for all QC samples in the negative and positive ionizations modes for all run sequences. Therefore, both the repeatability and stability of the global experimental performances were high and acceptable.

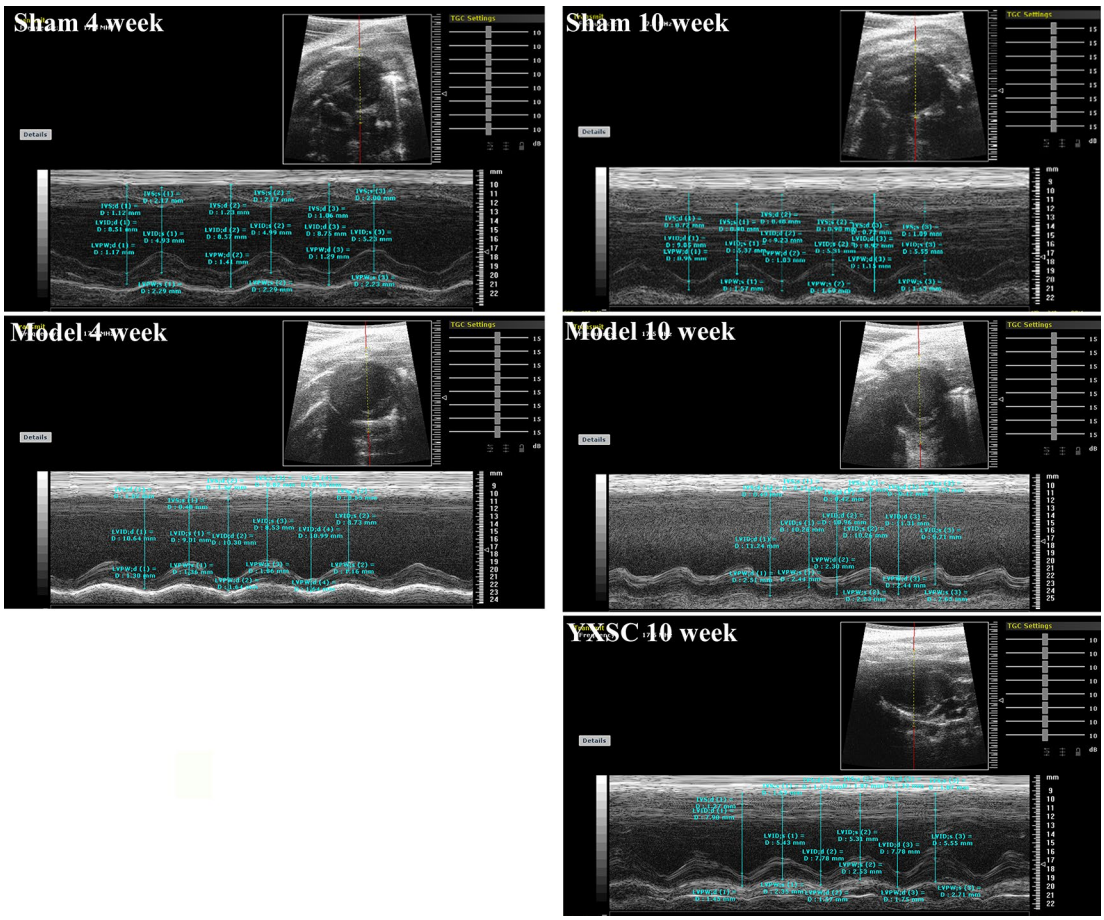

FIGURE 1 | Representative echocardiographic in sham group, model group and YXSC group.

TABLE 1 | Echocardiographic parameters of rats at 4th and 10th week.

	4th week		10th week		
	Sham	**Model**	**Sham**	**Model**	**YXSC**
LVEDd (mm)	8.05 ± 0.31	9.72 ± 1.22**	8.71 ± 0.30	10.15 ± 1.41**	9.13 ± 0.65#
LVEDs (mm)	5.24 ± 0.29	7.68 ± 1.27**	5.15 ± 0.27	7.98 ± 0.98**	6.26 ± 0.81#
EF (%)	69.00 ± 1.58	42.18 ± 5.74**	69.24 ± 1.56	41.49 ± 10.28**	54.89 ± 5.15#
FS (%)	43.32 ± 1.64	21.35 ± 3.25**	40.61 ± 1.25	21.75 ± 6.11**	32.28 ± 5.96##

*LVEDd: left ventricle end-diastolic diameter; LVEDs: left ventricle end-systolic diameter; EF: ejection fraction; FS: fractional shortening; *p < 0.05, **p < 0.01, model group vs. sham group; #p < 0.05, ##p < 0.01, YXSC group vs. model group.*

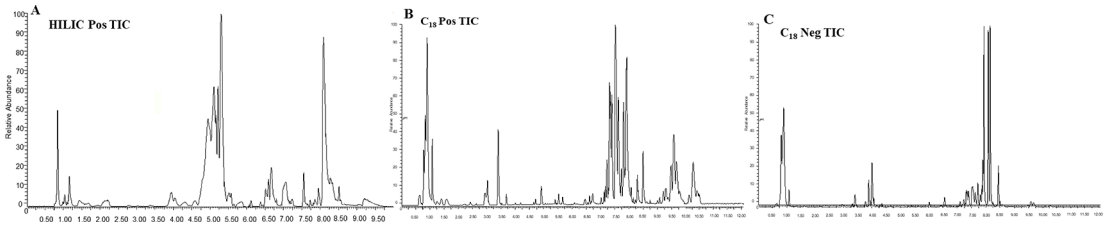

FIGURE 2 | Typical TIC of the rat plasma obtained in ESI positive and negative mode based on HILIC-MS and RPLC-MS. **(A)** HILIC-MS TIC in positive mode; **(B)** RPLC-MS TIC in positive mode; **(C)** RPLC-MS TIC in negative mode.

Statistical Analysis and Identification of Potential Biomarkers

After deconvolution, alignment, and normalization using the Progenesis QI software, all ion signals of HILIC-MS and RPLC-MS chromatograms both in positive and negative ionization modes were extracted and merged in an excel file. Then the merged data were imported into the SIMCA-P software for multivariate statistical analysis. In order to eliminate any non-specific effects of the operative technique and to uncover the metabolic biomarkers, OPLS-DA was applied to compare metabolic changes in the model group with the sham group. As a supervised pattern recognition technology, OPLS-DA can be used to improve biomarker discovery efforts and separate samples into two blocks. This technique can then be used to improve discrimination between the two groups. The data were standardized using a Pareto-scaling technique for OPLS-DA.

Score plots from OPLS-DA (**Figures 3 A1–A3**) indicated an obvious separation between the sham group and the corresponding model group of the 2nd, 4th, and 10th week after permanent occlusion, suggesting that blood metabolic perturbation significantly occurred in the model groups after permanent occlusion. From the corresponding S plots (**Figures 3B1–B3**), the ions (the dots in the figure) furthest away from the origin contributed significantly to be responsible for the separation between sham and model group and may be therefore regarded as the differentiating metabolites for HF. After combining the results of the S plots, the VIP value (VIP > 1) obtained from the OPLS-DA analysis, and the *t*-test ($p < 0.05$), the corresponding metabolites could be selected. Finally, common metabolite markers between the sham group and model group of the 2nd, 4th, and 10th week after permanent occlusion were selected as listed in **Table 2**. The chemical structures of the metabolites were identified according to online databases of the Human Metabolome Database (www.hmdb.ca), Metlin (https://metlin.scripps.edu) and the Mass Bank (www.massbank.jp) vWhen necessary, further confirmation was obtained through comparisons with authentic standards, including retention times and MS/MS fragmentation patterns.

As shown in **Table 2**, detail information on the filtered common metabolic markers is listed, including the applied chromatographic columns, names, retention times, measured mass (m/z), and the relative contents at the 10th week after permanent occlusion. Of the total 21 metabolic markers, 6 PCs, 3 fatty acids, 3 bile acids, 2

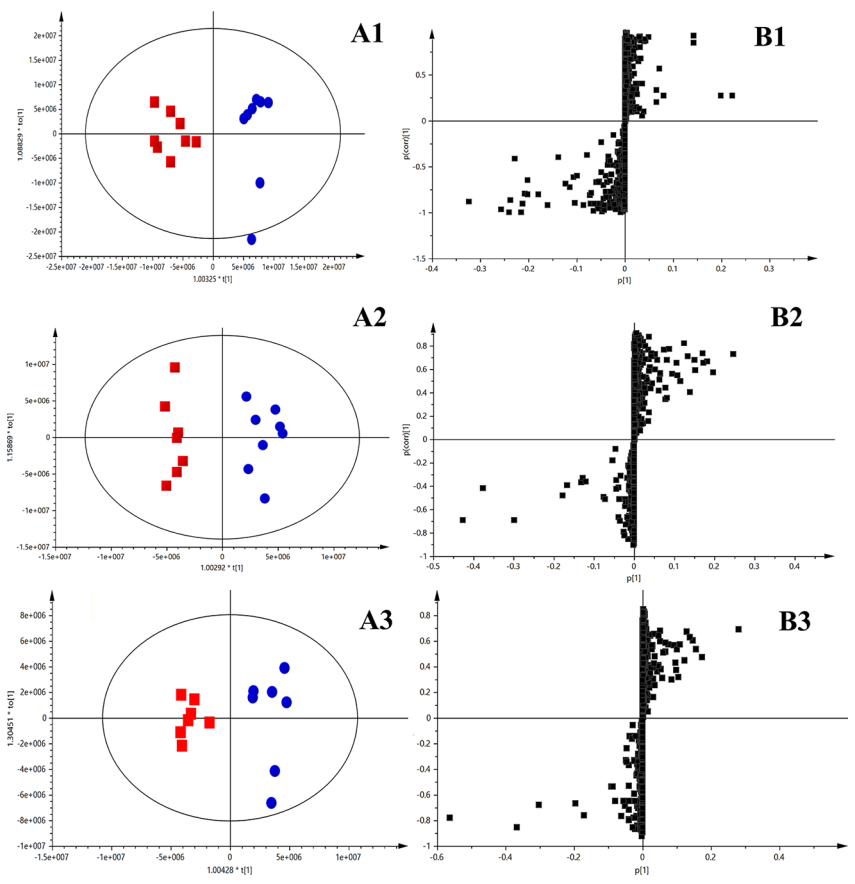

FIGURE 3 | OPLS-DA results between the sham group and model group based on the merged data of plasma untargeted metabolic profiles. **(A)** OPLS-DA scores plot, sham group (blue) vs. model group (red); **(A1)**, 2nd week after occlusion; **(A2)**, 4th week after occlusion; **(A3)**, 10th week after occlusion; **(B)** S-plot constructed from OPLS-DA; **(B1)**, 2nd week; **(B2)**, 4th week; **(B3)**, 10th week. The ions (black square) furthest away from the origin contribute significantly to be responsible for the separation between sham and model group.

TABLE 2 | Identified common metabolic markers between the sham group and model group of the 2nd, 4th, and 10th week after permanent occlusion.

No.	Column	Name	Retention time(min)	Mean measured mass (Da)	Elemental composition	Normalized content (×10000) at the tenth week after MI		
						Sham	Model	YXSC
1	Waters UPLC HSS T3 column	PC(20:4/18:2)	9.34	806.5690 $[M+H]^+$	$C_{46}H_{80}NO_8P$	440.37 ± 14.20	348.28 ± 30.85↓***	474.34 ± 36.61↑###
2		PC(20:4/20:4)	9.26	830.5687 $[M+H]^+$	$C_{48}H_{80}NO_8P$	346.10 ± 34.55	307.64 ± 92.14↓^	304.21 ± 108.18
3		PC(18:2/16:0)	9.72	758.5695 $[M+H]^+$	$C_{42}H_{80}NO_8P$	1548.02 ± 89.64	1282.69 ± 95.20↓**	1662.92 ± 70.04↑###
4		PC(18:0/18:2)	10.45	786.6009 $[M+H]^+$	$C_{44}H_{84}NO_8P$	727.59 ± 104.42	540.20 ± 108.59↓*	711.10 ± 76.11↑#
5		PC(20:4/18:0)	10.32	810.6000 $[M+H]^+$	$C_{46}H_{84}NO_8P$	1910.97 ± 207.55	1617.89 ± 163.09↓*	1656.79 ± 731.39↑
6		PC(22:6/18:0)	10.17	834.5979 $[M+H]^+$	$C_{48}H_{84}NO_8P$	482.14 ± 70.77	405.19 ± 52.18↓^	487.59 ± 40.83↑#
7		3-Methyl-2-oxovaleric acid	3.92	129.0554 $[M-H]^-$	$C_6H_{10}O_3$	67.33 ± 14.16	82.67 ± 16.09↑^	67.71 ± 11.70↓
8		Palmitoleic acid	7.85	253.2168 $[M-H]^-$	$C_{16}H_{30}O_2$	55.05 ± 9.61	82.82 ± 4.61↑***	69.71 ± 11.39↓#
9		Palmitic acid	8.13	255.2326 $[M-H]^-$	$C_{16}H_{32}O_2$	626.17 ± 137.94	689.71 ± 77.81↑^	594.43 ± 30.87↓#
10		Chenodeoxycholic acid	6.48	391.2847 $[M-H]^-$	$C_{24}H_{40}O_4$	24.34 ± 18.57	11.29 ± 5.38↓^	33.56 ± 16.49↑#
11		Taurochenodesoxycholic acid	6.64	498.2889 $[M-H]^-$	$C_{26}H_{45}NO_6S$	5.53 ± 0.49	3.35 ± 1.04↓**	4.31 ± 2.94↑
12		Arachidonic acid	7.94	303.2325 $[M-H]^-$	$C_{20}H_{32}O_2$	223.80 ± 30.08	277.56 ± 16.26↑**	234.89 ± 16.79↓##
13		Taurocholic acid	6.07	514.2837 $[M-H]^-$	$C_{26}H_{45}NO_7S$	49.41 ± 3.43	20.52 ± 1.37↓***	34.18 ± 22.37↑
14		Lactic acid	1.11	89.0243 $[M-H]^-$	$C_3H_6O_3$	15.16 ± 4.51	29.15 ± 4.42↑**	19.41 ± 1.54↓##
15		Citric acid	1.10	191.0193 $[M-H]^-$	$C_6H_8O_7$	97.99 ± 15.72	74.35 ± 10.84↓*	90.27 ± 5.78↑#
16		Uric acid	1.11	167.0206 $[M-H]^-$	$C_5H_4N_4O_3$	16.14 ± 1.86	28.49 ± 3.36↑***	21.17 ± 1.63↓##
17	Waters UPLC BEH Amide column	Valine	6.73	118.086255$[M+H]^+$	$C_5H_{11}NO_2$	88.77 ± 25.20	39.26 ± 65.22↓*	87.05 ± 27.22↑#
18		Edetic acid	8.11	293.098824$[M+H]^+$	$C_{10}H_{16}N_2O_8$	171.64 ± 21.51	149.48 ± 160.70↓^	277.37 ± 20.52↑###
19		Creatine	7.57	132.076753$[M+H]^+$	C4H9N3O2	34.71 ± 4.09	23.09 ± 31.67↓**	39.26 ± 9.12↑##
20		L-acetylcarnitine	5.10	204.123034$[M+H]^+$	$C_9H_{17}NO_4$	161.58 ± 34.87	148.53 ± 154.90↓^	250.98 ± 66.68↑##
21		N1-Methyl-2-pyridone-5-carboxamide	8.52	170.093359$[M+NH_4]^+$	$C_7H_8N_2O_2$	12.85 ± 2.01	10.37 ± 12.49↓^	16.67 ± 2.85↑##

** $p < 0.05$, ** $p < 0.0$, *** $p < 0.001$ and ^ VIP > 1; model group vs. sham group.*

#$p < 0.05$, ## $p < 0.01$, ###$p < 0.001$; YXSC group vs. model group.

amino acids, and 7 other basic metabolites including lactic acid, citric acid, uric acid, etc., could be identified.

The levels of six PCs [PC (20:4/18:2), PC (20:4/20:4), PC (18:2/16:0), PC (18:0/18:2), PC (20:4/18:0), PC(22:6/18:0)], three bile acids (chenodeoxycholic acid, taurocholic acid and taurochenodesoxycholic acid), two amino acids (valine and creatine), and four other basic metabolites (edetic acid, citric acid, L-acetylcarnitine and N1-Methyl-2-pyridone-5-carboxamide) obviously decreased in the model group compared to the sham group ($p < 0.05$ or VIP > 1). However, the levels of three fatty acid species (palmitoleic acid, palmitic acid, and arachidonic acid) and three other basic metabolites (lactic acid, uric acid, and 3-methyl-2-oxovaleric acid) showed incremental changes in the model group compared to the sham group ($p < 0.05$ or VIP > 1).

After administration of YXSC, among the total of 21 metabolic markers, the levels of 16 metabolites (4 PCs, 3 fatty acids, 2 amino acids, 1 bile acids and 6 other metabolites) showed significant changes in the YXSC group compared to the model group and were found to return to normal levels as listed in **Table 2**.

In Situ Mass Spectrometry Imaging

In situ MALDI-MS ionization was applied to verify plasma metabolite markers at the apoptosis region of the heart. As shown in **Figures 4 A1**, **B1**, and **C1**, TUNEL stained images were used to locate the apoptosis region of heart induced by ischemia. Then, the parallel section from the same rat hearts (n = 5) was subjected to MALDI-MS. Imaging data were acquired in the negative ionization mode at a spatial resolution of 200 μm. As shown in **Figures 4 A2**, **B2**, and **C2**, based on total ion current, the image reflects a relative modification of all metabolite levels at the apoptosis region of the heart between the sham group, model group, and YXSC group. Furthermore, the target metabolite markers found in the plasma were extracted by exact mass search as listed in **Table 1**, using the high accuracy of m/z determined by TOF-MS. The identification was further confirmed by MS/MS fragmentation. Finally, four metabolites were selected, including palmitoleic acid, palmitic acid, arachidonic acid, and lactic acid, for verification in the heart tissue. **Figure 5** showed the ion intensity of palmitoleic acid, palmitic acid, arachidonic acid, and lactic acid at the apoptosis region of the heart in the sham group, model group, and YXSC group. It can be seen from inspection of **Figure 5** that the ion intensities of palmitoleic acid, palmitic acid, arachidonic acid, and lactic acid in the model group were all higher than those in the sham group. Furthermore, a tendency for returning to baseline values in YXSC group ($p < 0.05$) could be determined, consistent to the variation trends in the plasma.

Correlation Network of Differential Metabolic Markers

In order to investigate the latent relationships of the metabolic markers of HF in the plasma, a correlation network diagram was constructed based on the KEGG database. As shown in **Figure 6**, the network diagram showed the interrelationship based on the identified metabolic pathways including 12 metabolic markers. The metabolic pathways of glycerophospholipid metabolism, arachidonic acid metabolism, fatty acid metabolism, primary bile acid biosynthesis, glycolysis or gluconeogenesis, pyruvate metabolism, purine metabolism, and amino acid metabolism are related to each other *via* acetyl coenzyme A (Acetyl-CoA) and the citric acid cycle. In the network diagram shown in **Figure 5**, the metabolites in red and blue indicate changes, i.e., amount increase and decrease, in the blood of HF rats compared to the sham groups, respectively. Importantly, the asterisk mark indicates that the metabolic markers showed

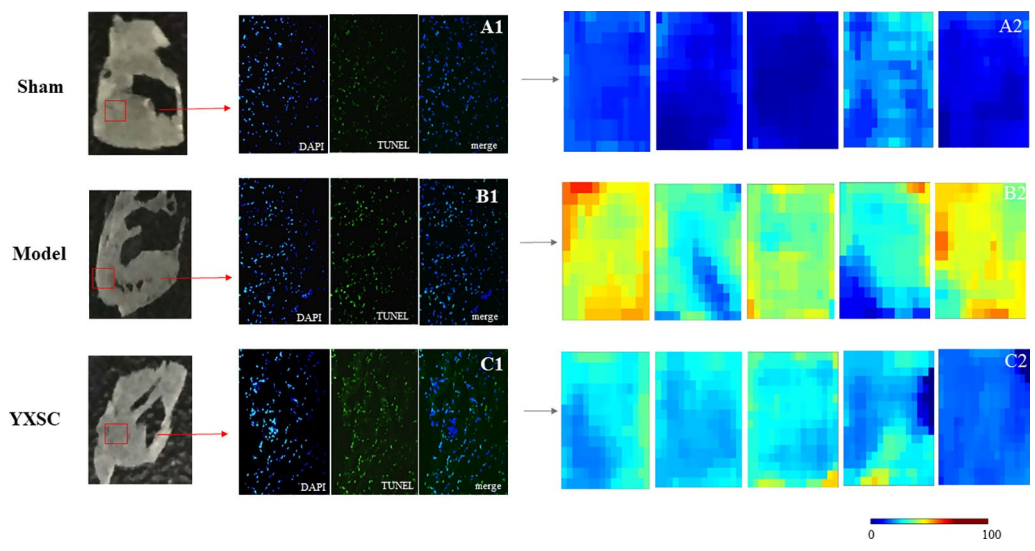

FIGURE 4 | *In situ* MALDI-MS and the levels of all metabolites at the apoptotic section of the hearts from sham group, model group, and YXSC group. Microscope images for whole Tunel stained heart sections from sham group **(A1)**, model group **(B1)**, and YXSC group **(C1)** (40 X). Heat map describing the total ion intensity at the region of apoptosis on the heart section from sham group **(A2)**, model group **(B2)**, and YXSC group **(C2)**.

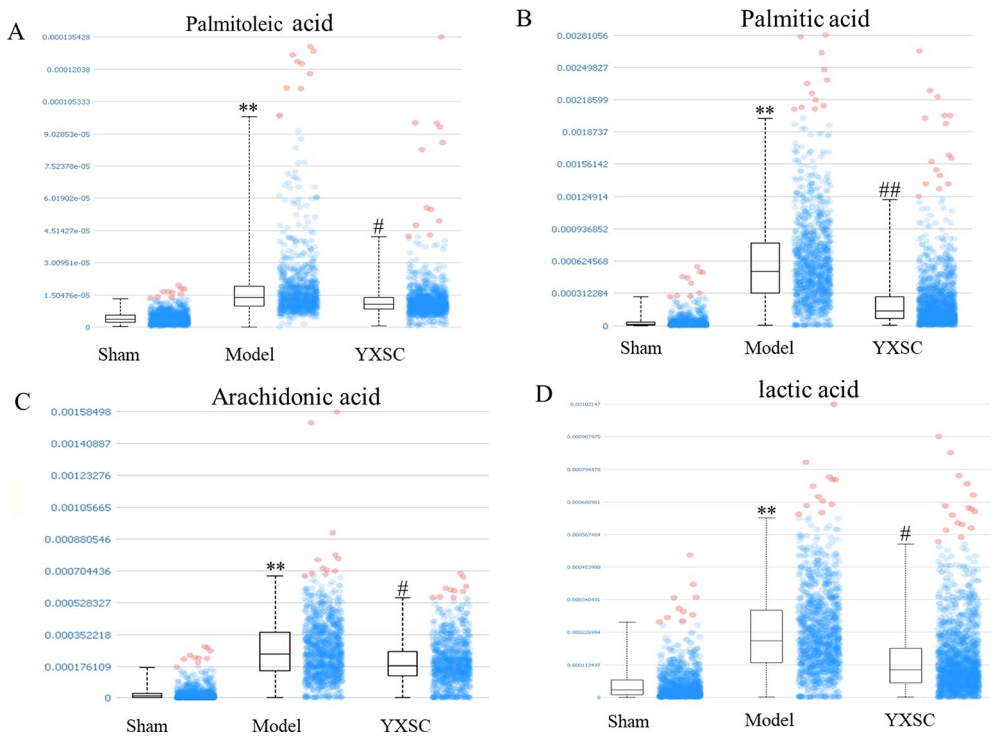

FIGURE 5 | The ion intensity of palmitoleic acid, palmitic acid, arachidonic acid, and lactic acid extracted from the region of apoptosis on the heart section. Data were shown as the mean ± SD (n = 5). Asterisk mark and octothorpe mark indicate significant differences (** $p < 0.01$, sham group versus model group; ## $p < 0.01$, # $p < 0.05$, model group versus YXSC group). **(A)** (Palmitoleic acid, $[M-H]^-$ m/z 253.217), **(B)** (Palmitic acid, $[M-H]^-$ m/z 255.237), **(C)** (Arachidonic acid, $[M-H]^-$ m/z 303.234), **(D)** (lactic acid $[M-H]^-$ m/z 89.025).

a tendency for returning to baseline values in the YXSC group. Moreover, metabolites in the heart tissue highlighted by a yellow rectangle were further validated by MALDI-MS.

DISCUSSION

To this day, the optimization of cardiac substrate metabolism to improve cardiac function and to slow the progression of HF, without causing any direct negative hemodynamic or inotropic effects, is believed to represent an attractive therapeutic approach. Although the consequences of metabolic dysfunction in HF are poorly understood, there is growing evidence to support the concept that alterations in substrate metabolism significantly contribute to contractile dysfunction and the progression of left ventricular (LV) remodeling. The metabolic markers identified in this study may offer an improved understanding of the complex pathogenesis of HF and the potential YXSC mechanism *in vivo*.

Fatty Acid and Pyruvate Metabolism

Plasma fatty acid concentration is generally regulated by the net release of fatty acids from triglycerides in adipocytes, reflecting the net balance between triglyceride breakdown by hormone-sensitive lipase and synthesis by glycerol phosphate acyltransferase (Lopaschuk et al., 1994). Under conditions of metabolic stress, such as ischemia, diabetes, or starvation, plasma free fatty acid concentrations may reach significantly increased levels. Furthermore, elevated fatty acid levels in the plasma can result in a cardiac specific "lipotoxicity," characterized by accumulation of neutral lipids (triglycerides) and ceramides, which are associated with apoptosis, and contractile dysfunction (Stanley et al., 2005). It has already been shown that ceramide, a critical second messenger in the regulation of signal transduction associated with apoptosis, participates in various biochemical processes including lipid peroxidation, bile acid biosynthesis, fatty acid biosynthesis, fatty acid metabolism, and lipid transport (Djoumbou Feunang et al., 2016).

Palmitic acid represents one of the most common saturated fatty acids and serves as precursor of ceramide synthesis as well as inhibitor of mitochondrial adenine nucleotide translocase. Palmitic acid is generally associated with apoptosis in the heart and has pro-apoptotic properties in cardiomyocytes (Vries et al., 1997; Sparagna et al., 2004; Miller et al., 2005). Palmitoleic acid, an unsaturated fatty acid, is positively associated with hypertension, inflammation, and cardiovascular mortality, critical risk factors for HF (Zheng et al., 1999; Warensjö et al., 2008; Mozaffarian et al., 2010; Djousse et al., 2012). In clinical study, the levels of palmitoleic acid have been shown to be significantly elevated in HF patients (Lopaschuk et al., 1994; Fosshaug et al., 2015; Ruiz et al., 2017). In the study reported herein, the levels of

palmitoleic acid and palmitic acid in the plasma were found to be increased in HF rats. Furthermore, using MALDI-MS, both levels could also be detected with the same variation tendency in the heart. The results were consistent with published reports and further suggest that palmitoleic acid and palmitic acid may represent important metabolic markers for fatty acid metabolism disorder in HF.

In addition, generally appreciated is the notion that the energy required for heart function mainly results from fatty acids metabolism and carbohydrate metabolism. Myocardial ischemia has been shown to disturb the net balance of "glucose-fatty acid cycle," resulting in a decreased mitochondrial ATP production, increased glucose anaerobic glycolysis, lactic acid accumulation, and cytotoxicity (Randle et al., 1963; Randle et al., 1964). Therefore, increasing the oxidation of glucose and lactic acid and thereby converting the energy metabolism of cardiomyocytes from fatty acids to glucose metabolism may contribute to improve cardiac function. As shown in **Figure 6**, lactic acid is produced from pyruvate *via* the enzyme lactate dehydrogenase (LDH) in the pyruvate metabolism. In this study, the plasma metabolic profiles analysis and MALDI-MS imaging of the heart both showed that the level of lactic acid was increased in HF rats. After treatment with YXSC, the levels of palmitoleic acid, palmitic acid, and lactic acid all showed a tendency for returning to baseline values in the YXSC group ($p < 0.05$). This important finding indicates that administration of YXSC may lead to the regulation of the fatty acid metabolism as well as pyruvate metabolism during HF. Additionally, L-acetylcarnitine, which reduces fatty acid oxidation, contributes to the improved recovery of the cardiac output in isolated perfused rat hearts subjected to global ischemia (Paulson et al., 1986). In this study, the level of L-acetylcarnitine was determined to be significantly reduced in the model group compared with the sham group. After treatment with YXSC, the level of L-acetylcarnitine showed a tendency for returning to baseline values in the YXSC group ($p < 0.05$).

Phosphatidylcholines and Bile Acids Metabolism

Phosphatidylcholines (PCs), a major lipid component of membranes, play an important role in physiology and pathophysiology (Kim et al., 2015). There are reports that the imbalance of phosphatidylcholines metabolism may lead to functional impairment of the heart involving plaque development and progression associated with atherosclerotic cardiovascular disease (Meikle et al., 2014). In this study, a series of six PC species was found to decrease in the model group compared with the sham group, indicating that the degradation of PCs was activated in the model group.

Arachidonic acid, a polyunsaturated omega-6 fatty acid, represents a constituent of animal phosphatides. Arachidonic acid and its metabolites such as prostaglandins and leukotrienes are considered intracellular messengers. Arachidonic acid mediates inflammation and the functioning of several organs, including the heart either directly or upon its conversion into eicosanoids (Nixon, 2009). For example, 20-hydroxyecostearonic acid (20-HETE) metabolized from arachidonic acid contributes to platelet aggregation and vasoconstriction (Jarrar et al., 2019). Inflammation cytokines such as TNF-α and IL-1β triggered $Ca2^{+}$ imbalance contribute to cardiac remodeling, cardiomyocyte hypertrophy, cardiomyocyte apoptosis, and often lead to detrimental

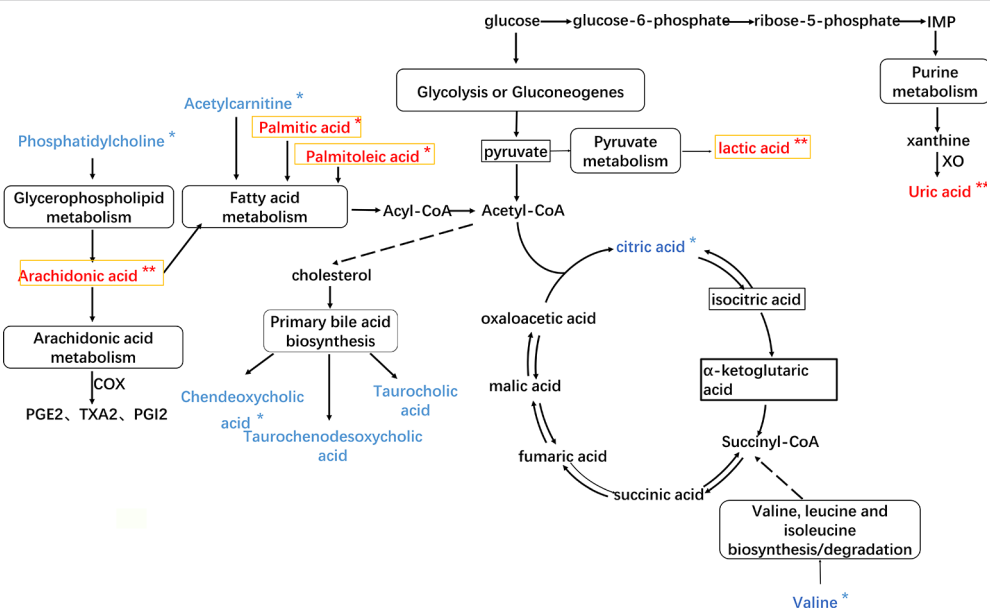

FIGURE 6 | The HF imbalanced network of the metabolic markers in plasma of rat. Metabolites in red and blue represent increase and decrease changes in HF rats; metabolites in yellow rectangle represent validation by MALDI-MS. ⟶ Direct interaction, - - -▶ Indirect interaction, ** $p < 0.01$, *$p < 0.05$, YXSC group versus model group.

effects (Schirone et al., 2017). The disturbance of arachidonic acid metabolites is often related to the development of cardiovascular diseases, such as hypertension (Bloom et al., 2017). In this study, the level of arachidonic acid increased in the model group compared with the sham group using UPLC-Q/TOF-MS and MALDI-MS.

Bile acids (BAs), the end products of cholesterol metabolism, served as mediators of cellular signals such as the regulator of lipid and energy metabolism (Claudel et al., 2005; Mayerhofer et al., 2017). As reported in the literature, BAs exhibit effects on the function of the cardiovascular system, including the formation of atherosclerotic plaque, influencing myocardial conduction and contraction by means of interaction with myocytes (Khurana et al., 2011). In this study, the levels of BAs found in the plasma, including chenodeoxycholic acid, taurochenodesoxycholic acid, and taurocholic acid, were reduced ($p < 0.05$ or VIP > 1) in model group compared with sham group, further demonstrating that the consumption of BAs might accelerate plaque aggregation.

After administration of YXSC, the levels of four PC species including PC (20:4/18:2), PC(18:2/16:0), PC(18:0/18:2), PC(22:6/18:0), arachidonic acid and taurocholic acid returned to normal levels. This result provided further evidence for the protective effects of YXSC, potentially due to suppressing the degradation of PCs and regulating of inflammatory reactions as well as the bile acid metabolism.

Amino Acid Metabolism

Amino acids, forming the basic units of all proteins as well as energy-providing substrates, feature critical roles in cell signaling, biosynthesis, transportation, and key metabolic pathways. Recently reported literature data indicate that branched-chain amino acids (BCAAs) catabolic defects are associated with HF (Tanada et al., 2015; Sun et al., 2016). 3-Methyl-2-oxovaleric acid, formed from the incomplete breakdown of branched-chain amino acids, represents an abnormal metabolite and a neurotoxin (Yudkoff et al., 2005). In this study, the levels of valine, one of the BCAAs, as well as 3-methyl-2-oxovaleric acid found in the plasma showed both decreased and increased concentrations in the model group compared to the sham group.

Another amino acid, creatine, is critically involved in energy metabolism. In the context of HF, ATP levels were reported to decrease with mitochondrial abnormalities (Meyer et al., 1984; Starling et al., 1998; Sabbah, 2016). The creatine kinase (CK) system plays a vital role in buffering the cellular ATP and ADP concentrations through transferring high-energy phosphates from phosphocreatine (PCr) to ADP. The predominance of creatine is a consequence of maintaining ATP and PCr levels (Meyer et al., 1984; Zhang et al., 2014). A recent study based on ^{1}H-NMR spectroscopy has demonstrated creatine depletion in human HF (Ingwall and Weiss, 2004). In a similar fashion, we observed significantly declined levels of creatine in the model group. These changes in creatine levels are closely associated with impaired cardiac function. Moreover, after treatment with YXSC, the levels of valine and creatine both showed apparent tendencies to return back to normal concentration levels.

CONCLUSION

In this study, a metabonomic approach using an integrated UPLC-Q/TOF-MS technique and MALDI-MS was carried out to explore potential metabolic biomarkers and to increase the understanding of HF as well as to assess the potential mechanism of YXSC in an ischemia-induced HF rat model. Plasma metabolic profiles were analyzed by UPLC-Q/TOF-MS, with complementary HILIC and reversed-phase liquid chromatography. In an effort to identify more reliable potential metabolic biomarkers, common metabolic markers found at different time points of the 2nd, 4th, and 10th week after permanent occlusion were selected through multivariate data analysis. Furthermore, MALDI-MS was applied to identify the identified metabolic markers in the bloodstream at the apoptotic position of the heart tissue.

Based on echocardiographic assessment, in this rat model, HF could be observed at the fourth week after permanent occlusion. Moreover, clear separations could be detected between the sham group and model group by the loading plots of OPLS-DA at different time points after permanent occlusion. The potential markers of interest were extracted from the combining S-plots, variable VIP values (VIP > 1) and t-test ($p < 0.05$). In doing so, 21 common metabolic biomarkers over the course of the development and progression of HF after permanent occlusion could be identified that were mainly related to disturbances in the fatty acid metabolism, phosphatidylcholines metabolism, bile acids metabolism, amino acids metabolism, and pyruvate metabolism. Of the biomarkers, 16 metabolites such as palmitoleic acid, arachidonic acid, and lactic acid showed obvious changes ($p < 0.01$) and a tendency for returning to baseline values in YXSC-treated HF rats at the 10th week after permanent occlusion. Moreover, four biomarkers of palmitoleic acid palmitic acid, arachidonic acid, and lactic acid could be further validated by MALDI-MS at the apoptotic position of the coronal heart slice.

To summarize, an integrated UPLC-Q/TOF-MS technique and MALDI-MS strategy may provide a significant contribution and a potential analytical tool for understanding of the complex pathogenesis of various disease states. Moreover, the results obtained throughout this study may help develop novel strategies to explore the mechanism of HF and may also be useful for the study of potential biochemical mechanisms associated with YXSC effects.

DATA AVAILABILITY STATEMENT

The datasets analyzed in this manuscript are not publicly available. Requests to access the datasets should be directed to whw9905012@163.com.

ETHICS STATEMENT

The animal study was reviewed and approved by the Academy of Chinese Medical Science's Administrative Panel on Laboratory Animal Care. Written informed consent was obtained from the owners for the participation of their animals in this study.

AUTHOR CONTRIBUTIONS

Participated in research design: HWW, HY, GL, ST. Conducted experiments of bioanalysis: XYL, JW, XQL, HWW. Conducted experiments of HF rats: JX, FZ, LT, DL, YZ, XT, HHW. Performed data analysis: JX, FZ, ST. Wrote or contributed to the writing of the manuscript: HWW, JX.

FUNDING

This study was financially supported by the National Natural Science Foundation of China (No. 81973711, No. 81573726, No.81673700) and the National Science and Technology Major Project (2014ZX09201021-009).

SUPPLEMENTARY MATERIAL

The Supplementary Material for this article can be found online at: https://www.frontiersin.org/articles/10.3389/fphar.2019.01474/full#supplementary-material

REFERENCES

Birkenfeld, A. L., Jordan, J., Dworak, M., Merkel, T., and Burnstock, G. (2018). Myocardial metabolism in heart failure: purinergic signalling and other metabolic concepts. *Pharmacol. Ther.* 194, 132–144. doi: 10.1016/j.pharmthera.2018.08.015

Bloom, M. W., Greenberg, B., Jaarsma, T., Januzzi, J. L., Lam, C. S. P., Maggioni, A. P., et al. (2017). Heart failure with reduced ejection fraction. *Nat. Rev. Dis. Primers* 3, 17058. doi: 10.1038/nrdp.2017.58

Bloom, M. W., Greenberg, B., Jaarsma, T., Januzzi, J. L., Lam, C. S. P., Maggioni, A. P., et al. (2017). Heart failure with reduced ejection fraction. *Nat. Rev. Dis. Primers* 3, 17058. doi: 10.1038/nrdp.2017.58

Carubelli, V., Castrini, A. I., Lazzarini, V., Gheorghiade, M., Metra, M., and Lombardi, C. (2015). Amino acids and derivatives, a new treatment of chronic heart failure? *Heart Fail Rev.* 20 (1), 39–51. doi: 10.1007/s10741-014-9436-9

Chinese Pharmacopoeia Commission. (2015). Chinese Pharmacopoeia (2015 edition), China Medical Science Press, 1, 1400.

Claudel, T., Staels, B., and Kuipers, F. (2005). The Farnesoid X receptor: a molecular link between bile acid and lipid and glucose metabolism. *Arterioscler. Thromb. Vasc. Biol.* 25 (10), 2020–2030. doi: 10.1161/01.ATV.0000178994.21828.a7

Djoumbou Feunang, Y., Eisner, R., Knox, C., Chepelev, L., Hastings, J., Owen, G., et al. (2016). ClassyFire: automated chemical classification with a comprehensive, computable taxonomy. *J. Cheminform.* 8, 61. doi: 10.1186/s13321-016-0174-y

Djousse, L., Weir, N. L., Hanson, N. Q., Tsai, M. Y., and Gaziano, J. M. (2012). Plasma phospholipid concentration of cis-palmitoleic acid and risk of heart failure. *Circ. Heart Fail* 5 (6), 703–709. doi: 10.1161/CIRCHEARTFAILURE.112.967802

Doenst, T., Nguyen, T. D., and Abel, E. D. (2013). Cardiac metabolism in heart failure: implications beyond ATP production. *Circ. Res.* 113 (6), 709–724. doi: 10.1161/CIRCRESAHA.113.300376

Fosshaug, L. E., Dahl, C. P., Risnes, I., Bohov, P., Berge, R. K., Nymo, S., et al. (2015). Altered levels of fatty acids and inflammatory and metabolic mediators in epicardial adipose tissue in patients with systolic heart failure. *J. Card Fail* 21 (11), 916–923. doi: 10.1016/j.cardfail.2015.07.014

Fu, F., Zhao, K., Li, J., Xu, J., Zhang, Y., Liu, C., et al. (2015). Direct evidence that myocardial insulin resistance following myocardial ischemia contributes to post-ischemic heart failure. *Sci. Rep.* 5, 17927. doi: 10.1038/srep17927

Guo, N., Yang, D., Wang, X., Dai, J., Wang, M., and Lei, Y. (2014). Metabonomic study of chronic heart failure and effects of Chinese herbal decoction in rats. *J. Chromatogr. A.* 1362, 89–101. doi: 10.1016/j.chroma.2014.08.028

Huang, N. F., Sievers, R. E., Park, J. S., Fang, Q., Li, S., and Lee, R. J. (2006). A rodent model of myocardial infarction for testing the efficacy of cells and polymers for myocardial reconstruction. *Nat. Protoc.* 1 (3), 1596–1609. doi: 10.1038/nprot.2006.188

Ingwall, J. S., and Weiss, R. G. (2004). Is the failing heart energy starved? on using chemical energy to support cardiac function. *Circ. Res.* 95 (2), 135–145. doi: 10.1161/01.RES.0000137170.41939.d9

Jackson, C. E., Castagno, D., Maggioni, A. P., Kober, L., Squire, I. B., Swedberg, K., et al. (2015). Differing prognostic value of pulse pressure in patients with heart failure with reduced or preserved ejection fraction: results from the MAGGIC individual patient meta-analysis. *Eur. Heart J.* 36 (18), 1106–1114. doi: 10.1093/eurheartj/ehu490

Jarrar, Y. B., Cho, S. A., Oh, K. S., Kim, D. H., Shin, J. G., and Lee, S. J. (2019). Identification of cytochrome P450s involved in the metabolism of arachidonic acid in human platelets. *Prostaglandins Other Lipid Mediat.* 141, 14–21. doi: 10.1016/j.plefa.2013.06.008

Khurana, S., Raufman, J. P., and Pallone, T. L. (2011). Bile acids regulate cardiovascular function. *Clin. Transl. Sci.* 4 (3), 210–218. doi: 10.1111/j.1752-8062.2011.00272.x

Kim, J., Lampe, J. W., Yin, T., Shinozaki, K., and Becker, L. B. (2015). Phospholipid alterations in the brain and heart in a rat model of asphyxia-induced cardiac arrest and cardiopulmonary bypass resuscitation. doi: 10.1007/s11010-015-2505-0

Liu, H., Chen, R., Wang, J., Chen, S., Xiong, C., Wang, J., et al. (2014). 1,5-diaminonaphthalene hydrochloride assisted laser desorption/ionization mass spectrometry imaging of small molecules in tissues following focal cerebral ischemia. *Anal. Chem.* 86 (20), 10114–10121. doi: 10.1021/ac5034566

Lopaschuk, G. D., Collins-Nakai, R., Olley, P. M., Montague, T. J., McNei, G., Gayle, M., et al. (1994). Plasma fatty acid levels in infants and adults after myocardial ischemia. *Am. Heart J.* 128 (1), 61–67. doi: 10.1016/0002-8703(94)90010-8

Lopaschuk, G. D., Belke, D. D., Gamble, J., Itoi, T., and Schönekess, B. O. (1994). Regulation of fatty acid oxidation in the mammalian heart in health and disease. *Biochim. Biophys. Acta* 1213, 263–276. doi: 10.1016/0005-2760(94)00082-4

Mayerhofer, C. C. K., Ueland, T., Broch, K., Vincent, R. P., Cross, G. F., Dahl, C. P., et al. (2017). Increased secondary/primary bile acid ratio in chronic heart failure. *J. Card Fail* 23 (9), 666–671. doi: 10.1016/j.cardfail.2017.06.007

Meikle, P. J., Wong, G., Barlow, C. K., and Kingwell, B. A. (2014). Lipidomics: potential role in risk prediction and therapeutic monitoring for diabetes and cardiovascular disease. *Pharmacol. Ther.* 143 (1), 12–23. doi: 10.1016/j.pharmthera.2014.02.001

Meyer, R. A., Sweeney, H. L., and Kushmerick, M. J. (1984). A simple analysis of the "phosphocreatine shuttle". *Am. J. Physiology-Cell Physiol.* 246 (5), C365–C377. doi: 10.1152/ajpcell.1984.246.5.C365

Miller, T. A., LeBrasseur, N. K., Cote, G. M., Trucillo, M. P., Pimentel, D. R., Ido, Y., et al. (2005). Oleate prevents palmitate-induced cytotoxic stress in cardiac myocytes. *Biochem. Biophys. Res. Commun.* 336 (1), 309–315. doi: 10.1016/j.bbrc.2005.08.088

Mozaffarian, D., Cao, H., King, I. B., Lemaitre, R. N., Song, X., Siscovick, D. S., et al. (2010). Circulating palmitoleic acid and risk of metabolic abnormalities and new-onset diabetes. *Am. J. Clin. Nutr.* 92 (6), 1350–1358. doi: 10.3945/ajcn.110.003970

Nixon, G. F. (2009). Sphingolipids in inflammation: pathological implications and potential therapeutic targets. *Br. J. Pharmacol.* 158 (4), 982–993. doi: 10.1111/j.1476-5381.2009.00281.x

Ohn, J. A. N. C., and Ognoni, G. I. T. (2001). A randomized trial of the angiotensin-receptor blocker. *New Engl. J. Med.* 345, 1667–1675. doi: 10.1056/NEJMoa010713

Paulson, D. J., Traxler, J., Schmidt, M., Noonan, J., and Shug, A. L. (1986). Protection of the ischaemic myocardium by L-propionylcarnitine: effects on the recovery of cardiac output after ischaemia and reperfusion, carnitine transport, and fatty acid oxidation. *Cardiovasc. Res.* 20 (7), 536–541. doi: 10.1093/cvr/20.7.536

Pfeffer, M. A. S. K., Granger, C. B., Held, P., McMurray, J. J., Michelson, E. L., Olofsson, B., et al. (2003). Effects of candesartan on mortality and morbidity

in patients with chronic heart failure: the CHARM-overall programme. *Lancet* 362 (9386), 754–755. doi: 10.1016/S0140-6736(03)14282-1

Ponikowski, P., Voors, A. A., Anker, S. D., Bueno, H., Cleland, J. G. F., Coats, A. J. S., et al. (2016). 2016 ESC Guidelines for the diagnosis and treatment of acute and chronic heart failure: the task force for the diagnosis and treatment of acute and chronic heart failure of the European Society of Cardiology (ESC) Developed with the special contribution of the Heart Failure Association (HFA) of the ESC. *Eur. Heart J.* 37 (27), 2129–2200. doi: 10.1093/eurheartj/ehw128

Randle, P. J., Newsholme, E. A., and Garland, P. B. (1964). Regulation of glucose uptake by muscle. 8. Effects of fatty acids, ketone bodies and pyruvate, and of alloxan-diabetes and starvation, on the uptake and metabolic fate of glucose in rat heart and diaphragm muscles. *Biochem. J.* 93, 652–665. doi: 10.1042/bj0930652

Randle, P. J., Garland, P. B., Hales, C. N., and Newsholme, E. A. (1963). The glucose fatty-acid cycle, Its role in insulin sensitivity and the metabolic disturbances of diabetes mellitus. *Lancet* 281 (7285), 785–789. doi: 10.1016/S0140-6736(63)91500-9

Ruiz, M., Labarthe, F., Fortier, A., Bouchard, B., Thompson Legault, J., Bolduc, V., et al. (2017). Circulating acylcarnitine profile in human heart failure: a surrogate of fatty acid metabolic dysregulation in mitochondria and beyond. *Am. J. Physiol. Heart Circ. Physiol.* 313 (4), H768–H781. doi: 10.1152/ajpheart.008202016

Sabbah, H. N. (2016). Targeting mitochondrial dysfunction in the treatment of heart failure. *Expert Rev. Cardiovasc. Ther.* 14 (12), 1305–1313. doi: 10.1080/14779072.2016.1249466

Savarese, G., Costanzo, P., Cleland, J. G., Vassallo, E., Ruggiero, D., Rosano, G., et al. (2013). A meta-analysis reporting effects of angiotensin-converting enzyme inhibitors and angiotensin receptor blockers in patients without heart failure. *J. Am. Coll. Cardiol.* 61 (2), 131–142. doi: 10.1016/j.jacc.2012.10.011

Schirone, L., Forte, M., Palmerio, S., Yee, D., Nocella, C., Angelini, F., et al. (2017). A review of the molecular mechanisms underlying the development and progression of cardiac remodeling. *Oxid. Med. Cell Longev.* 2017, 3920195. doi: 10.1155/2017/3920195

Sparagna, G. C., Hickson-Bick, D. L., Buja, L. M., and McMillin, J. B. (2004). Fatty Acid-Induced apoptosis in neonatal cardiomyocytes: redox signaling. *Antioxidants Redox Signaling* 3 (1), 71–79. doi: 10.1089/152308601750100524

Stanley, W. C., Recchia, F. A., and Lopaschuk, G. D. (2005). Myocardial substrate metabolism in the normal and failing heart. *Physiol. Rev.* 85 (3), 1093–1129. doi: 10.1152/physrev.000062004

Starling, R. C., Hammer, D. F., and Altschuld, R. A. (1998). Human myocardial ATP content and in vivo contractile function. *Mol. Cell. Biochem.* 180 (1-2), 171–177. doi: 10.1023/A.1006876031121

Sun, H., Olson, K. C., Gao, C., Prosdocimo, D. A., Zhou, M., Wang, Z., et al. (2016). Catabolic defect of branched-chain amino acids promotes heart failure. *Circulation* 133 (21), 2038–2049. doi: 10.1161/CIRCULATIONAHA.115.020226

Sun, Z., Li, Z., Zuo, L., Wang, Z., Zhou, L., Shi, Y., et al. (2017). Qualitative and quantitative determination of YiXinShu Tablet using ultra high performance liquid chromatography with Q Exactive hybrid quadrupole orbitrap high-resolution accurate mass spectrometry. *J. Sep. Sci.* 40 (22), 4453–4466. doi: 10.1002/jssc.201700619

Tanada, Y., Shioi, T., Kato, T., Kawamoto, A., Okuda, J., and Kimura, T. (2015). Branched-chain amino acids ameliorate heart failure with cardiac cachexia in rats. *Life Sci.* 137, 20–27. doi: 10.1016/j.lfs.2015.06.021

Tanai, E., and Frantz, S. (2015). Pathophysiology of Heart Failure. *Compr. Physiol.* 6 (1), 187–214. doi: 10.1002/cphy.c140055

Turer, A. T. (2013). Using metabolomics to assess myocardial metabolism and energetics in heart failure. *J. Mol. Cell Cardiol.* 55, 12–18. doi: 10.1016/j.yjmcc.2012.08.025

Vries, J. E. D., Vork, M. M., Roemen, T. H. M., Jong, Y. F. D., Cleutjens, J. P. M., Vusse, G. J. V. D., et al. (1997). Saturated but not mono-unsaturated fatty acids induce apoptotic cell death in neonatal rat ventricular myocytes. *J. Lipid Res.* 38, 1384–1394. doi: 10.1016/S0929-7855(97)00009-6

Wang, H., Chen, C., Liu, Y., Yang, X., and Xiao, H. (2015). Metabolic profile of Yi-Xin-Shu capsule in rat by ultra-performance liquid chromatography coupled with quadrupole time-of-flight tandem mass spectrometry analysis. *RSC Adv.* 5 (98), 80583–80590. doi: 10.1039/C5RA14260A

Wang, J., Qiu, S., Chen, S., Xiong, C., Liu, H., Wang, J., et al. (2015). MALDI-TOF MS imaging of metabolites with a N-(1-naphthyl) ethylenediamine dihydrochloride matrix and its application to colorectal cancer liver metastasis. *Anal. Chem.* 87 (1), 422–430. doi: 10.1021/ac504294s

Warensjö, E., Sundström, J., Vessby, B., and Risérus, T. C. U. (2008). Markers of dietary fat quality and fatty acid desaturation as predictors of total and cardiovascular mortality: a population-based prospective study. *Am. J. Clin. Nutr.* 88 (1), 203–209. doi: 10.1093/ajcn/88.1.203

Wei, J., Guo, F., Zhang, M., Xian, M., Wang, T., Gao, J., et al. (2019). Signature-oriented investigation of the efficacy of multicomponent drugs against heart failure. *FASEB J.* 33 (2), 2187–2198. doi: 10.1096/fj.201800673RR

Yang, D., Wang, X., Wu, Y., Lu, B., Yuan, A., Leon, C., et al. (2015). Urinary metabolomic profiling reveals the effect of shenfu decoction on chronic heart failure in rats. *Molecules* 20 (7), 11915–11929. doi: 10.3390/molecules200711915

Yudkoff, M., Daikhin, Y., Nissim, I., Horyn, O., Luhovyy, B., Lazarow, A., et al. (2005). Brain amino acid requirements and toxicity: the example of Leucine. *J. Nutr.* 135 (6), 15315–15385. doi: 10.1093/jn/135.6.1531S

Zhang, F., Zhan, Q., Dong, X., Jiang, B., Sun, L., Gao, S., et al. (2014). Shengxian decoction in chronic heart failure treatment and synergistic property of Platycodonis Radix: a metabolomic approach and its application. *Mol. Biosyst.* 10 (8), 2055–2063. doi: 10.1039/C4MB00055B

Zhang, J., Geng, Y., Guo, F., Zhang, F., Liu, M., Song, L., et al. (2017). Screening and identification of critical transcription factors involved in the protection of cardiomyocytes against hydrogen peroxide-induced damage by Yixin-shu. *Sci. Rep.* 7 (1), 13867. doi: 10.1038/s41598-017-10131-5

Zhang, M., Wu, H., Guo, F., Yu, Y., Wei, J., Geng, Y., et al. (2017). Identification of active components in Yixinshu Capsule with protective effects against myocardial dysfunction on human induced pluripotent stem cell-derived cardiomyocytes by an integrative approach. *Mol. Biosyst.* 13 (8), 1469–1480. doi: 10.1039/C6MB00813E

Zhao, Y., Xu, L., Qiao, Z., Gao, L., Ding, S., Ying, X., et al. (2016). YiXin-Shu, a ShengMai-San-based traditional Chinese medicine formula, attenuates myocardial ischemia/reperfusion injury by suppressing mitochondrial mediated apoptosis and upregulating liver-X-receptor alpha. *Sci. Rep.* 6, 23025. doi: 10.1038/srep23025

Zheng, Z. J., Folsom, A. R., Ma, J., Arnett, D. K., McGovern, P. G., and Eckfeldt, J. H. (1999). Plasma fatty acid composition and 6-year incidence of hypertension in middle-aged adults. *Am. J. Epidemiol.* 150 (5), 492–500. doi: 10.1093/oxfordjournals.aje.a010038

Conflict of Interest: The authors declare that the research was conducted in the absence of any commercial or financial relationships that could be construed as a potential conflict of interest.

frontiers in Pharmacology

ORIGINAL RESEARCH
published: 17 January 2020
doi: 10.3389/fphar.2019.01529

β-Asarone Inhibits Amyloid-β by Promoting Autophagy in a Cell Model of Alzheimer's Disease

Nanbu Wang[1†], *Haoyu Wang*[2†], *Lingyu Li*[2†], *Yunchuan Li*[3] *and Ronghua Zhang*[1,3*]

[1] The First Affiliated Hospital, Jinan University, Guangzhou, China, [2] College of Traditional Chinese Medicine, Jinan University, Guangzhou, China, [3] College of Pharmacy, Jinan University, Guangzhou, China

OPEN ACCESS

Edited by:
Yue Liu,
Xiyuan Hospital, China

Reviewed by:
Sheng-feng Lu,
Nanjing University of Chinese Medicine, China
Miao Qu,
Capital Medical University, China

***Correspondence:**
Ronghua Zhang
tzrh@jnu.edu.cn

[†]These authors have contributed equally to this work and share first authorship

Specialty section:
This article was submitted to Ethnopharmacology, a section of the journal Frontiers in Pharmacology

Received: 25 August 2019
Accepted: 26 November 2019
Published: 17 January 2020

Citation:
Wang N, Wang H, Li L, Li Y and Zhang R (2020) β-Asarone Inhibits Amyloid-β by Promoting Autophagy in a Cell Model of Alzheimer's Disease. Front. Pharmacol. 10:1529. doi: 10.3389/fphar.2019.01529

Alzheimer's disease (AD) is one of the most common types of dementia that causes memory, thinking, and behavior problems. The most important feature of AD is the gradual irreversible loss of cognitive ability through the formation of amyloid β (Aβ) plaques and neurofibrillary tangles composed of tau protein. The metabolism of Aβ and tau proteins is closely related to and is affected by autophagy. Current research speculates that autophagy dysfunction leads to an increase in harmful proteins in AD. β-Asarone is the main constituent of *Acorus tatarinowii* Schott and has important effects on the central nervous system. In this paper, we primarily explored the effects of β-asarone on the clearance of noxious proteins and the associated potential mechanisms *via* autophagy in a PC12 cell AD model. A CCK-8 assay and LDH experiments were used to assess cell viability/toxicity, and SPiDER-βGal was used to detect cellular senescence. The important proteins associated with the pathogenesis of AD including APP, PS1, Aβ, BACE1, and SYN1 were analyzed by immunofluorescence (IF) and Western blot analysis. Antimycin A (A3) and cyclosporine A (CSA) were selected as the activators and inhibitors of autophagy, respectively. LC3, BECN, P62, PINK1, and Parkin protein expression were also examined by IF and Western blot analysis. The data showed that β-asarone administration significantly dose-dependently increased cell proliferation and decreased cytotoxicity; moreover, β-asarone inhibited SA-βGal and improved cell senescence. The results further showed that, compared to the model, APP, PS1, Aβ, BACE1, and p62 were reduced, while SYN1, BECN1, and LC3 were increased after treatment with β-asarone. The results of Canonical Correlation Analysis (CCA) showed a highly significant relationship between the pathological factors of AD and the protein expression of autophagy. In conclusion, our study demonstrated that β-asarone can inhibit Aβ, and this effect may occur by promoting autophagy in a cell model of AD.

Keywords: β-asarone, amyloid β, Alzheimer's disease(AD), PC12, autophagy

INTRODUCTION

Alzheimer's disease (AD) is the most frequent cause of dementia, and this disease is gradually escalating into a global epidemic among older adults. The major neuropathological features of AD are widely described: amyloid β (Aβ) plaques and neurofibrillary tangles, but no treatment has changed its progression (Loera-Valencia et al., 2019; Reddy et al., 2019). Apart from these clear pathological lesions, the brain's immune response also undergoes dramatic changes, including dramatic changes in microglia and astrocyte phenotypes (Henstridge et al., 2019). Although research on the pathogenesis of AD continues to be controversial, the Aβ peptide is considered to be a central player (Vassa, 2004). The drugs that have successfully completed clinical trials and are approved for the clinical treatment of AD are all based on the neuroprotective hypothesis, that is, they are all agonists or antagonists of neurotransmitter production or neurotransmitter receptors, they are based on the drugs developed by other hypotheses and are still in the stages of basic research and early clinical trials, and their prospects are still unclear (Tricco et al., 2018; von Arnim et al., 2019). Donepezil (Aricept) is a centrally acting reversible acetyl cholinesterase (AChE) inhibitor which could increase the content of ACh and improving the cognitive function of patients with AD (Reardon, 2018).

Autophagy dysfunction may lead to an increase in harmful proteins in the AD brain (Steele and Gandy, 2013; Uddin et al., 2018). Studies have reported that in AD, the maturation of autophagosomes and their retrograde pathways to neuronal bodies are impeded (Nixon, 2007). Mitophagy is the selective degradation of mitochondria by autophagy. Studies have shown that Aβ inhibits mitophagy while mitophagy induction reduces Aβ in AD *Caenorhabditis elegans*, mice, and humans (Palikaras et al., 2015; Fang et al., 2019).

On the other hand, *Acorus tatarinowii* Schott (ATS) is a commonly used herbal medicine. Previous studies have shown that this herb has positive effects on neurodegenerative diseases, such as Parkinson's disease and AD, hypoxic-ischemic encephalopathy, and cerebrovascular diseases (Fang et al., 2003; Li et al., 2010). During the previous study, researchers found the main component of ATS volatile oil is β-asarone, followed by α-asarone and γ-asarone, as determined by the total ion current (TIC). β-Asarone (cis-2,4,5-tri-methoxy-1-allyl phenyl) is the main constituent of ATS and plays an important role in the central nervous system (Deng et al., 2016; Ning et al., 2019). Our previous study showed that β-asarone may help cancer treatment by promoting temozlomide's entry into glioma U251 cells (Wang et al., 2017). At the same time, it can affect autophagy for the therapy of antitumor and lead the drug through the blood–brain barrier (BBB) or the membrane (Wang et al., 2018). Here, we report preliminary data showing that β-asarone can protect PC12 cells against $A\beta_{42}$ induced injury. At the same time, we used antimycin A (A3) as the autophagy activator and cyclosporine A (CSA) and 3-methyladenine (3MA) as autophagy inhibitors. Here we propose that β-asarone could protect a PC12 cell model against $A\beta_{1\text{-}42}$ damage, and this process should occur by promoting autophagy.

MATERIALS AND METHODS

Reagents

The $A\beta_{1\text{-}42}$ used in these experiments was acquired from Life Technologies (USA); β-asarone was purchased from NIFDC (Beijing, China), and the purity value is 96.8%; donepezil was obtained from the First Affiliated Hospital of Jinan University (Guangzhou, China); A3 was purchased from Santa Cruz Biotechnology (Santa Cruz, CA, USA); CSA was purchased from Selleck (Houston, Texas, USA); 3MA, high-glucose DMEM, FBS, trypsin, and PBS were obtained from Gibco (Gaithersburg, MD, USA); Cell Counting Kit-8 (CCK-8), Cytotoxicity LDH Assay Kit—WST (LDH), and Cellular Senescence Detection Kit—SPiDER-βGal were obtained from Dojindo Molecular Technologies, Inc. (Tokyo, Japan); the bicinchoninic acid (BCA) protein assay kit, Immunol Fluorescence Staining Kit, and Immunohistochemistry Staining Kit were obtained from Beyotime (Shanghai, China); anti-SQSTM1/P62, anti-BECN, anti-LC3 II, anti-beta amyloid, anti-BACE1, anti-synapsin1, anti-Parkin, anti-Pink1, anti-APPL, and anti-PS1 were obtained from Abcam (Cambridge, UK).

Cell Culture and Handing

Highly differentiated PC12 cell was purchased from Shanghai BCB (TCR9). The cells were maintained in DMEM containing 10% FBS and 1% penicillin/streptomycin at 37°C in a humidified 5% CO_2 atmosphere.

Preparation of Oligomerization $A\beta_{1\text{-}42}$

$A\beta_{1\text{-}42}$ is the component found in amyloid plaques, and it has 42 amino acids. First, we allow lyophilized $A\beta_{1\text{-}42}$ to equilibrate at room temperature for 30 min to avoid condensation upon opening the peptide vial. Under the fume hood, re-suspend $A\beta_{1\text{-}42}$ peptide in ice-cold HFIP to obtain a 1 mM solution and vortex the solution for a few seconds. Using a glass GasTight Hamilton syringe with Teflon plug, quickly divide the $A\beta_{1\text{-}42}$/HFIP solution equally into three polypropylene vials and seal the vials. It was dissolved to a concentration of 100 μg/μl in 100% DMSO and kept at 4°C. Then it was resuspended in 100% DMSO, dissolved to a concentration of 100 μg/μl, and transferred to 4°C for 24 h to prepare an oligomer for use.

$A\beta_{1\text{-}42}$ is the component found in amyloid plaques, and it has 42 amino acids. We used gradient concentrations of $A\beta_{1\text{-}42}$ (0, 2.215, 4.43, 8.86, 17.72 μM) induced PC12 cell for 6, 12, 24, and 48 h (Neta et al., 2019). Cellular viability and toxicity were detected by CCK8 and LDH assays.

For cell growth and pharmacodynamics analyses, the cells were divided into six groups: normal group (PC12 cells), model group (culture with 7 μM $A\beta_{1\text{-}42}$), β-asarone 24, 36, 72 μM, and donepezil 9.6 μM groups. For autophagy analyses, the cells were divided into six groups: normal group (PC12 cells); model group (cultured with 7 μM $A\beta_{1\text{-}42}$); β-asarone 36 μM, A3 1 μM, CSA 20 μM, and 3MA 200 μM.

Cell Proliferation and Cytotoxicity

Cell viability was detected using the CCK-8 assay. For the CCK-8 assay, PC12 cells were seeded in 96-well plates and cultured

for 24 h. The absorbances were measured at 450 nm. Each group of experiments included six replicates and was repeated three times.

Cell damage was assessed by measuring LDH activity in PC12 cell supernatants using the LDH kit according to the manufacturer's protocol. In brief, 10 μl lysis buffer was added to high control at 24 h after drug treatment and incubated for 30 min at room temperature. Subsequently, 100 μl of working solution was added to each well. The plate was protected from light and incubated at 37°C for 30 min.

Cellular Senescence Detection

PC12 cells were treated as the above groups. The culture medium was discarded, and the cells were washed with 2 ml HBSS once. Bafilomycin A1 working solution and SPiDER-βGal 1 ml were added in sequence to the culture for 1 h and 30 min, respectively. Then, the cells were washed with HBSS once again. All the data were observed under a fluorescence microscope.

Immunofluorescence Analysis

We examined the expression of BACE1, APP, PS1, SYN1, LC3, BECN, and P62 with immunofluorescence (IF). PC12 cells were treated by grouping. Then, endogenous peroxidase activity was quenched for 10 min in PBS containing 3% H_2O_2, and the cells were chilled in water, and then immersed for 5 min in PBS. Sections were then incubated in anti-rabbit BACE1 (diluted 1:200), APP (diluted 1:100), PS1 (diluted 1:100), SYN1 (diluted 2:100), LC3 (diluted 1:100), BECN (diluted 1:100), and P62 (diluted 1:100) for 60 min at 37°C. Then the slides were set with SABC-FITC (diluted 1:200) and DAPI (1:5,000) for 5 min. Next, the cells were mounted with an anti-fluorescent quencher and blocked, and the specimen was visualized using a fluorescence microscope.

All the data were analyzed with ImageJ with integrated density. Each column in the results table calculates and displays the mean, standard deviation, minimum, and maximum of the values in that column.

Western Blot Analysis

The AD pathology-related proteins BACE1, APP, PS1, Aβ, and SYN1 and the autophagy/mitophagy-related proteins LC3, BECN, P62, PINK1, and Parkin were also detected with WB. The cells were cultured in six-well plates for the above six groups. Protein samples were extracted from the cells by suspension in radioimmunoprecipitation assay (RIPA) buffer. Then the protein concentrations were determined using the Bradford protein method and the BCA protein assay kit. The membranes were washed twice, blocked for 10 min, and incubated for 24 h with antibodies to detect BACE1 (1:1,000), APPL (1:1,000), PS1 (1:1,000), Aβ (1:1,000), SYN1 (1:1,000), LC3 (1:400), BECN1 (1:2,000), PINK1 (1:1,000), Parkin (1:1,000), and actin (1:5,000). Then followed by horseradish peroxidase (HRP)–conjugated secondary antibodies (1:2,000). The membranes were washed three times, and then visualized by enhanced chemiluminescence kit prior to analysis with photographic imaging equipment. All the data were analyzed with Image lab; all bands were compared with actin first.

Statistical Analysis

All data were expressed as the means ± standard deviation. Differences between two groups were analyzed using the t-test, and differences among three or more groups were analyzed using single-factor analysis of variance (one-way ANOVA) with SPSS. Differences were considered statistically significant at $P < 0.05$.

Since two sets of variables existed and the outcome set included more than one variable, the Canonical Correlation Analysis (CCA) method was performed (RStudio). We used the IF results of APP, PS1, BACE1, and SYN1 compared to BECN, P62, and LC3. The results and coefficients of the correlation analysis are expressed in heat maps.

RESULTS

$A\beta_{1\text{-}42}$ Induced PC12 Cell Model of AD in Gradient Concentrations and Times

To establish the AD cell model, we cultured PC12 cells *in vitro*, and $A\beta_{1\text{-}42}$ was added into the medium in different concentrations and time points. As the concentration of $A\beta_{1\text{-}42}$ and time increased, PC12 cell viability decreased in a dose-dependent manner; at the same time, cytotoxicity LDH increased (**Figures 1A, B**). We calculated LD50 with the Quest Graph™ LD50 Calculator (MLA, 2019) and chose 7 μM at 12 h as the experiment condition. The normal PC12 cells have a clear outline, and the shape is mostly round, spindle-shaped, and elliptical. The cells were also clustered while the dendrites were clearly visible. While the cells were damaged by 7 μM $A\beta_{1\text{-}42}$ for 12 h, the appearances of cells were shrinking and flat, and protuberances disappeared (**Figure 1C**). Moreover, senescent cells also clearly increased in cells treated with $A\beta_{1\text{-}42}$ (**Figure 1D**, n = 6).

B-Asarone Inhibited Cell Damage in the $A\beta_{1\text{-}42}$ PC12 Cell Model of AD

After we established a stable AD cell model, we investigated the effects of gradient concentrations of β-asarone (12, 24, 36, 72, 144 μM) or donepezil (10, 20, 40 μM). We found that the protective effect of β-asarone on cell proliferation was dose-dependent; the low-dose group showed better protective effect than the high-dose group. PC12 cells grew dose-dependent in 12 to 36 μM; when the concentration was increased to 72 μM, the proliferation capacity of PC12 cells started to decrease (**Figure 2A**). We chose 24, 36, and 72 μM of β-asarone and 9.6 μM of donepezil as the working concentration, respectively. Compared with model cells, β-asarone and donepezil both improved cell proliferation and decreased cell damage (**Figures 2B, C**). At the same time, they also decreased the cell senescence rate (**Figure 2D**).

β-Asarone Suppressed the Expression of APP, PS1, Aβ, and BACE1 While Promoting SYN1

Overexpression of Aβ plaques deposition is the major neuropathological feature of AD. Aβ generation is initiated by the proteolysis of APP by BACE1. Synaptophysin (SYN) is a

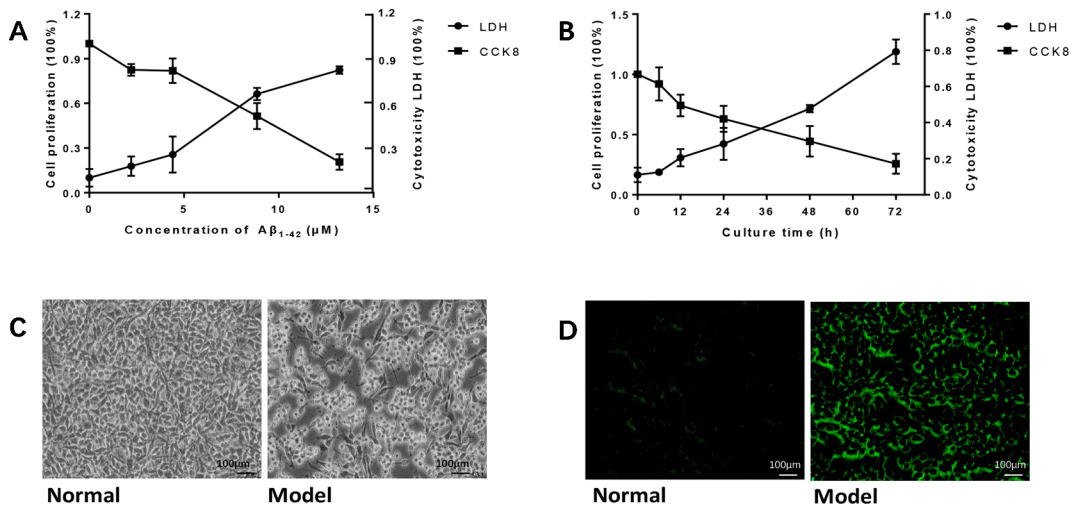

FIGURE 1 | Amyloid $\beta_{1\text{-}42}$ ($A\beta_{1\text{-}42}$) induced PC12 cell model of Alzheimer's disease (AD) in gradient concentrations and times. **(A)** PC12 cells were cultured with $A\beta_{1\text{-}42}$ 0, 2.215, 4.43, 8.86, 17.72 μM; $A\beta_{1\text{-}42}$ decreased cell viability and increase cytotoxicity in a dose-dependent manner; 1/2 LD_{50} was 7 μM (Quest Graph™ LD_{50} Calculator. **(B)** PC12 cells were cultured with 7 μM $A\beta_{1\text{-}42}$ for 6, 12, 24, 48, and 72 h; 12h was the best as 1/2 LD_{50}. **(C)** Cell morphology was also clearly changed while the cells were cultured by $A\beta_{1\text{-}42}$ for 12 h (×150), scale bar 100 μm; the appearances of cells were shrinking and flat, and protuberances disappeared. **(D)** Cellular senescence (green) was observed by fluorescence microscopy (excitation: 488 nm, emission: 500–600 nm), scale bar 100 μm. Senescent cells also increased in model group. The experiments were repeated twice independently with similar results.

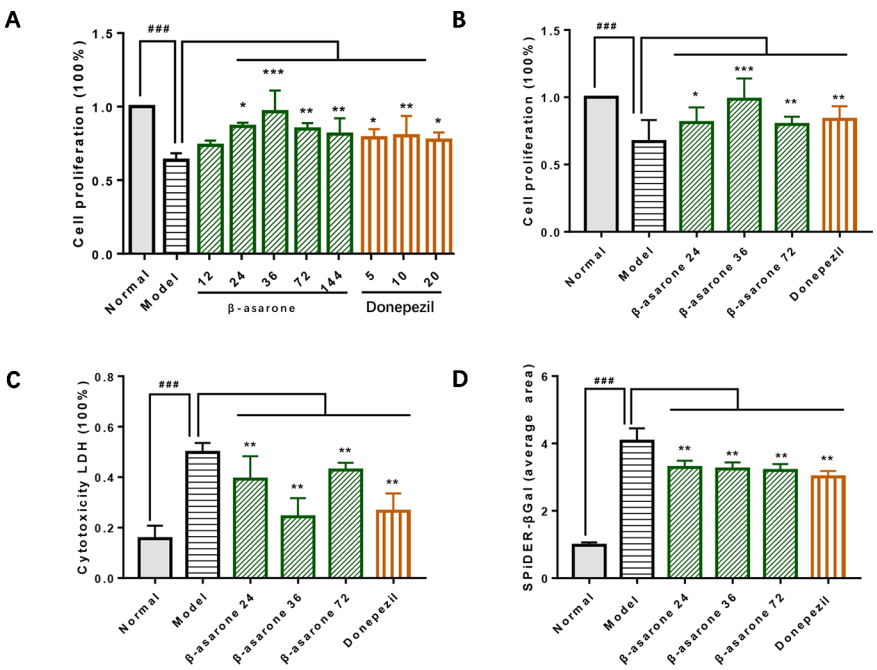

FIGURE 2 | β-Asarone inhibited cell damage in $A\beta_{1\text{-}42}$ PC12 cell model of AD. **(A)** PC12 cells were treated with 7 μM $A\beta_{1\text{-}42}$ for 12 h; then we cultured cells with β-asarone 12, 24, 36, 72, 144 μM or donepezil 10, 20, 40 μM for another 12 h. Cell proliferation was examined with CCK8; β-asarone 24, 36, and 72 μM and donepezil 9.6 μM were the optimal dosage in inhibiting cell damage. **(B)** After culturing with the above group dosage, CCK8 analysis showed that cell proliferation was improved in β-asarone 24, 36, and 72 μM and donepezil 9.6 μM. **(C)** Cytotoxicity LDH was also detected; cell damage was improved in β-asarone 24, 36, and 72 μM and donepezil 9.6 μM. **(D)** The average area of SPiDER-βGal was examined with ImageJ; the senescent cells were all mitigated significantly compared with model cells. (Compared with normal group, $^{\#}P < 0.05$, $^{\#\#}P < 0.01$, $^{\#\#\#}P < 0.001$; compared with model group, $^{*}P < 0.05$, $^{**}P < 0.01$, $^{***}P < 0.001$; one-away ANOVA, n = 9).

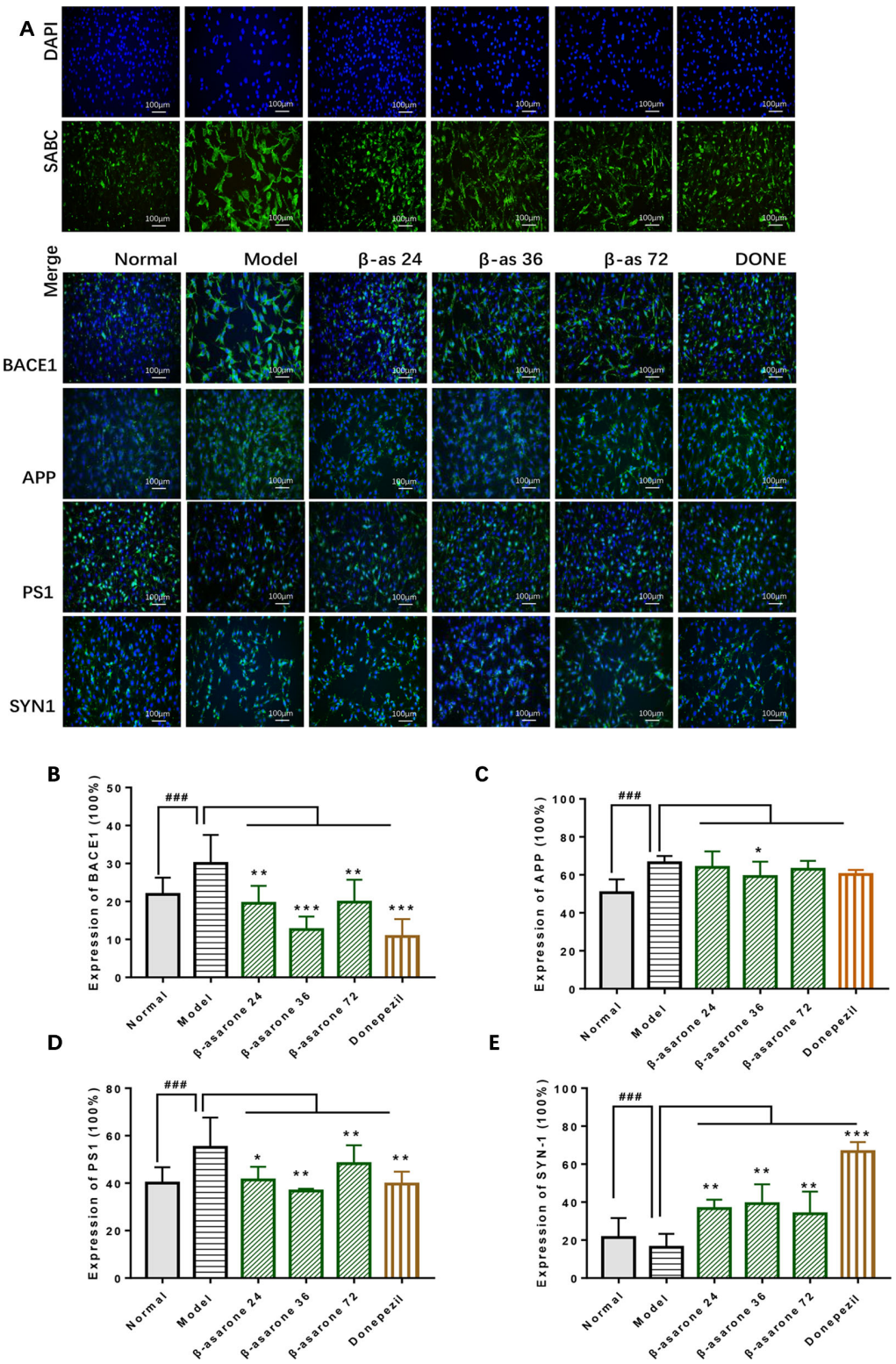

FIGURE 3 | Continued

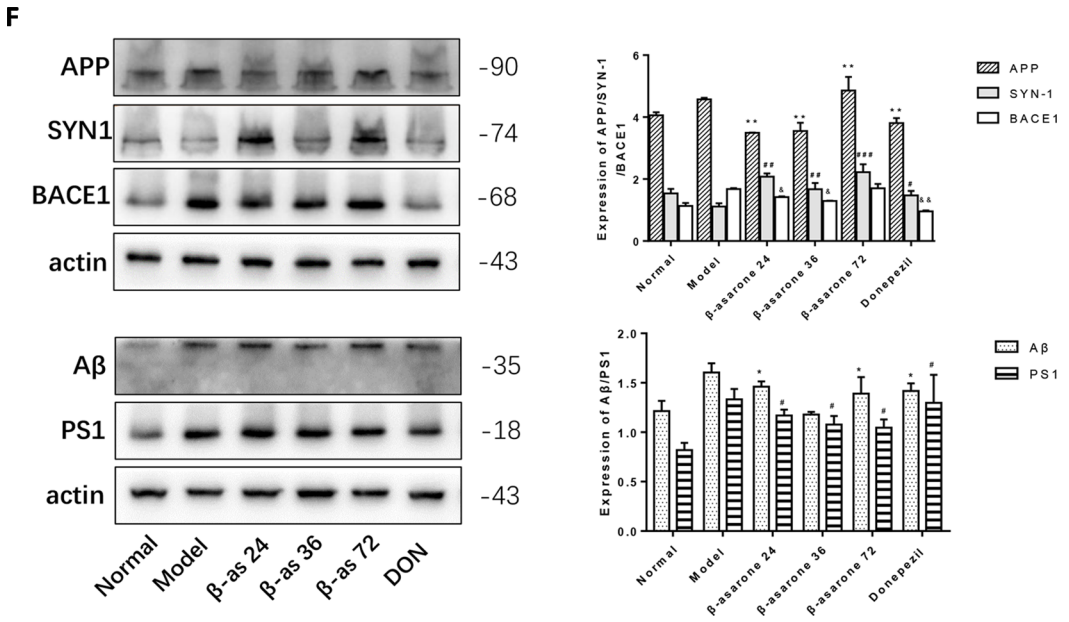

FIGURE 3 | β-Asarone induction ameliorated Aβ pathology and synaptic damage in $Aβ_{1-42}$ PC12 cell model of AD. PC12 cells were treated with 7 μM $Aβ_{1-42}$ for 12 h; then we cultured the model cells with β-asarone 24, 36, 72 μM or donepezil 9.6 μM for another 12 h. **(A)** IF microscopy and data analysis of BACE1 **(B)**, APP **(C)**, PS1 **(D)**, and SYN-1 **(E)** showed: compared with normal group, APP, PS1, and BACE1 all increased significantly. β-asarone could decrease the expression of BACE1, APP, and PS1; donepezil was effective in reducing the expression of BACE1 and PS1. SYN-1 were all improved after culture with them. (Compared with normal group, $^{\#}P < 0.05$, $^{\#\#}P < 0.01$, $^{\#\#\#}P < 0.001$; compared with model group, $^{*}P < 0.05$, $^{**}P < 0.01$, $^{***}P < 0.001$; one-away ANOVA, n = 6). **(F)** Western blot data showed the effects of β-asarone on the expression levels of proteins involved, APP, SYN-1, BACE1, Aβ, and PS1. β-asarone suppressed the expression of APP, PS1, Aβ, and BACE1 and promoted SYN1. (Compared with model group, $^{*}P < 0.05$, $^{**}P < 0.01$, $^{***}P < 0.001$; one-away ANOVA, n = 6).

major integral membrane glycoprotein of neuronal synaptic vesicles, is present in virtually all synapses, and shows a high degree of evolutionary conservation across mammals. To investigate the protective role of β-asarone against AD pathology, we monitored the effects of β-asarone and donepezil in cell model with IF (**Figures 3A, F**) and Western blotting. β-Asarone suppressed the expression of BACE1 (**Figure 3B**), APP (**Figure 3C**), PS1 (**Figure 3D**), and Aβ (**Figure 3F**), while it promoted SYN1 (**Figure 3E**).

β-Asarone Promoted the Expression of LC3 I/II, BECN, PINK1, and Parkin While It Inhibited P62

In the PC12 cell AD model, we found that autophagy was inhibited. The Western blot expression levels of LC3 I/II and BECN were decreased while P62 showed the opposite effect (**Figure 4A**). We used A3 as an autophagy activator and CSA and 3MA as autophagy inhibitors. Hence, to choose the optimal dosage, we detected them in gradient concentrations and analyzed the data. The final concentrations we selected of A3 (**Figure 4B**), CSA (**Figure 4C**), and 3MA (**Figure 4D**) were 1, 20, and 200 μM, respectively.

PINK1 and Parkin were shown to mediate the degradation of damaged mitochondria *via* selective autophagy (mitophagy). We next examined whether β-asarone could affect autophagy and mitophagy function with IF and Western blot. Clearly we could declare from the IF result (**Figure 5A**) that β-asarone could promote autophagy *via* an increase in the expression of LC3 I/II and BECN (**Figures 5C, D**). But p62 has little change (**Figure 5B**). Moreover, we preliminary found β-asarone could induce PINK1 (**Figure 5E**). Because autophagy failure was supposed to be the major driver of cell death in AD, our results suggested that β-asarone could protect AD cells by promoting autophagy in a model of AD.

Autophagy Defects Have a Critical Role in the Formation of the AD Pathological State

Compared with model group, β-asarone and A3 both decreased the expression of PS1. β-Asarone can promote the occurrence of autophagy and reduce PS1 (**Figure 6A**). This also gives us some hints that β-asarone can promote the occurrence of autophagy; at the same time, it can reduce the expression of AD-related proteins. To further prove this result, we did a correlation analysis. The results of CCA showed a highly significant relationship between the pathological factors of AD and the autophagy proteins expressed (**Figure 6B**). Basically, of the core proteins in autophagy that we chose, P62 was negatively correlated with BECN and LC3. PS1 was negative with BECN and LC3, which suggests that the increase in PS1 is most likely due to the destruction of autophagy. On the other hand, SYN1 was also negatively correlated with PS1 (**Figure 6C**).

DISCUSSION

AD is one of the most common causes of mental deterioration in elderly adults, accounting for approximately 50%–60% of the

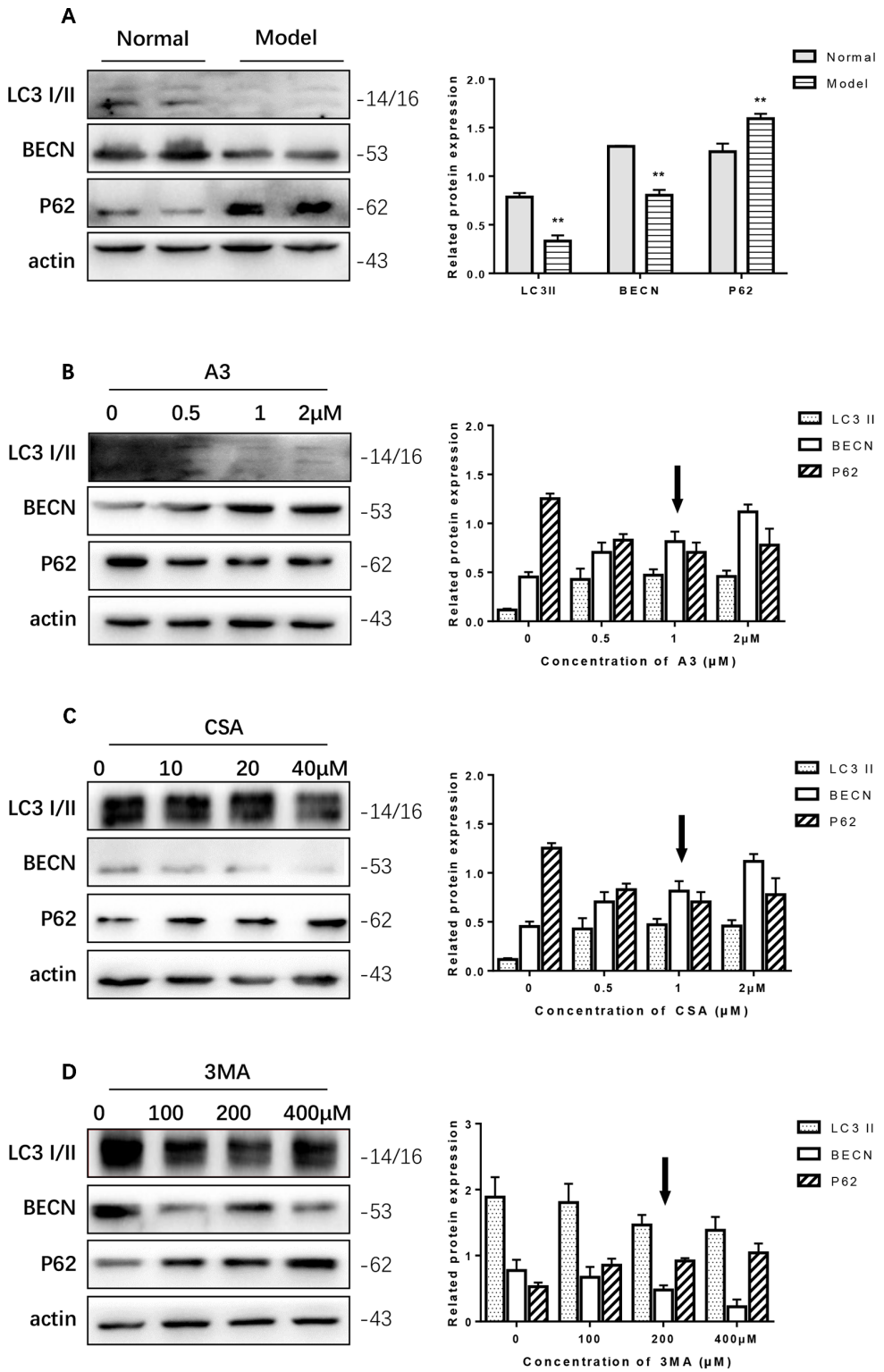

FIGURE 4 | Optimum concentration of antimycin A (A3), cyclosporine A (CSA), and 3-methyladenine (3MA) for $A\beta_{1-42}$ PC12 cell model of AD. **(A)** Autophagy-related protein changed in AD cell model. Compared with normal pc12 cells, the expression of LC3 I/II and Beclin-1 increased while p62 decreased after culturing with 7 μM $A\beta_{1-42}$ for 12 h. (Compare with the normal group, **P < 0.01). AD cells were treated with **(B)** A3 0.5, 1.2 μM, **(C)** CSA 10, 20, 40 μM, **(D)** 3MA 100, 200, 400 μM for 12 h. Then the autophagy-related proteins were examined with Western blot. The optimum concentration of them were as follows: A3 1 μM, CSA 20 μM, and 3MA 200 μM respectively.

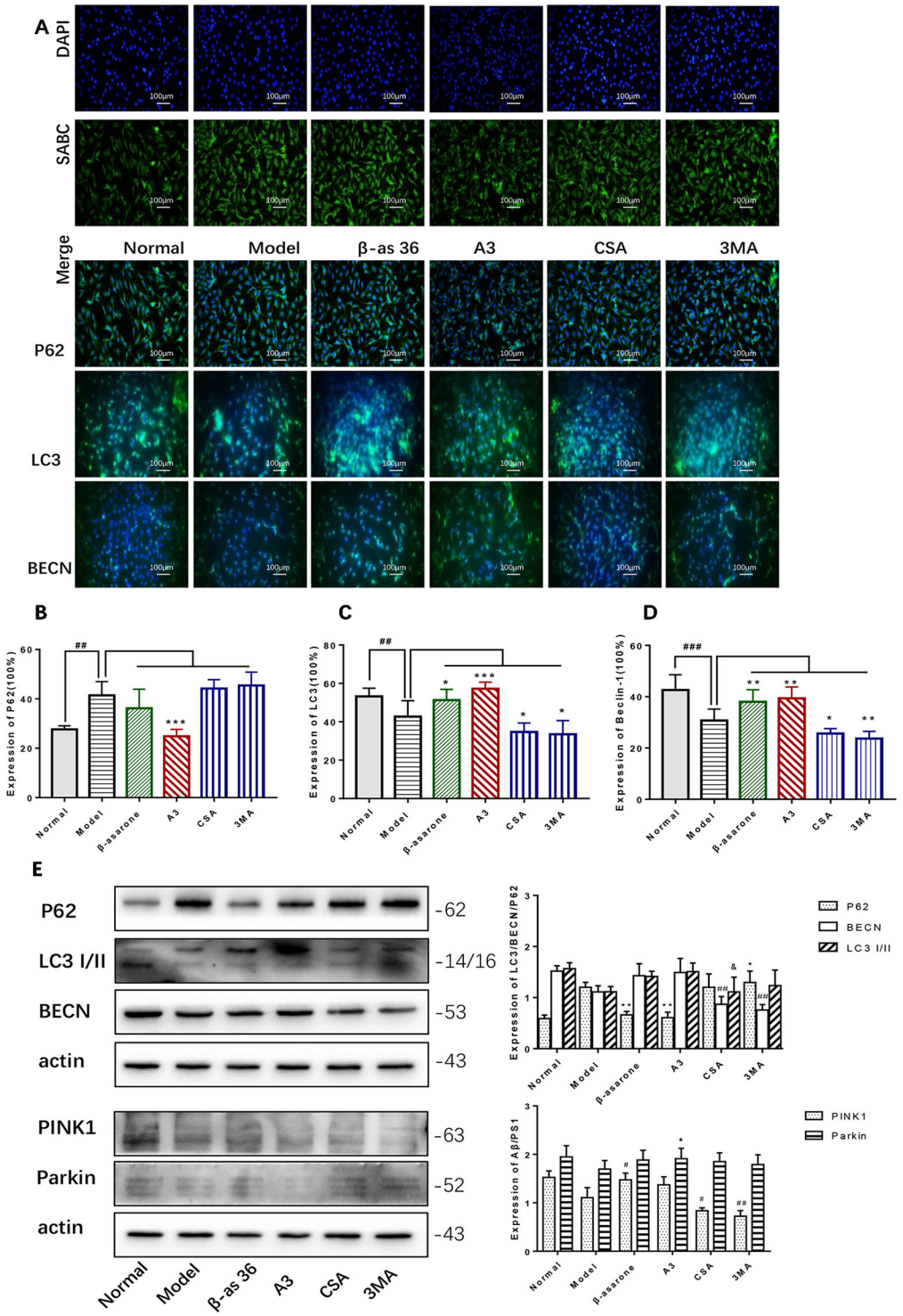

FIGURE 5 | β-asarone promoted autophagy- and mitophagy-related proteins in $A\beta_{1\text{-}42}$ PC12 cell model of AD. PC12 cell was treated with 7 μM $A\beta_{1\text{-}42}$ for 12 h; then we cultured the model cells with β-asarone 36 μM, A3 1 μM, CSA 20 μM, and 3MA 200 μM respectively for another 12 h. **(A)** Immunofluorescence (IF) microscopy and data analysis of P62 **(B)**, LC3 **(C)**, and BECN **(D)** showed: compared with normal group, P62 increased while LC3 and BECN decreased; β-asarone could improve the expression of LC3 and BECN. (Compared with normal group, $^{\#}P < 0.05$, $^{\#\#}P < 0.01$, $^{\#\#\#}P < 0.001$; compared with model group, $^{*}P < 0.05$, $^{**}P < 0.01$; one-away ANOVA, n = 6). **(E)** Western blot data showed the effects of β-asarone on the expression levels of proteins involved P62, LC3, BECN, PINK1, and Parkin. β-asarone showed effect on reducing P62 and improving PINK1. (Compared with model group, $^{\#}P < 0.05$, $^{\#\#}P < 0.01$; $^{*}P < 0.05$, $^{**}P < 0.01$; $^{\&}P < 0.05$; one-away ANOVA, n = 6).

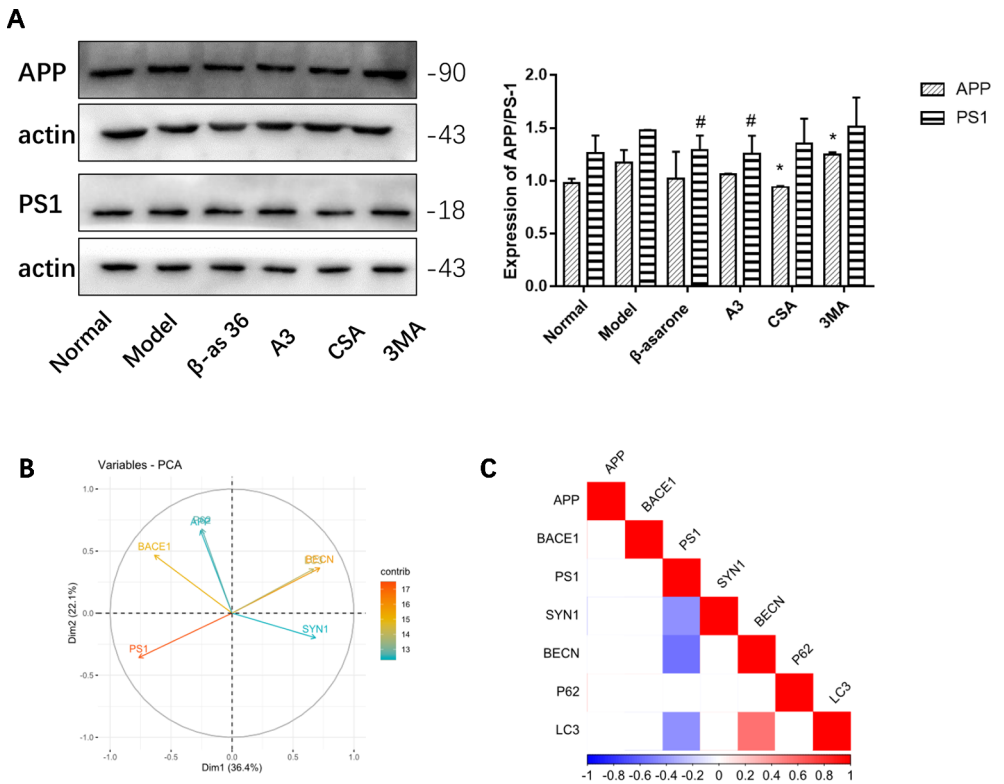

FIGURE 6 | The relationships of AD and autophagy factors. **(A)** Representative Western blotting bands using total protein extracts from the cells. Compared with model group, β-asarone and A3 both decreased the expression of PS1. β-asarone can promote the occurrence of autophagy and reduce PS1. (Compare with normal group ,$^{\#}p < 0.05$; compare with model group, $^{*}p < 0.05$; one-away ANOVA, n=6). **(B)** The results of Canonical Correlation Analysis (CCA) showed a highly significant relationship between the pathology factor of AD and protein expression of autophagy. **(C)** $P < 0.05$ was not shown; basically P62 was negatively correlated with BECN (r = –0.68, $P = 0.149$) and LC3 (r = –0.119, $P = 0.06$); BECN and LC3 were positively related ($r^2 = 0.547$, $P = 0.006$). PS1 was negatively correlated with BECN1 ($r^2 = –0.556$, $P = 0.005$) and LC3 ($r^2 = –0.430$, $P = 0.040$). Furthermore, PS1 was also negatively correlated with SYN1 ($r^2 = –0.424$, $P = 0.041$) (Pearson correlation coefficient, n = 28).

total dementia in people over 65 years of age (Park et al., 2019). In the past two decades, researchers have made great efforts to explore and discover the cause of AD, and ultimately hope to develop safe and effective therapeutic drugs (Pansieri et al., 2019). There are different hypotheses about the onset of the disease so far; the clinical drugs developed for AD are all based on protecting cholinergic and non-cholinergic neurons from the neurochemical and histopathological changes that occur in AD. Currently, there are no treatments available to alleviate AD or control its progression. The discovery and development of cholinesterase inhibitors of AD is recognized as one of the most effective treatments to improve mood changes and reduce movement disorders. However, clinical follow-up studies have found that these treatments do not effectively prevent AD progression, and do not perform well in improving patients' memory impairment and daily life.

Aβ fulfills a central role in AD pathogenesis, and reduction in Aβ levels should prove beneficial for AD treatment. The generation of Aβ is initiated by the proteolysis of APP by BACE1 (Cole and Vassar, 2008). As such, many institutes have been experimenting with blocking this production by producing BACE1 inhibitors. However, over the years, these have proven unsuccessful for a variety of reasons. Several trials of BACE1 inhibitors have been suspended due to their inability to improve AD symptoms or because of adverse side effects, despite reducing Aβ plaque formation. Many scientists think that BACE inhibitors fail as they prevent amyloid production later in the course of illness and may be more effective if used earlier. Trials failing on safety issues may be due to the structure of the drug (MLA, 2018).

As a commonly used herb belonging to the Acoraceae family, ATS has been reported in the literature for its effects on nervous system diseases such as neurodegenerative diseases, hypoxic-ischemic encephalopathy, and cerebrovascular diseases (Zhu et al., 2014). β-Asarone is the main effective component of ATS volatile oil. The molecular mass of β-asarone is 208. It is fat soluble and can easily pass the BBB and distribute mainly into the brain (Ning et al., 2019).

In this study, we focused on the pharmacological activities of β-asarone in a stable AD cell model. Groups included gradient concentrations of β-asarone and donepezil. Donepezil hydrochloride is the only new drug approved by both the FDA

and MCA for the symptomatic treatment of mild and moderate AD, so we chose it as positive control drug (Petersen et al., 2005). The cell proliferation and LDH experiments showed that both β-asarone and donepezil could improve the growth of model cells. Furthermore, it could also affect BACE1, and whether this could be an effective BACE inhibitor needs to be further verified with experimentation.

Based on the above results, we confirmed that this mechanism is the basis of the protective effect of β-asarone in AD. We also demonstrated that it has a significant therapeutic effect against toxic protein deposition. At the same time, β-asarone could also improve the expression of SYN1, which should destroy the superoxide anion radicals produced in cells that are toxic to biological systems. So, it plays a dual role of inhibition and promoting binding by eliminating metabolic toxicants and nutritional synapses.

Here we used LC3 I/II, BECN, P62, PINK1, and Parkin as indicators to detect autophagy. As the most important marker of autophagy, LC3 is now widely used to monitor autophagy. Thus, the detection of LC3 conversion (LC3-I to LC3-II) analysis is more correct because the amount of LC3-II is related to the number of autophagosomes (Mizushima and Yoshimori, 2007). BECN was the first mammalian gene which plays a role in mediating autophagy (Sun and Peng, 2008). P62 is a selective substrate for autophagy and delivers aggregates for autophagy degradation *via* LC3 interaction regions (Johansen and Lamark, 2011). Recently, PINK1 and Parkin have been implicated in the same signaling pathway to regulate mitochondrial clearance through the recruitment of Parkin by the stabilization of PINK1 on the outer membrane of depolarized mitochondria (Lazarou et al., 2015). The PINK1-dependent pathway also eliminates proinflammatory cytokines in AD microglia (Ye et al., 2015).

Our study's statistical significance and effect sizes demonstrate that there is a remarkable relationship between AD and autophagy. These findings provide evidence that autophagy is suppressed in an AD cell model, and that β-asarone plays a critical role in restoring autophagy. More broadly, we also detected the expression of PINK1 and Parkin; β-asarone can also affect mitophagy and improve energy metabolism.

However, it also raises many important questions, such as: (1) Does β-asarone only work by clearing the misfolded protein? (2) AD is a progressively aggravating disease. When is the best time for the application of β-asarone? While it is difficult to address these questions with cell models, we are conducting related animal experiments to further explain this problem.

CONCLUSION

In conclusion, our analyses provided evidence that autophagy defects have a critical role in AD development and progression. β-Asarone could protect the PC12 cell model against the formation and damage of $A\beta_{1\text{-}42}$, and this process should occur by promoting autophagy. Therefore, targeting autophagy at the neuronal and biological levels may be a promising therapeutic approach.

DATA AVAILABILITY STATEMENT

All datasets generated for this study are included in the article/ **Supplementary Material**.

ETHICS STATEMENT

All the experiments complied with ARRIVE guidelines and were carried out in strict accordance with the recommendations in the Guide for the Care and Use of Laboratory Cells of Jinan University.

AUTHOR CONTRIBUTIONS

Study design: RZ and NW. Study conduct: NW, HW, and YL. Data collection: HW, LL, and YL. Data analysis: NW and HW. Data interpretation: NW. Drafting manuscript: NW, HW, YL, and LL. Approving the final version of the manuscript: all authors.

FUNDING

This work was supported by the National Natural Science Foundation of China (81903971), General Program of China Postdoctoral Science Foundation (2018M643377), and National Key R&D Program of China (2018YFC2002500).

SUPPLEMENTARY MATERIAL

The Supplementary Material for this article can be found online at: https://www.frontiersin.org/articles/10.3389/fphar.2019.01529/full#supplementary-material

REFERENCES

Cole, S. L., and Vassar, R. (2008). The role of amyloid precursor protein processing by BACE1, the beta-secretase, in Alzheimer disease pathophysiology. *J. Biol. Chem.* 283 (44), 29621–29625. doi: 10.1074/jbc.R800015200

Deng, M., Huang, L., Ning, B., Wang, N., Zhu, C., and Fang, Y. (2016). β-asarone improves learning and memory and reduces Acetyl Cholinesterase and Beta-amyloid 42 levels in APP/PS1 transgenic mice by regulating Beclin-1-dependent autophagy. *Brain Res.* 1652, 188–194. doi: 10.1016/j.brainres.2016.10.008

Fang, Y., Li, L., and Wu, Q. (2003). Effects of beta-asaron on gene expression in mouse brain. *Zhong Yao Cai* 26 (9), 650–652.

Fang, E. F., Hou, Y., Palikaras, K., Adriaanse, B. A., Kerr, J. S., Yang, B., et al. (2019). Mitophagy inhibits amyloid-β and tau pathology and reverses cognitive deficits in models of Alzheimer's disease. *Nat. Neurosci.* 22 (3), 401–412. doi: 10.1038/s41593-018-0332-9

Henstridge, C. M., Hyman, B. T., and Spires-Jones, T. L. (2019). Beyond the neuron-cellular interactions early in Alzheimer disease pathogenesis. *Nat. Rev. Neurosci.* 20 (2), 94–108. doi: 10.1038/s41583-018-0113-1

Johansen, T., and Lamark, T. (2011). Selective autophagy mediated by autophagic adapter proteins. *Autophagy* 7 (3), 279–296. doi: 10.4161/auto.7.3.14487

Lazarou, M., Sliter, D. A., Kane, L. A., Sarraf, S. A., Wang, C., Burman, J. L., et al. (2015). The ubiquitin kinase PINK1 recruits autophagy receptors to induce mitophagy. *Nature* 524 (7565), 309–314. doi: 10.1038/nature14893

Li, C., Xing, G., Dong, M., Zhou, L., Li, J., Wang, G., et al. (2010). Beta-asarone against beta-amyloid-induced neurotoxicity in PC12 cells *via* JNK signaling and modulation of Bcl-2 family proteins. *Eur. J. Pharmacol.* 635 (1–3), 96–102. doi: 10.1016/j.ejphar.2010.03.013

Loera-Valencia, R., Cedazo-Minguez, A., Kenigsberg, P., Page, G., Duarte, A., Giusti, P., et al. (2019). Current and emerging avenues for Alzheimer's disease drug targets. *J. Intern. Med.* 286, 398–437. doi: 10.1111/joim.12959

Mizushima, N., and Yoshimori, T. (2007). How to interpret LC3 immunoblotting. *Autophagy* 3 (6), 542–545. doi: 10.4161/auto.4600

MLA. (2018). *Another BACE inhibitor fails in phase III trials* (AAT Bioquest Corporate: Drug Development Technology, Inc). https://www.drugdevelopment-technology.com/comment/another-bace-inhibitor-fails-phase-iii-trials/.

MLA. (2019). *Quest Graph™ LD50 Calculator* (AAT Bioquest, Inc). https://www.aatbio.com/tools/ld50-calculator.

Neta, Z.-H., Michal, R., Michal, R., Ronen, Y., Hadas, S., et al. (2019). Neuroprotective effect of nerve growth factor loaded in porous silicon nanostructures in an Alzheimer's Disease model and potential delivery to the brain. *Small.* 15 (45), e1904203. doi: 10.1002/smll.201904203

Ning, B., Zhang, Q., Wang, N., Deng, M., and Fang, Y. (2019). β-Asarone regulates ER stress and autophagy via inhibition of the PERK/CHOP/Bcl-2/Beclin-1 Pathway in 6-OHDA-induced parkinsonian rats. *Neurochem. Res.* 44 (5), 1159–1166. doi: 10.1007/s11064-019-02757-w

Nixon, R. A. (2007). Autophagy, amyloidogenesis and Alzheimer disease. *J. Cell Sci.* 120 (Pt 23), 4081–4091. doi: 10.1242/jcs.019265

Palikaras, K., Lionaki, E., and Tavernarakis, N. (2015). Coordination of mitophagy and mitochondrial biogenesis during ageing in C. elegans. *Nature* 521 (7553), 525–528. doi: 10.1038/nature14300

Pansieri, J., Josserand, V., Lee, S. J., Rongier, A., Imbert, D., Sallanon, M. M., et al. (2019). Ultraviolet–visible–near-infrared optical properties of amyloid fibrils shed light on amyloidogenesis. *Nat. Photonics* 13 (7), 473–479. doi: 10.1038/s41566-019-0422-6

Park, J. S., Lee, J., Jung, E. S., Kim, M. H., Kim, I. B., Son, H., et al. (2019). Brain somatic mutations observed in Alzheimer's disease associated with aging and dysregulation of tau phosphorylation. *Nat. Commun.* 10 (1), 3090. doi: 10.1038/s41467-019-11000-7

Petersen, R. C., Thomas, R. G., Grundman, M., Bennett, D., Doody, R., Ferris, S., et al. (2005). Vitamin E and donepezil for the treatment of mild cognitive impairment. *N. Engl. J. Med.* 352 (23), 2379–2388. doi: 10.1056/NEJMoa050151

Reardon, S. (2018). Frustrated Alzheimer's researchers seek better lab mice. *Nature* 563 (7733), 611–612. doi: 10.1038/d41586-018-07484-w

Reddy, A. P., Ravichandran, J., and Carcaci-Salli, N. (2019). Neural regeneration therapies for Alzheimer's and Parkinson's disease-related disorders. *Biochim. Biophys. Acta Mol. Basis Dis.* doi: 10.1016/j.bbadis

Steele, J. W., and Gandy, S. (2013). Latrepirdine (Dimebon®), a potential Alzheimer therapeutic, regulates autophagy and neuropathology in an Alzheimer mouse model. *Autophagy* 9 (4), 617–618. doi: 10.4161/auto.23487

Sun, Y., and Peng, Z. L. (2008). Autophagy, beclin-1, and their relation to oncogenesis. *Lab. Med.* 39 (5), 287–290. doi: 10.1309/8L1X4X1WF3UGK77U

Tricco, A. C., Ashoor, H. M., Soobiah, C., Rios, P., Veroniki, A. A., Hamid, J. S., et al. (2018). Comparative effectiveness and safety of cognitive enhancers for treating Alzheimer's Disease: systematic review and network metaanalysis. *J. Am. Geriatr. Soc.* 66 (1), 170–178. doi: 10.1111/jgs.15069

Uddin, M. S., Stachowiak, A., Mamun, A. A., Tzvetkov, N. T., Takeda, S., Atanasov, A. G., et al. (2018). Autophagy and Alzheimer's Disease: from molecular mechanisms to therapeutic implications. *Front. Aging Neurosci.* 30 (10), 04. doi: 10.3389/fnagi.2018.00004

Vassa, R. (2004). BACE1: the beta-secretase enzyme in Alzheimer's disease. *J. Mol. Neurosci.* 23 (1-2), 105–114. doi: 10.1385/JMN:23:1-2:105

von Arnim, C. A. F., Bartsch, T., Jacobs, A. H., Holbrook, J., Bergmann, P., Zieschang, T., et al. (2019). Diagnosis and treatment of cognitive impairment. *Z. Gerontol. Geriatr.* 52 (4), 309–315. doi: 10.1007/s00391-019-01560-0

Wang, N., Zhang, Q., Ning, B., Luo, L., and Fang, Y. (2017). β-Asarone promotes Temozolomide's entry into glioma cells and decreases the expression of P-glycoprotein and MDR1. *BioMed. Pharmacother.* 90, 368–374. doi: 10.1016/j.biopha.2017.03.083

Wang, N., Zhang, Q., Luo, L., Ning, B., and Fang, Y. (2018). β-asarone inhibited cell growth and promoted autophagy *via* P53/Bcl-2/Bclin-1 and P53/AMPK/mTOR pathways in Human Glioma U251 cells. *J. Cell Physiol.* 233 (3), 2434–2443. doi: 10.1002/jcp.26118

Ye, X., Sun, X., Starovoytov, V., and Cai, Q. (2015). Parkin-mediated mitophagy in mutant hAPP neurons and Alzheimer's disease patient brains. *Hum. Mol. Genet.* 24 (10), 2938–2951. doi: 10.1093/hmg/ddv056

Zhu, M., Zhu, H., Tan, N., Zeng, G., Zeng, Z., Chu, H., et al. (2014). The effects of Acorus tatarinowii Schott on 5-HT concentrations, TPH2 and 5-HT1B expression in the dorsal raphe of exercised rats. *J. Ethnopharmacol.* 158 Pt A, 431–436. doi: 10.1016/j.jep.2014.10.026

Conflict of Interest: The authors declare that the research was conducted in the absence of any commercial or financial relationships that could be construed as a potential conflict of interest.

frontiers in Pharmacology

ORIGINAL RESEARCH
published: 20 February 2020
doi: 10.3389/fphar.2020.00065

Neuroprotective Effects of Qingnao Dripping Pills Against Cerebral Ischemia *via* Inhibiting NLRP3 Inflammasome Signaling Pathway: *In Vivo* and *In Vitro*

*Chen Fu[1], Xinyang Zhang[2], Zixiu Zeng[2], Yang Tian[2], Xianglan Jin[3], Fengli Wang[1], Zhenmin Xu[2], Baoxin Chen[3], Hong Zheng[1] and Xuemei Liu[1]**

[1] Central Laboratory, Dongfang Hospital, Beijing University of Chinese Medicine, Beijing, China, [2] Department of Traditional Chinese Internal Medicine, Beijing University of Chinese Medicine, Beijing, China, [3] Neurology Department, Dongfang Hospital, Beijing University of Chinese Medicine, Beijing, China

OPEN ACCESS

Edited by:
Yue Liu,
Xiyuan Hospital, China

Reviewed by:
Junfa Li,
Capital Medical University, China
Hongyi Qi,
Southwest University, China

***Correspondence:**
Xuemei Liu
liuxuemeitcm@163.com

Specialty section:
This article was submitted to Ethnopharmacology, a section of the journal Frontiers in Pharmacology

Received: *11 December 2019*
Accepted: *22 January 2020*
Published: *20 February 2020*

Citation:
Fu C, Zhang X, Zeng Z, Tian Y, Jin X, Wang F, Xu Z, Chen B, Zheng H and Liu X (2020) Neuroprotective Effects of Qingnao Dripping Pills Against Cerebral Ischemia via Inhibiting NLRP3 Inflammasome Signaling Pathway: In Vivo and In Vitro. Front. Pharmacol. 11:65. doi: 10.3389/fphar.2020.00065

Ischemic stroke patients suffer from relatively limited treatment options. Studies have shown that in cerebral ischemia, NOD-like receptor family pyrin domain containing 3 (NLRP3) inflammasome is a key mediator in mediating inflammatory responses and results in activation of apoptosis signaling pathways. Here we assessed the *in vivo* and *in vitro* effects of Qingnao Dripping Pills (QNDP), a traditional Chinese prescription, on inflammatory responses and apoptosis. Our results showed that QNDP could significantly decrease cerebral ischemia injury, improve neurological function and inhibit apoptosis in rats impaired by middle cerebral artery occlusion (MCAO). Further, we found that QNDP inhibited NLRP3 inflammasome expression both in MCAO rats and in SH-SY5Y cells under OGD. Moreover, the levels of inflammatory cytokines including interleukin-1β (IL-1β) and IL-18, which mediated by NLRP3 inflammasome and increased in MCAO rats, could be reduced by QNDP, suggesting that QNDP could protect the neurons against inflammation through a mechanism mediated by NLRP3 inflammasome. Nuclear factor-kappa B (NF-κB) was also involved in the anti-inflammatory effect of QNDP. In conclusion, QNDP had neuroprotective effects against cerebral ischemia *via* inhibiting NLRP3 inflammasome signaling pathway, and was a potential candidate for the future treatment of ischemic stroke.

Keywords: cerebral ischemia, NOD-like receptor family pyrin domain containing 3 inflammasome, inflammatory response, apoptosis, middle cerebral artery occlusion, Qingnao dripping pills

INTRODUCTION

Stroke is a leading cause of mortality and permanent disability globally, and the economic costs and post-stroke care are substantial (Collaborators, 2019). However, there are still relatively limited treatment options for ischemic stroke patients, largely because the molecular and

cellular mechanisms underlying continue to be poorly understood (Wang et al., 2019). Recently, previous studies have found increasing amounts of evidence showing the critical role played by the inflammasome in cerebral ischemia (Gao et al., 2017).

The inflammatory response and apoptosis are essential processes which can cause cellular damage and cell death after stroke (Radak et al., 2017; Pan et al., 2018; Jayaraj et al., 2019). It has previously been observed that in response to cerebral ischemia, NOD-like receptor family pyrin domain containing 3 (NLRP3) inflammasome may be a key mediator in mediating inflammatory responses and result in activation of apoptosis signaling pathways (Guo et al., 2016; Pan et al., 2018; Hong et al., 2019). NLRP3 inflammasome is a large multi-protein complex that is composed of NLRP3, the adaptor apoptosis-associated speck-like protein containing a CARD domain (ASC), and pro-caspase-1(Banoth and Sutterwala, 2017). After assembly and activation of NLRP3 inflammasome, pro-caspase-1 clustering will permit autocleavage and formation of the active caspase-1(Lamkanfi et al., 2007). Moreover, the active caspase-1 converts interleukin-1β (IL-1β) and interleukin-18 (IL-18) into their mature forms to engage in immune defense (Guo et al., 2015; Gao et al., 2017), and also initiates activation of apoptosis, which is involved with Caspases family and B-cell lymphoma-2 (Bcl-2) Family and results in DNA fragmentation, degradation of cytoskeletal and nuclear proteins, cross-linking of proteins death receptor ligation, and lysosomal protease activation (Radak et al., 2017; Pan et al., 2018). Thus, it is necessary and meaningful to identify a drug that can control NLRP3 inflammasome activation in cerebral ischemia.

Qingnao dripping pills (QNDP) is a traditional Chinese prescription consisting of *Gardenia jasminoides* Ellis (Chaozhizi), *Panax notoginseng* (Burk.) F. H. Chen (Sanqi), and borneol (Bingpian). Its main functions include resuscitation, clearing heat, dredging meridians, and treating stroke caused by phlegm and blood stasis, dysphasia, hemiplegia, and facial paralysis (Zeng et al., 2019). A clinical study in China found that QNDP could ameliorate the neurological function and alleviate a series of symptoms in stroke patients, such as headache, thirst, constipation, etc. (Han et al., 2007). In addition, our previous work has shown QNDP could reduce infarct size in rat models of middle cerebral artery occlusion (MCAO) by mediating the levels of inflammatory factors (TNF-a, IL-1β, and IL-10) and inhibiting the mitogen-activated protein kinase (MAPK) signaling pathway, which is associated with inflammation and apoptosis(Liu et al., 2016; He et al., 2019a; Zeng et al., 2019). However, the effect of QNDP on NLRP3 inflammasome has not been explored at present.

In the present study, we assessed the potential roles of QNDP on NLRP3 inflammasome in cerebral ischemia. We demonstrate that QNDP could reduce inflammatory response and apoptosis *via* inhibiting NLRP3 inflammasome signaling pathway in cerebral ischemia *in vivo* and *in vitro*, further suggesting that QNDP is a novel treatment candidate for ischemic stroke.

MATERIALS AND METHODS

Drug Preparations

QNDP is a specification of 0.038 g/pill, which is composed of *Gardenia jasminoides* Ellis (stir fried fruit), *Panax notoginseng* (Burk.) F. H. Chen (root), and *borneol* at a weight ratio of 70:30:1. *Gardenia jasminoides* Ellis (stir fried fruit) and *Panax notoginseng* (Burk.) F. H. Chen (root) were purchased from Hebei Ju Ren Tang Co., Ltd. (Hebei, China), and *borneol* was purchased from Guizhou Minzu Medicine Co., Ltd. (Guizhou, China). Raw drugs were authenticated by Professor Yuan Zhang according to Chinese Pharmacopeia 2015, morphologically and chemically. The voucher specimens were deposited in School of Chinese Materia Medica, Beijing University of Chinese Medicine and the scan of the vouchers were given in **Supplementary Table 1**. The voucher numbers for *Gardenia jasminoides* Ellis, *Panax notoginseng* (Burk.) F. H. Chen, and *borneol* specimens were 18-BUCM-Q3-1, 18-BUCM-Q1-2, and 18-BUCM-Q4-3, respectively.

The QNDP was produced by the Scientific Research Institute of Beijing Tong Ren Tang Co., Ltd. (Beijing, China). *Gardenia jasminoides* Ellis and *Panax notoginseng* (Burk.) F. H. Chen were extracted with ethanol, separated and purified, concentrated into dry powder, then added appropriate amounts of *borneol* to make the mixture. The QNDP was made by adding the polyethylene glycol 6000 and 4000 to the mixture. The clinical trial (No.2008L11182) of QNDP has been approved by the China Food and Drug Administration (CFDA) at 2008. *Geniposide* is the primary active constituent in QNDP, and it was the marker component for controlling the quality of QNDP by the company. According to the ultra-performance liquid chromatography (UPLC) analysis, the content of *Geniposide* ($C_{17}H_{24}O_{10}$) should be no lower than 1.5mg/pill (**Supplementary Figure 1**).

The chromatography samples were prepared as follows: dissolve QNDP with 50% methanol according to 1:10, centrifuge to take 50 μL of the supernatant and added 450 μL of 50% methanol to dilute, then take 100 μL of the supernatant and added the mixture (methanol: acetonitrile = 1: 1) 300 μL, spin and mix for 60 s, centrifuge at 13000 rpm for 10 min, and take 100 μL for the liquid chromatography-tandem mass spectrometry (LC-MS) analysis.

Animals

Adult male Sprague-Dawley rats were provided by Vital River Co. Ltd. (Beijing, China), weighing between 220 and 240 g. All rats were fed five per cage under controlled temperature (22 ± 2°C), with 12 h light/dark cycle and free access to food and water. The study was approved by the Animal Care and Use Committee of Dongfang hospital, Beijing university of Chinese Medicine.

Materials and Reagents

Geniposide (lot number: 110749-201718), Ginsenoside Rg1 (lot number:110703-201832), Ginsenoside Re (lot number:1110754-201626), Notoginsenoside R1 (lot number: 110745-201619) were

purchased from the National Institutes for Food and Drug Control (Beijing, China).

NLRP3 inflammasome inhibitor (MCC950) and 2% 2,3,5-triphenyltetrazolium chloride (TTC) solution were purchased from Sigma-Aldrich (USA). The primary antibodies were provided as follows: mouse monoclonal anti-Bad antibody (sc-8044), mouse monoclonal anti-ASC antibody (sc-271054) were purchased from Santa Cruz Biotechnology (USA). Rat monoclonal anti-BcL-XL (2764), anti-Caspase 1 (4199) were purchased from Cell Signaling Technology (USA). Rabbit polyclonal anti-IL-1β antibody (ab9722), rabbit polyclonal anti-IL-18 antibody (ab71495) and mouse monoclonal anti-NeuN antibody (ab104224) were purchased from Abcam (USA). Rabbit polyclonal Anti-NLRP3 antibody was purchased from Novus (USA). GAPDH (YM3029) was purchased from Immunoway (USA).

LC-MS Analysis

One hundred microliter of the homogenate were used for detection using a QE-Orbitrap high-resolution mass spectrometer (Thermo, USA). Mobile phase A was 0.1% formic acid and 2 mmoL/L ammonium formatted in water, and mobile phase B was acetonitrile. The gradient elution procedure was as follows: 0–1.0 min, 30–60% B; 1.0–1.5 min, 60–90% B; 1.5–3.5 min, 90% B; 3.5–3.6 min, 90–30% B; 3.6–5.5min, 30% B. Other conditions of the procedure were as follows: analysis time, 0–5.5 min, 5 μL per injection; flow rate, 0.3 mL/min; the chromatography column was Thermo Hypersil Gold C18 (3 μm, 2.1×100 mm), the column temperature was 30°C, and the automatic sampler temperature was maintained at 4°C. They were detected using ESI in the negative ion modes. Other conditions were as follows: spray voltage, 3,000 V, evaporation temperature, 350°C; sheath gas, 40 Arb; auxiliary gas, 10 Arb; capillary temperature, 320°C; S-lens RF, 80, CE: 35.

Cerebral Ischemia–Reperfusion Model

Cerebral ischemia–reperfusion was produced following the suture middle cerebral artery occlusion (MCAO) method and modified as previously described(Longa et al., 1989; Zeng et al., 2019). Briefly, rats were separated the branches of the left common carotid artery, and subjected to MCAO for 1.5 h and followed by 24 h. After surgery, rats were allowed to stay in their cages with free access to food and water. Before study, rats were randomly divided into sham group or MCAO group, and for MCAO group, they were further randomized to receive either QNDP or NLRP3 inhibitor or QNDP and NLRP3 inhibitor. In the sham group, this same operation was performed but no sutures were inserted. All rats were scarified at 24 h of reperfusion. In accordance with the previous experiments(Zeng et al., 2019), based on clinical usage, we used different doses of QNDP, the results showed that the effective dose of QNDP for rats was 0.15 g/kg (**Supplementary Figure 2**). QNDP was dissolved in (0.9%) saline solution for the experiments. Glycol 6,000 and 4,000 were dissolved by 0.9% sodium chloride as vehicle treatment.

Rats were randomly divided into five groups (eight animals each): (1) sham group (sham), administered glycol 6,000 and 4,000 (1 mL/100 g, i.g.). (2) MCAO group (MCAO), administered glycol 6,000 and 4,000 (1 mL/100 g, i.g.). (3) QNDP group (QNDP), administered QNDP (0.15 g/kg, i.g.) 2 h after surgery, and then once a day. (4) NLRP3 inhibitor group (NLRP3 inhibitor), administered NLRP3 inflammasome inhibitor MCC950 (100 nM, i.p.) 30 min prior to surgery, as a positive control, and then administered glycol 6 000 and 4 000 after surgery 2 h (1 mL/100 g, i.g.). (5) QNDP and NLRP3 inhibitor group (QNDP+ NLRP3 inhibitor), administered NLRP3 inflammasome inhibitor MCC950 (100 nM, i.p.) 30min prior to surgery and then administered QNDP (0.15 g/kg, i.g.) once a day.

Evaluation of Neurological Deficits

The neurological deficits of MCAO rats after 24 h reperfusion were evaluated by an operator blinded to the experimental conditions. Neurologic deficits were evaluated with a modified method according to Garcia score (Garcia et al., 1995). The Garcia score, an 18-point neurobehavioral scoring system, was divided into 6 subjects, which includes spontaneous activity, movement symmetry of 4 limbs, symmetry of forepaw outstretching, climbing a wire cage, body proprioception and response to touching the vibrissae. Rats demonstrated normally were assigned as the highest score (18 scores) and the severe neurological impaired were assigned as the lowest score (3 score).

Measurement of Infarct Volume

Twenty-four hours after reperfusion, rats were anesthetized by 10% chloral hydrate (3.5 mL/kg, i.p.), and the brains were immediately removed and frozen at −20°C for 15 min. Brains were cut into five 2-mm-thick coronal sections, incubated in 2% TTC at 37°C for 30 min in the dark, and then fixed in 4% paraformaldehyde solution at 4°C for 24 h. Brain slices were photographed and analyzed by ImageJ analysis software (version 6.0, NIH). The infarct volume was calculated as follows: the left infarct volume/whole brain volume × 100%.

Brain Water Content

Brains were quickly weighed on the electronic analytical balance and recorded the wet weight. Then whole brains were dried at 110°C for 24 h to obtain the dry weight. The percent brain water content was calculated as follows: (wet weight-dry weight)/wet weight×100%.

Cell Culture and Lentivirus Transfection

The human neuroblastoma cell line (SH-SY5Y cells) were purchased from the American Type Culture Collection. The cells were cultured in RPMI 1640 medium (Hyclone, Thermo Fisher Scientific) containing 10% fetal bovine serum (Hyclone) in a humidified atmosphere at 37°C with 5% CO_2. Cells were incubated in neurobasal medium, supplemented with 2% B27 supplement (17504-044, Gibco) and 0.5 mM L-glutamine (35050-061, Gibco). 3 days of plating, cells were added 10 M

retinoic acid (0695, Sigma) to the medium, and induced to differentiate into a homogeneous population of the cells with neuronal morphological structure (Kume et al., 2008). After 7–8 days, cells were used in the experiments.

The lentivirus for knock down NLRP3 and the control lentivirus (LV-scramble) was synthesized by Genechem (Shanghai, China). A plasmid expressing shRNA that targeting human NLRP3 was constructed using the GV248 vector. The shRNA target sequence was designed follows: 5′-GTGCGTTA GAAACACTTCA-3′. The shRNA (100 nmol/L) were transfected into the cells using Lipofectamine 2000 reagent (11668, Invitrogen) according to the manufacturer's instructions. After 6 h of transfection, the medium was replaced by RPMI 1640 medium for 24 h and then treated with or without OGD deprivation.

OGD Model

After transfection, the cells were exposed to oxygen–glucose deprivation. For OGD, cells were exposed to hypoxia (95%N_2/ 5%CO_2) at 37°C for 12 h and normal culture conditions (95% air, 5% CO_2) for an additional 12 h. (**Supplementary Figure 3**). At the OGD same time, added different concentrations of QNDP into cells. The result showed that the effective concentration of QNDP was 5μg/mL for SH-SY5Y cells expose to OGD (**Supplementary Figure 4**). The SH-SY5Y cells were randomly divided into the following groups: (1) normal control group (CON); (2) OGD group OGD; (3) QNDP group (OGD+QNDP); (4) sh-NLRP3 in normal cells group (CON+ sh-NLRP3); (5) sh-NLRP3 under OGD deprivation group (OGD+ sh-NLRP3); (6) sh-NLRP3 under OGD deprivation (OGD+ sh-NLRP3) and treated with QNDP group (OGD+QNDP+sh-NLRP3).

Cell Viability

CCK-8 assay was performed to evaluate cell viability of SH-SY5Y cells. The cells were seeded into 96-well plates at a density of 1×10^5 cells per well for 24 h. In brief, CCK-8 buffer (10 μL) was added into each well. The cells were incubated 37°C for 4 h. The absorbance measurements were taken at 450 nm on a microplate reader (Bio-Tek, USA).

Quantitative Real-Time Polymerase Chain Reaction (qRT-PCR)

Total RNA was extracted from left cerebral samples using TRIzol reagent (DP405-02, TIANGEN, China). cDNA was amplified by sequence-specific primers. Total RNA (1 μg) was reverse transcribed into cDNA using Reverse Transcriptase M-MLV Kit (2641B, TaKaRa, Japan). The qRT-PCR was performed with the ABI 7500 sequence detection system (Applied Bio-systems) using SYBR® Premix Ex Taq™ II (Tli RNaseH Plus) (RR82LR, TaKaRa). Primer sequences for IL-1β and IL-18 were synthesized and obtained from Sangon Biotech (Shanghai, China). Primers were provided as follows: IL-1β: Forward, 5′-TCATTGTGGCTGTGGAGAAG-3′ and Reverse, 5′-CTAT GTCCCGACCATTGCTG-3′; IL-18: Forward, 5′-GGATCTTGCGTCAATTCAAGG-3′ and Reverse, 5′-TTGG CTGTCTTTTGTCAACGA-3′. GAPDH: Forward, 5′-CC ATCACTGCCACTCAGAAGA-3′ and Reverse, 5′-CATGAGGTCCACCACCCTGT-3′. The relative mRNA expression was quantified using the $2^{-\Delta\Delta Ct}$ method, GAPDH as housekeeping gene. All reactions were performed in triplicate.

Immunofluorescent Staining

For images from *in vivo* brain tissues, brains were removed following MCAO, and post-fixed using 4% PFA. After preparing the frozen sections, the brain sections were cut into 15μm thick coronal slices. For images from *in vitro*, the SH-SY5Y cells were fixed by 95% acetone for 30 min, permeabilized by Triton X-100 for 10 min, blocked with 5% goat serum for 1h. Immunostaining was performed using rabbit anti-NLRP3 antibody (1:200 dilution) and mouse anti-NeuN antibody (1:1,000 dilution) overnight at 4° C. After washed by PBST, goat anti-mouse IgG H&L (Alexa Fluor® 488) (1:1,000 dilution, Abcam) and goat anti-rabbit IgG H&L (Alexa Fluor® 555) (1:1,000 dilution, Abcam) was incubated for 2 h at room temperature. Then, the cells or sections were incubated DAPI (10 μg/ml) for 5 min. Images were required by a fluorescence microscopy (BX71, Olympus, Tokyo, Japan).

Western Blotting

The protein from the left cerebral tissues and SH-SY5Y cells was prepared and extracted as previously described (Zeng et al., 2019). Briefly, protein samples (40 μg/lane) were loaded in a 4–12% Bis-Tris SDS-PAGE, and then transferred to the 0.22 μm polyvinylidene fluoride (PVDF) membrane, and subsequently blocked with 5% non-fat milk for 1 h, incubated with the primary antibodies overnight at 4°C: Bad (1:1,000), Bcl-xL (1:1,000), cleaved caspase-3 (1:1,000), NLRP3 (1:1,000), ASC (1:500), cleaved caspase 1 (1:500), IL-1β (1:500), IL-18 (1:500). Membranes were washed with TBST three times and incubated with goat anti-rabbit IgG secondary antibody (1:5,000) for 1hour at the room temperature. GAPDH, or β-actin were used as internal control. Detection was performed with an Odyssey Infrared Imaging System (LI-COR, USA). Western blotting bands were analyzed using the ImageJ software (National Institutes of Health, USA). All experiments were performed in triplicate.

Statistical Analysis

The date are shown as mean ± standard deviation (SD). Statistical analysis was used SPSS 25.0 statistical software. Statistical analysis was performed using Student's t test and one-way ANOVA for comparisons between and among different groups. $P < 0.05$ was indicated statistically significant.

RESULTS

Concentrations of the Major Effective Components of QNDP

According to LC-MS analysis, the identification of 4 major chemical ingredients of QNDP was performed, the mass spectrograms and chemical formulas of the main ingredients were shown in **Supplementary Figures 5** and **6**. According to

the chromatograms results, their concentrations in QNDP were also determined as follows: Geniposide (145.6 ± 18.86) mg/g, Ginsenoside Rg1 (77.1 ± 2.4) mg/g, Notoginsenoside R1 (5.8 ± 0.2) mg/g, Ginsenoside Re (4.9 ± 0.3) mg/g (**Supplementary Table 2**).

QNDP Was Neuroprotective *In Vivo*

To investigate the neuroprotective effect of QNDP against cerebral ischemia injury, we examined the effect of QNDP on cerebral infarct volume, neurological scores and brain water content. As shown in **Figures 1A, B**, the quantitative assessment of TTC staining sections showed that MCAO group had an infarct volume of (39.89% ± 2.43%) ($p < 0.01$ vs. sham group). QNDP resulted in a significant decrease in cerebral infarct volume (22.32% ± 1.75%) as compared with MCAO group ($p < 0.01$). NLRP3 inhibitor group (21.65% ± 1.62%) and QNDP+NLRP3 inhibitor group (18.65% ± 1.37%) were also decreased in cerebral infarct volume, compared with MCAO group ($p < 0.01$). Neurological defects are shown in **Figure 1C**. The neurological scores in the QNDP group were significantly improved ($p < 0.01$) compared to the MCAO group. NLRP3 inhibitor group and QNDP+NLRP3 inhibitor group were increased in neurological scores, compared with MCAO group ($p < 0.01$). The brain water content in the MCAO group was significantly increased ($p < 0.01$) compared with the sham group. QNDP, NLRP3 inhibitor, QNDP+NLRP3 inhibitor markedly reduced the brain water content, data as shown in **Figure 1D** ($p < 0.01$). These results suggested that QNDP could significantly decrease cerebral ischemia injury and improve neurological function.

QNDP Inhibited Apoptosis in Ischemic Cortex After Cerebral Ischemia *In Vivo*

We examined apoptosis in ischemic cortex using Bad, Bcl-xL, cleaved caspase 3 by western blotting. The results showed that expression of Bad, Bcl-xL, cleaved caspase 3 were significantly increased, compared to sham group ($p < 0.01$). Compare to MCAO group, QNDP decreased the expression of Bad and cleaved caspase 3, while increased the expression of Bcl-xL ($p < 0.01$). The results in QNDP+ NLRP3 inhibitor group as

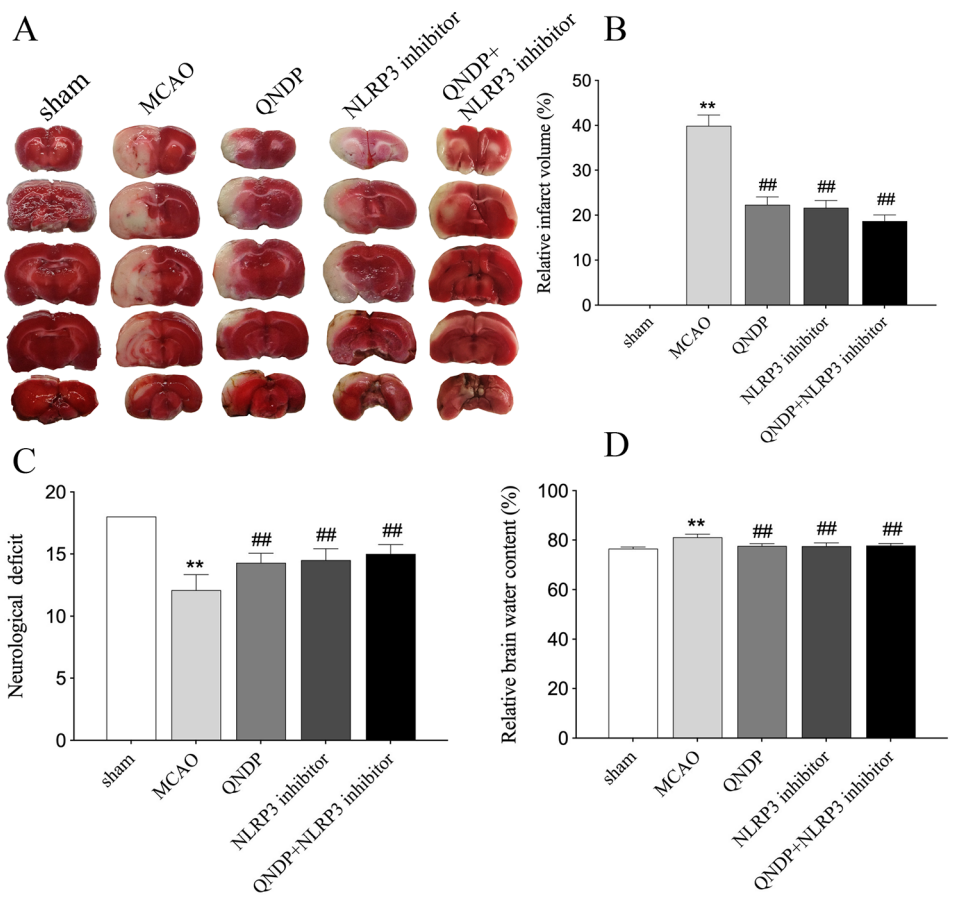

FIGURE 1 | QNDP is neuroprotective in MCAO rats. **(A)** Images of cerebral infarction (white, infarct tissue; red, non-infarct tissue) were TTC-stained brain sections. **(B)** The infarct volume was quantified with Image J analysis and expressed as a percentage of the damaged ipsilateral hemisphere. **(C)** Neurological deficit by Garcia JH scores. **(D)** Brain water content. Data are presented as means ± SEM, n = 8 per group, $^{**}p < 0.01$ compared with the sham group, $^{\#\#}p < 0.01$ compared with the MCAO group.

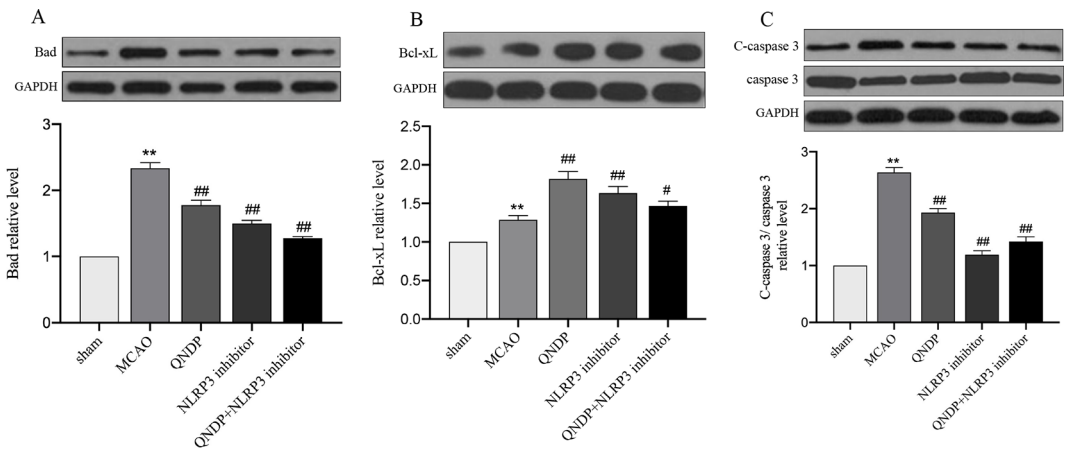

FIGURE 2 | Effect of QNDP on the protein expression of Bad, Bcl-xL, and cleaved caspase 3/caspase 3 in MCAO rats. Representative immunoblots and quantification illustrating the effect of QNDP on protein expression of Bad, Bcl-xL, and C-caspase 3/caspase 3. Data are presented as the mean ± SEM, n = 3 per group, $^{**}p < 0.01$ compared with the sham group, $^{\#}p < 0.05$, $^{\#\#}p < 0.01$ compared with the MCAO group.

same as QNDP group, compared to MACO group ($p < 0.01$). The date are shown in **Figures 2A–C**. The above data are indicated that QNDP could inhibits cortical apoptosis.

QNDP Inhibited NLRP3 Inflammasome Expression *In Vivo*

NLRP3 inflammasome has been demonstrated to be associated with neuroinflammation and cerebral ischemia, and plays an important role in cerebral ischemia and peaks 24 h after MCAO (Tang et al., 2010; Wang et al., 2019). To clarify whether QNDP inhibits NLRP3 inflammasome expression, we detected the expression of NLRP3 inflammasome at 24 h after MCAO following treatment with QNDP and sh-NLRP3 by immunofluorescence staining and western blotting. *In vivo*, as shown in **Figures 3A–C**, western blotting was detected the protein expression of NLRP3 inflammasome, ASC, cleaved caspase 1 in the ischemic cortex. The protein expression of NLRP3, ASC, and cleaved caspase 1 were significantly increased in the MCAO group, compared to the sham group ($p < 0.01$). QNDP treatment could significantly inhibit NLRP3, ASC, and cleaved caspase 1 expression ($p < 0.01$). However, compared to MCAO group, QNDP+NLRP3 inhibitor was significantly decreased the expression of NLRP3 and cleaved caspase 1 ($p < 0.01$), but it is interesting that NLRP3 inhibitor and QNDP+NLRP3 inhibitor has no significant with ASC. Furthermore, we examined NLRP3 expression in neurons in brain slices. Immunofluorescence staining showed that NLRP3 was mainly localized in the ischemic cortex. The images showed that the positive NLRP3 in QNDP and QNDP+NLRP3 inhibitor was less than those in MCAO group (**Figure 3D**). The **Figure 3D** was consistent with western blotting results. Double staining of NLRP3 and NeuN in brain slices demonstrated that NLRP3 partly co-localized with NeuN-immunoreactive neurons. In general, cerebral ischemia significantly elevated the expression of NLRP3 inflammasome, which was decreased by treatment with QNDP or QNDP+NLRP3 inhibitor. These results are indicated that QNDP may alleviate cerebral ischemia injury by inhibiting the NLRP3 inflammasome.

QNDP Inhibited NLRP3 Inflammasome Expression *In Vitro*

To determine whether the effects of QNDP on NLRP3 inflammasome activated in SH-SY5Y cells under OGD, we analyzed expression of NLRP3 inflammasome *in vitro* by western blotting and immunofluorescence staining. As shown in **Figure 4**, the data showed an increase in protein expression of NLRP3, ASC, and cleaved caspase1 during OGD. Compared to OGD group, QNDP and QNDP+NLRP3 inhibitor were obviously decreased the protein expression of NLRP3, ASC, and cleaved caspase 1 ($p < 0.05$ or 0.01, **Figures 4 A–E**). Next, we detected cell viability using CCK-8 assay. The data showed that OGD leads to a significant reduction in cell viability ($p < 0.01$, **Figure 4B**), while QNDP and QNDP+sh-NLRP3 were significantly increased *via* OGD group ($p < 0.01$). To further confirm the expression and activation of the NLRP3, we observed NLRP3 levels in the SH-SY5Y cells by immunofluorescence staining. Images showed NLRP3 appeared in the cytoplasm, and its fluorescence intensity was significantly enhanced by OGD (**Figure 4F**). QNDP or QNDP+sh-NLRP3 was significantly reduced the fluorescence intensity. These results are consistent with those derived from western blotting. The above data are shown that QNDP may inhibit the NLRP3 inflammasome in SH-SY5Y cells.

QNDP Decreased the Inflammatory Cytokines Level by Inhibiting IL-1β, and IL-18 After Cerebral Ischemia *In Vivo*

It is known that NLRP3 inflammasome activation promotes the secretion of IL-1β, IL-18 (He et al., 2017). We next examined

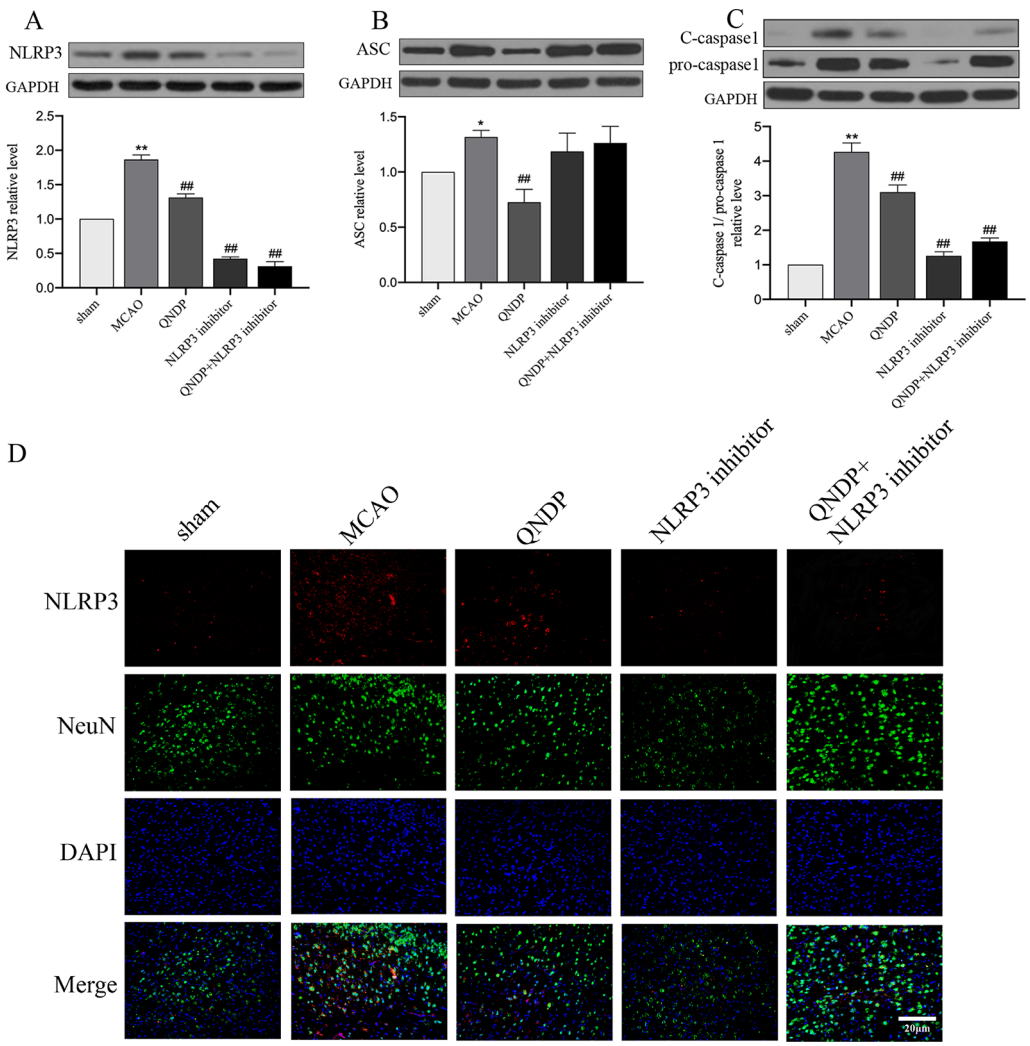

FIGURE 3 | Effect of QNDP on the expression of NLRP3, ASC, and cleaved caspase 1/pro-caspase 1 in MCAO rats. **(A)** Western blotting analysis of NLRP3, **(B)** Western blotting analysis of ASC, **(C)** Western blotting analysis of C-caspase 1/pro-caspase 1, **(D)** Immunofluorescent staining for NLRP3 (red), NeuN (green), the nuclei were stained blue with DAPI. Scale bar indicates 20 μm. Data are presented as the mean ± SEM, n = 3 per group, $^{*}p < 0.05$, $^{**}p < 0.01$ compared with the sham group, $^{\#\#}p < 0.01$ compared with the MCAO group.

whether QNDP affects effectors downstream of the NLRP3 inflammasome. To determine the effect of QNDP on pro-inflammatory cytokines after cerebral ischemia in rats, we detected the mRNA levels of IL-1β, IL-18 in the ischemic cortex by real time PCR (**Figures 5A, B**). Compared to the sham group, the mRNA levels of IL-1β and IL-18 were significantly increased in MCAO group ($p < 0.01$). In the QNDP group, the mRNA levels of IL-1β and IL-18 were significantly decreased ($p < 0.05$ or 0.01). When QNDP add NLRP3 inhibitor group, the results as same as QNDP alone. There was no statistical difference between the QNDP group and the QNDP+NLRP3 inhibitor group ($p > 0.05$). Similar to the results of real time PCR results, those of western blotting data were showed that the expression of IL-1β and IL-18, were obviously higher in the MCAO group than in the sham group ($p < 0.01$). QNDP and QNDP+NLRP3 inhibitor proudly decreased the expression of IL-1β and IL-18 ($p < 0.01$, **Figures 5C, D**). These findings are suggested that QNDP may alleviate cerebral ischemia injury by inhibiting the NLRP3 inflammasome-mediated release of cytokines, such as IL-1β, and IL-18.

QNDP Inhibited NF-κB Pathway After Cerebral Ischemia *In Vivo*

It is widely known that mRNA transcription of inflammatory cytokines depends on NF-κB activation. The priming step of NLRP3 inflammasome activation triggered by activating NF-κB signaling which induces NLRP3 transcription (He et al., 2019b). To further test the hypothesis that the effects of QNDP on the regulation of NLRP3 inflammasome activation are mediated by

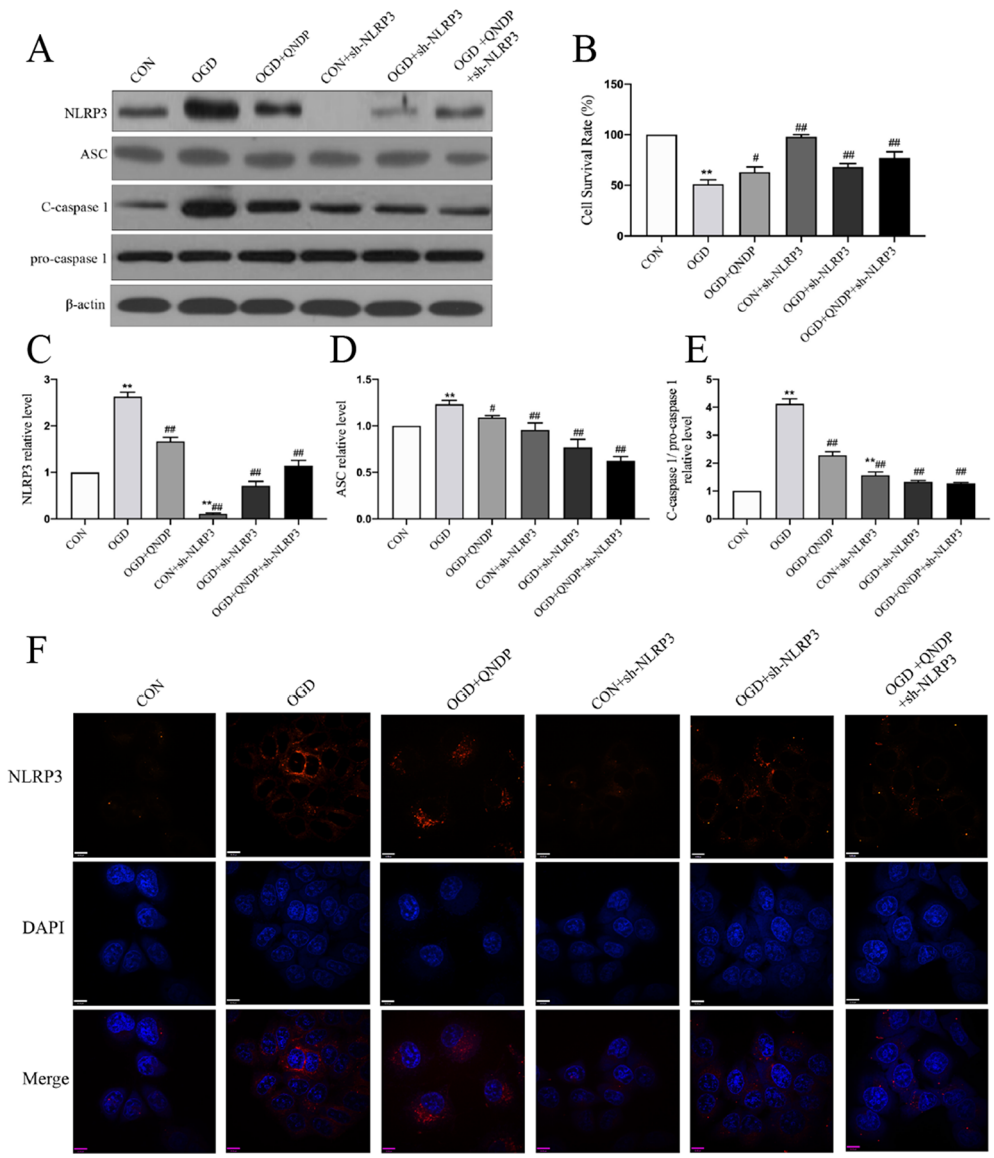

FIGURE 4 | Effect of QNDP on the expression of NLRP3, ASC, and cleaved caspase 1 following OGD in SH-SY5Y cells. **(A)** Western blotting bands of NLRP3, ASC, C-caspase 1, pro-caspase 1, **(B)** Cell survival rate using CCK-8 assay. Western blotting analysis of NLRP3 **(C)**, ASC **(D)**, C-caspase 1/pro-caspase 1 **(E)**. **(F)** Immunocytochemical staining for NLRP3 (red), the nuclei were stained blue with DAPI. Scale bar indicates 10 μm. Data are presented as the mean ± SEM, n = 3-5 batches of cells, $^{**}p < 0.01$ compared with the sham group, $^{\#}p < 0.05$, $^{\#\#}p < 0.01$ compared with the MCAO group.

NF-κB. Since IL-1β, IL-18, and NLRP3 inflammasome were up-regulated in the cortex after MCAO and obviously decreased by QNDP, we detected the expression of phosphorylation protein of NF-κB p65 (p-NF-κB) and IκBα in ischemic cortex. As shown in **Figure 6**, compared to the sham group, the p-NF-κB, and IκBα expression were significantly increased in the MACO group ($p < 0.01$, **Figures 6A, B**), which were markedly decreased by QNDP or QNDP+NLRP3 inhibitor, compared to the MCAO group ($p < 0.01$). These results are suggested that QNDP inhibiting NLRP3 inflammasome activation and cleaved-caspase 1, IL-1β, and IL-18 levels may be related with suppressing NF-κB pathway.

DISCUSSION

The present study generated three findings: (i) the important contribution of inflammatory response and apoptosis in cerebral ischemia injury, (ii) the anti-inflammatory and anti-apoptotic effect of QNDP in cerebral ischemia injury with evidence from both *in vivo* and *in vitro* models, and (iii) the crucial role of NLRP3 signaling pathway in mediating inflammatory response and apoptosis as an underlying mechanism for the effect of QNDP. These results suggest that QNDP is a potential candidate for the future treatment of ischemic stroke.

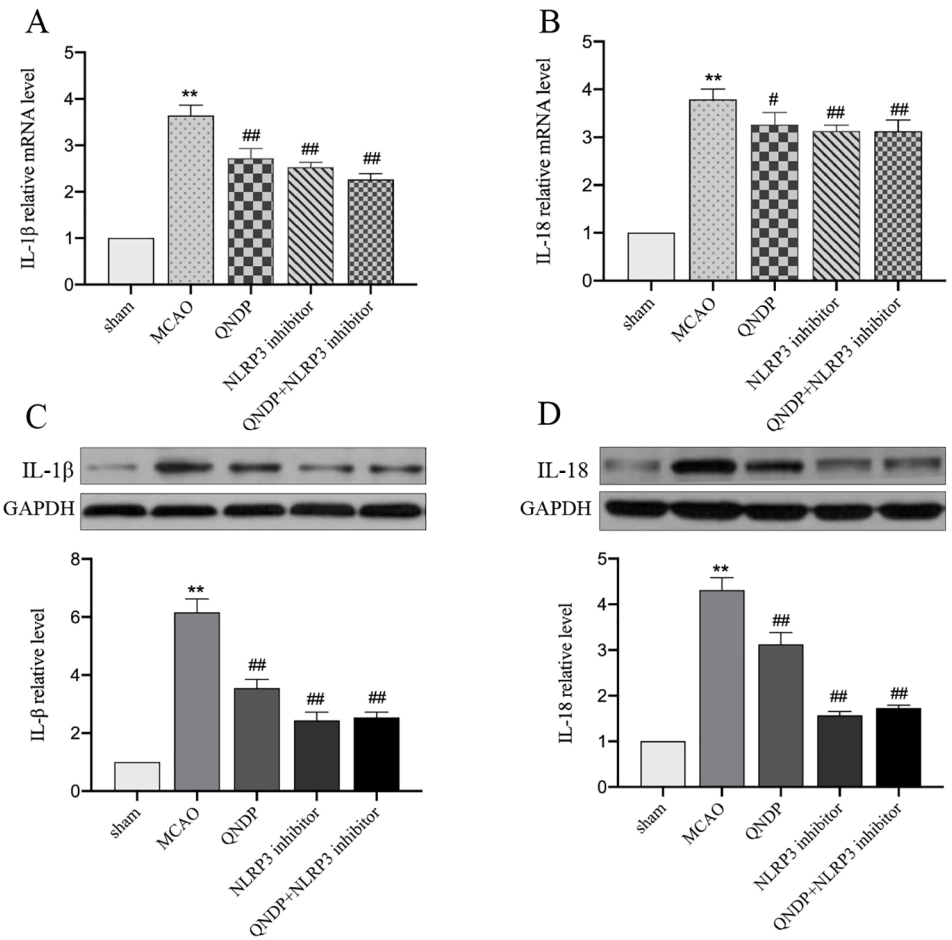

FIGURE 5 | Effect of QNDP on the expression of IL-1β and IL-18 in MCAO rats. Real- time PCR analysis of IL-1β **(A)**, IL-18 **(B)**. n = 8 per group. Western blotting analysis of IL-1β **(C)**, IL-18 **(D)**, n = 3 per group. Data are presented as the mean ± SEM, $^{**}p < 0.01$ compared with the sham group, $^{\#}p < 0.05$, $^{\#\#}p < 0.01$ compared with the MCAO group.

Stroke is a major cause of death and disability worldwide, and inflammation and apoptosis are key factors that cause and promote the cerebral ischemia injury (Lakhan et al., 2009). Importantly, apoptosis contributes to a significant proportion of neuron death in cerebral ischemia (Radak et al., 2017). The previous studies have illustrated that neuron apoptosis was initiated by activation of caspase molecules(Nijboer et al., 2008), and the inhibition of caspase 3 could prevent neuron apoptosis to protect against cerebral ischemia injury (Wang et al., 2014b). Besides, Bcl-2 family proteins are also critical in apoptosis, some members of which inhibit apoptosis (such as Bcl-2 and Bcl-xL), whereas others promote cell death (such as Bax and Bad) (Youle and Strasser, 2008; Jonas et al., 2014). A number of studies have suggested that Bcl-2 family proteins involved in the occurrence and development of stroke and played a role as a regulator of the apoptosis pathway in cerebral ischemia (Martinou et al., 1994; Hata et al., 1999; Wiessner et al., 1999; Qi et al., 2015). In this study, QNDP reduced infarct volume in MCAO rats, the same as the results of our previous study (Zeng et al., 2019). In addition, QNDP increased levels of Bcl-xL, and decreased levels of Bad and caspase 3, which meant QNDP alleviated apoptosis in cerebral ischemia injury. Our results suggested that QNDP can effectively protect against ischemic stroke by inhibiting apoptosis.

It is known that the inflammatory process is inherent across the whole time course of stroke(Iadecola and Anrather, 2011; Barrington et al., 2017), and understanding inflammatory mechanism can be helpful and meaningful for finding potential treatment opinions(Jayaraj et al., 2019). Following the acute stroke, sterile inflammation brings about the production of pro-inflammatory cytokines, such as IL-1β and IL-18, which exacerbates brain damage through activation of resident cells (i.e., microglia) and recruitment of inflammatory cells (Barrington et al., 2017; Hao et al., 2019; Jayaraj et al., 2019). Several studies have found that inhibition of IL-1β could cause significantly decreases in infarct volume (up to 60% to 70%) in MCAO mice and rats (Boutin et al., 2001; Touzani et al., 2002; Lambertsen et al., 2012), and increased level of IL-18 may

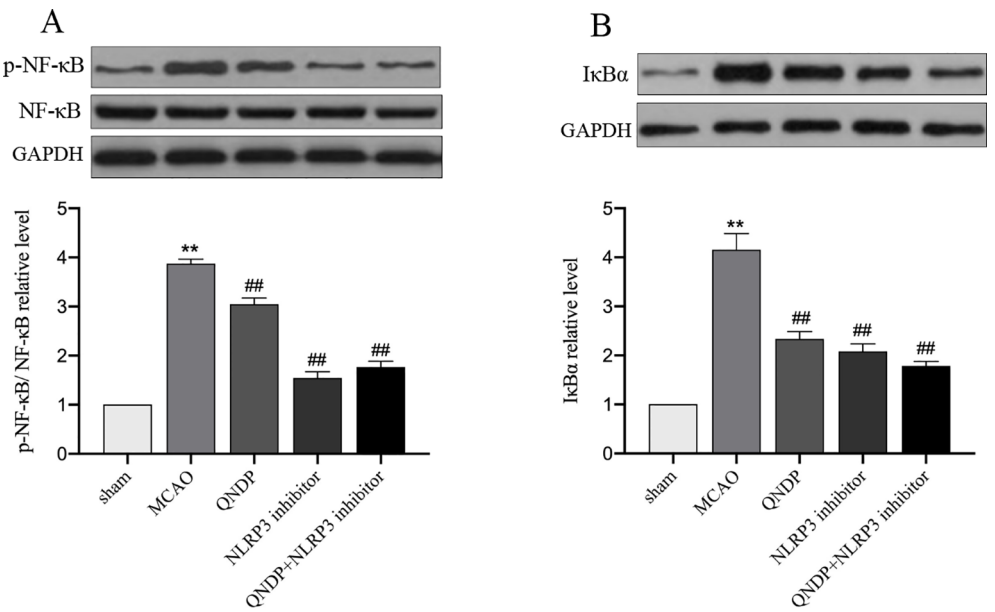

FIGURE 6 | Effect of QNDP on the protein expression of p-NF-κB, NF-κB and IκBα in MCAO rats. Representative immunoblots and quantification illustrating the effect of QNDP on protein expression of p-NF-κB/NF-κB and IκBα. Data are presented as the mean ± SEM, n=3 per group, $^{**}p < 0.01$ compared with the sham group, $^{\#\#}p < 0.01$ compared with the MCAO group.

contribute to the development and severity of ischemic stroke (Hao et al., 2019).This study referred that QNDP therapy obviously decreased the protein and mRNA expression of IL-1β and IL-18, and further demonstrated the notable intervention of QNDP on inflammatory response in cerebral ischemia based on our precious study(Zeng et al., 2019).

In recent years, there has been a growing interest in the role of inflammasome in cerebral ischemia. Inflammasome as a newly identified pattern-recognition receptors, was firstly described in detail by Martinon in 2002 (Martinon et al., 2002; Shao et al., 2015). It has been identified numerous inflammasomes, such as including NLRP3, NLRP1, NLRC4, AIM2, and so on(Yang et al., 2019). Among them, the NLRP3 inflammasome is one of most widely in the research. The NLRP3 inflammasome comprises the sensor molecule NLRP3, the adaptor protein ASC, and pro-caspase 1. Once activation, the NLRP3 protein interacts with ASC through the PYD domain, then the CARD domain of ASC recruits and activates pro-caspase 1, to form NLRP3–ASC–pro-caspase-1 complex (Guo et al., 2015). NLRP3 inflammasome acts a principal role in the pathogenesis of various inflammatory diseases. The studies reported that the activation of the NLRP3 inflammasome leads to the development and release of inflammatory cytokines IL-1β and IL-18, suggesting the role for the NLRP3 inflammasome in the initiation and development of cerebral ischemia (Rathinam et al., 2012; Gao et al., 2017). Accumulating amounts of evidence have indicated that NLRP3 inflammasome activation was closely related with post-ischemic inflammation after stroke, which was critical in neuronal cell death in ischemic stroke (Zhang et al., 2017; Alishahi et al., 2019).

The studies found that the levels of NLRP3 inflammasome proteins, IL-1β and IL-18 were elevated in stroke patients, and also increased in ipsilateral brain tissues of MCAO C57BL/6J mice and primary cortical neurons exposed to OGD (Fann et al., 2013; Wang et al., 2014a). The study found the highest level of NLRP3 inflammasome occurred at 24 h after ischemia–reperfusion injury (Hou et al., 2018). Gong et al. found that NLRP3 inflammasomes were first activated in microglia soon after cerebral ischemia injury onset and then were expressed in microvascular endothelial cells and neurons later, but they were mainly in neurons(Gong et al., 2018). Based on the above results, it can be deduced that NLRP3 inflammasome were rapidly activated and simultaneously activated inflammation, leading to neurons damaged after ischemic injury. When NLRP3 inflammasome was upregulated, following also IL-1β and IL-18 increased, and neurons are partly damaged from the ischemic insult. Consistent with these reports, our data demonstrate NLRP3, ASC and cleaved caspase 1 were substantially upregulated in the ischemic cortex in MCAO rats and SH-SY5Y cells exposed to OGD. In addition, IL-1β and IL-18 protein and mRNA levels in the ischemic cortex were also markedly elevated *in vivo*. Conversely, when NLRP3 inflammasome was blocked, neurons progress toward better. It was clarified that that NLRP3 inflammasome is harmful in ischemic stroke again. Hou et al. had reported that NLRP3 siRNA was reduced the infarct volume and improve neurological deficit, may be related with decrease the expression of the NLRP3 inflammasome and downstream IL-1β, and IL-18 of inflammation factors (Hou et al., 2018). Another research from Yu et al. reported that the inhibition of NLRP3 inflammasome

activation, which was reduced infarct volumes, decreased edema formation, has a neuroprotective effect in cerebral ischemia injury (Yu et al., 2017). These data suggested that NLRP3 inflammasome might be an inflammation contributor to cerebral ischemia injury. Those studies were in accordance with our results. We using NLRP3 shRNA or QNDP found that QNDP or QNDP and sh-NLRP3 obviously inhibited the levels of NLRP3, ASC and cleaved-caspase 1, then to regulate the inflammatory cytokines and inhibit apoptosis in cerebral ischemia *in vivo* and *in vitro*. In addition, we found that not all NeuN-immunoreactive neurons in the brain slices expressed NLRP3 after cerebral ischemia, which is worth exploring in depth. In our present study, QNDP could reduce the expression of NLRP3, cleaved caspase-1, IL-1β, and IL-18, alleviate brain edema, and improve the neurological function after cerebral ischemia. These results indicated that QNDP protects the neurons and alleviates brain injury against inflammation through a mechanism mediated by NLRP3 inflammasome partly.

NF-κB signal pathway is considered to be a vital regulator of inflammation response and is critical to the regulation of apoptosis, plays the important role in ischemic stroke (Harari and Liao, 2010; Li et al., 2019; Liu et al., 2019). NF-κB further promotes the production of NLRP3 and IL-1β and enhancing inflammation (Minutoli et al., 2016; Chen et al., 2019). Among various studies, NF-κB could regulate NLRP3 inflammasome activity (Pan et al., 2018). Fann et al. provided the results that both the NF-κB and MAPK signaling pathways play a pivotal role in regulating the expression and activation of NLRP3 inflammasomes in primary cortical neurons and brain tissue under ischemic conditions (Fann et al., 2018). In our previous study, we had illustrated activation MAPK signaling pathways was partly responsible for inducing cerebral ischemia. QNDP could inhibit MAPK pathway to alleviate cerebral ischemia injury. We focused on NLRP3 inflammasome in the current study to explore the relationship between NF-κB and the NLRP3 inflammasome in cerebral ischemia injury. We observed that the activation of NF-κB was increased, expression of the NLRP3 inflammasome also elevated, and the levels of downstream inflammatory factors as IL-1β, and IL-18. QNDP or QNDP +sh-NLRP3 had an opposite tendency.

CONCLUSION

QNDP displayed an inhibitory activity on the activation of NLRP3 inflammasome in MCAO rats and SH-SY5Y cells exposed to OGD. QDNP also inhibited the levels of mRNA and protein expression of IL-1β, and IL-18 in MCAO rats. Above all, the research suggests that QNDP shows an inhibitory activity on blocking the activation of NLRP3 inflammasome *in vivo* and *in vitro*, may be related with suppressing NF-κB pathway. QDNP significantly decreases cerebral ischemia injury and improve neurological function, protects the neurons against inflammation through a mechanism mediated by NLRP3 signaling. Furthermore, we want to do some more study to clarify which active components of QNDP plays the key role with NLRP3 inflammasome.

DATA AVAILABILITY STATEMENT

The datasets generated for this study can be available on request to the corresponding author.

ETHICS STATEMENT

The animal study was reviewed and approved by the Animal Care and Use Committee of Dongfang Hospital, Beijing University of Chinese Medicine.

AUTHOR CONTRIBUTIONS

CF performed the experiment and wrote the manuscript. XZ and ZZ assisted in the *in vivo* experiments and data analysis. YT and ZX assisted in the *in vitro* experiments. FW and HZ supervised the experiments. XJ and BC assisted in data analysis. XL conceived the study, designed the experiments and wrote the manuscript. All the authors reviewed and approved the manuscript.

FUNDING

This work was supported by the Natural Science Foundation of China (No. 81973788), the Beijing National Science Foundation (No.7182099), the Natural Science Foundation of China (No.81202683) and the International Science and Technology Cooperation Program of China (No. 2015DFA31130).

SUPPLEMENTARY MATERIAL

The Supplementary Material for this article can be found online at: https://www.frontiersin.org/articles/10.3389/fphar.2020.00065/full#supplementary-material

REFERENCES

Alishahi, M., Farzaneh, M., Ghaedrahmati, F., Nejabatdoust, A., Sarkaki, A., and Khoshnam, S. E. (2019). NLRP3 inflammasome in ischemic stroke: as possible therapeutic target. *Int. J. Stroke* 14 (6), 574–591. doi: 10.1177/1747493019841242

Banoth, B., and Sutterwala, F. S. (2017). Confounding role of tumor necrosis factor in cryopyrin-associated periodic syndromes. *J. Clin. Invest.* 127 (12), 4235–4237. doi: 10.1172/jci98322

Barrington, J., Lemarchand, E., and Allan, S. M. (2017). A brain in flame; do inflammasomes and pyroptosis influence stroke pathology? *Brain Pathol.* 27 (2), 205–212. doi: 10.1111/bpa.12476

Boutin, H., LeFeuvre, R. A., Horai, R., Asano, M., Iwakura, Y., and Rothwell, N. J. (2001). Role of IL-1alpha and IL-1beta in ischemic brain damage. *J. Neurosci.* 21 (15), 5528–5534. doi: 10.1523/JNEUROSCI.21-15-05528.2001

Chen, X., Liu, G., Yuan, Y., Wu, G., Wang, S., and Yuan, L. (2019). NEK7 interacts with NLRP3 to modulate the pyroptosis in inflammatory bowel disease *via* NF-kappaB signaling. *Cell Death Dis.* 10 (12), 906. doi: 10.1038/s41419-019-2157-1

Collaborators, G. S. (2019). Global, regional, and national burden of stroke 1990-2016: a systematic analysis for the Global Burden of Disease Study 2016. *Lancet Neurol.* 18 (5), 439–458. doi: 10.1016/s1474-4422(19)30034-1

Fann, D. Y., Lee, S. Y., Manzanero, S., Tang, S. C., Gelderblom, M., Chunduri, P., et al. (2013). Intravenous immunoglobulin suppresses NLRP1 and NLRP3 inflammasome-mediated neuronal death in ischemic stroke. *Cell Death Dis.* 4, e790. doi: 10.1038/cddis.2013.326

Fann, D. Y., Lim, Y. A., Cheng, Y. L., Lok, K. Z., Chunduri, P., Baik, S. H., et al. (2018). Evidence that NF-kappaB and MAPK Signaling Promotes NLRP Inflammasome Activation in Neurons Following Ischemic Stroke. *Mol. Neurobiol.* 55 (2), 1082–1096. doi: 10.1007/s12035-017-0394-9

Gao, L., Dong, Q., Song, Z., Shen, F., Shi, J., and Li, Y. (2017). NLRP3 inflammasome: a promising target in ischemic stroke. *Inflammation Res.* 66 (1), 17–24. doi: 10.1007/s00011-016-0981-7

Garcia, J. H., Wagner, S., Liu, K. F., and Hu, X. J. (1995). Neurological deficit and extent of neuronal necrosis attributable to middle cerebral artery occlusion in rats. Statistical validation. *Stroke* 26 (4), 627–634. doi: 10.1161/01.str.26.4.627

Gong, Z., Pan, J., Shen, Q., Li, M., and Peng, Y. (2018). Mitochondrial dysfunction induces NLRP3 inflammasome activation during cerebral ischemia/reperfusion injury. *J. Neuroinflammation* 15 (1), 242. doi: 10.1186/s12974-018-1282-6

Guo, H., Callaway, J. B., and Ting, J. P. (2015). Inflammasomes: mechanism of action, role in disease, and therapeutics. *Nat. Med.* 21 (7), 677–687. doi: 10.1038/nm.3893

Guo, Z., Yu, S., Chen, X., Ye, R., Zhu, W., and Liu, X. (2016). NLRP3 Is Involved in Ischemia/Reperfusion Injury. *CNS Neurol. Disord. Drug Targets* 15 (6), 699–712. doi: 10.2174/1871527315666160321111829

Han, Z., Zhang, Y., Shi, R., and Wang, Y. (2007). Clinical observation on the treatment of 66 cases of acute lacunar cerebral infarction. *Liaoning J. Trad. Chin. Med.* 34, 433–435. doi: 10.13192/j.ljtcm.2007.04.53.hanzhy.029

Hao, Y., Ding, J., Hong, R., Bai, S., Wang, Z., Mo, C., et al. (2019). Increased interleukin-18 level contributes to the development and severity of ischemic stroke. *Aging (Albany NY)* 11 (18), 7457–7472. doi: 10.18632/aging.102253

Harari, O. A., and Liao, J. K. (2010). NF-kappaB and innate immunity in ischemic stroke. *Ann. N Y Acad. Sci.* 1207, 32–40. doi: 10.1111/j.1749-6632.2010.05735.x

Hata, R., Gillardon, F., Michaelidis, T. M., and Hossmann, K. A. (1999). Targeted disruption of the bcl-2 gene in mice exacerbates focal ischemic brain injury. *Metab. Brain Dis.* 14 (2), 117–124. doi: 10.1023/a:1020709814456

He, Q., Li, Z., Wang, Y., Hou, Y., Li, L., and Zhao, J. (2017). Resveratrol alleviates cerebral ischemia/reperfusion injury in rats by inhibiting NLRP3 inflammasome activation through Sirt1-dependent autophagy induction. *Int. Immunopharmacol.* 50, 208–215. doi: 10.1016/j.intimp.2017.06.029

He, F., Zeng, Z., Zhang, X., and X., L. (2019a). Qingnao Dripping Pills antagonise apoptopsis of C6 Glial Cells induced by oxygen-glucose deprivation and reoxygenation *via* down-regulating HIF-1α/BNIP3 expression. *Chin. J. Integr. Traditional West. Med.* 39 (1), 92–96. doi: 10.7661/j.cjim.20180623.181

He, R., Li, Y., Han, C., Lin, R., Qian, W., and Hou, X. (2019b). L-Fucose ameliorates DSS-induced acute colitis *via* inhibiting macrophage M1 polarization and inhibiting NLRP3 inflammasome and NF-kB activation. *Int. Immunopharmacol.* 73, 379–388. doi: 10.1016/j.intimp.2019.05.013

Hong, P., Gu, R. N., Li, F. X., Xiong, X. X., Liang, W. B., You, Z. J., et al. (2019). NLRP3 inflammasome as a potential treatment in ischemic stroke concomitant with diabetes. *J. Neuroinflammation* 16 (1), 121. doi: 10.1186/s12974-019-1498-0

Hou, Y., Wang, Y., He, Q., Li, L., Xie, H., Zhao, Y., et al. (2018). Nrf2 inhibits NLRP3 inflammasome activation through regulating Trx1/TXNIP complex in cerebral ischemia reperfusion injury. *Behav. Brain Res.* 336, 32–39. doi: 10.1016/j.bbr.2017.06.027

Iadecola, C., and Anrather, J. (2011). The immunology of stroke: from mechanisms to translation. *Nat. Med.* 17 (7), 796–808. doi: 10.1038/nm.2399

Jayaraj, R. L., Azimullah, S., Beiram, R., Jalal, F. Y., and Rosenberg, G. A. (2019). Neuroinflammation: friend and foe for ischemic stroke. *J. Neuroinflammation* 16 (1), 142. doi: 10.1186/s12974-019-1516-2

Jonas, E. A., Porter, G. A., and Alavian, K. N. (2014). Bcl-xL in neuroprotection and plasticity. *Front. Physiol.* 5, 355. doi: 10.3389/fphys.2014.00355

Kume, T., Kawato, Y., Osakada, F., Izumi, Y., Katsuki, H., Nakagawa, T., et al. (2008). Dibutyryl cyclic AMP induces differentiation of human neuroblastoma SH-SY5Y cells into a noradrenergic phenotype. *Neurosci. Lett.* 443 (3), 199–203. doi: 10.1016/j.neulet.2008.07.079

Lakhan, S. E., Kirchgessner, A., and Hofer, M. (2009). Inflammatory mechanisms in ischemic stroke: therapeutic approaches. *J. Transl. Med.* 7, 97. doi: 10.1186/1479-5876-7-97

Lambertsen, K. L., Biber, K., and Finsen, B. (2012). Inflammatory cytokines in experimental and human stroke. *J. Cereb Blood Flow Metab.* 32 (9), 1677–1698. doi: 10.1038/jcbfm.2012.88

Lamkanfi, M., Kanneganti, T. D., Franchi, L., and Nunez, G. (2007). Caspase-1 inflammasomes in infection and inflammation. *J. Leukoc Biol.* 82 (2), 220–225. doi: 10.1189/jlb.1206756

Li, X., Huang, L., Liu, G., Fan, W., Li, B., Liu, R., et al. (2019). Ginkgo diterpene lactones inhibit cerebral ischemia/reperfusion induced inflammatory response in astrocytes *via* TLR4/NF-kappaB pathway in rats. *J. Ethnopharmacol*, 112365. doi: 10.1016/j.jep.2019.112365

Liu, X., Wang, J., Zhao, J., Wang, F., and Liang, X. (2016). Effects of Qingnao dripping pills on dynamic changes of inflammatory factors after cerebral ischemia-reperfusion in rats. *World Chin. Med.* 11 (1), 33–36. doi: 10.3969/j.issn.1673-7202.2016.01.007

Liu, H., Wu, X., Luo, J., Wang, X., Guo, H., Feng, D., et al. (2019). Pterostilbene Attenuates Astrocytic Inflammation and Neuronal Oxidative Injury After Ischemia-Reperfusion by Inhibiting NF-kappaB Phosphorylation. *Front. Immunol.* 10, 2408. doi: 10.3389/fimmu.2019.02408

Longa, E. Z., Weinstein, P. R., Carlson, S., and Cummins, R. (1989). Reversible middle cerebral artery occlusion without craniectomy in rats. *Stroke* 20 (1), 84–91. doi: 10.1161/01.str.20.1.84

Martinon, F., Burns, K., and Tschopp, J. (2002). The inflammasome: a molecular platform triggering activation of inflammatory caspases and processing of proIL-beta. *Mol. Cell* 10 (2), 417–426. doi: 10.1016/s1097-2765(02)00599-3

Martinou, J. C., Dubois-Dauphin, M., Staple, J. K., Rodriguez, I., Frankowski, H., Missotten, M., et al. (1994). Overexpression of BCL-2 in transgenic mice protects neurons from naturally occurring cell death and experimental ischemia. *Neuron* 13 (4), 1017–1030. doi: 10.1016/0896-6273(94)90266-6

Minutoli, L., Puzzolo, D., Rinaldi, M., Irrera, N., Marini, H., Arcoraci, V., et al. (2016). ROS-Mediated NLRP3 Inflammasome Activation in Brain, Heart, Kidney, and Testis Ischemia/Reperfusion Injury. *Oxid. Med. Cell Longev* 2016, 2183026. doi: 10.1155/2016/2183026

Nijboer, C. H., Heijnen, C. J., Groenendaal, F., May, M. J., van Bel, F., and Kavelaars, A. (2008). A dual role of the NF-kappaB pathway in neonatal hypoxic-ischemic brain damage. *Stroke* 39 (9), 2578–2586. doi: 10.1161/strokeaha.108.516401

Pan, Z., Cui, M., Dai, G., Yuan, T., Li, Y., Ji, T., et al. (2018). Protective Effect of Anthocyanin on Neurovascular Unit in Cerebral Ischemia/Reperfusion Injury in Rats. *Front. Neurosci.* 12, 947. doi: 10.3389/fnins.2018.00947

Qi, Z., Dong, W., Shi, W., Wang, R., Zhang, C., Zhao, Y., et al. (2015). Bcl-2 phosphorylation triggers autophagy switch and reduces mitochondrial damage in limb remote ischemic conditioned rats after ischemic stroke. *Transl. Stroke Res.* 6 (3), 198–206. doi: 10.1007/s12975-015-0393-y

Radak, D., Katsiki, N., Resanovic, I., Jovanovic, A., Sudar-Milovanovic, E., Zafirovic, S., et al. (2017). Apoptosis and Acute Brain Ischemia in Ischemic Stroke. *Curr. Vasc. Pharmacol.* 15 (2), 115–122. doi: 10.2174/1570161115666161104095522

Rathinam, V. A., Vanaja, S. K., and Fitzgerald, K. A. (2012). Regulation of inflammasome signaling. *Nat. Immunol.* 13 (4), 333–342. doi: 10.1038/ni.2237

Shao, B. Z., Xu, Z. Q., Han, B. Z., Su, D. F., and Liu, C. (2015). NLRP3 inflammasome and its inhibitors: a review. *Front. Pharmacol.* 6, 262. doi: 10.3389/fphar.2015.00262

Tang, J., Li, Y. J., Li, Q., Mu, J., Yang, D. Y., and Xie, P. (2010). Endogenous tissue plasminogen activator increases hemorrhagic transformation induced by heparin after ischemia reperfusion in rat brains. *Neurol. Res.* 32 (5), 541–546. doi: 10.1179/174313209x414560

Touzani, O., Boutin, H., LeFeuvre, R., Parker, L., Miller, A., Luheshi, G., et al. (2002). Interleukin-1 influences ischemic brain damage in the mouse

independently of the interleukin-1 type I receptor. *J. Neurosci.* 22 (1), 38–43. doi: 10.1523/JNEUROSCI.22-01-00038.2002

Wang, C. P., Zhang, L. Z., Li, G. C., Shi, Y. W., Li, J. L., Zhang, X. C., et al. (2014a). Mulberroside A protects against ischemic impairment in primary culture of rat cortical neurons after oxygen-glucose deprivation followed by reperfusion. *J. Neurosci. Res.* 92 (7), 944–954. doi: 10.1002/jnr.23374

Wang, G. H., Lan, R., Zhen, X. D., Zhang, W., Xiang, J., and Cai, D. F. (2014b). An-Gong-Niu-Huang Wan protects against cerebral ischemia induced apoptosis in rats: up-regulation of Bcl-2 and down-regulation of Bax and caspase-3. *J. Ethnopharmacol* 154 (1), 156–162. doi: 10.1016/j.jep.2014.03.057

Wang, Y., Meng, C., Zhang, J., Wu, J., and Zhao, J. (2019). Inhibition of GSK-3beta alleviates cerebral ischemia/reperfusion injury in rats by suppressing NLRP3 inflammasome activation through autophagy. *Int. Immunopharmacol.* 68, 234–241. doi: 10.1016/j.intimp.2018.12.042

Wiessner, C., Allegrini, P. R., Rupalla, K., Sauer, D., Oltersdorf, T., McGregor, A. L., et al. (1999). Neuron-specific transgene expression of Bcl-XL but not Bcl-2 genes reduced lesion size after permanent middle cerebral artery occlusion in mice. *Neurosci. Lett.* 268 (3), 119–122. doi: 10.1016/s0304-3940(99)00392-4

Yang, Y., Wang, H., Kouadir, M., Song, H., and Shi, F. (2019). Recent advances in the mechanisms of NLRP3 inflammasome activation and its inhibitors. *Cell Death Dis.* 10 (2), 128. doi: 10.1038/s41419-019-1413-8

Youle, R. J., and Strasser, A. (2008). The BCL-2 protein family: opposing activities that mediate cell death. *Nat. Rev. Mol. Cell Biol.* 9 (1), 47–59. doi: 10.1038/nrm2308

Yu, C., He, Q., Zheng, J., Li, L. Y., Hou, Y. H., and Song, F. Z. (2017). Sulforaphane improves outcomes and slows cerebral ischemic/reperfusion injury *via* inhibition of NLRP3 inflammasome activation in rats. *Int. Immunopharmacol.* 45, 74–78. doi: 10.1016/j.intimp.2017.01.034

Zeng, Z., Zhang, Y., Liang, X., Wang, F., Zhao, J., Xu, Z., et al. (2019). Qingnao dripping pills mediate immune-inflammatory response and MAPK signaling pathway after acute ischemic stroke in rats. *J. Pharmacol. Sci.* 139 (3), 143–150. doi: 10.1016/j.jphs.2018.12.009

Zhang, S., Jiang, L., Che, F., Lu, Y., Xie, Z., and Wang, H. (2017). Arctigenin attenuates ischemic stroke *via* SIRT1-dependent inhibition of NLRP3 inflammasome. *Biochem. Biophys. Res. Commun.* 493 (1), 821–826. doi: 10.1016/j.bbrc.2017.08.062

Conflict of Interest: The authors declare that the research was conducted in the absence of any commercial or financial relationships that could be construed as a potential conflict of interest.

frontiers in Pharmacology

REVIEW
published: 21 February 2020
doi: 10.3389/fphar.2020.00118

Roles and Mechanisms of Hawthorn and Its Extracts on Atherosclerosis: A Review

Min Wu[1†], Longtao Liu[2†], Yanwei Xing[1], Shengjie Yang[1], Hao Li[3] and Yu Cao[3*]*

[1] Guang'anmen Hospital, China Academy of Chinese Medical Sciences, Beijing, China, [2] Xiyuan Hospital, China Academy of Chinese Medical Sciences, Beijing, China, [3] Institute of Geriatrics, Xiyuan Hospital, China Academy of Chinese Medical Sciences, Beijing, China

Cardiovascular disease (CVD), especially atherosclerosis, is a leading cause of morbidity and mortality globally; it causes a considerable burden on families and caregivers and results in significant financial costs being incurred. Hawthorn has an extensive history of medical use in many countries. In China, the use of hawthorn for the treatment of CVD dates to 659 AD. In addition, according to the theory of traditional Chinese medicine, it acts on tonifying the spleen to promote digestion and activate blood circulation to dissipate blood stasis. This review revealed that the hawthorn extracts possess serum lipid-lowering, anti-oxidative, and cardiovascular protective properties, thus gaining popularity, especially for its anti-atherosclerotic effects. We summarize the four principal mechanisms, including blood lipid-lowering, anti-oxidative, anti-inflammatory, and vascular endothelial protection, thus providing a theoretical basis for further utilization of hawthorn.

Keywords: hawthorn, *Crataegus*, atherosclerosis, oxidative stress, inflammation, endothelial dysfunction

OPEN ACCESS

Edited by:
Youhua Xu,
Macau University of Science and Technology, Macau

Reviewed by:
Guilin Zhang,
Macau University of Science and Technology, Macau
Yong Wang,
Beijing University of Chinese Medicine, China

***Correspondence:**
Hao Li
xyhplihao1965@126.com
Yu Cao
yu.cao-xiyuan@foxmail.com

[†]These authors have contributed equally to this work

Specialty section:
This article was submitted to Ethnopharmacology, a section of the journal Frontiers in Pharmacology

Received: *12 November 2019*
Accepted: *28 January 2020*
Published: *21 February 2020*

Citation:
Wu M, Liu L, Xing Y, Yang S, Li H and Cao Y (2020) Roles and Mechanisms of Hawthorn and Its Extracts on Atherosclerosis: A Review. Front. Pharmacol. 11:118. doi: 10.3389/fphar.2020.00118

INTRODUCTION

Cardiovascular disease (CVD), especially atherosclerosis, is a leading cause of morbidity and mortality worldwide. CVD imposes a considerable burden on families and primary caregivers, along with a high financial cost to society. During past decades in China, ischemic heart disease and stroke are the top two causes of death (Yang et al., 2013). With a rapidly aging population, the absolute number of deaths due to CVD increased by 46% in China, a figure four and three times higher than those in the United States and Western Europe, respectively (Du et al., 2019). Beyond conventional medical treatment, herbal plants have several natural compounds for the prevention and treatment of various diseases. Herbal medicine, such as adjuvants, has also been popular worldwide. It is estimated by the World Health Organization that in the developing countries, nearly four billion people consume herbal medications as a primary source of healthcare (Bodeker and Ong, 2005). Therefore, the use of herbal remedies in complementary and alternative medicines has been widely embraced in many countries (Ekor, 2014).

Crataegus sp., commonly known as hawthorn, or hawberry, is a large genus of thorny shrubs and trees belonging to the family *Rosaceae*, comprising approximately 280 species, native to zones with a mild climate in Europe, East Asia, and North America (Hobbs and Foster, 1994). Hawthorn has been used for centuries worldwide as both food and folk medicine. Hawthorn is one of the recognized medicinal plants in European medicine, as Dioscorides primarily described its cardiovascular actions in the first century

(Petrovska, 2012). Currently, countries such as China, Germany, and France have officially recorded some species in their pharmacopeias (Chang et al., 2002).

In China, the bright red berries of hawthorn, also called *Shanzha* (**Figure 1**), have been extensively used to treat various ailments given their medicinal properties. It was mentioned first for "treating dysentery" in *Tang Materia Medica* (*Tang Ben Cao*) dating back to 659 AD, the first known official pharmacopeia in the world. As described in the *Compendium of Materia Medica (Bencao Gangmu)*, which is regarded as the most complete and comprehensive herbal monograph, the dried berry of *Crataegus pinnatifida* was described with healing efficacy for thoracalgia, hernia, indigestion, blood stagnation, and hematochezia (Liu et al., 2011). Currently, considerable efforts are underway to identify bioactive components from different parts of the plants and to unveil potential mechanisms of their pharmaceutical actions.

Crataegus sp: Chemical Constituents, Pharmacology, Potential Applications, and Toxicity

Presently, in traditional Chinese medicine (TCM), the fruits of both *C. pinnatifida* Bge. var. *major* N.E.Br and *C. pinnatifida* Bge are the only two medicinal species documented in Chinese pharmacopeia, which are used to promote digestion and improve blood circulation. Other species, such as *Crataegus monogyna* and *C. azarolus*, were also used as focal medicine in other countries. Different parts of the plant, i.e., flowers, leaves, seeds, and berries, have long been recorded for their traditional medical use in either decoction or powder form as folk medicine in many countries, such as Serbia, France, Chile, Turkey, and China, for the treatment of various diseases (e.g., antispasmodic, cardiotonic, diuretic, hypotensive, and anti-atherosclerotic) (Cloud et al., 2019; Dehghani et al., 2019).

In the past 20 years, greater than 150 chemical compounds, including flavonoids, triterpenoids, oligomeric proanthocyanidins, and organic acids, were separated and characterized in the berries, leaves, and flowers of *C. pinnatifida* (Özcan et al., 2005; Wu et al., 2014) (**Figures 2–4**). Moreover, the pectin in fresh hawthorn fruit was reported to be as high as 20.5% (Wang et al., 2007). Pectin oligosaccharides with 2–11 polymers show antioxidant, hypolipidemic, antiglycation, and antibiotic properties (Li et al., 2010; Li et al., 2013a; Li et al., 2014; Zhu et al., 2019). Interestingly, one study showed the contribution of total polyphenolics, rather than the total flavonoids or anthocyanins to the antioxidant capacity of the hawthorn drinks (made from *C. pinnatifida*) (Liu et al., 2016). Besides, heat and microwave exposure could increase the level of anthocyanins, such as cyanidin-3-galactoside (Liu et al., 2016). In other species such as *C. monogyna* and *C. azarolus*, similar types of phenolic compounds were present and categorized into four subclasses: phenolic acids including hydroxycinnamic acids and hydroxybenzoic acid, flavonoids, which are the most abundant components, including flavones and glucosylated flavonols, anthocyanins, such as glycosides of cyanidin, of which cyanidin-3-O-glucoside is the most abundant (Mraihi et al., 2015). Another study identified seven neolignans in the ethanol extract of the *C. pinnatifida* seeds, which elicited antioxidant and anti-inflammatory effects (Peng et al., 2016).

These results show that hawthorn fruits could serve as promising healthcare supplements and also as a potential source of antioxidant and cardiotonic phenolic materials. One study identified the phenolic compounds in the *Crataegus pubescens* fruit, and the most abundant substances were (+)-catechin, (−)-epicatechin, and chlorogenic acid, which could be used as nutraceutical and functional foods (González-Jiménez et al., 2018).

With expanding global interest, modern research validated the presence of multiple biological and pharmacological activities in the extracts of hawthorn fruits, leaves, and flowers, including cardiovascular protective ability, hypolipidemic activity, and anti-oxidative capacity (Pittler et al., 2003; Wang H. et al., 2011; Zhang et al., 2014). WS® 1442 is the most studied compound consisting of 20% oligomeric procyanidins extracted from the leaves and flowers (45% ethanol extract) of *C. monogyna* and *Crataegus laevigata* (Holubarsch et al., 2008). In the United States and European countries, WS® 1442 has been recommended for treating congestive heart failure stages I–III based on the classification of the New York Heart Association (NYHA) (Tauchert, 2002; Pittler et al., 2003).

Crataegus sp. has a long history of cardioprotective ability, which is extended for first-line clinical practice. Due to its

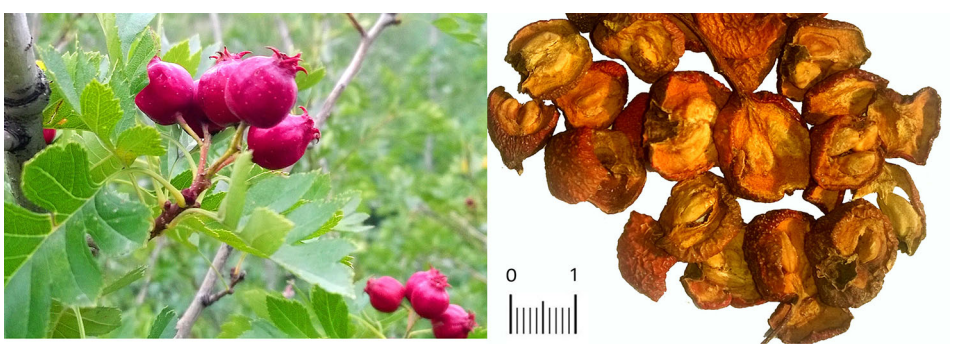

FIGURE 1 | *Crataegus pinnatifida* tree and fruits (left). Traditional Chinese herb *Shanzha* (Fructus *Crataegus*, prepared pieces of *Crataegus pinnatifida* var. *major*) fruit pieces (right).

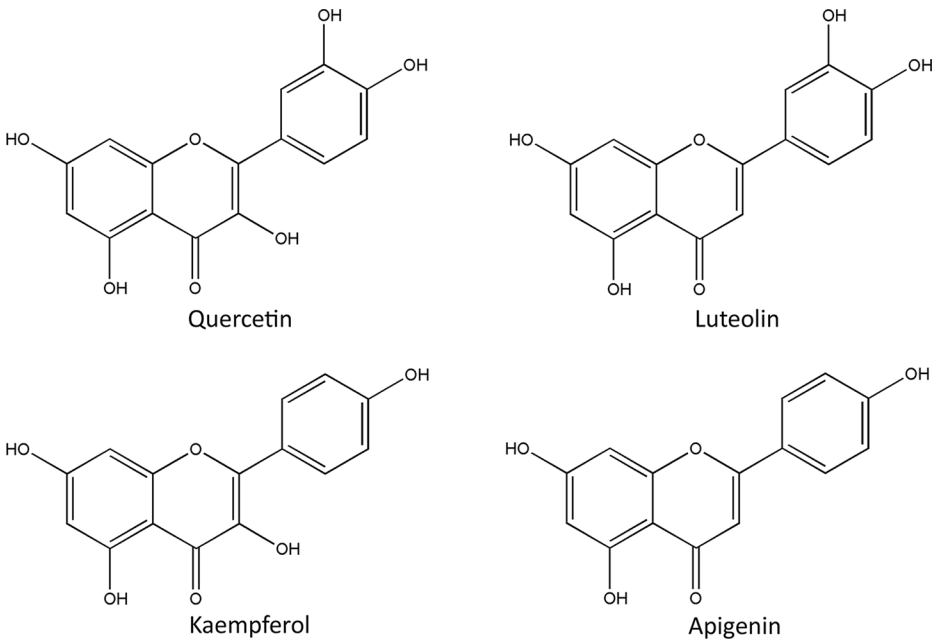

FIGURE 2 | Chemical structures of representative flavonoids in *Crataegus pinnatifida*.

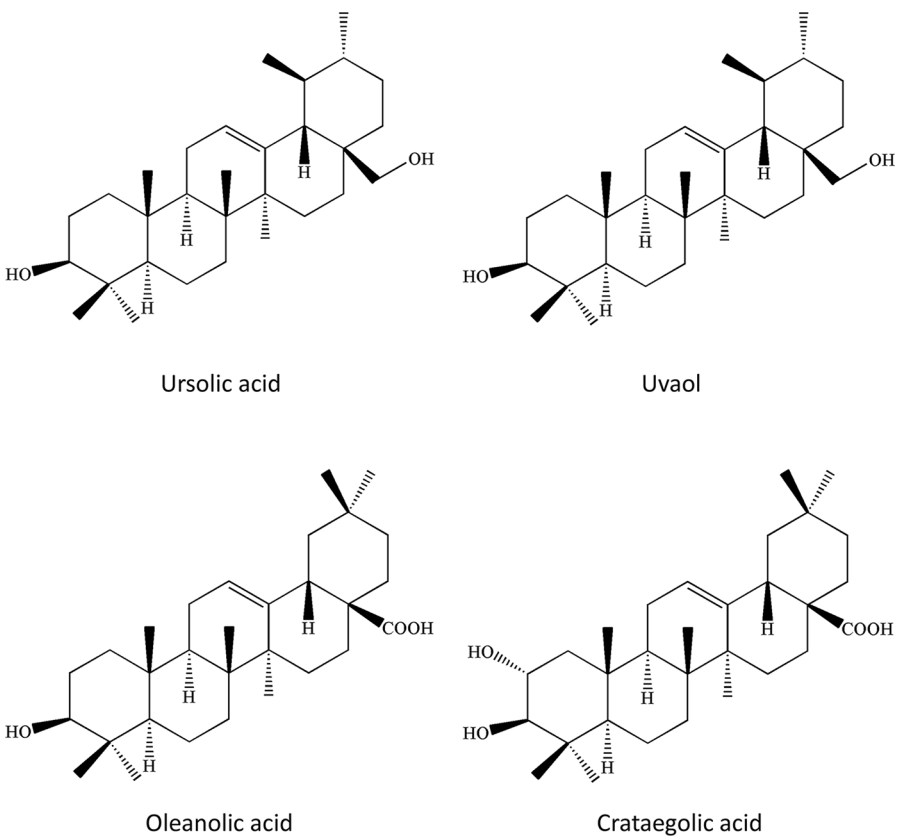

FIGURE 3 | Chemical structures of representative triterpenoids in *Crataegus pinnatifida*.

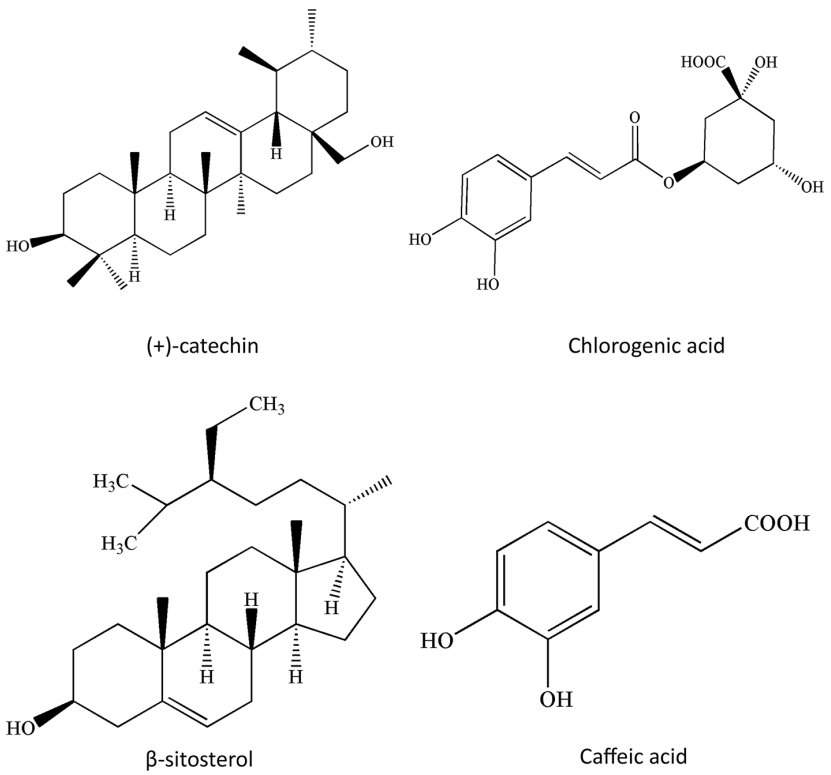

FIGURE 4 | Chemical structures of other compounds in *Crataegus pinnatifida*.

popularity and efficacy, the extracts of *Crataegus* sp. were assessed in several clinical trials. In addition to its well-known cardiotonic properties, *Crataegus oxyacantha* has also been reported to exert various other pharmacological activities such as anxiolytic, hypotensive, hypolipidemic, antioxidant, hypoglycemic, immunomodulatory, and antimutagenic activities. This article focuses mainly on the anti-atherosclerotic effects of hawthorn and summarizes the mechanisms involved in these effects.

Although no adverse events are reported in its current clinical use, *C. oxyacantha* extracts exhibit genotoxic and mutagenic effects in different cultured cell lines (de Quadros et al., 2017), as well as mild genotoxicity in mice (Yonekubo et al., 2018). Intriguingly, several studies showed a protective effect of *C. microphylla* extracts on a variety of genotoxic insults in lymphoid lineage cells (Hosseinimehr et al., 2006; Hosseinimehr et al., 2008; Hosseinimehr et al., 2009; Hosseinimehr et al., 2011). These results suggest caution regarding prolonged or high-dose use.

Hypolipidemic Activity

CVDs have been the leading cause of mortality and morbidity globally for decades. The primary pathogenesis of CVDs is atherosclerosis, which could lead to dramatic clinical events, such as unstable angina or myocardial infarction (Reiner et al., 2011). The underlying pathophysiological mechanisms of atherosclerosis are oxidative stress damage, lipid deposition, inflammatory responses, and vascular endothelial dysfunction (Libby et al., 2002; Weber and Noels, 2011). Multiple risk factors associated with the development of atherosclerotic plaque are diabetes mellitus, dyslipidemia, hypertension, obesity, and cigarette smoking (Folsom et al., 1997; Hackam and Anand, 2003; Mannarino and Pirro, 2008). Among the risk factors identified in epidemiological studies, only apolipoprotein (apo)-B containing lipoproteins, including low-density lipoproteins (LDLs) and very-low-density lipoproteins (VLDLs), cause atherosclerosis in both humans and experimental animals (Skålén et al., 2002).

Once the LDL traverses to the sub-endothelium, it binds to the chondroitin sulfate (CS) and dermatan sulfate (DS) site of the matrix proteoglycans, further leading to entrapment and phagocytosis by macrophages and other cells, eventually forming the foam cells and lipid core to initiate the local inflammatory response (Little et al., 2007). Lipid retention is an essential and critical initial step in the atherosclerotic cascade, and without this event, atherosclerosis could not be induced in animal models (Olofsson and Boren, 2005).

A 6-month clinical observation of 64 patients with carotid artery atherosclerosis showed that the ingestion of hawthorn extract at a dose of 5.0 mg/kg reduces the level of serum lipid and promotes plaque stability (Liu et al., 2014). *C. pinnatifida* extracts that primarily contain flavonoids showed promising hypolipidemic activity in different experimental animals. Flavonoid extracts from the leaves of *C. pinnatifida* considerably decreased level of the serum lipids, such as total cholesterol (TC)

and triglyceride (TG) in rats, mice, and rabbits (Zhang et al., 2002b; Luo et al., 2009; Zhang et al., 2013). The reduction in the level of serum total cholesterol and TG is a complex process involving multiple steps in cholesterol metabolism. First, it inhibits cholesterol absorption by downregulating the expression and activity of intestinal acyl-CoA cholesterol acyltransferase (ACAT). Intestinal ACAT is a critical regulator involved in cholesterol absorption by esterification of cholesterol before absorption (Zhang et al., 2002a). Second, the total flavonoids attenuate the expression of two essential liver enzymes involved in lipid biosynthesis, hydroxy methylglutaryl coenzyme A reductase (HMG-CoA) and cholesterol-7-alpha-hydroxylase (CYP7α) (Zhang et al., 2002a; Kwok et al., 2013). Moreover, the total flavonoids of *C. pinnatifida* inhibit the mature adipocyte secretion of the leptin and plasminogen activator inhibitor (PAI)-1 (Liu et al., 2009c) and decrease adipogenesis-related gene expression, including sterol regulatory element-binding proteins-1c (SREBP), fatty acid synthase (FAS), triacylglycerol hydrolase (TGH), and hormone-sensitive TG lipase (HSL) (Xie et al., 2009). A more recent study showed consistent results using extracts derived from the leaves of *C. pinnatifida* [Hawthorn leaf flavonoids (HLF)]. HLF decreased serum lipid levels, including total TGs, cholesterols, and lipoproteins, such as VLDLs and LDLs in Apoe$^{-/-}$ mice due to the involvement of the hepatic lipid metabolism-related genes, including peroxisome proliferator-activated receptor (PPAR)α, SREBP-1c, CPT-1, and HMG-CoAR reductase (Dong et al., 2017). *In vitro* data showed HLF inhibited the formation of foam cells by promoting cellular cholesterol efflux *via* the upregulation of the ATP-binding cassette transporter A1 (ABCA1), PPARγ, and downregulation of CD36, thus preventing the progression of atherosclerotic lesions (Liu et al., 2009a). Another line of research showed that pectin oligosaccharides and pectin hydrolysates fractionated from *C. pinnatifida* could restore unbalanced cholesterol metabolism and serum lipid overload in mice or hamsters that are fed a high-fat diet (HFD) (Li et al., 2010; Li et al., 2014; Zhu et al., 2015). This is specifically by the involvement of hepatic enzymes, such as glycerol 3-phosphate acyltransferase (GPAT), SREBP-2, phosphatidate phosphohydrolase (PAP), cholesterol-7α-hydroxylase (Zhu et al., 2013; Li et al., 2014), and hepatic fatty acid oxidation-related enzyme activities of acyl-CoA oxidase, 3-ketoacyl-CoA thiolase, 2,4-dienoyl-CoA reductase, and carnitine palmitoyltransferase I (Li et al., 2013b), and these results are consistent with earlier reported data. For example, pectin penta-oligogalacturonide was shown to increase the expression of CYP7A1, bile salt export pump, but not the sodium-taurocholate co-transporting polypeptide (Zhu et al., 2017). Similarly, pectin also reportedly downregulated the abnormal activity of high fat-induced SREBF-1c, suppressing the protein expression levels, pyruvate kinase, acetyl-CoA carboxylase, and fatty acid synthase enzyme activities (Li et al., 2017). Altogether, these data showed that pectin and its derivatives may be promising candidates for the treatment of hyperlipidemia and atherosclerosis.

Most of the research was conducted with the European and East Asian species. There exists little knowledge on plants native to other parts of the world. One study on the extracts from berries and leaves of *Crataegus chrysocarpa*, a species native to North America, showed that a reduced serum fasting LDL-C improved heart function by elevating the nitric oxide (NO) levels (Diane et al., 2016).

Anti-Oxidative Activity

Although elevated serum lipid levels are essential for atherosclerosis progression, LDLs in their native state cannot trigger the lipid retention cascade before oxidization by free radicals. Therefore, oxidative stress is crucial to illustrate atherogenic mechanisms. Oxidative stress is a state of unbalanced tissue oxidation due to the disturbed equilibrium between pro-oxidant and antioxidant molecules, an essential step in the pathophysiological development of atherosclerosis (Stocker and Keaney, 2004). Analysis of the atherosclerotic lesion compositions showed the oxidative products of protein and lipid such as F2α-isoprostanes, chlorinated lipid hydroperoxides, short-chain aldehydes, nitrated amino acids, oxidized phospholipids, and oxysterols as the major constituents (Heinecke, 1998). Recent studies, both *in vivo* and *in vitro*, showed that the extracts of *C. pinnatifida* eliminate free radicals to attenuate LDL oxidation (Wang T. et al., 2011; Cheng et al., 2013; Bedreag et al., 2014). In contrast to native LDLs, only the modified or oxidized LDLs can drive the development of atherosclerosis. It has been demonstrated that extracts from *C. pinnatifida* exert potent scavenging properties against DPPH, hydroxyl radicals, and copper-II and peroxyl radical-induced LDL cholesterol oxidation (Zhang et al., 2001; Liu et al., 2009b), as well as hydrogen peroxide and superoxide species (Bahorun et al., 1996), which is partially due to interactions with antioxidant enzymes, such as superoxide dismutase (SOD) and glutathione peroxidase (GSH-px) (Wang W. et al., 2011; Zhang et al., 2014). The pectin oligosaccharides of the *C. pinnatifida* fruit also reduced the aberrant oxidative state in a mouse model of experimental hyperlipidemia, as indicated by reduced serum synthesis and accumulation of malondialdehyde and increased SOD levels (Li et al., 2010). Metabolomic results showed that seedless hawthorn fruit extracts increased the levels of 11 different metabolites related to oxidative responses, as well as the concentration of NO and the activity of NO synthase, which are known factors that prevent against oxidative impairments (Zheng et al., 2019). The mechanism may involve the nuclear factor erythroid 2–related factor (Nrf2)/heme oxygenase-1 (HO-1) signaling pathway, major sentinels, and effectors in response to the oxidative status (Yoo et al., 2016). Similarly, another study provided evidence that the total flavones of hawthorn mitigate the endothelial cell impairment after coronary bypass graft operation by reducing the oxidative stress (Zhu et al., 2018). In addition, extracts of *C. oxyacantha* attenuate the ischemia–reperfusion insults, and the potential mechanism might be attributed to a reduction in the oxidative stress level, which increases after ischemia–reperfusion injury (Ranjbar et al., 2018). Furthermore, vitexin (an extract from hawthorn leaves) suppressed doxorubicin (DOX)-induced oxidative stress, inflammation, apoptosis, and myocardial damage through a mechanism involving increased cellular expression of p-FoxO3a (Sun et al., 2016). Thus, the Akt/FoxO3a signaling

pathway may be a novel target for the development of drugs to reduce DOX-induced cardiotoxicity.

Endothelium Protection

Endothelium dysfunction is a well-known independent risk factor for coronary heart disease and is closely associated with its clinical outcome (Daiber et al., 2017). Endothelium dysfunction occurs in the early stages of atherogenesis, characterized by a reduction of NO-mediated vasodilator responses and increased vasoconstriction due to excess endothelin (ET)-1 synthesis, resulting in enhanced vascular permeability. Such alterations lead to increased cell permeability, the release of pro-inflammatory factors, such as adhesion molecules and cytokines leukocyte adherence, platelet hyper-activation, enhanced low-density lipoprotein oxidation, as well as vascular smooth muscle cell proliferation and migration (Corte et al., 2016; Costantino et al., 2016; Jamwal and Sharma, 2018).

Hawthorn extracts resulted in decreased ET-1 and elevated NO levels in both human and animal experiments (Asher et al., 2012; Zhang et al., 2013). Endothelial NO synthase (eNOS) is a critical regulator of NO synthesis. The translocation from the cell membrane results in increased phosphorylation of serine residue 1177 or decreased phosphorylation of threonine residue 495, which are pathways for activating eNOS. Hawthorn extracts could induce vasorelaxation by increasing the phosphorylation of serine residue 1177 (Brixius et al., 2006). Hawthorn extract WS® 1442 increases cytosolic $[Ca^{2+}]$ i by suppressing sarcoplasmic/endoplasmic reticulum Ca^{2+} ATPase (SERCA) and activating the inositol 1,4,5-trisphosphate (IP3) pathway, but without affecting the barrier function or endothelial cell contraction. More importantly, it does not induce store-operated calcium entry (Willer et al., 2012).

In other pathological conditions attributed to atherogenesis, such as diabetes, aging, and hypertension, hawthorn extracts have shown a promising effect in maintaining the integrity and normal endothelial function both *in vitro* and *in vivo* (Xiyun and Yaofa, 2002; Bubik et al., 2012; Idris-Khodja et al., 2012; Peters et al., 2012; Topal et al., 2013).

Anti-Inflammatory Activity

Over the past decades, lipid retention and oxidation are regarded as the *sine qua non* of the atherosclerosis (Moriya, 2019), and how and where the lipid oxidation occurs have not been identified. Chemical analysis of the modified lipids and proteins, using human atheroma samples, does not necessarily correspond to the transition metal-mediated oxidized lipoproteins *in vitro*; also, randomized clinical trials failed to validate the effectiveness of antioxidant therapy (Pascual-Teresa et al., 2010; Myung et al., 2013).

Recent atherosclerosis studies focused on inflammation, thus providing new insight into the mechanisms of this disease. Inflammation participates at all stages of atherosclerosis development. Clinical research has identified the critical role of inflammation in the development and progression of coronary artery disease. Immune cells are present in early atherosclerotic lesions, and their effector chemicals drive the development of the lesions. The hyper-activated inflammatory response can lead to acute coronary syndromes (Gimbrone and García-Cardeña, 2016; Ferrucci and Fabbri, 2018; Ridker, 2019). Our previous study showed that hawthorn extracts alleviated atherosclerosis by inhibiting inflammation and apoptosis-related factors (Wang et al., 2019).

An *in vitro* study on mouse macrophage cell line showed that an aqueous extract of hawthorn fruit suppressed expression of inflammatory cytokines, such as interleukin (IL)-1β, tumor necrosis factor (TNF)-α, and IL-6 (Kim et al., 2011), which may be regulated by the nuclear factor (NF)-κB, a well-known mediator for its role in pro- and anti-inflammatory regulation and for controlling the expression of inflammatory genes including adhesion molecules, cytokines, and chemokines. Data from *Crataegus aronia* extracts showed inhibition of the nuclear accumulation of NF-κB and NLRP-3 protein levels and caspase-1 in HFD-induced aortic vascular inflammation in rats, thus suggesting inhibition of the NLRP3 inflammasome-mediated pathway (Shatoor and Al Humayed, 2019). The monocyte/macrophage is a major immunocyte involved in atherosclerosis, which scavenges modified LDLs and accelerates the local inflammatory response (Kao et al., 2005). One study reported that water extracts of *C. pinnatifida* inhibited NO production and inflammatory gene expression, including TNF-α, COX-2, IL-1β, and IL-6 in lipopolysaccharide (LPS)-stimulated RAW 264.7 cells (Li and Wang, 2011). In addition, ethanol extracts of *C. pinnatifid*a seeds elicit a potent NO and TNF-α inhibitory effect, hence regarded as a promising and reliable source of antioxidants and inhibitors of inflammation (Peng et al., 2016). Clinical evidence showed that when metformin was combined with hawthorn, the level of body mass index (BMI), HbA1c, FPG, 2hPG, TG, and hs-CRP remarkably reduced in patients with prediabetes complicated by nonalcoholic fatty liver disease (Gao et al., 2019). Altogether, these studies demonstrate that hawthorn extracts may be a promising drug for the treatment and prevention of atherosclerosis.

In addition to the activities mentioned above, the newly identified norditerpenoids from the leaves of *C. pinnatifid*a exert antithrombotic activities both *in vitro* and *in vivo* (Gao et al., 2017). The norditerpenoids prevent adenosine diphosphate-induced platelet accumulation, mediated in response to the purinergic P2Y receptor, and delay thrombocyte aggregation induced by $FeCl_3$ in the caudal vessels of zebrafish (Gao et al., 2017). Antiplatelet and antithrombotic treatment is a critical approach for the treatment of acute coronary artery syndrome and secondary prevention of coronary heart disease, as recommended by the global guidance for CVD (Vandvik et al., 2012; Stewart et al., 2017).

However, hawthorn ingestion could lead to higher bleeding risk, and a clinical study of patients who underwent cardiac surgery reported that hawthorn extract consumption may increase the postoperative bleeding rate, the amount of chest tube output after cardiac surgery, and most importantly, the overall mortality (Rababa'h et al., 2016). Since the use of antiplatelet and antithrombotic medications are quite common in the treatment of CVDs, such as atherosclerosis, arrhythmia, and post-percutaneous coronary intervention, patients with such diseases should exercise caution while using hawthorn as an adjuvant medication. Further high-grade evidence is also

required to assess the safety of hawthorn products in the treatment of CVDs.

Apart from these actions, one more recent study showed that a 16-week oral administration of *C. pinnatifida* leaf extracts suppressed the overall apoptotic level in the aorta, as indicated by the alternations of the expressions of Bcl-2 (B-cell lymphoma 2) and BAX (BCL2-associated X protein) (Wang et al., 2019). Besides, hawthorn extracts were reported to process an antiapoptotic effect in ischemic myocardial damage (Jayachandran et al., 2010; Ranjbar et al., 2018), a common result due to atherosclerotic lesions invading coronary arteries. This may attribute to the activation of Akt and HIF-1 (hypoxia-inducible factors) signaling pathways (Jayachandran et al., 2010). Myocardial apoptosis is known as a key pathological feature under ischemic conditions. Strategies against apoptotic cascades have been proposed for the treatment of ischemic heart disease (Perricone and Vander Heide, 2014). To this end, hawthorn extracts may be promising complementation for the treatment of cardiac ischemic injuries as well as post myocardial infarction rehabilitation. (The cardiovascular effects are shown in **Table 1** and **Figure 5**.)

CONCLUSIONS

Medicinal plants possessing considerable quantities of therapeutic natural products are considered a promising source of medicine and chemicals. Herbal plants are becoming the top-selling phytotherapeutics globally. A plethora of preclinical studies have shown that hawthorn extracts possess cardioprotective and anti-atherosclerotic properties and contain major bioactive components identified as flavonoids, polyphenols, and oligomeric procyanidins. The underlying mechanisms are associated with reduced serum lipid contents, which involve inhibition of lipid absorption in intestines and cholesterol *de novo* synthesis in the liver, as well as promoting cholesterol efflux, which subsequentially suppresses lipid retention and plaque formation. Reduced lipid

TABLE 1 | Major effects and targets of *Crataegus* in atherosclerosis.

Effects	Species	Materials	Subjects	Targets	Reference
Lipid-lowering effect	*C. pinnatifida*	Freeze-dried fruit powder	ApoE$^{-/-}$ mice	ACAT SREBP-1c HMG-CoAR, CYP7α FAS PPARα, CPT-1	Zhang et al., 2014
		Fruit powder	New Zealand rabbits	HMG-CoAR, CYP7α ACAT	Zhang et al., 2002b
		Ethanol extracts	Syrian golden hamsters	HMG-CoAR ACAT	Zhang et al., 2002a
		Total flavonoids	3T3-L1 cells	Leptin	Liu et al., 2009c
	C. pinnatifida var. *major*	50% ethanol extracts of leaf	Macrophage of ApoE$^{-/-}$ mice	PPARγ, ABCA1, CD36	Liu et al., 2009a
Antioxidant effect	*C. pinnatifida*	Freeze-dried fruit powder	ApoE$^{-/-}$ mice	SOD1, SOD2, Gpx3	Zhang et al., 2014
	C. pinnatifida var. *major*	Aqueous extracts of fruits	Wistar rats	SOD, MDA	Wang W. et al., 2011
Endothelial protection	*C. pinnatifida* var. *major*	Aqueous extracts	Wistar rats	NO, ET 6-keto-PGF1α, TXB2	Zhang et al., 2013
	C. monogyna and *C. laevigata*	WS® 1442	Rat aorta and human internal mammary artery	Serine 1177 residual of eNOS	Brixius et al., 2006
			HUVECs, C57 mice	cAMP/Epac1/Rap1 pathway Ca^{2+}/PKC/RhoA signaling pathway	Bubik et al., 2012
			HUVECs	IP3 Sarcoplasmic/endoplasmic reticulum Ca^{2+} ATPase	Willer et al., 2012
Anti-inflammatory effect	*C. pinnatifida* var. *major*	50% ethanol extracts of leaf	Carotid artery atherosclerosis patients	CRP	Liu et al., 2014
		Aqueous extracts of fruits	Wistar rats	IL-18 CRP, IL-1β, IL-8	Zhang et al., 2013
	C. oxyacantha	Hawthorn vinegar	Cardiovascular risk patients	CRP	Kadas et al., 2014
	C. pinnatifida var. *typica*	Methanol extracts	RAW 264.7 cell	TNF-α, IL-1β, IL-6	Tauchert, 2002
	C. pinnatifida var. *major*	50% ethanol extracts of leaf	ApoE$^{-/-}$ mice	CRP, NF-κB	Zheng and Wang, 2010
Anti-apoptotic effect	*C. pinnatifida* var. *major*	50% ethanol extracts	ApoE$^{-/-}$ mice	BAX, Bcl-2	Wang et al., 2019
	C. oxyacantha	Heartcare™ tablets	Wistar rats	Akt and HIF-1 signaling pathways	Jayachandran et al., 2010

6-keto-PGF1α, 6-keto-prostaglandin F1α; ABCA1, ATP-binding cassette transporter 1; ACAT, acyl-CoA cholesterol acyltransferase; Bcl-2, B-cell lymphoma 2; BAX, BCL2-associated X protein; CPT-1, carnitine palmitoyltransterase-1; CRP, C-reactive protein; ET, endothelin; Gpx3, glutathione peroxidase 3; HIF-1, hypoxia-inducible factor 1; HUVECs, human umbilical vein endothelial cells; MDA, malondialdehyde; NF-κB, nuclear factor κB; NO, nitric oxide; PPAR, peroxisome proliferator-activated receptor; SOD, superoxide dismutase; TNF-α, tumor necrosis factor α; TXB2, thromboxane B2.

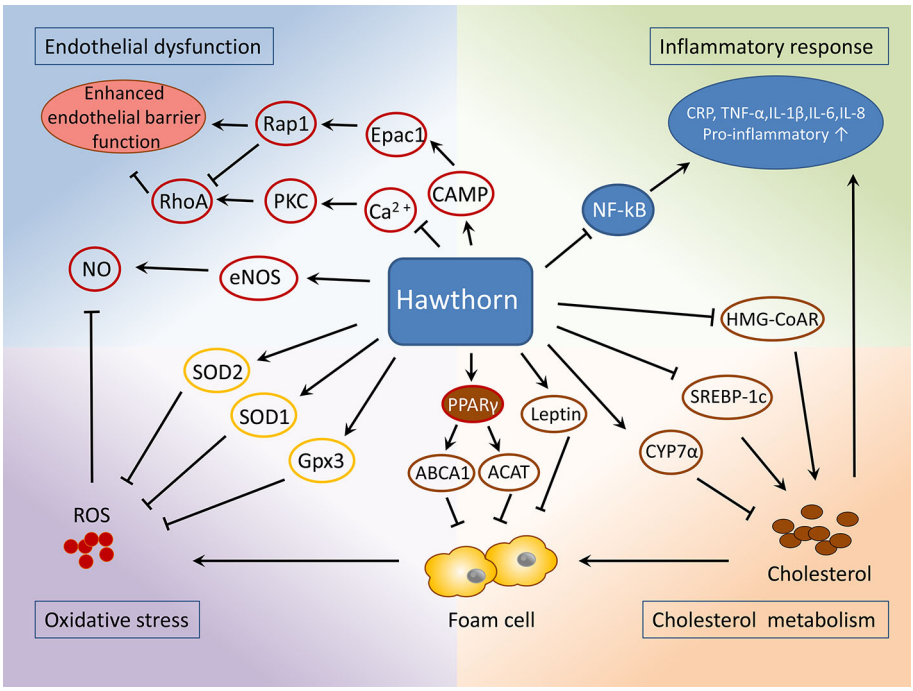

FIGURE 5 | Mechanisms of the protective role of hawthorn in the treatment of atherosclerosis.

retention then results in a lower number of foam cells, which is the major source of reactive oxygen species (ROS) and inflammatory cytokines. This also helps to maintain the normal function of endothelial cells, including its permeability, which in turn halts the lipid and circulating macrophage/monocyte infiltration.

These cardioprotective actions of the hawthorn target various pathological conditions associated with atherosclerosis, which may offer great potential for synergistic effects. In addition to these experimental data, a great deal of knowledge has been acquired regarding the benefits of hawthorn on other CVDs, including heart failure and primary hypertension (Wang et al., 2013; Holubarsch et al., 2018). However, little known is about its effects on coronary atherosclerosis in the clinical arena.

The current guidelines for the treatment of acute coronary syndrome and secondary prevention recommend medications such as inhibitor of platelet activation and aggregation, lipid modification drugs, β-blockers, and inhibitors of the renin-angiotensin-aldosterone system (RAAS) (Amsterdam et al., 2014; Roffi et al., 2016; Chinese Medical Association Cardiovascular Branch & Editorial Board of Chinese Journal of Cardiovascular Diseases, 2017). The biological effects of hawthorns may serve the needs of these strategies. The pathophysiology of atherosclerosis is complex; therefore, a therapeutic approach capable of targeting multiple arms of the cardioprotective aspects would likely elicit greatest efficacy in reducing the morbidity and mortality associated with atherosclerosis. However, the lack of investigation on its synergistic effects, and explanations on the specific underlying mechanisms, raises controversies with respect to its therapeutic efficacy. This calls for further clarification on whether the mixture of hawthorn extracts may exert synergistic benefits compared to the pure compound or rather exacerbate side effects.

It is worth noting that extracts from hawthorn leaves have been recorded in the European pharmacopoeia (European Pharmacopoeia, 2017) and in the pharmacopoeia of the People's Republic of China (Chinese Pharmacopoeia Commission, 2015), such as WS® 1442 which has been extensively investigated in both preclinical and clinical studies. However by now, none of its effects on patients with coronary heart disease was reported. In China, several hawthorn leaf products for the treatment of angina and coronary heart disease have been approved by the National Medical Products Administration for sale (http://www.nmpa.gov.cn/WS04/CL2042/). Nevertheless, clinical and pharmacological data of these drugs are not enough to evaluate its efficacy at the present moment.

Furthermore, the current consensus on the primary and secondary prevention of coronary heart disease requires long-term use of various medications interacting with multiple targets. The combined application of the hawthorn with other medications may give rise to unexpected effects. Hence, high-quality trials with long-term follow-up are warranted to provide more compelling evidence of its safety and efficacy.

Taken together, the cardiovascular activities and clinical implications of hawthorn extracts have been extensively studied. Current evidence shows its potential as a phytotherapeutic agent adjuvant in conventional management of coronary heart disease. This requires further efforts to explore its clinical efficacy and safety for the treatment of atherosclerosis.

AUTHOR CONTRIBUTIONS

MW and LL contributed equally to this manuscript. YC, HL, MW, LL, SY, and YX participated in the conception of the review. YC and HL drafted the initial full manuscript. MW and LL edited the manuscript.

FUNDING

This work was funded by the Beijing Natural Science Foundation (No.7172185), the National Key R&D Program of China (2018YFC1704901), and the National Natural Science Foundation of China (No. 81202805, 81973689, and 81573821).

REFERENCES

Özcan, M., Hacıseferoğulları, H., Marakoğlu, T., and Arslan, D. (2005). Hawthorn (*Crataegus* spp.) fruit: some physical and chemical properties. *J. Food Eng.* 69, 409–413. doi: 10.1016/j.jfoodeng.2004.08.032

Amsterdam, E. A., Wenger, N. K., Brindis, R. G., Casey, D. E., Ganiats, T. G., Holmes, D. R., et al. (2014). 2014 AHA/ACC guideline for the management of patients with non–ST-elevation acute coronary syndromes: a report of the american college of cardiology/american heart association task force on practice guidelines. *J. Am. Coll. Cardiol.* 64, e139–e228. doi: 10.1161/CIR.0000000000000134

Asher, G. N., Viera, A. J., Weaver, M. A., Dominik, R., Caughey, M., and Hinderliter, A. L. (2012). Effect of hawthorn standardized extract on flow mediated dilation in prehypertensive and mildly hypertensive adults: a randomized, controlled cross-over trial. *BMC Complem. Altern. Med.* 12, 26. doi: 10.1186/1472-6882-12-26

Bahorun, T., Gressier, B., Trotin, F., Brunet, C., Dine, T., Luyckx, M., et al. (1996). Oxygen species scavenging activity of phenolic extracts from hawthorn fresh plant organs and pharmaceutical preparations. *Arzneimittelforsch* 46, 1086–1089.

Bedreag, C. F., Trifan, A., Vasincu, A., Miron, S. D., Aprotosoaie, A. C., and Miron, A. (2014). *In vitro* screening of Crataegus succulenta extracts for free radical scavenging and 15-lipoxygenase inhibitory activities. *Rev. Med. Chir. Soc Med. Nat. Iasi* 118, 544–550.

Bodeker, G., and Ong, C. K. (2005). *WHO global atlas of traditional, complementary and alternative medicine* (Kobe, Japan: World Health Organization).

Brixius, K., Willms, S., Napp, A., Tossios, P., Ladage, D., Bloch, W., et al. (2006). Crataegus special extract WS® 1442 induces an endothelium-dependent, NO-mediated vasorelaxation *via* eNOS-phosphorylation at serine 1177. *Cardiovasc. Drugs Ther.* 20, 177–184. doi: 10.1007/s10557-006-8723-7

Bubik, M. F., Willer, E. A., Bihari, P., Jürgenliemk, G., Ammer, H., Krombach, F., et al. (2012). A novel approach to prevent endothelial hyperpermeability: the Crataegus extract WS® 1442 targets the cAMP/Rap1 pathway. *J. Mol. Cell Cardiol.* 52, 196–205. doi: 10.1016/j.yjmcc.2011.10.020

Chang, Q., Zuo, Z., Harrison, F., and Chow, M. S. S. (2002). Hawthorn. *J. Clin. Pharmacol.* 42, 605–612. doi: 10.1177/00970002042006003

Cheng, N., Wang, Y., Gao, H., Yuan, J., Feng, F., Cao, W., et al. (2013). Protective effect of extract of Crataegus pinnatifida pollen on DNA damage response to oxidative stress. *Food Chem. Toxicol.* 59, 709–714. doi: 10.1016/j.fct.2013.07.015

Chinese Medical Association Cardiovascular Branch, Editorial Board of Chinese Journal of Cardiovascular Diseases (2017). Guidelines for the diagnosis and treatment of non - ST - segment elevation acute coronary syndrome, (2016). *Chin. J. Cardiol.* 45, 359–376. doi: 10.3760/cma.j.issn.0253-3758.2017.05.003

Chinese Pharmacopoeia Commission (2015). *Pharmacopoeia of the People's Republic of China. Part I* (Beijing: China Medical Science Press).

Cloud, A. M. E., Vilcins, D., and McEwen, B. J. (2019). The effect of hawthorn (*Crataegus* spp.) on blood pressure: a systematic review. *Adv. Integr. Med.* doi: 10.1016/j.aimed.2019.09.002

Corte, V. D., Tuttolomondo, A., Pecoraro, R., Di Raimondo, D., Vassallo, V., and Pinto, A. (2016). Inflammation, endothelial dysfunction and arterial stiffness as therapeutic targets in cardiovascular medicine. *Curr. Pharm. Des.* 22, 4658–4668. doi: 10.2174/1381612822666160510124801

Costantino, S., Paneni, F., and Cosentino, F. (2016). Ageing, metabolism and cardiovascular disease. *J. Physiol.* 594, 2061–2073. doi: 10.1113/JP270538

Daiber, A., Steven, S., Weber, A., Shuvaev, V. V., Muzykantov, V. R., Laher, I., et al. (2017). Targeting vascular (endothelial) dysfunction. *Br. J. Pharmacol.* 174, 1591–1619. doi: 10.1111/bph.13517

de Quadros, A. P. O., Mazzeo, D. E. C., Marin-Morales, M. A., Perazzo, F. F., Rosa, P. C. P., and Maistro, E. L. (2017). Fruit extract of the medicinal plant Crataegus oxyacantha exerts genotoxic and mutagenic effects in cultured cells. *J. Toxicol. Environ. Health A.* 80, 161–170. doi: 10.1080/15287394.2016.1272517

Dehghani, S., Mehri, S., and Hosseinzadeh, H. (2019). The effects of Crataegus pinnatifida (Chinese hawthorn) on metabolic syndrome: a review. *Iran J. Basic Med. Sci.* 22, 460–468. doi: 10.22038/IJBMS.2019.31964.7678

Diane, A., Borthwick, F., Wu, S., Lee, J., Brown, P. N., Dickinson, T. A., et al. (2016). Hypolipidemic and cardioprotective benefits of a novel fireberry hawthorn fruit extract in the JCR: LA-cp rodent model of dyslipidemia and cardiac dysfunction. *Food Funct.* 7, 3943–3952. doi: 10.1039/C6FO01023G

Dong, P., Pan, L., Zhang, X., Zhang, W., Wang, X., Jiang, M., et al. (2017). Hawthorn (Crataegus pinnatifida Bunge) leave flavonoids attenuate atherosclerosis development in apoE knock-out mice. *J. Ethnopharmacol.* 198, 479–488. doi: 10.1016/j.jep.2017.01.040

Du, X., Patel, A., Anderson, C. S., Dong, J., and Ma, C. (2019). Epidemiology of Cardiovascular Disease in China and Opportunities for Improvement: JACC International. *J. Am. Coll. Cardiol.* 73, 3135–3147. doi: 10.1016/j.jacc.2019.04.036

Ekor, M. (2014). The growing use of herbal medicines: issues relating to adverse reactions and challenges in monitoring safety. *Front. Pharmacol.* 4, 177. doi: 10.3389/fphar.2013.00177

European Pharmacopoeia (2017). *Europäisches Arzneibuch* Vol. 9.0 (Stuttgart, Germany: Deutscher Apotheker Verlag), 2359–2360.

Ferrucci, L., and Fabbri, E. (2018). Inflammageing: chronic inflammation in ageing, cardiovascular disease, and frailty. *Nat. Rev. Cardiol.* 15, 505–522. doi: 10.1038/s41569-018-0064-2

Folsom, A. R., Wu, K. K., Rosamond, W. D., Sharrett, A. R., and Chambless, L. E. (1997). Prospective study of hemostatic factors and incidence of coronary heart disease: the Atherosclerosis Risk in Communities (ARIC) Study. *Circulation* 96, 1102–1108. doi: 10.1161/01.CIR.96.4.1102

Gao, P. Y., Li, L. Z., Liu, K. C., Sun, C., Sun, X., Wu, Y. N., et al. (2017). Natural terpenoid glycosides with *in vitro*/vivo antithrombotic profiles from the leaves of *Crataegus pinnatifida*. *Rsc Adv.* 7, 48466–48474. doi: 10.1039/C7RA10768D

Gao, Z., Xie, M., Wang, N., Chen, L., and Huang, X. (2019). Effects of combination treatment of metformin and hawthorn in patients with prediabetes complicated by nonalcoholic fatty liver disease. *Int. J. Clin. Exp. Med.* 12, 1979–1984.

Gimbrone, M. A. Jr., and García-Cardeña, G. (2016). Endothelial cell dysfunction and the pathobiology of atherosclerosis. *Circ. Res.* 118, 620–636. doi: 10.1161/CIRCRESAHA.115.306301

González-Jiménez, F. E., Salazar-Montoya, J. A., Calva-Calva, G., and Ramos-Ramírez, E. G. (2018). Phytochemical characterization, *in vitro* antioxidant activity, and quantitative analysis by micellar electrokinetic chromatography of hawthorn (*Crataegus pubescens*) fruit. *J. Food Qual.* 2018, 2154893. doi: 10.1155/2018/2154893

Hackam, D. G., and Anand, S. S. (2003). Emerging risk factors for atherosclerotic vascular disease: a critical review of the evidence. *JAMA* 290, 932–940. doi: 10.1001/jama.290.7.932

Heinecke, J. W. (1998). Oxidants and antioxidants in the pathogenesis of atherosclerosis: implications for the oxidized low density lipoprotein hypothesis. *Atherosclerosis* 141, 1–15. doi: 10.1016/S0021-9150(98)00173-7

Hobbs, C., and Foster, S. (1994). Hawthorn: a literature review. *Herbal Gram.* 22, 19–33.

Holubarsch, C. J., Colucci, W. S., Meinertz, T., Gaus, W., Tendera, M., Survival,, et al. (2008). The efficacy and safety of Crataegus extract WS® 1442 in patients

with heart failure: the spice trial. *Eur. J. Heart Fail.* 10, 1255–1263. doi: 10.1016/j.ejheart.2008.10.004

Holubarsch, C. J., Colucci, W. S., and Eha, J. (2018). Benefit-risk assessment of Crataegus extract WS 1442: an evidence-based review. *Am. J. Cardiovasc. Drug* 18, 25–36. doi: 10.1007/s40256-017-0249-9

Hosseinimehr, S. J., Azadbakht, M., Mousavi, S. M., Mahmoudzadeh, A., and Akhlaghpoor, S. (2006). Radioprotective effects of hawthorn fruit extract against gamma irradiation in mouse bone marrow cells. *J. Radiat. Res.* 48, 63–68. doi: 10.1269/jrr.06032

Hosseinimehr, S. J., Azadbakht, M., and Abadi, A. J. (2008). Protective effect of hawthorn extract against genotoxicity induced by cyclophosphamide in mouse bone marrow cells. *Environ. Toxicol. Pharmacol.* 25, 51–56. doi: 10.1016/j.etap.2007.08.006

Hosseinimehr, S. J., Mahmoudzadeh, A., Azadbakht, M., and Akhlaghpoor, S. (2009). Radioprotective effects of Hawthorn against genotoxicity induced by gamma irradiation in human blood lymphocytes. *Radiat. Environ. Biophys.* 48, 95–98. doi: 10.1007/s00411-008-0190-z

Hosseinimehr, S. J., Azadbakht, M., Tanha, M., Mahmodzadeh, A., and Mohammadifar, S. (2011). Protective effect of hawthorn extract against genotoxicity induced by methyl methanesulfonate in human lymphocytes. *Toxicol. Ind. Health* 27, 363–369. doi: 10.1177/0748233710387010

Idris-Khodja, N., Auger, C., Koch, E., and Schini-Kerth, V. (2012). Crataegus special extract WS® 1442 prevents aging-related endothelial dysfunction. *Phytomedicine* 19, 699–706. doi: 10.1016/j.phymed.2012.04.005

Jamwal, S., and Sharma, S. (2018). Vascular endothelium dysfunction: a conservative target in metabolic disorders. *Inflamm. Res.* 67, 391–405. doi: 10.1007/s00011-018-1129-8

Jayachandran, K. S., Khan, M., Selvendiran, K., Devaraj, S. N., and Kuppusamy, P. (2010). Crataegus oxycantha extract attenuates apoptotic incidence in myocardial ischemia-reperfusion injury by regulating Akt and HIF-1 signaling pathways. *J. Cardiovasc. Pharmacol.* 56, 526–531. doi: 10.1097/FJC.0b013e3181f64c51

Kadas, Z., Evrendilek, G. A., and Heper, G. (2014). The metabolic effects of hawthorn vinegar in patients with high cardiovascular risk group. *J. Food Nutr. Res.* 2, 539–545. doi: 10.12691/jfnr-2-9-2

Kao, E. S., Wang, C. J., Lin, W. L., Yin, Y. F., Wang, C. P., Tseng, T. H., et al. (2005). Anti-inflammatory potential of flavonoid contents from dried fruit of *Crataegus pinnatifida in vitro* and *in vivo*. *J. Agric. Food. Chem.* 53, 430–436. doi: 10.1021/jf040231f

Kim, S. J., Um, J. Y., Hong, S. H., and Lee, J. Y. (2011). Anti-inflammatory activity of hyperoside through the suppression of nuclear factor-κB activation in mouse peritoneal macrophages. *Am. J. Chin. Med.* 39, 171–181. doi: 10.1142/S0192415X11008737

Kwok, C. Y., Li, C., Cheng, H. L., Ng, Y. F., Chan, T. Y., Kwan, Y. W., et al. (2013). Cholesterol lowering and vascular protective effects of ethanolic extract of dried fruit of *Crataegus pinnatifida*, hawthorn (Shan Zha), in diet-induced hypercholesterolaemic rat model. *J. Funct. Foods.* 5, 1326–1335. doi: 10.1016/j.jff.2013.04.020

Li, C., and Wang, M. H. (2011). Anti-inflammatory effect of the water fraction from hawthorn fruit on LPS-stimulated RAW 264.7 cells. *Nutr. Res. Pract.* 5, 101–106. doi: 10.4162/nrp.2011.5.2.101

Li, T., Li, S., Du, L., Wang, N., Guo, M., Zhang, H., et al. (2010). Effects of haw pectic oligosaccharide on lipid metabolism and oxidative stress in experimental hyperlipidemia mice induced by high-fat diet. *Food Chem.* 121, 1010–1013. doi: 10.1016/j.foodchem.2010.01.039

Li, S., Li, T., Zhu, R., Wang, N., Song, Y., Wang, S., et al. (2013a). Antibacterial action of haw pectic oligosaccharides. *Int. J. Food Prop.* 16, 706–712. doi: 10.1080/10942912.2011.565904

Li, T. P., Zhu, R. G., Dong, Y. P., Liu, Y. H., Li, S. H., and Chen, G. J. (2013b). Effects of pectin pentaoligosaccharide from Hawthorn (*Crataegus pinnatifida* Bunge. var. *major*) on the activity and mRNA levels of enzymes involved in fatty acid oxidation in the liver of mice fed a high-fat diet. *J. Agric. Food. Chem.* 61, 7599–7605. doi: 10.1021/jf400283w

Li, T., Li, S., Dong, Y., Zhu, R., and Liu, Y. (2014). Antioxidant activity of penta-oligogalacturonide, isolated from haw pectin, suppresses triglyceride synthesis in mice fed with a high-fat diet. *Food Chem.* 145, 335–341. doi: 10.1016/j.foodchem.2013.08.036

Li, S., Huang, Z., Dong, Y., Zhu, R., and Li, T. (2017). Haw pectin pentaglaracturonide inhibits fatty acid synthesis and improves insulin sensitivity in high-fat-fed mice. *J. Funct. Foods.* 34, 440–446. doi: 10.1016/j.jff.2017.04.030

Libby, P., Ridker, P. M., and Maseri, A. (2002). Inflammation and atherosclerosis. *Circulation* 105, 1135–1143. doi: 10.1161/hc0902.104353

Little, P. J., Ballinger, M. L., and Osman, N. (2007). Vascular wall proteoglycan synthesis and structure as a target for the prevention of atherosclerosis. *Vasc. Health Risk. Manage.* 3, 117–124.

Liu, M., Zhang, W., and Liu, L. (2009a). Effect on PPARγ, ABCA1 and CD36 mRNA in macrophage of apoprotein e knock out mice with extractive of giant knotweed rhizome and hawthorn [J]. *Chin. J. Arterioscler.* 17, 902–906.

Liu, P., Kallio, H., Lu, D., Zhou, C., Ou, S., Yang, B., et al. (2009b). Acids, sugars, and sugar alcohols in Chinese hawthorn (*Crataegus* spp.) fruits. *J. Agric. Food. Chem.* 58, 1012–1019. doi: 10.1021/jf902773v

Liu, X., Zhou, L., Liang, R., and Wang, P. (2009c). Study on lipid regulation mechanism of total flavonoids from Folium crataegi by 3T3-L1 cells. *Chin. Arch. Tradit. Chin. Med.* 27, 1066–1068.

Liu, P., Kallio, H., Lü, D., Zhou, C., and Yang, B. (2011). Quantitative analysis of phenolic compounds in Chinese hawthorn (*Crataegus* spp.) fruits by high performance liquid chromatography–electrospray ionisation mass spectrometry. *Food Chem.* 127, 1370–1377. doi: 10.1016/j.foodchem.2011.01.103

Liu, L., Zheng, G., Zhang, W., Guo, G., and Wu, M. (2014). Clinical study on treatment of carotid atherosclerosis with extraction of Polygoni Cuspidati Rhizoma et Radix and Crataegi Fructus: a randomized controlled trial. *China J. Chin. Mater. Med.* 39, 1115–1119.

Liu, S., Chang, X., Liu, X., and Shen, Z. (2016). Effects of pretreatments on anthocyanin composition, phenolics contents and antioxidant capacities during fermentation of hawthorn (Crataegus pinnatifida) drink. *Food Chem.* 212, 87–95. doi: 10.1016/j.foodchem.2016.05.146

Luo, Y., Chen, G., Li, B., Ji, B., Xiao, Z., Yi, G., et al. (2009). Dietary intervention with AHP, a functional formula diet, improves both serum and hepatic lipids profile in dyslipidemia mice. *J. Food Sci.* 74, H189–H195. doi: 10.1111/j.1750-3841.2009.01241.x

Mannarino, E., and Pirro, M. (2008). Endothelial injury and repair: a novel theory for atherosclerosis. *Angiology* 59 (2_suppl), 69S–72S. doi: 10.1177/0003319708320761

Moriya, J. (2019). Critical roles of inflammation in atherosclerosis. *J. Cardiol.* 73, 22–27. doi: 10.1016/j.jjcc.2018.05.010

Mraihi, F., Hidalgo, M., de Pascual-Teresa, S., Trabelsi-Ayadi, M., and Cherif, J.-K. (2015). Wild grown red and yellow hawthorn fruits from tunisia as source of antioxidants. *Arab. J. Chem.* 8, 570–578. doi: 10.1016/j.arabjc.2014.11.045

Myung, S. K., Ju, W., Cho, B., Oh, S. W., Park, S. M., Koo, B. K., et al. (2013). Efficacy of vitamin and antioxidant supplements in prevention of cardiovascular disease: systematic review and meta-analysis of randomised controlled trials. *Br. Med. J.* 346, f10. doi: 10.1136/bmj.f10

Olofsson, S. O., and Boren, J. (2005). Apolipoprotein B: a clinically important apolipoprotein which assembles atherogenic lipoproteins and promotes the development of atherosclerosis. *J. Intern. Med.* 258, 395–410. doi: 10.1111/j.1365-2796.2005.01556.x

Pascual-Teresa, D., Moreno, D. A., and García-Viguera, C. (2010). Flavanols and anthocyanins in cardiovascular health: a review of current evidence. *Int. J. Mol.* 11, 1679–1703. doi: 10.3390/ijms11041679

Peng, Y., Lou, L. L., Liu, S. F., Zhou, L., Huang, X. X., Song, S. J., et al. (2016). Antioxidant and anti-inflammatory neolignans from the seeds of hawthorn. *Bioorg. Med. Chem.* 26, 5501–5506. doi: 10.1016/j.bmcl.2016.10.012

Perricone, A. J., and Vander Heide, R. S. (2014). Novel therapeutic strategies for ischemic heart disease. *Pharmacol. Res.* 89, 36–45. doi: 10.1016/j.phrs.2014.08.004

Peters, W., Drueppel, V., Kusche-Vihrog, K., Schubert, C., and Oberleithner, H. (2012). Nanomechanics and sodium permeability of endothelial surface layer modulated by hawthorn extract WS 1442. *PloS One* 7, e29972. doi: 10.1371/journal.pone.0029972

Petrovska, B. B. (2012). Historical review of medicinal plants' usage. *Pharmacogn. Rev.* 6, 1–5. doi: 10.4103/0973-7847.95849

Pittler, M. H., Schmidt, K., and Ernst, E. (2003). Hawthorn extract for treating chronic heart failure: meta-analysis of randomized trials. *Am. J. Med.* 114, 665–674. doi: 10.1016/S0002-9343(03)00131-1

Rababa'h, A. M., Altarabsheh, S. E., Haddad, O., Deo, S. V., Obeidat, Y., and Al-Azzam, S. (2016). Hawthorn herb increases the risk of bleeding after cardiac

surgery: an evidence-based approach. *Heart Surg. Forum.* 19, E175–E179. doi: 10.1532/hsf.1570

Ranjbar, K., Zarrinkalam, E., Salehi, I., Komaki, A., and Fayazi, B. (2018). Cardioprotective effect of resistance training and Crataegus oxyacantha extract on ischemia reperfusion–induced oxidative stress in diabetic rats. *BioMed. Pharmacother.* 100, 455–460. doi: 10.1016/j.biopha.2018.02.021

Reiner, Ž., Catapano, A. L., De Backer, G., Graham, I., Taskinen, M. R., Wiklund, O., et al. (2011). ESC/EAS guidelines for the management of dyslipidaemias: the task force for the management of dyslipidaemias of the European Society of Cardiology (ESC) and the European Atherosclerosis Society (EAS). *Eur. Heart J.* 32, 1769–1818. doi: 10.1093/eurheartj/ehr158

Ridker, P. M. (2019). Anticytokine agents: targeting interleukin signaling pathways for the treatment of atherothrombosis. *Circ. Res.* 124, 437–450. doi: 10.1161/CIRCRESAHA.118.313129

Roffi, M., Patrono, C., Collet, J. P., Mueller, C., Valgimigli, M., Andreotti, F., et al. (2016). 2015 ESC guidelines for the management of acute coronary syndromes in patients presenting without persistent st-segment elevation: task force for the management of acute coronary syndromes in patients presenting without persistent st-segment elevation of the European Society of Cardiology (ESC). *Eur. Heart J.* 37, 267–315. doi: 10.1093/eurheartj/ehv320

Shatoor, A. S., and Al Humayed, S. (2019). The protective effect of crataegus aronia against high-fat diet-induced vascular inflammation in rats entails inhibition of the nlrp-3 inflammasome pathway. *Cardiovasc. Toxicol.* 20, 82–99. doi: 10.1007/s12012-019-09534-9

Skålén, K., Gustafsson, M., Rydberg, E. K., Hultén, L. M., Wiklund, O., Innerarity, T. L., et al. (2002). Subendothelial retention of atherogenic lipoproteins in early atherosclerosis. *Nature* 417, 750–754. doi: 10.1038/nature00804

Stewart, J., Manmathan, G., and Wilkinson, P. (2017). Primary prevention of cardiovascular disease: a review of contemporary guidance and literature. *JRSM Cardiovasc. Dis.* 6, 2048004016687211. doi: 10.1177/2048004016687211

Stocker, R., and Keaney, J. F. Jr. (2004). Role of oxidative modifications in atherosclerosis. *Physiol. Rev.* 84, 1381–1478. doi: 10.1152/physrev.00047.2003

Sun, Z., Yan, B., Yu, W., Yao, X., Ma, X., Sheng, G., et al. (2016). Vitexin attenuates acute doxorubicin cardiotoxicity in rats *via the* suppression of oxidative stress, inflammation and apoptosis and the activation of FOXO3a. *Exp. Ther. Med.* 12, 1879–1884. doi: 10.3892/etm.2016.3518

Tauchert, M. (2002). Efficacy and safety of crataegus extract WS 1442 in comparison with placebo in patients with chronic stable New York heart association class-III heart failure. *Am. Heart J.* 143, 910–915. doi: 10.1067/mhj.2002.121463

Topal, G., Koç, E., Karaca, Ç., Altuğ, T., Ergin, B., Demirci, C., et al. (2013). Effects of crataegus microphylla on vascular dysfunction in streptozotocin-induced diabetic rats. *Phytother. Res.* 27, 330–337. doi: 10.1002/ptr.4726

Vandvik, P. O., Lincoff, A. M., Gore, J. M., Gutterman, D. D., Sonnenberg, F. A., Alonso-Coello, P., et al. (2012). Primary and secondary prevention of cardiovascular disease: antithrombotic therapy and prevention of thrombosis: american college of chest physicians evidence-based clinical practice guidelines. *Chest* 141, e637S–e668S. doi: 10.1378/chest.11-2306

Wang, N., Zhang, C., Qi, Y., and Li, T. (2007). Extraction and food chemical characterizations of haw pectins. *Sci. Technol. Food Ind.* 11, 87–92.

Wang, H., Zhang, Z., Guo, Y., Sun, P., Lv, X., and Zuo, Y. (2011). Hawthorn fruit increases the antioxidant capacity and reduces lipid peroxidation in senescence-accelerated mice. *Eur. Food Res. Technol.* 232, 743–751. doi: 10.1007/s00217-011-1435-7

Wang, T., Zhang, P., Zhao, C., Zhang, Y., Liu, H., Hu, L., et al. (2011). Prevention effect in selenite-induced cataract *in vivo* and antioxidative effects *in vitro* of *Crataegus pinnatifida* leaves. *Biol. Trace Elem. Res.* 142, 106–116. doi: 10.1007/s12011-010-8752-8

Wang, W., Yang, B., Wang, L., Liang, R., Chen, C., Hu, N., et al. (2011). Antiatherogenic effect of Radix Salviae Miltiorrhizae and Fructus Crataegi on experimental atherosclerosis in rats. *China J. Chin. Mater. Med.* 36, 784–789.

Wang, J., Xiong, X., and Feng, B. (2013). Effect of crataegus usage in cardiovascular disease prevention: an evidence-based approach. *Evid. -Based Complementary Altern. Med.* 2013, 149363. doi: 10.1155/2013/149363

Wang, S., Wu, M., Chen, K., Liu, Y., Sun, J., Sun, Z., et al. (2019). Hawthorn extract alleviates atherosclerosis through regulating inflammation and apoptosis related factors: an experimental study. *Chin. J. Integr. Med.* 25, 108–115. doi: 10.1007/s11655-018-3020-4

Weber, C., and Noels, H. (2011). Atherosclerosis: current pathogenesis and therapeutic options. *Nat. Med.* 17, 1410. doi: 10.1038/nm.2538

Willer, E. A., Malli, R., Bondarenko, A. I., Zahler, S., Vollmar, A. M., Graier, W. F., et al. (2012). The vascular barrier-protecting hawthorn extract WS® 1442 raises endothelial calcium levels by inhibition of SERCA and activation of the IP3 pathway. *J. Mol. Cell Cardiol.* 53, 567–577. doi: 10.1016/j.yjmcc.2012.07.002

Wu, J., Peng, W., Qin, R., and Zhou, H. (2014). *Crataegus pinnatifida*: chemical constituents, pharmacology, and potential applications. *Molecules* 19, 1685–1712. doi: 10.3390/molecules19021685

Xie, W., Sun, C., and Liu, S. (2009). Effect of hawthorn flavanone on blood-fat and expression of lipogenesis and lipolysis genes of hyperlipidemia model mouse. *China J. Chin. Mater. Med.* 34, 224–229.

Xiyun, Y., and Yaofa, W. (2002). Protective effects of hawthorn leaves flavonoids on oxidation induced damages of vascular endothelial cells *in vitro*. *Chin. J. Mod. Appl. Pharm.* 4, 265–268.

Yang, G., Wang, Y., Zeng, Y., Gao, G., Liang, X., Zhou, M., et al. (2013). Rapid health transition in China 1990–2010: findings from the global burden of disease study 2010. *Lancet* 381, 1987–2015. doi: 10.1016/S0140-6736(13)61097-1

Yonekubo, B. T., Alves, H. M. C., de Souza Marques, E., Perazzo, F. F., Rosa, P. C. P., Gaivão, I. O. M., et al. (2018). The genotoxic effects of fruit extract of Crataegus oxyacantha (hawthorn) in mice. *J. Toxicol. Environ. Health A.* 81, 974–982. doi: 10.1080/15287394.2018.1503982

Yoo, J. H., Liu, Y., and Kim, H. S. (2016). Hawthorn fruit extract elevates expression of Nrf2/HO-1 and improves lipid profiles in ovariectomized rats. *Nutrients* 8, 283. doi: 10.3390/nu8050283

Zhang, Z., Chang, Q., Zhu, M., Huang, Y., Ho, W. K., and Chen, Z. Y. (2001). Characterization of antioxidants present in hawthorn fruits. *J. Nutr. Biochem.* 12, 144–152. doi: 10.1016/S0955-2863(00)00137-6

Zhang, Z., Ho, W. K., Huang, Y., and Chen, Z. Y. (2002a). Hypocholesterolemic activity of hawthorn fruit is mediated by regulation of cholesterol-7α-hydroxylase and acyl CoA: cholesterol acyltransferase. *Food. Res. Int.* 35, 885–891. doi: 10.1016/S0963-9969(02)00099-6

Zhang, Z., Ho, W. K., Huang, Y., James, A. E., Lam, L. W., and Chen, Z. Y. (2002b). Hawthorn fruit is hypolipidemic in rabbits fed a high cholesterol diet. *J. Nutr.* 132, 5–10. doi: 10.1093/jn/132.1.5

Zhang, J., Liang, R., Wang, L., Yan, R., Hou, R., Gao, S., et al. (2013). Effects of an aqueous extract of *Crataegus pinnatifida* Bge. var. *major* NE Br. fruit on experimental atherosclerosis in rats. *J. Ethnopharmacol.* 148, 563–569. doi: 10.1016/j.jep.2013.04.053

Zhang, Y., Zhang, L., Geng, Y., and Geng, Y. (2014). Hawthorn fruit attenuates atherosclerosis by improving the hypolipidemic and antioxidant activities in apolipoprotein e-deficient mice. *J. Atheroscler. Thromb.* 21, 119–128. doi: 10.5551/jat.19174

Zheng, G. j., ZHU, Y., and Wang, T. (2010). Effect of polygonum cuspidatum and hawthorn on anti-atherosclerosis unstable plaque. *Chin. J. Pathophysio.* 26, 635–639.

Zheng, X., Li, X., Chen, M., Yang, P., Zhao, X., Zeng, L., et al. (2019). The protective role of hawthorn fruit extract against high salt-induced hypertension in Dahl salt-sensitive rats: impact on oxidative stress and metabolic patterns. *Food Funct.* 10, 849–858. doi: 10.1039/C8FO01818A

Zhu, R., Li, T., Dong, Y., Liu, Y., Li, S., Chen, G., et al. (2013). Pectin pentasaccharide from hawthorn (*Crataegus pinnatifida* Bunge. var. *major*) ameliorates disorders of cholesterol metabolism in high-fat diet fed mice. *Food Res. Int.* 54, 262–268. doi: 10.1016/j.foodres.2013.07.010

Zhu, R. G., Sun, Y. D., Li, T. P., Chen, G., Peng, X., Duan, W. B., et al. (2015). Comparative effects of hawthorn (*Crataegus pinnatifida* Bunge) pectin and pectin hydrolyzates on the cholesterol homeostasis of hamsters fed high-cholesterol diets. *Chem.-Biol. Interact.* 238, 42–47. doi: 10.1016/j.cbi.2015.06.006

Zhu, R. G., Sun, Y. D., Hou, Y. T., Fan, J. G., Chen, G., and Li, T. P. (2017). Pectin penta-oligogalacturonide reduces cholesterol accumulation by promoting bile

acid biosynthesis and excretion in high-cholesterol-fed mice. *Chem.-Biol. Interact.* 272, 153–159. doi: 10.1016/j.cbi.2017.05.018

Zhu, Y., Feng, B., He, S., Su, Z., and Zheng, G. (2018). Resveratrol combined with total flavones of hawthorn alleviate the endothelial cells injury after coronary bypass graft surgery. *Phytomedicine* 40, 20–26. doi: 10.1016/j.phymed.2017.12.037

Zhu, R., Zhang, X., Wang, Y., Zhang, L., Wang, C., Hu, F., et al. (2019). Pectin oligosaccharides from hawthorn (*Crataegus pinnatifida* Bunge. var. *major*): molecular characterization and potential antiglycation activities. *Food Chem.* 286, 129–135. doi: 10.1016/j.foodchem.2019.01.215

Conflict of Interest: The authors declare that the research was conducted in the absence of any commercial or financial relationships that could be construed as a potential conflict of interest.

frontiers in Pharmacology

ORIGINAL RESEARCH
published: 26 February 2020
doi: 10.3389/fphar.2020.00121

Shenfu Injection Promotes Vasodilation by Enhancing eNOS Activity Through the PI3K/Akt Signaling Pathway *In Vitro*

Jinqiang Zhu[1,2], *Wanshan Song*[3], *Shixin Xu*[4,5], *Yan Ma*[3], *Baoyu Wei*[1,2], *Hongwu Wang*[6] *and Shengyu Hua*[1,2,7*]

[1] Institute of Traditional Chinese Medicine, Tianjin University of Traditional Chinese Medicine, Tianjin, China, [2] Tianjin State Key Laboratory of Modern Chinese Medicine, Tianjin University of Traditional Chinese Medicine, Tianjin, China, [3] Encephalopathy Acupuncture Department, Second Affiliated Hospital of Tianjin University of Traditional Chinese Medicine, Tianjin, China, [4] Medical Experiment Center, First Teaching Hospital of Tianjin University of Traditional Chinese Medicine, Tianjin, China, [5] Tianjin Key Laboratory of Translational Research of TCM Prescription and Syndrome, First Teaching Hospital of Tianjin University of Traditional Chinese Medicine, Tianjin, China, [6] Public Health Science and Engineering College, Tianjin University of Traditional Chinese Medicine, Tianjin, China, [7] College of Chinese Medicine, Tianjin University of Traditional Chinese Medicine, Tianjin, China

OPEN ACCESS

Edited by:
Yue Liu,
Xiyuan Hospital, China

Reviewed by:
Yaozu Xiang,
Tongji University, China
Yanfei Liu,
Beijing University of Chinese Medicine, China

***Correspondence:**
Shengyu Hua
bravo2008@163.com

Specialty section:
This article was submitted to Ethnopharmacology, a section of the journal Frontiers in Pharmacology

Received: *25 November 2019*
Accepted: *28 January 2020*
Published: *26 February 2020*

Citation:
Zhu J, Song W, Xu S, Ma Y, Wei B, Wang H and Hua S (2020) Shenfu Injection Promotes Vasodilation by Enhancing eNOS Activity Through the PI3K/Akt Signaling Pathway In Vitro. Front. Pharmacol. 11:121. doi: 10.3389/fphar.2020.00121

Vasomotor dysfunction is one of the key pathological aspects of shock and heart failure (HF). *Shenfu* injection (SFI) has been widely used for the treatment of shock and HF in China. Pharmacological studies have suggested that SFI can reduce peripheral circulation resistance and improve microcirculation. However, whether it has a regulatory effect on macrovascular has not been elucidated. In this study, we used thoracic aorta rings isolated from *Wistar* rats and the human umbilical vein cell line (EA.hy926) to explore the vasodilative activity of SFI and its potential mechanisms. The relaxation due to SFI was measured after pre-treatment with selective soluble guanylate cyclase (sGC) inhibitor or cyclooxygenase (COX) inhibitor and compared with the vasodilation effect of SFI only treated with norepinephrine (NE). The contents of NO, endothelin-1 (ET-1), endothelial nitric oxide synthase (eNOS), COX-1, 6-K-PGF$_{1\alpha}$, and caveolin-1 were evaluated respectively. Additionally, the level of eNOS mRNA and total eNOS and its phosphorylation were studied to investigate the potential mechanisms involved. Experimental results showed that SFI markedly attenuated NE-induced vasoconstriction but that this effect was significantly eliminated after pre-incubation with the selective sGC inhibitor 1-H-[1, 2, 4] oxadiazolo [4, 3-α] quinoxaline-1-one (ODQ), instead of the COX inhibitor indomethacin (INDO). SFI significantly increased the eNOS content and up-regulated the eNOS mRNA expression, while it did not affect the content of COX-1 and 6-K-PGF$_{1\alpha}$. SFI also markedly increased NO content but significantly reduced the content of ET-1 and caveolin-1 in the cell supernatant. Furthermore, it promoted the expression of total eNOS and the phosphorylation of eNOS at serine (Ser) 1177 but inhibited the phosphorylation at threonine (Thr) 495, which was significantly reversed by PI3K-specific inhibitor LY294002. In conclusion, our study showed the vasodilation effect of SFI in thoracic aorta is mediated entirely by enhancing eNOS

activity through the PI3K/Akt signaling pathway, providing novel knowledge on the effect of SFI on shock and HF for future clinical applications.

Keywords: *Shenfu* injection, vasodilation, nitric oxide (NO), endothelial nitric oxide synthase (eNOS), PI3K/Akt signaling pathway

INTRODUCTION

Cardiovascular disease (CVD) is currently the leading cause of death, and around 17.5 million people died of the disease worldwide in 2015, accounting for 31% of deaths in the whole world (Mendis et al., 2015). Although more and more single-component and single-target chemical medicines are being developed, it is still difficult to prevent the increasing rate of morbidity and mortality of CVD; this may be because of serious adverse reactions and high medical costs. Traditional Chinese medicine and its compound may have advantages in treating CVD owing to its multi-component, multi-target, multi-effect features (Dong et al., 2017; Li et al., 2019).

Shenfu injection (SFI), a traditional Chinese herbal medicine, is composed of Red Ginseng (the dried root or rootstalk of *Panax ginseng* C. A. Mey) and Fuzi (the lateral root of *Aconitum carmichaeli* Debx) (Zhang, 2016). It is approved by the Chinese State Food and Drug Administration (medicine manufacturing approval number: Z51020664) and has been widely used in the treatment of patients with shock and heart failure (HF) in China (Huang et al., 2019; Wang et al., 2019). The occurrence and development of shock and HF are closely related to vascular activity (Widlansky et al., 2003; Penna et al., 2006; Gulati, 2016). It was reported that SFI could effectively improve microcirculation in shocked rats (Li et al., 2017), improve the microvascular blood flow and coronary perfusion pressure (CPP) during ventricular fibrillation (VF) and cardiopulmonary resuscitation (CPR), and reduce the shocks and duration of CPR (Wu et al., 2016). In addition, SFI can dilate the coronary through promoting NO release (Li et al., 2014) and effectively reduce the damage of vascular endothelial cells (VECs) (Huang et al., 2011).

Endothelial nitric oxide (NO), synthesized by L-arginine catalyzed by endothelial nitric oxide synthase (eNOS) in VECs, was reported to have a significant effect on maintaining the balance of circulation and modulating the vascular tone (Yao et al., 2013). The production of endothelial NO mainly depends on the activity of eNOS. Phosphorylation of eNOS is one of the key factors determining its activity, which is closely related to the phosphatidylinositol 3-kinase/protein kinase B (PI3K/Akt) signaling pathway (Ohkita et al., 2012). Previous studies have shown that vasoactive intestinal polypeptide has a vasorelaxation effect on rat isolated pulmonary artery rings through the PI3K/Akt/eNOS signaling pathway (Zhang et al., 2010), which suggested that this signaling pathway plays a vital role in regulating the vascular activity. Our previous research showed that SFI could dose-dependently inhibit the vasoconstriction induced by potassium chloride (KCl) and norepinephrine (NE) in endothelium-intact thoracic aorta rings but not in the removal of endothelium thoracic aorta rings and that treatment with 1 μM L-NAME eliminated SFI-induced relaxation (Zhu et al., 2013). In the light of the important role of NO in vasomotor function, we aim to evaluate whether the endothelium-dependent vascular relaxation (EDVR) of the thoracic aorta in response to SFI is mediated entirely by NO and whether its mechanism that it promotes eNOS activation through the PI3K/Akt signaling pathway.

MATERIALS AND METHODS

Shenfu Injection

SFI, produced by Ya'an Sanjiu Pharmaceutical Co., Ltd., is composed of Red Ginseng (the dried root or rootstalk of *Panax ginseng* C. A. Mey, 1 mg/ml) and Fuzi (the tuber of *Aconitum carmichaelii* Debeaux, 2 mg/ml). The workflow of SFI preparation is presented in previous research (Liu et al., 2019), and its quality was strictly controlled in compliance with the standard of the China Food and Drug Administration (approval No: WS3-B-3427-98-2013) and ensured by using fingerprint technology during production (Liu et al., 2019). The main active ingredients of SFI are ginsenosides and aconitine. Their chemical structures are shown in the **Supplementary Figure 1** (Wu et al., 2016). Furthermore, 12 ginsenosides and two aconitum alkaloids in 22 batches of SFIs (number of batches: 120609, 110804, 131006010, 131005010, 131013010, 131008010, 130902010, 130813010, 130812010, 130904010, 130905010, 130903010, 130505010, 130506010, 130508010, 130606010,130605010, 130604010, 130713010, 130715010, 130705010, and 130703010, Sichuan, China) were identified by Dr. Yanxu Chang, a member of our team from Tianjin University of Traditional Chinese Medicine (Tianjin, China) and their concentration calculated by the traditional method. The experimental results show that the types and contents of the chemical components in the 22 batches of SFIs were extremely stable. The chemical fingerprint of SFI (number of batch: 110804, Sichuan, China) is shown in the **Supplementary Figure 2**, and the concentrations of the 12 ginsenosides (Re, Rg_1, Rf, S-Rg_2, S-Rh_1, Rb_1, Rc, Rb_2, Rb_3, Rd, S-Rg_3, and S-Rh_2) and two aconitum alkaloids (benzoylmesaconine and benzoylhypacoitine) were 60.0 μg/ml, 105μg/ml, 36.6μg/ml, 28.6μg/ml, 15.9μg/ml, 47.6μg/ml, 67.6μg/ml, 53.6μg/ml, 8.60μg/ml, 17.6μg/ml, 22.2μg/ml, 14.5μg/ml, 26.2μg/ml, and 2.24μg/ml, respectively (Ge et al., 2015).

Aortic Ring Preparation

This study was carried out in strict accordance with the recommendations in the Guidance Suggestions for the Care and Use of Laboratory Animals issued by the Ministry of Science and Technology of China. The protocol was approved

by the Laboratory Animal Ethics Committee of Tianjin University of Traditional Chinese Medicine (Permit Number: LAEC2013002). Male *Wistar* rats, 6–8 weeks, weighing 250–300 g, were killed by decapitation. The thoracic aorta was immediately isolated and immersed in an oxygenated Krebs-Henseleit (K-H) solution (in mM: NaCl, 118; KCl, 4.75; $MgSO_4{\cdot}7H_2O$, 1.2; KH_2PO_4, 1.2; $CaCl_2$, 2.5; $NaHCO_3$, 25; D-glucose, 11) (Xu, 1994) at room temperature. After careful removal of the adipose tissue, it was cut into several 2–3 mm wide segments from the distal and proximal ends (Zhu et al., 2013).

Measurement of Vascular Relaxation

According to previous experimental methods (Zhu et al., 2013), the aortic rings were suspended between two parallel stainless steel hooks in the organ bath (Radnoti, AD Instruments Pty Ltd., Australia). One hook was fixed, while the other was connected to a force transducer (AD Instruments Pty Ltd., Australia) for the measurement of isometric tension. To keep the blood vessels living, the organ bath was filled with 10 ml K-H solution, maintained at 37.0°C, pH 7.3–7.4, and bubbled with 95% O_2 and 5% CO_2. During the resting periods, the aortic rings were stretched progressively to a basal tension of 2.0 g and allowed to equilibrate for at least 90 min. The organ bath solution was replaced with a pre-warmed and oxygenated K-H solution every 15 min. Thereafter, to standardize the experiments after stabilization at the beginning of the experiments, each aortic ring was first repeatedly contracted with 60 mM KCl till the plateau of contractions remained within 5% between two consecutive contractions. After washing with pre-warmed and oxygenated K-H solution three times until muscle tension returned to the basal level, the aortic rings were incubated with α_1-adrenoceptor agonist norepinephrine (NE, 1 μM) to evoke a steady contraction and then relaxed by acetylcholine (ACh, 10 μM) for assessment of the endothelial function. Rings with less than 60% relaxation in response to ACh were excluded from this experiment. The contractility of vascular rings with endothelium intact was measured isometrically. After establishing a sustained plateau contraction with 1μM NE, different doses (0.l, 1, 2, or 10 μl/ml) of SFI (number of batches: 110804, Sichuan, China) were added cumulatively to induce a concentration-dependent relaxation in rings, and each dosage was added with an interval of 5 min. In order to assess the contribution of relaxation due to NO or PGI_2, after repeated wash-out and subsequent equilibration for about 45 min, some rings were respectively exposed to 10 μM selective soluble guanylate cyclase (sGC) inhibitor 1-H-[1,2,4]oxadiazolo [4,3-α] quinoxalin-1-one (ODQ) or 10 μM cyclooxygenase (COX) inhibitor indomethacin (INDO) for 20 min prior to application of NE.

Cell Culture

The vial contained EA.hy 926 cells (ATCC® Catalog No. CRL-2922™, Manassas, VA, USA), which were rapidly thawed within 2 min by gentle agitation in a 37 °C water bath. To avoid the possibility of contamination, the O-ring and cap were kept out of the water. The vial was removed as soon as the contents were thawed and decontaminated by dipping in or spraying with 70% ethanol. The vial contents was transferred to a centrifuge tube containing 9.0 ml complete culture medium (Dulbecco's Modified Eagle's Medium (DMEM) with high glucose (HyClone, USA) supplemented with 10% fetal bovine serum (FBS, HyClone, USA) and antibiotics including $1{\times}10^5$ U/L penicillin and $1{\times}10^5$ μg/L streptomycin) and centrifuged at 4 °C and 1000 rpm for 10 min. Cells were resuspended with the complete medium and dispensed into a 25-cm^2 or 75-cm^2 culture flask at a density of 10^4-10^5 cells/ml, then cultured at 37 °C in a 5% CO_2 incubator with a renewal of medium every 2–3 days. They were subcultured as soon as they grew into confluent monolayer cells. After discarding the culture medium, the cell layer was briefly rinsed with 0.25% phosphate-buffered saline (PBS, containing 8 g NaCl, 0.2 g KCl, 1.44 g $Na_2HPO_4{\bullet}12H_2O$ and 0.24 g KH_2PO_4 per liter, PH 7.4) to remove all traces of serum, which contains trypsin inhibitor. These cells were digested with an appropriate amount of mixed digestive enzymes of 0.25% Trypsin and 0.02% EDTA (mixed at 1:1) until the cell layer was seen to be dispersed by examining cells under an inverted microscope. Digestion was terminated by the complete medium containing 10% FBS. The following procedures including centrifuge, resuspension, and culture are the same as mentioned above.

Griess Assay

Nitrites are oxidized metabolites of NO, which was evaluated by the Griess assay kit (Beyotime Biotechnology Co., Ltd., Jiangsu, China) to reflect the content of NO in cell supernatant. EA.hy 926 cells (n = 6 donors) were seeded in a 96-well culture plate and analyzed separately. Upon confluency, the medium was changed to FBS-free DMEM and incubated overnight for synchronization prior to treatment. Cells were separately incubated with 1 μM sildenafil (Sigma, USA) and SFI at three concentrations (10, 20, or 40 μl/ml) for 24 h. The amount of accumulated nitrite derived from NO metabolism was determined according to the kit operating instructions. After incubation at room temperature for 10 min, absorbance was measured at 540 nm as the reference wavelength by a microcontent multifunction microplate reader (Infinite M200, NanoQuant, Switzerland). Nitrite concentrations were calculated using a $NaNO_2$ standard curve (0-100 μM in cell culture medium). A nitrite standard reference curve was established for each assay.

DAF-FMDA Fluorescence Indicator

EA.hy 926 cells were seeded at $1{\times}10^6$ cells per well in a six-well culture plate. Upon 90% confluency, cells were synchronized and then treated with 1μM sildenafil (Sigma, USA) and 10, 20, or 40 μl/ml SFI for 24 h. DAF-FMDA fluorescence indicator (Beyotime Biotechnology Co., Ltd., Jiangsu, China) was used to detect the intracellular NO content. According to the kit instructions, the method was as follow:

i. *In-situ* loading probe: DAF-FM DA was diluted, with its dilution provided in this kit at a 1:1000 ratio to a final concentration of 5 μM. The cell culture medium was removed, and the appropriate volume of diluted DAF-FMDA was added. Cells were incubated at 37 °C for 20 min and then washed three times with PBS (pH 7.4) to adequately remove the DAF-FM DA that did not enter the cells.

ii. Detection: The fluorescence intensity was directly observed by laser confocal microscopy or detected by fluorescence spectrophotometer, fluorescence microplate reader, or flow cytometry after collecting cells.
iii. Parameter setting: The intensity of fluorescence was measured before and after stimulation at a 495 nm excitation wavelength and 515 nm emission wavelength in real-time or at time point or single time point.

ELISA Assay

EA.hy 926 cells (n = 6 donors) were transferred to a 96-well culture plate. Upon 90% confluency, cells were synchronized and respectively treated with drugs as described above. The cell supernatant from each group of cells was collected, and the eNOS, ET-1, COX-1, 6-K-$PGF_{1\alpha}$, and caveolin-1 contents were measured according to the manufacturer's instructions (ELISA kit; R&D Systems, USA). Absorbance was detected at 450 nm as the reference wavelength using the microcontent multifunction microplate reader.

RT-PCR

EA.hy 926 cells were seeded at 1×10^6 cells per well in a six-well culture plate. Upon 90% confluency, cells were synchronized and respectively treated with 1 μM mevastatin (Sigma, USA) and 5, 10, or 20μl/ml SFI for 24 h. Total RNA was extracted from each sample using the High Pure RNA Isolation kit (Roche, USA) according to the manufacturer's instructions. RNA samples were subsequently reverse-transcribed to cDNA using SYBR® *Premix* Ex Taq™ Reverse Transcription Reagents (Roche, Switzerland) according to the manufacturer's instructions, and the resulting cDNA was used as a template for RT-PCR amplification. RT-PCR was performed with the ABI® PRISM 7500 Sequence Detection System (Applied Biosystems; Foster City, USA) using SYBR® Green PCR Master Mix reagent kits (Roche, Switzerland) and the specific primers (**Table 1**, Sangon Biotech (Shanghai) Co., Ltd., Shanghai, China). Relative quantification of gene expression between samples was determined using the $2^{-\triangle\triangle CT}$ method. All samples were run in triplicate from three independent experiments. The mean crossing threshold (CT) values for both the target and internal control genes in each sample were determined, and the $2^{-\triangle\triangle CT}$ calculations were performed. The fold change and mean were calculated for each sample (Livak and Schmittgen, 2001).

Western Blotting

EA.hy 926 cells were treated according to the protocols mentioned in the RT-PCR study. They were homogenized in ice-cold RIPA lysis buffer containing 1mM PMSF (Beijing Solarbio Science & Technology Co., Ltd, Beijing, China) with several shocks, and lysates were centrifugated at 4°C and 12,000 g for 5 min. We collected and detected the total protein concentration of the supernatants using the BCA assay method (Beijing Solarbio Science & Technology Co., Ltd, Beijing, China). Samples containing 20 μg protein were boiled for 5 min with 5% β-mercaptoethanol and separated on a 10% SDS-polyacrylamide gel by electrophoresis (SDS-PAGE). The protein was transferred to the membrane (immobilon-P polyvinylidene difluoride; Millipore Corp., Bedford, MA, USA) and blocked with 5% skimmed milk for 1–2 h. Primary antibodies against total eNOS (9572S, Cell Signaling Technology, Inc., CST, USA), phosphorylated eNOS at Ser1177 (9571S, Cell Signaling Technology, Inc., CST, USA) and Thr 495 (9574S, Cell Signaling Technology, Inc., CST, USA), and β-actin (4970S, Cell Signaling Technology, Inc., CST, USA) were used for overnight incubation at 4℃. Following three washes (10 min per time) with 0.1% Tween-20 in Tris-buffered saline (TBS), the blots were exposed to horseradish peroxidase-conjugated secondary antibodies for 1.5 h and then washed three times using the method above. An enhanced chemiluminescence detection system (ECL reagent, Amersham Pharmacia Biotech, Buckinghamshire, UK) was used to develop the membranes, and a documentation program (FluorChem, Alpha Innotech Corp., San Leandro, CA, USA) was used for densitometry measurement.

TABLE 1 | Primers of real-time RT-PCR.

Genes	Primer/Probe sequences(5' to 3') F, forward; R, reverse
β-actin	F: GGATCAGCAAGCAGGAGTA R: GGTGTAACGCAACTAAGTCATAG
eNOS	F: CTCATGGGCACGGTGATG R: ACCACGTCATACTCATCCATACAC

Statistical Analysis

We employed percentage relaxation relative to pre-contraction levels to NE in the statistical analysis of the relaxant responses. Data are shown as mean ± SD, and statistical significance was estimated by Student's *t*-test for unpaired observation between two groups or by one-way ANOVA test in comparison to multiple groups. A *p*-value of less than 0.05 was regarded to be significant.

RESULTS

The Vasodilation Effect of SFI Involves sGC but not COX-1

To explore the vasodilatation pathways of SFI, we pre-treated the isolated thoracic aorta with 10 μM selective sGC inhibitor ODQ or 10 μM COX inhibitor INDO and compared with the vasodilation effect of SFI only treated with NE. The results showed that SFI (1, 2, and 10 μl/ml) markedly attenuated NE-induced vasoconstriction compared with vasoconstriction in control rat aortas but that this effect was significantly eliminated after pre-incubation with ODQ instead of INDO (**Figure 1**).

SFI Increases eNOS Content and up-Regulates eNOS mRNA Expression, While it Does not Affect the Prostacyclin Pathway

We further explore the vasodilatation pathways of SFI on the molecular biological level. eNOS and COX-1 are the key enzymes in the NO pathway and prostacyclin pathway, respectively. eNOS catalyzes the generation of NO from L-arginine and promotes

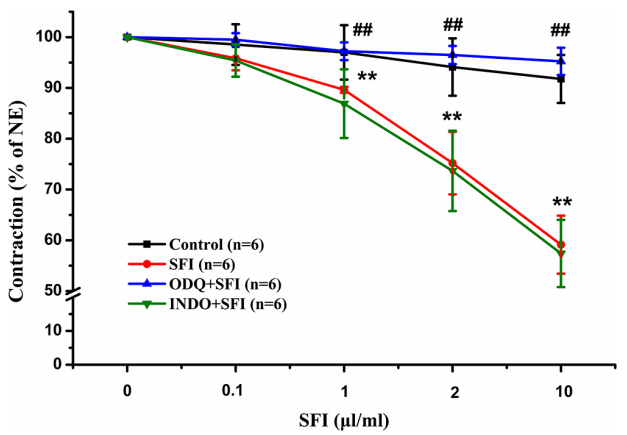

FIGURE 1 | Effects of selective sGC inhibitor ODQ and COX inhibitor INDO on relaxations induced by SFI in isolated thoracic aorta rings contracted with NE. The inhibition of NE (1 μM)-pre-contracted rat thoracic aorta rings with intact endothelium in response to cumulative addition of SFI (0.1, 1, 2 and 10 μl/ml) in the presence and absence of selective sGC inhibitor ODQ (10 μM) and COX inhibitor INDO (10 μM). ODQ, instead of INDO, can obviously restrain the vasorelaxation of SFI. Values are expressed as the mean ± SD, n = 6. $^{**}P < 0.01$ *vs.* Control (an equal volume K-H solution was added for the control group); $^{\#\#}P < 0.01$ *vs.* SFI.

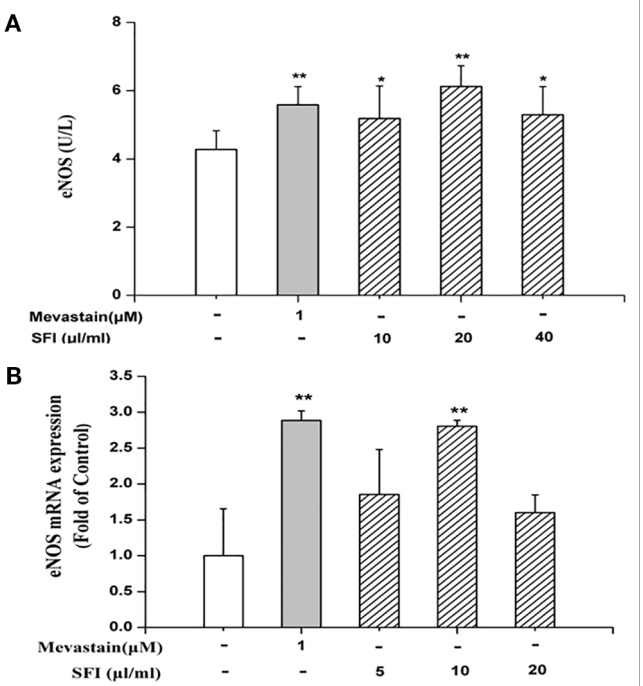

FIGURE 2 | Effect of SFI on eNOS content **(A)** and eNOS mRNA expression **(B)**. 10, 20, and 40 μl/ml of SFI and mevastatin significantly increased eNOS content **(A)**, and 10 μl/ml of SFI obviously up-regulated eNOS mRNA expression, as mevastatin **(B)**. Values are expressed as the mean ± SD, n = 6. $^{*}P < 0.05$, $^{**}P < 0.01$ *vs.* Control.

the conversion of arachidonic acid to prostacyclin (Moncada et al., 1991). PGI_2, an important vasodilator, is unstable, and it is rapidly degraded into 6-K-$PGF_{1\alpha}$ *in vivo* (Parkington et al., 2004). Thus, we tested the content of 6-K-$PGF_{1\alpha}$ instead of PGI_2 in the cell supernatant. The results of ELISA showed that 10, 20, and 40 μl/ml of SFI significantly increased eNOS content (**Figure 2A**), and RT-PCR showed that 10 μl/ml of SFI obviously up-regulated eNOS mRNA expression, as mevastatin (**Figure 2B**), while it had no effect on the content of COX-1 and 6-K-$PGF_{1\alpha}$ (**Supplementary Figures 3** and **4**).

SFI Increases NO Production and Reduces ET-1 Content

NO is the strongest diastolic vascular factor, and ET-1 is the strongest vasoconstrictor factor. We tested NO content in EA.hy 926 cells supernatant using Griess assay and in EA.hy 926 cells by DAF-FMDA fluorescence indicator, respectively, and detected the ET-1 content in EA.hy 926 cell supernatant by ELISA. After treatment with different dosages (10, 20, and 40 μl/ml) of SFI for 24 h, all doses of SFI markedly increased NO production in EA.hy 926 cell supernatant (**Figure 3A**), and 20μl/ml of SFI also increased the intracellular NO production (**Figures 3B, C**), like sildenafil, while 40μl/ml of SFI significantly reduced ET-1 content in EA.hy 926 cell supernatant (**Figure 4**).

Effects of SFI on the Phosphorylation Level of eNOS in the Endothelial Cells

Phosphorylation of protein residues is a major influencing factor on eNOS activity. Previous research shows that the phosphorylation of eNOS at Ser1177 can increase its activity. In contrast, the phosphorylation of eNOS at Thr495 can decrease its activity (Dimmeler et al., 1999; Fleming et al., 2001). The results of Western blotting showed that, compared with control, SFI promoted the expression of total eNOS (**Figures 5A, B**) and the phosphorylation of eNOS at Ser1177 (**Figures 5A, C**) but inhibited the phosphorylation at Thr495 (**Figures 5A, D**), which was significantly reversed by PI3K-specific inhibitor LY294002.

SFI Down-Regulates the Protein Expression of Caveolin-1

eNOS combined with caveolin-1 can inhibit its activity (Bucci et al., 2000). To preliminarily clarify the mechanism by which SFI regulates eNOS activity, we also measured the caveolin-1 content in the cell supernatant. The results showed that SFI significantly reduced the caveolin-1 content in the cell supernatant, like mevastatin (**Figure 6**).

DISCUSSION

To our best knowledge, this is the first systematic study of the mechanism behind the vasorelaxation effect of SFI. This study shows that SFI can exert endothelium-dependent vasodilatory effects through the NO-cGMP pathway on the vascular endothelium. Its mechanism is to up-regulate the expression of eNOS mRNA and protein, promote endothelial NO synthesis and release, reduce Cav-1 expression and ET-1 content, promote the phosphorylation of eNOS at Ser1177, and inhibit the

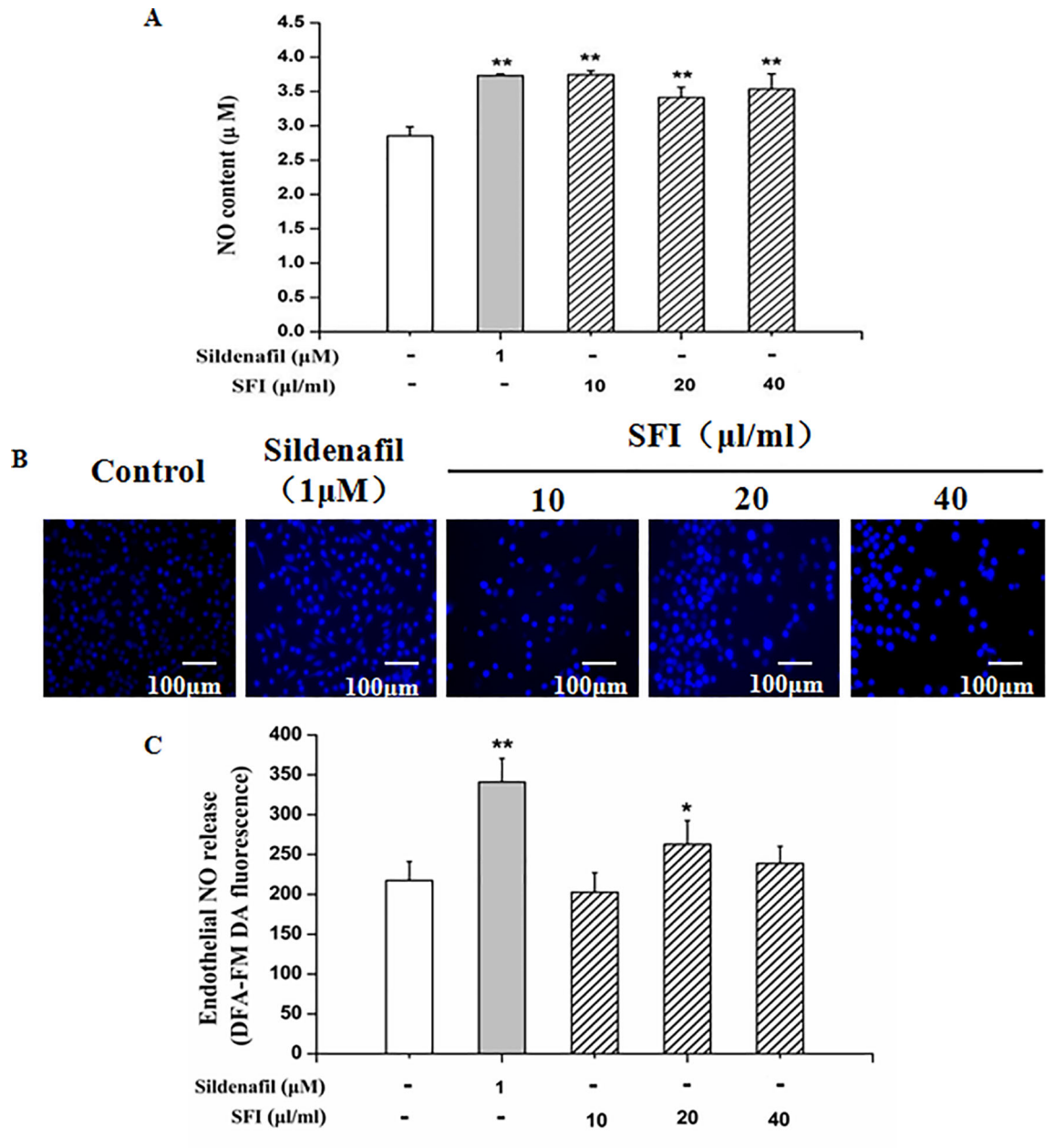

FIGURE 3 | Effect of SFI on extracellular **(A)** and intracellular **(B, C)** NO content. After treatment with different dosages (10, 20, and 40 μl/ml) of SFI for 24 h, all doses of SFI markedly increased NO production in EA.hy 926 cell supernatant **(A)**, and 20μl/ml of SFI also increased the intracellular NO production **(B, C)**, like sildenafil. Values are expressed as the mean ± SD, n = 6. $^{*}P < 0.05$, $^{**}P < 0.01$ *vs.* Control.

phosphorylation at Thr495, resulting in eNOS activation through the PI3K/Akt signal pathway.

Endothelial NO is generated in the VECs by L-arginine (L-Arg) catalyzed by eNOS and plays an important role in relaxing vascular smooth muscle, inhibiting smooth muscle cell proliferation and platelet adhesion and aggregation, which is important for maintaining the circulatory system and the internal environment (Cui et al., 2006; Jia et al., 2006). ET-1 is currently the most known vasoconstrictor substance (Nar et al., 2013). NO and ET-1 produced in VECs are the most important vasoconstrictor substances, and they are among the most important indicators reflecting the function of blood vessels. The dynamic balance between them is an important condition for the normal tension of blood vessels (Theodorakis et al., 2015).

When HF occurs, insufficient cardiac output leads to excessive activation of the sympathetic nervous system and rennin-angiotensin system and endothelial dysfunction, which manifests as a marked increase in vasoconstrictor substances, a marked

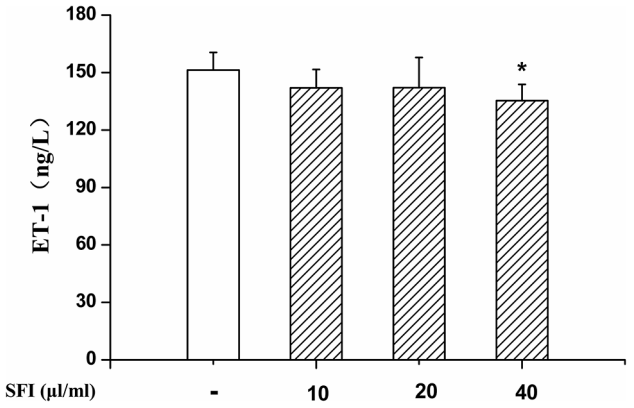

FIGURE 4 | Effect of SFI on ET-1 content. After treatment with different dosages (10, 20, and 40 μl/ml) of SFI for 24 h, 40 μl/ml of SFI significantly reduced ET-1 content in EA.hy 926 cell supernatant. Values are expressed as the mean ± SD, n = 6. *$P < 0.05$ *vs.* Control.

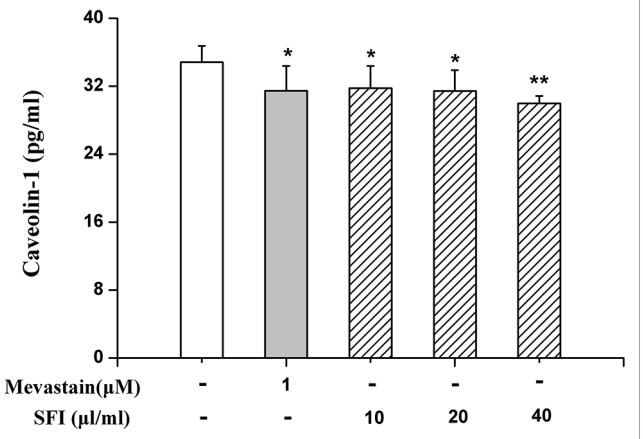

FIGURE 6 | Effect of SFI on the caveolin-1 content in the cell supernatant. SFI significantly reduced the caveolin-1 content in the cell supernatant, like mevastatin. Values are expressed as the mean ± SD, n = 6. *$P < 0.05$, **$P < 0.01$ *vs.* Control.

decrease in vasodilator substances, obvious damage to endothelium-dependent vasodilation, and abnormal contraction of blood vessels. All of this leads to increased systemic circulation and pulmonary circulation resistance, water and sodium retention, and increased cardiac preload and cardiac after-load; at the same time, endothelial dysfunction increases peripheral resistance and cardiac after-load through the peripheral effect (Widlansky et al., 2003; Penna et al., 2006). During the compensatory phase of shock, under the influence of shock factors, EDRF/NO secreted in VECs increases, which exerts a protective effect on systemic tissues and organs;

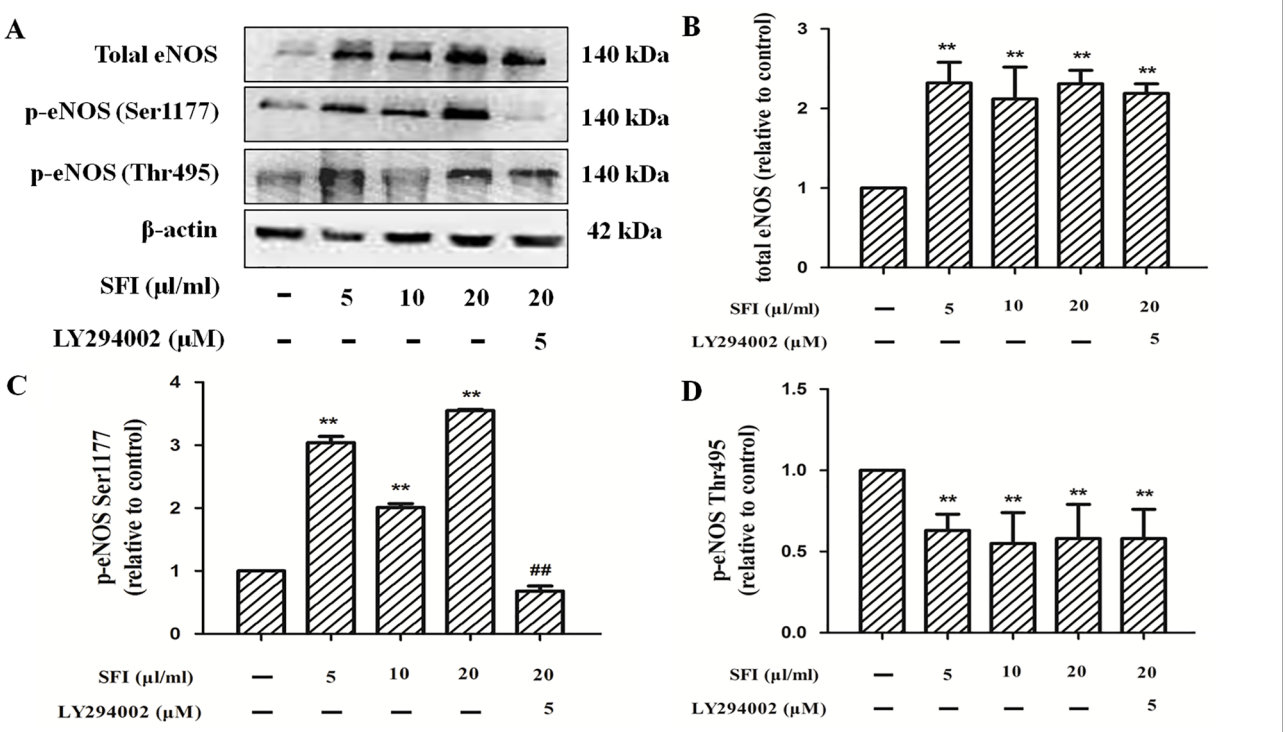

FIGURE 5 | Effect of SFI on the expression of total eNOS and the phosphorylation of eNOS at Ser1177 and Thr 495. Representative blot images demonstrating total eNOS, p-eNOS Ser 1177, p-eNOS Thr 495, and β-actin protein expression levels **(A)**. SFI promoted the expression of total eNOS **(B)** and the phosphorylation of eNOS at Ser1177 **(C)** but inhibited the phosphorylation at Thr495 **(D)**, which was significantly reversed by PI3K-specific inhibitor LY294002. Values are expressed as the mean ± SD, n = 3. **$P < 0.01$ *vs.* Control; $^{\#\#}P < 0.01$ *vs.* SFI (20 μl/ml).

during the decompensation period of shock, EDRF/NO continues to be excessive, and the steady state between vasoactive substances is destroyed, which guides, facilitates, or synergizes with vasodilators, such as adrenomedullin, and then causes an enhancement of vascular over-dilation and cell damage, which forms a vicious cycle, leading to irreversible shock (Wang et al., 2000). Therefore, vasomotor function plays an important role in the pathological process of shock and HF.

The regulation of vasomotor functions is mainly through NO-cGMP and PGI_2 pathways. The NO synthesized in VECs rapidly enters vascular smooth muscle cells (VSMCs) and acts on soluble guanylate cyclase (sGC) to convert guanosine triphosphate (GTP) to cyclic guanosine monophosphate (cGMP), then activates cGMP-dependent proteases, which causes the dephosphorylation of the myosin light chain, decreases intracellular free Ca^{2+} levels, and reduces the binding of contractile proteins to Ca^{2+}, resulting in smooth muscle relaxation and vasodilation (Moncada et al., 1991). PGI_2 is generated in the VECs by arachidonic acid under the action of COX and prostacyclin synthase and binds to the tissue-specific G protein-coupled receptor PGI_2 receptor on the cell membrane, which can activate adenylate cyclase, increase the content of cyclic adenosine monophosphate (cAMP), activate protein kinase A (PKA), promote the opening of K^+ channels, and thus exert vasodilation (Parkington et al., 2004; Fetalvero et al., 2006). PGI_2 is extremely unstable in aqueous solution and readily hydrolyzes to 6-K-PGF_1. Our previous studies suggested that SFI has NO-related endothelium-dependent vasodilatory effects (Zhu et al., 2013). This study used an isolated vascular ring experimental method to further clarify the pathway of its vasodilation. The results show that the sGC inhibitor ODQ can significantly eliminate the vasodilation of SFI, while the COX inhibitor INDO has no such effect, which suggested that the endothelium-dependent vasodilation of SFI is related to the NO-cGMP pathway. Moreover, the results of the *in vitro* cell experiments in this study show that SFI can significantly increase the expression of eNOS but that it has no significant effect on the content of COX-1 and PGI_2 metabolite 6-K-PGF_1, further verifying that the vasodilation effect of SFI is through the NO-cGMP pathway. On this basis, we investigated the effect of SFI on intracellular and extracellular NO content and extracellular ET-1 content. The results showed that SFI significantly increased NO synthesis and release and decreased ET-1 content, suggesting that SFI can modulate the balance of NO/ET-1, thereby effectively improving vasomotor function.

Since the half-life of NO is very short (about 6–30 s), the NO production in the endothelium mainly depends on the activity of the key enzyme eNOS (Laspas et al., 2014). The regulation mechanism of eNOS activity is extremely complex. i) The expression of eNOS mRNA directly affects the amount of eNOS synthesis and thus regulates eNOS activity. ii) The binding of CaM to eNOS enhances the activity of eNOS; conversely, the combination of Cav-1 and eNOS decreases the activity of eNOS (Feron et al., 1996; Garcia-Cardeña et al., 1997; Ghosh et al., 1998). iii) eNOS is readily phosphorylated at serine, threonine, and tyrosine residues. Phosphorylation at Thr495 reduces the binding of CaM to eNOS, thereby inhibiting the activity of eNOS (Fleming et al., 2001), while phosphorylation at Ser1177 can enhance the catalytic ability of eNOS by inhibiting the separation of CaM from eNOS and enhancing the internal electron transfer rate of eNOS (Gallis et al., 1999; McCabe et al., 2000). Akt (i.e., PKB) is an important determinant of

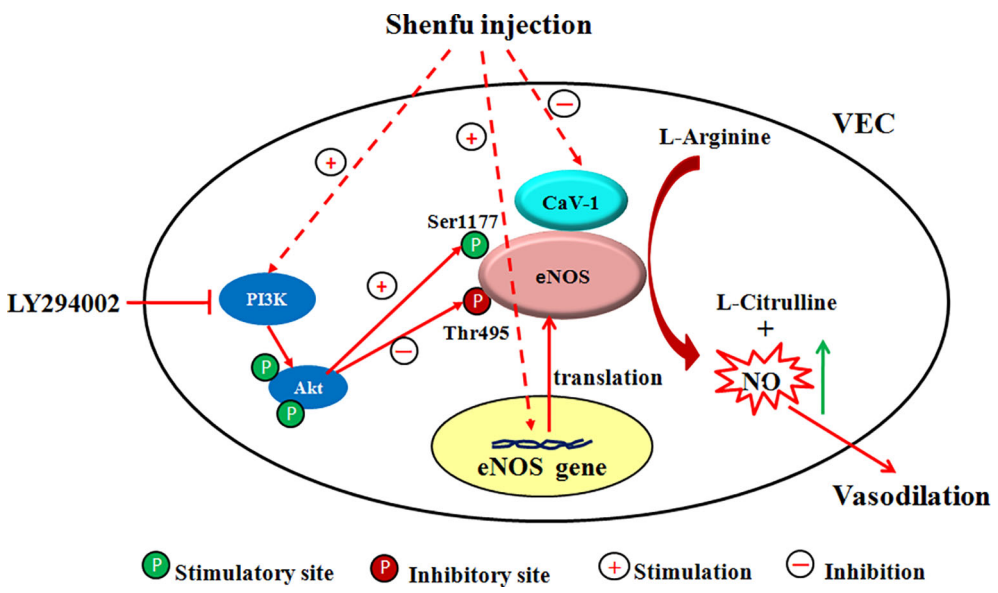

FIGURE 7 | Scheme of the proposed mechanism by which SFI increases eNOS activity. Administration of SFI results in an increase in the gene and protein expression of eNOS and promotes the eNOS phosphorylation at Ser1177 but inhibits the eNOS phosphorylation at Thr 495 and decreases the Cav-1 content, ultimately resulting in enhanced NO production. This effect was antagonized by the PI3K/Akt signaling pathway inhibitor LY294002. The inhibitor used and its location of action is also indicated.

phosphorylation at the eNOS Ser 1177, which is involved in the basic activation of eNOS and agonist-induced activation (Fulton et al., 1999; Bauer et al., 2003). It is mainly present in the cytoplasm in an inactive form and must translocate to the cell membrane to activate itself and phosphorylate eNOS (Gonzalez et al., 2002). In addition, it is directly controlled by the PI3K-dependent phosphorylation pathway, and PI3K recruits Akt to the cell membrane, thereby phosphorylating it (Vanhaesebroeck et al., 1997). To investigate the mechanism by which SFI regulates eNOS activity, we used EA.hy926, a fusion of primary cultured human umbilical vein cells with thioguanine-resistant A549 clone under PEG stress, to detect the gene and protein expression of eNOS, the protein expression of Cav-1, total eNOS, and the phosphorylation of eNOS at Ser1177 and Thr495. The results showed that SFI significantly up-regulated the gene and protein expression of eNOS, decreased the Cav-1 content in the cell supernatant, and promoted the phosphorylation of eNOS at Ser 1177 but inhibited the phosphorylation of eNOS at Thr495, thereby enhancing eNOS activity. This effect was antagonized by the PI3K/Akt signaling pathway inhibitor LY294002, which suggested that SFI may promote the phosphorylation of eNOS through the PI3K/Akt signaling pathway (**Figure 7**).

Although this study preliminarily revealed that the mechanism behind SFI's endothelium-dependent vasodilatation is that it enhances eNOS activity through the PI3K/Akt signaling pathway *in vitro*, the mechanism of eNOS activation is extremely complex and can be divided into gene regulation (regulation of promoter and mRNA stability) and protein regulation (eNOS intracellular translocation, eNOS complex formation, and the phosphorylation of eNOS amino acid residue) (Dias et al., 2011; Zhu et al., 2015). Various regulatory mechanisms are interconnected to form a complex network structure. Therefore, more comprehensive and systematic research on other regulatory mechanisms is needed in the future to fully elucidate the mechanism by which SFI regulates eNOS activity.

It is well-known that vasomotor function is not only related to vascular endothelium but also requires co-regulation of vascular smooth muscle (Dias et al., 2011). Therefore, it is necessary to explore the effect of SFI on signal transduction between VECs and VSMCs in the future to clarify its mechanism of diastolic vasodilation further.

CONCLUSION

Our study revealed for the first time that endothelium-dependent vasodilatation effect of SFI occurs through the NO-cGMP pathway but not the PGI_2 pathway. Moreover, we found that the vasorelaxation effect of SFI is mediated through the PI3K/Akt/eNOS/NO signaling pathway in VECs. Overall, this study provides a scientific basis for the treatment of shock and HF with SFI and lays a foundation for the expansion of its clinical application and secondary development.

DATA AVAILABILITY STATEMENT

All datasets generated for this study are included in the article/**Supplementary Material**.

ETHICS STATEMENT

This study was carried out in strict accordance with the recommendations in the Guidance Suggestions for the Care and Use of Laboratory Animals issued by the Ministry of Science and Technology of China. The protocol was approved by the Laboratory Animal Ethics Committee of Tianjin University of Traditional Chinese Medicine (Permit Number: LAEC2013002).

AUTHOR CONTRIBUTIONS

JZ and BW carried out the experiments. JZ, WS, SX, YM, and HW performed analysis and interpretation of the data. JZ and SH designed the experiments. JZ wrote and revised the manuscript. All of the authors gave final approval to the work.

FUNDING

We are grateful for the financial support from the National Natural Science Foundation of China (No. 81973626, 81473381) and the Training Project of Tianjin Institution "Innovation Team" (TD13-5049).

SUPPLEMENTARY MATERIAL

The Supplementary Material for this article can be found online at: https://www.frontiersin.org/articles/10.3389/fphar.2020.00121/full#supplementary-material

REFERENCES

Bauer, P. M., Fulton, D., Boo, Y. C., Sorescu, G. P., Kemp, B. E., Jo, H., et al. (2003). Compensatory phosphorylation and protein-protein interactions revealed by loss of function and gain of function mutants of multiple serine phosphorylation sites in endothelial nitric-oxide synthase. *J. Biol. Chem.* 278 (17), 14841–14849. doi: 10.1074/jbc.M211926200

Bucci, M., Gratton, J. P., Rudic, R. D., Acevedo, L., Roviezzo, F., Cirino, G., et al. (2000). In vivo delivery of the caveolin-1 scaffolding domain inhibits nitric oxide synthesis and reduces inflammation. *Nat. Med.* 6 (12), 1362–1367. doi: 10.1038/82176

Cui, Y. Y., Tang, C. S., and Geng, B. (2006). Restraint stress down-regulates L-Arg/NOS/NO pathway of platelet and aortic intima in rats. *J. Peking Univ. (Health Sciences)* 38 (3), 231–235.doi:10.1097, 00024382-200610001-00089

Dias, R. G., Negrao, C. E., and Krieger, M. H. (2011). Nitric oxide and the cardiovascular system: cell activation, vascular reactivity and genetic variant. *Arq Bras. Cardiol.* 96 (1), 68–75. doi: 10.1590/S0066-782X2011000100012

Dimmeler, S., Fleming, I., Fisslthaler, B., Hermann, C., Busse, R., and Zeiher, A. M. (1999). Activation of nitric oxide synthase in endothelial cells by Akt-dependent phosphorylation. *Nature* 399 (6736), 601–605. doi: 10.1038/21224

Dong, Y., Wang, P., Feng, X., Li, B., Wang, Z., and Li, H. (2017). The role of chinese herbal medicines and bioactive ingredients targeting myocardial KCa and KATP channels in cardiovascular diseases. *Curr. Pharm. Des.* 23 (7), 1070–1076. doi: 10.2174/1381612823666161122141755

Feron, O., Belhassen, L., Kobzik, L., Smith, T. W., Kelly, R. A., and Michel, T. (1996). Endothelial nitric oxide synthase targeting to caveolae. Specific interactions with caveolin isoforms in cardiac myocytes and endothelial cells. *J. Biol. Chem.* 271 (37), 22810–22814. doi: 10.1074/jbc.271.37.22810

Fetalvero, K. M., Shyu, M., Nomikos, A. P., Chiu, Y. F., Wagner, R. J., Powell, R. J., et al. (2006). The prostacyclin receptor induces human vascular smooth muscle cell differentiation *via the* protein kinase A pathway. *Am. J. Physiol. Heart Circ. Physiol.* 290 (4), H1337–H1346. doi: 10.1152/ajpheart.00936.2005

Fleming, I., Fisslthaler, B., Dimmeler, S., Kemp, B. E., and Busse, R. (2001). Phosphorylation of Thr(495) regulates Ca(2+)/calmodulin-dependent endothelial nitric oxide synthase activity. *Circ. Res.* 88 (11), 68–75. doi: 10.1161/hh1101.092677

Fulton, D., Gratton, J. P., McCabe, T. J., Fontana, J., Fujio, Y., Walsh, K., et al. (1999). Regulation of endothelium-derived nitric oxide production by the protein kinase Akt. *Nature* 399 (6736), 597–601. doi: 10.1038/21218

Gallis, B., Corthals, G. L., Goodlett, D. R., Ueba, H., Kim, F., Presnell, S. R., et al. (1999). Identification of flow-dependent endothelial nitric-oxide synthase phosphorylation sites by mass spectrometry and regulation of phosphorylation and nitric oxide production by the phosphatidylinositol 3-kinase inhibitor LY294002. *J. Biol. Chem.* 274 (42), 30101–30108. doi: 10.1074/jbc.274.42.30101

Garcia-Cardeña, G., Martasek, P., Masters, B. S., Skidd, P. M., Couet, J., Li, S., et al. (1997). Dissecting the interaction between nitric oxide synthase (NOS) and caveolin. Functional significance of the NOS caveolin binding domain *in vivo*. *J. Biol. Chem.* 272 (41), 25437–25440. doi: 10.1074/jbc.272.41.25437

Ge, A. H., Li, J., Donnapee, S., Bai, Y., Liu, J., He, J., et al. (2015). Simultaneous determination of 2 aconitum alkaloids and 12 ginsenosides in Shenfu injection by ultraperformance liquid chromatography coupled with a photodiode array detector with few markers to determine multicomponents. *J. Food Drug Anal.* 23 (2), 267–278. doi: 10.1016/j.jfda.2014.10.013

Ghosh, S., Gachhui, R., Crooks, C., Wu, C. Q., Lisanti, M. P., and Stuehr, D. J. (1998). Interaction between caveolin-1 and the reductase domain of endothelial nitric-oxide synthase- consequences for catalysis. *J. Biol. Chem.* 273 (35), 22267–22271. doi: 10.1074/jbc.273.35.22267

Gonzalez, E., Kou, R., Lin, A. J., Golan, D. E., and Michel, T. (2002). Subcellular targeting and agonist-induced site-specific phosphorylation of endothelial nitric-oxide synthase. *J. Biol. Chem.* 277 (42), 39554–39560. doi: 10.1074/jbc.M207299200

Gulati, A. (2016). Vascular endothelium and hypovolemic shock. *Curr. Vasc. Pharmacol.* 14 (2), 187–195. doi: 10.2174/1570161114666151202210221

Huang, Y., Pan, J., Lin, G., Zhang, J., Zhang, X., Jin, H., et al. (2011). Effects of the serum in shock rats and shenfu injection on the endothelial cell protein C receptor. *Chin. J. Emergency Med.* 20 (2), 168–172. doi: 10.3760/cma.j.issn.1671-0282.2011.02.014

Huang, P., Guo, Y., Feng, S., Zhao, G., Li, B., and Liu, Q. (2019). Efficacy and safety of Shenfu injection for septic shock: a systematic review and meta-analysis of randomized controlled trials. *Am. J. Emerg. Med.* 37 (12), 2197–2204. doi: 10.1016/j.ajem.2019.03.032

Jia, Y. X., Pan, C. S., Yang, J. H., Liu, X. H., Yuan, W. J., Zhao, J., et al. (2006). Altered L-arginine/nitric oxide synthase/nitric oxide pathway in the vascular adventitia of rats with sepsis. *Clin. Exp. Pharmacol. Physiol.* 33 (12), 1202–1208. doi: 10.1111/j.1440-1681.2006.04498.x

Laspas, P., Goloborodko, E., Sniatecki, J. J., Kordasz, M. L., Manicam, C., Wojnowski, L., et al. (2014). Role of nitric oxide synthase isoforms for ophthalmic artery reactivity in mice. *Exp. Eye Res.*, 127, 1–8. doi: 10.1016/j.exer.2014.06.018

Li, Y. H., Yu, B., Duan, Z. Z., Akinyi, O. M., Yu, J. H., Zhou, K., et al. (2014). The coronary dilation effect of shen fu injection was mediated through NO. *PloS One* 9 (3), e92415. doi: 10.1371/journal.pone.0092415

Li, J., Yu., L. B., Rong, Y., Zhengrong, Y., Xiaojun, Y., and Guoliang, X. (2017). The Effect of Shenfu Injection on the microcirculatory disturbance in rats with heart ligation. *Pharmacol. Clinics Chin. Material Med.* 33 (1), 2–6. doi: CNKI:SUN:ZYYL.0.2017-01-001

Li, J., Guan, X. K., and Liu, R. X. (2019). Role of chinese herbal medicines in regulation of energy metabolism in treating cardiovascular diseases. *Chin. J. Integr. Med.* 25 (4), 307–315. doi: 10.1007/s11655-018-2943-5

Liu, X., Liu, R., Dai, Z., Wu, H., Lin, M., Tian, F., et al. (2019). Effect of Shenfu injection on lipopolysaccharide (LPS)-induced septic shock in rabbits. *J. Ethnopharmacol.*, 234, 36–43. doi: 10.1016/j.jep.2019.01.008

Livak, K. J., and Schmittgen, T. D. (2001). Analysis of relative gene expression data using real-time quantitative PCR and the 2(T)(-Delta Delta C) method. *Methods* 25 (4), 402–408. doi: 10.1006/meth.2001.1262

McCabe, T. J., Fulton, D., Roman, L. J., and Sessa, W. C. (2000). Enhanced electron flux and reduced calmodulin dissociation may explain "calcium-independent" eNOS activation by phosphorylation. *J. Biol. Chem.* 275 (9), 6123–6128. doi: 10.1074/jbc.275.9.6123

Mendis, S., Davis, S., and Norrving, B. (2015). Organizational update: the world health organization global status report on noncommunicable diseases 2014; one more landmark step in the combat against stroke and vascular disease. *Stroke* 46 (5), e121–e122. doi: 10.1161/STROKEAHA.115.008097

Moncada, S., Palmer, R. M., and Higgs, E. A. (1991). Nitric oxide: phsiology, pathophysiology and pharmacology. *Pharmacol. Rev.* 43 (2), 109–142.

Nar, G., Soylu, M., Akcay, O., Gulel, S., Yuksel, M., Meric, M., et al. (2013). Evaluation of the relationship between arterial blood pressure, aortic stiffness andserum endothelin-1 levels in patients with essential hypertension. *Clin. Exp. Hypertens.* 35 (8), 589–594. doi: 10.3109/10641963.2013.776565

Ohkita, M., Tawa, M., Kitada, K., and Matsumura, Y. (2012). Pathophysiological roles of endothelin receptors in cardiovascular diseases. *J. Pharmacol. Sci.* 119 (4), 302–313. doi: 10.1254/jphs.12r01cr

Parkington, H. C., Coleman, H. A., and Tare, M. (2004). Prostacyclin and endothelium-dependent hyperpolarization. *Pharmacol. Res.* 49 (6), 509–514. doi: 10.1016/j.phrs.2003.11.012

Penna, C., Rastaldo, R., Mancardi, R., Capello, S., Pagliaro, P., Westerfold, N., et al. (2006). Effect of endotheliums on the cardiovascular system. *J. Cardiovasc. Med. (Hagerstown)* 7 (9), 645–652. doi: 10.2459/01.JCM.0000242996. 19077.ba.

Theodorakis, N., Maluccio, M., and Skill, N. (2015). Murine study of portal hypertension associated endothelin-1 hypo-response. *World J. Gastroenterol.* 21 (16), 4817–4828. doi: 10.3748/wjg.v21.i16.4817

Vanhaesebroeck, B., Leevers, S. J., Panayotou, G., and Waterfield, M. D. (1997). Phosphoinositide 3-kinases: a conserved family of signal transducers. *Trends Biochem. Sci.* 22 (7), 267–272. doi: 10.1016/s0968-0004(97)01061-x

Wang, F., Li, B., and Sun, S. (2000). Vasoactive substances and shock. *Bull. Med. Res.* 29 (7), 32–34.

Wang, X., Zhao, Z., Mao, J., Du, T., Chen, Y., Xu, H., et al. (2019). Randomized, double-blinded, multicenter, placebo-controlled trial of shenfu injection for treatment of patients with chronic heart failure during the acute phase of symptom aggravation (Yang and Qi Deficiency Syndrome). *Evid. Based Complement. Alternat. Med.* 2019, 9297163. doi: 10.1155/2019/9297163

Widlansky, M. E., Gokce, N., Keaney, J. F.Jr., and Vita, J. A. (2003). The clinical implications of endothelial dysfunction. *J. Am. Coll. Caidiol.* 42 (7), 1149–1160. doi: 10.1016/s0735-1097(03)00994-x

Wu, J., Li, C., and Yuan, W. (2016). Effects of Shenfu injection on macrocirculation and microcirculation during cardiopulmonary resuscitation. *J. Ethnopharmacol.* 180, 97–103. doi: 10.1016/j.jep.2016.01.027

Xu, X. (1994). *Pharmacological experiments methodology* (Beijing: People's Health Publishing House).

Yao, L., Lu, P., Li, Y. M., Yang, L. J., Feng, H. X., Huang, Y., et al. (2013). Osthole relaxes pulmonary arteries through endothelial phosphatidylinositol 3-kinase/Akt-eNOS-NO signaling pathway in rats. *Eur. J. Pharmacol.* 699 (1-3), 23–32. doi: 10.1016/j.ejphar.2012.11.056

Zhang, S. A., Liu, Y., Guo, S. L., Zhang, J. N., Chu, X. J., Jiang, C., et al. (2010). Vasoactive intestinal polypeptide relaxes isolated rat pulmonary artery rings through two distinct mechanisms. *J. Physiol. Sci.* 60 (6), 389–397. doi: 10.1007/s12576-010-0107-x

Zhang, N. (2016). *Study on the chemical substance base of Shenfu injection and the ingredient of Qishen granules. (doctor)* (Beijing: Beijing University of Chinese Medicine).

Zhu, J., Kang, L., Ye, Q., Fan, G., Liang, Y., Yan, C., et al. (2013). Effects of Shenfu injection and its main components on the contraction of isolated rat thoracic aortic rings. *PloS One* 8 (10), e78026. doi: 10.1371/journal.pone.0078026

Zhu, J. Q., Song, W. S., Hu, Z., Ye, Q. F., Liang, Y. B., and Kang, L. Y. (2015). Traditional Chinese medicine's intervention in endothelial nitric oxide

synthase activation and nitric oxide synthesis in cardiovascular system. *Chin. J. Integr. Med*, 1–9. doi: 10.1007/s11655-015-1964-1

Conflict of Interest: The authors declare that the research was conducted in the absence of any commercial or financial relationships that could be construed as a potential conflict of interest.

frontiers in Pharmacology

MINI REVIEW
published: 03 March 2020
doi: 10.3389/fphar.2020.00171

Phytochemical Profile, Pharmacological Attributes and Medicinal Properties of *Convolvulus prostratus* – A Cognitive Enhancer Herb for the Management of Neurodegenerative Etiologies

Acharya Balkrishna[1,2], *Pallavi Thakur*[1] *and Anurag Varshney*[1,2]*

[1] Drug Discovery and Development Division, Patanjali Research Institute, Haridwar, India, [2] Department of Allied and Applied Sciences, University of Patanjali, Haridwar, India

OPEN ACCESS

Edited by:
Valentina Echeverria Moran, Bay Pines VA Healthcare System, United States

Reviewed by:
Sefirin Djiogue, University of Yaounde I, Cameroon
Vivekananda Mandal, Guru Ghasidas Vishwavidyalaya, India

***Correspondence:**
Anurag Varshney
anurag@prft.co.in

Specialty section:
This article was submitted to Ethnopharmacology, a section of the journal Frontiers in Pharmacology

Received: *16 September 2019*
Accepted: *07 February 2020*
Published: *03 March 2020*

Citation:
Balkrishna A, Thakur P and Varshney A (2020) Phytochemical Profile, Pharmacological Attributes and Medicinal Properties of Convolvulus prostratus – A Cognitive Enhancer Herb for the Management of Neurodegenerative Etiologies. Front. Pharmacol. 11:171. doi: 10.3389/fphar.2020.00171

Convolvulus prostratus Forssk., a nootropic herb used in traditional medicinal systems, is also frequently known by its taxonomic synonym *Convolvulus pluricaulis*. In Indian medicinal system – *Ayurveda* – it is named as *Shankhpushpi*. According to the ancient literature, this herb has been attributed with several therapeutic properties, such as anxiolytic, neuroprotective, antioxidant, analgesic, immunomodulatory, antimicrobial, antidiabetic and cardioprotective activities. This medicinal herb has been reported to contain many bioactive phytoconstituents, such as, alkaloid (convolamine), flavonoid (kaempferol) and phenolics (scopoletin, β-sitosterol and ceryl alcohol), that have been ascribed to the observed medicinal properties. Several research teams across the globe have highlighted the neuro-pharmacological profile of *C. prostratus*, wherein, the neuroprotective, nootropic and neuro-modulatory roles have been described. Besides, role of *C. prostratus* extracts in neurodegeneration has been well demonstrated. Despite of such elaborative preclinical pharmacological profile, detailed clinical investigations and mechanistic mode-of-action studies of this important herb are yet to be executed. The present review is attempted to showcase the phytochemical profile, pharmacological attributes and medicinal information of *C. prostratus*; with comprehensive research gap analysis. It is hoped that the scientific update on the ethnomedicinal aspects of this herb would thrive research propagation and development of the CNS phytopharmaceuticals, originated from *C. prostratus*.

Keywords: *Convolvulus prostratus*, *Shankhpushpi*, natural product, Ayurveda, neuroprotective, nootropic

INTRODUCTION

In recent years, non-communicable diseases (NCDs) have become an emerging cause of morbidity and mortality (~ 12% global prevalence) (Islam et al., 2014). Neurological disorders constitute a significant proportion as the leading causes of death among all the other non-communicable diseases (Gourie-Devi, 2014). The most common disorders of the nervous system are schizophrenia (~ 40% prevalence in India) and epilepsy (~ 45% prevalence in India), which are clinically presented by dysfunction of the interneurons, misbalancing neuronal homeostasis, ultimately leading to neurophysiological disintegration (Gururaj et al., 2005). It is estimated that by next decade, mental and behavioural disorders will lead to a reduction in the average life expectancy, nearly by one-fifth proportion (Lopez and Murray, 1998). In India, an average of 65 people out of 1,000 inhabitants suffer from mental and behavioural disorders, wherein, maximum prevalence has been recorded for alcohol dependency afflicted mental disorders (~ 6% prevalence), child and adolescent behavioural disorders (~ 4.3% prevalence) and mood disorders (~ 1.6% prevalence). These statistics makes it obvious that the prevalence of neurodegenerative disorders is escalating, however, effective and safe treatment modalities are still under infancy (Gururaj et al., 2005).

The chemotherapeutic moieties used currently for the treatment of neurological disorders face a daunting challenge of systemic delivery of the drugs to the central nervous system. Moreover, crossing the blood brain barrier after strenuous systemic administration is another challenge. Ultimately, the bioavailability of these drugs becomes low and therefore, lead to below- optimal efficacies (Tonda-Turo et al., 2018). Several drug delivery vehicles and nano-formulations have been devised so as to facilitate the targeted delivery of the drug to the site of action, *i.e.*, the central nervous system, thereby bypassing the blood brain barrier (Saraiva et al., 2016; Tonda-Turo et al., 2018). However, these strategies have also shown little success. Most of the neurodegenerative disorders are progressive in nature, and the cycle of etiological events usually have an early-onset which might get unnoticed or under-detected. In such a case, the therapies initiated after the onset of neuropathological asymptomatic etiologies will only have limited value for the patients (Solanki et al., 2016). Moreover, the foresaid neuropathological conditions are manifested with several additional etiologies, wherein the chemotherapeutic modalities act typically on a single target, thereby providing only palliative care (Chen and Pan, 2014). Hence, natural compounds serve as the holistic option which act on multiple neural targets and are enriched with free radical scavenging polyphenolic compounds (Park et al., 2018). These phytoconstituents have well-described antioxidant and anti-inflammatory properties which aids in protecting the neuronal cells against oxidative stress. Additionally, the natural compounds, such as flavonoids also aid in modulating the neuronal cell signalling pathways (Solanki et al., 2016).

There are various herbs which are used in traditional medicine for the management of neurodegenerative diseases, for instance: *Centella asiatica* (L.) Urb., *Glycyrrhiza glabra* L., *Tinospora cordifolia* (Willd.) Hook. f. & Thomson, *Bacopa monnieri* (L.) Wettst. and *Nardostachys jatamansi* (D. Don) DC. (Kulkarni et al., 2012). One such example is *Convolvulus prostratus* Forssk. (Syn. *Convolvulus pluricaulis* Choisy), which is commonly known as *Shankhpushpi* in *Ayurveda* and is widely recognized for its anxiolytic, antidepressant and nootropic activities (Kulkarni et al., 2012). As per an ancient Indian medicinal scripture—*Charaka Samhita*—this plant is superior to other nootropic drugs (*Medhya rasayana*) of *Ayurveda*, however, a detailed ethnomedicinal update yet needs to be presented (Dev, 2006). The ensuing sections will provide an ethnomedicinal, phytochemical and pharmacological update of this cognitive booster herb, *C. prostratus* (CP).

ETHNOMEDICINAL UPDATE ON *C. prostratus*

C. prostratus belongs to Convolvulaceae family and is ubiquitous in the north-western regions of India (Nisar et al., 2012). In *Ayurveda*, this herb is classically described as a memory and intellect booster. Moreover, it is employed in a variety of formulations used for the treatment of nervous disorders, such as insanity, epilepsy, hysteria, insomnia, and psycho-neurosis (Khare, 2004). Mechanistically, it reduces the spontaneous motor activity, thereby controlling the refluxes and frightening responses. It ultimately acts as a sedative moiety which initiates a persistent fall in blood pressure and cardiac contraction, thereby managing neurological pathologies, such as anxiety, insanity and epilepsy (Chaudhary, 1996). The neuro-mechanistic aspects of this herb has been elucidated in **Figure 1A**. Besides, this plant has manifold therapeutic utilities, wherein, a decoction of its shoots is used as a remedy for anaemia and weakness (Singh et al., 2003). More specifically, in ancient texts, this plant has been mentioned as *sara*, *medhya*, *vrsya* and *rasayana*, which refers to the laxative, nootropic, aphrodisiac and rejuvenator properties of this herb, respectively. Additionally, one of the revered ancient Indian medical practitioner, *Acharya Charaka* had used white-flowered variety of *C. prostratus* (*Shankhpushpi*) along with the juice of *Bacopa monnieri* (*Brahmi*), *Acorus calamus* (*Vacha*) and *Saussurea lappa* (*Kushtha*) for alleviating insanity and epilepsy. Similar views had been presented in *Chikitsasangraha* written by *Chakradatta*; *Kaideva Nighantu*; and *Ayurveda Saar Sangraha* (Khare, 2004).

Besides *Ayurveda*, *C. prostratus* (CP) has also been used in *Siddha* system of medicine, wherein an oil obtained from this plant is used as a keratogenic agent for promoting hair growth (Gogte, 2012). It is also believed that a paste prepared from its roots and flowers act as anti-aging agents, thereby indicating its apparent anti-oxidant activity (Adams et al., 2007). Furthermore, in *Unani* medicinal system, a syrup prepared with *C. prostratus* and *Piper nigrum* is prescribed in bleeding piles and venereal diseases (Khare, 2004). All the above mentioned ethnomedicinal uses of *C. prostratus* have been tabulated in **Table 1**.

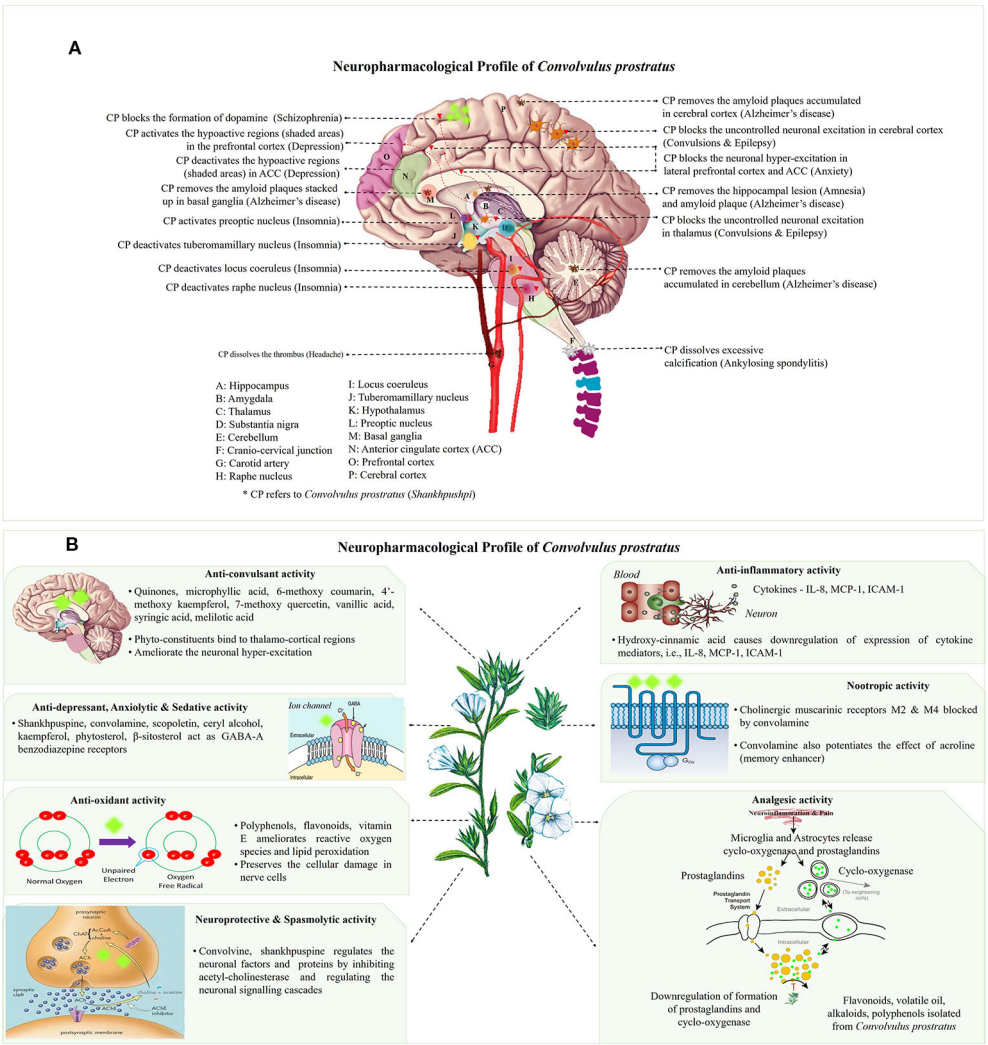

FIGURE 1 | (A) Neuro-mechanistic aspects of *Convolvulus prostratus* (CP). Schematic representations of *C. prostratus* (CP) target and mode of action in neural system. CP reduces the lesions formed in the hippocampus (A); and amyloid plaque accumulation in hippocampus (A), cortex (P), basal ganglia (M) and cerebellum (E). CP also acts as GABA-A agonists and binds to lateral prefrontal cortex (O) and anterior cingulate cortex (N). CP deactivates the wake promoting areas, namely, tuberomamillary nucleus (J) located in the hypothalamus (K), locus coeruleus (I) and raphe nucleus (H). It also activates the sleep inducing areas of the brain, namely, preoptic nucleus (L). Moreover, CP activates the hypoactive regions situated in the prefrontal cortex (shaded pink area; O), and deactivates hyperactive regions situated in the anterior cingulate cortex (shaded green area; N). CP blocks the excessive production of dopamine as produced *via* substantia nigra (D). CP also removes the excessive calcification formed at the cranio-cervical junction (F). Additionally, CP removes the formation of thrombus in the carotid artery (G). **(B)** Main mechanisms and phytoconstituents responsible for neuro-pharmacological activities of *C. prostratus* (CP). This herb exhibits anti-convulsant, anti-depressant, anxiolytic, sedative, anti-inflammatory, anti-oxidant, analgesic, nootropic, spasmolytic and neuroprotective activities. Phyto-constituents belonging to diverse chemical families, namely, coumarins, alkaloids and polyphenols (see **Table 2**) are responsible for such evident neuro-pharmacological profile of the CP plant (Nolte, 1999; Carter, 2014). Reported mechanisms of CNS action of CP phyto-constituents has been depicted in these schematics, with putative site of action has been marked with fluorescent green blobs.

INDUSTRIAL SIGNIFICANCE OF *C. prostratus*

C. prostratus is extensively used in pharmaceutical, cosmeceutical and nutraceutical industries (Jalwal et al., 2016). In the pharmaceutical industry, various extracts, syrups and tablets are produced, specifically for targeting neurodegenerative diseases, hypertension, hypercholesterolemia and gastric ulcers. A few examples of such marketed herbal pharmaceutical formulations include Patanjali Divya Shankhpushpi Churna™, Divya Pharmacy Shankhpushpi Sharbat™, Baidyanath Shankhpushpi Sharbat™, Dabur Shankhpushpi Syrup™, Biotrex Shankhpushpi™, Maxmind capsule™, Herbal Hills Shankhpushpi Tablets™ and many more (Bhowmik et al., 2012). Similarly, in the cosmeceutical industry, the CP herb is used as a general tonic for rejuvenating

TABLE 1 | Ethnomedicinal uses of *Convolvulus prostratus* (CP) with predominant plant parts and mode of herbal preparation.

Disease Targeted	Part(s) used	Method of Preparation and Dosage (if any)
Amnesia†	Whole plant	Decoction of this herb used along with milk (Bhalerao et al., 2014).
Anorexia	Leaf	Intact part used as such (Rizwan and Khan, 2014).
Anxiety†	Leaf, Flower	Intact parts used for treating anxiety neurosis (Mishra and Sethiya, 2010).
Arthritis	Whole plant	Whole plant used for the management of arthritis, osteoarthritis and rheumatic pain (Pan et al., 2009).
Asthma	Leaf	Intact part used as such (Mishra and Sethiya, 2010).
Blood disorders	Whole plant	Whole plant is used (Nisar et al., 2012).
Bone fracture	Leaf, Flower	Paste of flowers and leaves used for the management of fracture (Singh and Pandey, 1998).
Bronchitis	Leaf	Intact part used as such (Mishra and Sethiya, 2010).
Burning sensation†	Whole plant	Whole plant is used (Sethiya et al., 2009).
Calculi	Leaf	Intact part used as such (Mishra and Sethiya, 2010).
Constipation	Leaf, Stem	Intact parts used for the management of constipation (Malik et al., 2015).
Cough	Leaf	Intact part used as such (Rizwan and Khan, 2014).
Dementia†	Root, Flower	Paste of roots and flowers administered for the treatment of dementia (Adams et al., 2007).
Diabetes	Leaf	Paste of leaves (100 g) along with black pepper (3-4 grains) is to be administered once daily (Singh et al., 2003).
Dyspnoea	Leaf	Intact part used as such (Rizwan and Khan, 2014).
Dysuria	Whole plant	Jelly obtained from this plant (10 g) is mixed with honey (10 g) and is to be taken thrice a day (Bhutya, 2011).
Edema	Whole plant	Whole plant is used (Sethiya et al., 2009).
Emesis	Whole plant	Whole plant is used (Agarwa et al., 2014).
Enuresis	Whole plant	Powder of this plant along with *Hyoscyamus niger*, *Prunella vulgaris*, (l-2 g) and milk (100 mL) is to be taken along with twice a day (Bhutya, 2011).
Epilepsy†	Whole plant	Paste of this plant along with cumin seeds (l g) and milk thrice a day (Bhutya, 2011).
Gonorrhoea	Whole plant	Jelly obtained from this plant (10 g) is mixed with honey (10 g) and is to be taken thrice a day (Bhutya, 2011).
Haemoptysis	Leaf	Juice of the leaves has to be administered at a dose of 10 mL, thrice a day (Bhutya, 2011).
Haemorrhoid	Whole plant	Whole plant is used (Nisar et al., 2012).
Headache†	Whole plant	Powder of plant (3 g) mixed with sugar (5 g) and milk (20 ml) is to be taken twice daily (Bhutya, 2011).
Hematemesis	Whole plant	Whole plant is used (Dhingra and Valecha, 2007).
Hysteria†	Whole plant	Intact plant is used (Dhingra and Valecha, 2007).
Insomnia†	Whole plant	Whole plant is used (Dhingra and Valecha, 2007).
Leprosy	Whole plant	Whole plant is used (Nisar et al., 2012).
Leucoderma	Whole plant	Whole plant is used (Bhutya, 2011).
Menorrhagia	Whole plant	Paste of this plant is taken along with milk (Gupta, 2016).
Neurological disorders†	Whole plant	Decoction of this herb is used along with cumin and milk for treating attention deficit hyperactivity disorder (ADHD), mild convulsions, depression, emotional stress, mental debility, memory loss, mental hypersensitivity, schizophrenia and stress disorders (Mishra and Sethiya, 2010; Sultana et al., 2018).
Polydipsia	Leaf, Stem	Intact parts used for the management of excessive thirst (Malik et al., 2015).
Pyrexia	Root, Leaf	Intact parts used for alleviating fever (Bhalerao et al., 2014).
Pyrosis	Leaf, Stem	Intact parts used for the management of heart burn or pyrosis (Malik et al., 2015).
Scrofula	Whole plant	Decoction of this herb is used along with cumin and milk (Mishra and Sethiya, 2010).
Sexual debility	Whole plant	This plant (100 g) is ground with little water and taken with sugar or honey once daily, for 21 days (Bhutya, 2011).
Snake bite	Whole plant	Whole plant is used (Sethiya et al., 2009).
Stomachache	Whole plant	One tea spoon powder of dried plant is taken for the management of stomachache (Katewa and Jain, 2006).
Syphilis	Whole plant	Decoction of this herb is used along with cumin and milk (Mishra and Sethiya, 2010).
Ulcer	Root	Intact part used as such (Bhutya, 2011).
Urinary diseases	Leaf	Intact part used as such (Rizwan and Khan, 2014).
Vertigo†	Whole plant	A syrup prepared from this herb is used for the management of vertigo (Gogte, 2012).
Worm infestation	Whole plant	Whole plant is used (Gupta, 2016).
Wound	Whole plant	Whole plant is used (Trivedi, 2009).

†*Shaded rows indicate specific neurological diseases which can be managed by the administration of C. prostratus.*

the skin and hairs, thereby treating skin related ailments as well as keratogenic disorders. A few examples for elucidating the use of CP (Shankhpushpi) as cosmeceutical ingredients include Econature Shankhpushpi Hair oil™, Khadi Natural Shankhpushpi oil™ and Alps Shankhpushpi hair Mask Powder™. Moreover, the CP powder and juice, such as, Jain Shankhpushpi Powder™ and Axiom Jeevan Ras Shankhpushpi Juice™, are also being used as skin mask for rejuvenating the skin and managing skin problems such as acne, blemishes and sun spots (Hindu, 2012). Additionally, food grade CP powder and syrups are also available in the market for being used as a nutraceutical nootropic supplement, for example, Divya Pharmacy Shankhpushpi Sharbat™, Baidyanath Shankhpushpi Sharbat™, Shivalik Herbals Shankhpushpi Nutraceutical Capsules™ and Veg E Wagon *Shankhpushpi* Powder (Bhowmik et al., 2012). Such extensive industrial uses of CP further confirms the holistic significance of this nontoxic wonder herb (Jalwal et al., 2016).

PHYTOMEDICINAL FORMULATIONS CONTAINING *C. prostratus*

The CP herb has also been used as a phyto-ingredient of a polyherbal medicinal formulation: *Sankhahauli*, which contains leaves of *C. prostratus* (15 *g*); seeds of *Piper nigrum*

(3 *g*) and *Papaver somniferum* (20 *g*); whole plant of *Prunus amygdalus* (10 g), *Vitis vinifera* (20 g) and *Coriandrum sativum* (10 *g*). This formulation is mainly used for the management of insomnia, drug addiction and hypertension (Bhutya, 2011). Several such marketed herbal formulations containing CP are being used for the management of a variety of neurological ailments in India, for example., *Divya Medha Vati*, *Divya Medha Kwath* (Patanjali Ayurved Ltd.); BR-16A (Himalaya Drug Co. Ltd.); *Dimagheen* (Dawakhana Tibiya College); *Shankhpushpi* syrup (Unjha); *Shankhavali Churna* (Narnaryan Pharmacy); Brain tab and *Shankhpushpi* syrup (Baidyanath Pharmaceuticals) (Aggarwal et al., 2011; Sethiya et al., 2013; Amin et al., 2014).

CHEMICAL PROFILE OF *C. prostratus*

All of these stated medicinal utilities of *C. prostratus* (CP) have been attributed to various phytoconstituents, belonging to the chemical family of alkaloids, flavonoids, coumarins and polyphenols. Among these phytoconstituents, certain compounds are known to be present at a higher concentration (almost 20% w/w) and are known as major phyto-constituents. CP plant is known to contain kaempferol, β-sitosterol, N-hexacosanol, taraxerol, taraxerone, delphinidine and hydroxy-cinnamic acid as the major phyto-constituents, as depicted in **Table 2** (Billore et al., 2005; Amin et al., 2014). Moreover, an alkaloid, namely, Sankhpuspine has also been isolated from this plant and is known as a chemotaxonomic marker for this species (Basu and Dandiya, 1948; Saroya and Singh, 2018). CP plant also contains other alkaloids (convolamine, convosine, convoline, convolidine, convolvine, confoline, evolvine, phyllabine, subhirsine, sankhpuspine) (Agarwa et al., 2014; Balaji et al., 2014); anthroquinones; carbohydrates (D-glucose, sucrose, rhamnose, maltose) (Dhingra and Valecha, 2007; Bhowmik et al., 2012; Agarwa et al., 2014); coumarins (ayapanin, scopolin, scopoletin); flavonoids (kaempferol, quercetin) (Lal, 2014); glycosides (geranilan-3-ol-1-carboxylate-1-O-β-D-xylopyranosyl-(2′→1′′)-O-β-D-xylopyranoside (Sultana et al., 2018); phenolic compounds; steroids; tannins; and terpenoids (Ravichandra et al., 2013; Agarwa et al., 2014; Balaji et al., 2014; Malik et al., 2016).

Several other hydrocarbons, namely, 1- pentyl-2-tridecanyl cyclopentyl cyclohexane carboxylate, 1,2-benzenedicarboxylic acid, 10-bromodecanoic acid, 1-octadecanesulphonyl chloride, 2-butanone, 2-pentanol, 7- hydroxyheptadecanyl-1,7, 17-tricarboxylic acid, ascorbic acid, cyclononasiloxane, cyclo-octadecanyl methanol, decanoic acid, dicyclohexyl cyclo-octyl acetic acid, eicosane, heneicosane, hydroxy cinnamic acid, octatriacontyl pentafluoropropionate, pentadecyl 2-propyl ester, pentanoic acid, pentyl hexacosanoate, phthalic acid, silane, squalene, tetracyclohexanyl caproate and tridecane are also found in the extract of the CP plant (Bhalerao et al., 2014; Malik et al., 2016; Rachitha et al., 2018; Sultana et al., 2018).

In addition, CP is known to be a good source of vitamins and minerals, namely, calcium, copper, iron, magnesium, manganese, phosphorus, potassium, sulphur, zinc, vitamin C and E (Sethiya et al., 2010; Babu et al., 2015).

NEURO-PHARMACOLOGICAL PROFILE OF *C. prostratus*

Nootropic Activity

C. prostratus (CP) contains volatile oil; fatty alcohols; flavonoids, *i.e.* kaempferol; hydroxy cinnamic acid; β-sitosterol; and carbohydrates such as glucose, rhamnose, sucrose *etc.*, which endow this plant with nootropic capabilities. Moreover, an alkaloid, namely, convolvine present in this herb has also been found to block cholinergic muscarinic receptors: M2 and M4. Convolvine also aids in potentiating the effect of another muscarinic memory enhancer, namely, arecoline, thereby imparting nootropic abilities to CP (Sethiya et al., 2009). In a study, Rawat and Kothiyal have also found that the aquo-methanolic, ethanolic and petroleum ether extracts isolated from CP (50–400 mg/Kg) exhibited anxiolytic, memory-enhancing and nootropic activity as evaluated by using Elevated Plus Maze (EPM) and step-down models in mice. EPM test has mainly been used to investigate the interactions between aversive memory and anxiety responses of the mice. CP effects on EPM activity has been found to be comparable to the standard of care drug, Piracetam (Rawat and Kothiyal, 2011; Kaushik, 2017). Moreover, treatment with alcoholic extract of CP plant led to an increase in the average time-span spent by mice in the enclosed arm of plus maze model, and an escalation in the mean avoidance response on the jumping box model (Rawat and Kothiyal, 2011).

Neuroprotective Activity

The aqueous extract of the roots of *C. prostratus* inhibited the activity of acetylcholinesterase (AChE) within the cortex and hippocampus of male Wistar rats, that have been intoxicated with scopolamine. CP extract also posed evident anti-oxidant activity and elevated the levels of glutathione reductase, superoxide dismutase and reduced glutathione within the cortex and hippocampus (Kaushik, 2017). Similar results have been observed in case of aluminium chloride induced neurotoxicity in rat cerebral cortex. Regular administration of the CP root extracts (150 mg/Kg) for 3 months inhibited the decline in Na^+/K^+ ATPase activity and also preserved the mRNA expression levels of muscarinic acetylcholine receptor 1 (M1 receptor), choline acetyl transferase (ChAT) and nerve growth factor-tyrosine kinase A receptor (NGF-TrkA) (Bihaqi et al., 2009; Kaushik, 2017). The Na^+/K^+ ATPase pump aids in maintaining the osmotic equilibrium and membrane potential in neuronal cells (Forrest, 2014). Secondly, the muscarinic receptors bind to the neurotransmitter acetylcholine, thereby facilitating the transmission of electrical signals within the central nervous system (Brown, 2018). Furthermore, the choline acetyl transferase enzyme is essential for the synthesis of neurotransmitter acetylcholine; and the nerve growth factor-tyrosine kinase A receptor is necessary for binding of the neuronal trophic factors, thereby ensuring the survival of the neurons (Johnson et al., 2018; Indo, 2018).

In another experiments, it has been shown that the oral administration of the aqueous extract of the CP roots (150 mg/

TABLE 2 | Major phyto-constituents of *Convolvulus prostratus* (CP) with their reported medicinal utility.

Name of the compound	Category of phytoconstituent	Chemical structure†	Medicinal profile
Ayapanin	Coumarin	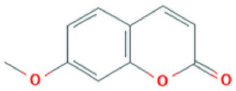	Improves scopolamine-induced spatial memory impairment (Zingue et al., 2018); anti-nociceptive activity (Cheriyan Sr et al., 2017).
Convolamine	Alkaloid	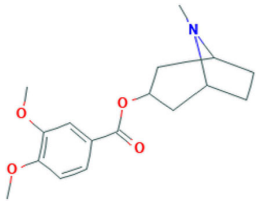	Antihypoxic, immune-modulating, and anti-inflammatory activity (Gapparov et al., 2011).
Convoline	Alkaloid	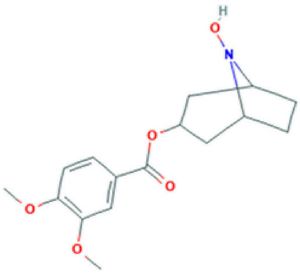	Anti-epileptic activity (Dubey et al., 2018).
Convolvine	Alkaloid	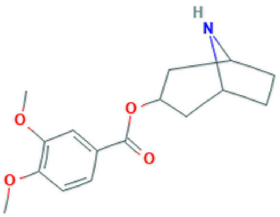	Antihypoxic, immune-modulating, and anti-inflammatory activity (Gapparov et al., 2011); blocks the M-receptors; exhibits nootropic, cytotoxic and sedative activity (Mirzaev and Aripova, 1998; Tseomashko et al., 2013).
Delphinidine	Anthocyanin	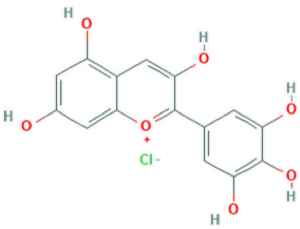	Antioxidant, anti-mutagenic, anti-inflammatory and antiangiogenic (Patel et al., 2013).
Hydroxy-cinnamic acid	Carboxylic acid	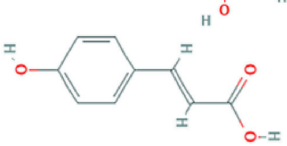	Antioxidant, photooxidant activity; strong inhibitory effect on the tumour U14 (Vinholes et al., 2015).
Kaempferol	Flavonoid	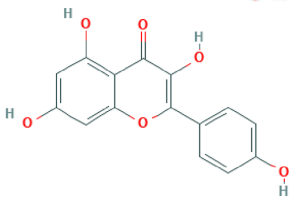	Activates LXR-β and suppresses SREBP-1 to enhance symptoms in metabolic syndromes; potent inhibitory effect on *in vitro* bone resorption; anti-inflammatory, anti-oxidant activity; inhibition of cancer cell invasion through blocking the PKCδ/MAPK/AP-1 (Wang et al., 2015; Hoang et al., 2015).
Quercetin	Flavonoid	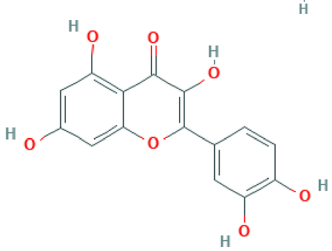	Antioxidant activity; stimulator of recombinant SIRT1 and also a PI3K inhibitor; attenuated the function VEGFR, androgen receptor and the expressions of NF-κB, IL Receptor, FAK, ERK, Nrf2 (Xing et al., 2001).

(Continued)

TABLE 2 | Continued

Name of the compound	Category of phytoconstituent	Chemical structure†	Medicinal profile
Scopoletin	Coumarin	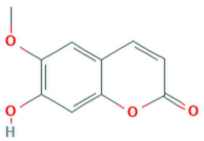	Antifungal, anti-allergic, anti-aging and hypouricemic activities (Sun et al., 2014; Nam and Kim, 2015).
Scopolin	Coumarin glucoside	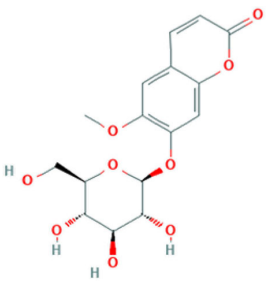	Antinociceptive activity; acetylcholinesterase (AChE) inhibitor; fungitoxic activity (Prats et al., 2006; Pan et al., 2009).
Taraxerol	Triterpenoid	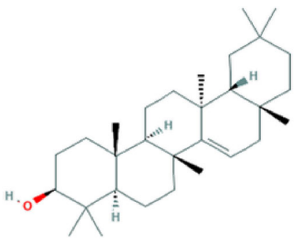	Anti-inflammatory; anti-cancerous activity (Swain et al., 2012).
β-sitosterol	Phytosterol	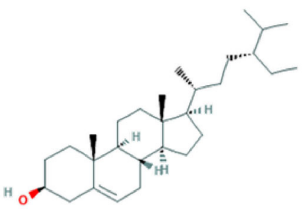	Anti-inflammatory; anti-proliferation; anti-pyretic; pro-apoptotic activity (Gupta et al., 1980; Park et al., 2007).

†*Source of Chemical structures: PubChem (https://pubchem.ncbi.nlm.nih.gov/).*

Kg) to scopolamine induced rats causes a marked reduction in the mRNA levels of tau protein (Bihaqi et al., 2012). Such reduction in the tau protein expression is responsible for causing an amelioration in the amyloid β-induced deficits in case of neurodegenerative disorders such as Alzheimer's disease (Vossel et al., 2010). Hence, the presence of phytoconstituents such as convolvine might be responsible for endowing CP with the abilities to regulate all the neuronal factors/proteins and enzymes, thereby showcasing its evident neuroprotective status (Sethiya et al., 2009; Ray and Ray, 2015).

Anxiolytic Activity

The ethanolic and chloroform extracts isolated from the aerial parts of CP showed significant anxiolytic activity as recorded using elevated plus maze test on experimental mice. There was increase in the time spent in open arms; and in the number of open arm entries upon the CP oral administration to mice at a dose of 200 mg/Kg (Bhalerao et al., 2014). Similar results have also been observed in case of the ethanolic extract of the CP flower petals at doses 200–400 mg/Kg in mice (Kaushik, 2017).

In another study, CP methanolic extract was evaluated for anxiolytic activity on Obsessive Compulsive Disorders (OCDs) in mice by employing marble burying behaviour analysis, hole board and rota-rod tests. The results have shown that the mice group treated with 200–400 mg/Kg CP methanolic extracts can modulate serotonin or dopaminergic levels, thereby harmonizing the major pathway involving serotonergic or dopaminergic receptors manifesting obsessive compulsive disorders (Subramani et al., 2013). Such anxiolytic activity can be linked with the hypotensive effect of this herb, which in turn is attributed to the presence of GABA-A-benzodiazepine agonists, such as convolamine and scopoletin (**Figure 1B**) (Malik et al., 2011; Amin et al., 2014; Siddiqui et al., 2014).

Anti-Convulsant Activity

The chloroform, ethanol and aqueous extracts of CP have been evaluated for anti-convulsant activity against strychnine induced as well as pentylene tetrazol (PTZ) induced convulsive seizures in different animal models. Five hundred mg/Kg concentration of the CP extracts have shown statistically significant ($p < 0.001$)

protection against strychnine and PTZ induced clonic convulsions (Ratha and Mishra, 2012; Siddiqui et al., 2014). Methanolic extract of this plant (500–1000 mg/Kg) also exhibited anti-convulsant activity, as characterized by reduction in the mean recovery time of convulsions in case of maximal electroshock seizure model in mice (Kaushik, 2017).

The fundamental mechanism behind such evident anti-convulsing activity of CP might be the presence of coumarins and triterpenoids (Quintans Júnior et al., 2008). Moreover, it has also been proposed that the anti-convulsant activity of a phyto-medicine is escalated by the presence of certain functional groups like, quinoline, quinazoline, thiazole, benzothiazines, oxadiazole, pyridine, pyrazole, imidazole, pyrimidine, phthalazine, triazine, triazoles, cyclopropane carboxylate, and oxime ether (Wei et al., 2015; Song and Deng, 2018). Indeed, many such functional groups have been found in the CP phyto-constituents (**Table 2**) for *e.g.*, quinones, microphyllic acid, 6-methoxy coumarin, 4'-methoxy kaempferol, 7-methoxy quercetin, vanillic acid, syringic acid and melilotic acid (Daniel, 2016).

Anti-Depressant Activity

Bhalerao and co-workers have found that the chloroform fraction isolated from the CP ethanolic extract reversed the reserpine-induced extension of immobility period of mice in Forced Swim Test (FST), and elicited a significant antidepressant effect by interaction with adrenergic, dopaminergic and serotonergic systems (Bhalerao et al., 2014). Similarly, a polyherbal formulation (Trans-01) containing *C. prostratus* (30%), *Valeriana wallichii* (45%), *Plumbago zeylanica* (7.5%), *Boswellia serrata* (15%) and *Acorus calamus* (3.5%) also exhibited similar anti-depressant properties as tested by employing the forced swim test (FST), tail suspension test (TST) and forced swimming stress (FSS)-induced alterations in serum corticosterone levels. In TST and FST, Trans-01 showed a dose-dependent decrease in immobility time. Moreover, Trans-01 significantly attenuated the elevated corticosteroid levels, thereby indicating a significant anti-depressant activity of this formulation (Shalam et al., 2007). CP herb is known to contain alkaloids (convolamine and scopoletin), flavonoids (kaempferol), and steroids (phytosterol and β-sitosterol). These phytoconstituents most probably act as GABA-A-benzodiazepine agonists and bind to the GABA-A-benzodiazepine receptors, thereby causing an increase in the chloride ion flux and consequent hyperpolarization of the postsynaptic membrane. Such hyperpolarization leads to a hypnotic effect and may alleviate depression (Siddiqui et al., 2014).

Anti-Inflammatory Activity

Hydroxy-cinnamic acid is a phenyl-propanoid compound found in CP. It is known to cause a downregulation in the expression of cytokine mediators such as IL-8, MCP-1 and ICAM-1, thereby blocking the expression of cytokine-mediated adhesion molecules and therefore the fundamental process of leukocyte–endothelial cell adhesion is deterred (Billore et al., 2005; Rathee et al., 2009). Hence, the CP herb may aid in ameliorating the conditions of neuro-inflammation and consequent cognitive impairment. Indeed, oral administration of the ethanolic extract of the CP leaves at dose of 800 mg/Kg, showed significant inhibition of rat paw edema, in the Carrageenan-induced paw edema and Cotton pellet-induced granuloma animal models (Agarwal et al., 2014).

Anti-Oxidant Activity

The reactive oxygen species are known to deteriorate the cellular physiology of nerve cells and ultimate lead to neurodegenerative disorders. Polyphenols, flavonoids and vitamin E present in the CP plant act as reactive oxygen species (ROS) scavengers and also ameliorate the lipid peroxidation, thereby attributing towards the anti-oxidant activity of CP (Nasri et al., 2015). It has also been observed that the ethyl acetate and methanolic extract of CP have shown appreciable results (IC_{50} ~ 0.07 mg/mL and 0.075 mg/mL, respectively), as observed in 2,2-diphenyl-1-picrylhydrazyl (DPPH) assay. Similarly, in Ferric Reducing Antioxidant Power (FRAP) analysis, aqueous CP extract has been found to be potentially active with anti-oxidant capacity of 460 ± 8 ascorbic acid equivalent/mg of the extract (Jain et al., 2011). Interestingly, the *Shankhpushpi* syrup and its isolated compounds (Scopoletin and Bacoside A) also exhibited evident anti-oxidant activity as evaluated by using DPPH assay with average IC_{50} value ranging from 0.94 - 2.39% v/v (Jain et al., 2017; Rachitha et al., 2018). Furthermore, the aqueous extract of CP roots diminished the endogenous levels of reactive oxygen species in tauopathy flies as induced by overexpression of τ-protein, thereby substantiating its oxidative stress ameliorative effect (Olakkaran and Antony, 2017).

Analgesic and Spasmolytic Activity

The ethanolic extract of CP at dose 750 mg/Kg showed statistically significant analgesic activity as compared to the standard analgesics like, morphine sulphate, when tested in hot plate method and tail-flick assays in rats (Agarwal et al., 2014). Such evident analgesic activity is cohesively attributed by flavonoids, volatile oils, alkaloids, polyphenols and organic acids by means of prevention of the formation of cyclooxygenase enzyme and prostaglandins, *i.e.*, mediators of pain sensitization. Hence, these CP phyto-constituents ultimately aid in ameliorating the neuronal pain and headache (Aleebrahim-Dehkordy et al., 2017).

The CP ethanolic extract has exhibited spasmolytic activity in isolated rabbit ileum, isolated rat uterus, intact intestine and tracheal muscles of dog (Barar and Sharma, 1965). Such anti-spasmodic action is linked to the inhibition of acetylcholine production which is mainly brought about by the specific alkaloid present in this CP herb, convolvine (Amin et al., 2014).

Sedative Activity

Interestingly, the ethanolic and aqueous extracts of the CP aerial parts showed statistical significant potentiation of sleeping time in rats induced with thiopental sodium (Siddiqui et al., 2014). In another similar experiment, the aqueous extract of the CP leaves and flowers showed an evident barbiturate hypnosis potentiation

in albino rats at a dose of 300 mg/Kg (Mudgal, 1975). Such sedative activity is directly linked to the presence of phytoconstituents like convolamine and scopoletin which act similarly to GABA-A agonists, thereby bringing about the effects of sedation (**Figure 1B**) (Siddiqui et al., 2014).

This CP herb has also been reported for several other pharmacological activities, including anti-diabetic, anti-hyperlipidemic, anti-hypertensive, anti-microbial, anti-platelet aggregation, anti-ulcer, cardio-vascular, hepatoprotective, and hypothyroidism (Barar and Sharma, 1965; Mudgal, 1975; Rizk et al., 1985; Mali, 1995; Jain et al., 2011; Ravichandra et al., 2013; Jalwal et al., 2016). Anti-diabetic activities of this plant might be attributed to the presence of tropane alkaloids which are known as potent inhibitor of α-glucosidases and R-galactosidases (Gaikwad et al., 2014; Rachitha et al., 2018). The polyphenols present in this species act as reactive oxygen species (ROS) quenchers, thereby ameliorating the oxidative stress that is generated as a diabetic manifestation. Additionally, the presence of vitamin E in this herb also aids in controlling the levels of protein oxidation and lipid peroxidation, thereby leading to an escalation in the antioxidant defense system (Cowan, 1999; Nasri et al., 2015; Domínguez-Avila et al., 2016; Foretz et al., 2018). Furthermore, the presence of GABA-A-benzodiazepine agonists, such as convolamine, scopoletin, ceryl alcohol, kaempferol, phytosterol, and β-sitosterol endow this herb with hypotensive and sedative activities (Malik et al., 2011; Siddiqui et al., 2014). More specifically, a compound, namely, 29-oxodotriacontanol, isolated from the CP herb has also been assessed to possess antimicrobial and anti-fungal activity (Amin et al., 2014). Certain flavonoids and phenyl-propanoids from CP have been shown to provide anti-platelet aggregation and anti-ulcerogenic activity by means of inhibition of cyclic nucleotide phosphodiesterase enzyme and clot retraction capabilities (Beretz and Cazenave, 1991; Tognolini et al., 2006). The anti-ulcerogenic effect was largely observed due to upregulation of mucosal defensive factors such as mucin and glycoprotein secretion, which in turn was induced by the flavonoids and steroids present in this herb (Srinivas et al., 2013). These flavonoids also pose the profound effects on the thyroid hormone regulation and deiodinase-1 inhibition, thereby endowing this herb with anti-thyroid activity (Nagarathna and Jha, 2013). Additionally, the fundamental principle responsible for the cardio-vascular activity of this herb has been proposed to be linked with it alkaloid derivative, evolvine hydrochloride, which is known to exhibit lobeline-like action on the cardiovascular system. This phytoconstituent acts as a cardiac depressant, ultimately leading to a fall in blood pressure, which gets gradually normalised (Dwoskin and Crooks, 2002; Sethiya et al., 2009).

Safety Profile of *C. prostratus*

The ethanolic and aqueous extracts of the CP leaves have been evaluated for acute oral toxicity study in albino Wistar rats. The animals did not show any toxicity or behavioural changes up to the dose of 5,000 mg/Kg (Agarwal et al., 2014). Similarly, the iron oxide nanoparticles of the CP herb exhibited maximum tolerable dose up to 2,000 mg/Kg in Swiss albino mice with no clinical signs of toxicity. The histopathology of brain also did not show any aberrations or degeneration of neurons. Furthermore, no inflammation was observed in the heart and liver (Ravichandra et al., 2013). These toxicological studies, therefore, confirmed that the administration of CP is safe for the vital organs within the respective treatment durations.

Summary and Way Forward

The use of herbal medicines continues to escalate rapidly with about 70% of the world population still relying upon traditional medicines for their primary healthcare needs. The natural plant products have negligible toxicities, if any, and are endowed with a multitude of phytoconstituents which are responsible for their holistic therapeutic action. Cognitive dysfunction is one of the major health problem in today's world, wherein the available synthetic chemotherapeutic modalities have proven to be non-absolute and, at times toxic in nature. In such a scenario, safer herbal alternative medicines play a vital role in managing the neurological etiologies. One such cognitive booster herb is *C. prostratus* Forssk., commonly known as *Shankhpushpi*, which is mainly endowed with neuroprotective, nootropic and neuro-modulatory activities (**Figure 1B**). Besides, it also possesses several other therapeutic properties, such as immunomodulatory, antimicrobial, antidiabetic and cardioprotective activities. The fundamental bioactive compounds responsible for the nootropic activities of this herb have been identified as 4'-methoxy kaempferol, 7-methoxy quercetin, convolamine, scopoletin, ceryl alcohol, β-sitosterol and hydroxy-cinnamic acid. Additionally, this herb did not exhibit any signs of toxicity and neurodegeneration up to a dose of 2000 mg/Kg in mice, thereby indicating its safety profile. A few initial clinical trials have conducted for CP, however, more detailed and controlled clinical trials are needed to establish and validate the neuro-pharmacological profile of *C. prostratus*. In addition, detailed mechanistic studies are yet to be executed to unravel the underlying mechanism of action for this cognition enhancing herb. Taken together, *C. prostratus* is likely to be the front runner for the clinical phyto-pharmaceutical status for treatment of neurological ailments.

AUTHOR CONTRIBUTIONS

AB conceived the presented research. PT analyzed the information, generated the artwork, and co-wrote the manuscript. AV investigated and supervised the findings of the work. AB and AV provided critical revision of this review article, and approved the manuscript for submission. All authors agreed with the final version of this manuscript.

FUNDING

The presented research work been funded by the research funds of Patanjali Research Foundation Trust (PRFT), Haridwar, India.

ACKNOWLEDGMENTS

The authors are grateful to Param Pujya Swami Ramdev Ji for institutional research facilities and supports. Authors gratefully acknowledge the efforts of Dr. Shivam Singh and Dr. Swami Narsingh Dev at Patanjali Research Institute, for their help in data collection and processing. We are also thankful to Mr. Gagan Kumar and Mr. Lalit Mohan for their swift administrative supports and encouragements.

REFERENCES

Adams, M., Gmünder, F., and Hamburger, M. (2007). Plants traditionally used in age related brain disorders—A survey of ethnobotanical literature. *J. Ethnopharmacol.* 113, 363–381. doi: 10.1016/j.jep.2007.07.016

Agarwa, P., Sharma, B., Fatima, A., and Jain, S. K. (2014). An update on Ayurvedic herb Convolvulus pluricaulis Choisy. *Asian Pac. J. Trop. Biomed.* 4, 245–252. doi: 10.1016/S2221-1691(14)60240-9

Agarwal, P., Sharma, B., and Alok, S. (2014). Screening of anti-inflammatory and anti-analgesic activity of Convolvulus pluricaulis choisy. *Int. J. Pharm. Sci. Res.* 5, 2458–2463. doi: 10.13040/IJPSR.0975-8232.5(6).2458-63

Aggarwal, B. B., Prasad, S., Reuter, S., Kannappan, R., R Yadav, V., Park, B., et al. (2011). Identification of novel anti-inflammatory agents from Ayurvedic medicine for prevention of chronic diseases: "reverse pharmacology" and "bedside to bench" approach. *Curr. Drug Targets* 12, 1595–1653. doi: 10.2174/138945011798109464

Aleebrahim-Dehkordy, E., Tamadon, M. R., Nasri, H., Baradaran, A., Nasri, P., and Beigrezaei, S. (2017). Review of possible mechanisms of analgesic effect of herbs and herbal active ingredient. *J. Young Pharm.* 9, 303–306. doi: 10.5530/jyp.2017.9.60

Amin, H., Sharma, R., Vyas, M., Prajapati, P. K., and Dhiman, K. (2014). Shankhapushpi (Convolvulus pluricaulis Choisy): Validation of the Ayurvedic therapeutic claims through contemporary studies. *Int. J. Green Pharm.* 8, 193–200. doi: 10.4103/0973-8258.142666

Babu, N. G., Raju, T. P., Srinivasu, Ch. Ch., Ramanamam, V., Ram, S. S., Sudershan, M., et al. (2015). Estimation of elemental concentrations of Indian medicinal plants using Energy dispersive X-ray fluorescence (EDXRF). *Int. J. Sci. Eng. Res.* 6, 1379–1387. Available at https://www.ijser.org/paper/Estimation-of-elemental-concentrations-of-Indian-medicinal-plants-using-Energy-dispersive-X-ray-fluorescence.html

Balaji, K., Hean, K. C., Ravichandran, K., and Shikarwar, M. (2014). In-Vitro Evaluation of Antioxidant Activity and Total Phenolic Content of Methanolic Extract of Convolvulus pluricaulis. *Res. J. Pharm. Biol. Chem. Sci.* 5, 959–964. doi: 10.1080/19390211.2018.1470126

Barar, F. S., and Sharma, V. N. (1965). Preliminary pharmacological studies on Convolvulus pluricaulis chois–an Indian indigenous herb. *Indian J. Physiol. Pharmacol.* 9, 99–102. Available at https://www.ijpp.com/IJPP%20archives/1965_9_2/99-102.pdf

Basu, N. K., and Dandiya, P. C. (1948). Chemical investigation of Convolvulus pluricaulis Chois. *J Am. Pharm. Assoc.* 37: 27–28. doi: 10.1002/jps.3030370108

Beretz, A., and Cazenave, J. P. (1991). Old and new natural products as the source of modern antithrombotic drugs. *Planta Med.* 57, S68–S72. doi: 10.1055/s-2006-960232

Bhalerao, S. A., Verma, D. R., Teli, N. C., and Trikannad, A. A. (2014). Ethnobotany, phytochemistry and pharmacology of Convolvulus pluricaulis, Choisy. *Res. J. Pharm. Biol. Chem. Sci.* 5, 629–636. Available at https://www.semanticscholar.org/paper/Ethnobotany%2C-Phytochemistry-and-Pharmacology-of-Bhalerao-Verma/62602df9affb6d3a5a27699015e1506aa34ef1bf

Bhowmik, D., Kumar, K., Paswan, S., Srivatava, S., Yadav, A., and Dutta, A. (2012). Traditional Indian herb Convolvulus Pluricaulis and its medicinal importance. *J. Pharmacogn. Phytochem.* 1, 44–51. Available at http://www.phytojournal.com/vol1Issue1/Issue_may_2012/4.pdf

Bhutya, R. K. (2011). *Ayurvedic medicinal plant of India* (Jodhpur, India: Scientific Publishers).

Bihaqi, S. W., Sharma, M., Singh, A. P., and Tiwari, M. (2009). Neuroprotective role of Convolvulus pluricaulis on aluminium induced neurotoxicity in rat brain. *J. Ethnopharmacol.* 124, 409–415. doi: 10.1016/j.jep.2009.05.038

Bihaqi, S. W., Singh, A. P., and Tiwari, M. (2012). Supplementation of Convolvulus pluricaulis attenuates scopolamine-induced increased tau and Amyloid precursor protein (AβPP) expression in rat brain. *Indian J. Pharmacol.* 44, 593–598. doi: 10.4103/0253-7613.100383

Billore, K. V., Yelne, M. B., Dennis, T. J., and Chaudhari, B. G. (2005). *Database on medicinal plants used in Ayurveda (Vol. 7)* (New Delhi, India: Central Council for Research in Ayurveda & Siddha).

Brown, D. A. (2018). Regulation of neural ion channels by muscarinic receptors. *Neuropharmacol.* 136, 383–400. doi: 10.1016/j.neuropharm.2017.11.024

Carter, R. (2014). *The human brain book: An illustrated guide to its structure, function, and disorders* (London: Penguin publishers).

Chaudhary, R. D. (1996). *Herbal drug industry* (Delhi, India: Eastern Publisher).

Chen, X., and Pan, W. (2014). "The treatment strategies for neurodegenerative diseases by integrative medicine. ,", vol. 1. *Integr. Med. Int,* 223–225. doi: 10.1159/000381546

Cheriyan, B. V.Sr., Kadhirvelu, P.Sr., Nadipelly, J.Jr., Shanmugasundaram, J., Sayeli, V.Sr., and Subramanian, V.Sr. (2017). Anti-nociceptive effect of 7-methoxy coumarin from Eupatorium Triplinerve vahl (Asteraceae). *Pharmacogn. Mag.* 13, 81–84. doi: 10.4103/0973-1296.197650

Cowan, M. M. (1999). Plant products as antimicrobial agents. *Clin. Microbiol. Rev.* 12, 564–582. doi: 10.1128/CMR.12.4.564

Daniel, M. (2016). "*Medicinal plants: chemistry and properties*," (Boca Raton, Florida, United States: CRC press).

Dev, S. (2006). *A selection of prime Ayurvedic plant drugs* (New Delhi, India: Anamaya Publishers).

Dhingra, D., and Valecha, R. (2007). Screening for antidepressant-like activity of Convolvulus pluricaulis Choisy in mice. *Pharmacol. Online* 1, 262–278. Available at https://www.semanticscholar.org/paper/SCREENING-FOR-ANTIDEPRESSANT-LIKE-ACTIVITY-OF-IN-Dhingra-Valecha/51168240f3c88647a52ce21a54878606c61a7c66

Domínguez-Avila, J., González-Aguilar, G., Alvarez-Parrilla, E., and de la Rosa, L. (2016). Modulation of PPAR expression and activity in response to polyphenolic compounds in high fat diets. *Int. J. Mol. Sci.* 17, E1002 1002. doi: 10.3390/ijms17071002

Dubey, S. K., Singhvi, G., Krishna, K. V., Agnihotri, T., Saha, R. N., and Gupta, G. (2018). Herbal medicines in neurodegenerative disorders: an evolutionary approach through novel drug delivery system. *J. Environ. Pathol. Toxicol.* 37, 199–208. doi: 10.1615/JEnvironPatholToxicolOncol.2018027246

Dwoskin, L. P., and Crooks, P. A. (2002). A novel mechanism of action and potential use for lobeline as a treatment for psychostimulant abuse. Biochem. *Pharmacol.* 63, 89–98. doi: 10.1016/s0006-2952(01)00899-1

Foretz, M., Even, P., and Viollet, B. (2018). AMPK activation reduces hepatic lipid content by increasing fat oxidation *in vivo*. *Int. J. Mol. Sci.* 19, E2826. doi: 10.3390/ijms19092826

Forrest, M. D. (2014). The sodium-potassium pump is an information processing element in brain computation. *Front. Physiol.* 5, 472–475. doi: 10.3389/fphys.2014.00472

Gaikwad, S. B., Krishna Mohan, G., and Sandhya Rani, M. (2014). Phytochemicals for diabetes management. *Pharm. Crop* 5, 11–28. doi: 10.2174/2210290601405010011

Gapparov, A. M., Okhunov, I. I., Aripova, S. F., Nabiev, A., and Khuzhaev, V. U. (2011). Derivatives of the alkaloid convolvine and their pharmacological activity. *Chem. Nat. Compd.* 47, 608–611. doi: 10.1007/s10600-011-0007-1

Gogte, V. M. (2012). *Ayurvedic pharmacology & therapeutic uses of medicinal plants* (Pune, India: Chaukhambha Sanskrit Sansthan).

Gourie-Devi, M. (2014). Epidemiology of neurological disorders in India: Review of background, prevalence and incidence of epilepsy, stroke, Parkinson's disease and tremors. *Neurol. India* 62, 588–598. doi: 10.4103/0028-3886

Gupta, M. B., Nath, R., Srivastava, N., Shanker, K., Kishor, K., and Bhargava, K. P. (1980). Anti-inflammatory and antipyretic activities of β-sitosterol. *Planta Med.* 39, 157–163. doi: 10.1055/s-2008-1074919

Gupta, V. K. (2016). *Traditional and folk herbal medicine: Recent researches (Vol. 3)* (New Delhi, India: Daya Publishing House).

Gururaj, G., Girish, N., and Isaac, M. K. (2005). *Mental, neurological and substance abuse disorders: Strategies towards a systems approach. Report submitted to the National Commission of Macroeconomics and Health* (Government of India, New Delhi: Ministry of Health and Family Welfare).

Hindu, V. (2012). Shanka Pushpi: A short review. *Int. Res. J. Pharm.* 3, 81–83. Available at https://irjponline.com/admin/php/uploads/794_pdf.pdf

Hoang, M. H., Jia, Y., Mok, B., Jun, H. J., Hwang, K. Y., and Lee, S. J. (2015). Kaempferol ameliorates symptoms of metabolic syndrome by regulating activities of liver X receptor-β. *J. Nutr. Biochem.* 26, 868–875. doi: 10.1016/j.jnutbio.2015.03.005

Indo, Y. (2018). NGF-dependent neurons and neurobiology of emotions and feelings: Lessons from congenital insensitivity to pain with anhidrosis. *Neurosci. Biobehav. Rev.* 87, 1–16. doi: 10.1016/j.neubiorev.2018.01.013

Islam, S. M. S., Purnat, T. D., Phuong, N. T. A., Mwingira, U., Schacht, K., and Fröschl, G. (2014). Non-Communicable Diseases (NCDs) in developing countries: a symposium report. *Global. Health* 10, 81–88. doi: 10.1186/s12992-014-0081-9

Jain, R., Pancholi, B., and Jain, S. C. (2011). Radical scavenging and antimicrobial activities of Convolvulus microphyllus. *Asian J. Chem.* 23, 4591–4594. Available at https://hero.epa.gov/hero/index.cfm/reference/details/reference_id/1109757

Jain, A., Kaur, J., Bansal, Y., Saini, B., and Bansal, G. (2017). WHO guided real time stability testing on Shankhpushpi Syrup. *J. Adv. Pharm. Technol. Res.* 5, 1–19. doi: 10.15415/jptrm.2017.51001

Jalwal, P., Singh, B., Dahiya, J., and Khokhara, S. (2016). A comprehensive review on shankhpushpi a morning glory. *Pharma Innov.* 5, 14–18. Available at http://www.thepharmajournal.com/archives/?year=2016&vol=5&issue=1&ArticleId=695

Johnson, C. D., Barlow-Anacker, A. J., Pierre, J. F., Touw, K., Erickson, C. S., Furness, J. B., et al. (2018). Deletion of choline acetyltransferase in enteric neurons results in postnatal intestinal dysmotility and dysbiosis. *FASEB J.* 32, 4744–4752. doi: 10.1096/fj.201701474RR

Katewa, S. S., and Jain, A. (2006). *Traditional folk herbal medicines* (Udaipur, India: Apex Publishing House).

Kaushik, R. (2017). Studying the pharmacological basis of an antiepileptic ayurvedic formulation-Sarasvata churna. *Int. J. Green Pharm.* 11, 62–68. Available at https://pdfs.semanticscholar.org/1dc0/39b0046a0caa7e211b7a64f0ec91596d4fef.pdf

Khare, C. P. (2004). *Encyclopedia of Indian medicinal plants* (New York, USA: Springer).

Kulkarni, R., Girish, K. J., and Kumar, A. (2012). Nootropic herbs (Medhya Rasayana) in Ayurveda: an update. *Pharmacogn. Rev.* 6, 147–153. doi: 10.4103/0973-7847.99949

Lal, B. (2014). Development of high performance thin layer chromatography method for the determination of scopolin in convolvulus pluricaulis chois. *PharmaTutor Mag.* 2 (11), 77–83. Available at https://www.pharmatutor.org/articles/development-high-performance-thin-layer-chromatography-method-for-determination-scopolin-convolvulus-pluricaulis-chois?page=1%2C1

Lopez, A. D., and Murray, C. C. (1998). The global burden of disease 1990–2020. *Nat. Med.* 4, 1241–1243. doi: 10.1038/3218

Mali, P. C. (1995). Hypolipidemic effect of Convolvulus microphyllus in cholesterol fed gerbils (Meriones hurrinae Jerdon). *J. Phytol. Res.* 8, 153–155. Available at https://www.researchgate.net/publication/266140204_Hypolipidemic_effect_of_Convolvulus_microphyllus_in_cholesterol_fed_gerbils_Meriones_hurrinae_Jerdon

Malik, J., Karan, M., and Vasisht, K. (2011). Nootropic, anxiolytic and CNS-depressant studies on different plant sources of shankhpushpi. *Pharm. Biol.* 49, 1234–1242. doi: 10.3109/13880209.2011.584539

Malik, S., Ahmad, S., Sadiq, A., Alam, K., Wariss, H. M., Ahmad, I., et al. (2015). A comparative ethno-botanical study of Cholistan (an arid area) and Pothwar (a semi-arid area) of Pakistan for traditional medicines. *J. Ethnobiol. Ethnomed.* 11, 31. doi: 10.1186/s13002-015-0018-2

Malik, J., Karan, M., and Vasisht, K. (2016). Attenuating effect of bioactive coumarins from Convolvulus pluricaulis on scopolamine-induced amnesia in mice. *Nat. Prod. Res.* 30, 578–582. doi: 10.1080/14786419.2015.1025398

Mirzaev, Y. R., and Aripova, S. F. (1998).). Neuro-and psychopharmacological investigation of the alkaloids convolvine and atropine. *Chem. Nat. Compd.* 34, 56–58. doi: 10.1007/BF02249687

Mishra, S. H., and Sethiya, N. K. (2010). Review on ethnomedicinal uses and phytopharmacology of memory boosting herb '*Convolvulus pluricaulis*' Choisy. *Aust. J. Med. Herb.* 22 (1), 19–25. Available at https://www.semanticscholar.org/paper/Review-on-ethnomedicinal-uses-and-of-memory-herb-Sethiya-Mishra/427692942318bd7bf5c9cd65e2cf8627aaa9c61f

Mudgal, V. (1975). Studies on medicinal properties of Convolvulus pluricaulis and Boerhaavia diffusa. *Planta Med.* 28, 62–68. doi: 10.1055/s-0028-1097830

Nagarathna, P. K. M., and Jha, D. K. (2013). Study on antithyroid property of some herbal plants. *Int. J. Pharm. Sci. Rev. Res.* 23, 203–211. Available at http://globalresearchonline.net/journalcontents/v23-2/36.pdf

Nam, H., and Kim, M. M. (2015). Scopoletin has a potential activity for anti-aging *via* autophagy in human lung fibroblasts. *Phytomedicine* 22, 362–368. doi: 10.1016/j.phymed.2015.01.004

Nasri, H., Shirzad, H., Baradaran, A., and Rafieian-Kopaei, M. (2015). Antioxidant plants and diabetes mellitus. *J. Res. Med. Sci.* 20, 491–502. doi: 10.4103/1735-1995.163977

Nisar, S. S., Khan, A. A., Maaz, M., and Shiffa, M. (2012). Review of sankhahauli (Convolvulus pluricaulis choisy) from traditional medicine to modern science. *Int. J. Institut. Pharm. Life Sci.* 2, 94–101. Available at https://www.semanticscholar.org/paper/REVIEW-OF-SANKHAHAULI-(CONVOLVULUS-PLURICAULIS-FROM-Nisar-Khan/0994b296aed35c7b9ccaa97be1505fddf55218e8

Nolte, J. (1999). *The human brain: an introduction to its functional anatomy (No. 798)* (United States: Mosby Inc.).

Olakkaran, S., and Antony, A. (2017). Convolvulus pluricaulis (Shankhapushpi) ameliorates human microtubule-associated protein tau (hMAPτ) induced neurotoxicity in Alzheimer's disease Drosophila model. *J. Chem. Neuroanat.* 95, 115–122. doi: 10.1016/j.jchemneu.2017.10.002

Pan, R., Dai, Y., Gao, X., and Xia, Y. (2009). Scopolin isolated from Erycibe obtusifolia Benth stems suppresses adjuvant-induced rat arthritis by inhibiting inflammation and angiogenesis. *Int. Immunopharmacol.* 9, 859–869. doi: 10.1016/j.intimp.2009.02.019

Park, C., Moon, D. O., Rhu, C. H., Choi, B. T., Lee, W. H., Kim, G. Y., et al. (2007). β-Sitosterol induces anti-proliferation and apoptosis in human leukemic U937 cells through activation of caspase-3 and induction of Bax/Bcl-2 ratio. *Biol. Pharm. Bull.* 30, 1317–1323. doi: 10.1248/bpb.30.1317

Park, G., Kusuma, I. W., and Kim, Y. U. (2018). Multiple Bioactivities of Traditional Medicinal Herbs for Treatment of Neurodegenerative Diseases. *Evid. Based Complement. Alternat. Med.* ,2018, 1–2. doi: 10.1155/2018/3075458

Patel, K., Jain, A., and Patel, D. K. (2013). Medicinal significance, pharmacological activities, and analytical aspects of anthocyanidins 'delphinidin': A concise report. *J. Acute Dis.* 2, 169–178. doi: 10.1016/S2221-6189(13)60123-7

Prats, E., Bazzalo, M. E., León, A., and Jorrín, J. V. (2006). Fungitoxic effect of scopolin and related coumarins on Sclerotinia sclerotiorum - A way to overcome sunflower head rot. *Euphytica* 147, 451–460. doi: 10.1007/s10681-005-9045-8

Quintans Júnior, L. J., Almeida, J. R., Lima, J. T., Nunes, X. P., Siqueira, J. S., Oliveira, L. E. G. D., et al. (2008). Plants with anticonvulsant properties: a review. *Rev. Bras. Farmacogn.* 18, 798–819. doi: 10.1590/S0102-695X2008000500026

Rachitha, P., Krupashree, K., Jayashree, G. V., Kandikattu, H. K., Amruta, N., Gopalan, N., et al. (2018). Chemical composition, antioxidant potential, macromolecule damage and neuroprotective activity of Convolvulus pluricaulis. *J. Tradit. Complement. Med.* 8, 483–496. doi: 10.1016/j.jtcme.2017.11.002

Ratha, K. K., and Mishra, S. S. (2012). Anticonvulsant activity of Shankhapuspi (Convolvulus pluricaulis Chois) on Strychnine induced seizure in experimental animals. *Int. J. Ayurvedic Med.* 3, 82–87. Available at https://www.ijam.co.in/index.php/ijam/article/view/163

Rathee, P., Chaudhary, H., Rathee, S., Rathee, D., Kumar, V., and Kohli, K. (2009). Mechanism of action of flavonoids as anti-inflammatory agents: a review. *Inflamm. Allergy Drug Targets* 8, 229–235. doi: 10.2174/187152809788681029

Ravichandra, V. D., Ramesh, C., and Sridhar, K. A. (2013). Hepatoprotective potentials of aqueous extract of Convolvulus pluricaulis against thioacetamide induced liver damage in rats. *Biomed. Aging Pathol.* 3, 131–135. doi: 10.1016/j.biomag.2013.06.005

Rawat, M. S. M., and Kothiyal, P. (2011). Comparative nootropic effect of Evolvulus alsinoides and Convolvulus pluricaulis. *Int. J. Pharma. Bio. Sci.* 2, 616–621. Available at https://ijpbs.net/abstract.php?article=NTk2

Ray, S., and Ray, A. (2015). Medhya rasayanas in brain function and disease. *Med. Chem.* 5, 505–511. doi: 10.4172/2161-0444.1000309

Rizk, A. M., Williamson, E. M., and Evans, F. J. (1985). Constituents of Plants Growing in Qatar VII An examination of Certain Plants for Anti-Inflammatory Activity. *Int. J. Crude Drug Res.* 23, 1–4. doi: 10.3109/13880208509070677

Rizwan, M., and Khan, A. A. (2014). Assessment of efficacy of Sankhahuli (Convolvulus pluricaulis Chois.) and gokhru (Tribulus terrestris L.) in the management of hypertension. *Indian J. Trad. Know.* 13, 313–318. Available at http://nopr.niscair.res.in/handle/123456789/27919

Saraiva, C., Praça, C., Ferreira, R., Santos, T., Ferreira, L., and Bernardino, L. (2016). Nanoparticle-mediated brain drug delivery: overcoming blood–brain barrier to treat neurodegenerative diseases. *J. Control. Release* 235, 34–47. doi: 10.1016/j.jconrel.2016.05.044

Saroya, A. S., and Singh, J. (2018). Phytopharmacology of Indian Nootropic Convolvulus pluricaulis, in *Pharmacotherapeutic Potential of Natural Products in Neurological Disorders*. (Singapore:Springer), 141–144. doi: 10.1007/978-981-13-0289-3_13

Sethiya, N. K., Nahata, A., Mishra, S. H., and Dixit, V. K. (2009). An update on Shankhpushpi, a cognition-boosting Ayurvedic medicine. *J. Chin. Integr. Med.* 7, 1001–1022. doi: 10.3736/jcim20091101

Sethiya, N. K., Trivedi, A., Patel, M. B., and Mishra, S. H. (2010). Comparative pharmacognostical investigation on four ethanobotanicals traditionally used as Shankhpushpi in India. *J. Adv. Pharm. Technol. Res.* 1, 388–395. doi: 10.4103/0110-5558.76437

Sethiya, N. K., Raja, M. M. M., and Mishra, S. H. (2013). Antioxidant markers based TLC-DPPH differentiation on four commercialized botanical sources of Shankhpushpi (A Medhya Rasayana): A preliminary assessment. *J. Adv. Pharm. Technol. Res.* 4, 25–30. doi: 10.4103/2231-4040.107497

Shalam, M. D., Shantakumar, S. M., and Narasu, M. L. (2007). Pharmacological and biochemical evidence for the antidepressant effect of the herbal preparation Trans-01. *Indian J. Pharmacol.* 39 (5), 231–234. doi: 10.4103/0253-7613.37273

Siddiqui, N. A., Ahmad, N., Musthaq, N., Chattopadhyaya, I., Kumria, R., and Gupta, S. (2014). Neuropharmacological profile of extracts of aerial parts of Convolvulus pluricaulis Choisy in mice model. *Open Neurol. J.* 8, 11–14. doi: 10.2174/1874205X01408010011

Singh, V., and Pandey, R. P. (1998). *Ethnobotany of Rajasthan* (Jodhpur, India: Scientific Publishers).

Singh, V. K., Govil, J. N., Hashmi, S., and Singh, G. (2003). *Recent progress in medicinal plants: Ethnomedicine & pharmacognosy II (Vol. 7)* (Texas, USA: Studium Press).

Solanki, I., Parihar, P., and Parihar, M. S. (2016). *Neurodegenerative diseases: from available treatments to prospective herbal therapy*.Neurochem. Int. 95, 100–108. doi: 10.1016/j.neuint.2015.11.001

Song, M. X., and Deng, X. Q. (2018). Recent developments on triazole nucleus in anticonvulsant compounds: a review. *J. Enzyme Inhib. Med. Chem.* 33, 453–478. doi: 10.1080/14756366.2017.1423068

Srinivas, T. L., Lakshmi, S. M., Shama, S. N., Reddy, G. K., and Prasanna, K. R. (2013). Medicinal plants as anti-ulcer agents. *J. Pharmacogn. Phytochem.* 2, 91–97. Available at http://www.phytojournal.com/archives/2013/vol2issue4/PartB/23.1.pdf

Subramani, R., Anand, M., and Muralidharan, P. (2013). *Effect of Convolvulus pluricaulis Choisy in obsessive compulsive disorder using animal models* (India: PharmaTutor EduLabs Publishing).

Sultana, S., Ali, M., Mir, S. R., and Iqbal, D. (2018). Isolation and characterization of glycosides from Convolvulus prostratus, Ficus virens, Phoenix dactifera, Spondias mangifera and Terminalia belerica. *Eur. J. Pharm. Med. Res.* 5, 310–318. Available at https://pdfs.semanticscholar.org/696f/2e4d7280727d2baba08bc7c6e3a7cd03ef3a.pdf

Sun, H., Wang, L., Zhang, B., Ma, J., Hettenhausen, C., Cao, G., et al. (2014). Scopoletin is a phytoalexin against Alternaria alternata in wild tobacco dependent on jasmonate signalling. *J. Exp. Bot.* 65, 4305–4315. doi: 10.1093/jxb/eru203

Swain, S. S., Rout, K. K., and Chand, P. K. (2012). Production of triterpenoid anti-cancer compound taraxerol in Agrobacterium-transformed root cultures of butterfly pea (Clitoria ternatea L.). *Appl. Biochem. Biotechnol.* 168, 487–503. doi: 10.1007/s12010-012-9791-8

Tognolini, M., Barocelli, E., Ballabeni, V., Bruni, R., Bianchi, A., Chiavarini, M., et al. (2006). Comparative screening of plant essential oils: phenylpropanoid moiety as basic core for antiplatelet activity. *Life Sci.* 78, 1419–1432. doi: 10.1016/j.lfs.2005.07.020

Tonda-Turo, C., Origlia, N., Mattu, C., Accorroni, A., and Chiono, V. (2018). Current Limitations in the Treatment of Parkinson's and Alzheimer's Diseases: State-of-the-Art and Future Perspective of Polymeric Carriers. *Curr. Med. Chem.* 25, 5755–5771. doi: 10.2174/0929867325666180221125759

Trivedi, P. C. (2009). *Medicinal plants: Utilization and conservation*. *2nd* (Jaipur, India: Aavishkar Publishers).

Tseomashko, N. E., Terent'Eva, E. O., Kodirova, D. B., Okhunov, I. I., Aripova, S. F., Khashimova, Z. S., et al. (2013). Synthesis of convolinine and cytotoxic activity of alkaloids of the genus Convolvulus and their derivatives. *Chem. Nat. Compd.* 48, 1039–1041. doi: 10.1007/s10600-013-0459-6

Vinholes, J., Silva, B. M., and Silva, L. R. (2015). "Hydroxycinnamic acids (HCAS): Structure, biological properties and health effects," in *Advances in Medicine and Biology*. Ed. LV Berhardt (India: Nova Science Publishers), 1–5.

Vossel, K. A., Zhang, K., Brodbeck, J., Daub, A. C., Sharma, P., Finkbeiner, S., et al. (2010). Tau reduction prevents Aβ-induced defects in axonal transport. *Science* 330, 198–198. doi: 10.1126/science.1194653

Wang, S. B., Jang, J. Y., Chae, Y. H., Min, J. H., Baek, J. Y., Kim, M., et al. (2015). Kaempferol suppresses collagen-induced platelet activation by inhibiting NADPH oxidase and protecting SHP-2 from oxidative inactivation. *Free Radic. Biol. Med.* 83, 41–53. doi: 10.1016/j.freeradbiomed.2015.01.018

Wei, C. X., Bian, M., and Gong, G. H. (2015). Current research on antiepileptic compounds. *Molecules* 20, 20741–20776. doi: 10.3390/molecules201119714

Xing, N., Chen, Y., Mitchell, S. H., and Young, C. Y. (2001). Quercetin inhibits the expression and function of the androgen receptor in LNCaP prostate cancer cells. *Carcinogenesis* 22, 409–414. doi: 10.1093/carcin/22.3.409

Zingue, S., Foyet, H. S., Djiogue, S., Ezo'o Ezo'o, Y., Abaïssou, H. H. N., Fachagbo, P., et al. (2018). Effects of Ficus umbellata (Moraceae) Aqueous Extract and 7-Methoxycoumarin on Scopolamine-Induced Spatial Memory Impairment in Ovariectomized Wistar Rats. *Behav. Neurol.* 2018, 5751864. doi: 10.1155/2018/5751864

Conflict of Interest: The authors declare that the research was conducted in the absence of any commercial or financial relationships that could be construed as a potential conflict of interest.

frontiers in Pharmacology

ORIGINAL RESEARCH
published: 13 March 2020
doi: 10.3389/fphar.2020.00223

Effect of Berberine on Atherosclerosis and Gut Microbiota Modulation and Their Correlation in High-Fat Diet-Fed ApoE−/− Mice

Min Wu[1†], Shengjie Yang[1†], Songzi Wang[2], Yu Cao[2], Ran Zhao[1,3], Xinye Li[1,3], Yanwei Xing[1] and Longtao Liu[2*]*

[1] Guang'anmen Hospital, China Academy of Chinese Medical Sciences, Beijing, China, [2] Xiyuan Hospital, China Academy of Chinese Medical Sciences, Beijing, China, [3] Beijing University of Chinese Medicine, Beijing, China

OPEN ACCESS

Edited by:
Youhua Xu,
Macau University of Science and Technology, Macau

Reviewed by:
Bin Geng,
Chinese Academy of Medical Sciences, China
Yanfei Liu,
Beijing University of Chinese Medicine, China

***Correspondence:**
Yanwei Xing
xingyanwei12345@163.com
Longtao Liu
liulongtao1976@126.com

[†] These authors have contributed equally to this work

Specialty section:
This article was submitted to Ethnopharmacology, a section of the journal Frontiers in Pharmacology

Received: 30 October 2019
Accepted: 18 February 2020
Published: 13 March 2020

Citation:
Wu M, Yang S, Wang S, Cao Y, Zhao R, Li X, Xing Y and Liu L (2020) Effect of Berberine on Atherosclerosis and Gut Microbiota Modulation and Their Correlation in High-Fat Diet-Fed ApoE−/− Mice. Front. Pharmacol. 11:223. doi: 10.3389/fphar.2020.00223

Atherosclerosis and its associated cardiovascular diseases (CVDs) are serious threats to human health and have been reported to be associated with the gut microbiota. Recently, the role of berberine (BBR) in atherosclerosis and gut microbiota has begun to be appreciated. The purposes of this study were to observe the effects of high or low doses of BBR on atherosclerosis and gut microbiota modulation, and to explore their correlation in ApoE$^{-/-}$ mice fed a high-fat diet. A significant decrease in atherosclerotic lesions was observed after treatment with BBR, with the effect of the high dose being more obvious. Both BBR treatments significantly reduced total cholesterol, APOB100, and very low-density lipoprotein cholesterol levels but levels of high/low-density lipoprotein cholesterol and lipoprotein (a) were only reduced by high-dose BBR. Decreased pro-inflammatory cytokines tumor necrosis factor-alpha, interleukin (IL)-1β, IL-6 and increased anti-inflammatory IL-10 and adiponectin levels were observed in the high-dose BBR group, but no decrease in IL-6 or increase in IL-10 was evident using the low-dose of BBR. 16S rRNA sequencing showed that BBR significantly altered the community compositional structure of gut microbiota. Specifically, BBR enriched the abundance of *Roseburia*, *Blautia*, *Allobaculum*, *Alistipes*, and *Turicibacter*, and changed the abundance of *Bilophila*. These microbiota displayed good anti-inflammatory effects related to the production of short-chain fatty acids (SCFAs) and were related to glucolipid metabolism. *Alistipes* and *Roseburia* were significantly enriched in high-dose BBR group while *Blautia* and *Allobaculum* were more enriched in low-dose, and *Turicibacter* was enriched in both BBR doses. Metagenomic analysis further showed an elevated potential for lipid and glycan metabolism and synthesis of SCFAs, as well as reduced potential of TMAO production after BBR treatment. The findings demonstrate that both high and low-dose BBR can improve serum lipid and systemic inflammation levels, and alleviate atherosclerosis induced by high-fat diet in ApoE$^{-/-}$ mice. The effects are more pronounced for the high dose. This anti-atherosclerotic effect of BBR may be partly attributed to changes in composition and functions of gut microbiota which may be associated with anti-inflammatory and metabolism of glucose and lipid. Notably, gut microbiota alterations showed different sensitivity to BBR dose.

Keywords: berberine, atherosclerosis, gut microbiota, inflammation, lipid metabolism

INTRODUCTION

Atherosclerosis is the common pathological basis of many cardiovascular diseases (CVDs). Although lipid-lowering drugs, interventional therapy, and other conventional treatments have been widely used to reduce the threats to human health, atherosclerosis and its associated CVDs are still the leading cause of death worldwide (Anderson et al., 1991; Vilahur et al., 2014). Atherosclerosis is accompanied by dyslipidemias, including elevated levels of low-density lipoprotein cholesterol (LDL-C), total cholesterol (TC), triglyceride (TG), etc. (Ju et al., 2018). Statins are the first-line pharmacotherapy for dyslipidemias and effectively control lipid levels and reduce major adverse cardiovascular events (MACE) (Catapano et al., 2016; Kobiyama and Ley, 2018). However, statins have been reported to be correlated with various adverse events related to myopathy, renal disease, hepatobiliary disorders, and other events (Law and Rudnicka, 2006). In addition, atherosclerosis is considered to be a chronic inflammatory disease of the large and medium arteries (Ross, 1999; Libby, 2002; Hansson, 2005), with changes in pro-inflammatory cytokines such as tumor necrosis factor-alpha (TNF-α),interleukin (IL)-6, and IL-1β, and anti-inflammatory cytokines including IL-10 (Tedgui and Mallat, 2006). The role of these cytokines in the development, progression, and complications of atherosclerosis has been reviewed (Tedgui and Mallat, 2006).

Studies in the past decade have shown that the gut microbiota is associated with certain human diseases, including obesity (Boulange et al., 2016), type 2 diabetes (Qin et al., 2012), hypercholesterolemia (Martinez et al., 2009) and CVDs (Tang et al., 2017), all of which are associated with atherosclerosis (Jonsson and Backhed, 2017). The role of the gut microbiota in atherosclerosis has begun to be appreciated in recent years, mainly including the regulation of inflammation and immunity, and cholesterol and lipid metabolism by gut microbiota and its metabolites (Jonsson and Backhed, 2017; Ma and Li, 2018). These findings have highlighted the great potential preventative and therapeutic benefits for atherosclerosis that might be realized by targeting the gut microbiome.

Berberine (BBR) is an isoquinoline alkaloid that can be isolated from various medicinal plants, such as *Coptis chinensis* Franch and *Cortex phellodendri*. BBR has various biological functions including anti-inflammatory activity, improvement of cholesterol levels and lipid metabolism, and prevention of metabolic diseases. These functions are also very important in anti-atherosclerosis effect. Nutraceuticals containing BBR can significantly reduce plasma LDL-C levels of elderly statin-intolerant hypercholesterolemic patients (Marazzi et al., 2011). Another study showed that when it plus low-dose statins and/or ezetimibe, most coronary artery disease (CHD) patients who were high-dose statin intolerant could achieve target LDL-C levels within 3 to 6 months (Marazzi et al., 2019).Of note, the therapeutic effects of BBR on these inflammatory and metabolic diseases, such as emergent mild diarrhea (Yue et al., 2019), ulcerative colitis (Cui et al., 2018), obesity (Xie et al., 2011; Zhang et al., 2015), hyperlipidemia (Wang et al., 2017) and diabetes (Zhang et al., 2012), appeared to be related to the regulation of the gut microbiota.

Previous studies have indicated that the anti-atherosclerotic effect of BBR may be associated with changes in the gut microbiota, specifically the increased abundance of *Akkermansia*, altered abundance of Firmicutes and Verrucomicrobia, and decreased serum trimethylamine *N*-oxide (TMAO) levels (Zhu et al., 2018; Shi et al., 2018). However, the specific linking of the role of BBR in gut microbiota with atherosclerosis and the potential mechanism are still unknown. Therefore, we investigated the correlation of the effect of BBR (high and low doses) on gut microbiota with the alleviation of atherosclerosis, including improvements in plaque area, serum lipid levels, and systemic inflammation. The results of 16S rRNA sequencing and metagenomic analysis showed that the anti-atherosclerotic effect of high and low-dose BBR may be partly attributed to the changes in composition and functions of the gut microbiota, which may be related to anti-inflammatory and the metabolism of glucose and lipid.

MATERIALS AND METHODS

Animal Model

All animal experimental procedures conformed to the ARRIVE guidelines, the United States National Institutes of Health Laboratory Animals Care and Use guidelines, and the Peking University Animal Investigation Committee guidelines. Six-week-old male ApoE$^{-/-}$ mice and C57BL/6J mice were purchased from the Jackson Laboratory (Bar Harbor, ME, United States) and were raised at the animal laboratory center of Peking University. The mice were housed in a specific pathogen-free environment with a room temperature at 22–24°C, relative humidity of 50%, 12 h light/dark cycle, and freely acquirable food and water. The ApoE$^{-/-}$ mice were fed with HFD containing 21% saturated fat and 0.15% cholesterol (Beijing Keao Xieli Feed Co., Ltd., Beijing, China) for 13 weeks. C57BL/6J mice (n = 12) were fed a normal-chow diet as the Control group. Mice fed with HFD were randomly divided into three groups (n = 12 in each group). The Model group was treated with 0.9% sterile saline by gavage once daily. The High group was given 100 mg/kg body weight BBR hydrochloride (97% purity, Xi'an Platt Biological Engineering Co., Ltd., Xi'an, China) by gavage once daily. The Low group was given 50 mg/kg body weight BBR by gavage once daily. Berberine were administrated for 13 weeks. C57BL/6J mice were administered with 0.9% sterile saline by gavage once daily. The experiment lasted 26 weeks.

Plaque Lesion Analysis

Heart tissues containing the aortic arch were excised from the proximal aortic root to the iliac artery branch and placed in a 4% paraformaldehyde environment for 6 h. The atherosclerotic lesion area of aorta was evaluated by *en face* Oil red O staining as previously described (Shi et al., 2018). Measurement of the lesion size was based on hematoxylin and eosin staining of sections of paraffin embedded aortic root. The area and size of the lesion were analyzed by a blind observer using Image J software.

Measurement of Serum Lipid Profiles

Blood samples were taken from the retro-orbital plexus after overnight fasting and centrifuged, and the serum was immediately stored at −80°C. Measurements of the levels of TC, TG, LDL-C, high density lipoprotein cholesterol (HDL-C), very LDL-C (VLDL-C), lipoprotein (a) [Lp (a)], Apolipoprotein B100 (ApoB100) and Apolipoprotein A-1 (APOA-1) were made using enzymatic methods in a model AD2700 automated biochemical analyzer (Olympus, Tokyo, Japan).

Measurement of Inflammatory Cytokines

The levels of serum inflammatory cytokines, including TNF-α, IL-1β, IL-6, IL-10, and adiponectin (ADPN), were measured using ELISA kits (Abcam, Cambridge, United Kingdom) according to the manufacturer's instructions. The level of high-sensitivity C-reactive protein (Hs-CRP) was measured by a nephelometry immunoassay.

Fecal DNA Extraction and PCR Amplification

Total genomic DNA was extracted from fecal samples using Omega Stool DNA Kit (Omega Bio-Tek, Norcross, GA, United States) following the manufacturer's instructions. The extracted fecal DNA was used as template. Amplification of the V3-V4 hypervariable regions of 16S rRNA gene was performed with the forward primer 338F(5′-ACTCCTACGGGAGGCAGCAG-3′) and reverse primer 806R(5′-GGACTACNNGGG TATCTAAT-3′). The PCR reaction system (total 25 μL) included 12.5 μL KAPA 2G Robust HotStart Ready Mix (Kapa Biosystems, Wilmington, MA, United States), 1 μL forward and 1 μL reverse primers (5 μM), 5 μL DNA template (30 ng), and 5.5 μL double-distilled water. The amplification procedure involved an initial denaturation at 95°C for 5 min, 28 cycles of denaturation at 95°C for 45 s, 50 s annealing at 55°C, 45 s elongation at 72°C, final extension at 72°C for 10 min, and storage at 4°C. PCR products were detected by 1% agarose gel electrophoresis to determine the size of the amplified target band and purified using Agencourt AMPure XP kit (Beckman Coulter, Brea, CA, United States). The library quality was assessed on the Qubit Fluorometer (Life Technologies, Carlsbad, CA, United States) and the Bioanalyzer 2100 system (Agilent, Santa Clara, CA, United States). Sequencing was performed on Illumina Miseq PE300 (Illumina Inc., San Diego, CA, United States) at Allwegene Technology Co., Ltd. (Beijing, China). All raw sequences have been submitted to the Sequences Read Archive database at the NCBI under accession number SRP226688.

High-Throughput Sequencing and Bioinformatics Analysis

USEARCH (Edgar, 2010), QIIME v.1.9.1 (Caporaso et al., 2010) and VSEARCH (Rognes et al., 2016) software were used to process the 16S rRNA gene sequence. Paired-end Illumina reads were quality controlled by FastQC v.0.11.5 (Andrews, 2010), and USEARCH was used to join the paired-end reads and rename. Removal of barcodes and primers, and quality filter were performed and non-redundancy reads were removed. All 16S rRNA chimeric sequences were detected and removed using the UCHIME algorithm against the RDP Gold database (Edgar, 2013). The non-chimeric sequences were sorted by abundance, and clustered into operational taxonomic units (OTUs) using the UNOISE algorithm (100% similarity threshold) with low abundant sequences removed (eight sequences). The OTU table was produced using VSEARCH software and the representative sequence of each OTU was classified by RDP classifier algorithm against the SILVA128 database with a confidence threshold of 70%.

Alpha (α) diversity analysis, including the Shannon index and Chao1 index, were carried out using the vegan (Oksanen et al., 2007) package in R. The beta (β) diversity was evaluated by Principal Coordinate Analysis (PCoA) based on the Bray Curtis distance algorithm. The LEfSe algorithm was used to identify microbes that differed significantly among groups at different taxonomy levels, with a linear discriminant analysis (LDA) score threshold of 4. The Statistical Analysis of Metagenomic Profiles (STAMP) software was used to analyze significant taxa between different groups using Welch's *t*-test with 0.95 confidence interval permutations (Parks et al., 2014). Differentially abundant OTUs were detected using the EdgeR package and depicted as volcano plots. Representative sequences from most abundant OTUs (relative abundance > 0.002) were selected to make a maximum likelihood phylogenetic tree (ML tree) using IQ-Tree software (Nguyen et al., 2015) with the following parameters: model gtr, 5000 Ultrafast bootstrap and 5000 SH-like approximate likelihood ratio test. Then, the tree was visualized by iTOL web software (Letunic and Bork, 2019) with annotations of relative abundance of groups[1]. Potential correlation between gut microbiota and serum levels of lipids and inflammatory cytokines was evaluated based on the Spearman rank correlation. Analysis and plotting were done using the vegan package.

Library Construction and Metagenomic Sequencing

The qualified DNA extract was broken to an average fragment of 300 bp size approximately with a Covaris S220 (Covaris, Inc., MS, United States) for paired-end library construction through NEBNext Ultra II DNA Library Prep Kit (NEB, Beijing, China). Paired-end sequencing was conducted on Illumina HiSeq4000 (Illumina Inc., San Diego, CA, United States) utilizing HiSeq 4000 Reagent Kits v2 under the manufacturer's instructions.

Sequence Quality Control and Genome Assembly

SeqPrep[2] was used to separate the adapter sequences from the 3′ and 5′ end of paired-end reads. Low-quality reads with insufficient length or quality value were eliminated with Sickle[3]. Reads were aligned to the host DNA sequences using the BWA[4], which removed contaminated reads with high alignment

[1]http://itol.embl.de

[2]https://github.com/jstjohn/SeqPrep

[3]https://github.com/najoshi/sickle

[4]http://bio-bwa.sourceforge.net

similarity. MEGAHIT (Li et al., 2015) was used to assemble the metagenomics data, and contigs which were over 300 bp in length were used as the final assembled result.

Gene Prediction, Taxonomy, and Functional Annotation

MetaGene (Noguchi et al., 2006) was employed on predicting open reading frames (ORFs) of the assembled contigs. Predicted ORFs which were over 100 bp in length were translated into amino acid sequences according to the translation table of the National Center for Biotechnology Information (NCBI).

All predicted genes were clustered using the CD-HIT (Fu et al., 2012) (parameters: 95% identity, 90% coverage). The representative sequences were selected from the longest sequences in each cluster to construct the non-redundant gene catalog. SOAPaligner (Li et al., 2008) was used to map the reads after quality control to the non-redundant gene catalog with 95% identity, and the gene abundance in the corresponding samples was evaluated.

Non-redundant gene catalog representative sequences were aligned to the NCBI NR database (truncating e-value to $1e^{-5}$) through BLASTP (Version 2.2.28 +) (Altschul et al., 1997) and further obtained taxonomic annotation. BLASTP against the Kyoto Encyclopedia of Genes and Genomes (KEGG) database was performed to determine the KEGG annotation. KOBAS 2.0 was used for functional annotation based on the comparison results.

Statistical Analyses

Data are expressed as mean ± SEM. Part of the 16S rRNA analysis was carried out in R software. In addition, differential levels of atherosclerotic plaques, lipids, inflammatory cytokines, and the abundance of potential gut biomarkers at the genus level were tested using one-way analysis of variance (ANOVA), followed by the Sidak multiple comparisons test. The Kruskal-Wallis rank sum test was used to test differential abundance of functional genus and KEGG pathways. A p-value < 0.05 was considered statistically significant. GraphPad Prism 8.0 (GraphPad, La Jolla, CA, United States) was used for the statistical analysis.

RESULTS

BBR Attenuates HFD-Induced Atherosclerosis

Oil Red O and H&E staining showed that the atherosclerotic plaques and lesions in the Model group were higher than those in the Control group (**Figures 1A,B**). However, significant reductions in atherosclerotic lesions after BBR treatment were observed in both the High and Low groups. Quantitative analysis also showed that atherosclerotic plaque area and lesion size decreased significantly in both the High and Low groups compared with the Model group (both $p < 0.001$). The decrease was more significant in the High group compared to the Low group ($p < 0.05$ for atherosclerotic plaque area and $p < 0.01$ for lesion size) (**Figures 1C,D**). These data suggested that HFD feeding markedly promoted the development of atherosclerosis, while the high or low dose of BBR could ameliorate HFD-induced atherosclerosis, with the effect of high dose being more pronounced.

BBR Ameliorates Serum Lipid Levels in HFD-Fed ApoE−/− Mice

Model group mice had significantly increased serum levels of TC ($p < 0.001$), TG ($p < 0.05$), HDL-C ($p < 0.001$), LDL-C ($p < 0.001$), APOB100 ($p < 0.001$), LP(a) ($p < 0.05$), and VLDL-C ($p < 0.001$), and significantly decreased APOA-1 levels ($p < 0.001$) compared with the Control group mice. In addition, both high and low doses of BBR significantly reduced TC, APOB100, and VLDL-C levels (all $p < 0.001$), with the decrease of TC ($p < 0.001$) and APOB100 ($p < 0.05$) being significantly different between the High and Low groups. TG ($p < 0.05$), HDL-C ($p < 0.001$), LDL-C ($p < 0.01$), and LP(a) ($p < 0.05$) were only significantly reduced in the High group compared with the Model group. However, there was no significant difference in serum APOA-1 levels after treatment with high or low doses of BBR ($p > 0.05$) (**Figure 2**).

BBR Improves Systemic Inflammation

Atherosclerosis is an inflammatory disease and inflammatory cytokines play an important role in the process of atherosclerosis. Here, we found that compared with the Control group mice, serum levels of TNF-α, IL-1β, IL-6 were significantly increased, and IL-10 and ADPN levels were significantly decreased in HFD-induced atherosclerosis mice (Model group; all $p < 0.001$). These changes could be reversed by BBR treatment. High dose BBR significantly reduced the levels of TNF-α, IL-1β, and IL-6, and significantly increased levels of IL-10 and ADPN (all $p < 0.001$). However, in the Low group, only TNF-α and IL-1β levels were decreased and ADPN levels were increased (all $p < 0.001$), while the decrease in IL-6 and increase in IL-10 levels were not significant ($p > 0.05$). Moreover, the levels of these inflammatory cytokines were significantly different between the High and Low groups ($p < 0.05$ or $p < 0.001$). Serum Hs-CRP level was higher in the Model group than in the Control group ($p < 0.05$), while there was no significant difference between the other groups ($p > 0.05$) (**Figure 3**).

Effect of BBR on Composition of Gut Microbiota

To determine the effects of BBR on gut microbiota composition, the Illumina Miseq PE300 high-throughput sequencing platform was used to conduct 16S rRNA amplicon paired-end sequencing. After sequence quality control and denoising, a total of 1,027,879 high-quality sequences were obtained from 30 samples. After removal of singleton (> 8) and non-bacteria sequences (such as mitochondria), 1085 OTUs were obtained with an average of 25,801 sequences per sample (range: 21,577-46,467), accounting for 75.3% of the total sequences.

The OTU table was normalized to the minimum number of reads (21,577) per sample and then diversity comparison

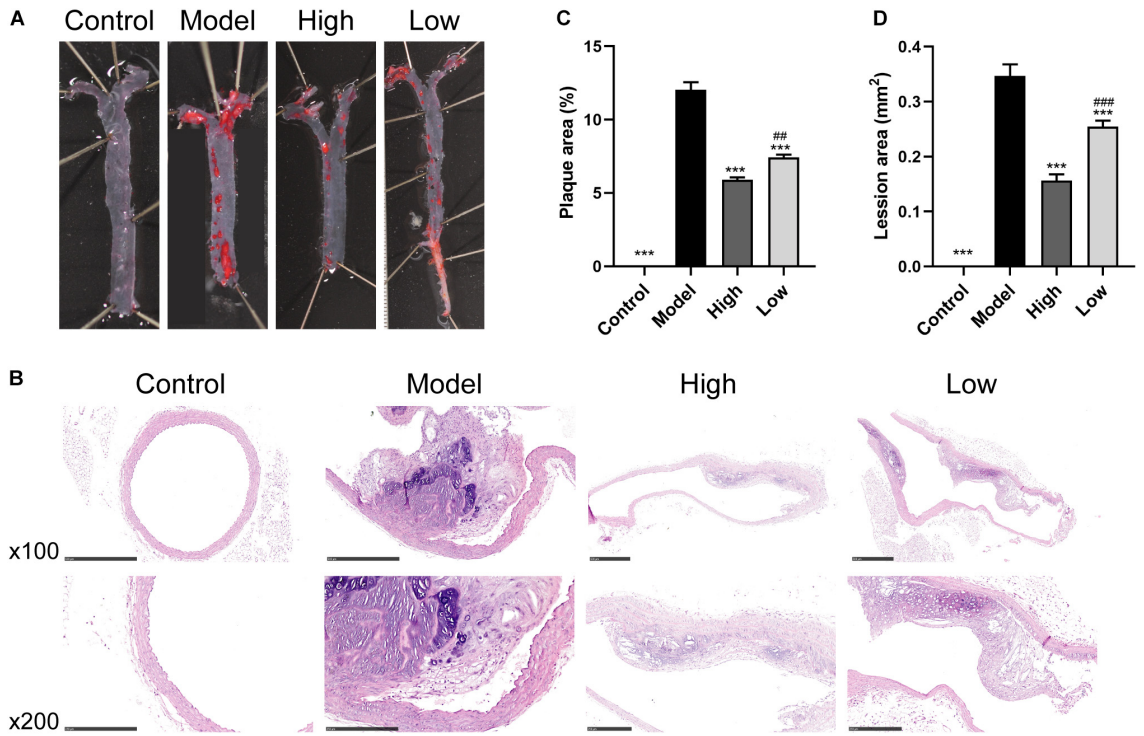

FIGURE 1 | Berberine attenuates HFD-induced atherosclerosis. **(A)** Representative images of *en face* Oil Red O staining of aorta. **(B)** H&E staining of aortic root. **(C** and **D)** Quantitative analysis of plaque area in aorta and lesion size in the aortic root (n = 6 per group). Data are expressed as mean ± SEM. Differences were assessed by one-way ANOVA. *** $p < 0.001$, vs Model; ## $p < 0.01$, ### $p < 0.001$, High vs Low.

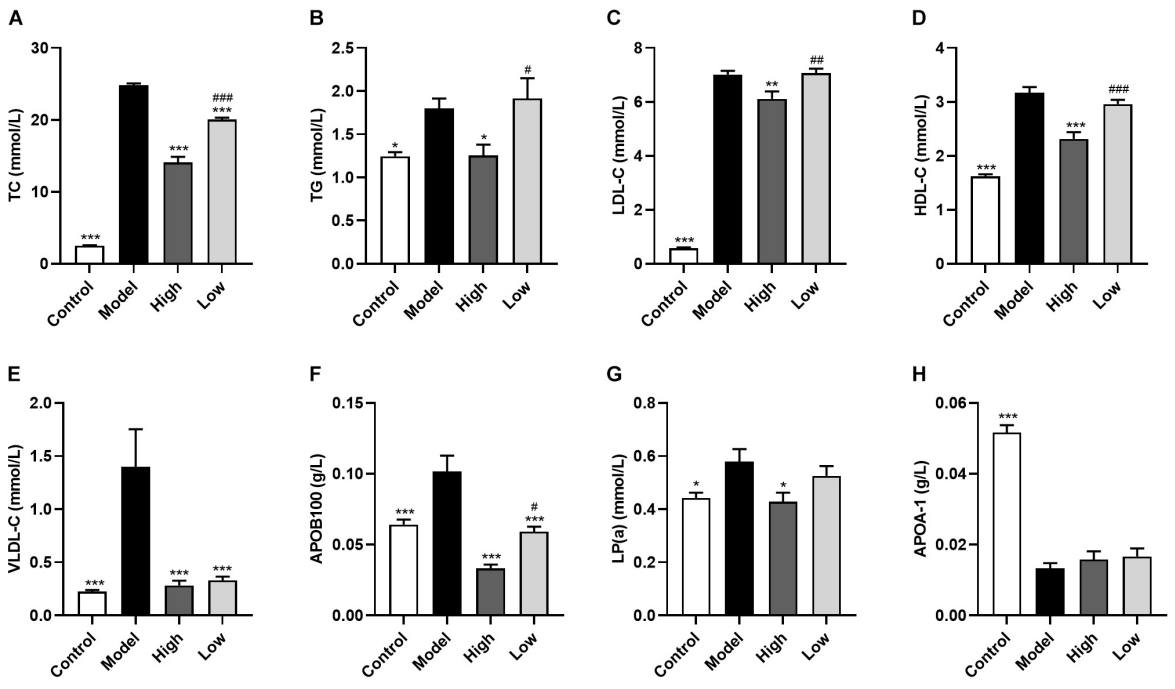

FIGURE 2 | Berberine ameliorates serum lipid levels in HFD-fed ApoE$^{-/-}$ mice. **(A)** Total cholesterol, **(B)** triglyceride, **(C)** low-density lipoprotein cholesterol, **(D)** high density lipoprotein cholesterol, **(E)** very low-density lipoprotein cholesterol, **(F)** lipoprotein (a), **(G)** Apolipoprotein B100, and **(H)** Apolipoprotein A-1. Data are expressed as mean ± SEM (n = 12). Differences among the groups were assessed by one-way ANOVA. * $p < 0.05$, ** $p < 0.01$, *** $p < 0.001$, vs Model; # $p < 0.05$, ## $p < 0.01$, ### $p < 0.01$, High vs Low.

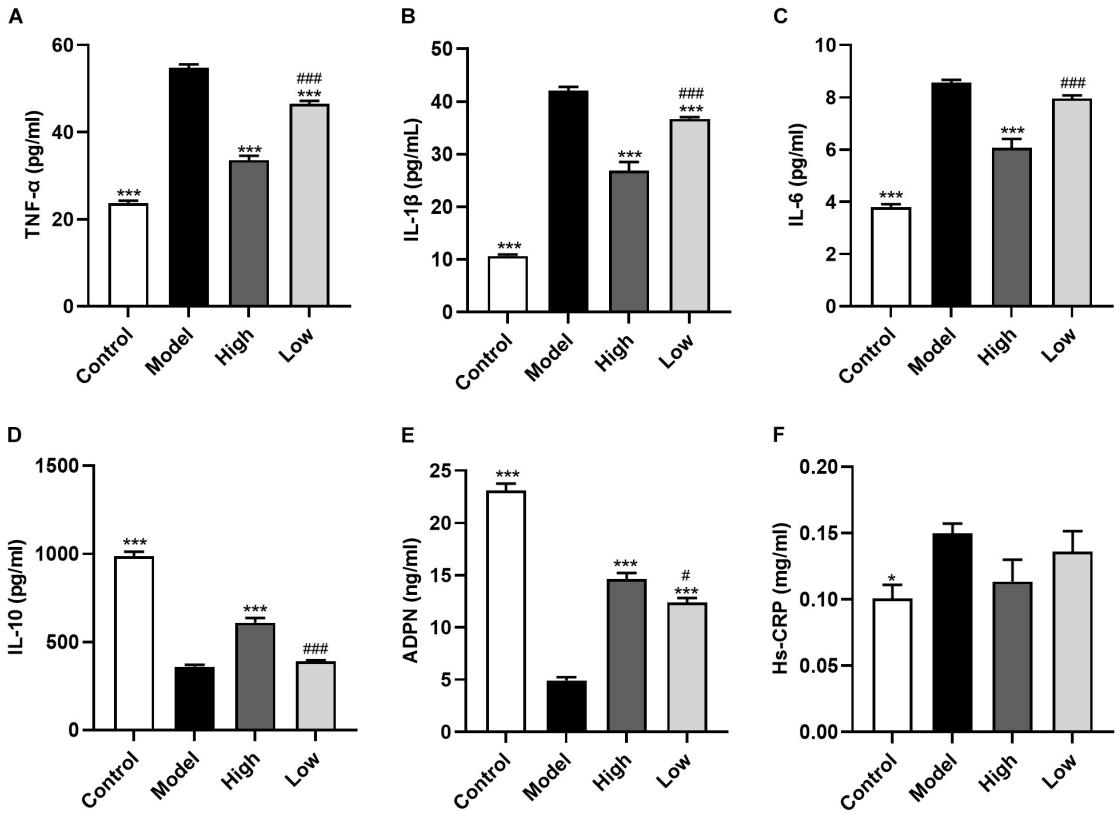

FIGURE 3 | Berberine improves systemic inflammation. **(A-F)** Serum levels of TNF-α, IL-1β, IL-6, Hs-CRP, IL-10, and ADPN. Data are expressed as mean ± SEM (n = 12). Differences among the groups were assessed by one-way ANOVA. * $p < 0.05$, *** $p < 0.001$, vs Model; # $p < 0.05$, ### $p < 0.001$, High vs Low.

was performed. Alpha diversity analysis revealed no significant difference in gut microbiota diversity between each group based on Chao 1 and Shannon indices ($p > 0.05$) (**Figures 4A,B**). PCoA based on Bray Curtis distance was used to visualize the dissimilarity in the compositions of the bacterial communities. The community compositional structure differed in the four groups, among which the High and Model groups and the Low and Model groups were significantly different ($p < 0.001$) (**Figure 4C**). A BBR dose-related difference was observed on PC2, in which the High group clustered separately from the Low group, and this explained 14.57% of the total variation in microbial composition. Mice treated with high or low doses of BBR showed similar microbial characteristics on PC1, which explained 22.05% of the total variation (**Figure 4C**).

Next, we investigated the differences of gut microbiota at different taxonomic levels. The compositions of gut microbiota at the phylum and genus levels in each group are shown in **Figures 4D,E**. At the phylum level, Firmicutes (75.4%) and Bacteroidetes (15.1%) were the two most dominant phyla, followed by Proteobacteria (3.3%) and Actinobacteria (2.5%) (**Figure 4D**). However, the abundance of these major phyla did not appear to differ significantly between the groups. One-way ANOVA analysis showed that only Proteobacteria and Actinobacteria had significant differences in abundance between the Control group and the High or Low group ($p < 0.05$), with decreased Proteobacteria abundance and increased Actinobacteria abundance after BBR treatment (**Figures 4F,G**).

We extracted all the representative sequences from OTUs with relative abundant > 0.2%. In total, 116 bacterial OTUs were selected and all the representative sequences were used to make an ML tree (**Supplementary Figure S1**). There were 116 OTUs annotated at the genus level, with color ranges identifying the phylum to which the OTUs belonged. These OTUs mainly distributed in Firmicutes and Bacteroidetes phylum, and *Lachnospiraceae_NK4A136_group* and unassigned genus. Heatmap was used to annotate the relative abundance of OTUs, and the OTUs with higher abundance were mainly distributed in *Allobaculum*, *Bacillus*, *Lachnospiraceae_NK4A136_group*, *Blautia*, etc. The outermost layer was added with circle annotation at the family level.

At the genus level, LEfSe analysis showed that *Turicibacter* and *Alistipes* were enriched in the High group, *Allobaculum* and *Blautia* were enriched in the Low group, and the abundance of *Bilophila* was relatively higher in the Control group than that in other groups (**Figure 5A**). Moreover, STAMP analysis revealed significant differences in *Roseburia* between the groups. Further analysis of the relative abundance of microbes that differed among groups revealed that the abundance of *Turicibacter* was higher, and *Bilophila* and *Blautia* were lower in the Model group than that in the Control group, but these differences

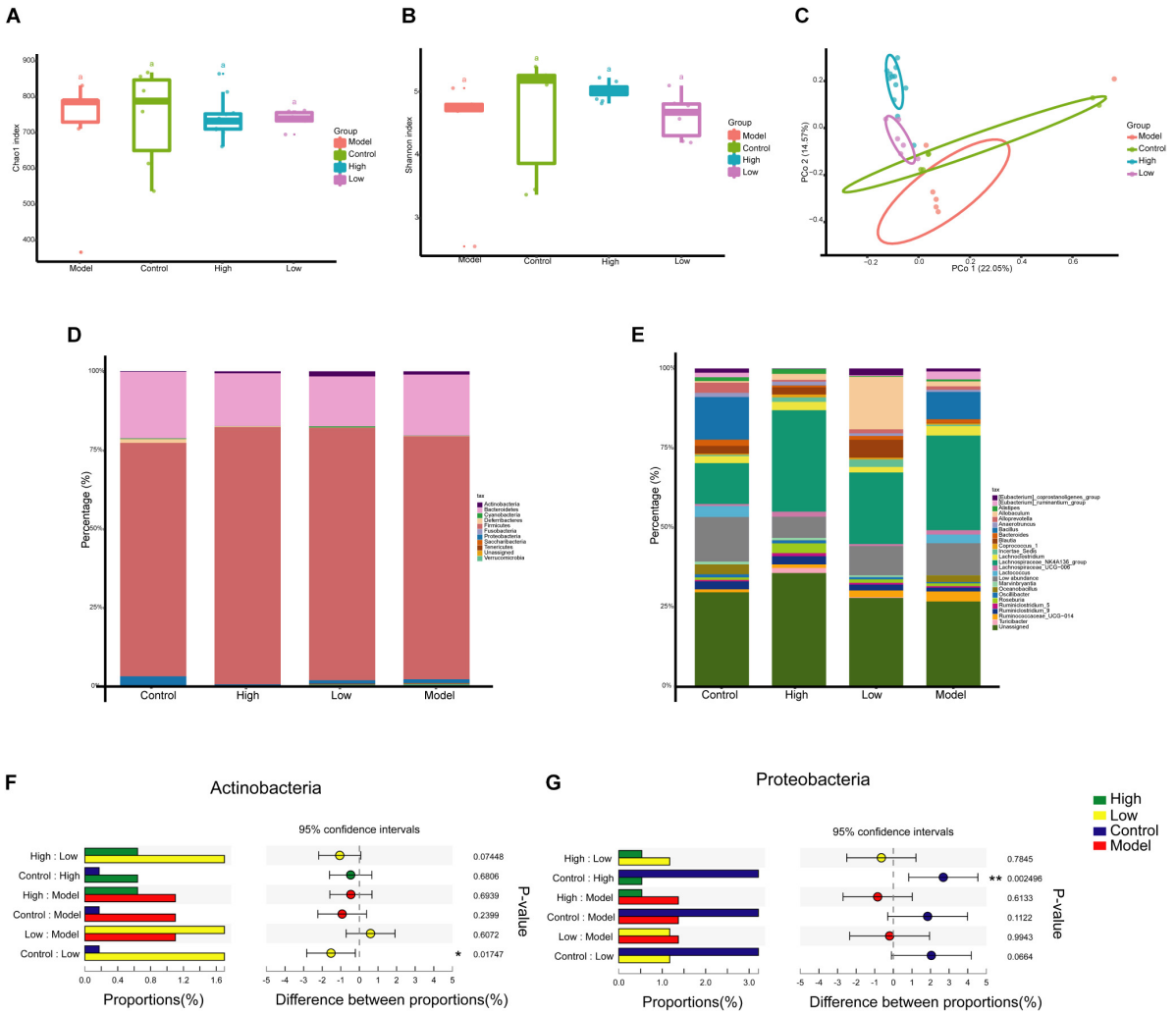

FIGURE 4 | Berberine significantly alters the composition of gut microbiota in HFD-induced atherosclerosis mice. **(A** and **B)** Diversity of the gut microbiome assessed by Chao1 and Shannon indices among the four groups. **(C)** Principal Coordinate Analysis (PCoA) based on the Bray Curtis distance algorithm. **(D)** Taxonomic composition of each group at the phylum level. **(E)** Taxonomic composition at the genus level. **(F** and **G)** Relative abundance of Proteobacteria and Actinobacteria in the one-way ANOVA bar plot on the phylum level. * $p < 0.05$, ** $p < 0.01$.

were not significant ($p > 0.05$). Both high and low doses of BBR increased the abundance of *Turicibacter*, and it was more obvious and significant at the high dose ($p < 0.05$) (**Figure 5B**). The abundance of *Alistipes* and *Roseburia* was only significantly enriched in the High group ($p < 0.05$ and < 0.01, respectively; **Figures 5C,D**). Of note, compared with the Model group, the abundance of both *Allobaculum* and *Blautia* was significantly increased when treated with low-dose BBR (both $p < 0.05$), but there was no significant change after high-dose BBR treatment ($p > 0.05$) (**Figures 5E,F**). In addition, the abundance of *Bilophila* decreased in the High group ($p < 0.05$) and increased in the Low group ($p < 0.01$) compared with the Model group (**Figure 5G**). These results showed that BBR significantly altered the composition of gut microbiota in HFD-induced atherosclerosis mice, and different doses of BBR showed different influence on specific microbes.

To further analyze these differences more precisely at the OTU level, we analyzed the number of significantly enriched and depleted OTUs in each group (**Supplementary Figure S2**). Compared with the Model group, 80 OTUs were enriched in the Control group, 213 OTUs were enriched in the Low group, and 228 OTUs were enriched in the High group. The number of OTUs with a significant difference increased obviously after BBR treatment, revealing an increasing change.

Correlation Between Gut Microbiota and Lipid Profile and Inflammatory Cytokines

As BBR significantly altered the composition of the gut microbiota and improved serum lipid levels and systemic inflammation in HFD-induced atherosclerotic mice, we further analyzed the correlation between gut microbiota and serum levels of lipids and inflammatory cytokines using the Spearman

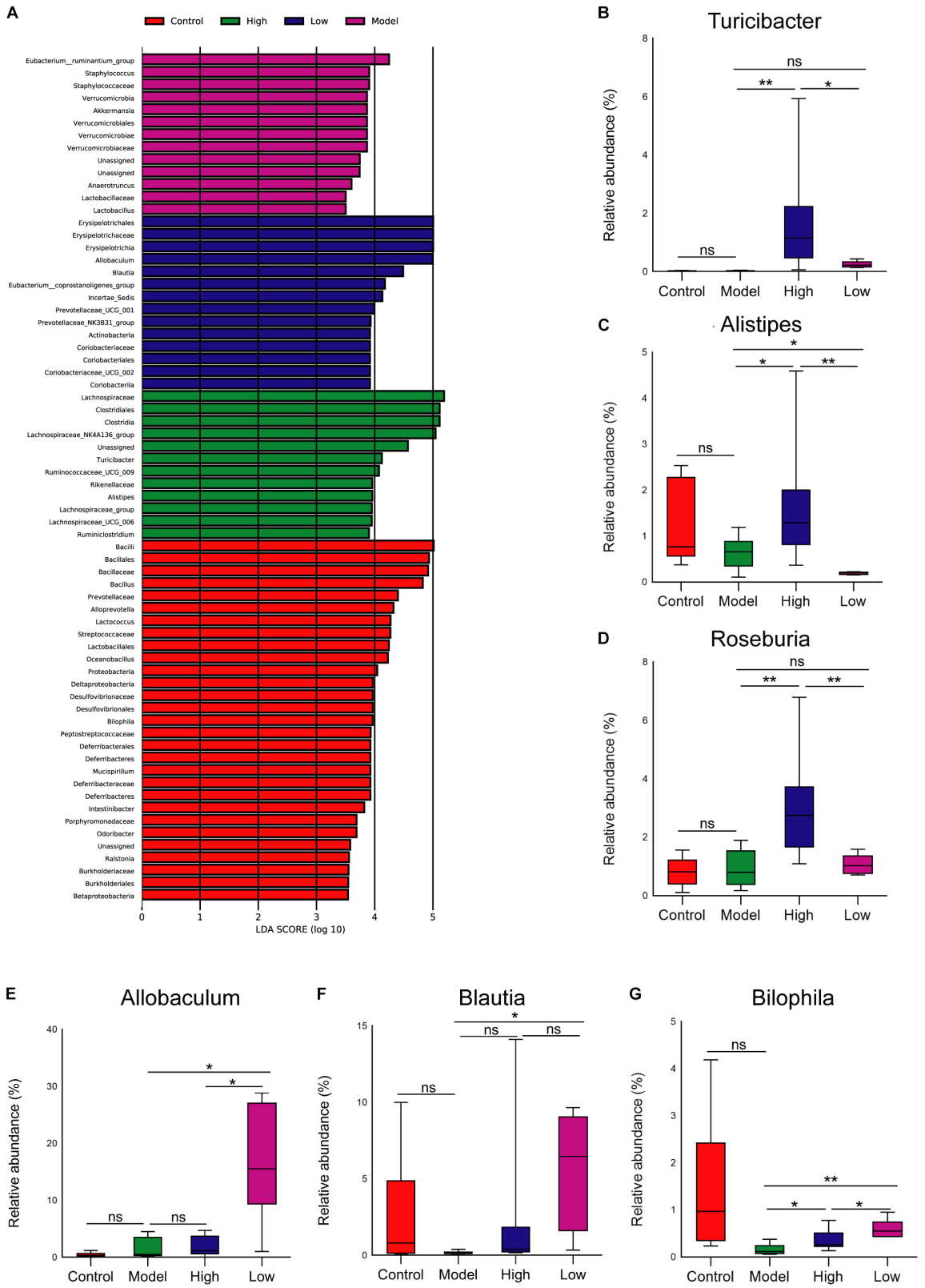

FIGURE 5 | (A) Gut microbiota comparisons among the four groups analyzed by LEfSe at different taxonomy levels, with taxa meeting LDA score threshold > 4 being listed. **(B-F)** The relative abundance of **(B)** *Turicibacter*, **(C)** *Alistipes*, **(D)** *Roseburia*, **(E)** *Allobaculum*, **(F)** *Blautia*, and **(G)** *Bilophila* at the genus level. * $p < 0.05$, ** $p < 0.01$; ns, not significant.

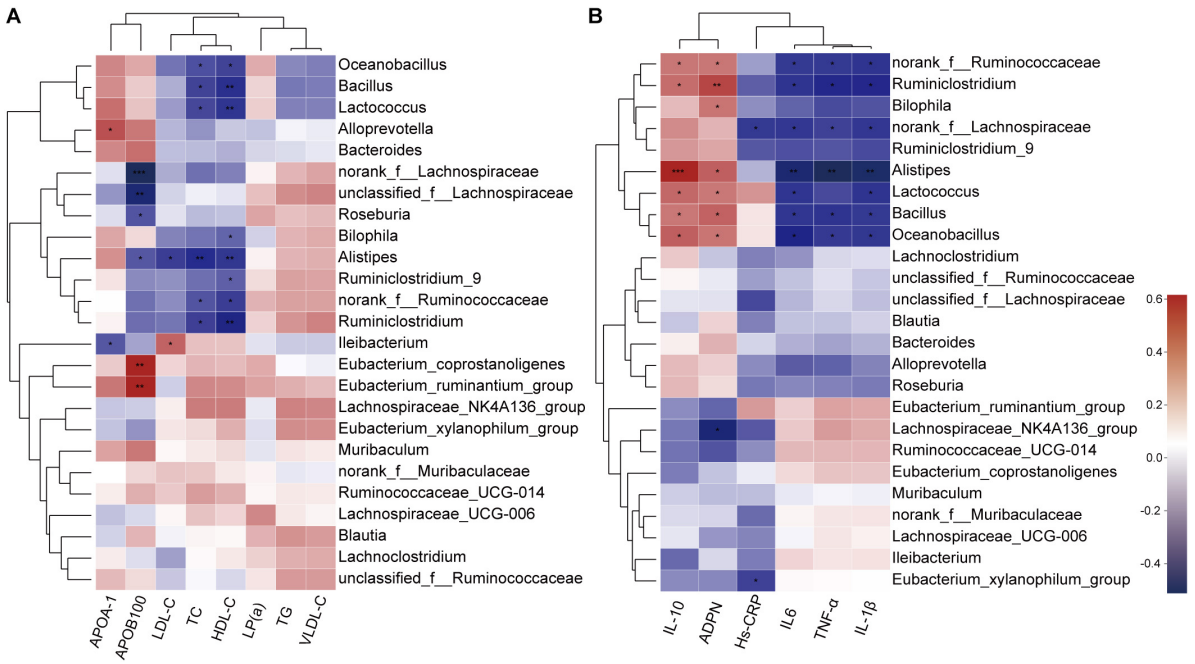

FIGURE 6 | Spearman rank correlations between gut microbiota abundance and serum levels of lipids **(A)** and inflammatory cytokines **(B)**. Red indicate being positive correlation and blue being negative. * $0.01 < p \leq 0.05$, ** $0.001 < p \leq 0.01$, *** $p \leq 0.001$.

rank correlation. We observed a significant negative correlation between serum levels of TC, HDL-C, LDL-C, APOB100 and the abundance of gut microbiota (at the genus level, in the top 25 genera), among which *Alistipes* showed the most significant negative correlation with lipid levels. Other potential genus-level biomarkers including *Roseburia* and *Bilophila* were also negatively correlated (**Figure 6A**). In addition, the anti-inflammatory cytokines IL-10 and ADPN displayed a positive correlation with gut microbiota, and pro-inflammatory cytokines IL-1β, IL-6, TNF-α and Hs-CRP were negatively correlated (**Figure 6B**). Notably, the correlation with *Alistipes* was still very significant.

Functional Alterations in Gut Microbiota Induced by BBR

To further investigate the effect of BBR on the functional changes of the gut microbiome in HFD-induced atherosclerotic mice, we determined the extent of different KEGG pathways and genes enriched in each group (three mice per group). LEfSe analysis was performed to detect the KEGG pathways with significantly different abundance between the four groups. At KEGG level 1, environmental information processing and cellular processes were significantly enriched in the model group, while the proportion of sequences related to metabolism was remarkably reduced (LDA > 2.5, $p < 0.05$, **Figure 7A**). This also supports the view that atherosclerosis is a disease that is closely associated with a variety of metabolic and cellular processes (Jie et al., 2017). At level 2, lipid metabolism, glycan biosynthesis and metabolism and carbohydrate metabolism are important components under the metabolism classification. The samples from the model group displayed reduced potential for lipid metabolism ($p < 0.01$) and glycan biosynthesis and metabolism ($p < 0.001$) compared with controls, while these were both increased after treatment with high or low dose BBR (all $p < 0.001$, **Figures 7B,C**). Differences between the high and low dose BBR groups were not significant. In addition, there was no significant difference in carbohydrate metabolism between groups ($p > 0.05$). Analysis of the relative contribution of species (at the genus level) to functional attributes found that (**Figure 7D**) *Bacteroides*, *Prevotella* and *Alistipes* were the major contributors to these functions. Consistent with the analysis results of the 16S rRNA sequencing, a lower abundance of *Alistipes* displayed a decreased functional contribution in the model group compared with the control group, and the functional contribution accordingly increased after high and low dose BBR treatment, with a higher abundance of *Alistipes*. Other potential genera that could be classified as gut biomarkers included *Roseburia*, *Allobaculum*, *Blautia,* and *Bilophila*; all of these were in the top thirty enriched genera with important contributions to lipid and glucose metabolism.

Short-chain fatty acids (SCFAs) are important metabolites of gut microbiota (den Besten et al., 2013) and have been reported to be closely related to inflammatory defense and anti-atherosclerosis (Ohira et al., 2017; Bultman, 2018). Sequences of SCFA-producing enzymes and associated enzymes identified by reference to the gut microbiota gene catalog were determined as previously described (Claesson et al., 2012; Jie et al., 2017). We screened the metagenomic data of enzymes related to the production of acetate (acetyl-CoA synthetase, K01895), propionate (propionyl-CoA: succinate-CoA transferase, K18118;

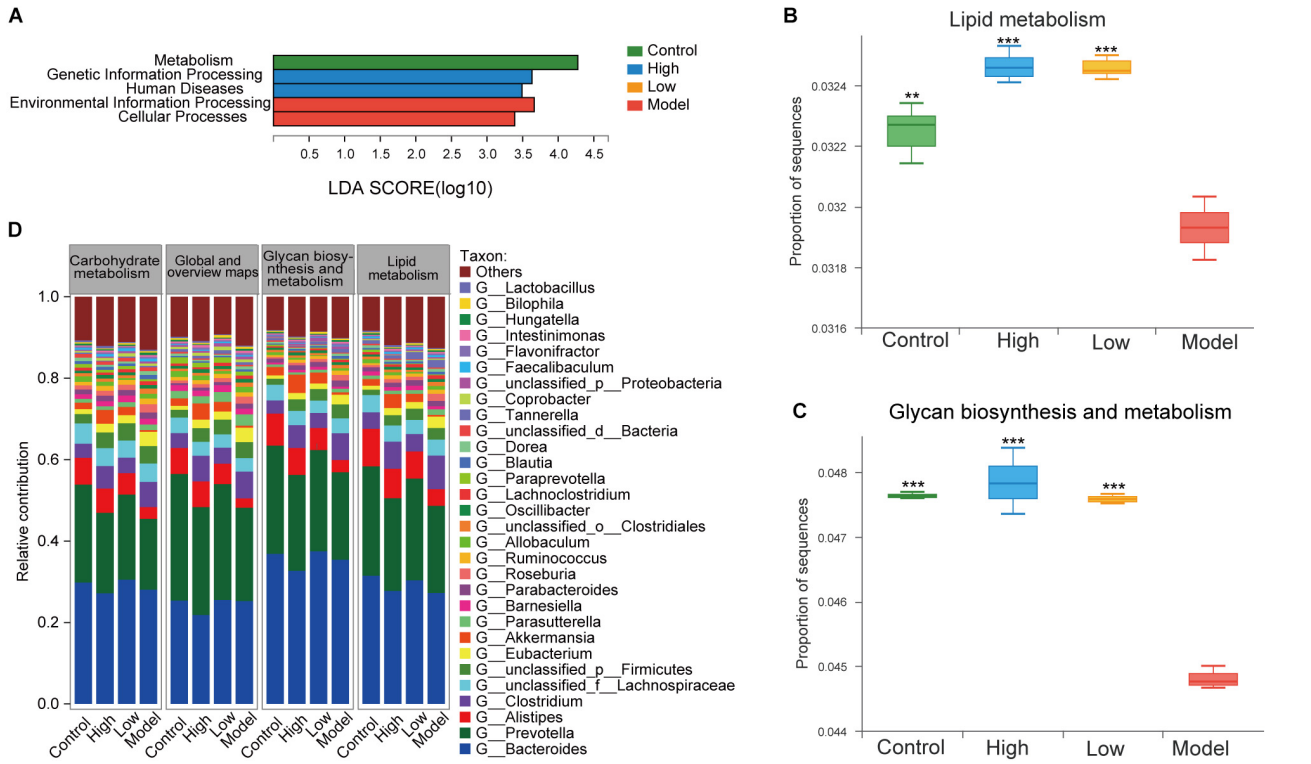

FIGURE 7 | (A) LEfSe analysis of KEGG pathways comparisons at levels 1 (LDA > 2.5, P < 0.05). **(B)** Differential abundance of lipid metabolism pathways. **(C)** Differential abundance of glycan biosynthesis and metabolism pathways. **(D)** The top 25 contributing species for functional genes related to metabolism at level 2. Differential abundance of KEGG pathways were assessed by Kruskal-Wallis rank sum test. ** $p < 0.01$, *** $p < 0.001$, vs Model.

propionate CoA transferase, K01026), and butyrate (acetyl-CoA hydrolase, K01067). Butyryl-CoA transferase was not successfully matched. We found that, compared with the model group, acetyl-CoA synthetase (K01895) was significantly enriched in the high and low dose BBR groups (all $p < 0.001$), indicating increased synthesis potential of acetate. This was more significant in the low dose BBR group than in the high ($p < 0.001$, **Figure 8A**). However, the abundance of K01026 was reduced in both the high and low dose BBR groups, which exhibited reduced potential for the synthesis of propionate compared with the model group ($p < 0.05$, **Figure 8B**). Another related gene, K18118, showed no significant difference between the groups ($p > 0.05$). Butyrate is produced through the condensation of two acetyl-CoA molecules and then reduction to butyryl-CoA, which is subsequently converted into butyrate via the classical pathway (Koh et al., 2016). Acetyl-CoA hydrolase(K01067) was observed to be more enriched in the model group compared with the high-dose ($p < 0.05$) and low-dose BBR groups ($p < 0.001$), suggesting a lower potential for butyrate synthesis in the model group (**Figure 8C**). In addition, pyruvate-formate lyase(K00656), a key enzyme in the biosynthesis of formate (Leonhartsberger et al., 2002), showed higher enrichment in the model group than in the BBR groups (all $p < 0.001$), which suggested that the gut microbiota in mice with atherosclerosis might produce more formate (**Figure 8D**). Previous studies have reported that formate was associated with hypertension and might be implicated in other atherosclerotic cardiovascular disease (ACVD)-related functions (Holmes et al., 2008; Goodrich et al., 2016). Spearman rank correlations (**Figure 8E**) showed that Alistipes, *Allobaculum, Blautia, Turicibacter,* and *Roseburia* exhibited a positive correlation with KEGG orthologues (KOs) related to SCFA production, while *Bilophila* exhibited a significant negative correlation with SCFA production ($p < 0.05$ or $p < 0.01$).

Trimethylamine N-oxide is an important pro-atherogenic metabolite produced by gut microbiota, and gut microbial enzymes were involved in the formation of its precursor trimethylamine (TMA) (Wang et al., 2011; Koeth et al., 2013). Previous studies confirmed that choline TMA lyase (K20038), betaine reductase (K21578, K21579) and *L*-carnitine CoA-transferase (K08298) are the main TMA-lyases involved in TMA production (Fennema et al., 2016; Zeisel and Warrier, 2017; Janeiro et al., 2018). Results at the KO level exhibited decreased abundance of betaine reductase (K21578, K21579) in both the high and low dose BBR groups compared to the model group, and was especially significantly in the low dose group (all $p < 0.01$, **Figures 9A,B**). The abundance of choline TMA lyase (K20038) and L-carnitine CoA-transferase (K08298) were also reduced after high or low dose BBR treatment, but were not significant ($p > 0.05$, **Figures 9C,D**).

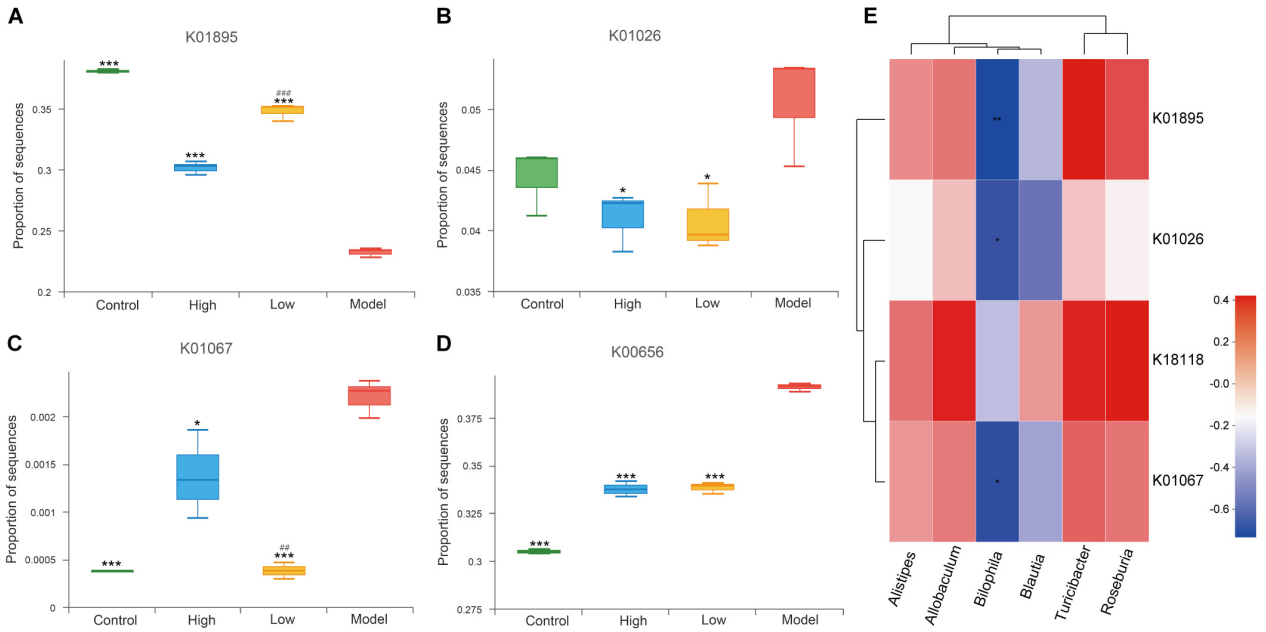

FIGURE 8 | (A–D) Differential enrichment of specific gut microbial KOs for SCFAs production among four groups. * $p < 0.05$, *** $p < 0.001$, vs Model. ### $p < 0.001$, High vs Low. **(E)** Spearman rank correlations between abundance of six biomarkers at genus level and SCFAs producing-related KOs. Red indicate being positive correlation and blue being negative.

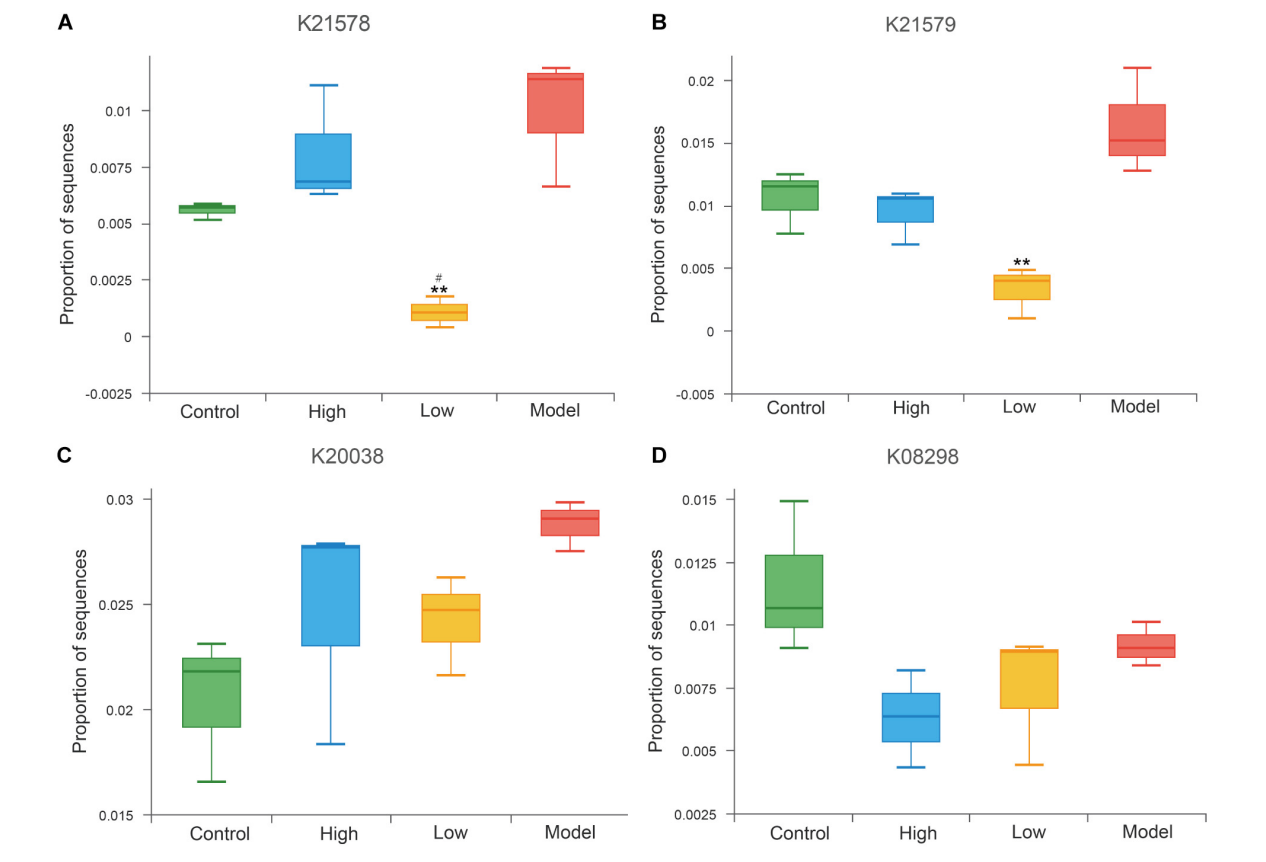

FIGURE 9 | Abundance differences in specific gut microbial KOs for TMAO production. ** $p < 0.01$, vs Model. # $p < 0.05$, High vs Low.

DISCUSSION

In this study, we investigated the effect of BBR on atherosclerosis in HFD-fed ApoE$^{-/-}$ mice. We observed the changes in serum levels of lipid and inflammatory cytokines as well as compositional structure and functions of gut microbiota after treatment with different doses of BBR, and correlated these changes with atherosclerosis. BBR treatment attenuated HFD-induced atherosclerosis, decreased atherosclerotic plaques and lesion areas, and ameliorated the level of serum lipids and inflammatory cytokines. The effects of the high dose of BBR were more significant than the effects of the low dose. 16S rRNA amplicon sequencing showed that BBR significantly altered the community compositional structure of the gut microbiota, and different doses of BBR showed different changes. Further analysis of environmental factor and metagenomic function displayed the effects of BBR on inflammation, glucose and lipid metabolism, and TMAO production in gut microbiota.

Elevated lipid levels are a major risk factor for atherosclerotic CVDs. Since Kong et al. (2004) identified BBR as a new cholesterol-lowering drug (Kong et al., 2004), the therapeutic effect of BBR on dyslipidemia has been confirmed and further explored in recent years (Kong et al., 2008; Zhang et al., 2008). Studies performed in dyslipidemia patients and hyperlipidemic mice showed that BBR significantly reduced serum TC, TG, and LDL-C levels (Kong et al., 2004; Zhang et al., 2008). In addition, these results were supported by two meta-analyses (Lan et al., 2015; Ju et al., 2018), which also reported increased HDL-C levels after BBR treatment. The current results demonstrated that both high and low doses of BBR significantly reduced the levels of TC, APOB100, and VLDL-C, while TG, HDL-C, LDL-C and LP (a) levels were reduced only in the High group. Our results do not indicate an increase in HDL-C after BBR treatment. APOA-1 has an anti-atherogenic effect, and injection of APOA-1 can reduce intracellular cholesterol levels in ApoE$^{-/-}$ mice (Pourcet and Staels, 2016; Gaddis et al., 2018). However, there was no significant increase in reduced APOA-1 levels in the atherosclerosis mice using the high or low dose of BBR in our study.

Atherosclerosis is a chronic inflammatory disease, and inflammation is constantly induced throughout the course of the disease (Libby, 2002; Hansson, 2005; Tedgui and Mallat, 2006). The anti-inflammatory effects of BBR, such as suppressing the expression of pro-inflammatory genes and improving HFD-induced systemic inflammation, have been widely reported (Jeong et al., 2009; Zhang et al., 2012). Previous studies in HFD-induced atherosclerosis mice reported that BBR administration remarkably reduced the mRNA expression of pro-inflammatory cytokines, including TNF-α, IL-1β, and IL-6, in ileal and carotid arteries (Shi et al., 2018; Zhu et al., 2018). Consistent with these results, serum levels of TNF-α, IL-1β, and IL-6 were significantly decreased by the high dose of BBR, while in the low dose group, only TNF-α and IL-1β levels were decreased. In addition, anti-inflammatory cytokines IL-10 (Han and Boisvert, 2015; Metghalchi et al., 2015) and insulin sensitizing hormone ADPN (Lin et al., 2015) have been shown to have anti-atherosclerosis effects. The production of IL-10 was increased in a mouse model of colitis induced by dextran sulfate sodium after BBR administration (Hong et al., 2012). Presently, ADPN levels increased significantly after both high and low dose BBR treatment compared to the Model group, but IL-10 levels were increased only by the high dose of BBR. Combined with previous reports, the present observations support the view that the alleviation of inflammation may be an important mechanism for the reduction of atherosclerosis in BBR-treated HFD-fed mice.

The role of the gut microbiota in atherosclerosis has begun to be studied in recent years. Multiple studies have identified a strong link between the gut microbiota and atherosclerosis (Law and Rudnicka, 2006; Catapano et al., 2016; Ju et al., 2018; Kobiyama and Ley, 2018). To explore the relationship between the anti-atherosclerosis effect of BBR and gut microbiota, 16S rRNA sequencing was used to observe the changes of gut microbiota in each group. Alpha diversity analysis did not reveal a significant decrease in fecal microbial diversity after BBR treatment, which is inconsistent with other research results (Zhang et al., 2015; Zhu et al., 2018). However, in our study beta diversity analysis showed that the community compositional structure was significantly different after treatment with the high or low dose of BBR, which do support the findings of a previous study (Shi et al., 2018). Presently, Firmicutes (75.4%) and Bacteroidetes (15.1%) are the two most dominant phylum at the phylum level, accounting for 90.5%. This was similar to the composition of human gut microbiota in prior studies, with Bacteroidetes and Firmicutes constituting more than 90% of the taxa (Qin et al., 2010; The Human Microbiome Project Consortium, 2012). In our study, the higher abundance was followed by Proteobacteria (3.3%) and Actinobacteria (2.5%), which is inconsistent with the prior finding of Proteobacteria and Verrucomicrobia (Shi et al., 2018). In addition, only decreased Proteobacteria abundance in High group and increased Actinobacteria abundance in Low group was significantly observed after BBR treatment compared with the Control group. These observations might be explained by the fact that, although the species abundance or number of the microbiota varied between individuals, the gut microbiota was semblable among individuals at higher taxonomic levels, such as the phylum level (Jonsson and Backhed, 2017).

At the genus level, LEfSe and STAMP analyses revealed significant differences between groups. Previous studies have shown that animal-based diets and HFD increases the abundance of *Alistipes* (David et al., 2014; Wan et al., 2019). Moreover, *Alistipes* has demonstrated a good anti-inflammatory effect in human and animal experiments. *Alistipes* is an obvious microbial characteristic of patients with inflammatory bowel disease (Schirmer et al., 2018) and increased *Alistipes* has been directly related to the improvement of colitis induced by dextran sulfate sodium in mice (Dziarski et al., 2016). In particular, a significant correlation was described between acetic acid production and the relative abundance of *Alistipes* (Yin et al., 2018). In addition, the genus *Roseburia* was reported to produce butyric acid and metabolize dietary plant polysaccharides, and its abundance was decreased in animal-based diets (David et al., 2014; Kim et al., 2018). In our

study, the abundance of *Alistipes* was also increased in the HFD-fed mice compared with the Control group, but not significantly, while no significant change was observed in the abundance of *Roseburia*. The high dose of BBR resulted in the significant increase in the abundance of *Alistipes* and *Roseburia*, which may be beneficial in the reduction of inflammation in BBR. Butyric acid and acetic acid are both SCFAs, and the role of SCFAs in relieving inflammation has been increasingly reported. For example, increased intake of SCFAs was proven to be beneficial in the treatment of colitis (Harig et al., 1989), and the anti-inflammation effect might be mediated by G-protein coupled receptor 43 (Maslowski et al., 2009). The SCFA-producing genera *Allobaculum* and *Blautia* were significantly enriched and systemic inflammation decreased in BBR-treated HFD-fed rats (Zhang et al., 2012). Our study supported the latter finding. However, it is worth noting that treatment with the low dose of BBR significantly increased the abundance of *Blautia* and *Allobaculum*, while the high dose of BBR did not.

Turicibacter is a genus that is associated with disorders of glucose and lipid metabolism, and is negatively correlated with random blood glucose in diabetic fatty rats (Lai et al., 2018; Zhou et al., 2019). *Turicibacter* has also been associated with intestinal butyric acid (Zhong et al., 2015), which could increase the secretion and sensitivity of insulin, and has significant anti-obesity and anti-inflammatory effects (Gao et al., 2009; Li et al., 2013; De Vadder et al., 2014). A meta-analysis showed that the decrease of *Turicibacter* is consistent with increased inflammation in obesity (Jiao et al., 2018). In addition, the decrease in *Turicibacter* has been associated with abundant dietary cholesterol and dietary fat (Everard et al., 2014; Zhong et al., 2015; Dimova et al., 2017). We found that both high and low doses of BBR enriched the abundance of *Turicibacter*, and the effect was significant and more pronounced at the high dose. This suggests that the anti-atherosclerosis effect may be related to the interference of BBR on glycolipid metabolism-related gut microbiota. Notably, the abundance of *Bilophila* decreased in HFD-fed mice, contrary to the prior finding that animal-based diets increased the abundance of *Bilophila* (David et al., 2014). *Bilophila* reportedly acts synergistically with HFD to promote higher inflammation and bile acid dysmetabolism, resulting in more serious glucose dysmetabolism and hepatic steatosis (David et al., 2014; Natividad et al., 2018). Presently, the abundance of *Bilophila* decreased in the high-dose BBR group and increased in the low-dose BBR group compared with the Model group. However, compared with normal control mice, the abundance of *Bilophila* was decreased after BBR treatment, although it was not obvious.

Environmental factor analysis helped us further determine the potential correlation between lipids, inflammatory cytokines, and the gut microbiota. In addition, metagenomic analysis based on functional changes of the gut microbiome showed that the potential for lipid metabolism and glycan biosynthesis and metabolism was elevated in atherosclerotic model mice after high or low dose BBR treatment. The analysis of species and functional contribution further highlighted the importance of these genus-level biomarkers for glucose and lipid metabolism, among which *Alistipes* contributed the most. SCFAs are known to be defensive players for inflammation and atherosclerosis (Ohira et al., 2017) and we observed an elevated potential for the synthesis of acetate and butyrate in both high and low-dose BBR groups compared to atherosclerosis model mice. Notably, the alteration of acetate was more significant in the low dose BBR group. However, the synthesis potential of propionate seemed to be decreased after BBR treatment, which was not consistent with the protective effects of propionate on hypertension, cardiovascular damage and anti-atherosclerosis (Bultman, 2018; Bartolomaeus et al., 2019). A heatmap showed that *Alistipes*, *Allobaculum*, *Blautia*, *Turicibacter* and *Roseburia* were positively correlated with SCFA production, while *Bilophila* was significantly negatively correlated. This supported the results that *Bilophila* acted synergistically with HFD to promote higher inflammation and more serious glucose dysmetabolism (David et al., 2014; Natividad et al., 2018). Consistently, the abundance of *Bilophila* decreased in the high-dose BBR group in our study. In addition, compared with the atherosclerotic mice, the abundance of TMAO-related enzymes was reduced in both the high and low dose BBR group, and betaine reductase decreased reduced more significantly in the low-dose BBR group. These results showed that different doses of BBR might have different inhibitory effects on TMAO production.

Our results suggested that high and low-dose BBR induced the alteration of abundance and function in certain gut microbiota that may be related to inflammation and glucose and lipid metabolism. These findings partially support the view that BBR may at least partly improve systemic inflammation and lipid level by regulating gut bacteria related to inflammation and glucolipid metabolism, thereby reducing HFD-induced atherosclerosis. Indeed, evidence is accumulating that gut microbiota and its metabolites, such as SCFAs, TMAO, and secondary bile acids, play a role in atherosclerosis by regulating inflammation and the metabolism of lipid, cholesterol and glucose (Barrington and Lusis, 2017; Jonsson and Backhed, 2017; Kasahara et al., 2017; Ma and Li, 2018). SCFAs have anti-atherogenic effect, in addition, it can inhibit the fat synthesis in enterocytes and adipocytes, and suppress biosynthesis of cholesterol and LDL formation in the liver, besides their anti-inflammatory effects (Chistiakov et al., 2015). The involvement of SCFAs in atherosclerosis has been reviewed (Brown and Hazen, 2018). The proatherogenic metabolite TMAO has been associated with the increased risk of atherosclerosis (Wang et al., 2011; Tang et al., 2013). Elevated TMAO levels contributed to foam cell formation and platelet hyperreactivity and inhibited reverse cholesterol transport in macrophages (Wang et al., 2011; Koeth et al., 2013; Zhu et al., 2016). Notably, previous study has shown that BBR treatment can significantly reduce serum TMAO levels (Shi et al., 2018).

Our study has some limitations. Considering the fact that sample quantity is relatively small, the persuasiveness of the results is limited. Although we explained the relationship between the regulation effect of BBR on gut microbiota and the reduction of atherosclerosis based on 16S rRNA sequencing and metagenomic analysis, further fecal bacteria transfer experiments are still needed to clarify the direct link of BBR on gut microbiota with atherosclerosis. This study was conducted in ApoE$^{-/-}$ mice fed with HFD. In the future study, we should extend to clinical

atherosclerosis patients to further well explore the relationship of effect of BBR on gut microbiota and atherosclerosis.

Nonetheless, our study increases the accumulating evidence that BBR can protect against atherosclerosis induced by HFD. Previous studies have shown that BBR could effectively reduce plasma LDL-C levels in patients with CHD and/or hypercholesterolemia who were statin intolerant (Marazzi et al., 2011, 2019). Studies performed in hyperlipidemia mice and meta-analyses also supported that BBR improved dyslipidemia (Lan et al., 2015; Ju et al., 2018). In addition, the anti-inflammatory effects of BBR, including the reduction of HFD-induced systemic inflammation and the suppression of proinflammatory gene expression, have been widely confirmed (Jeong et al., 2009; Zhang et al., 2012). However, the mechanism of these effects is still unclear due to the low BBR absorption rate. Recent studies suggested that the anti-atherosclerotic effect of BBR may be related to changes in gut microbiota, but the specific association and potential mechanism are still unknown (Shi et al., 2018; Zhu et al., 2018). The present study may provide a novel explanation. Our study ulteriorly supports the anti-atherogenic effect of BBR by targeting the gut microbiota at both the species and function levels. In some extent, this suggests the potential of BBR and certain gut microbiome as an alternative or adjuvant treatment strategy for atherosclerotic patients who are intolerant to conventional drugs (such as statins) or under an increased risk of adverse effects.

CONCLUSION

In conclusion, both high and low dose BBR can improve serum lipid and inflammation levels and alleviate atherosclerosis in a mouse model of HFD-induced atherosclerosis. This anti-atherosclerotic effect of BBR may be partly attributed to changes in composition and functions of gut microbiota which may be related to anti-inflammatory activity and the metabolism of glucose and lipid. In addition, different doses of BBR had different effects, among which the attenuation of atherosclerosis was more obvious at the high dose of BBR, but the alterations of composition and functions in gut microbiota showed different sensitivity to BBR dose.

DATA AVAILABILITY STATEMENT

The datasets generated for this study can be found in the Sequences Read Archive database at the NCBI under accession number PRJNA579048.

ETHICS STATEMENT

The animal study was reviewed and approved by the Animal Investigation Committee of Peking University.

AUTHOR CONTRIBUTIONS

MW, SY, LL and YX designed the experiment and wrote the manuscript. SW and YC aided in the design of the illustrations. RZ and XL commented on the manuscript. All authors approved the manuscript for publication.

FUNDING

The work was supported by the Be ijing Natural Science Foundation (7172185) and the National Natural Science Foundation of China (Grant Nos. 81202805, 81973689, and 81573821).

SUPPLEMENTARY MATERIAL

The Supplementary Material for this article can be found online at: https://www.frontiersin.org/articles/10.3389/fphar.2020.00223/full#supplementary-material

FIGURE S1 | Most abundant OTU members of the gut bacterial microbiome (Top 116).

FIGURE S2 | Differentially enriched and depleted OTUs between each group compared with the Model group. **(A)** Control vs Model; **(B)** Low vs Model; **(C)** High vs Model. Each point in the figure represents an individual OTU, of which the red points for significant enriched OTUs, green points for significant depleted OTUs, gray points for OTUs with no significant difference. The number labeled in the figure is the number of OTUs that significantly enriched or decreased.

REFERENCES

Altschul, S. F., Madden, T. L., Schaffer, A. A., Zhang, J., Zhang, Z., Miller, W., et al. (1997). Gapped BLAST and PSI-BLAST: a new generation of protein database search programs. *Nucleic Acids Res.* 25, 3389–3402. doi: 10.1093/nar/25.17.3389

Anderson, K. M., Odell, P. M., Wilson, P. W., and Kannel, W. B. (1991). Cardiovascular disease risk profiles. *Am. Heart J.* 121, 293–298.

Andrews, S. (2010). *FastQC: A Quality Control Tool for High Throughput Sequence Data*. Cambridge: Babraham Bioinformatics, Babraham Institute.

Barrington, W. T., and Lusis, A. J. (2017). Atherosclerosis: association between the gut microbiome and atherosclerosis. *Nat. Rev. Cardiol.* 14, 699–700. doi: 10.1038/nrcardio.2017.169

Bartolomaeus, H., Balogh, A., Yakoub, M., Homann, S., Marko, L., Hoges, S., et al. (2019). Short-chain fatty acid propionate protects from hypertensive cardiovascular damage. *Circulation* 139, 1407–1421. doi: 10.1161/circulationaha.118.036652

Boulange, C. L., Neves, A. L., Chilloux, J., Nicholson, J. K., and Dumas, M. E. (2016). Impact of the gut microbiota on inflammation, obesity, and metabolic disease. *Genome Med.* 8:42. doi: 10.1186/s13073-016-0303-2

Brown, J. M., and Hazen, S. L. (2018). Microbial modulation of cardiovascular disease. *Nat. Rev. Microbiol.* 16, 171–181. doi: 10.1038/nrmicro.2017.149

Bultman, S. J. (2018). Bacterial butyrate prevents atherosclerosis. *Nat. Microbiol.* 3, 1332–1333. doi: 10.1038/s41564-018-0299-z

Caporaso, J. G., Kuczynski, J., Stombaugh, J., Bittinger, K., Bushman, F. D., Costello, E. K., et al. (2010). QIIME allows analysis of high-throughput community sequencing data. *Nat. Methods* 7, 335–336.

Catapano, A. L., Graham, I., De Backer, G., Wiklund, O., Chapman, M. J., Drexel, H., et al. (2016). 2016 ESC/EAS guidelines for the management of dyslipidaemias. *Eur. Heart J.* 37, 2999–3058. doi: 10.1093/eurheartj/ehw272

Chistiakov, D. A., Bobryshev, Y. V., Kozarov, E., Sobenin, I. A., and Orekhov, A. N. (2015). Role of gut microbiota in the modulation of atherosclerosis-associated immune response. *Front. Microbiol.* 6:671. doi: 10.3389/fmicb.2015.00671

Claesson, M. J., Jeffery, I. B., Conde, S., Power, S. E., O'Connor, E. M., Cusack, S., et al. (2012). Gut microbiota composition correlates with diet and health in the elderly. *Nature* 488, 178–184. doi: 10.1038/nature11319

Cui, H., Cai, Y., Wang, L., Jia, B., Li, J., Zhao, S., et al. (2018). Berberine regulates Treg/Th17 balance to treat ulcerative colitis through modulating the gut microbiota in the colon. *Front. Pharmacol.* 9:571. doi: 10.3389/fphar.2018.00571

David, L. A., Maurice, C. F., Carmody, R. N., Gootenberg, D. B., Button, J. E., Wolfe, B. E., et al. (2014). Diet rapidly and reproducibly alters the human gut microbiome. *Nature* 505, 559–563. doi: 10.1038/nature12820

De Vadder, F., Kovatcheva-Datchary, P., Goncalves, D., Vinera, J., Zitoun, C., Duchampt, A., et al. (2014). Microbiota-generated metabolites promote metabolic benefits via gut-brain neural circuits. *Cell* 156, 84–96. doi: 10.1016/j.cell.2013.12.016

den Besten, G., van Eunen, K., Groen, A. K., Venema, K., Reijngoud, D. J., and Bakker, B. M. (2013). The role of short-chain fatty acids in the interplay between diet, gut microbiota, and host energy metabolism. *J. Lipid Res.* 54, 2325–2340. doi: 10.1194/jlr.R036012

Dimova, L. G., Zlatkov, N., Verkade, H. J., Uhlin, B. E., and Tietge, U. J. F. (2017). High-cholesterol diet does not alter gut microbiota composition in mice. *Nutr. Metab. (Lond)* 14:15. doi: 10.1186/s12986-017-0170-x

Dziarski, R., Park, S. Y., Kashyap, D. R., Dowd, S. E., and Gupta, D. (2016). Pglyrp-regulated gut microflora *Prevotella falsenii*, Para*bacteroides distasonis* and *Bacteroides eggerthii* enhance and *Alistipes finegoldii* Attenuates Colitis in mice. *PLoS One* 11:e0146162. doi: 10.1371/journal.pone.0146162

Edgar, R. C. (2010). Search and clustering orders of magnitude faster than BLAST. *Bioinformatics* 26, 2460–2461. doi: 10.1093/bioinformatics/btq461

Edgar, R. C. (2013). UPARSE: highly accurate OTU sequences from microbial amplicon reads. *Nat. Methods* 10, 996–998. doi: 10.1038/nmeth.2604

Everard, A., Lazarevic, V., Gaia, N., Johansson, M., Stahlman, M., Backhed, F., et al. (2014). Microbiome of prebiotic-treated mice reveals novel targets involved in host response during obesity. *ISME J.* 8, 2116–2130. doi: 10.1038/ismej.2014.45

Fennema, D., Phillips, I. R., and Shephard, E. A. (2016). Correction to "Trimethylamine and Trimethylamine N-oxide, a flavin-containing monooxygenase 3 (FMO3)-mediated host-microbiome metabolic axis implicated in health and disease". *Drug Metab. Dispos.* 44:1949. doi: 10.1124/dmd.115.070615err

Fu, L., Niu, B., Zhu, Z., Wu, S., and Li, W. (2012). CD-HIT: accelerated for clustering the next-generation sequencing data. *Bioinformatics* 28, 3150–3152. doi: 10.1093/bioinformatics/bts565

Gaddis, D. E., Padgett, L. E., Wu, R., McSkimming, C., Romines, V., Taylor, A. M., et al. (2018). Apolipoprotein AI prevents regulatory to follicular helper T cell switching during atherosclerosis. *Nat. Commun.* 9:1095. doi: 10.1038/s41467-018-03493-5

Gao, Z., Yin, J., Zhang, J., Ward, R. E., Martin, R. J., Lefevre, M., et al. (2009). Butyrate improves insulin sensitivity and increases energy expenditure in mice. *Diabetes* 58, 1509–1517. doi: 10.2337/db08-1637

Goodrich, J. K., Davenport, E. R., Beaumont, M., Jackson, M. A., Knight, R., Ober, C., et al. (2016). Genetic determinants of the gut microbiome in UK twins. *Cell Host Microbe* 19, 731–743. doi: 10.1016/j.chom.2016.04.017

Han, X., and Boisvert, W. A. (2015). Interleukin-10 protects against atherosclerosis by modulating multiple atherogenic macrophage function. *Thromb. Haemost.* 113, 505–512. doi: 10.1160/th14-06-0509

Hansson, G. K. (2005). Inflammation, atherosclerosis, and coronary artery disease. *N. Engl. J. Med.* 352, 1685–1695. doi: 10.1056/NEJMra043430

Harig, J. M., Soergel, K. H., Komorowski, R. A., and Wood, C. M. (1989). Treatment of diversion colitis with short-chain-fatty acid irrigation. *N. Engl. J. Med.* 320, 23–28. doi: 10.1056/nejm198901053200105

Holmes, E., Loo, R. L., Stamler, J., Bictash, M., Yap, I. K., Chan, Q., et al. (2008). Human metabolic phenotype diversity and its association with diet and blood pressure. *Nature* 453, 396–400. doi: 10.1038/nature06882

Hong, T., Yang, Z., Lv, C. F., and Zhang, Y. (2012). Suppressive effect of berberine on experimental dextran sulfate sodium-induced colitis. *Immunopharmacol. Immunotoxicol.* 34, 391–397. doi: 10.3109/08923973.2011.609887

Janeiro, M. H., Ramirez, M. J., Milagro, F. I., Martinez, J. A., and Solas, M. (2018). Implication of Trimethylamine N-oxide (TMAO) in disease: potential biomarker or new therapeutic target. *Nutrients* 10:e1398. doi: 10.3390/nu10101398

Jeong, H. W., Hsu, K. C., Lee, J. W., Ham, M., Huh, J. Y., Shin, H. J., et al. (2009). Berberine suppresses proinflammatory responses through AMPK activation in macrophages. *Am. J. Physiol. Endocrinol. Metab.* 296, E955–E964. doi: 10.1152/ajpendo.90599.2008

Jiao, N., Baker, S. S., Nugent, C. A., Tsompana, M., Cai, L., Wang, Y., et al. (2018). Gut microbiome may contribute to insulin resistance and systemic inflammation in obese rodents: a meta-analysis. *Physiol. Genomics* 50, 244–254. doi: 10.1152/physiolgenomics.00114.2017

Jie, Z., Xia, H., Zhong, S. L., Feng, Q., Li, S., Liang, S., et al. (2017). The gut microbiome in atherosclerotic cardiovascular disease. *Nat. Commun.* 8:845. doi: 10.1038/s41467-017-00900-1

Jonsson, A. L., and Backhed, F. (2017). Role of gut microbiota in atherosclerosis. *Nat. Rev. Cardiol.* 14, 79–87. doi: 10.1038/nrcardio.2016.183

Ju, J., Li, J., Lin, Q., and Xu, H. (2018). Efficacy and safety of berberine for dyslipidaemias: a systematic review and meta-analysis of randomized clinical trials. *Phytomedicine* 50, 25–34. doi: 10.1016/j.phymed.2018.09.212

Kasahara, K., Tanoue, T., Yamashita, T., Yodoi, K., Matsumoto, T., Emoto, T., et al. (2017). Commensal bacteria at the crossroad between cholesterol homeostasis and chronic inflammation in atherosclerosis. *J. Lipid Res.* 58, 519–528. doi: 10.1194/jlr.M072165

Kim, J. Y., Kwon, Y. M., Kim, I. S., Kim, J. A., Yu, D. Y., Adhikari, B., et al. (2018). Effects of the Brown Seaweed *Laminaria japonica* supplementation on serum concentrations of IgG, triglycerides, and cholesterol, and intestinal microbiota composition in rats. *Front. Nutr.* 5:23. doi: 10.3389/fnut.2018.00023

Kobiyama, K., and Ley, K. (2018). Atherosclerosis. *Circ. Res.* 123, 1118–1120. doi: 10.1161/circresaha.118.313816

Koeth, R. A., Wang, Z., Levison, B. S., Buffa, J. A., Org, E., Sheehy, B. T., et al. (2013). Intestinal microbiota metabolism of *L-carnitine*, a nutrient in red meat, promotes atherosclerosis. *Nat. Med.* 19, 576–585. doi: 10.1038/nm.3145

Koh, A., De Vadder, F., Kovatcheva-Datchary, P., and Backhed, F. (2016). From dietary fiber to host physiology: short-chain fatty acids as key bacterial metabolites. *Cell* 165, 1332–1345. doi: 10.1016/j.cell.2016.05.041

Kong, W., Wei, J., Abidi, P., Lin, M., Inaba, S., Li, C., et al. (2004). Berberine is a novel cholesterol-lowering drug working through a unique mechanism distinct from statins. *Nat. Med.* 10, 1344–1351. doi: 10.1038/nm1135

Kong, W. J., Wei, J., Zuo, Z. Y., Wang, Y. M., Song, D. Q., You, X. F., et al. (2008). Combination of simvastatin with berberine improves the lipid-lowering efficacy. *Metabolism* 57, 1029–1037. doi: 10.1016/j.metabol.2008.01.037

Lai, K. P., Ng, A. H., Wan, H. T., Wong, A. Y., Leung, C. C., Li, R., et al. (2018). dietary exposure to the environmental chemical, PFOS on the diversity of gut microbiota, associated with the development of metabolic syndrome. *Front. Microbiol.* 9:2552. doi: 10.3389/fmicb.2018.02552

Lan, J., Zhao, Y., Dong, F., Yan, Z., Zheng, W., Fan, J., et al. (2015). Meta-analysis of the effect and safety of berberine in the treatment of type 2 diabetes mellitus, hyperlipemia and hypertension. *J. Ethnopharmacol.* 161, 69–81. doi: 10.1016/j.jep.2014.09.049

Law, M., and Rudnicka, A. R. (2006). Statin safety: a systematic review. *Am. J. Cardiol.* 97, 52C–60C. doi: 10.1016/j.amjcard.2005.12.010

Leonhartsberger, S., Korsa, I., and Bock, A. (2002). The molecular biology of formate metabolism in enterobacteria. *J. Mol. Microbiol. Biotechnol.* 4, 269–276.

Letunic, I., and Bork, P. (2019). Interactive tree of life (iTOL) v4: recent updates and new developments. *Nucleic Acids Res.* 47, W256–W259. doi: 10.1093/nar/gkz239

Li, D., Liu, C. M., Luo, R., Sadakane, K., and Lam, T. W. (2015). MEGAHIT: an ultra-fast single-node solution for large and complex metagenomics assembly via succinct de Bruijn graph. *Bioinformatics* 31, 1674–1676. doi: 10.1093/bioinformatics/btv033

Li, H. P., Chen, X., and Li, M. Q. (2013). Butyrate alleviates metabolic impairments and protects pancreatic beta cell function in pregnant mice with obesity. *Int. J. Clin. Exp. Pathol.* 6, 1574–1584.

Li, R., Li, Y., Kristiansen, K., and Wang, J. (2008). SOAP: short oligonucleotide alignment program. *Bioinformatics* 24, 713–714. doi: 10.1093/bioinformatics/btn025

Libby, P. (2002). Inflammation in atherosclerosis. *Nature* 420, 868–874. doi: 10.1038/nature01323

Lin, Z., Pan, X., Wu, F., Ye, D., Zhang, Y., Wang, Y., et al. (2015). Fibroblast growth factor 21 prevents atherosclerosis by suppression of hepatic sterol regulatory

element-binding protein-2 and induction of adiponectin in mice. *Circulation* 131, 1861–1871. doi: 10.1161/circulationaha.115.015308

Ma, J., and Li, H. (2018). The role of gut microbiota in atherosclerosis and hypertension. *Front. Pharmacol.* 9:1082. doi: 10.3389/fphar.2018.01082

Marazzi, G., Cacciotti, L., Pelliccia, F., Iaia, L., Volterrani, M., Caminiti, G., et al. (2011). Long-term effects of nutraceuticals (berberine, red yeast rice, policosanol) in elderly hypercholesterolemic patients. *Adv. Ther.* 28, 1105–1113. doi: 10.1007/s12325-011-0082-5

Marazzi, G., Campolongo, G., Pelliccia, F., Calabro Md, P., Cacciotti, L., Vitale, C., et al. (2019). Usefulness of low-dose statin plus Ezetimibe and/or Nutraceuticals in patients with coronary artery disease intolerant to high-dose statin treatment. *Am. J. Cardiol.* 123, 233–238. doi: 10.1016/j.amjcard.2018.09.041

Martinez, I., Wallace, G., Zhang, C., Legge, R., Benson, A. K., Carr, T. P., et al. (2009). Diet-induced metabolic improvements in a hamster model of hypercholesterolemia are strongly linked to alterations of the gut microbiota. *Appl. Environ. Microbiol.* 75, 4175–4184. doi: 10.1128/aem.00380-09

Maslowski, K. M., Vieira, A. T., Ng, A., Kranich, J., Sierro, F., Yu, D., et al. (2009). Regulation of inflammatory responses by gut microbiota and chemoattractant receptor GPR43. *Nature* 461, 1282–1286. doi: 10.1038/nature08530

Metghalchi, S., Ponnuswamy, P., Simon, T., Haddad, Y., Laurans, L., Clement, M., et al. (2015). Indoleamine 2,3-dioxygenase fine-tunes immune homeostasis in atherosclerosis and colitis through repression of interleukin-10 production. *Cell Metab.* 22, 460–471. doi: 10.1016/j.cmet.2015.07.004

Natividad, J. M., Lamas, B., Pham, H. P., Michel, M. L., Rainteau, D., Bridonneau, C., et al. (2018). *Bilophila wadsworthia* aggravates high fat diet induced metabolic dysfunctions in mice. *Nat. Commun.* 9:2802. doi: 10.1038/s41467-018-05249-7

Nguyen, L. T., Schmidt, H. A., von Haeseler, A., and Minh, B. Q. (2015). IQ-TREE: a fast and effective stochastic algorithm for estimating maximum-likelihood phylogenies. *Mol. Biol. Evol.* 32, 268–274. doi: 10.1093/molbev/msu300

Noguchi, H., Park, J., and Takagi, T. (2006). MetaGene: prokaryotic gene finding from environmental genome shotgun sequences. *Nucleic Acids Res.* 34, 5623–5630. doi: 10.1093/nar/gkl723

Ohira, H., Tsutsui, W., and Fujioka, Y. (2017). Are short chain fatty acids in gut microbiota defensive players for inflammation and atherosclerosis? *J. Atheroscler. Thromb.* 24, 660–672. doi: 10.5551/jat.RV17006

Oksanen, J., Kindt, R., Legendre, P., O'Hara, B., Stevens, M. H. H., Oksanen, M. J., et al. (2007). The vegan package. *Community Ecol. Packag.* 10, 631–637.

Parks, D. H., Tyson, G. W., Hugenholtz, P., and Beiko, R. G. (2014). STAMP: statistical analysis of taxonomic and functional profiles. *Bioinformatics* 30, 3123–3124. doi: 10.1093/bioinformatics/btu494

Pourcet, B., and Staels, B. (2016). Perilipin2/adipophilin and ApoA-1 team up to combat atherosclerosis. *Cardiovasc. Res.* 109, 193–195. doi: 10.1093/cvr/cvv276

Qin, J., Li, R., Raes, J., Arumugam, M., Burgdorf, K. S., Manichanh, C., et al. (2010). A human gut microbial gene catalogue established by metagenomic sequencing. *Nature* 464, 59–65. doi: 10.1038/nature08821

Qin, J., Li, Y., Cai, Z., Li, S., Zhu, J., Zhang, F., et al. (2012). A metagenome-wide association study of gut microbiota in type 2 diabetes. *Nature* 490, 55–60. doi: 10.1038/nature11450

Rognes, T., Flouri, T., Nichols, B., Quince, C., and Mahe, F. (2016). VSEARCH: a versatile open source tool for metagenomics. *PeerJ* 4:e2584. doi: 10.7717/peerj.2584

Ross, R. (1999). Atherosclerosis–an inflammatory disease. *N. Engl. J. Med.* 340, 115–126. doi: 10.1056/nejm199901143400207

Schirmer, M., Franzosa, E. A., Lloyd-Price, J., McIver, L. J., Schwager, R., Poon, T. W., et al. (2018). Dynamics of metatranscription in the inflammatory bowel disease gut microbiome. *Nat. Microbiol.* 3, 337–346. doi: 10.1038/s41564-017-0089-z

Shi, Y., Hu, J., Geng, J., Hu, T., Wang, B., Yan, W., et al. (2018). Berberine treatment reduces atherosclerosis by mediating gut microbiota in apoE-/- mice. *Biomed. Pharmacother.* 107, 1556–1563. doi: 10.1016/j.biopha.2018.08.148

Tang, W. H., Kitai, T., and Hazen, S. L. (2017). Gut microbiota in cardiovascular health and disease. *Circ. Res.* 120, 1183–1196. doi: 10.1161/circresaha.117.309715

Tang, W. H., Wang, Z., Levison, B. S., Koeth, R. A., Britt, E. B., Fu, X., et al. (2013). Intestinal microbial metabolism of phosphatidylcholine and cardiovascular risk. *N. Engl. J. Med.* 368, 1575–1584. doi: 10.1056/NEJMoa1109400

Tedgui, A., and Mallat, Z. (2006). Cytokines in atherosclerosis: pathogenic and regulatory pathways. *Physiol. Rev.* 86, 515–581. doi: 10.1152/physrev.00024.2005

The Human Microbiome Project Consortium, (2012). Structure, function and diversity of the healthy human microbiome. *Nature* 486, 207–214. doi: 10.1038/nature11234

Vilahur, G., Badimon, J. J., Bugiardini, R., and Badimon, L. (2014). Perspectives: the burden of cardiovascular risk factors and coronary heart disease in Europe and worldwide. *Eur. Heart J. Suppl.* 16(Suppl. A), A7–A11.

Wan, Y., Wang, F., Yuan, J., Li, J., Jiang, D., Zhang, J., et al. (2019). Effects of dietary fat on gut microbiota and faecal metabolites, and their relationship with cardiometabolic risk factors: a 6-month randomised controlled-feeding trial. *Gut* 68, 1417–1429. doi: 10.1136/gutjnl-2018-317609

Wang, Y., Tong, Q., Shou, J. W., Zhao, Z. X., Li, X. Y., Zhang, X. F., et al. (2017). Gut microbiota-mediated personalized treatment of hyperlipidemia using berberine. *Theranostics* 7, 2443–2451. doi: 10.7150/thno.18290

Wang, Z., Klipfell, E., Bennett, B. J., Koeth, R., Levison, B. S., Dugar, B., et al. (2011). Gut flora metabolism of phosphatidylcholine promotes cardiovascular disease. *Nature* 472, 57–63. doi: 10.1038/nature09922

Xie, W., Gu, D., Li, J., Cui, K., and Zhang, Y. (2011). Effects and action mechanisms of berberine and *Rhizoma coptidis* on gut microbes and obesity in high-fat diet-fed C57BL/6J mice. *PLoS One* 6:e24520. doi: 10.1371/journal.pone.0024520

Yin, J., Li, Y., Han, H., Chen, S., Gao, J., Liu, G., et al. (2018). Melatonin reprogramming of gut microbiota improves lipid dysmetabolism in high-fat diet-fed mice. *J. Pineal Res.* 65:e12524. doi: 10.1111/jpi.12524

Yue, S. J., Liu, J., Wang, W. X., Wang, A. T., Yang, X. Y., Guan, H. S., et al. (2019). Berberine treatment-emergent mild diarrhea associated with gut microbiota dysbiosis. *Biomed. Pharmacother.* 116:109002. doi: 10.1016/j.biopha.2019.109002

Zeisel, S. H., and Warrier, M. (2017). Trimethylamine N-oxide, the microbiome, and heart and kidney disease. *Annu. Rev. Nutr.* 37, 157–181. doi: 10.1146/annurev-nutr-071816-064732

Zhang, X., Zhao, Y., Xu, J., Xue, Z., Zhang, M., Pang, X., et al. (2015). Modulation of gut microbiota by berberine and metformin during the treatment of high-fat diet-induced obesity in rats. *Sci. Rep.* 5:14405. doi: 10.1038/srep14405

Zhang, X., Zhao, Y., Zhang, M., Pang, X., Xu, J., Kang, C., et al. (2012). Structural changes of gut microbiota during berberine-mediated prevention of obesity and insulin resistance in high-fat diet-fed rats. *PLoS One* 7:e42529. doi: 10.1371/journal.pone.0042529

Zhang, Y., Li, X., Zou, D., Liu, W., Yang, J., Zhu, N., et al. (2008). Treatment of type 2 diabetes and dyslipidemia with the natural plant alkaloid berberine. *J. Clin. Endocrinol. Metab.* 93, 2559–2565. doi: 10.1210/jc.2007-2404

Zhong, Y., Nyman, M., and Fak, F. (2015). Modulation of gut microbiota in rats fed high-fat diets by processing whole-grain barley to barley malt. *Mol. Nutr. Food Res.* 59, 2066–2076. doi: 10.1002/mnfr.201500187

Zhou, W., Xu, H., Zhan, L., Lu, X., and Zhang, L. (2019). Dynamic development of fecal microbiome during the progression of diabetes mellitus in Zucker diabetic fatty rats. *Front. Microbiol.* 10:232. doi: 10.3389/fmicb.2019.00232

Zhu, L., Zhang, D., Zhu, H., Zhu, J., Weng, S., Dong, L., et al. (2018). Berberine treatment increases Akkermansia in the gut and improves high-fat diet-induced atherosclerosis in Apoe(-/-) mice. *Atherosclerosis* 268, 117–126. doi: 10.1016/j.atherosclerosis.2017.11.023

Zhu, W., Gregory, J. C., Org, E., Buffa, J. A., Gupta, N., Wang, Z., et al. (2016). Gut Microbial Metabolite TMAO Enhances Platelet Hyperreactivity and Thrombosis Risk. *Cell* 165, 111–124. doi: 10.1016/j.cell.2016.02.011

Conflict of Interest: The authors declare that the research was conducted in the absence of any commercial or financial relationships that could be construed as a potential conflict of interest.

frontiers in Pharmacology

REVIEW
published: 07 April 2020
doi: 10.3389/fphar.2020.00422

Herbal Medicine for Cardiovascular Diseases: Efficacy, Mechanisms, and Safety

Abdullah Shaito[1], Duong Thi Bich Thuan[2], Hoa Thi Phu[2], Thi Hieu Dung Nguyen[3], Hiba Hasan[4], Sarah Halabi[5], Samar Abdelhady[6], Gheyath K. Nasrallah[7], Ali H. Eid[7,8]* and Gianfranco Pintus[9,10]**

[1] Department of Biological and Chemical Sciences, Lebanese International University, Beirut, Lebanon, [2] Department of Biochemistry, University of Medicine and Pharmacy, Hue University, Hue City, Vietnam, [3] Department of Physiology, University of Medicine and Pharmacy, Hue University, Hue City, Vietnam, [4] Institute of Anatomy and Cell Biology, Justus Liebig University Giessen, Giessen, Germany, [5] Biology Department, Faculty of Arts and Sciences, American University of Beirut, Beirut, Lebanon, [6] Faculty of Medicine, Alexandria University, Alexandria, Egypt, [7] Department of Biomedical Sciences, College of Health Sciences, Qatar University, Doha, Qatar, [8] Department of Pharmacology and Toxicology, American University of Beirut, Beirut, Lebanon, [9] Department of Medical Laboratory Sciences, University of Sharjah, Sharjah, United Arab Emirates, [10] Department of Biomedical Sciences, Faculty of Medicine, University of Sassari, Sassari, Italy

OPEN ACCESS

Edited by:
Yue Liu,
Xiyuan Hospital, China

Reviewed by:
Guanwei Fan,
Tianjin University of Traditional Chinese Medicine, China
Yanfei Liu,
Beijing University of Chinese Medicine, China

***Correspondence:**
Ali H. Eid
ae81@aub.edu.lb
Gianfranco Pintus
gpintus@sharjah.ac.ae;
gpintus@uniss.it
Gheyath K. Nasrallah
gheyath.nasrallah@qu.edu.qa

Specialty section:
This article was submitted to Ethnopharmacology, a section of the journal Frontiers in Pharmacology

Received: *04 November 2019*
Accepted: *19 March 2020*
Published: *07 April 2020*

Citation:
Shaito A, Thuan DTB, Phu HT, Nguyen THD, Hasan H, Halabi S, Abdelhady S, Nasrallah GK, Eid AH and Pintus G (2020) Herbal Medicine for Cardiovascular Diseases: Efficacy, Mechanisms, and Safety. Front. Pharmacol. 11:422. doi: 10.3389/fphar.2020.00422

Cardiovascular diseases (CVDs) are a significant health burden with an ever-increasing prevalence. They remain the leading causes of morbidity and mortality worldwide. The use of medicinal herbs continues to be an alternative treatment approach for several diseases including CVDs. Currently, there is an unprecedented drive for the use of herbal preparations in modern medicinal systems. This drive is powered by several aspects, prime among which are their cost-effective therapeutic promise compared to standard modern therapies and the general belief that they are safe. Nonetheless, the claimed safety of herbal preparations yet remains to be properly tested. Consequently, public awareness should be raised regarding medicinal herbs safety, toxicity, potentially life-threatening adverse effects, and possible herb–drug interactions. Over the years, laboratory data have shown that medicinal herbs may have therapeutic value in CVDs as they can interfere with several CVD risk factors. Accordingly, there have been many attempts to move studies on medicinal herbs from the bench to the bedside, in order to effectively employ herbs in CVD treatments. In this review, we introduce CVDs and their risk factors. Then we overview the use of herbs for disease treatment in general and CVDs in particular. Further, data on the ethnopharmacological therapeutic potentials and medicinal properties against CVDs of four widely used plants, namely *Ginseng*, *Ginkgo biloba*, *Ganoderma lucidum*, and *Gynostemma pentaphyllum*, are gathered and reviewed. In particular, the employment of these four plants in the context of CVDs, such as myocardial infarction, hypertension, peripheral vascular diseases, coronary heart disease, cardiomyopathies, and dyslipidemias has been reviewed, analyzed, and critically discussed. We also endeavor to document the recent studies aimed to dissect the cellular and molecular cardio-protective mechanisms of the four plants, using recently reported *in vitro* and *in vivo* studies. Finally, we reviewed and reported the results of the

recent clinical trials that have been conducted using these four medicinal herbs with special emphasis on their efficacy, safety, and toxicity.

Keywords: herbal medicine, cardiovascular diseases, atherosclerosis, hypertension, medicinal plants, antioxidants, oxidative stress, inflammation

INTRODUCTION

Cardiovascular diseases (CVDs) are diseases of the heart or blood vessels. CVDs register a global annual toll of more than 17 million deaths. As a result, CVDs remain the world's most common cause of death and are a major economic and health burden, worldwide. The World Health Organization (WHO) reported that CVDs account for 31% of annual global deaths (World Health Organization, 2017). In Europe, CVDs account for 45% of all deaths according to the European Cardiovascular Disease Statistics 2017 (Martinet et al., 2019). The American Heart Association's current statistics estimate that around half of the population of the USA has a form of CVD (Benjamin et al., 2019).

CVDs are a variety of diseases including peripheral vascular diseases, coronary heart disease (CHD), heart failure, heart attack (myocardial infarction), stroke, cardiomyopathies, dyslipidemias, and hypertension, among others (**Figure 1**) (Toth, 2007; Reiner et al., 2019). CVDs majorly originate from a vascular dysfunction, which then leads to organ damage. For example, the heart can suffer a heart attack, or the brain can suffer a stroke due to vascular impairment. Major culprits in vascular impairment include atherosclerosis, thrombosis, and high blood pressure (BP). Common risk factors for CVDs include smoking, unhealthy diet, diabetes mellitus, hyperlipidemia, elevated levels of low-density lipoprotein cholesterol (LDL), suppressed levels of high-density lipoprotein cholesterol (HDL), and hypertension (**Figure 1**) (World Health Organization, 2017).

CVDs prevention is favored by a healthy vascular endothelium. A healthy endothelium exhibits vasodilatory, anti-atherogenic, and anti-inflammatory properties (Celermajer, 1997). Several risk factors for CVDs lead to endothelial cell (EC) dysfunction, which has been implicated as a key event in the pathogenesis of atherosclerosis, coronary vasoconstriction, and, probably, myocardial ischemia. Interestingly, EC dysfunction is a reversible phenomenon, which opens the door for CVD therapies based on its reversion (**Figure 1**) (Celermajer, 1997).

Recently, inflammation has been confirmed as a risk factor for CVDs, especially during atherosclerosis and coronary artery disease. High levels of high-sensitivity C-reactive protein (hs-

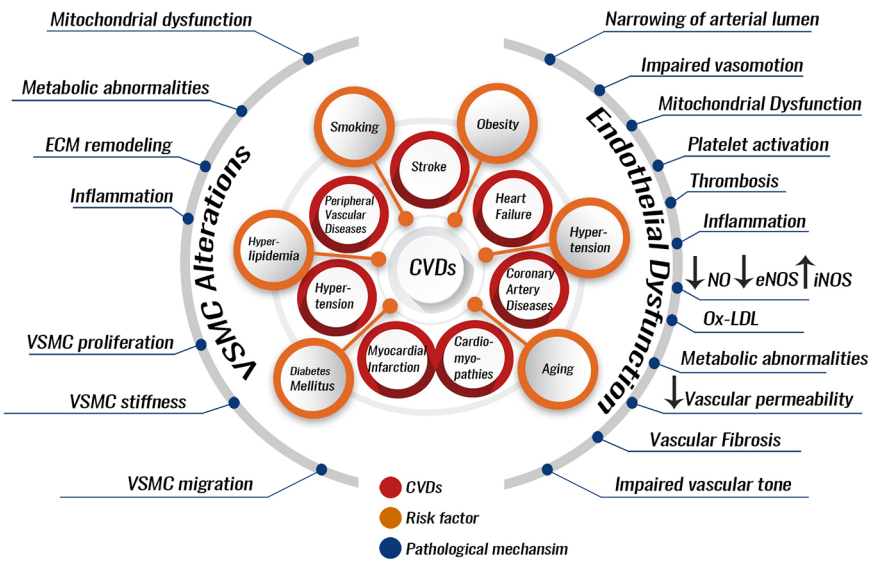

FIGURE 1 | Pathological processes involved in the development and progression of CVDs. Several risk factors can predispose to CVDs. These can include hypertension, smoking, dyslipidemia stemming from an unhealthy diet, or endocrinopathies like diabetes mellitus, hypothyroidism, and aging. The risk factors can lead to pathological alterations most of which can be due to endothelial dysfunction or VSMC alterations. Endothelial dysfunction or VSMC alterations increase the risk of developing atherosclerosis and hypertension. Atherosclerosis and hypertension are themselves CVDs risk factors and enhancers for the development of other CVDs like myocardial infarction, coronary artery diseases, or stroke. VSMC, vascular smooth muscle cell; ECM, extracellular matrix; NO, nitric oxide; eNOS, endothelial nitric oxide synthase; iNOS, inducible nitric oxide synthase; Ox-LDL, oxidized low-density lipoprotein.

CRP) and/or interleukin-6 (IL-6) are associated with higher absolute cardiovascular risk (Ridker et al., 1997; Ridker et al., 2000), where the CANTOS study, for the first time, established reduced rates of cardiovascular events following an anti-interleukin-1 beta (IL-1β) based therapy, independent of cholesterol levels (Ridker et al., 2017). Furthermore, common CVDs risk factors, such as diabetes or hypertension, can predispose to CVDs by the mediation of inflammation (Dokken, 2008; Aday and Ridker, 2018).

In the case of atherosclerosis, for example, inflammation can cause EC functional impairment. Dysfunctional ECs allow the accumulation of low-density lipoprotein (LDL) particles in the vessel wall intima where they become modified into oxidized LDL. Oxidized LDL can then activate the dysfunctional ECs to expose cell adhesion molecules (VCAM-1 and ICAM-1) that bind to and recruit inflammatory leukocytes (T-cells and monocytes) into the subendothelial space (Davies et al., 1993; Moore and Tabas, 2011). These inflammatory blood cells secrete interleukins and cytokines, produce reactive oxygen species (ROS) and thus form an inflamed microenvironment within the arterial wall. The inflamed microenvironment promotes vascular smooth muscle cell (VSMC) proliferation, matrix build-up, and lipid deposition, leading to the formation of an atherosclerotic plaque. The monocytes can reach the intima of the vessel, differentiate into macrophages, and uptake oxidized LDL to become foam cells (Tabas et al., 2007; Moore and Tabas, 2011; Douglas and Channon, 2014; Saleh Al-Shehabi et al., 2016; Martinet et al., 2019). Gradual intimal thickening takes place over the years and continues to expand causing decreased or complete occlusion of blood flow to organs, ultimately resulting in CVDs, such as myocardial infarction or stroke (Maguire et al., 2019). In addition, VSMCs proliferation leads to narrowing of the arterial lumen and dysregulation of the vasotone (Douglas and Channon, 2014). Usually several atherosclerotic plaques form in the intima and one of these may end up undergoing a necrotic breakdown, leading to acute luminal thrombosis, blood vessel occlusion, and cardiovascular complications, including myocardial infarction, unstable angina (chest pain caused by heart muscle ischemia), sudden cardiac death, or a stroke (Virmani et al., 2002). As a result, atherosclerosis is not only a risk factor but also a major contributor to CVD incidence. Around 50% of all deaths in developed countries are due to atherosclerosis (Tedgui and Mallat, 2006).

Hypertension also referred to as high BP, is a CVD and a major risk factor and contributor to other CVDs and other diseases (2017). Hypertension is an independent predisposing factor for heart failure, coronary artery disease, stroke, retinopathy, nephropathy, and peripheral arterial diseases (Sawicka et al., 2011; NCD Risk Factor Collaboration, 2017). Most of these diseases are associated with high mortality and morbidity (Abegaz et al., 2017). Additionally, hypertension is the single most significant risk factor for atherosclerosis, and any clinical outcome of atherosclerosis thereof (Sawicka et al., 2011). Hypertension is a "silent killer" as it does not show symptoms until later stages of the disease (Sawicka et al., 2011). Because of this, it is not surprising that hypertension affects 1.4 billion people and accounts for about 9.4 million deaths per year (Cooper et al., 2017; Egan et al., 2019). Lastly, hypertension prevalence is estimated to have a 30% worldwide increase by 2025 (Kearney et al., 2005).

The American Heart Association Hypertension Guidelines define hypertension as a persistent elevation of BP in the arteries [systolic BP (SBP) higher than 130/diastolic BP (DBP) higher than 80 mm Hg] (Muntner et al., 2018). If an elevated BP is left unmanaged, it can induce arterial remodeling; the walls of small vessels thicken, and the vessels lose their elasticity and become narrower. This process is called arteriosclerosis and can lead to "target organ damage" (TOD) (Triantafyllidi et al., 2010; Fan et al., 2017). TOD affects several organs such as the brain, kidney, or retina and may lead to death (Mensah, 2016; Abegaz et al., 2017). Arteriosclerosis can be witnessed in coronary vessels where it may cause a myocardial infarction (Rakugi et al., 1996). In the brain, arteriosclerosis can cause vessel lumen narrowing, vessel wall hardening, and blood clot formation, potentially causing a stroke (Johansson, 1999). Strokes have effects on cognitive and physical behaviors, and may result in dementia, paralysis, or death (Abegaz et al., 2017). Nephrosclerosis of the kidney is also due to arteriosclerosis which stiffens the nephron, ultimately affecting renal filtration and causing electrolyte imbalances (Bidani and Griffin, 2004; Lim et al., 2016). Overall, TOD proceed through hypertension-induced microvascular injuries in the cases of retinopathy and nephropathy and through hypertension-induced macrovascular injuries in the cases of stroke and myocardial infarctions (Nadar, 2011).

BP regulation, and therefore hypertension, depends on two main factors: cardiac output and systemic vascular resistance. Increased cardiac output or vascular resistance elevate BP. Cardiac output is majorly affected by sodium intake, renal function, and mineralocorticoids. Vascular resistance is affected by the sympathetic nervous system (SNS), rennin–angiotensin system (RAS), humoral factors, and local autoregulation (DiBona, 2013). SNS and RAS exert their effects mainly by eliciting vasoconstriction and inducing sodium retention. Humoral mediators can be vasoconstrictors like endothelin, angiotensin II, catecholamines, or vasodilators, for instance nitric oxide (NO), prostaglandins, and kinins (Oparil et al., 2003). Other factors that can modulate BP include blood flow velocity, blood viscosity, vascular wall stiffness, oxidative stress of VSMCs or ECs, VSMCs proliferation and shape changes, and EC health (Rodrigo et al., 2011).

Despite advances in CVD management and treatment, CVDs still claim more lives than the combination of all cancer forms (Mozaffarian et al., 2015). As a result, in recent years there has been major enforcement on CVD prevention (Reiner et al., 2019). Therefore, new treatment options are urgently warranted for all types of CVDs, considering the continued burden stemming from CVDs is still substantial.

HERBAL AND PLANT PRODUCTS AS MEDICINAL DRUGS

Traditional medicine and ethnomedicine, defined as the study of the traditional medicines practiced by various ethnic groups, are as old as human history. Traditional medicine historically relied on natural resources as medications. Historically, herbs, generally defined as any form of plant or plant product (Tachjian et al., 2010), and plant extracts formed the basis of the first drugs used in traditional medicine systems of many cultures and civilizations. Plants and herbs have always been a common source of medications, either in the form of traditional extracts or as pure active compounds (Fabricant and Farnsworth, 2001). Evidently, nature is a very important source for finding new drugs that leads to the treatment of diseases. Famous drugs from herbal and plant sources include aspirin from the *Salix alba* L. tree, digoxin (cardiac glycoside) from *Digitalis purpurea*, ephedrine from *Ephedra sinica*, lovastatin from *Monascus purpureus* L., taxol from *Taxus brevifolia*, reserpine from *Rauvolfia serpentina*, and many others (Harvey, 2000; Frishman et al., 2009; Cragg and Newman, 2013). Interestingly, reserpine is still an effective treatment for hypertension (Weber et al., 2014). Notably, the discovery of antimalarial drugs, quinine from the bark of *Cinchona* species and artemisinin from *Artemisia annua* L., represent a typical example of how ethnomedicine can guide drug discovery (Cragg and Newman, 2013).

The earliest records of drugs of natural origin, found in Mesopotamia (from around 2600 BCE), describe the use of approximately 1000 plant-derived compounds. The best record of using natural extracts in therapy is the Egyptians' Ebers Papyrus (from 1500 BCE), which documents more than 700 natural drugs, mainly of plant origin. The Chinese Materia Medica record (BCE 1100) describes 52 natural medicinal preparations, and the Indian Ayurvedic record (BCE 1000) describes more than 800 natural medicinal extracts (Cragg and Newman, 2013; Otvos et al., 2019). Hippocrates also applied phytotherapy, or healing with herbs, in his treatments (Otvos et al., 2019).

In 1985 WHO estimated that around 65% of the world population mostly depended on plant-derived traditional medicines (Farnsworth et al., 1985). People in different countries have come to use identical or comparable plants or herbal preparations for the prevention and/or treatment of physical and mental illnesses. Traditional Medicine Centers of the WHO identified 122 compounds to be commonly used in the Center's host countries. Interestingly, the 122 compounds have been reported to derive from only 94 plant species and are used for similar ethnomedical treatments in the different host countries (Farnsworth et al., 1985). Examples of such compounds include galegine, from *Galega officinalis* L., the base for the synthesis of metformin and similar bisguanidine-type antidiabetic drugs, and papaverine from *Papaver somniferum* which is the base for making the antihypertensive drug verapamil (Fabricant and Farnsworth, 2001). Commercially, drug production from natural products such as herbs is a viable commodity, where 39% of the 520 new drugs approved between 1983 and 1994 were natural compounds or derived from natural compounds and 60–80% of antibacterial and anticancer drugs were derived from natural products in that same period (Harvey, 2000).

Despite the many successes of using natural products for drug production, advances in combinatorial chemistry (in the late 1980s) shifted the focus of drug discovery efforts from natural products to synthesis at the laboratory bench (Cragg and Newman, 2013). This is mainly because natural product-based drug discovery and development is a complex endeavor demanding costly and highly integrated interdisciplinary approaches (Davison and Brimble, 2019; Otvos et al., 2019). Nonetheless, currently the use of natural products as drugs or as drug discovery platforms is "well and alive" (Newman and Cragg, 2016). In fact, traditional herbal and plant-derived extracts are becoming main stream as advances in scientific research are showing their importance in the prevention and treatment of diseases (Frishman et al., 2009).

Numerous and chemically diverse secondary metabolites have been purified from plant bioactives and have been optimized for exerting a biological effect, nonetheless, they are still away from exhaustive investigation for clinical use. However, recent published scientific evidence, technological advances, and research trends clearly point that naturally-derived compounds will be major sources of new drugs (Davison and Brimble, 2019; Otvos et al., 2019). This has provided a driving cause for the renewed popularity of traditional herbal and plant-derived medications among researchers, despite developments in combinatorial chemical synthesis and the production of modern synthetic drugs (Frishman et al., 2009).

Another reason for the regained interest in medicinal plant products is that, in their attempts to control diseases amid scarce socioeconomic resources, rural communities in developing countries have found resort in traditional herbal and plant-derived remedies. This is due to several factors, but in particular to the fact that plant-based medicines are a cheaper alternative with fewer side effects (Frishman et al., 2009; Tabassum and Ahmad, 2011). Herbal and plant remedies are not only economical, but they also contain thousands of bioactive components that have known therapeutic applications (Pan et al., 2013). Additionally, because herbs are viewed as food products, they are not subject to the same surveillance and regulation as conventional drugs. Moreover, herbal remedies are viewed by patients as being natural and therefore safe. However, more research efforts are required to validate the efficacy and the safety profile of such medicaments since many have adverse outcomes that can sometimes have life-threatening effects. It should also be noted that there is concern regarding herb–drug interaction (Tachjian et al., 2010; Anwar et al., 2016; Yuan et al., 2016).

One more reason for the revived interest in natural products is that the biological activity and structural diversity of natural products are unmatched by any available synthetic drug screening library (Davison and Brimble, 2019). Natural products have been selected by nature for bioactivity, over millions of years. As a result, natural product screening libraries need not be superfluously big, as is the case with synthetic drug screening libraries. In addition, natural products need only minor structural changes to optimize their drugability (Harvey, 2000; Gerry and Schreiber, 2018). As such, natural products offer "privileged scaffolds" and serve as

biologically "pre-validated platforms" for the design of compound candidate drug libraries (Davison and Brimble, 2019). Recent progress has focused on improving the potency, selectivity, and pharmacokinetics of bioactive natural products through structural modifications, which has led to the production of novel drug-like lead compounds. These structural changes are often required, as natural products usually show unfavorable toxicities and pharmacokinetics, limiting their clinical potential (Gerry and Schreiber, 2018; Davison and Brimble, 2019). Overall, natural products have been the single most productive source of drug leads even though little of nature's biodiversity has been tested for biological activity yet (Harvey, 2000).

We therefore address and expose the general rationale for using medicinal herbs in the therapy of diseases in general and CVDs in particular. Then, we move to discuss the medicinal potentials of four traditional herbs (*Ginseng*, *Ginkgo biloba*, *Ganoderma lucidum*, and *Gynostemma pentaphyllum*) for the treatment of CVDs, which are getting increasing popularity due to their commercial commodity in many markets worldwide and to their proven therapeutic potential in several settings including cardiovascular conditions. We describe and critically discuss their therapeutic benefits in terms of molecular, cellular, and metabolic properties in the context of CVDs. In addition, we highlight the major clinical trials in which these four herbs have been used, with an emphasis on their efficacy and safety.

MODERN MEDICINE MANAGEMENT OF ATHEROSCLEROSIS AND HYPERTENSION

Current health care guidelines emphasize prevention to minimize the risk of CVDs (Reiner et al., 2019). This is carried out by addressing the major CVD risk factors and trying to minimize their adverse outcomes. In atherosclerosis, most therapeutic approaches aim to control hypertension and hyperlipidemia or modulate hemostasis in order to avoid thrombotic complications (Weber and Noels, 2011). Hypercholesterolemia is a major contributor in atherosclerosis, so current conventional therapeutic approaches rely significantly on lowering LDL levels using statins (Ridker et al., 2017; Aday and Ridker, 2018; Reiner et al., 2019). In cases where statin therapy does not yield a significant reduction in LDL levels, an LDL-absorption inhibitor can be used, alone or in combination with statins depending on patient response. Clinical trials have clearly shown that such therapies are effective in lowering CVD risk (Reiner et al., 2019). Recently, pro-protein convertase subtilisin/kexin type 9 (PCSK9) inhibitors were approved by the regulatory bodies as a drug that can lower LDL level, and are recommended for use in patients with heart problems, where statins were not effective at lowering LDL levels (Ridker et al., 2017; Aday and Ridker, 2018). The CANTOS clinical trial (2017) has provided evidence that in patients with elevated inflammation (hsCRP > 2 mg/L), a combination therapy of statins and canakinumab (IL-1β antibody) may be necessary to lower atherosclerosis risk (Ridker et al., 2017; Aday and Ridker, 2018; Reiner et al., 2019). Prior to the recommendations of the CANTOS study, conventional therapy regimens have neglected the role of inflammation in atherosclerosis (Weber and Noels, 2011). It is very important to highlight that complementary and alternative medicine (CAM), including herbal remedies, have already tackled the inflammatory arm of atherosclerosis much earlier than the results of the CANTOS study (Frishman et al., 2009; Orekhov et al., 2013; Al-Shehabi et al., 2016), giving a hint as to why American patients visited CAM providers much more than primary care physicians (Eisenberg et al., 1998; Tachjian et al., 2010). Of relevance to this discussion is that herbal remedies are the most common type of CAM among CVD patients (Yeh et al., 2006; Tachjian et al., 2010).

Modern therapy regimens for hypertension involve controlling BP elevations in hypertensive patients. This usually requires the use of multiple antihypertensive drug agents in the majority of these patients (Guerrero-Garcia and Rubio-Guerra, 2018). Multiple classes of antihypertensive agents are available thus offering a practitioner the ability to prescribe highly effective drug combinations in order to reduce BP and protect target organs (Stewart et al., 2019). This combination therapy is of distinctive importance in resistant hypertension, which is highly prevalent worldwide (Noubiap et al., 2019; Samaha et al., 2019).

The major drug classes available for the management of hypertension are thiazide diuretics, angiotensin-converting enzyme (ACE) inhibitors, angiotensin receptor II blockers, and calcium channel blockers (Susalit et al., 2011; Munoz-Durango et al., 2016). Vasodilators, aldosterone antagonists, β-blockers, α-blockers, renin inhibitors, and central-acting agents are other agents that are occasionally used (Omboni and Volpe, 2018). These agents lower BP in patients and reduce their risk of hypertension-related CVD events, but do not prevent them thereby justifying the use of hypertension combination therapies (Rizvi, 2017).

Despite the availability of the aforementioned medications in modern-day health care systems, high BP is managed in only 34% of the patients (August, 2004; Wang and Xiong, 2012). Such an aspect appears to be mainly related not only to the cost of antihypertensive agents (Susalit et al., 2011), but also to their availability and accessibility (Wang and Xiong, 2012), their unwanted side effects (Susalit et al., 2011; Wang and Xiong, 2012), and their low patient compliance with the required dose (August, 2004). For these factors hypertension patients seek CAM medications, especially herbal-based medicaments to treat their CVDs in general and hypertension in particular (Yeh et al., 2006; Tachjian et al., 2010; Al Disi et al., 2016).

HERBAL MEDICINE MANAGEMENT OF ATHEROSCLEROSIS AND HYPERTENSION

Herbal extracts and their derivatives can favorably modulate and ultimately ameliorate the molecular events that contribute to hypertension or atherosclerosis, the two major contributors to CVDs incidence. Herbal remedies contain numerous bioactives

and, thus, have multi-modal cellular mechanisms of action. In fact, herbal remedies can have antioxidant, vasorelaxant, anti-inflammatory, anti-proliferative, or diuretic effects. Herbal remedies can also prevent VSMC phenotypic switching, inhibit endothelial dysfunction, platelet activation, lipid peroxidation, ROS production, and macrophage atherogenicity. Because of such a wide range of molecular and cellular targets, herbal preparations can be used to treat and manage a range of CVDs. For example, *Salvia miltiorrhiza* (Red sage), an annual sage traditionally used in Chinese medicine, has been used to treat a plethora of CVDs including CHD, myocardial infarction, atherosclerosis, and angina pectoris. The active compounds are mainly utilized as the dried root of the plant rhizome named Danshen (Gao et al., 2012). The plant bioactive compounds are the lipo-soluble Tanshinones and the water-soluble Phenolics (Ren et al., 2019). *S. miltiorrhiza* extracts have shown strong antioxidant capabilities with a high ability to scavenge free radicals, which seems the base of its strong cardio- and vascular-protective potential (Zhao et al., 2006).

Salvianolic acid B, one of the pure compounds that can be extracted from *S. miltiorrhiza*, is effective against fibrosis and ischemia–reperfusion injury (Lay et al., 2003). Danshen has a protective effect against homocysteine-induced adverse effects, where homocysteine imbalance is a high-risk factor for vascular diseases (Chan et al., 2004). In combination with *Pueraria montana* var. lobata. (Kudzu), Danshen has showed potent anti-hypertensive effects (Ng et al., 2011). In one clinical trial, Danshen capsules (1000 mg twice daily for 12 weeks) were able to significantly reduce SBP and pulse rate in patients with uncontrolled mild to moderate hypertension and under conventional antihypertensive treatment. It has also been found to be well-tolerated and considered to be safe in patients with hypertension (Yang et al., 2012).

Astragalus membranaceus (Synonym *Astragalus propinquus* Schischkin. in the Missouri Botanical Garden plant list), another Chinese herb, contains Astragaloside IV, which is the plant major bioactive compound widely used as an antioxidant and for protection against ischemic-associated CVDs (Zhang et al., 2006). *A. membranaceus* extract has been found to maintain cardiac functions by improving energy metabolism and inhibiting the production of free radicals in a myocardial ischemia reperfusion rat model (Zhou et al., 2000). By decreasing the levels of the oxidative stress marker malondialdehyde (MDA), maintaining superoxide dismutase (SOD) activity, and reducing free radicals-induced myocardial cell injury, *A. membranaceus* can also improve cardiac function and provide cardioprotection in a myocardial ischemic rat model (Ma et al., 2013). *A. membranaceus* extract also has angiogenic effects in the ischemic injury rat model (Zhang et al., 2011). Astragaloside IV has been found to provide a positive inotropic effect improving left ventricular ejection in patients with congestive heart failure (CHF) (Luo et al., 1995). The polysaccharide of *A. membranaceus* has also been shown to reduce insulin resistance and to possess anti-obesity and hypolipidemic effects (Mao et al., 2009).

Allium sativum (Garlic) is a classic example of herbs used in CVDs management and is quite known for its multifaceted properties against CVD-associated conditions such as hypertension, oxidative stress, inflammation, and hyperlipidemia (Ashraf et al., 2013; Jeong et al., 2016; Thomson et al., 2016). Indeed, by reducing total cholesterol and LDL levels, decreasing the content of lipid in arterial cells and inhibiting VSMCs proliferation, garlic can be used to manage atherosclerosis and hyperlipidemia (Sun Y. et al., 2018). Owing to its endothelial NO synthase (eNOS)-modulated vasorelaxation ability, *Crataegus oxyacantha* (Synonym *Crataegus rhipidophylla Gand.* Common name Hawthorn) is another example of herbs commonly used to manage hypertension (Brixius et al., 2006). Another herb, *Crocus sativus* (Saffron), can block Ca^{2+} channels *via* endothelium-independent mechanisms providing another vasodilator mechanism, in addition to its eNOS activating ability (Razavi et al., 2016). Among other medicinal plants *Hibiscus sabdariffa* (roselle), is known to reduce BP using its ability to inhibit ACE (Ojeda et al., 2010), while *Camellia sinensis* (Tea) extracts can reduce hypertension by significantly increasing brachial artery flow-mediated dilation (FMD) (Ras et al., 2011). Rosemary (*Rosmarinus officinalis*) exhibits neuroprotection by acting against ischemic stroke-associated cerebral insufficiency, which is characterized by a reduction of localized blood flow in the brain. Through its anti-inflammatory properties, rosemary can decrease the expression of inducible NO synthase (iNOS) and cyclooxygenase-2 (COX-2) as well as that other pro-inflammatory enzymes and mediators (Seyedemadi et al., 2016). The use of herbal plants extends to include CHF and atrial arrhythmias. Digitalis, extracted from the dried leaves of the common foxglove, is a potent inhibitor of Na^+/K^+-ATPase and can cause depolarization leading to smooth muscle contraction and vasoconstriction and hence can strengthen muscle heart contractions (Liu et al., 2016).

Given all these restorative abilities, it is not surprising that herbal remedies are being absorbed into evidence-based medicine for the prevention and/or treatment of CVDs. **Table 1** lists common herbal remedies and the form of CVDs that they can help alleviate.

Although herbs have been widely used in both traditional and modern medicine, a limited number of reviews that gather them and comprehensively focus on their mechanisms of action and safety in the context of CVDs are present. Many plant-based compounds appear to have cardiovascular protective effects, nevertheless, among the most effective compounds are flavonoids, terpenoids, saponins, and polysaccharides. These highly effective compounds are major components of four of the most recognized herbal preparations namely: Ginseng, *Ginkgo biloba*, *Ganoderma lucidum,* and *Gynostemma pentaphyllum,* which we decide to cover in this review.

TABLE 1 | Some herbal remedies traditionally used for the treatment of different forms of CVDs.

CVD form	Examples of herbal remedies used
Atherosclerosis and hyperlipidemia	Garlic (*Allium sativum*)
	Commiphora mukul
	Monascus purpureus
	Berberine (active compound of *Coptis chinensis*)
Systolic hypertension	Garlic (*Allium sativum*)
	Rauvolfia serpentina
	Panax species (Ginseng)
	Stephania tetrandra
	Veratrum species alkaloids
	Ligusticum wallichii (Synonym of *Ligusticum striatum* DC)
	Hawthorn from *Crataegus oxyacantha*
	Camelia sinensis
	Andrographis paniculata
	Apium graveolens
	Bidens pilosa L.
	Crocus sativus
	Cymbopogon citratus
	Hibiscus sabdariffa
	Nigella sativa
	Urtica dioica
	Viola odorata
	Mentha longifolia
	Salvia miltiorrhiza
	Uncaria Rhynchophylla
Venous insufficiency	*Aesculus hippocastanum*
	Ruscus aculeatus
Cerebral insufficiency	*Ginkgo biloba*
	Rosmarinus officinalis
Angina pectoris	*Crataegus species*
	Panax notoginseng
	Salvia miltiorrhiza
Congestive heart failure	*Digitalis purpurea*
	Digitalis lanata
	Crataegus species
	Adonis microcarpa and *Adonis vernalis*
	Berberine (active compound of *Coptis chinensis*)
	Salvia miltiorrhiza

The herbal remedies refer to the plant extract, unless otherwise indicated where the remedy may be a purified or partially purified active ingredient of the plant extract. Data were obtained from published data in (Valli and Giardina, 2002; Frishman et al., 2009; Al Disi et al., 2016; Al-Shehabi et al., 2016; Samaha et al., 2019).

GINSENG

Ginseng is an anciently cultivated plant (2000 years ago) partly due to its ritual use (**Figure 2**). Ginseng use in traditional medicine goes back to 20 centuries ago (Kim, 2012), but its use in Western medicine dates back to the early 20th century by two British physicians F. Porter Smith and G.A. Stuart who were exploring Chinese herbal remedies at the time (Shih-Chen et al., 1973). Ginseng habitats include Asian countries such as Korea, China, Japan, and Vietnam, and North American countries, mainly Canada and the United States. Korean red ginseng (KRG; *Panax ginseng C.A. Mey.*), Chinese ginseng (*Panax notoginseng* Burkill; F.H.Chen.), American ginseng (*Panax quinquefolium L.*), and Japanese ginseng (*Panax japonicas* C.A. Mey.) represent the most commonly used ginsengs.

Usually the roots of 5 to 7-year-old plants are either air-dried under the sun yielding "white ginseng" or steam-treated at 98–100°C for 2–3 h and then sun-dried to produce the "red ginseng" (Kim et al., 2000). During steaming, ginseng chemical constituents undergo changes that make red ginseng more pharmacologically effective than white ginseng (Kim et al., 2000). Currently, ginseng is prepared and used either in a liquid form: oil extracts or tea; or in a solid form: tablets, capsules, or dried roots (Valli and Giardina, 2002). However, extracts of ginseng root, berry, and leaf have been repeatedly demonstrated to have anti-obesity, anti-hyperglycemic, anti-hypertensive, insulin sensitization, and anti-hyperlipidemic effects (Kim, 2012).

More than 300 bioactives have been isolated from Ginseng. Ginsenosides, which are triterpene saponins, are the most bioactive constituents isolated from Ginseng extracts (Mahady et al., 2000). Of the 40 ginsenosides isolated so far, Rb1, Rg1, Rg3, Re, and Rd are the most frequently studied. Rg3, Rg5, and RK1 are unique to the red Korean Ginseng (**Figure 2**) (Lee and Kim, 2014). Research into Ginseng and its constituents has flourished so that currently there is a journal dedicated to Ginseng research: Journal of Ginseng Research (https://www.journals.elsevier.com/journal-of-ginseng-research). The study of the purified individual ginsenosides rather than the whole Ginseng root extract has gained recent interest (Kim, 2012). Ginseng and its ginsenoside constituents have vasorelaxation, anti-oxidation, anti-inflammation, and anti-cancer activities (Kim, 2012; Choi J. et al., 2013).

Ginseng at the Bench: Mechanism of Action in CVDs

In the context of CVDs, Ginseng has been used to manage hypertension. Ginseng has hypotensive effects due to its effect in the improvement of arterial functions. Interestingly, ginsenosides facilitate vasorelaxation of different vessels: rat aortas (Kim et al., 1999a), murine coronary arteries (Pan et al., 2013), and monkey cerebral arteries (Toda et al., 2001). Ginseng can increase eNOS expression and NO production while ginsenoside Rg3 activates eNOS (Valli and Giardina, 2002; Jang et al., 2011; Hong et al., 2012; Pan et al., 2013; Lee K. et al., 2016). KRG induces NO-dependent vasorelaxation improving vascular tone. These effects are mediated by the inhibition of arginase activity, the increase of NO generation, and the enhancement of eNOS dimer formation (Shin W. et al., 2013). The *Panax ginseng* G115 extract has also been shown to inhibit ACE activity in human umbilical vein endothelial cells (HUVECs) and angiotensin I-induced contractions of bovine mesenteric arteries (Persson et al., 2006). Other Ginseng CVDs management properties are its anti-oxidant (Lee et al., 2019a), anti-inflammatory (Keum et al., 2003; Shin Y. et al., 2013), and anti-hyperlipidemic (Park et al., 2005) effects, along with its ability to regulate Ca^{2+} channels (Lee and Kim, 2014).

The ginsenoside Rg3 can increase NO and cGMP levels, activate Ca^{2+}-gated potassium channels, inhibit ACE activity, and block Ca^{2+}-gated channels (Kim et al., 1999b; Persson et al., 2006; Park J. et al., 2014). Ginseng has also demonstrated an anti-inflammatory role by inhibiting the activation of activator

Ginsenoside PPD type	R1	R2
Rb1	-O-Glc-Glc	-O-Glc-Glc
Rd	-O-Glc-Glc	-O-Glc
Rb2	-O-Glc-Glc	-O-Glc-Ara (p)
Rg3	-O-Glc-Glc	OH
Compound K	OH	-O-Glc

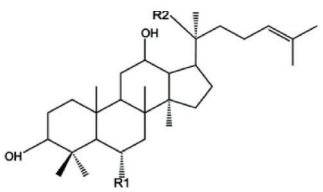

Ginsenoside PPT type	R1	R2
Re	-O-Glc-Rha	-O-Glc
Rf	-O-Glc-Glc	-O-Glc
Rg1	-O-Glc	-O-Glc

FIGURE 2 | Ginseng. **(A)** Roots have the healing properties (from https://pngtree.com/freepng). **(B)** Chemical structure of Ginsenosides. **(C)** Ginsenosides protopanaxadiol (PPD) and Ginsenoside protopanaxatriol (PPT). R1 and R2 are side chains in different ginsenosides. Glc, glucose; Ara, arabinose; Rha, rhamnose.

protein (AP-1) and nuclear factor-kappa B (NF-κB), ultimately reducing the expression of COX-2, IL-6, IL-1β, and tumor necrosis factor-α (TNF-α) (Keum et al., 2003; Shin Y. et al., 2013). In macrophages, Baek et al. demonstrated that each fraction of the KRG exerts anti-inflammatory actions through a different mechanism. For instance, the saponin fraction significantly suppressed NO production and reduced the expression of inflammatory genes such as iNOS, COX-2, TNF-α, and interferon-β. In contrast, all extracts, including water extracts, saponin, and non-saponin fractions, inhibit the activity of the kinase TBK1 and suppress both nuclear translocation and transcriptional activity of its downstream effector interferon regulatory factor 3 (IRF3) (Baek et al., 2016).

By inhibiting diacylglycerol liberation, dietary supplementation of KRG lowers blood cholesterol levels and reduces the formation of atherosclerotic lesions induced by a high cholesterol diet in rabbit (Hwang et al., 2008). Again, by up-regulating the adenosine triphosphate-binding cassette transporter A1, *the* saponin fraction of *P. notoginseng* can attenuate cholesterol esters in foam cells (Jia et al., 2010). In addition, Ginseng has shown a potent *in vivo* antithrombotic effect, which may be due to an antiplatelet activity rather than an anticoagulation activity, indicating that Ginseng intake may be beneficial for individuals with high risks of thrombosis and CVDs (Lee and Kim, 2014). In this context, the dihydro-ginsenoside Rg3 has been reported to potently inhibit platelet aggregation through the modulation of downstream intracellular signals such as cAMP and extracellular signal-regulated kinase 2 (Lee et al., 2008).

In Vivo Preclinical Evaluation of Ginseng in Animal Models of CVDs

Ginseng's hypotensive effects have been extensively demonstrated (Valli and Giardina, 2002; Lee et al., 2012; Mucalo et al., 2013; Al Disi et al., 2016). For example, Ginseng can reduce adrenal catecholamines secretion in hypertensive rats, thus contributing to vasorelaxation (Jang et al., 2011). However, there are reports of Ginseng being hypertensive (Jang et al., 2011; Kim, 2012). In fact, Ginseng may have biphasic concentration-dependent effects. Low doses of ginseng raise BP, while higher concentrations repress BP (Jang et al., 2011), a phenomenon that could be due to the varied action of different Ginseng extract constituents (Valli and Giardina, 2002).

Through their antioxidant properties, ginsenosides also mediate anti-hypertensive and anti-atherosclerotic effects. Ginsenosides exhibit free radical scavenging and metal ion chelating abilities. For instance, the lipid-soluble and water-soluble extracts from the North American Ginseng exhibit strong antioxidant activity (Kitts et al., 2000). Lu et al. showed that Rb1 could significantly and specifically alleviate hydroxyl radical and hypochlorous acid radical damaging effects (Lu et al., 2012). Aged rats, supplemented with the North American Ginseng for four months, had decreased production of both ROS and age-related oxidative damage in proteins of the heart and muscle fibers, a phenomenon mediated by SOD and glutathione peroxidase (GSH-Px) activation (Fu and Ji, 2003). The ginsenoside Rg3 can ameliorate mitochondrial dysfunction and promote enhanced expression of antioxidant

proteins, such as the nuclear factor erythroid 2-related factor-2 (Nrf2) and the heme oxygenase-1 (HO-1) (Lee et al., 2019a). By reducing hypertension- and atherosclerosis-associated inflammatory states, Ginseng can reduce CVD risk. To address the anti-inflammatory effects of Ginseng, Mohammadi et al. carried out a meta-analysis of data from randomized controlled trials. They report that Ginseng supplementation significantly lowered the levels of two key pro-inflammatory mediators IL-6 and TNF-α (Mohammadi et al., 2019). By modulating angiogenesis (decreased VEGF-A and FGF-2 expression), inflammatory (decreased CD68, TNFα, and MCP-1 expression) and matrix metalloproteinase (MMP) activity, Ginseng can inhibit ovariectomy-induced obesity, adiposity, and adipocyte hypertrophy (Lee H. et al., 2016).

Ginseng can lower the risk of atherosclerosis by inducing a better lipid profile. Ginseng's beneficial effects on lipid metabolism have been described more than three decades ago (Qureshi et al., 1983; Yamamoto et al., 1983). In humans and rats, red Ginseng supplementation improves lipid profiles by diminishing the total plasma levels of cholesterol, triglycerides, LDL-C, free fatty acids (FFA), and platelet adhesiveness and increasing HDL-C levels in total plasma (Deng et al., 2017; Singh et al., 2017). In rats, black Ginseng can ameliorate hypercholesterolemia by interfering with the expression of cholesterol metabolism genes (Saba et al., 2016). In addition, lipid profiles tend to improve in diabetic rats receiving Ginseng, suggesting that *Panax ginseng* can ameliorate diabetes mellitus-initiated dyslipidemias (Deng et al., 2017; Abdelazim et al., 2018). By modulating the secretion of lipoproteins, Ginseng can reduce the microsomal triglyceride transfer protein (MTTP) (Oh et al., 2012), which plays an essential role in lipid metabolism and transport (Deng et al., 2017).

KRG works as an agonist of peroxisome proliferator-activated receptor (PPAR), which is known to improve atherogenic dyslipidemia by augmenting liver PPAR-α mRNA and raising lipoprotein lipase mRNA levels (Park et al., 2005). Consistent with this study, Shin et al. demonstrated that Ginseng could prevent obesity and dyslipidemia in high-fat diet (HFD)-fed castrated mice. These processes were mediated through the inhibition of adipogenesis-related genes expression (SREBP-1C, PPAR-γ, FAS, SCD1, and ACC1) in visceral adipose tissues (Shin and Yoon, 2018). Ginseng extracts or ginsenosides can act synergistically with testosterone to further inhibit dyslipidemia (Shin and Yoon, 2018). Mollah et al. also showed that Ginseng can improve lipid profiles *via* PPAR pathway activation (Mollah et al., 2009; Yang and Kim, 2015). Further, ginsenoside Rg1 can activate the promoter of PPAR-α leading to the expression of its target genes carnitine palmitoyltransferase-1 (CPT-1) and acyl-CoA oxidase (ACO), which are involved in fatty acid oxidation. These findings indicate that Rg1-induced improvement of lipid profiles may be associated with increased fatty acid oxidation through PPAR-α activation (Park et al., 2011).

Ginseng to the Clinic

Numerous clinical trials have been conducted to assess the cardio-protective and beneficial effects of Ginseng and its constituents in CVD treatment. Checking the clinical trials on Ginseng, its extracts or ginsenosides on the U.S. National Library of Medicine www.clinicaltrials.gov reveals that there are 162 Ginseng clinical trials. Of the 162 trials, 47 were Phase 3 or 4 trials, 97 have been completed and the rest are ongoing. Importantly, a significant number of these trials addresses CVDs. For example, eight trials addressed hypertension, five addressed arterial occlusive diseases, and another five addressed strokes. One such clinical trial examined the vasorelaxation effects of Asian Ginseng (AG) and its ability to modulate vascular function. Trial participants were randomized to either the selected AG extract or placebo groups and received a daily dose of 3 g of AG for 12 weeks in combination with their usual antihypertensive and anti-diabetic therapy. Combining AG extract with conventional therapy in diabetics patients with concomitant hypertension decreased arterial stiffness and attenuated SBP (Mucalo et al., 2013). Another clinical trial found that Rg3 from KRG lowers central and peripheral arterial pressures in healthy adults (Jovanovski et al., 2014). In an acute, randomized, placebo-controlled, double-blind, crossover trial on participants with type 2 diabetes mellitus (T2DM), Shishtar et al. showed that acute administration of Korean white Ginseng appears to be safe and exhibits beneficial effects on the augmentations index, a cumulative indicator of arterial health (Shishtar et al., 2014a).

A 12-week intervention with KRG was conducted in patients with impaired fasting glucose, impaired glucose tolerance, or newly diagnosed with T2DM. Subjects were randomized in a double-blind, placebo-controlled trial. The trial results showed that 12 weeks of intervention with KRG supplementation (5 g/day) led to normalization of whole blood and serum glucose levels as well as serum insulin and CRP concentrations (Bang et al., 2014). Administration of *Panax Ginseng* extract (PGE) for 8 weeks (6 g/day) decreased serum triglycerides and total cholesterol and LDL levels, while increasing HDL levels. These results were attributed to PGE potent antioxidant effects (Kim and Park, 2003). In accordance, the effects of a low-dose (3 g/day) and a high-dose (6 g/day) of KRG supplementation for 8 weeks on antioxidant enzymes and oxidative stress markers in humans were assessed in a randomized, double-blind, placebo-controlled trial. Increased GSH-Px, SOD, and CAT activities were found in the high-dose group as compared to the placebo group. Plasma oxidized-LDL levels and DNA tail length and tail moment were significantly decreased in both high and low dose groups but increased in the placebo group. This led to the conclusion that supplementation with KRG upregulates antioxidant enzymes activities and consequently attenuates lymphocyte DNA damage (Lee et al., 2012).

The efficacy of Ginseng against T2DM is well documented. A meta-analysis of eight clinical trials showed that administration of Ginseng, in comparison to the placebo, improves fasting glucose levels, postprandial insulin levels, and insulin resistance. In these patients, ginseng was able to improve blood lipid profile lowering triglycerides, total cholesterol, and LDL levels. This meta-analysis concluded that Ginseng supplementation can improve the control of glucose levels and insulin sensitivity in patients with T2DM (Gui et al., 2016). Another meta-analysis of 16 randomized clinical trials

was conducted to assess the efficacy of Ginseng in controlling glycemic index by reporting the ability of Ginseng to reduce fasting blood glucose in both patients with and without diabetes (Shishtar et al., 2014a; Shishtar et al., 2014b). Interestingly, when Ginseng is combined with conventional drugs, its efficacy in the management of hypertension is more pronounced. Indeed, combining AG extract with conventional therapy in diabetic patients with concomitant hypertension decreased arterial stiffness and attenuated SBP (Mucalo et al., 2013).

Despite the numerous clinical trials showing the efficacy of Ginseng in CVDs management, this aspect yet remains controversial. In fact, some studies could not demonstrate Ginseng's beneficial effects against CVD. For example, a meta-analysis of 17 randomized clinical trials (1381 participants) found no significant effect of AG on arterial BP and hence no effect on CVDs risk (Komishon et al., 2016). Another clinical trial concluded that KRG intake (3 g/day) for 3 weeks had no beneficial effects on arterial stiffness in subjects with hypertension (Rhee et al., 2011). Yet, as mentioned above, when KRG was combined with conventional therapy it was able to control hypertension (Rhee et al., 2011).

Thus, Ginseng appears to be efficient in regulating several lipid profile parameters, and has shown positive effects in patients with T2D. Also, the efficacy of Ginseng in the management of hypertension is well documented when combined with conventional hypotensive medications.

Safety, Toxicity, and Side Effects of Ginseng

As mentioned earlier, the claimed safety of medicinal herbs has to be handled cautiously, and on a case-by-case basis for each herbal preparation. The safety of Ginseng has been experimentally approached using animal models and human clinical studies (Mahady et al., 2000). An abundant number of *in vitro* and *in vivo* studies, as well as human clinical trials have pointed out that Ginseng extracts have negligible side effects (Park K. et al., 2014). Few unfavorable symptoms were reported following long periods of administration of high doses of Ginseng extracts. This included morning diarrhea, skin eruption, nervousness, sleeplessness, hypertension, edema, decreased appetite, depression, and hypotension (Siegel, 1979; Kiefer and Pantuso, 2003). A systematic review on PGEs in randomized controlled trials highlighted the safety of Ginseng. The review identified 40 studies where adverse effects were reported, but analysis revealed that out of the 40 studies, 16 studies showed no adverse events and 24 studies had 135 minor events (Shergis et al., 2013). Lee et al. reported that *P. ginseng* extract (1 or 2 g/day) supplemented over the course of 4-weeks was safe, tolerable, and free of toxic effects in healthy volunteer subjects. Only non-significant changes were observed in hematological and biochemical tests (Lee et al., 2012). Recently, Song et al. performed a large-scale clinical study with 1000 participants randomly divided into two groups; a placebo and a group supplemented with 2 g/d of KRG. Their findings asserted the safety and tolerability of KRG (Song et al., 2018).

Along the same lines, the mutagenic and toxicity potentials of tissue cultured mountain Ginseng adventitious roots (TCMGARs) were tested. TCMGARs did not exhibit any mutagenic properties when tested in diverse strains of *Salmonella typhimurium* and *Escherichia coli*. This was further shown *in vivo* without any evidence of TCMGARs mutagenicity, such as chromosomal aberration and micronucleus appearance, in mice exposed to TCMGARs (Murthy et al., 2018). All these studies confirm the biosafety and non-toxicity of Ginseng at an average dietary consumption.

Ginseng supplements have also shown certain clinically relevant patterns of adverse cardiovascular reactions. There are reports of numerous cases where prolonged Ginseng use or misuse has led to potential side effects related to cardiovascular events such as increased BP (Coon and Ernst, 2002), long QT syndrome, or atrial fibrillation (AF) (Paik and Lee, 2015). For example, in a young man, 3-year Ginseng supplementation has been found to correlate with hypertension, shortness of breath, dizziness, and inability to concentrate, symptomatology that disappeared and did not recur after stopping the supplements. In another instance, a hypertensive female receiving no other medication than Ginseng (Ginzin tablets; Ferrosan) reported an increase in BP rather than a decrease. Interestingly, such Ginseng-associated BP increase remitted going back to pre-treatment levels 4 days after the cessation of Ginseng intake (Coon and Ernst, 2002). Although the observed effects appeared not to be clinically relevant, in a 30-subjects prospective, randomized, double-blind, placebo-controlled study, Ginseng was found to prolong the QTc interval and reduce DSB in healthy adults as early as 2 h after consumption (Caron et al., 2002). A 43-year-old healthy woman without familial history of sudden cardiac death and negative test of long QT mutations developed a long QT syndrome followed by polymorphic ventricular tachycardia. The woman admitted to the hospital revealed she was consuming 70 cL of caffeine and 4 L of Korean *Panax ginseng* daily for 6 months. Upon stopping Ginseng consumption, the patient had no subsequent events. Yet, it is not proven whether a higher dose of Ginseng or a synergistic effect of caffeine could further prolong QT leading to malignant dysrhythmias (Torbey et al., 2011). Additionally, an AF with slow ventricular rate developed after taking AG for 1-week in an 83-year old woman with chronic renal disease (Liao et al., 2010). Nevertheless, all these mentioned episodes are considered rare adverse reactions that mostly depend on inter-variability between patients (Paik and Lee, 2015).

Ginseng has been reported to interact with several drugs, yet its interaction with warfarin (blood-thinning drug) is the most documented (Yuan et al., 2004; Chua et al., 2015). A randomized, double-blind, placebo-controlled trial using 20 healthy patients concluded that a 2-week intake of American Ginseng (2 g/d; 1 g twice daily) significantly reduced peak international normalized ratio (INR) and peak plasma warfarin levels (Yuan et al., 2004). In a recent study performed on rats, ginsenosides were reported to significantly enhance the activity of two enzymes known to metabolize warfarin, P450 CYP3A4 and P450 CYP2C9, restoring the levels of coagulation factors II and VII and that of the protein

Z, that are usually suppressed by warfarin (Dong et al., 2017). The combined use of *Panax ginseng* with the monoamine oxidase inhibitor, phenelzine (Nardil), may result in manic-like symptoms (Vogler et al., 1999). Finally, although the efficacy and safety of Ginseng has been evidenced in numerous clinical studies, additional well-designed, large-scale randomized control trials are needed.

GINKGO BILOBA

Ginkgo biloba, also known as the maidenhair tree in English due to its resemblance to the foliage of the Maidenhair fern (**Figure 3**), is among the oldest seed plants. It is regarded as a "living fossil" because of its continued existence without dramatic changes for 270 million years. (Hori et al., 1997). Its place of origin is believed to be eastern China in Yangtze River Valley (Jaggy and Koch, 1997; Singh et al., 2008). From there, it became extensively distributed in Asia, Europe, North America, and New Zealand and is now widely cultivated (Kleijnen and Knipschild, 1992; Hori et al., 1997; Belwal et al., 2019). A remark about its leaf extract is included in the medical Dictionary of the Republic of China (Kimbel, 1992; Kleijnen and Knipschild, 1992; Kressmann et al., 2002). *Ginkgo biloba* is the only living species of the division Ginkgophyta probably due to its resistance to environmental stresses (Deng et al., 2006; Cao et al., 2012).

Ginkgo biloba is one of the most sold medicinal plants. It is one of the herbs mentioned in the Chinese Materia Medica more than 5000 years ago, where its seeds and leaves—fresh or dried—have been used for thousands of years in ancient herbal medicine. Current research on its therapeutic properties mainly uses *Ginkgo biloba* leaves and many pharmaceutical companies including those in the USA and Europe manufacture and sell extracts of the leaves (Kimbel, 1992; Kleijnen and Knipschild, 1992; Kressmann et al., 2002). The leaves can be used for the treatment of asthma and bronchitis in the form of a tea that is most commonly used by the Chinese people. More commonly, a standardized extract containing the most active constituents can be made from the leaves and then taken as a tablet, in liquid form, or given intravenously (Kleijnen and Knipschild, 1992).

The main constituents of *Gingko biloba* are flavonoids (ginkgo-flavone glycosides), terpenoids (ginkgolides and bilobalides), biflavones, and organic acids among other substances (**Figure 3**). Ginkgolides, being unique to *Gingko biloba,* are not synthesized by any other living species. Ginkgolides are classified into either A, B, C, J, or M types (**Figure 3**). *Gingko biloba* flavonoids include several

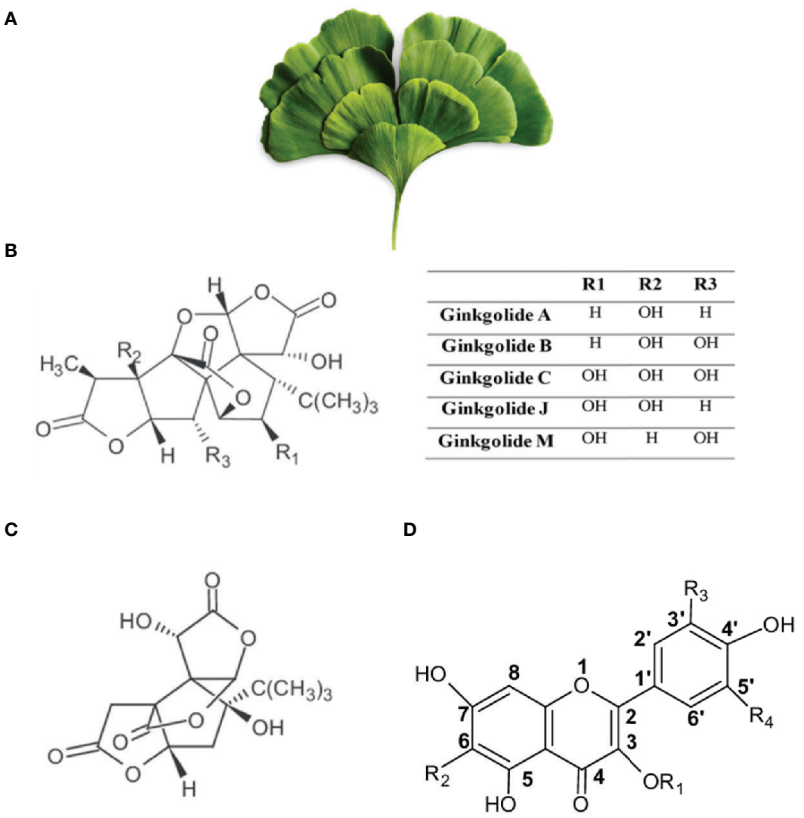

FIGURE 3 | *Ginkgo biloba*. **(A)** Leaves of *Ginkgo biloba* or Maiden Hair Tree (from https://pngtree.com/freepng). **(B)** Chemical structure of Ginkgolides. **(C)** Chemical structure of Bilobalides. **(D)** Structural skeleton of flavonoids. R1 and R2 are side chains.

representative glycosides, such as kaempferol, quercetin, and isorhamnetin (**Figure 3**). Flavonoids are known to reduce free radical generation and terpenoids are known to reduce inflammation and protect nerve cells against neuro-inflammation (Kleijnen and Knipschild, 1992; Ude et al., 2013; Isah, 2015). Through a multistep process, *Ginkgo biloba* dried leaves extracts are enriched for flavonoids and terpenoids and the unwanted substances are eliminated. At the final step, the liquid extract is dried to give 1 part extract from 50 parts of raw drug (leaves) (Kleijnen and Knipschild, 1992; Isah, 2015). The composition of *Gingko biloba* extracts may differ depending on the manufacturing process. Standardized extract forms have been developed and usually contain 24–36% flavone glycosides and 4–11% terpenoids. For example, standardized extract EGb761 is the most commonly used *Ginkgo biloba* extract (GBE), and it contains 24% ginkgo flavonoid glycosides, 6% terpene lactones, and 5–10% organic acids (Kressmann et al., 2002; Chan et al., 2007). These extracts have been used for various therapeutic purposes, including regulation of cerebral blood flow (Mashayekh et al., 2011), protection against free radicals (Oyama et al., 1996; Bridi et al., 2001), tinnitus treatment (Mahmoudian-Sani et al., 2017), protection of neurons (Mahdy et al., 2011), as well as enhancement of cognitive functions, such as memory and concentration problems (Weinmann et al., 2010; Tan et al., 2015).

Ginkgo biloba at the Bench: Mechanism of Action in CVDs

Ginkgo biloba's therapeutic effects and pharmacological actions are majorly due to its constituent flavonoids (ginkgo-flavone glycosides) and terpenoids (ginkgolides and bilobalide) (Lacour et al., 1991). These *Ginkgo biloba* constituents are well known for their antioxidant and anti-inflammatory effects. *Ginkgo biloba* antioxidant and anti-inflammatory effects are beneficial in a plethora of diseases that include cardiovascular, pulmonary, and central nervous systems.

Free radical generation contributes to the development and progression of numerous CVDs, including vascular injuries and atherosclerotic plaque formation. During CVD pathogenesis, the equilibrium between free radical generation and antioxidant defense is greatly shifted toward the former (Singh and Niaz, 1996; Witztum and Berliner, 1998; Fulton and Barman, 2016). GBE greatly restores the disturbed oxidative state equilibrium due to their antioxidant action, which helps to scavenge excessive free radicals as well as reduce free radical generation.

In addition, vasodilatory and antihypertensive properties of GBE can exert cardioprotective benefits (Perez-Vizcaino et al., 2009). In this regard, GBE has exhibited ACE inhibitory activities (Mansour et al., 2011), activation of cholinergic pathways, endothelial health improvement, inhibition of endothelium activation and adhesion (Mesquita et al., 2017), and serum lipid-lowering activities (Liou et al., 2015; Huang et al., 2018) among other reported effects that are beneficial in CVD.

By acting as an anti-atherothrombotic and anti-inflammatory agent, GBE can limit LPS-induced proliferation of VSMCs and their morphological alterations. Furthermore, GBE can regulate the inflammatory response in blood vessels by decreasing the activity of the ROS producing enzyme, nicotinamide adenine dinucleotide phosphate (NADPH) oxidase (NOX), and reducing the phosphorylation of mitogen-activated protein kinases (MAPKs). Subsequently, MAPKs suppress toll-like-receptor-4 (TLR-4) expression in human aortic smooth muscle cells (Lin et al., 2007). GBE can also decrease the production of the enzyme involved in the rupture of atherosclerotic plaques, MMP-1, in oxidized LDL- and 4-hydroxynonenal-induced human coronary smooth muscle cells (Akiba et al., 2007). In the same model, the GBE constituent, Ginkgolide B, attenuated endothelial dysfunction by inhibiting monocyte chemotactic protein-1 (MCP-1), intercellular adhesion molecule-1 (ICAM-1), and vascular cell adhesion molecule-1 (VCAM-1) production in oxidized-LDL-induced HUVECs. Additionally, Ginkgolide B treatment reduced the expression of several inflammatory cytokines in oxidized-LDL-induced mouse RAW264.7 macrophages (Feng et al., 2018). Ginkgolide C, another GBE constituent, can reduce adipogenesis and enhance lipolysis leading to suppression of lipid accumulation. Ginkgolide C treatment of 3T3-L1 adipocytes decreased the expression of PPAR adipogenesis-related transcription factors. Ginkgolide C also enhanced the Sirt1/AMPK pathway resulting in decreased activity of acetyl-CoA carboxylase and fatty acid synthesis. Moreover, Ginkgolide C stimulated the production of adipose triglyceride lipase and hormone-sensitive lipase, leading to elevated lipolysis levels (Liou et al., 2015). Similar results were obtained with human HepG2 hepatocyte cell line (Huang et al., 2018).

In Vivo Preclinical Evaluation of *Ginkgo biloba*

Ginkgo biloba has several cardioprotective effects, including improvement of atherosclerosis due to their ability to block platelet-activating factor and platelet aggregation in rats (Zeng et al., 2013; Huang et al., 2014).

eNOS is responsible for most of the vascular NO production, and NO acts as a protective molecule to maintain vasculature hemostasis and protection of the vascular endothelium (Forstermann and Munzel, 2006). eNOS production and activity are impaired in several CVDs, including hypertension (Chou et al., 1998), cardiac hypertrophy (Ozaki et al., 2002), myocardial infarction (Tsutsui et al., 2008), and heart failure (Couto et al., 2015). GBE can act as an antihypertrophic agent by the activation of the M_2 muscarinic receptors/NO pathway and of cholinergic signaling during cardiac hypertrophy. In a rat model of chronic β-adrenergic stimulation-induced cardiac hypertrophy, GBE was able to ameliorate the deleterious cardiac events associated with cardiac hypertrophy. These effects were mediated by the upregulation of M_2 receptors and the downregulation of β_1-adrenergic receptors. GBE also restored eNOS activity and consequently elevated NO levels (Mesquita et al., 2017). In addition, the anti-hypertensive effects of EGb761 supplementation were documented in hypertensive rats where SBP, DBP, and arterial BP were reduced. EGb761 supplementation also decreased inflammation and oxidative stress. While eNOS protein

expression levels were enhanced, protein levels of iNOS were decreased (Abdel-Zaher et al., 2018).

Vascular aging is commonly accompanied with low-grade inflammation and degenerative structural changes and stiffness of blood vessels and is considered a risk factor for the development of CVDs, such as CHD and hypertension (Franceschi et al., 2000; Lakatta and Levy, 2003). In the mesenteric arterioles of old rats, GBE had a protective effect that alleviated arterial stiffness and improved endothelial health (Cuong et al., 2019). In these aged mesenteric arterioles, GBE improved vascular elasticity by narrowing the EC gap, increasing curvature of inner elastic membrane and reducing the middle collagen fiber layer. These changes were accompanied by decreased phosphorylation levels of Akt/FoxO3a signaling components, which usually contributes to vascular dysfunction (Cuong et al., 2019).

Pre-treatment with EGb761 in rats that have undergone myocardial ischemia–reperfusion injury inhibited the apoptosis of myocardial cells, decreased the expression of caspase 3 and pro-apoptotic Bax and increased that of anti-apoptotic Bcl-2, and protected the myocardium by activating the endogenous Akt/Nrf2 antioxidant stress pathway. Akt/Nrf2 activation subsequently decreased oxidative stress leading to reduced lipid peroxidation and increased activities of the endogenous anti-oxidant defense enzymes, namely SOD, and GSH-Px. In addition, EGb761 pre-treatment increased the expression of the heat shock protein heme oxygenase 1 (HO-1) and repressed the expression of mediators of the inflammatory response, such as TNF-α, IL-6, and IL-1β (Chen et al., 2019). HO-1 degrades heme (a potent oxidant) to generate carbon monoxide, which has anti-inflammatory properties, bilirubin, which is an antioxidant derived from biliverdin, and iron (He et al., 2014). Similar *Ginkgo biloba* anti-oxidant properties have been reported in diabetic rats as well. Administration of GBE for 30 days can increase SOD, CAT, and GSH-Px activity along with glutathione (GSH) levels in the liver and pancreas of diabetic rats (Cheng et al., 2013). This enhanced anti-oxidant status might be responsible for improved glucose uptake *via* increased GLUT-4 expression (Shi et al., 2010). Furthermore, EGb761 oral supplementation of HFD-fed mice can dose-dependently enhance glucose tolerance, decrease insulin levels, and diminish parameters of insulin resistance (Cong et al., 2011).

The above reports point that GBE has a pleiotropic mechanism of action. Indeed, a metabolomic profiling study of the plasma and hearts of GBE-supplemented rats with myocardial infarction established that GBE acts *via* the regulation of multiple metabolic pathways. Metabolomic profiles of rats with MI showed disturbed metabolism in these rats because of modulated inflammatory reaction, oxidative stress, and structurally damaged pathways. However, GBE supplementation controlled the inflammatory reaction and oxidative stress pathways by regulating sphingolipid, phospholipid and glyceride metabolism and ameliorated the structural damage by downregulating amino acid metabolism (downregulation of urea cycle) and decreasing oxidative stress (Wang et al., 2016).

In addition to the above-mentioned effects, GBE was able to decrease calcium overload (Liu et al., 2013), the primary factor responsible for the irreversible myocardial injury (Moens et al., 2005). Rats with an ischemic myocardium and pre-treated with GBE50, an extract that matches EGb761, exhibited decreased intracellular calcium overload which could block arrhythmia. GBE could decrease the calcium overload and protect from an ischemic myocardium by inhibiting the Na^+/Ca^{2+} exchanger (Liu et al., 2013).

Ginkgo biloba to the Clinic

Given the above reported protective and therapeutic benefits of GBE *in vitro* and *in vivo*, several clinical trials have been conducted to test different formulations and doses of GBE in a plethora of diseases (DeKosky et al., 2008; Gardner et al., 2008; Kuller et al., 2010; Hashiguchi et al., 2015). A search of clinicaltrials.gov shows that there have been 88 reported clinical trials using various formulation of GBE. Of the 88 trials, 66 have been concluded, and there are 30 Phase 3 or 4 trials. Most of these trials dealt with neural and cognitive disorders, where GBE has been shown to have clinical promise. For GBE beneficial effects in CVDs, 7 out of the 88 trials were concerned with vascular diseases, 4 with stroke, 4 with arteriosclerosis, 2 with coronary disease, 1 with hypertension, and 1 with atherosclerosis.

GBE has vasorelaxation effects in human subjects. GBE was able to dilate forearm blood vessels causing changes in regional blood flow without affecting BP levels in 16 healthy subjects (Mehlsen et al., 2002). A small trial performed in normal glucose-tolerant subjects to determine the effects of GBE on glucose-stimulated pancreatic beta-cell function found that the ingestion of GBE for three months can decrease SBP and DBP. In these individuals, fasting plasma insulin and CRP were increased (Kudolo, 2000). A double-blind, placebo-controlled, parallel design trial was performed in patients with peripheral artery disease aimed to assess the effects of the supplementation of 300 mg/day of EGb761 to treadmill walking time and cardiovascular measures. In older adult patients, EGb761 produced a modest non-significant increase in maximal treadmill walking time and flow-mediated vasodilation. The authors suggested that a longer duration might be needed to observe significant beneficial effects (Gardner et al., 2008).

Kuller el al. used the Ginkgo Evaluation of Memory Study (GEM) to assess CVD as a secondary outcome. The GEM study was a double-blind trial that randomized 3069 participants whose ages were over 75 years to 120 mg of EGb761 twice daily (240 mg/day) or placebo. Data indicated that EGb761 did not affect the originally assessed primary outcome—the development of dementia or Alzheimer's disease (DeKosky et al., 2008). Also, there were no differences in the incidence of myocardial infarction, angina pectoris, or stroke between the GBE and placebo groups. After 6 years of monitoring, the study concluded that GBE does not reduce total CVD mortality or CVD events (Kuller et al., 2010).

Several clinical trials to assess the protective effects of GBE in CVDs are still ongoing. A 12-weeks randomized, double-blind, phase 3 clinical trial aimed to further evaluate the safety and efficacy of Rinexin® (Cilostazol 100mg, *Ginkgo biloba* leaf extract 80mg) which is widely used as an anti-platelet agent for the treatment of

peripheral artery disease (NCT03318276; clinicaltrials.gov). Most recently, efficacy and safety of *Ginkgo biloba* pills for CHD patients with impaired glucose regulation will be assessed in a Phase 4 randomized, double-blind, placebo-controlled clinical trial (NCT03483779; clinicaltrials.gov). Twelve patients will be recruited for a test period of 58 weeks. Pills of five different GBEs will be to administered three times a day (Sun M. et al., 2018).

The therapeutic effect GBE appears to be more evident in combination with modern medicine. The analysis of 23 randomized clinical trials (involving 2,529 patients) showed that when combined with routine Western medicine, GBE was more effective at the relief of angina pectoris as compared to the routine medicine alone (Sun et al., 2015). In addition, due to its platelet aggregation inhibitory effects, the combination of GBE and modern medicine was reported to posses beneficial effects against acute cerebral ischemia. In that study, platelet aggregation was found to be significantly lower in patients treated with ticlopidine and EGb 761 as compared with patients treated with ticlopidine alone (Hong et al., 2013). Combination of EGb 761 also had increased therapeutic effect in patients with uncontrolled diabetes. Indeed, a randomized controlled trial showed that the combination of EGb 761 with metformin is more effective than metformin alone in improving the outcomes of patients with uncontrolled T2DM (Aziz et al., 2018).

The GBE therapeutic potential in managing CVDs has not been always clinically observed. Using data obtained from the GEM study database, Brinkley et al. concluded that GBE does not reduce BP or the incidence of hypertension in older men and women (Brinkley et al., 2010). In accordance, another study reporting the analysis of 9 randomized clinical trials (1012 hypertensive patients) concluded that more rigorous trials are needed to draw a conclusion on the efficacy of GBE in managing hypertension (Xiong et al., 2014).

Based on these and other studies, the efficacy of GBE, despite being reported in many studies, is best documented and observed when combined with other known medications for the management of CVDs.

Safety, Toxicity, and Side Effects of *G. biloba*

Taken orally at the typical dosage, GBE may cause mild adverse effects, principal among which are mild gastrointestinal upset, headache, dizziness, constipation, and allergic skin reactions. Higher dosages, however, can result in restlessness, diarrhea, nausea, vomiting, and weakness (Diamond and Bailey, 2013). Noticeably, the therapeutic employment of this herb is also linked to adverse cardiovascular events. Fifteen published case reports described a temporal association between GBE intake and serious bleeding events, including intracranial bleeding (Bent et al., 2005), an effect that may be attributed to the platelet-activating factor antagonism exerted by ginkgolides, bilobalides, and other constituents present in the extract (Izzo and Ernst, 2009). These major bleeding events, including subarachnoid and intracranial hemorrhage, have been mostly described during the concomitant use of gingko and antiplatelet and/or anticoagulant medications (Matthews, 1998). Therefore, it is recommendable to stop GBE intake at least 2 weeks before surgical procedures. Always because of its anti-platelet properties, it has been suggested that GBEs (including seeds and leaves) should be used with caution during pregnancy, particularly around labor, and during lactation (Dugoua et al., 2006). Several case reports described cardiac adverse events associated with *Ginkgo biloba* leaf extracts. For example, 2 weeks GBE intake (40 mg, three times daily) has been reported to develop ventricular arrhythmia in a 49-year-old subject with good health (Cianfrocca et al., 2002), a symptom resolved upon the discontinuation of GBE supplementation (Cianfrocca et al., 2002).

A randomized placebo-controlled, double-blind pilot study of GBE reported more ischemic stroke and transient ischemic attack cases in the GBE group as compared with the placebo. The study lasted 42-month 118 cognitively intact subjects randomized to standardized GBE or placebo and its aim was to measure the effect of GBE on cognitive decline (Dodge et al., 2008). Another case report, attributed the frequent nocturnal palpitations reported by a 35-year old woman taking GBE supplementation to GBE (Russo et al., 2011). In addition to clinical trials, *Ginkgo biloba* safety has also been assessed *in vivo* in rats. Dietary intake of GBE (0.5% extract) for 4 weeks has been reported to significantly reduce heart rate and blood flow velocity in tail arteries of old spontaneously hypertensive (SH) rats as compared to the control group (Tada et al., 2008). Thus, in the elderly population with hypertension, the use of GBE may need to be assessed for effects on heart rate (Mei et al., 2017).

Furthermore, some of the components (ginkgolic acids) of EGb761 have been reported to elicit severe allergic reactions. However, this allergic reaction is not present as long as the carboxylic acid group of ginkgolic acids is intact (Chan et al., 2007). Yet, contact with *Ginkgo biloba* plants is associated with severe allergic reactions, including erythema and edema (Chiu et al., 2002)

Food poisoning by *Ginkgo biloba* seeds has been reported in Japan and China, where the main symptoms were convulsion, vomiting, and loss of consciousness. The poisoning is primarily due to the neurotoxic compound 4′-O-methylpyridoxine (MPN, also known as ginkgotoxin) which interferes with pyridoxine (vitamin B_6) metabolism, leading to serious neurological manifestations including neurotoxicity, seizures, and loss of consciousness (Wada et al., 1988; Wada, 2005). Ginkgotoxin is found in the ginkgo leaf at very low amounts. However, GBE is unlikely to contain this toxic component as ginkgotoxin is standardized to be too low in the extract (Arenz et al., 1996).

Several reports have described that GBE induces cytochrome P450 (CYP) in humans, shedding light on potential interactions between GBE and conventional drugs. *Ginkgo biloba* is known to decrease the plasma concentrations of omeprazole, ritonavir, and tolbutamide. It can interact with antiepileptics, acetylsalicylic acid, diuretics, ibuprofen, risperidone, rofecoxib, trazodone, and warfarin (Izzo and Ernst, 2009).

Considering that GBE is widely used in a plethora of diseases combined with the paucity of data from animal studies regarding

GBE toxicity and carcinogenicity, the National Institutes of Health (NIH) has performed a 2-year and 3-month toxicity and carcinogenicity study of GBE in B6C3F1/N mice and F344/N rats using different doses of GBE. The GBE used contained 24% flavonol glycosides and 6% terpene lactones, along with no more than five ppm ginkgolic acids. The study was performed by NIH National Toxicology Program (NTP) and concluded that GBE might elicit toxic and cancer-related consequences in rodents. The carcinogenic effects reported were stomach ulcers, organ modification including carcinogenic activity in the liver, liver and thyroid gland hypertrophy, liver hyperplasia, and hyperkeratosis (National Toxicology Program, 2013; Rider et al., 2014). These reports raised concerns about the safety of GBE. Following the NTP report, the International Agency for Research on Cancer (IARC) reported in 2014 that there is inadequate evidence in humans for the carcinogenicity of GBE (Grosse et al., 2013). Following this report, clinical and genomic safety of IDN 5933/ Ginkgoselect®Plus, a standardized GBE, was assessed in elderly subjects using a randomized placebo-controlled clinical trial. The treatment group was given 120-mg IDN 5933 twice-daily for 6 months. No adverse clinical effects or increase of liver injury markers were reported in the treatment group. Genomic testing revealed that there is no difference in micronucleus frequency or DNA breaks between the treated and placebo groups. The expression of genes known to be modulated in early carcinogenesis (c-*myb, p53*, and *ctnnb1* [β-catenin]) was not significantly different between groups at the beginning or the end of the study (Bonassi et al., 2018). Taken together these results support the safety of IDN 5933 at the used doses for a duration of 6 months. Overall, there is still controversy about the safety of GBE for long-term use in human subjects and additional well-designed clinical trials that assess the safety and efficacy of GBE are much needed.

GANODERMA LUCIDUM

Ganoderma lucidum, also known as "lingzhi" or "reishi," is a mushroom (**Figure 4**) whose different parts (mycelia, spores, and fruit body) are used to make different forms of commercial *G. Lucidum* for their medicinal benefits. Commercially, *G. Lucidum* is available as powders, dietary supplements, tea, among other forms. Historically, *G. Lucidum* medicinal use has been wide spread in Asian countries (mainly in China, Japan, and Korea) for more than 2000 years. Later, it was introduced to Western societies (Ahmad, 2018). Hot water or ethanol can be used to extract the bioactive compounds from the fruiting bodies, the mycelia, or the spores of the mushroom (Heleno et al., 2012). A wide array of bioactive compounds exist in *G. Lucidum* that include triterpenes (**Figure 4**), polysaccharides, nucleosides, steroids, fatty acids, alkaloids, proteins, peptides, amino acids, and inorganic elements (Ahmad, 2018).

Immunomodulation, anti-oxidation, liver protection, anti-proliferation, and anti-angiogenesis are among the various properties that *Ganoderma lucidum* bioactive compounds possess individually or synergistically (Sanodiya et al., 2009). The triterpenoids have hepatoprotective, anti-hypertensive, hypo-cholesterolemic, anti-histaminic, anti-tumor, and anti-angiogenic effects. In addition, *Ganoderma lucidum* triterpenoids have anti-platelet aggregation and complement inhibition effects. It should be noted that *G. Lucidum* is the only source of triterpene fatty acids called ganoderic acids. Of the 200 bioactive compounds that have been identified in *Ganoderma lucidum* extracts,

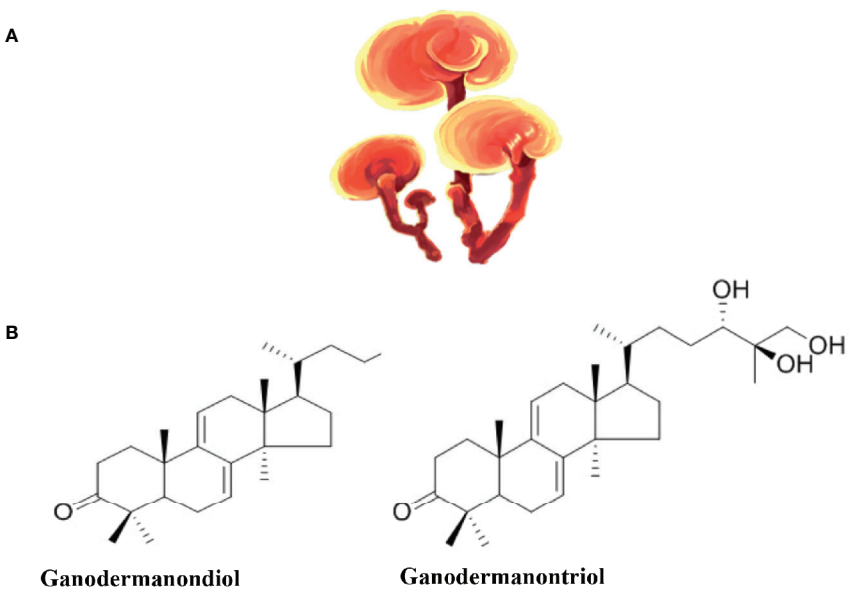

FIGURE 4 | *Ganoderma lucidum*. **(A)** *Ganoderma lucidum* (from https://pngtree.com/freepng). **(B)** Examples of the chemical structure of two Triterpenes from *Ganoderma lucidum*.

ganoderic acids A, B, and C have hypoglycemic effects (Hikino et al., 1985; Tomoda et al., 1986), while ganoderic acids F, B, D, H, K, S, and Y most likely have hypotensive effects (Morigiwa et al., 1986). *Ganoderma lucidum* polysaccharides (β-d-glucans) harbor anti-tumor properties due to their immunomodulation and anti-angiogenesis effects. They also exhibit anti-oxidant protective effects against free radicals and can decrease mutagen induced cell damage (Boh et al., 2007). *Ganoderma lucidum* β-d-Glucan polysaccharides were also identified as the active component in the polysaccharide peptide (PsP) usually found in *Ganoderma lucidum* extracts. There is no agreed dosage for *G. lucidum*, however, commonly used doses vary between 1.5 and 9 g of dried extract per day (Klupp et al., 2016).

G. lucidum at the Bench: Mechanism of Action in CVDs

As stated earlier, antioxidants are very important when it comes to the prevention of atherosclerosis. *G. lucidum* can act as an antioxidant; in the model organism *Caenorhabditis elegans, G. lucidum* protected *C. elegans* against paraquat and heavy metal-induced oxidative stress *via* the diet restriction pathway and the mTOR/S6K signaling pathway, respectively (Cuong et al., 2019). *G. lucidum* has been found to protect human lymphocyte DNA from hydrogen peroxide-induced oxidative damage (Shi et al., 2002). It was also found that *G. lucidum* regulates the expression of Nrf2 which in turn regulates antioxidants genes such as HO-1, GST, NQO-1; *G. lucidum* ethanol extract enhanced the phosphorylation of Nrf2 which upregulated HO-1 in C2C12 myoblasts (Lee Y. et al., 2016). Thus, the antioxidant power in *G. lucidum,* which is important for the prevention of atherosclerosis, can act on different signaling pathways.

Elevated BP can be detrimental to heart function. Three peptides (QLVP, QDVL, and QLDL), that can inhibit ACE activity and called ACE inhibitory peptides (ACEIPs), were extracted from *G. lucidum* and can be used to treat hypertension. QLVP can inhibit ACE by its interaction with Gln242 and Lys472 of ACE. QLVP also enhanced Angiotensin 1-mediated phosphorylation of eNOS and reduced mRNA and protein expression of the vasoconstrictor peptide endothelin-1 in HUVECs (Wu et al., 2019).

Selenium-enriched *G. lucidum* polysaccharide (Se-GLP) extracts have protective effects against oxidative damage in a mouse model of heart reperfusion injury. Se-GLP significantly reduced the ischemic reperfusion injury-induced serum levels of MDA as well as the levels of the proinflammatory molecule intercellular adhesion molecule-1. Heart and serum levels of the antioxidant enzymes SOD, CAT, and GSH-Px and the levels of GSH as well as total antioxidant capacity were rescued by Se-GLP (Shi et al., 2010). In another study, the protective effects of Ganoderic acid A, from *G. lucidum* extracts, was found to activate the PI3K/AKT signaling pathway causing increased proliferation and decreased apoptosis of rat H9c2 cardiomyocytes exposed to hypoxic injury, a phenomenon mediated by the activation of miR-182-5p and reduction of PTEN expression (Zhang et al., 2018). Similarly, a preclinical study using transverse aortic constriction mice as a model of pressure overload-caused cardiomyopathy reported improved cardiac function following treatment with spore oil extracted from *G. Lucidum* (Xie et al., 2016).

More research needs to be conducted on the possible mechanisms and signaling pathways that *G. Lucidum* bioactive derivatives employ to elicit their beneficial effects in order to get a more comprehensive sense of how these substances work.

In Vivo Preclinical Evaluation of *G. lucidum*

To study the cardioprotective effects of *G. lucidum* extract, global ischemia and reperfusion of isolated and perfused rat hearts were used. As a preventative treatment, 400 mg/kg body weight of *G. lucidum* extract was delivered to rats for 15 days. It was found that this treatment halted the necrotic death of the rat cardiomyocytes and reduced the reperfusion contracture (Lasukova et al., 2015). Interestingly, *G. lucidum* extract supplementation attenuated diastolic dysfunction and prevented irreversible cardiomyocyte damage (Lasukova et al., 2008).

Diabetes mellitus is a metabolic disease that has been correlated with a high incidence of CVDs, partly because high blood glucose levels can cause vascular damage (Klein et al., 2002; Fox et al., 2008; Shah et al., 2008). Thus, a supplement that can help manage diabetes would be of great benefit to decrease CVD risk. Thirty-five Wistar rats were supplemented with 50, 150, and 300 mg/kg of PsP from *G. lucidum* extracts. PsP induced endothelial repair process with 300 mg/kg being the most efficient dose. The findings showed that vascular damage was improved by PsP treatment in a rat model of T2DM (Heriansyah et al., 2019).

A diet high in fats is known to be a contributing risk factor to the development of CVDs (Fleming, 2002) and weight loss is an essential measure for the prevention of CVDs in obese people (Sowers, 2003). The water extract of *G. lucidum* can reduce the body weight, inflammation, and insulin resistance in HFD-fed mice (Chang et al., 2015). In another study, *G. lucidum* spores (GLSP) at a dose of 1 g/day supplemented orally for 4 weeks were used in adult male Sprague-Dawley rats. GLSP decreased total cholesterol and triglycerides in diabetic rats as well as attenuated the levels of oxidative stress; it is worth noting that there was an upregulation of genes related to lipid metabolism—acyl-CoA oxidase 1 (ACOX1), acetyl-CoA carboxylase (ACC), and Insig-1/2 gene expression. ACOX1 was activated more than 5-folds in the GLSP-treated diabetic rats which indicates an accelerated beta-oxidation of lipids in these rats (Wang et al., 2015).

Dyslipidemia is one of the major risk factors for CVDs (Miller, 2009). In experimental animal studies, *G. lucidum* showed anti-hyperlipidemic effects by lowering plasma total cholesterol, LDL, and triglyceride levels (Chen et al., 2005). Hydrogen peroxide free radicals are usually elevated during dyslipidemia, and thus the risk of atherosclerosis, so antioxidants are needed to prevent blood vessels damage. A study conducted in high cholesterol diet-supplemented Wistar rats that received 50, 150, and 300 mg/kg bodyweight of PsP derived from *G. Lucidum* found that PsP acted as a potent antioxidant. In addition, PsP may prevent the atherogenesis process in the context of dyslipidemia with the optimum dose being 300 mg/kg bodyweight (Wihastuti and Heriansyah, 2017).

Another study found that polysaccharides extracted from *G. Lucidum* significantly reduced the body-weight increases of mice fed an HFD suggesting its role as a hypolipidemic substance. In addition, it exhibited antioxidant and antiapoptotic effects in the HFD-fed mice (Liang et al., 2018).

With regard to regulation of high BP, a study conducted on adult male hypertensive rats that received *G. lucidum* water extracts intra-gastrically for seven weeks found that the experimental rats BP was reduced to a level comparable to that of rats on losartan (angiotensin II receptor antagonist) (Shevelev et al., 2018)

G. lucidum to the Clinic

Antioxidants are potentially therapeutic substances that can be used to prevent atherosclerosis as well as a variety of other diseases. Several *in vitro* and *in vivo* preclinical studies have shown that *G. lucidum* constituents possess antioxidant activities, but evidence for such activities in human subjects was lacking. Watchtel Galor et al. performed a follow-up study on the effects of *G. lucidum* supplementation on an array of parameters that included antioxidant biomarkers status and CHD risk. A double-blinded, crossover, placebo-controlled intervention study of 18 healthy people was conducted. There was an enhancement of plasma total antioxidant markers status as well as an improvement of CHD biomarkers after 10 days of supplementation. More importantly, there was no renal, liver, or DNA toxicity (Wachtel-Galor et al., 2004). To test *G. Lucidum* antioxidant potential, a crossover human intervention study was conducted on seven healthy people, and it was found that the plasma total antioxidant power was enhanced after the administration of a single dose of *G. Lucidum* extract. Lymphocytes harvested following blood collection, however, showed no signs of enhanced DNA repair (Wachtel-Galor et al., 2010). *G. lucidum* PsP was also examined for its antioxidant properties. A clinical trial was conducted with 37 high risk and 34 stable angina patients that were given PsP 750 mg/day for 90 days. PsP proved to be a potent antioxidant in the context of atherosclerosis in both the high angina risk and stable groups. PsP supplemented groups showed increased SOD, decreased MDA levels, and reduced counts of circulating endothelial cells (CEC) and endothelial progenitor cells (EPC) (Sargowo et al., 2018).

A double-blind, randomized, multicentered study was done to evaluate the effects and safety of *G. lucidum* polysaccharides on patients with CHD. Eighty-eight patients that constituted the experimental group were given *G. lucidum* polysaccharides for 12 weeks. The polysaccharides significantly enhanced the wellbeing of the patients evidenced as an improvement of their major symptoms (chest pain, shortness of breath, palpitations), and a decrease in BP and serum cholesterol levels (Gao et al., 2004). Another study found that PsP from *G. lucidum* had anti-inflammatory effects and vascular EC protection in patients with ST-elevation myocardial infarction and non-ST-elevation myocardial infarction with risk factors of dyslipidemia (Sargowo et al., 2019).

A randomized clinical trial was conducted on the use of *G. lucidum* for the treatment of cardiovascular risk factors of the metabolic syndrome. It was reported that using *G. lucidum* (3 g/d) for 16 weeks had no effect on glycosylated hemoglobin (HbA1c) and fasting plasma glucose (FPG). Further, consumption of *G. lucidum* was associated with the increased risk of a subset of mild events including headache, fatigue, and gastrointestinal events (Klupp et al., 2016).

None of the human studies reported above had any serious side effects thus highlighting *G. lucidum* as a potential therapeutic and preventative substance in the context of certain CVDs.

In a study examining 37 patients with high risk for atherosclerosis and on an ongoing conventional CVD medication, *G. lucidum* PsP was able to reduce the levels hs-CRP, IL-6, and TNF-α, as well as the levels of MDA (Widya et al., 2016). Another study involving 34 stable angina pectoris patients showed that administration of PsP in combination with previous medication is able to significantly reduce CECs and EPCs (markers for endothelial vascular injury) as well as the levels of total cholesterol (Ubaidillah et al., 2016).

The efficacy of *G. lucidum* in CVDs was tested in a prospective, double-blind, placebo-controlled trial. Eighty-four volunteers with T2DM and metabolic syndrome were supplemented with extracts of *G. lucidum, G. lucidum* with *Cordyceps sinensis*, or placebo in order to manage cardiovascular risk factors. Results from the study evidenced that *G. lucidum* failed to provide benefit against CVDs in patients with the metabolic syndrome (Klupp et al., 2016). Likewise, the analysis of five trials (398 total volunteers), concluded that *G lucidum* was not effective in treating elevated BP (Klupp et al., 2015).

Taken together, these data suggest that *G. lucidum* is most effective in providing cardiovascular protection when combined with conventional CVDs medications.

Safety, Toxicity, and Side Effects of *G. lucidum*

Numerous conducted studies and investigations pointed toward the safety of *G. Lucidum.* In both male and female rodents, *G. lucidum* shows no signs of toxicity even at a dose of up to 5000 mg/kg of body weight. No animal mortality was reported either (Smina et al., 2011). When compared to doxorubicin (a typical DNA intercalating agent used in chemotherapy), *G. lucidum* extracts were shown to act indirectly on DNA, thus adding more assurance to its safety (Gurovic et al., 2018).

Hemostatic parameters, platelet and global hemostatic functions, were not affected when a dose of 1.5 g/d of *G. lucidum* extract was given to healthy human volunteers for 4 weeks. In addition, the use of *G. lucidum* did not cause bleeding problems in the healthy subjects (Kwok et al., 2005). However, in another study, Tao and Feng volunteered 15 healthy subjects and 33 atherosclerotic patients and found that any dose above 3000 mg/day can inhibit platelet aggregation. As a result, caution is advised when supplementing *G. lucidum* to patients with low platelet count or patients that will undergo surgical procedures (Tao and Feng, 1990).

Safety of polysaccharides extracted from the fruiting body of *G. lucidum* was evaluated in Wistar rats and the results indicated no evidence of abnormal clinical symptoms, death or significant differences in body weight and food intake. No significant differences were found in the hematology value, clinical chemistry value and organ/body weight ratio. Additionally, no mutagenicity was detected in Kunming mice (Zhang et al., 2016).

However, high doses of *G. lucidum* polysaccharides modulated immune responses. The polysaccharides enhanced the primary immune response to sheep red blood cells but did not have significant effects on the phagocytic function or macrophages (Zhang et al., 2016). The *G. lucidum* polysaccharides-modulated immune responses were tested in another study where 16 participants supplemented with 2 g of *G. lucidum* extract twice daily took part in a 10-day controlled trial. In this study, there were no differences in CD4, CD8, and CD19 levels in the blood, though CD56 did increase, without achieving statistical significance, but it returned to baseline levels 10 days after intake of the extract (Wicks et al., 2007).

A 12-week trial performed on 23 dyslipidemic and mild hypertensive volunteers revealed that Lingzhi (1.44 g/day) had no effect on several clinical chemistry parameters as compared with the placebo. However, symptoms such as headache, influenza/running nose were found, although considered not clinically significant (Chu et al., 2012).

Whether these changes that are induced by *G. lucidum* have any clinical value remains to be addressed in future clinical trials especially after long-term administration of escalating doses of *G. lucidum* extracts to assess long-term safety. Further studies are still needed to examine the toxicity, side effects, and safety of *G. lucidum* for human consumption.

GYNOSTEMMA PENTAPHYLLUM

Gynostemma pentaphyllum (**Figure 5**), also known as Jiaogulan, is a herbaceous climbing vine. Originating in south China and now widely distributed in South and East Asia (Li et al., 2016), it is found in subtropical China, Japan, Myanmar, and India (Chen and Gilbert, 2006), growing near rivers and in the shade of forests that surround Yangtze River basin and the southern areas of China (Chen, 1995). It can be found as a health supplement in beverages, biscuits, face washes, and bath oils (Li et al., 2016). The herb has a low level of genetic diversity and a high level of variation among populations (Zhang et al., 2019).

Phytochemical analysis found that *G. pentaphyllum* extracts contain gypenoside saponins, flavonoids, polysaccharides, and amino acids (Zheng, 2004; Nookabkaew et al., 2006; Yan et al., 2013). Its biological effects can range from antimicrobial (Srichana et al., 2011), antioxidant (Muller et al., 2012), anticancer (Schild et al., 2010), anti-inflammatory (Wong et al., 2017), antidiabetic (Yeo et al., 2008; Huyen et al., 2012), antilipidemic (la Cour et al., 1995), and neuroprotective (Keilhoff et al., 2017) to anti-obesity effects (Gauhar et al., 2012; Park S. et al., 2014). It has been used to treat hepatitis and hypertension (Lin et al., 2000). Among the various bioactive compounds, dammarane-type triterpene saponins (gypenosides or gynosaponins) are major (Kim and Han, 2011).

G. pentaphyllum at the Bench: Mechanism of Action in CVDs

As already mentioned, antioxidants are important when it comes to the prevention of atherosclerosis. Four flavonoids—namely quercetin-3-O-(2″,6″-di-α-L-rhamnosyl)-β-D-galactopyranoside, quercetin-3-O-(2″,6″-di-α-L-rhamnosyl)-β-D-glucopyranoside, quercetin-3-O-(2″-α-L-rhamnosyl)-β-D-galactopyranoside, and quercetin-3-O-(2″-α-L-rhamnosyl)-β-D-glucopyranoside—with potent antioxidant effects against DPPH and OH free radicals, *in vitro,* were found in the extracts of *G. pentaphyllum.* These flavonoids also exhibited cytoprotection against AAPH-induced oxidative damage in pig kidney LLC-PK1 cells by suppressing the increase of MDA, and limiting the decrease of SOD and GSH (Lin et al., 2019). In another study, flavonoids from *G. pentaphyllum* were extracted and tested on human lung carcinoma A549 cells. It was found that the flavonoids protected A549 cells against hydrogen peroxide-induced oxidative damage by increasing the expression levels members of the endogenous antioxidant system including SOD, GSH, Nrf2, NQO1, and HO-1 (Wang et al., 2018). Another study evaluated the antioxidant potential of one *G. pentaphyllum* component, the phytoestrogen gypenoside XVII, it was found that the phytoestrogen alleviated atherosclerosis *via* the ERα-mediated PI3K/Akt pathway (Yang et al., 2017). A prior study evaluated the effects of gypenosides of *G. pentaphyllum* on hydrogen peroxide-induced oxidative damage in bovine pulmonary artery ECs. The gypenosides protected the ECs from oxidative injury further suggesting its potent antioxidant activity as well as its prospective use as a preventative supplement against atherosclerosis (Li and Lau, 1993).

Inflammation can contribute to the onset of atherosclerosis and other CVD risk factors, hence, reducing inflammation can act as a protective factor in CVDs. The gypenoside XLIX (Gyp-XLIX) from *G. pentaphyllum* has been studied for its anti-inflammatory properties. Gyp-XLIX inhibited LPS- and TNF-α-induced NF-κB activation in THP-1 monocytes and in HUVECs. Gyp-XLIX inhibition of NF-κB activation appears to be through a PPAR-α-dependent pathway (Huang et al., 2006). On the other hand, contradictory results were reported by Aktan et al., where *G. pentaphyllum* gypenosides attenuated NF-κB activation. In fact, the gypenosides extracted from *G. pentaphyllum* could suppress NO production by inhibiting iNOS activity and levels in murine macrophages. Gypenoside-mediated decrement of iNOS protein expression turned out to be mediated by the inhibition of NF-κB activation (Aktan et al., 2003). In a different study, Tanner et al. showed that *G. pentaphyllum* could elicit beneficial effects on vascular function by acting as an inducer of eNOS (Tanner et al., 1999).

Attenuating lipid accumulation may decrease CVDs incidence. A study assessed the role of ombuine, a dual agonist of PPAR-α and

PPAR-δ/β in lipid metabolism. Ombuine or mbuin-3-O-β-d-glucopyranoside, a flavonoid from *G. pentaphyllum,* were applied to HepG2 cells. Ombuine-stimulated HepG2 cells had activated PPAR-α and PPAR-δ/β, transcription factors that enhance lipolysis. Ombuine-mediated activation of PPAR-α and PPAR-δ/β significantly reduced intracellular concentrations of triglyceride and cholesterol as well as decreased lipogenic gene expression witnessed as decreased levels of sterol regulatory element binding protein-1c and stearoyl-CoA desaturase-1. These findings further our understanding of how *G. pentaphyllum* may be involved in lipid metabolism (Malek et al., 2013).

In a study that evaluated the role of total flavonoids of *G. pentaphyllum* on apoptosis in cardiomyocytes of neonatal rats, it was found that hypoxia-reoxygenation (H/R)-cardiomyocytes had an increased protein expression of apoptosis-associated Fas/FasL genes. Flavonoids of *G. pentaphyllum* could protect cardiomyocytes against H/R injury by decreasing the production of TNF-α and downregulating the protein levels of Fas/FasL genes leading to inhibition of myocyte apoptosis (Le et al., 2007).

In Vivo Preclinical Evaluations of *G. pentaphyllum*

Gypenosides are *G. pentaphyllum* key components with the ability to help prevent atherosclerosis. The anti-atherosclerotic effects of a mixture (HG) of *Fermentum rubrum* Hongqu and *G. pentaphyllum* gypenosides were investigated in Wistar rats. The study results revealed that the HG mixture had anti-atherosclerotic effects that were better than statin, simvastatin, treatment highlighting the anti-atherosclerotic potential of *G. pentaphyllum* (Gou et al., 2018). In addition, HG alleviated oxidative stress biomarkers by restoring antioxidant defense components and decreasing the serum levels of anti-inflammatory cytokines in male Sprague-Dawley rats with fatty liver disease. The HG mixture in this study displayed athero-protective characteristics (Gou et al., 2016).

Emphasizing the reported *G. pentaphyllum* gypenoside anti-inflammatory and antioxidant capabilities, Yu et al. demonstrated their beneficial effects in an ischemia–reperfusion injury rat model where they were found to inhibit apoptosis. Ischemia–reperfusion injury has detrimental outcomes in CHD. Yu et al. found that in ischemia reperfusion injured-rats, the administration of gypenosides decreased apoptotic rates as well as improved cardiac function. Gypenosides inhibited ER-stress and apoptosis through the blockade of the CHOP pathway and the activation of PI3K/Akt pathway (Yu et al., 2016b). In a different study, it was demonstrated that pretreatment with gypenosides limited the infarct size and relieved ischemia reperfusion-induced pathological changes in the myocardium, also in an ischemia reperfusion injury rat model. Additionally, left ventricle function was preserved. Molecularly, gypenosides pre-treatment reduced oxidative stress and restored the antioxidant machinery in the myocardium. The cardio-protective effects were also evidenced by the preservation of mitochondrial function in myocytes. In this regard, the maintenance of the mitochondrial membrane integrity inhibited the release of cytochrome c from the mitochondria into the cytosol. This further demonstrated the role of gypenosides from *G. pentaphyllum* as a cytoprotective agent against acute myocardial infarction and reperfusion injury (Yu et al., 2016a).

As elucidated to earlier, diabetes is positively correlated with the development of CVDs. The effect of *G. pentaphyllum* extracts on fasting blood sugar levels in diabetic mice was assessed. It was found that the extracts had inhibitory effects on α-glucosidase activity while affecting the protein expression of GLUT2 which highlights its potential to manage diabetes (Wang et al., 2019).

Attenuating obesity, a risk factor for developing CVDs, may decrease CVD incidence. *G. pentaphyllum* is largely used for the management of diseases such as hyperlipidemia, fatty liver, and obesity in China. *G. pentaphyllum* was found to affect lipid metabolism and elicit anti-hyperlipidemic effects by elevating the levels of phosphatidylcholine and decreasing the levels of trimethylamine N-oxide in the plasma and liver of rats (Wang et al., 2013). In addition, Gauhar et al. studied the effects of heat processed ethanol extracts of *G. pentaphyllum* on obese mice. They found that this extract decreased obesity in *ob/ob* mice by activating the AMP-activated protein kinase (AMPK) pathway. This study suggested a possible mechanism for fat-loss as well as a potential for the use of *G. pentaphyllum* as a weight-loss supplement (Gauhar et al., 2012). Gypenosides anti-hyperlipidemic effects were examined in rats with poloxamer P407-induced hyperlipidemia. Gypenosides at 250 mg/kg of body weight was orally administered to hyperlipidemic rats. Four and 12 days of gypenosides administration reduced plasma triglycerides levels by 53% and 85%, respectively. Similarly, total cholesterol levels were decreased by 10% and 44%, respectively. Interestingly enough, results were similar to atorvastatin cholesterol-lowering statin drugs. Additionally, LDL levels were reduced and HDL levels were increased by gypenoside, which also reversed the poloxamer P407 inhibition of lipoprotein lipase activity. This shows a promising therapeutic potential of *G. pentaphyllum* for lowering high triglyceride and cholesterol levels during acute hyperlipidemia (Megalli et al., 2005). In accordance, extracts from the plant also decreased triglyceride levels and LDL levels in obese Zucher rats (Megalli et al., 2006). By employing a new extraction technique, Lee et al. described some biological activity of a *G. pentaphyllum* extract with a higher content of gypenoside L (1.8% w/w), gypenoside LI (1.4% w/w), and ginsenoside Rg3 (0.15% w/w) (Lee et al., 2019b). While HFD-fed mice showed significant clinical effects such as increases in body weight, fat mass, white adipose tissue, and adipocyte hypertrophy as compared to the control group, the GPE-treated group failed to show them. GPE treatment also reduced serum levels of triglyceride, total cholesterol, and LDL-cholesterol, without affecting HDL-cholesterol. Mechanistically, the clinically observed GPE effects appeared due to increased AMPK activation and suppressed adipogenesis by decreasing the mRNA levels of CCAAT/enhancer binding protein-α (C/EBPα), PPARγ, SREBP-1c, PPARγ coactivator-1α, fatty acid synthase, adipocyte protein 2, and sirtuin 1, and increased levels of

carnitine palmitoyltransferase and hormone-sensitive lipase (Lee et al., 2019b).

G. pentaphyllum to the Clinic

In general, there are few human trials that addressed *G. pentaphyllum* extract therapeutic effects or safety. A search on clinicaltrials.gov shows that there are only four studies that use *G. pentaphyllum* extracts. One of the studies is on obese patients and three are on diabetes mellitus patients.

Actiponin, an extract of *G. pentaphyllum,* is a dietary supplement used for weight loss in obese individuals. During an interventional study, 80 randomized Korean participants took part in a double blind, parallel study for 12 weeks where the experimental group took Actiponin at a dose of 450 mg/day. The experimental group lost weight with no adverse effects, as compared to the placebo group (Park S. et al., 2014).

In another study, 1 mg/kg of the water extract of *G. pentaphyllum* was given to 44 patients with CVDs and 56 healthy individuals and the platelet aggregation was studied. It was revealed that the water extract elicited significant inhibition of the aggregation of platelets. This means that there is potential for the use of this supplement to prevent cardio-cerebrovascular diseases while being cautious not to give these supplements to patients who suffer from low platelet count or bleeding disorders (Juan and Shanzhang, 1995).

Some studies suggest there is a link between anxiety disorders and an increased risk of developing a CVD (Fan et al., 2008; Vogelzangs et al., 2010; Seldenrijk et al., 2011; Batelaan et al., 2014). For this reason, it is of interest to reduce anxiety in order to decrease the risk of developing CVD in predisposed individuals. It was shown that *G. pentaphyllum* ethanol extract had anti-anxiety effects on mice exposed to chronic stress (Choi H. et al., 2013). This finding was replicated in a double-blind, placebo-controlled clinical trial that had 72 healthy Korean individuals under chronic stressful conditions. Thirty-six participants were given 200 mg of *G. pentaphyllum* ethanol extract, twice a day for 8 weeks. The supplementation reduced the experimental group anxiety without any adverse drug effects suggesting its potential as a safe anti-anxiety supplement (Choi et al., 2019).

Although the proven pharmacological effects of *G. pentaphyllum* in *in vitro* studies and *in vivo* animal studies may not necessarily translate well into efficacy human subjects, there are positive studies. For instance, a set of studies conducted in T2DM patients supplemented with *G. pentaphyllum* tea showed improvements in insulin sensitivity and glycemia with no adverse side effects (Huyen et al., 2010; Huyen et al., 2013). In one of the trials, 24 drug-naïve T2DM patients were randomized to take either 6 g daily of *Gynostemma pentaphyllum* tea or placebo tea, during 1- week period. The authors measured FPG, insulin levels, and HbA1c levels before, during, and after the treatment. The study showed a prompt improvement of glycemia and insulin sensitivity, and suggested that *Gynostemma pentaphyllum* tea could be an effective, and safe approach to treat T2DM patients (Huyen et al., 2010). The same authors followed up with another study that used the same study design but enrolled only 16 drug-naïve T2DM patients. The authors measured the same parameters and came to the same conclusion that *Gynostemma pentaphyllum* tea exerted antidiabetic effects by improving insulin sensitivity (Huyen et al., 2013). These results were confirmed by another study where *G. pentaphyllum* was used together with sulfonylurea (Huyen et al., 2012). Thus far, the current data indicate that *G. pentaphyllum* is quite efficient at improving insulin sensitivity and blood sugar levels if administered solely and that its efficacy may be enhanced when combined with other medications.

Safety, Toxicity, and Side Effects of *G. pentaphyllum*

In a study evaluating the toxicity of *G. pentaphyllum* extract on female Sprague-Dawley rats, a single dose of up to 5000 mg/kg of the extract was given and subchronic toxicity tests were performed with 1000 mg/kg/day for 90 days. No rat death occurred nor did any signs of toxicity arise. Blood chemistry values, though statistically different from the control group, were within normal ranges in rats. Thus, no mortality nor abnormalities have risen from the *G. pentaphyllum* extract treatment (Chiranthanut et al., 2013). In addition, no toxicity or mortality was reported upon long-term administration of a dose up to 750 mg/kg body weight of *G. pentaphyllum* in rats (Attawish et al., 2004).

A Phase I clinical trial was conducted to evaluate the safety of *G. pentaphyllum* whereby three groups of healthy volunteers were administered 50, 200, and 400 mg twice daily with water extract of *G. pentaphyllum* for two months. No major immune adverse events such as significant changes in natural killer cell activities, number of CD3+, CD4+, and CD8+ cells, were reported. No biochemical parameters were significantly affected either. Such doses of *G. pentaphyllum* were deemed to be safe (Chavalittumrong et al., 2007). In another clinical trial, 537 bronchitic patients were treated three times a day with *G. pentaphyllum* (2.5–3 g, prepared as tablets or capsules). Adverse side effects that included vomiting, abdomen tension, diarrhea (or constipation), dizziness, blurred vision, and tinnitus effects were seen in a small number of patients. Notably, these symptoms were mild and did not stop the patients from taking the *G. pentaphyllum* extract (Razmovski-Naumovski et al., 2005). A very recent randomized, double-blind, placebo-controlled clinical trial utilizing *G. pentaphyllum* extract in 72 healthy adults revealed no adverse side effects of the ingestion of the ethanolic extract of *G. pentaphyllum* (Choi et al., 2019). Overall, consumption of *G. pentaphyllum* seems to be safe at the doses required to observe a therapeutic effect.

CONCLUSION

Despite the abundance of knowledge regarding CVDs, CVD prevalence continues to be on the rise. Thus, there is an immediate demand for new safe, effective, and relatively cheap drug candidates. Mounting evidence obtained from *in vitro* and *in vivo* studies suggests that the four traditionally used medicinal

B

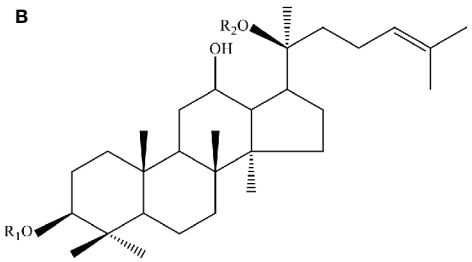

Gypenoside	R_1	R_2
20 S-Protopanaxadiol (PPD)	H	H
Gypenoside III	β-D-Glu(1→2) β-D-Glu	β-D-Glu(1→6) β-D-Glu
Gypenoside VIII	β-D-Glu(1→2) β-D-Glu	β-D-Glu

FIGURE 5 | *Gynostemma pentaphyllum*. **(A)** *Gynostemma pentaphyllum* (Source https://pngtree.com/freepng). Examples of the chemical structure of *Gynostemma pentaphyllum* Gypenoside that are usually synthesized 20 S-Protopanaxadiol (PPD). **(B)** example of some chemical structures of Gypenosides.

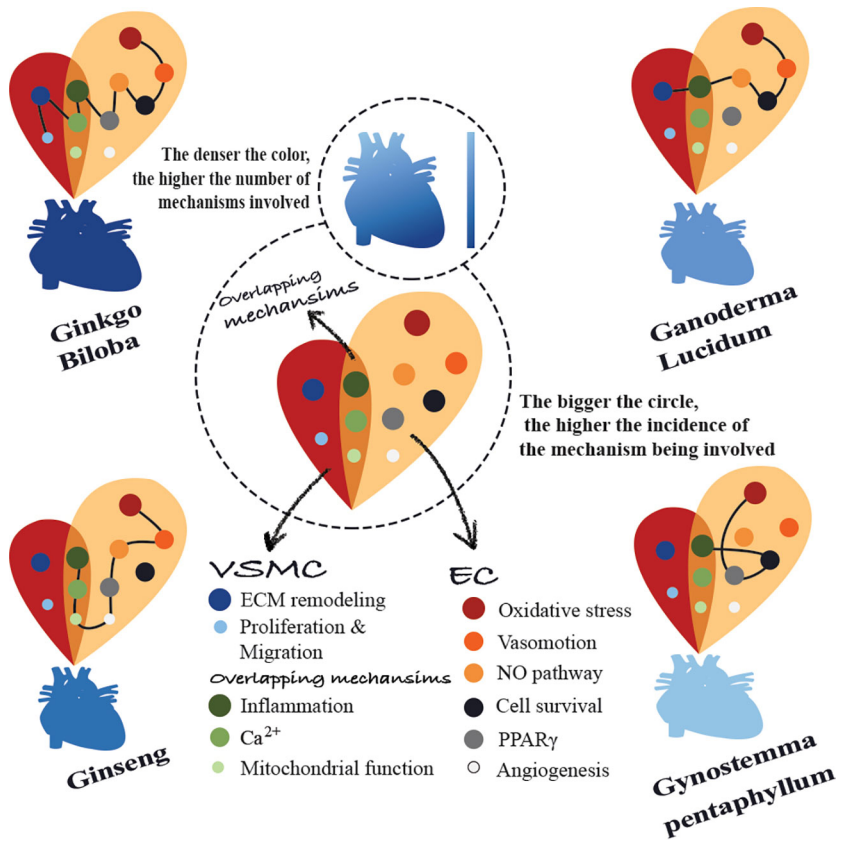

FIGURE 6 | Herbal therapies in the context of CVDs. Herbal preparations can exert protective effects by ameliorating the pathological effects exerted by CVDs risk factors. The herbal extracts can attenuate endothelial dysfunction and/or VSMC alterations by acting as, vasodilators, ROS scavengers, anti-oxidants, anti-inflammatory, anti-apoptotic, anti-hypertrophic, or anti-proliferative agents. This achieved through mechanisms that act in ECs only, VSMCs only, or through overlapping mechanism that act in both ECs and VSMCs. In ECs, herbal preparations can increase NO availability, decrease mitochondrial dysfunction and/or metabolic abnormalities as well as enhance angiogenesis. This can decrease the incidence of atherosclerosis and hypertension, which in return can decrease the risk of CVDs development. In VSMCs, the herbal extracts can modulate ECM deposition as well as cell migration, proliferation, and cell shape changes. VSMC, vascular smooth muscle cell; ECM, extracellular matrix; EC, endothelial cell; NO, nitric oxide; PPARY, peroxisome proliferator-activated receptor-gamma.

TABLE 2 | Summary of the mechanisms of action of the four discussed plants.

Plant		Mechanism of action	References
Ginseng	**Bioactive/active fractions:** Rb1, Rg1, Rg3, Re, and Rd **Commonly used extracts:** *Panax ginseng, Panax notoginseng*, *Panax quinquefolium L., Panax japonicas*	**Improves lipid profile** • By acting as an agonist of PPAR **Controls hypertension and improve endothelial function** • By Inhibition of ACE • By reducing adrenal catecholamines levels, elevating NO and cGMP levels • By activating Ca2+-gated potassium channels **Controls inflammation** • By inhibiting AP-1 and NF-κB • By reducing COX-2, IL-6, IL-1β, TNF-α, CD68, MCP-1 and MMP levels **Ameliorates oxidative stress** • By exhibiting free radical scavenging and metal ion chelating abilities • By promoting enhanced expression of antioxidant proteins, such as Nrf2 and HO-1 **Ameliorates mitochondrial dysfunction** **Modulates angiogenesis** • By decreasing VEGF-A and FGF-2 levels	(Kim et al., 1999b; Keum et al., 2003; Park et al., 2005; Persson et al., 2006; Shin Y. et al., 2013; Park J. et al., 2014; Lee H. et al., 2016; Deng et al., 2017; Singh et al., 2017; Lee et al., 2019a)
Gingko Biloba	**Bioactive/active fractions:** Ginkgolides classified into either A, B, C, J, or M types **Commonly used extracts:** EGb761	**Improves lipid profile** • By decreasing PPARs levels **Controls hypertension and improves endothelial function** • By decreasing ACE activity, activating cholinergic pathways, limiting LPS-induced proliferation of VSMCs • By decreasing ICAM-1 and VCAM-1 expression, decreasing phosphorylation of Akt/FoxO3a • By restoring eNOS activity, decreasing iNOS expression and consequently elevating NO levels **Controls inflammation** • By suppressing TLR-4 expression • By decreasing MMP-1, MCP-1, TNF-α, IL-6, or IL-1β **Ameliorates oxidative stress** • By decreasing NOX activity and level, activating endogenous Akt/Nrf2 antioxidant stress pathway • By increasing levels of HO-1, SOD and GSH-Px • By reducing the phosphorylation of MAPKs **Prevents hypertrophy** • By activating M2 muscarinic receptors/NO pathway • By decreasing calcium overload and inhibiting the Na^{+}/Ca^{2+} exchanger **Prevents apoptosis** • By decreasing caspase 3 and pro-apoptotic Bax expression and increasing anti-apoptotic Bcl-2 expression	(Akiba et al., 2007; Lin et al., 2007; Mansour et al., 2011; Liu et al., 2013; Liou et al., 2015; Mesquita et al., 2017; Abdel-Zaher et al., 2018; Huang et al., 2018; Chen et al., 2019).
Ganoderma lucidum	**Bioactive/active fractions:** ganoderic acids A, B, C, D, F, H, K, S, and Y, β-d-Glucan polysaccharides **Commonly used extracts:** Polysaccharide peptide (PsP) Ganoderma lucidum	**Controls hypertension and improves endothelial function** • By inhibition of ACE, enhancing Angiotensin 1-mediated phosphorylation of eNOS • By reducing the levels of vasoconstrictor peptide Endothelin-1 **Improves lipid profile** • By upregulating lipid metabolism (ACOX1 and ACC) **Ameliorates oxidative stress and inflammation** • By enhancing phosphorylation of Nrf2 which upregulates HO-1, GST, NQO-1, SOD, CAT, GSH-Px and GSH • By decreasing the levels of MDA and ICAM, and regulation of mTOR/S6K signaling pathways **Reduces necrosis** • By decreasing the levels of creatine phosphokinase	(Hikino et al., 1985; Tomoda et al., 1986; Shi et al., 2002; Shi et al., 2010; Lasukova et al., 2015; Wang et al., 2015; Wihastuti and Heriansyah, 2017; Cuong et al., 2019; Wu et al., 2019)

(Continued)

TABLE 2 | Continued

Plant		Mechanism of action	References
Gynostemma pentaphyllum	**Bioactive/active fractions:** dammarane-type triterpene saponins (gypenosides or gynosaponins) **Commonly used extracts:** Actiponin, Ombuine	**Improves lipid profile** • By activation of PPAR-α and PPAR-δ/β, decreasing the levels of sterol regulatory element binding protein-1c and stearoyl-CoA desaturase-1 • By activation of the AMPK pathway **Ameliorate oxidative stress and decreases apoptosis** • By decreasing the levels of MDA, increasing the levels of SOD, GSH, Nrf2, NQO-1 and HO-1 • By downregulating Fas/FasL, blocking CHOP pathway • By regulating the activation of PI3K/Akt pathway **Controls inflammation** • By decreasing LPS- and TNF-α-induced NF-κB through regulating PPAR-α	(Huang et al., 2006; Megalli et al., 2006; Malek et al., 2013; Yu et al., 2016b; Yang et al., 2017; Wang et al., 2018; Lin et al., 2019)

PPAR, peroxisome proliferator-activated receptor; ACE, acetylcholinesterase; NO, nitric oxide; AP-1, activator protein 1; NF-κB, nuclear factor kappa-light-chain-enhancer of activated B cells; COX, cyclooxygenase; IL, interleukin; TNF, tumor necrosis factor; CD, cluster of differentiation; MCP, monocyte chemoattractant; MMP, matrix metalloproteases; Nrf2, nuclear factor erythroid-2-related factor 2; HO-1, hemeoxygenase-1; VEGF, vascular endothelial growth factor; FGF, fibroblast growth factor; VSMCs, vascular smooth muscle cells; ICAM, intercellular adhesion molecule; VCAM, vascular cell adhesion molecule; Akt, protein kinase B; FoxO3a, forkhead box O; eNOS, endothelial nitric oxide synthase; iNOS, inducible nitric oxide synthase; TLR, toll-like receptor; NOC, nicotinamide adenine dinucleotide phosphate oxidase; SOD, superoxide dismutase; GSH-Px, glutathione peroxidase; MAPK, mitogen-activated protein kinase; ACOX1, peroxisomal acyl-coenzyme A oxidase 1; ACC, acetyl-CoA carboxylase; GST, glutathione S-transferase; NQO-1, NAD(P)H dehydrogenase (quinone); GSH, glutathione; MDA, malondialdehyde; mTOR, mammalian target of rapamycin complex; S6K, S6 kinase; AMPK, AMP-activated protein kinase; CHOP, C/EBP homologous protein.

plants discussed in this review significantly modulate key cellular, molecular, and metabolic mechanisms that control both CVDs pathogenesis and pathophysiology (**Figure 6**). Here are presented the recent findings, advances, and studies describing the therapeutic values of these plants in the context of several CVDs. Current evidence demonstrates that these herbal medicines have potent therapeutic properties and can ameliorate pathological conditions associated with CVDs (**Table 2** and **Figure 6**). However, clear clinical therapeutic benefits have not yet been secured. As such, these herbal treatments cannot be safely recommended as an alternative therapeutic medicine. In fact, the safety and toxicity of some of these plants have recently raised potential concerns (*eg. Gingko Biloba*). We conclude that better-designed studies and future clinical trials involving larger sample sizes are needed to investigate the role of different medicinal plants and their underlying mechanisms in the context of CVDs. Above all, the future clinical trials should address the safety and toxicity of these herbal remedies.

AUTHOR CONTRIBUTIONS

AS ideated and wrote the manuscript. DT, HP, TN, and GN contributed to manuscript writing and editing. SAH, HH, and SH contributed to manuscript writing and figures drawing. AE and GP contributed to manuscript ideation, revision, and editing

FUNDING

This work has been made possible thanks to grants (Ager S.O.S.) and (fondo di Ateneo per la ricerca 2019) to GP and Qatar University grant (IRCC-2019-007) to GN and GP.

REFERENCES

Abdelazim, A., Khater, S., Ali, H., Shalaby, S., Afifi, M., Saddick, S., et al. (2018). Panax ginseng improves glucose metabolism in streptozotocin-induced diabetic rats through 5'Adenosine mono phosphate kinase up-regulation. *Saudi J. Biol. Sci.* 26 (7), 1436–1441. doi: 10.1016/j.sjbs.2018.06.001

Abdel-Zaher, A. O., Farghaly, H. S., El-Refaiy, A. E., and Abd-Eldayem, A. M. (2018). Protective effect of the standardized leaf extract of G inkgo biloba (EGb761) against hypertension-induced renal injury in rats. *Clin. Exp. Hypertens.* 40 (8), 1–12. doi: 10.1016/j.sjbs.2018.06.001

Abegaz, T. M., Tefera, Y. G., and Befekadu Abebe, T. (2017). Target Organ Damage and the Long Term Effect of Nonadherence to Clinical Practice Guidelines in Patients with Hypertension: A Retrospective Cohort Study. *Int. J. Hypertens.* 2017, 2637051. doi: 10.1155/2017/2637051

Aday, A. W., and Ridker, P. M. (2018). Antiinflammatory Therapy in Clinical Care: The CANTOS Trial and Beyond. *Front. Cardiovasc. Med.* 5, 62. doi: 10.3389/fcvm.2018.00062

Ahmad, M. F. (2018). Ganoderma lucidum: Persuasive biologically active constituents and their health endorsement. *BioMed. Pharmacother.* 107, 507–519. doi: 10.1016/j.biopha.2018.08.036

Akiba, S., Yamaguchi, H., Kumazawa, S., Oka, M., and Sato, T. (2007). Suppression of oxidized LDL-induced PDGF receptor beta activation by ginkgo biloba extract reduces MMP-1 production in coronary smooth muscle cells. *J. Atheroscler. Thromb.* 14 (5), 219–225. doi: 10.5551/jat.e516

Aktan, F., Henness, S., Roufogalis, B. D., and Ammit, A. J. (2003). Gypenosides derived from Gynostemma pentaphyllum suppress NO synthesis in murine macrophages by inhibiting iNOS enzymatic activity and attenuating NF-kappaB-mediated iNOS protein expression. *Nitric Oxide* 8 (4), 235–242. doi: 10.1016/S1089-8603(03)00032-6

Al Disi, S. S., Anwar, M. A., and Eid, A. H. (2016). Anti-hypertensive herbs and their mechanisms of action: part I. *Front. Pharmacol.* 6, 323. doi: 10.3389/fphar.2015.00323

Al-Shehabi, T. S., Iratni, R., and Eid, A. H. (2016). Anti-atherosclerotic plants which modulate the phenotype of vascular smooth muscle cells. *Phytomedicine* 23 (11), 1068–1081. doi: 10.1016/j.phymed.2015.10.016

Anwar, M. A., Al Disi, S. S., and Eid, A. H. (2016). Anti-Hypertensive Herbs and Their Mechanisms of Action: Part II. *Front. Pharmacol.* 7, 50. doi: 10.3389/fphar.2016.00050

Arenz, A., Klein, M., Fiehe, K., Gross, J., Drewke, C., Hemscheidt, T., et al. (1996). Occurrence of neurotoxic 4'-O-methylpyridoxine in Ginkgo biloba leaves, Ginkgo medications and Japanese Ginkgo food. *Planta Med.* 62 (6), 548–551. doi: 10.1055/s-2006-957967

Ashraf, R., Khan, R. A., Ashraf, I., and Qureshi, A. A. (2013). Effects of Allium sativum (garlic) on systolic and diastolic blood pressure in patients with essential hypertension. *Pak. J. Pharm. Sci.* 26 (5), 859–863.

Attawish, A., Chivapat, S., Phadungpat, S., Bansiddhi, J., Techadamrongsin, Y., Mitrijit, O., et al. (2004). Chronic toxicity of Gynostemma pentaphyllum. *Fitoterapia* 75 (6), 539–551. doi: 10.1016/j.fitote.2004.04.010

August, P. (2004). Overview: mechanisms of hypertension: cells, hormones, and the kidney. *J. Am. Soc. Nephrol.* 15 (8), 1971–1973. doi: 10.1097/01.Asn.0000133197.23478.76

Aziz, T. A., Hussain, S. A., Mahwi, T. O., Ahmed, Z. A., Rahman, H. S., and Rasedee, A. (2018). The efficacy and safety of Ginkgo biloba extract as an adjuvant in type 2 diabetes mellitus patients ineffectively managed with metformin: a double-blind, randomized, placebo-controlled trial. *Drug Des. Devel. Ther.* 12, 735–742. doi: 10.2147/dddt.S157113

Baek, K. S., Yi, Y. S., Son, Y. J., Yoo, S., Sung, N. Y., Kim, Y., et al. (2016). In vitro and in vivo anti-inflammatory activities of Korean Red Ginseng-derived components. *J. Ginseng Res.* 40 (4), 437–444. doi: 10.1016/j.jgr.2016.08.003

Bang, H., Kwak, J. H., Ahn, H. Y., Shin, D. Y., and Lee, J. H. (2014). Korean red ginseng improves glucose control in subjects with impaired fasting glucose, impaired glucose tolerance, or newly diagnosed type 2 diabetes mellitus. *J. Med. Food* 17 (1), 128–134. doi: 10.1089/jmf.2013.2889

Batelaan, N. M., ten Have, M., van Balkom, A. J., Tuithof, M., and de Graaf, R. (2014). Anxiety disorders and onset of cardiovascular disease: the differential impact of panic, phobias and worry. *J. Anxiety Disord.* 28 (2), 252–258. doi: 10.1016/j.janxdis.2013.12.003

Belwal, T., Giri, L., Bahukhandi, A., Tariq, M., Kewlani, P., Bhatt, I. D., et al. (2019). "Ginkgo biloba," in *Nonvitamin and Nonmineral Nutritional Supplements*, vol. 241-250. (San Diego, California, United States: Elsevier).

Benjamin, E. J., Muntner, P., Alonso, A., Bittencourt, M. S., Callaway, C. W., Carson, A. P., et al. (2019). Heart Disease and Stroke Statistics-2019 Update: A Report From the American Heart Association. *Circulation* 139 (10), e56–e528. doi: 10.1161/cir.0000000000000659

Bent, S., Goldberg, H., Padula, A., and Avins, A. L. (2005). Spontaneous bleeding associated with ginkgo biloba: a case report and systematic review of the literature: a case report and systematic review of the literature. *J. Gen. Internal Med.* 20 (7), 657–661. doi: 10.1111/j.1525-1497.2005.0121.x

Bidani, A. K., and Griffin, K. A. (2004). Pathophysiology of hypertensive renal damage: implications for therapy. *Hypertension* 44 (5), 595–601. doi: 10.1161/01.Hyp.0000145180.38707.84

Boh, B., Berovic, M., Zhang, J., and Zhi-Bin, L. (2007). Ganoderma lucidum and its pharmaceutically active compounds. *Biotechnol. Annu. Rev.* 13, 265–301. doi: 10.1016/S1387-2656(07)13010-6

Bonassi, S., Prinzi, G., Lamonaca, P., Russo, P., Paximadas, I., Rasoni, G., et al. (2018). Clinical and genomic safety of treatment with Ginkgo biloba L. leaf extract (IDN 5933/Ginkgoselect(R)Plus) in elderly: a randomised placebo-controlled clinical trial [GiBiEx]. *BMC Complement. Alternat. Med.* 18 (1), 22. doi: 10.1186/s12906-018-2080-5

Bridi, R., Crossetti, F. P., Steffen, V. M., and Henriques, A. T. (2001). The antioxidant activity of standardized extract of Ginkgo biloba (EGb 761) in rats. *Phytother. Res.* 15 (5), 449–451. doi: 10.1002/ptr.814

Brinkley, T. E., Lovato, J. F., Arnold, A. M., Furberg, C. D., Kuller, L. H., Burke, G. L., et al. (2010). Effect of Ginkgo biloba on blood pressure and incidence of hypertension in elderly men and women. *Am. J. Hypertens.* 23 (5), 528–533. doi: 10.1038/ajh.2010.14

Brixius, K., Willms, S., Napp, A., Tossios, P., Ladage, D., Bloch, W., et al. (2006). Crataegus special extract WS 1442 induces an endothelium-dependent, NO-mediated vasorelaxation via eNOS-phosphorylation at serine 1177. *Cardiovasc. Drugs Ther.* 20 (3), 177–184. doi: 10.1007/s10557-006-8723-7

Cao, F., Cheng, H., Cheng, S., Li, L., Xu, F., Yu, W., et al. (2012). Expression of selected Ginkgo biloba heat shock protein genes after cold treatment could be induced by other abiotic stress. *Int. J. Mol. Sci.* 13 (5), 5768–5788. doi: 10.3390/ijms13055768

Caron, M. F., Hotsko, A. L., Robertson, S., Mandybur, L., Kluger, J., and White, C. M. (2002). Electrocardiographic and hemodynamic effects of Panax ginseng. *Ann. Pharmacother.* 36 (5), 758–763. doi: 10.1345/aph.1A411

Celermajer, D. S. (1997). Endothelial dysfunction: does it matter? Is it reversible? *J. Am. Coll. Cardiol.* 30 (2), 325–333. doi: 10.1016/s0735-1097(97)00189-7

Chan, K., Chui, S., Wong, D., Ha, W., Chan, C., and Wong, R. (2004). Protective effects of Danshensu from the aqueous extract of Salvia miltiorrhiza (Danshen) against homocysteine-induced endothelial dysfunction. *Life Sci.* 75 (26), 3157–3171. doi: 10.1016/j.lfs.2004.06.010

Chan, P. C., Xia, Q., and Fu, P. P. (2007). Ginkgo biloba leave extract: biological, medicinal, and toxicological effects. *J. Environ. Sci. Health C Environ. Carcinog. Ecotoxicol. Rev.* 25 (3), 211–244. doi: 10.1080/10590500701569414

Chang, C. J., Lin, C. S., Lu, C. C., Martel, J., Ko, Y. F., Ojcius, D. M., et al. (2015). Ganoderma lucidum reduces obesity in mice by modulating the composition of the gut microbiota. *Nat. Commun.* 6, 7489. doi: 10.1038/ncomms8489

Chavalittumrong, P. S. B., Kijphati, R., Jitjuk, B., Treesangsri, W., Phadungpat, S., Boonruad, T., et al. (2007). A phase I trial of Gynostemma pentaphyllum in healthy volunteers. *Songklanakarin J. Sci. Technol.* 29, 83–93.

Chen, J., and Gilbert, M. (2006). *Flora of China* (St Louis, MO and Beijing, China: Missouri Botanical Garden Press & Science Press, Beijing).

Chen, W. Q., Luo, S. H., Ll, H. Z., and Yang, H. (2005). [Effects of ganoderma lucidum polysaccharides on serum lipids and lipoperoxidation in experimental hyperlipidemic rats]. *Zhongguo Zhong Yao Za Zhi* 30 (17), 1358–1360.

Chen, X. J., Ren, S. M., Dong, J. Z., Qiu, C. G., Chen, Y. W., and Tao, H. L. (2019). Ginkgo biloba extract-761 protects myocardium by regulating Akt/Nrf2 signal pathway. *Drug Des. Dev. Ther.* 13, 647–655. doi: 10.2147/DDDT.S191537

Chen, S. (1995). A classificatory system and geographical distribution of the genus Gynostemma BL. (Cucurbitaceae). *Acta Phytotaxon. Sin.* 33, 403– 410.

Cheng, D., Liang, B., and Li, Y. (2013). Antihyperglycemic effect of Ginkgo biloba extract in streptozotocin-induced diabetes in rats. *Biomed. Res. Int.* 2013, 162724. doi: 10.1155/2013/162724

Chiranthanut, N., Teekachunhatean, S., Panthong, A., Khonsung, P., Kanjanapothi, D., and Lertprasertsuk, N. (2013). Toxicity evaluation of standardized extract of Gynostemma pentaphyllum Makino. *J. Ethnopharmacol.* 149 (1), 228–234. doi: 10.1016/j.jep.2013.06.027

Chiu, A. E., Lane, A. T., and Kimball, A. B. (2002). Diffuse morbilliform eruption after consumption of ginkgo biloba supplement. *J. Am. Acad. Dermatol.* 46 (1), 145–146. doi: 10.1067/mjd.2001.118545

Choi, H., Zhao, T., Shin, K., Kim, S., Hwang, B., Lee, C., et al. (2013). Anxiolytic effects of herbal ethanol extract from Gynostemma pentaphyllum in mice after exposure to chronic stress. *Molecules* 18 (4), 4342–4356. doi: 10.3390/molecules18044342

Choi, J., Kim, T. H., Choi, T. Y., and Lee, M. S. (2013). Ginseng for health care: a systematic review of randomized controlled trials in Korean literature. *PloS One* 8 (4), e59978. doi: 10.1371/journal.pone.0059978

Choi, E. K., Won, Y. H., Kim, S. Y., Noh, S. O., Park, S. H., Jung, S. J., et al. (2019). Supplementation with extract of Gynostemma pentaphyllum leaves reduces anxiety in healthy subjects with chronic psychological stress: A randomized, double-blind, placebo-controlled clinical trial. *Phytomedicine* 52, 198–205. doi: 10.1016/j.phymed.2018.05.002

Chou, T. C., Yen, M. H., Li, C. Y., and Ding, Y. A. (1998). Alterations of nitric oxide synthase expression with aging and hypertension in rats. *Hypertension* 31 (2), 643–648. doi: 10.1161/01.hyp.31.2.643

Chu, T. T., Benzie, I. F., Lam, C. W., Fok, B. S., Lee, K. K., and Tomlinson, B. (2012). Study of potential cardioprotective effects of Ganoderma lucidum (Lingzhi): results of a controlled human intervention trial. *Br. J. Nutr.* 107 (7), 1017–1027. doi: 10.1017/s0007114511003795

Chua, Y. T., Ang, X. L., Zhong, X. M., and Khoo, K. S. (2015). Interaction between warfarin and Chinese herbal medicines. *Singapore Med. J.* 56 (1), 11–18. doi: 10.11622/smedj.2015004

Cianfrocca, C., Pelliccia, F., Auriti, A., and Santini, M. (2002). Ginkgo biloba-induced frequent ventricular arrhythmia. *Ital. Heart J.* 3 (11), 689–691.

Cong, W.-n., Tao, R.-y., Tian, J.-y., Zhao, J., Liu, Q., and Ye, F. (2011). EGb761, an extract of Ginkgo biloba leaves, reduces insulin resistance in a high-fat-fed mouse model. *Acta Pharm. Sin. B* 1 (1), 14–20. doi: 10.1016/j.apsb.2011.04.006

Coon, J. T., and Ernst, E. (2002). Panax ginseng: a systematic review of adverse effects and drug interactions. *Drug Saf.* 25 (5), 323–344. doi: 10.2165/00002018-200225050-00003

Cooper, R. S., Kaufman, J. S., and Bovet, P. (2017). Global Burden of Disease Attributable to Hypertension. *JAMA* 317 (19), 2017–2018. doi: 10.1001/jama.2017.4213

Couto, G. K., Britto, L. R., Mill, J. G., and Rossoni, L. V. (2015). Enhanced nitric oxide bioavailability in coronary arteries prevents the onset of heart failure in rats with myocardial infarction. *J. Mol. Cell Cardiol.* 86, 110–120. doi: 10.1016/j.yjmcc.2015.07.017

Cragg, G. M., and Newman, D. J. (2013). Natural products: a continuing source of novel drug leads. *Biochim. Biophys. Acta* 1830 (6), 3670–3695. doi: 10.1016/j.bbagen.2013.02.008

Cuong, V. T., Chen, W., Shi, J., Zhang, M., Yang, H., Wang, N., et al. (2019). The anti-oxidation and anti-aging effects of Ganoderma lucidum in Caenorhabditis elegans. *Exp. Gerontol.* 117, 99–105. doi: 10.1016/j.exger.2018.11.016

Davies, M. J., Gordon, J. L., Gearing, A. J., Pigott, R., Woolf, N., Katz, D., et al. (1993). The expression of the adhesion molecules ICAM-1, VCAM-1, PECAM, and E-selectin in human atherosclerosis. *J. Pathol.* 171 (3), 223–229. doi: 10.1002/path.1711710311

Davison, E. K., and Brimble, M. A. (2019). Natural product derived privileged scaffolds in drug discovery. *Curr. Opin. Chem. Biol.* 52, 1–8. doi: 10.1016/j.cbpa.2018.12.007

DeKosky, S. T., Williamson, J. D., Fitzpatrick, A. L., Kronmal, R. A., Ives, D. G., Saxton, J. A., et al. (2008). Ginkgo biloba for prevention of dementia: a randomized controlled trial. *JAMA* 300 (19), 2253–2262. doi: 10.1001/jama.2008.683

Deng, Z., Wang, Y., Jiang, K., Liu, X., Wu, W., Gao, S., et al. (2006). Molecular cloning and characterization of a novel dehydrin gene from Ginkgo biloba. *Biosci. Rep.* 26 (3), 203–215. doi: 10.1007/s10540-006-9016-x

Deng, J., Liu, Y., Duan, Z., Zhu, C., Hui, J., Mi, Y., et al. (2017). Protopanaxadiol and protopanaxatriol-type saponins ameliorate glucose and lipid metabolism in type 2 diabetes mellitus in high-fat diet/streptozocin-induced mice. *Front. Pharmacol.* 8, 506. doi: 10.3389/fphar.2017.00506

Diamond, B. J., and Bailey, M. R. (2013). Ginkgo biloba: indications, mechanisms, and safety. *Psychiatr. Clin. North Am.* 36 (1), 73–83. doi: 10.1016/j.psc.2012.12.006

DiBona, G. F. (2013). Sympathetic nervous system and hypertension. *Hypertension* 61 (3), 556–560. doi: 10.1161/hypertensionaha.111.00633

Dodge, H. H., Zitzelberger, T., Oken, B. S., Howieson, D., and Kaye, J. (2008). A randomized placebo-controlled trial of Ginkgo biloba for the prevention of cognitive decline. *Neurology* 70 (19 Pt 2), 1809–1817. doi: 10.1212/01.wnl.0000303814.13509.db

Dokken, B. B. (2008). The Pathophysiology of Cardiovascular Disease and Diabetes: Beyond Blood Pressure and Lipids. *Diabetes Spectr.* 21 (3), 160–165. doi: 10.2337/diaspect.21.3.160

Dong, H., Ma, J., Li, T., Xiao, Y., Zheng, N., Liu, J., et al. (2017). Global deregulation of ginseng products may be a safety hazard to warfarin takers: solid evidence of ginseng-warfarin interaction. *Sci. Rep.* 7 (1), 5813. doi: 10.1038/s41598-017-05825-9

Douglas, G., and Channon, K. M. (2014). The pathogenesis of atherosclerosis. *Medicine* 42 (9), 480–484. doi: 10.1016/j.mpmed.2014.06.011

Dugoua, J. J., Mills, E., Perri, D., and Koren, G. (2006). Safety and efficacy of ginkgo (Ginkgo biloba) during pregnancy and lactation. *Can. J. Clin. Pharmacol.* 13 (3), e277–e284.

Egan, B. M., Kjeldsen, S. E., Grassi, G., Esler, M., and Mancia, G. (2019). The global burden of hypertension exceeds 1.4 billion people: should a systolic blood pressure target below 130 become the universal standard? *J. Hypertens.* 37 (6), 1148–1153. doi: 10.1097/HJH.0000000000002021

Eisenberg, D. M., Davis, R. B., Ettner, S. L., Appel, S., Wilkey, S., Van Rompay, M., et al. (1998). Trends in alternative medicine use in the United States 1990-1997: results of a follow-up national survey. *JAMA* 280 (18), 1569–1575. doi: 10.1001/jama.280.18.1569

Fabricant, D. S., and Farnsworth, N. R. (2001). The value of plants used in traditional medicine for drug discovery. *Environ. Health Perspect.* 109 (Suppl 1), 69–75. doi: 10.1289/ehp.01109s169

Fan, A. Z., Strine, T. W., Jiles, R., and Mokdad, A. H. (2008). Depression and anxiety associated with cardiovascular disease among persons aged 45 years and older in 38 states of the United States 2006. *Prev. Med.* 46 (5), 445–450. doi: 10.1016/j.ypmed.2008.02.016

Fan, X., Zhu, M., Chi, C., Yu, S., Xiong, J., Lu, Y., et al. (2017). Association of arteriosclerosis and/or atherosclerosis with hypertensive target organ damage in the community-dwelling elderly Chinese: the Northern Shanghai Study. *Clin. Interv. Aging* 12, 929–936. doi: 10.2147/cia.S133691

Farnsworth, N. R., Akerele, O., Bingel, A. S., Soejarto, D. D., and Guo, Z. (1985). Medicinal plants in therapy. *Bull. World Health Organ.* 63 (6), 965–981.

Feng, Z., Yang, X., Zhang, L., Ansari, I. A., Khan, M. S., Han, S., et al. (2018). Ginkgolide B ameliorates oxidized low-density lipoprotein-induced endothelial dysfunction via modulating Lectin-like ox-LDL-receptor-1 and NADPH oxidase 4 expression and inflammatory cascades. *Phytother. Res.* 32 (12), 2417–2427. doi: 10.1002/ptr.6177

Fleming, R. M. (2002). The effect of high-, moderate-, and low-fat diets on weight loss and cardiovascular disease risk factors. *Prev. Cardiol.* 5 (3), 110–118. doi: 10.1111/j.1520-037X.2002.01231.x

Forstermann, U., and Munzel, T. (2006). Endothelial nitric oxide synthase in vascular disease: from marvel to menace. *Circulation* 113 (13), 1708–1714. doi: 10.1161/CIRCULATIONAHA.105.602532

Fox, C. S., Pencina, M. J., Wilson, P. W., Paynter, N. P., Vasan, R. S., and D'Agostino, R. B. (2008). Lifetime risk of cardiovascular disease among individuals with and without diabetes stratified by obesity status in the Framingham heart study. *Diabetes Care* 31 (8), 1582–1584. doi: 10.2337/dc08-0025

Franceschi, C., Bonafe, M., Valensin, S., Olivieri, F., De Luca, M., Ottaviani, E., et al. (2000). Inflamm-aging. An evolutionary perspective on immunosenescence. *Ann. N. Y. Acad. Sci.* 908, 244–254. doi: 10.1111/j.1749-6632.2000.tb06651.x

Frishman, W. H., Beravol, P., and Carosella, C. (2009). Alternative and complementary medicine for preventing and treating cardiovascular disease. *Dis. Mon.* 55 (3), 121–192. doi: 10.1016/j.disamonth.2008.12.002

Fu, Y., and Ji, L. L. (2003). Chronic ginseng consumption attenuates age-associated oxidative stress in rats. *J. Nutr.* 133 (11), 3603–3609. doi: 10.1093/jn/133.11.3603

Fulton, D. J., and Barman, S. A. (2016). Clarity on the Isoform-Specific Roles of NADPH Oxidases and NADPH Oxidase-4 in Atherosclerosis. *Arterioscler. Thromb. Vasc. Biol.* 36 (4), 579–581. doi: 10.1161/ATVBAHA.116.307096

Gao, Y., Chen, G., Dai, X., Ye, J., and Zhou, S. (2004). A phase I/II study of ling zhi mushroom Ganoderma lucidum (W. Curt.: Fr.) Lloyd (Aphyllophoromycetideae) extract in patients with coronary heart disease. *Int. J. Med. Mushrooms* 6 (4).

Gao, S., Liu, Z., Li, H., Little, P. J., Liu, P., and Xu, S. (2012). Cardiovascular actions and therapeutic potential of tanshinone IIA. *Atherosclerosis* 220 (1), 3–10. doi: 10.1615/IntJMedMushr.v6.i1.20

Gardner, C. D., Taylor-Piliae, R. E., Kiazand, A., Nicholus, J., Rigby, A. J., and Farquhar, J. W. (2008). Effect of Ginkgo biloba (EGb 761) on treadmill walking time among adults with peripheral artery disease: a randomized clinical trial. *J. Cardiopulm. Rehabil. Prev.* 28 (4), 258–265. doi: 10.1097/01.HCR.0000327184.51992.b8

Gauhar, R., Hwang, S.-L., Jeong, S.-S., Kim, J.-E., Song, H., Park, D. C., et al. (2012). Heat-processed Gynostemma pentaphyllum extract improves obesity in ob/ob mice by activating AMP-activated protein kinase. *Biotechnol. Lett.* 34 (9), 1607–1616. doi: 10.1007/s10529-012-0944-1

Gerry, C. J., and Schreiber, S. L. (2018). Chemical probes and drug leads from advances in synthetic planning and methodology. *Nat. Rev. Drug Discov.* 17 (5), 333–352. doi: 10.1038/nrd.2018.53

Gou, S. H., Huang, H. F., Chen, X. Y., Liu, J., He, M., Ma, Y. Y., et al. (2016). Lipid-lowering, hepatoprotective, and atheroprotective effects of the mixture Hong-Qu and gypenosides in hyperlipidemia with NAFLD rats. *J. Chin. Med. Assoc.* 79 (3), 111–121. doi: 10.1016/j.jcma.2015.09.002

Gou, S. H., Liu, B. J., Han, X. F., Wang, L., Zhong, C., Liang, S., et al. (2018). Anti-atherosclerotic effect of Fermentum Rubrum and Gynostemma pentaphyllum mixture in high-fat emulsion- and vitamin D3-induced atherosclerotic rats. *J. Chin. Med. Assoc.* 81 (5), 398–408. doi: 10.1016/j.jcma.2017.08.018

Grosse, Y., Loomis, D., Lauby-Secretan, B., El Ghissassi, F., Bouvard, V., Benbrahim-Tallaa, L., et al. (2013). Carcinogenicity of some drugs and herbal products. *Lancet Oncol.* 14 (9), 807–808. doi: 10.1016/S1470-2045(13)70329-2

Guerrero-Garcia, C., and Rubio-Guerra, A. F. (2018). Combination therapy in the treatment of hypertension. *Drugs Context* 7, 212531. doi: 10.7573/dic.212531

Gui, Q. F., Xu, Z. R., Xu, K. Y., and Yang, Y. M. (2016). The Efficacy of Ginseng-Related Therapies in Type 2 Diabetes Mellitus: An Updated Systematic Review and Meta-analysis. *Medicine (Baltimore)* 95 (6), e2584. doi: 10.1097/MD.0000000000002584

Gurovic, M. S. V., Viceconte, F. R., Pereyra, M. T., Bidegain, M. A., and Cubitto, M. A. (2018). DNA damaging potential of Ganoderma lucidum extracts. *J. Ethnopharmacol.* 217, 83–88. doi: 10.1016/j.jep.2018.02.005

Harvey, A. (2000). Strategies for discovering drugs from previously unexplored natural products. *Drug Discovery Today* 5 (7), 294–300. doi: 10.1016/S1359-6446(00)01511-7

Hashiguchi, M., Ohta, Y., Shimizu, M., Maruyama, J., and Mochizuki, M. (2015). Meta-analysis of the efficacy and safety of Ginkgo biloba extract for the treatment of dementia. *J. Pharm. Health Care Sci.* 1, 14. doi: 10.1186/s40780-015-0014-7

He, M., Pan, H., Chang, R. C., So, K. F., Brecha, N. C., and Pu, M. (2014). Activation of the Nrf2/HO-1 antioxidant pathway contributes to the protective effects of Lycium barbarum polysaccharides in the rodent retina after ischemia-reperfusion-induced damage. *PloS One* 9 (1), e84800. doi: 10.1371/journal.pone.0084800

Heleno, S. A., Barros, L., Martins, A., Queiroz, M. J. R., Santos-Buelga, C., and Ferreira, I. (2012). Fruiting body, spores and in vitro produced mycelium of Ganoderma lucidum from Northeast Portugal: A comparative study of the antioxidant potential of phenolic and polysaccharidic extracts. *Food Res. Int.* 46 (1), 135–140. doi: 10.1016/j.foodres.2011.12.009

Heriansyah, T., Nurwidyaningtyas, W., Sargowo, D., Tjahjono, C. T., and Wihastuti, T. A. (2019). Polysaccharide peptide (PsP) Ganoderma lucidum: a potential inducer for vascular repair in type 2 diabetes mellitus model. *Vasc. Health Risk Manage.* 15, 419. doi: 10.2147/VHRM.S205996

Hikino, H., Konno, C., Mirin, Y., and Hayashi, T. (1985). Isolation and Hypoglycemic Activity of Ganoderans A and B, Glycans of Ganoderma lucidum Fruit Bodies1. *Planta Med.* 51 (4), 339–340. doi: 10.1055/s-2007-969507

Hong, S. Y., Kim, J. Y., Ahn, H. Y., Shin, J. H., and Kwon, O. (2012). Panax ginseng extract rich in ginsenoside protopanaxatriol attenuates blood pressure elevation in spontaneously hypertensive rats by affecting the Akt-dependent phosphorylation of endothelial nitric oxide synthase. *J. Agric. Food Chem.* 60 (12), 3086–3091. doi: 10.1021/jf204447y

Hong, J. M., Shin, D. H., Lim, Y. A., Lee, J. S., and Joo, I. S. (2013). Ticlopidine with Ginkgo Biloba extract: a feasible combination for patients with acute cerebral ischemia. *Thromb. Res.* 131 (4), e147–e153. doi: 10.1016/j.thromres.2013.01.026

Hori, T., Ridge, R. W., Tulecke, W., Del Tredici, P., Tremouillaux-Guiller, J., and Tobe, H. (1997). *Ginkgo biloba: a global treasure: from biology to medicine* (Japan: Springer).

Huang, T. H., Li, Y., Razmovski-Naumovski, V., Tran, V. H., Li, G. Q., Duke, C. C., et al. (2006). Gypenoside XLIX isolated from Gynostemma pentaphyllum inhibits nuclear factor-kappaB activation via a PPAR-alpha-dependent pathway. *J. Biomed. Sci.* 13 (4), 535–548. doi: 10.1007/s11373-006-9076-8

Huang, P., Zhang, L., Chai, C., Qian, X. C., Li, W., Li, J. S., et al. (2014). Effects of food and gender on the pharmacokinetics of ginkgolides A, B, C and bilobalide in rats after oral dosing with ginkgo terpene lactones extract. *J. Pharm. Biomed. Anal.* 100, 138–144. doi: 10.1016/j.jpba.2014.07.030

Huang, W. C., Chen, Y. L., Liu, H. C., Wu, S. J., and Liou, C. J. (2018). Ginkgolide C reduced oleic acid-induced lipid accumulation in HepG2 cells. *Saudi Pharm. J.* 26 (8), 1178–1184. doi: 10.1016/j.jsps.2018.07.006

Huyen, V., Phan, D., Thang, P., Hoa, N., and Östenson, C. (2010). Antidiabetic effect of Gynostemma pentaphyllum tea in randomly assigned type 2 diabetic patients. *Horm. Metab. Res.* 42 (05), 353–357. doi: 10.1055/s-0030-1248298

Huyen, V. T., Phan, D. V., Thang, P., Ky, P. T., Hoa, N. K., and Ostenson, C. G. (2012). Antidiabetic Effects of Add-On Gynostemma pentaphyllum Extract Therapy with Sulfonylureas in Type 2 Diabetic Patients. *Evid. Based Complement. Alternat. Med.* 2012, 452313. doi: 10.1155/2012/452313

Huyen, V., Phan, D., Thang, P., Hoa, N., and Östenson, C. (2013). Gynostemma pentaphyllum tea improves insulin sensitivity in type 2 diabetic patients. *J. Nutr. Metab.* 2013, 765383. doi: 10.1155/2013/765383

Hwang, S. Y., Son, D. J., Kim, I. W., Kim, D. M., Sohn, S. H., Lee, J. J., et al. (2008). Korean red ginseng attenuates hypercholesterolemia-enhanced platelet aggregation through suppression of diacylglycerol liberation in high-cholesterol-diet-fed rabbits. *Phytother. Res.* 22 (6), 778–783. doi: 10.1002/ptr.2363

Isah, T. (2015). Rethinking Ginkgo biloba L.: Medicinal uses and conservation. *Pharmacogn. Rev.* 9 (18), 140–148. doi: 10.4103/0973-7847.162137

Izzo, A. A., and Ernst, E. (2009). Interactions between herbal medicines and prescribed drugs: an updated systematic review. *Drugs* 69 (13), 1777–1798. doi: 10.2165/11317010-000000000-00000

Jaggy, H., and Koch, E. (1997). Chemistry and biology of alkylphenols from Ginkgo biloba L. *Pharmazie* 52 (10), 735–738.

Jang, S. J., Lim, H. J., and Lim, D. Y. (2011). Inhibitory Effects of Total Ginseng Saponin on Catecholamine Secretion from the Perfused Adrenal Medulla of SHRs. *J. Ginseng Res.* 35 (2), 176–190. doi: 10.5142/jgr.2011.35.2.176

Jeong, Y. Y., Ryu, J. H., Shin, J. H., Kang, M. J., Kang, J. R., Han, J., et al. (2016). Comparison of Anti-Oxidant and Anti-Inflammatory Effects between Fresh and Aged Black Garlic Extracts. *Molecules* 21 (4), 430. doi: 10.3390/molecules21040430

Jia, Y., Li, Z. Y., Zhang, H. G., Li, H. B., Liu, Y., and Li, X. H. (2010). Panax notoginseng saponins decrease cholesterol ester via up-regulating ATP-binding cassette transporter A1 in foam cells. *J. Ethnopharmacol.* 132 (1), 297–302. doi: 10.1016/j.jep.2010.08.033

Johansson, B. B. (1999). Hypertension mechanisms causing stroke. *Clin. Exp. Pharmacol. Physiol.* 26 (7), 563–565. doi: 10.1046/j.1440-1681.1999.03081.x

Jovanovski, E., Bateman, E. A., Bhardwaj, J., Fairgrieve, C., Mucalo, I., Jenkins, A. L., et al. (2014). Effect of Rg3-enriched Korean red ginseng (Panax ginseng) on arterial stiffness and blood pressure in healthy individuals: a randomized controlled trial. *J. Am. Soc. Hypertens.* 8 (8), 537–541. doi: 10.1016/j.jash.2014.04.004

Juan, Y., and Shanzhang, Y. (1995). Observation of Effects of Gynostemma Pentaphyllum on Platelet Disaggregation in Human. *J. Fujian Med. Univ.* (1995) (3), 03.

Kearney, P. M., Whelton, M., Reynolds, K., Muntner, P., Whelton, P. K., and He, J. (2005). Global burden of hypertension: analysis of worldwide data. *Lancet* 365 (9455), 217–223. doi: 10.1016/S0140-6736(05)17741-1

Keilhoff, G., Esser, T., Titze, M., Ebmeyer, U., and Schild, L. (2017). Gynostemma pentaphyllum is neuroprotective in a rat model of cardiopulmonary resuscitation. *Exp. Ther. Med.* 14 (6), 6034–6046. doi: 10.3892/etm.2017.5315

Keum, Y. S., Han, S. S., Chun, K. S., Park, K. K., Park, J. H., Lee, S. K., et al. (2003). Inhibitory effects of the ginsenoside Rg3 on phorbol ester-induced cyclooxygenase-2 expression, NF-kappaB activation and tumor promotion. *Mutat. Res.*, 523–524, 75-85. doi: 10.1016/s0027-5107(02)00323-8

Kiefer, D., and Pantuso, T. (2003). Panax ginseng. *Am. Fam. Physician* 68 (8), 1539–1542.

Kim, J. H., and Han, Y. N. (2011). Dammarane-type saponins from Gynostemma pentaphyllum. *Phytochemistry* 72 (11-12), 1453–1459. doi: 10.1016/j.phytochem.2011.04.003

Kim, S. H., and Park, K. S. (2003). Effects of Panax ginseng extract on lipid metabolism in humans. *Pharmacol. Res.* 48 (5), 511–513. doi: 10.1016/S1043-6618(03)00189-0

Kim, N. D., Kang, S. Y., Kim, M. J., Park, J. H., and Schini-Kerth, V. B. (1999a). The ginsenoside Rg3 evokes endothelium-independent relaxation in rat aortic rings: role of K+ channels. *Eur. J. Pharmacol.* 367 (1), 51–57. doi: 10.1016/s0014-2999(98)00899-1

Kim, N. D., Kang, S. Y., Park, J. H., and Schini-Kerth, V. B. (1999b). Ginsenoside Rg3 mediates endothelium-dependent relaxation in response to ginsenosides in rat aorta: role of K+ channels. *Eur. J. Pharmacol.* 367 (1), 41–49. doi: 10.1016/s0014-2999(98)00898-x

Kim, W. Y., Kim, J. M., Han, S. B., Lee, S. K., Kim, N. D., Park, M. K., et al. (2000). Steaming of ginseng at high temperature enhances biological activity. *J. Nat. Prod.* 63 (12), 1702–1704. doi: 10.1021/np990152b

Kim, J. H. (2012). Cardiovascular Diseases and Panax ginseng: A Review on Molecular Mechanisms and Medical Applications. *J. Ginseng Res.* 36 (1), 16–26. doi: 10.5142/jgr.2012.36.1.16

Kimbel, K. H. (1992). Ginkgo biloba. *Lancet* 340 (8833), 1474. doi: 10.1016/0140-6736(92)92668-6

Kitts, D. D., Wijewickreme, A. N., and Hu, C. (2000). Antioxidant properties of a North American ginseng extract. *Mol. Cell. Biochem.* 203 (1-2), 1–10. doi: 10.1023/a:1007078414639

Kleijnen, J., and Knipschild, P. (1992). Ginkgo biloba. *Lancet* 340 (8828), 1136–1139. doi: 10.1016/0140-6736(92)93158-j

Klein, B. E., Klein, R., and Lee, K. E. (2002). Components of the metabolic syndrome and risk of cardiovascular disease and diabetes in Beaver Dam. *Diabetes Care* 25 (10), 1790–1794. doi: 10.2337/diacare.25.10.1790

Klupp, N. L., Chang, D., Hawke, F., Kiat, H., Cao, H., Grant, S. J., et al. (2015). Ganoderma lucidum mushroom for the treatment of cardiovascular risk factors. *Cochrane Database Syst. Rev.* (2), CD007259. doi: 10.1002/14651858.CD007259.pub2

Klupp, N. L., Kiat, H., Bensoussan, A., Steiner, G. Z., and Chang, D. H. (2016). A double-blind, randomised, placebo-controlled trial of Ganoderma lucidum for

the treatment of cardiovascular risk factors of metabolic syndrome. *Sci. Rep.* 2 (6), 29540. doi: 10.1038/srep29540

Komishon, A. M., Shishtar, E., Ha, V., Sievenpiper, J. L., de Souza, R. J., Jovanovski, E., et al. (2016). The effect of ginseng (genus Panax) on blood pressure: a systematic review and meta-analysis of randomized controlled clinical trials. *J. Hum. Hypertens.* 30 (10), 619–626. doi: 10.1038/jhh.2016.18

Kressmann, S., Muller, W. E., and Blume, H. H. (2002). Pharmaceutical quality of different Ginkgo biloba brands. *J. Pharm. Pharmacol.* 54 (5), 661–669. doi: 10.1211/0022357021778970

Kudolo, G. B. (2000). The effect of 3-month ingestion of Ginkgo biloba extract on pancreatic beta-cell function in response to glucose loading in normal glucose tolerant individuals. *J. Clin. Pharmacol.* 40 (6), 647–654. doi: 10.1002/j.1552-4604.2000.tb05991.x

Kuller, L. H., Ives, D. G., Fitzpatrick, A. L., Carlson, M. C., Mercado, C., Lopez, O. L., et al. (2010). Does Ginkgo biloba reduce the risk of cardiovascular events? *Circ. Cardiovasc. Qual. Outcomes* 3 (1), 41–47. doi: 10.1161/circoutcomes.109.871640

Kwok, Y., Ng, K. F., Li, C. C., Lam, C. C., and Man, R. Y. (2005). A prospective, randomized, double-blind, placebo-controlled study of the platelet and global hemostatic effects of Ganoderma lucidum (Ling-Zhi) in healthy volunteers. *Anesth. Analg.* 101 (2), 423–426. doi: 10.1213/01.ANE.0000155286.20467.28

la Cour, B., Molgaard, P., and Yi, Z. (1995). Traditional Chinese medicine in treatment of hyperlipidaemia. *J. Ethnopharmacol.* 46 (2), 125–129. doi: 10.1016/0378-8741(95)01234-5

Lacour, M., Ez-Zaher, L., and Raymond, J. (1991). Plasticity mechanisms in vestibular compensation in the cat are improved by an extract of Ginkgo biloba (EGb 761). *Pharmacol. Biochem. Behav.* 40 (2), 367–379. doi: 10.1016/0091-3057(91)90568-m

Lakatta, E. G., and Levy, D. (2003). Arterial and cardiac aging: major shareholders in cardiovascular disease enterprises: Part II: the aging heart in health: links to heart disease. *Circulation* 107 (2), 346–354. doi: 10.1161/01.cir.0000048893.62841.f7

Lasukova, T. V., Arbuzov, A. G., Maslov, L. N., and Burkova, V. N. (2008). [Ganoderma lucidum extract in cardiac diastolic dysfunction and irreversible cardiomyocytic damage in ischemia and reperfusion of the isolated heart]. *Patol. Fiziol. Eksp. Ter.* (1), 22–25.

Lasukova, T., Maslov, L., Arbuzov, A., Burkova, V., and Inisheva, L. (2015). Cardioprotective activity of Ganoderma lucidum extract during total ischemia and reperfusion of isolated heart. *Bull. Exp. Biol. Med.* 158 (6), 739–741. doi: 10.1007/s10517-015-2851-7

Lay, S., Chiu, J.-H., Shiao, M.-S., Lui, W.-Y., and Wu, C.-W. (2003). Crude extract of Salvia miltiorrhiza and salvianolic acid B enhance in vitro angiogenesis in murine SVR endothelial cell line. *Planta Med.* 69 (01), 26–32. doi: 10.1055/s-2003-37034

Le, L., Gao, X. L., Ding, B. X., and Yuan, B. X. (2007). [Effect of total flaveos of Gymostemma pentaphyllum on protein expression of Fas/FasL genes and TNF-alpha concentration in cultured neonatal rat cardiomyocytes with hypoxia-reoxygenation]. *Zhongguo Zhong Yao Za Zhi* 32 (18), 1925–1927.

Lee, C. H., and Kim, J. H. (2014). A review on the medicinal potentials of ginseng and ginsenosides on cardiovascular diseases. *J. Ginseng Res.* 38 (3), 161–166. doi: 10.1016/j.jgr.2014.03.001

Lee, W. M., Kim, S. D., Park, M. H., Cho, J. Y., Park, H. J., Seo, G. S., et al. (2008). Inhibitory mechanisms of dihydroginsenoside Rg3 in platelet aggregation: critical roles of ERK2 and cAMP. *J. Pharm. Pharmacol.* 60 (11), 1531–1536. doi: 10.1211/jpp/60.11.0015

Lee, N. H., Yoo, S. R., Kim, H. G., Cho, J. H., and Son, C. G. (2012). Safety and tolerability of Panax ginseng root extract: a randomized, placebo-controlled, clinical trial in healthy Korean volunteers. *J. Altern. Complement. Med.* 18 (11), 1061–1069. doi: 10.1089/acm.2011.0591

Lee, H., Choi, J., Shin, S. S., and Yoon, M. (2016). Effects of Korean red ginseng (Panax ginseng) on obesity and adipose inflammation in ovariectomized mice. *J. Ethnopharmacol.* 178, 229–237. doi: 10.1016/j.jep.2015.12.017

Lee, K. H., Bae, I. Y., Park, S. I., Park, J. D., and Lee, H. G. (2016). Antihypertensive effect of Korean Red Ginseng by enrichment of ginsenoside Rg3 and arginine-fructose. *J. Ginseng Res.* 40 (3), 237–244. doi: 10.1016/j.jgr.2015.08.002

Lee, Y. H., Kim, J. H., Song, C. H., Jang, K. J., Kim, C. H., Kang, J. S., et al. (2016). Ethanol Extract of Ganoderma lucidum Augments Cellular Anti-oxidant Defense through Activation of Nrf2/HO-1. *J. Pharmacopuncture* 19 (1), 59–69. doi: 10.3831/KPI.2016.19.008

Lee, H., Hong, Y., Tran, Q., Cho, H., Kim, M., Kim, C., et al. (2019a). A new role for the ginsenoside RG3 in antiaging via mitochondria function in ultraviolet-irradiated human dermal fibroblasts. *J. Ginseng Res.* 43 (3), 431–441. doi: 10.1016/j.jgr.2018.07.003

Lee, H. S., Lim, S. M., Jung, J. I., Kim, S. M., Lee, J. K., Kim, Y. H., et al. (2019b). Gynostemma Pentaphyllum Extract Ameliorates High-Fat Diet-Induced Obesity in C57BL/6N Mice by Upregulating SIRT1. *Nutrients* 11 (10), 431–441. doi: 10.3390/nu11102475

Li, L., and Lau, B. H. (1993). Protection of vascular endothelial cells from hydrogen peroxide-induced oxidant injury by gypenosides, saponins of Gynostemma pentaphyllum. *Phytother. Res.* 7 (4), 299–304. doi: 10.1002/ptr.2650070408

Li, Y., Lin, W., Huang, J., Xie, Y., and Ma, W. (2016). Anti-cancer effects of Gynostemma pentaphyllum (Thunb.) Makino (Jiaogulan). *Chin. Med.* 11, 43. doi: 10.1186/s13020-016-0114-9

Liang, Z., Yuan, Z., Li, G., Fu, F., and Shan, Y. (2018). Hypolipidemic, antioxidant, and antiapoptotic effects of polysaccharides extracted from Reishi Mushroom, Ganoderma lucidum (Leysser: Fr) Karst, in mice fed a high-fat diet. *J. Med. Food* 21 (12), 1218–1227. doi: 10.1089/jmf.2018.4182

Liao, W. I., Lin, Y. Y., Chu, S. J., Hsu, C. W., and Tsai, S. H. (2010). Bradyarrhythmia caused by ginseng in a patient with chronic kidney disease. *Am. J. Emerg. Med.* 28 (4), 538.e535–536. doi: 10.1016/j.ajem.2009.08.006

Lim, L. M., Tsai, N. C., Lin, M. Y., Hwang, D. Y., Lin, H. Y., Lee, J. J., et al. (2016). Hyponatremia is Associated with Fluid Imbalance and Adverse Renal Outcome in Chronic Kidney Disease Patients Treated with Diuretics. *Sci. Rep.* 6, 36817. doi: 10.1038/srep36817

Lin, C. C., Huang, P. C., and Lin, J. M. (2000). Antioxidant and hepatoprotective effects of Anoectochilus formosanus and Gynostemma pentaphyllum. *Am. J. Chin. Med.* 28 (1), 87–96. doi: 10.1142/S0192415X00000118

Lin, F. Y., Chen, Y. H., Chen, Y. L., Wu, T. C., Li, C. Y., Chen, J. W., et al. (2007). Ginkgo biloba extract inhibits endotoxin-induced human aortic smooth muscle cell proliferation via suppression of toll-like receptor 4 expression and NADPH oxidase activation. *J. Agric. Food Chem.* 55 (5), 1977–1984. doi: 10.1021/jf062945r

Lin, M., Wang, Y. R., Zhai, X. F., Xing, S. F., and Piao, X. L. (2019). [Protective effects of flavonoids from Gynostemma pentaphyllum on oxidative damage in LLC-PK1 cells]. *Zhongguo Zhong Yao Za Zhi* 44 (6), 1193–1200. doi: 10.19540/j.cnki.cjcmm.20181226.019

Liou, C. J., Lai, X. Y., Chen, Y. L., Wang, C. L., Wei, C. H., and Huang, W. C. (2015). Ginkgolide C suppresses adipogenesis in 3T3-L1 adipocytes via the AMPK signaling pathway. *Evid. Based Complement. Alternat. Med.* 2015, 298635. doi: 10.1155/2015/298635

Liu, A. H., Bao, Y. M., Wang, X. Y., and Zhang, Z. X. (2013). Cardio-protection by Ginkgo biloba extract 50 in rats with acute myocardial infarction is related to Na(+)-Ca(2)(+) exchanger. *Am. J. Chin. Med.* 41 (4), 789–800. doi: 10.1142/S0192415X13500535

Liu, L., Wu, J., and Kennedy, D. J. (2016). Regulation of Cardiac Remodeling by Cardiac Na(+)/K(+)-ATPase Isoforms. *Front. Physiol.* 7, 382. doi: 10.3389/fphys.2016.00382

Lu, J. M., Weakley, S. M., Yang, Z., Hu, M., Yao, Q., and Chen, C. (2012). Ginsenoside Rb1 directly scavenges hydroxyl radical and hypochlorous acid. *Curr. Pharm. Des.* 18 (38), 6339–6347. doi: 10.2174/138161212803832254

Luo, H. M., Dai, R. H., and Li, Y. (1995). [Nuclear cardiology study on effective ingredients of Astragalus membranaceus in treating heart failure]. *Zhongguo Zhong Xi Yi Jie He Za Zhi* 15 (12), 707–709.

Ma, X., Zhang, K., Li, H., Han, S., Ma, Z., and Tu, P. (2013). Extracts from Astragalus membranaceus limit myocardial cell death and improve cardiac function in a rat model of myocardial ischemia. *J. Ethnopharmacol.* 149 (3), 720–728. doi: 10.1016/j.jep.2013.07.036

Maguire, E. M., Pearce, S. W. A., and Xiao, Q. (2019). Foam cell formation: A new target for fighting atherosclerosis and cardiovascular disease. *Vascul. Pharmacol.* 112, 54–71. doi: 10.1016/j.vph.2018.08.002

Mahady, G. B., Gyllenhaal, C., Fong, H. H., and Farnsworth, N. R. (2000). Ginsengs: a review of safety and efficacy. *Nutr. Clin. Care* 3 (2), 90–101. doi: 10.1046/j.1523-5408.2000.00020.x

Mahdy, H. M., Tadros, M. G., Mohamed, M. R., Karim, A. M., and Khalifa, A. E. (2011). The effect of Ginkgo biloba extract on 3-nitropropionic acid-induced neurotoxicity in rats. *Neurochem. Int.* 59 (6), 770–778. doi: 10.1016/j.neuint.2011.07.012

Mahmoudian-Sani, M. R., Hashemzadeh-Chaleshtori, M., Asadi-Samani, M., and Yang, Q. (2017). Ginkgo biloba in the treatment of tinnitus: An updated literature review. *Int. Tinnitus J.* 21 (1), 58–62. doi: 10.5935/0946-5448.20170011

Malek, M. A., Hoang, M. H., Jia, Y., Lee, J. H., Jun, H. J., Lee, D. H., et al. (2013). Ombuin-3-O-beta-D-glucopyranoside from Gynostemma pentaphyllum is a dual agonistic ligand of peroxisome proliferator-activated receptors alpha and delta/beta. *Biochem. Biophys. Res. Commun.* 430 (4), 1322–1328. doi: 10.1016/j.bbrc.2012.12.020

Mansour, S. M., Bahgat, A. K., El-Khatib, A. S., and Khayyal, M. T. (2011). Ginkgo biloba extract (EGb 761) normalizes hypertension in 2K, 1C hypertensive rats: role of antioxidant mechanisms, ACE inhibiting activity and improvement of endothelial dysfunction. *Phytomedicine* 18 (8-9), 641–647. doi: 10.1016/j.phymed.2011.01.014

Mao, X.-q., Yu, F., Wang, N., Wu, Y., Zou, F., Wu, K., et al. (2009). Hypoglycemic effect of polysaccharide enriched extract of Astragalus membranaceus in diet induced insulin resistant C57BL/6J mice and its potential mechanism. *Phytomedicine* 16 (5), 416–425. doi: 10.1016/j.phymed.2008.12.011

Martinet, W., Coornaert, I., Puylaert, P., and De Meyer, G. R. Y. (2019). Macrophage Death as a Pharmacological Target in Atherosclerosis. *Front. Pharmacol.* 10, 306. doi: 10.3389/fphar.2019.00306

Mashayekh, A., Pham, D. L., Yousem, D. M., Dizon, M., Barker, P. B., and Lin, D. D. (2011). Effects of Ginkgo biloba on cerebral blood flow assessed by quantitative MR perfusion imaging: a pilot study. *Neuroradiology* 53 (3), 185–191. doi: 10.1007/s00234-010-0790-6

Matthews, M. K.Jr. (1998). Association of Ginkgo biloba with intracerebral hemorrhage. *Neurology* 50 (6), 1933–1934. doi: 10.1212/wnl.50.6.1933

Megalli, S., Aktan, F., Davies, N. M., and Roufogalis, B. D. (2005). Phytopreventative anti-hyperlipidemic effects of Gynostemma pentaphyllum in rats. *J. Pharm. Pharm. Sci.* 8 (3), 507–515.

Megalli, S., Davies, N. M., and Roufogalis, B. D. (2006). Anti-hyperlipidemic and hypoglycemic effects of Gynostemma pentaphyllum in the Zucker fatty rat. *J. Pharm. Pharm. Sci.* 9 (3), 281–291.

Mehlsen, J., Drabaek, H., Wiinberg, N., and Winther, K. (2002). Effects of a Ginkgo biloba extract on forearm haemodynamics in healthy volunteers. *Clin. Physiol. Funct. Imaging* 22 (6), 375–378. doi: 10.1046/j.1475-097X.2002.00445.x

Mei, N., Guo, X., Ren, Z., Kobayashi, D., Wada, K., and Guo, L. (2017). Review of Ginkgo biloba-induced toxicity, from experimental studies to human case reports. *J. Environ. Sci. Health C Environ. Carcinog. Ecotoxicol. Rev.* 35 (1), 1–28. doi: 10.1080/10590501.2016.1278298

Mensah, G. A. (2016). Hypertension and Target Organ Damage: Don't Believe Everything You Think! *Ethnicity Dis.* 26 (3), 275–278. doi: 10.18865/ed.26.3.275

Mesquita, T. R. R., de Jesus, I. C. G., Dos Santos, J. F., de Almeida, G. K. M., de Vasconcelos, C. M. L., Guatimosim, S., et al. (2017). Cardioprotective Action of Ginkgo biloba Extract against Sustained beta-Adrenergic Stimulation Occurs via Activation of M2/NO Pathway. *Front. Pharmacol.* 8, 220. doi: 10.3389/fphar.2017.00220

Miller, M. (2009). Dyslipidemia and cardiovascular risk: the importance of early prevention. *QJM* 102 (9), 657–667. doi: 10.1093/qjmed/hcp065

Moens, A. L., Claeys, M. J., Timmermans, J. P., and Vrints, C. J. (2005). Myocardial ischemia/reperfusion-injury, a clinical view on a complex pathophysiological process. *Int. J. Cardiol.* 100 (2), 179–190. doi: 10.1016/j.ijcard.2004.04.013

Mohammadi, H., Hadi, A., Kord-Varkaneh, H., Arab, A., Afshari, M., Ferguson, A. J. R., et al. (2019). Effects of ginseng supplementation on selected markers of inflammation: A systematic review and meta-analysis. *Phytother. Res.* 33 (8), 1991–2001. doi: 10.1002/ptr.6399

Mollah, M. L., Kim, G. S., Moon, H. K., Chung, S. K., Cheon, Y. P., Kim, J. K., et al. (2009). Antiobesity effects of wild ginseng (Panax ginseng CA Meyer) mediated by PPAR-γ, GLUT4 and LPL in ob/ob mice. *Phytother. Res.* 23 (2), 220–225. doi: 10.1002/ptr.2593

Moore, K. J., and Tabas, I. (2011). Macrophages in the pathogenesis of atherosclerosis. *Cell* 145 (3), 341–355. doi: 10.1016/j.cell.2011.04.005

Morigiwa, A., Kitabatake, K., Fujimoto, Y., and Ikekawa, N. (1986). Angiotensin converting enzyme-inhibitory triterpenes from Ganoderma lucidum. *Chem. Pharm. Bull.* 34 (7), 3025–3028. doi: 10.1248/cpb.34.3025

Mozaffarian, D., Benjamin, E. J., Go, A. S., Arnett, D. K., Blaha, M. J., Cushman, M., et al. (2015). Heart disease and stroke statistics–2015 update: a report from the American Heart Association. *Circulation* 131 (4), e29–322. doi: 10.1161/cir.0000000000000152

Mucalo, I., Jovanovski, E., Rahelic, D., Bozikov, V., Romic, Z., and Vuksan, V. (2013). Effect of American ginseng (Panax quinquefolius L.) on arterial stiffness in subjects with type-2 diabetes and concomitant hypertension. *J. Ethnopharmacol.* 150 (1), 148–153. doi: 10.1016/j.jep.2013.08.015

Muller, C., Gardemann, A., Keilhoff, G., Peter, D., Wiswedel, I., and Schild, L. (2012). Prevention of free fatty acid-induced lipid accumulation, oxidative stress, and cell death in primary hepatocyte cultures by a Gynostemma pentaphyllum extract. *Phytomedicine* 19 (5), 395–401. doi: 10.1016/j.phymed.2011.12.002

Munoz-Durango, N., Fuentes, C. A., Castillo, A. E., Gonzalez-Gomez, L. M., Vecchiola, A., Fardella, C. E., et al. (2016). Role of the Renin-Angiotensin-Aldosterone System beyond Blood Pressure Regulation: Molecular and Cellular Mechanisms Involved in End-Organ Damage during Arterial Hypertension. *Int. J. Mol. Sci.* 17 (7), E797. doi: 10.3390/ijms17070797

Muntner, P., Carey, R. M., Gidding, S., Jones, D. W., Taler, S. J., Wright, J. T.Jr., et al. (2018). Potential U.S. Population Impact of the 2017 ACC/AHA High Blood Pressure Guideline. *J. Am. Coll. Cardiol.* 71 (2), 109–118. doi: 10.1016/j.jacc.2017.10.073

Murthy, H. N., Dandin, V. S., Park, S. Y., and Paek, K. Y. (2018). Quality, safety and efficacy profiling of ginseng adventitious roots produced in vitro. *Appl. Microbiol. Biotechnol.* 102 (17), 7309–7317. doi: 10.1007/s00253-018-9188-x

Nadar, S. (2011). "Target organ damage in hypertension," in *Hypertension (Oxford Cardiology Library)*. Eds. S. Nadar and G. Lip (London: Oxford University Press).

National Toxicology Program (2013). Toxicology and carcinogenesis studies of Ginkgo biloba extract (CAS No. 90045-36-6) in F344/N rats and B6C3F1/N mice (Gavage studies). *Natl. Toxicol. Program Tech. Rep. Ser.* (578), 1–183.

NCD Risk Factor Collaboration (NCD-RisC) (2017). Worldwide trends in blood pressure from 1975 to 2015: a pooled analysis of 1479 population-based measurement studies with 19.1 million participants. *Lancet* 389 (10064), 37–55. doi: 10.1016/s0140-6736(16)31919-5

Newman, D. J., and Cragg, G. M. (2016). Natural Products as Sources of New Drugs from 1981 to 2014. *J. Nat. Prod.* 79 (3), 629–661. doi: 10.1021/acs.jnatprod.5b01055

Ng, C., Koon, C., Cheung, D., Lam, M., Leung, P., Lau, C., et al. (2011). The anti-hypertensive effect of Danshen (Salvia miltiorrhiza) and Gegen (Pueraria lobata) formula in rats and its underlying mechanisms of vasorelaxation. *J. Ethnopharmacol.* 137 (3), 1366–1372. doi: 10.1016/j.jep.2011.08.006

Nookabkaew, S., Rangkadilok, N., and Satayavivad, J. (2006). Determination of trace elements in herbal tea products and their infusions consumed in Thailand. *J. Agric. Food Chem.* 54 (18), 6939–6944. doi: 10.1021/jf060571w

Noubiap, J. J., Nansseu, J. R., Nyaga, U. F., Sime, P. S., Francis, I., and Bigna, J. J. (2019). Global prevalence of resistant hypertension: a meta-analysis of data from 3.2 million patients. *Heart* 105 (2), 98–105. doi: 10.1136/heartjnl-2018-313599

Oh, J., Lee, H., Park, D., Ahn, J., Shin, S. S., and Yoon, M. (2012). Ginseng and its active components ginsenosides inhibit adipogenesis in 3T3-L1 cells by regulating MMP-2 and MMP-9. *Evid. Based Complement. Alternat. Med.* 2012, 265023. doi: 10.1155/2012/265023

Ojeda, D., Jimenez-Ferrer, E., Zamilpa, A., Herrera-Arellano, A., Tortoriello, J., and Alvarez, L. (2010). Inhibition of angiotensin convertin enzyme (ACE) activity by the anthocyanins delphinidin- and cyanidin-3-O-sambubiosides from Hibiscus sabdariffa. *J. Ethnopharmacol.* 127 (1), 7–10. doi: 10.1016/j.jep.2009.09.059

Omboni, S., and Volpe, M. (2018). Management of arterial hypertension with angiotensin receptor blockers: Current evidence and the role of olmesartan. *Cardiovasc. Ther.* 36 (6), e12471. doi: 10.1111/1755-5922.12471

Oparil, S., Zaman, M. A., and Calhoun, D. A. (2003). Pathogenesis of hypertension. *Ann. Intern. Med.* 139 (9), 761–776. doi: 10.7326/0003-4819-139-9-200311040-00011

Orekhov, A. N., Sobenin, I. A., Korneev, N. V., Kirichenko, T. V., Myasoedova, V. A., Melnichenko, A. A., et al. (2013). Anti-atherosclerotic therapy based on botanicals. *Recent Pat. Cardiovasc. Drug Discov.* 8 (1), 56–66. doi: 10.2174/1872208311307990008

Otvos, R. A., Still, K. B. M., Somsen, G. W., Smit, A. B., and Kool, J. (2019). Drug Discovery on Natural Products: From Ion Channels to nAChRs, from Nature to Libraries, from Analytics to Assays. *SLAS Discov.* 24 (3), 362–385. doi: 10.1177/2472555218822098

Oyama, Y., Chikahisa, L., Ueha, T., Kanemaru, K., and Noda, K. (1996). Ginkgo biloba extract protects brain neurons against oxidative stress induced by hydrogen peroxide. *Brain Res.* 712 (2), 349–352. doi: 10.1016/0006-8993(95)01440-3

Ozaki, M., Kawashima, S., Yamashita, T., Hirase, T., Ohashi, Y., Inoue, N., et al. (2002). Overexpression of endothelial nitric oxide synthase attenuates cardiac hypertrophy induced by chronic isoproterenol infusion. *Circ. J.* 66 (9), 851–856. doi: 10.1253/circj.66.851

Paik, D. J., and Lee, C. H. (2015). Review of cases of patient risk associated with ginseng abuse and misuse. *J. Ginseng Res.* 39 (2), 89–93. doi: 10.1016/j.jgr.2014.11.005

Pan, S. Y., Zhou, S. F., Gao, S. H., Yu, Z. L., Zhang, S. F., Tang, M. K., et al. (2013). New Perspectives on How to Discover Drugs from Herbal Medicines: CAM's Outstanding Contribution to Modern Therapeutics. *Evid. Based Complement. Alternat. Med.* 2013, 627375. doi: 10.1155/2013/627375

Park, M. Y., Lee, K. S., and Sung, M. K. (2005). Effects of dietary mulberry, Korean red ginseng, and banaba on glucose homeostasis in relation to PPAR-alpha, PPAR-gamma, and LPL mRNA expressions. *Life Sci.* 77 (26), 3344–3354. doi: 10.1016/j.lfs.2005.05.043

Park, J.-H., Lee, J.-Y., Yeo, J.-Y., Nam, J.-S., and Jung, M.-H. (2011). Antihyperlipidemic effect of ginsenoside Rg1 in type 2 diabetic mice. *J. Life Sci.* 21 (7), 932–938. doi: 10.5352/JLS.2011.21.7.932

Park, J. B., Kwon, S. K., Nagar, H., Jung, S. B., Jeon, B. H., Kim, C. S., et al. (2014). Rg3-enriched Korean Red Ginseng improves vascular function in spontaneously hypertensive rats. *J. Ginseng Res.* 38 (4), 244–250. doi: 10.1016/j.jgr.2014.05.011

Park, K. S., Park, K. I., Kim, J. W., Yun, Y. J., Kim, S. H., Lee, C. H., et al. (2014). Efficacy and safety of Korean red ginseng for cold hypersensitivity in the hands and feet: a randomized, double-blind, placebo-controlled trial. *J. Ethnopharmacol.* 158 (Pt A), 25–32. doi: 10.1016/j.jep.2014.09.028

Park, S. H., Huh, T. L., Kim, S. Y., Oh, M. R., Tirupathi Pichiah, P. B., Chae, S. W., et al. (2014). Antiobesity effect of Gynostemma pentaphyllum extract (actiponin): a randomized, double-blind, placebo-controlled trial. *Obesity* 22 (1), 63–71. doi: 10.1002/oby.20539

Perez-Vizcaino, F., Duarte, J., Jimenez, R., Santos-Buelga, C., and Osuna, A. (2009). Antihypertensive effects of the flavonoid quercetin. *Pharmacol. Rep.* 61 (1), 67–75. doi: 10.1016/S1734-1140(09)70008-8

Persson, I. A., Dong, L., and Persson, K. (2006). Effect of Panax ginseng extract (G115) on angiotensin-converting enzyme (ACE) activity and nitric oxide (NO) production. *J. Ethnopharmacol.* 105 (3), 321–325. doi: 10.1016/j.jep.2005.10.030

Qureshi, A. A., Abuirmeileh, N., Din, Z. Z., Ahmad, Y., Burger, W. C., and Elson, C. E. (1983). Suppression of cholesterogenesis and reduction of LDL cholesterol by dietary ginseng and its fractions in chicken liver. *Atherosclerosis* 48 (1), 81–94. doi: 10.1016/0021-9150(83)90019-9

Rakugi, H., Yu, H., Kamitani, A., Nakamura, Y., Ohishi, M., Kamide, K., et al. (1996). Links between hypertension and myocardial infarction. *Am. Heart J.* 132 (1 Pt 2 Su), 213–221. doi: 10.1016/S0002-8703(96)90556-6

Ras, R. T., Zock, P. L., and Draijer, R. (2011). Tea consumption enhances endothelial-dependent vasodilation; a meta-analysis. *PloS One* 6 (3), e16974. doi: 10.1371/journal.pone.0016974

Razavi, B. M., Amanloo, M. A., Imenshahidi, M., and Hosseinzadeh, H. (2016). The Relaxant Activity of Safranal in Isolated Rat Aortas is Mediated Predominantly via an Endothelium-Independent Mechanism: -Vasodilatory mechanism of safranal. *J. Pharmacopuncture* 19 (4), 329–335. doi: 10.3831/KPI.2016.19.034

Razmovski-Naumovski, V., Huang, T. H.-W., Tran, V. H., Li, G. Q., Duke, C. C., and Roufogalis, B. D. (2005). Chemistry and pharmacology of Gynostemma Pentaphyllum. *Phytochem. Rev.* 4 (2-3), 197–219. doi: 10.1007/s11101-005-3754-4

Reiner, Z., Laufs, U., Cosentino, F., and Landmesser, U. (2019). The year in cardiology 2018: prevention. *Eur. Heart J.* 40 (4), 336–344. doi: 10.1093/eurheartj/ehy894

Ren, J., Fu, L., Nile, S. H., Zhang, J., and Kai, G. (2019). Salvia miltiorrhiza in Treating Cardiovascular Diseases: A Review on Its Pharmacological and Clinical Applications. *Front. Pharmacol.* 10, 753. doi: 10.3389/fphar.2019.00753

Rhee, M. Y., Kim, Y. S., Bae, J. H., Nah, D. Y., Kim, Y. K., Lee, M. M., et al. (2011). Effect of Korean red ginseng on arterial stiffness in subjects with hypertension. *J. Altern. Complement. Med.* 17 (1), 45–49. doi: 10.1089/acm.2010.0065

Rider, C. V., Nyska, A., Cora, M. C., Kissling, G. E., Smith, C., Travlos, G. S., et al. (2014). Toxicity and carcinogenicity studies of Ginkgo biloba extract in rat and mouse: liver, thyroid, and nose are targets. *Toxicol. Pathol.* 42 (5), 830–843. doi: 10.1177/0192623313501235

Ridker, P. M., Cushman, M., Stampfer, M. J., Tracy, R. P., and Hennekens, C. H. (1997). Inflammation, aspirin, and the risk of cardiovascular disease in apparently healthy men. *N. Engl. J. Med.* 336 (14), 973–979. doi: 10.1056/nejm199704033361401

Ridker, P. M., Hennekens, C. H., Buring, J. E., and Rifai, N. (2000). C-reactive protein and other markers of inflammation in the prediction of cardiovascular disease in women. *N. Engl. J. Med.* 342 (12), 836–843. doi: 10.1056/nejm200003233421202

Ridker, P. M., Everett, B. M., Thuren, T., MacFadyen, J. G., Chang, W. H., Ballantyne, C., et al. (2017). Antiinflammatory Therapy with Canakinumab for Atherosclerotic Disease. *N. Engl. J. Med.* 377 (12), 1119–1131. doi: 10.1056/NEJMoa1707914

Rizvi, A. A. (2017). Addressing hypertension in the patient with type 2 diabetes mellitus: pathogenesis, goals, and therapeutic approach. *Eur. Med. J. Diabetes* 5 (1), 84–92.

Rodrigo, R., Gonzalez, J., and Paoletto, F. (2011). The role of oxidative stress in the pathophysiology of hypertension. *Hypertens. Res.* 34 (4), 431–440. doi: 10.1038/hr.2010.264

Russo, V., Rago, A., Russo, G. M., Calabro, R., and Nigro, G. (2011). Ginkgo biloba: an ancient tree with new arrhythmic side effects. *J. Postgrad. Med.* 57 (3), 221. doi: 10.4103/0022-3859.85214

Saba, E., Jeon, B. R., Jeong, D. H., Lee, K., Goo, Y. K., Kim, S. H., et al. (2016). Black ginseng extract ameliorates hypercholesterolemia in rats. *J. Ginseng Res.* 40 (2), 160–168. doi: 10.1016/j.jgr.2015.07.003

Saleh Al-Shehabi, T., Iratni, R., and Eid, A. H. (2016). Anti-atherosclerotic plants which modulate the phenotype of vascular smooth muscle cells. *Phytomedicine* 23 (11), 1068–1081. doi: 10.1016/j.phymed.2015.10.016

Samaha, A. A., Fawaz, M., Salami, A., Baydoun, S., and Eid, A. H. (2019). Antihypertensive Indigenous Lebanese Plants: Ethnopharmacology and a Clinical Trial. *Biomolecules* 9 (7), E292. doi: 10.3390/biom9070292

Sanodiya, B. S., Thakur, G. S., Baghel, R. K., Prasad, G. B., and Bisen, P. S. (2009). Ganoderma lucidum: a potent pharmacological macrofungus. *Curr. Pharm. Biotechnol.* 10 (8), 717–742. doi: 10.2174/138920109789978757

Sargowo, D., Ovianti, N., Susilowati, E., Ubaidillah, N., Widya Nugraha, A., Vitriyaturrida,, et al. (2018). The role of polysaccharide peptide of Ganoderma lucidum as a potent antioxidant against atherosclerosis in high risk and stable angina patients. *Indian Heart J.* 70 (5), 608–614. doi: 10.1016/j.ihj.2017.12.007

Sargowo, D., Rahmah, F. N., Nugroho, F. W., Kamila, P. A., Irawan, D., Sitio, M., et al. (2019). "The role of PSP (policakarida peptida) as anti inflammation therapy and vascular endotel cell protectors in dislipidemic patients with or without diabetes through IL1, TNF-α, Cr Cr, EPC, CEC in STEMI and NSTEMI patients," in *AIP Conference Proceedings* (AIP Publishing), 020044.

Sawicka, K., Szczyrek, M., Jastrzębska, I., Prasał, M., Zwolak, A., and Daniluk, J. (2011). Hypertension – The Silent Killer. *J. Pre Clin. Clin. Res.* 5 (2), 43–46.

Schild, L., Chen, B. H., Makarov, P., Kattengell, K., Heinitz, K., and Keilhoff, G. (2010). Selective induction of apoptosis in glioma tumour cells by a Gynostemma pentaphyllum extract. *Phytomedicine* 17 (8-9), 589–597. doi: 10.1016/j.phymed.2009.12.002

Seldenrijk, A., van Hout, H. P., van Marwijk, H. W., de Groot, E., Gort, J., Rustemeijer, C., et al. (2011). Depression, anxiety, and arterial stiffness. *Biol. Psychiatry* 69 (8), 795–803. doi: 10.1016/j.biopsych.2010.12.034

Seyedemadi, P., Rahnema, M., Bigdeli, M. R., Oryan, S., and Rafati, H. (2016). The Neuroprotective Effect of Rosemary (Rosmarinus officinalis L.) Hydro-alcoholic Extract on Cerebral Ischemic Tolerance in Experimental Stroke. *Iran J. Pharm. Res.* 15 (4), 875–883.

Shah, B. R., Retnakaran, R., and Booth, G. L. (2008). Increased risk of cardiovascular disease in young women following gestational diabetes mellitus. *Diabetes Care* 31 (8), 1668–1669. doi: 10.2337/dc08-0706

Shergis, J. L., Zhang, A. L., Zhou, W., and Xue, C. C. (2013). Panax ginseng in randomised controlled trials: a systematic review. *Phytother. Res.* 27 (7), 949–965. doi: 10.1002/ptr.4832

Shevelev, O. B., Seryapina, A. A., Zavjalov, E. L., Gerlinskaya, L. A., Goryachkovskaya, T. N., Slynko, N. M., et al. (2018). Hypotensive and neurometabolic effects of intragastric Reishi (Ganoderma lucidum)

administration in hypertensive ISIAH rat strain. *Phytomedicine* 41, 1–6. doi: 10.1016/j.phymed.2018.01.013

Shi, Y. L., James, A. E., Benzie, I. F., and Buswell, J. A. (2002). Mushroom-derived preparations in the prevention of H2O2-induced oxidative damage to cellular DNA. *Teratog. Carcinog. Mutagen.* 22 (2), 103–111. doi: 10.1002/tcm.10008

Shi, W.-L., Han, H., Chen, G.-Z., Chen, X., Hong, Y.-K., Chen, L.-K., et al. (2010). Extraction, characterization of the polysaccharide extracts from Se-enriched G. lucidum (Se-GLP) and its inhibition against oxidative damage in ischemic reperfusion mice. *Carbohydr. Polym.* 80 (3), 774–778. doi: 10.1016/j.carbpol.2009.12.027

Shih-Chen, L., Smith, F., and Stuart, G. (1973). *Chinese medicinal herbs*. (San Francisco: Georgetown Press).

Shin, S. S., and Yoon, M. (2018). Korean red ginseng (Panax ginseng) inhibits obesity and improves lipid metabolism in high fat diet-fed castrated mice. *J. Ethnopharmacol.* 210, 80–87. doi: 10.1016/j.jep.2017.08.032

Shin, W., Yoon, J., Oh, G. T., and Ryoo, S. (2013). Korean red ginseng inhibits arginase and contributes to endotheliumdependent vasorelaxation through endothelial nitric oxide synthase coupling. *J. Ginseng Res.* 37 (1), 64–73. doi: 10.5142/jgr.2013.37.64

Shin, Y. M., Jung, H. J., Choi, W. Y., and Lim, C. J. (2013). Antioxidative, anti-inflammatory, and matrix metalloproteinase inhibitory activities of 20(S)-ginsenoside Rg3 in cultured mammalian cell lines. *Mol. Biol. Rep.* 40 (1), 269–279. doi: 10.1007/s11033-012-2058-1

Shishtar, E., Jovanovski, E., Jenkins, A., and Vuksan, V. (2014a). Effects of Korean White Ginseng (Panax Ginseng CA Meyer) on vascular and glycemic health in type 2 diabetes: results of a randomized, double blind, placebo-controlled, multiple-crossover, acute dose escalation trial. *Clin. Nutr. Res.* 3 (2), 89–97. doi: 10.7762/cnr.2014.3.2.89

Shishtar, E., Sievenpiper, J. L., Djedovic, V., Cozma, A. I., Ha, V., Jayalath, V. H., et al. (2014b). The effect of ginseng (the genus panax) on glycemic control: a systematic review and meta-analysis of randomized controlled clinical trials. *PloS One* 9 (9), e107391. doi: 10.1371/journal.pone.0107391

Siegel, R. K. (1979). Ginseng abuse syndrome. Problems with the panacea. *JAMA* 241 (15), 1614–1615. doi: 10.1001/jama.1979.03290410046024

Singh, R. B., and Niaz, M. A. (1996). Antioxidants, oxidants and free radical stress in cardiovascular disease. *J. Assoc. Physicians India* 44 (1), 43–48.

Singh, B., Kaur, P., Gopichand,, Singh, R. D., and Ahuja, P. S. (2008). Biology and chemistry of Ginkgo biloba. *Fitoterapia* 79 (6), 401–418. doi: 10.1016/j.fitote.2008.05.007

Singh, R. K., Lui, E., Wright, D., Taylor, A., and Bakovic, M. (2017). Alcohol extract of North American ginseng (Panax quinquefolius) reduces fatty liver, dyslipidemia, and other complications of metabolic syndrome in a mouse model. *Can. J. Physiol. Pharmacol.* 95 (9), 1046–1057. doi: 10.1139/cjpp-2016-0510

Smina, T. P., Mathew, J., Janardhanan, K. K., and Devasagayam, T. P. (2011). Antioxidant activity and toxicity profile of total triterpenes isolated from Ganoderma lucidum (Fr.) P. Karst occurring in South India. *Environ. Toxicol. Pharmacol.* 32 (3), 438–446. doi: 10.1016/j.etap.2011.08.011

Song, S. W., Kim, H. N., Shim, J. Y., Yoo, B. Y., Kim, D. H., Lee, S. H., et al. (2018). Safety and tolerability of Korean Red Ginseng in healthy adults: a multicenter, double-blind, randomized, placebo-controlled trial. *J. Ginseng Res.* 42 (4), 571–576. doi: 10.1016/j.jgr.2018.07.002

Sowers, J. R. (2003). Obesity as a cardiovascular risk factor. *Am. J. Med.* 115 (8), 37–41. doi: 10.1016/j.amjmed.2003.08.012

Srichana, D., Taengtip, R., and Kondo, S. (2011). Antimicrobial activity of Gynostemma pentaphyllum extracts against fungi producing aflatoxin and fumonisin and bacteria causing diarrheal disease. *Southeast Asian J. Trop. Med. Public Health* 42 (3), 704–710.

Stewart, M. H., Lavie, C. J., and Ventura, H. O. (2019). Emerging Therapy in Hypertension. *Curr. Hypertens. Rep.* 21 (3), 23. doi: 10.1007/s11906-019-0923-1

Sun, T., Wang, X., and Xu, H. (2015). Ginkgo Biloba extract for angina pectoris: a systematic review. *Chin. J. Integr. Med.* 21 (7), 542–550. doi: 10.1007/s11655-015-2070-0

Sun, M., Chai, L., Lu, F., Zhao, Y., Li, Q., Cui, B., et al. (2018). Efficacy and Safety of Ginkgo Biloba Pills for Coronary Heart Disease with Impaired Glucose Regulation: Study Protocol for a Series of N-of-1 Randomized, Double-Blind, Placebo-Controlled Trials. *Evid. Based Complement. Alternat. Med.* 2018, 7571629. doi: 10.1155/2018/7571629

Sun, Y. E., Wang, W., and Qin, J. (2018). Anti-hyperlipidemia of garlic by reducing the level of total cholesterol and low-density lipoprotein: A meta-analysis. *Medicine (Baltimore)* 97 (18), e0255. doi: 10.1097/MD.0000000000010255

Susalit, E., Agus, N., Effendi, I., Tjandrawinata, R. R., Nofiarny, D., Perrinjaquet-Moccetti, T., et al. (2011). Olive (Olea europaea) leaf extract effective in patients with stage-1 hypertension: comparison with Captopril. *Phytomedicine* 18 (4), 251–258. doi: 10.1016/j.phymed.2010.08.016

Tabas, I., Williams, K. J., and Boren, J. (2007). Subendothelial lipoprotein retention as the initiating process in atherosclerosis: update and therapeutic implications. *Circulation* 116 (16), 1832–1844. doi: 10.1161/circulationaha.106.676890

Tabassum, N., and Ahmad, F. (2011). Role of natural herbs in the treatment of hypertension. *Pharmacogn. Rev.* 5 (9), 30–40. doi: 10.4103/0973-7847.79097

Tachjian, A., Maria, V., and Jahangir, A. (2010). Use of herbal products and potential interactions in patients with cardiovascular diseases. *J. Am. Coll. Cardiol.* 55 (6), 515–525. doi: 10.1016/j.jacc.2009.07.074

Tada, Y., Kagota, S., Kubota, Y., Nejime, N., Nakamura, K., Kunitomo, M., et al. (2008). Long-term feeding of Ginkgo biloba extract impairs peripheral circulation and hepatic function in aged spontaneously hypertensive rats. *Biol. Pharm. Bull.* 31 (1), 68–72. doi: 10.1248/bpb.31.68

Tan, M. S., Yu, J. T., Tan, C. C., Wang, H. F., Meng, X. F., Wang, C., et al. (2015). Efficacy and adverse effects of ginkgo biloba for cognitive impairment and dementia: a systematic review and meta-analysis. *J. Alzheimers Dis.* 43 (2), 589–603. doi: 10.3233/JAD-140837

Tanner, M. A., Bu, X., Steimle, J. A., and Myers, P. R. (1999). The direct release of nitric oxide by gypenosides derived from the herb Gynostemma pentaphyllum. *Nitric. Oxide* 3 (5), 359–365. doi: 10.1006/niox.1999.0245

Tao, J., and Feng, K. Y. (1990). Experimental and clinical studies on inhibitory effect of ganoderma lucidum on platelet aggregation. *J. Tongji Med. Univ.* 10 (4), 240–243. doi: 10.1007/bf02887938

Tedgui, A., and Mallat, Z. (2006). Cytokines in atherosclerosis: pathogenic and regulatory pathways. *Physiol. Rev.* 86 (2), 515–581. doi: 10.1152/physrev.00024.2005

Thomson, M., Al-Qattan, K. K., Js, D., and Ali, M. (2016). Anti-diabetic and anti-oxidant potential of aged garlic extract (AGE) in streptozotocin-induced diabetic rats. *BMC Complement. Altern. Med.* 16, 17. doi: 10.1186/s12906-016-0992-5

Toda, N., Ayajiki, K., Fujioka, H., and Okamura, T. (2001). Ginsenoside potentiates NO-mediated neurogenic vasodilatation of monkey cerebral arteries. *J. Ethnopharmacol.* 76 (1), 109–113. doi: 10.1016/s0378-8741(01)00217-3

Tomoda, M., Gonda, R., Kasahara, Y., and Hikino, H. (1986). Glycan structures of ganoderans b and c, hypoglycemic glycans of ganoderma lucidum fruit bodies. *Phytochemistry* 25 (12), 2817–2820. doi: 10.1016/S0031-9422(00)83748-6

Torbey, E., Abi Rafeh, N., Khoueiry, G., Kowalski, M., and Bekheit, S. (2011). Ginseng: a potential cause of long QT. *J. Electrocardiol.* 44 (3), 357–358. doi: 10.1016/j.jelectrocard.2010.08.007

Toth, P. P. (2007). Making a case for quantitative assessment of cardiovascular risk. *J. Clin. Lipidol.* 1 (4), 234–241. doi: 10.1016/j.jacl.2007.07.002

Triantafyllidi, H., Tzortzis, S., Lekakis, J., Ikonomidis, I., Arvaniti, C., Trivilou, P., et al. (2010). Association of target organ damage with three arterial stiffness indexes according to blood pressure dipping status in untreated hypertensive patients. *Am. J. Hypertens.* 23 (12), 1265–1272. doi: 10.1038/ajh.2010.156

Tsutsui, M., Nakata, S., Shimokawa, H., Otsuji, Y., and Yanagihara, N. (2008). Spontaneous myocardial infarction and nitric oxide synthase. *Trends Cardiovasc. Med.* 18 (8), 275–279. doi: 10.1016/j.tcm.2008.12.002

Ubaidillah, N., Widya, A., Vittryaturida,, Siwi, K., Failasufi, M., Ramadhan, F., et al. (2016). "The novel effect of polysaccharide peptides ganoderma lucidum in endothelial dysfuction on stable angina patients," in *European Heart Journal Supplements* (Oxford, England: Oxford Univ Press), B39–B39.

Ude, C., Schubert-Zsilavecz, M., and Wurglics, M. (2013). Ginkgo biloba extracts: a review of the pharmacokinetics of the active ingredients. *Clin. Pharmacokinet.* 52 (9), 727–749. doi: 10.1007/s40262-013-0074-5

Valli, G., and Giardina, E. G. (2002). Benefits, adverse effects and drug interactions of herbal therapies with cardiovascular effects. *J. Am. Coll. Cardiol.* 39 (7), 1083–1095. doi: 10.1016/s0735-1097(02)01749-7

Virmani, R., Burke, A. P., Kolodgie, F. D., and Farb, A. (2002). Vulnerable plaque: the pathology of unstable coronary lesions. *J. Interv. Cardiol.* 15 (6), 439–446. doi: 10.1111/j.1540-8183.2002.tb01087.x

Vogelzangs, N., Seldenrijk, A., Beekman, A. T., van Hout, H. P., de Jonge, P., and Penninx, B. W. (2010). Cardiovascular disease in persons with depressive and

anxiety disorders. *J. Affect. Disord.* 125 (1-3), 241–248. doi: 10.1016/j.jad.2010.02.112

Vogler, B. K., Pittler, M. H., and Ernst, E. (1999). The efficacy of ginseng. A systematic review of randomised clinical trials. *Eur. J. Clin. Pharmacol.* 55 (8), 567–575. doi: 10.1007/s002280050674

Wachtel-Galor, S., Tomlinson, B., and Benzie, I. F. (2004). Ganoderma lucidum ("Lingzhi"), a Chinese medicinal mushroom: biomarker responses in a controlled human supplementation study. *Br. J. Nutr.* 91 (2), 263–269. doi: 10.1079/BJN20041039

Wachtel-Galor, S., Wong, W.-c., Choi, S.-W., and Benzie, I. F. (2010). Antioxidant Power and DNA Repair Effects of Lingzhi or Reishi Medicinal Mushroom, Ganoderma lucidum (W. Curt.: Fr.) P. Karst.(Aphyllophoromycetideae), in Human Acute Post-ingestion Study. *Int. J. Med. Mushrooms* 12 (4), 359–366. doi: 10.1615/IntJMedMushr.v12.i4.30

Wada, K., Ishigaki, S., Ueda, K., Take, Y., Sasaki, K., Sakata, M., et al. (1988). Studies on the constitution of edible and medicinal plants. I. Isolation and identification of 4-O-methylpyridoxine, toxic principle from the seed of Ginkgo biloba L. *Chem. Pharm. Bull.* 36 (5), 1779–1782. doi: 10.1248/cpb.36.1779

Wada, K. (2005). [Ginkgo seed food poisoning]. *Chudoku Kenkyu* 18 (1), 11–16.

Wang, J., and Xiong, X. (2012). Outcome measures of chinese herbal medicine for hypertension: an overview of systematic reviews. *Evid. Based Complement. Alternat. Med.* 2012, 697237. doi: 10.1155/2012/697237

Wang, M., Wang, F., Wang, Y., Ma, X., Zhao, M., and Zhao, C. (2013). Metabonomics study of the therapeutic mechanism of Gynostemma pentaphyllum and atorvastatin for hyperlipidemia in rats. *PloS One* 8 (11), e78731. doi: 10.1371/journal.pone.0078731

Wang, F., Zhou, Z., Ren, X., Wang, Y., Yang, R., Luo, J., et al. (2015). Effect of Ganoderma lucidum spores intervention on glucose and lipid metabolism gene expression profiles in type 2 diabetic rats. *Lipids Health Dis.* 14, 49. doi: 10.1186/s12944-015-0045-y

Wang, Z., Zhang, J., Ren, T., and Dong, Z. (2016). Targeted metabolomic profiling of cardioprotective effect of Ginkgo biloba L. extract on myocardial ischemia in rats. *Phytomedicine* 23 (6), 621–631. doi: 10.1016/j.phymed.2016.03.005

Wang, Y. R., Yang, K., Cui, W. Y., and Piao, X. L. (2018). [Effects of flavonoids from Gynostemma pentaphyllum on A549 cells damaged by hydrogen peroxide]. *Zhongguo Zhong Yao Za Zhi* 43 (5), 1014–1020. doi: 10.19540/j.cnki.cjcmm.2018.0034

Wang, Z., Zhao, X., Liu, X., Lu, W., Jia, S., Hong, T., et al. (2019). Anti-diabetic activity evaluation of a polysaccharide extracted from Gynostemma pentaphyllum. *Int. J. Biol. Macromol.* 126, 209–214. doi: 10.1016/j.ijbiomac.2018.12.231

Weber, C., and Noels, H. (2011). Atherosclerosis: current pathogenesis and therapeutic options. *Nat. Med.* 17 (11), 1410–1422. doi: 10.1038/nm.2538

Weber, M. A., Schiffrin, E. L., White, W. B., Mann, S., Lindholm, L. H., Kenerson, J. G., et al. (2014). Clinical practice guidelines for the management of hypertension in the community a statement by the American Society of Hypertension and the International Society of Hypertension. *J. Hypertens.* 32 (1), 3–15. doi: 10.1097/hjh.0000000000000065

Weinmann, S., Roll, S., Schwarzbach, C., Vauth, C., and Willich, S. N. (2010). Effects of Ginkgo biloba in dementia: systematic review and meta-analysis. *BMC Geriatr.* 10, 14. doi: 10.1186/1471-2318-10-14

Wicks, S. M., Tong, R., Wang, C. Z., O'Connor, M., Karrison, T., Li, S., et al. (2007). Safety and tolerability of Ganoderma lucidum in healthy subjects: a double-blind randomized placebo-controlled trial. *Am. J. Chin. Med.* 35 (3), 407–414. doi: 10.1142/S0192415X07004928

Widya, A., Ubaidillah, N., Vittryaturida,, Siwi, K., Failasufi, M., Ramadhan, F., et al. (2016). "An experimental study of beta-D-Glucans exctract of Ganoderma lucidum polysaccharide peptides as anti-inflammation and anti-oxidant in patients at high-risk of atherosclerosis," in *European Heart Journal Supplements* (Oxford, England: Oxford Univ Press), B19–B19.

Wihastuti, T. A., and Heriansyah, T. (2017). The inhibitory effects of polysaccharide peptides (PsP) of Ganoderma lucidum against atherosclerosis in rats with dyslipidemia. *Heart Int.* 12 (1), e1–e7. doi: 10.5301/heartint.5000234

Witztum, J. L., and Berliner, J. A. (1998). Oxidized phospholipids and isoprostanes in atherosclerosis. *Curr. Opin. Lipidol.* 9 (5), 441–448. doi: 10.1097/00041433-199810000-00008

Wong, W. Y., Lee, M. M., Chan, B. D., Ma, V. W., Zhang, W., Yip, T. T., et al. (2017). Gynostemma pentaphyllum saponins attenuate inflammation in vitro and in vivo by inhibition of NF-kappaB and STAT3 signaling. *Oncotarget* 8 (50), 87401–87414. doi: 10.18632/oncotarget.20997

World Health Organization (2017). *Cardiovascular Diseases (CVDs)* (World Health Organization). Available: https://www.who.int/news-room/fact-sheets/detail/cardiovascular-diseases-(cvds) [Accessed 26-06-2019].

Wu, Q., Li, Y., Peng, K., Wang, X. L., Ding, Z., Liu, L., et al. (2019). Isolation and Characterization of Three Antihypertension Peptides from the Mycelia of Ganoderma Lucidum (Agaricomycetes). *J. Agric. Food Chem.* 67 (29), 8149–8159. doi: 10.1021/acs.jafc.9b02276

Xie, Y. Z., Yang, F., Tan, W., Li, X., Jiao, C., Huang, R., et al. (2016). The anti-cancer components of Ganoderma lucidum possesses cardiovascular protective effect by regulating circular RNA expression. *Oncoscience* 3 (7-8), 203–207. doi: 10.18632/oncoscience.316

Xiong, X. J., Liu, W., Yang, X. C., Feng, B., Zhang, Y. Q., Li, S. J., et al. (2014). Ginkgo biloba extract for essential hypertension: a systemic review. *Phytomedicine* 21 (10), 1131–1136. doi: 10.1016/j.phymed.2014.04.024

Yamamoto, M., Uemura, T., Nakama, S., Uemiya, M., and Kumagai, A. (1983). Serum HDL-cholesterol-increasing and fatty liver-improving actions of Panax ginseng in high cholesterol diet-fed rats with clinical effect on hyperlipidemia in man. *Am. J. Chin. Med.* 11 (1-4), 96–101. doi: 10.1142/S0192415X83000161

Yan, W., Niu, Y., Lv, J., Xie, Z., Jin, L., Yao, W., et al. (2013). Characterization of a heteropolysaccharide isolated from diploid Gynostemma pentaphyllum Makino. *Carbohydr. Polym.* 92 (2), 2111–2117. doi: 10.1016/j.carbpol.2012.11.074

Yang, J.-W., and Kim, S. S. (2015). Ginsenoside Rc promotes anti-adipogenic activity on 3T3-L1 adipocytes by down-regulating C/EBPα and PPARγ. *Molecules* 20 (1), 1293–1303. doi: 10.3390/molecules20011293

Yang, T. Y., Wei, J. C., Lee, M. Y., Chen, C. M., and Ueng, K. C. (2012). A randomized, double-blind, placebo-controlled study to evaluate the efficacy and tolerability of Fufang Danshen (Salvia miltiorrhiza) as add-on antihypertensive therapy in Taiwanese patients with uncontrolled hypertension. *Phytother. Res.* 26 (2), 291–298. doi: 10.1002/ptr.3548

Yang, K., Zhang, H., Luo, Y., Zhang, J., Wang, M., Liao, P., et al. (2017). Gypenoside XVII Prevents atherosclerosis by attenuating endothelial apoptosis and oxidative stress: Insight into the ERα-mediated PI3K/Akt pathway. *Int. J. Mol. Sci.* 18 (2), 77. doi: 10.3390/ijms18020077

Yeh, G. Y., Davis, R. B., and Phillips, R. S. (2006). Use of complementary therapies in patients with cardiovascular disease. *Am. J. Cardiol.* 98 (5), 673–680. doi: 10.1016/j.amjcard.2006.03.051

Yeo, J., Kang, Y. J., Jeon, S. M., Jung, U. J., Lee, M. K., Song, H., et al. (2008). Potential hypoglycemic effect of an ethanol extract of Gynostemma pentaphyllum in C57BL/KsJ-db/db mice. *J. Med. Food* 11 (4), 709–716. doi: 10.1089/jmf.2007.0148

Yu, H., Guan, Q., Guo, L., Zhang, H., Pang, X., Cheng, Y., et al. (2016a). Gypenosides alleviate myocardial ischemia-reperfusion injury via attenuation of oxidative stress and preservation of mitochondrial function in rat heart. *Cell Stress Chaperones* 21 (3), 429–437. doi: 10.1007/s12192-016-0669-5

Yu, H., Zhang, H., Zhao, W., Guo, L., Li, X., Li, Y., et al. (2016b). Gypenoside Protects against Myocardial Ischemia-Reperfusion Injury by Inhibiting Cardiomyocytes Apoptosis via Inhibition of CHOP Pathway and Activation of PI3K/Akt Pathway In Vivo and In Vitro. *Cell Physiol. Biochem.* 39 (1), 123–136. doi: 10.1159/000445611

Yuan, C. S., Wei, G., Dey, L., Karrison, T., Nahlik, L., Maleckar, S., et al. (2004). Brief communication: American ginseng reduces warfarin's effect in healthy patients: a randomized, controlled Trial. *Ann. Intern. Med.* 141 (1), 23–27. doi: 10.7326/0003-4819-141-1-200407060-00011

Yuan, H., Ma, Q., Ye, L., and Piao, G. (2016). The Traditional Medicine and Modern Medicine from Natural Products. *Molecules* 21 (5), E559. doi: 10.3390/molecules21050559

Zeng, Z., Zhu, J., Chen, L., Wen, W., and Yu, R. (2013). Biosynthesis pathways of ginkgolides. *Pharmacogn. Rev.* 7 (13), 47–52. doi: 10.4103/0973-7847.112848

Zhang, W.-D., Chen, H., Zhang, C., Liu, R.-H., Li, H.-L., and Chen, H.-Z. (2006). Astragaloside IV from Astragalus membranaceus shows cardioprotection during myocardial ischemia in vivo and in vitro. *Planta Med.* 72 (01), 4–8. doi: 10.1055/s-2005-873126

Zhang, L., Yang, Y., Wang, Y., and Gao, X. (2011). Astragalus membranaceus extract promotes neovascularisation by VEGF pathway in rat model of ischemic injury. *Pharmazie* 66 (2), 144–150.

Zhang, J., Gao, X., Pan, Y., Xu, N., and Jia, L. (2016). Toxicology and immunology of Ganoderma lucidum polysaccharides in Kunming mice and Wistar rats. *Int. J. Biol. Macromol.* 85, 302–310. doi: 10.1016/j.ijbiomac.2015.12.090

Zhang, X., Xiao, C., and Liu, H. (2018). Ganoderic Acid A Protects Rat H9c2 Cardiomyocytes from Hypoxia-Induced Injury via Up-Regulating miR-182-5p. *Cell Physiol. Biochem.* 50 (6), 2086–2096. doi: 10.1159/000495053

Zhang, X., Su, H., Yang, J., Feng, L., Li, Z., and Zhao, G. (2019). Population genetic structure, migration, and polyploidy origin of a medicinal species Gynostemma pentaphyllum (Cucurbitaceae). *Ecol. Evol.* 9 (19), 11145–11170. doi: 10.1002/ece3.5618

Zhao, G.-R., Xiang, Z.-J., Ye, T.-X., Yuan, Y.-J., and Guo, Z.-X. (2006). Antioxidant activities of Salvia miltiorrhiza and Panax notoginseng. *Food Chem.* 99 (4), 767–774. doi: 10.1016/j.foodchem.2005.09.002

Zheng, X. J. (2004). [Composition analysis and dominance test of three kinds of raw variety of Gynostemma pentaphyllum]. *Zhongguo Zhong Yao Za Zhi* 29 (4), 317–319.

Zhou, J., Fan, Y., Kong, J., Wu, D., and Hu, Z. (2000). Effects of components isolated from Astragalus membranaceus Bunge on cardiac function injured by myocardial ischemia reperfusion in rats. *Zhongguo Zhong Yao Za Zhi* 25 (5), 300–302.

Conflict of Interest: The authors declare that the research was conducted in the absence of any commercial or financial relationships that could be construed as a potential conflict of interest.

frontiers in Pharmacology

REVIEW
published: 08 April 2020
doi: 10.3389/fphar.2020.00403

Medicinal Plants as a Potential and Successful Treatment Option in the Context of Atherosclerosis

Tatiana V. Kirichenko[1,2,3], *Vasily N. Sukhorukov*[1,2,3], *Alexander M. Markin*[1], *Nikita G. Nikiforov*[2,3], *Ping-Yen Liu*[4,5], *Igor A. Sobenin*[1,3], *Vadim V. Tarasov*[6], *Alexander N. Orekhov*[1,2] *and Gjumrakch Aliev*[6,7,8,9*]

[1] Laboratory of Infection Pathology and Molecular Microecology, Research Institute of Human Morphology, Moscow, Russia, [2] Laboratory of Angiopathology, Institute of General Pathology and Pathophysiology, Moscow, Russia, [3] Laboratory of Medical Genetics, National Medical Research Center of Cardiology, Moscow, Russia, [4] Institute of Clinical Medicine, College of Medicine, National Cheng Kung University, Tainan, Taiwan, [5] Division of Cardiology, College of Medicine, National Cheng Kung University Hospital, Tainan, Taiwan, [6] Sechenov First Moscow State Medical University (Sechenov University), Moscow, Russia, [7] Institute of Physiologically Active Compounds, Russian Academy of Sciences, Chernogolovka, Russia, [8] GALLY International Research Institute, San Antonio, TX, United States, [9] Laboratory of Molecular Pathology, Research Institute of Human Morphology, Moscow, Russia

OPEN ACCESS

Edited by:
Yue Liu,
Xiyuan Hospital, China

Reviewed by:
Ali H. Eid,
American University of Beirut, Lebanon
Yanfei Liu,
Beijing University of Chinese Medicine, China

***Correspondence:**
Gjumrakch Aliev
aliev03@gmail.com;
cobalt55@gallyinternational.com

Specialty section:
This article was submitted to Ethnopharmacology, a section of the journal Frontiers in Pharmacology

Received: *06 December 2019*
Accepted: *17 March 2020*
Published: *08 April 2020*

Citation:
Kirichenko TV, Sukhorukov VN, Markin AM, Nikiforov NG, Liu P-Y, Sobenin IA, Tarasov VV, Orekhov AN and Aliev G (2020) Medicinal Plants as a Potential and Successful Treatment Option in the Context of Atherosclerosis. Front. Pharmacol. 11:403. doi: 10.3389/fphar.2020.00403

Atherosclerosis is a chronic multifactorial disease characterized by mainly changes of blood lipids profile and inflammation in vessel wall. The cardiovascular disease based on atherosclerosis is currently the leading cause of mortality in developed countries. Therefore, timely prevention and therapy of atherosclerosis are able to reduce the risk of the development of its clinical manifestations. Anti-atherosclerotic activity of medicinal plants mainly appears in their multiple effects such as anti-inflammatory, antioxidant, anti-atherogenic, hypotensive, lipid-lowering, anti-thrombotic. Moreover, most of medicinal plants are characterized by their pleiotropic anti-atherosclerotic action. In addition, the medicinal plants-derived pharmacological substances and/or compounds are characterized by relative safety and fewer side effects that allows considering them as one of potential anti-atherosclerotic effective agents. The direct anti-atherosclerotic effect of some medicinal plants was confirmed in clinical trials of carotid Intima-media thickness (IMT) progression during long-term medication with medicinal plants. This review attempted to determine the current status of the databases PubMed and Scopus (until November, 2019) to investigate the medicinal plants possessing anti-atherosclerotic activity in experimental and clinical studies.

Keywords: medicinal plants, atherosclerosis, cardiovascular risk, anti-atherosclerotic mechanisms, carotid IMT

Abbreviations: LDL, low-density lipoproteins; HDL, high-density lipoproteins; TC, total cholesterol; Tg, triglycerides; hs-CRP, high-sensitive C-reactive protein; cIMT, intima-media thickness of carotid arteries; VCAM-1, Vascular cell adhesion molecule-1; ICAM-1, Intercellular adhesion molecule-1; TNF, tumor-necrosis factor; IL, interleukin; HLA-DR - human leukocyte antigen - DR isotype; HUVECs, human umbilical vein endothelial cells; NO, nitric oxide; HMG-CoA, 3-hydroxy-3-methyl-glutaryl coenzyme A reductase; SREBP-1c, sterol regulatory element binding protein-1c (); COX-2, cyclooxygenase-2; BMI, body mass index; T2D, type 2 diabetes mellitus; DBP, diastolic blood pressure; SBP, systolic blood pressure; ACAT, Acyl-CoA-cholesterol-acyltransferase); PPAR, peroxisome proliferator-activated receptors.

INTRODUCTION

Atherosclerosis is a chronic multifactorial disease characterized by dyslipidemia and inflammation. Nowadays it is one of the key reasons of cardiovascular disease that is currently the leading cause of mortality in developed countries (Libby et al., 2011; Fredman and Spite, 2013). Atherosclerosis develops in the human arteries for many years, and remains asymptomatic for a long time. Patients very often learn about the presence of atherosclerotic lesions when they seek medical attention because of the development of cardiovascular disease, that is a complication of the atherosclerotic process. However, initial atherosclerotic lesions can be identified at the subclinical stage by modern diagnostic methods, which make it possible to start prevention timely. Anti-atherosclerotic therapy is very important for the prevention of diseases of this group and their complications. Non-drug methods of prevention exist and apply. They are based on the prevention of the development of cardiovascular disease by changing lifestyle, keeping a diet, and administration of courses of medicinal plants and natural products that possess anti-atherosclerotic properties (Pogosova et al., 2017).

In general, atherosclerosis can be also described as a type of immunological disorder, in which immune cells are activated along the inflammatory pathway and migrate into the vascular intima. After that, atherosclerotic lesion may develop in this place (Frostegard, 2013). Recent data indicate that the prevailing beliefs about the decisive role of high cholesterol in the development of atherosclerosis are not entirely correct. High blood cholesterol does not always clearly correlate with the presence of atherosclerotic lesions in arterial wall and complications of atherosclerosis process (Orekhov and Ivanova, 2017).

Currently, a strategy for the correction of lipid metabolism disorders is widely used around the world to treat atherosclerosis. But at the same time, researchers are developing methods to counteract inflammatory processes in the vessel wall at cellular level. The viability of these methods is indicated by the latest data from studies of the pathogenesis of atherosclerotic lesions. This process begins in the intima layer of large and medium arteries, especially in places of bifurcation. Vascular wall of such areas experiences increased stress due to the turbulent effects of blood flow. This causes damage to the cells of endothelial layer of intima, resulting in attracting of immune cells due to the production of adhesion molecules. (Koch and Zernecke, 2014). At the same time, low-density lipoproteins (LDL) undergo modification (Nikifirov et al., 2017; Alipov et al., 2017) and acquire the ability to penetrate and accumulate at the subendothelial level of the arterial wall. There they can additionally undergo oxidation, turning into oxidized LDL. Monocytes attracted by endothelial cells in the intimal space differentiate into macrophages and absorb oxidized LDL. However, in the event of a violation of the processes of cholesterol metabolism in macrophages, they are transformed into foam cells (Pirillo et al., 2013; Lopes-Virella and Virella, 2013; Witztum and Lichtman, 2014; Akhter et al., 2016; Tabas and Lichtman, 2017).

Thus, the activation of cascades of immune and inflammatory reactions is crucial for the progression of atherosclerotic lesions. In attempt to influence these processes, several new strategies for the treatment of atherosclerosis, based on the use of various therapeutic agents to inhibit the pro-inflammatory activation of immune cells or stimulate signals to the anti-inflammatory activity of body systems, have recently appeared. They can be used as an addition to conventional methods of treating cardiovascular diseases based on the use of lipid-lowering preparations (Li et al., 2017; Chistiakov et al., 2018). However, the most common preparations used for anti-atherosclerotic therapy are currently statins since they possess multiple anti-atherosclerotic properties (Davignon, 2012; Tian et al., 2012; Oesterle et al., 2017), but their prescription is still limited because of prolonged administration of preparations of this group leads to a risk of undesirable side effects so statins are traditionally prescribed to patients with hypercholesterolemia (Stroes et al., 2015; Beckett et al., 2015).

Nowadays, there are no preparations that can be used for long-term prevention and treatment of atherosclerosis without the risk of developing pronounced side effects. This leads to the extremely high relevance of the study and use of medicinal plants for long-term anti-atherosclerotic therapy. Actually, the medical properties of various plants have been known since ancient times. A large number of herbal preparations are capable of exerting inhibitory effects in pathological immune reactions, and some of them have traditionally been used for the modulation of atherosclerosis progression. It can be explained by their relative safety, fewer side effects, and, in a sense, their greater effectiveness. Since cytokines are the main mediators in all types of inflammation, that is a significant factor at all phases of the atherosclerosis progression, the studies of the use of medicinal plants for modulation of cytokines production are very relevant in the field of atherosclerosis medication (Ramji and Davies, 2015; Fatkhullina et al., 2016). In addition, medicinal plants are widely used for the correction of conventional risk factors of atherosclerosis such as hyperlipidemia, hypertension, and etc. (Tariq et al., 2016; Chukwuma et al., 2019). The variety of clinical trials' results of various research groups studying medicinal plants can be partially explained by the multiple mechanisms of action on various cardiovascular risk factors. In addition, some visualization methods give encouraging results. For example, evaluation of the carotid intima-media thickness (CIMT) indicator (intima-media thickness of the carotid arteries) using ultrasound investigation can quantify the progression of atherosclerotic lesions and evaluate the direct effect of these preparations on atherosclerosis (Bots et al., 2016; Katakami et al., 2019).

This review reflects current views on how medicinal plants are used to reduce the risk of atherosclerosis development, their direct or indirect anti-atherosclerotic effects. English scientific literature was searched using electronic databases PubMed and Scopus by keywords “medicinal plants”, “natural products”, “atherosclerosis”, “intima-media thickness”, “cardiovascular risk”, “clinical trial” in different combinations until November,

2019, with first focus on medicinal plants with proven direct anti-atherosclerotic activity in patients with carotid atherosclerosis and natural products possessing cardioprotective effects in clinical trials, and further their anti-atherosclerotic mechanisms of action were reviewed. We will focus on medicinal plants and the products created on their base, used in modern practice meeting the principles of evidence-based medicine.

POSSIBLE ANTI-ATHEROSCLEROTIC MECHANISMS OF MEDICINAL PLANTS

Atherosclerosis is a multifactorial process, and despite the great progress in understanding the mechanisms of the development of atherosclerotic lesions in the last decades, the pathogenesis of atherosclerosis is the subject of study by a large circle of scientists around the world. Nevertheless, the key points of the pathogenesis of atherosclerosis are known, and the possible pathogenetic mechanisms of the anti-atherosclerotic effects of medicinal plants are being studied in cell cultures, animal models, and human studies. **Figure 1** summarizes plausible effects of medicinal plants reviewed in this article, on different stages of atherosclerosis development. The effects of the most promising natural anti-atherosclerotic agents are noteworthy.

Numerous studies describe the contribution of pro-inflammatory cytokines to the formation of atherosclerotic lesions in arterial wall. Evidence from these studies underlies the potential use of anti-cytokine therapy that can become a promising direction for the correction of changes at early stages of the atherosclerosis development. Thanks to recent studies, it was found that components of a large number of medicinal plants are capable of modulating the pathways of the inflammatory response. Many of these natural products have anti-cytokine mechanism of action, and most of them do not possess pronounced side effects and can be used for long-term prevention and treatment of atherosclerosis. In particular, herbal preparation Inflaminat, mixture of black elder (*Sambucus nigra* L.), violet tricolor (*Viola tricolor* L.), and calendula (*Calendula officinalis* L.), significantly inhibits the expression of inflammatory cytokines *via* inhibiting IL-6 and TNF-α expression and alleviates serum atherogenic activities *via* unknown mechanism in *ex vivo* model (Kirichenko et al., 2016).

There are some beneficial data of multiple anti-inflammatory and anti-atherosclerotic effects of glabridin, a flavonoid isolated

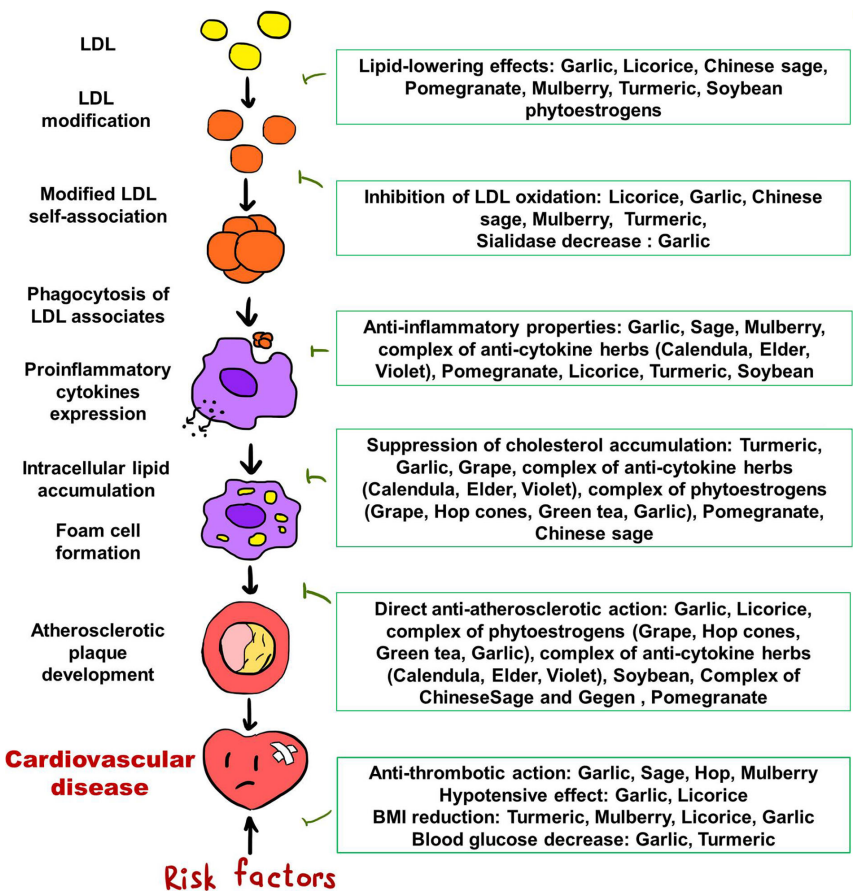

FIGURE 1 | Plausible effects of medicinal plants on different stages of atherosclerosis development.

from licorice (*Glycyrrhiza glabra* L.). Glabridin possesses anti-inflammatory action by preventing TNF-α-stimulated gene expression of VCAM-1 (vascular cell adhesion molecule-1) and ICAM-1 (intercellular adhesion molecule-1) *via* blocking JNK and NF-κB (Kwon et al., 2007; Cook-Mills et al., 2011). Glabridin possesses anti-cytokine activity, since it suppresses the LPS-stimulated secretion of inflammatory cytokines TNF-α and IL-1β in microglial cells (Park et al., 2010) and TNF-α- stimulated production of adhesion molecules in human umbilical vein endothelial cells (Jong et al., 2006; Chang et al., 2010). In addition to anti-inflammatory properties, glabridin can inhibits LDL oxidation by suppression of 2,2-azobis(2-amidinopropane) hydrochloride (AAPH)–stimulated production of cholesteryl linoleate hydroperoxide in LDL, and the reduction of LDL oxidation by glabridin was confirmed in *ex vivo* model: the ability to oxidize LDL in cell culture of mice peritoneal macrophages decreased after accumulation of glabridin (Rosenblat et al., 1999; Kang et al., 2015).

Garlic (Allium sativum L.) possesses multiple anti-atherosclerotic effects. Allicor, garlic powder, inhibits inflammation signaling (like TNF, IL-1β, ICAM-1, and HLA-DR expression and secretion) (Karagodin et al., 2016a). Garlic also exhibits hypotensive activity through the inhibition of angiotensin-converting enzyme (Asdaq and Inamdar, 2010), positive activation of the growth suppressor p27, descent of ERK1/2 phosphorylation (Castro et al., 2010), and down-regulation of angiotensin II receptor (Mansour et al., 2013), reduction of vasoconstrictor prostanoids synthesis (Al-Qattan et al., 2001), stimulation of hydrogen sulfide (H2S) production (Al-Qattan et al., 2006), and regulation of endothelial nitric oxide (NO) synthesis (Ried and Fakler, 2014; Karagodin et al., 2016a). Garlic antithrombotic activity revealed through suppression of cyclooxygenase (Ali et al., 2000), diminished production of thromboxane B2 and vasoconstrictors like prostaglandin E2 and leukotriene C4 by platelets (Vilahur and Badimon, 2013), control of membrane phospholipases activity, and serotonin and coagulation factor IV secreting from platelets (Rahman, 2007). Aged garlic extract also prevented platelet aggregation by increasing cyclic nucleotides (Allison et al., 2012; Rahman et al., 2016), the quantity of both extracellular ATP and intra- and extracellular thromboxane B2, by inhibiting GPIIb/IIIa receptor and fibrinogen binding, and by abolishing phosphorylation of collagen-induced ERK, JNK, and p38 (Morihara and Hino, 2017). Moreover, antioxidant activity, synthesis of connective tissue matrix components, and cellular proliferative activity are suppressed, and LDL becomes less prone to oxidation thanks to the anti-atherosclerotic activity of garlic extracts (Orekhov et al., 2013; Orekhov et al., 2015). Garlic powder preparations inhibited neointimal thickening in cholesterol-fed rabbit models (Sobenin et al., 2016a). Garlic powder obviated neointimal thickening in cholesterol-fed rabbits, and Allicor (garlic tablet) decreased the accumulation of cholesterol in cell cultures incubated with serum from patients with atherosclerosis (Orekhov et al., 2013; Orekhov et al., 2015; Sobenin et al., 2016a). Garlic extracts were demonstrated to impede sialidase activity in blood plasma, which causes atherogenic LDL formation (Aksenov et al., 2007; Venkataiah et al., 2016; Sobenin et al., 2017). Diallyl disulfide, a component of garlic oil, is able to inhibit 3-hydroxy-3-methylglutaryl CoA reductase (HMGR) activity due to significant decrease in the mRNA levels and protein expression of HMGR. (Rai et al., 2009). It was shown in rat models that garlic consumption led to down-regulation of genes related to lipid metabolism: acetyl-CoA carboxylase (ACC), acyl-CoA cholesterol acyltransferase (ACAT), HMGR, fatty acid synthase (FAS), sterol regulatory element-binding protein-1c (SREBP-1c), and glucose-6-phosphate dehydrogenase (G6PD) (Ha et al., 2015). Thus, garlic can cause the lowering of total cholesterol and triglycerides in the blood. It was reported in review of Shouk et al., that bioactive components of garlic possess antihypertensive activity through modulating various parameters implicated in the pathogenesis of hypertension, in particular, proliferation of vascular smooth muscle cells, nitric oxide bioavailability, hydrogen sulfide production, angiotensin converting enzyme activity, expression of nuclear factor-κB (Shouk et al., 2014).

Phytoestrogens, plant-derived estrogens, can be used as an alternative estrogen replacement therapy for Cardiovascular disease (CVD) and osteoporosis prevention. Phytoestrogens, bioflavonoids characterized by similar structure to endogenous estrogens, can be found in different plants like soybean, pomegranate, spinach, etc (Franke et al., 1998; Kirichenko et al., 2017). Soybean contents a lot of isoflavones, which are selective estrogen receptor modulators (Franke et al., 1998; Oseni et al., 2008). Soybean consumption leads to the suppression of VCAM-1 expression (Kim et al., 2019) and elevation of the number of endothelial progenitor cells thus improving endothelial function (Chan et al., 2011). The flavanone 8-prenylnaringenin from hop flowers possessed anti-aggregatory and anti-adhesive effects on human platelets, acting as an inhibitor of platelet aggregation stimulated by different agonists and platelet adhesion to collagen matrix, a direct activator of intracellular cAMP and cGMP production, and VASP phosphorylation promoter (Di Vito et al., 2012). Grape phytoestrogens consumption helps to reduce serum atherogenicity, namely, intracellular cholesterol accumulation in primary culture of human blood-derived monocytes (Nikitina et al., 2006).

In traditional Chinese medicine plants and their mixtures are actively used to treat cardiovascular diseases, including atherosclerosis. Recently researches on the functions of several popular Chinese plants were conducted but they didn't reveal the exact mechanism of action for many of these plants (Hao et al., 2015; Hao et al., 2017; Sedighi et al., 2017). In overall, Chinese plants may influence all pathogenic mechanisms underlying atherosclerosis, including lowering plasma LDL-cholesterol, reduction of oxidative stress in endothelium, attenuation of endothelial proinflammatory activation, inhibition of endothelial cells apoptosis, anti-inflammatory activity, activation of macrophages M2 polarization, decrease of foam cells formation, inhibition of platelet activation and aggregation. Most important Chinese plants are turmeric (*Curcuma longa* L.),

Chinese sage or danshen (*Salvia miltiorrhiza* Bge), flowering plants of the barberry family (*Berberidaceae family* Juss.), green chireta (*Andrographis paniculate* Nees.), oak leaves (*Quercus dentata* Thunb.), garlic (*Allium sativum* L.), and jiaogulan (*Gynostemma pentaphylla* Thunb.) (Qiao and Chen, 2018). For example, curcuma may reduce cholesterol accumulation in arterial wall by inhibiting SR-A-mediated oxidized LDL uptake and promoting cholesterol efflux through activation of AMPK-SIRT1-LXRα signaling (Zhao et al., 2012; Lin et al., 2015). Curcumin, which is an active component of turmeric, exhibits its anti-inflammatory properties *via* negative regulation of pro-inflammatory interleukins (IL-1, IL-2, IL-6, IL-8, and IL-12), cytokines (TNF-a), MCP-1) by inhibiting expression of JAK/STAT signaling pathway. Moreover, curcumin may regulate the inflammatory response by suppressing activity of iNOS, COX-2, lipoxygenase, and xanthine oxidase, and activation of NF-kB (Kocaadam and Şanlier, 2017).

Chinese sage has a potential to inhibit foam cell formation caused by oxidized LDL through down-regulating of CD36 expression and up-regulating of Prdx1/ABCA1 signaling (Bao et al., 2012; Yang et al., 2018). Tanshiones, a group of lipophilic abietane diterpene compounds from Salvia miltiorrhiza, stabilized plaques or even attenuated plaque formation through inhibition of NF-kB pathway (Liu et al., 2015; Yang et al., 2016; Zhao D. et al., 2016; Zhao W. et al., 2016), suppressed endothelial apoptosis *via* lncRNA TUG1 up-regulating miR-26a expression (Chen et al., 2016). Tanshiones also protect from oxidation stress by increasing NO production and superoxide dismutase activity, inhibiting ROS production (Lin et al., 2006; Yang et al., 2011; Chen et al., 2012; Joe et al., 2012). Salvia compounds possess anti-thrombotic activity since they inhibit phosphoinositide 3-kinase and that's why decrease platelet activation (Huang et al., 2010). Chinese sage and gegen (*Pueraria lobate* Willd.) radix is a herbal formula suppress the expression of ICAM-1 and VCAM-1 and production of MCP-1 in TNF-α stimulated human umbilical vein endothelial cells (Koon et al., 2011). Sage also has antihypertensive activity as it was shown that sage extract increased nitric oxide production and relaxed endothelium-intact rings in experiments on isolated thoracic aorta from rats (Anwar et al., 2017).

Berberine from Huang Liang (*Coptis chinensis* Franch.) decreased plasma LDL-cholesterol by upregulating LDLR, and apoE expression and downregulating HMGR expression (Kong et al., 2004; Chang et al., 2012). Berberine exhibits cytoprotective effect on endothelial cells (EC) by blocking JNK phosphorylation (Guo et al., 2016) and increases plaque stability by inhibiting MMP-9 and EMMPRIN by suppressing the activation of p38 pathway (Huang et al., 2011) and NF-kB activation (Huang et al., 2012). Foam cell formation can be reduced by berberine *via* enhancing LXRα-ABCA1-dependent cholesterol efflux (Lee et al., 2010). Berberine activates the AMPK-SIRT1-PPAR-γ pathway and, respectively, reduces the uptake of oxidized LDL (Chi et al., 2014). Coptis chinensis extract can induce macrophage autophagy *via* AMPK/mTOR and PI3K/AKT/mTOR pathways (Fan et al., 2015; Kou et al., 2017). More Chinese herbs, their influence on atherosclerosis and underlying mechanism were thoroughly described in recent reports (Zhao et al., 2012; Hao et al., 2015; Qiao and Chen, 2018).

Mulberry (*Morus alba* L.) leaf extract provides anti-platelet and antithrombotic effects *via* blocking of platelet activation and aggregation, thromboxane B2 formation, serotonin secretion, and thrombus formation. Granule secretion and extracellular-signal-regulated kinase and Akt phosphorylation underlie the mechanism of this anti-platelet activity (Kim et al., 2014). Mulberry leaf extract protects lymphocyte DNA from oxidative damage, prevents ROS-mediated endothelial cell dysfunction *via* downregulating intracellular redox-dependent signaling pathways. It also has anti-inflammatory effects through the modulation of AP-1, NF-κB, PPARs, and STAT3 signaling (Chao et al., 2013).

The last but not the least medicine plant in this review is pomegranate (*Punica granatum* L.), which extracts possess multiple anti-atherosclerotic activities. Thus, ellagic acid promotes cholesterol removal by regulating LXR/PPAR-ABCA1 pathway (Zhao S. et al., 2016). Pomegranate peel extract and punicalgin up-regulate mRNA expression of LXRα and ABCA1 (Zhao et al., 2014). Ellagic acid and punicalagin cause anti-oxidant effect by reducing ROS level produced by mitochondria (Hwang et al., 2010; Zou et al., 2014). Moreover, pomegranate possesses obvious anti-inflammatory effect since pomegranate peel, flower, and seed oil may reduce plasma levels of IL-6 and TNFa, pomegranate flower may increase the anti-inflammatory cytokine IL-10 (Harzallah et al., 2016) and, in addition, pomegranate extract diminishes the translocation of NF-κB from the cytosol to the nucleus (Mandal et al., 2017). Pomegranate ellagic acid, peel polyphenols, and punicalagin lower LPS-induced pro-inflammatory cytokine activation (Du et al., 2018).

The most common pathogenetic mechanisms of anti-atherosclerotic action of medicinal plants are presented in **Table 1**.

REDUCTION OF THE ATHEROSCLEROSIS RISK FACTORS WITH MEDICINAL PLANTS

Conventional risk factors for cardiovascular diseases, in particular, hyperlipidemia, arterial hypertension, type 2 diabetes mellitus (T2D), smoking, obesity, etc., explain more than 50% of the variability of atherosclerosis, so represent the most significant factor in atherosclerosis development. In this regard, cardiovascular risk factors are the most important target in the process of timely prevention and treatment of atherosclerosis.

Medicinal plants have long been widely studied as anti-atherosclerotic agents; to date, sufficient data have been obtained on the effect of natural products on various traditional risk factors (**Table 2**). Nowadays natural products are known to have the greatest potential for long-term prevention of atherosclerosis.

TABLE 1 | Possible Anti-Atherosclerotic Mechanisms of Action of Medicinal Plants.

Effect	Plants/complex of plants	Mechanism
Anti-inflammatory (suppression of inflammatory mediators expression and signal pathway)	1) Inflaminat (Calendula *(Calendula officinalis* L.) + Black Elder (*Sambucus nigra* L.) + Violet (*Viola tricolor* L.))	Inhibiting expression of IL-1β and TNF (Kirichenko et al., 2016)
	Licorice (*Glycyrrhiza glabra* L.)	- JNK and NF-κB signaling blocking (Kwon et al., 2007; Cook-Mills et al., 2011)
		- TNF-α, IL-1β production suppression (Park et al., 2010)
		- Adhesion molecules suppression (Jong et al., 2006; Chang et al., 2010)
	Garlic (*Allium sativum* L.)	- Inflammation signaling inhibiting (like TNF-α, IL-1β, ICAM-1 and HLA-DR) (Karagodin et al., 2016a)
	Turmeric (*Curcuma longa* L.)	- Inhibiting expression of JAK/STAT signaling pathway (Kocaadam and Şanlier, 2017)
		- Suppressing activity of iNOS, COX-2, lipoxygenase, and xanthine oxidase (Kocaadam and Şanlier, 2017)
		- Activation of NF-kB (Kocaadam and Şanlier, 2017)
	Chinese sage (*Salvia miltiorrhiza*)	- Inhibition of NF-kB pathway (Yang et al., 2016; Zhao D. et al., 2016)
	Chinese sage (*Salvia miltiorrhiza*) and gegen (*Pueraria lobate* Willd.)	- Inhibition of adhesion molecules expression (Koon et al., 2011)
		- Suppression of MCP-1secretion (Koon et al., 2011)
	Huang Liang (*Coptis chinensis* Franch.)	- JNK phosphorylation (Guo et al., 2016)
		- Activation of p38 pathway (Huang et al., 2011)
		- NF-kB activation (Huang et al., 2012)
	Mulberry *(Morus alba* L.)	- Modulation of AP-1, NF-κB, PPARs, and STAT3 signaling (Kim et al., 2014)
	Pomegranate (*Punica granatum* L.)	- Reduction plasma levels of IL-6 and TNFa and increase IL-10 (Harzallah et al., 2016)
Antioxidant (Inhibition of LDL oxidation)	Licorice extract (*Glycyrrhiza glabra* L.)	- Inhibiting of LDL oxidation by suppression of AAPH-induced formation of cholesteryl linoleate hydroperoxide in LDL particle (Rosenblat et al., 1999; Kang et al., 2015)
	Chinese sage (*Salvia miltiorrhiza* Bge.)	- Inhibiting ROS production (Lin et al., 2006; Huang et al., 2010; Yang et al., 2011; Joe et al., 2012)
	Mulberry *(Morus alba* L.)	- Down-regulating intracellular redox-dependent signaling pathways (Chao et al., 2013)
	Pomegranate (*Punica granatum* L.)	- Reducing ROS level production by mitochondria (Harzallah et al., 2016; Mandal et al., 2017)
Antithrombotic activity (prevention of platelet aggregation)	Garlic (*Allium sativum* L.)	- Suppression of cyclooxygenase-2 (Ali et al., 2000)
		- Reducing synthesis of vasoconstrictors such as prostaglandin E2 and leukotriene C4 (Vilahur and Badimon, 2013)
		- Regulation of serotonin and coagulation factor IV production (Rahman, 2007)
		- Supression of platelet aggregation by increasing of cyclic nucleotides (Allison et al., 2012; Rahman et al., 2016)
		- Inhibiting the GPIIb/IIIa receptor and fibrinogen binding (Morihara and Hino, 2017)
		- Suppressing the phosphorylation of collagen-induced ERK, JNK and p38 (Morihara and Hino, 2017)
	Hop flowers (*Hunulus lupulus* L.)	- Increasing of intracellular cAMP and cGMP lexpression, promotion of VASP phosphorylation (Di Vito et al., 2012)
	Chinese sage (*Salvia miltiorrhiza* Bge.)	- Inhibition of phosphoinositide 3-kinase (Huang et al., 2010)
	Mulberry *(Morus alba* L.)	- Blocking of platelet activation and aggregation, thromboxane B2 formation (Kim et al., 2014)
Anti-atherogenic (suppression of Intracellular cholesterol accumulation in cultured cells)	Garlic (*Allium sativum* L.)	- Down-regulation of HMGR, FAS, SREBP-1c, G6PDH, acetyl-CoA carboxylase, and ACAT (Rai et al., 2009)
		- Inhibiting HMGR activity (Venkataiah et al., 2016)
	Turmeric (*Curcuma longa* L.)	- Inhibiting of SR-A-mediated oxidized LDL uptake (Zhao et al., 2012; Lin et al., 2015)
		- Promoting ABCA1-dependent cholesterol efflux through activation of AMPK-SIRT1-LXRα signaling (Zhao et al., 2012; Lin et al., 2015)
	Chinese sage (*Salvia miltiorrhiza* Bge.)	- Down-regulating of CD36 expression (Bao et al., 2012; Yang et al., 2018)
		- Up-regulating of Prdx1/ABCA1 signaling (Bao et al., 2012; Yang et al., 2018)
	Huang Liang (*Coptis chinensis* Franch.)	- Up-regulating of LDLR (Kong et al., 2004; Chang et al., 2012)
		- Up-regulating apoE expression (Kong et al., 2004; Chang et al., 2012)
		- Down-regulating HMGR expression (Kong et al., 2004; Chang et al., 2012)

(Continued)

TABLE 1 | Continued

Effect	Plants/complex of plants	Mechanism
	Pomegranate (*Punica granatum* L.)	- Enhancing LXRα-ABCA1-dependent cholesterol efflux (Lee et al., 2010) - Activating the AMPK-SIRT1-PPAR-γ pathway (Chi et al., 2014) - Regulating LXR/PPAR-ABCA1 pathway (Zhao S. et al., 2016) - Up-regulation of LXRα and ABCA1 expression (Zhao et al., 2014)
Hypotensive effects	Garlic (*Allium sativum* L.)	- Inhibition of angiotensin-converting enzyme (Asdaq and Inamdar, 2010) - Activation of the growth suppressor p27 (Castro et al., 2010) - Down-regulation of angiotensin II receptor (Mansour et al., 2013) - Reduction of vasoconstrictor prostanoids synthesis (Al-Qattan et al., 2001) - Stimulation of H2S production (Al-Qattan et al., 2006) - Regulation of endothelial NO synthesis (Ried and Fakler, 2014; Karagodin et al., 2016b)

Chinese medicine has achieved significant results in reducing the risk factors of atherosclerosis. Studies of the traditional Chinese formula Danshen Salvia miltiorrhiza + Gegen Radix puerariae in showed a significant decrease in plasma total cholesterol (TC) and LDL in postmenopausal women with hypercholesterolemia after 12 months of daily intake of 1 g of the drug in a randomized placebo-controlled trial (Koon et al., 2013). A randomized, double-blind, placebo-controlled pilot trial involving patients with type 2 diabetes showed that daily intake of 9 g of YH1-formula (Rhizoma Coptidis (*Coptis chinensis* Franch.) and Shen-Ling-Bai-Zhu-San (complex of *Salvia miltiorrhiza* Bge., *Atractylodis macrocephalae* DC., *Glycyrrhiza glabra* L., *Poria* Pers., *Citrus reticulata* Blanco., *Nelumbinis* Adans., *Platycodon* A.DC., *Amomum* Roxb., *Coix lacryma-jobi* L., *Dolichos* L.) led to a significant reduction of not only HbA1c and glucose levels, but also plasma Tg, TC, LDL levels (Huang et al., 2019). Another study of the JTTZ formula {Chinese sage [*Salvia miltiorrhiza* Bge.], Aloe vera [*Aloe vera* (L.) Burm.f.], Huanglian [*Coptis chinensis* Franch.], Rhizoma Anemarrhenae [*Anemarrhena asphodeloides* Bge.], red yeast [*Monascus purpureus* Went., 1895], Kugua [*Momordica charantia* L.], Wuweizi [*Schisandra chinensis* (Turcz.) Baill.], and dried ginger [*Zingiber officinale* Roscoe.]}, involving patients with type 2 diabetes, not only reduced HbA1c and normalized the lipid profile of blood plasma, but also led to weight loss (Yu et al., 2018).

Garlic powder is characterized by significant effects on many risk factors of atherosclerosis. In a randomized placebo-controlled trial performed by Zeb F. et al., the weight loss of the subjects was demonstrated (Zeb et al., 2018). In this and other studies, administration of garlic powder caused a significant lipid-lowering effect (Higashikawa et al., 2012; Ahmad Alobaidi, 2014; Alali et al., 2017; Xu et al., 2018; Choudhary et al., 2018). Several clinical trials also confirmed hypotensive effect of garlic. In particular, it was shown in the randomized, placebo-controlled, clinical study of Mahdavi-Roshan et al. that 3-months administration of garlic powder pills (equal to 800 mg garlic daily) results in significant reduction of systolic blood pressure by 12.0 mm Hg in patients with mild arterial hypertension in comparison with placebo (Mahdavi-Roshan et al., 2016). A similar hypotensive effect was demonstrated by other randomized placebo-controlled clinical studies (Ashraf et al., 2013; Al Disi et al., 2016). Treatment with 600 mg garlic powder pills (Allicor) led to a significant decrease of both systolic and diastolic blood pressure by 7.0 and 3.8mmHg (95% CI: 2.7–4.8), respectively (Sobenin et al., 2009). Interestingly, Aalami-Harandi R et al. in their randomized, double-blind, placebo-controlled trial at risk for pre-eclampsia involving pregnant women demonstrated that administration of 400 mg garlic daily for 9 weeks resulted in reduced levels of serum high sensitivity C-reactive protein (hs-CRP) (-1425.90 versus 1360.50 ng/ml, $p = 0.01$) in comparison with placebo (Aalami-Harandi et al., 2015).

Phytoestrogens are characterized by lipid-lowering and hypotensive effects. Villa P et al. in their pilot randomized trial involving ninety women in menopausal transition showed that administration of phytoestrogen substances in addition to vitamins and passionflower herbal preparation during 6 months led to TC decrease in blood plasma (Saadati et al., 2019). Eight-week of soy nut diet helped to decrease of fasting blood glucose as well as to improve blood lipids profile, significantly decreasing TC and LDL (Fogelman et al., 2016). Other 6-month randomized controlled trial showed the LDL and hs-CRP reduction effects of daily 40 g phytoestrogen-rich soy flour treatment of equol-producing postmenopausal women (Zeb et al., 2018). Other randomized controlled study has shown the hypotensive effect of isoflavones manifesting in a significant decrease of blood pressure (Alali et al., 2017). In a double-blind, randomized, placebo-controlled trial, 50 mg of isoflavone-rich preparation Rimostil resulted in significant serum LDL cholesterol reduction in perimenopausal women (Clifton-Bligh et al., 2015). Plant-derived flavonoids are well-documented to play important vasculoprotective role and it was demonstrated in several randomized controlled trials that catechins and quercetin have significant blood pressure lowering effect (Maaliki et al., 2019).

Turmeric also has lipid, hs-CRP, BMI, and glucose lowering effects observing during treatment of type 2 diabetes. Curcumin, a natural polyphenol from turmeric was tested in a randomized, double-blind, placebo-controlled trial on patients with diabetes who consumed 1,5 g curcumin daily for 10 weeks. Adibian M et al. have found significant hs-CRP and Tg-lowering effects (Adibian

TABLE 2 | Medicinal Plants in Cardiovascular Risk Improvement.

Plant/complex of plants	Study design and results	References
Chinese sage (*Salvia miltiorrhiza* Bge.) and Gegen Radix (*Pueraria lobate* Willd.)	12-months randomized, placebo-controlled trial in postmenopausal women with hypercholesterolemia: - lipid-lowering effect (TC -6.2% and LDL - 7.3%)	Koon et al. (2013)
YH1 (*Coptis chinensis* Franch., *Salvia miltiorrhiza* Bge., *Atractylodis macrocephalae* DC., *Glycyrrhiza glabra* L., *Poria* Pers., *Citrus reticulata* Blanco., *Nelumbinis* Adans., *Platycodon* A.DC., *Amomum* Roxb., *Coix lacryma-jobi* L., *Dolichos* L.)	12-week randomized, double-blind, placebo-controlled pilot trial in 46 patients with T2D: - reduction in HbA1c (-11.1%) - postprandial glucose decrease (-26.2%) - lipid-lowering effect (Tg -29.5%, TC -21.6%, LDL -17.4%)	Huang et al. (2019)
JTTZ formula (*Salvia miltiorrhiza* Bge., *Aloe vera* (L.) Burm.f., *Coptis chinensis* Franch., *Anemarrhena asphodeloides* Bge., *Monascus purpureus* Went., 1895, *Momordica charantia* L., *Schisandra chinensis* (Turcz.) Baill., *Zingiber officinale* Roscoe.	12-week randomized, positive-controlled (metformin), open-label trial in 450 patients with T2D, obesity and hyperlipidemia: - reduction of HbA1c (-0.75 ± 1.32%) - lipid-lowering effect (Tg -0.64 ± 2.37 mmol/L) - Weight decrease (-2.47 ± 2.71 kg)	Yu et al., (2018)
Allicor (*Allium sativum* L.)	4-week randomized, double-blind, placebo-controlled trial in 42 men: - lipid-lowering effect (TC -7.6 ± 2.4%, LDL -11.8 ± 4.5%, Tg -7.7 ± 9.0%)	Sobenin et al. (2008a)
	16-weeks randomized, placebo-controlled, double-blind trial in 84 men with moderate hypertension: - hypotensive (SBP -9.3 ± 0.7 mmHg, DBP -3.8 ± 0.5 mmHg)	Sobenin et al. (2009)
	4-weeks randomized double-blinded placebo-controlled outpatient clinical trial of 60 T2D patients: - blood glucose decrease (-1.8 ± 0.5mmol/l)	Sobenin et al. (2008)
Garlic (*Allium sativum* L.)	6-weeks randomized, double-blind, placebo-controlled trial in 51 patients with obesity: - LDL-lowering effect (p=0.05)	Xu et al. (2018)
Raw crushed garlic	4-weeks open-label trial in 40 patients with metabolic syndrome: - blood pressure decrease ($p < 0.001$) - Tg -lowering effect ($p < 0.01$) - blood glucose decrease ($p < 0.001$) - HDL increase ($p < 0.001$)	Choudhary et al. (2018)
Aged black garlic	12-weeks open-label trial in 60 patients with with mild hypercholesterolemia: - HDL increase ($p < 0.001$)	Jung et al. (2014)
Galois (garlic powder tablet)	3-months randomized, double-blind, placebo-controlled trial in 56 patients with coronary artery disease: - SBP decrease (p=0.04)	Mahdavi-Roshan et al. (2016)
Phytoestrogens (*Glycine max* (L.) Merr. + *Passiflora* L.) with vitamins	6-months pilot randomized trial in 90 women in menopausal transition: - TC-lowering effect ($p < 0.05$)	Villa et al. (2017)
Soy nut (*Glycine max* (L.) Merr.)	8-week randomized placebo-controlled trial in 70 patients with T2D - lipid-lowering effect (TC($p < 0.01$) and LDL (p=0.01) decrease) - blood glucose decrease ((p=0.03)	Sedaghat et al. (2019)
Karinat (*Vitis vinifera* L., *Camellia sinensis* L., *Hunulus lupulus* L., *Allium sativum* L.)	12-months randomized double-blind placebo-controlled study in 157 postmenopausal women: - lipid-lowering effect (TC -6.3% (p=0.011), LDL -7.6% (p=0.040)	Myasoedova et al. (2016)
Isoflavones from soybean (*Glycine max* (L.) Merr.)	2-year double-blind randomized study in 200 early postmenopausal women: - SBP-reduction (-3.2 mmHg, $p < 0.01$)	Sathyapalan et al. (2018)
Curcumin	10-weeks randomized double-blind placebo-controlled trial in 44 T2D patients: - hs-CRP decrease (-2.5 ± 4.3 mg/L) - Tg–lowering (-14.2 ± 30.6 mg/dl)	Adibian et al. (2019)
Curcuminoids	8-weeks 80 hyperlipidemic in T2D patients: - BMI and lipid-lowering effect (Tg, TC and LDL decrease, $p < 0.05$)	Adab et al. (2019)
Curcumin formulation	3-months randomized double-blind placebo-controlled trial in 100 T2D patients: - blood glucose decrease, -9 ± 16 mg/dL	Panahi et al. (2018)
	12-weeks randomized, placebo-controlled trial in 50 patients with non-alcoholic fatty liver disease - BMI decrease ($p < 0.001$) - TNF-α reduction (< 0.001)	Saadati et al. (2019)
Licorice root extract	12-months randomized placebo-controlled study in 110 patients with hypercholesterolemia: - lipid-lowering effect (TC -7.8%, LDL -4.9%) - hypotensive (SBP -13 ± 13 mmHg, DBP -8 ± 10 mmHg)	Fogelman et al. (2016)

et al., 2019). Adab Z et al. have demonstrated that administration of turmeric (2,1 g powdered rhizome of turmeric daily for 8 weeks) significantly decreased BMI as well as plasma Tg, TC, and LDL (Adab et al., 2019). Panahi Y et al. also observed lipid-lowering effect in their randomized controlled trial using curcuminoids (1 g/day plus piperine 10mg/day) treatment of diabetes patients for 12 weeks (Panahi et al., 2018). Finally, a treatment with amorphous dispersion curcumin formulation (500 mg/day equivalent to 70-mg curcumin) of non-alcoholic fatty liver patients for 8 weeks resulted in BMI-reduction as well as plasma Tg, LDL, and glucose levels lowering (Saadati et al., 2019).

In the placebo-controlled clinical study of the effect of 1-year licorice root extract consumption on cardiovascular risk factors, beneficial results were demonstrated, namely, the significant reduction of TC and LDL levels as well as hypotensive activity (Fogelman et al., 2016).

POTENTIAL DIRECT ANTI-ATHEROSCLEROTIC EFFICACY OF MEDICINAL PLANTS

The intima-media thickness of common carotid arteries is often used as a direct quantitative characteristic of atherosclerosis in clinical studies of the effectiveness of anti-atherosclerotic preparations. Currently, a number of medicinal plants have been studied using ultrasound scanning of the carotid arteries, that allows evaluating not only the indirect anti-atherosclerotic effect of these natural products by conversion of cardiovascular risk factors, but also studying their effect on carotid atherosclerosis development. **Table 3** demonstrates the results of clinical trials evaluating the effect of medicinal plants on carotid IMT dynamics during long-term administration.

Several medicinal plants that are widely used in Chinese traditional medicine have been studied in clinical trials in patients with carotid atherosclerosis. Chinese herbal formula—complex of Chinese sage (*Salvia miltiorrhiza* Bge.) and gegen radix (*Pueraria lobate* Willd.), that is often used for cardiovascular protection, caused the reduction of cIMT by –0.012mm after 1-year administration in 165 postmenopausal women (Kwok et al., 2014). Similar results of this herbal preparation (D&G) were obtained in a parallel study in high-risk hypertensive patients (Woo et al., 2013). Clinical study of the other Chinese complex: Reynoutria japonica rhizoma (*Polygonum cuspidatum* Siebold & Zucc.) and hawthorn fruits (*Crataegus*Tourn.ex L.) also demonstrates a significant reduction of cIMT after 6 months of follow-up (Liu et al., 2014).

Among a number of medicinal plants that have been studied in terms of anti-atherosclerotic mechanisms of action, garlic seems to be one of the most studied, its effectiveness is also investigated in clinical trials evaluating its direct anti-atherosclerotic action on carotid atherosclerosis. For the first time in 1999 the effect of 4-year garlic powder dragees administration on atherosclerosis plaque dynamics was evaluated by B-mode ultrasound of carotid and femoral arteries and the significant reduction of plaque volume increase during follow-up period in garlic-receiving group in comparison with placebo was shown (Koscielny et al., 1999). Atherosclerosis Monitoring and Atherogenicity Reduction (AMAR) study was designed to evaluate effect of time-released garlic powder pills Allicor on dynamics of carotid IMT. It was shown in 2-year double-blinded placebo-controlled trial that Allicor administration leads to cIMT reduction by –0.022mm per year

TABLE 3 | Carotid IMT in Studies of the Direct Anti-atherosclerotic Effect of Medicinal Plants.

Plants/complex of plants	Carotid IMT dynamics	References
Chinese herbal formula (danshen *Salvia miltiorrhiza* Bge., gegen radix *Pueraria lobate* Willd.)	12-months cIMT reduction: –0.012 mm ($p < 0.001$)	Woo et al. (2013); Kwok et al. (2014)
Chinese herb extraction (Reynoutria japonica rhizoma *Polygonum cuspidatum* Siebold & Zucc., hawthorn fruits *Crataegus* Tourn.ex L.)	6-months cIMT reduction ($p < 0.05$)	Liu et al. (2014)
Allicor (garlic powder *Allium sativum* L.)	annual cIMT change at 2-year study: Allicor –0.022 vs. placebo +0.015 mm/year ($p < 0.05$)	Karagodin et al. (2016a) (clinical trial registration number NCT01734707, http://clinicaltrials.gov/)
Garlic powder tablets (*Allium sativum* L.)	3-months cIMT dynamics: Garlic –0.009 mm vs. placebo +0.004 mm	Mahdavi-Roshan et al. (2013) (clinical trial registration number NCT01948453, http://clinicaltrials.gov/)
Karinat (*Vitis vinifera* L., *Camellia sinensis* L., *Hunulus lupulus* L., *Allium sativum* L.)	12-month cIMT progression: Karinat +0.006 mm vs. placebo +0.011 mm	Myasoedova et al. (2016) (clinical trial registration number NCT01742000, http://clinicaltrials.gov/)
Soybean (*Glycine max* (L.) Merr.) - isoflavone soy protein	annual cIMT change at 2-year study: ISP +0.002 vs. placebo +0.006 mm/year ($p=0.05$)	Hodis et al. (2011)
Inflaminat (Calendula flowers *Calendula officinalis* L., Black elder berries *Sambucus nigra* L., Violet herb *Viola tricolor* L.)	annual cIMT change at 2-year study: Inflaminat +0.006 vs. placebo +0.022 mm/year ($p=0.045$)	Kirichenko et al. (2016) (clinical trial registration number NCT01743404, http://clinicaltrials.gov/)
Licorice root extract (*Glycyrrhiza glabra* L.)	3-months cIMT dynamics: Licorice –0.008 mm vs. placebo +0.003 mm	Fogelman et al. (2016)
Pomegranate (*Punica granatum* L.)		Davidson et al. (2009) (clinical trial registration number NCT00728299, http://clinicaltrials.gov/)

while in placebo group the progression of cIMT was observed with mean annual rate +0.015mm ($p < 0.001$) (Orekhov et al., 2013; Karagodin et al., 2016b). Another study of garlic powder tablets efficacy on carotid atherosclerosis showed the similar beneficial data, cIMT dynamics differed significantly between verum and placebo groups ($p < 0.001$): 3-month cIMT reduction –0.009mm in garlic-administrated group vs. 3-months cIMT progression +0.004mm in placebo-administrated group; only preliminary results of this study were published for this moment (Mahdavi-Roshan et al., 2013).

An important area of research is the correction of atherosclerotic changes in postmenopausal women. It is known that women of childbearing age are less likely to suffer from atherosclerosis than men of this age. However, after menopause, this situation evens out. There is evidence of the ability of preparations containing isoflavonoids (phytoestrogens) to inhibit the formation of new atherosclerotic lesions and slow down the development of existing ones. The data of some studies (Myasoedova et al., 2016; Sobenin et al., 2016b) indicate that the use of isoflavonoid-rich herbal preparations, such as Karinat (grape seeds *Vitis vinifera* L., green tea *Camellia sinensis* L., hop cone *Hunulus lupulus* L., garlic *Allium sativum* L.), has therapeutic potential for the prevention of cardiovascular disease in postmenopausal women and in the perimenopausal period. The significant reduction of annual rate of cIMT progression was demonstrated in 2-year double-blinded placebo-controlled study in postmenopausal women – 0.006 vs. 0.011 mm/year in placebo group ($p < 0.001$) (Myasoedova et al., 2016). Soybean [*Glycine max* (L.) Merr.] is one of the richest sources of phytoestrogens so it's widely used for therapy of climacteric syndrome and it's also successfully used for cardiovascular protection in women after menopause (Sathyapalan et al., 2018). In the study of Hodis HN et al. the annual rate of cIMT progression differed significantly in the group with isoflavone soy protein (ISP) supplementation in comparison with placebo and was +0.002 and +0.006 mm/year, respectively, ($p=0.05$); but such effect was observed in subgroup of women within 5 years of menopause, and in the total group of men and women the difference in cIMT progression between ISP and placebo control was not significant (Hodis et al., 2011). It was shown in another study that higher habitual soy food consumption is associated with decreased cIMT in middle-aged Chinese adults, wherein a significant interaction between sex and soy food intake on cIMT was observed ($p=0.008$) (Zhang et al., 2008).

Several studies of the herbal preparation Inflaminat that suppresses inflammatory cytokines expression as well as inhibits intracellular cholesterol accumulation in *ex vivo* models as was described above, has been conducted. Based on them, an optimal dosage regimen of the preparation was developed to achieve a stable anti-inflammatory effect. In patients with subclinical atherosclerosis, a clinical study was designed to evaluate anti-atherosclerotic properties of Inflaminat. As a criterion for assessing the development of atherosclerotic lesions was also used the cIMT indicator. As it turned out, Inflaminat possesses direct anti-atherosclerotic activity since significantly reduces of the cIMT progression during 2-years of administration. It was demonstrated that annual rate of cIMT progression was +0.006 mm/year in Inflaminat-treated group and +0.022 mm/year in placebo group ($p=0.045$) (Kirichenko et al., 2016). Among other medicinal plants that possess multiple anti-atherosclerotic effects in atherosclerosis models, several products have been also studied in clinical trials of direct anti-atherosclerotic activity. In particular, in the clinical study of Fogelman Y. et al., the effect of 1-year licorice-root extract (*Glycyrrhiza glabra* L.) consumption on cIMT dynamics was examined in 94 participants aged 41–80 years. It was demonstrated that cIMT reducted by - 0.008 mm in licorice-treated group and increased by +0.003 mm in placebo group (Fogelman et al., 2016). In clinical trial of Davidson M.H. et al., the pomegranate juice consumption decreased cIMT progression only in patients with dyslipidemia, but not in total group (Davidson et al., 2009).

Based on this evidence in our knowledge prevention and treatment of atherosclerosis with medicinal plants has certain limitations. The most important fact is that natural products have multiple therapeutic effects, and it will be almost impossible to know which exact nature of the mechanism of action has led to a beneficial effect. This is especially true for natural complexes in which plants can potentiate and/or attenuate the effects of each other due to various multiple mechanisms of action. Almost all studies have a sufficient number of limitations, very few of them are registered, so it is difficult to assess the main outcome indicators and adverse reaction. Most researchers report that there are no side effects, but protocol requirements for recording any side effects are usually not given; moreover, possible interactions with prescription preparations practically are not describe. Therefore, given the importance of long-term prevention of atherosclerosis and reduction of cardiovascular risk, it is recommended to use the medicinal plants possessing pleiotropic anti-atherosclerotic effects in experimental studies those have shown atheroprotective activity in registered clinical trials.

CONCLUSION

Critical analysis of the current literature, demonstrate that the accumulated knowledge of traditional herbal based medicine and modern approaches to studying the action of medicinal plants open a veil of secrecy over the mechanisms of action and possible ways of creating and using preparations based on medicinal plants. Medicinal plants facilitate the treatment of atherosclerosis using different pathway and various mechanisms of the action, a number of medicinal plants have prospects for the prevention or treatment of atherosclerosis. However, direct anti-atherosclerosis activity of preparations based on garlic powder was studied wider than others natural products, their ameliorating effect on the progression of cIMT was proved in randomized double-blinded placebo-controlled trials, registrated on https://clinicaltrials.gov/

(Hodis et al., 2011; Mahdavi-Roshan et al., 2013; Karagodin et al., 2016a Karagodin et al., 2016b). Garlic preparations have the most interesting and obvious cardio-protective properties since garlic is able to ameliorate the blood lipids profile by inhibiting cholesterol biosynthesis, reducing of LDL, modulate arterial hypertension, and inhibit platelet aggregation (Sobenin et al., 2008a; Sobenin et al., 2008b; Sobenin et al., 2009; Jung et al., 2014; Mahdavi-Roshan et al., 2016; Myasoedova et al., 2016; Villa et al., 2017; Choudhary et al., 2018; Sathyapalan et al., 2018; Panahi et al., 2018; Xu et al., 2018; Sedaghat et al., 2019; Adibian et al., 2019; Adab et al., 2019). In laboratory experiments, garlic extract inhibits proliferative and inflammatory cellular reactions, possesses anti-cytokine properties, has pronounced antioxidant activity, so reduces the oxidation of LDL, activates the hydralase of cholesterol esters and inhibit ACAT, so reduces the content of cholesterol esters in cells. Thus, currently garlic seems to be the most promising plant for atherosclerosis prevention and treatment. Further comprehensive study of the mechanisms of influence of natural products on key links in the chain of development of atherosclerosis is an important and necessary step on the way to the development of new safe and effective preparations based on medicinal plants. But even modern data already indicate the possibility of using many medicinal plants as an additional therapy for patients with atherosclerosis and as a preventive measure for subjects with high cardiovascular risk.

AUTHOR CONTRIBUTIONS

AO and GA conceived and designed the review. TK, VS, NN, IS, VT, and P-YL contributed with the bibliographic research. TK, VS, AM, and NN wrote the manuscript. TK and IS provided table design. P-YL, VT, AO, and GA—review final version approval. AO, VT, and GA also contributed with the paper organization.

FUNDING

This work was supported by Russian Science Foundation (Grant #19-15-00010). This research was also supported within the framework of the grant provided by CSP Ministry of the Health Russian Federation, and by the IPAC RAS State Targets Project # 0090-2019-0005" for Gjumrakch Aliev. This work partially was also supported by the Russian Academic Excellence Project "5-100" for the Sechenov University, Moscow, Russia (for Gjumrakch Aliev and Vadim V. Tarasov).

REFERENCES

Aalami-Harandi, R., Karamali, M., and Asemi, Z. (2015). The favorable effects of garlic intake on metabolic profiles, hs-CRP, biomarkers of oxidative stress and pregnancy outcomes in pregnant women at risk for pre-eclampsia: randomized, double-blind, placebo-controlled trial. *J. Matern. Fetal Neonatal Med.* 28 (17), 2020–2027. doi: 10.3109/14767058.2014.977248

Adab, Z., Eghtesadi, S., Vafa, M. R., Heydari, I., Shojaii, A., Haqqani, H., et al. (2019). Effect of turmeric on glycemic status, lipid profile, hs-CRP, and total antioxidant capacity in hyperlipidemic type 2 diabetes mellitus patients. *Phytother. Res.* 33 (4), 1173–1181. doi: 10.1002/ptr.6312

Adibian, M., Hodaei, H., Nikpayam, O., Sohrab, G., Hekmatdoost, A., and Hedayati, M. (2019). The effects of curcumin supplementation on high-sensitivity C-reactive protein, serum adiponectin, and lipid profile in patients with type 2 diabetes: a randomized, double-blind, placebo-controlled trial. *Phytother. Res.* 33 (5), 1374–1383. doi: 10.1002/ptr.6328

Ahmad Alobaidi, A. H. (2014). Effect of Nigella sativa and Allium sativum coadminstered with simvastatin in dyslipidemia patients: a prospective, randomized, double-blind trial. *Antiinflamm. Antiallergy Agents Med. Chem.* 13 (1), 68–74. doi: 10.2174/18715230113129990013

Akhter, F., Khan, M. S., Alatar, A. A., Faisal, M., and Ahmad, S. (2016). Antigenic role of the adaptive immune response to d-ribose glycated LDL in diabetes, atherosclerosis and diabetes atherosclerotic patients. *Life Sci.* 151, 139–146. doi: 10.1016/j.lfs.2016.02.013

Aksenov, D. V., Kaplun, V. V., Tertov, V. V., Sobenin, I. A., and Orekhov, A. N. (2007). Effect of plant extracts on trans-sialidase activity in human blood plasma. *Bull. Exp. Biol. Med.* 143, 46–50. doi: 10.1007/s10517-007-0013-2

Al Disi, S. S., Anwar, M. A., and Eid, A. H. (2016). Anti-hypertensive Herbs and their Mechanisms of Action: Part I. *Front. Pharmacol.* 19;6, 323. doi: 10.3389/fphar.2015.00323

Alali, F. Q., El-Elimat, T., Khalid, L., Hudaib, R., Al-Shehabi, T. S., and Eid, A. H. (2017). Garlic for Cardiovascular Disease: Prevention or Treatment? *Curr. Pharm. Des.* 23 (7), 1028–1041. doi: 10.2174/1381612822666161010124530

Ali, M., Thomson, M., and Afzal, M. (2000). Garlic and onions: their effect on eicosanoid metabolism and its clinical relevance. *Prostaglandins Leukot. Essent. Fatty Acids* 62 (2), 55–73. doi: 10.1054/plef.1999.0124

Alipov, V. I., Sukhorukov, V. N., Karagodin, V. P., Grechko, A. V., and Orekhov, A. N. (2017). Chemical composition of circulating native and desialylated low density lipoprotein: what is the difference? *Vessel Plus* 1, 107–115. doi: 10.20517/2574-1209.2017.20

Allison, G. L., Lowe, G. M., and Rahman, K. (2012). Aged garlic extract inhibits platelet activation by increasing intracellular cAMP and reducing the interaction of GPIIb/IIIa receptor with fibrinogen. *Life Sci.* 91, 1275–1280. doi: 10.1016/j.lfs.2012.09.019

Al-Qattan, K. K., Khan, I., Alnaqeeb, M. A., and Ali, M. (2001). Thromboxane-B2, prostaglandin-E2 and hypertension in the rat 2-kidney 1-clip model: a possible mechanism of the garlic induced hypotension. *Prostaglandins Leukot. Essent. Fatty Acids* 64, 5–10. doi: 10.1054/plef.2000.0232

Al-Qattan, K. K., Thomson, M., Al-Mutawa'a, S., Al-Hajeri, D., Drobiova, H., and Ali, M. (2006). Nitric Oxide Mediates the Blood-Pressure Lowering Effect of Garlic in the Rat Two-Kidney, One-Clip Model of Hypertension. *J. Nutr.* 136, 774S–776S. doi: 10.1093/jn/136.3.774S

Anwar, M. A., Samaha, A. A., Ballan, S., Saleh, A. I., Iratni, R., and Eid, A. H. (2017). Salvia fruticosa Induces Vasorelaxation In Rat Isolated Thoracic Aorta: Role of the PI3K/Akt/eNOS/NO/cGMP Signaling Pathway. *Sci. Rep.* 7 (1), 686. doi: 10.1038/s41598-017-00790-9

Asdaq, S. M., and Inamdar, M. N. (2010). Potential of garlic and its active constituent, S-allyl cysteine, as antihypertensive and cardioprotective in presence of captopril. *Phytomedicine* 17, 1016–1026. doi: 10.1016/j.phymed.2010.07.012

Ashraf, R., Khan, R. A., Ashraf, I., and Qureshi, A. A. (2013). Effects of Allium sativum (garlic) on systolic and diastolic blood pressure in patients with essential hypertension. *Pak. J. Pharm. Sci.* 26 (5), 859–863.

Bao, Y., Wang, L., Xu, Y., Yang, Y., Wang, L., Si, S., et al. (2012). Salvianolic acid B inhibits macrophage uptake of modified low density lipoprotein (mLDL) in a scavenger receptor CD36-dependent manner. *Atherosclerosis* 223, 152–159. doi: 10.1016/j.atherosclerosis.2012.05.006

Beckett, R. D., Schepers, S. M., and Gordon, S. K. (2015). Risk of new-onset diabetes associated with statin use. *SAGE Open Med.* 3, 2050312115605518. doi: 10.1177/2050312115605518

Bots, M. L., Evans, G. W., Tegeler, C. H., and Meijer, R. (2016). Carotid Intima-media Thickness Measurements: Relations with Atherosclerosis, Risk of

Cardiovascular Disease and Application in Randomized Controlled Trials. *Chin. Med. J. (Engl.)* 129 (2), 215–226. doi: 10.4103/0366-6999.173500

Castro, C., Lorenzo, A. G., González, A., and Cruzado, M. (2010). Garlic components inhibit angiotensin II-induced cell-cycle progression and migration: involvement of cell-cycle inhibitor p27Kip1 and mitogen-activated protein kinase. *Mol. Nutr. Food Res.* 54, 781–787. doi: 10.1002/mnfr.200900108

Chan, Y. H., Lam, T. H., Lau, K. K., Yiu, K. H., Siu, C. W., Li, S. W., et al. (2011). Dietary intake of phytoestrogen is associated with increased circulating endothelial progenitor cells in patients with cardiovascular disease. *Eur. J. Cardiovasc. Prev. Rehabil.* 18, 360–368. doi: 10.1177/1741826710389385

Chang, Y. L., Chen, C. L., Kuo, C. L., Chen, B. C., and You, J. S. (2010). Glycyrrhetinic acid inhibits ICAM-1 expression via blocking JNK and NF-B pathways in TNF-α-activated endothelial cells. *Acta Pharmacol. Sin.* 31, 546–553. doi: 10.1038/aps.2010.34

Chang, X. X., Yan, H. M., Xu, Q., Xia, M. F., Bian, H., Zhu, T. F., et al. (2012). The effects of berberine on hyperhomocysteinemia and hyperlipidemia in rats fed with a long-term high-fat diet. *Lipids Health Dis.* 11, 86. doi: 10.1186/1476-511X-11-86

Chao, P.-Y., Lin, K.-H., Chiu, C.-C., Yang, Y.-Y., Huang, M.-Y., and Yang, C.-M. (2013). Inhibitive Effects of Mulberry Leaf-Related Extracts on Cell Adhesion and Inflammatory Response in Human Aortic Endothelial Cells. *Evid. Based Complement. Alternat. Med.* 2013, 1–14. doi: 10.1155/2013/267217

Chen, W., Tang, F., Xie, B., Chen, S., Huang, H., and Liu, P. (2012). Amelioration of atherosclerosis by tanshinone IIA in hyperlipidemic rabbits through attenuation of oxidative stress. *Eur. J. Pharmacol.* 674, 359–364. doi: 10.1016/j.ejphar.2011.10.040

Chen, C., Cheng, G., Yang, X., Li, C., Shi, R., and Zhao, N. (2016). Tanshinol suppresses endothelial cells apoptosis in mice with atherosclerosis via lncRNA TUG1 up-regulating the expression of miR-26a. *Am. J. Transl. Res.* 8, 2981–2991.

Chi, L., Peng, L., Pan, N., Hu, X., and Zhang, Y. (2014). The anti-atherogenic effects of berberine on foam cell formation are mediated through the upregulation of sirtuin 1. *Int. J. Mol. Med.* 34, 1087–1093. doi: 10.3892/ijmm.2014.1868

Chistiakov, D. A., Grechko, A. V., Myasoedova, V. A., Melnichenko, A. A., and Orekhov, A. N. (2018). The role of monocytosis and neutrophilia in atherosclerosis. *J. Cell Mol. Med.* 22, 1366–1382. doi: 10.1111/jcmm.13462

Choudhary, P. R., Jani, R. D., and Sharma, M. S. (2018). Effect of Raw Crushed Garlic (Allium sativum L.) on Components of Metabolic Syndrome. *J. Diet. Suppl.* 15 (4), 499–506. doi: 10.1080/19390211.2017.1358233

Chukwuma, C. I., Matsabisa, M. G., Ibrahim, M. A., Erukainure, O. L., Chabalala, M. H., and Islam, M. S. (2019). Medicinal plants with concomitant anti-diabetic and anti-hypertensive effects as potential sources of dual acting therapies against diabetes and hypertension: A review. *J. Ethnopharmacol.* 235, 329–360. doi: 10.1016/j.jep.2019.02.024

Clifton-Bligh, P. B., Nery, M. L., Clifton-Bligh, R. J., Visvalingam, S., Fulcher, G. R., Byth, K., et al. (2015). Red clover isoflavones enriched with formononetin lower serum LDL cholesterol-a randomized, double-blind, placebo-controlled study. *Eur. J. Clin. Nutr.* 69 (1), 134–142. doi: 10.1038/ejcn.2014.207

Cook-Mills, J. M., Marchese, M. E., and Abdala-Valencia, H. (2011). Vascular Cell Adhesion Molecule-1 Expression and Signaling During Disease: Regulation by Reactive Oxygen Species and Antioxidants. *Antioxid. Redox Signal.* 15, 1607–1638. doi: 10.1089/ars.2010.3522

Davidson, M. H., Maki, K. C., Dicklin, M. R., Feinstein, S. B., Witchger, M., Bell, M., et al. (2009). Effects of consumption of pomegranate juice on carotid intima-media thickness in men and women at moderate risk for coronary heart disease. *Am. J. Cardiol.* 104 (7), 936–942. doi: 10.1016/j.amjcard.2009.05.037

Davignon, J. (2012). Pleiotropic effects of pitavastatin. *Br. J. Clin. Pharmacol.* 73, 518–535. doi: 10.1111/j.1365-2125.2011.04139.x

Di Vito, C., Bertoni, A., Nalin, M., Sampietro, S., Zanfa, M., and Sinigaglia, F. (2012). The phytoestrogen 8-prenylnaringenin inhibits agonist-dependent activation of human platelets. *Biochim. Biophys. Acta* 1820 (11), 1724–1733. doi: 10.1016/j.bbagen.2012.06.018

Du, L., Li, J., Zhang, X., Wang, L., and Zhang, W. (2018). Pomegranate peel polyphenols inhibits inflammation in LPS-induced RAW264.7 macrophages via the suppression of MAPKs activation. *J. Funct. Foods* 43, 62–69. doi: 10.1016/j.jff.2018.01.028

Fan, X., Wang, J., Hou, J., Lin, C., Bensoussan, A., Chang, D., et al. (2015). Berberine alleviates ox-LDL induced inflammatory factors by up-regulation of autophagy via AMPK/mTOR signaling pathway. *J. Transl. Med.* 13, 92. doi: 10.1186/s12967-015-0450-z

Fatkhullina, A. R., Peshkova, I. O., and Koltsova, E. K. (2016). The role of cytokines in the development of atherosclerosis. *Biochemistry (Mosc.)* 81 (11), 1358–1370. doi: 10.1134/S0006297916110134

Fogelman, Y., Gaitini, D., and Carmeli, E. (2016). Antiatherosclerotic effects of licorice extract supplementation on hypercholesterolemic patients: decreased CIMT, reduced plasma lipid levels, and decreased blood pressure. *Food Nutr. Res.* 60, 30830. doi: 10.3402/fnr.v60.30830

Franke, A. A., Custer, L. J., Wang, W., and Shi, C. Y. (1998). HPLC analysis of isoflavonoids and other phenolic agents from foods and from human fluids. *Proc. Soc. Exp. Biol. Med.* 217, 263–273. doi: 10.3181/00379727-217-44231

Fredman, G., and Spite, M. (2013). Recent advances in the role of immunity in atherosclerosis. *Circ. Res.* 113, e111–e114. doi: 10.1161/CIRCRESAHA.113.302986

Frostegard, J. (2013). Immunity, atherosclerosis and cardiovascular disease. *BMC Med.* 11, 117. doi: 10.1186/1741-7015-11-117

Guo, J., Wang, L., Wang, L., Qian, S., Zhang, D., Fang, J., et al. (2016). Berberine Protects Human Umbilical Vein Endothelial Cells against LPS-Induced Apoptosis by Blocking JNK-Mediated Signaling. *Evid. Based Complement. Alternat. Med.* 2016, 6983956. doi: 10.1155/2016/6983956

Ha, A. W., Ying, T., and Kim, W. K. (2015). The effects of black garlic (Allium satvium) extracts on lipid metabolism in rats fed a high fat diet. *Nutr. Res. Pract.* 9, 30–36. doi: 10.4162/nrp.2015.9.1.30

Hao, P. P., Jiang, F., Chen, Y. G., Yang, J., Zhang, K., Zhang, M. X., et al. (2015). Evidence for traditional Chinese medication to treat cardiovascular disease. *Nat. Rev. Cardiol.* 12, p374. doi: 10.1038/nrcardio.2014.177-c2

Hao, P., Jiang, F., Cheng, J., Ma, L., Zhang, Y., and Zhao, Y. (2017). Traditional Chinese Medicine for Cardiovascular Disease: Evidence and Potential Mechanisms. *J. Am. Coll. Cardiol.* 69, 2952–2966. doi: 10.1016/j.jacc.2017.04.041

Harzallah, A., Hammami, M., Kępczyńska, M. A., Hislop, D. C., Arch, J. R. S., Cawthorne, M. A., et al. (2016). Comparison of potential preventive effects of pomegranate flower, peel and seed oil on insulin resistance and inflammation in high-fat and high-sucrose diet-induced obesity mice model. *Arch. Physiol. Biochem.* 122, 75–87. doi: 10.3109/13813455.2016.1148053

Higashikawa, F., Noda, M., Awaya, T., Ushijima, M., and Sugiyama, M. (2012). Reduction of serum lipids by the intake of the extract of garlic fermented with Monascus pilosus: a randomized, double-blind, placebo-controlled clinical trial. *Clin. Nutr.* 31 (2), 261–266. doi: 10.1016/j.clnu.2011.10.008

Hodis, H. N., MacK, W. J., Kono, N., Azen, S. P., Shoupe, D., Hwang-Levine, J., et al. (2011). Isoflavone soy protein supplementation and atherosclerosis progression in healthy postmenopausal women: a randomized controlled trial. *Stroke* 42, 3168–3175. doi: 10.1161/STROKEAHA.111.620831

Huang, Z. S., Zeng, C. L., Zhu, L. J., Jiang, L., Li, N., and Hu, H. (2010). Salvianolic acid A inhibits platelet activation and arterial thrombosis via inhibition of phosphoinositide 3-kinase. *J. Thromb. Haemost.* 8, 1383–1393. doi: 10.1111/j.1538-7836.2010.03859.x

Huang, Z., Wang, L., Meng, S., Wang, Y., Chen, T., and Wang, C. (2011). Berberine reduces both MMP-9 and EMMPRIN expression through prevention of p38 pathway activation in PMA-induced macrophages. *Int. J. Cardiol.* 146, 153–158. doi: 10.1016/j.ijcard.2009.06.023

Huang, Z., Meng, S., Wang, L., Wang, Y., Chen, T., and Wang, C. (2012). Suppression of oxLDL-induced MMP-9 and EMMPRIN expression by berberine via inhibition of NF-κB activation in human THP-1 macrophages. *Anat. Rec.* 295, 78–86. doi: 10.1002/ar.21489

Huang, Y. H., Chen, S. T., Liu, F. H., Hsieh, S. H., Lin, C. H., Liou, M. J., et al. (2019). The efficacy and safety of concentrated herbal extract granules, YH1, as an add-on medication in poorly controlled type 2 diabetes: A randomized, double-blind, placebo-controlled pilot trial. *PloS One* 14 (8), e0221199. doi: 10.1371/journal.pone.0221199

Hwang, J. M., Cho, J. S., Kim, T. H., and Lee, Y. I. (2010). Ellagic acid protects hepatocytes from damage by inhibiting mitochondrial production of reactive oxygen species. *BioMed. Pharmacother.* 64, 264–270. doi: 10.1016/j.biopha.2009.06.013

Joe, Y., Zheng, M., Kim, H. J., Kim, S., Uddin, M. J., Park, C., et al. (2012). Salvianolic acid B exerts vasoprotective effects through the modulation of heme

oxygenase-1 and arginase activities. *J. Pharmacol. Exp. Ther.* 341, 850–858. doi: 10.1124/jpet.111.190736

Jong, S. K., Yeo, D. Y., Mi, H. H., Han, S. B., Lee, K., Ki, H. L., et al. (2006). Glabridin suppresses intercellular adhesion molecule-1 expression in tumor necrosis factor-α-stimulated human umbilical vein endothelial cells by blocking sphingosine kinase pathway: Implications of Akt, extracellular signal-regulated kinase, and nuclear factor-κB/Rel signaling pathways. *Mol. Pharmacol.* 69, 941–949. doi: 10.1124/mol.105.017442

Jung, E. S., Park, S. H., Choi, E. K., Ryu, B. H., Park, B. H., Kim, D. S., et al. (2014). Reduction of blood lipid parameters by a 12-wk supplementation of aged black garlic: a randomized controlled trial. *Nutrition* 30 (9), 1034–1039. doi: 10.1016/j.nut.2014.02.014

Kang, M. R., Park, K. H., Oh, S. J., Yun, J., Lee, C. W., Lee, M. Y., et al. (2015). Cardiovascular protective effect of glabridin: implications in LDL oxidation and inflammation. *Int. Immunopharmacol.* 29, 914–918. doi: 10.1016/j.intimp.2015.10.020

Karagodin, V. P., Sobenin, I. A., and Orekhov, A. N. (2016a). Antiatherosclerotic and Cardioprotective Effects of Time-Released Garlic Powder Pills. *Curr. Pharm. Des.* 22, 196–213. doi: 10.2174/1381612822666151112153351

Karagodin, V. P., Sobenin, I. A., and Orekhov, A. N. (2016b). Antiatherosclerotic and Cardioprotective Effects of Time-Released Garlic Powder Pills. *Curr. Pharm. Des.* 22 (2), 196–213. doi: 10.2174/1381612822666151112153351

Katakami, N., Matsuoka, T. A., and Shimomura, I. (2019). Clinical utility of carotid ultrasonography: application for the management of patients with diabetes. *J. Diabetes Invest.* 10 (4), 883–898. doi: 10.1111/jdi.13042

Kim, D.-S., Ji, H. D., Rhee, M. H., Sung, Y.-Y., Yang, W.-K., Kim, S. H., et al. (2014). Antiplatelet Activity of Morus alba Leaves Extract, Mediated via Inhibiting Granule Secretion and Blocking the Phosphorylation of Extracellular-Signal-Regulated Kinase and Akt. *Evid. Based Complement. Alternat. Med.* 2014, 1–11. doi: 10.1155/2014/639548

Kim, J. S., Kim, J. H., Palaniyandi, S. A., Lee, C. C., You, J. W., Yang, H., et al. (2019). Yak-Kong Soybean (Glycine max) Fermented by a Novel Pediococcus pentosaceus Inhibits the Oxidative Stress-Induced Monocyte-Endothelial Cell Adhesion. *Nutrients* 11 (6), 1380. doi: 10.3390/nu11061380

Kirichenko, T. V., Sobenin, I. A., Nikolic, D., Rizzo, M., and Orekhov, A. N. (2016). Anti-cytokine therapy for prevention of atherosclerosis. *Phytomedicine* 23, 1198–1210. doi: 10.1016/j.phymed.2015.12.002

Kirichenko, T. V., Myasoedova, V. A., Orekhova, V. A., Ravani, A. L., Nikitina, N. A., Grechko, A. V., et al. (2017). Phytoestrogen-Rich Natural Preparation for Treatment of Climacteric Syndrome and Atherosclerosis Prevention in Perimenopausal Women. *Phytother. Res.* 31, 1209–1214. doi: 10.1002/ptr.5841

Kocaadam, B., and Şanlier, N. (2017). Curcumin, an active component of turmeric (Curcuma longa), and its effects on health. *Crit. Rev. Food Sci. Nutr.* 57, 2889–2895. doi: 10.1080/10408398.2015.1077195

Koch, M., and Zernecke, A. (2014). The hemostatic system as a regulator of inflammation in atherosclerosis. *IUBMB Life.* 66, 735–744. doi: 10.1002/iub.1333

Kong, W., Wei, J., Abidi, P., Lin, M., Inaba, S., Li, C., et al. (2004). Berberine is a novel cholesterol-lowering drug working through a unique mechanism distinct from statins. *Nat. Med.* 10, 1344–1351. doi: 10.1038/nm1135

Koon, C. M., Woo, K. S., Leung, P. C., and Fung, K. P. (2011). Salviae Miltiorrhizae Radix and Puerariae Lobatae Radix herbal formula mediates anti-atherosclerosis by modulating key atherogenic events both in vascular smooth muscle cells and endothelial cells. *J. Ethnopharmacol.* 138, 175–183. doi: 10.1016/j.jep.2011.08.073

Koon, C. M., Ko, C. H., Sun, X. X., Hoi, S. W., Tam, J. C., Cheung, D. W., et al. (2013). Gene expression profiling on the molecular action of danshen-gegen formula in a randomized placebo-controlled trial of postmenopausal women with hypercholesterolemia. *Evid. Based Complement. Alternat. Med.* 2013, 703705. doi: 10.1155/2013/703705

Koscielny, J., Klüssendorf, D., Latza, R., Schmitt, R., Radtke, H., Siegel, G., et al. (1999). The antiatherosclerotic effect of Allium sativum. *Atherosclerosis* 144 (1), 237–249. doi: 10.1016/S0021-9150(99)00060-X

Kou, J. Y., Li, Y., Zhong, Z. Y., Jiang, Y. Q., Li, X. S., Han, X. B., et al. (2017). Berberine-sonodynamic therapy induces autophagy and lipid unloading in macrophage. *Cell Death Dis.* 8 (1), e2558. doi: 10.1038/cddis.2016.354

Kwok, T., Leung, P. C., Lam, C., Ho, S., Wong, C. K., Cheng, K. F., et al. (2014). A randomized placebo controlled trial of an innovative herbal formula in the prevention of atherosclerosis in postmenopausal women with borderline hypercholesterolemia. *Complement. Ther. Med.* 22 (3), 473–480. doi: 10.1016/j.ctim.2014.03.010

Kwon, H. M., Choi, Y. J., Choi, J. S., Kang, S. W., Bae, J. Y., Kang, I. J., et al. (2007). Blockade of cytokine-induced endothelial cell adhesion molecule expression by licorice isoliquiritigenin through NF-κB signal disruption. *Exp. Biol. Med.* 232, 235–245.

Lee, T.-S., Pan, C.-C., Peng, C.-C., Kou, Y. R., Chen, C.-Y., Ching, L.-C., et al. (2010). Anti-atherogenic effect of berberine on LXRα-ABCA1-dependent cholesterol efflux in macrophages. *J. Cell Biochem.* 111, 104–110. doi: 10.1002/jcb.22667

Li, B., Li, W., Li, X., and Zhou, H. (2017). Inflammation: A Novel Therapeutic Target/Direction in Atherosclerosis. *Curr. Pharm. Des.* 23, 1216–1227. doi: 10.2174/1381612822666161230142931

Libby, P., Ridker, P. M., and Hansson, G. K. (2011). Progress and challenges in translating the biology of atherosclerosis. *Nature* 473, 317–325. doi: 10.1038/nature10146

Lin, R., Wang, W. R., Liu, J. T., Yang, G. D., and Han, C. J. (2006). Protective effect of tanshinone IIA on human umbilical vein endothelial cell injured by hydrogen peroxide and its mechanism. *J. Ethnopharmacol.* 108, 217–222. doi: 10.1016/j.jep.2006.05.004

Lin, X. L., Liu, M. H., Hu, H. J., Feng, H. R., Fan, X. J., Zou, W. W., et al. (2015). Curcumin Enhanced Cholesterol Efflux by Upregulating ABCA1 Expression Through AMPK-SIRT1-LXRα Signaling in THP-1 Macrophage-Derived Foam Cells. *DNA Cell Biol.* 34, 561–572. doi: 10.1089/dna.2015.2866

Liu, L. T., Zheng, G. J., Zhang, W. G., Guo, G., and Wu, M. (2014). Clinical study on treatment of carotid atherosclerosis with extraction of polygoni cuspidati rhizoma et radix and crataegi fructus: a randomized controlled trial. *Zhongguo Zhong Yao Za Zhi* 39 (6), 1115–1119.

Liu, Z., Xu, S., Huang, X., Wang, J., Gao, S., Li, H., et al. (2015). Cryptotanshinone, an orally bioactive herbal compound from Danshen, attenuates atherosclerosis in apolipoprotein E-deficient mice: Role of lectin-like oxidized LDL receptor-1 (LOX-1). *Br. J. Pharmacol.* 172, 5661–5675. doi: 10.1111/bph.13068

Lopes-Virella, M. F., and Virella, G. (2013). Pathogenic role of modified LDL antibodies and immune complexes in atherosclerosis. *J. Atheroscl. Thromb.* 20, 743–754. doi: 10.5551/jat.19281

Maaliki, D., Shaito, A. A., Pintus, G., El-Yazbi, A., and Eid, A. H. (2019). Flavonoids in hypertension: a brief review of the underlying mechanisms. *Curr. Opin. Pharmacol.* 45, 57–65. doi: 10.1016/j.coph.2019.04.014

Mahdavi-Roshan, M., Zahedmehr, A., Mohammad-Zadeh, A., Sanati, H. R., Shakerian, F., Firouzi, A., et al. (2013). Effect of garlic powder tablet on carotid intima-media thickness in patients with coronary artery disease: a preliminary randomized controlled trial. *Nutr. Health* 22 (2), 143–155. doi: 10.1177/0260106014563446

Mahdavi-Roshan, M., Nasrollahzadeh, J., Mohammad Zadeh, A., and Zahedmehr, A. (2016). Does Garlic Supplementation Control Blood Pressure in Patients with Severe Coronary Artery Disease? A Clinical Trial Study. *Iran Red Crescent Med. J.* 18 (11), e23871. doi: 10.5812/ircmj.23871

Mandal, A., Bhatia, D., and Bishayee, A. (2017). Anti-Inflammatory Mechanism Involved in Pomegranate-Mediated Prevention of Breast Cancer: the Role of NF-κB and Nrf2 Signaling Pathways. *Nutrients* 9, 436. doi: 10.3390/nu9050436

Mansour, M. H., Al-Qattan, K., Thomson, M., and Ali, M. (2013). Garlic (Allium sativum) down-regulates the expression of angiotensin II AT1 receptor in adrenal and renal tissues of streptozotocin-induced diabetic rats. *Inflammopharmacology* 21, 147–159. doi: 10.1007/s10787-012-0139-3

Morihara, N., and Hino, A. (2017). Aged garlic extract suppresses platelet aggregation by changing the functional property of platelets. *J. Nat. Med.* 71, 249–256. doi: 10.1007/s11418-016-1055-4

Myasoedova, V. A., Kirichenko, T. V., Melnichenko, A. A., Orekhova, V. A., Ravani, A., Poggio, P., et al. (2016). Anti-atherosclerotic effects of a phytoestrogen-rich herbal preparation in postmenopausal women. *Int. J. Mol. Sci.* 17 (8), 1318. doi: 10.3390/ijms17081318

Nikifirov, N. G., Zakiev, E. R., Elizova, N. V., Sukhorukov, V. N., and Orekhov, A. N. (2017). Multiple-modified low-density lipoprotein as atherogenic factor of patients' blood: Development of therapeutic approaches to reduce blood atherogenicity(Review). *Curr. Pharm. Des.* 23, 932–936. doi: 10.2174/1381612823666170124112918

Nikitina, N. A., Sobenin, I. A., Myasoedova, V. A., Korennaya, V. V., Mel'nichenko, A. A., Khalilov, E. M., et al. (2006). Antiatherogenic effect of

grape flavonoids in an ex vivo model. *Bull. Exp. Biol. Med.* 141 (6), 712–715. doi: 10.1007/s10517-006-0260-7

Oesterle, A., Laufs, U., and Liao, J. K. (2017). Pleiotropic Effects of Statins on the Cardiovascular System [published correction appears in Circ Res. *Circ. Res.* 120, 229–243. doi: 10.1161/CIRCRESAHA.116.308537

Orekhov, A. N., and Ivanova, E. A. (2017). Introduction of the special issue Atherosclerosis and Related. *Dis. Vessel Plus* 1, 163–165. doi: 10.20517/2574-1209.2017.33

Orekhov, A. N., Sobenin, I. A., Korneev, N. V., Kirichenko, T. V., Myasoedova, V. A., Melnichenko, A. A., et al. (2013). Anti-atherosclerotic therapy based on botanicals. *Recent Pat. Cardiovasc. Drug Discov.* 8 (1), 56–66. doi: 10.2174/1872208311307990008

Orekhov, A. N., Sobenin, I. A., Revin, V. V., and Bobryshev, Y. V. (2015). Development of Antiatherosclerotic Drugs on the basis of Natural Products Using Cell Model Approach. *Oxid. Med. Cell Longev.* 2015, 463797. doi: 10.1155/2015/463797

Oseni, T., Patel, R., Pyle, J., and Jordan, V. C. (2008). Selective estrogen receptor modulators and phytoestrogens. *Planta Med.* 74, 1656–1665. doi: 10.1055/s-0028-1088304

Panahi, Y., Khalili, N., Sahebi, E., Namazi, S., Simental-Mendía, L. E., Majeed, M., et al. (2018). Effects of Curcuminoids Plus Piperine on Glycemic, Hepatic and Inflammatory Biomarkers in Patients with Type 2 Diabetes Mellitus: A Randomized Double-Blind Placebo-Controlled Trial. *Drug Res. (Stuttg.)* 68 (7), 403–409. doi: 10.1055/s-0044-101752

Park, S. H., Kang, J. S., Yoon, Y. D., Lee, K., Kim, K. J., Lee, K. H., et al. (2010). Glabridin inhibits lipopolysaccharide-induced activation of a microglial cell line, BV-2, by blocking NF-κB and AP-1. *Phytother Res.* 1, S29–S34. doi: 10.1002/ptr.2872

Pogosova, N. V., Oganov, R. G., Boytsov, S. A., Ausheva, A. K., Sokolova, O. Y., Kursakov, A. A., et al (2017). Efficiency of primary prevention for diseases caused by atherosclerosis in patients at high cardiovascular risk in Russia and other European countries (Part 2). *Kardiologiia* 57, (83) 5–16. doi: 10.18087/cardio.2412

Pirillo, A., Norata, G. D., and Catapano, A. L. (2013). LOX-1, OxLDL, and atherosclerosis. *Mediators Inflamm.* 2013, 152786. doi: 10.1155/2013/152786

Qiao, L., and Chen, W. (2018). Atheroprotective effects and molecular targets of bioactive compounds from traditional Chinese medicine. *Pharmacol. Res.* 135, 212–229. doi: 10.1016/j.phrs.2018.07.012

Rahman, K., Lowe, G. M., and Smith, S. (2016). Aged Garlic Extract Inhibits Human Platelet Aggregation by Altering Intracellular Signaling and Platelet Shape Change. *J. Nutr.* 146, 410S–415S. doi: 10.3945/jn.114.202408

Rahman, K. (2007). Effects of garlic on platelet biochemistry and physiology. *Mol. Nutr. Food Res.* 51 (11), 1335–1344. doi: 10.1002/mnfr.200700058

Rai, S. K., Sharma, M., and Tiwari, M. (2009). Inhibitory effect of novel diallyldisulfide analogs on HMG-CoA reductase expression in hypercholesterolemic rats: CREB as a potential upstream target. *Life Sci.* 85 (5-6), 211–219. doi: 10.1016/j.lfs.2009.05.020

Ramji, D. P., and Davies, T. S. (2015). Cytokines in atherosclerosis: key players in all stages of disease and promising therapeutic targets. *Cytokine Growth Factor Rev.* 26 (6), 673–685. doi: 10.1016/j.cytogfr.2015.04.003

Ried, K., and Fakler, P. (2014). Potential of garlic (Allium sativum) in lowering high blood pressure: Mechanisms of action and clinical relevance. *Integr. Blood Press. Control* 7, 71–82. doi: 10.2147/IBPC.S51434

Rosenblat, M., Belinky, P., Vaya, J., Levy, R., Hayek, T., Coleman, R., et al. (1999). Macrophage enrichment with the isoflavan glabridin inhibits NADPH oxidase-induced cell-mediated oxidation of low density lipoprotein. A possible role for protein kinase C. *J. Biol. Chem.* 274, 13790–13799. doi: 10.1074/jbc.274.20.13790

Saadati, S., Sadeghi, A., Mansour, A., Yari, Z., Poustchi, H., Hedayati, M., et al. (2019). Curcumin and inflammation in non-alcoholic fatty liver disease: a randomized, placebo controlled clinical trial. *BMC Gastroenterol.* 19 (1), 133. doi: 10.1186/s12876-019-1055-4

Sathyapalan, T., Aye, M., Rigby, A. S., Thatcher, N. J., Dargham, S. R., Kilpatrick, E. S., et al. (2018). Soy isoflavones improve cardiovascular disease risk markers in women during the early menopause. *Nutr. Metab. Cardiovasc. Dis.* 28 (7), 691–697. doi: 10.1016/j.numecd.2018.03.007

Sedaghat, A., Shahbazian, H., Rezazadeh, A., Haidari, F., Jahanshahi, A., Mahmoud Latifi, S., et al. (2019). The effect of soy nut on serum total antioxidant, endothelial function and cardiovascular risk factors in patients with type 2 diabetes. *Diabetes Metab. Syndr.* 13 (2), 1387–1391. doi: 10.1016/j.dsx.2019.01.057

Sedighi, M., Bahmani, M., Asgary, S., Beyranvand, F., and Rafieian-Kopaei, M. (2017). A review of plant-based compounds and medicinal plants effective on atherosclerosis. *J. Res. Med. Sci.* 22, 30. doi: 10.4103/1735-1995.202151

Shouk, R., Abdou, A., Shetty, K., Sarkar, D., and Eid, A. H. (2014). Mechanisms underlying the antihypertensive effects of garlic bioactives. *Nutr. Res.* 34 (2), 106–115. doi: 10.1016/j.nutres.2013.12.005

Sobenin, I. A., Andrianova, I. V., Demidova, O. N., Gorchakova, T. V., and Orekhov, A. N. (2008a). Lipid-lowering Effects of Time-Released Garlic Power Tablets in Double-Blinded Placebo-Controlled Randomized Study. *J. Atheroscler. Thromb.* 15 (6), 334–338. doi: 10.5551/jat.E550

Sobenin, I. A., Nedosugova, L. V., Filatova, L. V., Balabolkin, M. I., Gorchakova, T. V., and Orekhov, A. N. (2008b). Metabolic effects of time-released garlic powder tablets in type 2 diabetes mellitus: the results of double-blinded placebo-controlled study. *Acta Diabetol.* 45 (1), 1–6. doi: 10.1007/s00592-007-0011-x

Sobenin, I. A., Andrianova, I. V., Fomchenkov, I. V., Gorchakova, T. V., and Orekhov, A. N. (2009). Time-released garlic powder tablets lower systolic and diastolic blood pressure in men with mild and moderate arterial hypertension. *Hypertens. Res.* 32 (6), 433–437. doi: 10.1038/hr.2009.36

Sobenin, I. A., Andrianova, I. V., Lakunin, K. Y., Karagodin, V. P., Bobryshev, Y. V., and Orekhov, A. N. (2016a). Anti-atherosclerotic effects of garlic preparation in freeze injury model of atherosclerosis in cholesterol-fed rabbits. *Phytomedicine* 23, 1235–1239. doi: 10.1016/j.phymed.2015.10.014

Sobenin, I. A., Myasoedova, V. A., and Orekhov, A. N. (2016b). Phytoestrogen-Rich Dietary Supplements in Anti-Atherosclerotic Therapy in Postmenopausal Women. *Curr. Pharm. Des.* 22 (2), 152–163. doi: 10.2174/1381612822666151112150520

Sobenin, I. A., Galitsyna, E. V., Grechko, A. V., and Orekhov, A. N. (2017). Small dense and desialylated low density lipoprotein in diabetic patients. *Vessel Plus* 1, 29–37. doi: 10.20517/2574-1209.2016.12

Stroes, E. S., Thompson, P. D., Corsini, A., Vladutiu, G. D., Raal, F. J., Ray, K. K., et al. (2015). Statin-associated muscle symptoms: impact on statin therapy-European Atherosclerosis Society Consensus Panel Statement on Assessment, Aetiology and Management. *Eur. Heart J.* 36 (17), 1012–1022. doi: 10.1093/eurheartj/ehv043

Tabas, I., and Lichtman, A. H. (2017). Monocyte-macrophages and T cells in atherosclerosis. *Immunity* 47, 621–634. doi: 10.1016/j.immuni.2017.09.008

Tariq, S., Imran, M., Mushtaq, Z., and Asghar, N. (2016). Phytopreventive antihypercholesterolmic and antilipidemic perspectives of zedoary (Curcuma Zedoaria Roscoe.) herbal tea. *Lipids Health Dis.* 15, 39. doi: 10.1186/s12944-016-0210-y

Tian, J., Gu, X., Sun, Y., Ban, X., Xiao, Y., Hu, S., et al. (2012). Effect of statin therapy on the progression of coronary atherosclerosis. *BMC Cardiovasc. Disord.* 12, 70. doi: 10.1186/1471-2261-12-70

Venkataiah, V., Vickram,, Thirumalarao, K. R., Raiker, V. G., and Puttaswamy, S. H. (2016). Effects of diaceto-dipropyl-disulphide on plasma sialic acid and renal tissue thiol levels in alloxan diabetic rats. *J. Clin. Diagn. Res.* 10, BF06–BF08. doi: 10.7860/JCDR/2016/19241.8058

Vilahur, G., and Badimon, L. (2013). Antiplatelet properties of natural products. *Vascul. Pharmacol.* 59 (3-4), 67–75. doi: 10.1016/j.vph.2013.08.002

Villa, P., Amar, I. D., Bottoni, C., Cipolla, C., Dinoi, G., Moruzzi, M. C., et al. (2017). The impact of combined nutraceutical supplementation on quality of life and metabolic changes during the menopausal transition: a pilot randomized trial. *Arch. Gynecol. Obstet.* 296 (4), 791–801. doi: 10.1007/s00404-017-4491-9

Witztum, J. L., and Lichtman, A. H. (2014). The influence of innate and adaptive immune responses on atherosclerosis. *Annu. Rev. Pathol.* 9, 73–102. doi: 10.1146/annurev-pathol-020712-163936

Woo, K. S., Yip, T. W., Chook, P., Kwong, S. K., Szeto, C. C., Li, J. K., et al. (2013). Cardiovascular Protective Effects of Adjunctive Alternative Medicine (Salvia miltiorrhiza and Pueraria lobata) in High-Risk Hypertension. *Evid. Based Complement. Alternat. Med.* 2013, 132912. doi: 10.1155/2013/132912

Xu, C., Mathews, A. E., Rodrigues, C., Eudy, B. J., Rowe, C. A., O'Donoughue, A., et al. (2018). Aged garlic extract supplementation modifies inflammation and immunity of adults with obesity: A randomized, double-blind, placebo-controlled clinical trial. *Clin. Nutr. ESPEN* 24, 148–155. doi: 10.1016/j.clnesp.2017.11.010

Yang, T. L., Lin, F. Y., Chen, Y. H., Chiu, J. J., Shiao, M. S., Tsai, C. S., et al. (2011). Salvianolic acid B inhibits low-density lipoprotein oxidation and neointimal hyperplasia in endothelium-denuded hypercholesterolaemic rabbits. *J. Sci. Food Agric.* 91, 134–141. doi: 10.1002/jsfa.4163

Yang, J. X., Pan, Y. Y., Ge, J. H., Chen, B., Mao, W., Qiu, Y. G., et al. (2016). Tanshinone II A Attenuates TNF-α-Induced Expression of VCAM-1 and ICAM-1 in Endothelial Progenitor Cells by Blocking Activation of NF-κB. *Cell Physiol. Biochem.* 40, 195–206. doi: 10.1159/000452537

Yang, Y., Li, X., Peng, L., An, L., Sun, N., Hu, X., et al. (2018). Tanshindiol C inhibits oxidized low-density lipoprotein induced macrophage foam cell formation via a peroxiredoxin 1 dependent pathway. *Biochim. Biophys. Acta* 1864, 882–890. doi: 10.1016/j.bbadis.2017.12.033

Yu, X., Xu, L., Zhou, Q., Wu, S., Tian, J., Piao, C., et al. (2018). The Efficacy and Safety of the Chinese Herbal Formula, JTTZ, for the Treatment of Type 2 Diabetes with Obesity and Hyperlipidemia: A Multicenter Randomized, Positive-Controlled, Open-Label Clinical Trial. *Int. J. Endocrinol.* 2018, 9519231. doi: 10.1155/2018/9519231

Zeb, F., Safdar, M., Fatima, S., Khan, S., Alam, S., Muhammad, M., et al. (2018). Supplementation of garlic and coriander seed powder: Impact on body mass index, lipid profile and blood pressure of hyperlipidemic patients. *Pak. J. Pharm. Sci.* 31 (5), 1935–1941.

Zhang, B., Chen, Y. M., Huang, L. L., Zhou, X. X., Chen, C. G., Ye, Y. B., et al. (2008). Greater habitual soyfood consumption is associated with decreased carotid intima-media thickness and better plasma lipids in Chinese middle-aged adults. *Atherosclerosis* 198 (2), 403–411. doi: 10.1016/j.atherosclerosis.2007.10.001

Zhao, J. F., Ching, L. C., Huang, Y. C., Chen, C. Y., Chiang, A. N., Kou, Y. R., et al. (2012). Molecular mechanism of curcumin on the suppression of cholesterol accumulation in macrophage foam cells and atherosclerosis. *Mol. Nutr. Food Res.* 56, 691–701. doi: 10.1002/mnfr.201100735

Zhao, W., Li, J., He, X., Lv, O., Cheng, Y., and Liu, R. (2014). In vitro steatosis hepatic cell model to compare the lipid-lowering effects of pomegranate peel polyphenols with several other plant polyphenols as well as its related cholesterol efflux mechanisms. *Toxicol. Rep.* 1, 945–954. doi: 10.1016/j.toxrep.2014.10.013

Zhao, W., Wu, C., and Chen, X. (2016). Cryptotanshinone inhibits oxidized LDL-induced adhesion molecule expression via ROS dependent NF-κB pathways. *Cell Adhes. Migr.* 10, 248–258. doi: 10.1080/19336918.2015.1119361

Zhao, D., Tong, L., Zhang, L., Li, H., Wan, Y., and Zhang, T. (2016). Tanshinone II A stabilizes vulnerable plaques by suppressing RAGE signaling and NF-κB activation in apolipoprotein-E-deficient mice. *Mol. Med. Rep.* 14, 4983–4990. doi: 10.3892/mmr.2016.5916

Zhao, S., Li, J., Wang, L., and Wu, X. (2016). Pomegranate peel polyphenols inhibit lipid accumulation and enhance cholesterol efflux in raw264.7 macrophages. *Food Funct.* 7, 3201–3210. doi: 10.1039/C6FO00347H

Zou, X., Yan, C., Shi, Y., Cao, K., Xu, J., Wang, X., et al. (2014). Mitochondrial Dysfunction in Obesity-Associated Nonalcoholic Fatty Liver Disease: The Protective Effects of Pomegranate with Its Active Component Punicalagin. *Antioxid. Redox Signal.* 21, 1557–1570. doi: 10.1089/ars.2013.5538

Conflict of Interest: GA was employed by GALLY International Biomedical Research LLC.

The remaining authors declare that the research was conducted in the absence of any commercial or financial relationships that could be construed as a potential conflict of interest.

frontiers in Pharmacology

REVIEW
published: 26 May 2020
doi: 10.3389/fphar.2020.00699

Aniba canelilla (Kunth) Mez (Lauraceae): A Review of Ethnobotany, Phytochemical, Antioxidant, Anti-Inflammatory, Cardiovascular, and Neurological Properties

Fabio J. C. Souza-Junior[1], *Daniele Luz-Moraes*[1,2], *Felype S. Pereira*[1,2], *Mayra A. Barros*[1], *Luanna M. P. Fernandes*[1], *Letícia Y. Queiroz*[1], *Cristiane F. Maia*[1,2], *José Guilherme S. Maia*[2] *and Enéas A. Fontes-Junior*[1,2]*

[1] *Laboratório de Farmacologia da Inflamação e do Comportamento, Universidade Federal do Pará, Belém-PA, Brazil,* [2] *Programa de Pós-Graduação em Ciências Farmacêuticas, Instituto de Ciências da Saúde, Universidade Federal do Pará, Belém-PA, Brazil*

OPEN ACCESS

Edited by:
Yue Liu,
Xiyuan Hospital, China

Reviewed by:
Maria A. Deli,
Hungarian Academy of Sciences (MTA), Hungary
Yanfei Liu,
Beijing University of Chinese Medicine, China

***Correspondence:**
Enéas A. Fontes-Junior
efontes@ufpa.br

Specialty section:
This article was submitted to Ethnopharmacology, a section of the journal Frontiers in Pharmacology

Received: *02 December 2019*
Accepted: *28 April 2020*
Published: *26 May 2020*

Citation:
Souza-Junior FJC, Luz-Moraes D, Pereira FS, Barros MA, Fernandes LMP, Queiroz LY, Maia CF, Maia JGS and Fontes-Junior EA (2020) Aniba canelilla (Kunth) Mez (Lauraceae): A Review of Ethnobotany, Phytochemical, Antioxidant, Anti-Inflammatory, Cardiovascular, and Neurological Properties. Front. Pharmacol. 11:699. doi: 10.3389/fphar.2020.00699

Aniba canelilla (Kunth) Mez, popularly known as "casca preciosa" (precious bark), falsa canela (cinnamon-scented) Casca-do-maranhão (bark of maranhão), and Folha-preciosa (precious leaf), is an aromatic species of the Lauraceae family, widely distributed in the Amazon region. In traditional medicine, it is indicated for the treatment of a great diversity of diseases, including digestive, respiratory, inflam]matory, painful, and central nervous system disorders, it is administered mainly in the form of tea or decoction orally. Its essential oil is referred to as a natural antioxidant for food preservation and disease control, showing great potential for use in the cosmetics, perfumery, and pharmaceutical products sector. The present review aimed to discuss critically and comprehensively the ethnobotanical characteristics, phytochemical constitution, and scientifically tested biological properties of *A. canelilla*, systematizing the knowledge about the species and proposing new perspectives for research and development. The chemical composition of *A. canelilla* includes 1-nitro-2-phenylethane, metyleugenol, eugenol, safrol, anabasin, anbin, tannin, α-pinene, b-pinene, b-felandren, b-caryophyllene, b-sesquifelandren, p-cymene, linalool, α-copaene, and spatulenol. Researches with ethanolic extracts, essential oils, and major constituents (1-nitro-2-phenylethane and metyleugenol) have revealed antioxidant, antinociceptive, anti-inflammatory, cardio-modulating, hypotensive (vasorelaxant), hypnotic, anxiolytic, anticholinesterase, and antibiotic properties (trypanomicidal, leishmanicidal, and antifungal). Some of these effects are potentially beneficial for aging-related diseases treatment, such as cardio and cerebrovascular,

chronic inflammatory, neurological, and degenerative diseases. However, it is necessary to advance in the research of its clinical use and development of therapeutic products.

Keywords: *Aniba canelilla* (Kunth) Mez, folk medicine, biological activities, toxicity, 1-nitro-2-phenylethane, methyleugenol

INTRODUCTION

The increase in human longevity, as well as population growth, is a result of its social and technological evolution. This phenomenon, however, represents a growing public health challenge due to the proportional increase in the incidence of chronic inflammatory, neurological, and cardiovascular diseases. Such pathological conditions often require chronic polymedication which are sometimes marked by intense adverse reactions and are not always effective, leading to deterioration of patients' quality of life or discontinuation of therapy. There are still cases where current therapy consists only of palliative measures, with little effect on disease progression (Boccardi, 2019). This reality drives the scientific community in search of safer and more effective drugs.

Finding a solution for the future, however, may be related to our ability to investigate the past, valuing all traditional knowledge about plant species with therapeutic potential but lacking studies on their safety and effectiveness. In fact, medical plants have been a valuable source of herbal medicines and bioactive molecules for drug development (Samy et al., 2008). Brazilian forests, especially the Amazon rainforest, represent the largest source of plant species in the world, many of which have medicinal benefits. Along with such biodiversity, the Brazilian population also has a very rich folk medicine, preserved by traditional communities, which provides valuable information, useful to the selection of species for pharmacological screening (Hegde et al., 2014; Moraes et al., 2019).

Among the plants inserted in the Amazonian culture, *Aniba canelilla* (Kunth) Mez [syn. *Aniba elliptica* A.C. Sm., *Cryptocarya canelilla* Kunth, and others] stands out for its diversity economic and medicinal applications. This species of Lauraceae is an aromatic medium-sized tree, native from solid ground and semi-deciduous forests of South America, known as *casca-preciosa* (precious bark), *falsa-canela* (fake cinnamon), *casca-do-maranhão* (maranhão bark), and *folha-preciosa* (precious leaf), (Gottlieb and Magalhães, 1960b; Kubitzki and Renner, 1982; Ribeiro et al., 1999; Franciscon et al., 2018; Tropicos.org, 2019). Among its characteristics, the cinnamon-like aroma stands out, is even linked to the history of its discovery. Around Brazil discovery period, when Portuguese and Spanish navigators entered the Amazon River in search of cinnamon (*Cinnamomum verum* J.Presl) thought they had found a lot of this plant, instead what they had found was Casca-preciosa trees (Pinto, 1995). In folk medicine, this species is often used to treat painful and inflammatory conditions, gastrointestinal disorders, and neurological and psychiatric diseases, in addition to the treatment of infections (Maia et al., 2001; De Filipps et al., 2004; Sousa et al., 2009; Manhães et al., 2012). Some of these applications have been studied, elucidating their main constituents and ratifying their anti-inflammatory, antinociceptive, antihypertensive, and antioxidant potential, among others.

Nevertheless, it is noted that much remains to be elucidated about the therapeutic potential of *A. canelilla*, including the safety of its use, medical applications, and mechanisms of action. In this sense, the present study aims to review critically and comprehensively the current knowledge about the ethnobotany, phytochemical, pharmacological, and toxicological characteristics of *A. canelilla* and its derivatives (extracts, essential oil, and major constituents), identifying perspectives for new research and exploring its potential for neurological and cardiovascular diseases treatment (Graphical abstract—**Figure S1**). Data collection on *A. canelilla* was carried out electronically, based on articles published in peer-reviewed journals, abstracts published in conference proceedings, theses, and ethnobotanical textbooks. The research was carried out in the Google Scholar, Science Direct, Scopos, and PubMed databases.

ETHNOBOTANY

Taxonomy and Botanical Aspects

Lauraceae is a family of trees and shrubs recorded since the Cretaceous period, which includes 52 genera and approximately 2,500 to 3,500 species, distributed in tropical and subtropical areas, as well as in temperate climates, as America, tropical Asia, Australia, and Madagascar (Van der Werff, 1991; Kubitzki et al., 1993; Hu et al., 2007). This family gathers medium to large trees, but some species have characteristics of shrubs or small trees, with a diameter between 1 and 5 cm and their height rarely exceeds 8 m (Ribeiro et al., 1999). Several species of Lauraceae have economic use, providing wood, essential oils, and chemical compounds, relevant to civil construction and for the food and pharmaceutical industries (Barbosa et al., 2012). In Brazil, 24 genera and 441 species have been identified (Quinet et al., 2015). Some genera of Lauraceae are highlighted by having aromatic species, that is, plants that produce essential oils (EO) or resins rich in volatile compounds, as *Aniba*, *Nectandra*, *Ocotea*, *Licaria*, and *Dicypellium* (Marques, 2001).

As previously mentioned, the species *A. canelilla* is an aromatic plant with a characteristic odor, which is easily confused with cinnamon. Historically this characteristic is portrayed in the expeditions of Pizzarro and Orellana, in 1540, to the Amazon River, and Humbolt and Bonpland to the Orinoco River in 1800. In both cases, it was considered that excellent sources of the coveted spice were found, when in fact they found *Casca-preciosa* (Naranjo et al., 1981; Pinto, 1995; Lahlou et al., 2005). Its proper botanical designation was made by Carl Kunth, a German botanist, from samples collected by Humbolt and Bonpland. In his description, the botanist

emphasized the aromatic characteristic of the plant and its similarity to cinnamon. Initially called *Aniba canelilla* by Kunth, it was later registered and published by Carl Mez (1889), being officially identified as *Aniba canelilla* (Kunth) Mez (Gottlieb and Magalhães, 1960b; Almeida et al., 2017).

This prominent tree reaches up to 35 m in height and has a retinal trunk, with a diameter between 40 and 60 cm. Its branches are glabrous and lenticelated, with 8 to 16 cm leaves (thin petioles, grayish and dense garment, and secondary veins flattened and slightly prominent at the bottom), small flowers, and oblong capsular fruit (De Siqueira et al., 2010).

Distribution and Traditional Uses

Native to the plains and solid ground forests of the Amazon rainforest and Guyana, *A. canelilla* is adaptable to different types of soils, including regions of solid or semi-deciduous forests, lowland areas, rocky outcrops and rocky soils, poorly drained soils, and clay and sandy soils (Franciscon et al., 2018). This species extends from the Antilles, Guyana high lands to the dry lands of Brazil. In fact, it presents a wide distribution in the Amazon region, which predominates from the East of French Guiana, Suriname, Venezuela, Colombia to the Peruvian Amazon, rarely found in Central America (Kubitzki and Renner, 1982; Van der Werff, 1991; Ribeiro et al., 1999; Quinet et al., 2015; **Figure 1**). **Table 1** summarizes the various popular names attributed to *A. canelilla*, by geographic location.

A. canelilla is present in several aspects of the culture of these peoples. Its wood is used for civil construction (Lupe, 2007) and its EO and extracts are consumed as spices, cosmetics, and perfumes, as the product known as "Cheiro-de-santarém" (Maia et al., 2011; Araújo et al., 2007; Lorenzi and Matos, 2008; Barbosa et al., 2017).

In folk medicine, multiple ethnopharmacological indications have been found, with variations in the form of use. The most

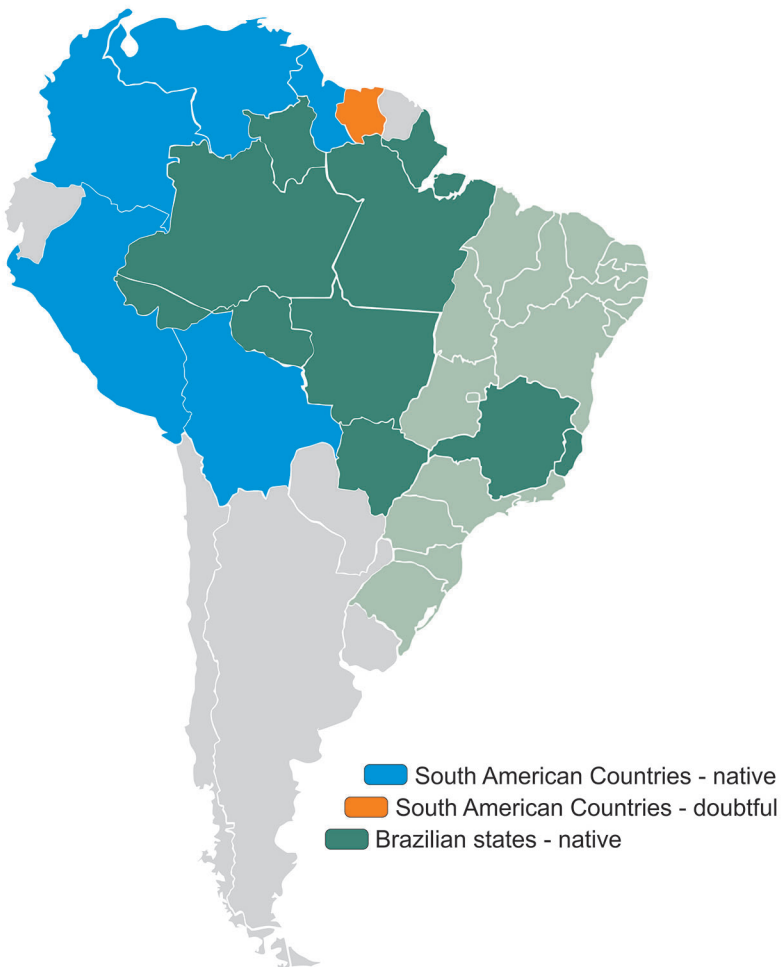

FIGURE 1 | Distribution of *Aniba canelilla* in South America. Blue color in cartogram indicates coutries where the *A. canelilla* tree is native, Orange color indicates countries where its native presence is doubtful, and the dark green color highlights the states of Brazil where it is native. Adapted from Quinet et al., 2015.

TABLE 1 | Popular names of *Aniba canelilla* according to its geographical location.

Popular name	Geographic location	Reference
Amapaima	Guiana	De Filipps et al., 2004
Ashmud	Guiana	De Filipps et al., 2004
Canela	Brazil: Pará	Herrero-Jaurégui et al., 2009
Canelão	Brazil: Manaus	Costa, 2013
Canelón	Bolivia[1], Peru[2]	Fournet et al., 1994[1]; Organismo Andino de Salud, 2014[2]
Casca-do-maranhão	Brazil: Maranhão	Madaleno, 2011
Casca-preciosa	Brazil: Pará[1], Manaus[2], Rondônia[3] Guiana[4]	Elisabetsky and Castilhos, 1990[1]; Bitencourt et al., 2014[1]; Santos et al., 2016[1]; Lima et al., 2004[2]; Silva et al., 2011[3]; De Filipps et al., 2004[4]
Chorecho	Bolivia	Fournet et al., 1994; Guze et al., 2014
Guarimán	Venezuela	Francisco and Ortega, 1994
Koto chojlla	Bolivia	Thomas and Vandebroek, 2006
Pokaneragi	Bolivia	Thomas and Vandebroek, 2006
Preciosa	Brazil: Amazonas[1], Maranhão[2], Pará[3]	Quignard et al., 2003[1]; Madaleno, 2011[2]; Branch and Silva, 1983[3]; Almeida et al., 2013[3]; Lima et al., 2011[3]
Showoyaja	Bolivia	Thomas and Vandebroek, 2006

Superscript 1-4, numbering is used to correlate the items in the same row as columns 2 and 3, pointing out the reference (column 3) corresponding to the information (column 2).

frequently mentioned form was the infusion of the barks, used to treat stomach inflammation, pain, and ulcers (De Almeida et al., 2013). Interestingly, the plant has been cited as a natural soothing, and still cited by indigenous communities as tranquilizer (Oger et al., 1994; Almeida et al., 2013; Santos et al., 2016), in contrast to some studies that point a stimulating and antidepressant effect (Rodrigues and Carlini, 2006; Bitencourt et al., 2014). There were also indications for the treatment of colds, cough, headache, and nausea (Taylor, 2005). Topical applications of bark extracts have been cited for the treatment of skin diseases, injuries, and infections (Mors et al., 2000; Taylor, 2005). *A. canelilla* EO (AcEO) also has a wide range of indications. According to Barbosa et al. (2017), the AcEO has therapeutic properties similar to those attributed to the infusions of bark, leaves, and branches, and there are also citations of its use to treat acne, dermatitis, fever, and various types of infections and injuries (Taylor, 2005). Another interesting finding is the use of smoke produced by barks burning, by the Tiryó Indians (Suriname), to treat diarrhea (De Filipps et al., 2004). References of the use of this species as analgesic, anti-inflammatory, antispasmodic, anti-anemic, anti-dysenteric, and antibiotic are also frequent. Additional uses of *A. canelilla* in folk medicine are summarized in **Table 2**.

PHYTOCHEMICAL COMPOSITION

Extracts

There are few studies dedicated to elucidate the phytochemical composition of *A. canelilla* extracts and carried out studies present only screens of the metabolite classes. For example, the study conducted by Mesquita et al. (2014) demonstrated the presence of phenolic compounds, tannins, flavonoids, and saponins in ethanol extracts obtained from leaves and branches. Despite the typical presence of benzyltetrahydroisoquinoline alkaloids in Lauraceae species, such as reticulin, coclaurine, and noranicanine (Oger et al., 1992; Oger et al., 1993; Custódio and Veiga Junior, 2014), the evaluation of the ethanolic extracts of *A. canelilla* did not detect alkaloids, as well as steroids and triterpenes.

Essential Oil

AcEO, unlike other extracts, has been well characterized. It is a yellowish-brown oil, denser than water, which have the characteristic aroma of the specie. It can be extracted from the trunk wood, branches, leaves, thin stems, and barks, by steam distillation or hydrodistillation, using a Clevenger-type apparatus, with a yield between 0.2 to 1.3% (Gottlieb and Magalhães, 1960a; Oger et al., 1994; Taveira et al., 2003; Da Silva et al., 2007; Silva et al., 2009; Silva et al., 2014; Barbosa et al., 2017; Giongo et al., 2017). Several factors, such as humidity and incidence of light, physiological, and geographical variations, environmental conditions, and genetic factors, can influence the production of AcOE. The available studies demonstrate higher oil yield in rainy periods, in the initial periods of development of plant organs, and in conditions where there is a greater supply of light. Regarding the parts of the plant, its yield of the stem is higher in the dry seasons. Leaf yield, however, does not appear to be influenced by such factors (Taveira et al., 2003; Manhães et al., 2012).

Its chemical composition has two main constituents, 1-nitro-2-phenylethane (1N2PE), the first known natural nitro derivative which is generally pointed as the major component and is responsible for the cinnamon-like odor characteristic of the species, and methyleneugenol (Gottlieb and Magalhães, 1959; Gottlieb and Magalhães, 1960a; Oger et al., 1994; Maia et al., 2001; Taveira et al., 2003; Lima et al., 2004; Da Silva et al., 2007; Maia and Andrade, 2009; Silva et al., 2009; Sousa, 2011; Manhães et al., 2012; Vale et al., 2013; Almeida et al., 2017; Farias et al., 2017; Giongo et al., 2017). These substances were identified both in the stem wood, bark, and leaves. Other identified constituents are eugenol, safrole, anabasine, anbin, tannin, α-pinene, b-pinene, b-felandren, b-caryophyllene, b-sesquifelandren, p-cymene, linalool, α-copaene, and spatulenol (Sangwan et al., 2001; Figueiredo et al., 2008). The main chemical constituents present in AcEO are listed in **Figure 2**.

As well as the oil yield, its composition also suffers seasonal influence. In the rainy period, the 1N2PE concentrations reach near 95%, while methyleugenol remain below 18%. In the dry period, 1N2PE decrease to less than 40%, while methyleugenol reaches 45%. The greatest value of 1N2PE (95.3%) and the least value of methyleugenol (0.2%) were observed in the leaves, during the rainy season (Taveira et al., 2003). Silva et al. (2009), otherwise, found no variation in 1N2PE concentration from the rainy to the dry seasons in samples collected on Reserva Adolpho Ducke, AM, Brazil. Additionally, methyleugenol was not detected in oils (Silva et al., 2009). Regarding the parts of the plant, Taveira et al. (2003) has found higher percentage of 1N2PE in leaves, while Manhães et al. (2012) found higher

TABLE 2 | Traditional uses of *Aniba canelilla*.

Popular indication	Part of the plant	Preparation	Administration	Reference
Arthritis, dyspepsia, infection, weakness, chest stimulant	Bark Leaves	Not stated	Not stated	Botsaris, 2007
Malaria	Bark[1,2] Leaves[1,2] Seeds[1]	Not stated	Not stated	Quignard et al., 2003[1]; Botsaris, 2007[2]
Sinusitis	Bark	Tea	Oral	Silva et al., 2011
Intestinal colic	Bark[1,2] Leaves[2]	Not stated	Not stated	Deharo et al., 2001[1]; Botsaris, 2007[2]
Fever	Bark[1,2,3] Leaves[3]	Maté[1] Decoction [2]	Oral	Fournet et al., 1994[1]; De Filipps et al., 2004[2]; Botsaris, 2007[3]
Calmative	Bark	Tea	Oral	Almeida et al., 2013; Santos et al., 2016
Migraine	Bark	Maté	Oral	Fournet et al., 1994
Dysentery	Bark[1,2,3] Leaves[1] Seeds[1]	Maté Decocção[2] Tea[3]	Oral	Quignard et al., 2003[1]; De Filipps et al., 2004[2]; Bitencourt et al., 2014[3]
Diarrhea	Bark	Maté[1]	Oral	Fournet et al., 1994[1]; Thomas and Vandebroek, 2006; Luziatelli et al., 2010
Vomiting	Bark	Not stated	Not stated	Thomas and Vandebroek, 2006
Stomachache	Bark	Decoction[1,3] Tea[2]	Oral	Elisabetsky and Castilhos, 1990; Bourdy et al., 2000[1]; Deharo et al., 2001; Almeida et al., 2013[2]; Thomas and Vandebroek, 2006; Costa, 2013[3]
Postpartum recovery	Bark	Not stated	Not stated	Deharo et al., 2001
Syphilis	Bark Seeds Leaves	Not stated	Not stated	Quignard et al., 2003
Inflammation	Bark[1,2] Leaves[2]	Tea	Oral	Almeida et al., 2013[1]; Organismo Andino de Salud, 2014[2]
Pain	Bark Leaves	Not stated	Not stated	Organismo Andino de Salud, 2014
Gout, catarrh	Bark	Tea	Oral	Bitencourt et al., 2014
Ulcer	Bark	Tea	Oral	Almeida et al., 2013
Against human hookworm	Bark	Extract (cooblation)	Not stated	Marques, 2001
Alzheimer's disease	Not stated	Not stated	Not stated	Madaleno, 2011
Antidepressant/stimulant	Bark [1]	Tea[1]	Oral	Rodrigues and Carlini, 2006; Bitencourt et al., 2014[1]

Superscript 1-4, numbering is used to correlate the items in the same row as columns 2, 3 and 5, pointing out the reference (column 5) corresponding to the information (column 2).

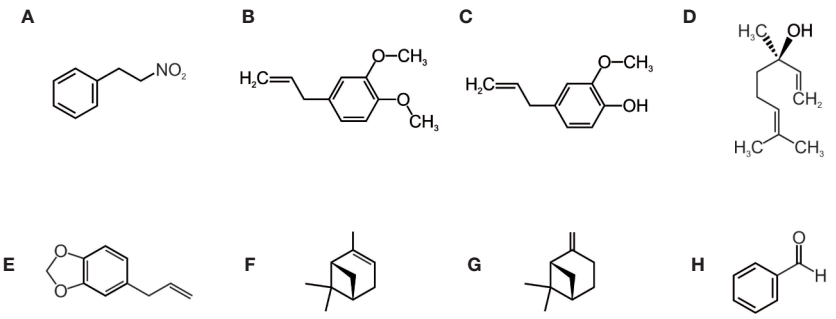

FIGURE 2 | Substances present in the *Aniba canelilla* essential oil: 1-nitro-2-phenylethane **(A)**, methyleugenol **(B)**, eugenol **(C)**, linalool **(D)**, safrole **(E)**, α-pinene **(F)**, β-pinene **(G)**, benzaldehyde **(H)**. Adapted from: Sugimoto et al. (2017), Sipe et al. (2014), Tsuchiya (2017), Rianjanu et al. (2018), Silva et al. (2012).

concentrations in stems. The content of 1N2PE and methyleugenol in leaves and fine stems are comparable to the content observed in the trunk wood and bark of *A. canelilla*. Thus, the extraction of essential oil from leaves and branches becomes an alternative to prevent the overthrow of the trunk to produce essential oils from this specie (Barbosa et al., 2017).

1-Nitro-2-Phenylethane

1N2PE ($C_8H_9NO_2$, MW 151.16) is a nitro compound formed through the biotransformation of phenylalanine by enzymes of the CYP superfamily (cytochrome P450) (Gottlieb and Magalhães, 1959; Gottlieb, 1972; Matsuo et al., 1972; Wittstock and Halkier, 2000). It is also found in two other species, *Ocotea*

pretiosa (Nees & Mart.) Mez (Lauraceae) (Gottlieb and Magalhães, 1959), present in São Paulo, Rio de Janeiro, Minas Gerais and Santa Catarina (Brazil) states, where it is known as *Canela-sassafrás*, and *Dennettia tripetala* G. Baker (Annonaceae) (Okogun and Ekong, 1969; Oyemitan et al., 2013). Due to the characteristic odor generated by the nitro compound, *O. pretiosa* can be confused with *A. canelilla*. EO samples from *O. pretiosa* collected in the warmer regions Brazilian southeastern showed 1N2PE and methyleugenol with main constituents (Gottlieb and Magalhães, 1959), while samples collected in the south, colder region, showed higher proportions of safrole (Gottlieb and Magalhães, 1960a).

Methyleugenol

Chemically referred to as 1-allyl-3,4-dimethoxybenzene ($C_{11}H_{14}O_2$, MW 178.23), methyleugenol is a yellowish oily compound with the characteristic of clove aroma and bitter taste, present in a wide variety of EOs. It is soluble in several organic solvents and insoluble in water. Methyleugenol is formed from the methylation of eugenol, another minor phenolic compound found in the AcEO (Gottlieb and Magalhães, 1959; Lahlou et al., 2004; Burdock, 2005; Barbosa et al., 2017). Concerning its occurrence in the parts of the plant, it is mainly concentrated in the trunk wood, where it has already been quantified at the concentration of 45.8% (Taveira et al., 2003). In the state of Pará, Brazil, it is considered a chemical marker for the AcEO, is also a significant constituent in other Lauraceae species, such as *O. pretiosa* from Southeastern Brazilian States (Gottlieb and Magalhães, 1960a; Silva et al., 2009; Manhães et al., 2012).

BIOLOGICAL PROPERTIES

Traditional communities attribute a variety of therapeutic properties to *A. canelilla*, being applied to the treatment of painful and inflammatory conditions, gastrointestinal and respiratory diseases, microbial infections, and parasitosis, in addition to neuropsychiatric disorders, as detailed above. Therefore, based on the medicinal culture of these people, much has been explored in scientific research, even though most of these studies have little depth. The studies identified in this review addressed mainly the toxicity antioxidant, antinociceptive, anti-inflammatory, cardiovascular, and neuropharmacological activities of *A. canelilla* EO and extracts in murine or *in vitro* models. Evidence of anticholinesterase and antibiotic activity was also verified (**Table 3**).

Toxicity

Characterizing the safety of using a therapeutic agent is as important as ensuring its effectiveness, being a requirement for the registration of herbal agents. The present review identified *in vitro,* and *in vivo* toxicological tests that aimed to characterize acute and subacute toxicity of *A. canelilla* derived products.

The cytotoxicity of AcEO and its two main constituents was tested by Giongo et al. (2017) in primary lymphocyte culture. AcEO, 1N2PE, and methyleugenol were tested in concentrations of 0.5%, 1%, and 2%, producing no cytotoxicity on those cells. However, the samples treated with a mixture of 1N2PE and methyleugenol in the concentration of 2% showed an average reduction of 21% in cell viability, pointing to the potential risk of the association of these constituents in high concentrations. In the brine shrimp bioassay, Silva et al. (2007) performed the analysis of plant samples collected in the Brazilian states of Para and Amazonas in rainy season. Methanolic extracts and EO from the trunks wood were tested, as well as 1N2PE isolated from EO. Products presented medium lethal concentration (LC_{50}) of 91.38 ± 7.20 μg/mL, 21.61 ± 1.21 μg/mL, and 20.37 ± 0.99 μg/mL, respectively, highlighting that 1N2PE showed equivalent activity to EO, and methanolic extract presented toxicity about four times lower.

AcEO oral toxicity was tested in an acute and subacute pattern of administration in murine models by Sousa et al. (2009). In the acute evaluation, performed with mice, the authors presented a medium lethal dose (LD_{50}) of 720 ± 66.4 mg/kg, despite declaring that the "study does not show any toxic symptoms, changes in behavior or mortality at the tested doses." For 1N2PE, LD50 of 712 ± 17.39 mg/kg for oral administration (Lima, 2008) and 490 mg/kg for intraperitoneal (ip) administration were identified in mice (Oyemitan et al., 2013).

Subacute toxicity (30 days of treatment) was tested in rats, with doses equivalent to 5% (36 mg/kg) and 10% (72 mg/kg) of LD_{50}, evaluating the incidence of deaths and behavioral, hematological (red cells, hematocrit, hemoglobin, MCV, HCM, MCCH, leukocytes, segmented cells, lymphocytes, and monocytes), biochemical (glucose, urea, creatinine, triglycerides, cholesterol, ALT, AST, and alkaline phosphatases), and histopathological markers. AcEO did not promote deaths in tested doses, nor did it promote significant changes in animals' behavior, as well as in the biochemical and hematological parameters tested. The vital organs showed no histological changes, except for the liver, which presented necrotic foci, apoptotic cells, and mononuclear infiltrate. There was also evidence of tissue regeneration, which, together with the absence of changes in biochemical markers, indicates adaptation of the organ to aggression. Together, these findings classify AcEO and 1N2PE as class 4 xenobiotics (low toxicity) (OECD, 2001).

Antioxidant Activity

The genesis and evolution of chronic degenerative diseases, as well as several pathologies, are strongly related to the imbalance between reactive oxygen species (ROS) production and the body's enzymatic and non-enzymatic antioxidant agents, a state called oxidative stress. Several EOs are recognized for their antioxidant potential, used for food preservation, but it also has pharmaceutical interest (Ruberto and Baratta, 2000; Miliauskas et al., 2004; Mimica-Duric et al., 2004). Such properties have been associated with the presence of phenolic compounds, such as flavonoids, phenolic acids, and phenolic diterpenes in aromatic plants. Studies carried out with *A. canelilla* highlight its potential, related to the presence of antioxidant phenolic compounds and coumarins, for the development of cosmetic, anti-corrosion products for the metallurgical industry and pharmaceutical products

TABLE 3 | Biological activities of *Aniba Canelilla* extracts, essential oil, and 1-nitro-2-phenylethane.

Experimental model	Part of the plant	Evaluated drug	Dose/Conc. interval	Activity	References
Nociception in mice	Bark	1N2PE	15–50 mg/kg	Antinociceptive	Lima et al., 2009
Writhing test					
Formalin test					
Hotplate test					
Inflammation in rats	Bark	1N2PE	25–50 mg/kg	Antiedematogenic	Vale et al., 2013
Dextran paw edema					
Carrageenan paw edema					
Croton oil ear edema					
In vitro isolated rat aorta	Bark	EO	1–600 µg/mL	Vasorelaxant	Lahlou et al., 2005
	Bark	1N2PE	1–300 µg/mL		De Siqueira et al., 2010
Normotensive rats	Bark	EO	1–20 mg/kg	Bradycardic and hypotensive	Lahlou et al., 2005
	Bark	1N2PE	1–10 mg/kg		De Siqueira et al., 2010
Hypertensive rats	Bark	EO	10–20 mg/kg	Bradycardic and hypotensive	Interaminense et al., 2010;
		1N2PE	5–10 mg/kg		Interaminense et al., 2013
Neuropharmacological evaluations in mice	–	1N2FE	50–400 mg/kg	Hypnotic,	Oyemitan et al., 2013
Sleeping time			25–200 mg/kg	Anticonvulsant	
PTZ-induced convulsion			5–20 mg/kg	Anxiolytic	
Elevated plus-maze					
In vitro acetylcholinesterase activity assay	Trunk wood	EO	0.01–1,000 ng/spot	Anticholinesterase	Silva et al., 2014
		1N2PE			
Tripomastigotes culture	Wood	EO	0.5–2.0%	Trypanocide	Giongo et al., 2017
Trypanosoma evansi		1N2PE			
In vitro antileishmanial assay	Leaves	EO	40 µg/mL*	Leishmanicide	Silva et al., 2009
Leishmania amazonensis					
In vitro microdilution test	Bark	1N2PE	170 µg/mL**	Antifungal	Oger et al., 1994
Candida albicans			360 µg/mL**		
C. tropicalis			720 µg/mL**		
C. parapsilosis			1500 µg/mL**		
Aspergillus. fumigatus					
Challerger test	Leaves Branches	EO	2 mg/mL	Antifungal	Silva, 2012
Candida albicans					
Didymella bryoniae					

**Median inhibitory concentration (IC_{50}).*
***Minimum inhibitory concentration (MIC).*
EO, essential oil; 1N2PE, 1-nitro-2-phenilethane; ETEX, ethanolic extract; PTZ, pentylenetetrazol.

(Da Silva et al., 2007; Silva, 2012; Mesquita et al., 2014; Farias et al., 2017; Barros et al., 2018).

Despite the potential of its phytochemical constituents, until now only chemical tests have been used to evaluate the antioxidant capacity of *A. canelilla* derivatives, based on its ability to eliminate DPPH (2,2-diphenyl-1-picrylhydrazyl) radicals, an assay aimed to screen non-enzymatic antioxidant agents candidate scavenger activity, using the Trolox (6-hydroxy-2,5,7,8-tetramethylchroman-2-carboxylic acid), ascorbic acid, and/or quercetin as activity patterns. Da Silva et al. (2007), using Trolox as standard, demonstrated an DPPH inhibition of 32 to 93% for samples of AcEO (110 to 1,400 µg/mL) obtained from Amazonas and Pará state (Brazil) plants. Methanolic extracts (2 to 10 µg/mL) obtained from same plants showed an DPPH inhibition of 25 to 93%, and 11.47 to 63.19% of inhibition was found for 1N2PE (200 to 1000 µg/mL). Such findings suggest a greater antioxidant capacity for the methanolic extract, up to fifty times higher than that of AcEO and equivalent to Trolox. For ethanolic extract of the plant branches and leaves, Mesquita et al. (2014) demonstrated a greater scavenger activity in leaf extract, that showed 34.97% of ascorbic acid activity. This finding was similar to the one found by Silva (2012), who noticed that the ethanolic extract of the leaves had about one-third of ascorbic acid activity. In the same study, the hydroalcoholic extract presented similar results. The results by Martins et al. (2016), on the other hand, demonstrated equivalence between ascorbic acid and the ethanolic extract from the bark of *A. canelilla*. They also demonstrated that the extracts had photoprotective effect.

In this context, considering the preliminary character of these findings and the identification of secondary metabolites, phenolic compounds, and coumarins, related to antioxidant activity and the reduction of the risk of various diseases, in products obtained from *A. canelilla* (Bubols et al., 2013; Mesquita et al., 2014; Serino and Salazar, 2019), we believe it is essential to explore biological models to evaluate its effects on enzymes with oxidizing [nicotinic adenine dinucleotide phosphate oxidase (NOX), nitric oxide synthase (NOS), monoxides, and xanthine oxidoreductase (XO), etc.] and antioxidant [catalase, glutathione (GPx), superoxide dismutase (SOD), etc.] activities, as well as on the formation of ROS and oxidative injury markers (lipid peroxidation, carbonylated proteins, etc.) (Awad et al., 2018) to determine its real benefit for the prevention or treatment of chronic and/or degenerative metabolic, cardiovascular, neural,

and other diseases, whose mechanisms of genesis and evolution comprise of an important oxidative component (for review: Uttara et al., 2009; Liguori et al., 2018).

Antinociceptive and Anti-Inflammatory Activity

Inflammation is another key pathophysiological process in the origin and development of numerous diseases. Considering not only the chronic inflammatory conditions that are increasing in function of aging, but it has also been widely discussed in cardiovascular and neuropsychiatric diseases context, showing clinical benefits with anti-inflammatory drugs use. Pain is involved in worsening the patient's quality of life, requiring non-pharmacological and pharmacological care aimed at its adequate control. In this context, *A. canelilla* has shown promise, since published studies have ratified, in murine models, its antinociceptive and anti-inflammatory properties referred in traditional use.

The study initially conducted by Lima (2008), later expanded and published in two other articles (Lima et al., 2009; Vale et al., 2013), demonstrated antinociceptive and anti-inflammatory activity using a fraction of the AcEO containing 1N2PE with 97.5 to 99% purity. This product was therefore applied to classic models of antinociceptive activity (abdominal contortions, hot plaque, and formalin) and antiedematogency (croton oil ear edema, paw edema by carrageenan or dextran), in addition to performing a theoretical study of functional density calculations. Regarding nociception, 1N2PE showed antinociceptive activity in a dose-dependent pattern (15, 25, and 50 mg/kg) when administered ip. The screening proceeded also revealed that it modulates only peripheral components of nociception, despite apparently involving opioid receptors in its mechanism of action (Lima et al., 2009). In inflammatory context, the results indicate the reduction of edema induced by croton oil, carrageenan, and dextran, with oral doses of 25 and 50 mg/kg (Vale et al., 2013). A possible mechanism related to these effects was pointed out by a conformational study conducted by Vale et al. (2013) who demonstrated that 1N2PE molecule had a favorable configuration for interaction with prostaglandin endoperoxide synthase.

Methyleugenol, the second major compound in AcEO, it also shows evidence of antinociceptive, anesthetic, and anti-inflammatory activity. According to Yano et al. (2006) research, its oral administration (10 mg/kg) reduces the second stage nociceptive response in formalin test. This effect was inhibited by bicuculline, a GABAa receptor antagonist, indicating that its activity would be related to the activation of these receptors. On the other hand, it did not promote any activity on cyclooxygenases 1 and 2. These findings seem to corroborate with Carlini et al. (1981) study, that attributed anesthetic activity to methyleugenol (200 and 300 mg/kg). Additionally, Choi et al. (2010) demonstrated a reduction in the expression of pro-inflammatory (IL-1B, IL-6, TNFα, and iNOS) and increased expression of anti-inflammatory (IL-10, TGF-B) mediators in rat and cell culture models of cerebral ischemia. In view of these results, there is still much to be done in elucidating mechanisms of its antinociceptive and anti-inflammatory properties. Also taking advantage of central nervous system activity evidences to better characterize its potential anti-neuroinflammatory effect.

Cardiovascular Activities

Cardiovascular effects of AcEO and its major components were elucidated through a partnership between researchers from the federal universities of Ceará and Pará (Brazil). The work developed by those groups initially demonstrated hypotension and bradycardia being promoted by intravenous (i.v.) injection of AcEO in normotensive rats, triggering in a dose-dependent pattern. According to the authors, such effects were linked, at least in part, to endothelial integrity factors, also identifying the participation of endothelial muscarinic receptors and stimulation of nitric oxide (NO) production, regulated by calcium flow (Lahlou et al., 2005). The same pattern was observed with i.v. administration of a concentrated fraction (98%) of 1N2PE (1, 3, 5, and 10 mg/kg) in normotensive anesthetized rats, indicating that 1N2PE was responsible for the vasorelaxant and bradycardic properties of AcEO (De Siqueira et al., 2010). According to the authors, this effect was a vago-vagal bradycardiac and depressor reflex generated by excitation of pulmonary afferent type C fibers. Also, 1N2PE has a direct effect on the vascular smooth muscle, promoting its relaxation. Thus, the authors demonstrated that the i.v. treatment with AcEO actively promoted vascular relaxation and consequent hypotension, not associated with the sympathetic tone (Lahlou et al., 2005; De Siqueira et al., 2010). In the next research stage, cardiovascular effects of AcEO and 1N2PE were tested in spontaneously hypertensive rats. Under these conditions, the i.v. administration of both AcEO (1, 5, 10, and 20 mg/kg) and 1N2PE (1, 3, 5, and 10 mg/kg) retained the same pattern of biphasic effect, composed of the vago-vagal bradycardic reflex (phase 1) and the direct vasodilatory action (phase 2; **Figure 3**) (Interaminense et al., 2010; Interaminense et al., 2013).

The biochemical pathways involved on those effects were investigated by Brito et al. (2013) who reported that 1N2PE would raise the levels of cyclic guanosine monophosphate (cGMP) in smooth muscle cells, suggesting a possible stimulation of guanylate cyclase (sGC). In addition, blocking the production of cyclic adenosine monophosphate (cAMP) or NO did not interfere with 1N2PE effects. Such evidence reveals the potential of 1N2PE for the treatment of cardiovascular diseases, such as systemic arterial hypertension and pulmonary arterial hypertension, and cerebrovascular diseases, such as stroke.

Neuropharmacological Activities

Despite the references of *A. canelilla* tea traditional use for the treatment of central nervous system-related conditions, such as Alzheimer's disease and depression, in addition to indication as calming (Rodrigues and Carlini, 2006; Madaleno, 2011; Almeida et al., 2013; Bitencourt et al., 2014; Santos et al., 2016), no studies were identified that explored such properties in this specie.

However, studies on the neuropharmacological properties of the two major constituents of AcEO, 1N2PE and methyleugenol, have been identified. 1N2PE, isolated (93% pure) from *Dennettia tripetala* G. Baker EO, an African Annonaceae species, promoted hypnotic effect in doses between 100 and 400 mg/kg (ip) in mice,

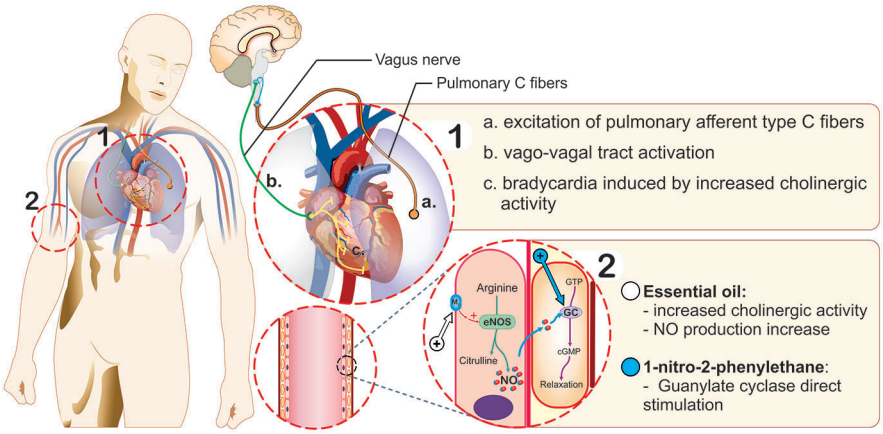

FIGURE 3 | Proposed mechanism for the antihypertensive and bradycardic effects of *Aniba canelilla* essential oil and 1-nitro-2-phenylethane.

reducing sleep latency with potency higher than pentobarbitone sodium (50 mg/kg; ip) and diazepam (20 mg/kg; ip). It also promoted a dose-dependent increase in sleep time, reaching an effect equivalent to diazepam (standard drug) at 400 mg/kg. 1N2PE also promoted protection in the model of Pentylenetetrazol (PTZ)-induced convulsions in mice. At a dose of 20 mg/kg, 20% protection was observed, while at doses above 50 mg/kg, seizures were fully inhibited. Pretreatment with flumazenil (2 mg/kg; ip) blocked the protection provided by 1N2PE, indicating a likely involvement of γ-aminobutyric acid (GABA) pathways in its effect. Finally, evidence of an anxiolytic effect was also evaluated in the plus-maze model at doses between 5 and 20 mg/kg (ip) with equivalent potency to diazepam (20 mg/kg) (Oyemitan et al., 2013). Silva et al. (2014), in turn, demonstrated that 1N2PE, isolated from AcEO, is a strong acetylcholinesterase blocker, with potency equivalent to physostigmine. Its effect was related to the positioning of its nitro group next to the enzyme catalytic serine residue, forming a potent hydrogen bond with its hydroxyl group.

Methyleugenol, in turn, has been described as a central nervous system depressant, with anticonvulsant and anesthetic effects (Dallmeier Zelger et al., 1983; Sayyah et al., 2002). In this context Ding et al. (2014) demonstrates in cultured hippocampal neurons the agonist property of this substance on GABAa receptors. Considering the majority presence of these constituents in AcEO, they can be the basis of the traditional indications described as calming. However, there are still other properties to be investigated, such as the influence on neurodegeneration, memory, and depressive behaviors.

Other Biological Activities

In addition to the effects addressed above, *A. canelilla* and its constituents have also been investigated for its antibiotic properties. Giongo et al. (2017), described the trypanomicidal effect of AcEO from bark, 1N2PE, and methyleugenol in a culture of *Trypanosoma evansi*, suggesting that may be a viable alternative for the treatment of this protozoosis. Silva et al. (2009), in turn, demonstrated the leishmanicidal effect of AcEO and 1N2PE on *Leishmania amazonensis*.

Antifungal activity has also been described. Evaluating EOs, hydrolates, ethanolic extract, and hexane and dichloromethane fractions of plant leaves or branches in the culture of bacteria (*Staphylococcus aureus* and *Pseudomonas aeruginosa*), human pathogenic fungi (*Candida albicans*), and phytopathogens (*Didymella bryoniae* and *Corynespora cassiicola*), reported that only EOs promoted growth inhibition and exclusively against *C. albicans* and *D. bryoniae*. These antifungal properties have been attributed mainly to 1N2PE (Oger et al., 1994; Silva, 2012).

POTENTIAL FOR AGING-RELATED DISEASES TREATMENT

The human aging process involves the progressive alteration of the cell repair and proliferation capacity, in addition to nuclear and mitochondrial DNA alterations, constituting a progressively favorable context for the development of diseases. Among the events related to this senescence process is the so-called inflammating, a state caused by the increase in the production/release of inflammatory mediators and oxidative stress, caused by the imbalance between the production of ROS and the body's antioxidant capacity. The studies in this area discuss the cause and consequence relationships between the aging process and these two mechanisms, however, agree on the principle that they are key factors in the genesis and evolution of aging-related diseases, among which stands out the cancer, diabetes, and cardiovascular, respiratory, and neurological diseases (Khansari et al., 2009; Zuo et al., 2019) (**Figure 4**).

In this context, *A. canelilla* has great potential, as it brings together a set of advantageous activities for the treatment of clinical conditions related to inflammation and oxidative stress. The reviewed studies demonstrate the ability of the plant derivatives to modulate the inflammatory process by inhibiting

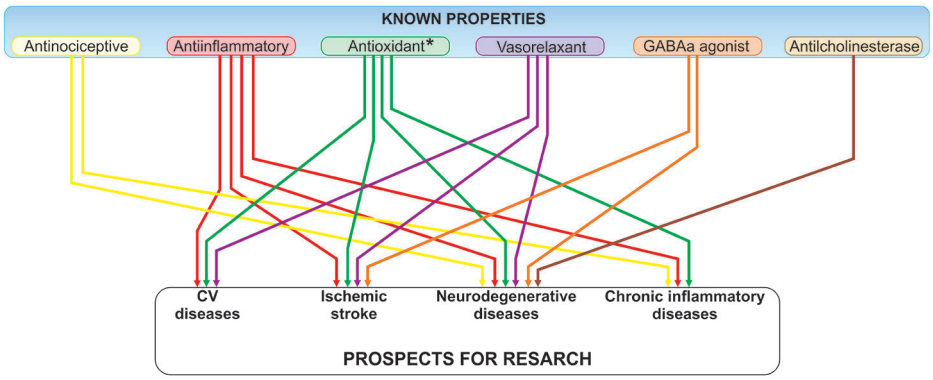

FIGURE 4 | Prospects for assessing the therapeutic potential of *Aniba canelilla* in aging-related diseases, based on current knowledge. *Needs to be confirmed in biological models.

pro-inflammatory and inducing anti-inflammatory cytokines, preventing edema formation and leukocyte migration to the focus of aggression (Lima, 2008; Choi et al., 2010; Vale et al., 2013). Based on these findings, much can be explored concerning the diversity of inflammatory diseases that can be benefited by their actions. Therefore, it is necessary to expand the studies on such actions, exploring its influences on the cellular inflammatory response, diapedesis mechanisms, and intracellular signaling pathways. Studies about its antioxidant properties, as previously mentioned, were limited to chemical DPPH tests (Silva et al., 2007; Silva, 2012; Mesquita et al., 2014; Martins et al., 2016), so we consider essential studies on its effects on ROS production, pro (NOX, NOS, XO, etc.) and antioxidant (Catalase, GPx, SOD, etc.) enzymes activity and macromolecules oxidation (lipid peroxidation, protein carbonylation, nucleic acid damage, etc.).

Regarding cardiovascular diseases (CVD), which emerge worldwide as the main cause of death (WHO, 2018), significant cardio modulatory and vasorelaxant effects of AcEO and its major constituent have been reported, leading to a reduction in blood pressure in hypertensive rats, through vago-vagal response and sGC stimulation, with consequent increase in cGMP production (Interaminense et al., 2010; Interaminense et al., 2013). It is important, however, to advance in the search for these effects. Antioxidant and anti-inflammatory properties of the plant could also promote additional benefits, reducing vascular remodeling, endothelial dysfunction, and atherosclerosis, which are induced/aggravated by inflammation and oxidative stress (Garcia et al., 2017; Zuo et al., 2019).

In view of the combination of vascular, anti-inflammatory, and antioxidant properties, we consider it is interesting to study its effects on the outcome of ischemic strokes (Kim et al., 2016). This condition is marked by rapid and intense neuronal death by apoptosis in ischemic core. In penumbra area, neuron death is triggered by glutamatergic excitotoxicity and oxidative stress, in addition to an important neuroinflammatory event, with the development of microgliosis and astrogliosis, and the release of pro-inflammatory cytokines (Fontes-Junior et al., 2016).

In fact, the interaction between oxidative stress and inflammation has been widely explored, identifying the interfaces between these mechanisms, that is, the state of "inflamming" increases the ROS production, favoring oxidative stress, in the same way as oxidative stress promotes the activation of inflammatory pathways and together are involved in chronic and degenerative conditions (Reuter et al., 2010). In addition, based on the evidence of the *A. canelilla* constituents action on central nervous system and traditional indications of use for the treatment of neurodegenerative conditions, such as Alzheimer's disease (AD), and depression (Rodrigues and Carlini, 2006; Madaleno, 2011), we consider it as a possible research line to be explored. The anticholinesterase effect attributed to 1N2PE may justify, at least in part, the use of *A. canelilla* for AD treatment, but there are no studies about its benefits on memory or disease progression, topic which assemble multiple mechanisms and must be elucidated in future studies. On behavior and emotionality, evidence of anxiolytic activity was observed (Oyemitan et al., 2013), but no study has yet explored traditional indications for depression treatment, considered an inflammatory disease too, or the supposed stimulating effect.

FINAL CONSIDERATIONS

Studies on the aromatic species *A. canelilla*, popularly known as "Casca preciosa," have ratified several of its traditional indications, showing its commercial and therapeutic potential, including antioxidant, antinociceptive, anti-inflammatory, anticholinesterase, anxiolytic, anticonvulsant, hypnotic, cardio modulatory, vasorelaxant, and antibiotic properties, through the application of its EO, extracts, and major constituents (1N2PE and Methyleugenol). However, it is necessary to advance in characterization of its mechanisms of action, pharmacokinetic, and clinical potential applications arising from each property. Special attention should also be paid to possible synergisms resulted from combined properties, such as antioxidant (needs

to be confirmed in biological models), anti-inflammatory, and cardiovascular, which open new therapeutic possibilities on aging-related diseases, such as the treatment of cerebrovascular, neurobehavioral, and chronic degenerative diseases.

AUTHOR CONTRIBUTIONS

The review was conceived and designed by EF-J, FS-J, and DL-M. Data collection were performed by FS-J, DL-M, FP, MB, LF, and LQ. Data were analyzed by EF-J, FS-J, DL-M, CM, and JM. Drafting of the manuscript: FS-J, DL-M, FP, MB, LF, and LQ. Critical revision of the manuscript: EF-J, CM, and JM. All authors revised and approved the final version of the manuscript.

ACKNOWLEDGMENTS

We thank to Universidade Federal do Pará (UFPA) and Coordenação de Aperfeiçoamento de Pessoal de Nível Superior (CAPES) for the financial support for this project. Thanks to Mr. Valter Vinicius Silva Monteiro for his contribution to English review.

SUPPLEMENTARY MATERIAL

The Supplementary Material for this article can be found online at: https://www.frontiersin.org/articles/10.3389/fphar.2020.00699/full#supplementary-material

FIGURE S1 | Graphical abstract.

REFERENCES

Almeida, M. R., Fidelis, C. H. V., Barata, L. E. S., and Poppi, R. J. (2013). Classification of Amazonian rosewood essential oil by Raman spectroscopy and PLS-DA with reliability estimation. *Talanta* 117, 305–311. doi: 10.1016/j.talanta.2013.09.025

Almeida, M. R., Martinez, S. T., and Pinto, A. C. (2017). Chemistry of natural products: Plants that witness histories. *Rev. Virtual Quimica.* 9, 1117–1153. doi: 10.21577/1984-6835.20170068

Araújo, V. F., De Petry, A. C., Echeverria, R. M., Fernandes, E. C., and Pastore, F. (2007). *Plantas da Amazônia para Produção Cosmética: uma abordagem química - 60 espécies do extrativismo florestal não-madeireiro da Amazônia*. Brasília, 244: Universidade de Brasilia.

Awad, M. A., Aldosari, S. R., and Ruhul Abid, M. (2018). Genetic Alterations in Oxidant and Anti-Oxidant Enzymes in the Vascular System. *Front. Cardiovas. Med.* 117. doi: 10.3389/fcvm.2018.00107

Barbosa, T. D. M., Baitello, J. B., and Moraes, P. L. R. (2012). A família Lauraceae Juss. no município de Santa Teresa, Espírito Santo. *Bol. Mus. Biol. Mello Leitão* 30, 5–178.

Barbosa, P. C. S., Fernandes, K. S., Manhães, A. P., Carneiro, S. B., Sampaio, P., de, T. B., et al. (2017). New and sustainable essential oils obtained from the long-term explored cinnamomum-like Aniba canelilla. *J. Appl. Res. Med. Aromatic Plants* 5, 60–71. doi: 10.1016/j.jarmap.2016.11.002

Barros, I. B., Bonfim, R., and Friburgo, N. (2018). The inhibitory action of *Aniba Canelilla* (H.B.K.) Mez extracts on the corrosion of carbon steel in hydrochloric acid medium. *Mater. Res.* 21, 1–8. doi: 10.1590/1980-5373-mr-2017-0786

Bitencourt, B. L. G., Lima, P. G. C., and Barros, F. B. (2014). *Comércio e uso de plantas e animais de importância mágico-religiosa e medicinal no mercado público do Guamá, Belém do Pará.* Revista Faculdade Santo Agostinho. 11 (3), 96–158. doi: 10.12819/2014.11.3.5

Bizzo, H. R., Ana Maria, C. H., and Rezende, C. M. (2009). Óleos essenciais no brasil: aspectos gerais, desenvolvimento e perspectivas. *Quimica Nova.* 32, 588–594. doi: 10.1590/S0100-40422009000300005

Boccardi, V. (2019). Population Ageing: The Need for a Care Revolution in a World 2.0. *Geriatrics* 4, 47. doi: 10.3390/geriatrics4030047

Botsaris, A. S. (2007). Plants used traditionally to treat malaria in Brazil: the archives of Flora Medicinal. *J. Ethnobiol. Ethnomed.* 3 (18), 1–8. doi: 10.1186/1746-4269-3-18

Bourdy, G., DeWalt, S. J., Chávez de Michel, L. R., Roca, A., Deharo, E., Muñoz, V., et al. (2000). Medicinal plants uses of the Tacana, an Amazonian Bolivian ethnic group. *J. Ethnopharmacol.* 70, 87–109. doi: 10.1016/S0378-8741(99)00158-0

Branch, L. C., and Silva, M. F. (1983). Folk medicine in alter do Chão, Pará Brasil. *Acta Amaz* 13, 737797. doi: 10.1590/1809-4392135737

Brito, T. S., Lima, F. J. B., Aragão, K. S., De Siqueira, R. J. B., Sousa, P. J. C., Maia, J. G. S., et al. (2013). The vasorelaxant effects of 1-nitro-2-phenylethane involve stimulation of the soluble guanylate cyclase-cGMP pathway. *Biochem. Pharmacol.* 85, 780–788. doi: 10.1016/j.bcp.2012.12.012

Bubols, G. B., Vianna, D. R., Medina-Remón, A., Von Poser, G., Lamuela-Raventos, R. M., Eifler-Lima, V. L., et al. (2013). The antioxidant activity of coumarins and flavonoids, Mini-Rev. *Med. Chem.* 13, 318–334. doi: 10.2174/138955713804999775

Burdock, G. A. (2005). *Fenaroli´s Handbook of Flavor Ingredients,* Sixth Edition. (New York: CRC Press). doi: 10.1201/9781439847503-c3

Carlini, E. A., Dallmeier, K., and Zelger, J. L. (1981). Methyleugenol as a Surgical Anesthetic in Rodents. *Experientia* 37, 37–38. doi: 10.1007/BF01990065

Choi, Y. K., Cho, G.-S., Hwang, S., Kim, B. W., Lim, J. H., Lee, J.-C., et al. (2010). Methyleugenol reduces cerebral ischemic injury by suppression of oxidative injury and inflammation. *Free Radical Res.* 44, 925–935. doi: 10.3109/10715762.2010.490837

Costa, P. S. P. (2013). *Estudo etnobotânico e farmacognóstico de plantas antimaláricas de uso popular na comunidade cèu do Mapiá, Pauini- AM* [masters dissertation]. [Manaus] Universidade Federal do Amazonas, Faculdade de Ciências Farmacêuticas. Available in: https://tede.ufam.edu.br/handle/tede/5324

Custódio, D. L., and Veiga Junior, V. F. (2014). Lauraceae alkaloids. *RCS Adv.* 4, 21864–21890. doi: 10.1039/C4RA01904K

Da Silva, J. K. R., Sousa, P. J. C., Andrade, E. H. A., and Maia, J. G. S. (2007). Antioxidant capacity and cytotoxicity of essential oil and methanol extract of Aniba canelilla (H.B.K.) Mez. *J. Agric. Food Chem.* 55, 9422–9426. doi: 10.1021/jf071928e

Dallmeier Zelger, K. R., Zelger, J. L., and Carlini, E. A. (1983). New anticonvulsants derived from 4-allyl-2-methoxyphenol (Eugenol): comparison with common antiepileptics in mice. *Pharmacology* 27, 40–49. doi: 10.1159/000137828

De Almeida, L. S., Gama, J. R. V., Oliveira, F., de, A., Ferreira, M. S. G., De Menezes, A. J. E. A., et al. (2013). Uso de Espécies Da Flora Na Comunidade Rural Santo Antônio, BR-163, Amazônia Brasileira. *Floresta e Ambiente* 20, 435–446. doi: 10.4322/floram.2013.044

De Filipps, R. A., Maina, S. L., and Crepin, J. (2004). *Medicinal plants of the Guianas (Guyana, Surinam, French Guiana)* Washington, D.C.: Dept. of Botany, National Museum of Natural History, Smithsonian Institution.

De Siqueira, R. J. B., Macedo, F. I. B., Interaminense, L., de, F. L., Duarte, G. P., Magalhães, P. J. C., et al. (2010). 1-Nitro-2-phenylethane, the main constituent of the essential oil of Aniba canelilla, elicits a vago-vagal bradycardiac and depressor reflex in normotensive rats. *Eur. J. Pharmacol.* 638 (13), 90–98. doi: 10.1016/j.ejphar.2010.03.060

Deharo, E., Bourdy, G., Quenevo, C., Muñoz, V., Ruiz, G., and Sauvain, M. (2001). A search for natural bioactive compounds in Bolivia through a multidisciplinary approach. Part V. Evaluation of the antimalarial activity of plants used by the Tacana Indians. *J. Ethnopharmacol.* 77, 91–98. doi: 10.1016/S0378-8741(01)00270-7

Ding, J., Huang, C., Peng, Z., Xie, Y., Deng, S., Nie, Y. Z., et al. (2014). Electrophysiological characterization of methyleugenol: A novel agonist of GABA(A) receptors. *ACS Chem. Neurosci.* 5, 803–811. doi: 10.1021/cn500022e

Elizabetsky, E., and Castilhos, Z. C. (1990). Plants Used as Analgesics by Amazonian Caboclos as a Basis for Selecting Plants for Investigation. *Int. J. Crude Drug Res.* 28 (4), 309–320. doi: 10.3109/13880209009082838

Farias, A. B., Fernandes, F. S., Santos, R. A., Souza, E. S., and Souza, J. V. B. (2017). Estudo fitoquímico e análise de fotoproteção dos extratos eóleos essenciais de aniba canelilla (H.B.K) Mez. *J. Engr. Exact Sci.* 3 (4), 0614–0620. doi: 10.18540/2446941603042017061 4

Figueiredo, A. C., Barroso, J. G., Pedro, L. G., and Scheffer, J. J. C. (2008). Factors affecting secondary metabolite production in plants: volatile components and essential oils. *Flavour Frag J.* 23 (4), 213226. doi: 10.1002/ffj.1875

Fontes-Júnior, E. A., Maia, C. S. F., Fernandes, L. M. P., Gomes-Leal, W., Costa-Malaquias, A., Lima, R. R., et al. (2016). Chronic Alcohol Intoxication and Cortical Ischemia: Study of Their Comorbidity and the Protective Effects of Minocycline. *Oxid. Med. Cell. Longevity* 2016, 110. doi: 10.1155/2016/1341453

Fournet, A., Barriosb, A. A., and Muiiozb, V. (1994). Leishmanicidal and trypanocidal activities of Bolivian medicinal plants. *J. Ethnopharm.* 41, 19–37. doi: 10.1016/0378-8741(94)90054-X

Francisco, J., and Ortega, M. (1994). *La etnobotánica en el descubrimiento del Río Apure (1648)* Antropologica 85, 3–72.

Franciscon, C. H., Miranda, I., and de, S. (2018). Distribution and conservation of Aniba aubl. (Lauraceae Jussieu) species in brazil. *Biota Neotropica.* 18, 1–16. doi: 10.1590/1676-0611-BN-2017-0362

García, N., Zazueta, C., and Aguilera-Aguirre, L. (2017). Oxidative Stress and Inflammation in Cardiovascular Disease. *Oxid. Med. Cell. Longevity* 2017, 2–4. doi: 10.1155/2017/5853238

Giongo, J. L., Vaucher, R. A., Da Silva, A. S., Oliveira, C. B., de Mattos, C. B., Baldissera, M. D., et al. (2017). Trypanocidal activity of the compounds present in Aniba canelilla oil against Trypanosoma evansi and its effects on viability of lymphocytes. *Microbial. Pathogenesis* 103, 13–18. doi: 10.1016/j.micpath.2016.12.006

Gottlieb, O. R., and Magalhães, M. T. (1959). Communications occurrence of 1-nitro-2-phenylethane in *Ocotea pretiosa* and *Aniba canelilla*. *J. Org. Chem.* 24, 2070–2071. doi: 10.1021/jo01094a050

Gottlieb, O. R., and Magalhães, M. T. (1960a). Essential oil of the bark and wood of *Aniba canelilla*. *Perfum. Essent. Oil Rec.* 51, 69–70.

Gottlieb, O. R., and Magalhães, M. T. (1960b). Physiological varieties of *Ocotea pretiosa.* II. *Perfumer Essential Oil Record.* 51, 18–21.

Gottlieb, O. R. (1972). Chemosystematics of the Lauraceae. *Phytochemistry* 5, 1537–1570. doi: 10.1016/0031-9422(72)85001-5

Guze, M., Luz, A. C., Paneque-Gálvez, J., Macía, M. J., Orta-Martínez, M., Pino, J., et al. (2014). Are Ecologically Important Tree Species the Most Useful? A Case Study from Indigenous People in the Bolivian Amazon. *Econ. Bot.* 20 (10), 1–15. doi: 10.1007/s12231-014-9257-8

Hegde, K. S., Chandrashekhar, S., Rao, S. N., and Manikkoth, S. (2014). Preclinical screening of phyllanthus amarus ethanolic extract for its analgesic and antimicrobial activity. *Pharmacogn. Res.* 7, 378–384. doi: 10.4103/0974-8490.159577

Herrero-Jáuregui, C., García-Fernández, C., Sist, P. L. J., and Casado, M. A. (2009). Conflict of use for multi-purpose tree species in the state of Pará, eastern Amazonia, Brazil. Biodivers. *Conserv.* 18 (4), 10191044–285. doi: 10.1007/s10531-008-9456-7

Hu, Y.-Q., Ferguson, D. K., Li, C.-S., Xiao, Y.-P., and Wang, Y.-F. (2007). Alseodaphne (Lauraceae) From the Pliocene of China and its paleoclimatic significance. *Rev. Palaeobot. Palynol.* 146, 277–285. doi: 10.1016/j.revpalbo.2007.06.002

Interaminense, L. D. F. L., Siqueira, R. J., and Xavier, F. E. (2010). Cardiovascular effects of 1-nitro-2-phenylethane, the main constituent of the essential oil of Aniba canelilla, in spontaneously hypertensive rats. *Fund. Clin. Pharmacol.* 25 (6), 661–669. doi: 10.1111/j.1472-8206.2010.00891.x

Interaminense, L. D. F. L., Dos, Ramos-Alves, F. E., De Siqueira, R. J. B., Xavier, F. E., Duarte, G. P., et al. (2013). Vasorelaxant effects of 1-nitro-2-phenylethane, the main constituent of the essential oil of Aniba canelilla, in superior mesenteric arteries from spontaneously hypertensive rats. *Eur. J. Pharmaceut. Sci.* 48, 709–716. doi: 10.1016/j.ejps.2012.12.0337

Khansari, N., Shakiba, Y., and Mahmoudi, M. (2009). Chronic Inflammation and Oxidative Stress as a Major Cause of Age-Related Diseases and Cancer. *Recent Patents Inflammation Allergy Drug Discovery* 3, 73–80. doi: 10.2174/187221309787158371

Kim, J., Fann, D. Y., Seet, R. C., Jo, D. G., Mattson, M. P., and Arumugam, T. V. (2016). Phytochemicals in Ischemic Stroke. *Neuromol. Med.* 18, 283–305. doi: 10.1007/s12017-016-8403-0

Kubitzki, K., and Renner, S. (1982). *Lauraceae l (Aniba and Aiouea): Flora Neotropica, Monograph* Vol. 31 (New York: The New York Botanical Garden), 1–84.

Kubitzki, K., Rohwer, J. G., and Bittrich, V. (1993). *The families and genera of vascular plants II* (Berlin: Springer-Verlag Berlin Heidelberg).

Lahlou, S., Figueiredo, A. F., Magalhães, P. J. C., Leal-Cardoso, J. H., and Gloria, P. D. (2004). Cardiovascular effects of methyleugenol, a natural constituent present in many plant essential oils, in normotensive rats. *Life Sci.* 74, 2401–2412. doi: 10.1016/j.lfs.2003.09.063

Lahlou, S., Caldas Magalhães, P. J., Bezerra De Siqueira, R. J., Figueiredo, A. F., Leal Interaminense, L. F., Soares Maia, J. G., et al. (2005). Cardiovascular effects of the essential oil of Aniba canelilla bark in normotensive rats. *J. Cardiovasc. Pharmacol.* 46, 412–421. doi: 10.1097/01.fjc.0000175876.25296.f4

Liguori, I., Russo, G., Curcio, F., Bulli, G., Aran, L., Della-Morte, D., et al. (2018). Oxidative stress, aging, and diseases. *Clin. Interv. Aging.* 13, 757–772. doi: 10.2147/CIA.S158513

Lima, M., da, P., Silva, T. M. D., da Silva, J. D., Zoghbi, M., das, G. B., et al. (2004). Essential oil composition of leaf and fine stem of Aniba canelilla (Kunth) Mez from Manaus, Brazil. *Acta Amazonica* 34, 329–330. doi: 10.1590/s0044-59672004000200019

Lima, A. B., Santana, M. B., Cardoso, A. S., Silva, J. K. R., Maia, J. G. S., Carvalho, J. C. T., et al. (2009). Antinociceptive activity of 1-nitro-2-phenylethane, the main component of *Aniba canelilla* essential oil. *Phytomedicine* 16, 555–559. doi: 10.1016/j.phymed.2008.10.007

Lima, A. B. (2008). Estudo da ação antinociceptiva e antiinflamatória do 1-nitro-2-feniletano, principal constituinte da *Aniba canelilla*. [dissertação/dissertação de mestrado]. Belém (PA): Universidade Federal do Pará.

Lima, P. G. C., Coelho-Ferreira, M., and Oliveira, R. (2011). Plantas medicinais em feiras e mercados públicos do Distrito Florestal Sustentável da BR-163, estado do Pará, BrasilActa Bot. Bras. 25(2), 422–434. doi: 10.1590/S0102-33062011000200018

Lorenzi, H., and Matos, F. J. A. (2008). *Medicinal Plants in Brazil: Native and Exotic* (Nova Odessa, Brazil: Publisher Plantarum Institute).

Lupe, F. A. (2007). *Estudo da composição química de óleos essenciais de plantas aromáticas da Amazônia* [dissertação/dissertação de mestrad] [Campinas (SP)]: Universidade Estadual de Campinas, Instituto de Química.). http://repositorio.unicamp.br/jspui/handle/REPOSIP/248371

Luziatelli, G., Sorensen, M., Theilade, I., and Molgaard, P. (2010). Asháninka medicinal plants: a case study from the native community of Bajo Quimiriki, Junín, Peru. *J. Ethnobiol. Ethnomed.* 6 (21), 1–23. doi: 10.1186/1746-4269-6-21

Madaleno, I. M. (2011). Plantas da medicina popular de São Luís, Brasil. Boletim Do Museu Paraense Emílio Goeldi. *Ciências Humanas.* 6, 273–286. doi: 10.1590/s1981-81222011000200002

Maia, O. G. S., and Andrade, L. H. A. (2009). Database of the amazon aromatic plants and their essential oils. *Quimica Nova.* 32, 595–622. doi: 10.1590/S0100-40422009000300006

Maia, J. G., Zoghbi, M. G., and Andrade, E. H. (2001). *Plantas aromáticas na Amazônia e seus óleos essenciais* (Belém: Série Adolpho Ducke, Museu Paraense Emílio Goeldi).

Manhães, A. P., da Veiga-Júnior, V. F., Wiedemann, L. S. M., Fernandes, K. S., and De Tarso Barbosa Sampaio, P. (2012). Biomass production and essential oil yield from leaves, fine stems and resprouts using pruning the crown of Aniba canelilla (H.B.K.) (Lauraceae) in the Central Amazon. *Acta Amazonica.* 42, 355–362. doi: 10.1590/s0044-59672012000300007

Marques, C. A. (2001). Importância econômica da família Lauraceae Lindl. *Floresta e Ambiente* 8, 195–206.

Martins, F. J., Caneschi, C. A., Vieira, J. L. F., Barbosa, W., and Raposo, N. R. B. (2016). Antioxidant Activity and Potential Photoprotective from Amazon Native Flora Extracts. *J. Photochem. Photobiol. B.: Biol.* 161, 34–39. doi: 10.1016/j.jphotobiol.2016.05.012

Matsuo, M., Kirkland, D. F., and Underhill, E. W. (1972). 1-Nitro-2-phenylethane: a possible intermediate in the biosynthesis of benzyl glucosinolate. *Phytochemistry* 11, 697–701. doi: 10.1016/0031-9422(72)80034-7

Mesquita, T. J. B., Silva, G. F., Albuquerque, P. M., and Duvoisin-Júnior, S. (2014). *Análise fitoquímica e determinação da capacidade antioxidante em extratos de Aniba canelilla (H.B.K.) Mez. Anais do XX Congresso Brasileiro de Engenharia Química.* Florianópolis, Santa Catarina, Brasil, p. 8. doi: 10.5151/chemeng-cobeq2014-2075-15962-176825

Mez, C. (1889). Lauraceae Americanae. *Jahrb. Königl. Bot. Gart. Berlin* 5, 1–556.

Miliauskas, G., Van Beek, T. A., Venskutonis, P. R., Linssen, J. P. H., and De Waard, P. (2004). Antioxidative activity of Geranium macrorrhizum. *Eur. Food Res. Technol.* 218, 253–261. doi: 10.1007/s00217-003-0836-7

Mimica-Dukic, N., Bozin, B., Sokovic, M., and Simin, N. (2004). Antimicrobial and Antioxidant Activities of Melissa officinalis L. (Lamiaceae) Essential Oil. *J. Agric. Food Chem.* 52, 2485–2489. doi: 10.1021/jf030698a

Moraes, L. L., Freitas, J. L., Filho, J. R. M., Silva, R. B., Borges, C. H., and Santos, A. C. (2019). Ethno-knowledge of medicinal plants in a community in the eastern Amazon. *Rev. Ciências Agrárias.* 42, 565–573. doi: 10.19084/rca.15625

Morais, A. A., Rezende, C. M. A. M., Bulow, M. V. V., Moura, J. C., Gottlieb, O. R., Marx, M. C., et al. (1972). Óleos essenciais de espécies do genero Aniba. *Acta Amazônica* 2, 41–44. doi: 10.1590/1809-43921972021041

Mors, W. B., Rizzini, C. T., and Pereira, N. A. (2000). *Medicinal plants of Brazil* (Michigan: Reference Publications, Inc).

Naranjo, P., Kijoa, A., Giesbrecht, A. M., and Gottlieb, O. R. (1981). *Ocotea quixos*, American cinnamon. *J. Ethnopharmacol.* 4, 233–236. doi: 10.1016/0378-8741(81)90038-6

OECD - and The Organization of Economic Cooperation Development (2001). *The OECD Guideline No. 407 for Testing of Chemical - Repeated Dose Oral Toxicity - Rodent: 28-Day or 14-Day Study* (Paris, France: OECD), 1–7.

Oger, J. M., Duval, O., Richomme, P., Bruneton, J., Guinaudeau, H., and Fournet, A. (1992). Noranicanine a new type of trioxygenated benzylisoquinoline isolation and synthesis. *Heterocycles* 34, 17.

Oger, J. M., Fardeau, A., Richomme, P., Guinaudeau, H., and Fournet, A. (1993). Nouveaux alcaloïdes isoquinoléiques isolés d'une Lauraceae bolivienne: *Aniba canelilla* H.B.K. *Can. J. Chem.* 71, 1128. doi: 10.1139/v93-149

Oger, J. M., Richomme, P., Guinaudeau, H., Bouchara, J. P., and Fournet, A. (1994). Aniba canelilla (H.B.k.) mez essential oil: Analysis of chemical constituents, fungistatic properties. *J. Essential Oil Res.* 6, 493–497. doi: 10.1080/10412905.1994.9698432

Okogun, J. I., and Ekong, D. E. U. (1969). Essential oil of *Dennettia tripetala*. *Chem. Industry* 8 (3), 669–671.

Organismo Andino de Salud. (2014). Plantas medicinales de la subregión andina. Peru: Convenio Hipólito Unanue. Available in: https://www.orasconhu.org/sites/default/files/LIBRO%20PLANTAS%20MEDICINALES%20DE%20LA%20SUBREGI%C3%93N.pdf

Oyemitan, I. A., Elusiyan, C. A., Akanmu, M. A., and Olugbade, T. A. (2013). Hypnotic, anticonvulsant and anxiolytic effects of 1-nitro-2-phenylethane isolated from the essential oil of Dennettia tripetala in mice. *Phytomedicine* 20, 1315–1322. doi: 10.1016/j.phymed.2013.07.005

Pinto, A. C. (1995). O Brasil dos viajantes e dos exploradores e a química de produtos naturais brasileira. *Química Nova.* 18, 608–615.

Quignard, E. L. J., Pohlit, A. M., Nunomora, S. M., Pinto, A. C. S., Santos, E. V. M., and Morais, S. K. R. (2003). Screening of plants found in amazonas state for lethality towards brine shrimp *Acta Amaz.* 33 (1), 93–104. doi: 10.1590/1809-4392200331104

Quinet, A., Baitello, J. B., Moraes, P. L. R., de Assis, L., and Alves, F. M. (2015). *Lauraceae, in Lista de Espécies da Flora do Brasil, Jardim Botânico do Rio de Janeiro*. http://floradobrasil.jbrj.gov.br/jabot/floradobrasil/FB143 [accessed in March 2019].

Reuter, S., Gupta, S. C., Chaturvedi, M. M., and Aggarwal, B. B. (2010). Oxidative stress, inflammation, and cancer: How are they linked?. *Free Radical Biol. Med.* 49 (11), 16031616. doi: 10.1016/j.freeradbiomed.2010.09.006

Rianjanu, A., Roto, R., Julian, T., Hidayat, S., Kusumaatmaja, A., Suyono, E., et al. (2018). Polyacrylonitrile Nanofiber-Based Quartz Crystal Microbalance for Sensitive Detection of Safrole. *Sensors* 18 (4), 1150. doi: 10.3390/s18041150

Ribeiro, J. E. L. S., Hopkins, M. J. G., Vicentini, A., Sothers, C. A., Costa, M. A. S., Brito, J. M., et al. (1999). *Flora da Reserva Ducke: Guia de identificação das plantas vasculares de uma floresta de terra-firme na Amazônia Central* (Manaus: INPA).

Rodrigues, E., and Carlini, E. A. (2006). Plants with possible psychoactive actions used by the Krahô Indians, Brazil. *Revista Brasileira de Psiquiatria.* 28 (4, 277–282. doi: 10.1590/S1516-44462006005000014

Ruberto, G., and Baratta, M. T. (2000). Antioxidant activity of selected essential oil components in two lipid model systems. *Food Chem.* 69, 167–174. doi: 10.1016/S0308-8146(99)00247-2

Samy, R. P., Pushparaj, P. N., and Gopalakrishnakone, P. (2008). A compilation of bioactive compounds from Ayurveda. *Bioinformation* 3, 100–110. doi: 10.6026/97320630003100

Sangwan, N. S., Farooqi, A. H. A., Shabih, F., and Sangwan, R. S. (2001). Regulation of essential oil production in plants. *Plant Growth Regulation* 34, 3–21. doi: 10.1023/A:1013386921596

Santos, J. X., Reis, A. R. S., Parry, S. M., Leão, F. M., and Carvalho, J. C. (2016). Caracterização Etnobotânica de Essências Florestais com Fins Medicinais Utilizadas pela Etnia Xipaya, no Município de Altamira-PA. *Biota Amazônia* 6, 1–8. doi: 10.18561/2179-5746/biotaamazonia.v6n2p1-8

Santos, E. R. Q. (2017). *Óleos essenciais ricos em linalol (*Aniba rosaeodora, A. parviflora *e* Aeollanthus suaveolens*) na amazônia e seus efeitos neurocomportamentais em roedores*. [dissertação/dissertação de mestrado]. Belém (PA): Universidade Federal do Pará.

Sayyah, M., Valizadeh, J., and Kamalinejad, M. (2002). Anticonvulsant activity of the leaf essential oil of Laurus nobilis against pentylenetetrazole- and maximal electroshock-induced seizures. *Phytomedicine* 9, 212–216. doi: 10.1078/0944-7113-00113

Serino, A., and Salazar, G. (2019). Protective Role of Polyphenols against Vascular Inflammation, Aging and Cardiovascular Disease. *Nutrients* 11, 1–23. doi: 10.3390/nu11010053

Silva, J. R., d, A., do Carmo, D. F. M., Reis, E. M., Machado, G. M. C., Leon, L. L., et al. (2009). Chemical and biological evaluation of essential oils with economic value from lauraceae species. *J. Braz. Chem. Soc.* 20, 1071–1076. doi: 10.1590/S0103-50532009000600011

Silva, N. N. S., Silva, J. R. A., Alves, C. N., Andrade, E. H. A., Da Silva, J. K. R., and Maia, J. G. S. (2014). Acetylcholinesterase inhibitory activity and molecular docking study of 1-nitro-2-phenylethane, the main constituent of Aniba canelilla essential oil. *Chem. Biol. Drug Design* 84, 192–198. doi: 10.1111/cbdd.12304

Silva, G. F. (2012). *Estudo do potencial biotecnológico de* Aniba canelilla *(H.B.K) Mez para obtenção de cosméticos*. [dissertação/dissertação de mestrado]. Manaus (AM): Universidade do Estado do Amazonas.

Silva, A. G., Lima, R. A., Silva, L. P., and Souza, A. C. R. (2011). Uso, conservação e diversidade de plantas aromáticas, condimentares e medicinais para fins medicinais na comunidade Vila Princesa, Porto Velho-RO. Revista Pesquisa & Criação. [dissertação/dissertação de mestrado]. 10:2, 21–35. Avaliable in: http://www.periodicos.unir.br/index.php/propesq/article/view/409/448

Silva, A. C. R., da, Lopes, P. M., Azevedo, M. M. B., de, Costa, D. C., Alviano, C. S., and Alviano, D. S. (2012). Biological Activities of a-Pinene and β-Pinene Enantiomers. *Molecules* 17 (6), 63056316. doi: 10.3390/molecules17066305

Sipe, H. J., Lardinois, O. M., and Mason, R. P. (2014). Free Radical Metabolism of Methyleugenol and Related Compounds. *Chem. Res. Toxicol.* 27 (4), 483489. doi: 10.1021/tx400256b

Sousa, P. J. C., Araujo, J. S., Pereira, L. L. S., Modro, M. N. R., Maia, J. G. S., Araujo, M. T. F., et al. (2009). Phytochemical and toxicological evaluations of the essential oil from the bark of aniba canellila (h.B.K.) Mez. *J. Essential Oil Res.* 21, 381–384. doi: 10.1080/10412905.2009.9700197

Sousa, D. P. (2011). Analgesic-like Activity of Essential Oils Constituents. *Molecules* 16, 2233–2252. doi: 10.3390/molecules16032233

Sugimoto, M., de Jesus Amazonas da Silva, M., Froede Brito, L., dos Santos Borges, R., Amaral, F., de Araujo Boleti, A., et al. (2017). Anti-Inflammatory Potential of 1-Nitro-2-Phenylethylene. *Molecules* 22 (11), 1977. doi: 10.3390/molecules22111977

Taveira, F. S. N., Lima, W. N., Andrade, E. H. A., and Maia, J. G. S. (2003). Seasonal essential oil variation of *Aniba canelilla*. *Biochem. Syst. Ecol.* 31, 69–75. doi: 10.1016/S0305-1978(02)00088-1

Taylor, L. (2005). Rosewood (*Aniba canelilla*, *Aniba rosaeodora*. In *The Healing Power of Rainforest Herbs. A Guide to Understanding and Using Herbal Medicinals*. Square One Publishers, Inc., New York. http://www.rain-tree.com/rosewood.htm [accessed March 2019].

Thomas, E., and Vandebroek, I. (2006). *Guía de Plantas Medicinales: de los Yuracarés y Trinitarios del Territorio Indígena Parque Nacional Isiboro-Sécure, Bolivia*. Bolívia: Imprenta Sirena.

Tropicos.org (2019). *Missouri Botanical Garden*. http://www.tropicos.org/Name/40014791 [Acessed November 2019].

Tsuchiya, H. (2017). Anesthetic Agents of Plant Origin: A Review of Phytochemicals with Anesthetic Activity. *Molecules* 22 (8), 1369. doi: 10.3390/molecules22081369

Uttara, B., Singh, A. V., Zamboni, P., and Mahajan, R. T. (2009). Oxidative Stress and Neurodegenerative Diseases: A Review of Upstream and Downstream Antioxidant Therapeutic Options. *Curr. Neuropharmacol.* 7, 65–74. doi: 10.2174/157015909787602823

Vale, J. K. L., Lima, A. B., Pinheiro, B. G., Cardoso, A. S., Silva, J. K. R., Maia, J. G. S., et al. (2013). Evaluation and theoretical study on the anti-inflammatory mechanism of 1-nitro-2-phenylethane. *Planta Med.* 79, 628–633. doi: 10.1055/s-0032-1328402

Van der Werff, H. (1991). A key to the genera of Lauraceae in the New World. *Ann. Missouri Bot. Garden.* 78, 377–387. doi: 10.2307/2399567

Wittstock, U., and Halkier, B. A. (2000). Cytochrome P450 CYP79A2 fromArabidopsis thalianaL. Catalyzes the Conversion of l-Phenylalanine to Phenylacetaldoxime in the Biosynthesis of Benzylglucosinolate. *J. Biol. Chem.* 275 (19), 1465914666. doi: 10.1074/jbc.275.19.14659

World Health Organization (2018). *Top 10 causes of death. Global Health Observatory*. Avaliable in: https://www.who.int/gho/mortality_burden_disease/causes_death/top_10/en/

Yano, S., Suzuki, Y., Yuzurihara, M., Kase, Y., Takeda, S., Watanabe, S., et al. (2006). Antinociceptive effect of methyleugenol on formalin-induced hyperalgesia in mice. *Eur. J. Pharmacol.* 553, 99–103. doi: 10.1016/j.ejphar.2006.09.020

Zuo, L., Prather, E. R., Stetskiv, M., Garrison, D. E., Meade, J. R., Peace, T. I., et al. (2019). Inflammaging and Oxidative Stress in Human Diseases: From Molecular Mechanisms to Novel Treatments. *Int. J. Mol. Sci.* 20, 1–39. doi: 10.3390/ijms20184472

Conflict of Interest: The authors declare that the research was conducted in the absence of any commercial or financial relationships that could be construed as a potential conflict of interest.

frontiers in Pharmacology

REVIEW
published: 05 June 2020
doi: 10.3389/fphar.2020.00852

A Review on the Potential Use of Medicinal Plants From Asteraceae and Lamiaceae Plant Family in Cardiovascular Diseases

Jennifer Michel, Nur Zahirah Abd Rani and Khairana Husain *

Drug and Herbal Research Centre, Faculty of Pharmacy, Universiti Kebangsaan Malaysia, Kuala Lumpur, Malaysia

Cardiovascular diseases are one of the most prevalent diseases worldwide, and its rate of mortality is rising annually. In accordance with the current condition, studies on medicinal plants upon their activity on cardiovascular diseases are often being encouraged to be used in cardiovascular disease management, due to the availability of medicinal values in certain dedicated plants. This review was conducted based on two plant families, which are Asteraceae and Lamiaceae, to study on their action in cardiovascular disease relieving activities, to review the relationship between the phytochemistry of Asteraceae and Lamiaceae families and their effect on cardiovascular diseases, and to study their toxicology. The medicinal plants from these plant family groups are collected based on their effects on the mechanisms that affect the cardiovascular-related disease which are an antioxidant activity, anti-hyperlipidemic or hypocholesterolemia, vasorelaxant effect, antithrombotic action, and diuresis effect. In reference to various studies, the journals that conducted *in vivo* or *in vitro* experiments, which were used to prove the specific mechanisms, are included in this review. This is to ensure that the scientific value and the phytochemicals of the involved plants can be seen based on their activity. As a result, various plant species from both Asteraceae and Lamiaceae plant family have been identified and collected based on their study that has proven their effectiveness and uses in cardiovascular diseases. Most of the plants have an antioxidant effect, followed by anti-hyperlipidemia, vasorelaxant, antithrombotic, and diuretic effect from the most available to least available studies, respectively. These are the mechanisms that contribute to various cardiovascular diseases, such as heart attack, stroke, coronary heart disease, and hypertension. Further studies can be conducted on these plant species by identifying their ability and capability to be developed into a new drug or to be used as a medicinal plant in treating various cardiovascular diseases.

Keywords: cardiovascular diseases, coronary heart disease, stroke, Asteraceae, Lamiaceae, hypertension, heart failure, medicinal plants

OPEN ACCESS

Edited by:
Ameenah Gurib-Fakim, Independent Researcher, Quatre Bornes, Mauritius

Reviewed by:
Riana Kleynhans, Tshwane University of Technology, South Africa
Sarri Madani, University of M'sila, Algeria

***Correspondence:**
Khairana Husain
khairana@ukm.edu.my

Specialty section:
This article was submitted to Ethnopharmacology, a section of the journal Frontiers in Pharmacology

Received: *15 July 2019*
Accepted: *22 May 2020*
Published: *05 June 2020*

Citation:
Michel J, Abd Rani NZ and Husain K (2020) A Review on the Potential Use of Medicinal Plants From Asteraceae and Lamiaceae Plant Family in Cardiovascular Diseases. Front. Pharmacol. 11:852. doi: 10.3389/fphar.2020.00852

INTRODUCTION

Cardiovascular diseases (CVD) are known as the most frequent and common cause of death worldwide. World Health Organization (WHO) reported that the total number of people who died from CVDs in 2012 was estimated to be around 17.5 million people representing 31% worldwide population. Disorders of heart and blood vessels, including coronary heart disease (CHD), cerebrovascular disease (stroke), increase in blood pressure (hypertension) and myocardial infarction are the precursor that causes CVD (Rastogi et al., 2016). CVD diseases involve the cardiovascular system that comprises of heart and veins. They are the main source of death universally, and its incidence is rising rapidly globally (Gaziano et al., 2010).

CVD diseases that often being suffered by people are heart failure, coronary heart disease (CHD), stroke, myocardial infarction, and hypertension. CHD and stroke, which responsible for 80% of CVD patients' death, are caused by the lack of oxygen to the brain and heart. The accumulation of fatty deposits within the blood vessel causes the blocking of cerebral and coronary arteries hence narrows their pathway size (Roth et al., 2017). CHD contributes to almost 75% of worldwide death, which occurs both in low- and middle-income countries, due to few factors such as their socio-economy variations and risk factors, due to lifestyle modification (Gaziano et al., 2010).

Heart failure is caused by any functional or structural damage to ventricular filling or in the blood ejection (Klein et al., 2003). It is known as a leading cause of mortality in the western globe and tends to develop when cardiac injury or cardiac insult impairs the heart's ability to maintain and pump tissue perfusion (Lymperopoulos et al., 2013). Hypertension, which is also known as a common CVD, is a crucial concern in health in diverse parts of the world. When the arterial pressure rises above 140/90 mm Hg., it is known as arterial hypertension (Malik et al., 2018).

Stroke is a heterogeneous disease, which includes the hemorrhage of cerebral and the pathogenic subtypes of ischemic stroke (Sacco et al., 2013). In the contribution of the major cause of death, stroke is one of the lead diseases. Among the stroke cases, 85% of them are ischemic stroke, and the other 15% is the hemorrhage stroke, which is also known as an intracerebral stroke (Woodruff et al., 2011). A clinical study shows that warfarin is being effective in preventing ischemic stroke in patients that are suffering from atrial fibrillation, which has reduced the risk of intracranial hemorrhage (Go et al., 2003). Hemorrhage is the rupture of the blood vessel that causes the blood to escape from its blood vessel. One of the main causes of stroke is due to blood coagulation. When the clotting blood accumulates in the blood vessel, the blood refuses to flow to the brain, and the brain tends to be lack of oxygen that leads to ischemic stroke. In this condition, an anticoagulant will avoid the blood from clotting and allow the ease of blood flow throughout the body and brain from the heart. Based on these regards, plants with anticoagulant activity will help treat cardiovascular diseases of these mechanisms.

Throughout human history, medicinal plants have always been used as medicine to treat various diseases. Almost 80% who live in developed countries are said to be depended on the practice of traditional medicine (Abdala et al., 2012). A report from the World Health Organization (WHO) comes out with a percentage of 80% of the global population tend to rely on traditional medicines. Most of the therapies use extracts and active compounds of the medicinal plant (Craig, 1999). Currently, there is a rise in medicinal plant consumption in the world, due to the proven effectiveness of medicinal plants, in curing certain diseases and claims that shows it is safe to be used (Perez Gutierrez and Baez, 2009). Medicinal plants play a major role in medication since the beginning of human civilization and also contribute to the manufacturing of drugs these days (Rastogi et al., 2016).

Asteraceae plant family is also used to be known as the Compositae plant family, is known as one of the largest plant families with thousands of plant species. Its large production as angiosperm phylogeny is in Asterideae. The Asteraceae plant family consists of 24,000 accepted species. It also has about 1,600 to 1,700 of its genera is distributed around the world, excluding Antarctica. This family is also known as a cosmopolitan family, as it has a great concentration of species in different areas such as temperate, cold-temperate, and subtropical. Asteraceae consists of three subfamilies; Asteroideae, Barnadesioideae, and Cichorioideae (Medeiros-Neves et al., 2018). The Lamiaceae plant family is also called a Labiatae family, which is often uttered as the mint family, and the plant family of flowering plants. They consist of shrubs or herbs which produce and release the aromatic smell, which consists of more than 3,000 species in the Lamiaceae plant family. The largest genera of Lamiaceae plant family are Salvia, Scutellaria, and Stachys (Cantino et al., 1992).

Plant species in Asteraceae and Lamiaceae family are being used to cured various diseases. Satureja species exhibits analgesic, antimicrobial, antiviral, antioxidant, antiproliferative, anti-inflammatory, and vasodilatory activities (Momtaz and Abdollahi, 2008). Meanwhile, *Crassocephalum crepidioides* (Benth.) S. Moore were used to cure epilepsy, indigestion, hepatotoxicity, swollen lips, tumor, and sleeping sickness (Bahar et al., 2016). Despite their variation in botanical features and traditional values, both Asteraceae and Lamiaceae plant family species exhibits mechanisms of improving cardiovascular disease. The seeds of *Gundelia tournefortti* L. (Asteraceae) are often used as pickles, and it is an effective diuretic (Çoruh et al., 2007). *Achillea millefolium* L., which is a plant species from the Asteraceae plant family, also exhibited diuretics effect in a hypertension group (De Souza et al., 2013). It is often found in Brazil and used as the Brazilian folk medicine, usually for kidney and heart diseases. *Emilia praetermissa* Milne-Redh. reduced hyperlipidemic conditions as an anticoagulant agent through a clinical study (Memariani et al., 2018). *Salvia miltiorrhiza* Bunge exerts the potential vasodilator effect on the cardiovascular system (Li et al., 1990). *S. miltiorrhiza* lowered whole blood viscosity, improved the peripheral circulation, and fastened erythropoiesis of erythrocytes (Lei and Chiou, 1986).

Medicinal plants are currently being used in developing a new hypertension drug, and one of them is *Marrubium vulgare* L.

from Lamiaceae plant family. The crude oil of the plant was examined its hypotensive effect, and due to the presence of diterpenoids in the plant, it has potential cardiovascular activity, which was caused due to relaxation of vessels and reduces systolic blood pressure which are the mechanisms involved in hypertension (Bardai et al., 2001). The second example is *Cynara cardunculus* L. (syn. *Cynara scolymus* L.) from the Asteraceae plant family, which is also known as an artichoke. It is one of the oldest medicinal drugs for its cardiovascular effects. It exhibits a lipid-lowering effect and inhibits the biosynthesis of cholesterol (Fintelmaan, 1996). These drugs prove that medicinal plants can be developed into drugs or for as a treatment for therapeutic purposes. New drugs from the available medicinal plant can treat the disease more efficiently, as a safer and more efficient drug can be discovered in the future, which may benefit the patient (Bardai et al., 2001). Based on the traditional uses and the developed drug, it showed that the plant families have a high potential in alleviating cardiovascular diseases. Thus, an in-depth compilation of the activity and mechanism of the plant family on cardiovascular diseases needs to be examined.

A review on phytochemistry and pharmacological of medicinal plants related to cardiovascular diseases specifically on *Asteraceae* and *Lamiaceae* family were conducted by using searching engines such as Google Scholar, Scopus, ScienceDirect, ProQuest, Karger, and Molecule. The literature taken range from the year 1979 to 2018 and was evaluated and tabulated in this review. The keywords used during searching includes "cardiovascular diseases," "coronary heart disease," "stroke," "myocardial infarction," "hypertension," "heart failure," "antioxidant," "anti-hyperlipidemia," "antithrombotic," "medicinal plants," "plants," "herbs," "*in vivo,*" "*in vitro*" alone and in different combinations. This review specifically focuses on the identification and collection of the information on medicinal plants from the Asteraceae and Lamiaceae family, with proven *in vivo* or *in vitro* studies upon cardiovascular diseases. **Tables 1** and **2** show the plant species from Asteraceae and Lamiaceae family with their medicinal uses. **Tables 3** and **4** are on the mechanisms of the Asteraceae and Lamiaceae family plant species that are involved in cardiovascular diseases. Meanwhile, **Figure 1** is composed of chemical compounds derived from the two species that have potential as the lead drug in cardiovascular diseases.

INHIBITORY ACTIVITY ON CARDIOVASCULAR DISEASES

Antioxidant Activity

The chemical substances that reduce or prevent oxidation are known as antioxidants. Antioxidants can resist the free radicals from causing damaging effects in tissues. They are often used to safeguard cerebrovascular diseases (Bandyopadhyay et al., 2007). The oxidative stress that occurs at the cellular level acts as the prime pathogenic factor for cardiovascular diseases. It occurs due to the free radical's toxic being released by the vascular smooth muscle cells and endothelial cells (Fearon and Faux, 2009). Apart from that, cardiovascular diseases are caused by oxidative stress by reactive oxygen species (ROS) such as uncoupled nitric oxide synthases, xanthine oxidase, and NADPH oxidases (Taleb et al., 2018). ROS voluntarily attack and cause oxidative damage to various biomolecules such as lipoproteins, lipids, protein, and DNA.

This oxidative harm is an essential etiological figure that ensnared a few endless human sicknesses. Examples are cardiovascular illnesses, rheumatism, diabetes mellitus, cerebrovascular infections, and malignant growth. The damage of DNA and oxidative stress may be caused by oxidized low-density lipoproteins (oxLDL) or by hypercholesterolemia due to individual diet lifestyle (Ceaser et al., 2003). One of the lead causes of atherosclerosis is oxygen-free radicals that reduce the cells' capacity to inhibit the oxidation. This can leads to fatal inflammation disorder.

Most of the plants from the Asteraceae and Lamiaceae plant family were proven to possess the antioxidant effect *via in vitro* assay such as 2,2-diphenyl-1-picrylhydrazyl (DPPH) assay. The plants from the Asteraceae family that shows antioxidant effect based on this study are *Achillea tenuifolia* Lam. (syn. *Achillea santolina* L.), *Anthemis melampodina* subsp. *deserti* (Boiss.) Eig (syn. *Anthemis deserti* Boiss), *Artemisia absinthium* L., *Baccharis trimera* (Less.) DC, *C. crepidioides* (Benth.) S. Moore, *Helichrysum leucocephalum* Ausfeld, *Laggera decurrens* (Vahl) Hepper and J. R. I. Wood, *Senecio ovatus* subsp. *stabianus* (Lacaita) Greuter (syn. *Senecio stabianus* Lacaita), and *Silybum marianum* (L.) Gaertn. The plants from Lamiaceae that show antioxidant activities are *Ajuga iva* (L.) Schreb., *Ballota glandulosissima* Hub. -Mor. and Patzak, *Dracocephalum moldavica* L., *H. leucocephalum* Ausfeld, *Lavandula angustifolia* Mill., *Lavandula stoechas* L., *Micromeria macrosiphon* Coss. (syn. *Satureja macrosiphon* (Coss.) Maire), *Origanum vulgare* L., *Plectranthus monostachyus* (P. Beauv.) B. J. Pollard (syn. *Solenostemon monostachyus* (P. Beauv.) Briq), and *Salvia officinalis* L. These plants had shown the antioxidant effect, with its scientific value. Based on the studies, antioxidant properties were mostly exhibited by phenolic compounds due to their tendency to scavenge the free-radicals. The phenolic compounds act by chelating the metal ions, improving the endogenous antioxidant system, and avoiding the formation of free radicals. Due to this, studies on the search for natural antioxidants from plant origin have become more intense in recent years (Seyoum et al., 2006). Other chemical compounds in these plants that mainly contribute to its antioxidant activity are flavonoids, flavanols, and diterpenes.

Achillea tenuifolia Lam. is known for its free radical scavenging activity. The ferric thiocyanate test was conducted to determine the antioxidant activity of *A. tenuifolia* extract (ATE) by measuring peroxide concentration during the early stage of lipid peroxidation (Ardestani and Yazdanparast, 2007). ATE concentration of 200 and 400 μg/mL suppress the lipid peroxidation by the extension on the lag phase and the reduction of the propagation rate, which reflects the typical chain-breaking

TABLE 1 | Medicinal uses of Asteraceae plant family species in cardiovascular diseases.

Plant Name	Country/ Region	Common Name	Medicinal Uses	Part/s Used	Mode of Usage/Preparation	References
***Achillea arabica* Kotschy (syn. *Achillea biebersteinii* Hub.-Mor.)**	Mediterranean	Qaysoum	Hypolipidemic	Aerial parts	–	(Mais et al., 2016)
***Achillea millefolium* L.**	Europe, North America, Australia, and Asia	Mil-folhas	Diuretic and hypotensive actions	Aerial parts (leaves, stalks, and stems)	Aqueous extract	(De Souza et al., 2013)
***Achillea tenuifolia* Lam. (syn. *Achillea santolina* L.)**	Europe	Yarrow	Antioxidant	Aerial parts	–	(Ardestani and Yazdanparast, 2007)
***Ageratum conyzoides* (L.) L.**	Brazil	Billygoat-weed	Hypolipidemic	Leaf, stem, and root	–	(Atawodi et al., 2017)
***Anthemis melampodina* subsp. *deserti* (Boiss.) Eig (syn. *Anthemis deserti* Boiss)**	Saudi Arabia	–	Antioxidant	Whole plant	Aqueous extract	(Shahat et al., 2014)
***Artemisia absinthium* L.**	Europe, North America, and Asia	Wormwood	Antioxidant	Aerial parts (leaves, stalks, and stems)	Methanolic extract	(Bora and Sharma, 2011)
***Artemisia campestris* L.**	Eastern Morocco	–	Antihypertensive and vasorelaxant	Aerial parts	–	(Dib et al., 2017)
***Baccharis trimera* (Less.) DC**	South America	Carqueja	Vasorelaxant	Whole plants	Infusions, decoctions, and tinctures of its aerial parts	(Sabir et al., 2017)
***Bidens pilosa* L.**	South America	Spanish needles, beggar's ticks, devil's needles	Antihypertensive, vasodilation	Leaf	Dry powder, decoction, maceration or tincture	(Dimo et al., 2001)
***Chamaemelum nobile* (L.) All.**	Roman chamomile	–	Hypotensive and diuretics	Whole plant	–	(Zeggwagh et al., 2009)
Chromolaena odorata* (L.) *R. M. King and H. Rob.	South and Central America, India	Ahihia eliza or Siam Weed	Anti-hyperlipidemic	Leaves	Fresh leaves or decoction	(Ikewuchi and Ikewuchi, 2011)
***Chrysanthemum* x *morifolium* Ramat. Hemsl.**	Japan	Chrysanthemum	Vasodilation	Flowers	Extract	(Gao et al., 2016)
***Crassocephalum crepidioides* (Benth.) S. Moore**	Africa	Okinawa Spinach, Red flower	Antioxidant and anti-hyperlipidemic	Aerial Parts (leaves, stalks, and stems)	Maceration	(Bahar et al., 2016)
***Cynara cardunculus* L. (syn. *Cynara scolymus* L.)**	Mediterranean	Global artichoke	Hypolipidemic	Leaf	Aqueous extract	(Mocelin et al., 2016)
***Eclipta prostrata* (L.) L.**	India, Nepal, China, and Brazil	False daisy	Hypolipidemic	Leaves	Herb or plant juice taken orally	(Dhandapani, 2007)
***Emilia praetermissa* Milne-Redh**	Sierra Leone and Nigeria	Kipo or Koyagipo	Lipid-lowering effect	Leaves	Orally consumed as fresh salads or cooked. Maceration for improving heart conditions.	(Ngozi et al., 2013)
***Erigeron canadensis* L.**	North America and Central America	Conyza canadensis	Antithrombotic	Flowering parts	Raw material	(Pawlaczyk et al., 2011)
***Flaveria bidentis* (L.) Kuntze**	South America	Coastal plain yellowtops	Anticoagulant	Leaves	–	(Guglielmone et al., 2002)
***Gundelia tournefortti* L.**	South America	Kuub	Hypolipidemic	Seeds	Oil extract	(Sharaf and Ali, 2004)
***Gymnanthemum amygdalinum* (Delile) Sch. Bip. (syn. *Vernonia amygdalina* Delile)**	Africa	Bitter leaf	Hypolipidemia and antioxidant	Leaf	Orally consumed	(Audu et al., 2012)
***Helichrysum leucocephalum* Ausfeld**	Eurasia, Africa, and Australi	Curry plant or Italian strawflower	Antioxidant	Aerial parts (leaves, stalks, and stems)	Extract	(Goldansaz et al., 2018)
***Inula racemosa* Hook F.**	India, Asian	Pushkarmool	Hypotensive, antihyperlipidemic and antioxidant	Roots	Administered orally for rheumatic pains	(Mangathayaru et al., 2009)
***Laggera decurrens* (Vahl) Hepper and J. R. I. Wood.**	Africa	Fwimba	Antioxidant	Aerial parts	Traditional herb	(Mothana et al., 2011)

(Continued)

TABLE 1 | Continued

Plant Name	Country/ Region	Common Name	Medicinal Uses	Part/s Used	Mode of Usage/Preparation	References
***Launaea intybacea* (Jacq.) Beauverd (syn. *Lactuca runcinata* DC.)**	India	Lettuce	Anti-hyperlipidemic	Whole plant	Ethanolic extract	(Devi and Muthu, 2015)
***Leuzea carthamoides* Willd. DC.**	Russian	Maral root	Antiplatelet	Leaves	–	(Koleckar et al., 2008)
***Pectis brevipedunculata* Sch. Bip**	Brazil, America	Lemongrass	Vasorelaxant	Aerial parts	Orally consumed as tea, juice drinks or spices	(Pereira et al., 2013)
***Senecio nutans* Sch. Bip**	South America	Senecio graveolens	Hypotensive and antihypertensive effect	Braches and leaves	Extract	(Cifuentes et al., 2016)
***Senecio ovatus* subsp. *stabianus* (Lacaita) Greuter (syn. *Senecio stabianus* Lacaita)**	Italy	–	Antioxidant	Aerial parts	Extract	(Tundis et al., 2012)
***Silybum marianum* (L.) Gaertn.**	Mediterranean region of Europe	Milk thistle, Mary thistle	Antioxidant, anti-cholesterolemia	Seed	Extract	(Taleb et al., 2018)
***Solidago chilensis* eyen**	Southern America	Arnica-do-brazil	Hypolipidemic and antioxidant	Aerial parts	–	(Schneider et al., 2015)
***Sphaeranthus indicus* L.**	India	Gorakhmundi	Antihyperlipidemic	Flower	Extract	(Pande and Dubey, 2009)
***Tagetes erecta* L. (syn. *Tagetes patula* L.)**	France	Jafri	Hypotensive	Roots (nematocidal thiophenes)	Perfume	(Saleem et al., 2004)
***Tanacetum vulgare* L.**	Europe and Asia	Tansy	Diuretics	Leaves	–	(Lahlou et al., 2007)
***Tridax procumbens* (L.) L.**	India	Ghamra or coat buttons	Antithrombotic	Leaves	–	(Naqash and Nazeer, 2011)
***Vernonia elaeagnifolia* DC**	Asia and Europe	Toran vel, curtain creeper	Anti-hyperlipidemic	Leaf	Aqueous extract	(Khandekar et al., 2015; Sultana et al., 2017)

antioxidant characteristics. The activity was determined using a linoleic acid system. The peroxidation activity was measured using the thiocyanate method by using the absorbance at 500 nm to determine the peroxide values. The study showed that the ATE contained 55 mg ascorbic acid equivalents per gram of extract with the EC_{50} value of 55 μg/mL (Ardestani and Yazdanparast, 2007). Besides consists of gallic acid **(1)** and catechin **(2)**, this plant also contains phenols and flavonoid, which induce the antioxidant activity in nature (Khafagy et al., 1976).

The methanolic extract of *A. melampodina* subsp. *deserti* (Boiss.) Eig in the concentration of 25, 50, and 100 μg/mL showed more significant DPPH radical scavenging activity, compared to the positive controls, L-ascorbic acid, and butylated hydroxytoluene, BHT (Shahat et al., 2014). The DPPH radical scavenging activity and chelating effect of the plant were concentration-dependent. The plant extract at the concentration of 400 μg/mL showed a 100% chelating effect. The ferrous ion chelating effect of the extract was measured to determine the capacity of the extract to bind to the ferrous ion to catalyze oxidation in lipid peroxidation. The extract also possessed superoxide anion radicals scavenging capacity. It has a potent anion scavenging power at each concentration tested with a range from 25 μg/mL to 400 μg/mL (Shahat et al., 2014).

Artemisia absinthium L. methanolic (MAB) extract at the concentration from 25 to 100 μg/mL showed scavenging activity on superoxide anion radicals produced from the PMS-NADH system (Bora and Sharma, 2011). When the MAB was administered orally at doses of 100 or 200 mg/kg, it restored superoxide dismutase (SOD) and glutathione (GSH) levels and decreased the thiobarbituric acid reactive substances (TBARS) level. As a whole, it causes inhibitory activity on oxidative stress induced by cerebral ischemia and reperfusion. GSH is known as a central component in the antioxidant and known as the defense cells. It acts by detoxifying ROS directly and as a substrate for various peroxides (Bora and Sharma, 2011). The plant extract consists of quercetin **(3)**, rutin, and vanillic acids **(4)**. It was reported that the plant manages to alleviate stroke disease by reducing SOD activity in the serum (Spranger et al., 1997). Its antioxidant activity has potential in the acute treatment of cerebral ischemia.

Ballota glandulosissima Hub. -Mor. and Patzak is a Turkish Ballota species, collected from Kumluca. The aerial parts of *B. glandulosissima* were extracted using ethanolic extract and were determined its antioxidant activity *via in vitro* (Citoglu et al., 2004). The extract showed remarkable anti-superoxide anion formation by inhibiting the activity with an IC_{50} value of 0.51 mg/mL. In inhibiting lipid peroxidation, the extract exhibited a

TABLE 2 | Medicinal uses of Lamiaceae plant family species in cardiovascular diseases.

Plant Name	Country/ Region	Common Name	Medicinal Uses	Part/s Used	Mode of Usage/ Preparation	References
***Agastache mexicana* (Kunth.) Lint. and Epling.**	Mexico	Mexican giant hyssop	Vasorelaxant	Aerial parts	–	(Hernandez-Abreu et al., 2013)
***Ajuga integrifolia* Buch.-Ham. ex D. Don (syn. *Ajuga remota* Benth.)**	Ethiopia	Armagusa	Diuretics	Leaves	Methanolic extract	(Hailu and Engidawork, 2014)
***Ajuga iva* (L.) Schreb.**	Mediterranean	Southern Bugle	Antioxidant and hypolipidemic	Whole plant	Aqueous extract	(Taleb-Senouci et al., 2009)
***Ballota glandulosissima* Hub. -Mor. and Patzak**	Turkey	Horehound	Antioxidant	Aerial parts	External use or aerial parts used internally	(Citoglu et al., 2004)
***Clerodendrum volubile* P.Beauv**	Nigeria	Marugbo	Antihyperlipidemic	Leaves	Leaf extract (dried and blended fresh leaves)	(Akinpelu et al., 2016)
***Clinopodium vulgare* L. (syn. *Calamintha vulgaris* (L.) Druce)**	Pakistan	Wild basil	Antihypertensive and vasodilation	Aerial parts	Crude extract and methanolic extract	(Khan et al., 2018)
***Dracocephalum moldavica* L.**	Central Asia	Moldavian dragonhead	Antioxidant and cardioprotective	Aerial parts	Oral consumption as food or tea	(Jiang et al., 2014)
***Isodon rugosus* (Wall. ex Benth) Codd**	Pakistan	Wall. ex Benth	Vasorelaxant and antioxidant	Aerial parts	–	(Janbaz et al., 2014)
***Lagenaria siceraria* (Mol.) Standl**	African	Long melon, New Guinea bean and Tasmania bean	Cardioprotective, antihyperlipidemic, and diuretic activities.	Fruit	Fruit powder	(Mali et al., 2012)
***Lallemantia royleana* (Benth.) Benth.**	Iran	Balangu	Hypolipidemic	Seed	Oral consumption	(Ghannadi et al., 2015)
***Lavandula angustifolia* Mill.**	Iran	Ostokhoddus	Antioxidant	Aerial parts	Essential oil	(Ziaee et al., 2015)
***Lavandula stoechas* L.**	Morocco	French lavender	Antioxidant	Aerial parts	–	(Ezzoubi et al., 2014)
***Leonotis leonurus* (L.) R. Br.**	South Africa	Lion's tail/Wild dagga	Anticoagulant and antiplatelet	Leaves	Organic extract	(Mnonopi et al., 2011)
***Leonurus cardiaca* L.**	Europe	Matthiolus	Antiarrhythmic	Aerial parts	–	(Ritter et al., 2010)
***Lepechinia caulescens* (Ortega) Epling**	Mexico	Island pitchersage	Antihypertensive and vasorelaxant	Aerial parts	Oral beverage or tea	(Estrada-Soto et al., 2012)
***Leucas aspera* (Willd.) Link**	India	Thumbai	Antihyperlipedimia	Leaf	Ethanolic extract	(Kumar, 2016)
***Melissa officinalis* L.**	Anatolia and Mediterranean	Lemon balm	Vasodilation	Leaves	Consumed orally as tea	(Ersoy et al., 2008)
***Micromeria macrosiphon* Coss. (syn. *Satureja macrosiphon* (Coss.) Maire)**	Morocco	Maire	Antioxidant	Aerial parts	Extract	(Amiri, 2011)
***Origanum vulgare* L.**	Europe, North Africa, America	Oregano	Antioxidant	Whole plants	Traditional medicine	(Zhang et al., 2014)
***Orthosiphon aristatus* (Blume) Miq. (syn. *Orthosiphon stamineus* Benth.)**	Indonesia, Asia	Kumis kucing, Misai kusing	Antihypertensive and vasorelaxant	Leaves, whole plant	Water decoction, extract	(Matsubara et al., 1999; Akowuah et al., 2005; Yam et al., 2016; Yam et al., 2018)
***Phlomoides bracteosa* (Royle ex Benth.) Kamelin and Makhm. (syn. *Phlomis bracteosa* (Royle ex Benth.) Kamelin and Makhm.)**	Pakistan	Jerusalem sage	Vasodilation	Whole plant	Methanolic extract	(Khan et al., 2012)
***Plectranthus hadiensis* (Forssk.) Schweinf. ex Sprenger (syn. *Coleus forskohlii* Willd.)**	India	Plectranthus barbatus	Antihypertensive and vasodilation	Whole plant	Ethanolic extract	(Dubey et al., 1981)
***Plectranthus monostachyus* (P. Beauv.) B. J. Pollard (syn. *Solenostemon monostachyus* (P. Beauv.) Briq.)**	Ivory coast	Coleus	Antioxidant and antihypertensive	Leaves	Ethanolic extract	(Fidele et al., 2012)
***Pogostemon elsholtzioides* Benth.**	Eastern Himalaya	Nakhrang sheng	Vasorelaxant and antihypertensive	Leaves	Leaf decoction	(Shiva Kumar et al., 2017)

(Continued)

TABLE 2 | Continued

Plant Name	Country/ Region	Common Name	Medicinal Uses	Part/s Used	Mode of Usage/ Preparation	References
***Prunella vulgaris* L.**	–	Self-heal	Antihyperlipidemic and antioxidant	Rhizome/ root	Hydroalcoholic and aqueous extract	(Zargar et al., 2017)
***Rosmarinus officinalis* L.**	Mediterranean countries	–	Anti-hypercholesterolemic	Leaves	Water decoction	(Belmouhoub et al., 2017)
***Salvia miltiorrhiza* Bunge**	China and Japan	Danshen	Antithrombosis	Root	Oral consumption of dried root	(Fan et al., 2010)
***Salvia officinalis* L.**	Mediterranean	Sage	Antioxidant	Shoots	Raw material, essential oils or extract	(Santos-Gomes et al., 2002)
***Salvia scutellarioides* Kunth**	Colombia	Mastranto	Antihypertensive and diuretic effects	Leaves and stem	Aqueous extract	(Ramirez et al., 2006)
***Satureja cuneifolia* Ten. (syn. *Satureja obovata* Lag.)**	Lanjoran	Thin savory	Vasodilation and vasorelaxant	Whole plant	Extract	(De Rojas et al., 1999)
***Sideritis raeseri* Boiss. and Heldr.**	Mediterranean	Ironwort, mountain tea, and shepherd's tea	Hypotension and vasodilatation	Aerial parts	–	(Kitic et al., 2012)
***Teucrium polium* Linn.**	South-western Asia and Europe	Felty germander	Hypolipidemic	Aerial parts	Aqueous extract	(Rasekh et al., 2001)
***Thymus dreatensis* Batt. (syn. *Thymus atlanticus* (Ball) Pau)**	Morocco	Thyme, German thyme	Antihyperlipidemic and anticoagulant	Whole plant	Extract	(Ramchoun et al., 2012)
***Thymus saturejoides* Coss.**	Morocco	Thyme borneol	Antioxidant	–	–	(Khouya et al., 2015)
***Thymus serpyllum* Linn.**	Europe and North America	Breckland thyme	Antihypertensive	Whole plant	Culinary herb	(Katalinic et al., 2006)
Thymus zygis L.	Morocco	Thyme, sauce thyme	Anticoagulant	Whole plant	Extract	(Ocana and Reglero, 2012; Khouya et al., 2015)
***Vitex megapotamica* (Spreng.) Moldenke**	South America	Forest olive	Antihyperlipidemic	Leaves	Extract	(Pires et al., 2018)
***Ziziphora clinopodioides* Lam.**	China	Blue mint bush	Vasodilation and antihypertensive	Whole plant	Decoction of whole plant	(Senejoux et al., 2010)

strong inhibitory capacity and potent scavenging property (IC_{50}, 15 mg/mL) compared to α-tocopherol (IC_{50}, 3 mg/mL) (Citoglu et al., 2004).

The antioxidant activity of methanolic extract of aerial part of *C. crepidioides* (Benth.) S. Moore was determined by measuring its total phenol and flavonoid content, reducing capacity and radical scavenging activity on DPPH assay (Bahar et al., 2016). The plant consisted of various phytochemicals such as flavonoids, alkaloids, tannins, saponins, glycosides, and reducing sugar which, contributed to the extract's antioxidant activity. The activity reported was lower (IC_{50}: 130.32 μg/mL) compared to ascorbic acid (IC_{50}: 11.24 μg/mL). The aerial part extract of the plant consists of gallic acid **(1)** and quercetin **(3)**, which tends to cause the antioxidant effect (Bahar et al., 2016).

Dracocephalum moldavica L. contains antioxidant compounds with cardioprotective effects (Jiang et al., 2014). The total flavonoid extract (5 μg/mL) from *D. moldavica* pre-treatment had caused improvement in the heart rate and coronary flow by decreasing lactate dehydrogenase levels, creatinine kinase levels, and caused a rise on left ventricular developed pressure. In the concentration of higher than 70 mg/L, the total flavonoid extract exhibited a higher DPPH radical scavenging activity than vitamin E. The study showed that *D. moldavica* exhibited protection against myocardial ischemia/ reperfusion(I/R)-induced injury by enhancing GSH/GSSG ratio and SOD activity and attenuating malondialdehyde (MDA) production (Jiang et al., 2014). The ethanolic extract of *H. leucocephalum* Ausfeld aerial parts showed an antioxidant effect *via in vitro* assay. The extract exhibited antioxidant activity with an IC_{50} value of 69.94 ± 0.17 μg/mL. The high amount of phenolic compounds from this plant showed a sufficient antioxidant activity in the DPPH assay (Goldansaz et al., 2018).

Laggera decurrens (Vahl) Hepper and J. R. I. Wood. contains 46.3% of oxygenated monoterpenes and among them are thymol (5.7%) and 3-methoxy-2-methyl-5-(1-methylethyl)-2,5-cyclohexadiene-1,4-dione (3-methoxythymoquinone) (28.1%) (Mothana et al., 2011). The oil consisted of 22.7% oxygenated sesquiterpenes with caryophyllene oxide (3.4%), T-cadinol (5.1%) and eudesma-11-en-4a-ol (7.0%) as the main compounds. The essential oil, especially, at a concentration of 500 μg/mL, exhibited strong antioxidant activity by causing a reduction in DPPH concentration which is comparable to ascorbic acid activity due to the presence of carvacrol, 3-methoxymoquinone, and thymol (Mothana et al., 2011).

Lavandula angustifolia Mill. from the Lamiaceae family consists of essential oil that can inhibit isoproterenol-induced myocardial infarction in rats (Ezzoubi et al., 2014). It protected the myocardium against isoproterenol-induced myocardial infarction at the concentration of 20 mg/kg of the essential oil. This amount of oil had caused the reduction in the ST-elevation

TABLE 3 | Mechanism of action of Asteraceae family plant species.

Plant Name	Parts Used	Isolated Compound/ Extract	Class	*In Vivo*/ *In Vitro*	Mechanism of Action	References
***Achillea arabica* Kotschy (syn. *Achillea biebersteinii* Hub.-Mor.)**	Aerial parts	Ethanolic extract	Sesquiterpene lactones, polyphenols, and flavonoids.	*In vivo*	The extract at a dose of 400 mg/kg showed a significant decrease in the levels of serum cholesterol, triglycerides, and LDL. It also significantly decreased hepatic total cholesterol and triglycerides.	(Mais et al., 2016)
***A. millefolium* L.**	Aerial parts (leaves, stalks, and stems)	Hydroethanolic extract (HEAM), Dichloromethane (DCM), and armetin	Flavonoid	*In vivo*	With the dose of 300 mg/kg of HEAM, it increased the diuresis around 30–60% between 4 and 8 h after administration. The diuresis effect decreased systemic vascular resistance. The extract also reduced blood volume and cardiac output. A single dose of HEAM (100 mg/kg), which was administered to the rats 3 h before measurement, showed a lower MAP reading by 13 ± 1 mm Hg. Increasing the dose to 300 mg/kg, decreased MAP by 14 ± 3 mm Hg.	(De Souza et al., 2013)
***A. tenuifolia* Lam. (syn. *Achillea santolina* L.)**	Aerial	Hydroalcoholic extract (ASE)	Phenol and flavonoid	*In vitro*	At high concentrations (200 and 400 kg/mL), ASE suppressed lipid oxidation, by extending the lag phase and reducing the propagation rate. It reflects a typical characteristic of a chain-breaking antioxidant, similar to that of known antioxidants.	(Ardestani and Yazdanparast, 2007)
***Ageratum conyzoides* (L.) L.**	Leaf, stem, and root	Methanolic extract	Alkaloids, carbohydrate, cardiac glycosides, flavonoids, saponins, tannins, steroids, and triterpenes	*In vivo*	The leaves and stem extracts (100 mg/kg) lowered total cholesterol, LDL-C, and triglycerides level.	(Atawodi et al., 2017)
***A. melampodina* subsp. *deserti* (Boiss.) Eig (syn. *Anthemis deserti* Boiss)**	Whole plant	Methanolic extract	Flavonoid	*In vitro*	The extract exhibited antioxidant capacity at 400 μg/mL. All concentrations of the extract tested possessed radical scavenging activity. Higher concentrations of the extract showed similar activity as standards.	(Shahat et al., 2014)
***Artemisia absinthium* L.**	Aerial parts	Quercetin **(3)**, rutin, isoquercitrin, quercitin-3-*O*-β-D-glucoside, glucoside, chlorogenic, syringic, coumaric, salicylic, and vanillic acids **(4)**.	Flavonoids, flavonoid glycosides, phenolic acid	*In vitro*	The extract showed a significant ($p < 0.05$) activity at the dose of 100 μg/mL in the scavenging of superoxide anion radical. Pre-treatment of ischemic brain mouse with the extract significantly ($p < 0.05$) decreased the elevated TBARS concentration in brain mitochondrial and supernatant fractions as compared to the control group. Reducing power of the extract data suggests that it contributes significantly to the observed antioxidant effect.	(Bora and Sharma, 2011)
***Artemisia campestris* L.**	Aerial parts	3,5-dicaffeoylquinic (isochlorogenic A) acid, 5-caffeoylquinic (chlorogenic) acid, and vicenin-2 **(16)**.	Flavonoids	*In vivo*	The extract at the dose of 150 mg/kg/day prevented hypertension on hypertensive rats and reduced SBP from 172 mm Hg to 144 mm Hg. At the dose of 40 mg/kg, the extract reduced SBP, DBP, and MAP, without affecting the heart rate. The extract (10^{-2}–2 mg/mL) relaxed the pre-contracted aorta by 95.8 ± 1.3%.	(Dib et al., 2017)
***Baccharis trimera* (Less.) DC**	Whole plant	Aqueous extracts (rutin and quercetin **(3)**)	Flavonoids and terpenes	*In vitro*	The aqueous extract showed higher efficiency in eliminating DPPH radical with an IC_{50} value of 415 ± 12.1 μg/mL. The extract was capable of reducing deoxyribose damage at all concentrations by its ability to chelate iron by greater than 50% at the extract concentration of 100 μg/mL.	(Sabir et al., 2017)
***Bidens pilosa* L.**	Leaf	Aqueous and methylene chloride extracts	Flavonoids, alkaloids, saponins, phenyl acetylenes, and terpenes	*In vivo*	Aqueous extract (150 or 350 mg/kg) and methylene chloride extract (150 mg/kg or 300 mg/kg) of *B. pilosa* completely blocked the elevation of blood pressure in fructose-treated rats and provoked a decline toward control values. The extracts reversed the increase in SBP.	(Dimo et al., 2001)
***Chamaemelum nobile* (L.) All.**	Whole plant	Aqueous extract	–	*In vitro* and	Single oral administration of the extract (140 mg/kg) produced a significant reduction in SBP. Daily oral administration of the extract (140 mg/kg) during three weeks, produced a significant reduction in SBP in day eight of treatment.	(Zeggwagh et al., 2009)

(Continued)

TABLE 3 | Continued

Plant Name	Parts Used	Isolated Compound/ Extract	Class	*In Vivo*/ *In Vitro*	Mechanism of Action	References
				in vivo	The extract produced a significant increase in urinary output and electrolytes excretion.	
Chromolaena odorata* (L.) *R. M. King* and *H. Rob.	Leaves	Aqueous extract	–	*In vivo*	100 mg/kg of aqueous extract reduced triglycerides, LDL, VLDL, non-HDL, and total cholesterol. The HDL-C level of the treated animals was significantly higher.	(Ikewuchi and Ikewuchi, 2011)
***Chrysanthemum* x *morifolium* Ramat. Hemsl.**	Flower	*C. morifolium* extract (CME)	Polyphenols	*In vivo*	Polyphenol-rich CME alleviated hypertensive cardiac hypertrophy in rats through the reduction of blood pressure. Administration of CME at the dose of 75–150 mg/kg for four weeks lowered the SBP.	(Gao et al., 2016)
***C. crepidioides* (Benth.) S. Moore**	Aerial parts	Aerial methanolic extract, coumarin, and reducing sugar	Alkaloids, glycosides, cardiac steroids, tannins, flavonoids, saponins, and glycosides	*In vitro* and *in vivo*	Increasing concentration of the methanolic extract increased its DPPH radical scavenging activity. The Wistar albino rats were administered with plant extract (150 and 300 mg/kg/day) orally. It significantly reduced the serum total cholesterol, triglycerides, LDL-C, VLDL-C levels, and significantly increased serum HDL-C level compared with a positive control group. The dose of 300 mg/kg showed significant ($p < 0.01$) antihyperlipidemic activity compared with the positive control group.	(Bahar et al., 2016)
***C. cardunculus* L. (syn. *Cynara scolymus* L.)**	Leaf	Quercetin **(3)**	Phenols and flavonoids	*In vitro* and *in vivo*	The extract exhibited a free radical scavenging effect. Hyperlipidemic rat administered with the extract of 150 to 600 mg/kg decreased triglyceride and LDL-C levels. It also reduced HMG-CoA reductase enzyme activity, hence reduced the formation of VLDL from the liver.	(Mocelin et al., 2016)
***Eclipta prostrata* (L.) L.**	Leaves	Leaf extract	Alkaloids, phytosterols, flavonoids, saponins, tannins, sugar	*In vivo*	The extract reduced total cholesterol, triglyceride, protein, and increased HDL-C. The extract (100 and 200 mg/kg) showed a significant hypolipidemic effect.	(Dhandapani, 2007)
***E. praetermissa* Milne-Redh**	Leaves	Aqueous extract	Tannins, cardiac glycosides, flavonoids, terpenoids	*In vivo*	The aqueous extract significantly reduced the triglyceride level (47.80 ± 4.75 mg/dl to 37.22 ± 2.18 mg/dl) at a dose of 200 mg/kg after 2 h. The level of HDL was significantly increased (48.44%) by 400 mg/kg of the extract. The extract (100 mg/kg) caused significant reductions in LDL level when it was administered concomitantly with 15 and 30 mg/kg atorvastatin, respectively.	(Ngozi et al., 2013)
***Erigeron canadensis* L.**	Flowering parts	Plant extract (polysaccharide-polyphenolic)	Flavonoids and tannins	*In vitro* *In vivo*	The extract inhibited thrombin and factor Xa amidolytic activities in the presence of antithrombin. The plant preparation inhibits plasma clot formation in aPTT at the concentration as low as 390 μg/mL of standardized human blood plasma, and in PT test at the concentration of 1.56 mg/mL. The strong anticoagulant effect was observed after 40 min after the administration, with the clotting time almost three times longer than control measurement.	(Pawlaczyk et al., 2011)
***Flaveria bidentis* (L.) Kuntze**	Leaves	Quercetin 3-acetyl-7,3′,4′-trisulfate (ATS) and quercetin 3,7,3′,4′-tetrasulfate (QTS)	Flavonoids	*In vitro*	QTS has higher activity than ATS in activating heparin cofactor II (HCII), indicating that these flavonoids act as agonists of this inhibitor. The flavonoids also increased PT with a concentration of 1 mM of QTS (25.2 ± 0.8 s, $p < 0.01$) and ATS (22.2 ± 0.7 s, $p < 0.04$). It also prolonged aPTT at the concentration of 112 ± 11 and 53 ± 2, respectively.	(Guglielmone et al., 2002)
***G. tournefortti* L.**	Seeds	Tyramine	Saponin and alkaloid	*In vivo*	The oil extract (90 mg/kg) possessed a hypolipidemic effect by reducing plasma total lipid, total cholesterol, VLDL-cholesterol, LDL-cholesterol, and atherogenic indices. It also increased the HDL value and reduced the total cholesterol level in the liver.	(Sharaf and Ali, 2004)
***Gymnanthemum amygdalinum* (Delile) Sch. Bip. (syn. *Vernonia amygdalina* Delile)**	Leaf	Aqueous extract	Flavonoids and phenolics	*In vivo*	The extract caused a decrease in plasma total cholesterol, LDL, triacylglycerol, and VLDL and an increase in plasma HDL-C concentration of hyperlipidemic animals.	(Audu et al., 2012)

(Continued)

TABLE 3 | Continued

Plant Name	Parts Used	Isolated Compound/ Extract	Class	*In Vivo*/ *In Vitro*	Mechanism of Action	References
***H. leucocephalum* Ausfeld**	Aerial parts (leaves, stalks, and stems)	Chalcones, phthalides, α-pyron derivatives, essential oils, volatiles, and fatty acids	Phenol, terpenoids, and flavonoids	*In vitro* and *In vivo*	The extracts exhibited scavenging activity towards DPPH radicals.	(Goldansaz et al., 2018)
***Inula racemosa* Hook F.**	Roots	Alcohol extract (essential oil of the roots), phenyl acetonitrile and phenyl ethanol	Sesquiterpenes and phenolics	*In vivo*	IrA decreased total cholesterol, triglycerides, LDL-C, and the atherogenic index, and increased HDL-C compared with the positive control. It also reduced GSH in both the tested tissues, levels of endogenous antioxidants SOD and GPX in the heart. It inhibited lipid peroxidation, and reduced lipid uptake, resulting in a reduction of fatty streak formation, *via* decreased foam cell formation.	(Mangathayaru et al., 2009)
***L. decurrens* (Vahl) Hepper and J. R. I.Wood.**	Aerial parts	Essential oil (3-methoxythymoquinone, thymol, and carvacrol)	Monoterpenes, Phenols	*In vitro*	The extract (500 μg/mL) exhibited high antioxidant activity (91%) by scavenging DPPH.	(Mothana et al., 2011)
***Launaea intybacea* (Jacq.) Beauverd (syn. *Lactuca runcinata* DC.)**	Whole plant	Ethanolic extract	–	*In vivo*	At a dose of 200 mg/kg, the extract reduced the level of plasma total cholesterol, ester cholesterol, free cholesterol, free fatty acid phospholipids, and triglycerides in comparison with AD rat. Whereby at a dose of 400 mg/kg, the extract increased the rats' HDL-C level. The reduction of the plasma lipid and lipoprotein profile was due to the presence of phenolic and flavonoids compounds. HDL reversing cholesterol transport, inhibiting the oxidation of LDL and neutralizing the atherogenic effects of oxidized LDL.	(Devi and Muthu, 2015)
***Leuzea carthamoides* Willd. DC.**	Leaves	Eriodictyol **(21)** and patuletin **(22)**	Flavonoid	*In vitro*	Eriodictyol **(21)** and patuletin **(22)** exhibited antiplatelet activity. They inhibited COL- and AA-induced platelet aggregation.	(Koleckar et al., 2008)
***Pectis brevipedunculata* Sch. Bip**	Aerial parts	Essential oil (Citral, geranial **(19),** limonene, and α-pinene)	Monoterpene compounds, hydrocarbons, sesquiterpenes, alcohols and aldehydes	*In vitro*	The essential oil caused vasorelaxation activity. The citral possessed vasodilator activity towards KCl-contracted aorta. Citral attenuated the contracture induced by Ca^{2+} in the depolarized aorta. EOPB and citral elicited vasorelaxation on thoracic aorta by affecting the NO/cyclic GMP pathway and the calcium influx through voltage-dependent L-type Ca^{2+} channels.	(Pereira et al., 2013)
***Senecio nutans* Sch. Bip**	Branches and leaves	Hydroalcoholic extract, dihydroeuparin,p-hydroxy acetophenone	Terpenes and flavonoids	*In vivo*	The plant extract (40 mg/kg) caused a reduction in SBP and DBP by 23% and 35%, respectively. The extract also decreased MAP and heart rate by intravenous (IV) route administration, in addition to prolonged dilatation time.	(Cifuentes et al., 2016)
***S. ovatus* subsp. *stabianus* (Lacaita) Greuter (syn. *Senecio stabianus* Lacaita)**	Aerial parts	Plant extract	Phenol and flavonoid	*In vitro*	Ethyl acetate extract showed the highest activity with IC_{50} values of 35.5 and 32.7 mg/mL on the DPPH test and ABTS test, respectively.	(Tundis et al., 2012)
***Silybum marianum* (L.) Gaertn.**	Seeds	Silybin (the main component of Silymarin mixture)	Polyphenols	*In vivo*	Silymarin **(12)** acts as a free radical scavenger such as (OH, O_2) and it enhances the antioxidant enzymes CAT, SOD, and GPx. Thus, it increased the antioxidant cell defense and the activity of the mitochondrial enzyme. It caused activation of Nrf2 and inhibited NF-kB, and expressions of eNOS and MAPK (ERK1, 2, JNK). It activated the ribosome and increased protein synthesis to regenerate cardiovascular tissues. It also scavenged free radicles in the cytoplasm and increased ribosomal RNA synthesis. A dose of 200 mg/kg of silymarin **(12)** reduced the ROS level of rats when given intraperitoneally. 100 mg/kg of silymarin **(12)** increased HDL-cholesterol and decreased liver cholesterol of hypercholesterolemic rats.	(Taleb et al., 2018)
***Solidago chilensis* Meyen**	Aerial parts	Hydroalcoholic extract	Flavonoids	*In vitro*	The extract exhibited antioxidant properties with an IC_{50} value of 59.12 ± 3.14 μg/mL.	(Schneider et al., 2015)

(Continued)

TABLE 3 | Continued

Plant Name	Parts Used	Isolated Compound/ Extract	Class	*In Vivo*/ *In Vitro*	Mechanism of Action	References
				In vivo	The extract at the dose of 125, 250, or 500 mg/kg decreased the total cholesterol of rats.	
***Sphaeranthus indicus* L.**	Flower	Ethanolic extract	Tannin	*In vivo*	The extract of dose 500 mg/kg/day given in rat orally for eight days caused a decrease in body weight, total cholesterol, triglycerides, LDL, and VLDL. It showed a rise in HDL level resembling its use in atherosclerosis conditions.	(Pande and Dubey, 2009)
***Tagetes erecta* L. (syn. *Tagetes patula* L.)**	Roots	Citric acid **(24)**, dimethyl citrate, and malic acid	Tricarboxylic acid	*In vivo*	The citric acid **(24)** reduced the blood pressure of normotensive rats in a dose-dependent manner. It caused 17–21% and 32–35% fall in MABP at the corresponding doses of 3 and 30 mg/kg, respectively.	(Saleem et al., 2004)
***T. vulgare* L.**	Leaves	Plant extract	–	*In vivo*	Administration of 10 mg/kg of the leaf extract caused an increase in urine output. The levels of Na^+ and K^+ in the urine increased, but the plasma Na^+ and K^+ were not affected in this activity.	(Lahlou et al., 2007)
***Tridax procumbens* (L.) L.**	Leaves	Extract	Sulfated polysaccharide	*In vitro*	The sulfated polysaccharides prolonged aPTT (113 s) at a dose of 100 μg/mL, which was approximately 4.0-fold compared with the saline group.	(Naqash and Nazeer, 2011)
***Vernonia elaeagnifolia* DC.**	Leaf	Ethanolic extract	Flavonoids, phenolic compounds, tannins, terpenoids, phytosterols, alkaloids, and coumarins	*In vivo*	The extract restored the levels of LDL and HDL cholesterol of albino rabbits.	(Sultana et al., 2017)

of the myocardial infarction situation, resembled its effectiveness in cardiovascular disease, and indicated its protective effects on cell membrane functions (Ezzoubi et al., 2014).

The essential oils and subfractions of *M. macrosiphon* Coss. methanolic extract were examined their antioxidative properties *via in vitro* study (Amiri, 2011). In examining the effect of *M. macrosiphon* on DPPH assay, the polar subfraction of the flowering stage was more potent with an EC_{50} value of 57.0 ± 0.6 mg/mL. In contrast, the essential oil of the flowering stage was more potent (EC_{50}: 91.7 ± 1.2 mg/mL) in inhibiting α-carotene oxidation with almost similar inhibitory activity compared to the positive control, BHT. The oxidation of α-carotene was determined by observing its discoloration caused by coupled oxidation of linoleic acid and α-carotene that generates free radicals.

The phenolic compounds isolated from the ethanolic extract of the whole plant of *O. vulgare* L. were determined their antioxidant activity. From the study, *O. vulgare* consists of phenol compounds such as 2,5-dihydroxybenzoic acid, 3,4-dihydrobenzoic acid, rosmarinic acid **(5)**, origanoside, maltol, *E*-caffeic acid **(6)**, apigenin **(7)**, luteolin **(8),** and didymin (Zhang et al., 2014). Based on the *in vitro* test, the phenolic compounds of *O. vulgare* showed potent antioxidant activity. The SC_{50} values of the compounds ranged from 16.7 ± 1.1 to 221.8 ± 49.0 μM. The scavenging activity of the compound that consists of 3,4-dihydroxyphenyl and gastrodin moiety was higher than its positive control, the ascorbic acid. The highest radical scavenging activities were exhibited by compounds with danshensu moieties with SC_{50} values 17.5 ± 1.1 μM and 16.7 ± 1.1 μM. The phenolic structure is responsible for the scavenging activity by donating the hydroxyl group to the free radicals (Graf, 1992). The ferric reduced antioxidant power (FRAP) assay also showed similar antioxidant activity of the phenolic compounds. The FRAP values of the compounds ranged from 143.0 ± 4.0 and 201.0 ± 8.0, with the highest activity exhibited by origanoside and apigenin **(7)** (Zhang et al., 2014).

Salvia officinalis L., which is also known as sage, contains phenolic compounds in its shoot part (Santos-Gomes et al., 2002). The antioxidant extract of the shoots contains phenolic acids such as gallic acid **(1)**, rosmarinic acid **(5)**, caffeic acid **(6)**, 5-*O*-caffeoylquinic acid, and 3-*O*- caffeoylquinic acid. The identified flavonoids in the extract are hesperetin, genkwanin, hispidulin, cirsimaritin, and apigenin **(7)**. Whereas, the phenolic diterpenes are methyl carnosate, rosmanol **(9)**, epirosmanol, epiisorosmanol ethyl ether, epirosmanol methyl ether, carnosic acid, rosmadial, and carnosol**(10)**. The rosmarinic acid **(5)**, carnosic acid, and carnosol **(10)** contributed to *S. officinalis* inhibitory activity on lipid peroxidation (Santos-Gomes et al., 2002). The ethanolic leaves extract of the plant contains a high amount of chlorogenic acid **(11)** and rosmarinic acid **(5)**. The compounds exhibited strong antioxidant activity due to the ability of their phenols structure to donate hydrogen atoms to free radicals. (Ramu et al., 2012).

Senecio ovatus subsp. *stabianus* (Lacaita) Greuter was used an *in vitro* assay to examine its antioxidant activity by conducting azino-bis(3-ethylbenzthiazoline-6-sulphonate) (ABTS) and DPPH assay (Tundis et al., 2012). The study showed that the

TABLE 4 | Mechanism of action of Lamiaceae family plant species.

Plant Name	Parts Used	Isolated Compound/ Extract	Class	*In Vivo*/ *In Vitro*	Mechanism of Action	References
***Agastache mexicana* (Kunth.) Lint. and Epling.**	Aerial parts	Acacetin, oleanolic acid **(25)**, and ursolic acid	–	*In vivo*	Each hypertensive mouse received an intragastric dose of ursolic acid (50 mg/kg). It inhibited vasoconstriction induced by KCl and noradrenaline bitartrate (NA) in endothelium-denuded aortic rings, and also inhibited the concentration-response contraction of NA in a nonparallel manner and depressed its maximal response. The extract at the dose of 112, 200, and 625 µg/mL possessed Ca_{2+}entry blocking activity.	(Hernandez-Abreu et al., 2013)
***Ajuga integrifolia* Buch.-Ham. ex D. Don (syn. *Ajuga remota* Benth.)**	Leaves	phenolic compounds, tannins, saponins, flavonoids, terpenoids, steroids, and cardiac glycosides	–	*In vivo*	80% methanolic extract produced significant diuresis ($p < 0.01$), while the aqueous extract had shown diuresis both at the middle ($p < 0.01$) and higher ($p < 0.01$) doses by the end of the fifth hour of administration.	(Hailu and Engidawork, 2014)
***Ajuga iva* (L.) Schreb.**	Whole plant	Aqueous extract	Ecdysone, terpenoid, flavonoid	*In vitro*	The extract (1 mg/mL) reduced plasma cholesterol and triacylglycerol. It also reduced TBARS concentration, the lipid peroxidation product. Product concentration was reduced	(Taleb-Senouci et al., 2009)
***Ballota glandulosissima* Hub. -Mor. and Patzak**	Aerial parts	kumatakenin, pachypodol, 5-hydroxy-7,3′,4′-trimethoxyflavone, velutin, corymbosin, retusine	Flavonoid	*In vivo*	The extract inhibited lipid peroxidation with an IC_{50} value of 12 to 20 mg/mL.	(Sever, 2000; Citoglu et al., 2004)
***Clerodendrum volubile* P. Beauv**	Leaf	Leaf extract (alkaloids, saponins, tannins, flavonoids, steroids, and cardiac glycosides)	–	*In vivo*	The extract (250 and 500 mg/kg) significantly lowered the total cholesterol, LDL, VLDL, and triglycerides, and increased HDL level dose-dependently, in both phyto-preventive and curative animals.	(Akinpelu et al., 2016)
***C. vulgare* L. (syn. *C. vulgaris* (L.) Druce)**	Aerial parts	Crude extract	Phenolic and flavonoid	*In vivo* and *in vitro*	The extract and fractions showed an antihypertensive effect at doses of 10 and 30 mg/kg, respectively, by reducing the MAP of hypertensive rats.	(Khan et al., 2018)
***Dracocephalum moldavica* L.**	Aerial parts	Plant extract	Flavonoid	*In vitro*	The flavonoids fraction, at the concentration of more than 70 mg/L, exhibited a higher DPPH radical scavenging activity than vitamin E. The flavonoids fraction also possessed scavenging activity on DPPH, hydroxyl radicals, and superoxide anion radicals.	(Jiang et al., 2014)
***Isodon rugosus* (Wall. ex Benth) Codd**	Aerial parts	Crude extract	–	*In vivo* and *in vitro*	The crude extract (0.01–0.3 mg/mL) possessed a relaxant effect on isolated rabbit jejunum, trachea, and aorta preparations. The mechanism of action was assumed to be by the Ca^{2+} channel blockade.	(Janbaz et al., 2014)
***Lagenaria siceraria* (Mol.) Standl**	Fruit	C-glycosides	Flavone	*In vivo*	*L*-NAME was used to induce hypertension in rats. Concomitant treatment of *L. siceraria* fruit powder (LS) and *L*-NAME for 28 days reduced cholesterol level but did not reduce triglycerides levels. It also reduced SBP, DBP, and MABP significantly. LS, as well as L-arginine treatment, produced significant ($p <0.001$) attenuation of the hypertensive effect of *L*- NAME.	(Mali et al., 2012)
***Lallemantia royleana* Benth. in Wall.**	Seeds	Oleic, linoleic, and linolenic acid content	–	*In vivo*	Administration of the seeds for 12 weeks decreased ($p < 0.05$) the rabbit's total serum cholesterol and triglycerides. It also significantly decreased LDL-C and HDL-C of the hypercholesterolemic group ($p < 0.05$).	(Ghannadi et al., 2015)
***Lavandula angustifolia* Mill.**	Aerial parts	Essential oil (linalool, linalyl acetate camphor **(14)**, 1,8-cineol, luteolin **(8)**, triterpenoids like ursolic are and coumarin)	Mono and sesquiterpenes, flavonoids	*In vivo*	The essential oil (10 mg/kg) significantly decreased heart to body weight ratio ($p < 0.001$). Treatment with 10 and 20 mg/kg of essential oil demonstrated a profound reduction ($p < 0.001$) in the ST-segment elevation.	(Ziaee et al., 2015)
***Lavandula stoechas* L.**	Aerial parts	Ethanolic extract	–	*In vitro*	The extract exhibited antioxidant activity by scavenging DPPH with an IC_{50} value of 1.2 µg/mL while the IC_{50} value of the reference standard, BHT was 0.2 µg/mL.	(Ezzoubi et al., 2014)
***Leonotis leonurus* (L.) R. Br.**	Leaves	Marrubiin **(20)** and organic extract	Diterpenoids	*In vivo*	The extract (25–2,000 µg/mL) and marrubiin **(20)** (1.25–100 µg/mL) inhibited platelet aggregation by suppressing the	(Mnonopi et al., 2011)

(Continued)

TABLE 4 | Continued

Plant Name	Parts Used	Isolated Compound/ Extract	Class	*In Vivo*/ *In Vitro*	Mechanism of Action	References
				and *in vitro*	binding of fibrinogen to the surface receptor GP2b/3a. They also inhibited collagen and thrombin-induced calcium mobilization. Diterpenoids inhibited the extracellular receptor kinase (ERK) 1/2 signaling pathway.	
***Leonurus cardiaca* L.**	Aerial parts	Leonurus cardiaca refined extract (LCRE) Cardioactive lavandulifolioside and verbascoside	Phenylethanoid glycosides	*In vitro* and *in vivo*	LCRE at the dose of 1.0 to 2.0 mg/mL was infused intracoronary for 10 min before mapping its epicardial potential. It reduced the left ventricular pressure in a dose-dependent manner and elevated the relative coronary flow.	(Ritter et al., 2010)
***Lepechinia caulescens* (Ortega) Epling**	Aerial parts	Methanolic extract (ursolic acid, terpinene- 4-ol, salvigenin, and spathuleno)	–	*In vivo* and *in vitro*	Methanolic extract *L. caulescens* (MELc) at 38 and 120 mg/kg induced a significant decrease in heart rate, SBP, and DBP in comparison with control, captopril (30 mg/kg). MELc (120 mg/Kg) induced a long-term antihypertensive and vasorelaxant effect.	(Estrada-Soto et al., 2012)
***L. aspera* (Willd.) Link**	Leaf	Ethanolic extract of leaf	Phytosterols and alkaloids	*In vivo*	The ethanolic extract of leaves (200 and 400 mg/kg) showed significant inhibition against dexamethasone-induced hyperlipidemia in rats by maintaining the serum levels of cholesterol and triglycerides near to normal levels.	(Kumar, 2016)
***M. officinalis* L.**	Leaves	Hydroxycinnamic acid derivatives (rosmarinic acid **(5)** and caffeic acids **(6)**)	Phenol	*In vitro*	The aqueous extract (1–1,000 μg/mL) exhibited concentration-dependent relaxation in phenylephrine-precontracted endothelium intact thoracic rings. Rosmarinic acid **(5)** possessed a dose-dependent vasorelaxant effect.	(Ersoy et al., 2008)
***M. macrosiphon* Coss. (syn. *S. macrosiphon* (Coss.) Maire)**	Aerial parts	Methanolic extract (carvacrol, thymol, flavonoids, beta-caryophyllene, gamma-terpinene, and linalool)	Isopropanoids	*In vitro*	The methanolic extract of its flowering stage possessed higher activity in inhibiting α-carotene oxidation with an EC_{50} value of 57.0 ± 0.6 mg/mL.	(Amiri, 2011)
***O. vulgare* L.**	Whole plants	Flavonoids and phenolic acids, rosmarinic acid **(5)**, origanoside	Phenolic compounds	*In vitro*	The *in vitro* test of the phenolic compounds exhibited potent DPPH radical scavenging activities with SC_{50} values ranging from 16.7 ± 1.1 to 221.8 ± 49.0 μM.	(Zhang et al., 2014)
***Orthosiphon aristatus* (Blume) Miq. (syn. *Orthosiphon stamineus* Benth.)**	Leaves	Methylripariochromene (MRC)	–	*In vivo*	MRC (50 and 100 mg/kg) reduced SBP and heart rate of the mice *via* the subcutaneous route. The MRC reduced BP due to the dilation of the blood vessel decreased in cardiac output. It also has suppressive actions to contractions.	(Matsubara et al., 1999)
	Whole plant	Sinensetin **(17)**, eupatorin **(26)**, flavonoid	–	*In vitro*	Sinensetin **(17)** (0.03–2.11 μM) caused concentration-dependent vasorelaxation of phenylephrine-contracted endothelium-intact aortic rings. *O. aristatus* caused aortic ring that was pre-contracted with phenylephrine in the presence and absence of endothelium to be relaxed. It also caused relaxation to the aortic ring that was pre-contracted with potassium chloride in the endothelium-intact aortic ring.	(Yam et al., 2016; Yam et al., 2018)
***Phlomoides bracteosa* (Royle ex Benth.) Kamelin and Makhm. (syn. *Phlomis bracteosa* (Royle ex Benth.) Kamelin and Makhm.)**	Whole plant	Marrubiin **(20)** (labdane-type diterpene) and phlomeoic acid (tricyclic clerodane-type diterpenoid)	–	*In vitro*	It exhibited a vasodilator effect mediated through dual Ca^{2+} channel inhibition (endothelium-independent) and nitric oxide (NO) generation (endothelium-dependent) pathways. Marrubiin **(20)**, phlomeoic acid, RA, and RB inhibited the K^+ and PE-induced contractions in endothelium-denuded rings with different patterns.	(Khan et al., 2012)
***Plectranthus hadiensis* (Forssk.) Schweinf. ex Sprenger (syn. *Coleus forskohlii* Willd.)**	Whole plant	Ethanolic extract	Diterpene	*In vivo*	Coleonol produced well-marked and sustained hypotension in the anesthetized cat in a dose range of 0.1–1.0 mg/kg, given intravenously in the smooth muscle. A close intra-arterial injection of coleonol (0.1 mg) increased the blood flow in the femoral artery.	(Dubey et al., 1981)
P. monostachyus* (P. Beauv.) B. J. Pollard (syn. *S.	Leaves	Ethanolic extract	flavonoids, coumarin, polyphenol	*In vivo*	The extract (0.6–17.6 mg/kg bw) induced a significant decrease in arterial blood pressure (EC_{50} = 2.5 ± 0.15 mg/kg b.w) in a dose-dependent manner ($p < 0.001$). The extract	(Fidele et al., 2012)

(Continued)

TABLE 4 | Continued

Plant Name	Parts Used	Isolated Compound/ Extract	Class	*In Vivo*/ *In Vitro*	Mechanism of Action	References
***monostachyus* (P. Beauv.) Briq.)**					(10^{-2}-1 mg/mL) inhibited aorta smooth muscle contraction suggesting calcium channel blocking action with a major inhibitory effect on L-type voltage-operated Ca^{2+} channels.	
***Pogostemon elsholtzioides* Benth.**	Leaves	Essential oil (Curzerene, majority sesquiterpenes)	–	*In vitro*	The essential oil of *P. elsholtzioides* induced dose-dependent vasodilation in pre-contracted aortic rings against contraction evoked by Phe (10^{-3}M). Injection of the essential oil at the dose level 20 mg/kg induced a significant decrease in MAP and heart rate.	(Shiva Kumar et al., 2017)
***P. vulgaris* L.**	Whole plant	Rosemarinic acid	–	*In vivo* and *in vitro*	The aqueous extract showed a substantial increase in the HDL level. The extract exhibited radical scavenging activity towards superoxide, hydroxyl, and hydrogen peroxide.	(Zargar et al., 2017)
***R. officinalis* L.**	Leaves	*n*-butanol extract	Flavonoids and phenolic	*In vivo*	The *n*-butanol extract (400 mg/kg) significantly reduced ($p < 0.01$) the plasma total cholesterol level of diabetic mice group by 51.85% reduction.	(Belmouhoub et al., 2017)
***S. miltiorrhiza* Bunge**	Root	Salvianolic acid **(23)**	Phenolic acids	*In vivo* *In vitro*	Salvianolic acid **(23)** reduced thrombus weight and increased plasma CAMP level. Salvianolic acid **(23)** (2.5–10 mg/kg) administered inhibited the platelet aggregation in a dose-dependent manner. The acid inhibited various agonists that stimulate platelet aggregation. It also induced CAMP levels in platelets that were activated by ADP. induce a rise in CAMP level in platelets activated by ADP.	(Fan et al., 2010)
***S. officinalis* L.**	Shoots	Phenolic acids, carnosol derivatives, and flavonoids, namely, rosmarinic acid **(5)**, carnosic acid, and carnosol **(10)** followed by caffeic acid **(6)**, rosmanol **(9)**, rosmadial, genkwanin, and cirsimaritin	Phenolic compound and flavonoids	*In vitro*	It exhibited scavenging activity towards active oxygen's such as superoxide anion radicals, hydroxyl radicals, and singlet oxygen, and inhibits lipid peroxidation.	(Masaki et al., 1995; Santos-Gomes et al., 2002)
***Salvia scutellarioides* Kunth**	Leaves and stem	Aqueous plant extract	–	*In vivo*	Intravenous consumption of 1 and 2 g/kg of the extract produced a significant increase in diuresis. It increased the urinary excretion of potassium and chloride. High tubular concentrations of potassium stimulated the activity of the Na^+/K^+ ATPase pump in the basolateral membrane of the tubular epithelial cells, decreasing the sodium concentration in the urine.	(Ramirez et al., 2006)
***Satureja cuneifolia* Ten. (syn. *Satureja obovata* Lag.)**	Whole plant	Eriodictyol **(21)**	Flavonoid	*In vitro*	Eriodictyol **(21)** inhibited the KCl and noradrenaline-induced contraction in a concentration-dependent manner. Eriodictyol **(21)** (10^5, 5×10^5, 10^4, and 5×10^4 M) added before the contraction reduced the tonic phase of contraction.	(De Rojas et al., 1999)
***Sideritis raeseri* Boiss. and Heldr.**	Aerial parts	Plant extract	Terpenoids, sterols, coumarins, flavonoid aglycones, and glycosides	*In vivo* *In vitro*	The extract (0.025–7.5 mg/kg) caused a dose dependent decrease of the arterial pressure and heart rate, with an EC_{50} value of 24.31 ± 3.87 mg/kg and 88.14 ± 7.51 mg/kg, respectively Extract of *S. raeseri* (0.005–1.5 mg/mL) elicited a vasodilator action (EC_{50}: 0.11 ± 0.008 mg/mL).	(Kitic et al., 2012)
***T. polium* L.**	Aerial parts	Aqueous extract	Diterpenoids, flavonoids, iridoids, sterols, and terpenoids	*In vivo*	Administration of 50 to 150 mg/kg of the extract for ten days significantly reduced the serum levels of cholesterol and triglycerides in hyperlipidemic rats dose-dependently.	(Rasekh et al., 2001)
***Thymus saturejoides* Coss.**	Whole plant	Caffeic acid **(6)** Rosmarinic acid **(5)** Quercetin **(3)**	Polyphenolic compound	*In vivo* and *in vitro*	The extract exhibited a hypolipidemic effect. Injection of 0.2 g/100 g of the extract significantly lowered both plasma triglycerides and cholesterol levels after 24 h of treatment. The reduction of plasma total cholesterol was associated with a decrease in the LDL fraction. It suppressed the elevated blood concentrations of triglycerides.	(Ramchoun et al., 2012; Khouya et al., 2015)
***Thymus serpyllum* L.**	Whole plant	GAE, and rosmarinic and caffeic acids **(6)**	Phenols and flavonoids	*In vivo*	The injection *via* bolus of 100 mg/kg body weight produced a significant decrease in SBP, DBP, and total peripheral	(Katalinic et al., 2006;

(Continued)

TABLE 4 | Continued

Plant Name	Parts Used	Isolated Compound/ Extract	Class	*In Vivo*/ *In Vitro*	Mechanism of Action	References
				In vitro	resistance. Rosmarinic acid **(5)** portrayed a dose-dependent antioxidant activity against *in vitro* LDL oxidation. It inhibited the formation of conjugated dienes and TBARS. The thyme extract (1 mg/mL) exhibited nitric oxide (NO) scavenging activity of 63.43%, with the IC_{50} value of 122.36 µg/mL.	Mihailovic-Stanojevic et al., 2013)
***Thymus zygis* L.**	Whole plant	Caffeic acid **(6)** and rosmarinic acid **(5)**	–	*In vivo*	In the aPTT test, it completely inhibited the plasma clot formation in the concentration of 5.72 mg/mL in the clotting mixtures and prolongs the clotting time at the concentration of 0.18 mg/mL In the PT test, it completely inhibited the clotting process at a concentration of 11.43 mg/mL.	(Khouya et al., 2015)
***Vitex megapotamica* (Spreng.) Moldenke**	Leaves	Crude extract	Flavonoid	*In vivo*	The hydroethanolic extract (500 or 1,000 mg/kg/day) significantly reduced the levels of total cholesterol, triglycerides, LDL-C, and the atherogenic index. The atherosclerotic plaque formation was impaired only by the lower dose of the hydroethanolic extract.	(Pires et al., 2018)
***Ziziphora clinopodioides* Lam.**	Whole plant	Caffeic acid **(6)**, luteolin **(8)**, 7-methylsudachitin, thymonin	Phenolic and flavonoid	*In vitro*	The extract exhibited relaxation on the vascular smooth muscle cells through intracellular and extracellular Ca^{2+} mobilization. It acts on voltage-dependent K^{+}channels.	(Senejoux et al., 2010)

ethyl acetate extract of the plant exhibited the strongest activity on ABTS (IC_{50} value: 32.7 mg/mL) and DPPH (IC_{50} value: 35.5 mg/mL) assay. Based on the Folin-Ciocalteu method, the plant contains total phenol of 76.3 mg chlorogenic acid **(11)** equivalent per gram of the plant. Whereas, based on the formation of the flavonoid-aluminum complex method, the plant contains a total flavonoid of 11.8 mg quercetin **(3)** equivalent per gram of the plant. Thus, it was assumed that the antioxidant activity of the plant due to its flavonoids content (Tundis et al., 2012).

Silybum marianum (L.) Gaertn. contains silymarin **(12),** which is one of the polyphenolic antioxidants. Administration of 200 mg/kg silymarin **(12)** by intraperitoneal on rats reduced ROS level and protected the rats from supra celiac abdominal aorta ischemia or reperfusion injury. (Kocarslan et al., 2016). Administration of 100 mg/kg silymarin **(12)** on the rats reduced iron and oxidative stress level of the rats' blood. Besides, the phenolic structure of silymarin **(12)** caused the compound to has a strong scavenger activity towards hypochlorous acid (HOCI). It inhibited hydroxyl radical formation, which is essential for the inhibition of xanthine oxidase activity (Varga et al., 2006). A low concentration of silymarin **(12)** caused inhibition of the NF-kB pathway by treating and attenuating the inflammatory reaction that stimulates atherosclerosis.

Antihyperlipidemia, Hypolipidemia, and Hypocholesterolemia Activity

The rise in both blood cholesterol and triglyceride that may be due to hereditary factors is known as hyperlipidemia. One of the CVD that is caused by hyperlipidemia is atherosclerosis. It is the condition where the lipids or fat substances which are denoted as plagues hardened the arteries. These plagues will be built up in the walls of arteries and lead to the narrowing of the arteries. It will diminish the ability of blood flow in the artery that usually associated with vascular diseases, heart disease, and stroke (Akinpelu et al., 2016). The role of substance that possesses the antihyperlipidemic effect is to reduce the total cholesterol level in the body by reducing triglycerides, very low-density lipoprotein (VLDL) and low-density lipoprotein (LDL). The antihyperlipidemic possessing substance also has a role in increasing the high-density lipoprotein (HDL) level in the body, which is known as the good cholesterol in the body that alleviates the risk of CVD.

A few plants from the plant family of Asteraceae and Lamiaceae plant family possess an antihyperlipidemic effect. Of such, the plants from Asteraceae *are Achillea arabica* Kotschy (syn. *Achillea biebersteinii* Hub.-Mor.), *Ageratum conyzoide* L., *Chromolaena odorata* (L.) R. M. King and H.Rob., *C. crepidioides* (Benth). S. Moore, *C. cardunculus* L. (syn. *Cynara scolymus* L.), *Eclipta prostrata* (L.) L., *E. praetermissa* Milne-Redh, *Gundelia tournefortti* L., *Gymnanthemum amygdalinum* (Delile) Sch. Bip. (syn. *Vernonia amygdalina* Delile), *Inula racemosa* Hook F., *Launaea intybacea* (Jacq.) Beauverd (syn. *Lactuca runcinata* DC.), *Solidago chilensis* Meyen, *Sphaeranthus indicus* L., and *Vernonia elaeagnifolia* DC. The plants from the Lamiaceae family are *Clerodendrum volubile* P. Beauv., *Lagenaria siceraria* (Mol.) Standl., *Lallemantia royleana* Benth., *Leucas aspera* (Willd.) Link, *Prunella vulgaris* L., *Rosmarinus officinalis* L., *Teucrium polium* L., *Thymus dreatensis* Batt. (syn. *Thymus atlanticus* (Ball) Pau), and *Vitex megapotamica* (Spreng.) Moldenke. These plants' extracts from different solvents, such as ethanol, methanol, and water lower the lipid markers concentration in the body either *via in vivo* or *in vitro* assays.

Achillea arabica Kotschy ethanolic extract was used to test its hypolipidemic effect in animals (Mais et al., 2016). The extract was from the aerial parts of the plant taken during its flowering

phase. The high-fat diet was fed to adult male Golden-Syrian hamsters for ten days to cause hyperlipidemia. The dose of 400 mg/kg of the *A. arabica* ethanolic extract had reduced VLDL, cholesterol, LDL, and triglycerides level in the hamsters' serum. It had no significant effect on HDL. Total cholesterol and triglycerides in the hepatic were also reduced. The plant extract contains flavonoids, sesquiterpene lactones, and polyphenols. Whereas, its essential oil contains a high amount of eucalyptol **(13)** (10.98%), camphor **(14)** (12.46%) and piperitone **(15)** (31.06%). These may act as an inducer for the hypolipidemic effect of *A. arabica* upon the experimental hyperlipidemic hamster (Mais et al., 2016). Few reports had documented that flavonoids and phenolic compounds have antioxidant, antihyperlipidemic, and antihypertensive activity as their pharmacological effect (Rouhi-Boroujeni et al., 2015).

In vivo study of methanolic extracts of *Ageratum conyzoide* L. root, leaf, and stem were carried out on rats to examine its hypolipidemic activity (Atawodi et al., 2017). The extracts contain flavonoids, alkaloids, cardiac glycosides, triterpenes, saponins, carbohydrates, and tannins. Meanwhile, the leaf also consists of steroids. Fiber, saponins, and flavonoids have an underlying antihyperlipidemic effect. The methanolic extract in a concentration of 100 mg/kg was treated on rats. The extract reduced serum lipids, which is one of the insulin-releasing factors. Insulin inhibits lipolysis, thus causing a rise in uptake of fatty acids into adipose tissue and triglyceride synthesis. The diabetic rat had shown a significant reduction in total cholesterol, triglycerides, low-density lipoprotein cholesterol (LDL-C) levels, and increased high-density lipoprotein cholesterol (HDL-C) (cardioprotective lipid) levels (Atawodi et al., 2017).

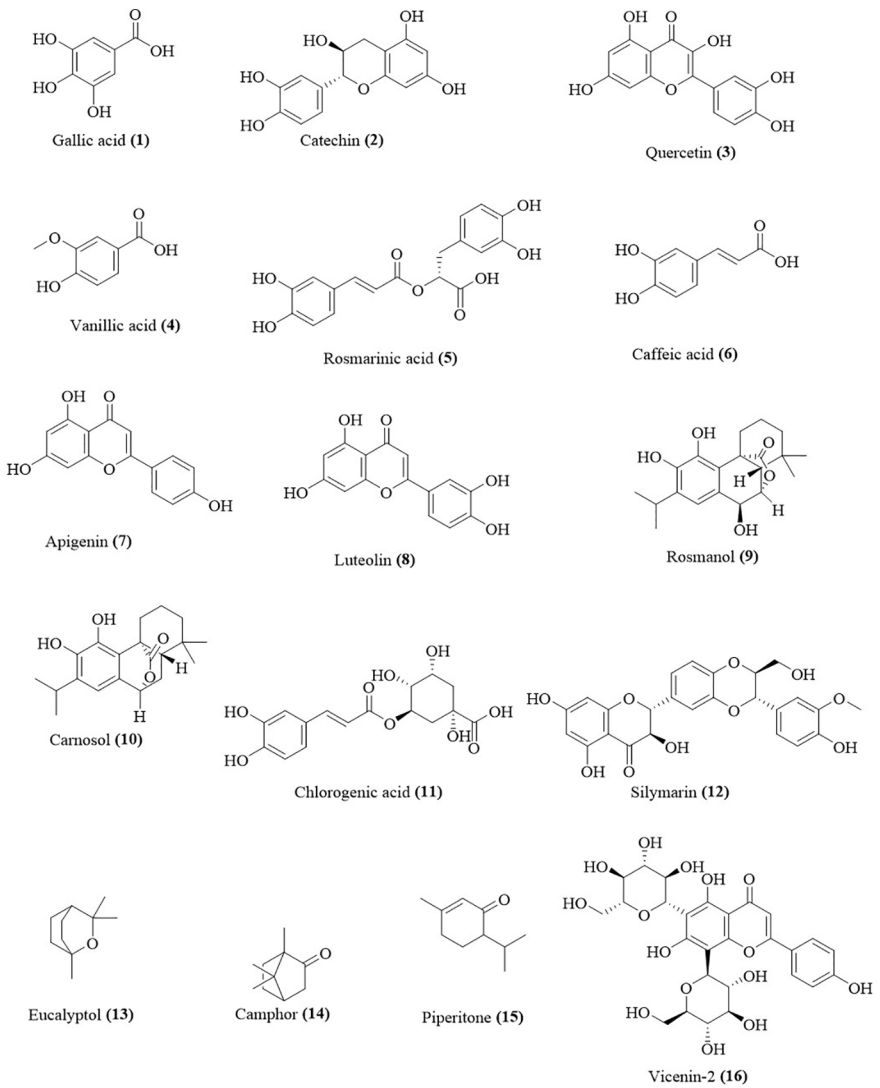

FIGURE 1 | Continued

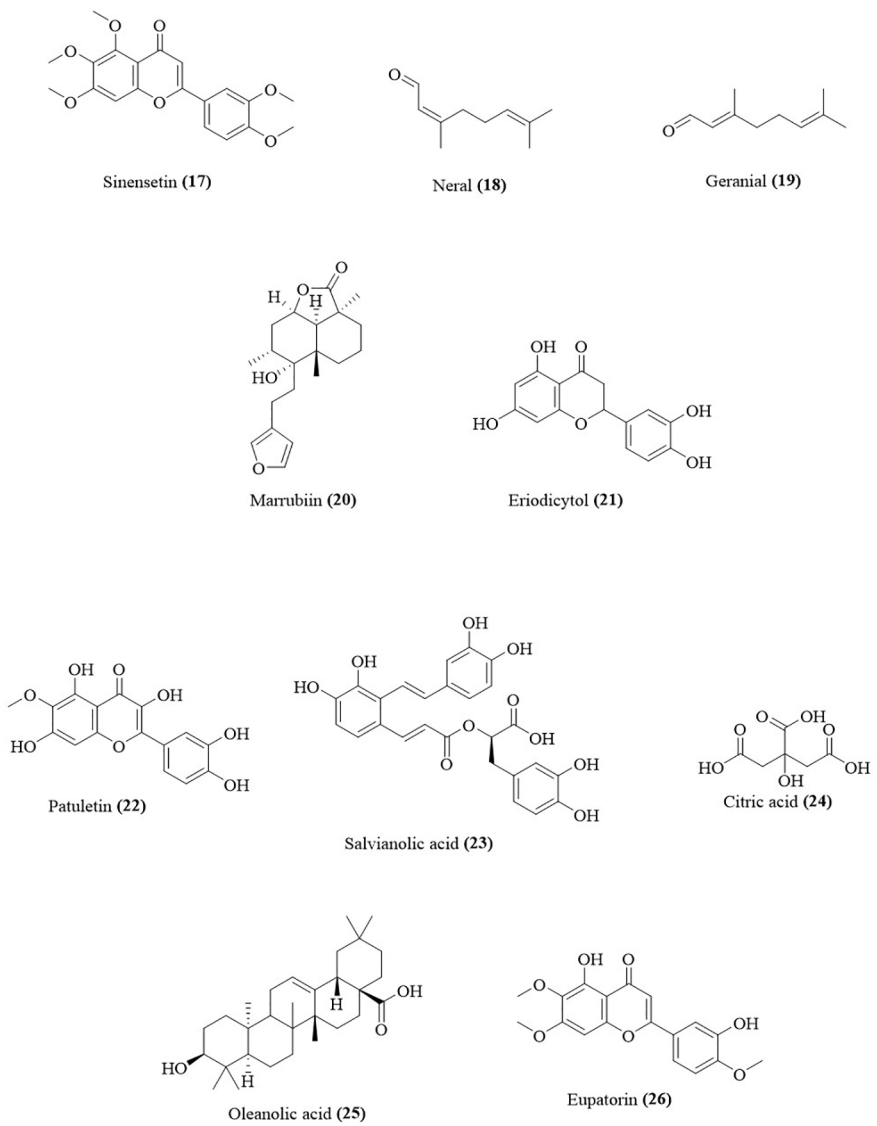

FIGURE 1 | Chemical structures of phytochemicals with inhibitory activity on cardiovascular diseases from Asteraceae and Lamiaceae species.

Chromolaena odorata (L.) R. M. King and H.Rob. leaves aqueous extract was examined its atherogenic indices and plasma lipid profiles on rats that have fed loaded with cholesterol (Ikewuchi and Ikewuchi, 2011). The intra-gastric gavages of the plant extract (100 mg/kg body weight) was administered to the rats. As a result, there was a significant reduction in total cholesterol, LDL, non-HDL, VLDL, and plasma's triglyceride levels. The HDL-C level in the plasma was high once being treated with the extract. The extract contains saponin, which was reported to have a hypercholesterolemic activity (Soetan, 2008). The extract significantly reduced ($p < 0.05$) the atherogenic index of plasma, cardiac risk ration, and atherogenic coefficient compared to the control group. Thus, the study showed that *C. odorata* could reduce the risk of heart diseases (Ikewuchi and Ikewuchi, 2011).

Ethanolic leaf extract of *C. volubile* P. Beauv. was evaluated by its anti-hyperlipidemic activity (Akinpelu et al., 2016). *Clerodendrum volubile* ethanolic leaf extract contains cardiac glycosides, saponins, flavonoids, alkaloids, tannins, and steroids. The extract contains phenolic compounds as the major constituents, followed by flavonoids and alkaloids. The lowest constituent of the extract was tannin, followed by saponin. The extract with a concentration of 250 and 500 mg/kg was administered to the hyperlipidemic animal. The extract significantly reduced the triglycerides, VLDL, total cholesterol, and LDL level in curative and phyto-preventive animals in addition to increased their HDL level (Akinpelu et al., 2016).

The methanolic extract of the aerial parts of *C. crepidioides* (Benth.) S. Moore had shown an antihyperlipidemic activity (Bahar et al., 2016). The albino rats were induced with a high-fat

diet to mimic hyperlipidemia model. The methanolic extract in a concentration of 150 and 300 mg/kg were administered orally to the rats. As a result, the extract increased HDL-C level while reduced VLDL-C, LDL-C, total cholesterol, and triglycerides levels compared to the positive group. The extract in a concentration of 300 mg/kg showed potent antihyperlipidemic activity compared to the positive control group (Bahar et al., 2016).

Cynara cardunculus L. is known for its antiatherogenic and hypolipidemic effects. Hypercholesterolemic rats were fed with *C. cardunculus* leaves aqueous extract at the amount of 150, 300, and 60 mg/kg (Mocelin et al., 2016). The extracts exhibited DPPH scavenging activity with an IC_{50} value of 57.40 ± 2.05 μg/mL. After four weeks of treatment, the serum lipid profile showed that there was a decrease in total cholesterol and LDL-C levels. The flavonoids and phenols content decreased the activities of acyl-CoA acetyltransferase and HMG-CoA reductase in the hypercholesterolemic rats. It decreased the availability of cholesterol esters to form VLDL, which caused a reduction in the secretion of VLDL from the liver (Mocelin et al., 2016).

Eclipta prostrata (L.) L. leaf extract was measured its hypolipidemic activity (Dhandapani, 2007). The phytochemical screening had shown the presence of saponins, alkaloids, flavonoids, phytosterols, and tannins in the leaf extract. Atherogenic diet caused an increase in total cholesterol and total protein and decreased serum HDL-cholesterol level in rats. Daily administration of the aqueous extract in the dose 100 and 200 mg/kg increased the rats' HDL level and reduced protein level, triglycerides, and total cholesterol significantly. It had also shown an increase in the atherogenic index. The saponins may contribute to the hypolipidemic effect of the plant extract (Dhandapani, 2007).

Emilia praetermissa Milne-Redh had shown its antihyperlipidemic effect *via* its aqueous leaf extract. The extract at doses of 100 mg/kg, 200 mg/kg, and 400 mg/kg were fed to male albino rats. As a result, the extract reduced the levels of plasma atherogenic index, total cholesterol, LDL, and triglycerides, and raised the level of HDL significantly when compared with the hyperlipidemic group. The hypolipidemic activity might due to the cholesterol-lowering effect of the extract, which may be portrayed by tannins, terpenoids, and flavonoids content. Terpenoid acts as an intermediate in cholesterol synthesis. It regulates the degradation of HMG-CoA reductase activity, which is the main enzyme in cholesterol synthesis (Ngozi et al., 2013).

Alcohol extract (IrA) and hexane extract (IrH) of *Inula racemosa* Hook F. roots at the dose of 100 mg/kg was administered to guinea pigs to observe the extracts' hypolipidemic effect (Mangathayaru et al., 2009). IrA showed antihyperlipidemic activity by reducing lipid peroxidation and lipid uptake. It decreased foam cell formation and led to a reduction of fatty streak formation. Meanwhile, IrH exhibited more significant activity in enhancing HDL-C ($p < 0.001$) than in reducing LDL levels. Based on the effects of the extracts on coronary artery histopathology, IrA and IrH had shown a replacement in a muscular pattern which is the type of primary medial destruction in early atherosclerosis. It also caused the cardiac tissue to be devoid of fatty degeneration. The presence of the phenolic compounds contributes to the inhibition of LDL oxidation and prevent the degradation and uptake of oxidized LDL by macrophages (Mangathayaru et al., 2009).

Launaea intybacea (Jacq.) Beauverd exhibited curative and preventive activity against hyperlipidemia (Devi and Muthu, 2015). Its ethanolic extract of the whole plant reduced cardiac risk ration, plasma lipid, and lipoprotein profile. It increased the HDL level, which responsible for neutralizing atherogenic effects of oxidized LDL, in addition to inhibiting LDL oxidation and reversing cholesterol transport. It also reduced free cholesterol and ester levels. Its lipid-lowering activity was due to its inhibition of hepatic cholesterogenesis or due to its ability to increase fecal sterol excretion (Devi and Muthu, 2015).

Vasorelaxant and Vasodilation Action

Excessive contraction of vessels can cause increases in pressure that may lead to hypertension. Vasorelaxant facilitates the vasodilation of the contracted vessel to ensure the ease of blood flow through the blood vessels. Vascular smooth muscle relaxation is one of the mechanisms for treatment and prevention of hypertension, with most of the treatments were focusing on impeding vascular smooth muscle contraction (Goodman, 1996). A few plant species from Asteraceae and Lamiaceae exhibited vasorelaxant activity. The plants from the Asteraceae family are *Artemisia campestris* L., *Bidens pilosa* L., *Chrysanthemum* x *morifolium* Ramat. Hemsl., and *Pectis brevipedunculata* Sch. Bip. The plants from the Lamiaceae family are *Agastache mexicana* (Kunth.) Lint. and Epling, *C. vulgare* L. (syn. *Calamintha vulgaris* (L.) Druce), *Isodon rugosus* (Wall. Ex Benth.) Codd, *Lepechinia caulescens* (Ortega) Epling, *Melissa officinalis* L., *Orthosiphon aristatus* (Blume) Miq. (syn. *Orthosiphon stamineus* Benth.), *Phlomoides bracteosa* (Royle ex Benth.) Kamelin and Makhm. (syn. *Phlomis bracteosa* (Royle ex Benth.) Kamelin and Makhm.), *Plectranthus hadiensis* (Forssk.) Schweinf. ex Sprenger (syn. *Coleus forskohlii* Willd.), *Pogostemon elsholtzioides* Benth, *Satureja cuneifolia* Ten. (syn. *Satureja obovata* Lag.), *Sideritis raeseri* Boiss. and Heldr., and *Ziziphora clinopodioides* Lam.

Agastache mexicana (Kunth.) Lint. and Epling is a medicinal plant species from the Lamiaceae family that can treat hypertension and anxiety conditions. The antihypertensive activity of the dichloromethane extract of *A. mexicana* (DEAm) and its isolated compound, ursolic acid were determined in the male rat (Flores-Flores et al., 2016). The extract exhibited relaxant activity on noradrenaline bitartrate 0.1 μM and potassium chloride (KCl) 80 mM pre-contracted aortic rings which suggest that the extract exhibited vasodilation effect through several receptors, such as the augment of free cytosolic Ca^{2+}levels. The extract inhibited the vasoconstriction caused by noradrenaline bitartrate and potassium chloride (Hernandez-Abreu et al., 2013). Ursolic acid evoked a significant decrease in systolic blood pressure (SBP) and

diastolic blood pressure (DBP) with no change in the hypertensive rat. This action was due to its diuretic effect in relieving the hypertension condition (Somova et al., 2003).

The aqueous extract of *Artemisia campestris* L. aerial parts (AcAE) has a hypotensive and antihypertensive effect due to its vasodilatory effect (Dib et al., 2017). The extract contains a high amount of polyphenols such as mono-and di-cinnamoyl compounds with the highest concentration of 3,5-dicaffeoylquinic (isochlorogenic A) as its constituent. Meanwhile, the major flavonoids in the extract were (5-caffeoylquinic) chlorogenic acid **(11)** and vicenin-2 (apigenin 6,8-di-C-glucoside) **(16)**. Daily administration of 150 mg/kg of AcAE on *L*-NAME hypertensive rats prevented hypertension by reducing SBP from 170 to 114 mm Hg. The extract at the dose of 40 mg/kg reduced SBP and DBP without affecting heart rate. The extract caused vasorelaxation *via* inhibition of calcium influx through voltage-operated calcium channels and the calmodulin-NO-sGC-PKG pathway. Besides, the extract also activated intracellular calcium mobilization into the sarcoplasmic reticulum (Dib et al., 2017).

Based on one of the studies on *Bidens pilosa* L., the plant exhibited a vasorelaxant effect on precontracted rat aorta induced by the KCl (Nguelefack et al., 2005). Besides, it also exhibited vasodilating activity on norepinephrine-induced tonic contraction. The endothelium of the vascular managed to secrete contractile factors and relaxant that caused regulation of vascular tone. The chemical and physical stimulations are responded by the endothelial cells, by producing prostacyclin, nitric oxide, and bradykinin which are the relaxant factors (Corvol et al., 1993; Dimo et al., 2001).

Clinopodium vulgare L. was used in *in vivo* and *in vitro* studies to understand its antihypertensive activity (Khan et al., 2018). The administration of *C. vulgaris* crude extract and fractions on normotensive and high salt-induced hypertensive rats reduced the rats' mean arterial pressure (MAP). It has a distinct effect on hypertensive rats compared to the normotensive rats. At the dose of 1, 3, 10, and 30 mg/kg, the extract had shown an antihypertensive effect in hypertensive rats with the most significant activity exhibited by the extract at the dose of 10 and 30 mg/kg. The vasodilatory effect of the extract (EC_{50}:0.27 mg/mL) in the extracted rat aorta was endothelium-dependently. The extracts worked by inhibiting the high K^+ precontraction and rightward shifted Ca^{2+} concentration-response curves which have an identical mechanism to verapamil. The antihypertensive effect that was showed by *C. vulgaris* is due to the vasodilation effect that involves muscarinic receptor-linked NO and activation of tetraethylammonium (TEA)-sensitive K^+ channels, Ca^{2+} antagonism, and prostacyclin. The methanolic extract of the plant consists of quercetin **(3)** and rutin, which may act as the substance that possesses the vasodilatory effect (Khan et al., 2018).

Flower extract of *Chrysanthemum* x *morifolium* Ramat. Hemsl. exhibited a vasodilatory effect by reducing the blood pressure of cardiac hypertrophy rats (Gao et al., 2016). The major phytochemicals in this extract are 4,5-di-caffeoylquinic acid, 3,5-dicaffeoylquinic acid, luteolin-7-β-glucoside, 3-chlorogenic acid **(11)**, and apigenin-7-*O*-glucoside. A range of 75 to 150 mg/kg extract was fed to the rats for four weeks to study the effect of the extract on the rats' SBP. The dose of 150 mg/kg showed a reduction in the SBP, which was about 4% by the second week. One month administration of the extract caused a reduction in the serum-free fatty acid (FFA) by 18.9% to 29.8%, and myocardial FFA level by 5.4% to 16.0%. In addition to the extract activity in inhibiting myocardial hypoxia-inducible factor-1α (HIF-1α) expression, the extract also caused subsequent modulation of some peroxisome proliferator-activated receptor α (PPARα)-mediated gene expression; a decreased in the glucose transporter-4 (GLUT-4) protein expression and an increased in the pyruvate dehydrogenase kinase-4 (PDK-4) and carnitine palmitoyltransferase-1a (CPT-1a) protein expression. (Gao et al., 2016).

Orthosiphon aristatus (Blume) Miq. contains sinensetin **(17),** which is essential for vasorelaxation activity (Yam et al., 2016; Yam et al., 2018). The studies measured the vasorelaxant effect of the compound by conducting a pre-contraction aortic ring assay. The presence of antagonists has shown the mechanism of the vasorelaxant effect of sinensetin **(17)**. Sinensetin **(17)** had exhibited a relaxation effect of potassium chloride-induced endothelium-intact aortic rings and phenylephrine-induced aortic ring with or without the endothelium. The study showed that sinensetin **(17)** exhibited a vasorelaxant effect *via* antagonization of aortic ring contraction through direct and indirect vasorelaxation. The pathways that were involved in this vasorelaxant activity were NO/sGC/cGMP pathways. Sinensetin **(17)** at a dose of 0.262 μg/mL caused the vasodilatory effect (Yam et al., 2016; Yam et al., 2018).

The vasodilatory effect of essential oil of the *Pectis brevipedunculata* Sch. Bip aerial parts (EOPB) was identified (Pereira et al., 2013). The essential oil is rich with citral content, which consists of neral **(18)** and geranial **(19),** followed by limonene and α-pinene. The vasodilator activity of EOPB and citral was measured using aortic rings obtained from Wistar Kyoto (WKY) rats. EOPB and citral exhibited relaxation to the phenylephrine-induced endothelium-intact aortic rings with an IC_{50} value of 0.044 ± 0.006% and 0.024 ± 0.004%, respectively. Meanwhile, EOPH and citral exhibited relaxation to the phenylephrine-induced denuded aortic rings with an IC_{50} value of 0.093 ± 0.015% and 0.021 ± 0.004%, respectively. The extract mechanism of activity was through the NO/cyclic GMP pathway. Meanwhile, the citral mechanism of activity was by blocking voltage-dependent L-type Ca^{2+} channels that reduced calcium influx. The high concentrations of EOPB caused vasorelaxation of endothelium-independent which predominated the endothelium-dependent pathway (Pereira et al., 2013).

Phlomoides bracteosa (Royle ex Benth) Kamelin and Makhm. has few phytochemicals which had the vasorelaxant effects, which are marrubiin **(20)**, phlomeoic acid, and new components (RA and RB) (Khan et al., 2012). The whole plant was powdered and extracted using methanol to produce its extract and examined its activity using rat thoracic aorta. The EC_{50} values of 23.4 and 36.7 μg/mL of marrubiin **(20)** had shown a relaxant effect upon the phenylephrine-induced contraction

and inhibited the K^+. Marrubiin **(20)** in the concentration of 3.0 to 10 μg/mL induced rightward shift of the Ca^{2+} channels. Marrubiin **(20)**, phlomeoic acid, and RA exhibited a more potent effect against K^+-induced contractions, compared with phenylephrine, which indicated that it had a greater efficacy in blocking the voltage-sensitive Ca^{2+} channels. Among all four phytochemicals studied, the marrubiin **(20)** was most potent for its vasodilator activity. It can be used in further studies to test its extent of vasodilation activity in the future (Khan et al., 2012).

Satureja cuneifolia Ten. is a plant species from the Satureja genus. Its constituent, eriodictyol **(21)**, possessed a vasodilatory effect in the rat aorta (De Rojas et al., 1999). The concentration of eriodictyol **(21)** 10^5 M and 5×10^5 M showed the inhibitory effect of calcium chloride, $CaCl_2$ in the concentration-response curve. It possessed a weak inhibition in the calcium from the sarcoplasmic reticulum whereby showing off a light relaxant effect. The final results of the study indicated that the partial mechanism of the vasodilatory effect was due to its inhibition of enzyme protein such as myosin light chain kinase that related to protein kinase C or inhibition of calcium influx (De Rojas et al., 1999).

The dichloromethane extract of *Ziziphora clinopodioides* Lam. (ZDCE) had shown a significant effect on the inhibition of extracellular Ca^{2+} induced contraction in the pre-contracted rings by high KCl and phenylephrine. It also caused an inhibition of intracellular Ca^{2+} release to the phenylephrine. Among the hexane, dichloromethane, and aqueous extracts, ZDCE had shown the endothelium-independent vasodilation properties that occurs due to the extracellular Ca^{2+} influx *via* the voltage and receptor-operated Ca^{2+} channels, causing Ca^{2+} inhibition from the stores of the intracellular and lastly *via* opening the K^+ channels which are voltage-dependent (Senejoux et al., 2010).

Anticoagulation and Anti-Thrombosis Activity

A series of zymogens are involved in the blood coagulation process. Proteolysis caused the conversion of zymogens into active enzymes that caused the production of thrombin, which can lead to the conversion of fibrinogen into fibrin (Rand et al., 1996). Enzymes are involved in mediating the blood coagulation of damaged tissues. Factor VII (FVII) binds to uncovered tissue factor (TF), which triggers the development of thrombin that causes coagulation of blood. Anticoagulant inhibits thrombin generation and fibrin formation. An ideal clinical anticoagulant should inhibit thrombin activity without induced bleeding. Platelets and other mediators play an important role in thrombosis and cardiovascular diseases. Based on reported studies, few plants from the plant family of Asteraceae and Lamiaceae plant family possess an anticoagulant effect. The plants' species from the family of Asteraceae are *Erigeron canadensis* L., *Flaveria bidentis* (L.) Kuntze, *Leuzea carthamoides* Willd. DC., and *Tridax procumbens* (L.) L. The plants' species from the Lamiaceae family are *Leonotis leonurus* (L.) *R.Br., S. miltiorrhiza Bunge,* and *Thymus zygis* L.

Erigeron canadensis L. consists of different types of flavonoids and tannins on top of the essential oil that is present. Its polyphenolic-polysaccharide preparation was isolated from its flowering part and was determined its anticoagulant activity *via in vivo* assay (Pawlaczyk et al., 2011). The plant preparation had shown its anti-platelet activity specifically towards the cyclooxygenase pathway that was induced by the arachidonic acid (AA), which is similar to acetylsalicylic acid activity. The assay was conducted on standardized human plasma by measuring prothrombin time (PT) and partial thromboplastin time (aPTT). The plant preparation inhibited plasma clot formation in aPTT and PT at the concentration of 390 μg/mL and 1.56 mg/mL, respectively. The plant preparation also exhibited significant anti-IIa activity mediated by the cofactor II of heparin. Further fractionation of the plant preparation at the concentration of 50 μg/mL, showed higher anticoagulation activity in aPTT test corresponded to 7 to 9 IU/mg of 5^{th} International Standard for Unfractionated Heparin (ISUH). *In vivo* studies also showed that the dose of 50 mg/mL of the plant preparation has the anticoagulant effect in the rat. These anticoagulant activities are essential in patients suffering from deep vein thrombosis, and those had already been resistant to the acetylsalicylic derivatives drugs (Pawlaczyk et al., 2011).

From the plant *Flaveria bidentis* (L.) Kuntze, the anticoagulant activity of its sulfated flavonoids, quercetin 3,7,3′,4′-tetrasulfate (QTS) and quercetin 3-acetyl-7,3′,4′-trisulfate (ATS) was investigated (Guglielmone et al., 2002). Thrombin time (TT), aPTT, antithrombin III (ATIII), PT, and heparin cofactor II (HCII) activation were measured. The flavonoids exhibited HCII activation by acting as agonists with higher activation observed exhibited by QTS than ATS (Guglielmone et al., 2002).

Marrubiin **(20)** was isolated from *Leonotis leonurus* (L.) R. Br., and both were tested *via in vivo* and *in vitro* studies to determine their anticoagulation reaction (Mnonopi et al., 2011). The marrubiin **(20)** and the plant extract suppressed the inflammatory markers, platelet aggregation, and coagulation marker while prolonged aPTT. The extract and marrubiin **(20)** in the concentration of 100 μg/mL were administered on rats. It was observed that the platelet adhesion was reduced in a dose-dependent manner, together with a depletion in protein secretion, fibrin formation, and d-dimer. The intracellular levels of Ca^{2+} were also reduced in a concentration-dependent manner and inhibited the calcium mobilization that was induced by thrombin by 50 to 200 μg/mL. This study shows that marrubiin **(20)** and the extract may have a direct inhibitory effect upon the synthase activity of cyclooxygenase or thromboxane due to the suppression of thromboxane B2 production (Mnonopi et al., 2011).

Leuzea carthamoides Willd. DC. consists of eriodictyol **(21)** and patuletin **(22),** which have similar antiplatelet activity (Koleckar et al., 2008). The leaf parts of the plant exhibited antiplatelet activity by inhibiting arachidonic acid and collagen-induced platelet aggregation. It showed a more potent antiplatelet activity in the collagen-induced aggregation compared to the arachidonic acid-induced aggregation. The mechanism that was exhibited by eriodictyol **(21)** is the decrease in antiplatelet potency that was caused by glucosylation process. Based on the study, apigenin and

quercetin formed from the glycosylation process exhibited a lesser activity compared to their aglycons (Guerrero et al., 2005). Based on the study, the extract of the *L. carthamoides* has a potent antithrombotic effect due to the presence of the antithrombotic agents, not due to the effect of the specific flavonoids that are present in the extract. The plant had shown a strong inhibition activity upon the platelet aggregation that was induced by adenosine diphosphate (ADP) (Koleckar et al., 2008).

Salvia miltiorrhiza Bunge consists of phenolic acid that is water-soluble, which is the salvianolic acid **(23)** (SAA). The study examined the effect of SAA in the antiplatelet and antithrombotic effect (Fan et al., 2010). In the *in vitro* assay, Tyrode's solution was used to study the antiplatelet properties using a platelet aggregometer. The maximum height reached *via* the aggregation curves determines the extent of platelet aggregation of SAA. All tests showed that SAA had an inhibitory effect on ADP, thrombin, and platelet aggregation that was induced by AA. The compound inhibited ADP-induced platelet aggregation of rats with an IC_{50} value of 390 μg/mL, whereby it inhibited the thrombin-induced platelet aggregation with an IC_{50} value of 912 μg/mL. SAA (1,000 μg/mL) exhibited mild inhibitory activity on AA-induced platelet aggregation. In the *in vivo* study, the administration of SAA at dose 2.5, 5, and 10 mg/kg *via* intravenous caused dose-dependent inhibition upon the platelet aggregation in the rats. A similar observation with the *in vitro* study was observed. This study claimed that the SAA antiplatelet activity was due to the interference to a common signaling pathway, then directly binding to thrombin, ADP or AA to their respective receptors. The inhibition of ADP from dense granules of activated platelet might be one of the factors of the anti-aggregating properties of SAA (Fan et al., 2010).

The anticoagulant activity of *Tridax procumbens* (L.) L. was examined (Naqash and Nazeer, 2011). Sulfated polysaccharide isolated from the leaf extract of *T. procumbens* acts as an anticoagulant on heparin and chondroitin sulfate. Based on the *in vivo* assay, the activated aPTT had been prolonged to 113 s at 100 μg/mL by the sulfated polysaccharides from *T. procumbens*, which is almost 4-fold higher than the standard group. The sulfate group causes the anticoagulant activity but it is dependent on the sulfate group position in the chemical structure (Naqash and Nazeer, 2011).

Diuresis Action

Diuresis is an important mode of treatment for cardiovascular diseases, such as hypertension. It can increase the urinary volume and has a fewer side effect compared to others. Diuretics usually used as an independent drug or a combination with other drugs of the same mechanism of action in easing various conditions such as congestive heart failure, ascites, and pulmonary edema as well. Thus, few of the available diuretics cause adverse effects such as an imbalance of electrolytes, alterations in metabolic status, and some may impair the sexual function (Gupta and Neyses, 2005; Morganti, 2005).

Based on the previous studies of Asteraceae and Lamiaceae plant species, the number of plant species that exhibits diuretic effects is lesser than those other mechanisms, such as antioxidants, antihyperlipidemic, and vasorelaxant. The plant species that possess diuretic effect from the Asteraceae family are *Chamaemelum nobile* (L.) All., *Chrysanthemum* x *morifolium* Ramat. Hemsl., and *Tanacetum vulgare* L. and the plant species from Lamiaceae family are *Ajuga integrifolia* Buch.-Ham. ex D. Don (syn. *Ajuga remota* Benth.), *Anisomeles indica* (L.) Kuntze, and *Plectranthus amboinicus* (Lour) Spreng. The diuretic effect of *C. nobile* was assessed by examining the rats' urine after fasted overnight (Zeggwagh et al., 2009). After repeated oral administration of 140 mg/kg aqueous plant extract for three weeks, the extract showed a diuretic and hypotensive effect.

Plectranthus amboinicus (Lour) Spreng is a plant species from the Lamiaceae family. Its leaf aqueous, alcoholic, and ethyl acetate extracts increased urine volume and decreased serum sodium level of albino rats after 24 h compared to the moduretic drug (El-Hawary et al., 2012). Meanwhile, the extracts did not show any significant effect on the rats' potassium level. Based on the study, the ethyl acetate fraction was more potent as a diuretic group with better electrolyte balance (El-Hawary et al., 2012).

Tanacetum vulgare L. leaf extract was studied on its ability to act as a diuretic on rats (Lahlou et al., 2007). Water extract of the plant at a dose of 100 mg/kg was administered orally to the male Wistar rats. An increase in urine output was identified after 24 h of administration of the extract with a similar amount compared to furosemide administration. The extract had caused an increased level of Na^+ and K^+ in the urine, compared to furosemide, which has only an increase in Na^+. In contrast, the extract does not affect Na^+ and K^+ levels of the plasma. The diuretic effect occurs due to the renal tubular suppression upon its tendency for reabsorption of electrolytes and water into the bloodstream. The plant extract does not cause any renal toxicity as repeated dosing upon the rat for nine consecutive days. Thus, it requires a clinical study to ensure that its safety profile matches up with the physiology of humans and the long duration that patients usually take on diuretics. Different studies have shown that *T. vulgare* consists of flavonoids, tri- and sesquiterpene lactones and isoprenoids, polysaccharides, saponins, and polyphenols. Thus, it is unsure of which compound contributes to the diuretic effect of this extract (Lahlou et al., 2007).

TOXICOLOGICAL STUDIES

There are plenty of pharmacological studies on the Asteraceae and Lamiaceae plant species on its cardiovascular effects, while the toxicological aspects of these species have yet to be explored. Most of the people believe that medicines that are from medicinal plants or herbal medicines are always safe, simply due to the belief that all plants are safe to be consumed. This does not apply to all the medicinal plants. Medicinal plants have their toxicity nature depending on their dosage and method of extraction (Chanda et al., 2015).

Based on the studies in this review, few had included its toxicology test results and had herbal drug interaction during the administration of the medicinal plant extract in specific conditions. Traditional preparation methods of the medicinal plants into a consumable substance take different toxicity levels. The level of toxicity differs according to the solvents used. Thus it

is important to choose the appropriate solvent either for *in vivo* or *in vitro* experiments.

Acute toxicity test of *Artemisia campestris* L. showed no symptoms of toxicity upon its aqueous extract administration of doses 1, 2, 4, and 6 g/kg (Dib et al., 2017).Based on the acute toxicological studies on *C. crepidioides* (Benth.) S. Moore, it showed that consumption of the plant extract at a dose of 2500 mg/kg was safe. During the observation on the first 8 h, within the interval of every 8 h and upon the next 72 h, no significant change in the animal behavior or mortality was observed (Bahar et al., 2016). It showed that the dose is safe in the *in vivo* testing.

Acute toxicity study was conducted on the ethanolic extract of *Launaea intybacea* (Jacq.) Beauverd (syn. *Lactuca runcinata* DC.) in 1% gum acacia upon rats (Devi and Muthu, 2015). Subsequent administration of the extract at dose 2,000 mg/kg body weight of rats for 14 days showed no toxicity effect, and this dose had helped in the reduction of total cholesterol and elevated the HDL level.

The plant in this study that showed toxicity is *Leonurus cardiaca* L. Lavandulifolioside, the active component of *L. cardiaca,* showed moderate toxicity at the amount of 1,000 mg/kg on the LD_{50} when given intravenously (Wojtyniak et al., 2013). The butanol extract of the plant showed higher toxicity with LD_{50} of 400 mg/kg when administered intravenously compared to LD_{50} of 2,000 mg/kg when administered orally. This showed that the intake of this drug *via* intravenous possess a higher toxicity possibility than *via* oral intake (Wojtyniak et al., 2013).

Aqueous extract of *Salvia scutellarioides* Kunth was administered on mice in two doses of 1 or 2 g/kg for 28 days (Ramirez et al., 2007). The administration showed no mortality. The study also claimed that if *S. scutellarioides* is taken together with other diuretics drug, it might worsen hypokalemia symptoms or increase in digoxin related arrhythmias in patients because of the herb-drug interactions. (Ramirez et al., 2007). *Teucrium polium* L. is known for its risk of hepatotoxicity due to hepatocyte necrosis occurs massively in the central lobular area such as lymphocyte inflammatory inflate, bile duct proliferation, and bile retention. Clinical signs are often seen in the usage of this plant; thus, proper usage of this plant on the therapeutic range would resolve the problem.

CONCLUSION

The last few decades have witnessed several rapid changes in the traditional use of the medicinal plant in developing countries. However, some of the traditional use of the medicinal plant is undocumented that results in the decline of knowledge and making it unreliable. Therefore, it has become necessary to document the knowledge and shared them entirely to ensure their quality and preservation. Based on this review, medicinal plants were widely consumed using decoction or taken orally as a raw product of fruits, leaves, and roots. Most of the plants from Asteraceae and Lamiaceae family are rich in flavonoids and terpenoids, together with other phytochemicals that act as the inducer of the mechanism in alleviating cardiovascular diseases. The plants have a strong antioxidant effect, followed by anti-hyperlipidemic, vasodilation, antithrombotic, and diuretic effects which are mechanisms that are closely related in resolving cardiovascular diseases such as coronary heart diseases (CHD), atherosclerosis, hypertension, and others. As the medicinal plant being beneficial for treating human ailments, we should not waste these resources by leaving them to grow wild and perish, without utilizing them for better pharmaceutical development in the future.

FUTURE STUDIES

Based on the evidence-based review on the use of medicinal plant from the plant family of Asteraceae and Lamiaceae in cardiovascular diseases, we hope that information from this review will facilitate future research initiatives to develop new medicinal plant-based medication for cardiovascular disease treatment or continue with any clinical studies to prove the effectiveness of this medicinal plant upon humans. The clinical trial needs to be performed to have a better knowledge of their safety and efficacy to ensure that it can be beneficial to the human race.

AUTHOR CONTRIBUTIONS

JM obtained the pieces of literature and wrote the manuscript while NA and KH edited the manuscript.

ACKNOWLEDGMENTS

The authors would like to thank Universiti Kebangsaan Malaysia (UKM) for the financial support under grant number DIP-2018-029 and for allowing us to use all its facilities.

REFERENCES

Çoruh, N., Sag˘Dıçog˘Lu Celep, A. G., Özgökçe, F., and İşcan, M. (2007). Antioxidant Capacities of Gundelia Tournefortii L. Extracts and Inhibition on Glutathione- S-Transferase Activity. *Food Chem.* 100, 1249–1253. doi: 10.1016/j.foodchem.2005.12.008

Abdala, S., Martin-Herrera, D., Benjumea, D., and Gutierrez, S. D. (2012). Diuretic Activity of Some Smilax Canariensis Fractions. *J. Ethnopharmacol.* 140, 277–281. doi: 10.1016/j.jep.2012.01.017

Akinpelu, B., Apata, J., Iwalewa, E., and Ovedapo, O. (2016). Evaluation of Anti-Hyperlipidemic Potential of Ethanolic Leaf Extract of *Clerodendrum volubile* P. Beauv. Ife. *J. Sci.* 18, 789–800.

Akowuah, G. A., Ismail, Z., Norhayati, I., and Sadikun, A. (2005). The Effects of Different Extraction Solvents of Varying Polarities on Polyphenols of Orthosiphon Stamineus and Evaluation of the Free Radical-Scavenging Activity. *Food Chem.* 93, 311–317. doi: 10.1016/j.foodchem.2004.09.028

Amiri, H. (2011). The in Vitro Antioxidative Properties of the Essential Oils and Methanol Extracts of Satureja Macrosiphonia Bornm. *Natural Prod. Res.* 25, 232–243. doi: 10.1080/14786410903374694

Ardestani, A., and Yazdanparast, R. (2007). Antioxidant and Free Radical Scavenging Potential of Achillea Santolina Extracts. *Food Chem.* 104, 21–29. doi: 10.1016/j.foodchem.2006.10.066

Atawodi, S. E., Adepoju, O. A., and Nzelibe, H. C. (2017). Antihyperglycaemic and Hypolipidemic Effect of Methanol Extracts of Ageratum Conyzoides L (Asteraceae) in Normal and Diabetic Rats. *Trop. J. Pharmaceut. Res.* 16, 989–996. doi: 10.4314/tjpr.v16i5.4

Audu, S., Taiwo, A., Ojuolape, A., Sani, A., Bukola, A., and Mohammed, I. (2012). A Study Review of Documented Phytochemistry of Vernonia Amygdalina (Family Asteraceae) as the Basis for Pharmacologic Activity of Plant Extract. *J. Natural Sci. Res.* 2, 1–9.

Bahar, E., Siddika, M. S., Nath, B., and Yoon, H. (2016). Evaluation of in Vitro Antioxidant and in Vivo Antihyperlipidemic Activities of Methanol Extract of Aerial Part of *Crassocephalum crepidioides* (Asteraceae) Benth S Moore. *Trop. J. Pharmaceut. Res.* 15, 481–488. doi: 10.4314/tjpr.v15i3.8

Bandyopadhyay, M., Chakraborty, R., and Raychaudhuri, U. (2007). A Process for Preparing a Natural Antioxidant Enriched Dairy Product (Sandesh). *LWT-Food Sci. Technol.* 40, 842–851. doi: 10.1016/j.lwt.2006.05.007

Bardai, S. E., Lyoussi, B., Wibo, M., and Morel, N. (2001). Pharmacological Evidence of Hypotensive Activity of *Marrubium vulgare* and *Foeniculum vulgare* in Spontaneously Hypertensive Rat. *Clin. Exp. Hypertension* 23, 329–343. doi: 10.1081/CEH-100102671

Belmouhoub, M., Chebout, I., and Iguer-Ouada, M. (2017). Antidiabetic and Anti-Hypercholesterolemic Effects of Flavonoid-Rich Fractions of *Rosmarinus officinalis* in Streptozotocin-Induced Diabetes in Mice. *Phytotherapie* 16 (4), 1–7. doi: 10.1007/s10298-017-1103-6

Bora, K. S., and Sharma, A. (2011). Evaluation of Antioxidant and Free-Radical Scavenging Potential of Artemisia Absinthium. *Pharmaceut. Biol.* 49, 1216–1223. doi: 10.3109/13880209.2011.578142

Cantino, P., Harley, R., and Wagstaff, S. (1992). "Genera of Labiatae Status and Classification" in *Advances in Labiate Science* Eds. R. M. Harley and T. Reynolds (Royal Botanic Gardens Kew), 511–522.

Ceaser, E., Ramachandran, A., Levonen, A., and Darley-Usmar, V. (2003). Oxidized low-density lipoprotein and 15-deoxy-delta 12,14-PGJ2 increase mitochondrial complex I activity in endothelial cells. *Am. J. Physiol. Heart Circulatory Physiol.* 285, H2298–H2308. doi: 10.1152/ajpheart.00508.2003

Chanda, S., Parekh, J., Vaghasiya, Y., Dave, R., Baravalia, Y., and Nair, R. (2015). Medicinal Plants-from Traditional Use to Toxicity Assessment: A Review. *Int. J. Pharmaceut. Sci. Res.* 6, 2652–2670. doi: 10.13040/IJPSR.0975-8232.6 (7).2652-70

Cifuentes, F., Paredes, A., Palacios, J., Munoz, F., Carvajal, L., Nwokocha, C. R., et al. (2016). Hypotensive and Antihypertensive Effects of a Hydroalcoholic Extract from Senecio Nutans Sch. Bip. (Compositae) in Mice: Chronotropic and Negative Inotropic Effect, a Nifedipine-Like Action. *J. Ethnopharmacol.* 179, 367–374. doi: 10.1016/j.jep.2015.12.048

Citoglu, G. S., Coban, T., Sever, B., and Iscan, M. (2004). Antioxidant Properties of Ballota Species Growing in Turkey. *J. Ethnopharmacol.* 92, 275–280. doi: 10.1016/j.jep.2004.03.012

Corvol, P., Alhenc-Gelas, F., and Soubrier, F. (1993). L'endothélium, Site De Production Et De Métabolisme Des Peptides Vaso-Actifs. doi: 10.4267/10608/2808

Craig, W. J. (1999). Health-Promoting Properties of Common Herbs. *Medecine/Sciences 9, 1050-1060. Am. J. Clin. Nutr.* 70, 491s–499s. doi: 10.1093/ajcn/70.3.491s

De Rojas, V. R. S., Somoza, B., Ortega, T., Villar, A. M., and Tejerina, T. (1999). Vasodilatory Effect in Rat Aorta of Eriodictyol Obtained from Satureja Obovata. *Planta Med* 65, 234–238. doi: 10.1055/s-1999-13986

De Souza, P., Crestani, S., Da Silva, R. D. C. V., Gasparotto, F., Kassuya, C. ,. A. L., Da Silva-Santos, J. E., et al. (2013). Involvement of Bradykinin and Prostaglandins in the Diuretic Effects of *Achillea millefolium* L. (Asteraceae). *J. Ethnopharmacol.* 149, 157–161. doi: 10.1016/j.jep.2013.06.015

Devi, J., and Muthu, A. K. (2015). Hypolipidemic Effect of Ethanolic Extract from Whole Plant of Lactuca Runcinata (Dc.) in Atherogenic Diet Induced Hyperlipidemic Rats. *Afr. J. Pharm. Pharmacol.* 9, 1080–1087. doi: 10.5897/AJPP2015.4447

Dhandapani, R. (2007). Hypolipidemic Activity of Eclipta Prostrata (L.) L. Leaf Extract in Atherogenic Diet Induced Hyperlipidemic Rats. *Indian J. Exp. Biol.* 45 (7), 617–619.

Dib, I., Tits, M., Angenot, L., Wauters, J. N., Assaidi, A., Mekhfi, H., et al. (2017). Antihypertensive and Vasorelaxant Effects of Aqueous Extract of Artemisia Campestris L. From Eastern Morocco. *J. Ethnopharmacol.* 206, 224–235. doi: 10.1016/j.jep.2017.05.036

Dimo, T., Azay, J., Tan, P. V., Pellecuer, J., Cros, G., Bopelet, M., et al. (2001). Effects of the Aqueous and Methylene Chloride Extracts of Bidens Pilosa Leaf on Fructose-Hypertensive Rats. *J. Ethnopharmacol.* 76, 215–221. doi: 10.1016/S0378-8741(01)00229-X

Dubey, M. P., Srimal, R. C., Nityanand, S., and Dhawan, B. N. (1981). Pharmacological Studies on Coleonol, a Hypotensive Diterpene from Coleus Forskohlii. *J. Ethnopharmacol.* 3, 1–13. doi: 10.1016/0378-8741(81)90010-6

El-Hawary, S. S., El-Sofany, R. H., Abdel-Monem, A. R., Ashour, R. S., and Sleem, A. A. (2012). Polyphenolics content and biological activity of Plectranthus amboinicus (Lour.) spreng growing in Egypt (Lamiaceae). *Pharmacogn J.* 4, 45–54. doi: 10.5530/pj.2012.32.9

Ersoy, S., Orhan, I., Turan, N., Sahan, G., Ark, M., and Tosun, F. (2008). Endothelium- Dependent Induction of Vasorelaxation by *Melissa officinalis* L. Ssp. Officinalis in Rat Isolated Thoracic Aorta. *Phytomedicine* 15, 1087–1092. doi: 10.1016/j.phymed.2008.05.007

Estrada-Soto, S., Navarrete-Vazquez, G., Leon-Rivera, I., Rios, M., Aguilar-Guadarrama, B., Castillo-Espana, P., et al. (2012). Antihypertensive Effect of Lepechinia Caulescens Extract on Spontaneously Hypertensive Rats. *Phytopharmacol* 2, 170–178.

Ezzoubi, Y., Bousta, D., Lachkar, M., and Farah, A. (2014). Antioxidant and Anti-Inflammatory Properties of Ethanolic Extract of Lavandula Stoechas L. From Taounate Region in Morocco. *Int. J. Phytopharmacol* 5, 21–26.

Fan, H. Y., Fu, F. H., Yang, M. Y., Xu, H., Zhang, A. H., and Liu, K. (2010). Antiplatelet and Antithrombotic Activities of Salvianolic Acid A. *Thromb. Res.* 126, e17–e22. doi: 10.1016/j.thromres.2010.04.006

Fearon, I. M., and Faux, S. P. (2009). Oxidative Stress and Cardiovascular Disease: Novel Tools Give (Free) Radical Insight. *J. Mol. Cell. Cardiol.* 47, 372–381. doi: 10.1016/j.yjmcc.2009.05.013

Fidele, K. Z., Andre, K. B., Yao, D. J., and Michel, O. A. (2012). Action of Hydroethanolic Leaves Extract of *Solenostemon monostachyus* (Lamiaceae) on Cardiovascular System of Mammalians: Blood Pressure Lowering Effects. *Int. J. Pharm. Biol. Sci.* 2, 310–320.

Fintelmaan, V. (1996). Antidyspeptic and Lipid-Lowering Effect of Artichoke Leaf Extract. *Z. Fur Allgemeinmed* 72, 3–19.

Flores-Flores, A., Hernandez-Abreu, O., Rios, M. Y., Leon-Rivera, I., Aguilar-Guadarrama, B., Castillo-Espana, P., et al. (2016). Vasorelaxant mode of action of dichloromethane soluble extract from Agastache mexicana and its main bioactive compounds. *Pharmaceut. Biol.* 54 (12), 2807–2813. doi: 10.1080/13880209.2016.1184690

Gao, T., Zhu, Z.-Y., Zhou, X., and Zxie, M.-L. (2016). Chrysanthemum Morifolium Extract Improves Hypertension-Induced Cardiac Hypertrophy in Rats by Reduction of Blood Pressure and Inhibition of Myocardial Hypoxia Inducible Factor-1alpha Expression. *Pharmaceut. Biol.* 54, 2895–2900. doi: 10.1080/13880209.2016.1190764

Gaziano, T. A., Bitton, A., Anand, S., Abrahams-Gessel, S., and Murphy, A. (2010). Growing Epidemic of Coronary Heart Disease in Low- and Middle-Income Countries. *Curr. Problems Cardiol.* 35, 72–115. doi: 10.1016/j.cpcardiol.2009.10.002

Ghannadi, A., Movahedian, A., and Jannesary, Z. (2015). Hypocholesterolemic Effects of Balangu (Lallemantia Royleana) Seeds in the Rabbits Fed on a Cholesterol- Containing Diet. *Avicenna J. Phytomed.* 5, 167–173. doi: 10.22038/ajp.2015.3913

Go, A. S., Hylek, E. M., Chang, Y., Philips, K. A., Henault, L. E., Capra, A. M., et al. (2003). Anticoagulation Therapy for Stroke Prevention in Atrial Fibrillation: How Well Do Randomized Trials Translate into Clinical Practice? *Jama* 290, 2685–2692. doi: 10.1001/jama.290.20.2685

Goldansaz, S. M., Mahboubi, A., Yazdi-Nejad, A., Jahanbakshi, M., and Mojab, F. (2018). Investigation on Total Phenolic Content, Antibacterial, and Antioxidant Activity of Ethanolic Extract of *Helichrysum leucocephalum* Boiss. *Am. J. Essential Oils Natural Prod.* 6, 20–24.

Goodman, L. S. (1996). *Goodman and Gilman"s the Pharmacological Basis of Therapeutics* (New York: McGraw-Hill).

Graf, E. (1992). Antioxidant Potential of Ferulic Acid. *Free Radical Biol. Med.* 13, 435–448. doi: 10.1016/0891-5849(92)90184-I

Guerrero, J., Lozano, M., Castillo, J., Benavente-Garcia, O., Vicente, V., and Rivera, J. (2005). Flavonoids Inhibit Platelet Function through Binding to the Thromboxane A2 Receptor. *J. Thromb. Haemostasis* 3, 369–376. doi: 10.1111/j.1538-7836.2004.01099.x

Guglielmone, H. A., Agnese, A. M., Montoya, S. C. N., and Cabrera, J. L. (2002). Anticoagulant Effect and Action Mechanism of Sulphated Flavonoids from Flaveria Bidentis. *Thromb. Res.* 105, 183–188. doi: 10.1016/S0049-3848(01)00419-4

Gupta, S., and Neyses, L. (2005). Diuretic Usage in Heart Failure: A Continuing Conundrum in 2005. *Eur. Heart J.* 26, 644–649. doi: 10.1093/eurheartj/ehi176

Hailu, W., and Engidawork, E. (2014). Evaluation of the Diuretic Activity of the Aqueous and 80% Methanol Extracts of Ajuga Remota Benth (Lamiaceae) Leaves in Mice. *BMC Complementary Altern. Med.* 14, 1–8. doi: 10.1186/1472-6882-14-135

Hernandez-Abreu, O., Torres-Piedra, M., Garcia-Jimenez, S., Ibarra-Barajas, M., Villalobos-Molina, R., Montes, S., et al. (2013). Dose-Dependent Antihypertensive Determination and Toxicological Studies of Tilianin Isolated from Agastache Mexicana. *J. Ethnopharmacol.* 146, 187–191. doi: 10.1016/j.jep.2012.12.029

Ikewuchi, J. C., and Ikewuchi, C. C. (2011). Anti-Cholesterolemic Effect of Aqueous Extract of the Leaves of Chromolaena Odorata (L) King and Robinson (Asteraceae): Potential for the Reduction of Cardiovascular Risk. *Pacific J. Sci. Technol.* 12, 385–391.

Janbaz, K. H., Arif, J., Saqib, F., Imran, I., Ashraf, M., Zia-Ul-Haq, M., et al. (2014). In-Vitro and in-Vivo Validation of Ethnopharmacological Uses of Methanol Extract of Isodon Rugosus Wall. Ex Benth. (Lamiaceae). *BMC Complementary Altern. Med.* 14, 1–12. doi: 10.1186/1472-6882-14-71

Jiang, J., Yuan, X., Wang, T., Chen, H., Zhao, H., Yan, X., et al. (2014). Antioxidative and Cardioprotective Effects of Total Flavonoids Extracted from Dracocephalum Moldavica L. Against Acute Ischemia/Reperfusion-Induced Myocardial Injury in Isolated Rat Heart. *Cardiovasc. Toxicol.* 14, 74–82. doi: 10.1007/s12012-013-9221-3

Katalinic, V., Milos, M., Kulisic, T., and Jukic, M. (2006). Screening of 70 Medicinal Plant Extracts for Antioxidant Capacity and Total Phenols. *Food Chem.* 94, 550–557. doi: 10.1016/j.foodchem.2004.12.004

Khafagy, S., Sabri, N., Soliman, F., Abou-Donia, A., and Mosandl, A. (1976). Isolation of Two Flavonoids from Achillea Santolina L. Growing in Egypt. *Pharmazie* 31, 894–895.

Khan, A.-U., Ullah, R., Khan, A., Mustafa, M. R., Hussain, J., Murugan, D. D., et al. (2012). Vasodilator Effect of Phlomis Bracteosa Constituents Is Mediated through Dual Endothelium-Dependent and Endothelium-Independent Pathways. *Clin. Exp. Hypertension* 34, 132–139. doi: 10.3109/10641963.2011.601383

Khan, S., Khan, T., and Shah, A. J. (2018). Total Phenolic and Flavonoid Contents and Antihypertensive Effect of the Crude Extract and Fractions of *Calamintha vulgaris*. *Phytomedicine* 47, 174–183. doi: 10.1016/j.phymed.2018.04.046

Khandekar, U., Tippat, S., Ghongade, R., and Dudhe, K. (2015). Chemical Composition and Pharmacognostic Study of Crude Plant Extract of Vernonia Elaeagnifolia. *Int. J. Pharma Bio Sci.* 6, B7–B15.

Khouya, T., Ramchoun, M., Hmidani, A., Amrani, S., Harnafi, H., Benlyas, M., et al. (2015). Anti-Inflammatory, Anticoagulant and Antioxidant Effects of Aqueous Extracts from Moroccan Thyme Varieties. *Asian Pacific J. Trop. Biomed.* 5, 636–644. doi: 10.1016/j.apjtb.2015.05.011

Kitic, D., Brankovic, S., Radenkovic, M., Savikin, K., Zdunic, G., Kocic, B., et al. (2012). Hypotensive, Vasorelaxant and Cardiodepressant Activities of the Ethanol Extract of Sideritis Raeseri Spp. Raeseri Boiss & Heldr. *J. Physiol. Pharmacol.* 63, 531–535.

Klein, L., O'connor, C. M., Gattis, W. A., Zampino, M., De Luca, L., Vitarelli, A., et al. (2003). Pharmacologic Therapy for Patients with Chronic Heart Failure and Reduced Systolic Function: Review of Trials and Practical Considerations. *Am. J. Cardiol.* 91, 18–40. doi: 10.1016/S0002-9149(02)03336-2

Kocarslan, A., Kocarslan, S., Aydin, M. S., Gunay, S., Karahan, M. A., Taskin, A., et al. (2016). Intraperitoneal Administration of Silymarin Protects End Organs from Multivisceral Ischemia/Reperfusion Injury in a Rat Model. *Braz. J. Cardiovasc. Surg.* 31, 434–439. doi: 10.5935/1678-9741.20160072

Koleckar, V., Brojerova, E., Rehakova, Z., Kubikova, K., Cervenka, F., Kuca, K., et al. (2008). In Vitro Antiplatelet Activity of Flavonoids from Leuzea Carthamoides. *Drug Chem. Toxicol.* 31, 27–35. doi: 10.1080/01480540701688444

Kumar, G. V. (2016). Antihyperlipidemic Activity of Leaf Extracts of *Leucas aspera* Linn. Against Dexamethasone-Induced Hyperlipidemia in Rats. *Asian J. Pharmaceut.* 10, S408–S413. doi: 10.22377/ajp.v10i03.781

Lahlou, S., Tahraoui, A., Israili, Z., and Lyoussi, B. (2007). Diuretic Activity of the Aqueous Extracts of Carum Carvi and *Tanacetum vulgare* in Normal Rats. *J. Ethnopharmacol.* 110, 458–463. doi: 10.1016/j.jep.2006.10.005

Lei, X.-L., and Chiou, G. C. (1986). Studies on Cardiovascular Actions of *Salvia miltiorrhiza*. *Am. J. Chin. Med.* 14, 26–32. doi: 10.1142/S0192415X86000053

Li, C., Yung, K., and Chiu, K. (1990). Hypotensive Action of *Salvia miltiorrhiza* Cell Culture Extract. *Am. J. Chin. Med.* 18, 157–166. doi: 10.1142/S0192415X90000204

Lymperopoulos, A., Rengo, G., and Koch, W. J. (2013). Adrenergic Nervous System in Heart Failure: Pathophysiology and Therapy. *Circ. Res.* 113, 739–753. doi: 10.1161/CIRCRESAHA.113.300308

Mais, B., Yaser, A. M., and Ream, N. (2016). Hypolipidemic Effect of Achillea Biebersteinii Ethanolic Extract in Hamsters with Diet-Induced Hypercholesterolemia. *Int. J. Pharmacogn Phytochem. Res.* 8, 1555–1559.

Mali, V. R., Mohan, V., and Bodhankar, S. L. (2012). Antihypertensive and Cardioprotective Effects of the Lagenaria Siceraria Fruit in N G-Nitro-L-Arginine Methyl Ester (L- Name) Induced Hypertensive Rats. *Pharmaceut. Biol.* 50, 1428–1435. doi: 10.3109/13880209.2012.684064

Malik, K., Ahmad, M., Bussmann, R. W., Tariq, A., Ullah, R., Alqahtani, A. S., et al. (2018). Ethnobotany of Anti- Hypertensive Plants Used in Northern Pakistan. *Front. Pharmacol.* 9, 1–18. doi: 10.3389/fphar.2018.00789

Mangathayaru, K., Kuruvilla, S., Balakrishna, K., and Venkhatesh, J. (2009). Modulatory Effect of Inula Racemosa Hook. F.(Asteraceae) on Experimental Atherosclerosis in Guinea-Pigs. *J. Pharm. Pharmacol.* 61, 1111–1118. doi: 10.1211/jpp.61.08.0016

Masaki, H., Sakaki, S., Atsumi, T., and Sakurai, H. (1995). Active-Oxygen Scavenging Activity of Plant Extracts. *Biol. Pharmaceut. Bull.* 18, 162–166. doi: 10.1248/bpb.18.162

Matsubara, T., Bohgaki, T., Watarai, M., Suzuki, H., Ohashi, K., and Shibuya, H. (1999). Antihypertensive Actions of Methylripariochromene a from Orthosiphon Aristatus, an Indonesian Traditional Medicinal Plant. *Biol. Pharmaceut. Bull.* 22, 1083–1088. doi: 10.1248/bpb.22.1083

Medeiros-Neves, B., Teixera, H. F., and Von Poser, G. L. (2018). The Genus Pterocaulon (Asteraceae) – a Review on Traditional Medicinal Uses, Chemical Constituents and Biological Properties. *J. Ethnopharmacol.* 224, 451–464. doi: 10.1016/j.jep.2018.06.012

Memariani, Z., Moeini, R., Hamedi, S. S., Gorji, N., and Mozaffarpur, S. A. (2018). Medicinal Plants with Antithrombotic Property in Persian Medicine: A Mechanistic Review. *J. Thromb. Thrombolysis* 45, 158–179. doi: 10.1007/s11239-017-1580-3

Mihailovic-Stanojevic, N., Belscak-Cvitanovic, A., Grujic-Milanovic, J., Ivanov, M., Jovovic, D., Bugarski, D., et al. (2013). Antioxidant and Antihypertensive Activity of Extract from Thymus Serpyllum L. In Experimental Hypertension. *Plant Foods Hum. Nutrition* 68, 235–240. doi: 10.1007/s11130-013-0368-7

Mnonopi, N., Levendal, R.-A., Davies-Coleman, M. T., and Frost, C. L. (2011). The Cardioprotective Effects of Marrubiin, a Diterpenoid Found in Leonotis Leonurus Extracts. *J. Ethnopharmacol.* 138, 67–75. doi: 10.1016/j.jep.2011.08.041

Mocelin, R., Marcon, M., Santo, G. D., Zanatta, L., Sachett, A., Schonell, A. P., et al. (2016). Hypolipidemic and Antiatherogenic Effects of Cynara Scolymus in Cholesterol-Fed Rats. *Rev. Bras. Farmacognosia* 26, 233–239. doi: 10.1016/j.bjp.2015.11.004

Momtaz, S., and Abdollahi, M. (2008). A Systematic Review of the Biological Activities of Satureja L. Species. *Pharmacologyonline* 2, 34–54.

Morganti, A. (2005). Should a Diuretic Always Be the First Choice in Patients with Essential Hypertension? The Case for No. *J. Am. Soc. Nephrol* 16, S70–S73. doi: 10.1681/ASN.2004110964

Mothana, R. A., Alsaid, M. S., and Al-Musayeib, N. M. (2011). Phytochemical Analysis and in Vitro Antimicrobial and Free-Radical-Scavenging Activities of the Essential Oils from *Euryops arabicus* and *Laggera decurrens*. *Molecules* 16, 5149–5158. doi: 10.3390/molecules16065149

Naqash, S. Y., and Nazeer, R. (2011). Anticoagulant, Antiherpetic and Antibacterial Activities of Sulphated Polysaccharide from Indian Medicinal Plant Tridax Procumbens L.(Asteraceae). *Appl. Biochem. Biotechnol.* 165, 902–912. doi: 10.1007/s12010-011-9307-y

Ngozi, A. O., Josephine, O. O., and Felicity, E. (2013). Anti-Hyperlipidemic Effect of Aqueous Leaf Extract of *Emilia praetermissa* Milne-Redh (Asteraceae) in Rats. *Int. J. Biosci.* 3, 68–77. doi: 10.12692/ijb/3.5.68-77

Nguelefack, T. B., Dimo, T., Nguelefack Mbuyo, E. P., Tan, P. V., Rakotonirina, S. V., and Kamanyi, A. (2005). Relaxant Effects of the Neutral Extract of the Leaves of Bidens pilosa Linn on Isolated Rat Vascular Smooth Muscle. *Phytother. Res.* 19, 207–210. doi: 10.1002/ptr.1646

Ocana, A., and Reglero, G. (2012). Effects of Thyme Extract Oils (from *Thymus vulgaris*, Thymus Zygis, and Thymus Hyemalis) on Cytokine Production and Gene Expression of Oxldl-Stimulated Thp-1-Macrophages. *J. Obesity* 2012, 1–11. doi: 10.1155/2012/104706

Pande, V., and Dubey, S. (2009). Antihyperlipidemic Activity of Sphaeranthus Indicus on Atherogenic Diet Induced Hyperlipidemia in Rats. *Int. J. Green Pharmacy* 3, 159–161. doi: 10.4103/0973-8258.54911

Pawlaczyk, I., Czerchawski, L., Kuliczkowski, W., Karolko, B., Pilecki, W., Witkiewicz, W., et al. (2011). Anticoagulant and Anti-Platelet Activity of Polyphenolic- Polysaccharide Preparation Isolated from the Medicinal Plant Erigeron Canadensis L. *Thromb. Res.* 127, 328–340. doi: 10.1016/j.thromres.2010.11.031

Pereira, S., Marques, A., Sudo, R. T., Kaplan, M. A., and Zapata-Sudo, G. (2013). Vasodilator Activity of the Essential Oil from Aerial Parts of Pectis Brevipedunculata and Its Main Constituent Citral in Rat Aorta. *Molecules* 18, 3072–3085. doi: 10.3390/molecules18033072

Perez Gutierrez, R. M., and Baez, E. G. (2009). Cardioactive Agents from Plants. *Mini Rev. Med. Chem.* 9, 878–899. doi: 10.2174/138955709788452612

Pires, V. A., Cardozo-Junior, E. L., Ortmann, C. F., Maraschin, J. C., Favreto, W., Donaduzzi, C. M., et al. (2018). Lipid-Lowering and Antiatherogenic Effects of Vitex Megapotamica (Spreng.) Moldenke in a Mice Experimental Model. *J. Ethnopharmacol.* 215, 14–20. doi: 10.1016/j.jep.2017.12.030

Ramchoun, M., Harnafi, H., Alem, C., Buchele, B., Simmet, T., Rouis, M., et al. (2012). Hypolipidemic and Antioxidant Effect of Polyphenol-Rich Extracts from Moroccan Thyme Varieties. *e-SPEN J.* 7, e119–e124. doi: 10.1016/j.clnme.2012.02.005

Ramirez, J. H., Palacios, M., and Gutierrez, O. (2006). Efecto Diurético De La Especie Salvia Scutellarioides En Ratas. *Biomedica* 26, 145–149. doi: 10.7705/biomedica.v26i1.1403

Ramirez, J. H., Palacios, M., Tamayo, O., Jaramillo, R., and Gutierrez, O. (2007). Acute and Subacute Toxicity of Salvia Scutellarioides in Mice and Rats. *J. Ethnopharmacol.* 109, 348–353. doi: 10.1016/j.jep.2006.07.040

Ramu, G., Mohan, G. K., Jayaveera, K. N., Dhanapal, S. P., and Senthilkumar, G. (2012). Preliminary Phytochemical and Antioxidant Study of Hydroalcoholic Extracts from Selected Genera of Indian Lamiaceae. *Asian Pacific J. Trop. Biomed.* 2, S685–S688. doi: 10.1016/S2221-1691(12)60296-2

Rand, M. D., Lock, J., Van't Veer, C., Gaffney, D., and Mann, K. (1996). Blood Clotting in Minimally Altered Whole Blood. *Blood* 88, 3432–3445. doi: 10.1182/blood.V88.9.3432.bloodjournal8893432

Rasekh, H. R., Khoshnood-Mansourkhani, M. J., and Kamalinejad, M. (2001). Hypolipidemic Effects of *Teucrium polium* in Rats. *Fitoterapia* 72, 937–939. doi: 10.1016/S0367-326X(01)00348-3

Rastogi, S., Pandey, M. M., and Rawat, A. K. S. (2016). Traditional Herbs: A Remedy for Cardiovascular Disorders. *Phytomedicine* 23, 1082–1089. doi: 10.1016/j.phymed.2015.10.012

Ritter, M., Melichar, K., Strahler, S., Kuchta, K., Schulte, J., Sartiani, L., et al. (2010). Cardiac and Electrophysiological Effects of Primary and Refined Extracts from Leonurus Cardiaca L.(Ph. Eur.). *Planta Med* 76, 572–582. doi: 10.1055/s-0029-1240602

Roth, G. A., Johnson, C., Abajobir, A., Abd-Allah, F., Abera, S. F., Abyu, G., et al. (2017). Global, Regional, and National Burden of Cardiovascular Diseases for 10 Causes 1990 to 2015. *J. Am. Coll. Cardiol.* 70, 1–25. doi: 10.1016/j.jacc.2017.04.052

Rouhi-Boroujeni, H., Rouhi-Boroujeni, H., Heidarian, E., Mohammadizadeh, F., and Rafieian-Kopaei, M. (2015). Herbs with Anti-Lipid Effects and Their Interactions with Statins as a Chemical Anti-Hyperlipidemia Group Drugs: A Systematic Review. *ARYA Atherosclerosis* 11, 244–251.

Sabir, S. M., Athayde, M. L., Boligon, A. A., and Rocha, J. B. T. (2017). Antioxidant Activities and Phenolic Profile of Baccharis Trimera, a Commonly Used Medicinal Plant from Brazil. *South Afr. J. Bot.* 113, 318–323. doi: 10.1016/j.sajb.2017.09.010

Sacco, R. L., Kasner, S. E., Broderick, J. P., Caplan, L. R., Connors, J., Culebras, A., et al. (2013). An Updated Definition of Stroke for the 21st Century: A Statement for Healthcare Professionals from the American Heart Association/American Stroke Association. *Stroke* 44, 2064–2089. doi: 10.1161/STR.0b013e318296aeca

Saleem, R., Ahmad, M., Naz, A., Siddiqui, H., Ahmad, S. I., and Faizi, S. (2004). Hypertensive and Toxicological Study of Citric Acid and Other Constituents Fromtagetes Patula Roots. *Arch. Pharmacal. Res.* 27, 1037–1042. doi: 10.1007/BF02975428

Santos-Gomes, P. C., Seabra, R. M., Andrade, P. B., and Fernandes-Ferreira, M. (2002). Phenolic Antioxidant Compounds Produced by in Vitro Shoots of Sage (*Salvia officinalis* L.). *Plant Sci.* 162, 981–987. doi: 10.1016/S0168-9452(02)00052-3

Schneider, M., Sachett, A., Schonell, A. P., Ibagy, E., Fantin, E., Bevilaqua, F., et al. (2015). Hypoglycemic and Hypolipidemic Effects of Solidago Chilensis in Rats. *Rev. Bras. Farmacognosia* 25, 258–263. doi: 10.1016/j.bjp.2015.05.001

Senejoux, F., Girard, C., Kerram, P., Aisa, H. A., Berthelot, A., Bevalot, F., et al. (2010). Mechanisms of Vasorelaxation Induced by Ziziphora Clinopodioides Lam. (Lamiaceae) Extract in Rat Thoracic Aorta. *J. Ethnopharmacol.* 132, 268–273. doi: 10.1016/j.jep.2010.08.028

Sever, B. (2000). *The Investigation of Diterpenoid and Flavonoid Contents of Ballota Species Growing in Turkey.* (Ankara: Ankara University).

Seyoum, A., Asres, K., and El-Fiky, F. K. (2006). Structure–Radical Scavenging Activity Relationships of Flavonoids. *Phytochemistry* 67, 2058–2070. doi: 10.1016/j.phytochem.2006.07.002

Shahat, A. A., Ibrahim, A. Y., and Elsaid, M. S. (2014). Polyphenolic Content and Antioxidant Activity of Some Wild Saudi Arabian Asteraceae Plants. *Asian Pacific J. Trop. Biomed.* 7, 545–551. doi: 10.1016/S1995-7645(14)60091-2

Sharaf, K. H., and Ali, J. S. (2004). Hypolipemic Effect of Kuub (Gundelia Tourefotti A.) Oil and Clofibrate on Lipid Profile of Atherosclerotic Rats. *Veterinarski Arhiv* 74, 359–369. doi: 10.4314/ajb.v7i25.59660

Shiva Kumar, A., Jeyaprakash, K., Chellappan, D. R., and Murugan, R. (2017). Vasorelaxant and Cardiovascular Properties of the Essential Oil of Pogostemon Elsholtzioides. *J. Ethnopharmacol.* 199, 86–90. doi: 10.1016/j.jep.2017.01.036

Soetan, K. (2008). Pharmacological and Other Beneficial Effects of Antinutritional Factors in Plants-A Review. *Afr. J. Biotechnol.* 7, 4713–4721.

Somova, L., Nadar, A., Rammanan, P., and Shode, F. (2003). Cardiovascular, Antihyperlipidemic and Antioxidant Effects of Oleanolic and Ursolic Acids in Experimental Hypertension. *Phytomedicine* 10, 115–121. doi: 10.1078/094471103321659807

Spranger, M., Krempien, S., Schwab, S., Donneberg, S., and Hacke, W. (1997). Superoxide Dismutase Activity in Serum of Patients with Acute Cerebral Ischemic Injury: Correlation with Clinical Course and Infarct Size. *Stroke* 28, 2425–2428. doi: 10.1161/01.STR.28.12.2425

Sultana, A., Khaliq, T., Rehman, A. U., Majeed, W., Faisal, M. N., Aslam, B., et al. (2017). Pharmacological Evaluation of Vernonia Elaeagnifolia (Asteraceae) Leaves in Hyperlipidemic Albino Rabbits. *Trop. J. Pharmaceut. Res.* 16, 1077–1083. doi: 10.4314/tjpr.v16i5.15

Taleb, A., Ahmad, K. A., Ihsan, A. U., Qu, J., Lin, N., Hezam, K., et al. (2018). Antioxidant Effects and Mechanism of Silymarin in Oxidative Stress Induced Cardiovascular Diseases. *Biomed. Pharmacother.* 102, 689–698. doi: 10.1016/j.biopha.2018.03.140

Taleb-Senouci, D., Ghomari, H., Krouf, D., Bouderbala, S., Prost, J., Lacaille-Dubois, M., et al. (2009). Antioxidant Effect of Ajuga Iva Aqueous Extract in Streptozotocin-Induced Diabetic Rats. *Phytomedicine* 16, 623–631. doi: 10.1016/j.phymed.2008.12.004

Tundis, R., Menichini, F., Loizzo, M. R., Bonesi, M., Solimene, U., and Menichini, F. (2012). Studies on the Potential Antioxidant Properties of Senecio Stabianus Lacaita (Asteraceae) and Its Inhibitory Activity against Carbohydrate-Hydrolysing Enzymes. *Natural Prod. Res.* 26, 393–404. doi: 10.1080/14786419.2010.488233

Varga, Z., Seres, I., Nagy, E., Ujhelyi, L., Balla, G., Balla, J., et al. (2006). Structure Prerequisite for Antioxidant Activity of Silybin in Different Biochemical Systems in Vitro. *Phytomedicine* 13, 85–93. doi: 10.1016/j.phymed.2004.06.019

Wojtyniak, K., Szymanski, M., and Matlawska, I. (2013). Leonurus Cardiaca L.(Motherwort): A Review of Its Phytochemistry and Pharmacology. *Phytotherapy* 27, 1115–1120. doi: 10.1002/ptr.4850

Woodruff, T. M., Thundyil, J., Tang, S.-C., Sobey, C. G., Taylor, S. M., and Arumugam, T. V. (2011). Pathophysiology, Treatment, and Animal and Cellular Models of Human Ischemic Stroke. *Mol. Neurodegeneration* 6, 11–29. doi: 10.1186/1750-1326-6-11

Yam, M. F., Tan, C. S., Ahmad, M., and Ruan, S. (2016). Vasorelaxant Action of the Chloroform Fraction of Orthosiphon Stamineus Via NO/cGMP Pathway, Potassium and Calcium Channels. *Am. J. Chin. Med.* 44, 1413–1439. doi: 10.1142/S0192415X16500798

Yam, M. F., Tan, C. S., and Shibao, R. (2018). Vasorelaxant Effect of Sinensetin Via the NO/sGC/cGMP Pathway and Potassium and Calcium Channels. *Hypertension Res.* 41, 787–797. doi: 10.1038/s41440-018-0083-8

Zargar, B. A., Ahmad, B., Bhat, M. F., and Masoodi, M. H. (2017). *Prunella vulgaris* Linn. As Antihyperlipidemic and Antioxidant against High-Fat Diet Induced Oxidative Stress in Wistar Rats. *J. Pharmacogn Phytochem.* 6, 1097–1103.

Zeggwagh, N. A., Moufid, A., Michel, J. B., and Eddouks, M. (2009). Hypotensive Effect of Chamaemelum Nobile Aqueous Extract in Spontaneously Hypertensive Rats. *Clin. Exp. Hypertension* 31, 440–450. doi: 10.1080/10641960902825453

Zhang, X.-L., Guo, Y.-S., Wang, C.-H., Li, G.-Q., Xu, J.-J., Chung, H. Y., et al. (2014). Phenolic Compounds from *Origanum vulgare* and Their Antioxidant and Antiviral Activities. *Food Chem.* 152, 300–306. doi: 10.1016/j.foodchem.2013.11.153

Ziaee, M., Khorrami, A., Ebrahimi, M., Nourafcan, H., Amiraslanzadeh, M., Rameshrad, M., et al. (2015). Cardioprotective Effects of Essential Oil of Lavandula Angustifolia on Isoproterenol-Induced Acute Myocardial Infarction in Rat. *Iranian J. Pharmaceut. Res.* 14, 279–289.

Conflict of Interest: The authors declare that the research was conducted in the absence of any commercial or financial relationships that could be construed as a potential conflict of interest.

Advantages of publishing in Frontiers

OPEN ACCESS
Articles are free to read for greatest visibility and readership

FAST PUBLICATION
Around 90 days from submission to decision

HIGH QUALITY PEER-REVIEW
Rigorous, collaborative, and constructive peer-review

TRANSPARENT PEER-REVIEW
Editors and reviewers acknowledged by name on published articles

Frontiers
Avenue du Tribunal-Fédéral 34
1005 Lausanne | Switzerland

Visit us: www.frontiersin.org
Contact us: info@frontiersin.org | +41 21 510 17 00

REPRODUCIBILITY OF RESEARCH
Support open data and methods to enhance research reproducibility

DIGITAL PUBLISHING
Articles designed for optimal readership across devices

FOLLOW US
@frontiersin

IMPACT METRICS
Advanced article metrics track visibility across digital media

EXTENSIVE PROMOTION
Marketing and promotion of impactful research

LOOP RESEARCH NETWORK
Our network increases your article's readership